

M.Y.H. Bangash

Earthquake Resistant Buildings

Dynamic Analyses, Numerical Computations, Codified Methods, Case Studies and Examples

Springer

www.EngineeringBooksPDF.com

Earthquake Resistant Buildings

www.EngineeringBooksPDF.com

www.EngineeringBooksPDF.com

M.Y.H. Bangash

Earthquake Resistant Buildings

Dynamic Analyses, Numerical Computations, Codified Methods, Case Studies and Examples

Springer

www.EngineeringBooksPDF.com

M.Y.H. Bangash
Consulting Engineer in Advanced
Structural Analysis
London, UK

ISBN 978-3-540-93817-0 e-ISBN 978-3-540-93818-7
DOI 10.1007/978-3-540-93818-7
Springer Heidelberg Dordrecht London New York

Library of Congress Control Number: 2010920825

© 2011 M.Y.H. Bangash; London, UK
Published by: Springer-Verlag Berlin Heidelberg 2011
This work is subject to copyright. All rights are reserved, whether the whole or part of the material is concerned, specifically the rights of translation, reprinting, reuse of illustrations, recitation, broadcasting, reproduction on microfilm or in any other way, and storage in data banks. Duplication of this publication or parts thereof is permitted only under the provisions of the German Copyright Law of September 9, 1965, in its current version, and permission for use must always be obtained from Springer. Violations are liable to prosecution under the German Copyright Law.
The use of general descriptive names, registered names, trademarks, etc. in this publication does not imply, even in the absence of a specific statement, that such names are exempt from the relevant protective laws and regulations and therefore free for general use.

Cover design: deblik, Berlin

Printed on acid-free paper

Springer is part of Springer Science + Business Media (www.springer.com)

www.EngineeringBooksPDF.com

Preface

This book provides a general introduction to the topic of three-dimensional analysis and design of buildings for resistance to the effects of earthquakes. It is intended for a general readership, especially persons with an interest in the design and construction of buildings under servere loadings.

A major part of design for earthquake resistance involves the building structure, which has a primary role in preventing serious damage or structural collapse. Much of the material in this book examines building structures and, specifically, their resistance to vertical and lateral forces or in combinations. However, due to recent discovery of the vertical component of acceleration of greater magnitude in the kobes' earthquake the original concept of "lateral force only" has changed. This book does advocate the contribution of this disastrous component in the global analytical investigation.

When the earthquake strikes, it shakes the whole building and its contents. Full analysis for design layout and type of earthquakes, therefore, must include considerations for the complete building construction, the building contents and the building occupants.

The work of designing for earthquake effects is formed by a steady stream of studies, research, new technologies and the cumulative knowledge gained from forensic studies of earthquake-damaged buildings. Design and construction practices, regulating codes and professional standards continuously upgraded due to the flow of this cumulative knowledge. Hence, any book on this subject must regularly be updated. Since the effects are not the same, the earthquake forces are always problematic.

Over the years, earthquake has been the cause of great disasters in the form of destruction of property and injury and loss of life to the population. The unpredictability and sudden occurrence of earthquakes make them somewhat mysterious, both to the general public and to professional building designers. Until quite recently, design for earthquakes – if consciously considered at all – was done with simplistic methods and a small database. Extensive study and research and a great international effort and cooperation have vastly improved design theories and procedures. Accordingly, most buildings in earthquake-prone areas today are designed in considerable detail for seismic resistance.

www.EngineeringBooksPDF.com

Despite the best efforts of scientists and designers, most truly effective design methods are those reinforced by experience. This experience, unfortunately, grown by leaps when a major earthquake occurs and strongly affects regions of considerable development – notably urban areas. Observation of damaged buildings by experts in forensic engineering adds immeasurably to our knowledge base. While extensive research studies are ongoing in many testing laboratories, the biggest laboratory remains the real world and real earthquakes.

Design decisions that affect the seismic response of buildings range from broad to highly specific ones. While much of this design work may be performed by structural engineers, many decisions are made by, or are strongly affected by, others. Building codes and industry standards establish restrictions on the use of procedures for analysis of structural behaviour and for the selection of materials and basic systems for construction. Decisions about site development, building placement on sites, building forms and dimensions and the selection of materials and details for construction are often made by so many others too.

On this respect it was necessary that the reader should look into codes of practice in certain countries prone to major earthquakes. Some codes including the Eurocode-8 are given together with numerical and analytical methods for comparative studies. This approach enhances the design quality and creates confidence in the designer on his/her work.

While ultimate collapse of the Building structure is a principal concern, the building's performance during an earthquake must be considered in many other ways as well. If the structure remains intact, but structural part of the building sustains critical damage, occupants are traumatized or injured, and it is infeasible to restore the building for continued use; the design work may not be viewed as success. However, the necessity sometimes governs. Some countries may not have sophisticated tools and resources. Others must assist to provide them.

The work in this book is mostly analytical and hence should be accessible to the broad range of people in the building design and construction fields. This calls for some compromise since all are trained highly in some areas and less – or not at all – in others. The readers should have general knowledge of building codes, current construction technology, principal problems of planning buildings and at least an introduction to design of simple structures for earthquake-prone buildings. Most of all, readers need some real motivation for learning about making buildings safer during earthquakes. Many design examples and case studies are included to make the book fully attractive to all and sundry.

Readers less prepared may wish to strengthen their backgrounds in order to get the most from the work in this book. The author gives a vast bibliography at the end of this book and a list of references after each chapter so that the reader can carryout an in-depth study on a specific area missed out in detail. The reader hopefully will understand the need for grappling with this complex subject.

This book addresses the perplexing problem of how to maintain operability of equipment after a major earthquake. The programme is often more complicated than simple anchorage. Some critical types of equipment, for example,

www.EngineeringBooksPDF.com

are likely to fail operationally (false signalling of switches, etc.) even if adequate base anchorage has been provided. It is the goal of this book to point out to the reader with a plan whereby equipment must be classified and subsequently qualified for the postulated seismic environment in a manner that best suits the individual piece of equipment. In some cases this qualification and analysis can be accomplished only by sophisticated seismic testing programme, while at the other end of the spectrum, equipment sometimes may be qualified simply by adequate architectural detailing. All too often, professional design teams and owners rely on an electric plug and gravity to keep a critical piece of equipment in place during an earthquake and functional afterwards. Obviously, this is less than desirable situation. One part of the suggestion is devoted to the qualification procedures which include

- Testing
- Analyses
- Designer's judgement
- Prior experience
- Design earthquakes
- Seismic categories for equipment
- Design specification procedures

The reader can easily be advised to refer to relevant codes such as Eurocode 8 and its supplements and parts. This book does not go into details regarding the above procedures but only concentrates on the analytical/design methodology.

The discussion of these topics leaves the designer with a complete course of action for qualifying all types of equipments, such as seismic devices to control the building structures during earthquakes. The author for this reason gives a comprehensive chapter on the subject.

One major measure to mitigate the earthquake hazards is to design and build structures through better engineering practices, so that these structures possess adequate earthquake-resistant capacity. Considerable research efforts have been carried out in the USA, Japan, China and other countries in the last few decades to advance earthquake engineering knowledge and design methods. This book summarizes the state-of-the-art knowledge and worldwide experiences, particularly those from China and the USA, and presents them systematically in one volume for possible use by engineers, researchers, students, and other professionals in the field of earthquake engineering. Considering the active research and rapid technological advances which have taken place in this field, there has been a surprising shortage of suitable textbooks for senior level or graduate level students. This book also attempts to help fill such a gap.

The book consists of 10 major parts: engineering seismology and earthquake-resistant analyses and design. Special attention is placed on bridging the gap between these disciplines. For the convenience of the reader, fundamentals of seismology, earthquake engineering and random processes, which, can be useful tools to describe the three-dimensional ground motions are given to assess the structural or soil response to them. Vast chapters are included.

www.EngineeringBooksPDF.com

This is followed by describing earthquake intensity, ground motions and its damaging effects. In the ensuing chapters concerning the earthquake-resistant design, both fundamental theories and new research problems and design standards are introduced. In this book stochastic methods are introduced because of their potential to offer a new dimension in earthquake engineering applications. These two areas have been subjected to intensive research in recent years and there is a potential in them to provide solutions to some special problems which might not be amenable to conventional approaches. Appendices are given for supporting analyses. Computer subroutines, which can be used with any known packages to suit the reader.

Although this book may appear to present a daunting amount of material, it is, nevertheless, just a toe in the door of the vast library of knowledge that exists. Readers may use this book to gain general awareness of the field or to launch a much more exhaustive programme of study.

On design sides, many codified methods have been briefly mentioned. The Eurocode EC-8 and the American codes with examples have been highlighted.

The book will serve as a useful text for teachers preparing design syllabi for undergraduate and postgraduate courses. Each major section contains a full explanation which allows the book to be used by students and practicing engineers, particularly those facing formidable task of having to design/detail complicated building structures with unusual boundary conditions. Contractors will also find this book useful in the preparation of construction drawings, and manufacturers will be interested in the guidance even in the text recording codified and newly developed methods and the manufacture of earthquake resistant devices.

London, UK M.Y.H. Bangash

www.EngineeringBooksPDF.com

Acknowledgments

The author is indebted to many individuals, institutions, organizations and research establishments mentioned in the text for helpful discussions and for providing useful practical data and research materials.

The author owes a special debt of gratitude to his family who, for the third time, provided unwavering support.

The author also acknowledges the following private communications:

Aerospace Daily (Aviation and Aerospace Research), 1156 15th Street NW, Washington, 20005, USA.
Azad Kashmir, Disaster Management Centre. Reports Jan. 2008–2009.
Afghan Agency Press, 33 Oxford Street, London, UK.
Agusta SpA, 21017 Cascina Costa di Samarate (VA), Italy.
Ailsa Perth Shipbuilders Limited, Harbour Road, Troon, Ayrshire KA10 6DN, Scotland.
Airbus Industrie, 1 Rond Point Maurice Bellonte, 31707 Blagnac Cédex, France.
Allison Gas Turbine, General Motors Corporation, Indianapolis, Indiana 46 206–0420, USA.
AMX International, Aldwych House, Aldwych, London, WC2B 4JP, UK.
Arizona State University, Tempe AZ, USA.
Azad Kashmir office for Earthquake Management Pakistan, 2009. Pakistan, (Pukhtoon Khawa) *N.W.F.P. Pákistan, Peshawar, Earthquake Division, 2009*, Pakistan
Bogazici, University, Turkey.
Bremer Vulkan AG, Lindenstrasse 110, PO Box 750261, D-2820 Bremen 70, Germany.
British Library, Kingcross, London, UK.
Catic, 5 Liang Guo Chang Road, East City District (PO Box 1671), Beijing, China.
Chantiers de l'Atlantique, Alsthom-30, Avenue Kléber, 75116 Paris, France.
Chemical and Engineering News, 1155 16th Street NW, Washington DC 20036, USA.
Chinese State Arsenals, 7A Yeutan Nanjie, Beijing, China.

www.EngineeringBooksPDF.com

Conorzio Smin, 52, Villa Panama 00198, Rome, Italy.
CITEFA, Zufratequ y Varela, 1603 Villa Martelli, Provincia de Buenos Aires, Argentina.
Daily Muslim, Abpara, Islamabad, Pakistan.
Daily Telegraph, Peterborough Court, South Quay Plaza, Marshwall, London E14, UK.
Dassault-Breguet, 33 Rue de Professeur Victor Pauchet, 92420, Vaucresson, France.
Défense Nationale, 1 Place Joffre, 75700, Paris, France.
Der Spiegel, 2000 Hamburg 11, Germany.
Department of Engineering Sciences, University of California, San Diego, CA, USA.
Earthquake Hazard Prevention Institute, Wasada University, Shinju Ko-Ku, Tokyo, Japan
Earthquake Research Institute, University of Tokyo, Japan
Evening Standard, Evening Standard Limited, 118 Fleet Street, London EC4P 4DD, UK.
Financial Times, Bracken House, 10 Cannon Street, London EC4P 4BY.
Fokker, Corporate Centre, PO Box 12222, 1100 AE Amsterdam Zuidoost, The Netherlands.
Fukuyama University, Gakuen-Cho, Fukuyama, Hiroshima, Japan
General Dynamic Corporation, Pierre Laclede Centre, St Louis, Missouri 63105, USA (2003–2009).
General Electric, Neumann Way, Evendale, Ohio 45215, USA.
Graduate School of Engineering, Kyoto University, Kyoto, Japan
Guardian, Guardian Newspapers Limited, 119 Farringdon Road, Londo EC1R 3ER, UK.
Hawker Siddeley Canada Limited, PO Box 6001, Toronto AMF, Ontario L5P 1B3, Canada.
Hindustan Aeronautics Limited, Indian Express Building, PO Box 5150, Bangalore 560 017, India (Dr Ambedkar Veedhil).
Howaldtswerke Deutsche Werft, PO Box 146309, D-2300 Kiel 14, Germany.
Imperial College Earthquake Engineering Centre, London, U.K. The Indian institute of Technology, Bombay, India (2009).
Independent, 40 City Road, London EC1Y 2DB, UK. (2007–2009)
Information Aéronautiques et Spatiales, 6 Rue Galilee, 75116, Paris, France.
Information Resources Annual, 4 Boulevard de 1'Empereur, B-1000, Brussels, Belgium.
Institute Für Ange Nandte Mechanik, Techniche Universität Braunschweig. D-38106, Braunschweig, Germany (2009).
Institutodi Energetica, Universitâ degdi studi Reggio Calibria, Reggio, Calibria, Italy
International Aero-engines AG, 287 Main Street, East Hartford, Connecticut 06108, USA.

www.EngineeringBooksPDF.com

Israel Aircraft Industries Limited, Ben-Gurion International Airport, Israel 70100.
Israel Ministry of Defence, 8 David Elazar Street, Hakiryah 61909, Tel Aviv, Israel.
KAL (Korean Air), Aerospace Division, Marine Centre Building 18FL, 118-2 Ga Namdaernun-Ro, Chung-ku, Seoul, South Korea.
Kangwon Industrial Company Limited, 6-2-KA Shinmoon-Ro, Chongro-ku, Seoul, South Korea.
Kawasaki Heavy Industries Limited, 1–18 Nakamachi-Dori, 2-Chome, Chuo-ku, Kobe, Japan.
Konoike Construction Co Limited, Osaka, Japan
Korea Tacoma Marine Industries Limited, PO Box 339, Masan, Korea.
Krauss-Maffei AG, Wehrtocknik GmbH Krauss-Maffei Strasse 2, 8000 Munich 50, Germany.
Krupp Mak Maschinenbau GmbH, PO Box 9009, 2300 Kiel 17, Germany.
Laboratory for Earthquake Engineering, National Technical University of Athens, Athens, Greece
Limited, Quadrant House, The Quadrant, Sutton, Surrey SM2 5AS, UK.
Lockheed Corporation, 4500 Park Granada Boulevard, Calabasas, California 91399-0610, USA.
Matra Defense, 37 Avenue Louis-Bréguet BP1, 78146 Velizy-Villa Coublay Cédex, France.
Massachusetts Institute of Technology, USA (2003–2009).
McDonnell Douglas Corporation, PO Box 516, St Louis, Missouri 63166, USA.
Mitsubishi Heavy Industries Limited, 5-1 Marunouchi, 2-Chome, Chiyoda-ku, Tokyo 100, Japan.
Muto Institute of Earthquake Engineering Tokyo, Japan (2001–2010).
NASA, 600 Independence Avenue SW, Washington DC 20546, USA.
Nederlandse Verenigde Scheepsbouw Bureaus, PO Box 16350, 2500 BJ, The Hague, The Netherlands.
Netherland Naval Industries Group, PO Box 16350, 2500 BJ, The Hague, The Netherlands.
New York Times, 229 West 43rd Street, New York, NY 10036, USA.
Nuclear Engineering International, c/o Reed Business Publishing House
Observer, Observer Limited, Chelsea Bridge House, Queenstown Road, London SW8 4NN, UK.
Offshore Engineer, Thomas Telford Limited, Thomas Telford House, 1 Heron Quay, London E14 9XF, UK.
OTO Melara, Via Valdilocchi 15, 19100 La Spezia, Italy.
Pakistan Aeronautical Complex, Kamra, District Attock, Punjab Province, Pakistan.
Plessey Marine Limited, Wilkinthroop House, Templecombe, Somerset BA8 ODH, UK.
Princeton University U.S.A.

www.EngineeringBooksPDF.com

Promavia SA, Chaussée de Fleurs 181, 13-6200 Gosselies Aéroport, Belgium.
SAC (Shenyang Aircraft Company), PO Box 328, Shenyang, Liaoning, China. Short Brothers pic, PO Box 241, Airport Road, Belfast BT3 9DZ, Northern Ireland.
Seismological Society of America, U.S.A.
Sikorsky, 6900 North Main Street, Stratford, Connecticut 06601-1381, USA. Soloy Conversions Limited, 450 Pat Kennedy Way SW, Olympia, Washington 98502, USA.
Soltam Limited, PO Box 1371, Haifa, Israel.
SRC Group of Companies, 63 Rue de Stalle, Brussels 1180, Belgium.
State University of Newyork at Buffalo, U.S.A.
Tamse, Avda, Rolon 1441/43, 2609 Boulgone sur Mer, Provincia de Buenos Aires, Argentina.
Technische Universität Berlin, Sekr B7, D1000, Berlin 12, Germany.
The American Society of Civil Engineers, U.S.A.
The Institution of Civil Engineers, Great George Street, Westminster, London SW1, UK.
The Institution of Mechanical Engineers, 1 Bird Cage Walk, Westminster, London SW1, UK.
The National University of Athens, Greece.
The World Conferences on Earthquake Engineering–Management 1960–2002. California Institute, California, U.S.A.
Thomson-CSF, 122 Avenue du General Leclerc, 92105 Boulogne Billancourt, France.
Texas A&M university, U.S.A.
Textron Lycoming, 550 Main Street, Stratford, Connecticut 06497, USA.
*Times Index,*Research Publications, PO Box 45, Reading RGl 8HF, UK.
Turbomeca, Bordes, 64320 Bizanos, France.
Universitâ degdi studi di cantania, Italy.
University of Perugia, Loc. Pentima Bassa, 21, Terni, Italy
USSR Public Relations Offices, Ministry of Defence, Moscow, USSR.

www.EngineeringBooksPDF.com

Dedicated Acknowledgement

(a) Acknowledgement to Scholars in Earthquake Engineering. There are a number of people who worked for life cannot be left alone. It is difficult to name all of them here. The authors heart goes out for them and their work. They richly deserve their place. The following are chosen for the dedicated acknowledgement:

- Professor Thomas. A. Jaeger Bundesomstalt für material prufung, Berlin, Germany
- Dr. Bruno A. Boley, Northwestern University, Illinois, U.S.A.
- Dr. M. Watabe, Ibaraki, Japan
- V.V. Bertera, University of California, U.S.A.
- Professor H.B. Seed, Earthquake Engineering Center, University of California, U.S.A.
- Professor H. Shibata, University of Tokyo, Japan.
- Professor J. Lysmer, Earthquake Engineering Center, University of California, Berkeley, California U.S.A.
- Professor R. Clough, University of California, U.S.A.
- Professor H. Ambarasy, Impertial College, London, U.K.
- Professor G.W. Housner, California Institute of Technology, U.S.A.
- Dr. J. Blume, University of California, U.S.A.

(b) Acknowledgement Companies and Research Establishments in Earthquake Engineering. Their help is enormous.

- Toda Construction Company Ltd, Tokyo, Japan
- Tennessee Valley Authority, Tennessee, U.S.A.
- Nuclear Regulatory Commission (NRG) Washingtons DC. U.S.A.
- Lawrence Livermore Laboratory, Livermore, University of California, U.S.A.
- Saap 2000, University of California Computer Center, University of California U.S.A.
- The Architectural Institute of Japan, Tokyo, Japan

www.EngineeringBooksPDF.com

- Carnegie Institute of Washington, Washington D.C., U.S.A.
- Institute de Ingeniera, UNAM, Mexico, U.S.A.
- Ministry of Construction, Tokyo, Japan
- Kyoto University Disaster Prevention Laboratory, Kyoto, Japan

www.EngineeringBooksPDF.com

Contents

1 Introduction to Earthquake with Explanatory Data 1
1.1 Earthquake or Seismic Analysis and Design Considerations 1
1.1.1 Introduction. 1
1.2 Plate Tectonic and Inner Structure of Earth 1
1.3 Types of Faults 6
1.4 Seismograph And Seismicity 7
1.5 Seismic Waves. 8
1.6 Magnitude of the Earthquake 9
1.6.1 Seismic Magnitude 10
1.7 The World Earthquake Countries and Codes of Practices . . . 11
1.8 Intensity Scale. 23
1.8.1 Earthquake Intensity Scale 24
1.8.2 Intensity Distribution 25
1.8.3 Abnormal Intensity Region. 31
1.8.4 Factors Controlling Intensity Distribution 31
1.9 Earthquake Intensity Attenuation 32
1.9.1 Epicentral Intensity and Magnitude 32
1.10 Geotechnical Earthquake Engineering. 32
1.11 Liquefaction 33
1.11.1 Introduction. 33
1.11.2 Types of Damage. 34
1.12 Earthquake-Induced Settlement. 34
1.13 Bearing Capacity Analyses for Earthquakes 35
1.14 Slope Stability Analysis for Earthquakes. 35
1.15 Energy Released in an Earthquake 36
1.16 Earthquake Frequency 37
1.17 Impedance Contrast 40
1.18 Glossary of Earthquake/Seismology 41
1.19 Artificial Generation of Earthquake 45
1.20 Net Result. 45
Bibliography 46

www.EngineeringBooksPDF.com

2 Existing Codes on Earthquake Design with and Without Seismic Devices and Tabulated Data 51
2.1 Existing Codes on Earthquake Design 51
2.1.1 Algeria: RPA (1989) 51
2.1.2 Argentina : INPRES-CIRSOC 103 (1991) 53
2.1.3 Australia: AS11704 (1993) 57
2.1.4 China: TJ 11-78 and GBJ 11-89 60
2.1.5 Europe: 1-1 (Oct 94); 1-2 (Oct 94); 1-3 (Feb 95); Part 2 (Dec 94); Part 5 (Oct 94); Eurocode 8 64
2.1.6 India and Pakistan: IS-1893 (1984) and PKS 395-Rev (1986) 75
2.1.7 Iran: ICRD (1988) 77
2.1.8 Israel: IC-413 (1994) 79
2.1.9 Italy: CNR-GNDT (1986) and Eurocode EC8 is Implemented 83
2.1.10 Japan: BLEO (1981) 84
2.1.11 Mexico: UNAM (1983) M III (1988) 88
2.1.12 New Zealand: NZS 4203 (1992) and NZNSEE (1988) 92
2.1.13 USA: UBC-91 (1991) and SEAOC (1990) 95
2.1.14 Codes Involving Seismic Devices and Isolation Techniques 100
Bibliography 136

3 Basic Structural Dynamics 143
3.1 General Introduction 143
3.2 Structural Dynamics 143
3.2.1 General Introduction to Basic Dynamics 143
3.2.2 Single-Degree-of-Freedom Systems – Undamped Free Vibrations 144
3.2.3 Summary and Conclusions 149
3.2.4 Multi-Degree-of-Freedom System 152
3.2.5 Dynamic Response of Mode Superposition 159
3.3 Examples of Dynamic Analysis of Building Frames and Their Elements Under Various Loadings and Boundary Conditions 162
3.3.1 Example 3.1 163
3.3.2 Example 3.2 165
3.3.3 Example 3.3 167
3.3.4 Example 3.4 169
3.3.5 Example 3.5 172
3.3.6 Example 3.6 179
3.3.7 Example 3.7 181
3.3.8 Example 3.8 182
3.3.9 Example 3.9 184

www.EngineeringBooksPDF.com

3.3.10 Example 3.10 185
3.3.11 Example 3.11 190
3.3.12 Generalized Numerical Methods in Structural Dynamics 195

4 Earthquake Response Spectra With Coded Design Examples 207
4.1 Introduction 207
4.2 Fourier Spectrum 208
4.3 Combined Spectrum S_d-V-S_a 218
4.4 Construction of Response Spectrum 219
4.5 Design Examples 220
4.5.1 Example 4.1 American Practice 221
4.5.2 Example 4.2 American and Other Practices 224
4.5.3 Example 4.3 Algeria and Argentina Practices 229
4.5.4 Example 4.4 American Practice 236
4.5.5 Example 4.5 American Practice 237
4.5.6 Example 4.6 American Practice 242
4.5.7 Elastic Design Spectrum: Construction of Design Spectrum 244
4.6 Earthquake Response of Inelastic Systems 252
4.6.1 General 252
4.6.2 De-amplification Factors 254
4.6.3 Response Modification Factors 256
4.6.4 Energy Content and Spectra 257
4.6.5 Example 4.7 American Practice 259
4.6.6 Example 4.8 American Practice 261
4.6.7 Example 4.9 European Practice 271
4.6.8 Example 4.10 British Practice 281
4.6.9 Yield Strength and Deformation from the Response Spectrum (American Practice) 284
4.7 Equivalent Static Force Method Based on Eurocode-8 286
4.7.1 General Introduction 286
4.7.2 Evaluation of Lumped Masses to Various Floor Levels 286
4.7.3 Response Spectrum Method 288
4.7.4 Example 4.12 Step-by-Step Design Analysis Based on EC8 293

5 Dynamic Finite Element Analysis of Structures 305
5.1 Introduction 305
5.2 Dynamic Equilibrium 305
5.2.1 Lumped Mass system 305
5.3 Solution of the Dynamic Equilibrium Equations 306
5.3.1 Mode Superposition Method 307
5.4 Step-By-Step Solution Method 312

www.EngineeringBooksPDF.com

5.4.1 Fundamental Equilibrium Equations 312
5.4.2 Supplementary Devices 313
5.5 Runge–Kutta Method 315
5.5.1 Introduction. 315
5.6 Non-linear Response of Multi-Degrees-of-Freedom Systems: Incremental Method 317
5.7 Summary of the Wilson-θ Method. 320
5.8 Dynamic Finite Element Formulation with Base Isolation . . . 322
5.9 Added Viscoelastic Dampers (VEDs) in Seismic Buildings . . . 323
5.9.1 Introduction. 323
5.9.2 Generalized Equation of Motion when Dampers Are Used 324
5.9.3 System Dynamic Equation with Friction Dampers . . 324
5.10 Non-linear Control of Earthquake Buildings with Actuators . . 327
5.10.1 Introduction. 327
5.10.2 Analysis Involving Actuators 327
5.11 Spectrum Analysis with Finite Element 332
5.11.1 Calculation by Quadratic Integration 334
5.11.2 Calculation by Cubic Integration 334
5.11.3 Cubic Integration. 334
5.11.4 Mode Frequency Analysis using Finite Element. 335
5.11.5 Dynamic Analysis: Time-Domain Technique 338
5.12 Sample Cases 350
5.12.1 Plastic Potential of the Same Form as the Yield Surface. . . 350
5.12.2 von Mises Yield Surface Associated with Isotropic Hardening 351
5.12.3 Dynamic Local and Global Stability Analysis 360
5.13 Dynamic Analysis of Buildings in Three Dimensions 362
5.13.1 General Introduction. 362
5.13.2 Finite Element Analysis of Framed Tubular Buildings Under Static and Dynamic Load Influences. 364
5.14 Finite Element Modelling of Building Structures – Step by Step Formulations Incorporating All Previous Sections 365
5.14.1 Introduction. 365
5.14.2 Solid Isoparametric Element Representing Concrete . . 366
5.14.3 The Shape Function 368
5.14.4 Derivatives and the Jacobian Matrix 368
5.14.5 Determination of Strains. 370
5.14.6 Determination of Stresses 371
5.14.7 Load Vectors and Material Stiffness Matrix. 371
5.14.8 The Membrane Isoparametric Elements 375
5.14.9 Isoparametric Line Elements. 379
5.14.10 Element Types, Shape Functions, Derivatives, Stiffness Matrices for Finite Element 387

www.EngineeringBooksPDF.com

5.15 Criteria for Convergence and Acceleration 393
5.15.1 Introduction. 398
5.15.2 Hallquist et al. Method 398
Bibliography 400

6 Geotechnical Earthquake Engineering and Soil–Structure Interaction 405
6.1 General Introduction 405
6.2 Concrete Structures – Seismic Criteria, Numerical Modelling of Soil–Building Structure Interaction and Isolators. 406
6.2.1 Structural Design Requirements for Building Structures. 406
6.2.2 Structure Framing Systems 407
6.3 Combination of Load Effects. 413
6.4 Deflection and Drift Limits 414
6.5 Equivalent Lateral Force Procedure 415
6.5.1 General 415
6.5.2 Seismic Base Shear. 415
6.5.3 Period Determination 416
6.5.4 Vertical Distribution of Seismic Forces. 417
6.6 Horizontal Shear Distribution 418
6.6.1 Torsion. 418
6.6.2 Overturning (determined by all codes) 419
6.7 Drift Determination and $P-\Delta$ Effects. 419
6.7.1 Storey Drift Determination (determined by all codes) 419
6.7.2 $P-\Delta$ Effects (determined according to all codes) 420
6.8 Modal Analysis Procedure: Codified Approach 420
6.8.1 Introduction. 420
6.8.2 Modal Base Shear as by Codified Methods 421
6.8.3 Modal Forces, Deflection and Drifts 422
6.8.4 Soil–Concrete Structure Interaction Effects 423
6.9 Methods of Analysis Using Soil-Structure Interaction 426
6.9.1 General Introduction. 426
6.9.2 Response-Spectrum Analysis. 426
6.9.3 Time-History Analysis. 427
6.9.4 Characteristics of Interaction 427
6.10 Site Response – A Critical Problem in Soil–Structure Interaction Analyses for Embedded Structures 430
6.10.1 Vertical Earthquake Response and $P-\Delta$ Effect 430
6.10.2 $P-\Delta$ Effects. 430
6.10.3 Frequency Domain Analysis of an MDF System 433
6.10.4 Some Non-linear Response Spectra 434
6.10.5 Soil–Structure Interaction Numerical Technique 435
6.10.6 Substructure Method in the Frequency Domain. 436

www.EngineeringBooksPDF.com

6.11 Mode Superposition Method – Numerical Modelling 438
6.12 Mass Moments of Inertia 439
6.12.1 Energies 441
6.13 Modelling of Isolators with Soil–Structure Interaction 441
6.13.1 Introduction 441
6.13.2 Isolation System Components 443
6.13.3 Numerical Modelling of Equations of Motion with Isolators 443
6.13.4 Displacement and Rotation of Isolation Buildings 444
Bibliography 451

7 Response of Controlled Buildings – Case Studies 455
7.1 Introduction 455
7.2 Building With Controlled Devices 457
7.2.1 Special Symbols with Controlled Devices 459
7.2.2 Seismic Waveforms and Spectra 460
7.2.3 Maximum Acceleration and Magnification 462
7.2.4 Three-Dimensional Simulation of the Seismic Wave Field 462
7.3 Evaluation of Control Devices and the Response-Control Technique 462
7.3.1 Initial Statistical Investigation of Response-Controlled Buildings 462
7.3.2 Permutations and Combinations 469
7.4 Permutations and Combinations of Devices 472
7.5 Seismic Design of Tall Buildings in Japan – A Comprehensive Study 523
7.5.1 General Introduction 523
7.5.2 Resimulation Analysis of SMB Based on the Kobe Earthquake Using Three-Dimensional Finite Element Analysis 523
7.5.3 Data I 529
7.5.4 Data II 530

8 Seismic Criteria and Design Examples Based on American Practices 555
8.1 General Introduction 555
8.2 Structural Design Requirements for Structures 555
8.2.1 Introduction to the Design Basis 555
8.3 Drift Determination and $P-\Delta$ Effects 556
8.3.1 Storey Drift Determination 556
8.4 $P-\Delta$ Effects 556
8.5 Modal Forces, Deflection and Drifts 557
8.6 Soil–Concrete Structure Interaction Effects 557
8.6.1 General 557

www.EngineeringBooksPDF.com

8.7 Equivalent Lateral Forces Procedure 557
8.7.1 Base Shear 558
8.7.2 Effective Structural Period 559

9 Design of Structural Elements Based on Eurocode 8 565
9.1 Introduction 565
9.2 Existing Codes 565
9.2.1 Explanations Based on Clause 4.2.3 of EC8 Regarding Structural Regularity. A Reference is Made to Eurocode 8: Part 1 – Design of Structures for Earthquake Resistance 567
9.2.2 Seismological Actions (Refer Clause 3.2 of EC8) 567
9.3 Avoidance in the Design and Construction in Earthquake Zones: Contributing Factors Responsible for Collapse Conditions 568
9.4 Superstructure and Structural Systems 569
9.4.1 Regularity 569
9.4.2 Structural Systems 569
9.5 Response Spectra Based on EU Code 8 572
9.5.1 The Behaviour Factor q 574
9.6 Seismic Design Philosophy of Building Frames Using Eurocode 8 575
9.6.1 General Introduction 575
9.7 Load Combinations and Strength Verification 578
9.7.1 Design Strength 578
9.7.2 Capacity Design Effects: Method Stated in the Eurocode-8 578
9.7.3 Design Provisions for Earthquake Resistance of Structures 580
9.7.4 Second-Order Effects 581
9.7.5 Resistance Verification of Concrete Sections 581
9.8 Analysis and Design of a Steel Portal Frame under Seismic Loads. A Reference is Made to Fig. 9.6 596
9.8.1 Data on Loadings 596
9.8.2 Bending Moments, Vertical and Horizontal Reactions 597
9.8.3 Ultimate Design Moments and Shears (Moment-Capacity Design) 597

10 Earthquake–Induced Collision, Pounding and Pushover of Adjacent Buildings 601
10.1 General Introduction 601
10.2 Analytical Formulation for the Pushover 604
10.3 Linear Response 605
10.3.1 Post-contact Conditions 609

www.EngineeringBooksPDF.com

10.4 Calculation of Building Separation Distance 612
10.4.1 Minimum Separation Distance Required to Avoid Structural Pounding 612
10.5 Data for Buildings 614
10.6 Discussion on Results 614
Bibliography 618

Additional Extensive Bibliography 623

Appendix A Subroutines for Program ISOPAR and Program F-Bang . . 645

Appendix B KOBE (Japan) Earthquake Versus Kashmir (Pakistan) Earthquake 705

www.EngineeringBooksPDF.com

Generalised Notation

In advanced analysis and numerical modelling certain welknown notations are used universaly. These together with the ones given in the text are to be adopted. Where ever additional notations are necessary, especially in the codes for the design of structural elements, they should be defined clearly in this area.

Based on specific analyses, the analyst has the options to substitute any notations which are clearly defined in the analytical or computational work.

A	Constant
A	Projected area, hardening parameter
A_0	Initial surface area
A_{ST}	Surface area of the enclosure
A_V	Vent area
$\bar{A}$	Normalized vent area
a	Radius of the gas sphere
a_0	Loaded length, initial radius of gas sphere
B	Burden
$[B]$	Geometric compliance matrix
BG	Blasting gelatine
b	Spaces between charges
b_l	Distance between two rows of charges
C_D, C_d	Drag coefficient or other coefficients
C'_d	Discharge coefficient
C_f	Charge size factor, correction factor
C_l	A coefficient which prevents moving rocks from an instant velocity
$[C_{in}]$	Damping coefficient matrix
C_p	Specific heat capacity at constant pressure
C_r	Reflection coefficient
C_v	Specific heat capacity at constant volume
$c_a, c_l, c_\psi, c_\theta$	Coefficients for modes

www.EngineeringBooksPDF.com

D	Depth of floater, diameter
$[D]$	Material compliance matrix
D_a	Maximum aggregate size
D_i	Diameter of ice
D_p	Penetration depth of an infinitely thick slab
DIF	Dynamic increase factor
d	Depth, diameter
d_0	Depth of bomb from ground surface
E	Young's modulus
E_b	Young's modulus of the base material
ΔE_{er}	Maximum energy input occurring at resonance
E_{ic}	Young's modulus of ice
E_K	Energy loss
E_{na}	Energy at ambient conditions
E_{ne}	Specific energy of explosives
E_R	Energy release
E_t	Tangent modulus
e	Base of natural logarithm
e	Coefficient of restitution, efficiency factor
F	Resisting force, reinforcement coefficient
F_{ad}	The added mass force
$F_1(t)$	Impact
$F(t)$	Impulse/impact
F_s	Average fragment size shape factor
f	Function
f	Frequency (natural or fundamental), correction factor
f_a	Static design stress of reinforcement
f_c	Characteristic compressive stress
f'_c	Static ultimate compressive strength of concrete at 28 days
f^*_{ci}	Coupling factor
f_d	Transmission factor
f'_{dc}	Dynamic ultimate compressive strength of concrete
f_{ds}	Dynamic design stress of reinforcement
f_{du}	Dynamic ultimate stress of reinforcement
f_{dyn}	Dynamic yield stress of reinforcement
f^*_{TR}	Transitional factor
f_u	Static ultimate stress of reinforcement
f_y	Static yield stress of reinforcement
G	Elastic shear modulus
G_a	Deceleration
G_f	Energy release rate

www.EngineeringBooksPDF.com

G_m, G_s	Moduli of elasticity in shear and mass half space
g	Acceleration due to gravity
H	Height
H_s	Significant wave height
HE	High explosion
HP	Horsepower
h	Height, depth, thickness
I	Second moment of area, identification factor
$[I]$	Identity matrix
I_1	The first invariant of the stress tensor
i_p	Injection/extraction of the fissure
J_1, J_2, J_3	First, second and third invariants of the stress deviator tensor
J_F, J	Jacobian
K	Vent coefficient, explosion rate constant, elastic bulk modulus
$[K_c]$	Element stiffness matrix
K_p	Probability coefficients
K_s	Stiffness coefficient at impact
K_{TOT}	Composite stiffness matrix
K_W	Reduction coefficient of the charge
K_σ	Correction factor
KE	Kinetic energy
k_{cr}	Size reduction factor
k_r	Heat capacity ratio
k_t	Torsional spring constant
L	Length
L'	Wave number
L_i	Length of the weapon in contact
ln, $\log_e$	Natural logarithm
l_x	Projected distance in x direction
M	Mach number
$[M]$	Mass matrix
M'	Coefficient for the first part of the equation for a forced vibration
${}^*M_A$	Fragment distribution parameter
M_p	Ultimate or plastic moment or mass of particle
m	Mass
N	Nose-shaped factor
N_c	Nitrocelluloid

www.EngineeringBooksPDF.com

N_f	Number of fragments
N'	Coefficient for the second part of the equation for a forced vibration
NG	Nitroglycerine
n	Attenuation coefficient
P_i	Interior pressure increment
P_m	Peak pressure
P_u	Ultimate capacity
PE	Potential energy
PETN	Pentaerythrite tetra-nitrate
p	Explosion pressure
p_a	Atmospheric pressure
p_d	Drag load
p_{df}	Peak diffraction pressure
p_{gh}	Gaugehole pressure in rocks
p_{pa}	Pressure due to gas explosion on the interface of the gases and the medium
p_r	Reflected pressure
p_{ro}	Reflected overpressure
p'_s	Standard overpressure for reference explosion
p_{so}	Overpressure
P_{stag}	Stagnation pressure
Q_{sp}	Explosive specific heat (TNT)
q_{do}	Dynamic pressure
R	Distance of the charge weight gas constant, Reynolds number, Thickness ratio
R'	Radius of the shock front
$\{R(t)\}$	Residual load vector
R_T	Soil resistance
R_{vd}	Cavity radius for a spherical charge
R_w, r_s	Radius of the cavity of the charge
r	Radius
r_o, r_ψ, r_ϕ	Factors for translation, rocking and torsion
S_i	Slip at node i
S_{ij}	Deviatoric stress
S_L	Loss factor
$S_{\eta\eta}(f)$	Spectral density of surface elevation
s	$\pm i\omega t$ or distance or wave steepness, width, slope of the semi-log
T	Temperature, period, restoring torque
T_a	Ambient temperature
T_d	Delayed time

www.EngineeringBooksPDF.com

T'_{i}	Ice sheet thickness
T_{ps}	Post shock temperature
$[T'']$	Transformation matrix
TR	Transmissibility
t	Time
t_{A}	Arrival time
t_{av}	Average time
t_{c}	Thickness of the metal
t_{d}	Duration time
t_{exp}	Expansion time
t_{i}	Ice thickness
t_{p}	Thickness to prevent penetration, perforation
t_{sc}	Scabbing thickness, scaling time
t_{sp}	Spalling thickness
U	Shock front velocity
u	Particle velocity
V	Volume, velocity
V'	Velocity factor
$V_{\mathrm{R}n}$	Velocity at the end of the nth layer
v_{b}	Fragment velocity or normalized burning velocity
v_{bt}	Velocity affected by temperature
v_{c}	Ultimate shear stress permitted on an unreinforced web
v_{con}	Initial velocity of concentrated charges
v_{f}	Maximum post-failure fragment velocity
v_{in}, v_0	Initial velocity
v_{l}	Limiting velocity
v_{m}	Maximum mass velocity for explosion
v_{p}	Perforation velocity
v_{pz}	Propagation velocities of longitudinal waves
v_{RZ}	Propagation velocities of Rayleigh waves
v_{r}	Residual velocity of primary fragment after perforation or $\sqrt{E/p}$
v_{s}	Velocity of sound in air or striking velocity of primary fragment or missile
v_{so}	Blast-generated velocity at initial conditions
v_{su}	Velocity of the upper layer
v_{sz}	Propagation velocities of transverse waves
v_{szs}	Propagation velocity of the explosion
v'_{xs}	Initial velocity of shock waves in water
v_{z}	Phase velocity
v_{zp}	Velocity of the charge

www.EngineeringBooksPDF.com

W	Charge weight
$W^{1/3}$, Y	Weapon yield
W_t	Weight of the target material
w_a	Maximum weight
w_f	Forcing frequency
X	Amplitude of displacement
$\dot{X}$	Amplitude of velocity
$\ddot{X}$	Amplitude of acceleration
X_f	Fetch in metres
$X_{(x)}$	Amplitude of the wave at a distance x
X_0	Amplitude of the wave at a source of explosion
x	Distance, displacement, dissipation factor
x	Relative distance
$\dot{x}$	Velocity in dynamic analysis
$\ddot{x}'$	Acceleration in dynamic analysis
$\{x\}^*$	Displacement vector
x_{cr}	Crushed length
x_i	Translation
x_n	Amplitude after n cycles
x_p	Penetration depth
x_r	Total length
Z	Depth of the point on the structure
α	Cone angle of ice, constant for the charge
$\alpha_a, \alpha_l, \alpha_\psi$	Spring constants
α_B	Factor for mode shapes
α'	Angle of projection of a missile, constant
$\bar{\alpha}$	Constant
β	Constant for the charge, angle of reflected shock
$\bar{\beta}$	Constant
γ	Damping factor, viscosity parameter
γ_f	ω_f/ω
δ	Particle displacements
$\bar{\delta}$	Pile top displacement
δ_{ij}	Kronecker delta
$\delta_m, \delta'_m, \delta''_m$	Element displacement
δ_{st}	Static deflection
δ_t	Time increment
ϵ	Strain
$\dot{\varepsilon}$	Strain rate
ϵ_d	Delayed elastic strain
η	Surface profile
θ	Deflection angle

www.EngineeringBooksPDF.com

θ_g	Average crack propagation angle
λ	A constant of proportionality
μ_f	Jet fluid velocity
ν	Poisson's ratio
ρ_a	Mass density of stone
ρ_w	Mass density of water
σ	Stress
σ_c	Crushing strength
σ_{cu}	Ultimate compressive stress
σ_f	Ice flexural strength
$(\sigma_{nn})^c$	Interface normal stress
$(\sigma_{nt})^c$	Interface shear stress
σ_{pi}	Peak stress
σ_t	Uniaxial tensile strength
τ_o	Crack shear strength
ϕ	Phase difference
ψ	Circumference of projectile
ω	Circular frequency
$l, m, n, p,$ q, r, s, t	Direction cosines
$X, Y, Z;$ x, y, z	Cartesian coordinates
(ξ, η, ζ)	Local coordinates

www.EngineeringBooksPDF.com

www.EngineeringBooksPDF.com

Conversion Tables

Weight

1 g	= 0.0353 oz	1 oz	= 28.35 g
1 kg	= 2.205 lbs	1 lb	= 0.4536 kg
1 kg	= 0.197 cwt	1 cwt	= 50.8 kg
1 tonne	= 0.9842 long ton	1 long ton	= 1.016 tonne
1 tonne	= 1.1023 short ton	1 short ton	= 0.907 tonne
1 tonne	= 1000 kg	1 stone	= 6.35 kg

Length

1 cm	= 0.394 in	1 in	= 2.54 cm = 25.4 mm
1m	= 3.281 ft	1 ft	= 0.3048m
1m	= 1.094 yd	1 yd	= 0.9144m
1 km	= 0.621 mile	1 mile	= 1.609 km
1 km	= 0.54 nautical mile	1 nautical mile	= 1.852 km

Area

1 cm^2	= 0.155 in^2	1 in^2	= 6.4516 cm^2
1 dm^2	= 0.1076 ft^2	1 ft^2	= 9.29 dm^2
1m^2	= 1.196 yd^2	1 yd^2	= 0.8361m^2
1 km^2	= 0.386 sq mile	1 sq mile	= 2.59 km^2
1 ha	= 2.47 acres	1 acre	= 0.405 ha

Volume

1 cm^3	= 0.061 in^3	1 in^3	= 16.387 cm^3
1 dm^3	= 0.0353 ft^3	1 ft^3	= 28.317 dm^3
1m^3	= 1.309 yd^3	1 yd^3	= 0.764m^3
1m^3	= 35.4 ft^3	1 ft^3	= 0.0283m^3
1 litre	= 0.220 Imp gallon	1 Imp gallon	= 4.546 litres
1000 cm^3	= 0.220 Imp gallon	1 US gallon	= 3.782 litres
1 litre	= 0.264 US gallon		

www.EngineeringBooksPDF.com

Density

$1\ kg/m^3 = 0.6242\ lb/ft^3$ $1\ lb/ft^3 = 16.02\ kg/m^3$

Force and pressure

1 ton = 9964 N
1 lbf/ft = 14.59 N/m
$1\ lbf/ft^2 = 47.88\ N/m^2$
1 lbf in = 0.113Nm
1 psi = $1 lbf/in^2 = 6895\ N/m^2 = 6.895\ kN/m^2$
$1\ kgf/cm^2 = 98070\ N/m^2$
1 bar = $14.5\ psi = 10^5\ N/m^2$
$1\ mbar = 0.0001\ N/mm^2$
1 kip = 1000 lb

Temperature, energy, power

$1°C = 5/9(°F - 32)$
$0\ K = -273.16°C$
$0°R = -459.69°F$

1 J = 1 milli-Newton
1 HP = 745.7 watts
1 W = 1 J/s

1 BTU = 1055 J

Notation

lb = pound weight
Lbf = pound force
in = inch
cm = centimetre
m = metre
km = kilometre
d = deci
ft = foot
ha = hectare
s = second
°C = centigrade = Celsius
K = Kelvin
°R = Rankine
°F = Fahrenheit
oz = ounce
cwt = one hundred weight
g = gram
kg = kilogram
yd = yard
HP = horsepower
W = watt
N = Newton
J = Joule

www.EngineeringBooksPDF.com

Chapter 1
Introduction to Earthquake with Explanatory Data

1.1 Earthquake or Seismic Analysis and Design Considerations

1.1.1 Introduction

Earthquakes can cause local soil failure, surface ruptures, structural damage and human deaths. The most significant earthquake effects on buildings or their structural components result from the seismic waves that propagate outwards in all directions from the earthquake focus. These different types of waves can cause significant ground movements up to several hundred miles from the source. The movements depend on the intensity, sequence, duration and the frequency content of the earthquake-induced ground motions. For design purposes ground motion is described by the history of hypothesized ground acceleration and is commonly expressed in terms of the response spectrum derived from that history. When records are unavailable or insufficient, smoothed response spectra are devised for design purposes to characterize the ground motion. In principle, the designers describe the ground motion in terms of two perpendicular horizontal components and a vertical component for the entire base of the structure

When the history of ground shaking at a particular site or the response spectrum derived from this history is known, a building's theoretical response can be calculated by various methods; these are described later. Researchers (2107–2141) have carried out thorough assessments of structures under earthquakes. This chapter includes plate tectonics, earthquake size, earthquake frequency and energy, seismic waves, local site effects on the ground motion and interior of the Earth

1.2 Plate Tectonic and Inner Structure of Earth

The Earth is roughly spherical with an average radius of around 6,400 km. Its inner structure was determined from the propagation of earthquake waves. The Earth consists of three spherical shells of quite different physical properties. The

M.Y.H. Bangash, *Earthquake Resistant Buildings*,
DOI 10.1007/978-3-540-93818-7_1, © M.Y.H. Bangash 2011

www.EngineeringBooksPDF.com

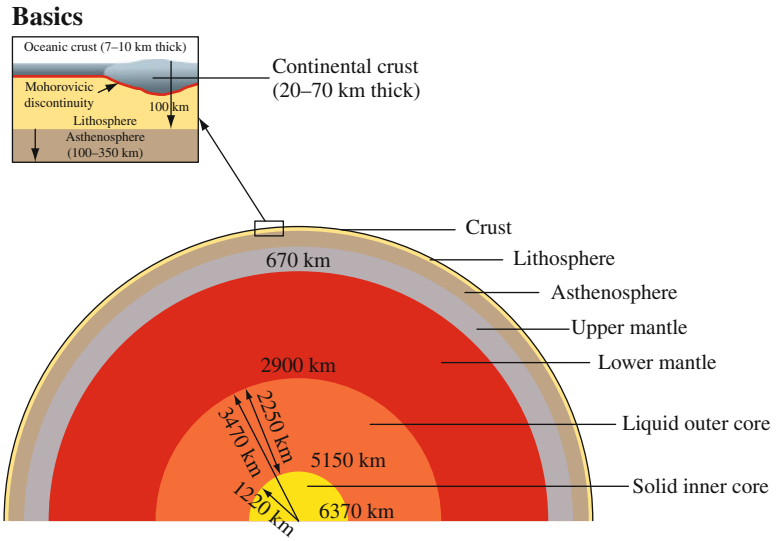
outer shell is a thin crust of thickness varying from a few kilometres to a few tens of kilometres; the middle shell is the mantle, about 2,900 km thick, and the Moho (Mohorovicic) discontinuity is its interface with the crust; the innermost shell contains the core, of radius approximately 3,500 km. The crust is made of various types of rock, differing in composition and thickness in its oceanic and continental parts. The crust in the continental part consists of two layers, granitic in the outer and basaltic in the inner layer, with total thickness about 30–40 km, but reaching 70 km under high mountains, such as in the Qing-Zang plateau of west China. The crust under the oceans is basaltic only, with no granitic deposit, with a thickness of only about 5 km. The mantel consists mainly of comparatively uniform ultrabasic olivine rock; its outer 40–70 km shell together with the crust is usually referred to as the lithosphere, directly under which is a layer of soft viscoelastic asthenosphere a few hundreds of kilometres in thickness. The wave velocity in the asthenosphere is obviously lower than those in its neighbouring rocks, perhaps due to its viscoelastic, or creep, property under high temperature and confining pressure. The lithosphere and asthenosphere together form the upper mantle. Below, the lower mantle extends a further 1,900 km or so. The core consists of outer and inner cores. Because it is found that no transverse wave can propagate through the outer core, it is agreed that the outer core is in a liquid state.

Temperature increases from crust to core. The temperature is about 600°C at a depth of 20 km, 1,000–1,500°C at 100 km, 2,000°C at 700 km and 4,000–5,000°C in the core. The high temperature comes from the heat release from radioactive material inside the Earth. The distributions of the radioactive material under ocean or under the continents may be different, and this is considered to be the cause of current movement of materials in the mantle.

Pressure increases also from crust to core, perhaps 89.676 KN/cm^2 in the upper mantle, 139.49 KN/cm^2 in the outer core and 36,867 KN/cm^2 in the inner core.

Plate tectonics was developed on the hypothesis of sea-floor spreading during the past few decades. According to this concept, the rigid lithosphere, consisting of six major plates, drifts on the rheological asthenosphere, like a ship on the ocean, but with a very slow speed. The six plates are the Eurasian, Pacific, American, African, Indian and Antarctic. Each plate may then be subdivided into smaller plates. The relative movements of the plates are roughly a few centimetres per year and has continued for at least 200 million years. The theory can be described as follows: (1) Material flows out from the upper mantel through the lithosphere at ocean ridges where the crust is thin and pushes the lithosphere, whose thickness is a few kilometres, (2) drifting horizontally on the asthenosphere, which shows rheological properties under high temperature, high pressure and permanent horizontal pushing. When two tectonic plates collide, one thrusts under the other and comes back to the lithosphere, which forms a deep ocean trench and subduction zone at the junction of two plates and volcanoes and mountains on the plate which remains on the Earth's surface. A reference is made to the basics given in Plates 1.1, 1.2 and 1.3.

www.EngineeringBooksPDF.com



Structure of the earth crust

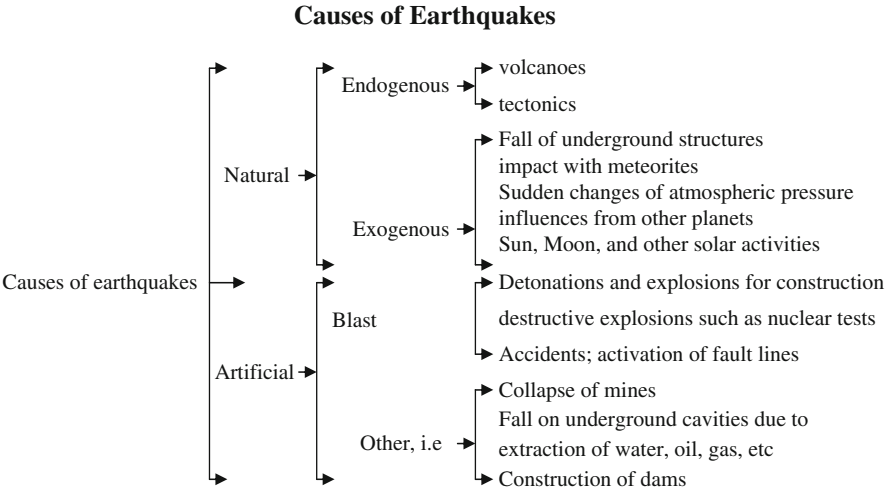


Plate 1.1 An earthquake is a transient violent movement of the Earth's surface that follows a release of energy in the Earth's crust

The following four facts support this theory:

- matching of the geology, palaeontology and geometry of the continents;
- imprinting of historical traces of magnetic fluctuations;
- characteristics of ocean ridges and trenches;
- instrumental earthquake evidence.

www.EngineeringBooksPDF.com

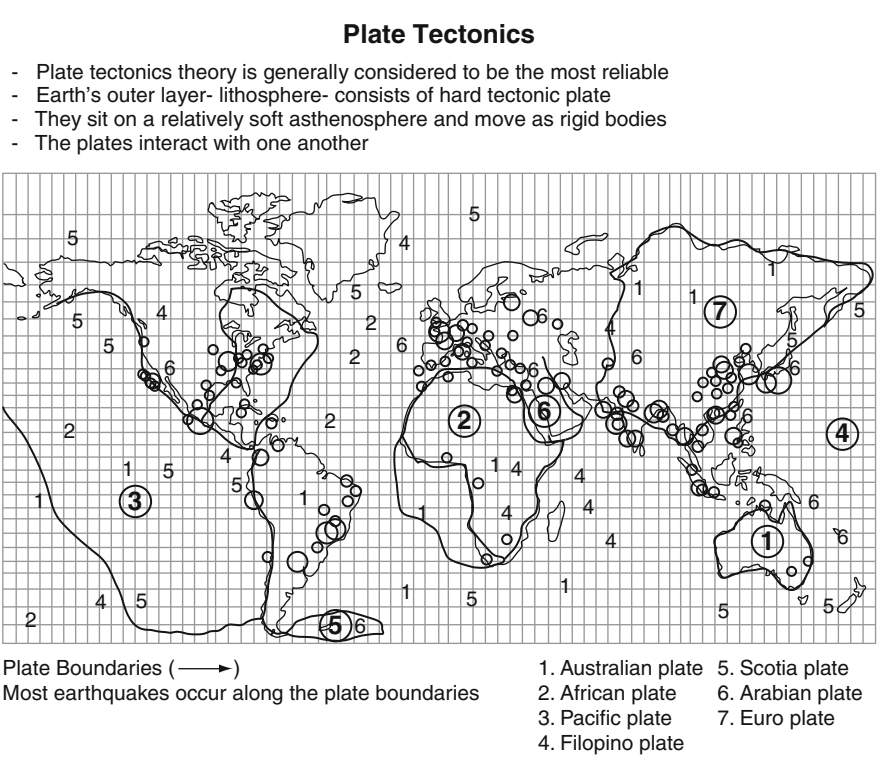


Plate 1.2 Plate Tectonics

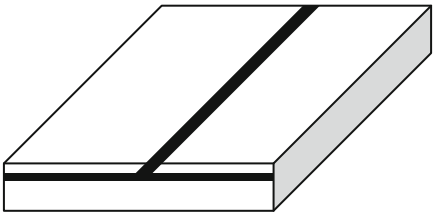
The traces of magnetic fluctuations in the ocean plates are all parallel to the ocean ridge and can be correlated and dated by radioactive methods and explained only by the sea-floor spreading theory.

Various seismological stations now cover almost the whole world, and about 1,000 earthquakes of magnitude not smaller than 5.0 are recorded each year. Most of these earthquakes are concentrated along plate boundaries. Earthquake-concentrated zones are called earthquake belts. There are two major earthquake belts on the Earth (Fig. 1.2). One is the Circum-Pacific belt, which is very active, with 75% of earthquakes concentrated on it. The other one is the Eurasian or Alpide-Asiatic, with about 22% of earthquakes occurring on it. Earthquakes on these two major belts are interplate earthquakes. The remaining 3% of the earthquakes occur inside the plates and are thus intraplate earthquakes.

Intraplate earthquakes are also caused by plate movements. Because the thickness and rigidity of the crust, the Moho discontinuity surface and the driving force of the ocean plates are not uniform, the relative displacements

www.EngineeringBooksPDF.com

Tectonic Plate Positioning



1. Where two plates move apart from one another causing spreading and rifting,



tensile stress occurs (Divergent Plate Boundary)

2. Where two plates converge each other compression occurs together with plate instability



(Convergent Plate Boundary)

3. Where two plates shear each other or slide past one another, shear stresses occur



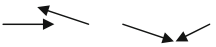
(Transform Plate Boundary) faults at shallow depth

4. Where several plates collide, known as continental collisions, mountains occur



(Continental collision)

5. Where one plate overrides or subducts another, pushing it downwards into the mantel where it melts, submarine trench is formed. They are shallow to deep earthquakes. They can be ocean to ocean subduction. They can be ocean to continent subduction.



(Subduction)

Faults

Fault – a fracture in the Earth's crust along which two blocks of the crust can slip relative to each other.

Faults – classified according to the direction of slippage:

1. Strike-slip fault– if the movement or slippage is primarily horizontal
   - They are essentially vertical fault planes
   - The strike is the direction of the fault line relative to north

2. Dip-slip fault – if the movement or slippage is vertical
   - The dip of the fault is the angle that the fault makes with the horizontal plane

Plate 1.3 Tectonic Plate Positioning

and velocities between plates vary both in space and in time. A plate is usually under complex stress condition; one part may be under tension, causing depression, and the other part under compression, causing mountain uplift, or under shear, causing horizontal deformation.

www.EngineeringBooksPDF.com

Compared with interplate earthquakes, continental earthquakes have the following three features:

a. They are less frequent and less concentrated.
b. They are more dangerous to humans.
c. The source mechanism varies and is more complicated.

Because the continental plate remains on the Earth's surface and is of varying thickness, it is full of faults and folds under long-term tectonic action, and earthquakes occur with much more scattering.

Deformation due to plate tectonics is a very slow but persisting process. In a very long time period, deformation accumulates elastic strain in the crust. Crust material may be elastic somewhere but rheologic in other places. If the crust is elastic, strain energy may be accumulated and it may crack suddenly when the strength of rock is overcome and the accumulated energy is transferred into earthquake waves, and an earthquake occurs. This is the elastic rebound theory of earthquakes.

The rigidity and brittleness of rocks are higher in the crust, and the rock behaves like an elastic and brittle material. When stress or strain is over the limit capacity, the rock breaks and the stress drops suddenly from its maximum σ_0 at time t_0 instantly to a minimum value $\sigma_{\min}$. This value can recover to some other value of σ in between at time t_1.

1.3 Types of Faults

Faults may range in length from less than a metre to many hundreds of kilometres. In the field, geologists commonly find many discontinuities in rock structures, which they interpret as faults, and these are drawn on geological maps as continuous or broken lines. The presence of such faults indicates that, at some time in the past, movements took place along them. One now knows that such movement can be either slow slip, which produces no ground shaking, or sudden rupture, which results in perceptible vibrations – an earthquake. For example, one of the most famous examples of sudden faults rupture is the San Andreas Fault in April 1906. However, the observed surface faulting of most shallow focus earthquakes is much shorter in length and shows much less offset in this case. In fact, in the majority of earthquakes, fault rupture does not reach the surface and is thus not directly visible. The faults seen at the surface sometimes extend to considerable depths in the outermost shell of the Earth, called the crust. This rocky skin, from 5 to 60 km thick, forms the outer part of the lithosphere.

It must be emphasized that slip no longer occurs at most faults plotted on geological maps. The last displacement to occur along a typical fault may have taken place tens of thousands or even millions of years ago. The local disruptive forces in the Earth nearby may have subsided long ago, and chemical processes involving water movement may have cemented the ruptures, particularly at shallow depths. Such an inactive fault is now not the site of earthquakes and may never be again.

www.EngineeringBooksPDF.com

The primary interest is of course in active faults, along which crustal displacements can be expected to occur. Many of these faults are in rather well-defined tectonically active regions of the Earth, such as the mid-oceanic ridges and young mountain ranges. However, sudden fault displacements can also occur away from regions of clear present tectonic activity.

Whether on land or beneath the oceans, fault displacements can be classified into three types. The plane of the fault cuts the horizontal surface of the ground along a line whose direction from the north is called the strike of the fault. The fault plane itself is usually not vertical but dips at an angle down into the Earth. When the rock on that side of the fault hanging over the fracture slips downwards, below the other side, we have a normal fault. The dip of a normal fault may vary from 0° to 90°. When, however, the hanging wall of the fault moves upwards in relation to the bottom or footwall, the fault is called a reverse fault. A special type of reverse fault is a thrust fault in which the dip of the fault is small. The faulting in mid-oceanic ridge earthquakes is predominantly normal, whereas mountainous zones are the sites of mainly thrust-type earthquakes.

Both normal and reverse faults produce vertical displacements – seen at the surface as fault scarps – called dip-slip faults. By contrast, faulting that causes only horizontal displacements along the strike of the fault is called transcurrent or strike-slip. It is useful in this type to have a simple term that tells the direction of slip. For example, the arrows on the strike-slip fault show a motion that is called left-lateral faulting. It is easy to determine if the horizontal faulting is left-lateral or right-lateral. Imagine that one is standing on one side of the fault and looking across it. If the offset of the other side is from right to left, the faulting is left-lateral, whereas if it is from left to right, the faulting is right-lateral. Of course, sometimes faulting can be a mixture of dip-slip and strike-slip motion.

In an earthquake, serious damage can arise not only from the ground shaking but also from the fault displacement itself, although this particular earthquake hazard is very limited in area. It can usually be avoided by the simple expedient of obtaining geological advice on the location of active faults before construction is undertaken. These concepts are clearly indicated in the world conferences on Earthquake Engineering, mostly held in California Institute of Technology, California.

1.4 Seismograph And Seismicity

Seismicity is a description of the relationship of time, space, strength and frequency of earthquake occurrence within a certain region and its understanding is the foundation of earthquake study. Since there is still no practical way to control earthquakes, one can only try to understand and follow their nature wisely to prepare for possible strong earthquakes through prediction, earthquake engineering and society or governmental efforts of disaster reduction.

www.EngineeringBooksPDF.com

The most popular way to study seismicity is empirically or statistically. A seismic belt is defined first to have a similar past earthquake distribution and geological and tectonic background, with dimensions somewhat similar to the ones already familiar.

Although earthquake-recording instruments, called seismographs, are now more sophisticated, the basic principle employed is the same. A mass on a freely movable support can be used to detect both vertical and horizontal shaking of the ground. The vertical motion can be recorded by attaching the mass to a spring hanging from an anchored instrument frame; the bobbing of the frame (as with a kitchen scale) will produce relative motion. When the supporting frame is shaken by earthquake waves, the inertia of the mass causes it to lag behind the motion of the frame, and this relative motion can be recorded as a wiggly line by pen and ink on paper wrapped around a rotating drum (alternatively the motion is recorded photographically or electromagnetically on magnetic tape or as discrete digital samples for direct computer input). For measurements of the sideways motion of the ground, the mass is usually attached to a horizontal pendulum, which swings like a door on its hinges. Earthquake records are called seismograms. A seismograph appears to be no more than a complicated series of wavy lines, but from these lines a seismologist can determine the hypocentre location, magnitude and source properties of an earthquake. Although experience is essential in interpreting seismograms, the first step in understanding the lines is to remember the following principles. First, earthquake waves consist predominantly of three types – P-waves and S-waves, which travel through the Earth, and a third type, surface waves, which travel around the Earth. If you look closely enough, you will find that almost always each kind of wave is present on a seismogram, particularly if it is recorded by a sensitive seismograph at a considerable distance from the earthquake source. Each wave type affects the pendulums in a predetermined way. Second, the arrival of a seismic wave produces certain telltale changes on the seismogram trace: The trace is written more slowly or rapidly than just before; there is an increase in amplitude; and the wave rhythm (frequency) changes. Third, from past experience with similar patterns, the reader of the seismogram can identify the pattern of arrivals of the various phases.

A common time standard must be used to compare the arrival times of seismic waves between earthquake observatories around the world. Traditionally, seismograms are marked in terms of Universal Time (UT) or Greenwich Mean Time (GMT), not local time. The time of occurrence of an earthquake in UT can easily be converted to local time, but be sure to make allowance for Daylight Saving Time when this is in effect.

1.5 Seismic Waves

Human understanding of earthquakes, and of other physical sciences, comes first from macroseismic phenomena, but ultimately from instrumental observation. It is the instrumental data for seismic waves that provide quantitative

www.EngineeringBooksPDF.com

understanding of the earthquake source mechanism and of the interior construction of the Earth. Although the Earth's materials show rheological properties under static forces from plate tectonic movement, they show elastic properties under the dynamic action of seismic waves from earthquakes; the weak viscosity under dynamic forces can be considered in terms of energy-absorbing damping added to the elastic properties.

Nowadays, for the great majority of earthquakes, the location is determined from the time taken by P seismic waves (and sometimes S-waves) to travel from the focus to a seismograph. Many hundreds of modern seismographs are operated worldwide continuously and reliably for this and other purposes. In some seismic areas, special local networks of seismographic stations have been installed to locate the foci of even very small earthquakes.

Today, almost everyone is familiar with the concept of digital signals rather than continuous recordings, the latter provided by the continually varying electric currents that drove the old-style pen-and-ink (or even magnetic tape) recording seismographs. New technology allows modern seismographs to record the continuous ground motions as a finely spaced series of separate numbers; such discrete numerical sampling is defined by the binary number or "bits". This form makes the recordings, unlike analog seismograms, immediately accessible for computer processing. In the 1970s, seismologists began to take full advantage of this emerging digital technology; now it is commonplace.

The first global project of any size to convert globally distributed seismographs began in the 1970s. The digital samples had 14 bits. This number provided the dynamic range of frequencies that spanned what is called a broadband seismographic system – that is, from periods of a fraction of a second to the periods of free vibrations of the Earth (approximately 1 h) – and even out to the tidal deformations of the Earth (days). The intensity of shaking is observed to vary greatly with the direction around a fault rupture. The physical reason is that the seismic source is a moving energy emitter – like the whistle on a moving train. The energy increases as the source approaches and decreases as it moves away. A simple comparison of seismograms from the 1992 Landers, California, earthquake has been plotted. The shaking is represented as ground acceleration, velocity and displacement.

1.6 Magnitude of the Earthquake

The first known seismic instrument, the Houfeng seismometer, made in the year AD 132 in the Late Han dynasty by the ancient Chinese scientist Heng Zhang, successfully recorded an earthquake in AD 138. The modern type of seismograph started in the eighteenth century and includes three subsystems: sensor, amplifier and recorder. For the special requirements of the seismologist, the seismograph records usually the displacement of the ground motion due to an earthquake.

www.EngineeringBooksPDF.com

There are usually three sensors, arranged in two perpendicular horizontal directions and one vertical direction. The most important property of a seismograph is the dynamic amplification spectrum. The pass bandwidth of currently used seismographs is usually not very wide and with maximum amplification not less than a few thousands, mostly at periods not less that 0.7 s; both amplitude (Table 1.1) and phase characteristics may be rather different for different frequency components.

Table 1.1 Amplitude–frequency characteristics of Wood–Anderson torsional seismograph

Period T (s)	Amplification
0.1	2,786
0.2	2,745
0.4	2,557
0.6	2,199
0.7	1,972
0.8	1,750
0.9	1,538
1.0	1,350
1.4	807
2.0	424

Seismographs are in operation 24 h a day, and records are produced continuously on a roll paper. Accuracy of timing is about 0.1 s.

There are several typical seismographs currently in use. One is for local and weak earthquake observation, with natural period around 1 s and amplification around 10^4–10^5. The Wood–Anderson torsional seismograph is also used for near-earthquake observation, with a natural period 0.8 s and near-critical damping (0.8) but with an amplification of only 2,800. The long-period seismographs of natural period longer than 10 s are for distant and strong earthquake observations.

1.6.1 Seismic Magnitude

In 1935, Richter first introduced the idea of magnitude to give a quantitative measure of an earthquake through instrumental records. The Wood–Anderson torsional seismograph was in common use in southern California. Richter discovered that the curves of $\log A - \Delta$ for many earthquakes in that region were almost parallel to each other and he suggested the following definition of a local magnitude:

$$M_{\mathrm{L}} = \log A(\Delta) - \log A_0(\Delta) \tag{1.1}$$

where A is the average of the maximum displacements (in μ) of two horizontal components at epicentral distance $\Delta = 100\,\mathrm{km}$ and A_0 is an empirical

www.EngineeringBooksPDF.com

correction for the effect of local conditions on attenuation of ground motion. As shown in Table 1.1, the amplification at period $T = 1.0$ s drops to about half of that of $T = 0.1$ s; this definition is therefore made for magnitude on the basis of short-period ground motion and is adequate for local small earthquakes.

Since seismic stations are not normally so densely allocated as in southern California, Gutenberg followed the same idea and defined a surface wave magnitude for shallow and distant earthquakes as follows:

$$M_s = \log A(\Delta) - \log A_0(\Delta) \tag{1.2}$$

At a distance of about 2,000 km, the primary wave is a surface wave of period about 20 s; A is defined as the maximum vector of the horizontal displacement in μ of a 20 s period wave.

Since M_s cannot be used for deep earthquakes, he defined the following body wave magnitude:

$$m_b = \log(A/T)_{max} - Q(\Delta, h) \tag{1.3}$$

where $(A/T)_{max}$ may be the maximum ratio (A/T) of P, PP or S waves, either the vertical or horizontal vector displacement in μ, and T in seconds is the period corresponding to A. But in practice, most seismographs have a natural period of 1 s and A of the vertical component is used to define the body wave.

Empirical conversion relations have been suggested between these magnitudes, such as

$$M_s = 1.59m_b - 40 = 1.27(M_L - 1.0) - 0.16M_L^2 \tag{1.4}$$

In China, when these definitions are used, the correction term $\log A_0$ or $Q(\Delta, h)$ includes also the instrument correction; the conversion relation used is

$$M_s = 1.13M_L - 1.08 \tag{1.5}$$

1.7 The World Earthquake Countries and Codes of Practices

A reference is made to the Author's book on "Proto type Building Structures" (Thomas Telford, London) for many details. Table 1.2 and 1.3 give the list of countries with lethal earthquakes with average return periods. The statistics recording casualties due to earthquake include a wide range of events such as fires, tsunamis generated by offshore events, rockfalls, landslides and other hazards triggered by earthquakes. Most large-scale disasters given by Table 1.4 due to earthquakes result from the collapse of buildings. The number of significant earthquakes can also be viewed in Fig. 1.1.

www.EngineeringBooksPDF.com

Table 1.2 The world's earthquake countries

Earthquake ranking	No. of lethal earthquakes 1900–2008	Average return period (years)	Earthquake ranking	No. of lethal earthquakes 1900–2008	Average return period (years)
1. China	1958	0.6	40. New Zealand	6	15
2. Japan	201	1	41. Uganda	1	100+
3. Italy	43	2	42. Lebanon	1	100+
4. Iran	135	1	43. Portugal	4	23
5. Turkey	135	1	44. Puerto Rico	1	100+
6. CIS (USSR)	46	2	45. Dominican		
7. Peru	53	2	Republic	1	100+
8. Pakistan	248	5	46. Zaire	3	30
9. Chile	34	3	47. Ethiopia	3	30
10. Indonesia	148	2	48. Solomon Islands	2	50
11. Guatemala	14	7	49. Canada	3	30
12. India	221	4	50. Bangladesh	5	18
13. Nicaragua	3	31	51. Panama	2	50
14. Morocco	2	46	52. France	2	50
15. Nepal	14	23	53. Cyprus	2	50
16. Philippines	55	4	54. South Africa	6	15
17. Mexico	71	2	55. Mongolia	1	100+
18. Taiwan	49	2	56. Egypt	13	30
19. Ecuador	26	4	57. Ghana	1	100+
20. Argentina	22	8	58. Tunisia	1	100+
21. Algeria	41	5	59. Australia	2	50
22. Yemen	3	31	60. Malawi	1	100+
23. El Salvador	13	7	61. Cuba	18	50
24. Romania	4	23	62. Haiti	8	50
25. Costa Rica	7	13	63. Spain	15	23
26. Yugoslavia	18	5	64. Bolivia	4	23
27. Colombia	29	3	65. Poland	2	50
28. Afghanistan	41	8	66. Tanzania	2	50
29. USA	32	3	67. Honduras	3	30
30. Greece	51	2	68. Czechoslovakia	1	100+
31. Jamaica	2	50	69. Hungary	2	50
32. Burma	31	9	70. Belgium	1	100+
33. Venezuela	16	6	71. Iceland	1	100+
34. Albania	24	7	72. Germany	1	100+
35. Papua New			73. Israel	12	–
36. Guinea	15	10	74. Burundi	1	–
37. Bulgaria	6	15	75. Iraq	6	–
38. Jordan	2	50	76. Sudan	5	–
39. Libya	2	50	77. Syria	5	–

Note: Data collected by the author from reports, newspapers and television records by the author.

www.EngineeringBooksPDF.com

Table 1.3 Major earthquakes: magnitudes and fatalities

Date	Location	Magnitude (Richter scale)	Fatalities
26 January 2001	India	7.9	>13,000
21 September 1999	Taiwan	7.6	2,400
17 August 1999	Western Turkey	7.4	17,000
25 January 1999	Western Colombia	6	1,171
4 February 1998	Northeast Afghanistan	6.1	5,000
10 May 1997	Northern Iran	7.1	1,500
17 January 1995	Kobe, Japan	7.2	>6,000
30 September 1993	Latur, India	6.0	>10,000
21 June 1990	Northwest Iran	7.3–7.7	50,000
7 December 1988	Northwest Armenia	6.9	25,000
19 September 1985	Central Mexico	8.1	>9,500
16 September 1978	Northeast Iran	7.7	25,000
28 July 1976	Tangshan, China	7.8–8.2	755,000
4 February 1976	Guatemala	7.5	22,778
26 December 1939	Erzincan province, Turkey	7.9	33,000
24 January 1939	Chillan, Chile	8.3	28,000
1 September 1923	Tokyo-Yokohama, Japan	8.3	200,000
16 December 1920	Gansu, China	8.6	100,000
16 August 1906	Valparaiso, Chile	8.6	20,000
18–19 April 1906	San Francisco (CA), USA	7.7–7.9	3,000 and fire
28 December 1908	Messina, Italy	7.5	83,000
13 January 1915	Avezzano, Italy	7.5	29,980
22 May 1927	Nan-Shan, China	8.3	200,000
26 December 1932	Gansu, China	7.6	70,000
31 May 1935	Quetta, India	7.5	60,000
6 October 1948	Iran/USSR	7.3	100,000
15 August 1950	Assam, India	8.7	1,530
29 February 1960	Agadir, Morocco	5.7	12,000
1 September 1962	Northwestern Iran	7.1	12,000
26 July 1963	Skopje, Yugoslavia	6.0	1,100
27 March 1964	Anchorage (AL), USA	9.2	131
31 August 1968	Northeastern Iran	7.4	11,600
5 January 1970	Yunan Province, China	7.7	10,000
31 May 1970	Chimbote, Peru	7.8	67,000
23 December 1972	Managua, Nicaragua	6.2	5,000
6 May 1976	Friuli, Italy	6.5	939

Note: Data from reports, newspapers and T.V. records by the author.

www.EngineeringBooksPDF.com

Table 1.3 (continued)

Date	Location	Magnitude (Richter scale)	Fatalities
4 March 1977	Romania	7.5	1,541
10 October 1980	Northern Algeria	7.7	3,000
23 November 1980	Southern Italy	7.2	4,800
13 December 1982	Northern Yemen	6.0	1,600
17 October 1989	San Francisco (CA), USA	7.1	62
16 July 1990	Luzon, Philippines	7.7	1,660
29 September 1993	Maharashtra, India	6.3	9,800
13–16 October 1993	Papua New Guinea	6.8	>60
6 June 1994	Cauca, Colombia	6.8	1,000
16 January 1995	Kobe, Japan	7.2	5,500
14 June 1995	Sakhalin Island, Russia	7.6	2,000
28 February 1997	Baluchistan Province, Pakistan	7.3	>100
7 September 1999	Athens, Greece	5.9	125
26 December 2003	Bam, Iran	6.6	30,000
8 October 2005	Kashmir, Pakistan	8.5	>76,000
23 January 2005	Sulawesi, Indonesia	6.2	1
25 January 2005	Turkey/Iraq Border	5.9	2
2 February 2005	Jara, Indonesia	4.8	1
5 February 2005	Celebes Sea	7.1	2
22 February 2005	Central Iran	6.4	612
9 March 2005	South Africa	5.0	2
20 March 2005	Kyushu, Japan	6.6	1
28 March 2005	Northern Sumatra	8.7	1,313
12 December 2005	Hindu Kush, Afghanistan	6.5	5
14 December 2005	Uttaranchal, India	5.3	1
1 April 2006	Taiwan	6.2	>42
4 April 2006	Pakistan, N.W.F.P	4.7	>28
14 April 2006	Norwegiansca	3.3	–
20 April 2006	Koryakia, Russia	7.6	40
25 April 2006	Tasmania, Australia	2.2	4
29 April 2006	Koryakia, Russia	6.6	–
30 April 2006	Atacama, Chile	6.7	–
30 April 2006	Atacama, Chile	6.5	–
3 May 2006	Tonga	7.9	–
7 May 2007	Central Iran	4.8	–
16 May 2006	Kermadec Islands	7.4	–
16 May 2006	Nias, Indonesia	6.8	–
22 May 2006	Koryakia, Russia	6.6	–

Note: Data collected and tabulated from reports, newspapers and T.V. records by the author.

www.EngineeringBooksPDF.com

Table 1.3 (continued)

Date	Location	Magnitude (Richter scale)	Fatalities
15 Jan 2010	Haiti	7.2	>100,000
23 May 2006	Anglesev	1.5	–
26 May 2006	Java, Indonesia	6.3	5,749
28 May 2006	Papua New Guinea	6.5	–
3 June 2006	Southern Iran	5.4	2
8 June 2006	Shieldaig	2.9	–
11 June 2006	Kyushhu, Japan	6.3	–
13 June 2006	Albania	4.5	–
20 June 2006	Gansu, China	5.1	–
28 June 2006	Southern Iran	5.8	9
14 May 2008	China	7.9	50,000

Note: Data Collected from various reports, newspapers and television records by the author.

Table 1.4 Locations of large-scale earthquakes: types, magnitudes and fatalities

Date	Location	Magnitude	Fatalities	Comments
23 January 1556	Shansi, China	8	830,000	–
26 December 2004	Sumatra	9.1	283,106	Deaths from earthquake and tsunami
27 July 1976	Tangshan, China	7.5	255,000	Estimated death toll as high as 655,000
9 August 1138	Aleppo, Syria		230,000	
22 December 856	Damghan, Iran		200,000	
22 May 1927	Tsinghai, China	7.9	200,000	Large fractures
16 December 1920	Gansu, China	7.8	200,000	Major fractures, landslides
23 March 893	Ardabil, Iran		150,000	
1 September 1923	Kanto (Kwanto), Japan	7.9	143,000	Great Tokyo fire
5 October 1948	USSR (Turkmenistan, Ashgabat)	7.3	110,000	
28 December 1908	Messina, Italy	7.2	70,000 – 100,000 (estimated)	Deaths from earthquake and tsunami
September 1290	Chihli, China		100,000	
8 October 2005	Pakistan	7.6	80,361	
November 1667	Shemakha, Caucasia		80,000	
18 November 1727	Tabriz, Iran		77,000	
25 December 1932	Gansu, China	7.6	70,000	
1 November 1755	Lisbon, Portugal	8.7	70,000	Great tsunami
31 May 1970	Peru	7.9	66,000	$530,000,000
Haiti	–	7.1	>100,000	damage, great slide, floods

Note: Data from various reports by the author.

www.EngineeringBooksPDF.com

Table 1.4 (continued)

Date	Location	Magnitude	Fatalities	Comments
30 May 1935	Quetta, Pakistan	7.5	30,000 – 60,000	Quetta almost completely destroyed
11 January 1693	Sicily, Italy		60,000	
1268	Silicia, Asia Minor		60,000	
20 June 1990	Western Iran	7.7	40,000 – 50,000	Landslides
4 February 1783	Calabria, Italy		50,000	
19 April 1902	Guatemala 14 N 91 W	7.5	2,000	–
16 December 1902	Turkestan 40.8 N 72.6 E	6.4	4,500	–
19 April 1903	Turkey 39.1 N 42.4 E		1,700	
28 April 1903	Turkey 39.1 N 42.5 E	6.3	2,200	–
4 April 1905	Kangra, India 33.0 N 76.0 E	7.5	19,000	–
8 September 1905	Calabria, Italy 39.4 N 16.4 E	7.9	2,500	–
31 January 1906	Colombia-Ecuador 1 N 81.5 W	8.8	1,000	–
16 March 1906	Formosa, Kagi (Taiwan) 23.6 N 120.5 E	7.1	1,300	–
18 April 1906	San Francisco, California 38.0 N 123.0 W	7.8	about 3,000	Deaths from earthquake and fire
17 August 1906	Valparaiso, Chile 33 S 72 W	8.2	20,000	–
14 January 1907	Kingston, Jamaica 18.2 N 76.7 W	6.5	1,600	–
21 October 1907	Central Asia 38 N 69 E	8.1	12,000	–
28 December 1908	Messina, Italy 38 N 15.5 E	7.2	70,000 – 100,000 (estimated)	Deaths from earthquake and tsunami
23 January 1909	Iran 33.4 N 49.1 E	7.3	5,500	–
9 August 1912	Marmara Sea 40.5 N 27 E	7.8	1950	–
13 January 1915	Avezzano, Italy 42 N 13.5 E	7.5	29,980	–
21 January 1917	Bali, Indonesia 8.0 S 115.4 E		15,000	–
30 July 1917	China 28.0 N 104.0 E	6.5	1,800	–
13 February 1918	Kwangtung (Guangdong), China 23.5 N 117.0 E	7.3	10,000	–

Note: Data collected and tabulated from reports, newspapers and T.V. records by the author.

www.EngineeringBooksPDF.com

Table 1.4 (continued)

Date	Location	Magnitude	Fatalities	Comments
16 December 1920	Gansu, China 35.8 N 105.7 E	7.8	200,000	Major fractures, landslides
24 March 1923	China 31.3 N 100.8 E	7.3	5,000	–
25 May 1923	Iran 35.3 N 59.2 E	5.7	2,200	–
1 September 1923	Kanto (Kwanto), Japan 35.0 N 139.5 E	7.9	143,000	Great Tokyo fire
16 March 1925	Yunnan, China 25.5 N 100.3 E	7.1	5,000	Talifu almost completely destroyed
7 March 1927	Tango, Japan 35.8 N 134.8 E	7.6	3,020	–
22 May 1927	Tsinghai, China 36.8 N 102.8 E	7.9	200,000	Large fractures
1 May 1929	Iran 38 N 58 E	7.4	3,300	–
6 May 1930	Iran 38.0 N 44.5 E	7.2	2,500	–
23 July 1930	Italy 41.1 N 15.4 E	6.5	1,430	–
31 March 1931	Nicaragua 13.2 N 85.7 W	5.6	2,400	–
25 December 1932	Gansu, China 39.7 N 97.0 E	7.6	70,000	–
2 March 1933	Sanriku, Japan 39.0 N 143.0 E	8.4	2,990	–
25 August 1933	China 32.0 N 103.7 E	7.4	10,000	–
15 January 1934	Bihar-Nepal, India 26.6 N 86.8 E	8.1	10,700	–
20 April 1935	Formosa 24.0 N 121.0 E	7.1	3,280	–
30 May 1935	Quetta, Pakistan 29.6 N 66.5 E	7.5	30,000 – 60,000	Quetta almost completely destroyed
16 July 1935	Taiwan 24.4 N 120.7 E	6.5	2,700	–
25 January 1939	Chillan, Chile 36.2 S 72.2 W	7.8	28,000	–
26 December 1939	Erzincan, Turkey 39.6 N 38 E	7.8	30,000	–
10 November 1940	Romania 45.8 N 26.8 E	7.3	1,000	–
26 November 1942	Turkey 40.5 N 34.0 E	7.6	4,000	–
20 December 1942	Erbaa, Turkey 40.9 N 36.5 E	7.3	3,000	Some reports of 1,000 killed
10 September 1943	Tottori, Japan 35.6 N 134.2 E	7.4	1,190	–

www.EngineeringBooksPDF.com

Table 1.4 (continued)

Date	Location	Magnitude	Fatalities	Comments
26 November 1943	Turkey 41.0 N 33.7 E	7.6	4,000	–
15 January 1944	San Juan, Argentina 31.6 S 68.5 W	7.8	5,000	Reports of as many as 8,000 killed
1 February 1944	Turkey 41.4 N 32.7 E	7.4	2,800	Reports of as many as 5,000 killed
7 December 1944	Tonankai, Japan 33.7 N 136.2 E	8.1	1,000	–
12 January 1945	Mikawa, Japan 34.8 N 137.0 E	7.1	1,900	–
27 November 1945	Iran 25.0 N 60.5 E	8.2	4,000	–
31 May 1946	Turkey 39.5 N 41.5 E	6.0	1,300	–
10 November 1946	Ancash, Peru 8.3 S 77.8 W	7.3	1,400	Landslides, great destruction
20 December 1946	Tonankai, Japan 32.5 N 134.5 E	8.1	1,330	–
28 June 1948	Fukui, Japan 36.1 N 136.2 E	7.3	5,390	–
5 October 1948	USSR (Turkmenistan, Ashgabat) 38.0 N 58.3 E	7.3	110,000	–
5 August 1949	Ambato, Ecuador 1.2 S 78.5 E	6.8	6,000	Large landslides, topographical changes
15 August 1950	India, Assam–Tibet 28.7 N 96.6 E	8.6	1,530	Great topographical changes, landslides, floods
18 March 1953	Western Turkey 40.0 N 27.5 E	7.3	1,103	Yenice destroyed and major damages at Gonen and Can. Felt throughout the Aegean Islands and southern Greece. Microseismic area estimated at 2,000 square miles. Damage estimated about $3,570,000.

www.EngineeringBooksPDF.com

Table 1.4 (continued)

Date	Location	Magnitude	Fatalities	Comments
9 September 1954	Orleansville, Algeria 36 N 1.6 E	6.8	1,250	–
27 June 1957	USSR (Russia) 56.3 N 116.5 E		1,200	–
2 July 1957	Iran 36.2 N 52.7 E	7.4	1,200	–
13 December 1957	Iran 34.4 N 47.6 E	7.3	1,130	–
29 February 1960	Agadir, Morocco 30 N 9 W	5.7	10,000 – 15,000	Occurred at shallow depth
22 May 1960	Chile 39.5 S 74.5 W	9.5	4,000 – 5,000	Tsunami, volcanic activity, floods
1 September 1962	Qazvin, Iran 35.6 N 49.9 E	7.3	12,230	–
26 July 1963	Skopje, Yugoslavia 42.1 N 21.4 E	6.0	1,100	Occurred at shallow depth just undefined
19 August 1966	Varto, Turkey, 39.2 N 41.7 E	7.1	2,520	–
31 August 1968	Iran 34.0 N 59.0 E	7.3	12,000 – 20,000	–
25 July 1969	Eastern China 21.6 N 111.9 E	5.9	3,000	–
4 January 1970	Yunnan Province, China 24.1 N 102.5 E	7.5	10,000	–
28 March 1970	Gediz, Turkey 39.2 N 29.5 E	6.9	1,100	–
31 May 1970	Peru 9.2 S 78.8 W	7.9	66,000	$530,000,000 damage, great rock floods
22 May 1971	Turkey 38.83 N 40.52 E	6.9	1,000	–
10 April 1972	Southern Iran 28.4 N 52.8 E	7.1	5,054	–
23 December 1972	Managua, Nicaragua 12.4 N 86.1 W	6.2	5,000	–
10 May 1974	China 28.2 N 104.0 E	6.8	20,000	–
28 December 1974	Pakistan 35.0 N 72.8 E	6.2	5,300	–
4 February 1975	China 40.6 N 122.5 E	7.0	10,000	–
6 September 1975	Turkey 38.5 N 40.7 E	6.7	2,300	–
4 February 1976	Guatemala 15.3 N 89.1 W	7.5	23,000	–
6 May 1976	Northeastern Italy 46.4 N 13.3 E	6.5	1,000	–

www.EngineeringBooksPDF.com

Table 1.4 (continued)

Date	Location	Magnitude	Fatalities	Comments
25 June 1976	West Irian (New Guinea) 4.6 S 140.1 E	7.1	422	5,000 – 9,000 missing and presumed dead
27 July 1976	Tangshan, China 39.6 N 118.0 E	7.5	255,000 (official)	Estimated death toll as high as 650,000
16 August 1976	Mindanao, Philippines 6.3 N 124.0 E	7.9	8,000	–
24 November 1976	Northwest Iran–USSR border 39.1 N 44.0 E	7.3	5,000	Deaths estimated
4 March 1977	Romania 45.8 N 26.8 E	7.2	1,500	–
16 September 1978	Iran 33.2 N 57.4 E	7.8	15,000	–
10 October 1980	El Asnam (formerly Orleansville), Algeria 36.1 N 1.4 E	7.7	3,500	–
23 November 1980	Southern Italy 40.9 N 15.3 E	7.2	3,000	–
11 June 1981	Southern Iran 29.9 N 57.7 E	6.9	3,000	–
28 July 1981	Southern Iran 30.0 N 57.8 E	7.3	1,500	–
13 December 1982	Western Arabian Peninsula 14.7 N 44.4 E	6.0	2,800	–
30 October 1983	Turkey 40.3 N 42.2 3 E	6.9	1,342	–
19 September 1985	Michoacan, Mexico 18.2 N 102.5 W	8.0	9,500 (official)	Estimated death toll as high as 30,000
10 October 1986	El Salvador 13.8 N 89.2 W	5.5	1,000	–
6 March 1987	Colombia–Ecuador 0.2 N 77.8 W	7.0	1,000	–
20 August 1988	Nepal–India border region 26.8 N 86.6 E	6.8	1,450	–
7 December 1988	Spitak, Armenia 41.0 N 44.2 E	6.8	25,000	–
20 June 1990	Western Iran 37.0 N 49.4 E	7.7	40,000 – 50,000	Landslides
16 July 1990	Luzon, Philippine Islands 15.7 N 121.2 E	7.8	1,621	Landslides, subsidence and sand.

www.EngineeringBooksPDF.com

Table 1.4 (continued)

Date	Location	Magnitude	Fatalities	Comments
19 October 1991	Northern India 30.8 N 78.8 E	7.0	2,000	–
12 December 1992	Flores Region, Indonesia 8.5 S 121.9 E	7.5	2,500	Tsunami ran inland 300 m, water height 25 m
29 September 1993	Latur-Killari, India 18.1 N 76.5 E	6.2	9,748	–
16 January 1995	Kobe, Japan 34.6 N 135 E	6.9	5,502	Landslide, liquefaction
27 May 1995	Sakhalin Island 52.6 N 142.8 E	7.5	1,989	–
10 May 1997	Northern Iran 33.9 N 59.7 E	7.5	1,560	4,460 injured, 60,000 homeless
4 February 1998	Tajikistan Border Region-Afghanistan 37.1 N 70.1 E	6.1	2,323	818 injured, 8,094 houses destroyed
30 May 1998	Tajikistan border region–Afghanistan 37.1 N 70.1 E	6.9	4,000	At least 4,000 people killed, many thousands injured and homeless in Badakhshan and Takhar province in Afghanistan
17 July 1998	Papua New Guinea 2.96 S 141.9 E	7.0	2,183	Thousands injured, about 9,500 homeless and about 500 missing as a result of tsunami with maximum wave height estimated at 10 m
25 January 1999	Colombia 4.46 N 75.82 W	6.2	1,185	Over 700 missing and presumed killed. Over 4,750 injured and about 250,000 homeless
17 August 1999	Turkey 40.7 N 30.0 E	7.6	17,118	At least 50,000 injured, thousands homeless. Damage estimated at 3 billion USD

www.EngineeringBooksPDF.com

Table 1.4 (continued)

Date	Location	Magnitude	Fatalities	Comments
20 September 1999	Taiwan 23.7 N 121.0 E	7.7	2,297	Over 8,700 injured, over 600,000 homeless. Damage estimated at 14 million USD
26 January 2001	India 23.3 N 70.3 E	7.7	20,023	166,836 injured, 600,000 homeless
25 March 2002	Hindu Kush Region, Afghanistan 35.9 N 3.71 E	6.1	1,000	4,000 injured, 1,500 houses destroyed in the Nahrin area. Approx. 2,000 people homeless
21 May 2003	Northern Algeria 36.90 N 3.71 E	6.8	2,266	10,261 injured, 150,000 homeless, more than 1,243 buildings damaged or destroyed
26 December 2003	Southeastern Iran 28.99 N 58.31 E	6.6	26,200	30,000 injured, 85% of buildings damaged or destroyed and infrastru-cture damaged in the Bam area
26 December 2004	Sumatra 3.30 N 95.87 E	9.1	283,106	Deaths from earthquake and tsunami
28 March 2005	Northern Sumatra, Indonesia 2.07 N 97.01 E	8.7	1,313	–
8 October 2005	Pakistan 34.53 N 73.58 E	7.6	80,361	–
26 May 2006	Indonesia -7.961 110.446	6.3	5,749	At least 5,749 people were killed

Note: Some sources list an earthquake that killed 300,000 people in Calcutta, India, on October. Recent studies indicate that these casualties were most likely due to a cyclone, not an earthquake. (Source: The 1737 Calcutta Earthquake and Cyclone Evaluated by Roger Bilham, BSSA, October 1994)

Data collected from reports newspapers and television records by the author over a period of times.

www.EngineeringBooksPDF.com

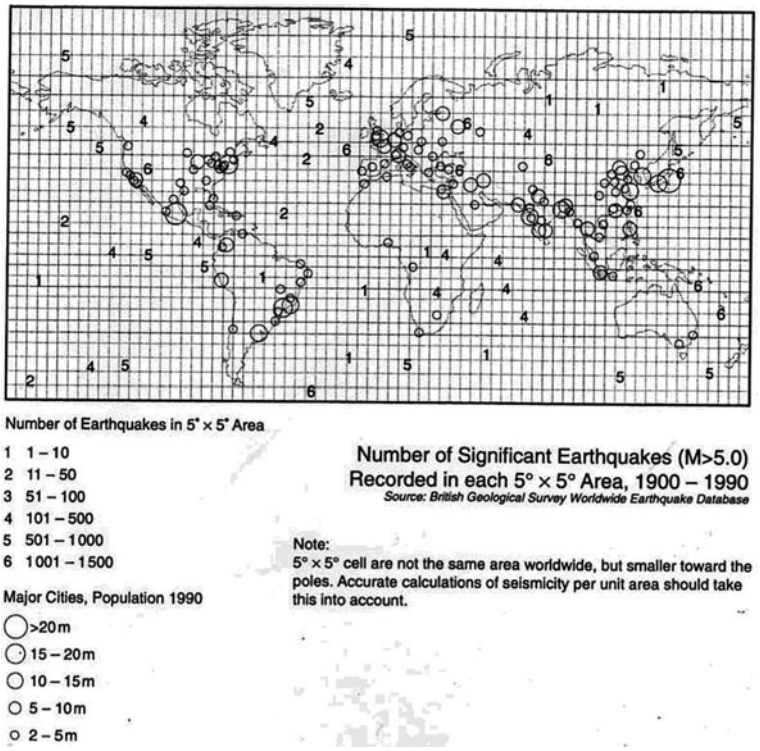


Fig. 1.1 Seismicity of the world (courtesy of Cartographic Data Atlas version 1.02, British Geological Survey Worldwide Earthquake Database)
(Ref. Prototype Building Structures, Thomas Telford, London 1993.)

1.8 Intensity Scale

The word "intensity" may be defined qualitatively as "the quality or condition of being intense" or quantitatively as "magnitude, as of energy or a force per unit of area or time". The term earthquake intensity was introduced to be a physical quantity, but through qualitative or fuzzy definitions. In the earthquake engineering field, some consider it a qualitative rating through the intensity scale, but many engineers consider it an equivalent of ground peak acceleration intensity.

There are three properties of earthquake intensity defined by macroseismic phenomena:

1. A composite measure of multiple scales: intensity is defined through the levels of human response, structural damage, changes in natural phenomena and behaviour of objects during or after an earthquake. Each of these four responses is a scale, and intensity ratings are specified in each scale. When the measurements of each individual scale differ from each other as

www.EngineeringBooksPDF.com

usually happens, a subjective decision is made, such as in China, by individuals who rate the intensity, but the maximum rating is taken in Europe.
2. A ranking and fuzzy measure through macroseismic description: on each individual scale, the scaling is not quantitative but qualitative in terms of fuzzy ranks, such as a "few", "some", "many", "most", for the number of items considered; "slight", "moderate", "heavy", "serious", for strength of response. These are typical fuzzy set terms, i.e. they are defined through qualitative description, and the boundaries between ranks are not clear but fuzzy.
3. Indirectness of defining a cause through the results if intensity means ground motion: many building design codes still define intensity as ground motion. It is quite clear that ground motion is the cause of its effects on objects. The relation between cause and effects must be rough or fuzzy if the objects, as well as the cause and effects, are not clearly defined as in the case of an intensity scale.

The term earthquake intensity has been used for more than 170 years before the term earthquake magnitude and is still widely used. Its usage includes the following three aspects:

4. As a simple measure of earthquake damage: after a strong earthquake, government and society want to know the general level of damage and its distribution in order to take emergency action. It is relatively easy to estimate after an earthquake and to be understood by ordinary people, just like wind intensity.
5. As a simple macroseismic scale for the strength of earthquake motion for the seismologist: historical earthquake data are damage data, which have been used to study past seismicity. Without damage data, the history of earthquakes would cover only a few decades, too short to know the spatial and temporal distribution of earthquakes or their seismicity.
6. As a rough but convenient index to sum up experience to earthquake engineering construction and to depict zones of seismic hazard (Hu, C1983): many countries use intensity as index for zonation, such as Russia, China and several European countries, and many countries have previously used it, such as the United States, Canada and India.

1.8.1 Earthquake Intensity Scale

The macroseismic idea of earthquake intensity was a natural product 170 years ago when no instruments were available to measure any physical quantity of ground motion and the requirement of earthquake description was also simple,

www.EngineeringBooksPDF.com

just a scale or a single number or grade to describe its strength or magnitude. The earliest record of earthquake intensity may be traced back to 1564 in Europe. When discussing the effect of an earthquake, different colours are used to show different effects on a map. Up to the nineteenth century, there appeared many earthquake intensity scales, mostly used to grade the local damage or effect. During the early period, macroseismic phenomena were the only means possible to define the indices of the intensity scale. As an example, the one commonly used is the abridged Modified Mercalli (MM) intensity scale, from which a general and brief idea of intensity may be obtained. A reference is made to Tables 1.1, 1.2, 1.3, 1.4, 1.5, 1.6 and 1.7.

An effective earthquake-resisting design for buildings in an area subject to seismic activity depends on the characteristics of earthquakes, namely frequency content, intensity and duration. The type of construction, soil conditions and a number of other complex factors concerning dynamic modelling, load–structure– soil interactions, etc. are additional areas which need to be investigated.

The genealogy of the intensity scales is described in a step-by-step manner in Figs. 1.1 and 1.2. The most well-known intensity scales, Modified Mercalli (Richter) and Medvedev–Sponheuer–Karnik (MSK), are fully described in Tables 1.3, 1.4 and 1.5. These tables are needed to assess the damage to structures such as buildings and their components. A guide to earthquake magnitude is given in Tables 1.3, 1.4, 1.5, 1.6 and 1.7.

1.8.2 Intensity Distribution

1.8.2.1 Isoseismal Map

The intensity contour or isoseismal map is a simple way to show the general damage to a strong earthquake on a map. After field investigations an isoseismal map is drawn in the following two stages:

1. The original intensity ratings of all sites investigated are indicated on a detailed map.
2. Contour lines of equal intensities are drawn which group sites of the same intensity in the same zone.

For the design of buildings three approaches are specified and are given below:

(a) Seismic coefficient method: Various codes recommend this method. Flexibility or stiffness methods are employed. Specified shear distribution as cubic parabola in various building storeys is recommended. This approach is adopted for buildings no more than 40 m high.
(b) Modal analysis: Modal analysis using average acceleration spectra and a multiplying factor is adopted for buildings within the range of 40–90 m height.

www.EngineeringBooksPDF.com

Table 1.5 Modified Mercalli intensity scale

I.	Not felt except by a very few under exceptionally favourable circumstances.
II.	Felt by persons at rest, on upper floors, or favourably placed.
III.	Felt indoors; hanging objects swing; vibration similar to passing of light trucks; duration may be estimated; may not be recognized as an earthquake.
IV.	Hanging objects swing; vibration similar to passing of light trucks; or sensation of a jolt similar to a heavy ball striking the walls; standing motor cars rock; windows, dishes and doors rattle; glasses clink and crockery clashes; in the upper range of IV wooden walls and frames creak.
V.	Felt outdoors; direction may be estimated; sleepers wakened, liquids disturbed, some spilled; small unstable objects displaced or upset; doors swing, close or open; shutters and pictures move; pendulum clocks stop, start or change rate.
VI.	Felt by all; many frightened and run outdoors; walking unsteady; windows, dishes and glassware broken; knick-knacks, books, etc., fall from shelves and pictures from walls; furniture moved or overturned; weak plaster and masonry D* cracked; small bells ring (church or school); trees and bushes shaken (visibly, or heard to rustle).
VII.	Difficult to stand; noticed by drivers of motor cars; hanging objects quiver; furniture broken; damage to masonry D, including cracks; weak chimneys broken at roof line; fall of plaster, loose bricks, stones, tiles, cornices (also unbraced parapets and architectural ornaments); some cracks in masonry C*; waves on ponds; water turbid with mud; small slides and caving in along sand or gravel banks; large bells ring; concrete irrigation ditches damaged.
VIII.	Steering of motor cars affected; damage to masonry C or partial collapse; some damage to masonry B*; none to masonry A*; fall of stucco and some masonry walls; twisting and fall of chimneys, factory stacks, monuments, towers and elevated tanks; frame houses moved on foundations if not bolted down; loose panel walls thrown out; decayed piling broken off; branches broken from trees; changes in flow or temperature of springs and wells; cracks in wet ground and on steep slopes.
IX.	General panic; masonry D destroyed; masonry C heavily damaged, sometimes with complete collapse; masonry B seriously damaged; general damage to foundations; frame structures if not bolted shifted off foundations; frames racked; serious damage to reservoirs; underground pipes broken; conspicuous cracks in ground; in alluviated areas sand and mud ejected, earthquake fountains and sand craters appear.
X.	Most masonry and frame structures destroyed with their foundations; some well-built wooden structures and bridges destroyed; serious damage to dams, dykes and embankments; large landslides; water thrown on banks of canals, rivers, lakes, etc.; sand and mud shifted horizontally on beaches and flat land; rails bent slightly.
XI.	Rails bent greatly; underground pipelines completely out of service.
XII.	Damage nearly total; large rock masses displaced; lines of sight and level distorted; objects thrown into the air.

Masonry A: Good workmanship, mortar and design; reinforced, especially laterally, and bound together by using steel, concrete, etc., designed to resist lateral forces.

Masonry B: Good workmanship and mortar; reinforced but not designed in detail to resist lateral forces.

Masonry C: Ordinary workmanship and mortar; no extreme weaknesses like failing to tie in at corners, but neither reinforced nor designed against horizontal forces.

Masonry D: Weak materials, such as adobe; poor mortar; low standards of workmanship; weak horizontally.

www.EngineeringBooksPDF.com

Table 1.6 Seismic intensity scale MSK-81 Medvedev–Sponheuer–Karnik 1981 Revision

Intensity degree I: Not noticeable

The intensity of the vibration is below the limit of sensibility; the tremor is detected and recorded by seismographs only.

Intensity degree II: Scarcely noticeable (very slight)

Vibration is felt only by individual people at rest in houses, especially on upper floors of buildings.

Intensity degree III: Weak

The earthquake is felt indoors by a few people, outdoors only in favourable circumstances. The vibration is weak. Attentive observers notice a slight swinging of hanging objects, somewhat more heavily on upper floors.

Intensity degree IV: Largely observed

The earthquake is felt indoors by many people, outdoors by a few. Here and there people are awakened, but no one is frightened. The vibration is moderate. Windows, doors and dishes rattle. Floors and walls creak. Furnitures begin to shake. Hanging objects swing slightly. Liquids in open vessels are slightly disturbed. In standing motor cars the shock is noticeable.

Intensity degree V: Strong

Effects on people and surroundings: The earthquake is felt indoors by most, outdoors by many. Many sleeping people are awakened. A few run outdoors. Animals become uneasy. Buildings tremble throughout. Hanging objects swing considerably. Pictures swing out of place. Occasionally pendulum clocks stop. Unstable objects may be overturned or shifted. Open doors and windows are thrust open and slam back again. Liquids spill in small amounts from well-filled open containers. The vibration is strong, resembling sometimes the fall of a heavy object in the building.

Effects on structures: Damage of grade 1 in a few buildings of type A is possible.

Effects on nature: Sometimes change in flow of springs.

Intensity degree VI: Slight damage

Effects on people and surroundings: Felt by most indoors and outdoors. Many people in buildings are frightened and run outdoors. A few persons lose their balance. Domestic animals run out of their stall. In a few instances dishes and glassware may break. Books fall down. Heavy furniture may possibly move and small steeple bells may ring.

Effects on structures: Damage of grade 1 is sustained in single buildings of type B and in many of type A. Damage in few buildings of type A is of grade 2.

Effects on nature: In a few cases cracks up to widths of 1 cm are possible in wet ground; in mountains occasional landslips; changes in flow of springs and in level of well water are observed.

Intensity degree VII: Damage to buildings

Effects on people and surroundings: Most people are frightened and run outdoors. Many find it difficult to stand. Persons driving motor cars notice the vibration. Large bells ring.

Effects on structures: In many buildings of type C damage of grade 1 is caused; in many buildings of type B damage is of grade 2. Many buildings of type A suffer damage of grade 3, a few of grade 4. In some instances landslips of roadway on steep slopes occur; local cracks in roads and stonewalls.

Effects on nature: Waves are formed on water, and water is made turbid by mud stirred up. Water levels in wells change, and the flow of springs changes. In a few cases dry springs have their flow restored and existing springs stop flowing. In isolated instances parts of sandy or gravelly banks slip off.

Intensity degree VIII: Destruction of buildings

Effects on people and surroundings: General fright; a few people show panic, also persons driving motor cars are disturbed. Here and there branches of trees break off. Even heavy furniture moves and partly overturns. Hanging lamps are in part damaged.

www.EngineeringBooksPDF.com

Table 1.6 (continued)

Effects on structures: Many buildings of type C suffer damage of grade 2 and a few of grade 3. Many buildings of type B suffer damage of grade 3 and a few of grade 4. Many buildings of type A suffer damage of grade 4 and a few of grade 5. Memorials and monuments move and twist. Tombstones overturn. Stone walls collapse.

Effects on nature: Small landslips on hollows and on banked roads on steep slopes; cracks in ground up to widths of several centimetres. New reservoirs come into existence. Sometimes dry wells refill and existing wells become dry. In many cases change in flow and level of water or wells.

Intensity degree IX: General damage to buildings

Effects on people and surroundings: General panic; considerable damage to furniture. Animals run to and fro in confusion and cry.

Effects on structures: Many buildings of type C suffer damage of grade 3 and a few of grade 4. Many buildings of type B show damage of grade 4, a few of grade 5. Many buildings of type A suffer damage of grade 5. Monuments and columns fall. Reservoirs may show heavy damage. In individual cases railway lines are bent and roadways damaged.

Effects on nature: On flat land overflow of water, sand and mud is often observed. Ground cracks to widths of up to 10 cm, in slopes and river banks more than 10 cm; furthermore, a large number of slight cracks in ground; falls of rock, many landslides and earth flows; large waves on water.

Intensity degree X: General destruction of buildings

Effects on structures: Many buildings of type C suffer damage of grade 4, a few of grade 5. Many buildings of type B show damage of grade 5, most of type A collapse. Dams, dykes and bridges may show severe to critical damage. Railway lines are bent slightly. Road pavements and asphalt show wary folds.

Effects on nature: In ground, cracks up to widths of several decimetres, sometimes up to 1 m. Broad fissures occur parallel to water courses. Loose ground slides from steep slopes. Considerable landslides are possible from river banks and steep coast. In coastal areas displacement of sand and mud; water from canals, lakes, river, etc., thrown on land. New lakes occur.

Intensity degree XI: Catastrophe

Effects on structures: Destruction of most and collapse of many buildings of type C. Even well-built bridges and dams may be destroyed and railway lines largely bent, thrusted or bucked; highways become unusable; underground pipes destroyed.

Effects on nature: Ground fractured considerably by broad cracks and fissures, as well as by movement in horizontal and vertical directions; numerous landslides and fall of rocks. The intensity of the earthquake requires to be investigated especially.

Intensity degree XII: Landscape changes

Effects on structures: Practically all structures above and below ground are heavily damaged or destroyed.

Effects on nature: The surface of the ground is radically changed. Considerable ground cracks with extensive vertical and horizontal movement are observed. Fall of rocks and slumping of river banks over wide areas; lakes are dammed; waterfalls appear, and rivers are deflected. The intensity of the earthquake requires to be investigated especially.

Type of structures (building not antiseismic)

A Buildings of fieldstone, rural structures, adobe houses, clay houses.

B Ordinary brick buildings, large block construction, half-timbered structures, structures of hewn blocks of stone.

C Precast concrete skeleton construction, precast large panel construction, well-built wooden structures.

www.EngineeringBooksPDF.com

Table 1.6 (continued)

Classification of damage to buildings
Grade 1: Slight damage: fine cracks in plaster; fall of small pieces of plaster.
Grade 2: Moderate damage: small cracks in walls; fall of fairly large pieces of plaster; pantiles slip off; cracks in chimneys; parts of chimneys fall down.
Grade 3: Heavy damage: large and deep cracks in walls; fall of chimneys.
Grade 4: Destruction: gaps in walls; parts of buildings may collapse; separate parts of the buildings lose their cohesion; inner walls and filled-in walls of the frame collapse.
Grade 5: Total damage: total collapse of buildings.

Table 1.7 A guide to earthquake magnitude

Magnitudes less than 4.5
Magnitude 4.5 represents an energy release of about 10^8 kJ and is the equivalent of about 10 t of TNT being exploded underground. Below about magnitude 4.5, it is extremely rare for an earthquake to cause damage, although it may be quite widely felt. Earthquakes of magnitude 3 and magnitude 2 become increasingly difficult for seismographs to detect unless they are close to the event. A shallow earthquake of magnitude 4.5 can generally be felt for 50–100 km from the epicentre.
Magnitude 4.5–5.5 – local earthquakes
Magnitude 5.5 represents an energy release of around 10^9 kJ and is the equivalent of about 100 t of TNT being exploded underground. Earthquakes of magnitude 5.0–5.5 may cause damage if they are shallow and if they cause significant intensity of ground shaking in areas of weaker buildings. Earthquakes up to magnitude of about 5.5 can occur almost anywhere in the world – this is the level of energy release that is possible in normal non-tectonic geological processes such as weathering and land formation. An earthquake of magnitude 5.5 may well be felt 100–200 km away.
Magnitude 6.0–7.0 – large magnitude events
Magnitude 6 represents an energy release of the order of 10^{10} kJ and is the equivalent of exploding about 6,000 t of TNT underground. A magnitude 6.3 is generally taken as being about equivalent to an atomic bomb being exploded underground. A magnitude 7.0 represents an energy release of 10^{12} kJ. Large magnitude earthquakes of magnitude 6.0 and above are much larger energy releases associated with tectonic processes. If they occur close to the surface they may cause intensities at their centre of VIII, IX or even X, causing very heavy damage or destruction if there are towns or villages close to their epicentre. Some of these large magnitude earthquakes, however, are associated with tectonic processes at depth and may be relatively harmless to people on the Earth's surface. There are about 200 large magnitude events somewhere in the world each decade. A magnitude 7.0 earthquake at shallow depth may be felt at distances 500 km or more from its epicentre.
Magnitudes 7.0–8.9 – great earthquakes
A magnitude 8 earthquake releases around 10^{13} kJ of energy, equivalent to more than 400 atomic bombs being exploded underground, or almost as much as a hydrogen bomb. The largest earthquake yet recorded, magnitude 8.9, released 10^{14} kJ of energy. Great earthquakes are the massive energy releases caused by long lengths of linear faults rupturing in on break. If they occur at shallow depths they cause slightly stronger epicentral intensities than large magnitude earthquakes but their great destructive potential is due to the very large areas that are affected by strong intensities.

www.EngineeringBooksPDF.com

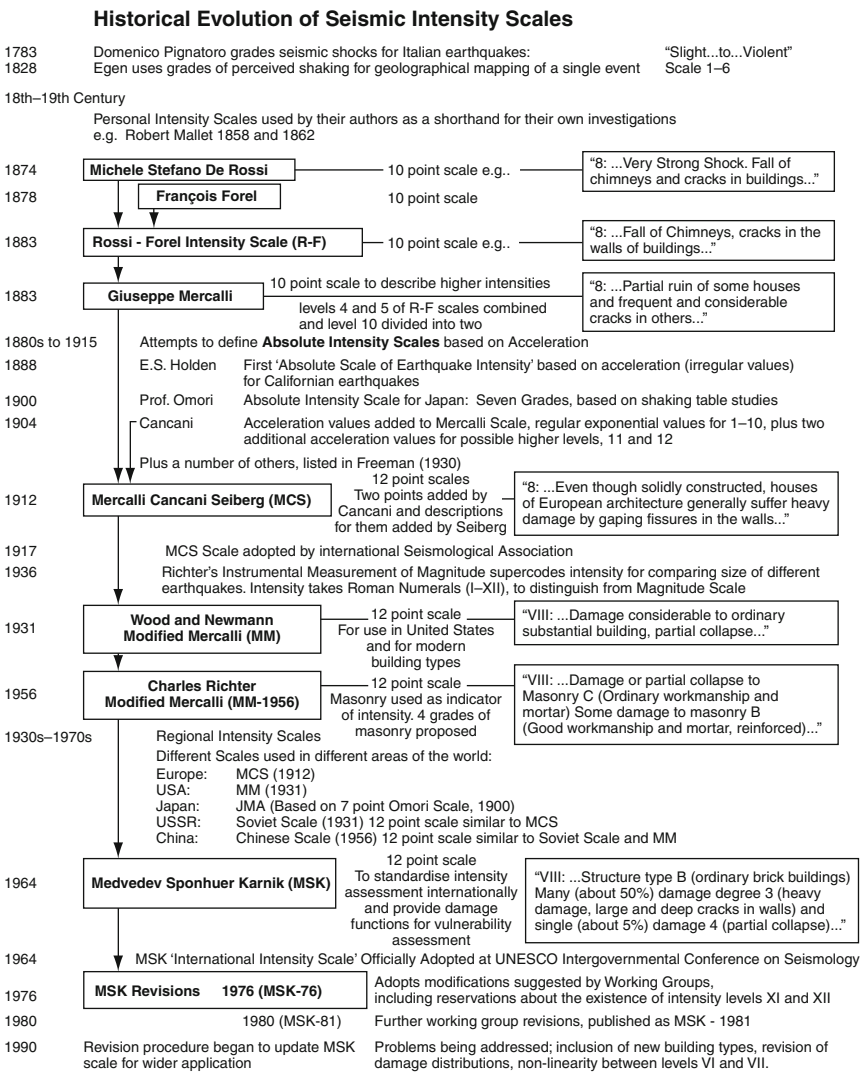


Fig. 1.2 The "genealogy" of seismic intensity scales

The response spectra are given in this section. Direct integration method is recommended as a method of solving various differential equations.

(c) Detailed dynamic analysis: Here the building structure is dynamically analysed using actual earthquake accelerogram and time-wise integration of the dynamic response for tall buildings of more than 90 m. The response spectra can be elastic or inelastic. Finite element and other methods associated with static and dynamic condensation techniques are employed to solve for large building structures located in seismic zones.

www.EngineeringBooksPDF.com

A greater detail of such methods is given in Part B of the book, Methods of Analysis, and in the Appendix.

Design for drift and lateral stability is important and should be addressed in the early stages of the building design development. The concept of lateral stability and its relationship to drift and the $P - \Delta$ effect has been codified. In an earthquake area the relative displacement of buildings is measured by an overall drift ratio or index. This ratio is either of the following:

(i) the ratio of the relative displacement of a particular floor to the storey height at that level;
(ii) relative displacement between two adjacent floors.

The *drift index* is the drift divided by the storey height.

Stability analysis sections and the Appendix provide details for drift, lateral stability and $P - \Delta$. The limitations of these are given by various codes.

Because of the wide scattering of data, judgement is necessary for the second stage. The routine compromise is to have one set of isoseismals starting from the epicentral area with the highest intensity and decreasing outwards by a decrement of one grade with fairly smooth contours and some individual contours scattered almost randomly. The former is considered to represent the general intensity distribution, which reflects attenuation of damage away from the epicentre, and the latter as abnormal intensity areas, which reflect the local variations of site conditions and other effects.

If intensity is rated by the highest indication of an intensity scale, the isoseismals will be the envelope of intensity scale; as the Chinese do, the isoseismals will be some average.

1.8.3 Abnormal Intensity Region

Since site conditions over a wide region change quite often, abnormal intensity areas are actually quite common and can be found in almost any strong earthquake. In mountainous regions, local topography and soil conditions are mainly responsible; in alluvial plains, soft and weak soils are the major cause of abnormality. There are areas where abnormal intensities have been reported for several historical earthquakes. For example, the Yutian area, about 50 km northwest of Tangshan City, was an area of abnormally low intensity in both the 1679 Sanhe-Pinggu and the 1976 Tangshan earthquakes.

1.8.4 Factors Controlling Intensity Distribution

1.8.4.1 Source Effect

The term "earthquake source" is used here for the whole region where strain energy is released in the form of earthquake waves during one earthquake. Energy density, geometry of the source and its position in space are the

www.EngineeringBooksPDF.com

controlling factors of intensity distribution. The overall shape of isoseismals is controlled by the source. For example, small earthquakes have small sources and the isoseismals are usually circular; but very large earthquakes have in general extended sources, i.e. with one horizontal dimension much longer than the other, and the isoseismals of higher intensities are usually elongated or elliptical. For example, the surface faulting of the 1970 Tonghai earthquake was about 60 km long and the isoseismals of intensities VII, VIII, IX and X were very narrow, with a short-axis/long-axis ratio less than one-third.

1.8.4.2 Distance Effect

The effect of distance is clear and it is the main factor of attenuation. There are several definitions of distance and their distinction is important for the near field, i.e. the epicentre and the neighbouring areas. The epicentral distance depends on the definition of epicentre. The instrumental epicentre is the easiest to use with instrumental records, but it has the lowest correlation with intensity distribution. The fault distance or the shortest distance to the fault is even better when surface faulting can be found.

1.9 Earthquake Intensity Attenuation

The relationship of intensity variation with magnitude and distance is usually referred to as the attenuation law.

1.9.1 Epicentral Intensity and Magnitude

The epicentral intensity I_0 was used to represent the size of an earthquake before the earthquake magnitude was suggested. Although epicentral intensity also depends on focal depth h, it can still be used for a certain specified narrow range of focal depth, say 10–30 km, which is the rough average of most strong earthquakes. To estimate the magnitude of historical earthquakes, the relation between epicentral intensity I_0 and magnitude M that given by Gutenberg and Richter (1956) for the southern California region is useful.

1.10 Geotechnical Earthquake Engineering

Geotechnical earthquake engineering can be defined as that subspecialty within the field of geotechnical engineering which deals with the design and construction of projects in order to resist the effects of earthquakes. Geotechnical earthquake engineering requires an understanding of basic geotechnical principles as well as geology, seismology and earthquake engineering. In a broad sense, seismology can

www.EngineeringBooksPDF.com

be defined as the study of earthquakes. This would include the internal beheviour of the Earth and the nature of seismic waves generated by the earthquake.

The first step in geotechnical earthquake engineering is often to determine the dynamic loading from the anticipated earthquake (the anticipated earthquake is also known as the design earthquake). For the analysis of earthquakes, the types of activities that may need to be performed by the geotechnical engineer include the following:

- Investigating the possibility of liquefaction at the site. Liquefaction can cause a complete loss of the soil's shear strength, which could result in a bearing capacity failure, excessive settlement or slope movement.
- Calculating the settlement of the structure caused by the anticipated earthquake.
- Checking the design parameters for the foundation, such as the bearing capacity and allowable soil bearing pressures, to make sure that the foundation does not suffer a bearing capacity failure during the anticipated earthquake.
- Investigating the stability of slopes for the additional forces imposed during the design earthquake. In addition, the lateral deformation of the slope during the anticipated earthquake may need to be calculated.
- Evaluation of the effect of the design earthquake on the stability of structures.
- Analysing other possible earthquake effects, such as surface faulting and resonance of the structure.
- Developing site improvement techniques to mitigate the effects of the anticipated earthquake. These include ground stabilization and groundwater control.
- Determining the type of foundation, such as a shallow or deep foundation.
- Assisting the structural engineer by investigating the effects of ground movement due to seismic forces on the structure and by providing design parameters or suitable structural systems to accommodate the anticipated displacement.

1.11 Liquefaction

1.11.1 Introduction

The final three sections of this chapter deal with secondary effects, which are defined as non-tectonic surface processes that are directly related to earthquake shaking. Examples of secondary effects are liquefaction, earthquake-induced slope failures and landslides, tsunamis and seiches.

This section deals with liquefaction. The typical subsurface soil condition that is susceptible to liquefaction is loose sand, which has been newly deposited or placed, with a groundwater table near ground surface. During an earthquake, the propagation of shear waves causes the loose sand to contract, resulting in an

www.EngineeringBooksPDF.com

increase in pore water pressure. Because the seismic shaking occurs so quickly, the cohesionless soil is subjected to an undrained loading. The increase in pore water pressure causes an upward flow of water to the ground surface, where ti emerges in the form of mud spouts or sand boils. The development of high pore water pressures due to the ground shaking and the upward flow of water may turn the sand into a liquefied condition, which has been termed liquefaction. For this state of liquefaction, the effective stress is zero and the individual soil particles are released from any confinement, as if the soil particles were floating in water.

Because liquefaction typically occurs in soil with a high groundwater table, its effects are most commonly observed in low-lying areas or adjacent rivers, lakes, bays and oceans.

Structures on top of the loose sand deposit that has liquefied during an earthquake can sink or fall over, and buried tanks will float to the surface when the loose sand is liquefied.

After the soil has liquefied, the excess pore water pressure will start to dissipate the length of time that the soil will remain in a liquefied state, which depends on two main factors: (1) the duration of the seismic shaking from the earthquake and (2) the drainage condition of the liquefied soil. The longer and the stronger the cyclic shear stress application from earthquake, the longer the state of liquefaction persists. Likewise, if the liquefied soil is confined by an upper and a lower clay layer, then it will take longer for the excess water pressures to dissipate by the flow of water from the liquefied soil. After the liquefaction process is complete, the soil will be in a somewhat denser state.

1.11.2 Types of Damage

As previously mentioned, there could also be liquefaction-induced ground damage, which causes settlement of structures.

There are two main aspects to the ground surface damage:

1. *Sand boils*: There could be liquefaction-induced ground loss below the structures as the loss of soil through the development of ground surface sand boils. Often liquefaction, and sand boils are observed at ground surface. A row of sands often develops at the location of cracks or fissures in the ground.
2. *Surface fissures*: The liquefied soil could also cause the development of ground face fissures which break the overlying soil into blocks that open and close during earthquakes. Note that the liquefied soil actually flowed out of the fissures.

1.12 Earthquake-Induced Settlement

Buildings founded on solid rocks are least likely to experience earthquake-induced differential settlement. However, buildings on soils could be subjected to many different types of earthquake-induced settlement;

www.EngineeringBooksPDF.com

where the earthquake-induced settlement exists the following conditions must be satisfied:

(a) Settlement versus the factor of safety against liquefaction and is acceptable
(b) Liquefaction–induced ground damage has been successfully evaluated and is ok
(c) Volumetric compression is satisfied
(d) Settlement due to dynamic loads caused by rocking is within permissible limits given in various codes.

1.13 Bearing Capacity Analyses for Earthquakes

A bearing capacity failure is defined as a foundation failure that occurs when the shear stresses in the soil exceed the shear strength of the soil. For both static and seismic cases bearing capacity failures of foundations can be grouped into three categories:

– General shear strength
– Punching shear strength
– Local shear strength

1.14 Slope Stability Analysis for Earthquakes

It is necessary to have a shaking threshold that is needed to produce earthquake-induced slope movement. The inertia slope stability analysis is prefered for those materials that retain their shear strength during the earthquake. Examples of these types of soil and rock are as follows:

(a) Massive crystalline bedrock and sedimentary rock
(b) Soils that tend to dilate during seismic shaking: examples are very stiff to hard clay
(c) Soils that have a stress–strain curve that does not exhibit a significant reduction in shear strength with strains. Earthquake-induced slope movement in these soils often takes the form of soil slumps or soil block slides
(d) Clay that has a low sensitivity
(e) Soils located above the groundwater table. They have negative pore water pressure due to capillary action
(f) Landslides that have a distinct rupture surface. Cases such as shear strength along the rupture surface can be equal to the drained residual shear strength

Tables 1.8 and 1.9 give earthquake-induced slope movements in rocks and soils with appropriate threshold values.

www.EngineeringBooksPDF.com

Table 1.8 Earthquake-induced slope movement in rock

Types of slope movement	Subdivisions	Material type	Minimum slope inclination	Threshold values
Falls	Rockfalls	Rocks weakly cemented, intensely fractured or weathered; contain conspicuous planes of weakness dipping out of slope or contain boulders in a weak matrix	40° (1.2:1)	$M_L = 4.0$
Slides	Rock slides	Rocks weakly cemented, intensely fractured or weathered; contain conspicuous planes of weakness dipping out of slope or contain boulders in a weak matrix	35° (1.4:1)	$M_L = 4.0$
	Rock intensely fractured and exhibiting one of the following	avalanches	Rocks	
		properties: significant weathering, planes of weakness dipping out of slope, weak cementation or evidence of previous landsliding	25° (2.1:1)	$M_L = 6.0$
	Rock slumps	Intensely fractured rocks, preexisting rock slump deposits, shale and other rocks containing layers of weakly cemented or intensely weathered material	15° (3.7:1)	$M_L = 5.0$
Rock block slides	Rocks having	conspicuous bedding planes or similar planes of weakness dipping out of slopes	15° (3.7:1)	$M_L = 5.0$

Note: Data collected by the author from references to the World Congress on Earthquakes held at CALTECH, California, U.S.A.

1.15 Energy Released in an Earthquake

The earthquake magnitude is defined in terms of logarithm of the amplitude of recorded seismic wave, and energy of a wave is proportional to the square of its amplitude. So, there should be no surprise that the magnitude is also related to the logarithm of the energy. Several equations have been proposed for this relationship in the past. An empirical formula worked out by Gutenberg and Richter (1945; Gutenberg, 1956) relates the energy release E to the surface wave magnitude M_s

$$\log_{10} E = 4.4 + 1.5\, M_s \tag{1.6}$$

where E is in Joules. An alternative version of the energy–magnitude relation, suggested by Bath (1966) for magnitudes $M_s > 5$, is

$$\log_{10} E = 5.24 + 1.44\, M_s \tag{1.7}$$

www.EngineeringBooksPDF.com

Table 1.9 Earthquake-induced slope movement in soil

Types of slope movement	Subdivisions	Material type	Minimum slope inclination	Threshold values
Falls	Soil falls	Granular soils that are slightly cemented or contain clay binder	40° (1.2:1)	$M_L = 4.0$
Slides	Soil	avalanches	Loose,	
		unsaturated sands	25° (2.1:1)	$M_L = 6.5$
	Disrupted soil slides	Loose, unsaturated sands	15° (3.7:1)	$M_L = 4.0$
	Soil slumps	Loose, partly to completely saturated sand or silt; uncompacted or poorly compacted artificial fill composed of sand, silt or clay, preexisting soil slump	10° (5.7:1)	$M_L = 4.5$
Soil block slides	Loose, partly or	completely saturated sand or silt; uncompacted or slightly compacted artificial fill composed of sand or silt, bluffs containing horizontal or subhorizontal layers of loose, saturated sand or silt	5° (11:1)	$M_L = 4.5$
Flow slides	Slow earth flows	Stiff, partly to completely saturated clay and preexisting earth flow deposits	10° (5.7:1)	$M_L = 5.0$
	Flow slides	Saturated, uncompacted or slightly compacted artificial fill composed of sand or sandy silt (including hydraulic)	2.3° (25:1)	$M_L = 5.0$ $a_{max} = 0.10$ g

The logarithmic nature of each formula means that the energy release increases very rapidly with magnitude. For example, when the magnitudes of two earthquakes differ by 1, their corresponding energies differ by a factor 28 ($= 10^{1.44}$) according to Bath's equation or 32 ($10^{1.5}$) according to the Gutenberg–Richter formula.

More recently, Kanamori came up with a relationship between seismic moment and seismic wave energy:

$$\text{Energy} = \text{Moment}/20,000 \tag{1.8}$$

For this relation moment is in units of dyne-cm and energy is in units of erg.

1.16 Earthquake Frequency

On this globe, the annual frequency of small earthquakes is very large and that of large earthquakes is very small (Table 1.10). According to a compilation published by Gutenberg and Richter in 1954, the mean annual number of earthquakes in the

www.EngineeringBooksPDF.com

Table 1.10 Seismic waves

Seismic waves are classified into two groups: **body waves**, which travel through the Earth in all directions and to all depths, and **surface** waves, whose propagation is limited to a volume of rock within a few sesmic wavelengths of the Earth's surface.

1 Body waves

Two types of body waves exist: **compressional waves** (P) and **shear waves**(S). P-waves are similar to sound waves. They obey all the physical laws of the science of acoustics. The mass particle motion of a P-wave is in the direction of the propagation of the wave. In addition, P-waves cause a momentary volume change in the material through which they pass, but no concomitant momentary shape change occurs in the material.

S-waves, or **shear waves**, as they are commonly called, move in a direction of particle motion. Vertically and horizontally polarized S-waves are known as SV-wave and SH-wave, respectively. They are sometimes called secondary waves.

2 Surface waves

A disturbance at the free surface of a medium propagates away from its source partly as seismic surface waves. Surface waves, sometimes known as L-waves, are subdivided into Rayleigh (L_R) and Love waves (L_Q). These surface waves are distinguished from each other by the type of motion of particles on their wave fronts.

Rayleigh waves

Lord Rayleigh (1885) described the propagation of Rayleigh wave along the free surface of semi-infinite elastic half-space. In the homogeneous half-space, vertical and horizontal components of particle motion are 90° out of phase in such a way that as the wave propagates, the particle motion describes a retrograde ellipse in the vertical plane, with its major axis vertical and minor axis in the direction of wave propagation

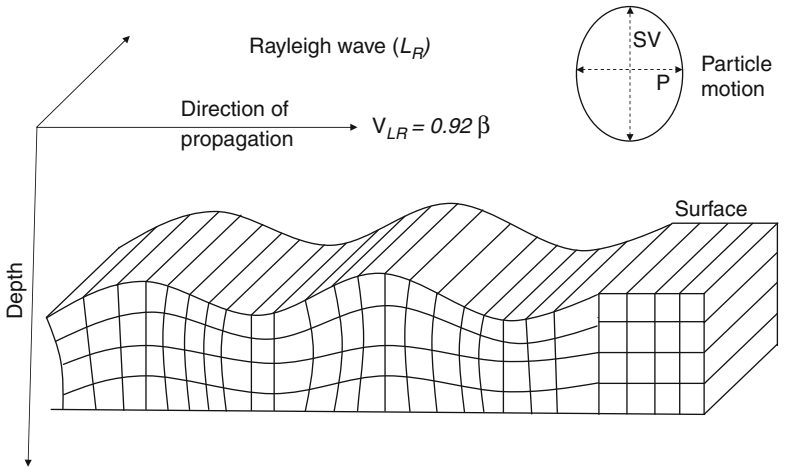


Fig. 1.3 Schematic representation of movement of particle during Rayleigh agation (after Lowrie, 1997)

www.EngineeringBooksPDF.com

Table 1.10 (continued)

Love waves

A.E.H. Love (1911) explained the mechanism of generation of Love waves in horizontal soil layer overlying the half-space. When the angle of reflection at the base of the soil layer is more than the critical angle, SH-waves are trapped in the soil layer. The constructive interference of reflected SH-waves from the top and bottom of the soil layer generates horizontally travelling Love waves. The particle motion is in horizontal plane and transverse to the direction of wave propagation. The velocity of Love wave lies between the velocity of S-wave in the soil layer and in the half-space. The velocity of Love wave with short wavelength is close to the velocity of S-wave in soil layer and velocity of longer wavelength Love wave is close to the S-wave velocity in half-space. This dependence of velocity on wavelength is termed dispersion. Love waves are always dispersive, because they can only propagate in a velocity-layered medium.

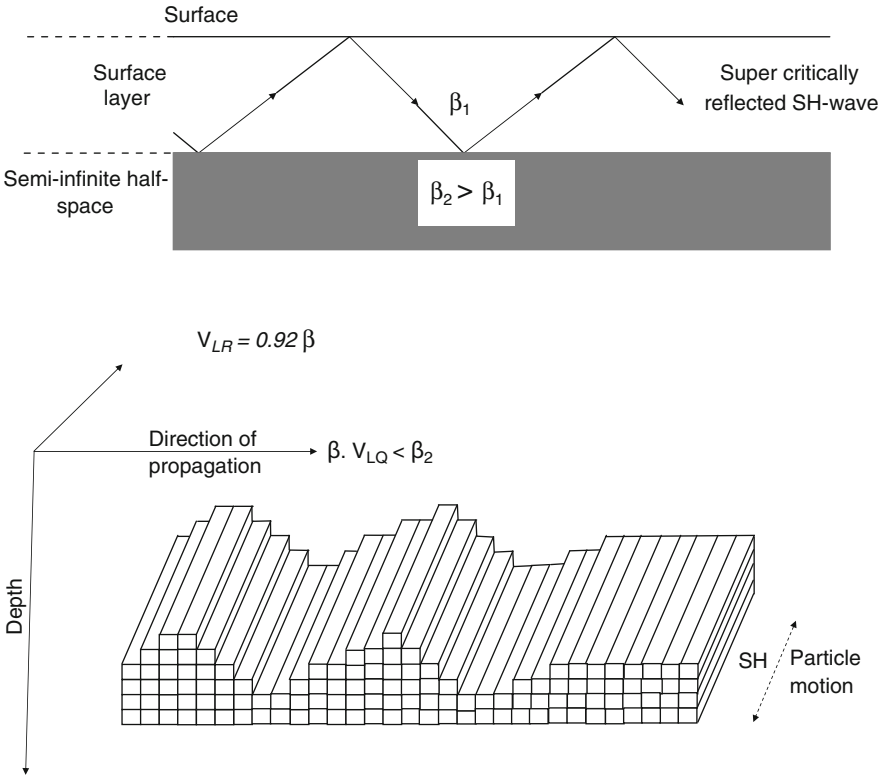


Fig. 1.4 Schematic representation of movement of particle during Love wave

www.EngineeringBooksPDF.com

years 1918–1945 with magnitudes 4–4.9 was around 6,000, while there were only on average about 100 earthquakes per year with magnitudes 6–6.9. The relationship between annual frequency (N) and magnitude is shown below:

Earthquake magnitude	Number per year	*Annual energy* ($10^{15}J^{-1}$)
≥8.0	0–1	0–600
7–7.9	18	200
6–6.9	120	43
5–5.9	800	12
4–4.9	6,200	3
3–3.9	49,000	1
2–2.9	≈350,000	0.2
1–1.9	≈3,000,000	0.1

The relationship between annual frequency (N) and magnitude (M_s) is logarithmic and is given by an equation of the form

$$\log N = a - bM_s \tag{1.9}$$

The value of "a" varies between about 8 and 9 from one region to another, while "b" is approximately unity for regional and global seismicity. Most of the time "b" is assumed to be equal to 1; "b" > 1 in an area generally means that small earthquakes occur frequently; "b" < 1 indicates an area that is more prone for a larger earthquake. In volcanic areas where there are lots of earthquake swarms "b" > 1. Along subduction zones and continental rifts the value of "b" < 1. The mean annual numbers of earthquakes in different magnitude ranges are listed in Table 1.10.

1.17 Impedance Contrast

Seismic waves travel faster in hard rocks than in softer rocks and sediments. As the seismic waves pass from hard medium to soft medium, their celerity decreases, so they must get bigger in amplitude to carry the same amount of energy. If the effects of scattering and material damping are neglected, the conservation of elastic wave energy requires that the flow of energy (energy flux, $\rho V_s v^2$) from depth to the ground service be constant. Therefore, with decrease in density (ρ) and S-wave velocity (V_s) of the medium, as waves approach the ground surface, the particle velocity (v) must increase. Thus, shaking tends to be stronger at sites with softer soil layers.

Resonance: Tremendous increase in ground motion amplification occurs when there is resonance of signal frequency with the fundamental frequency or higher harmonics of the soil layer. Various spectral peaks characterize resonance patterns. For one-layer one-dimensional structures, this relation is very simple:

www.EngineeringBooksPDF.com

$$f_0 = V_{s1}/4h \text{ (fundamental model} \quad \text{and} \quad f_n = (2n+1))\, f_0 \text{ (harmonics)}$$

where V_{s1} is the S-wave velocity in the surficial soil layer and h is the thickness. The amplitudes of these spectral peaks are related mainly to the impedance contrast and sediment damping.

Damping in soil: Absorption of energy occurs due to imperfect elastic properties of medium in which the collision between neighbouring particles of the medium is not perfectly elastic and a part of the energy in the wave is lost instead of being transferred through the medium. This type of attenuation of the seismic waves is referred to as anelastic damping. The damping of seismic waves is described by a parameter called as **quality factor** (Q). It is defined as the fractional loss of energy per cycle, $2\pi/Q = -\Delta E/E$, where $\Delta E$is the energy lost in one cycle and E is the total elastic energy stored in the wave. If we consider the damping of a seismic wave as a function of the distance and the amplitude of seismic wave, we have

$$A = A_0 \exp\left(-\frac{\pi r}{Q\lambda}\right) = A_0 \exp(-\alpha r) \tag{1.10}$$

where $\alpha = \omega/2QV$ is the absorption coefficient. This relation implies that higher frequencies will be absorbed at a faster rate.

1.18 Glossary of Earthquake/Seismology

- **Active fault**. A fault that is likely to have another earthquake sometime in the future. Faults are commonly considered to be active if they have moved one or more times in the past.
- **Aftershocks**. Earthquakes that follow the largest shock of an earthquake sequence. They are smaller than the mainshock and continue over a period of weeks, months or years. In general, the larger the mainshock, the larger and more numerous the aftershocks, and the longer they will continue.
- **Alluvium**. Loose gravel, sand, silt or clay deposited by streams.
- **Aseismic**. This term describes a fault on which no earthquakes have been observed.
- **Attenuation**. When you throw a pebble in a pond, it makes waves on the surface that move out from the place where the pebble entered the water. The waves are largest where they are formed and gradually get smaller as they move away. This decrease in size, or amplitude, of the waves is called attenuation.
- **Basement**. Harder and usually older igneous and metamorphic rocks that underlie the main sedimentary rock sequences (softer and usually younger) of a region and extend downwards to the base of the crust.

www.EngineeringBooksPDF.com

- **Bedrock**. Relatively hard, solid rock that commonly underlies softer rock, sediment or soil; a subset of the basement.
- **Benioff zone**. A dipping planar (flat) zone of earthquakes that is produced by the interaction of a downgoing oceanic crustal plate with a continental plate. These earthquakes can be produced by slip along the subduction thrust fault or by slip on faults within the downgoing plate as a result of bending and extension as the plate is pulled into the mantle. Also known as the Wadati–Benioff zone.
- **Body wave**. A seismic wave that moves through the interior of the Earth, as opposed to the surface waves that travel near the Earth's surface. P- and S-waves are body waves.
- **Core**. The innermost part of the Earth. The outer core extends from 2,500 to 3,500 miles below the Earth's surface and is liquid metal. The inner core is the central 500 miles and is solid metal.
- **Crust**. The outermost major layer of the Earth, ranging from about 10 to 65 km in thickness worldwide. The uppermost 15–35 km of crust is brittle enough to produce earthquakes.
- **Earthquake**. This term is used to describe both sudden slip on a fault and the resulting ground shaking and radiated seismic energy caused by the slip, or by volcanic or magmatic activity, or other sudden stress changes in the Earth.
- **Earthquake hazard**. Anything associated with an earthquake that may affect the normal activities of people. This includes surface faulting, ground shaking, landslides, liquefaction, tectonic deformation, tsunamis and seiches.
- **Earthquake risk**. The probable building damage and number of people that are expected to be hurt or killed if a likely earthquake on a particular fault occurs. Earthquake risk and earthquake hazard are occasionally used interchangeably.
- **Epicentre**. The point on the Earth's surface vertically above the point in the crust where seismic rupture begins.
- **Fault**. A fracture along which the blocks of crust on either side have moved relative to one another parallel to the fracture. **Strike-slip faults** are vertical (or nearly vertical) fractures where the blocks have mostly moved horizontally. If the block opposite to an observer looking across the fault moves to the right, the slip style is termed right-lateral; if the block moves to the left, the motion is termed left-lateral. **Dip-slip faults** are inclined fractures where the blocks have mostly shifted vertically. If the rock mass above an inclined fault moves down, the fault is termed **normal**, whereas if the rock above the fault moves up, the fault is termed **reverse (or thrust)**. Oblique-slip faults have significant components of both slip styles.
- **Foreshocks**. Foreshocks are relatively smaller earthquakes that precede the largest earthquake in a series, which is termed the mainshock. Not all mainshocks have foreshocks.
- **Hypocentre**. The point within the Earth where an earthquake rupture starts. Also commonly termed the focus.

www.EngineeringBooksPDF.com

- **Intensity**. A number (written as a Roman numeral) describing the severity of an earthquake in terms of its effects on the Earth's surface and on humans and their structures. There are many intensity values for an earthquake, depending on where you are, unlike the magnitude, which is one number for each earthquake.
- **Intraplate and crust plate**. **Intraplate** pertains to process within the Earth's crustal plates. **Interplate** pertains to process between the plates.
- **Isoseismal**. A contour or line on a map bounding points of equal intensity for a particular earthquake.
- **Left-lateral**. If you were to stand on the fault and look along its length, this is a type of strike-slip fault where the left block moves towards you and the right block moves away.
- **Lithosphere**. The outer solid part of the Earth, including the crust and uppermost mantle. The lithosphere is about 100 km thick, although its thickness is age dependent (older lithosphere is thicker). The lithosphere below the crust is brittle enough at some locations to produce earthquakes by faulting, such as within a subducted oceanic plate.
- **Love wave**. A type of seismic surface wave having a horizontal motion that is transverse (or perpendicular) to the direction the wave is travelling.
- **Magnitude**. A number that characterizes the relative size of an earthquake. Magnitude is based on measurement of the maximum motion recorded by a seismograph. Several scales have been defined, but the most commonly used are (1) local magnitude (M_L), commonly referred to as "Richter magnitude", (2) surface wave magnitude (M_S), (3) body wave magnitude (M_B) and (4) moment magnitude (M_W).
- **Mainshock**. The largest earthquake in a sequence, sometimes preceded by one or more foreshocks and almost always followed by many aftershocks.
- **Mantle**. The part of the Earth's interior between the metallic outer core and the crust.
- **Moho**. The boundary between the crust and the mantle in the Earth. The boundary is between 25 and 60 km deep beneath the continents and between 5 and 10 km deep beneath the ocean floor.
- **Oceanic spreading ridge**. A fracture zone along the ocean bottom where molten mantle material comes to the surface, thus creating new crust. This fracture can be seen beneath the ocean as a line of ridges that form as molten rock reaches the ocean bottom and solidifies.
- **Oceanic trench**. A linear depression of the sea floor caused by the subduction of one plate under another.
- **P-wave**. A seismic body wave that shakes the ground back and forth in the same direction and the opposite direction as the wave is moving.
- **Plate tectonics**. A theory supported by a wide range of evidence that considers the Earth's crust and upper mantle to be composed of several large, thin, relatively rigid plates that move relative to one another. Slip on faults that define the plate boundaries commonly results in earthquakes. Several styles of faults bound the plates, including thrust faults along

www.EngineeringBooksPDF.com

which plate material is subducted or consumed in the mantle, oceanic spreading ridges along which new crystal material is produced and transform faults that accommodate horizontal slip (strike-slip) between adjoining plates.

- **Rayleigh wave**. A seismic surface wave causing the ground to shake in an elliptical motion, with no transverse or perpendicular motion.
- **Recurrence interval**. The average time span between large earthquakes at a particular site. Also termed return period.
- **Reflection**. The energy or wave from an earthquake that has been returned (reflected) from a boundary between two different materials within the Earth, just as a mirror reflects light.
- **Refraction**. The deflection, or bending, of the ray path of a seismic wave caused by its passage from one material to another having different elastic properties. Bending of a tsunami wave front owing to variations in the water depth along a coastline.
- **Right-lateral**. If you were to stand on the fault and look along its length, this is a type of strike-slip fault where the right block moves towards you and the left block moves away.
- **Ring of fire**. The zone of earthquakes surrounding the Pacific Ocean which is called the Circum-Pacific belt, about 90% of the world's earthquakes occur there. The next most seismic region (5–6% of earthquakes) is the Alpide belt (extends from Mediterranean region, eastwards through Turkey, Iran and northern India).
- **S-wave**. A seismic body wave that shakes the ground back and forth perpendicular to the direction the wave is moving, also called a shear wave.
- **Sand boil**. Sand and water that come out onto the ground surface during an earthquake as a result of liquefaction at shallow depth.
- **Seismic gap**. A section of a fault that has produced earthquakes in the past but is now quiet. For some seismic gaps, no earthquakes have been observed historically, but it is believed that the fault segment is capable of producing earthquakes on some other basis, such as plate-motion information or strain measurements.
- **Seismicity**. The geographic and historical distribution of earthquakes.
- **Seismic moment**. A measure of the size of an earthquake based on the area of fault rupture, the average amount of slip and the force that was required to overcome the friction sticking the rocks together that were offset by faulting. Seismic moment can also be calculated from the amplitude spectra of seismic waves.
- **Seismic zone**. An area of seismicity probably sharing a common cause. Example: "The Himalayan Zone".
- **Seismogenic**. Capable of generating earthquakes.
- **Seismogram**. A record written by a seismograph in response to ground motions produced by an earthquake, explosion or other ground motion sources.
- **Seismology**. The study of earthquakes and the structure of the Earth by both naturally and artificially generated seismic waves.

www.EngineeringBooksPDF.com

1.19 Artificial Generation of Earthquake

Back in the period of cold war, the Soviet Union (now Russia), along with the satellite countries, developed a methodology for the creation of underground warfare. The basis of this warfare was the artificial generation of earthquakes of any magnitude, their intention was to destroy ALASKA by reactivating the live or dead fault lines. Depending on the depth of placing nuclear explosives, the main concept was to produce various energy waves. The fault lines can easily be re-activated. This was treated as the cheapest way to destroy any part of a country with sensative establishment. To a large extent this research was a success. ALASKA was onetime a part of Soviet Union and was sold to America. It was by Soviet Union as a great danger, owing to its close proximity. In case of the Third World War, they could easily have destroyed ALASKA without the world knowing that who was responsible.

To create successfully on environment for the artificial generation of earthquake, the following parameters are essentially to be known as indicated from the archives:

1. Site survey and geological maps inclusive of the geometry of fault lines.
2. Aseismic data and data of aftershock.
3. Possibilities of sudden slip on a fault line.
4. Tactonic data and soil samples plates.
5. Epicentre and Hypocentre data of past earthquakes if any. Site seismology.
6. The depth of placement to produce required energy and waves from nuclear explosives.
7. Seismic Zones inclusive of faults and their geometry and positioning.
8. The method of production and direction's of waves.
9. Seismograph.
10. The nature and magnitude and producing waves.
11. The calculation of wave intensity.
12. Control of the waves to the extent demanded.
13. Instrumentations and Equipment related to.

1.20 Net Result

This technology has not been effectively tried. However it is a widespread believe that one portion of Kashmir, known as AZAD KASHMIR, had been experimented upon successfully. One occupied part of Kashmir was turned out to be safe while AZAD KASHMIR was totally destroyed.

www.EngineeringBooksPDF.com

Bibliography

Abe, K. Tsunami and mechanism of great earthquakes. *Phys. Earth Planet Interiors* 1973; 7:143–153.

Aki, K. Local site effects on strong ground motion. In *Earthquake Engineering and Soil Dynamics II – Recent Advances in Ground Motion Evaluation* (Von Thun, J. L., ed.), Geotechnical Special Publication No. 20, 103–155, American Society of Civil Engineering, New York, 1988.

Aki, K., and Chouet, B. Origin of coda waves: Source, attenuation and scattering effects. *J. Geophys. Res.* 1975; 80: 3322.

Algermisen, S.T., and Perkins, D.M. A technique for seismic zoning-general consideration and parameter. In *Proceedings of the International Conference of Microzonation for Safer-Construction, Research and Application*, Vol. II, pp. 865–878, Seattle, Washington, 1972.

Ambraseys, N.N. The correlation of intensity with ground motions. In *Advances in Engineering Seismology in Europe*, Trieste, 1974.

Barazangi, M., and Dorman, J. World seismicity map compiled from ESSA, coat and geodetic survey, epicenter data, 1961–1967. *Bull. Seismol. Soc. Am.* 1969; 59: 369–380.

Bard, P.Y., and Bouchon, M. The seismic response of sediment-filled valleys – Part 1: The case of incident SH waves. *Bull. Seismol. Soc. Am.* 1980a; 70: 1263–1286.

Bard, P.Y., and Bouchon, M. The seismic response of sediment-filled valleys – Part 2: The case of incident P and SV waves. *Bull. Seismol. Soc. Am.* 70: 1921–1941, 1980b.

Bard, P.Y., and Bouchon, M. The two-dimensional resonance of sediment-filled valleys. *Bull. Seismol. Soc. Am.* 1985; 75: 519–541.

Basu, S. Statistical analysis of seismic data and seismic risk analysis of Indian Peninsula. *Ph.D. thesis*, Department of Civil Engineering, IIT Kanpur, India, 1977.

Bath, M. Earthquake energy and magnitude. *Phys. Chem. Earth*. Ahren, L.H. Press, 1966; 115–165.

Bolt, B.A., and Abrahamson, N.A. New attenuation relations for peak and expected accelerations of ground motion. *Bull. Seismol. Soc. Am.* 1982; 72, 2307–2321.

Boore, D.M., Joyner, W.B., and Fumal, T.E. Equations for estimating horizontal response spectra and peak acceleration for western north American earthquakes: A summary of recent works. *Seismol. Res. Lett.* 1997; 68(1), 128–140.

Bullen, E., and Bolt, B.A. *An Introduction to the Theory of Seismology*, Cambridge University Press, Cambridge, 1985.

Burridge, R., and Knopoff, L. Body force equivalents for seismic dislocation. *Bull. Seismol. Soc. Am.* 54: 1875–1888, 1964.

Campbell, K.W. Empirical near-source attenuation relationships for horizontal and vertical components of peak ground acceleration, Peak Ground Velocity, and Pseudo-absolute Acceleration Response Spectra. *Seismol. Res. Lett.* 1997; 68(1), 154–179.

Celebi, M. Topographical and geological amplifications determined from strong-motion and aftershock records of the 3 March 1985 Chile earthquake. *Bull. Seismol. Soc. Am.* 1987; 77: 1147–1167.

Conrad, V., Laufzeitkurven Des Tauernbebens, vom 28: 59: 1–23, Mitt. Erdb. –Komm. Wien, 1925.

Cornell, C.A. Engineering seismic risk analysis. *Bull. Seismol. Soc. Am.* 1968; 58, 1583–1606.

DeMets, C. et al. *Curr. Plate Motions* 1990; 101, 425–478.

Esteva, L. Bases Para la Formulacion de Decisiones de Diseno Sismico. *Technical Report*, INstitute de Ingenieria, UNAM, Mexico, 1968.

Esteva, L., and Villaverde, R. Seismic risk design spectra and structural reliability. In *Proceedings of the Fifth World Conference on Earthquake Engineering*, Rome, pp. 2586–2596, 1974.

www.EngineeringBooksPDF.com

Faccioli, E., Seismic Amplification in the presence of geological and topographic irregularities. *Proceedings of the 2nd International Conference on Recent Advances in Geotechnical Earthquake Engineering and Soil Dynamics*, St. Louis, Missouri, 1991; 2: 1779–1797.

Geli, L., Bard, P.Y., and Jullien, B. The effect of topography on earthquake ground motion: A review and new results. *Bull. Seismol. Soc. Am.* 1988; 78: 42–63.

Gutenberg, B. *The Energy of Earthquakes* 1945; 112: 1–14.

Gutenberg, B. Magnitude determination for deep focus earthquakes. *Bull. Seismol. Soc. Am.* 1956; 35: 117–130.

Gutenberg, B., and Richter, C.F., *Seismicity of Earth and Related Phenomenon*, Princeton University Press, Princeton, NJ, 1945.

Hanks, T.C., and Kanamori, H. A moment magnitude scale. *J. Geophys. Res.* 1979; 84(B5), 2348–2350.

Hatayama, K., Matsunami, K. Iwata, T., and Irikura, K. Basin-induced love wave in the eastern part of the Osaka basin. *J. Phys. Earth* 1995; 43, 131–155.

Housner, G.W. Calculating the response of an oscillator to arbitrary ground motion. *Bull. Seismol. Soc. Am.* 31: 143–149, 1941.

Housner, G.W. Measures of severity of earthquake ground shaking. In *Proceedings of the US National Conference on Earthquake Engineering*, Earthquake Engineering Institute, Ann Arbor, Michigan, pp. 25–33, 1975.

Hutton, L.K., and Boore, D.M. The M scale in Southern California. *Bull. Seismol. Soc. Am.* 77: 6: 2074–2094, 1987.

IS:1893. *Indian Standard Criteria for Earthquake Resistant Design of Structures*, Part 1, Bureau of Indian Standards, New Delhi, 2002.

Jibson, R. Summary on research on the effects of topographic amplification of earthquake shaking on slope stability. *Open-File-Report-87-268*, USGS, California, 1987.

Joyner, W.B., and Boore, D.M. Peak horizontal acceleration and velocity from strong-motion records including records from the 1979 Imperial Valley, California Earthquake. *Bull. Seismol. Soc. Am.* 71: 2011–2038, 1981.

Kanamori, H. Mechanisms of tsunami earthquake. *Phys. Planet Interiors* 1972; 6, 246–259.

Kanamori, H. The energy release in great earthquakes. *Tectonophysics* 1977; 93, 185–199.

Kawase, H. The cause of damage belt in Kobe: 'The basin-edge effect', constructive interference of the direct S-waves with the basin induced diffracted/Rayleigh waves. *Seismol. Res. Lett.* 1996; 67, 25–34.

Kawase, H., and Aki, K. Topography effect at the critical SV wave incidence: Possible explanation of damage pattern by the Whitter narrow. Earthquake of 1 October 1987. *Bull. Seismol. Soc. Am.* 1990; 80: 1–22, California.

Kennet, B.L.N., and Engdahl, E.R. Trabel ties for global earthquake location and phase identification. *Int. J. Geophys.* 1991; 105, 429–465.

Khan, P.K. Recent seismicity trend in India and adjoining regions. ISET, *New Lett.*, October 2003–July 2004, 10–14, 2004.

Kim, W.Y. The M scale in Eastern North America. *Bull. Seismol. Soc. Am.* 1998; 88, 935–951.

Langston, C.A. Brazier, R., Nyblade, A.A., and Owens, T.J. Local magnitude scale and seismicity rate for Tanzania, East Africa. *Bull. Seismol. Soc. Am.* 1998; 88, 712–721.

Levret, A., Loup, C., and Goula, X. The Provence Earthquake of June 11, 1909 (France): New assessment of near field effects. *Proceedings of the 8th European Conference of Earthquake Engineering*, Lisbon, 2, p. 4.2.79, 1986.

Love, A.E.H. *Some Problems of Aerodynamics*, Cambridge University Press, Cambridge, 1911.

Lowrie, W., *Fundamentals of Geophysics*, Cambridge University Press, Cambridge, 1997.

MacMurdo, J. Papers relating to the earthquake which occurred in India in 1819. *Philos. Mag.* 1824; 63, 105–177.

www.EngineeringBooksPDF.com

Maruyama, T. On the force equivalents of dynamic elastic dislocations with reference to the earthquake mechanism. *Bulletin of Earthquake Research Institute*, Tokyo University 1963; 41, 467–486.

McGuire, R.K. Seismic design spectra and mapping procedures using hazard analysis based directly on oscillator response. *Earthquake Eng. Struct. Dyn.* 1977; 5, 211–234.

Moczo, P., and Bard, P.Y. Wave diffraction, amplification and differential motion near strong lateral discontinuities. *Bull. Seismol. Soc. Am.* 83: 85–106, 1993.

Mohorovicic, A. Das Beben Vom 8 x 1909. *Jb. Met. Obs. Zagreb* 1909; 9, 1–63.

Mohraz, B. A study of earthquake response spectra for different geologic condition. *Bull. Seismol. Soc. Am.* 66: 915–932, 1976.

Murphy, J.R., and O'Brien, L.J. The correlation of peak ground acceleration amplitude with seismic intensity and other physical parameters. *Bull. Seismol. Soc. Am.* 1977; 67, 877–915.

Mussett, A.E., and Khan, M.A., *Looking into the Earth: An Introduction to Geological Geophysics*. Cambridge University Press, Cambridge, 2000.

Narayan, J.P, Sharma, M.L., and Ashwani K. A Seismological Report on the January 26, 2001 Bhuj, India Earthquake. *Seismol. Res. Lett.* 2002; 73, 343–355.

Narayan, J.P. 2.5D Simulation of basin-edge effects on the ground motion characteristics. *Proc. Indian Acad. Sci. (Science of the Earth Planet)*, 2003a; 112: 463–469.

Narayan, J.P. 3D Simulation of basin-edge effects on the ground motion characteristics. *13WCEE*, August 1–6, Paper No. 3333, Vancouver, Canada, 2004.

Narayan, J.P. Simulation of ridge weathering effects on the ground motion characteristics. *J. Earthquake Eng.* 2003b; 7: 447–461.

Narayan, J.P. Study of basin-edge effects on the ground motion characteristics using 2.5-D modelling. *Pure Appl. Geophys.* 2005; 162, 273–289.

Narayan, J.P., and Prasad Rao, P.V. Two and half dimensional simulation of ridge effects on the ground motion characteristics. *Pure Appl. Geophys.* 2003; 160, 1557–1571.

Narayan, J.P., and Rai, D.C. An observational study of local site effects in the Chamoli earthquake. *Proceedings of Workshop on Recent Earthquakes of Chamoli and Bhuj*, 273–279, 2001.

Narayan, M.P. Site specific strong ground motion prediction using 2.5-D modelling. *Geophys. J. Int.* 2001; 146, 269–281.

NEHRP. Recommended Provisions for Seismic Regulation for New Buildings and Other Structures. *Technical Report*, Building Safety Council for Federal Emergency Management, Washington D.C., 1997.

Newmark, N.M. and Rosenblueth, E., *Fundamentals of Earthquake Engineering*. Prentice Hall, Inc., Englewood Cliffs, NJ, 1971.

Newmark, N.M., and Hall, W.J. Earthquake spectra and design. *Technical Report*, Earthquake Engineering Research Institute, Berkeley, California, 1982.

Newmark, N.M., Blume, J.A., and Kapur, K.K. Seismic design spectra for nuclear power plants. *J. Power Division*, ASCE 1973; 99(02), 873–889.

Oldham, R.D. A catalogue of Indian earthquakes from the earliest times to the end of A.D. 1869. *Memoir X*, Geological Survey of India, 1883.

Oldham, R.D. The constitution of the interior of the earth, as revealed by earthquakes. *Quar. J. Geo. Soc. London* 1906; 62, 456–75.

Pederson, H., Hatzfield, D., Campillo, M., and Bard, P.Y. Ground motion amplitude across ridges. *Bull. Seismol. Soc. Am.* 84: 1786–1800, 1994.

Pitarka, A. Irikura, K., Iwata, T., and Sekiguchi, H. Three-dimensional Simulation of the near fault ground motion for 1995. Hyogo-ken Nanbu (Kobe), Japan earthquake, *Bull. Seismol. Soc. Am.* 88: 428–440, 1998.

Plesinger, A., Zmeskal, M., and Zednik, J. *Automated Pre-processing of Digital Seismograms: Principles and Software*. Version 2.2, E. Bergman (Ed.), Prague and Golden, 1996.

Rayleigh, L. On-wave propagated along the plane surface of an elastic solid. *Proc. London Math. Soc.* 1885; 17, 4–11.

www.EngineeringBooksPDF.com

Reid, H.F. The elastic rebound theory of earthquakes. *Bull. Dept. Geol* 6: 413–444, University of Berkeley, 1911.

Reid, H.F., *The California Earthquake of April 18, 1906*, Publication 87, 21 Carnegie Institute of Washington, D.C., 1910.

Richter, C.F. An instrumental earthquake magnitude scale. *Bull. Seismol. Soc. Am.* 25: 1–32, 1935.

Richter, C.F., *Elementary Seismology*. W.H. Freeman and Co., San Francisco, CA, 1958.

Sanchez-Sesma, F.J. Elementary solutions for the response of a wedge-shaped medium to incident SH and SV waves. *Bull. Seismol. Soc. Am.* 80: 737–742, 1990.

Satake, K., *Tsunamis, International Handbook of Earthquake and Engineering Seismology-Part B*, Lee et al. (Eds.), 437–451, 2002.

Seed, H.B., and Idriss, I.M. Ground motions and soil liquefaction during earthquakes. *Technical Report*, Earthquake Engineering Research Institute, Berkeley, California, 1982.

Seed, H.B., Ugas, C., and Lysmer, J. Site dependent spectra for earthquake-resistant design. *Bull. Seismol. Soc. Am.* 66: 221–243, 1976.

Siro, L. Southern Italy November 23, 1980 Earthquake. *Proceedings of the 7th European Conference on Earthquake Engineering*, Athens, Greece, 1982.

Slemmons, D.B. Determination of design earthquake magnitudes for Microzonation. in *Proceedings of 3rd International Earthquake Microzonation Conference*, pp. 119–130, 1982.

Tocher, D. Earthquake energy and ground breakage. *Bull. Seismol. Soc. Am.* 1958; 48(2): 147–153.

Trifunac, M.D., and Brady, A.G. A study of the duration of strong earthquake ground motion. *Bull. Seismol. Soc. Am.* 65: 581–626, 1975.

Trifunac, M.D., and Brady, A.G. On the correlation of seismic intensity with peaks of recorded strong motion. *Bull. Seismol. Soc. Am.* 65: 139–162, 1975.

Wells, D.L., and Coppersmith, K.J. New empirical relationships among magnitude, rupture length, rupture width, rupture area and surface displacement. *Bull. Seismol. Soc. Am.* 1994; 84(4): 974–1002.

Wood, H.O. Distribution of apparent intensity in San Francisco, in the California Earthquake of April 18, 1906. *Report of the State Earthquake Investigation Commission*, 1: 220–245, Carnegie Institute of Washington, Washington, D.C., 1908.

www.EngineeringBooksPDF.com

www.EngineeringBooksPDF.com

Chapter 2
Existing Codes on Earthquake Design with and Without Seismic Devices and Tabulated Data

2.1 Existing Codes on Earthquake Design

Some well-known codes are discussed in brief and they are classified under items such as seismic actions, dynamic characteristics, seismic weights, forces, moments, storey drift ($P - \Delta$ effect), seismic factors, site characteristics and building categories. These are only briefs and for detailed codified design, a reference is made to individual codes where detailed applications are available from the references given at the end of this chapter.

2.1(a) Existing Codes–Comparative Study

They are briefly mentioned below as given by the different countries:

2.1.1 Algeria: RPA (1989)

Seismic actions/dynamic characteristics

Load combination

$$G + Q + E \quad \text{or} \quad 0.8G + E \quad \text{or} \quad G + Q + 1.2E \tag{2.1}$$

$G =$ dead load
$Q =$ live load
$E =$ seismic load
$N =$ number of storeys
$h =$ height of the building
$T = 0.1\,N$ s (building frames with shear walls)
$T = \dfrac{0.09\,h}{\sqrt{L}}$ (other buildings)

M.Y.H. Bangash, *Earthquake Resistant Buildings*,
DOI 10.1007/978-3-540-93818-7_2, © M.Y.H. Bangash 2011

www.EngineeringBooksPDF.com

Table 2.1 Seismic factors

A/BC	Seismic coefficient		
	I	II	III
1	0.12	0.25	0.35
2	0.08	0.15	0.25
3	0.05	0.10	0.15

Seismic weights, forces and moments

$$F_k = \text{equivalent lateral force} = \frac{(V - F_t)W_k h_k}{\sum_{i=1}^{N} W_i h_i} \tag{2.2}$$

$$V = ADB\bar{Q}W \tag{2.3}$$

Where

A = seismic coefficient = 0.05−0.25
W = seismic weight

$$\text{Quality factor } \bar{Q} = 1 + \sum_{1}^{6} Pq \qquad B = 0.20-0.5 \tag{2.4}$$

$F_t = 0$

$$T \leq 0.7\,\text{s} = 0.07TV \leq 0.25\,V \quad \text{for } T > 0.7\,\text{s} \tag{2.5}$$

F_t = additional force at the building top

Storey drift/*P*–Δ effect

$$\Delta_i = X_i - X_{i-1} \qquad \text{with } X_0 = 0 \tag{2.6}$$

X_i = lateral displacement at b
$\Delta \nsucceq 0.0075 \times$ storey height

$$P_F = \text{performance factor} = 0.2-0.67 \tag{2.7}$$

Building category (BC)
Category 1 (500 year return)
Category 2 (100 year return)
Category 3 (50 year return)

Table 2.2 Site characteristics/building categories

Zone	Seismicity zone
0	Negligible
I	Low
II	Average
III	High

www.EngineeringBooksPDF.com

2.1.2 Argentina : INPRES-CIRSOC 103 (1991)

Seismic actions/dynamic characteristics

Horizontal seismic spectra

$$\left.\begin{aligned} S_a &= a_s + (b - a_s)\frac{T}{T_1} && \text{for } T \le T_1 \\ S_a &= b && \text{for } T_1 \le T \le T_2 \\ S_a &= b\left[\frac{T_2}{T_1}\right]^{2/3} && \text{for } T \ge T_2 \end{aligned}\right\} \tag{2.8}$$

$$\left.\begin{aligned} S_a &= a_s + (f_A b - a_s)\frac{T}{T_1} && \text{for } T \le T_1 \\ S_a &= f_A b && \text{for } T_1 \le T \le T_2 \\ S_a &= \left[1 + (f_A - 1)\frac{T_2}{T_1}\right]\left[b\left\{\frac{T_2}{T_1}\right\}^{2/3}\right] && \text{for } T \ge T_2 \end{aligned}\right\} \tag{2.9}$$

ξ = damping 5%
T = fundamental period
f_A = amplification factor due to ξ

$$= \sqrt{\frac{5}{\xi}} \text{ for } 0.5\% \le \xi \le 5\% \tag{2.10}$$

ξ = relative damping = percentage of critical damping

$$T_0 = 2\pi\sqrt{\frac{\sum_{i=1}^{n} W_i u_i^2}{g\sum_{i=1}^{n} \bar{F}_i u_i}} \tag{2.11}$$

W_i = gravity load at level i
g = acceleration
u_i = displacement at i
$\bar{F}_i$ = normal horizontal force

For regular building level height equals

$$T_0 = \frac{h_n}{100}\sqrt{\frac{W_n u_n}{g\bar{F}_n}} \tag{2.12}$$

Alternative empirical formula is

$$T_{0l} = \frac{h_n}{100}\sqrt{\frac{30}{L} + \frac{2}{1 + 300}} \tag{2.13}$$

www.EngineeringBooksPDF.com

T_{0l} = fundamental period
h_n = height of the building
L = length of the building
d = density of the wall

Torsional effects

$$M_{ti} = \text{torsional moment at level } i = (1.5e_1 + 0.10L)V_i \tag{2.14}$$

or

$$M_{ti} = (e_1 - 0.10L)V_i \tag{2.15}$$

e_1 = distance between CS at level i and the line of action of the shear force measured perpendicular to the analysed direction
L = maximum dimension in plan measured perpendicular to the direction of V_i

Seismic weights, forces and moments

$$\bar{F}_i = \frac{W_i h_i}{\sum_{i=1}^{n} W_i h_i} \tag{2.16}$$

W_i = seismic weight at level $i = G_i + \eta L_i$
$\eta = 0{-}1.0$
h_i = height of the storey level i above the base level
n = number of levels in the building
G_i and ηL_i = dead and live loads respectively

Vertical seismic actions

$$S_{aV} = f_V S_a \tag{2.17}$$

f_V	Seismic zone
0.6	4
0.6	3
0.5	2
0.4	1
0.4	0

Load states

$1.3E_W \pm E_S$ $E_W =$ actions due to gravitational loads

$0.85E_W \pm E_S$ $E_S =$ seismic actions

www.EngineeringBooksPDF.com

Building separation due to hammering

$$Y_i = \text{ separation between adjacent structures} = \delta_i + f_S h_i \tag{2.18}$$

$$Y_i \geq f_0 h_i + 1 \text{ cm} \tag{2.19}$$

$$Y_i \geq 2.5 \text{ cm} \tag{2.20}$$

f_S = factor depending on foundation soil = 0.001−0.0025
f_0 = different soils in seismic zones = 0.003−0.010

$$V_i = \text{storey shear force} = \sum_{k=1}^{n} F_k \tag{2.21}$$

$$M_i = \text{overturning moment} = \alpha \sum_{k=i+1}^{n} F_k (h_k^* - h_i^*) \tag{2.22}$$

where

$$h_k^*, h_i^* = \text{heights at level } k \text{ and } i \text{ from the foundation level} \quad i = 0, 1, 2, 3, ..., n-1 \tag{2.23}$$

$$V_0 = \text{base shear force} = CW = C \sum_{i=1}^{n} W_i \tag{2.24}$$

$$C = \frac{S_a \gamma_d}{R} \tag{2.25}$$

$$F_i = \text{lateral force} = \frac{W_i h_i V_0}{\sum_{k=1}^{n} W_k h_k} \tag{2.26}$$

$$F_V = \text{vertical seismic forces} = \pm C_V \gamma_d W \tag{2.27}$$

Storey drift/P−Δ effect

Lateral displacements δ and storey drift Δ

$$\Delta_i = \delta_i - \delta_{i-1} \quad \text{with } \delta_0 = 0 \tag{2.28}$$

Alternatively

$$\delta_i = \frac{g}{4\pi^2} \frac{T^2 F_i}{W_i} \tag{2.29}$$

$\delta =$ horizontal displacements at levels i

www.EngineeringBooksPDF.com

Limiting values for storey drift
Non-structural elements attached are damaged

Group A_0	Group A	Group B
0.01	0.011	0.014

Non-structural elements attached are not damaged

0.01	0.015	0.019

$P-\Delta$ effect

$$\beta_i = \frac{P_i \Delta_i}{V_i H_i} \geq 0.08 \tag{2.30}$$

$P_i =$ total seismic weight at level i
$V_i =$ shear force at storey i
$H_i =$ storey height i
$\psi =$ amplification factor for forces and displacements

$$= \frac{1}{1-\beta_{\max}}$$

$\beta_{\max}$ is the $\beta_{i\max}$ value.

Reduction factor R
A factor for the dissipation of the energy by inelastic deformation:

$$R = 1 + (\mu - 1)\frac{T}{T_1} \quad \text{for } T \leq T_1 \tag{2.31}$$

$$R = \mu \quad \text{for } T \leq T_1 \tag{2.32}$$

μ varies from 6 to 1.

Table 2.3 Seismic factors γ_d defines the risk factor:

Group	γ_d
A_0	1.4
A	1.3
B	1.0

Table 2.4 Site characteristics/building categories
Seismic zones

Zone	Seismicity
0	Negligible
I	Low
II	Average
III	High

www.EngineeringBooksPDF.com

Table 2.5 Seismic zone

Zone	Risk
0	Very low
1	Low
2	Moderate
3	High
4	Very high

Table 2.6 Building classifications

Group	Classification
A_0	Important centres
A	Hotels, stadia, etc.
B	Private, commercial, industrial buildings
C	Containers, silos, sheds, stables

Zone	a_s	b	T_1	T_2
4	0.35	1.05	0.2–0.4	0.35–1.0
3	0.25	0.75	0.2–0.4	0.35–0.1
2	0.16–0.18	0.48–0.54	0.2–0.4	0.5–1.0
1	0.08–0.10	0.24–0.30	0.2–0.4	0.6–1.2
0	0.04	0.12	0.10	1.2–1.6

Table 2.7 Vertical seismic coefficient (C_V)

Zone	Balcony and cantilevers	Roof and large spans
4	1.20	0.65
3	0.86	0.47
2	0.52	0.28
1	0.24	0.13

Building category (BC)

Category 1 (500 year return)
Category 2 (100 year return)
Category 3 (50 year return)

2.1.3 Australia: AS11704 (1993)

Seismic actions/dynamic characteristics

Bearing walls and frames where k_d = deflection amplification factor

www.EngineeringBooksPDF.com

Bearing walls	1.25–4.0
Building frame	1.50–4.0
Moment-resisting frame	2.0–5.5
Dual system with a special moment-resisting frame	4.0–6.5
Dual system with intermediate moment frame (steel or concrete)	4.5–5.0

Torsional effects

$e_{d1} = A_1 e_S + 0.05b$
$e_{d2} = A_2 e_S - 0.05b$
A_S = dynamic eccentricity factors
e_S = eccentricity
$A_1 = 2.6 - \frac{3.6 e_S}{b} \geq 1.4 = 2.6$
$A_2 = 0.5$
b = maximum dimension at level i

Seismic weights, forces and moments

$$V = \text{total horizontal force (kN)} = ZIKCSW \tag{2.33}$$

I = occupancy importance factor
= 1.2 essential facilities
= 1.0 other buildings
W = total dead load + 0.25 live load

$$V = \text{seismic base shear} = \frac{ICS}{R_f} Gg$$

$$V_i = \text{horizontal shear force} = \sum_{x=i}^{n} F_x$$

$$M_0 = \text{overturning moment} = \alpha \sum_{i=1}^{n} F_i h_i$$

i = levels number
$\alpha = 0.75$ general
$\alpha = 1.0$ at base
$\alpha = 0.5$ at top

Base shear distribution

$$F_x = C_{Vx} \cdot V \tag{2.34}$$

$$C_{Vx} = \frac{G_{gs} h_x^k}{\sum_{i=1}^{n} G_{gi} \cdot h_i^k} \tag{2.35}$$

www.EngineeringBooksPDF.com

$x = i$ levels
$k = 1\ T \leq 0.5$ s
$Gg =$ gravity load $= G + \psi Q$
$G =$ dead load (kN)
$Q =$ live load (kN)

Storey drift/$P-\Delta$ effect

$$\begin{aligned} \delta_x &= \text{interstorey drift} = k_\mathrm{d}\delta_{xe} \\ \delta_{xe} &= \text{lateral displacement at levels } i \end{aligned} \tag{2.36}$$

$$= a_i\left(\frac{T}{2\pi}\right)^2 = \frac{gF_i}{G_{gi}}\left(\frac{T}{2\pi}\right)^2 \tag{2.37}$$

$P-\Delta$ effect
To allow for $P-\Delta$ effect, the storey drift is increased by

$$\frac{0.9}{(1-m)} \geq 1.0 \tag{2.38}$$

When $m < 0.1$ there is no effect

$$m = \text{stability coefficient} = \frac{P_x\Delta_x}{V_x h_{sx} k_\mathrm{d}} \tag{2.39}$$

$P_x =$ total vertical design load

Seismic factors

$$C = \text{seismic response factor} = \frac{1}{15\sqrt{T}} \leq 0.12 \tag{2.40}$$

$a =$ acceleration coefficient $= 0.05-0.11$

$$C = \frac{1.25a}{T^{2/3}} \tag{2.41}$$

$$T = \frac{h_0}{46}\ \text{(main direction)} \tag{2.42}$$

$$T = \frac{h_0}{58}\ \text{(orthogonal direction)} \tag{2.43}$$

$\psi = 0.4-0.6$
$R_\mathrm{f} =$ response modification factor $= 1.5-8.0$

www.EngineeringBooksPDF.com

k = horizontal force factor
= 0.75 (ductile)
= 3.2 (brittle)
Z = zone factor
= 0 for zone A ductile
= 0.09 for zone A non-ductile
= 0.18 for zone 1
= 0.36 for zone 2

Site characteristics/building categories

S = soil structure resonance factor = 1.5 if not calculated

Building classification

Type I Domestic and not more than two storeys
Type II Buildings with high occupancy (schools, theatres, etc.)
Type III Buildings for essential functions (power stations, tall structures, hospitals, etc.)

Table 2.8 Seismic design categories

a_S	III	II	I	Domestic
$a_S \geq 0.20$	E	D	C	H_3
$0.10 \leq a_S \leq 0.20$	D	C	B	H_2
$a_S < 0.10$	C	B	A	H_1

C = static analysis
D = static and dynamic analysis
E = static and dynamic analysis
S = site factor varies from 0.67 to 2.0

2.1.4 China: TJ 11-78 and GBJ 11-89

Seismic actions/dynamic characteristics

S = total effect of horizontal seismic action

$$= \sqrt{\sum_{j=1}^{N} S_j^2} \tag{2.44}$$

T_1 = fundamental period
S_j = modal effect caused by seismic forces of the jth mode
N = number of modes

www.EngineeringBooksPDF.com

δ_n values

$$\left.\begin{array}{lll} Tg & T_1 > 1.47\,g & T_1 \le 1.4Tg \\ \le 0.25 & 0.08T_1 + 0.07 & \text{no need to consider} \\ 0.3 - 0.4 & 0.08T_1 + 0.01 & \\ \ge 0.55 & 0.08T_1 - 0.02 & \end{array}\right\} \text{concrete building} \tag{2.45}$$

Horizontal seismic action

$$F_{xji} = \alpha_j \gamma_{tj} W_i \qquad F_{yji} = \alpha_j \gamma_{tj} Y_{ji} W_i \tag{2.46}$$

$$F_{tji} = \alpha_j \gamma_{tj} r_i^2 \phi_{ji} W_i \tag{2.47}$$

ϕ_{ji} = angular rotation at ith floor jth mode
x, j, t = directions in x, y and angular direction
r_i = mass radius of gyration
α_j = seismic coefficient
$i = 1, 2, ..., n$
$j = 1, 2, ..., m$

Torsional effects

Modelling with degrees of freedom including two orthogonal horizontal displacements and one angular rotation for each level. The complete quadratic combination (CQC) can be used to obtain the response "S" (force, moment and displacement) given by

$$S = \sqrt{\sum_{j=1}^{n} \sum_{k=1}^{n} \rho_{jk} S_j S_k} \tag{2.48}$$

S_j, S_k = effects caused by seismic forces

$$\rho_{jk} = \frac{0.02(1 + \lambda_T)(\lambda_T)^{1.5}}{(1 - \lambda_T^2)^2 + 0.01(1 + \lambda_T)^2 \lambda_T} \tag{2.49}$$

where λ_T = ratio of the periods of the kth and jth modes.

Seismic weights, forces and moments

Base shear force:

$$F_{EK} = \alpha W_{eq} = \alpha \sum_{i=1}^{n} W_i \tag{2.50}$$

F_i = horizontal seismic forces at i level

$$= \frac{W_i H_i}{\sum_{j=1}^{n} W_j H_j} F_{EK}(1 - \delta_n) \tag{2.51}$$

www.EngineeringBooksPDF.com

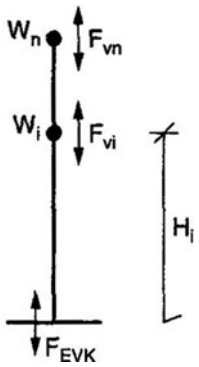


Fig. 2.1 Seismic actions at various levels

ΔF_n = additional seismic force applied to the top level of the building.

$$= \delta_n F_{\mathrm{EK}} \tag{2.52}$$

H = height from the base

$$M_i = \text{overturning moment} = \sum_{j=i+1}^{n} f_j(H_j - H_i) \tag{2.53}$$

$$F_{\mathrm{EVK}} = \text{vertical seismic action force} = \alpha_{\mathrm{V_{max}}} W_{\mathrm{eq}} \tag{2.54}$$

At ith level (see Fig. 2.1)

$$F_{\mathrm{V}i} = \frac{W_i H_i}{\sum_{j=1}^{n} W_j H_j} F_{EVK} \tag{2.55}$$

Storey drift/P–Δ effect

The elastic relative displacement is

$$\Delta U_{\mathrm{e}} \leq [\theta_{\mathrm{e}}] H \tag{2.56}$$

where θ_{e} = elastic drift limitation.

Elasto-plastic deformation

$$\Delta U_{\mathrm{p}} = \eta_{\mathrm{p}} \Delta U_{\mathrm{e}} \tag{2.57}$$

Table 2.9 Values of θ_{e}

Structure frame	θ_{e}
Brick infill walls	1/550
Others	1/450
Public buildings	1/800
Frame shear walls	1/650

www.EngineeringBooksPDF.com

Table 2.10 The value of θ_p

θ_p	Structure
1/30	Single-storey RC frame
1/50	Frame with infill
1/70	Frame in the first storey of a brick building

or

$$\Delta U_p = \mu \Delta U_y = \frac{\eta_p \Delta U_y}{\xi_y} \tag{2.58}$$

ΔU_y = storey yield displacement
ΔU_e = elastically calculated storey displacement
η_p = amplification coefficient

$$U_p \leq [\theta_p] H \tag{2.59}$$

Seismic factors

$$\alpha = \text{seismic coefficient}$$

$$\alpha = \alpha_{max}(5.5T_1 + 0.45) \quad \text{for } T_1 \leq 0.1\text{s} \tag{2.60}$$

$$\alpha = \alpha_{max} \quad \text{for } 0.1 < T_1 \leq 0.1Tg$$

$$\alpha = \left(\frac{Tg}{T_1}\right)^{0.9} \alpha_{max} \quad \text{for } Tg < T_1 < 3\text{s} \tag{2.61}$$

δ_n = additional seismic action coefficient
γ_{tj} = the mode participation factor of the jth mode
ρ_{jk} = coupling coefficient for jth and kth modes
μ = storey ductility coefficient

$$\xi_y = \text{storey yield strength coefficient} = \frac{F_y}{Q_e} \tag{2.62}$$

Table 2.11 α_{max} values for various intensities

Intensity	α_{max}		
VI	VII	VIII	IX
0.04	0.08	0.16	0.32

www.EngineeringBooksPDF.com

Table 2.12 Values of Epicentre at different sites

Epicentre	Site			
	I	II	III	IV
Near	0.2	0.3	0.4	0.65
Remote	0.25	0.40	0.55	0.85

Table 2.13 The values of ξ_y

Structure	ξ_y			
	0.5	0.4	0.3	0.2
2−4 storeys	1.3	1.4	1.6	2.1
5−7 storeys	1.5	1.65	1.8	2.4
8−12 storeys	1.8	2.0	2.2	2.8
Single storey	1.3	1.6	2.0	2.6

$F_y = 2Q_{y1} + (m-2) \times Q_{y2}$
m = total number of columns in a storey
$Q_{y1}Q_{y2}$ = average yield strength of exterior and interior columns, respectively

Site characteristics/building categories

Building classifications

Type A Structures not failing beyond repair. Important structures.
Type B Buildings and structures in the main city.
Type C Structures not included in A, B, D.
Type D Structures of less importance not likely to cause deaths, injuries or economic losses.

Tg = characteristic period of vibration

2.1.5 Europe: 1-1 (Oct 94); 1-2 (Oct 94); 1-3 (Feb 95); Part 2 (Dec 94); Part 5 (Oct 94); Eurocode 8

Note: From these parts minimum items are given. For details see the entire codes and parts.

Seismic actions/dynamic characteristics

Horizontal seismic action: two orthogonal components with the same response spectrum.

Vertical seismic action:

$T < 0.15$ s the vertical ordinates $= 0.15 \times$ horizontal
$T > 0.15$ s the vertical ordinates $= 0.5 \times$ horizontal

T between 0.15 and 0.5 s − linear interpolation.

www.EngineeringBooksPDF.com

$$S_e(T) = \text{elastic response spectrum} \quad 0 \le T \le T_B \tag{2.63}$$

$$S_e(T) = a_g \cdot S\left[1 + \frac{T}{T_B}(\xi B_0 - 1)\right] \; T_B \le T \le E \tag{2.64}$$

$$S_e(T) = a_g S \xi B_0 \; T_C \le T \le T_D \tag{2.65}$$

$$S_e(T) = a_g S \xi B_0 \left[\frac{T_C}{T}\right]^{K_1} \; T_D = T \tag{2.66}$$

$$S_e(T) = a_g S \xi B_0 \left[\frac{T_C}{T_D}\right]^{K_1} \left[\frac{T_D}{T}\right]^{K_2} \tag{2.67}$$

At A $= a_g \cdot S$
At B $= a_g \cdot S \cdot \xi B_0$

where

$S_e(T)$	ordinate of the elastic response spectrum,
T	vibration period of a linear single-degree-of-freedom system,
a_g	design ground acceleration for the reference return period,
T_B, T_C	limits of the constant spectral acceleration branch,
T_D	value defining the beginning of the constant displacement range of the spectrum,
S	soil parameter
η	damping correction factor with reference value $\eta = 1$ for 5% viscous damping,

B_0 = spectral acceleration amplification factor for 5% viscous damping,
K_1, K_2 = exponents that influence the shape of the spectrum for vibration at T_D and T_C (see Fig. 2.2).

For the three subsoil classes A, B and C the values of the parameters B_0, T_B, T_C, T_D, S are given in Table 2.14 reproduced from the code.

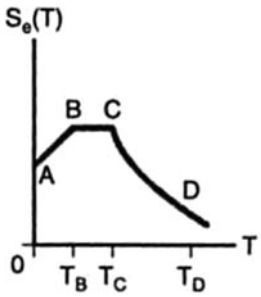


Fig. 2.2 Response spectrum

www.EngineeringBooksPDF.com

Table 2.14 Values of the parameters describing the elastic response spectrum

Sub-soil class	S	β_0	k_1	k_2	T_B[s]	T_C[s]	T_D[s]
A	[1,0]	[2,5]	[1,0]	[2,0]	[0,10]	[0,40]	[3,0]
B	[1,0]	[2,5]	[1,0]	[2,0]	[0,15]	[0,60]	[3,0]
C	[0,9]	[2,5]	[1,0]	[2,0]	[0,20]	[0,80]	[3,0]

These values are selected so that the ordinates of the elastic response spectrum have a uniform probability of exceedance over all periods (uniform risk spectrum) equal to 50%.

Design spectrum

Here, a_g is replaced by α and $S_e(T)$ by$S_d(T)$

$$\xi = \frac{1}{q} \tag{2.68}$$

K_1 and K_2 are replaced by K_{d1} and K_{d2}, respectively

$$T_C = T_D \geq 0.2\alpha \tag{2.69}$$

Combinations of seismic actions

$$\sum G_{Kj} + \sum \psi_{Ei} Q_{Ki} \tag{2.70}$$

$\sum \psi_{Ei} =$ combination coefficients for variable actions $i = 0.5-1.0$

G and Q are characteristic values of actions

$\psi_{Ei} = \phi\psi_{2i}$ $\phi = 0.5-1.0$

Design seismic coefficient $= 0.2$

Seismic weights, forces and moments

$$M_{1it} = e_{1j} F_i \tag{2.71}$$

e_{1i} = accidental torsional eccentricity
L_i = floor dimensions perpendicular to seismic action

$$\text{seismic base shear} = F_b = V = S_e(T_1) W \tag{2.72}$$

$W = W_t =$ total weight
$T_1 \leq 4T_C$ (fundamental period)

www.EngineeringBooksPDF.com

$$F_i = F_b \frac{S_i W_i}{\sum S_j \cdot W_j} \tag{2.73}$$

when horizontal displacement is increasing linearly.

$$F_i = F_b \frac{Z_i W_i}{\sum Z_j \cdot W_j} \tag{2.74}$$

S_i, S_j = displacement of masses M_i and M_j in the fundamental mode shape

For sites with ground conditions not matching the three subsoil classes A, B, C special studies for the definition of the seismic action may be required.

The value of the damping correction factor η can be determined by the expression

$$\eta = \sqrt{7/(2+\xi)} \geq 0,7 \tag{2.75}$$

where ξ is the value of the viscous damping ratio of the structure, expressed in percent. If for special studies a viscous damping ratio different from 5% is to be used, this value will be given in the relevant parts of Eurocode 8.

Peak ground displacement

1. Unless special studies based on the available information indicate otherwise the value $U = d_g$ of the peak ground displacement may be estimated by means of the following expression:

$$U = d_g = [0,05] \cdot a_g \cdot S \cdot T_C \cdot T_D \tag{2.76}$$

with the values of a_g, S, T_C, T_D defined as

W_i, W_j = corresponding weights
Z_i, Z_j = heights of masses M_i and M_j, respectively
d_S = displacement induced by design seismic action
= $q_d d_e \gamma_I$
q_d = displacement behaviour factor
d_e = displacement from the linear analysis
F_a = horizontal force on non-structural element
W_a = weight of the element
q_a = $\bar{B}$ = behaviour factor
= 1.0–2.0 = q

Storey drift/P–Δ effect

P–Δ effect is not considered if the following is satisfied:

$$\phi = \frac{P_{tot} \cdot d_r}{V_{tot} \cdot h_i} \leq 0.10 \tag{2.77}$$

www.EngineeringBooksPDF.com

d_r = Δ in other literature
h_i = interstorey height
P_{tot} = total gravity load at and above the storey
V_{tot} = total seismic storey shear

For buildings with non-structural elements

$$\frac{d_r}{\bar{R}_d} \leq 0.004\,h \tag{2.78}$$

When structural deformation is restricted

$$\frac{d_r}{\bar{R}_d} \leq 0.006\,h \tag{2.79}$$

where $0.1 < \theta \leq 0.2$ increases the seismic action effects by

$$\frac{1}{(1-\theta)} \nrightarrow 0.3 \tag{2.80}$$

Seismic factors

$I = \gamma_I = 0.8{-}1.5$
$B_0 = 5\%$ viscous damping
ξ = damping acceleration factor ≥ 0.7
S = soil parameter = 1.0 for 5% damping
$q = \bar{B}$ = behaviour factor

$$S_a = \text{seismic coefficient} = \frac{\alpha \times 3\left(1+\frac{z}{h}\right)}{\left[1+\left(1-\frac{T_a}{T_1}\right)^2\right]} \tag{2.81}$$

$$a = \frac{a_g}{a} \tag{2.82}$$

T_a for non-structural elements
T for structural elements
z = height of the non-structural element
$\bar{R}_D = v$

Site characteristics/building categories

Subsoil Class A

$$V_S = 100 \text{ m/s} \quad 5\,\text{m}$$
$$= 400 \text{ m/s} \quad 10\,\text{m}$$

www.EngineeringBooksPDF.com

Table 2.15 K-values

Class	K_{d1}	K_{d2}	K_1	K_2
A	2/3	5/3	1	2
B	2/3	5/3	1	2
C	2/3	5/3	1	2

Table 2.16 S_1, B_0, T_B, T_C, T_D and $\bar{R}_D$ values

S_1	B_0	T_B	T_C	T_D
1.0	2.5	0.10	0.40	3.0
1.0	2.5	0.15	0.60	3.0
0.9	2.5	0.20	0.80	3.0

Subsoil Class B

$$V_S = 200 \text{ m/s} \quad 10\,\text{m}$$
$$= 350 \text{ m/s} \quad 50\,\text{m}$$

Subsoil Class C

$$V_S = 200 \text{ m/s } 20\,\text{m}$$

Ground acceleration $a_g \nsucc 0.10$ g

$$d_g = \text{peak ground displacement} = 0.5 a_g S \cdot T_C T_D \tag{2.83}$$

Building categories versus $\bar{R}_D$

	$\bar{R}_D$
I	2.5
II	2.5
III	2.0
IV	2.0

2.1.5.1 Symbols

In addition to the symbols listed in Part 1-1, the following symbols are used in Part 1-2 with the following meanings:

E_E effect of the seismic action;
E_{Edx}, E_{Edy} design values of the action effects due to the horizontal components of the seismic; action;
E_{Edz} design value of the action effects due to the vertical component of the seismic action;
F horizontal seismic force;

www.EngineeringBooksPDF.com

F_a horizontal seismic force acting on a non-structural element (appendage);
H building height;
R_d design resistance;
T_1 fundamental vibration period of a building;
T_a fundamental vibration period of a non-structural element (appendage);
W weight;
W_a weight of a non-structural element (appendage);
d displacement;
d_r design interstorey drift;
e_1 accidental eccentricity of a storey mass from its nominal location;
h interstorey height;
m mass;
q_a behaviour factor of a non-structural element;
q_d displacement behaviour factor;
s displacement of a mass m in the fundamental mode shape of a building;
z height of the mass m above the level of application of the seismic action;
γ_a important factor of a non-structural element;
θ interstorey drift sensitivity coefficient.

2.1.5.2 Characteristics of Earthquake-Resistant Buildings

Basic Principles of Conceptual Design

(1) P The aspect of seismic hazard shall be taken into consideration in the early stages of the conceptual design of the building.
(2) The guiding principles governing this conceptual design against seismic hazard are
  – structural simplicity,
  – uniformity and symmetry,
  – redundancy,
  – bidirectional resistance and stiffness,
  – torsional resistance and stiffness,
  – diaphragmatic action at storey level,
  – adequate foundation.
(3) Commentaries to these principles are given in Annex B.

Structural Regularity

General

(1) P For the purpose of seismic design, building structures are distinguished as regular and non-regular.

www.EngineeringBooksPDF.com

(2) This distinction has implications on the following aspects of the seismic design:
- method of analysis such as power spectrum, non-linear time history and frequency domain
- the value of the behaviour factor 'q'
- geometric non-linearity exceeding the limit by the Eurocode 8
- Non-regular distribution of overstrength in elevation exceeding the limit by Eurocode 8
- Criteria describing regularity in plan and in elevation

Safety Verifications

General

(1) P For the safety verifications the relevant limit states and specific measures (see Clause 2.2.4 of Part 1-1) shall be considered.
(2) For building of importance categories II–IV (see Table 3.3) the verifications prescribed in Sects. 4.2 and 4.3 may be considered satisfied if the following two conditions are met:

(a) The total base shear due to the seismic design combination (see Clause 4.4 of Part 1-1), calculated with a behaviour factor $q = [1,0]$, is less than that due to the other relevant action combinations for which the building is designed on the basis of a linear elastic analysis.
(b) The specific measures described in Clause 2.2.4 of Part 1-1 of the code are taken, with the exception that the provisions contained in Clause 2.2.4.1 (2)–(3) of Part 1-1 need not be demonstrated as having been met.

Ultimate Limit State

General

(1) P The safety against collapse (ultimate limit state) under the seismic design situation is considered to be ensured if the following conditions regarding resistance, ductility, equilibrium, foundation stability and seismic joints are met.

Resistance Condition

(1) P The following relation shall be satisfied for all structural elements – including connections – and the relevant non-structural elements:

$$E_d \leq R_d \tag{2.84}$$

where

$$E_d = E\left\{\sum G_{kj}, \gamma_I \cdot A_{ED}, P_K, \sum \psi_{2i} \cdot Q_{ki}\right\}$$

www.EngineeringBooksPDF.com

is the design value of the action effect due to the seismic design situation (see Clause 4.4 of Part 1-1), including – if necessary – second-order effects, and

$$R_d = R\{f_k/\gamma_M\} \tag{2.85}$$

is the corresponding design resistance of the element, calculated according to the rules specific to the pertinent material (characteristic value of property f_k and partial safety factor γ_M) and according to the mechanical models which relate to the specific type of structural system.

(2) Second-order effects ($P-\Delta$ effects) need not be considered when the following condition is fulfilled in all storeys:

$$\theta = \frac{P_{\text{tot}} \cdot d_r}{V_{\text{tot}} \cdot h} \leq 0.10 \tag{2.86}$$

where

θ interstorey drift sensitivity coefficient,
P_{tot} total gravity load at and above the storey considered, in accordance with the assumptions made for the computation of the seismic action effects,
d_r design interstorey drift, evaluated as the difference of the average lateral displacements at the top and bottom of the storey under consideration,
V_{tot} total seismic storey shear,
h interstorey height.

(3) In cases when $0.1 < \theta \leq 0.2$, the second-order effects can approximately be taken into account by increasing the relevant seismic action effects by a factor equal to $1/(1-\theta)$.

(4) P The value of the coefficient θ shall not exceed 0.3.

Ductility Condition

(1) P It shall be verified that both the structural elements and the structure as a whole possess adequate ductility taking into account the expected exploration of ductility, which depends on the selected system and the behaviour factor.

(2) P Specific material-related requirements as defined in Part 1-3 shall be satisfied, including – when indicated – capacity design provisions in order to obtain the hierarchy of resistance of the various structural components necessary for ensuring the intended configuration of plastic hinges and for avoiding brittle failure modes.

(3) P Capacity design rules are presented in detail in Part 1-3.

www.EngineeringBooksPDF.com

Equilibrium Condition

(1) P The building structure shall be stable under the set of actions given by the combination rules of Clause 4.4 of Part 1-1. Herein are included such effects as overturning and sliding.
(2) P In special cases the equilibrium may be verified by means of energy balance methods or by geometrically non-linear methods with the seismic action defined as described in Clause 4.3.2 of Part 1-1 of the code.

Resistance of Horizontal Diaphragms

(1) P Diaphragms and bracings in horizontal planes shall be able to transmit with sufficient overstrength the effects of the design seismic action to the various lateral load resisting systems to which they are connected.
(2) Paragraph (1) is considered satisfied if for the relevant resistance verifications the forces obtained from the analysis are multiplied by a factor equal to 1.3.

Resistance of Foundations

(1) P The foundation system shall be verified according to Clause 5.4 of Part 5 and to Eurocode 7.
(2) P The action effects for the foundations shall be derived on the basis of capacity design considerations accounting for the development of possible overstrength, but they need not exceed the action effects corresponding to the response of the structure under the seismic design situation inherent to the assumption of an elastic behaviour ($q = 1.0$).
(3) If the action effects for the foundation have been determined using a behaviour factor $q \leq [1,\ 5]$, no capacity design considerations according to (2) P are required.

Seismic Joint Condition

(1) P Building shall be protected for collisions with adjacent structures induced be earthquakes.
(2) Paragraph (1) is deemed to be satisfied if the distance from the boundary line to the potential points of impact is not less than the maximum horizontal displacement.
(3) If the floor elevations of a building under design are the same as those of the adjacent building, the above referred distance may be reduced by a factor of [0,7].
(4) Alternatively, this separation distance is not required if appropriate shear walls are provided on the perimeter of the building to act as collision walls ("bumpers"). At least two such walls must be placed at each side subject to pounding and must extend over the total height of the building. They must be perpendicular to the side subject to collisions and they can end on the boundary line. Then the separation distance for the rest of the building can be reduced to [4,0] cm.

www.EngineeringBooksPDF.com

Serviceability Limit State

General

(1) P The requirement for limiting damage (serviceability limit state) is considered satisfied if – under a seismic action having a larger probability of occurrence than the design seismic action – the interstorey drifts are limited according to 4.3.2 of the code.
(2) Additional verifications for the serviceability limit state may be required in the case of buildings important for civil protection or containing sensitive equipment.

Limitation of Interstorey Drift

(1) P Unless otherwise specified in Part 1-3, the following limits shall be observed:

(a) for buildings having non-structural elements of brittle materials attached to the structure

$$d_r/v \leq [0,004] \cdot h \tag{2.87}$$

(b) for buildings having non-structural elements fixed in a way so as not to interfere with structural deformations

$$d_r/v \leq [0,006] \cdot h \tag{2.88}$$

where

d_r design interstorey drift as defined in 4.2.2.(2) of the code,
h storey height,
v reduction factor to take into account the lower return period of the seismic event associated with the serviceability limit state.

(2) The reduction factor can also depend on the importance category of the building. Values of v are given in Table 2.17.
(3) Different values of v may be required for the various seismic zones of a country. The code provides methodologies in detail for buildings and their elements made in concrete steel, timber and masonry. Design concepts, material properties, building systems, dissipative zones and structural types of behaviour factors are dealt with in greater depths in the code.

Table 2.17 Values of the reduction factor v

Importance category	I	II	III	IV
Reduction factor v	[2,5]	[2,5]	[2,0]	[2,0]

www.EngineeringBooksPDF.com

2.1.6 India and Pakistan: IS-1893 (1984) and PKS 395-Rev (1986)

Seismic actions/dynamic characteristics

T (moment-resisting frame, shear walls) $= 0.1n$

$$T \text{ (other buildings)} = 0.09H/\sqrt{d} \tag{2.89}$$

$n =$ number of storeys
$d =$ maximum base dimension
$H =$ height of the building

Response spectrum

S_a/g versus T when $\xi = 5\%$, $\xi = 10\%$, $\xi = 20\%$ (2.90)

$F_{ir} =$ seismic design lateral force at the ith floor level corresponding to the rth mode

$$= K\beta I F_0 \phi_{ir} C_r \frac{S_{ar}}{g} W_i \tag{2.91}$$

$\phi_{ir} =$ mode shape coefficient

$$C_r = \sum_{j=i}^{n} \frac{W_j \phi_{jr}}{\sum_{j=1}^{n} W_j \left[\phi_{jr}\right]^2} \tag{2.92}$$

Seismic weights, forces and moments

$$V = \text{design base shear} = KC\beta I \alpha_0 W \quad \text{(India)} \tag{2.93}$$

$$V = \text{design base shear} = C_S \omega_t \quad \text{(Pakistan)} \tag{2.94}$$

$$C_S = ZISM\gamma_d Q \tag{2.95}$$

$$Z = ACF \tag{2.96}$$

Table 2.18 S_a/g versus T(s)

S_a/g	T (s)	T (s)
0	0.16	0.2
0.1	1.00	1.9
0.2	0.30	1.18
0.3	_	0.80
0.4	_	0.60
0.5	_	0.50
0.6	_	0.40
0.7	_	0.15

From the above, the average acceleration coefficient S_a/g is obtained.

www.EngineeringBooksPDF.com

$$F_i = V\frac{W_i h_i^2}{\sum_{j=1}^{n} \omega_j h_j^2} \tag{2.97}$$

W = total load = dead + appropriate live loads
F_i = lateral force at the ith floor = P_i
W_i = gravity load
h_i = from the base to the ith floor
n = number of storeys = N
W_j = individual floor load

India

F_i = force in the ith frame to resist torsion

$$= \frac{M_t(K_i r_i)}{\sum K_i r_i^2} \tag{2.98}$$

where

K_i = stiffness of the ith frame
r_i = distance of the ith frame from the centre of the stiffness

$$M_t = \text{torsional moment} = 1.5\,eV \tag{2.99}$$

Pakistan

$$W_i = D_i + nL_i \tag{2.100}$$

$$\eta = 0.25\text{–}0.50$$

$$M_i = \text{overturning moment} \tag{2.101}$$

$$= \sum_{i+1}^{n} F_i(h_i - h_j) + F_i(h_n - h_j)$$

Torsional effects

$$e_a = 1.5e + 0.1b \quad \text{or} \quad e_a = e - 0.1b \tag{2.102}$$

b = the largest distance or dimension
e = eccentricity
e_a = eccentricity for torsional moment
L_i = live load at ith level

Storey drift/P–Δ effect

$\Delta_{\max}$ between two floors $\nprec 0.004 \times h_i$ for height >40 m (India)

www.EngineeringBooksPDF.com

$$\left.\begin{aligned} \delta_i &= \frac{g}{4\pi^2}\frac{T^2 F_i}{W_i} \\ \Delta &= \delta_i - \delta_{i-1} \qquad \delta_0 = 0 \\ P &- \Delta \text{ effect} \\ \theta_{\mathrm{i}} &= \frac{W_i \Delta_j}{V_i h_i} \nless 0.3 \end{aligned}\right\} \text{(Pakistan)} \tag{2.103}$$

Seismic factors

F_0 = seismic zone factor
α_0 = basic horizontal seismic coefficient
$C = 5\%$
$A = 0{-}0.08$
M = material factor = 0.8–1.2
Q = construction factor = 1.0
$S = 0.67{-}3.2$
$\alpha_0 = 0.01{-}0.08$
I = importance factor = 1.0–1.5
$\beta = 0.01{-}0.08$

For different soil foundations:

Site characteristics/building categories

Table 2.19 Height versus γ_d

γ_d	Height (m)
0.4	up to 20
0.6	40
0.8	60
1.0	90

Table 2.20 Values of α_0 and F_0 for various zones

Zone	α_0	F_0
V	0.08	0.40
IV	0.05	0.25
III	0.04	0.20
II	0.02	0.10
I	0.01	0.05

2.1.7 Iran: ICRD (1988)

Seismic actions/dynamic characteristics

Design methodologies: Analyses

(a) Equivalent static
(b) Pseudo-dynamic

www.EngineeringBooksPDF.com

(c) Dynamic analysis using acceleration data

$$T = 0.09\frac{h}{\sqrt{L}} \text{ /> } T \leq 0.06\,h^{3/4} \tag{2.104}$$

$$T = 0.08\,h^{3/4} \quad \text{(steel frame)} \tag{2.105}$$

$$T = 0.07\,h^{3/4} \quad \text{(RC frame)} \tag{2.106}$$

$$F_V = \text{vertical seismic action} = \frac{2AI}{R_V} W_P \tag{2.107}$$

R_V = reaction coefficient
= 2.4 for steel
= 2.0 for concrete

$$W_p = G_i + L_i + \text{total} \tag{2.108}$$

Seismic weights, forces and moments

$$V = \text{minimum base shear force} = CW_t \tag{2.109}$$

$$C = \frac{A\bar{R}I}{\bar{B}} \tag{2.110}$$

Lateral forces

$$F_i = (V - F_t)\frac{W_i h_i}{\sum_{j=1}^{n} W_j h_j} \tag{2.111}$$

F_t = additional lateral force at top level

$$= 0 \quad \text{if } T \leq 0.7\,\text{s} \tag{2.112}$$

$$= 0.07 \quad \text{if } T_V \leq 0.25\,V \tag{2.112a}$$

$$M_i = F_t(h_N - h_i) + \sum_{j=i+1}^{N} F_j(h_j - h_i) \quad i = 0 \text{ to } N-1 \tag{2.113}$$

$$M_{ti} = \sum_{j=1}^{n} e_{ij}F_j + M_{\text{ta}} \tag{2.114}$$

M_{ta} = accidental torsional moment

Storey drift/P–Δ effect

The lateral drift is $\succ 0.005h_i$. Both lateral forces and torsional moment effects are coupled.

www.EngineeringBooksPDF.com

Seismic factors

$$W_t = G_i + \eta L_I \tag{2.115}$$

$$\eta = 20\text{–}40\% \tag{2.116}$$

$$A = \text{design base acceleration} = 0.35\text{–}0.20 \tag{2.117}$$

$$\bar{R} = 2.0\left(\frac{T_0}{T}\right)^{2/3} \qquad 0.6 \le \bar{R} \le 2.0 \tag{2.118}$$

$$I = 0.8\text{–}1.2$$

$$\bar{B} = 5\text{–}8$$

Site characteristics/building categories

1. High-priority buildings
2. Medium-priority buildings
3. Low-priority buildings

Classification

(a) Regularity in plan
(b) Regularity in elevation

Soil Classification
I to IV where

$$T_0 = \text{characteristic period on site} = 0.3\text{–}0.7$$

2.1.8 Israel: IC-413 (1994)

Seismic actions/dynamic characteristics

$$\begin{aligned} T &= 0.073\,h^{3/4} \quad \text{(concrete)} \\ &= 0.085\,h^{3/4} \quad \text{(steel)} \\ &= 0.049\,h^{3/4} \quad \text{(others)} \end{aligned} \tag{2.119}$$

Vertical seismic action

$$F_r = \pm\frac{2}{3}ZW \quad \text{cantilevers} \tag{2.120}$$

$$= W_{\min} - 1.52ISW \quad \text{for concrete beams} \tag{2.121}$$

www.EngineeringBooksPDF.com

Modal lateral force $= F_{i\mathrm{m}}$ at level i

$$F_{i\mathrm{m}} = \frac{V_{\mathrm{m}}[W_i \phi_{i\mathrm{m}}]}{\sum_{i=1}^{n} W_i \phi_{i\mathrm{m}}} \tag{2.122}$$

Modal displacements

$$\delta_{i\mathrm{m(max)}} = \pm K \sum_{j=0}^{i} \Delta_{j\mathrm{m}} \tag{2.123}$$

or

$$\delta_{i\mathrm{m(max)}} = \frac{g}{4\pi^2} \frac{T_{\mathrm{m}}^2 F_{i\mathrm{m}}}{W_i} \tag{2.124}$$

where $T_{\mathrm{m}} = m$th natural period.

Seismic weights, forces and moments

$$V = C_{\mathrm{d}} \sum_{i=1}^{N} W_i \tag{2.125}$$

$$\left.\begin{array}{l} C_{\mathrm{d}} = \dfrac{R_{\mathrm{a}} I Z}{\bar{R}} \\ \text{or } \geq \dfrac{SIZ}{\sqrt{3\bar{R}}} \end{array}\right\} \nsim \begin{array}{ll} 0.3I & \text{low} \\ 0.2I & \text{medium} \\ 0.1I & \text{high ductility} \end{array} \tag{2.126}$$

Lateral forces

$$F_t = 0.07TV \leq 0.25V \tag{2.127}$$

$$F_i = \frac{(V - F_t) W_i h_i}{\sum_{i=1}^{N} W_i h_i} \quad \text{at the top level } F_N + F_t \tag{2.128}$$

$$\begin{aligned} e &= \text{torsional accidental eccentricity} \\ &= \pm 0.05L \end{aligned} \tag{2.129}$$

$$3.0 \geq A_{\mathrm{T}} = 2.75 \left(\frac{\delta_{\max}}{\delta_{\max} + \delta_{\min}} \right)^2 \geq 1.0 \tag{2.130}$$

$$\begin{aligned} \xi &= \text{multiplying factor applied to lateral load at each stiffness} \\ &\quad \text{element to account for torsional effect} \\ &= 1.0 + 0.6 \tfrac{y}{L} \end{aligned} \tag{2.131}$$

www.EngineeringBooksPDF.com

Modal overturning moment

$$M_{i\mathrm{m}} = \sum_{j=i+1}^{N} F_{\mathrm{pm}}\left(h_j - h_i\right) \tag{2.132}$$

Modal torsional moment

$$= M_{t\dot{i}\mathrm{m}} = (d_i \pm e_i) V_{i\mathrm{m}} \tag{2.133}$$

d_i = eccentricity
e_i = accidental eccentricity

Modal weight

$$W_{\mathrm{m}} = \frac{\left(\sum_i W_i \phi_{i\mathrm{m}}\right)^2}{\sum_i W_i \phi_{i\mathrm{m}}^2} \tag{2.134}$$

$\phi_{i\mathrm{m}}$ = amplitude at ith level of mth mode

Storey drift/$P-\Delta$ effect

$P-\Delta$ effect

$$\theta_i > 1.0 \tag{2.135}$$

$$\theta_i = W \Delta_{\mathrm{el},i} \frac{K}{V_i h_i} \tag{2.136}$$

$$V_i = \sum_{j=i}^{N} F_j \quad \text{(storey shear force)} \tag{2.137}$$

$$\Delta_{\mathrm{el},i} = \left[\sum_{m=1}^{N} \left(\Delta_{\mathrm{el},\,i\mathrm{m}}\right)^2\right]^{1/2} \tag{2.138}$$

$$\begin{aligned} \Delta_{\mathrm{el},\,i\mathrm{m}} &= \text{elastic modal drift at the level of } i \\ V_i &= \text{modal shear force at } i \\ &= \left[\sum_{m=1}^{N} \left(V_{i\mathrm{m}}\right)^2\right]^{1/2} \end{aligned} \tag{2.139}$$

Drift limitations

$$\text{for } T \le 0.7\,\mathrm{s} \quad \Delta_{i,\mathrm{lim}} = \min\left(\frac{h_i}{40K};\quad \frac{h_i}{200}\right) \tag{2.140}$$

www.EngineeringBooksPDF.com

$$\text{for } T > 0.7\,\text{s} \quad \Delta_{i,\text{lim}} = \min\left(\frac{0.75h_i}{40K};\quad \frac{h_i}{250}\right) \tag{2.141}$$

$$\text{maximum displacement } \delta_{t_{\max}} = \pm K\sum_{i=0}^{i}\Delta_i \tag{2.142}$$

$\Delta_i =$ computed interstorey displacement

Storey drift

$$\Delta_{i\text{m}} = \delta_{i\text{m}} - \delta_{(i-j)\text{m}} \tag{2.143}$$

Seismic factors

$$\begin{aligned}
\bar{R} &= \text{steel } 4-8,\ \text{concrete } 3.5-7\\
W_i &= G_i + K_g(Q_i + A_i \cdot q_i) \qquad (2.144)\\
Q_i &= \text{concrete load}\\
q_i &= \text{UDL}\\
A_i &= \text{area}\\
K_g &= \text{live load factor}\\
&= 0.2 \quad \text{(dwellings)}\\
&= 0.5 \quad \text{(stores, etc.)}\\
&= 1.0 \quad \text{(storage)}\\
I &= 1.0-1.4\\
C_\text{d} &= \text{seismic coefficient}\\
R_\text{a} &= \text{spectral amplification factor}
\end{aligned}$$

$$R_\text{a}(T) = \frac{1.255}{T^{2/3}} \qquad 2.5 \geq R_\text{a}(T) \geq 0.2\,K \tag{2.145}$$

Table 2.21 Z values for various zones

Seismic zones	Z
I	0.075
II	0.075
III	0.10
IV	0.15
V	0.25
VI	0.30

$S = 1.0-2.0$

www.EngineeringBooksPDF.com

Site characteristics/building categories

Regular structures
Category B < 80 m high
Category C < 80 m high

with normalized seismic zones $Z \leq 0.075$.

2.1.9 Italy: CNR-GNDT (1986) and Eurocode EC8 is Implemented

Seismic actions/dynamic characteristics

Structure	Maximum height (m)		
Frame	$S = 6$	$S = 9$	$S = 12$
Frame	No limitation		
Masonry	16.0	11.0	7.5
Walls	32.0	25.0	15.0
Timber	10.0	7.0	7.0

Seismic index $S = 6$, 9 and 12
Fundamental period T_0

$$T_0 > 0.8\,\text{s} \quad \bar{R} = 0.862/T_0^{2/3} \tag{2.146}$$

$$T_0 \leq 0.8\,\text{s} \quad \bar{R} = 1.0 \tag{2.147}$$

$$T_0 = 0.1\frac{h}{\sqrt{L}} \quad \text{for a framed structure} \tag{2.148}$$

Lateral and vertical effects

$$\alpha = \left[\alpha_h^2 + \alpha_v^2\right]^{1/2} \tag{2.149}$$

$$\bar{\eta} = \left[\eta_h^2 + \eta_v^2\right]^{1/2} \tag{2.150}$$

α = single force component
h, v = subscripts for horizontal and vertical
η = single displacement component

Combination of modal effects

$$\alpha = \sqrt{\sum_{\alpha} \alpha_i^2} \tag{2.151}$$

www.EngineeringBooksPDF.com

$$\eta = \sqrt{\sum_n n_i^2} \tag{2.152}$$

α_{tot} = combined total force = $\alpha \pm \alpha_p$
α_p = action due to non-seismic loads such as permanent loads and live load fraction
$\alpha_{tot} = \alpha \pm \alpha_{p1}$ (non-seismic loads)
$= \alpha \pm \alpha_{p2}$ (fraction of live load)
η_r = actual displacement for design purpose in elastic situation
$= \eta_p \pm \phi\eta$
η_p = elastic displacement due to non-seismic loads
$\phi = 6$ if displacements obtained from static analysis
$= 4$ if displacements obtained from dynamic analysis

2.1.10 Japan: BLEO (1981)

Seismic actions/dynamic characteristics

R_t = spectral coefficient = 0.4

$$= 1 - 0.2\left(\frac{T}{x} - 1\right)^2 \tag{2.153}$$

$x = 0.4$ (hard soil)
$= 0.6$ (medium soil)
$= 0.8$ (soft soil)
$T = h(0.02 + 0.18)$ s
h = full height of the building

$$Q_{bi} = (1 + 0.7\beta_i)Q_i \tag{2.154}$$

$$Q_{bi} \leq 1.5Q_i \tag{2.154a}$$

Q_{bi} = lateral shear strength

$$\beta_i = \frac{\text{lateral shear in bracings}}{\text{total storey shear}} \tag{2.155}$$

$$Q_i = C_i\bar{W}_i \tag{2.156}$$

$$Q_{ui} = D_S F_{es} Q_i \quad \text{[ultimate shear strength (lateral)]} \tag{2.157}$$

D_S = structural coefficient

www.EngineeringBooksPDF.com

$$F_{es} = F_E \cdot F_S \tag{2.158}$$

Seismic intensity

Elastic response	0.15–0.25g
Elasto-plastic response	0.30–0.5g

Seismic weights, forces and moments

Lateral seismic shear force

$$Q_i = C_i \bar{W}_i \tag{2.159}$$

$\bar{W}_i$ = portion of the total seismic weight at the level i

$$C_i = Z R_t A_i C_0 \tag{2.160}$$

$$A_i = 1 + \left(\frac{1}{\sqrt{\alpha_i}} - \alpha_i\right)\frac{2T}{1+3T} \tag{2.161}$$

$$\alpha_i = \frac{\bar{W}_i}{W_0} = 0\text{–}1.0 \tag{2.162}$$

W_0 = weight above ground floor
$C_0 = 0.2$ (moderate earthquake motion)
$= 1.0$ (severe earthquake motion)

$$q = KW \tag{2.163}$$

$$M_i = \sum_{j=i+1}^{n} F_j\left(h_j - h_i\right) \tag{2.164}$$

or

$$= \sum_{j=i+1}^{n} Q_j h_j \tag{2.165}$$

h_j = interstorey height

$$Q_B = \text{horizontal seismic shear at the basement} = Q_p + KW_B \tag{2.166}$$

W_B = weight of the basement
q = horizontal seismic shear force
$= KW$ (for appendages such as penthouse, chimneys)

www.EngineeringBooksPDF.com

Torsional stiffness

$$r_{ex} = \left[\frac{J_{xy}}{\sum_{i=1}^{N_x} K_{xi}}\right]^{1/2} \tag{2.167}$$

$$r_{ey} = \sqrt{\frac{J_{xy}}{\sum_{i=1}^{N_y} K_{yi}}} \tag{2.168}$$

Eccentricity ratio

$$R_{ex} = \frac{e_x}{\gamma_{ex}} \leq 0.15 \tag{2.169}$$

$$R_{ey} = \frac{e_y}{\gamma_{ey}} \leq 0.15 \tag{2.170}$$

For the x and y directions

$$J_{xy} = \sum_{i=1}^{N_x} K_{xi} y_i^2 + \sum_{i=1}^{N_y} K_{yi} x_i^2 \tag{2.171}$$

where N_x, N_y = number of resisting elements.

Connections

$$M_u = \alpha M_p \tag{2.172}$$

$\alpha = 1.2-1.3$
M_p = full plastic moment of the column or beam
M_u = maximum bending strength of the connection

Storey drift/$P-\Delta$ effect

$$\text{Seismic lateral forces} = F_i = Q_i - Q_{i+1} \tag{2.173}$$

$\Delta \nsucceq \frac{1}{200} h_i$ or equal to $\frac{1}{120} h_i$ for non-structural elements for buildings not exceeding 60 m height, i.e. $h \nsucceq 60$ m.

For steel buildings $\nsucceq 31$ m

$$\Delta \nsucceq \frac{1}{200} h_i \tag{2.174}$$

$$R_e \leq 0.15 \quad R_s \geq 0.6$$

Q_i is increased by Q_{bi}

www.EngineeringBooksPDF.com

Seismic factors

R_t = spectral coefficient
A_i = distribution factor
Z = seismic coefficient = 0.7–1.0

Seismic coefficient K of the basement

$$\geq 0.1\left(1 - \frac{H}{40}\right) \times Z \tag{2.175}$$

H = depth of the basement in metres ($\succ$20 m).

Site characteristics/building categories

$$\text{Type 1} \quad \text{Hard soil} \quad \frac{0.64}{T} \tag{2.176}$$

$$\text{Type 2} \quad \text{Medium soil} \quad \frac{0.96}{T} \tag{2.177}$$

$$\text{Type 3} \quad \text{Soft soil} \quad \frac{1.28}{T} \tag{2.178}$$

T = 0–2.0 s
T_C for Type 1 soil = 0.4
T_C for Type 2 soil = 0.6
T_C for Type 3 soil = 0.8

D_S = structural coefficients
= 0.25–0.5 (for steel)
= 0.30–0.55 (for RC)

F_e = function of eccentricity
= 1.0 for $R_e < 0.15$
= 1.5 for $R_e > 0.3$

F_S = function of stiffness ratio R_x
= 1.0 $R_S > 0.6$
= 1.5 $R_S < 0.3$ (2.179)

Buildings
Those of one to two-storeys: wooden $\succ$500 m^2
Special building $\succ$100 m^2

www.EngineeringBooksPDF.com

RC buildings

$$25\sum A_{\mathrm{W}} + 7\sum A_{\mathrm{C}} \geq Z\bar{W}_i A_i \quad \text{for} \quad h \nleq 20 \text{ m} \tag{2.180}$$

$$25\sum A_{\mathrm{W}} + 7\sum A_{\mathrm{C}} + 10\sum A'_{\mathrm{C}} \geq 0.75 Z A_i \bar{W}_i \quad \text{for} \quad h \nleq 31 \text{ m} \tag{2.181}$$

Steel buildings

(1) Not exceeding three storeys
$h \leq 13$ m span ≤ 6 m
total floor area ≤ 500 m^2
$C_0 = 0.3$
(2) Not exceeding 60 m

$$Q_{\mathrm{u}i} \leq Q_{\mathrm{u}} \tag{2.182}$$

$\sum A_{\mathrm{C}}$ = summation of total column areas
$\sum A_{\mathrm{W}}$ = summation of total horizontal cross-sectional areas of walls

2.1.11 Mexico: UNAM (1983) M III (1988)

Seismic actions/dynamic characteristics

$$T_0 = 4\sum_i \frac{t_i}{\beta_{\mathrm{l}i}} \tag{2.183}$$

Design spectra
Referring to Fig. 2.3:

$$a = \left(1 + \frac{3T'}{T\alpha}\right)\frac{C}{4} \quad \text{for } T \leq T_{\mathrm{a}} \text{ s} \tag{2.184}$$

$$a = C \qquad \text{for } T_{\mathrm{a}} < T \leq T_{\mathrm{b}} \text{ s} \tag{2.185}$$

$$a = \left(\frac{T_{\mathrm{b}}}{T}\right)^r c \qquad \text{for } T > T_{\mathrm{b}} \text{ s} \tag{2.186}$$

$$T \text{ (reduced lateral forces)} = 0.63\left(\sum_{i=1}^{N} \frac{W_i x_i^2}{g\sum_{i=1}^{N} F_i x_i}\right)^{1/2} \tag{2.187}$$

x = displacements
F_i = force at ith level
a = spectral acceleration

www.EngineeringBooksPDF.com

Dynamic analysis
Modal analysis accepted by the code:

$$V_0 \geq \frac{0.8aW_0}{Q'} \tag{2.188}$$

$$\begin{aligned} \bar{R} &= \text{total response} = S \\ &= \sqrt{\sum S_i^2} \\ S_i &= \text{modal responses} \end{aligned} \tag{2.189}$$

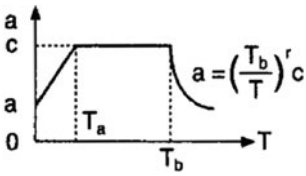


Fig. 2.3 Design spectra: acceleration versus time

Table 2.22

				Seismic zone			
Zone	T_a	T_b	r	A	B	C	D
				c values			
I	0.2	0.6	$\frac{1}{2}$	0.08	0.16	0.24	0.48
II	0.3	1.5	$\frac{2}{3}$	0.12	0.20	0.30	0.56
III	0.6	3.9	1.0	0.16	0.24	0.36	0.64

Seismic weights, forces and moments

Seismic loads
Dead loads as prescribed (DL)
Live loads = 90–180 kg/m^2 (LL)
Load combinations

$$\begin{aligned} \text{UIF} &= \text{ultimate internal forces} \\ &= 1.1(\text{DL} \pm \text{LL} \pm \text{ELL} \pm 0.3\text{ELT}) \end{aligned} \tag{2.190}$$

or

$$= 1.1(\text{DL} \pm \text{LL} \pm 0.3\text{ELL} \pm \text{ELT}) \tag{2.191}$$

where

ELL = earthquake loads (longitudinal)
ELT = earthquake loads (transverse)

www.EngineeringBooksPDF.com

Static method
Lateral forces

$$F_i = \frac{W_i h_i}{\sum_{j=1} W_j h_j} V_0 \tag{2.192}$$

$$V_0 = \frac{c}{Q'} W_0 \tag{2.193}$$

$W_0 = W_t$ = total weight

If $T < T_b \leftarrow$ delimiting period, the response spectrum F_i (reduced) will be obtained by changing

$$V_0 = \frac{a}{Q'} W_0 \tag{2.194}$$

If $T > T_b$

$$F_i(\text{reduced}) = W_i\left(K_i h_i + K_2 h_i^2\right) \frac{a}{Q'} \tag{2.195}$$

$$K_1 = \left(\frac{T_b}{T}\right)^r \left\{1 - r\left[1 - \left(\frac{T_b}{T}\right)^r\right]\right\} \frac{W_0}{\sum_{j=1}^{N} w_j h_j} \tag{2.196}$$

$$K_2 = 1.5r\left(\frac{T_b}{T}\right)\left\{1 - \left(\frac{T_b}{T}\right)^r\right\} \times \frac{W_0}{\sum_{j=1}^{N} w_j h_j^2} \tag{2.197}$$

Torsional effects

$$e = 1.5e_s + 0.1L \tag{2.198}$$

$$e = e_s - 0.1L \tag{2.199}$$

e_s = static eccentricity
e = torsional eccentricity
L = plan dimensions of a storey

The factor of 1.5 is reduced to take into account dynamic modifications of torsional motion.

Overturning moment

www.EngineeringBooksPDF.com

$$M_i = \sum_{j=i+1}^{N} F_j\left(h_j - h_i\right) \quad i = 0 \text{ to } N-1 \tag{2.200}$$

$$M_i \text{ is multiplied by } R_{\mathrm{m}} = 0.8 + 0.2z \text{ where} \tag{2.201}$$

$$z = \frac{\text{height above ground}}{h}$$

Storey drift/$P-\Delta$ effect

$$\Delta \nsucceq 0.006h_i \quad \text{(main structural elements)} \tag{2.202}$$

$$\Delta \nsucceq 0.012 \qquad \text{(for partition)} \tag{2.203}$$

$P-\Delta$ effect

When $\Delta > 0.08V/W$, this effect should be considered (2.204)

V = calculated shear force
W = total weight of the part of the structure above that storey

Seismic factors

$$R_{\mathrm{d}} = \bar{Q} \tag{2.205}$$

$$Q' = Q \qquad T \geq T_{\mathrm{a}} \tag{2.206}$$

$$Q' = 1 + \left(\frac{T}{T_{\mathrm{a}}}\right) \times (Q-1) \quad T < T_{\mathrm{a}} \tag{2.207}$$

$$Q = 4 \text{ to } 1 \quad \text{for } Q \geq 3 \tag{2.208}$$

The point of application of the shear force

$$e_{\mathrm{r}} \geq e_{\mathrm{s}} - 0.2L \quad \text{if } Q = 3 \tag{2.209}$$

$$e_{\mathrm{r}} \geq e_{\mathrm{s}} - 0.1b \quad \text{if } Q > 3 \tag{2.210}$$

Site characteristics/building categories

Building classification
Group A Important buildings
Group B Ordinary buildings

www.EngineeringBooksPDF.com

Table 2.23 Seismic zones: soil types

Seismic zones	Soil types
I	Hill zone, stiff rock, soft clays
II	Transition zone, sandy, silty sands < 20 m
III	Lake bed zone, clays, silty clay

sands > 50 m

$$\beta_i = \frac{\sum_i t_i}{\sum_i \frac{t_i}{\beta_{1i}}} \tag{2.211}$$

t_i = thickness of soil layers i
G_i = shear modulus tons/m^2
γ_i = unit weight tons/m^3

$$\beta_1 = \sqrt{\frac{gG_i}{\gamma_i}} \quad \text{for Class II} \tag{2.212}$$

$$\beta_1 < 700 - 550T_0 \tag{2.213}$$

For outside Mexico

$$a = a_0 + (c - a_0)\frac{T}{T_a} \quad \text{for } T \le T_a \tag{2.214}$$

2.1.12 New Zealand: NZS 4203 (1992) and NZNSEE (1988)

Seismic actions/dynamic characteristics

Methods

(a) Equivalent static method
(b) Modal response spectrum
(c) Numerical integration time – history analysis

$$T = 2\pi \left[\frac{\sum_{i=1}^{N} W_i u_i^2}{\sum_{i=1}^{N} W_i u_i}\right]^{1/2} \tag{2.215}$$

$$T = 0.042 \tag{2.216}$$

$u_i = 1.0$ for one storey
$= 0.85$ for six or more storeys
= for fewer than six storeys interpolate between 1.0 and 0.85
u_i = lateral displacement at level i
δ_t = lateral displacement in millimetres at the top of the building

www.EngineeringBooksPDF.com

Modal response spectrum

$$C_1(T_m) = S_m C_b(T_m, 1)\bar{R}Zf_L \tag{2.217}$$

S_m = response spectrum scaling factor
T_m = modal period

Seismic weights, forces and moments

Basic shear force

$$V = CW \tag{2.218}$$

W = total weight

$$C = C_b(T, \mu)\bar{R}Zf_L > 0.025 \quad T > 0.4\,\text{s} \tag{2.219}$$

$$C = C_b(0.4, \mu)RZf_L > 0.025 \quad T \leq 0.4\,\text{s} \tag{2.220}$$

$\mu = 6$ (structural steel)
$= 5$ [concrete (RC or prestressed)]
$= 4$ (masonry)
$= 3–4$ (timber)

Equivalent static force F_i at level i

$$F_i = 0.92V\frac{W_i h_i}{\sum_{j=1}^{N} W_j h_j} \tag{2.221}$$

Seismic weight with additional top force

$$F_t = 0.08V \tag{2.222}$$

Storey drift/P–Δ effect

Δ = storey drift (2.223)

$$\frac{\Delta}{h} \quad 0, 0.2, 0.4, 0.6 \quad (\%) \tag{2.224}$$

$\Delta_{max} = 600$

P–Δ effects
Ultimately it should satisfy

(a) $T < 0.4\,\text{s}$ (2.225)
(b) $h \nrightarrow 15\,\text{m}$ for $T < 0.8\,\text{s}$ (2.226)
(c) $\mu < 1.5$
(d)

$$\frac{u_i - u_{i-1}}{h_i - h_{i-1}} \leq \frac{V_i}{7.5\sum_{j=1}^{N} W_i} \tag{2.227}$$

V_i = storey shear

$$= F_t + \sum_{i=1}^{N} F_j \tag{2.228}$$

www.EngineeringBooksPDF.com

Seismic factors

Risk factor $\bar{R}$ is given by

$$\begin{aligned}
\text{I} &= 1.3\\
\text{II} &= 1.2\\
\text{III} &= 1.1\\
\text{IV} &= 1.0\\
\text{V} &= 0.6\\
C &= \text{lateral force coefficient}\\
f_{\text{L}} &= \text{limit state}\\
&= 1.0 \quad \text{(ultimate)}\\
&= 1/6 \quad \text{(serviceability)}\\
Z &= \text{zone factor}
\end{aligned}$$

$$\begin{aligned}
C_{\text{b}}(T,\mu) &= \text{basic seismic acceleration factor}\\
&= 0-1.0 \quad \text{for } T = 0-4\,\text{s and } \mu = 1.0-0.6
\end{aligned} \tag{2.229}$$

$$S_{\text{m}_1} = \frac{C_{\text{b}}(T,\mu)}{C_{\text{b}}(T,1)} \text{ for } T > 0.4\,\text{s} \tag{2.230}$$

$$S_{\text{m}_1} = \frac{C_{\text{b}}(0.4,\mu)}{C_{\text{b}}(0.4,1)} \text{ for } T \leq 0.4\,\text{s} \tag{2.231}$$

$$S_{\text{m}_1} = 1.0 \text{ for the limit state of serviceability}$$

$$\text{S}_{\text{m}_2} = \frac{K_{\text{m}} CW}{V_1} \tag{2.232}$$

$$K_{\text{m}} = 0.8 \quad \text{for } \mu = 1.0$$

Site characteristics/building categories

Building categories

I Important buildings
II Holding crowds
III Building with highly valued contents
IV Buildings not included in any category
V Secondary nature

Soil category

(1) Rock or stiff soils
(2) Normal soil sites
(3) Flexible deep soil sites

www.EngineeringBooksPDF.com

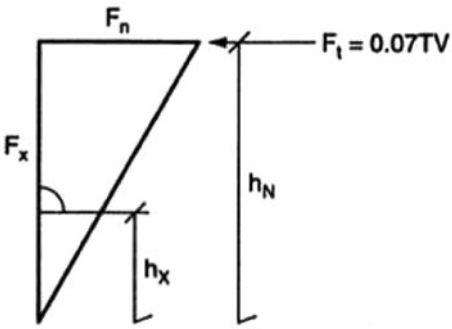


Fig. 2.4 Shear force distribution

2.1.13 USA: UBC-91 (1991) and SEAOC (1990)

Seismic actions/dynamic characteristics

Referring to Fig. 2.4

$$T = \text{fundamental period} = C_t[h_N]^{3/4} \tag{2.233}$$

$h_N = h =$ total height

$C_t = 0.035$ (steel moment-resisting frame)
$= 0.030$ (RC moment-resisting frame)
$= 0.020$ (for Rayleigh's formula)

Alternatively

$$T = 2\pi\left(\frac{\sum_{i=1}^{N} W_i\delta_i^2}{g\sum_{i=1}^{N} f_i\delta_i}\right)^{1/2} \tag{2.234}$$

$f_i =$ lateral force distribution
$V_x =$ storey shear force at x

$$= F_t + \sum_{i=x}^{N} F_i \tag{2.235}$$

F_x is evaluated under seismic weights.

Dynamic method
Using modal shapes

$$[K] - \omega^2[M]\{\phi\} = \{0\} \tag{2.236}$$

work out ω, f and T and finally modal shape $[\phi]$.

Spectral accelerations

www.EngineeringBooksPDF.com

Scaled down by peak one of $0.3g/R_w = 12$:

$$S_{a1} = 0.034g \quad S_{a2} = 0.063g \tag{2.237}$$

$$S_{a3} = 0.061g \quad S_{a4} = 0.05g \tag{2.238}$$

Seismic weights, forces and moments

$$V = \text{basic shear force} = \frac{ZICW}{R_w} \tag{2.239}$$

$$C = \frac{1.25S}{T^{2/3}} \leq 2.75 \tag{2.240}$$

R_w = structural factor = 4–12

$$F_x = \frac{(V - F_t)W_x h_x}{\sum_{i=1}^{N} W_i h_i} \quad \text{at level } x \text{ from the base} \tag{2.241}$$

$$F_t = 0.07TV \leq 0.25V \quad \text{for } T > 0.7\,\text{s} \tag{2.242}$$

$$F_t = 0 \quad \text{for } T \leq 0.7\,\text{s}$$

$$V = F_t + \sum_{i=1}^{N} F_i \tag{2.243}$$

Storey shear force

$$V_x = F_t + \sum_{i=x}^{N} F_i \tag{2.244}$$

M_x = overturning moment, thus

$$M_x = F_t(h_N - h_x) + \sum_{i=x+1}^{N} F_i(h_i - h_x) \quad \text{where } x = 0, 1, 2, \ldots, N-1 \tag{2.245}$$

Torsional moment
Torsional (based on UBC-91) irregularities in buildings are considered by increasing the accidental torsion by A_x (amplification factor)

$$A_x = \left(\frac{\delta_{\max} \text{ at } x}{1.20\delta_{avg}}\right)^2 \leq 3.0 \tag{2.246}$$

δ_{avg} = the average displacement at extreme points at level x.

www.EngineeringBooksPDF.com

The floor and the roof diaphragms shall resist the forces determined by the following formula:

$$F_{px} = \frac{F_t + \sum_{i=x}^{N} F_i}{\sum_{i=x}^{N} W_i} W_{px} \tag{2.247}$$

where

W_{px} = weight of the diaphragm and attached parts of the building.

$$\text{Correspondingly } F_{px} \nless 0.75ZIW_{px} \text{ and } \nless 0.35ZIW_{px} \tag{2.248}$$

Storey drift/P–Δ effect

$$\text{Drift calculated} \nless \frac{0.04}{R_w} \times h_i \tag{2.249}$$

$$\text{or} \quad \nless 0.005h_i \quad \text{for } T < 0.7\,\text{s}$$

$$\text{or} \quad \nless 0.004h_i \quad \text{for } T \geq 0.7\,\text{s}$$

$P-\Delta$ effect
Secondary moment formula drift
Primary moment due to lateral forces

$$\frac{M_{xs}}{M_{sp}} \nless 0.10 \quad \text{not considered for greater values} \tag{2.250}$$

$$\theta_x = \frac{M_{xs}}{M_{sp}} = \frac{P_x \Delta_x}{V_x H_x} \tag{2.251}$$

Subscript x means to the level of storey x.

Elastic storey drift

$$\Delta_{ie} = \frac{V_i}{K_i} \tag{2.252}$$

Δ_i = inelastic storey drift

$$= \frac{\Delta_{ie}}{K} \quad (K < 1.0) \tag{2.253}$$

or

$$\Delta_i = R\Delta_{ie} \tag{2.254}$$

$$\delta_i = \text{lateral displacement} = \sum_{i=1}^{N} \Delta_i \tag{2.255}$$

www.EngineeringBooksPDF.com

Total displacement

$$\delta_{px} = \delta_{ix} - \theta Y_p \tag{2.256}$$

$$\delta_{py} = \delta_{iy} + \theta Y_p \tag{2.257}$$

δ_{ix}, δ_{iy} = lateral displacement in x and y directions
θ = storey rotation
δ_{px}, δ_{py} = lateral displacement in x and y directions
δ_p = total displacement at a selected point P
$= \left(\delta_{px}^2 + \delta_{py}^2\right)^{1/2}$

Seismic factors

Z = seismic zone factor
$Z = 0.075$ Zone I
$= 0.15$ Zone IIA
$= 0.20$ Zone IIB
$= 0.30$ Zone III
$= 0.40$ Zone IV
I = occupancy or importance factor = 1.0−1.25

Site characteristics/building categories

S_1 type

$$S_a = 1 + 10T \quad 0 < T \leq 0.15\,\text{s} \tag{2.258}$$

$$S_a = 2.5T \qquad 0.15 < T \leq 0.39\,\text{s} \tag{2.259}$$

$$S_a = \frac{0.975}{T} \qquad T > 0.39\,\text{s} \tag{2.260}$$

S_2 type

$$\begin{aligned} S_a &= 1 + 10T \quad 0 < T \leq 0.15\,\text{s} \quad (2.261) \\ S_a &= 2.5T \quad 0.15 < T \leq 0.585\,\text{s} \quad (2.262) \end{aligned} \tag{2.261}$$

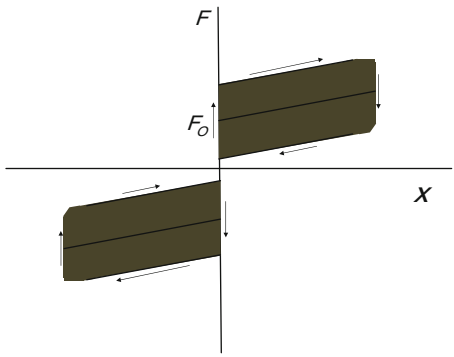
Table 2.24 Soils in seismic zones

Seismic zones		Soil S*
I	Rock like	1.0 (S_1)
IIA	Dense stiff	1.2 (S_2)
IIB		
II	Soft-medium clay	1.5 (S_3)
IV	Soft clay	2.0 (S_4)

S* = site coefficient

www.EngineeringBooksPDF.com

Fig. 2.5 F versus X



$$S_a = \frac{1.463}{T} \quad T > 0.585\,\text{s} \tag{2.262}$$

S_3 type

$$S_a = 1 + 75T \quad 0 < T \leq 0.2\,\text{s} \tag{2.263}$$

$$S_a = 2.5T \quad 0.2 < T \leq 0.915\,\text{s} \tag{2.264}$$

$$S_a = \frac{2.288}{T}T \quad T > 0.915\,\text{s} \tag{2.265}$$

K = spring parameter of the damper
C = viscous constant of the damper
α = parameter of the damper, α usually varies between 0.1 and 0.4

Parameters should be experimentally calibrated by the supplier.

Additional deliberations on viscoelastic dampers

A convenient way to improve the dynamic performance of a structure subjected to wind or earthquake loading vibration is to incorporate mechanical dampers to augment the structural damping. This damping increase yields a reduction in the expected structural damage through a significant reduction of the interstory drifts of the structure during the dynamic event.

Although the developments in research and analysis techniques, paralleled by significant improvements and refinements of device hardware, make the mechanical dampers totally suitable for consideration in new or retrofit design, there are still relatively few applications to buildings (Mahmoodi 1969; Aiken and Kelly 1990; Tsai and Lee 1993; Inaudi et al. 1993; Inaudi and Kelly 1995; Lai et al. 1995; Shen and Soong 1995; Makri et al. 1995).

Among a number of viable types of energy dissipation devices proposed, the viscoelastic dampers have found several successful applications for wind-induced vibration reduction of the tall buildings. Remarkable examples are the 110-story twin towers of the World Trade Center, in New York City, the

www.EngineeringBooksPDF.com

73-story Columbia SeaFirst Building and the 60-story Number Two Union Square Building, both in Seattle.

The implementation of viscoelastic dampers (VEDs) for seismic protection has been investigated only in the last few years (Zhang et al. 1989; Zhang and Soong 1992; Bergman and Hanson 1993; Hanson 1993; Tsai 1993; Chang et al. 1993; Kasai et al. 1993; Abbas and Kelly 1993; Chang et al. 1995; Munshi and Kasai 1995).

An accurate model for the mechanical behaviour of VEDs subjected to seismic loading must incorporate the variability of the material's physical properties with the deformation amplitude, the excitation frequency and the temperature conditions during dynamic service.

2.1.14 Codes Involving Seismic Devices and Isolation Techniques

2.1.14.1 General Introduction

Although the excessive vibrations can be based on active, semi-active or passive control techniques, the use of them depends on a number of factors. The passive control device is presently the most common, reliable and economic technical solution. Among many passive control devices are tuned mass dampers (TMDs), tuned liquid mass dampers (TLMDs) and fluid viscous dampers (FVDs). The general principles for the design of a damping system are

a. It should be accessible
b. It should have a low maintenance
c. Its design must take into account corrosion
d. Where high amplitude oscillations exist, buffers should be associated
e. It should allow a later adjustment
f. Its design must be accompanied with experimental tests

Different types of possible damping systems are discussed in this section.

2.1.14.2 Different types of Damper Devices

a. *Pendulum damper* (horizontal tuned mass damper)

For movement in the horizontal plane, a pendulum is clearly a simple system with one degree of freedom, the spring constant and a natural frequency, which depends on the length of its hanger l (g – acceleration due to gravity)

$$K_d = \frac{m_d g}{l}; \quad f_d = \frac{1}{2\pi}\sqrt{\frac{g}{l_d}}; \quad l_d = \frac{g}{4\pi^2 f_d^2} \tag{2.266}$$

where f_d = pendulum frequency
l_d = pendulum length
g = acceleration due to gravity

www.EngineeringBooksPDF.com

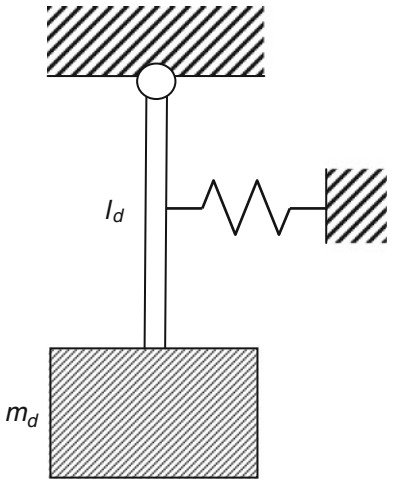


Fig. 2.6 Damper idealization

If the problem exists in construction and damping system, the pendulum length can be calculated as

$$l_d = \frac{g}{(2 \cdot \pi \cdot f)^2 - \frac{c}{m}} \tag{2.267}$$

For a given pendulum length, the spring constant c of the damping system can be derived as

$$c = \left[(2 \cdot \pi \cdot f)^2 - \frac{g}{l_d}\right] \cdot m \tag{2.268}$$

The necessary damping ξ_D can be provided by hydraulic dampers, friction-type dampers and the maximum swing period of the damper.

Absorber T_{abs} should be (Anagnostopoulos 2002)

$$T_D = 2(T_{\text{str}} + \tau) \tag{2.269}$$

where T_{str} is the period of the vibration of the structure; τ is the duration of the impact, introduced as 0.01–0.1 s.

b. *Ball damper*

The idea of the dynamic vibration absorber arranged as a rolling ball is not quite new and in the Czech Republic was already designed for the first time at the beginning of the 1990s. In the application transversal vibrations of a suspended pre-stressed concrete footbridge spanning 252 m were shown, the natural frequency of which was 0.15 Hz. Pimer M and Urus hadze (Eurodyn 2005) mill press Rotterdam (2005) suggested, the relationship between damper mass and modal mass of structures

$$\mu = \frac{m_d}{m_{\text{str}}} \tag{2.270}$$

www.EngineeringBooksPDF.com

ranging from 0 to 1 for logarithmic decrement ϑ of 01004 where m_d is the mass of the ball and m_{str} is the mass of the structure. Initial amplitudes are 100, 200 and 300 mm.

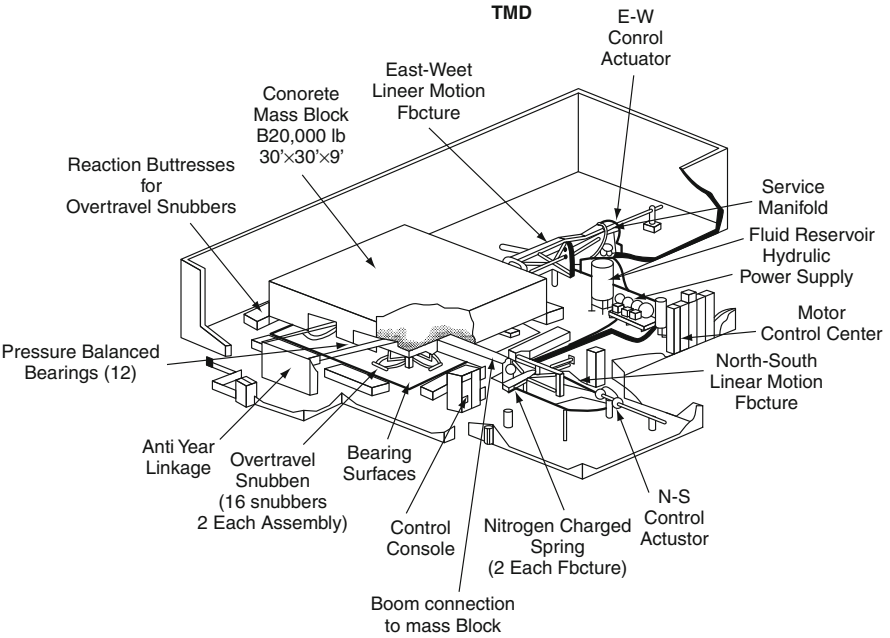


Fig. 2.7 TMD in Citicorp Center (Petersen, 1980, 1981)

The natural frequency of the rolling of the sphere is

$$f_{ds} = \frac{1}{2\pi}\sqrt{\frac{g}{(R-r)(1+(I_{\text{sph}}/m_{\text{sph}}r^2))}} \tag{2.271}$$

where $I_{\text{sph}} =$ moment of inertia of the rolling sphere and $f_{ds} =$ natural frequencies of the rolling sphere.

The horizontal (H) and tangential forces (T) have been computed by Petersen et al as

$$H = -m_{\text{sph}} g \sin\varphi\cos\varphi + \frac{1}{1+\dfrac{I_{\text{sph}}}{m_{\text{sph}}r^2}} \tag{2.272}$$

$$T = mg\sin\varphi - \frac{mg\sin\varphi}{m+\dfrac{I_{\text{sph}}}{mr^2}} \tag{2.273}$$

www.EngineeringBooksPDF.com

Table 2.25 Tuned mass dampers in John Hancock Tower, Boston, and Citicorp Center, New York

		John Hancock Boston, MA	Citicorp Center New York, NY
Typical floor size	(ft)	343 × 105	160 × 160
Floor area	(sq ft)	36,015	25,600
Building height	(ft)	800	920
Building model weight	(tons)	47,000	20,000
Building period 1st mode	(s)	7.00	6.25
Design wind storm	(years)	100	30
Mass block weight	(tons)	2×300	373
Mass block size	(ft)	18×18×3	30×30×8
Mass block material	(type)	lead/steel	concrete
TMD/AMD stroke	(ft)	±6.75*	±4.50*
Max spring force	(kips)	135	170
Max actuator force	(kips)	50	50
Max hydraulic supply	(gms)	145	190
Max operating pressure	(psi)	900	900
Operating trigger – acceleration	(g)	0.002	0.003
Max power	(HP)	120	160
Equivalent damping	(%)	4.0%	4.0%

* Including overtravel.

Note: Collected data and then tabulated. Data provided by Boston and New York Borough councils. They have been checked from literature.

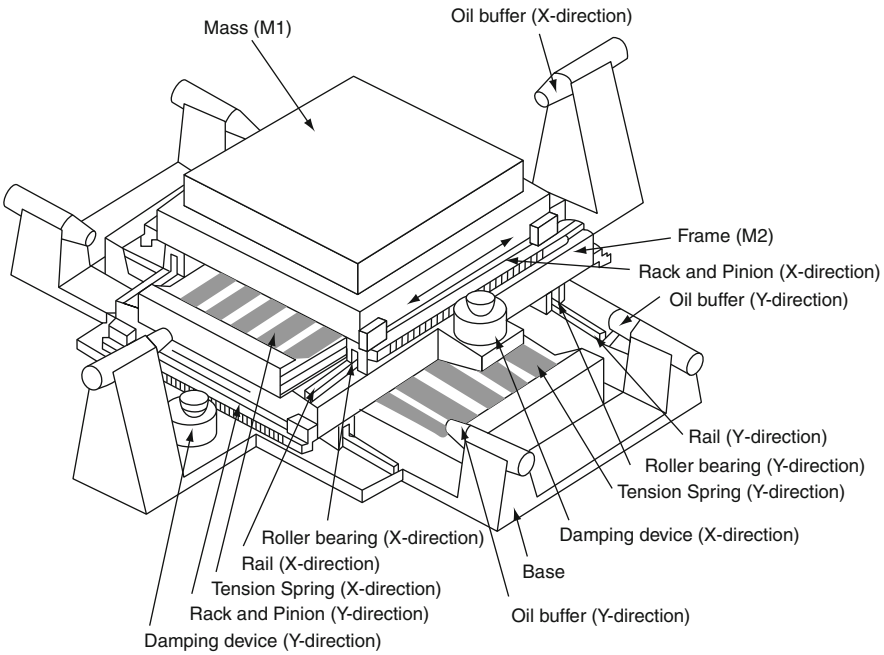


Fig. 2.8 TMD in Chiba Port Tower (Ohtake et al. 1992)

www.EngineeringBooksPDF.com

c. *Tuned mass damper*

Petersen [1995] provides a method design for tuned mass dampers using equation (2.279)

Calculation of damper mass:

$$m_d = m_h \cdot \mu \tag{2.274}$$

Calculation of optimum turning K_{opt} and of optimum damping ratio ξ_{opt}:

$$K_{\text{opt}} = 1/1 + \mu \tag{2.275}$$

$$\xi_{\text{opt}} = \sqrt{3} \cdot \mu/8 \cdot (1 + \mu)^3 \tag{2.276}$$

Calculation of the optimum damping frequency, f_d:

$$f_d = K_{\text{opt}} \cdot f_h \tag{2.277}$$

Calculation of the spring constant of the damping element, k_d:

$$k_d = (2 \cdot \pi \cdot f_d)^2 \cdot m_d \tag{2.278}$$

Calculation of the damping coefficient of the damping element, ${}^{\text{d}}\text{d}_{\text{c}}$:

$${}^{\text{d}}\text{d}_{\text{c}} = 2 \cdot m_d \cdot (2 \cdot \pi \cdot f_d) \cdot \xi_{\text{opt}} \tag{2.279}$$

d. *Viscous dampers*

Viscous elastic dampers or dry friction dampers use the action of solids to dissipate the oscillatory energy of a structure. It is also possible to use a fluid for obtaining the same goal.

The immediate device is the one derived from the "dashpot". In such a device, the dissipation is obtained by the conversion of the mechanical energy into heat with the help of a piston that deforms and displaces a very viscous substance such as silicon. Another family of dampers is based on the flow of a fluid in a closed container. The piston not only deforms the viscous substance but also forces the passage of the fluid through calibrated orifices. As in the preceding case, the dissipation of the energy results in development of the heat.

The main difference between these two techniques is the following. In the "dashpot" damper, the dissipative force is a function of the viscosity of the fluid, while in the other one that force is principally due to the volumic mass of the fluid. This means that the dampers with orifices are more stable against temperature variations in comparison with the "dashpot" ones.

Viscous dampers must be placed between two points of the structure with differential displacement between them. They can be either on an element linking a pier and the deck or on the horizontal wind bracing of the deck.

www.EngineeringBooksPDF.com

Several recent studies have shown that supplement fluid viscous damping effectively reduces the seismic responses of asymmetric plan systems. However, these investigations examined the behaviour of asymmetric plan systems with linear fluid viscous dampers. Non-linear fluid viscous dampers (velocity exponent less than one) have the apparent advantage of limiting the peak damper force at large velocities while still providing sufficient supplemental damping for linear dampers, the damper force increasing linearly with damper velocity.

A recent investigation examined the seismic response of asymmetric systems with non-linear viscous and viscoelastic dampers. It was found that structural response is weakly affected by damper non-linearity, and non-linear dampers achieve essentially the same reduction in response but with much smaller damper force compared to linear dampers; reductions up to 20% were observed for edge deformations and plan rotations of short-period systems. Furthermore, it was shown that the earthquake response of the asymmetric systems with non-linear dampers can be estimated with sufficient degree of accuracy by analysing the same asymmetric systems with equivalent linear dampers. A simplified analysis procedure for asymmetric plan systems with non-linear dampers has also been developed.

The investigation by Lin and Chopra examined the effects of damper non-linearity on edge deformations and damper forces. For asymmetric plan systems, however, other important response quantities of interest for design purposes include base shear, base torque and base torque generated by asymmetric distribution of dampers. Therefore, it is useful to investigate the effects of damper non-linearity on these responses.

e. *Viscous elastic dampers*

The use of viscous elastic materials for the control of vibrations goes back to the 1950s. Their application in structural engineering dates back to the 1960s.

The viscous elastic materials are principally polymers dissipating the energy by shear. The characteristics of viscous elastic dampers depend not only on frequency but also on temperature. The damping coefficient is expressed by

$$C = \frac{W_d}{\pi \cdot \Omega \cdot x^2} \tag{2.280}$$

where W_d = energy dissipation in the structure per cycle
Ω = circular frequency of excitation
x = (piston) displacement

To calculate the effect of dampers in the structure a time history dynamic analysis could be carried out. Viscoelastic damper's behaviour could be represented with the following simplified model:

$$F = F_0 + Kx + Cv^\alpha \tag{2.281}$$

www.EngineeringBooksPDF.com

where F = force transmitted by damper
F_0 = preloading force
x = (piston) displacement
v = velocity

f. *Tuned liquid dampers*

Tuned liquid dampers are fluid-filled containers and provide an interesting possibility for footbridge damping systems. Accelerations of the container cause inertial and damping forces that can be used as system damping. The damping forces are dependent on the viscosity of the fluid and the texture of the container walls. Figure 2.9 a – d is referred to as tuned liquid column dampers while Fig. 2.9e and f is referred to as tuned sloshing dampers.

The natural frequency of the liquid dampers as in Fig. 2.9a and b can be expressed as

$$f = \frac{1}{2\pi}\sqrt{\frac{2g}{L_f}} \tag{2.282}$$

where L_f = total length of fluid column and g = acceleration due to gravity.

The natural frequency of the liquid damper as in Fig. 2.9e and f can be expressed as

$$f = \frac{1}{2\pi}\sqrt{\alpha \cdot \frac{g}{L} \cdot \tanh\left(\alpha \cdot \frac{H}{L}\right)} \tag{2.283}$$

where $\alpha = \pi/2$ for a rectangular container and 1.84 for a cylindrical container.

H and L can be determined from Fig. 2.9. The radius of the cylinder can be replaced by L in (2.288) for cylindrical containers.

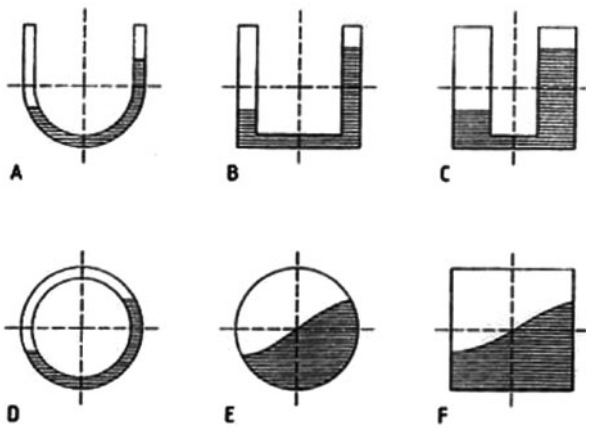


Fig. 2.9 Various types of tuned liquid dampers

www.EngineeringBooksPDF.com

The effectiveness of a fluid damper depends on the ratio between modal mass of the damper and the structure and the detuning. The dimensions of the container, height of fluid and the viscosity of the fluid also play an important role. For larger accelerations, the behaviour of the fluid damper is non-linear. Petersen recommends an experimental tuning of the fluid damper. Contrary to a number of high-rise buildings, it seems that no footbridge has been equipped with this type of damper yet.

Frictional damping systems
Frictional damping systems use friction between surfaces to achieve a damping effect. Frictional damping systems have been used in the footbridges in Germany. A total of eight dampers are generally installed near the bearings, providing frictional damping in the vertical and longitudinal directions.

Isolators

(a) *Natural rubber bearings*
Figure 2.10 shows the devices known as bearings made in natural rubber. They are either round or square in shape. The main construction is that such a bearing is composed of laminated rubber bearings with inner steel plates and flange plate. Sometimes it is encased by a layer of surface rubber.

Dynamic Characteristics

The vertical stiffness Kv of the natural rubber is given by

$$Kv = \alpha \cdot \frac{A_r}{t} \cdot \frac{E_r(1 + 2kS_1^2)G_b}{E_r(1 + 2kS_1^2) + G_b} \tag{2.284}$$

where A_r : cross-sectional area of laminated rubber
t : total rubber thickness
S_1 : primary shape factor
α_e: correction modulus of longitudinal elasticity
E_r : longitudinal elastic modulus of rubber

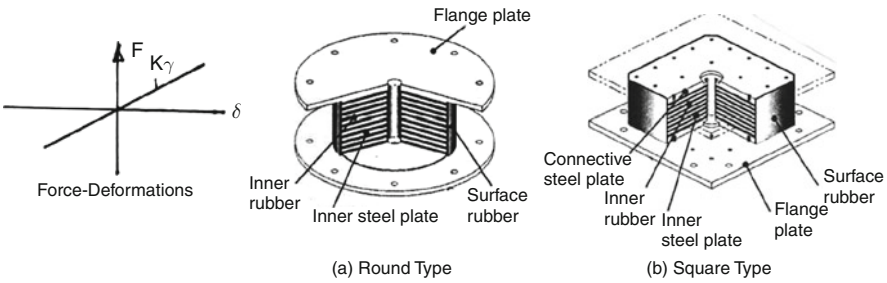


Fig. 2.10 Natural rubber bearings – isolators

www.EngineeringBooksPDF.com

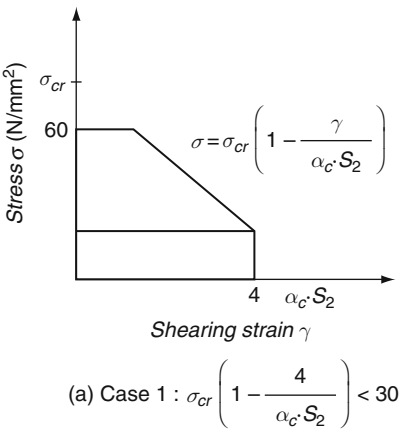


Fig. 2.11 Stress versus shearing strain for case 1

γ : Shear strain $= \epsilon_s$
G_b: bulk modulus of rubber
K : correction modulus of rubber hardness

The maximum compressive strength at critical level is 60 N/mm^2. Maximum shearing strain $T_{r(\max)}$ is 400%.

σ_{cr} : compressive critical strength for shearing strain $= 0$

$$\sigma_{cr} = \xi \cdot G_r \cdot S_1 \cdot S_2 \tag{2.285}$$

$$\text{where } \xi = \begin{cases} 0.85 & (S_1 \geq 30) \quad \text{damping} \\ 0.90 & (S_1 < 30) \quad \text{factor} \end{cases} \tag{2.286}$$

G_r: shear modulus of rubber

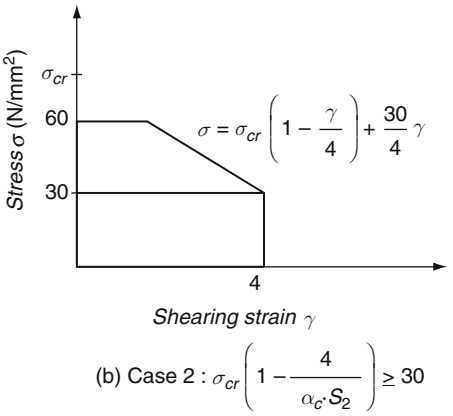


Fig. 2.12 Stress versus shearing strain – for case 2

www.EngineeringBooksPDF.com

$$\alpha_c = \begin{cases} 1 & (S_2 < 4) \\ 0.1(S_2 - 3) + 1 & (S_2 \geq 4) \end{cases} \tag{2.287}$$

S_2 : secondary shape factor

$$S_2 = \begin{cases} S_2 & (S_2 \leq 6) \\ 6 & (S_2 > 6) \end{cases} \tag{2.288}$$

When $\gamma \neq 0$, then the maximum stresses are determined.

$\sigma_{cr}\left(1 - \frac{4}{\alpha_c \cdot S_2}\right) < 30$ (Case 1):

$\sigma = \sigma_{cr}\left(1 - \frac{\gamma}{\alpha_c \cdot S_2}\right)$ (The maximum value of σ is 60 $\mathrm{N/mm^2}$):

$\sigma_{cr}\left(1 - \frac{4}{\alpha_c \cdot S_2}\right) \geq 30$ (Case 2):

$\sigma = \sigma_{cr}\left(1 - \frac{\gamma}{4}\right) + \frac{30}{4}\gamma$ (The maximum value of σ is 60 $\mathrm{N/mm^2}$):

The lateral stiffness K_r at 15° is given for the hysteresis loop model as

$$K_r = G_r \cdot \frac{A_r}{t} \tag{2.289}$$

where G_r = shear modulus of the rubber.

Selecting dimension, the F-8 relation can be achieved using the analysis and a typical experiment.

(b) *High damping rubber bearing*
A procedure similar to (a) stated for natural rubber bearing on page 105 shall be adopted and the hysteresis shear stress versus shear strain can be drawn.

(c) *Lead-rubber bearing*
Fundamental dynamic characteristics

$$K_d = C_{Kd}\left(K_r + K_p\right) \quad (\text{at } 15°) \tag{2.290}$$

where K_r : lateral stiffness

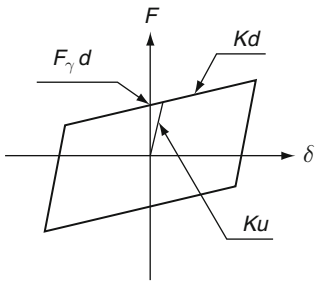


Fig. 2.13 Hysteresis loop model of lead-rubber bearing

www.EngineeringBooksPDF.com

$$K_r = G_r \cdot \frac{A_r}{t} \tag{2.291}$$

where A_r : cross-section of laminated rubber
K_p : additional stiffness by lead plug

$$K_p = \alpha \cdot \frac{Ap}{H} \tag{2.292}$$

F_{yd} = yield force
K_u = initial stiffness
K_d = secondary stiffness
C_{kd} = modification modulus k_d

where α: shear modulus of lead
A_p: cross-section area of plug
C_{Kd} : modification modulus on K_d by strain dependency

$$C_{Kd} = \begin{cases} 0.779\gamma \ [\gamma < 0.25] & (2.293) \\ \gamma \ [0.25 \le \gamma < 1.0] & (2.294) \\ \gamma \ [1.0 \le \gamma < 2.5] & (2.295) \end{cases}$$

The yield force F_{yd} is determined as

$$F_{yd} = C_{yd}\sigma_{pb}A_p \text{ at } 15^\circ \tag{2.296}$$

2.1.14.3 Seismic Isolation Codes and Techniques

General Introduction

After the 1994 Northridge earthquake in the USA, the 1995 Hyogo-Ken Nanbu earthquake in Japan and the 1999 Chi-Chi earthquake in Taiwan, the number of seismically isolated buildings has increased rapidly. Over the same period, building codes have been revised and updated to include requirements for design of seismically isolated buildings. In the USA, seismic isolation provisions have been included in building codes since first appearing in the 1991 Uniform Building Code. The current US provisions are contained in the International Building Code, IBC 2003, which makes reference to the requirements of ASCE 7-02. In Japan, the most recent building code provisions took effect in 2000 and in China and Taiwan in 2002.

In this section, a test study on a seismically isolated building is presented in order to understand and illustrate the difference in the isolation provisions of the building codes of Japan, China, the USA, Italy and Taiwan. The concept of the design spectrum in each code is summarized first. To consider the seismic region coefficients, the target construction sites are assumed to be in Tokyo,

www.EngineeringBooksPDF.com

Beijing, Los Angeles, Potenza and Taipei, respectively. A fixed soil profile is assumed in all cases where the average shear wave velocity within the top 30 m is about 209 m/s.

If the control device needs external energy to modify the vibration properties of a structure, a closed-loop control system can be used, which does not affect many properties of external vibrations. In the case of an open loop control system external vibrations are sensed as soon as they reach the foundation and before they are incident on the building. The control is exercised in such a way that the building does not vibrate in resonance with the severe changes in seismic motion. The usefulness of the open-loop system depends on the proper functioning of the brain unit which recognizes the information from various sensors and generates signals to counter the earthquake.

Various devices are being considered for the control mechanism. The main mechanisms being discussed are (a) variable stiffness mechanism where stiffness of the structure is varied according to the seismic motion striking the foundation of the building so that the building does not attain resonance condition and (b) a mechanism requiring external energy or a mechanism with additional control power which actively and effectively absorbs the energy incident on the building according to the response and which can restore the deformation caused in the building due to the action of the seismic force.

Design Spectrum

In general, seismic load is expressed by a 5% damped design spectrum as follows:

$$S(T) = IS_{\mathrm{a}}(T) \tag{2.297}$$

where

I: occupancy importance factor, which is taken as 1.0 in this study
T: fundamental period of the structure
$S_{\mathrm{a}}(T)$: the design spectrum on site.

The design spectrum generally consists of two parts, namely, a uniform acceleration portion in the short-period range and a uniform velocity portion in the longer period range.

In the Chinese code, spectrum in the constant velocity portion is additionally increased to ensure the safety of structures having long natural periods, such as high-rise buildings or seismically isolated buildings.

A two-stage design philosophy is introduced in the Japanese, Chinese and Italian codes. The two stages are usually defined as damage limitation (level 1) and life safety (level 2). In this chapter, response analyses in the life safety stage will be discussed. In addition, an extremely large earthquake with 2% probability of exceedance in 50 years is defined to check the maximum design displacement of the isolation system in the US and Italian codes.

www.EngineeringBooksPDF.com

China Codified Method

Plate 2.1 gives an overall specification of the design spectrum. The response spectrum for isolated buildings requires design spectrum.

Time history analysis is suggested to calculate the response.

- The first branch for periods less than 0.1 s.
- The constant design spectrum branch, with amplitude listed in Plate 2.1 between 0.1s and the characteristic period of ground motion T_g.
- The third branch, which decreases over the period range T_g to five times T_g.
- The fourth decreasing branch for periods greater than T_g and defined up to 6 s.

Plate 2.1

Country: China

Design spectrum

There are four site classes which are classified by characteristic period Tg shown in Table

$$\alpha(g) = \begin{cases} (0.45 + \frac{\eta_2 - 0.45}{0.1} T)\alpha_{\max} & T \le 0.1 \quad (2.298) \\ \eta_2 \alpha_{\max} & 0.1 < T \le T_g \\ (\frac{T_g}{T})^{\gamma} \eta_2 \alpha_{\max} & T_g < T \le 5T_g \\ [\eta_2 0.2^{\gamma} - \eta_1 (T - 5T_g)]\alpha_{\max} & 5T_g < T \le 6.0 \end{cases}$$

where

$\alpha_{\max}$: zone factor

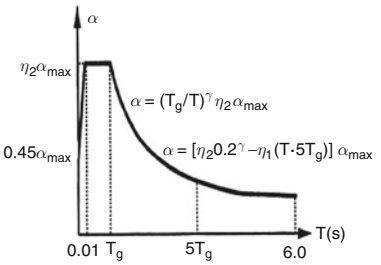
η_1, γ : shape coefficients;

η_2 : response reduction factor defined in Equation

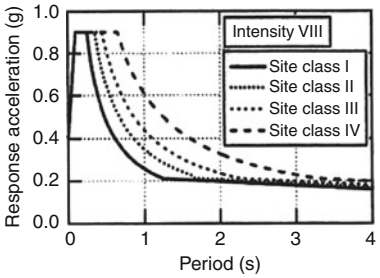
Return period Level 1 50 years
Level 2 1600-2500 years

Storey drift, 1/550

Spectral acceleration versus period



Design response spectrum (China)



Site spectra for the four kind site classes (China)

Zone factor $\alpha_{\max}$ (g) based on Seismie Intensity (China)

	Intensity			
Level	VI	VII	VIII	IX
Level 1	0.04	0.08 (0.12)	0.16 (0.24)	0.32
Level 2		0.50 (0.72)	0.90 (1.20)	1.40

( ): regions where the amplitude of design basic acceleration is 0.15 g or 0.30 g.

Characteristic period T_g related to site class (China)

	Site			
Zone	I	II	III	IV
1	0.25	0.35	0.45	0.65
2	0.30	0.40	0.55	0.75
3	0.35	0.45	0.65	0.90

T_g: characteristic period related to the site soil profile: ζ: effective damping.

$\gamma = 0.9 + \frac{0.05 - \zeta}{0.5 + 5\zeta}$

$\eta_1 = 0.02 + (0.05 - \zeta)/8, \eta_1 \ge 0$

$\eta_2 = 1 + \frac{0.05 - \zeta}{0.06 + 1.7\zeta}, \eta_2 \ge 0.55 \quad (2.299)$

Fortification intensity		6	7	8	9
α_{max}	Frequently occurred earthquake	0.04	0.08(0.12)	0.16(0.24)	0.32
	Seldom occurred earthquake	0.28	0.50(0.72)	0.90(1.20)	1.40
	Design basis earthquake	0.05	0.10(0.15)	0.20(0.30)	0.40

Note: In the items of α_{max} the values in brackets are used for the regions which Design Basis Earthquake acceleration values are 0.15 g or 0.30 g.

www.EngineeringBooksPDF.com

Table 2.26 The peak value of acceleration based on time history analysis

Seismic intensity/peak acc. (gal)	6	7	8	9
Frequently occurred earthquake	18	35 (55)	70 (110)	140
Seldom occurred earthquake		220 (310)	400 (510)	620

Japan

Introduction

Japan is situated at the complex intersection of the Eurasian, North American, Pacific and Philippine tectonic plate boundaries, a region that is considered as having one of the highest risks of severe seismic activity of any area in the world. Nearly 60% of Japan's population is concentrated in the three largest cities of the Kanto, Chubu and Kansai regions. The Kanto region includes Japan's two largest cities, Tokyo and Yokohama, the Chubu region includes Nagoya and the Kansai area includes Kyoto, Osaka and Kobe. In an east – west area these three regions are situated along the subduction zone of the Philippine and Pacific plates and have experienced many large earthquakes such as the 1854 Ansei-Tokai earthquake (M8.4), the 1923 Kanto earthquake (M7.9). All of these cities have suffered destructive damage in the past earthquakes. The northwestern coast of Japan lies on the boundaries of the Eurasian and North American plates. The 1964 Niigata Prefecture earthquake (M6.8) had occurred almost all over Japan.

The severe seismic threat faced by the entire country has led to the extensive development of the field of earthquake engineering and resulted in widespread innovation and application of innovative seismic structural technologies in Japan.

Recent applications of seismic isolation have extended beyond implementing the plane of isolation at the base of a building to mid-story isolation and also to applying isolation to high-rise buildings with heights greater than 60 m. Moreover, seismic isolation has been utilized as a means to realize architectural design aesthetics, a realm that hitherto was much restricted in traditional Japanese earthquake-resistant design.

The Japan Society of Seismic Isolation (JSSI) published "the Guideline for Design of Seismically Isolated Buildings" in 2005 summarizing the basic concepts and approach for performing time history analysis of seismically isolated buildings.

In the 1995 Hyogo-Ken Nanbu earthquake, a large number of condominium buildings suffered severe damage, but mostly they did not collapse. Subsequently, many complex issues arose between the engineer and residence owners in deciding whether or not to demolish or to repair the damaged buildings. These difficulties called developer's attention to the importance of maintaining a building's function or limiting damage to a low and repairable level, even after a severe earthquake.

www.EngineeringBooksPDF.com

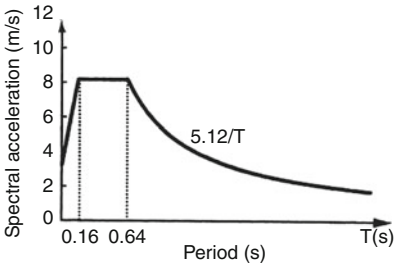
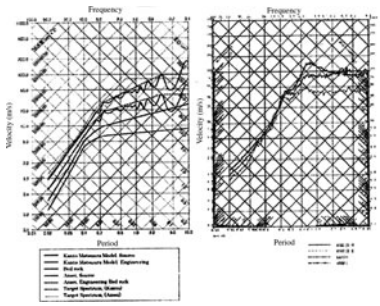
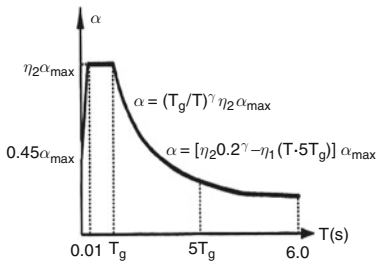
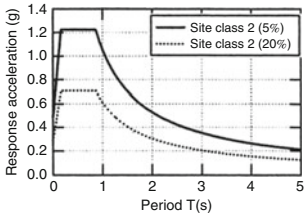
Japanese Codified Method

The basic parameters are indicated briefly in Plate 2.2 and give the response factor at ground face for three features of devices. Plate 2.2 gives also the relatives for ground characteristics together with the isolation devices.

The verification response values. The response acceleration, ${}_eS_a$, is determined as the value of the vertical axis at the corresponding natural period calculated as shown. The response displacement ${}_e\delta$ at gravity centre is determined as follows:

$$ {}_e\delta = {}_e Q/K_{eq} = \frac{M_e S_a}{K_{eq}} \tag{2.300} $$

Plate 2.2 Design spectrum adopted in Japan

Country	Design spectrum	Spectral acceleration versus period
Japan	In general, the five percent-damped spectral acceleration, $s_a(T)$ is: $S_a(T) = ZG_1(T)S_0(T)$ where Z: the seismic hazard zone factor. $Gst(T)$: a soil amplification factor dependent on the soil profile. $S_0(T)$: the design spectral acceleration at engineering bedrock defined in Equation (3.3) which is shown in Figure for Level 2 $S_a(m/s^2) = \begin{cases} 3.2 + 30T & T \le 0.16 \\ 8.0 & 0.16 < T \le 0.64 \\ 5.12/T & 0.64 < T \end{cases}$ Storey drift, 1/200 Return year period 50 – 500	 Design spectral acceleration at the engineering bedrock ($V_S > 400$m/s) (Japan)
	 	

www.EngineeringBooksPDF.com

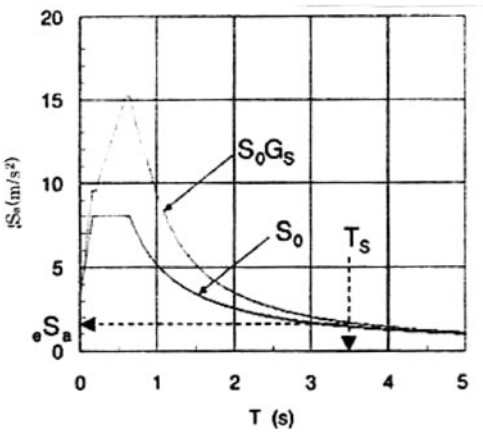


Fig. 2.14 Response spectrum at ground surface

Considering the layout of isolation devices, which cause eccentricities between the gravity centre and stiffness centre, the overall response displacement of the isolation interface ${}_{e}\delta_{r}$ is obtained as follows:

$$ {}_{e}\delta = 1.1{}_{e}\delta_{r} < (\delta_{s}) $$

$$ {}_{e}\delta_{r} = \alpha_{e}\delta $$

Table 2.27 Features of devices

	NRB700	LRB800	LRB850
Diameter (mm)	700	800	850
Inner diameter (mm)	15	160	170
Rubber sheet (mm) *Layer	4.7×30	5.1×33	5.25×32
Area (cm^2)	3,847	4,825	5,448
Steel plate (mm)	3.1×29	4.4×32	4.4×31
Height of rubber (mm)	141	168	168
1 st shape factor	36.4	39.2	40.5
2 nd shape factor	5	4.8	5.1
Diameter of lead core (mm)	–	160	170
Diameter of flange (mm)	1,000	1,150	1,200
Flange thickness (mm)	28 – 22	32 – 24	32 – 24
Height (mm)	286.9	373.1	368.4
Weight (kN)	6.4	11.5	12.7
Total number	2	4	6

Table 2.28 Eccentricities of isolation interface

	Gravity		Rigidity		Eccentricity		Eccentricity	
Story	g_x(m)	g_y(m)	I_x(m)	I_y(m)	e_x(m)	e_y(m)	R_{ex}	R_{ey}
$\gamma = 1.0$	1148.3	708.2	1121.4	707.4	26.8	0.8	0.001	0.029
$\gamma = 1.5$	1148.3	708.2	1121.3	689.6	27.0	18.6	0.020	0.029

www.EngineeringBooksPDF.com

Table 2.29 Relation for ground characteristics

	Formulae	Minimum values
$T \leq 0.8T_2$	$G_s = G_{s2}\frac{T}{0.8T_2}$	1.2
$0.8T_2 < T \leq 0.8T_1$	$G_s = \frac{G_{s1}-G_{s2}}{0.8(T_1-T_2)}T + G_{s2} - 0.8\frac{G_{s1}-G_{s2}}{0.8(T_1-T_2)}T_2$	1.2
$0.8T_1 < T \leq 1.2T_1$	$G_s = G_{s1}$	1.2
$1.2T_1 < T$	$G_s = \frac{G_{s1}-1}{\frac{1}{1.2T_1}-0.1}\cdot\frac{1}{T} + G_{s1} - \frac{G_{s1}-1}{\frac{1}{1.2T_1}-0.1}\cdot\frac{1}{1.2T_1}$	1.0

Note: Data provided by the Japanese manufacturers for devices.

Table 2.30 Dimensions of dampers

		Steel bar damper	Lead damper
Rod	Rod diameter (mm)	ϕ90	ϕ180
	Number of rods	4	1
	Loop diameter	ϕ760	–
	Material (Standard No.)	SCM415 (JIS G 4105)	Lead (JIS H 2105)
	Number of dampers	16	6

Table 2.31 Characteristics of isolation devices

	Item	Rubber bearings		Steel rod damper	Lead damper
		ϕ 800	ϕ 800A		
Horizontal stiffness (kN/m)	Initial stiffness K_1	1,060	860	7,110	12,000
	Secondary stiffness K_2	–	–	0	0
	Yield load (kN)	–	–	290	90
	Yield displacement (m)	–	–	0.0408	0.0075

where α is the safety factor for temperature-dependent stiffness changes and property dispersions in manufacturing of devices and superstructures, which must be smaller than their strength and allowable stress, respectively.

The United States of America

Introduction

This section presents an overview of seismic isolation and passive energy dissipation technologies in the USA. A historical survey of seismic isolation and energy dissipation applications is presented with descriptions of selected notable projects. The types of devices that are most commonly used in the USA are described along with a brief overview of research on the technologies and the evolution of code regulations governing their use. The section concludes with comments on the future direction of the technologies.

www.EngineeringBooksPDF.com

Overview of Seismic Isolation Applications in the USA

Construction of the first seismically isolated building in the USA was completed in 1985 and by mid-2005 there were approximately 80 seismically isolated buildings in the USA. Some of the most significant early projects are discussed below, along with examples of several more recent projects.

Buildings

The first building in the USA to be seismically isolated, the Foothill Communities Law and Justice Center in Rancho, California, was completed in 1985, a four-storey plus basement building. The realization of the project was the culmination of the efforts of numerous parties. The use of high-damping rubber bearings was the first application in the world of this type of isolation system.

The US Court of Appeals building, in San Francisco, is another example of a large historic building retrofit of numerous other monumental building structures, including City Hall in Oakland and State Capitols in South Carolina and Utah.

Seismic isolation has been used throughout the US buildings up and down the country; many reports exist on the testing facilities of passive energy dissipation systems. However, code provisions for seismic isolation and passive energy systems are briefly dealt with below.

Current Status and Future Development

Seismic isolation. Given the 20-year application history of seismic isolation in the USA, the approximately 80 projects completed is a modest total. While many notable projects, particularly the retrofit of a number of landmark historic buildings, have been undertaken, fewer projects of this type are expected in the future. Seismic isolation has not moved into the mainstream as a widely accepted and used seismic-resistant technology.

Somewhat unfairly, seismic isolation has suffered under the conventional wisdom that it is an expensive technology. Many of the most prominent early isolation projects were large and costly retrofits of historic buildings, projects that would have been expensive regardless of whether or not isolation was used. Nonetheless, the general belief has evolved that seismic isolation is expensive and that it is not economically feasible to consider for typical buildings.

Codified Method

According to IBC 2003, the general design response spectrum curve with various equations are indicated in Plate 2.3.

Apart from these parameters, the values of the site coefficient F_a as a function of the site class and mapped spectra response acceleration at short period (S) would be needed and they are given below:

www.EngineeringBooksPDF.com

Plate 2.3 Design spectrum and Data (U.S.A)

Country	Design spectrum	Spectral acceleration versus period

USA

According to the IBC 2003, the general design response spectrum curve is as shown in Figure and is defined by Equation

$$S_a = \begin{cases} 0.6\frac{S_{DS}}{T_0} + 0.4S_{DS} & T \le T_0 \\ S_{DS} & T_0 \le T \le T_S \\ \frac{S_{D1}}{T} & T_S < T \end{cases}$$

where:
S_{DS}, S_{D1}: the design spectral response acceleration at short periods and one second period, respectively, as determined by Equation (3.8).

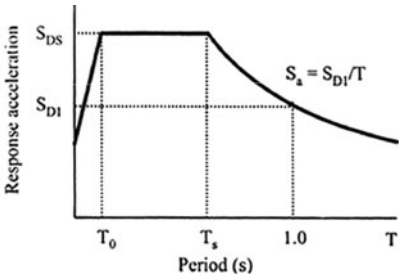
$T_0 = 0.2S_{D1}/S_{DS}$; $T_S = S_{D1}/S_{DS}$

$S_{DS} = \frac{2}{3}S_{MS} = \frac{2}{3}F_aS_S$

$S_{D1} = \frac{2}{3}S_{M1} = \frac{2}{3}F_vS_1$

$S_S \sim 1.55\,g$; $S_1 = 0.623\,g$

Where: F_a, F_v: site coefficients defined in Tables and, respectively. S_s, S_1: the mapped spectral accelerations for short periods and one second period.

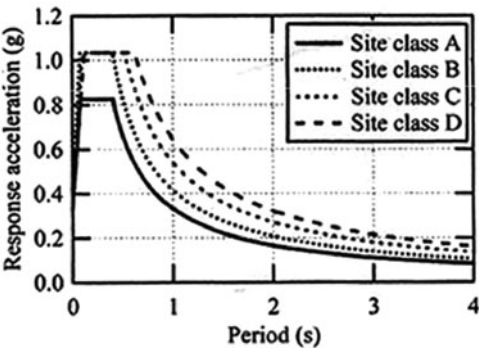


Design response spectrum, IBC 2003 (USA)

Table Values of the site coefficient F_a as a functions of the class and mapped spectral response acceleration at short period (S_s)[a]

Site Class	Mapped spectral accelerations at short periods $S_s \le 0.25$	$S_s = 0.50$	$S_s = 0.75$	$S_s = 1.00$	$S_s \le 1.25$
A	0.8	0.8	0.8	0.8	0.8
B	1.0	1.0	1.0	1.0	1.0
C	1.2	1.2	1.1	1.0	1.0
D	1.6	1.4	1.2	1.1	1.0
E	2.5	1.7	1.2	0.9	0.9
F	Note b	Note b	Note b	Note b	Note b

a Use straight line interpolation for intermediate values of mapped spectral acceleration at short period
b. Site specific geotechnical investigation and dynamic site response analyses shall be performed.



Site spectra at the four kinds of site classes (USA)

Table Values of site coefficient Fa as a function of site class and mapped spectral response acceleration at short period (S_t)[a]

Site Class	Mapped spectral accelerations at one second period $S_t \le 0.1$	$S_t = 0.2$	$S_t = 0.3$	$S_t = 0.4$	$S_t \le 0.5$
A	0.8	0.8	0.8	0.8	0.8
B	1.0	1.0	1.0	1.0	1.0
C	1.74	1.6	1.5	1.4	1.3
D	2.4	2.0	1.8	1.6	1.5
E	3.5	3.2	2.8	2.4	2.4
F	Note b	Note b	Note b	Note b	Note b

Values of site coefficient F_a as a function of site class and mapped spectral response are given in tables provided by the code.

Based on ISO, the following information is required if one goes on using the code:

Acceleration at short period (Ss)[a]
Mapped spectral accelerations at short periods

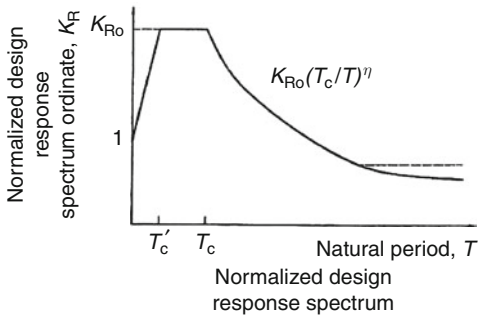
Site Class
A reference is made to the code

www.EngineeringBooksPDF.com

ISO 3010: 2001E. Plate 2.4 indicate the relationships for normalised response spectra.

Sheet No. S 2.4 to 2.5.3 give brief information on this subject based on the ISO requirements. These sheets are available.

Plate 2.4 Design spectrum based on ISO

Country	Design spectrum	Spectral acceleration versus period
ISO 3010: 2001E		T_c, T'_c

Eurocode-8

Introduction

The seismic protection of conventional structures is based on the favourable changes of their dynamic characteristics, induced by yielding and damage occurring in structural and non-structural elements under intense seismic action. Such changes can be essentially described as an increase of flexibility and of damping. Due to the usual spectral characteristics of earthquakes and/or to the energy dissipation occurring in the structure, these changes give rise to a considerable reduction in the structural mass accelerations and, then, of the inertia forces. This makes it possible for a ductile structure to survive a "destructive" earthquake without collapsing.

In the last two to three decades, new strategies have been developed which still rely upon deformation and energy dissipation capabilities. These properties, however, are concentrated in special devices, in the form of rubber or sliding bearings, of energy dissipating and/or re-centring viscous or hysteretic devices. Such devices are incorporated in the structure so as to store and dissipate most of the input energy. The inertia forces acting on the structure during a strong earthquake are considerably reduced, so that no damage to structural and non-structural elements is in principle required to further reduce them, and hence higher levels of seismic protection are obtained.

The two most frequently used "passive control" strategies for buildings are

– energy dissipation
– seismic isolation

www.EngineeringBooksPDF.com

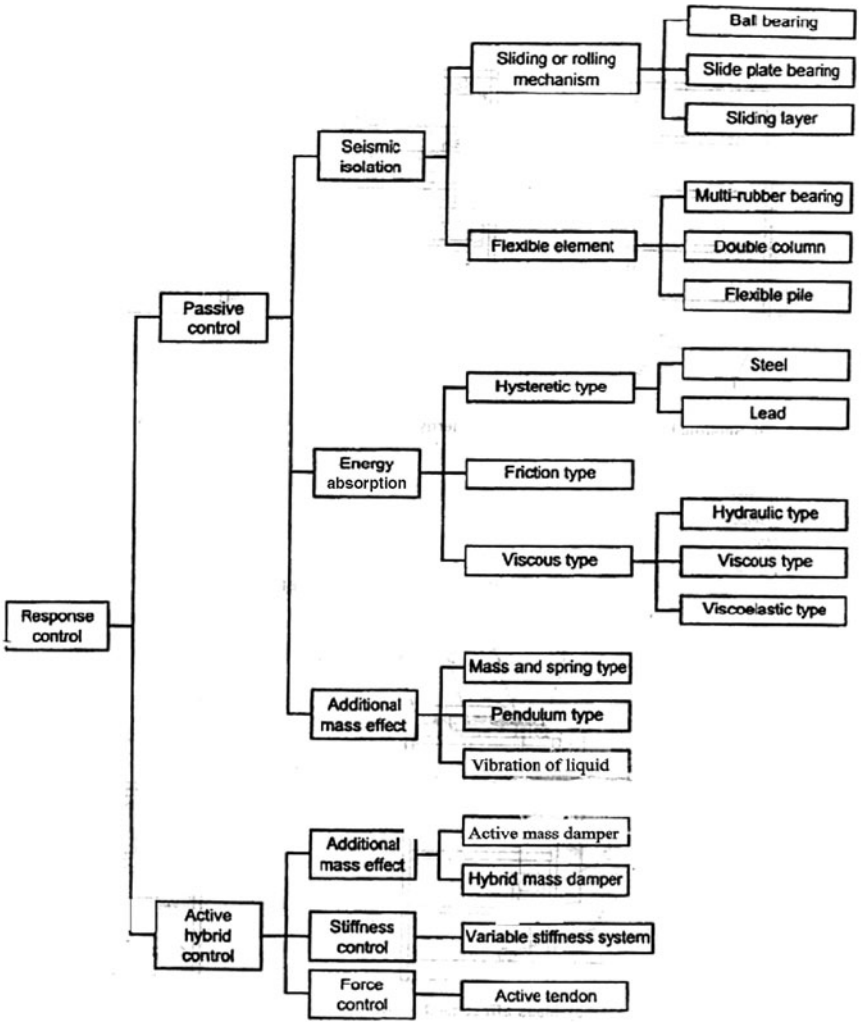
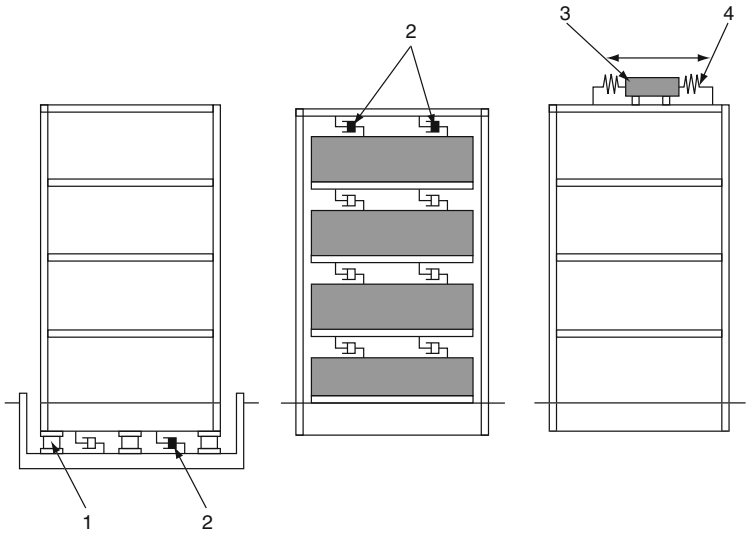


Fig. 2.15 Classification of response-control systems

The energy dissipation strategy consists of the introduction within the structural system of elements specifically designed to dissipate energy in the dynamic deformation of the structure. These elements may take the form of dissipative steel bracings separate for the structure and working in parallel with it or they can be obtained by the use of friction devices, viscous dampers or elasto-plastic steel components.

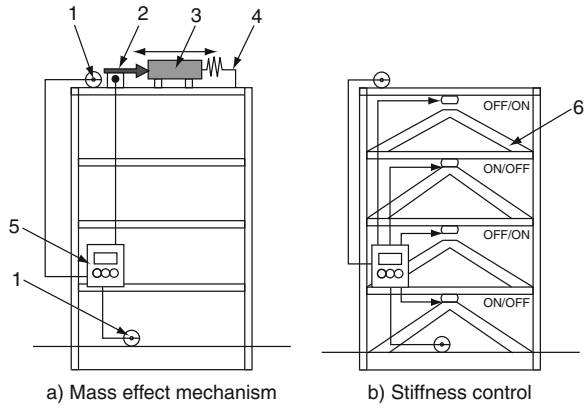
Seismic isolation essentially uncouples the structural movement from the ground motion by introducing a strong discontinuity in the lateral stiffness distribution along the height of the structure (usually at their base in buildings). The structure is thus subdivided into two parts: the substructure, rigidly

www.EngineeringBooksPDF.com



Key
1 Isolator
2 Damper
3 Mass
4 Spring

Fig. 2.16 Example of passive control system



Key
1 Sensor
2 Actuator
3 Mass
4 Spring
5 Computer
6 Brace

Fig. 2.17 Example of active control system

www.EngineeringBooksPDF.com

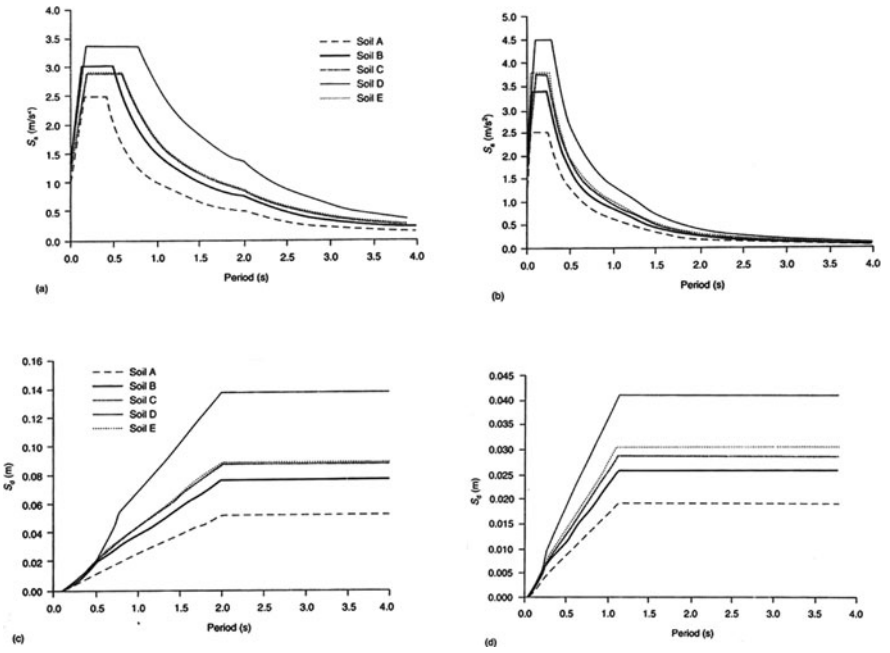


Plate 2.5 Eurocode 8 elastic response spectra for 5% damping: (a, b) pseudo-acceleration spectra; (c, d) displacement spectra; (a, c) recommended spectra of type 1; (b, d) recommended spectra of type 2.
Note: these diagrams are taken from Eurocode 8 with indebtedness and compliment

connected to the ground, and the superstructure. They are separated by the isolation interface, which includes the isolation system.

After a careful consideration of the Eurocode-8, four diagrams covering elastic response spectra, pseudo-acceleration spectra and displacement spectra are given in Plate 2.5

Classification and Characteristics of Response-Controlled Structures

In general there is a great non-uniformity in the classification of response-controlled structure. Various methodologies have been delivered. Some are listed in Plate 2.5.

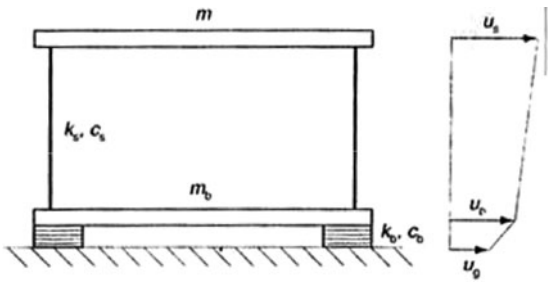


Fig. 2.18 Simplified two-degrees-of-freedom model of a base-isolated structure

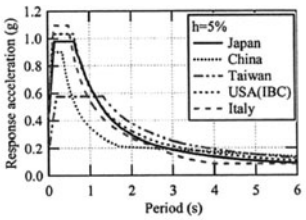
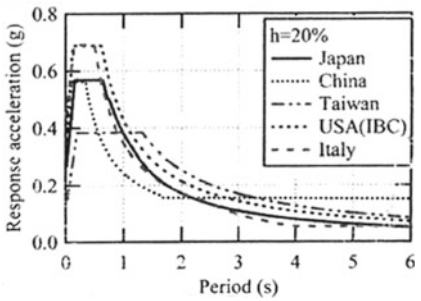
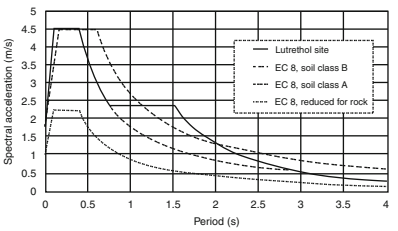
www.EngineeringBooksPDF.com

A Comparative Study of Seismic Codes

Introduction

Plate 2.6 gives a brief comparison of response acceleration versus period based on a fixed soil profile using isolation techniques adopted in Japan, China, the USA, Italy and Eurocode 8. The Far East countries data were compared with 5 and 20% damping. Where the effective damping rate is greater than 15%, the reduction factor in the Japanese is comparatively smaller. The dynamic characteristics of the soils such as the relationship between G (shear stiffness), γ (shear strain) and effective damping have been

Plate 2.6 Design spectra–a comparative study

Country	Design spectrum	Spectral acceleration versus period
Comparison Japan China Taiwan The USA Italy Euro 8	 Five percent-damped acceleration response spectra for Tokyo, Beijing, Los Angeles, Potenza and Taipei Five percentamped acceleration response spectra for Tokyo, Beijing. Los Angles, Potenza and Taipei   Ref. seismic conceptual Design of Buildings. Prof Hugo Backman DFA and DETEC, Switzerland BBL publications, BWG 2003.	In order to evaluate the differences in the spectral accelerations, a comparison study is conducted. For this study, the building sites are assumed to be in Tokyo, Beijing, Los Angeles, Potenza and Taipei. A fixed soil profile is assumed, where $V_{s,\ average} = 209$ m/s. Typically, seismically isolated buildings should be located on relatively stiff ground, such as that defined. In the Japanese code, an iterative procedure is used to calculate the site amplification coefficient, rather than using the amplification coefficients defined in the code. The detailed procedure is shown in Section 5.3.2. The dynamic characteristics of the soils such as the relationship between shear stiffness G and shear strain and the relationship between effective damping and shear strain were obtained from the site investigation. Ground surface 5% damped acceleration response spectra given by the five different codes. In the short-period range, less than about 0.5 s, Sa, Italy, is the largest. For periods longer than about 0.6 s, Sa, USA and Sa, Japan, have approximately the same value. Beyond about 1.2 s, Sa, Taiwan, has the largest value due to the Taipei basin geology. Soong et al. ( ) used a fixed soil profile for comparison. It is seen that for structures having natural periods longer than 3 s, the spectral acceleration level is about the same for all five codes, with the exception of the Italian code, which gives slightly lower values Soil Profile used for study, where $V_{s\ average} = 209$ m/s Layer / Depth (m) / Vs (m/s) / γ (t/m^3) 1 / 0.00 / 120 / 1.85 2 / 2.85 / 120 / 1.50 3 / 5.90 / 120 / 1.80 4 / 8.95 / 310 / 1.90 5 / 14.35 / 220 / 1.85 6 / 18.55 / 380 / 2.00 7 / 23.50 / 320 / 1.75 8 / 28.50 / 400 / 1.95

www.EngineeringBooksPDF.com

Table 2.32 Examples of response-controlled structures in Japan and other countries

No.	Name of building	Location	No. of floors	Built-up area, m^2	Structure	Application	Year of construction	Remarks (details of response control)
1	2	3	4	5	6	7	8	9
1	M.I.E. building					Computer room floor		Ball bearing support
2	Dynamic floor					Computer room floor		Teflon sheets
3	Fudochokin Bank (now Kyowa Bank)	Himeji	+3, –1	791	RCC	Bank branch	1934	Sway-type hinge column
		Shimonoseki Tokyo	+3	641	RCC	Bank branch	1934	
4	Tokyo Science University	Auckland, New Zealand	+17, –1	14,436	Steel	School	1981	Double columns
5	Union House	Skopje, Yugoslavia	+12, –1		RCC	Office	1984	Double columns
6	Pestaloci Elementary School	California, USA	+3		RCC	School	1969	Rubber
7	Foothill Law and Justice Center	Wellington, New Zealand	+4, –1		Steel	Court	1986	Laminated rubber
8	W. Clayton Building	France	+4		RCC	Office	1983	Laminated rubber
9	Cruas Atomic Power Plant	South Africa			RCC	Atomic furnace	1984	Laminated rubber
10	Koeberg Atomic Power Plant	Chiba, Japan			RCC	Atomic furnace	1983	Laminated rubber
11	Hachiyodai Apartments	Tochigi, Japan	+2	114	RCC	Housing	1983	Laminated rubber
12	Okumura group, Okumura Research Center, Japan office wing	Miyagi, Japan	+4	1,330	RCC	Research centre	1986	Laminated rubber
13	Tohoku University, Shimizu Construction Laboratory		+3	200	RCC	Observatory	1986	Laminated rubber, viscous response control
14	Obayashi group, Technical Research Center, 61st Laboratory	Tokyo	+5, –1	1,624	RCC	Laboratory	1986	Laminated rubber
15	Fujizawa Industries, Fujizawa Plant, TC wing	Kanagawa, Japan	+5	4,765	RCC	Laboratory, office	1986	Laminated rubber
16	Funabashi Taketomo Dormitory	Chiba, Japan	+3	1,530	RCC	Dormitory	1987	Laminated rubber
17	Kashima Constructions Research Laboratory, West Chofu, Acoustic Laboratory	Tokyo	+2	655	RCC	Research laboratory	1986	Laminated rubber
18	Christian Data Bank	Kanagawa, Japan	+2	293	RCC	Data center	1988	Laminated rubber
19	Chiba Port Tower	Chiba, Japan	125 m	2,308	Steel	Tower	1986	Dynamic response control

Note: Data are collected from the earthquake reports, newspapers and T.V. records. They are put in the current format.

www.EngineeringBooksPDF.com

Table 2.32 (continued)

No.	Name of building	Location	No. of floors	Built-up area, m^2	Structure	Application	Year of construction	Remarks (details of response control)
1	2	3	4	5	6	7	8	9
20	Sydney Tower	Australia	325 m		Steel	Tower	1975	Dynamic response control
21	Citicorp Center	New York, USA	+59		Steel	Office	1977	Tuned mass response control
22	Hitachi Headquarters	Tokyo	+20, –3	57,487	Steel	Office	1983	Steel response control
23	World Trade Center	New York, USA	+110		Steel	Office	1976	VEM damper (viscous elastic mass)
24	Columbia Center	Seattle, USA	+76		Steel	Office	1985	VEM damper (viscous elastic mass)
25	Radar Construction	Chiba, Japan			Steel	Instrument Platform	1980	Roller bearing
26	Christchurch Chimney	Christchurch, New Zealand	35 m		RCC	Chimney		Steel response control
27	Commerce, Cultural Center	Saitama, Japan	+30		Steel	Office	1987	Friction response control
28	Fujita Industries Technical Research Laboratory, (6th Laboratory)	Kanagawa, Japan	+3	3,952	RCC	Research Center	1987	Laminated rubber
29	Shibuya Shimizu No. 1 Building	Tokyo	+5, –1	3,385	RCC	Office	1988	Laminated rubber
30	Fukumiya Apartments	Tokyo	+4	682	RCC	Cooperative housing	1988	Laminated rubber
31	Lambeso C.E.S.	France	+3	4,590	RC prefab	School	1978	Laminated rubber
32	Lambeso C.E.S.	France	+3	4,590	RC prefab	School	1978	Laminated rubber
33	Pestaloci Elementary School	Skopje, Yugoslavia	+3		RCC	School	1969	Laminated rubber
34	Cruas Atomic Power Plant	France			RCC	Atomic furnace		Laminated rubber
35	Kousberg Atomic Power Plant	South Africa			RCC	Atomic furnace		Laminated rubber
36	Pestaloci Elementary School	Skopje, Yugoslavia	+3		RCC	School	1969	Laminated rubber
37	Foothill Law and Justice Center	California, USA	+4, –1		Steel	Court	1983	Laminated rubber
38	W. Clayton Building	Wellington, New Zealand	+4		RCC	Office	1984	Laminated rubber
39	Hachiyodai Apartments	Chiba, Japan	+2	114	RCC	Housing	1983	Laminated rubber
40	Okumura group, Namba Research Center, Office Wing	Tochigi, Japan	+4	1,330	RCC	Research center	1986	Laminated rubber

www.EngineeringBooksPDF.com

Table 2.32 (continued)

No.	Name of building	Location	No. of floors	Built-up area, m^2	Structure	Application	Year of construction	Remarks (details of response control)
1	2	3	4	5	6	7	8	9
41	Obayashi group, Technical Research Center, 61 Laboratory	Tokyo	+5, –1	1,024	RCC	Laboratory	1986	Laminated rubber
42	Oires Industries, Fujizawa Plant, TC wing	Kanagawa, Japan	+5	4,765	RCC	Laboratory, Office	1986	Laminated rubber
43	Funabashi Taketomo Dormitory	Chiba, Japan	+3	1,530	RCC	Dormitory	1987	Laminated rubber
44	Kashima Constructions Research Laboratory, West Chofu, Acoustic Laboratory	Tokyo, Japan	+2	655	RCC	Research Laboratory	1986	Laminated rubber
45	Christian Data Bank	Kanagawa, Japan	+2	293	RCC	Data center	1988	Laminated rubber
46	Tohoku University, Shimizu Construction Laboratory	Miyagi, Japan	+3	200	RCC	Observatory	1986	Laminated rubber
47	Fujita Industries Technical Research Laboratory, 6th Laboratory	Kanagawa, Japan	+3	3,952	RCC	Research center	1987	Laminated rubber
48	Shibuya Shimizu No. 1 Building	Tokyo, Japan	+5, –1	3,385	RCC	Office	1988	Laminated rubber
49	Fukumiya Apartments	Tokyo, Japan	+4	685	RCC	Housing	1988	Laminated rubber
50	Shimizu Constructions Tsuchiura Branch	Ibaraki, Japan	+4	637	RCC	Office	1988	Laminated rubber
51	Toranomon 3-chome building	Tokyo, Japan	+8	3,373	RCC	Office	1989	Laminated rubber
52	National Institute for Research in inorganic materials, vibration free special laboratory	Ibaraki, Japan	+1	616	RCC	Laboratory	1988	Laminated rubber
53	Fudochokin Bank (now Kyowa Bank)	Himeji, Japan	+3, –1	791	RCC	Bank branch	1933	Sway-type hinge column
54	Fudochokin Bank (now Kyowa Bank)	Shimonoscki, Japan		641				Sway-type hinge column
55	Tokyo Science University	Tokyo, Japan	+17, –1	14,436	Steel	School	1981	Double columns
56	Union House	Auckland, New Zealand	+12, –1		RCC	Office	1983	Double columns
57	A Certain Radar	Chiba, Japan	+9 Atop the building	711	Steel platform	Instrument	1980	Roller bearing
58	Taisei Construction, Technical Research Center, J Wing	Kanagawa, Japan	+4	1,029	RCC	Office	1988	Sliding support

www.EngineeringBooksPDF.com

Table 2.32 (continued)

No.	Name of building	Location	No. of floors	Built-up area, m^2	Structure	Application	Year of construction	Remarks (details of response control)
1	2	3	4	5	6	7	8	9
59	World Trade Center	New York, USA	+110		Steel	Office	1976	VEM damper (viscoelastic material)
60	Columbia Center	Seattle, USA	+76		Steel	Office	1985	VEM damper
61	Commerce, Cultural Center	Saitama, Japan	+31	105,060	Steel	Office	1988	Friction damper
62	1-Chome Complex, Office Wing	Tokyo, Japan	+22	34,650	Steel	Office	1990 [sic]	Friction damper
63	Sydney Tower	Australia	325 m		Steel	Tower	1975	Dynamic damper
64	Citicorp Center	New York, USA	+59		Steel	Office	1977	Tuned mass damper
65	Chiba Port Tower	Chiba, Japan	125 m	2,204	Steel	Tower	1986	Dynamic damper
66	Toyama Park Observation Tower	Aichi, Japan	134 m	2,929	Steel	Tower	1988	Dynamic damper
67	Gold Tower		136 m	1,193	Steel	Tower	1988	Aqua damper
68	Yokohama Marine Tower	Kanagawa, Japan	103 m	3,325	Steel	Tower	1988	Super sloshing-damper

Note: + indicates floors above ground and – indicates floors below ground.
Data collected from the reports, newspapers and television records. They have been put in the current order.
Individual information collected from reports, newspapers and television records. They are placed and put in this order.
The data are taken from newspapers such as Time Index and placed in the given order.

www.EngineeringBooksPDF.com

Table 2.33 Seismically isolated buildings in the USA

Building	Height/ storeys	Floor area (m^2)	Isolation system	Date
Foothill Communities Law and Justice Center	4	17,000	10% damped elastomeric bearings	1985/86
Salt Lake City and County Building (Retrofit)	5	16,000	Rubber and lead-rubber bearings	1987/88
Salt Lake City Manufacturing Facility (Evans and Sutherland Building)	4	9,300	Lead-rubber bearings	1987/88
USC University Hospital	8	33,000	Rubber and lead-rubber bearings	1989
Fire Command and Control Facility	2	3,000	10% damped elastomeric bearings	1989
Rockwell Building (Retrofit)	8	28,000	Lead-rubber bearings	1989
Kaiser Computer Center	2	10,900	Lead-rubber bearings	1991
Mackay School of Mines (Retrofit)	3	4,700	10% damped elastomeric bearings plus PTFE	1991
Hawley Apartments (Retrofit)	4	1,900	Friction pendulum/slider	1991
Channing House Retirement Home (Retrofit)	11	19,600	Lead-rubber bearings	1991
Long Beach VA Hospital (Retrofit)	12	33,000	Lead-rubber bearings	1991

Note: Data is obtained from various Newyork Times.

www.EngineeringBooksPDF.com

Table 2.34 Bridges seismically isolated in Italy

No. of bridges	Name/location	Range of lengths (m)	Total length (m)	Superstructure type	Isolating system	Date completed
1	Somplago, Udine-Tarvisio		1,240	Precast segments	EL (neoprene disc)	1974
5	Tiberina E45		1,700		OL	1974
16	Udine-Tarvisio	240–900	7,900	Box girders	Long: elastom. Sleeves Transv: elastom. discs	1981–1986
3	Udine-Tarvisio	400–830	1,600	Box girders	Long: EP dampers Transv: elastom. discs	1983
1	Cellino, Road SS251		580	Concrete beams	EL (neoprene)	1983
3	Udine-Tarvisio	480–900	2,100	Steel girders	OL	1983–1986
1	Sesia, Trafori Highway		2,100		OL	1984
1	Bruscata, Greco		70	Steel truss	EL	1984
1	Pontebba, Udine-Tarvisio		960	Box girders	EL (elastomer)	1984
2	Milano-Napoli	350–780	1,100	Box girders	EP (steel)	1985
12	*Napoli-Bari	70–720	5,700	PCB boxed, piers or framed RC columns	Long: EP devices on abutments or on each span. Transv: EP on pier	1985–1988
1	Slizza 3, Udine-Tarvisio		160	Steel girders	EL	1985
1	Vallone, railway		240	Steel girders	EL	1985
1	Rivoli Bianchi, Udine-Tarvisio		1,000	Concrete beams	Pneumatic dampers	1985
2	Salerno-Reggio	600	1,400	Concrete beams	OL	1988
3	Fiano-San Cesareo	300–1,200	1850	Concrete beams	RB + metal shock	1986–1987
5	Fiano-San Cesareo	120–700	1,400	Box girders	RB + metal shock	1986–1987
6	Fiano-San Cesareo	100–650	1,600	Box girders/concrete beams	EL (rubber discs)	1986–1987
2	Fiano-San Cesareo	300–700	1,000	PCB	Viscoelastic shock absorber	1986–1987
3	*Napoli-Bari	130–200	500	PCB	LRB (long and transv)	1986
2	Milano-Napoli		170	Concrete beams	LRB	1986
2	Salerno-Reggio	350–900	1,200	PCB	OL	1987
1	Sizzine, Trafori Highway		1,800	PCB	OL	1987
1	Aqua Marcia, Milano-Napoli		325	Box girders	Long: EP Transv: EL dampers	1987
4	Monte Vesuvio		6,000	PCB	EL dampers with mechanical dissipators	1987–1990
12	Roma-Firenze railway	200–2,700	12,400	Box girders	OL	1987–1989
1	Lontrano, Salerno-Reggio		550	Box girders	OL	1988
1	Tagliamento, Pontebbana		1,000	PCB	Viscoelastic	1988

Note: Data collected from the Italian Embassy in London by the author.

www.EngineeringBooksPDF.com

Table 2.34 (continued)

No. of bridges	Name/location	Range of lengths (m)	Total length (m)	Superstructure type	Isolating system	Date completed
6	Roma-L'Aquila-Teramo	128–450	1,800	Box girders	EL (rubber + metal shock)	1988
1	Calore, Caserta (railway)		100	PCB	EL dampers + mechanical dissipators	1988
1	Granola, railway overpass		120	Concrete slab	Bearings + EL buffers	1988
2	Viaducts, San Mango	600–640	1,200	Steel girders	OL	1988–1990
1	Morignano, A14 highway		450	PCB	EP dampers	1989
1	*Lenze-Pezze, Napoli-Bari		300	PCB	EP dampers	1989
2	Vittorio Veneto – Pian di Vedoia	210–2,100	2,300	PCB	Long: Viscoelastic. Trans: EP	1989
1	Pont Suaz, Aosta		240	PCB	EP shock absorber	1989
1	Flumicello, Bologna-Firenze		300	PCB	OL	1989
1	Temperino, Roma-L'Aquila		830	PCB	EP dampers	1989
1	S.Onofrio, Salerno-Reggio		450	PCB	OL	1989
3	Roma-L'Aquila	230–1,300	1,800	Box girders	OL + RB	1989
1	*D'Antico, Napoli-Bari		250	Composite deck	EP	1989
1	Viadotto, Targia-Siracusa		23	Concrete beams	EP	1989
3	Napoli-Bari (retrofitted)	160–390	720	PCB	EP	1989–1990
1	*3rd Line, Roma-Napoli		580	Concrete beams	LRB	1990
7	*Milano-Napoli	100–200	1,000	PCB	EP	1990–1991
1	Santa Barbara, railway overpass		120	Concrete slab	EP	1990
1	Tora, Firenze-Pisa-Livorno		5,000	Steel girders	EP multidirectional	1990
3	Roma-L'Aquila	230–500	1,200	Box girders	Pneudynamic + RB	1990–1991
2	Salerno-Reggio	190, 390	600	Concrete beams	OL	1990
1	Railway Rocca Avellino		400	Concrete beams	OL	1990
1	SS 206, Firenze-Pisa-Livorno		2,500	Steel girders	EP	1990
1	Tiasca, Trafori highway		1,610	PCB	Elastic buffers	1990
1	Vesuvio, SS 269		1,860	PCB	Elastic buffers	1990
3	Messina-Palermo	900	900	Prestressed concrete box girder	EP (long)	1990
1	Mortaiolo, Livorno-Civitavecchio		9,600	Prestressed concrete slabs	EP with shock absorbers	1990–1992
1	S Antonio, Bretella		700	Prestressed concrete	EP with shock absorbers	1991
2	Salerno-Reggio	350. 500	850	PCB	EP	1991
2	PN-Conigliano	500, 800	1,300	Prestressed concrete	EP	1991
1	Minuto, Fondo Valle Sele		1,000	PCB	OL	1991
3	Roma-L'Aquila-Teramo	200–300	700	Box girders	OL	1991–1992

www.EngineeringBooksPDF.com

Table 2.34 (continued)

No. of bridges	Name/location	Range of lengths (m)	Total length (m)	Superstructure type	Isolating system	Date completed
1	Poggio Ibema, Livorno-Civitavecchia		2,500	PCB	OL	1991–1992
3	Livorno-Cecina	600–1800	2,800	PCB	EP, EP + RB	1991–1992
1	*Rumeano, Via Salaria		340	PCB	EP	Retrofit designed
1	Viadotto No 2, Tangenziale Potenza		240	PCB	EP	1990
1	Angusta, Siracusa		450	Boxed RC beams	EL	1990
7	*Salerno-R Calabria	100–500	1,800	PCB with connecting slabs	EP	Retrofit designed
1	Fragneto		870	Steel box girder with RC slabs	EP devices on piers, with ST long. Highest piers connected	Designed
1	Ponte Nelle Alpi, Via Veneto-Pian di Vedoia		310	Steel box girder with RC slabs	Long: EP with ST Transv: EP on all piers	Designed

Key:
EP = Elastic – plastic behaviour
EL = Elastic
OL = Oleodynamic system (EP equivalent)
SL = Sliding support
ST = Shock transmitter system associated with SL
RB = Rubber bearings
LRB = Lead-rubber bearings
RC = Reinforced concrete
PCB = Prestressed concrete beams
Notes:
Where bridges are two-way, they have been regarded as a single bridge in estimating the length.
The total length of isolated bridges is thus greater than 100 km.
Of the more recent bridges (1985–1992), typical design values of the parameters are
Yield/weight ratio: 5–28%, with a representative value of 10%.
- Maximum seismic displacement: ±30 to ±150 mm, with a representative value of ±60 mm.
- Peak ground acceleration: 0.15–0.40 g, with a representative value of 0.25g.

Known retrofits are indicated with an asterisk (*)
Information and data collected from the Italian Embassy in London by the author.
Information collected from Research Library, Westminster, London by the author.
Research data from the Research Library, Westminster, London by the author.
Note: Research Data from the Times documents in Westminster Research Library, London by the author.

www.EngineeringBooksPDF.com

Table 2.35 Various applications and possibilities of using response-controlled structures in buildings

Effect/technical theme	Building application							
	Housing a	General office building b	Public high-rise building c	Disaster preventive building d	Art gallery/ museums facility e	Atomic power facility f	Hospital facility g	Modern industrial facility h
1. Ensure safety of building structure	Safe	Safe	Safe	Safe	Safe	Safe	Safe	Safe
2. Freedom in design of cross-section of members	Economy, design freedom	Economy, design freedom						
3. Prevent vibrations, sliding, rolling of contents	Safe	Satisfactory performance	Satisfactory performance	Satisfactory perfor-mance	Protect the exhibits	Protect contents. Satisfactory performance. Prevent hazardous discharge	Protect contents. Satisfactory performance. Prevent hazardous discharge	Satisfactory performance. Prevent hazardous discharge
4. Prevent loss of secondary materials	Safe economy, design freedom	Safe economy, design freedom	Satisfactory performance	Satisfactory performance	Satisfactory performance	Satisfactory performance	Satisfactory performance	Satisfactory performance
5. Sensitivity control when the vibrations are not comfortable	Satisfactory living conditions	Satisfactory living conditions	Satisfactory living conditions					
6. Maintain proper functioning of machinery, equipment, etc.	Satisfactory performance	Satisfactory performance	Satisfactory performance					

Note: They are collected and then placed in the correct order from numerous literature on earthquakes and buildings related to earthquakes. They are based on constructed facilities.

www.EngineeringBooksPDF.com

Table 2.36

Item	(0) Hachiya Apartments	(1) Christian Data Center	(2) Okumura group	(3) Obayashi Group Technical Research Center	(4) Dieres Industries Fujizawa site TC wing	(5) Funabashi Taketomo Dormitory	(6) Okumura Group
Designed by	Tokyo Building Research Center	Tokyo Building Research Center, Unitika	Tokyo Building Research Center, Okumura group	Obayashi group	Oires Industries, Symiono Constructions, Yasui Building	Takenaka Komyten	–
Design requirements		Antiseismic. Prevent any damage to goods stored	Antiseismic. Protect computer and stored data for technical	Antiseismic. Protection of computer and other laboratory equipment	Designers	Safety and fire resistance during earthquake	–
No. of floors	+2	+2, −1	+4	No. of floors	+5	+5	+3
Built-up area, m^2	60.18	226.21	348.18	Built-up area, m^2	351.92	1136.5	719.28
Application	Housing (residential	Data house	Research center	Application	Laboratory	Research laboratory and office	Dormitory
Structure	RCC frame (shear wall)	RCC frame (shear wall)	RCC frame	Structure	RC	RC	RC
Foundation	Raft foundation with cast in situ piles	Deep foundation	RCC cast in situ raft	Foundation	PHC tie (cement grout method)	Concrete in situ raft (each-drilling method)	Concrete in situ raft (earth-drilling method)
Isolator: Dimensions, mm	82 × 300 dia	Rubber 5 thick × 300 dia (12 layers)	Rubber 7 thick × 500 dia (14 layers)	Isolator: Dimensions, mm	Rubber 4.4 thick × 740 dia (61 layers)	Rubber 10 thick × 24 dia (H = 363), OD = 650, 700, 750, 800)	Rubber 7 thick × 670 dia (19 layers) (H = 187)
							Rubber 8 thick × 700 dia (18 layers) (H = 195)
Numbers	6	32	25	Numbers	14	35	14
Supporting force	σ = 45 kg/cm^2, 0.5 t/cm (32 t)	σ = 60 kg/cm^2, 0.5 t/cm (42.5 t)	σ = 60 kg/cm^2, 0.86 t/cm (120 t)	Supporting force	200 t		200 t → 6 Nos.
							150 t → 8 Nos.
Response-control device	Friction force between PC plates	Uses plastic deformation of steel bars bent to make a loop (8 Nos.)	Uses plastic deformation of steel bars bent to make a loop (12 Nos.)	Response-control device	Uses elasto-plastic recovery of steel bars (96 Nos.)	Lead plug inserted in laminated rubber	Viscous damper (8 Nos.)
Shear force coefficient used in design	0.2	0.15	0.15	Shear force coefficient used in design	0.15	0.2	0.15
Fundamental period Small deformation	1.83 s	14 s	1.4 s	Fundamental period Small deformation	X = 1.33 s	X = 0.895 s	X = 2.09 s
					Y = 1.24 s	Y = 0.908 s (at 50% deflection)	Y = 2.10 s
Large deformation		1.9 s	2.1 s	Large deformation	X = 3.12 s	X = 2.143 s	

Note: Data collected from the British Library in London by the author and placed in the given order.

www.EngineeringBooksPDF.com

Table 2.36 (continued)

Item	(0) Hachiya Apartments	(1) Christian Data Center	(2) Okumura group	(3) Obayashi Group Technical Research Center	(4) Dieres Industries Fujizawa site TC wing	(5) Funabashi Taketomo Dormitory	(6) Okumura Group
					$Y = 3.08$ s	$Y = 2.148$ s (at 100 % deflection)	
Incident seismic wave	El Centro 1940 (NS)	El Centro 1940 (NS)	El Centro 1940 (NS)	Incident seismic wave	El Centro 1940 (NS)	El Centro 1940 (NS)	El Centro 1940 (NS)
	Hachinohe 1968 (NS)	Hachinohe 1968 (NS)	Taft 1952 (EW)		Hachinohe 1968 (NS)	Hachinohe 1968 (NS)	Taft 1952 (EW)
	Hachinohe 1968 (EW)	Taft 1952 (EW)	Hachinohe 1968 (NS)		Hachinohe 1968 (EW)	Hachinohe 1968 (EW)	Tokyo 101 1956 (NS)
	Taft 1952 (EW)				Taft 1952 (EW)	Taft 1952 (EW)	Hachinohe 1968 (NS)
					Man-made earthquake two waves	KT 008 1980 (NS)	Man-made earthquake four waves
						Man-made earthquake two waves	
Input level	300 gal	300 gal, 450 gal	300 gal, 450 gal	Input level	25 cm/s, 50 cm/s	25 cm/s, 50 cm/s	25 cm/s, 50 cm/s
Item	(6) Kashima Constructions Research Center, Nishi Chofu Acciystue	(7) Christian Data Center (reapplied)	(8) Fukumiya Apartments	(9) Shibuya Shimizu Building No. 1	(10) Fujita Industries, 6th Laboratory		(11) Inorganic Materials Research Center, Vibration-Free Wing
1	2	3	4	5	6		7
Designed by	Kashima Constructions	Tokyo Building Research Center	Okumura group	Obayashi group	Fujita Kogyo		Secretariat of the Ministry of construction, Planning Bureau
Design requirements	Reduce seismic input and insulate (isolate) from Earth's vibrations	Anti-seismic. Prevent any damage to stored goods	Safety of building. Added value in business	Protect the main building and OA equipment installed therein	Protect the main building and the equipment stored therein such as laboratory equipment and computers		Protect the main building and research equipment stored therein
No. of floors	+2	+2	+4	+5, –2	+3		+1
Built-up area, m^2	379.10	149.43	225.40	560.30	102.21		8,341 (old – 7,725; new – 616)
Application	Research laboratory	Data house	Cooperative housing	Office	Research laboratory		Research center
Structure	RC	RC	RC	RCC	RCC		RCC

www.EngineeringBooksPDF.com

Table 2.36 (continued)

Item	(0) Hachiya Apartments	(1) Christian Data Center	(2) Okumura group	(3) Obayashi Group Technical Research Center	(4) Dieres Industries Fujizawa site TC wing	(5) Funabashi Taketomo Dormitory	(6) Okumura Group
Foundation	Concrete in situ raft (deep foundation)	Deep foundation	Concrete in situ raft (miniature earth-drilling method)	Concrete in situ raft (earth-drilling method)	PHC pile (type A, B) cement grout method		PHC raft (type A) blast method
Isolator: Dimensions, mm	320 × 1340 (48 thick × 5 dia); 308 × 1080 (38 thick × 6 dia)	4 thick × 435 dia (25 layers)		5.0 thick × 620 dia (50 layers); 6.0 thick × 740 dia (45 layers)	4.0 thick × 450 dia (44 layers)		3.2 thick × 420 dia (62 layers)
Numbers	18	12		20	4		32
Supporting force	165 t : 1340 dia	σ = 60 kg/cm^2; 0.55 t/cm (90 t)		100-150 t : 620 dia			65 t (max 80 t)
	100 t: 1080 dia			200-250 t : 740 dia			
Response-control device	Elasto-plastic damper using mild steel bars (14 Nos.)	Uses plastic deformation of steel bars bent to make a loop (6 Nos.)	Uses plastic deformation of steel bars bent to make a loop (7 Nos.)	Elasto-plastic damper using mild steel bars (48 Nos.)			Elasto-plastic damper using mild steel bars (108 nos.)
Shear force coefficient used in design	0.2	0.15	0.2	0.15: Basement, 1st floor; 0.183: 3rd floor ; 0.205: 5th floor	0.15: 1st floor, 0.17: 2nd floor; 0.20: 3rd floor		0.15
Primary period Small deformation	X = 0.828 s	1.3 s	1.4 s	X = 1.30 s	1.35 s		X = 1.17 s
	Y = 0.809 s			Y = 1.24 s			Y = 1.17 s
Large deformation	1.80 s	1.9 s	2.2 s	X = 2.99 s			X = 2.26 s
				Y = 2.97 s			Y = 2.26 s
Incident seismic wave	El Centro 1940 (NS)	El Centro 1940 (NS)	El Centro 1940 (NS)	El Centro 1940 (NS)	El Centro 1940 (NS)		El Centro 1940 (NS)
	Taft 1952 (EW)	Taft 1952 (EW)	Taft 1952 (EW)	Taft 1952 (EW)	Taft 1952 (EW)		Taft 1952 (EW)
	Tokyo 101 1956 (NS)	Hachinohe 1968 (NS)	Tokyo 101 1956 (NS)	Hachinohe 1968 (NS)	Hachinohe 1968 (NS)		Hachinohe 1968 (NS)
	Sendai THO38-1 1978 (EW)		Hachinohe 1968 (NS)	Hachinohe 1968 (EW)	Hachinohe 1968 (EW)		Hachinohe 1968 (EW)
				Sdkanrig, Sdkantig, Sdansrig } Man - made seismic waves	Artm 79L00 (seismic wave)	Tsukuba 85 NS, Tsukuba 85 EW, Tsukuba 86 NS, Tsukuba 86 EW }	Observed seismic waves
Input level	25 cm/s, 50 cm/s	300 gal, 450 gal	25 cm/s, 50 cm/s	25 cm/s, 50 cm/s	25 cm/s, 50 cm/s		25 cm/s, 50 cm/s

Notes:
Designers data collected by the author from stated companies in Japan.
Data collected from U.S.A and Japanese reports, British Library, Kingscross, London by the author. They are placed under topics.
Data collected from the companies in the reports available with British Library, London. They are placed under topics.

www.EngineeringBooksPDF.com

evaluated. The spectral acceleration level is about the same in all codes mentioned here. The velocity versus coverage (average) was taken by Soong et al. to be 210 m/s.

Data on Constructed Facilities

Some constructed building and other structural facilities have been examined with respect to the usage of seismic devices and are categorized on the basis of the types of structures and seismic devices installed to control and minimize various parameters inclusive of disastrous vibrations included by the earthquakes. Tables (2.34) to (2.36) give the details of the constructed facilities where various devices have been installed.

Bibliography

Abe, M., and Fujino, Y. Dynamic characteristics of multiple tuned mass dampers and some design formulas. *Earthquake Eng. Struct. Dyn.* 1994; 23(8), 813–836.

Algeria RPA (1999) Algerian Earthquake Resistant Regulation-Document Technique, Reglementaire (DTR) 1982

Argentina INPRESS-CIROSC 103 (1991) -Australian standard AS1170-4-1993 Minimum Design Roads on structures Pa A4, Earthquake loads 1996

Australia AS I 1704 (1993) -Australian standard AS1170-4-1993 Minimum Design Roads on structures Pa A4, Earthquake loads 1996

Beliayev, V.S., Vinogradov, V.V., and Guskov, V.D. Most recent development of the studies for seismic isolation of nuclear structures in Russia, International Post-Smirt Conference Seminar on Seismic Isolation, Passive Energy Dissipation and Control of Vibrations of Structures, Santiago, Chile, 1995.

Bishop, R.E.D. and Welbourn, D.B. The problem of the dynamic vibration absorber. *Engineering, London*, 1952, 174, 769.

Brock, J.E. A Note on the Damped Vibration Absorber. *J. Appl. Mech.* 13(4), A-284.

Carter, W.J., and Lin, F.C. Steady-state behavior of nonlinear dynamic absorber. *J. Appl. Mech.* 1961; 60-WA-14, 67–70.

Chang, J.C.H., and Soong, T.T. Structural control using active tuned mass dampers. *J. Eng. Mech. Div. ASCE* 1980; 106(EM6): 1091–1098.

China T J 11-78 and GB J11-89

Chowdhury, A.H., Iwuchukwu, M.D., and Garske, J.J. *The Past and Future of Seismic Effectiveness of Tuned Mass Dampers, Structural Control* (Leipholz, H.H.E., ed.), Martinus Nijhoff Publishers, Dordrecht, 1987; 105–127.

Clarke, A.J. Multiple passive tuned mass damper for reducing earthquake induced building motion, Proc. 9th Wld. Conf. Earthquake Eng., 5, Japan, 1988; 779–784.

Den Hartog, J.P. *Mechanical Vibrations*, 4th edition, McGraw-Hill, New York, 1956.

Ding, J.H., and Ou, J.P. Theoretical study and performance experiment for cylinder with holes viscous damper. *World Inf. Earthquake Eng.* 2001; 17(1): 30–35 (in Chinese).

Englekirk, R., *Seismic Design of Reinforcement and Precast Concrete Buildings*. Wiley, New York, 2003.

ENR. Hancock Tower Now to Get Dampers, Engineering News-Record, Oct. 30, 1975; 11.

ENR. Tower Cables Handle Wind, Water Tank Dampens It, Engineering News-Record, Dec. 9, 1971; 23.

Europ 1-1 OCT(94), Eurocode 8-Design provisions for Earthquake Resistance of structures ENV 1994–1998

www.EngineeringBooksPDF.com

Fajfar, P. Equivalent ductility factors taking into account low-cycle fatigue. *Earthquake Eng. Struct. Dyn.* 1992, 21, 837–848.

Falcon, K.C., Stone, B.J., Simcock, W.D., and Andrew, C. Optimization of vibration absorbers: A graphical method for use on idealized systems with restricting damping. *J. Mech. Eng. Sci.* 1967, 9, 374–381.

Frahm, H. Device for Damped Vibrations of Bodies, U.S. Patent No. 989958, Oct. 30, 1909.

Fu, Y., and Kasai, K. Comparative study of frames using viscoelastic and viscous dampers. *J. Struct. Eng., Am. Soc. Civil Eng.* 1998; 122(10), 513–522.

Fujita, T. Studies about vibration isolating floor using pre-stretched or pre-compressed springs (Part 2. Vibration characteristics and vibration isolator properties II.). *Seisan Kenkyu*, December, 1980; 32(10), 28–31.

Fujita, T., Hattori, S., and Ishida, J. Studies about vibration isolating floor using pre-stretched or pre-compressed springs (Part 1. Vibration characteristics and vibration isolator properties I.). *Seisan Kenkyu*, August, 1980; 32(8), 48–51.

Fujita, T., Hattori, S., and Ishida, J. Studies about vibration isolating floor using pre-stretched or pre-compressed springs (Part 3. Vibration characteristics and vibration isolator properties III.). *Seisan Kenkyu*, December, 1980; 32(12), 22–25.

Furukawa, Y., Kawaguchi, S., Sukagawa, M., Masaki, N., Sera, S., Kato, N., Washiyama, Y., and Mitsusaka, Y. Performance and quality control of viscous dampers. Proc. Structural Engineers World Congress (SEWC), Yokohama, JAPAN, CD-Rom, T3-3-3, 2002.

Garcia de Jalon, J., and Bayo, E. *Kinematic and Dynamic Simulation of Multibody Systems: The Real Time Challenge*. Springer, Berlin, 1994.

GB50011-2001. *Code for Seismic Design of Buildings*. China Building Industry Press, Beijing, China (in Chinese), 2001.

Housner, G.W. et al. Structural control: Past, present and future. *J. Struct. Eng. ASCE* 1997; 123(9): 897–971.

India Pakistan Criteria for Earthquake Resistant designing structures fifth revision Part I IS 1893 (Part 1) 2002

Iran ICSRD (1988) Iranian code for seismic design of Buildings 1988. Building Housing regional centre, Tehran.

Ishikawa, K., Okuma, K., Shimada, A., Nakamura, H., and Masaki, N. JSSI Manual for Building Passive Control Technology: Part-5 Performance and Quality Control of Viscoelastic Dampers (Companion Paper, Presented at 13WCEE).

ISO3010: 1988 Base for design of structures_Seismic Actions on Structures. Notification of No.1446 of Ministry of Construction, Japan/May 31, 2000. Notification of No.2009 of Ministry of Construction, Japan/May 31, 2000

Israel IC-413 (1994) SI 413 Design provision for Earthquake Resistant of structures. Standard Institute of Israel 1988.

Italy CNR-GNDT (1986) & Eurocode Technical Rulers for Constructions in seismic zones Public works ministry 2000.

Iwan, W.D., and Gates, N.C. Estimating earthquake response of simple hysteretic structures. *J. Eng. Mech. Div. ASCE* 1979; 105(EM3): 391–405.

Izumi, M. Mitsuhashi, H., Sasaki, T., Katsukura, H., and Aizawa, F. Studies about damping of vibrations in buildings. Basic studies about energy dissipation-type structure. *Nippon Kecnchiku Gakkai, Tohoku-shibu*, February, 1980; 85–88.

Jangid, R., and Londhe, Y. Effectiveness of elliptical rolling rods for base isolation. *J. Struct. Eng. (ASCE)* 1988; 124: 469–472.

Jangid, R.S. Response of pure-friction sliding structures to bi-directional harmonic ground motion. *Eng. Struct.* 1997; 19: 97–104.

Jangid, R.S. Seismic response of sliding structures to bi-directional earthquake excitation. *Earthquake Eng. Struct. Dyn.* 1996; 25: 1301–1306.

www.EngineeringBooksPDF.com

Japan BLEO (1981) Part 1, Earthquake Resistant Design of Structures Part 2, Earthquake Resistant Design of Building (Tokyo Japan, 2000)

JSSI Manual. Design and Construction Manual for Passively Controlled Buildings, Japan Society of Seismic Isolation (JSSI), First Edition, Tokyo, JAPAN, October (in Japanese, 405 pages), 2003.

Kanada, M., Kasai, K., and Okuma, K. Innovative passive control scheme: a Japanese 12-story building with stepping columns and viscoelastic dampers. Proc. Structural Engineers World Congress (SEWC), Yokohama, JAPAN, CD-ROM, T2-2-a-5, 2002.

Kasai, K., and Kibayashi, M. JSSI Manual for Building Passive Control Technology, Part-1 Manual Contents and Design Analysis Methods", 13WCEE, No.2989, 2004.

Kasai, K., and Kibayashi, M. JSSI Manual for Building Passive Control Technology: Part-1 Control Device and System (Companion Paper, Presented at 13WCEE).

Kasai, K., and Nishimura, T. Equivalent linearization of passive control system having oil damper bi-linearly dependent on velocity. *J. Struct. Constr. Eng.* (Transaction of AIJ), (in Review), (in Japanese), 2004.

Kasai, K., and Okuma, K. Accuracy enhancement of Kelvin-type modeling for linear viscoelastic dampers. A refined model including effect of input frequency on, 2002

Kasai, K., and Okuma, K. Kelvin-type formulation and its accuracy for practical modeling of linear viscoelastic dampers (Part1: One-Mass System Having Damper and Elastic / Inelastic Frame). *J. Struct. Constr. Eng.* (Transactions of AIJ), No. 550, 2001; 71–78, Dec. (in Japanese).

Kasai, K., Ito, H., and Watanabe, A. Peak response prediction rule for a SDOF elasto-plastic system based on equivalent linearization technique. J. Struct. Constr. Eng. (Transactions of AIJ), No. 571, 2003; 53–62, Sep. (in Japanese).

Kasai, K., Kibayashi, M., Takeuchi, T., Kimura, Y., Saito, Y., Nagashima, I., Mori, H., Uchikoshi, M., Takahashi, O., and Oohara, K. Principles and current status of manual for design and construction of passively-controlled buildings: Part-1: Background scope, and design concept. Proc. Structural Engineers World Congress (SEWC), Yokohama, JAPAN, CD-ROM, T2-2-a-1, 2002.

Kasai, K., Suzuki, A., and Oohara, K. Equivalent linearization of a passive control system having viscous dampers dependent on fractional power of velocity. J. Struct. Constr. Eng. (Transactions of AIJ), No. 574, 2003; 77–84, Dec. (in Japanese).

Kibayashi, M., Kasai, K., Tsuji, Y., Kato, S., Kikuchi, M., Kimura, Y., and Kobayashi, T. Principles and current status of manual for design and construction of passively-controlled buildings: Part-2: JSSI Criteria for Implementation of Energy Dissipation Devices. Proc. Structural Engineers World Congress (SEWC), Yokohama, JAPAN, CD-ROM, T3-3-1, 2002.

Kibayashi, M., Kasai, K., Ysuji, J., Kukuchi, M., Kimura, Y., Kobayashi, T., Nakamura, J., and Matsubsa, Y. JSSI Manual for Building Passive Control Technology, Part-2 Criteria for Implementation of Energy Dissipation Devices, 13WCEE, No. 2990, 2004.

Kobori, T, and Minai, R., Analytical study on active seismic response control: Seismic-response-controlled structure 1. *Trans. Architectural Inst. Japan* 1960; 66: 257–260 (in Japanese).

Kobori, T, and Minai, R., Condition for active seismic response control: seismic-response-controlled structure 2. *Trans. Architectural Inst. Japan* 1960; 66: 253–256 (in Japanese).

Kobori, T. Quake resistant and nonlinear problems of the structural vibrations to violent earthquake. *J. Kyoto University Disaster Prevention Laboratory*, 5th Anniversary Edition 1956; 116–124 (in Japanese).

Kobori, T. The direction of earthquake resistant engineering. *J. Architecture Building Sci.* 1958; 73: 5–9 (in Japanese).

Kobori, T., Koshika, N. Yamada, K., and Ikeda, Y. Seismic-response-controlled structure with active mass driver system. Part 1: Design. *Earthquake Eng. Struct. Dyn.* 1991; 20: 133–149.

www.EngineeringBooksPDF.com

Kobori, T., Koshika, N. Yamada, K., and Ikeda, Y. Seismic-response-controlled structure with active mass driver system. Part 2: Verification, Design. *Earthquake Eng. Struct. Dyn.* 1991; 20: 151–166.

Krieg, R.D., and Krieg, D.N. Accuracy of numerical solution methods for the elastic, perfectly plastic model. *Pres. Ves. Technol.* 1997; 99: 510–515.

Kumaya, K., Arano, T., Kurihara, M., and Sasai, H. Structure incorporating sliding elements and rubber in the foundations of buildings (Part 2. Rocking vibrations developed in a vibration isolator structure developed at the time of sliding). *Nippon Kikai Gakkai Koen Ronbun-shu*, No. 800–3, 1980; 89–91.

Kumaya, K., Arano, T., Kurihara, M., Sasai, H. Structure incorporating sliding elements and rubber in the foundations of buildings (Part 2. Methods of response analysis in a multi-freedom systems and comparison with experimental findings). *Nippon Kikai Gakkai Koen Ronbun-shu*, No. 800–3, 1980; 92–94.

Li, Z., Rossow, E.C., and Shah, S.P. Sinusoidal forced vibration of sliding masonry system. *Struct. Eng. ASCE* 1989; 115: 1741–1755.

Liaw, T.C., Tian, Q.L., and Cheung, Y.K., Structures on sliding base subjected to horizontal and vertical motions. *Struct. Eng. ASCE* 1988; 114: 2119–2129.

Lin, B.C., and Tadjbakhsh, I.G. Effect of vertical motion on friction driven systems. *Earthquake Eng. Struct. Dyn.* 1986; 14: 609–622.

Lin, T.W., Chern, C.C., and Hone, C.C. Experimental study of base isolation by free rolling rods. *Earthquake Eng. Struct. Dyn.* 1995; 24: 1645–1650.

Lu, L.Y., and Yang, Y.B. Dynamic response of equipment in structures with sliding support. *Earthquake Eng. Struct. Dyn.* 1997; 26: 61–77.

Makris, N., Dargush, G.F., and Constantinou, M.C. Dynamic analysis of viscoelastic fluid dampers. *J. Eng. Mech. ASCE*, 1995; 121(10), 1114–1121.

Masri, S.F., Bekey, G.A., and Caughey, T.K. On-line control of nonlinear flexible structures. *J. Appl. Mech. ASME* 1982; 49: 877–884.

Mathworks, Inc., MATLAB, Reference Guide. Natick, MA, 1999.

Matsushita, S., Nomura, M., and Sasaki, T. Recovery properties of steel pipe type response-control device. *Nippon Kenchiku Gakkai, Tohoku-shibu*, March, 1980; 129–132.

Mexico UNAM (1983) M111 (1988)

Miyazaki, N., and Mitsusaka, Y. Design of a building with 20% or greater damping, Tenth World Conf. Earthquake Eng., Madrid, 1992; 4143–4148.

Mokha, A., Constantinou, M.C., and Reinhorn, A.M. Verification of friction model of Teflon bearings under triaxial load. *Struct. Eng. ASCE* 1993; 119: 240–261.

Mori, M., Arano, T., Kataoka, T., Ochiai, K., and Sasai, H. Structure incorporating sliding elements and rubber in the foundations of buildings (Part 1). *Nippon Kikai Gakkai Koen Ronbun-shu*, No. 800–3, 1980; 88–91.

Mostaghel, N., and Khodaverdian, M. Dynamics of resilient-friction base isolator (R-FBI). *Earthquake Eng. Struct. Dyn.* 1987; 15: 379–390.

Mostaghel, N., and Tanbakuchi, J. Response of sliding structures to earthquake support motion. *Earthquake Eng. Struct. Dyn.* 1983; 11: 729–748.

Mostaghel, N., Hejazi, M., and Tanbakuchi, J. Response of sliding structure to harmonic support motion. *Earthquake Eng. Struct. Dyn.* 1983; 11: 355–366.

Nakagawa, K., Watanabe, S., and Shimaguchi. S. Experimental studies about dynamic floor system (Part 2) – Vibration experiment with a computer using vibration table. *Dairin-gumi gijutsu Kenkyusho-ho*, No. 17, 1978; 17–21.

Nakata, Y. Performance and quality control of steel hysteretic damper. Proc. Structural Engineers World Congress (SEWC), Yokohama, Japan, CD-ROM, T3-3-5, 2002.

Nakata, Y., Hirota, M., Shimizu, T., and Iida, T. JSSI manual for building passive control technology: Part-6 performance and quality control of steel dampers (Companion Paper, Presented at 13WCEE).

www.EngineeringBooksPDF.com

New Zealand NZS 4203 (1992) and NZNSEE (1988) general structures designs, design loading for buildings. Standards association of New Zealand 2004.
Nishitani, A. Application of active structural control in Japan. *Prog. Struct. Eng. Mater.* 1998; 1(3): 301–307.
Niwa, N., Kobori, T., Takahashi, M., Hatada, T., Kurino, H., and Tagami, J. Passive seismic response controlled high-rise building with high damping device. *Earthquake Eng. Struct. Dyn.* 1995, 24, 655–671.
Okuma, K., Ishikawa, K., Oku, T., Sone, Y., Nakamura, H., and Masaki, N. Performance and quality control of viscoelastic dampers. *Proc. Structural Engineers World Congress (SEWC)*, Yokohama, Japan, CD-ROM, T3-3-4, 2002.
Okuma, K., Kasai, K., and Tokoro, K. JSSI manual for building passive control technology: Part-10 time-history analysis model for viscoelastic dampers (Companion Paper, Presented at 13WCEE), 2002.
Oldham, K.B., and Spanier, J. *The Fractional Calculus*. Academic Press, New York, 1974.
Ooki, Y., Kasai, K., and Amemiya, K. JSSI manual for building passive control technology: Part-11 Time-history Analysis Model for Viscoelastic Dampers Combining Iso-Butylene and Stylene Polymers (Companion Paper, Presented at 13WCEE).
Ou, J.P., and Zou, X. Experimental study on properties of viscoelastic damper. *J. Vibration Shock* 1999; 18(3): 12–19 (in Chinese).
Ou, J.P., He, Z., Wu, B., and Long, X. Seismic damage performance design for RC structures. *J. Building* (in Chinese), 2001; 21:1, 63–73.
Ou, J.P., Niu, D., and Wang, G. Seismic damage estimation and optimal design of nonlinear RC structures. *J. Civil Eng.* (in Chinese), 1993; 26:5, 14–21.
Ou, J.P., Wu, B., and Long, X. Parameter analysis of passive energy dissipation systems. *Earthquake Eng. Vibration* 1998; 18(1): 60–70 (in Chinese).
Park, Y.J., and Ang, A. H.-S. Mechanistic seismic damage model for reinforced concrete. *J. Struct. Eng.* 1985; 111(4): 722–739.
Pekcan, G., Mander, J.B., and Chen, S.S. The seismic response of a 1:3 scale model R.C. structure with elastomeric spring dampers. *Earthquake Spectra*, 1995; 11(2), 249–267.
Press, W.H., Teukolsky, S.A., Vetterling, W.T., and Flannery, B.P. Numerical recipes in FORTRAN, Cambridge University Press, Cambridge, UK, 1992.
Petersen et al. Dynamic analysis with tuned mass dampers private communication (Two reports 1995).
Qumaroddin, M., Rasheedazzafar, Arya, A.S., and Chadra, B. Seismic response of masonry buildings with sliding substructure. *Struct. Eng. ASCE* 1986; 112: 2001–2011.
Reinhorn, A.M., and Li, C. Experimental and analytical investigation of seismic retrofit of structures with supplemental damping, Part III: Viscous Damping Walls, Technical Report NCEER-95-0013, National Centre for Earthquake Engineering Research, Buffalo, NY, 1995.
Reinhorn, A.M., Li, C., and Constantinou, M.C. Experimental and analytical investigation of seismic retrofit of structures with supplemental damping, Part I: Fluid Viscous Damping Devices, Technical Report NCEER-95-0001, National Centre for Earthquake Engineering Research, Buffalo, NY, 1995.
Schwahn, K.J., and Delinic, K. Verification of the reduction of structural vibrations by means of viscous dampers, Seismic Engineering, ASME, Pressure Vessel and Piping Conf., Pittsburgh, PA, 1988, 144, 87–95.
Sekiguchi, Y., Kasai, K., and Ooba, K. JSSI manual for building passive control technology: Part-13 Time-history Analysis Model for Viscous Dampers (Companion Paper, Presented at 13WCEE).
Sekiguchi, Y., Kasai, K., and Takahashi, O. JSSI manual for building passive control technology: Part-12 time-history analysis model for nonlinear oil dampers. (Companion Paper, Presented at 13WCEE).

www.EngineeringBooksPDF.com

Shames, I.H., and Dym, C.L. Energy and *Finite Element Methods in Structural Mechanics*. Hemisphere Publishing, New York, 1985.

Shimazu, T., and Hidco, A. Basic experimental studies on vibration isolator properties of layered walls. *Nippn Kenchiku Gakkai Taikai*, September, 1980; 755–757.

Soong, T.T., and Dargush, G.F. *Passive Energy Dissipation Systems in Structural Engineering*. Wiley, New York, 1997.

Spencer Jr. B.F., and Sain, M.K. Controlling buildings: A new frontier in feedback. IEEE Control Systems Magazine: Special Issue on Emerging Technologies (Samad, T. Guest ed.), 1997; 17(6): 19–35.

Suresh, S. *Fatigue of Materials*. Cambridge University Press, Cambridge, 1991.

Tanaka, K., Kawagushi, S., Sukagawa, M., Masaki, N., Sera, S., Washiyama, Y., and Mitsusaka, Y. JSSI manual for building passive control technology: Part-4 Performance and Quality Control of Viscous Dampers (Companion Paper, Presented at 13WCEE).

Taylor, D.P., and Constantinou, M.C. Fluid dampers for applications of seismic energy dissipation and seismic isolation. Proceedings of the Eleventh World Conference on Earthquake Engineering, Acapulco, Mexico, 1996.

Tezcan, S., and Civi, A. Reduction in Earthquake Response of Structures by Means of Vibration Isolators, Proc. Second U.S. National Conf. on Earthquake Engrg., Earthquake Engrg. Research Institute, Stanford Univ., California, 1979; 433–442.

Tsopelas, P., and Constantinou, M.C. NCEER-Taisei Corporation Research Program on Sliding Seismic Isolation Systems for Bridges: Experimental and Analytical Study of a System Consisting of Sliding Bearings and Fluid Restoring Force/Damping Devices, Technical Report NCEER-94-0014, National Centre for Earthquake Engineering Research, Buffalo, NY, 1994.

Tsuyuki, Y., Kamei, T., Gofuku, Y., Iiyama, F., and Kotake, Y. Performance and quality control of oil-damper. *Proc. Structural Engineers World Congress (SEWC)*, Yokohama, Japan, CD-ROM, T3-3-2, 2002.

Tsuyuki, Y., Kamei, T., Gofuku, Y., Kotake, Y., and Iiyama, F. JSSI manual for building passive control technology: Part-3 Performance and Quality Control of Oil Dampers (Companion Paper, Presented at 13WCEE).

USA UBC. 95 (1995) 2 SEAOC (1990) ASCE Minimum Design Loads for Buildings and other structures, ASCE, USA.

Vidic, T., Fajfar, P., and Fischinger, M. Consistent inelastic design spectra: Strength and displacement. Earthquake Eng. Struct. Dyn. 1992; 23: 507–521.

Warburton, G.B., and Soni, S.R. Errors in response calculations for non-classically damped structures. Earthquake Eng. Struct. Dyn. 1977, 5, 365–376.

Westermo, B., and Udwadia, F., Periodic response of a sliding oscillator system to harmonic excitation. *Earthquake. Eng. Struct. Dyn.* 1983; 11: 135–146.

Yang, J.N. Application of optimal control theory to civil engineering structures. *J. Eng. Mech. Div. ASCE* 1975; 101(6): 819–838.

Yang, Y.B., Lee, T.Y., and Tsai, I.C. Response of multi-degree-of-freedom structures with sliding supports. *Earthquake Eng. Struct. Dyn.* 19, 739–752, 1990

Yao, J.T.P. Concept of structural control. *J. Struct. Div. ASCE* 1972; 98(ST7): 1567–1574.

Yasui, H., and Iniwa, C. Experimental studies about dynamic floor system (Part1) – Sinusoidal forced damped vibration experiment on a large-scale model. Dairin-gumi Gijutsu Kenkyusho-ho, No. 16, 1978; pp. 46–50.

Yasunishi, K., and Tada, H. Discussions about aseismic isolator (steel, rubber lamination pad). *Nippon Kenchiku Gakkai Taikai*, September, 1980; 751–753.

Younis, C.J., and Tadjbakhsh, I.G. Response of sliding structure to base excitation. *Eng. Mech. ASCE* 1984; 110: 417–432.

www.EngineeringBooksPDF.com

www.EngineeringBooksPDF.com

Chapter 3
Basic Structural Dynamics

3.1 General Introduction

Most loads acting on structures are dynamic in origin. These loads can be suddenly applied or allowed to reach full magnitude after a considerable delay. On the other hand, the structures will have various degrees of freedom with unclamped or clamped free or forced vibrations. These need to be discussed prior to the introduction of earthquake analysis and design.

One of the most important applications of the theory of structural dynamics is in analysing the response of structures to ground shaking caused by an earthquake. In this chapter the reader can study the earthquake response of linear SDF systems to earthquake motions. By definition, linear systems are elastic systems and one shall also refer to them as linearly elastic systems to emphasize both properties. Because earthquakes can cause damage to many structures, one is also interested in the response of yielding or inelastic systems, the subject is known as non-linear structural dynamics.

The later part of this chapter is concerned with the earthquake response deformation, internal element forces, stresses and so on of simple structures as a function of time and how this response depends on the system parameters. Then one introduces the response spectrum concept, which is central to earthquake engineering, together with procedures to determine the peak response of systems directly from the response spectrum. This is followed by a study of the characteristics of earthquake response spectra, which lead into the design spectrum for the design of new structures and safety evaluation of existing structures against future earthquakes. A number of examples are given to the reader in order to understand the basis of structural dynamics in relation to earthquakes.

3.2 Structural Dynamics

3.2.1 General Introduction to Basic Dynamics

A number of textbooks and research papers have been written on the subject of structural dynamics in relation to earthquakes. Various mathematical models

M.Y.H. Bangash, *Earthquake Resistant Buildings*,
DOI 10.1007/978-3-540-93818-7_3, © M.Y.H. Bangash 2011

www.EngineeringBooksPDF.com

exist. In such models the number of independent coordinates specifies the position or configuration at any time. They are known as degrees of freedom. The structures can be idealized in some cases from a single degree of freedom to multiple degrees of freedom, depending on the nature of the problem. Sections 3.2.2, 3.2.3, 3.2.4 and 3.2.5 summarize these cases. They are included so that the reader becomes familiarized with the concepts of structural dynamics associated with seismic activities. Some case studies are included in the form of examples.

3.2.2 Single-Degree-of-Freedom Systems – Undamped Free Vibrations

3.2.2.1 The Mathematical Models

A mass M is suspended by a spring having a linear constant K (the force necessary to cause unit change of length, also called spring stiffness; units: lb/in or N/mm). Horizontal constraints are assumed, so that m can only be displaced vertically (Fig. 3.1):

$$\begin{aligned} W - K\Delta_{\mathrm{STAT}} &= 0 \\ W &= K\Delta_{\mathrm{STAT}} \end{aligned} \tag{3.1}$$

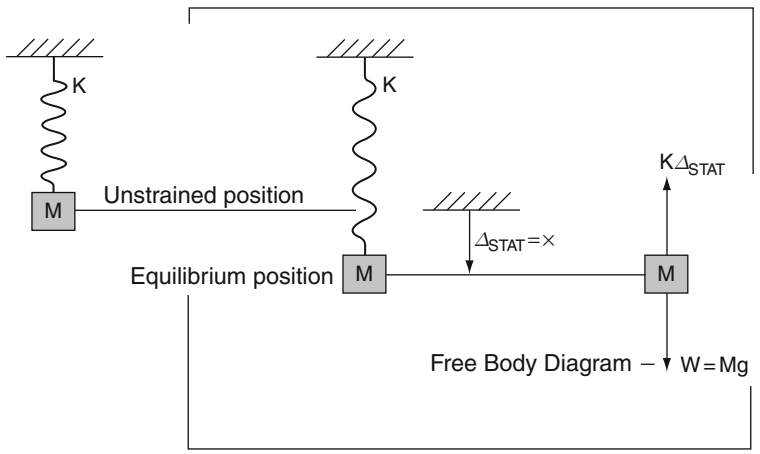


Fig. 3.1 The mass and its equilibrium position

The coordinate x defines the position of mass M at any time; positive δ is taken downwards, with the same sign convention for forces, accelerations, etc. (Fig. 3.2).

www.EngineeringBooksPDF.com

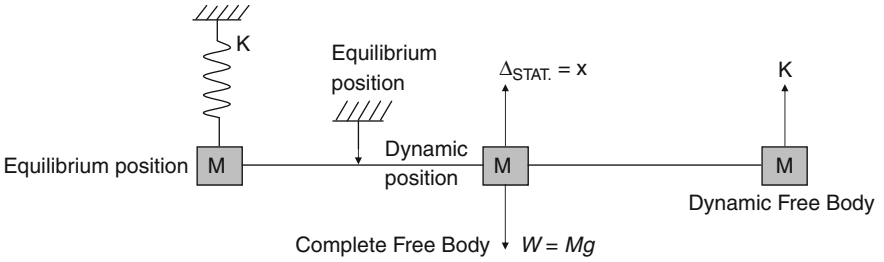


Fig. 3.2 Displacement of a mass from the equilibrium position and released

3.2.2.2 Setting Up the Differential Equation

(a) *By Newton's second law of motion*
The magnitude of the acceleration of a particle is proportional to the resultant force acting upon it and has the same direction and sense as this force:

$$\begin{aligned} \frac{dx}{dt} &= \dot{x} \text{ (velocity)} \\ \frac{d^2x}{dt^2} &= \ddot{x} \text{ (acceleration)} \\ \frac{d^2x}{dt^2} &= -K(\Delta_{\text{STAT}} + \delta) + W \\ \frac{d^2x}{dt^2} &= -Kx \end{aligned} \tag{3.2}$$

or

$$\ddot{x} + Kx = 0 \tag{3.3}$$

(b) By energy method
For a conservative system, the total energy of the system (potential and kinetic energy) is unchanged at all times.

$$\text{KE} + \text{PE} = \text{constant}$$

or

$$\frac{d}{dt} = (KE + PE) = 0 \tag{3.4}$$

$$KE = \frac{1}{2}Mx^2 \tag{3.5}$$

$$PE = \int_k^0 [w - k(\Delta_{\text{STAT}} + x)]dx = -\int_x^0 K_x d_x = \frac{K_{x^2}}{2} \tag{3.6}$$

$$\frac{d}{dt}\left(\frac{Mx^2}{2} + \frac{Kx^2}{2}\right) = 0 \text{ or } M\ddot{x} + Kx = 0 \tag{3.6a}$$

www.EngineeringBooksPDF.com

The motion defined is said to be harmonic, because of its sinusoidal form. The motion is repeated, with the time for one cycle being defined by the value ωt equals 2π. The *period* T or time for one cycle is

$$T = \frac{2\pi}{\omega} \tag{3.7}$$

The reciprocal of T is called *frequency* f (in cycles per unit time):

$$T = \frac{\omega}{2\pi} \tag{3.8}$$

The term ω is called *circular frequency*, and it is measured in radians per second:

$$\begin{aligned} \omega &= \sqrt{\frac{k}{M}} = \sqrt{\frac{k_g}{W}} = \sqrt{\frac{g}{\Delta_{\text{STAT}}}} \\ g &= 32.2\text{ft/s}^2\text{or } 386\text{ in/ s}^2\text{or } 9.81\text{m/s}^2 \\ \Delta_{\text{STAT}} &= \text{static deflection of the system} \end{aligned} \tag{3.9}$$

Remember to use consistent units when calculating ω or f. The last of the expressions (3.9) seems to be the most convenient in structural applications.

The velocity:

$$\begin{aligned} \dot{x} &= \dot{x}_0 \cos \omega t = x_0 \omega \ \sin \omega t \\ &= X\ \omega \cos(\omega t + \phi) = X\ \omega \sin(\omega t + \phi + \pi/2) \\ &= \dot{X} \cos(\omega t + \phi) \end{aligned} \tag{3.10}$$

amplitude of velocity:

$$\dot{X} = X\omega$$

acceleration:

$$\begin{aligned} \ddot{x} &= -\dot{x}_0 \omega \sin \omega t - x_0 \omega^2 \sin \omega t \\ &= -X\omega^2 \sin(\omega t + \phi) = X\omega^2 \sin(\omega t + \phi + \pi) \\ &= -\omega^2 x = -\ddot{X} \sin(\omega t + \phi) \end{aligned} \tag{3.11}$$

amplitude of acceleration:

$$\ddot{X} = X\ \omega^2$$

www.EngineeringBooksPDF.com

The velocity is ω times the displacement and leads it by 90°. The acceleration is ω^2 times the displacement and leads it by 180°.

Displacement, velocity, acceleration against ωt diagrams are shown in Fig. 3.3.

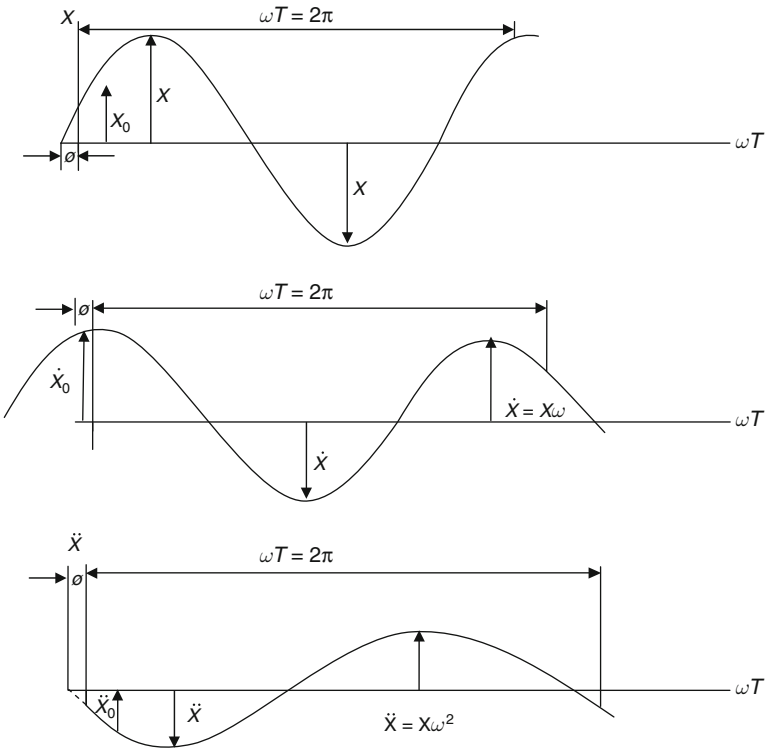


Fig. 3.3 Displacement, period, velocity and acceleration

The *phase angle* indicates the amount by which each curve is shifted ahead with respect to an ordinary sine curve:

$$\ddot{X} = X\,\omega \tag{3.12a}$$

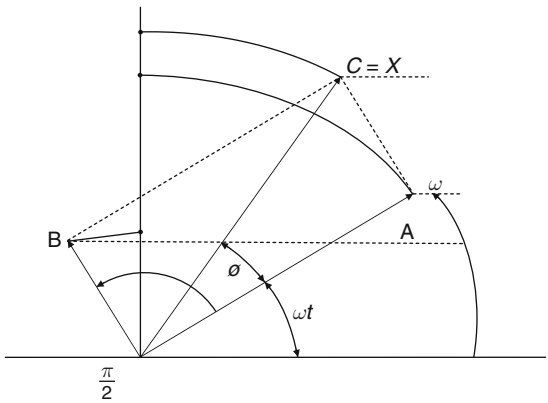
$$\ddot{X} = \dot{X}\,\omega = X\,\omega^2 \tag{3.12b}$$

The rotating vector concept: phase-plane solutions

The displacement x is given according to Figs. 3.4 and 3.5. Three vectors A, B and C whose relative positions are fixed rotate with angular velocity ω. Their angular position at any time t is ωt. A and B are at right angles and C leads A by

www.EngineeringBooksPDF.com

Fig. 3.4 The rotating vector



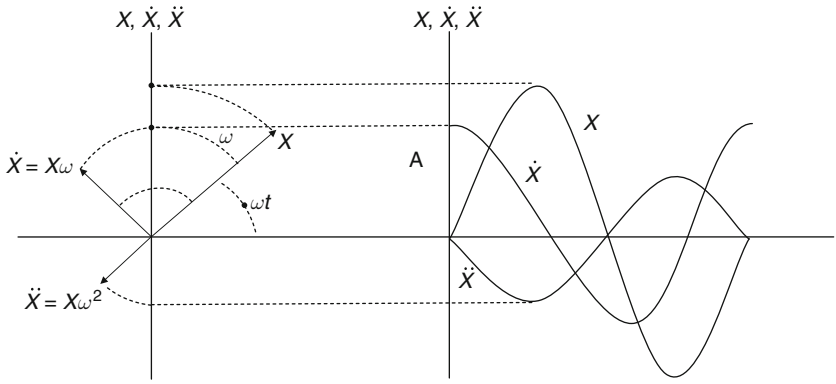


Fig. 3.5 Rotating displacements, velocities and accelerations

the phase angle ϕ. A graphical representation is obtained by vertically projecting the vectors onto the $x + \omega t$ graph.

$$\begin{aligned} \mathrm{A} &= \frac{x_0}{\omega} \\ \mathrm{B} &= x_0 \\ \mathrm{C} &= \sqrt{A^2 + B^2} = X \end{aligned} \tag{3.13a}$$

The velocity and acceleration curves, as well as the displacement, can be generated in this manner using rotating vectors $X, \dot{X}, \ddot{X}$. The velocity and acceleration vectors lead the displacement by 90° and 180°, respectively. Their relative position is fixed and they rotate with angular velocity ω:

www.EngineeringBooksPDF.com

$$
\begin{aligned}
x &= X\sin\omega t = \frac{\dot{x}_0}{\omega}\sin\omega t \qquad\qquad x_0 = 0!\\
\dot{x} &= X\,\omega\ \cos\ \omega t = \dot{X}\cos\omega t\\
\ddot{x} &= \omega^2 - X\sin\omega t = -X\sin\omega t
\end{aligned}
\tag{3.13b}
$$

3.2.3 Summary and Conclusions

3.2.3.1 Example

A beam with uniformly distributed mass m, and unit length, supporting a concentrated mass, M, at midspan is illustrated in Fig. 3.6.

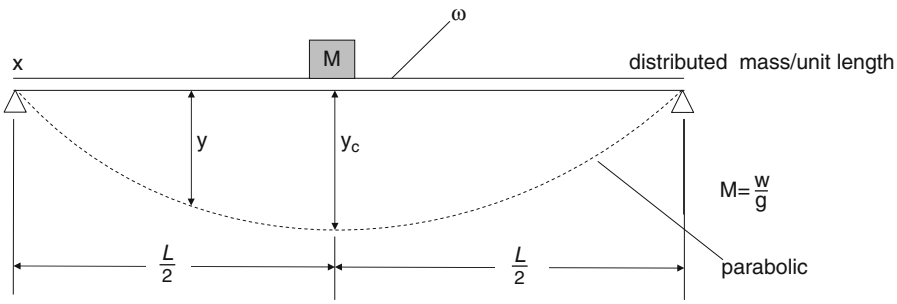


Fig. 3.6 Uniform mass on a beam

Making the assumption that the dynamic deflection curve is of the same shape as that due to the concentrated load acting statically on the beam, the vertical displacement at a distance x from the left support is

$$
y = y_c\frac{3xL^2 - 4x^3}{L^2} \tag{3.14}
$$

max KE (due to distributed mass)

$$
\begin{aligned}
&= 2\int_0^{L/2}\frac{\omega}{2g}\left(\dot{y}_c\frac{3xL^2 - 4x^3}{L^3}\right)dx\\
&= \frac{17}{35}\ \omega L\ \frac{\dot{y}_c^2}{2g}
\end{aligned}
\tag{3.15}
$$

$$
\max \mathrm{KE}\ (\text{due to concentrated load}) = \frac{1}{2}\ \frac{W}{g}\ \dot{y}_c^2 \tag{3.16}
$$

www.EngineeringBooksPDF.com

$$\begin{aligned} \max \text{SE} &= \tfrac{1}{2} K y_c^2 \\ \text{total energy} &= \text{KE} + \text{SE} = \text{constant} \end{aligned} \tag{3.17}$$

$$= \frac{1}{2}\dot{y}_c^2 \frac{\left(W + \frac{17}{35}\omega L\right)}{g} + \frac{1}{2} K y_c^2 = \text{constant} \tag{3.18}$$

$$\frac{\partial}{\partial \text{t}} = \dot{y}_c \left(\frac{W + \frac{17}{35}\omega L}{g} \ddot{y}_c + K y_c \right) = 0 \tag{3.19}$$

This expression is equivalent to (3.7) except that $\frac{17}{35}$ of the total mass of the beam is lumped with the concentrated mass. The natural frequency is

$$f = \frac{1}{2\pi} \sqrt{\frac{Kg}{W + \frac{17}{35}\omega L}} = \frac{1}{2\pi} \sqrt{\frac{g}{\Delta_{\text{STAT}}}} \tag{3.20}$$

where Δ_{STAT} is the static deflection under the concentrated load due to a total load of $W + \frac{17}{35}\omega L$ acting at the same point.

3.2.3.2 Estimate of the Fundamental Frequency of Multi-mass Systems by Rayleigh's Method

The mass of the beam or structure is assumed negligible or is "lumped" as in (3.20).

Assume again that the dynamic amplitude of the loads $W_1, W_2, \ldots, W_n$ is approximated by the static deflections of the structure $y_1,\ y_2, \ldots, y_n$ at the load points. Substitute into (3.16), remembering that the amplitude of the velocity is

$$\begin{aligned} \dot{y}_i &= \omega y \\ \max \text{SE} &= \sum \frac{W_i y_i}{2} \text{ by Clapeyron's theorem} \end{aligned} \tag{3.21}$$

$$\begin{aligned} \max \text{KE} &= \sum \frac{M_i y_i^2}{2} \text{ at the equilibrium position} \\ &= \sum \frac{M_i y_1^2}{2} = \sum \frac{M_i \omega^2 y_i^2}{2} = \frac{\omega^2}{g} \frac{\sum W_i y_i^2}{2} \end{aligned} \tag{3.22}$$

$$\sum \frac{W_i y_i}{2} = \frac{\omega^2}{g} \sum \frac{W_i y_i^2}{2} \tag{3.23}$$

www.EngineeringBooksPDF.com

Hence

$$\begin{cases} \omega = \sqrt{g}\sqrt{\dfrac{\Sigma W_i y_i}{\Sigma W_i y_i^2}} = \sqrt{g}\sqrt{\dfrac{W_1 y_1 + W_2 y_2 + \cdots}{W_1 y_1^2 + W_2 y_2^2 + \cdots}} \\ f = \dfrac{\omega}{2\pi} \end{cases} \tag{3.24}$$

The above provides a powerful method for the determination of the estimate of the fundamental frequency of many structural systems of practical importance:

(i) trusses: the masses and loads are lumped in the joints. The statical deflections may be in this case conveniently found from a Williot diagram (Fig. 3.7) or by calculation. The vertical deflections will usually be of interest.

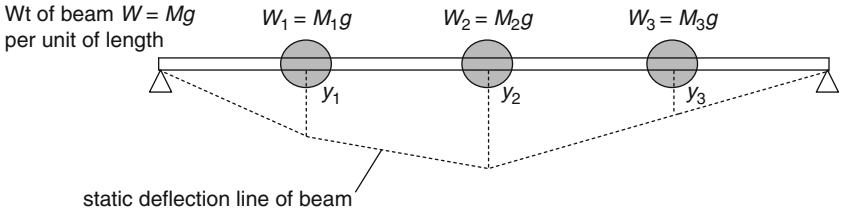


Fig. 3.7 Masses and static deflections

(ii) The shear building. Multistorey buildings, where the assumption is made that the floor construction is rigid, and the mass of the beams and loads carried can be lumped at the floor levels. The mass of the columns is usually neglected. In this case horizontal deflections at the floor levels will normally be required (Fig. 3.8).

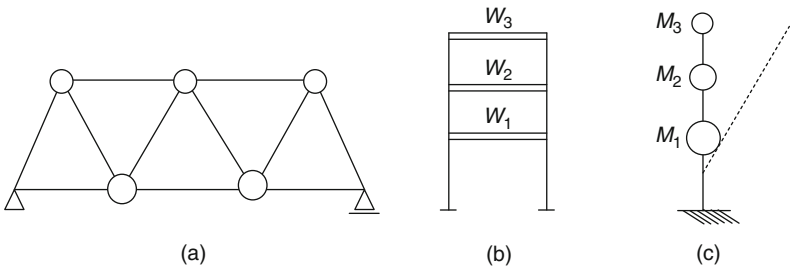


Fig. 3.8 Lump masses

An exact frequency analysis is much more laborious.

When the distributed mass of the structure is not quite negligible, the "static deflection method" can still be used, with some modifications, compared with (3.24):

www.EngineeringBooksPDF.com

$$\begin{aligned}\max \text{SE of distributed mass } (=\text{PE}) &= \int_0^L \frac{Wy\mathrm{d}x}{2}\\ \max \text{KE of distributed load} &= \int_0^L \frac{M\dot{y}^2\mathrm{d}x}{2}\\ &= \int_0^L \frac{M\omega^2 y^2\mathrm{d}x}{2}\\ &= \omega^2 \int_0^L \frac{W}{g}\,\frac{y^2\mathrm{d}x}{2}\end{aligned} \tag{3.25}$$

SE and KE for loads W are in (3.21) and (3.22), hence respectively

$$\frac{1}{2}\sum W_i y_i + \frac{1}{2}\int_0^L \omega y\mathrm{d}x = \frac{\omega^2}{2g}\sum W_i y_i^2 + \frac{\omega^2}{2g}\int_0^L \omega y_i^2\mathrm{d}x \tag{3.26}$$

$$\begin{aligned}\omega^2 &= \sum g\frac{\int \omega y\mathrm{d}x + W_i y_i}{\int \omega y^2\mathrm{d}x + \sum W_i y_i^2}\\ f &= \frac{\omega}{2\pi}\end{aligned} \tag{3.27}$$

The very practical formula now occurs throughout vibration literature in the symbolic forms:

$$\begin{Bmatrix} w \\ f \\ N \end{Bmatrix} = \begin{Bmatrix} 19.65 \\ 3.127 \\ 157.7 \end{Bmatrix} \sqrt{\frac{\Sigma Wy}{\Sigma Wy^2}} \begin{Bmatrix} \text{radius per s} \\ \text{cycles per s} \\ \text{cycles per s} \end{Bmatrix} \tag{3.28}$$

3.2.4 Multi-Degree-of-Freedom System

3.2.4.1 Systems of Masses, Springs and Dashpots

Consider the following equation grouping:

$$\left.\begin{aligned} m_1\ddot{x}_1 + c_1\dot{x}_1 + k_1x_1 + c_2(\dot{x}_1 - \dot{x}_2) + k_2(x_1 - x_2) &= P_1(t)\\ m_2\ddot{x}_2 + c_2(\dot{x}_2 - \dot{x}_1) + k_2(x_2 - x_1) + c_3(\dot{x}_2 - \dot{x}_3) &\\ +k_3(x_2 - x_3) &= P_2(t)\end{aligned}\right\}\begin{matrix}(a)\\(b)\\(c)\end{matrix}$$

$$\vdots$$

$$m_N\ddot{x}_N + c_N(\dot{x}_N - \dot{x}_{N-1}) + k_N(x_N - x_{N-1}) = P_N(t) \tag{3.29}$$

www.EngineeringBooksPDF.com

Changes due to the multi-degree-of-freedom system should be different from previous other degrees of freedom (see Fig. 3.9).

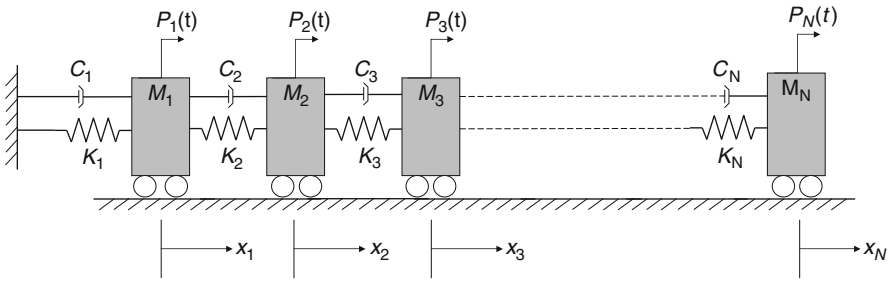


Fig. 3.9 Multi-degree-of-freedom system

These equations may be arranged in the matrix form:

$$M\ddot{x} + C\dot{x} + K\dot{x} = P_1(t) \ldots = P(t) \tag{3.30}$$

where

$$\text{mass matrix } M = \begin{bmatrix} M_1 & & & \\ & M_2 & & \\ & & \ddots & \\ & & & M_N \end{bmatrix} \text{ diagonal type} \tag{3.31}$$

all off-diagonal terms = 0

$$\text{damping matrix } C = \begin{bmatrix} c_1 + c_2 & -c_2 & & & \\ -c_2 & c_2 + c_3 & -c_3 & & \\ & & & \ddots & \\ & & & -c_N & c_N \end{bmatrix} \tag{3.32}$$

$$\text{stiffness matrix } K = \begin{bmatrix} k_1 + k_2 & -k_2 & & & \\ -k_2 & k_2 + k_3 & -k_3 & & \\ & & & \ddots & \\ & & & & -k_N \ldots k_N \end{bmatrix}$$

$$\text{displacement vector } x = \begin{Bmatrix} x_1 \\ \vdots \\ x_N \end{Bmatrix} \tag{3.33}$$

www.EngineeringBooksPDF.com

$$\text{load vector } P(t) = \begin{bmatrix} P_1(t) \\ \vdots \\ P_N(t) \end{bmatrix} \tag{3.34}$$

For example, when all masses move in phase with each other

$$x = X\sin(\omega t + \phi) \tag{3.35}$$

For a single degree of freedom $M\ddot{x} + Kx = 0$, it is written as

$$[K - \omega^2 M]X = 0 \tag{3.36}$$

The evaluation will be the determinant of $[K - \omega^2 M]$ which is

$$|K - \omega^2 M| = 0 \tag{3.37}$$

Because of the phase difference ϕ_N for all N masses, orthogonality for all normal modes of vibrations exists. The normalized mode shapes would be denoted by ϕ_N for N massed structures:

$$\phi_n = \begin{Bmatrix} \phi_{1n} \\ \phi_{2n} \\ \phi_{3n} \\ \vdots \\ \phi_{Nn} \end{Bmatrix}; \quad \frac{1}{X_{\max}} \begin{Bmatrix} X_{1n} \\ X_{2n} \\ X_{3n} \\ \vdots \\ X_{Nn} \end{Bmatrix} \tag{3.38}$$

The free vibration may be written as

$$\left[K\phi_n - \omega_n^2 M\phi_n\right] \tag{3.39}$$

$$K\phi_n - \omega_n^2 M\phi_n = q_n \tag{3.40}$$

where

ϕ_n = the nth mode shape

q_n = the inertial force $= \omega_n^2 M\phi_n$

$K\phi_n$ = stiffness equilibrium condition required when these forces are applied as loads on structures

www.EngineeringBooksPDF.com

3.2.4.2 Betti's Law

When the structure is subjected to alternate load systems, the work done by the first set of loads when moved through the displacements caused by the second set of loads is identical to the work done by the second set of loads when moved through the displacements caused by the first set of loads. Let us say for "m" mode, the inertial force will be q_m and the corresponding deflection ϕ_m according to Betti's law

$$\phi_m^T q_n = \phi_m^T qm \tag{3.41}$$

Shape factors must be transposed in order to carry out the appropriate matrix product

$$\omega_n^2 \phi_m^T M \phi_n = \omega_m^2 \phi_n^T M \phi_m \tag{3.42}$$

or

$$\left(\omega_n^2 - \omega_m^2\right) \phi_m^T M \phi_n = 0 \tag{3.43}$$

3.2.4.3 If Any Two Frequencies Are Not Equal Orthogonality conditions

$$\phi_m^T M \phi_n = 0 \quad \omega_m \neq \omega_n \quad \text{(first orthogonality)} \tag{3.44}$$

A *second orthogonality condition* by premultiplying (3.44) by ϕ_m^T

$$\phi_m^T K \phi_n = \omega_n^2 \phi_m^T M \phi_n \tag{3.45}$$

Because of (3.44) conditions

$$\phi_m^T K \phi_n = 0 \quad \omega_m \neq \omega_n \quad \text{(second orthogonality)} \tag{3.46}$$

The two orthogonality conditions, (3.44) and (3.46), have important considerations when *eigenvalue solution methods* are adopted and dynamic response is evaluated.

Standard eigenvalue
The *eigenvector* of a matrix is the vector when premultiplied by the matrix that yields another vector which is proportional to the original vector. This *constant of proportionality* is called *eigenvalue* and is expressed as

$$AX = \lambda x \tag{3.47}$$

www.EngineeringBooksPDF.com

where A is the square matrix of order N and X is the eigenvector of order N. λ is the corresponding eigenvalue where

$$(A - \lambda I)X = 0 \tag{3.48}$$

I is the identity matrix of the same order as A. In case of free vibration, the eigenvalue problem is represented by

$$KX = \lambda MX \tag{3.49}$$

in which $\lambda = \omega^2$.

The eigenvalues are both real and positive and eigenvalues can similarly be obtained using the orthogonality given above. Just take for X_m, X_n (eigenvectors), the corresponding values λ_m and λ_n and equations are solved for $\lambda_m \neq \lambda_n$, $m \neq n$, etc. Hence

$$\lambda_m = \frac{X_m^T K Y_m}{X_m^T M X_m}$$

The mass orthonormalization for scaling will be

$$\phi_m^T M \phi_M = 1 \tag{3.50}$$

Superposition

The basic eigenvectors of Nth order as in N-dimensional space can be represented by the superposition of N independent vectors also of order N. The superposition can be expressed as

$$\delta_s = \sum_{m=1}^{N} X_m \bar{W}_m \tag{3.50a}$$

where

$$\delta_s = \text{a vector of order} N$$

X_m is as defined above and $\bar{W}_m$ is a weighting factor

$$\begin{aligned} \delta_s &= \bar{X}\bar{W}_m \\ \bar{X} &= \sum_{m=1}^{N} X_m \end{aligned} \tag{3.50b}$$

The value of

www.EngineeringBooksPDF.com

$$f\bar{W}_m = (\bar{X})^{-1}\delta_s \tag{3.50c}$$

Since X_m vectors are independent, $(\bar{X})^{-1}$ must exist and can be equal to $(\bar{X})^T$. This mean the mode shapes obtained are also independent and are used in the representation of vectors δ_s. Hence

$$\begin{aligned}\delta_s &= \bar{W}_1 X_1 + \bar{W}_2 X_2 + \cdots + \bar{W}_N X_N \\ &= \phi_{ml} X_1 + \phi_{m2} X_2 + \cdots + \phi_{mN} X_N\end{aligned} \tag{3.50d}$$

$\bar{W}_m$ is written as

$$\frac{X_m^T M \delta_s}{X_m^T M X_m} \tag{3.50e}$$

Because $\phi_m^T M \phi_m = 1$, $\bar{W}_m$ is given by

$\bar{W}_m = \Phi M \delta_s$ for $m = 1, 2, 3, \ldots, N$

Rayleigh quotient
Let K, M and δ_s be the stiffness and mass matrices of order N and any arbitrary vector of order N. The scalar factor S_f, known as the Rayleigh quotient, is written as

$$S_f = \frac{\delta^T K \delta}{\delta^T M \delta} \tag{3.50f}$$

If $\delta = \Phi \bar{W}$ then

$$\begin{aligned}\delta^T M \delta &= (\bar{W})^T \Phi^T M \Phi \bar{W} = \sum_{m=1}^{N} (\bar{W}_m)^2 \\ \delta^T K \delta &= (\bar{W})^T \Phi^T K \Phi \bar{W} \\ &= (\bar{W})^T \Lambda \bar{W} = \sum_{m=1}^{N} \lambda_m (\bar{W}_m)^2\end{aligned} \tag{3.50g}$$

where Φ is a set of normalized modes.

The value of S_f is given by

$$\begin{aligned}S_f &= \frac{\lambda_1 (\bar{W}_1)^2 + \lambda_2 (\bar{W}_2)^2 + \cdots + \lambda_N (\bar{W}_N)^2}{(\bar{W}_1)^2 + (\bar{W}_2)^2 + \cdots + (\bar{W}_N)^2} \\ \bar{W}_1 &\le S_f\end{aligned} \tag{3.50h}$$

www.EngineeringBooksPDF.com

When a set of arbitrary vector δ are orthogonal to the first $s-1$ eigenvectors

$$\delta^T M\phi_m = 0 \quad m = 1, 2, \ldots, s-1 \tag{3.51}$$

and when δ is in expansion

$$\bar{W}_m = 0 \quad m = 1, 2, \ldots s-1 \tag{3.52}$$

the arbitrary vector δ used in obtaining or developing the expression for S_{f}, the eigenvectors were of approximate characteristics. The deviation from the true eigenvectors by $\varepsilon\bar{\delta}$ (ε^2, taken out) can be written as

$$\delta = \phi_m + \varepsilon\bar{\delta} \tag{3.53}$$

where

$\phi_m = m$th eigenvector

$\varepsilon\bar{\delta}$ = contribution from all other eigenvectors to δ

$$\bar{\delta} = \sum_{m=1}^{N} \alpha_m \phi_m \tag{3.54}$$

Numerator of the value of S_f

$$\delta^T K\delta = \left(\phi_m^T + \varepsilon\bar{\delta}^T\right) K\left(\phi_m + \omega\bar{\delta}\right) \tag{3.55}$$

Using the orthogonality principle described above

$$\left.\begin{aligned} \phi_m^T M\bar{\delta} = (\bar{\delta})^T K\phi_m = 0 \\ \phi_m^T K\bar{\delta} = (\bar{\delta})^T M\phi_m = 0 \\ \phi_m^T K\phi_m = \lambda_m \phi_m^T M\phi_m = \lambda_m \end{aligned}\right\} \tag{3.56}$$

then substituting into (3.55)

$$\delta^T K\delta = \lambda_m + \varepsilon^2\left(\alpha_1^2\lambda_1 + \alpha_2^2\lambda_2 + \cdots + \alpha_N^2\lambda_N\right) \tag{3.57}$$

Denominator of S_f

$$\begin{aligned} \delta^T M\delta &= \phi_m^T M\phi_m + \varepsilon\phi_m^T M\bar{\delta} + \varepsilon(\bar{\delta})^T M\phi_m + \varepsilon^2(\bar{\delta})^T M\bar{\delta} \\ &= 1 + \varepsilon^2\left(\alpha_1^2 + \alpha_2^2 + \cdots + \alpha_N^2\right) \end{aligned} \tag{3.58}$$

www.EngineeringBooksPDF.com

Hence

$$S_f = \lambda_m + \varepsilon^2\left\{\alpha_1^2(\lambda_1 - \lambda_m) + \alpha_2^2(\lambda_2 - \lambda_m) + \cdots + \alpha_N^2(\lambda_N - \lambda_m)\right\} \tag{3.59}$$

3.2.5 Dynamic Response of Mode Superposition

Multi-degree-of-freedom system is described by

$$M\ddot{x} + C\dot{x} + Kx = F = P \tag{3.60}$$

As stated, mode superposition is based on the fact that the deflected shape of the structure may be expressed as a linear combination of all the modes:

$$x = \phi_1 X_1 + \phi_2 X_2 + \phi_3 X_3 + \cdots \phi_N X_N = \sum_{n=1}^{N} \phi_n X_n \tag{3.61}$$

X_n are the modal amplitudes varying with time.

The motion of the ith mass is

$$_i x_i = \phi_{i1} X_1 + \phi_{i2} X_2 + \cdots + \phi_{in} X_n + \cdots + \phi_{iN} X_N$$

where

$$\phi_{in} = \text{displacement of the } i\text{th mode ofvibration}$$

Equation (3.61) may be written as

$$x = \Phi\Lambda$$

where Φ is the modal matrix whose columns are the mode shapes so that

$$\Phi = \{\Phi_2\Phi_2\Phi + \cdots + \Phi_N\}$$

X is a vector of the modal amplitudes

$$X^T = \{X_1, X_2, \ldots X_n, \ldots, X_N\}$$

They are always in generalized coordinates where x are natural coordinates.

Modal analysis is a process of decomposition (3.60) using generalized coordinates so as to obtain a set of differential equations that are uncoupled, each of which may be analysed as a single degree of freedom. Substituting Eq. (3.61) into (3.60) gives

www.EngineeringBooksPDF.com

$$M\sum_{n=1}^{N}\Phi_n\ddot{X}_n + C\sum_{n=1}^{N}\Phi_n\dot{X}_n + K\sum_{n=1}^{N}\Phi X_n = P \tag{3.62}$$

Φ_n *shape functions* are independent of time. Premultiplying Eq. (3.62) by Φ_m for the mth case of mode

$$\Phi_m^{T''}M\sum_{n=1}^{N}\Phi\ddot{X}_n + \phi_m^{T''}C\sum_{n=1}^{N}\Phi_n\dot{X}_n + \Phi_m^{T}K\sum_{n=1}^{N}\Phi_n N_n = \Phi_m^{T''}P \tag{3.63}$$

The first term can be expanded to

$$\Phi^{T''}M\Phi_1\ddot{X}_1 + \Phi_m^{T''}M\Phi_2\ddot{X}_2 + \cdots + \Phi_m^{T''}M\Phi_n\ddot{X}_n + \cdots \tag{3.64}$$

Referring to the first or orthogonality conditions every term in this series will be zero except for the case where $n = m$

$$\therefore\ \Phi_m^{T}\sum_{n=1}^{N}\Phi\ddot{X}_n = \Phi_m M\Phi_m\ddot{X}_m = M_m\ddot{X}_m \tag{3.65}$$

where M_m is a generalized mass of the mth mode. The reasoning applies to the stiffness term

$$\Phi_m^{T''}K\sum_{n=1}^{N}\phi_n X_n = \phi_m^{T''}M\phi_m X_m = K_m Y_m \tag{3.66}$$

where K_m is the generalized stiffness.

The generalized force Q_m will be

$$Q_{m=}\Phi_m^{T''}P \tag{3.67}$$

Damping C is a problem

Assume C is proportional to either M or K or a combination of both. The same effect of decomposition would be achieved

$$\phi_m C\sum_{n=1}^{N}\phi_n\dot{X}_n = C_m X_m \tag{3.68}$$

$$\text{Transpose} = \text{T}''$$

The damping ratios in the N modes are written as $\xi_1, \xi_2, \ldots, \xi_N$ and the transformed damping matrix is written as

www.EngineeringBooksPDF.com

$$C_{TRA} = \phi^T C \phi = \begin{bmatrix} 2\xi_1\omega_1 & 0 & \cdots & 0 \\ 0 & 2\xi_2\omega_2 & & \vdots \\ \vdots & \vdots & & \vdots \\ 0 & 0 & \cdots & 2\xi_N\omega_N \end{bmatrix} \tag{3.69}$$

where
C_{TRA} = transformed damping matrix.

Then

$$C = (\phi^{T''})^{-1} C_{TRA} \phi^{-1} \tag{3.70}$$

The values of ϕ^{-1} (obtained from orthogonality condition) $= \phi^T M$:

$$\phi^{T''} M \phi = I$$

Hence

$$C = M \phi C_{TRA} \phi^{T''} M \tag{3.71}$$

or

$$C = M \left(\sum_{m=1}^{N} 2\xi\omega\phi\phi^T \right) M \tag{3.72}$$

Equation (3.60) can be written in the form

$$M_m \ddot{X}_m + C_m \dot{X}_m + K_m X_m = P_m; \quad m = 1, 2, 3, \ldots, N \tag{3.73}$$

When a system is assumed to possess proportional *damping*, the mode superposition method is used. The damping matrix would then be diagonalized by a normal coordinate system. Let the damping matrix C be written as

$$C = \alpha_0 M \tag{3.74}$$

where α_0 is a constant of proportionality.

Pre-multiply Eq. (3.74) by $\phi_m^{T''}$ and post-multiply by ϕ_m

$$\phi_m^T C \phi_m = \alpha_0 \phi_m^{T''} M \phi_m = 0, \; m \neq n \tag{3.75}$$

or

www.EngineeringBooksPDF.com

$$C_m = 2\xi_m\omega_m = \phi_m^T C\phi_m$$
$$\alpha_0\phi_m^{T''} M\phi_m = 2\xi_m\omega_m \tag{3.76}$$
$$\alpha_0 = 2\xi_m\omega_m$$

$$\xi_m = \frac{\alpha_0}{2\omega_m} \tag{3.77}$$

If it is decided to choose a *stiffness proportional damping* rather than a *mass proportional damping*, the damping matrix C can be written as

$$C = \alpha_1 \mathrm{k}$$
$$\phi_{\mathrm{m}}^{\mathrm{T}''} C\phi_m = 2\xi_m\omega_m = \alpha_0 + \alpha_1\omega_m^2 \tag{3.78}$$

$$\phi_m^{T''} C\phi_n = 2\xi_m\omega_n = \alpha_0 + \alpha_1\omega_n^2 \tag{3.79}$$

A more generalized equation would be

$$C = \alpha_0 M + \alpha_1 K + \alpha_2 M^{-1} KM \tag{3.80}$$

Damping that leads to satisfying (3.80) is the *Rayleigh damping*.

Orthogonality condition is used

$$\phi_m^{T''} C\phi_m = 2\xi_m\omega_m = \alpha_0 + \alpha_1\omega_m^2 + \alpha_2\omega_m^4$$
$$\phi_m^{T''} C\phi_n = 2\xi_n\omega_n = \alpha_0 + \alpha_1\omega_n^2 + \alpha_2\omega_n^4 \tag{3.81}$$
$$\phi_p^{T''} C\phi_p = 2\xi_p\omega_p = \alpha_0 + \alpha_1\omega_p^2 + \alpha_2\omega_p^4$$

written in a matrix form and solving for them.

Alternatively for obtaining an orthogonal damping matrix use

$$\text{load vector} = \begin{Bmatrix} P_1(t) \\ \vdots \\ P_n(t) \end{Bmatrix} \tag{3.82}$$

3.3 Examples of Dynamic Analysis of Building Frames and Their Elements Under Various Loadings and Boundary Conditions

This section deals with solved examples of building frames and their elements subjected to dynamic loads. Examples selected are based on their day-to-day occurrence in various building problems. Readers are advised to also study

www.EngineeringBooksPDF.com

additional materials on dynamic analysis. These examples together with the dynamic analysis in Sect. 3.2 will hopefully pave the way to finally understanding and tackling earthquake problems.

3.3.1 Example 3.1

A beam of length L is subjected to a uniformly distributed load "q" as shown in Fig. 3.10. Assuming the vibration deflection curve is of the same form as the static deflection curve, determine the frequency for this beam when

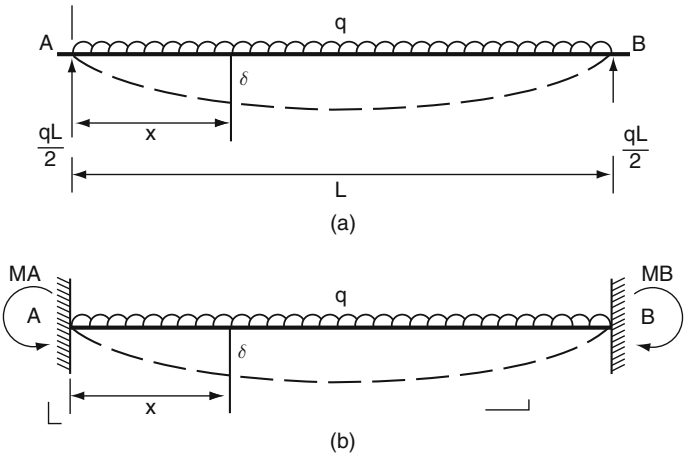


Fig. 3.10 A beam under uniform load

(a) supports are simple
(b) supports are fixed

Take EI as constant.
Solution
Beams with uniform load but with different boundary conditions.

(a)

$$EI\frac{d^2\delta}{dx^2} = M = \frac{qx^2}{2} - \frac{qLx}{2}$$

$$EI\frac{d\delta}{dx} = \frac{qx^3}{6} - \frac{qLx^2}{4} + A$$

$$EI\delta\frac{qx^4}{24} = \frac{qLx^3}{4} + A + B$$

www.EngineeringBooksPDF.com

when the boundary conditions are

$$x = 0 \ \delta = 0 \ B = 0$$

$$x = L \ \delta = 0 \ A = \frac{qL^3}{24}$$

$$EI\delta = 0 = \frac{qL^4}{24} - \frac{qL^4}{12} + AL$$

$$\delta = \frac{q}{24EI}(x^4 - 2Lx^3 + L^3x)$$

$$\int_0^L \delta \mathrm{d}x = \frac{qL^5}{120EI}$$

$$\int_0^L \delta^2 \mathrm{d}x = \frac{31}{360}L^9\left(\frac{q}{24EI}\right)^2$$

$$f = \frac{1}{2\pi}\sqrt{\left\{\frac{gqL^5}{120EI} \quad \frac{630}{31L^9} \quad \left(\frac{24EI}{q}\right)^2\right\}}$$

$$= 1.572\sqrt{\frac{EIg}{qL^4}} \ (Hz)$$

(b)

$$EI\ \frac{d^2\delta}{dx^2} = M = M_A + \frac{qx^2}{2} - \frac{qL}{2}x$$

$$EI\frac{d\delta}{dx} = M_A x + \frac{qx^3}{6} - qL\frac{x^2}{4} + A$$

$$EI\delta = \frac{1}{2}M_A x^2 + \frac{qx^4}{24} - \frac{qLx^3}{12} + Ax + B$$

Boundary conditions:

$$x = 0 \ \frac{\mathrm{d}\delta}{\mathrm{d}x} = 0 \ A = 0 \ B = 0 \ \delta = 0$$

$$x = L \ \frac{\mathrm{d}\delta}{\mathrm{d}x} = 0$$

$$EI\frac{\mathrm{d}\delta}{\mathrm{d}x} = M_A L + \frac{qL^3}{6} - \frac{qLx^2}{4} + 0$$

$$0 = M_A L + \frac{qL^3}{6} - \frac{qL^3}{4} \ \text{or} \ \ M_A = \frac{qL^3}{12}$$

$$\delta = \frac{q}{24EI}\ [L^2x^2 + x^4 - 2Lx^3]$$

www.EngineeringBooksPDF.com

$$\int_0^L \delta dx = \frac{q}{24EI}\,\frac{L^3}{30}$$

$$\int_0^L \delta^2 dx = \left(\frac{q}{24EI}\right)^2 \frac{L^q}{630}$$

$$\omega^2 = \text{circular frequency} = \frac{\delta \int_0^L \delta dx}{\int_0^L \delta^2 dx}$$

$$\omega^2 = \frac{504ELg}{qL^4}$$

$$f = \text{natural frequency} = \frac{\omega}{2\pi}$$

$$= \frac{1}{2\pi} g \sqrt{\frac{504EL}{qL^4}}$$

$$= 3.573\sqrt{\frac{ELg}{qL^4}(H_2)}$$

3.3.2 Example 3.2

A simply supported beam of weight q/m carries a central load W. Assuming that the vibration deflection curve is of the same form as the static deflection curve, determine deflection "δ" in terms of maximum deflection $\delta_{\max}$, load W and the inertia effects. Take EI as constant. Find the total central load for the beam in Fig. 3.10.

Solution A simply supported beam subjected to UDL and a centrally concentrated load:

$$EI\frac{d^2\delta}{dx^2} = M_x = \frac{1}{2}W_x$$

$$EI = \frac{d\delta}{dx} = \frac{1}{4}W_{x^2} + A_1$$

$$\delta = \frac{1}{EI}\left[\frac{1}{2}W_{x^3} + A_1 x + B_1\right]$$

Boundary conditions:

$$x = 0 \quad \delta = 0 \quad B_1 = 0$$

www.EngineeringBooksPDF.com

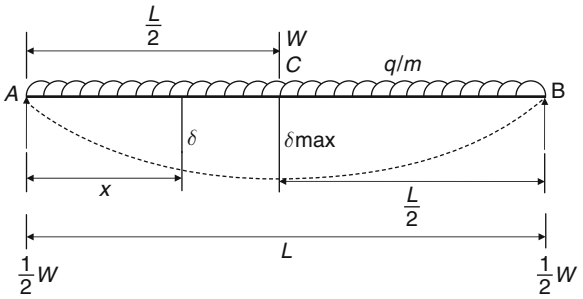


Fig. 3.11 A beam under concentrated load and self-weight

$$x = \frac{L}{2} \quad \frac{d\delta}{dx} = 0 \quad A_1 = \frac{1}{16}\, WL^2$$

When $x = \dfrac{L}{2}$

$$\delta_0 = \delta \max = \left[\frac{-W}{12}\left(\frac{L}{2}\right)^3 + \frac{WL^2}{16}\left(\frac{L}{2}\right)\right]\frac{1}{EI}$$

$$= \frac{WL^3}{48EI}$$

Hence

$$\delta = \frac{1}{EI}\left[\frac{WL^2}{16} - \frac{W_{x^3}}{12}\right] = \frac{W}{48EI}\left[3L^2x - 4x^3\right]$$

$$\frac{\delta}{\delta_{\max}} = \frac{x}{L^3}(3L^2 - 4x^2)$$

$$\delta = \delta \max \frac{x}{L^3}(3L^2 - 4x^2)$$

Kinetic energy due to element dx

$$= \frac{qdx\, v^2}{2g} = \frac{qdx\, q^2\, \delta^2}{2g}$$

Where $v = \delta$.
Total kinetic energy KE $= 2\int_0^L \frac{q}{2g} q^2\, \delta^2 dx$

$$= \frac{qv^2}{2g} \quad \underbrace{\frac{17}{35}}_{\text{Inertia effect}} \quad L$$

Total central load $=$ W $+ \frac{17}{35} qL = W'$
W′replaces W in the above analysis in order to compute "δ".

www.EngineeringBooksPDF.com

3.3.3 Example 3.3

Find the natural frequency of the beam/mass system lying in the plane as shown in Fig. 3.12, use the following data:

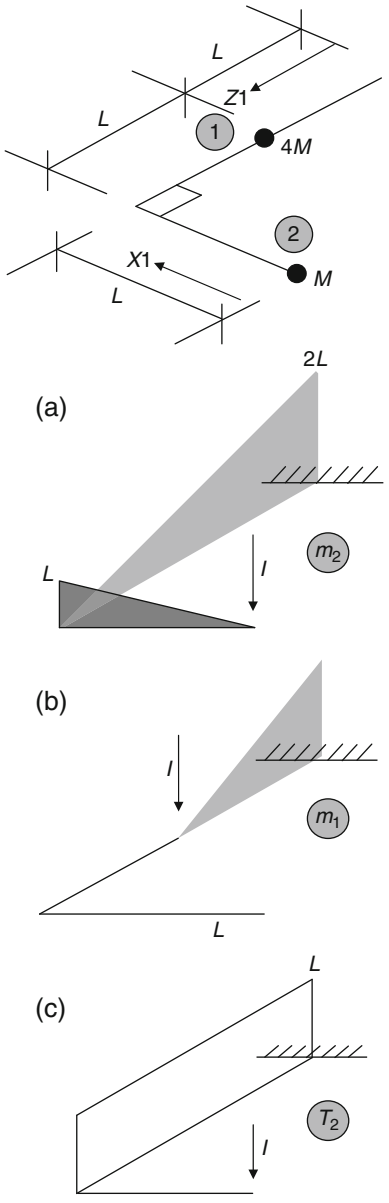


Fig. 3.12 Beam/mass system in bending and torsion

www.EngineeringBooksPDF.com

$$EI = \frac{3}{2}GJ$$

$$\delta = \mathrm{X}\sin\,\omega t$$

Reference coordinates are ② and ②. Use the flexibility method.
Solution
Bending + torsion: beam/mass system
Equations of motion

$$4\,M\ddot{\delta}_{10}f_{11} + M\ddot{\delta}_{20}f_{12} = -\delta_{10}$$
$$4\,M\ddot{\delta}_{21}10f_{21} + M\ddot{\delta}_{20}f_{22} = -\delta_{20}$$

Displacement due to bending and torsion

$$f_{ij} = \int \frac{m_i m_j}{EI}ds + \int \frac{T_i T_j}{GJ}ds$$

Flexibility coefficients

$$f_{11} = \int \frac{m_1^2 ds}{EI} + \int \frac{T_1^2 ds}{GJ} = \frac{L}{6EI}(2L^2) = \frac{L^3}{3EI}$$
$$F_{22} = \int \frac{m_2^2 ds}{EI} + \int \frac{T_2^2 ds}{GJ} = \frac{2L}{6EI}(2\times 4L^2) + \frac{2L}{6GJ}(6L^2) = \frac{6L^3}{EI}$$
$$f_{12} = f_{21} = \int \frac{m_1 m_1}{EI} + \int \frac{T_1 T_2}{GJ} = \frac{L}{6EI}\left[2(2L^2) + L^2\right] = \frac{5L^3}{6EI}$$
$$\delta_{10} = X_1\sin\,\omega t \quad \dot{\delta}_{10} = \omega X_1\cos\,\omega t \quad \ddot{\delta}_{10} = -\omega^2 X_1\sin\,\omega t = -\omega^2\delta_{10}$$
$$\delta_{20} = X_2\sin\,\omega t \quad \dot{\delta}_{20} = \omega X_2\cos\,\omega t \quad \ddot{\delta}_{20} = -\omega^2 X_2\,\sin\,\omega t = \omega^2\delta_{20}$$

All necessary values are substituted, the following determinant is obtained and is made equal to zero:

$$\begin{vmatrix} (1 - 4\,M\omega^2 f_{11}) & -M\omega^2 f_{22} \\ -4\,M\omega^2 f_{21} & 1 - M\omega^2 f_{22} \end{vmatrix} = 0$$

The solution of the determination yields

$$1 - \frac{22}{44}\,\bar{\mathrm{K}}\, - \frac{47}{9}(\bar{\mathrm{K}})^2 = 0 \quad \text{where } \bar{\mathrm{K}} = \frac{L^3\,M\omega^2}{EI}$$

$$\bar{\mathrm{K}} = 1.251 \text{ or } 0.163$$

$$\omega_1 = \sqrt{\frac{1.251\,EI}{ML^3}} \text{ or } \sqrt{\frac{0.163\,EI}{ML^3}}\ \text{(rad/s)}$$

www.EngineeringBooksPDF.com

$$f(\text{lowest}) = \frac{1}{2\pi}\sqrt{\left[\frac{0.163\,EI}{ML^3}\right]}$$

3.3.4 Example 3.4

A frame lying in a plane with a distributed mass of 1,500 kg/m is shown in Fig. 3.13. Using the flexibility method or otherwise, determine the natural frequency "f" for this frame. Use the following data:

$E = 14 \times 10^6\ \text{kN/m}^2$

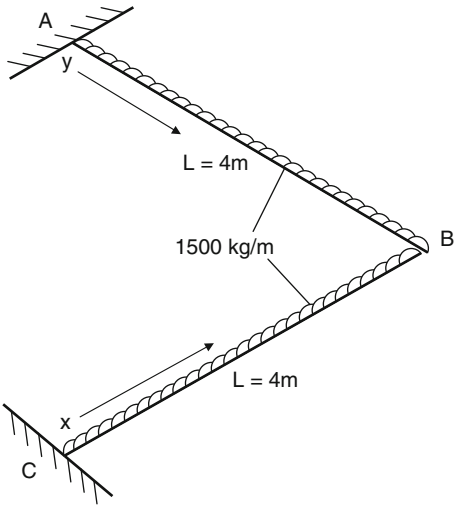


Fig. 3.13 A frame in-plane

$I = 2{,}600 \times 10^{-6}\ \text{m}^4$
$G = 6.4 \times 10^6\ \text{kN/m}^2$
$J = 1{,}800 \times 10^{-6}\ \text{m}^4$
$L = 4\text{m}$
$\delta = X \sin \omega\, t$
$EI = 14 \times 10^6\ \text{kN/m}^2 \times 2600 \times 10^{-6}$
$GJ = 6.4 \times 10^6\ \text{kN/m}^2 \times 1800 \times 10^{-6}$
Use the direct integration process.

Solution

A bent in-plane subject to a distributed mass. Different coordinate systems x and y apply:

www.EngineeringBooksPDF.com

$$fij = \int \frac{m_i m_j}{EI}\, ds + \int \frac{T_i T_j}{GJ}$$

$$\delta = -\omega^2 X \sin\, \omega t$$

Flexibility parameters	Limits
$m_1 = 1 \times L$	$0 \le y \le L$
$m_1 = 1 \times L$	$0 \le x \le L$
$m_2 = 1 \times L$	$0 \le y \le L$
$m_2 = 1 \times L$	$0 \le x \le L$
$T_1 = \frac{1}{2} L$	$0 \le y \le L$
$T_1 = \frac{1}{2} L$	$0 \le x \le L$
$T_2 = \frac{1}{2} L$	$0 \le y \le L$
$T_2 = \frac{1}{2} L$	$0 \le x \le L$

Flexibility coefficients

$$f_{11} = 2\int_0^L \frac{L^2}{EI}\, dL + 2\int_0^L \frac{L^2}{4GJ_2}\, dL = \frac{2L^3}{3EI} + \frac{L^3}{6GJ} = \frac{0.0021}{EI}$$

$$f_{22} = 2\int_0^L \frac{L dL}{EI} + 2\int_0^L \frac{L^2}{4GJ}\, dL = \frac{0.0014}{EI}$$

$$f_{12} = f_{21} = \frac{2}{EI}\int_0^L L^2 dL + \frac{2}{GJ}\int_0^L L^2\, dL = \frac{0.0021}{EI}$$

Equations of motion:

$$M_1\, \ddot{\delta}_{10} f_{11} + M_2\, \ddot{\delta}_{20} f_{12} = -\delta_{10}$$

$$M_1\, \ddot{\delta}_{10} f_{12} + M_2\, \ddot{\delta}_{20} f_{22} = -\delta_{20}$$

Substituting respective values, the following relations are established:

$$\begin{bmatrix} (0.1029\, w^2 - 1) & 0.062\, w^2 \\ 0.1029\, w^2 & (0.041\, w^2 - 1) \end{bmatrix} \begin{Bmatrix} X_1 \\ X_2 \end{Bmatrix} = \begin{Bmatrix} 0 \\ 0 \end{Bmatrix}$$

Solving the determinant of the matrix $X_1 \neq 0,\ X_2 \neq 0$ and making $K = \omega^2$

$$\bar{K} = \frac{-0.1439 \pm 0.1718}{0.0044}$$

$$\omega = 2.51(\text{the lowest rad /s})$$

$$F = \frac{\omega}{2\pi} = 0.4\text{Hz}$$

www.EngineeringBooksPDF.com

Plate 3.1 gives a suitable method of providing harmonic support motion of a beam.

Plate 3.1 Harmonic support motion

To represent a harmonic support motion of the beam shown in Fig. 3.15, assume

$$u_g = X \sin \Omega t = X \sin \beta\omega t \tag{1}$$

where $\beta = \Omega/\omega$ is the frequency ratio and X is vertical amplitude of the motion. Then, since $k = M\omega^2$, as is well known,

$$-M\phi\, \ddot{u}_g = k\beta^2 \phi X \sin \beta\omega t \tag{2}$$

Put (2) into the equation of motion,

$$M\ddot{u} + C\dot{u} + Ku = -M\phi\ddot{u}_g = K\beta^2\, \phi x \sin \beta\omega t \tag{3}$$

By identifying

$$p_0 \sin \beta\omega t = \left(k\beta^2\, \phi x\right) \sin \beta\omega t \tag{4}$$

differential Eq. (3) may be noted as similar to that for harmonically forced motion.

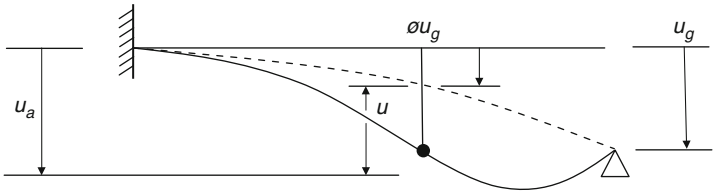


Fig. 3.15 Support motion of a beam

Displacement of the Beam Mass

The solution of (3) for the *steady-state relative displacement* $u'(t)$ is therefore

$$\begin{aligned} u'(t) = \frac{p_0}{k} F(t) &= \frac{p_0}{k}\left[C_1' \sin \beta\omega t + C_2' \cos \beta\omega t\right] \\ &= \beta^2 \phi X \left[\frac{\left(1-\beta^2\right) \sin \beta\omega t - 2\xi\beta \cos \beta\omega t}{\left(1-\beta^2\right)^2 + (2\xi\beta)^2}\right] \end{aligned} \tag{5}$$

www.EngineeringBooksPDF.com

from which the maximum value may be written as

$$u'_{\max} = \frac{p_0}{k} F_{\max} = \beta^2 \phi X F_{\max} \tag{6}$$

where

$$F_{\max} = \frac{1}{\sqrt{\left(i - \beta^2\right)^2 + (2\xi\beta)^2}} \tag{7}$$

Consequently, the *steady-state absolute displacement* $u_a(t)$ of the beam mass is given by

$$u_a(t) = \phi u_g(t) + u(t) = \phi x \frac{\left(1 - \beta^2 + 4\xi^2\beta^2\right) \sin\, \beta\omega t - 2\xi\beta^3 \cos\, \beta\omega t}{\left(1 - \beta^2\right)^2 + (2\xi\beta)^2} \tag{8}$$

and its maximum value is found (after manipulation) to be

$$\boxed{u_{\max} = \phi x F_{\max} \sqrt{1 + (2\xi\beta)^2}} \tag{9}$$

For most practical values of ξ and β the square root factor is almost equal to unity.

Equivalent Static Load on the Beam
From the equation of motion of the beam mass, the equivalent static load is

$$Pequiv = M\ddot{u}_a \tag{10}$$

$$Pequiv = Ku + C\dot{u} = K\left[u + \frac{2\xi}{\omega}\dot{u}\right] \tag{11}$$

Through the use of (8), (10) gives the following result:

$$Pequiv = \beta^2 k u_a(t) = \beta^2\, k\phi X \left[\frac{\left(1 - \beta^2 + 4\xi^2\beta^2\right) \sin\, \beta\omega t - 2\xi\beta^2 \cos\, \beta\omega t}{\left(1 - \beta^2\right)^2 + (2\xi\beta)^2}\right] \tag{12}$$

using (9), the maximum value can be achieved as

$$\boxed{Pequiv_{\max} = \beta^2\, k\phi \left[F_{\max} \sqrt{1 + (2\xi\beta)^2}\right]} \tag{13}$$

3.3.5 Example 3.5

A single-bay two-storey frame is shown in Fig. 3.14. Derive equations of motion.

For displacements x_1 and x_2, the tensions in the springs are

$$P_1 = k_1 x_1 \text{ and } P_2 = k_2(x_2 - x_1)$$

www.EngineeringBooksPDF.com

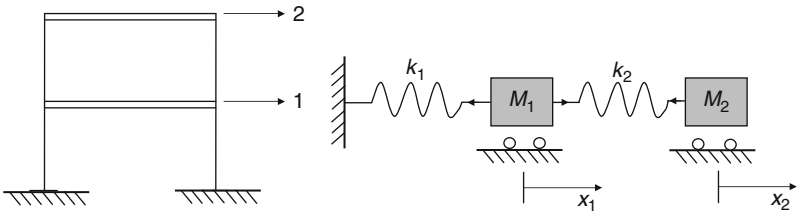


Fig. 3.14 (**a**) A two-storey frame. (**b**) Idealized mass/spring system

The dynamic equilibrium equations are

$$\text{for mass 1} \quad M_1\ddot{x}_1 + P_1 - P_2 = 0$$

$$\text{for mass 1} \quad M_2\ddot{x}_2 + P_2 - 0 = 0$$

Substituting for P_1 and P_2 gives

$$\text{for mass 1} \quad M_1\ddot{x}_1 + (k_1 + k_2)\ x_1 - k_2\, x_2 = 0$$

$$\text{for mass 2} \quad M_2\ddot{x}_2 - k_2 x_1 + k_2 x_2 = 0$$

In general for a two-degree-of-freedom system

$$\begin{aligned} M_1\ddot{x}_1 + k_{11}x_1 + k_{12}x_2 &= 0 \\ M_2\ddot{x}_2 + k_{12}x_1 + k_{22}x_2 &= 0 \end{aligned} \tag{3.83}$$

where k_{11}, k_{12}, k_{21} and k_{22} are the usual stiffness coefficients for the system.

Look for solutions having the form $x_1{=}X_1 \sin \omega t$, $x_2{=};X_2 \sin \omega t$; this implies

$$\ddot{x} = -X_1\omega^2 \sin\ \omega t,\ \ddot{x}_2 = -X_2\omega^2\ \sin\ \omega t.$$

Substituting in (3.83) for $x_1, x_2, \ddot{x}_1$ *and* $\ddot{x}_2$ and cancelling ωt throughout,

$$\begin{aligned} M_1\left(-X_1\omega^2\right) + k_{11}x_1 + k_{12}x_2 &= 0 \\ M_2\left(-X_2\omega^2\right) + k_{21}x_1 + k_{22}x_2 &= 0 \end{aligned}$$

or

$$\begin{aligned} \left(k_{11} - M_1\omega^2\right)X_1 + k_{12}x_2 &= 0 \\ k_{21} + X_1 + \left(k_{22} - M_2\omega^2\right)X_2 &= 0 \end{aligned} \tag{3.84}$$

Elimination X_2/X_1,

www.EngineeringBooksPDF.com

$$\left(k_{11} - M_1\omega^2\right)\left(k_{22} - M_2\omega^2\right) - k_{12}k_{21} = 0 \tag{3.85}$$

This is a quadratic in ω^2 whose two roots give the two natural circular frequencies.

For each root, back substitution into either one of (3.84) gives X_2/X_1, i.e. the mode shape.

In matrix form, (3.84) may be written as

$$\left(K - M\omega^2\right)X = 0$$

where

$$K = \begin{bmatrix} k_{11} & \mathrm{k}_{12} \\ k_{21} & \mathrm{k}_{22} \end{bmatrix} \quad \text{(the stiffness matrix)}$$

$$M = \begin{bmatrix} M_1 & 0 \\ 0 & M_2 \end{bmatrix} \quad \text{(the mass matrix)}$$

$$\mathrm{X} = \begin{bmatrix} X_1 \\ \mathrm{X}_2 \end{bmatrix}$$

3.3.5.1 Modal Analysis of Two-Storey Frames Under Lateral Loads

Plate 3.2 gives a complete analysis of such a frame under lateral loads $F_1(t)$ and $F_2(t)$ using modal coordinates. Plate 3.3 indicates a complete modal analysis of forced vibrations of the two-storey frame subjected to two loads laterally applied, one is an applied load of a triangular pulse placed at the top floor and the other is $F(t)$. The values are shown in Plate 3.3.

Plate 3.2 Free undamped virations of a two degree of freedom system-first and second harmonic frequencies

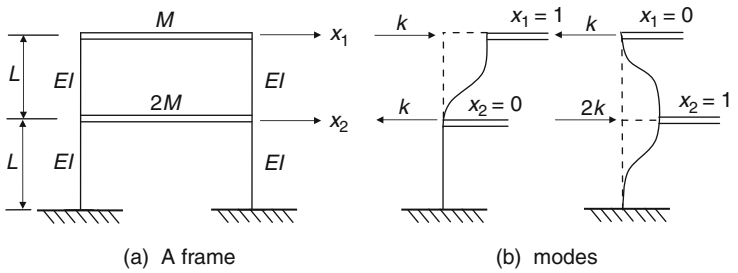


Fig. 3.16 A two-story single-bay frame

www.EngineeringBooksPDF.com

Equations of Motion

$$M\ddot{x} + kx = 0$$

$$\begin{bmatrix} M & 0 \\ 0 & 2M \end{bmatrix} \begin{bmatrix} \ddot{x}_1 \\ \ddot{x}_2 \end{bmatrix} + \begin{bmatrix} k & -k \\ -k & 2k \end{bmatrix} \begin{bmatrix} x_1 \\ x_2 \end{bmatrix} = \begin{bmatrix} 0 \\ 0 \end{bmatrix} \tag{1}$$

Trial Solution

$$x(t) = x(A \sin \omega t + B \cos \omega t)$$

$$\begin{bmatrix} x_1(t) \\ x_2(t) \end{bmatrix} \begin{bmatrix} x_1 \\ x_2 \end{bmatrix} (A \sin \omega t + B \cos \omega t) \tag{2}$$

The Eigenvalue Problem
By substituting (2) into (1), we obtain the necessary conditions for (2) to be a solution

$$\left[k - \omega^2 M\right] x = 0 \tag{3}$$

$$\begin{bmatrix} (1-\beta) & -1 \\ -1 & 2(1-\beta) \end{bmatrix} \begin{bmatrix} x_1 \\ x_2 \end{bmatrix} = \begin{bmatrix} 0 \\ 0 \end{bmatrix} \qquad \beta = \omega^2 M/k \tag{4}$$

Using nontrivial solutions to (3), i.e. solutions where the eigenvectors $\phi \neq 0$,

$$\left|k - \omega^2 M\right| = 0 \tag{5}$$

Equation (5) if the frequency equation from which the eigenvalues ω^2 can be obtained

$$2(1-\beta)^2 - 1 = 0 \;\; or \; 2\beta^2 - 4\beta + 1 = 0 \rightarrow \beta \mp \frac{1}{2}\sqrt{2} \tag{6}$$

$$\beta_1 = 0.2929, \;\; \beta_2 = 1.7071 \tag{7}$$

Natural Circular Frequencies and Natural Periods
First harmonic

$$\omega_1 \sqrt{\beta_1 k/M}, \qquad T_1 = \frac{2\pi}{\omega_1} \tag{8}$$

Second harmonic

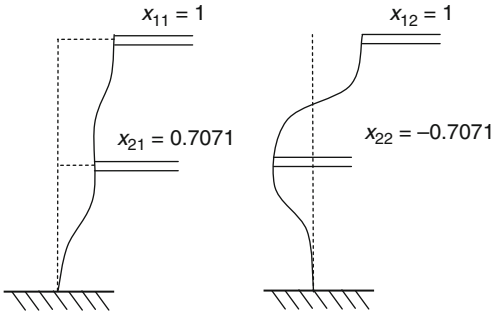
$$\omega_2 \sqrt{\beta_2 k/M}, \qquad T_2 = \frac{2\pi}{\omega_2} \tag{9}$$

www.EngineeringBooksPDF.com

Natural Modes for Free, Undamped Vibrations

1. Fundamental (first harmonic)
   $\beta_1 = 0.2929$ in (3), after normalisation and solve $x_{11} = 1,\ x_{21} = 0.7071$ (10)

2. Second Mode (second harmonic)
   $\beta_2 = 1.7071$ in (3), after normalisation and as in firstcase solve $x_{12} = 1$, $x_{22} = 0.7071$ (11)



Modal Matrix

The two natural modes may be displayed as the two columns of the modal matrix

$$x = \begin{bmatrix} x_{11} & x_{12} \\ x_{21} & x_{22} \end{bmatrix} = \begin{bmatrix} 1 & 1 \\ 0.7071 & -0.7071 \end{bmatrix} \tag{12}$$

General Solution for Free, Undamped Vibrations

Two different solutions, Eq. (2), have been obtained. Their sum therefore gives the general solution

$$\begin{bmatrix} x_1(t) \\ x_2(t) \end{bmatrix} = \begin{bmatrix} x_{11} \\ x_{21} \end{bmatrix} (A_1 \sin \omega_1 t + B_1 \cos \omega_1 t) + \begin{bmatrix} x_{11} \\ x_{21} \end{bmatrix} (A_2 \sin \omega_2 t + B_2 \cos \omega_2 t) \tag{13}$$

using Eq. (13) can also be written as $x(t) = \phi[D_1(t)A + D_2(t)B]$

$$\begin{bmatrix} x_1(t) \\ x_2(t) \end{bmatrix} = \begin{bmatrix} x_{11} & x_{12} \\ x_{21} & x_{22} \end{bmatrix} \begin{bmatrix} \sin \omega_1 t & 0 \\ 0 & \sin \omega_2 t \end{bmatrix} \begin{bmatrix} A_1 \\ A_2 \end{bmatrix} + \begin{bmatrix} \cos \omega_1 t & 0 \\ 0 & \cos \omega_2 t \end{bmatrix} \begin{bmatrix} B_1 \\ B_2 \end{bmatrix} \tag{14}$$

Free, Undamped Vibrations Based on Imposed Initial Conditions

The initial conditions be taken as

$$x_1(t = 0) = x_{10}, \tag{15}$$

www.EngineeringBooksPDF.com

$$x_2(t=0) = x_{20} \tag{16}$$

$$\dot{x}(t=0) = \dot{x}_{10}, \tag{17}$$

$$\dot{x}_2(t=0) = \dot{x}_{20}. \tag{18}$$

Upon substitution into (13) or (14), these condtions give

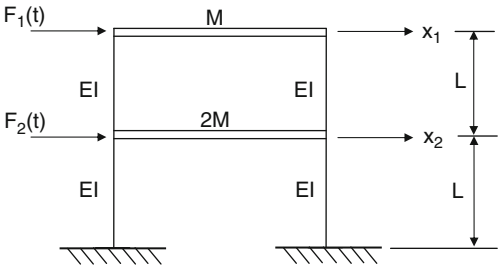
$$x(t) = xD_1(t)\omega^{-1}x^{-1}\dot{u}_0 + xD_2(t)x^{-1}u_0$$

$$\begin{bmatrix} x_1(t) \\ x_2(t) \end{bmatrix} = \begin{bmatrix} x_{11} & x_{12} \\ x_{21} & x_{22} \end{bmatrix} \begin{bmatrix} \sin\omega_1 t & 0 \\ 0 & \sin\omega_2 t \end{bmatrix} \begin{bmatrix} \frac{1}{\omega_1} & 0 \\ 0 & \frac{1}{\omega_2} \end{bmatrix} \frac{1}{x_{11}x_{22}-x_{12}x_{21}} \begin{bmatrix} x_{22} & x_{12} \\ -x_{21} & x_{11} \end{bmatrix} \begin{bmatrix} \dot{u}_{10} \\ \dot{u}_{20} \end{bmatrix} \tag{19}$$

$$+ \begin{bmatrix} x_{11} & x_{12} \\ x_{21} & x_{22} \end{bmatrix} \begin{bmatrix} \cos\omega_1 t & 0 \\ 0 & \cos\omega_2 t \end{bmatrix} \frac{1}{x_{11}x_{22}-x_{12}x_{21}} \begin{bmatrix} x_{22} & -x_{12} \\ -x_{21} & x_{11} \end{bmatrix} \begin{bmatrix} x_{10} \\ x_{20} \end{bmatrix}$$

It is necessary to use modal coordinates.

Plate 3.3 Motion expressed modal coordinates



DATA

$$M = 80 \text{ tonne}$$

$$k = 24\,EI/L^3 = 30 \times 10^6 \text{N/m}$$

Natural Circular Frequencies, using previous methods

$$\omega_1 = 10.480217\,\text{rad/s}$$

$$\omega_2 = 25.301483\,\text{rad/s}$$

$\longrightarrow$ Modal matrix ϕ

www.EngineeringBooksPDF.com

Equations of Motion

$$M\dot{x} + C\dot{x} + K\dot{x} = F(t)$$

$$\begin{bmatrix} M & 0 \\ 0 & 2M \end{bmatrix} \begin{bmatrix} \ddot{x}_1 \\ \ddot{x}_2 \end{bmatrix} + \begin{bmatrix} C_{11} & C_{12} \\ C_{21} & C_{22} \end{bmatrix} \begin{bmatrix} \dot{x}_1 \\ \dot{x}_2 \end{bmatrix} + \begin{bmatrix} K & -K \\ -K & 2K \end{bmatrix} \begin{bmatrix} x_1 \\ x_2 \end{bmatrix} = \begin{bmatrix} F_1(t) \\ F_2(t) \end{bmatrix} \quad (1)$$

Equations of Motion in Modal Coordinates with Classical Damping
Equation (1) can be transformed into the Modal equations

$$\phi^{T''} M\phi\ddot{q} + \phi^{T''} C\phi\dot{q} + \phi^{T''} K\phi q = \phi^{T''} F(t)$$

where T″ is transpose

$$\begin{bmatrix} M_1 & 0 \\ 0 & M_2 \end{bmatrix} \begin{bmatrix} \ddot{q}_1 \\ \ddot{q}_2 \end{bmatrix} + \begin{bmatrix} C_1 & 0 \\ 0 & C_2 \end{bmatrix} \begin{bmatrix} \dot{q}_1 \\ \dot{q}_2 \end{bmatrix} + \begin{bmatrix} K_1 & 0 \\ 0 & K_1 \end{bmatrix} \begin{bmatrix} q_1 \\ q_2 \end{bmatrix} = \begin{bmatrix} F_1(t) \\ F_2(t) \end{bmatrix} \quad (2)$$

With the assumption of classical damping, the matrix $\phi^{T''} C\phi$ becomes diagonal and (2) becomes uncoupled, i.e. the first equation involves the modal coordinate q_1 only while the second equation likewise involves only q_2. Each equation therefore represents a different (generalized) single-degree-of-freedom system.

Generalized or Modal Masses

$$M_1 = \sum M_i(\phi_{i1})^2 \quad (3a)$$

$$M_2 = \sum M_i(\phi_{i2})^2 \quad (3b)$$

Generalized or Modal Classical Damping Coefficients

$$C_1 = 2\xi_1\omega_1 M_1 \quad (4a)$$

$$C_2 = 2\xi_2\omega_2 M_2 \quad (4b)$$

Generalized or Modal Stiffnesses

$$K_1 = \omega_1^2 M_1 \quad (5a)$$

$$K_2 = \omega_2^2 M_2 \quad (5b)$$

Generalized or Modal Loads

$$P_1(t) = \sum \phi_{i1} p_i(t) \quad (6a)$$

$$P_2(t) = \sum \phi_{i2} p_i(t) \quad (6b)$$

www.EngineeringBooksPDF.com

3.3.6 Example 3.6

A rigidly jointed two-bay two-storey frame with relative masses at two floor levels is shown in Fig. 3.17. Assuming the horizontal members are infinitely

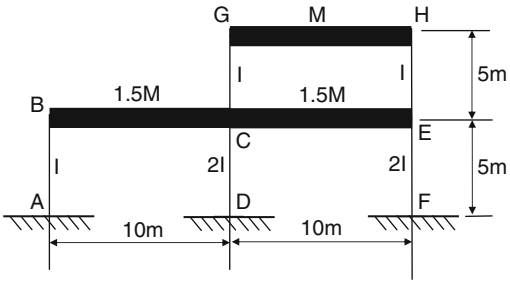


Fig. 3.17 A two-bay two-storey frame

stiff in comparison with the vertical members, determine two frequencies and their corresponding periods for this frame. Use the following data:

$$EI = 1.50 \times 10^6 \text{Nm}^2 \quad M = 10^5 \text{kg}$$

$$\delta = (A \sin \omega t + B \cos \omega t) \cdot D$$

where

δ = displacement of the frame
ω = circular frequency
D = column matrix for the deflected shape of the frame
A, B = constants

Referring to Fig. 3.17, it follows that

$$\ddot{\delta} = -\omega^2 \delta$$

$$\left[[k] - M\omega^2\right]\delta = 0$$

$$k_{11} = \frac{2 \times 12EI}{(5)^3} + \frac{2 \times 12E(2I)}{(5)^3} + \frac{12EI}{(5)^3}$$

$$= 0.672EI$$

$$k_{12} = k_{21} = -\frac{2 \times 12EI}{(5)^3} k_{12} = k_{21} = -\frac{2 \times 12EI}{(5)^3}$$

$$= -0.192EI$$

$$k_{22} = 2\left(\frac{12EI}{(5)^3}\right) = +0.192EI$$

www.EngineeringBooksPDF.com

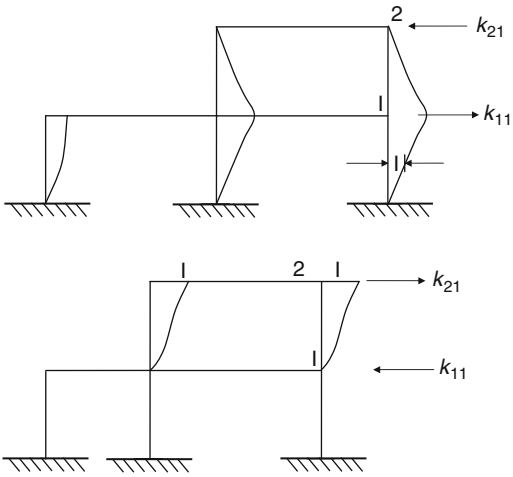


Fig. 3.18 Motion of vertical members

$$[k] = \begin{bmatrix} +0.672 & -0.192 \\ k_{11} & k_{12} \\ -0.192 & +0.192 \\ k_{21} & k_{22} \end{bmatrix} EI$$

$$[k - M\omega^2] \rightarrow \text{the determinant of this matrix} \begin{bmatrix} M & 0 \\ 0 & 3M \end{bmatrix} = 0$$

$$EI \begin{bmatrix} K_{11} - M_1\omega^2 & K_{12} \\ K_{21} & K_{22} - M_2\omega^2 \end{bmatrix}$$

$$= \begin{bmatrix} 0.672 - 10^5\omega^2 & -0.192 \\ -0.192 & 0.192 - 1.5 \times 10^5\omega^2 \end{bmatrix} EI$$

$$\begin{vmatrix} 0.672 - 10^5\omega^2 & -0.192 \\ -0.192 & 0.192 - 1.5 \times 10^5\omega^2 \end{vmatrix} EI = 0$$

$$\omega^2 = \bar{B}$$

$$\omega^4 - 29.6\omega^2 + 25.15 = 0$$

$$(\bar{B})2 - 29.6\bar{B} + 25.15 = 0$$

www.EngineeringBooksPDF.com

$$\bar{B} \rightarrow \omega^2 \rightarrow$$

$$f_1 = \frac{\omega_1}{2\pi} = 0.332\,Hz$$

$$f_2 = \frac{\omega_2}{2\pi} = 1.185\,Hz$$

$$T_1 = \frac{1}{f_1} = 3.012s$$

$$T_2 = \frac{1}{f_2} = 0.844s$$

3.3.7 Example 3.7

A single-bay single-storey frame with different leg heights is shown in Fig. 3.19, determine frequency and acceleration. Take $x = D\sin\omega t$ where x = displacements = δ; take $EI = 2 \times 10^6 Nm^2$

$$k_{total} = k_{AB} + k_{CD}$$

$$k_{AB} = \frac{12EI}{(4)^3} = \frac{12 \times 2 \times 10^6 Nm^2}{(4)^3}$$

$$k_{CD} = \frac{12EI}{(5)^3} = 375000$$

$$= \frac{12 \times 2 \times 10^6}{(5)^3} Nm^2 = \frac{192,000}{567,000}$$

$$[k_T]_{total} = 567,000\,N/m$$

$$k = N/m \rightarrow kg \text{ as meas}$$

$$\omega^2 = \sqrt{\frac{k_T}{m}} = \sqrt{\frac{567,000\,N/m}{2,000\,kg}}$$

$$= 16.84 \text{ rad/s}$$

$$T = \frac{2\pi}{\omega} = \frac{2\pi}{16.84} = 0.373\text{s}$$

$$f = \frac{1}{T} = \frac{1}{0.373} = 2.68 \text{ Hz}$$

$$F = \frac{6EI/L^2}{L/2} = \frac{12EI}{L^3}$$

www.EngineeringBooksPDF.com

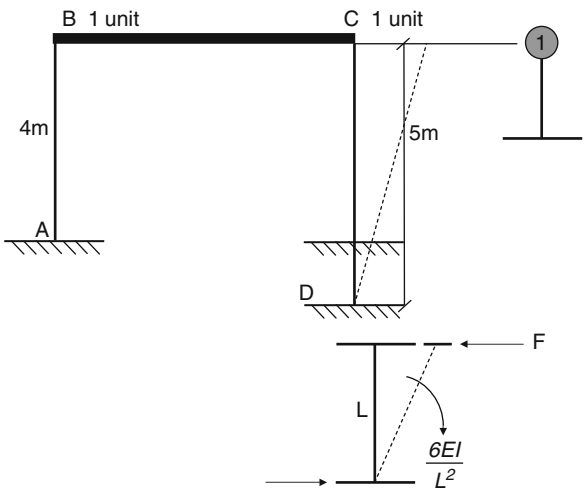


Fig. 3.19 Single frame with different heights of legs

When

$$F = \frac{12EI}{L^3}$$

$$k = \frac{12EI}{L^3}$$

$$D = \sqrt{A^2 + B^2} = 20\,mm = 0.02m$$

$$x = D \sin \omega t$$

$$= 0.02 \sin \omega t$$

$$= 0.2 \sin 16.84t$$

$$\frac{dx}{dt} = \dot{x} = 0.2 \times 16.84 \cos 16.84t$$

$$= 3.368 \cos 16.84t$$

$$\frac{dx^2}{dt^2} = \ddot{x} = -3.368 \times 16.84 \sin 16.84t$$

$$= -56.7 \sin 16.84t$$

3.3.8 Example 3.8

A typical rigidly jointed frame is shown in Fig. 3.20. The beam BCEG is assumed to be infinitely stiff. Assuming the frame is vibrating in a horizontal direction

www.EngineeringBooksPDF.com

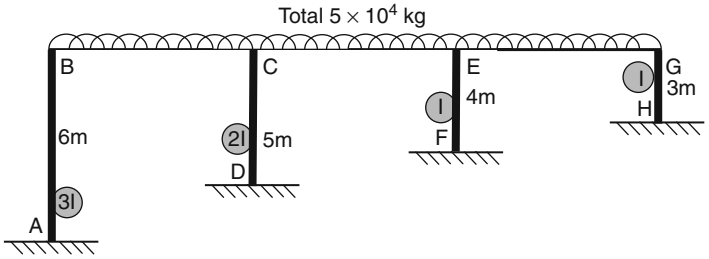


Fig. 3.20 A four-legged frame

determine the natural frequency for this frame. Take

$$\delta = X \sin \omega t$$

$$E = 200 \times 10^6 kN/m^2$$

$$I = 0.04m^4$$

Solution
A four-legged rigidly jointed frame:

$$K = \Sigma k = \Sigma k_{AB} + \Sigma k_{CD} + \Sigma k_{EF} + \Sigma k_{GH}$$

$$= \frac{12E(3I)}{(6)^3} + \frac{12E(2I)}{(5)^3} + \frac{12EI}{(4)^3} + \frac{12EI}{(3)^3}$$

$$= 0.9905EI$$

$$= 0.9905 \times 200 \times 10^6 \times 0.04$$

$$= 784.8722 \times 10^6$$

$$\delta = X \sin \omega t$$

$$\ddot{\delta} = -\omega^2 X \sin \omega t = \omega^2 \delta$$

$$M\ddot{\delta} + k\delta = 0$$

Substituting the values of $\ddot{\delta}, \delta$ and M, the above equation becomes

$$-M\omega^2\delta + k\delta = 0$$

$$(-M\omega^2 + k)\delta = 0$$

$$-M\omega^2 + K = 0$$

$$\omega = \sqrt{\frac{K}{M}} = \sqrt{\left\{\frac{784.8722 \times 10^6}{50000}\right\}}$$

$$= 0.036 \times 10^3 \, rad/s$$

$$f = \frac{\omega}{2\pi} = 5.73\mathrm{H_z}$$

www.EngineeringBooksPDF.com

3.3.9 Example 3.9

Figure 3.21 shows a multistorey frame with masses and second movement of areas (circled). With the indicated modes of vibration and the displacement $\delta = (A\sin\omega t - B\cos\omega t)$, determine natural frequencies and periods. Take $E = 200GN/m^2$; $I = 0.01m^4$. Reference coordinates are ① and ② as shown in the figure.

Solution

Multistorey frame

Stiffness coefficients:

$$k_{11} = 3\left\{\frac{12E(2I)}{(4.5)^3}\right\} = \frac{72EI}{(4.5)^3}$$

$$k_{12} = \frac{-72EI}{(4.5)^3}$$

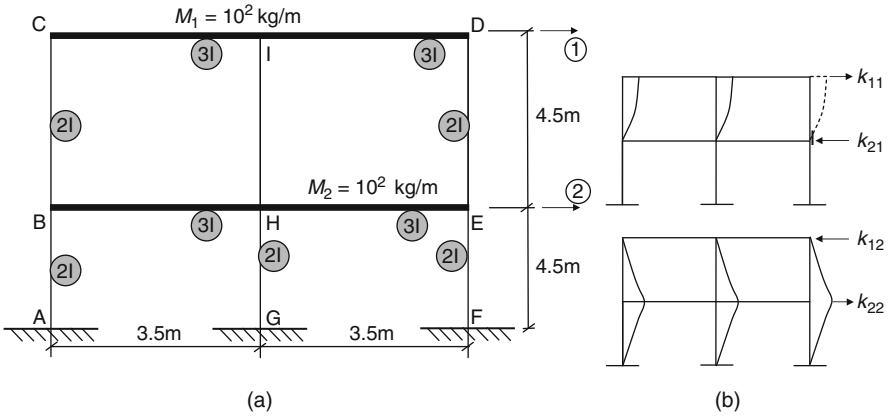


Fig. 3.21 A two-bay two-storey frame

$$k_{22} = 6\left(\frac{12E(2I)}{(4.5)^3}\right) = \frac{144EI}{(4.5)^3}$$

$$k_{12} = k_{21}$$

$$\dot{\delta} = A\cos\omega t - B\omega\sin\omega t$$

$$\ddot{\delta} = -A\omega^2\sin\omega t - B\omega^2\cos\omega t = -\omega^2\delta$$

Therefore,

$$\delta = -\omega^2\delta$$

www.EngineeringBooksPDF.com

Substituting various values in the equation of motion

$$M\ddot{\delta} + k\delta = 0$$

$$M(-\omega^2\delta) + k\delta = 0$$

or

$$k\delta - \omega^2 M\delta = 0$$

$$k - M\omega^2 = 0$$

The determinant of which is given below:

$$\begin{vmatrix} k_{11} - \omega^2 M_1 & k_{12} \\ k_{21} & k_{22} - \omega^2 M_2 \end{vmatrix} = 0$$

or

$$\begin{vmatrix} 1.6 \times 10^6 - 7 \times 10^3\omega^2 & -1.6 \times 10^6 \\ -1.6 \times 10^6 & 3.2 \times 10^6 - 14 \times 10^3\omega^2 \end{vmatrix} = 0$$

$$98\omega^4 - 44.8 \times 10^3\omega^2 + 2.56 \times 10^6 = 0$$

$$\omega^2 = \overline{k}$$

$$\overline{k} = 396 \quad \text{or} \quad 67$$

$$\omega_1 = 19.75 \quad \omega_2 = 8.186\,\text{rad/s}$$

$$f_1 = \frac{\omega_1}{2\pi} = 3.142\text{H}_\text{z} \quad f_2 = 1.3\,\text{Hz}$$

$$T_1 = \frac{1}{f_1} = 0.318\text{s} \quad T_2 = \frac{1}{f_2} = 0.77\text{s}$$

3.3.10 Example 3.10

A single-bay three-storey building with data given below is subjected to a horizontal dynamic load shown in Fig. 3.22. Calculate displacement at three levels as a multi-degree-of-freedom system.

www.EngineeringBooksPDF.com

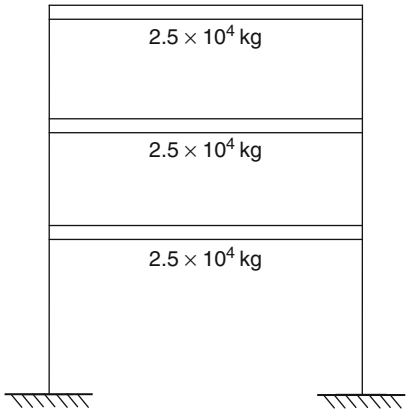


Fig. 3.22 A frame of a multi-degree-of-freedom system

Data

$$\phi = \begin{pmatrix} 1 & 1 & 1 \\ 0.533 & -1.51 & -3.2 \\ 0.155 & -1.24 & 4.5 \end{pmatrix} \text{m}$$

$$\omega = \begin{pmatrix} 2.0 \\ 13.10 \\ 35.26 \end{pmatrix} \text{rad/s}$$

$$M = \begin{pmatrix} 25 & 0 & 0 \\ 0 & 25 & 0 \\ 0 & 0 & 25 \end{pmatrix} \times 10^4 \text{ kg}$$

Equations of motion in matrix form

$$M\ddot{x} + Kx = P(t)$$

This equation is coupled due to the stiffness matrix. To uncouple equations, use an orthogonality relationship

$$\phi_i^T M \phi_i = 0$$

$$\text{If } i = j \quad \rightarrow \quad \omega_1^2 = \omega_j^2$$

$$\phi_i^T M \phi_i = L_1^2 \text{ (say a constant)}$$

$$L_1^2 = \phi_1^T M \phi_1$$

www.EngineeringBooksPDF.com

$$= (1,\ 0.533,\ 0.155)\begin{pmatrix} 25,000 & 0 & 0 \\ 0 & 25,000 & 0 \\ 0 & 0 & 25,000 \end{pmatrix}\begin{pmatrix} 1 \\ 0.533 \\ 0.155 \end{pmatrix}$$

$$=(25,000,\ 13,325,\ 38,75)\begin{pmatrix} 1 \\ 0.533 \\ 0.155 \end{pmatrix}$$

$$= 32,702.35 \Rightarrow L_1 = 180.84\ \text{kg}^{1/2}\text{m}$$

$$L_2^2 = \phi_2^T M \phi_2$$

$$= (1\ -1.51 - 1.24)\begin{pmatrix} 25,000 & 0 & 0 \\ 0 & 25,000 & 0 \\ 0 & 0 & 25,000 \end{pmatrix}\begin{pmatrix} 1 \\ -1.51 \\ -1.24 \end{pmatrix}$$

$$= (25,000\ -37,250\ -31,000)\begin{pmatrix} 1 \\ -1.51 \\ -1.24 \end{pmatrix}$$

$$= 120,442.5\ \Rightarrow\ L_2 = 347.048\text{kg}^{1/2}\text{m}$$

$$\text{L}_3^2 - \phi_3^{\text{T}} M \phi_3$$

$$= (1.0\ -3.2,\ 4.5)\begin{pmatrix} 25,000 & 0 & 0 \\ 0 & 25,000 & 0 \\ 0 & 0 & 25,000 \end{pmatrix}\begin{pmatrix} 1.0 \\ -3.2 \\ 4.5 \end{pmatrix}$$

$$= (25,000\ -80,000,\ 112,500)\begin{pmatrix} 1.0 \\ -3.2 \\ 4.5 \end{pmatrix}$$

$$= 787,250 \Rightarrow L_3 = 897.27\text{kg}^{1/2}\text{m}$$

The following can now be written:

$$z_i = \frac{\phi_i}{L_i}$$

which gives

$$z_i^T M z_i = \frac{\phi_i^T\ M\ \phi_i}{L_1^2} = 1$$

and

$$z_i^T\ M\ z_j = 0$$

www.EngineeringBooksPDF.com

because

$$\frac{\phi_i^T}{L_i}\ M\ \frac{\phi_i}{L_j} = 0$$

$$z = \begin{pmatrix} \frac{\phi_{11}}{L_1} & \frac{\phi_{21}}{L_2} & \frac{\phi_{31}}{L_3} \\ \frac{\phi_{12}}{L_1} & \frac{\phi_{22}}{L_2} & \frac{\phi_{32}}{L_3} \\ \frac{\phi_{13}}{L_1} & \frac{\phi_{23}}{L_2} & \frac{\phi_{33}}{L_3} \end{pmatrix}$$

$$= \begin{pmatrix} 5.53 & 2.88 & 1.127 \\ 2.95 & -4.35 & -3.60 \\ 0.857 & -3.573 & 5.071 \end{pmatrix} \times 10^{-3} \frac{\text{m}}{\text{kg}^{1/2}\text{m}} = \text{kg}^{-1/2}$$

From the equation of motion

$$K = M\omega^2$$

Hence $z^{\text{T}''} Kz = z^{\text{T}''} Mz\omega^2$. As $z^{\text{T}''}\ Mz = 1$, then

$$z^{\text{T}''} Kz = I\omega^2$$

where T″ is transpose.

At this stage, it is necessary to uncouple the equation of motion by introducing a check of coordinates by writing

$$x = zq$$

$$\dot{x} = z \cdot \dot{q}$$

$$\ddot{x} = z \cdot \ddot{q}$$

$$M\ddot{x} - Kx = P_{(t)}$$

$$Mz\ddot{q} - Kzq = P_{(t)}$$

Pre-multiplying by $z^{\text{T}''}$ the result is

$$\ddot{q} - \omega^2 q = z^{\text{T}} P_{(t)}$$

$$\omega = \begin{pmatrix} 20 & 0 & 0 \\ 0 & 13.10 & 0 \\ 0 & 0 & 35.26 \end{pmatrix} \text{rad/s}$$

$$P_{(t)} = \begin{pmatrix} 20 \\ 0 \\ 0 \end{pmatrix} \sin 0.3T\ (\text{kN})$$

www.EngineeringBooksPDF.com

$$z^{\mathrm{T}}P_{(t)} = \begin{pmatrix} 5.53 & 2.95 & 0.857 \\ 2.88 & -4.35 & -3.573 \\ 1.127 & -3.60 & 5.071 \end{pmatrix} \begin{pmatrix} 20 \\ 0 \\ 0 \end{pmatrix} \sin 0.3T$$

$$= \begin{pmatrix} 110.6 \\ 57.6 \\ 22.54 \end{pmatrix} \sin 0.3\mathrm{T}(\mathrm{z}[\mathrm{kg}^{-1/2}]10^{-3}P[N]10^{-3})[\mathrm{kg}^{1/2}/\mathrm{ms}^2]$$

The set of uncoupled equations:

$$= \begin{pmatrix} \ddot{q}_1 \\ \ddot{q}_2 \\ \ddot{q}_3 \end{pmatrix} - \begin{pmatrix} 2.0 & 0 & 0 \\ 0 & 13.10 & 0 \\ 0 & 0 & 35.26 \end{pmatrix} \begin{pmatrix} q_1 \\ q_2 \\ q_3 \end{pmatrix} = \begin{pmatrix} 110.6 \\ 57.6 \\ 22.54 \end{pmatrix} \sin 0.3\mathrm{T}$$

This is a set of three SDOF equations subjected to undamped $P_0 \sin \omega T$ motion and particular integral solution is given by

$$q_1(t) = \frac{P_i}{m\omega_i^2} \sin \omega t$$

$$q_1(t) = \frac{110.6}{4.0. \times 2.5 \times 10^4} \sin 0.3t = 1106 \sin 0.4t \times 10^{-3}\mathrm{kg}^{1/2}\mathrm{m}$$

$$\mathrm{q}_2(t) = \frac{57.6}{171.69 \times 2.5 \times 10^4} \sin 0.3t = 1.34 \sin 0.4t \times 10^{-5}\mathrm{kg}^{1/2}\mathrm{m}$$

$$\mathrm{q}_3(t) = \frac{22.54}{1243.36 \times 2.5 \times 10^4} \sin 0.3t = 7.25 \sin 0.3t \times 10^{-7}\mathrm{kg}^{1/2}\mathrm{m}$$

Now $x_i = z \cdot q_i$

$$\begin{pmatrix} x_1(t) \\ x_2(t) \\ x_3(t) \end{pmatrix} = \begin{pmatrix} 5.53 & 2.88 & 1.127 \\ 2.95 & -4.35 & -3.60 \\ 0.857 & -3.573 & 5.079 \end{pmatrix} \times 10^{-3} \begin{pmatrix} 1.106 \\ 0.0134 \\ 0.000725 \end{pmatrix} \sin 0.3t \times 10^3(\mathrm{m})$$

www.EngineeringBooksPDF.com

$$x_1(t) = 6.115 \sin 0.3t \times 10^{-6}\text{m}$$

(maximum displacement when $\sin 0.3t = 1$)

$$x_2(t) = 3.20 \sin 0.3t \times 10^{-6}\text{m}$$

$$\left(\text{maximum displacement when } 0.3t = \frac{m\pi}{2}\right)$$

$$x_3(t) = 0.923 \sin 0.3t \times 10^{-6}\text{m}$$

(maximum displacement when $t = m \times 5.23\text{s}$)

$$\text{x}_1 \text{ max} = 6.115 \times 10^6\text{m}$$

$$\text{x}_2 \text{ max} = 3.20 \times 10^6\text{m}$$

$$\text{x}_3 \text{ max} = 0.923 \times 10^6\text{m}$$

3.3.11 Example 3.11

A single-bay four-storey building frame with data is shown in Fig. 3.23. Calculate frequencies and modes of this frame with a multi-degree-of-freedom system.

Data

$$\text{Stiffness matrix} = \begin{pmatrix} 1 & -1 & 0 & 0 \\ -1 & 2 & -1 & 0 \\ 0 & -1 & 2 & -1 \\ 0 & 0 & -1 & 2 \end{pmatrix} \times 10^9\ \text{N/m}$$

$$\text{Flexibility matrix} = \begin{pmatrix} 4 & 3 & 2 & 1 \\ 3 & 3 & 2 & 1 \\ 2 & 2 & 2 & 1 \\ 1 & 1 & 1 & 1 \end{pmatrix} \times 10^6(\text{m/kN}) \text{ or } \times 10^{-9}\ \text{m/N}$$

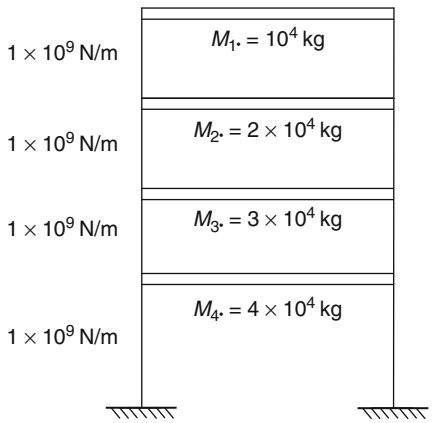


Fig. 3.23 A single-bay four-storey building frame of a multi-degree-of-freedom system

www.EngineeringBooksPDF.com

$$M = \begin{pmatrix} 1 & 0 & 0 & 0 \\ 0 & 2 & 0 & 0 \\ 0 & 0 & 3 & 0 \\ 0 & 0 & 0 & 4 \end{pmatrix} \times 10^4\, kg$$

$$H = F \times M = \begin{pmatrix} 4 & 6 & 6 & 4 \\ 3 & 6 & 6 & 4 \\ 2 & 4 & 6 & 4 \\ 1 & 2 & 3 & 4 \end{pmatrix} \times 10^{-5} m^2$$

(a) Stodola method
Based on equation of motion

$$\frac{1}{\omega^2} X = FMX$$

the initial mode shape is

$$X_1^0 = \begin{pmatrix} 1 \\ 1 \\ 1 \\ 1 \end{pmatrix}$$

Hence

$$\frac{1}{\omega^2} X_1^1 = HX_1^0$$

But $1/\omega^2$ is unknown, hence

$$\frac{1}{\omega^2} X = \bar{X}$$

Thus, it follows that

X_1^0	X_1^1	X_1^1	$\bar{X}_1^2$	X_1^2	$\bar{X}_1^3$	X_1^3	$\bar{X}_1^4$	X_1^4
1	20	1	96.5	1	15.98	1	15.90	1
1	19	0.95	15.5	0.939	14.98	0.937	14.90	0.937
1	16	0.8	12.6	0.764	12.11	0.758	12.03	0.757
1	10	0.5	7.3	0.442	6.938	0.434	6.884	0.433

www.EngineeringBooksPDF.com

Hence, the first mode shape is

$$\phi = \begin{pmatrix} 1 \\ 0.937 \\ 0.757 \\ 0.433 \end{pmatrix}$$

and

$$\omega_1^2 = \frac{X_{11}^3}{X_{11}^4} = \frac{1}{10^{-5} \times 15.9} = 6,239.3$$

Therefore,

$$\omega_1 = 79.3\,\text{rad/s}$$

for the second mode shape.

(i) Calculate sweeping matrix

$$Q_1 = I - \phi_1 \frac{\phi_1^T M}{\phi_1^T M \phi_1}$$

or for higher modes

$$Q_1 = I - \frac{1}{M_1} \phi_1 \phi_1^T M$$

$$M_1 = \phi_1^T M \phi_1$$

$$Q_m = Q_{m-n} - \phi_m \frac{\phi_m^T M}{\phi_m^T M \phi_m}$$

$$M_1 = (10\ 0.937,\ 0.757,\ 0.433) \begin{pmatrix} 1 & 0 & 0 & 0 \\ 0 & 2 & 0 & 0 \\ 0 & 0 & 3 & 0 \\ 0 & 0 & 0 & 4 \end{pmatrix} \begin{pmatrix} 1.0 \\ 0.937 \\ 0.757 \\ 0.433 \end{pmatrix}$$

$$= 5.226 \times 10^4\,\text{kg}$$

www.EngineeringBooksPDF.com

$$\phi_1\phi_1^T M = \begin{pmatrix} 10 \\ 0.937 \\ 0.757 \\ 0.433 \end{pmatrix} (10,\ 0.937,\ 0.757,\ 0.433) \begin{pmatrix} 1 & 0 & 0 & 0 \\ 0 & 2 & 0 & 0 \\ 0 & 0 & 3 & 0 \\ 0 & 0 & 0 & 4 \end{pmatrix}$$

$$= \begin{pmatrix} 1.0 & 1.874 & 2.271 & 1.732 \\ 0.937 & 1.756 & 2.123 & 1.624 \\ 0.757 & 1.418 & 1.719 & 1.312 \\ 0.433 & 0.812 & 0.984 & 0.748 \end{pmatrix} \times 10^4 \mathrm{Kg/m^2}$$

$$Q_1 = \begin{pmatrix} 0.808 & -0.358 & -0.434 & -0.331 \\ -0.279 & 0.664 & -0.407 & -0.311 \\ -0.145 & -0.279 & 0.671 & 0.259 \\ -0.083 & -0.155 & -0.188 & 0.357 \end{pmatrix}$$

(ii) Calculate matrix H_2 (which eliminates contribution of first mode from the assumed initial shape of the second mode X_1^0 which converges to a true shape)

$$H_2 = H_1 Q_n$$

For higher shapes

$$H_{n+1} = H_1 Q_n$$

$$H_3 = \begin{pmatrix} 4 & 6 & 6 & 4 \\ 3 & 6 & 6 & 4 \\ 2 & 4 & 6 & 4 \\ 1 & 2 & 3 & 4 \end{pmatrix} \begin{pmatrix} 0.808 & -0.358 & -0.454 & -0.339 \\ -0.179 & 0.664 & -0.407 & -0.311 \\ -0.145 & -0.279 & 0.679 & -0.251 \\ -0.083 & -0.155 & -0.188 & 0.857 \end{pmatrix}$$

$$\begin{pmatrix} 0.965 & 0.306 & -0.904 & -1.268 \\ 0.143 & 0.664 & -0.47 & -0.932 \\ -0.302 & -0.306 & 0.778 & 0.016 \\ -0.317 & -0.463 & 0.013 & 1.722 \end{pmatrix} \times 10^{-5}$$

(iii) Now determine second mode shape as before

$$X_2^0 = \begin{pmatrix} 1 \\ 1 \\ -1 \\ -1 \end{pmatrix}$$

$$\bar{X}_1^1 = H_2 \times X_2^0$$

www.EngineeringBooksPDF.com

X_2^0	$\bar{X}_2^1$	X_2^1	$\bar{X}_2^2$	X_2^2	$\bar{X}_2^3$	X_2^3	$\bar{X}_2^4$	X_2^4	$\bar{X}_2^5$	X_2^5
1	3.443	1	2.455	1	2.42	1.0	2.427	1	2.437	1
1	2.219	0.644	1.451	0.591	1.415	0.585	1.423	0.586	1.432	0.587
−1	−1.402	−0.407	−0.327	−0.336	−0.756	−0.312	−0.736	−0.303	−0.729	−0.299
−1	−2.515	−0.730	−1.877	−0.765	−1.912	−0.790	−1.952	−0.804	−1.926	−0.811

$$\phi_2 = \begin{pmatrix} 1 \\ 0.587 \\ -0.299 \\ -0.811 \end{pmatrix}$$

$$\omega_2^2 = \frac{X_2^4}{\bar{X}_2^5} = \frac{1}{10^{-5} \times 2,437} \Rightarrow \omega_2 = 202.56 \text{ rad/s}$$

(b) Holzer method

Evaluate second mode shape:

(i) ω_2 assumed $=$ 200 rad/s, $\omega_2^2 = 40,000$

(ii) Displacement of m_1 is taken as unity (i.e. $X_1 = 1$). Thus, new displacement of the next pass in the chain, M_2, is

$$X_2 = X_1 - \omega^2 \frac{M_1 X_1}{k_2}$$

now with mass

$$X_m = X_{m-n} - \frac{\omega^2}{k_m} \sum_{r=1}^{m-n} M, X,$$

Take $\omega^2 = 200 \left(\omega_2^2 = 40,000\right)$. Then it follows that

Level	X	$M_r X_r$	$\sum M_r X_r$	$\frac{\omega_1^2}{k} \sum M_r X_r$
1	1	10^4	10^4	0.4
2	0.6	12×10^4	22×10^4	0.88
3	−0.28	−8,400	13,600	0.544
4	−0.824	−32,960	−19,360	−0.774
5	0.05 mm	OK		

Displacement at level 5 should be 0 at next iteration. Thus

Level	X	$M_r X_r$	$\sum M_r X_r$	$\frac{\omega_1^2}{k_m} \sum M_r X_r$
1	1	10^4	10^4	0.41
2	0.589	1.178×10^4	21780	0.893
3	−0.30	−9000	12780	0.524
4	−0.824	−32974.8	−20194.8	−0.828
5	−0.0046 mm			

www.EngineeringBooksPDF.com

Both Stodola and Holzer's iterations converge to the same second mode shape:

$$\phi_2 \begin{pmatrix} 1 \\ 0.589 \\ -0.3 \\ -0.824 \end{pmatrix}$$

$$\omega = 202.56 \text{ rad/s}$$

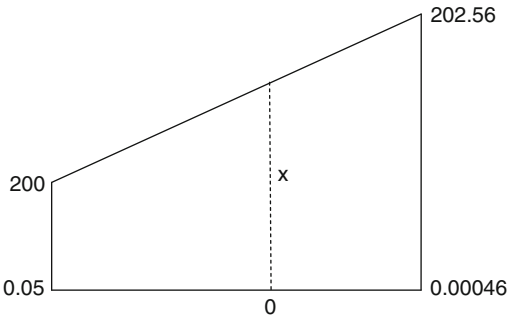


Fig. 3.24 Diagram for interpolation

We can interpolate to get better approximation for ω (see Fig. 3.24):

$$\omega = 202.34 \,\text{rad/s}$$

Section 3.3.12 gives analysis for the numerical methods used in the classical dynamic analysis.

3.3.12 Generalized Numerical Methods in Structural Dynamics

3.3.12.1 A Method of Continuous Distribution of Mass

Static law $p - m\frac{\partial^2 u}{\partial t^2} = -\frac{\partial^2}{\partial x^2} M(x,t)$

Kinematic Law $$k(x,t) = -\frac{\partial^2}{\partial x^2} u(x,t) \tag{3.86}$$

$M(x,t) = EI\{1 + c\frac{\partial}{\partial t}\}k(x,t)$

www.EngineeringBooksPDF.com

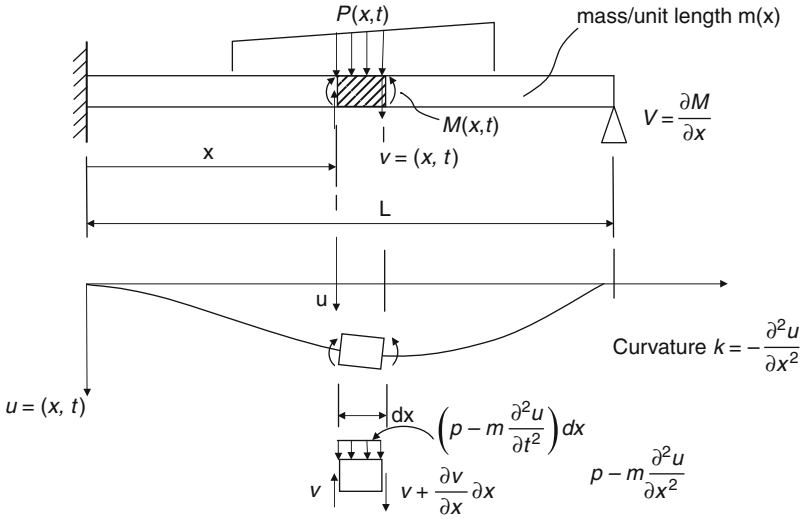
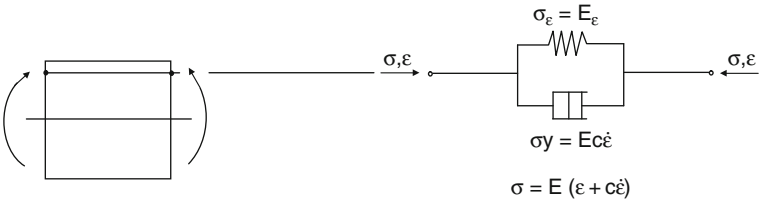


Fig. 3.25 Continuous mass distribution



$$\frac{\partial^2}{\partial x^2}\left\{EI\left(\frac{\partial^2 u}{\partial x^2}+c\frac{\partial^2 u}{\partial x^2\partial t}\right)\right\}+m\frac{\partial^2 u}{\partial t^2}=p \tag{3.87}$$

$$M(x,t)=-\left[EI\frac{\partial^2 u}{\partial x^2}+cEI\frac{\partial^3 u}{\partial x^2\partial t}\right] \tag{3.88}$$

$$V(x,t)=-\frac{\partial}{\partial x}\left[EI\frac{\partial^2 u}{\partial x^2}+cEI\frac{\partial^3 u}{\partial x^2\partial t}\right] \tag{3.89}$$

3.3.12.2 Free Vibrations of Prismatic Beams $P=0$ m,c, EI = const.

$$EI\frac{\partial^4 u}{\partial x^4}+dEI\frac{\partial^5 u}{\partial x^4\partial t}+m\frac{\partial^2 u}{\partial^2}=0 \tag{3.90}$$

www.EngineeringBooksPDF.com

Assume $u(x,t) = \phi(x)q(t)$ $[u(t) = \Phi q(t)]$
$EI^{iv}(x)q(t) + dEI\phi^{iv}(x)\dot{q}(t) + m\phi(x)\ddot{q}(t) = 0$ constant for all x and t

$$\frac{\phi^{iv}(x)}{\phi(x)} = \frac{m\ddot{q}(t)}{EI(q + c\dot{q})} \text{ i.e. } f(x) = g(t) \tag{3.91}$$

Therefore,

$$Hf = g = a^4 (\text{a constant}) \tag{3.92}$$

Two ODEs are thereby obtained:
ODE 1 in t

$$\frac{m\ddot{q}(t)}{EI(q + e\dot{q})} = \alpha^4 m\ddot{q} + (cEIa^4)\dot{q} + (EIa^4)q = 0 \tag{3.93}$$

Solution:

$$q(t) = e^{-\xi\omega t}\left[\frac{\dot{q}(0) + q(0)\xi\omega}{\omega_D}\sin\omega_D t + q(0)\cos\omega_D t\right] \tag{3.94}$$

$$\omega = \omega\sqrt{1 - \xi^2} \qquad m\omega^2 = EIa^4 \tag{3.95}$$

ODE 2 in x

$$\frac{\phi^{iv}}{\phi} = \alpha^4 \frac{\partial^4\phi}{\partial x^4} - a^4\phi = 0 \tag{3.96}$$

Solution:

$$\phi(x) = A_1 \sinh ax + A_2 \cosh ax + A_3 \sin ax + A_4 \cos ax \tag{3.97}$$

A_1 depends on end fixing of beam.

Plate 3.4 Numerical Integration of The Equation of Motion: The Newmark Method

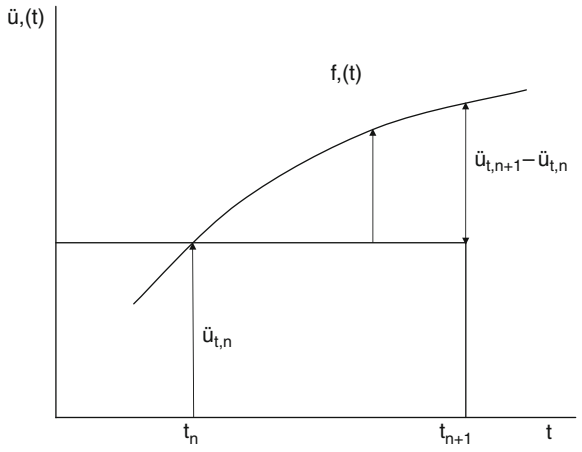


Fig. 3.26 Newmark method

Consider the variation of acceleration $\ddot{u}(t)$ in the interval $t_n \le t \le t_{n+1}$. Suppose that the $\ddot{u}_i(t)$ initial values $\ddot{u}(t = t_n) = \ddot{u}_n$ are known and the aim is to advance

www.EngineeringBooksPDF.com

the solution to t_{n+1}. Let $\ddot{u}(t) = \ddot{u}_n + f(t)$ (3.97a) where $f(t) = \{f_i(t)\}$ is a vector of approximating functions f_i , one for each degree of freedom i. Integrate (1) twice

$$\dot{u}(t) = b + \ddot{u}_n t + \int_{t_n}^{t} f(t)df \tag{3.98}$$

$$u(t) = a + bt + \frac{1}{2}\ddot{u}_n t^2 + \int_{t_n}^{t}\int_{t_n}^{t} f(t)dtdt \tag{3.99}$$

At $t = t_n$, the known velocities and displacements are $\dot{u}(t_n) = \dot{u}_n, u(t_n) = u_n$. Use these to eliminate arbitrary constant vectors a and b and write (3.98) and (3.99) at time t_{n+1}.

$$\dot{u}_{n+1} = \dot{u}_n + \ddot{u}_n(t_{n+1} - t_n) + \int_{t_n}^{t_{n+1}} f(t)dt \tag{3.100}$$

$$u_{n+1} = u_n + \ddot{u}_n(t_{n+1} - t_n) + \frac{1}{2}\ddot{u}_n(t_{n+1} - t_n)^2 \int_{t_n}^{t_{n+1}}\int_{t_n}^{t_{n+1}} f(t)dtdt \tag{3.101}$$

In these equations, $\Delta t = (t_{n+1} - t_n)$ is the selected *time-step*.

At the end of the time interval, it happens that $f_i(t_n) = 0$ and $f_i(t_{n+1}) = \ddot{u}_{i,n+1} - \ddot{u}_{i,n}$, but within the interval the approximating functions $f_i$are otherwise arbitrary. For each such f_i it may easily be written as

$$\int_{t_n}^{t_{n+1}}\int_{t_n}^{t_{n+1}} f(t)dtdt = Bi(\ddot{u}_{i,n+1} - \ddot{u}_{i;n})\Delta t^2 \tag{3.102}$$

$$\int_{t_n}^{t_{n+1}} f_i(t)dt = yi[\ddot{u}_{i,n+1} - \ddot{u}_{i,n}]\Delta t \tag{3.103}$$

in which the constants $\alpha_i (0 \le \alpha_i \le 1)$ and $\beta_i (0 \le \beta_i \le 1)$ depend only on the form of the f_i.

Assuming that the form of the functions f_i is the same for all degrees of freedom i, then the parameters β_i and γ_i reduce to two values, β and γ. This simplification, (3.100), (3.101), (3.102) and (3.103) can be

written as:

$$u_{n+1} = u_n + (1 - \beta)\ddot{u}_n\Delta t + \beta\ddot{u}_{n+1}\Delta t \tag{3.104}$$

$$u_{n+1} = u_n + u_n\Delta t + (\frac{1}{2} - \beta)\ddot{u}_n\Delta t^2 + \beta\ddot{u}_{n+1}\Delta t^2 \tag{3.105}$$

These are the basic equations of the *Newmark method,* and the choice of the parameters B, β, Δt significantly influences the numerical stability and accuracy of the method.

www.EngineeringBooksPDF.com

From Eq. (3.105) the incremental acceleration vector is obtained:

$$\Delta\ddot{u} = \ddot{u}_{n+1} - \ddot{u}_n = \frac{1}{\beta\Delta t^2}[u_{n+1,} - u_n] - \frac{1}{\beta\Delta t}u_n - \frac{1}{2\beta}\ddot{u}_n \tag{3.106}$$

Now substitute Eq. (3.106) to Eq. (3.104) gives the incremental velocity vector:

$$\Delta\dot{u} = \dot{u}_{n+1} - \dot{u}_n = \frac{\gamma}{\beta\Delta t}[u_{n+1} - u_n] - \frac{\gamma}{\beta}\dot{u}_n + (1 - \frac{\gamma}{2\beta})\ddot{u}_n\Delta t \tag{3.107}$$

At times t_{n+1} and t_n, the equations of motion may be written as:

$$m\ddot{u}_{n+1} + cu_{n+1} + ku_{n+1} = p_{n+1} \tag{3.108}$$

$$m\ddot{u}_n + cu_n + ku_n = p_n \tag{3.109}$$

Subtracting Eqs. (3.108) and (3.109) the equations of motion in incremental form can be written as

$$m\Delta\ddot{u} + c\Delta\dot{u} + k\Delta u = \Delta p \tag{3.110}$$

When Eqs (3.106) and (3.107) are substituted into (3.108) gives the incremental displacements:

$$\left[\frac{1}{\alpha\Delta t^2}m + \frac{y}{\alpha\Delta t}c + k\right]\Delta u = \Delta p + \left[\frac{1}{\alpha\Delta t}m + \frac{y}{\alpha}c\right]\dot{u}_u + \left[\frac{1}{2\alpha}m + \left\{\frac{y}{2\alpha}\right\}\Delta tc\right]\ddot{u}_n \tag{3.111}$$

Algorithm

For a structure having N degrees of freedom, choose the time step $\Delta t = 0.1T_N$, where T_N is the shortest natural period. Choose the parameters $\alpha = 0.25$ (constant average acceleration) and $\beta = 0.5$ (no algorithmic damping).

Plate No. 3.5 Eigenvalue analysis by inverse matrix iteration

In structural dynamics, the ith natural circular frequency ω_i and natural mode ϕ_i must satisfy

$$\mathbf{k}\phi_i = \omega_i^2\mathbf{m}\phi_i \tag{3.112}$$

Let s be a constant called the shift. Then, subtracting $s\mathbf{m}\phi_i$ from both sides of Eq. (1) gives

$$[\mathbf{k} - s\mathbf{m}]\phi_i = (\omega_i^2 - s)\mathbf{m}\phi_i \tag{3.113}$$

The modified stiffness matrix retains the same eigenvectors ϕ_i but shifts all the eigenvalues ω_i^2 by the same amount s.

www.EngineeringBooksPDF.com

Introduce the nth iterates $\lambda_i^{(n)}$ and $\mathbf{x}_i^{(n)}$ as approximations to ω_i^2 and ϕ_i, then Eq. (3.113) may be rewritten as a recurrence relation:

$$[\mathbf{k} - s\mathbf{m}]\left(\lambda_i^{(n+1)} - s\right)^{-1}\mathbf{x}_i^{(n+1)} = \mathbf{m}\mathbf{x}_i^{(n)} \tag{3.114}$$

$$\mathbf{y}_i^{(n)} = \mathbf{m}\mathbf{x}_i^{(n)} \tag{3.115}$$

and

$$\mathbf{x}_i^{(n+1)} = \left(\lambda_i^{(n+1)} - s\right)^{-1}\mathbf{x}_i^{(n+1)} \tag{3.116}$$

Let Eq. (3.114) becomes

$$[\mathbf{k} - s\mathbf{m}]\bar{\mathbf{x}}_i^{(n+1)} = \mathbf{y}_i^{(n)} \tag{3.117}$$

and the iteration can be commenced from any trial vector $\mathbf{y}_i^{(0)}$.

To solve Eq. (3.117) *without matrix inversion*, first that the symmetric matrix can be factorized as

$$[\mathbf{L}\mathbf{D}\mathbf{L}^{\mathbf{T}}]\bar{\mathbf{x}}_i^{(n+1)} = \mathbf{y}_i^{(n)} \tag{3.118}$$

Gaussian elimination will reduce Eq. (3.118) to

$$\mathbf{L}^{\mathbf{T}}\bar{\mathbf{x}}_i^{(n+1)} = \bar{\mathbf{v}}_i^{(n)} \tag{3.119}$$

The pivots of the elimination process form the diagonal matrix $\mathbf{D}$, and $\mathbf{L}^{\mathbf{T}}$ is an upper triangular matrix whose leading diagonal contains only unit elements. Eq. (3.119) can therefore be solved by a simple and accurate back substitution to obtain $\bar{\mathbf{x}}_i^{(n+1)}$. Hence

$$\bar{\mathbf{y}}_i^{(n+1)} = \bar{\mathbf{x}}_i^{(n+1)} \tag{3.120}$$

and multiply the resulting vector by a suitable normalizing constant:

$$\mathbf{y}_i^{(n+1)} = q_i^{(n+1)}\bar{\mathbf{y}}_i^{(n+1)} \tag{3.121}$$

Go back to the right-hand side of Eq. (3.118) and iterate until convergence is achieved in the $\mathbf{y}_i$.

An improved estimate of the eigenvalue may be obtained by pre-multiplying both sides of Eq. (3.113) by $\phi_i^{\mathbf{T}}$. Thus follows the Rayleigh quotient for $\omega_i^2 - s$, and from Eqs. (3.117) and (3.119)

$$\lambda_i^{(n+1)} - s = \frac{\mathbf{x}_i^{(n+1)T}[\mathbf{k} - s\mathbf{m}]\mathbf{x}_i^{(n+1)}}{\mathbf{x}_i^{(n+1)\mathbf{T}}\mathbf{m}\mathbf{x}_i^{(n+1)}} = \frac{\bar{\mathbf{x}}_i^{(n+1)T}[\mathbf{k} - s\mathbf{m}]\bar{\mathbf{x}}_i^{(n+1)}}{\bar{\mathbf{x}}_i^{(n+1)\mathbf{T}}\bar{\mathbf{x}}_i^{(n+1)}} = \frac{\bar{\mathbf{x}}_i^{(n+1)\mathbf{T}}\mathbf{y}_i^{(n)}}{\bar{\mathbf{x}}_i^{(n+1)\mathbf{T}}\bar{\mathbf{y}}_i^{(n+1)}} \tag{3.122}$$

An improved estimate of the eigenvector is then produced by normalizing the solution of Eq. (3.119):

$$\mathbf{x}_i^{(n+1)} = p_i^{(n+1)}\ \mathbf{x}_i^{(n+1)} \tag{3.123}$$

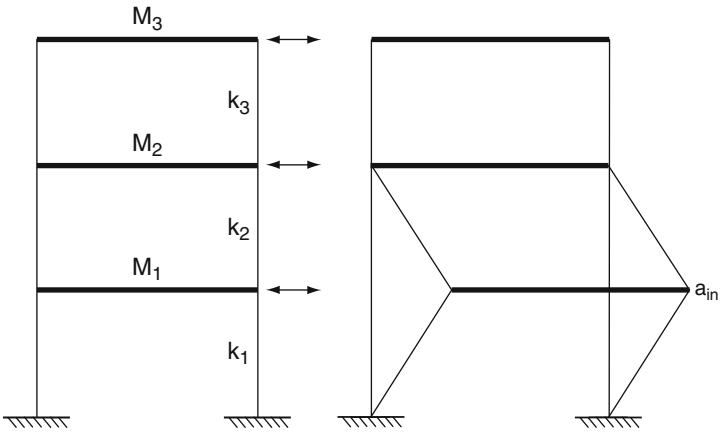
www.EngineeringBooksPDF.com

It can be shown that if s is made a sufficiently close estimate of the ith eigenvalue ω_i^2, then the process will converge on the ith eigenpair, i.e. as $n \to \infty$, so $\mathbf{x}_i^{(n)} \to \phi_i$ and $\lambda_i^{(n)} \to \omega_i^2$.

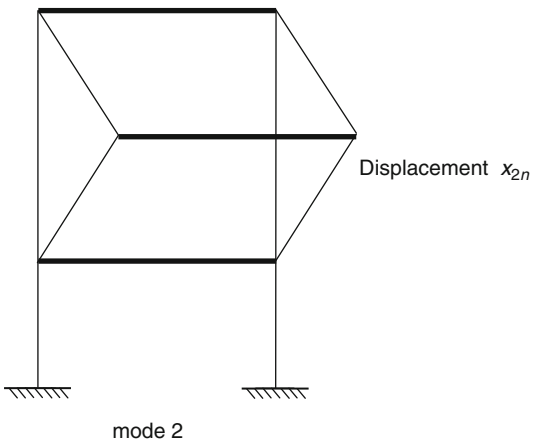
Use of the factorization Eq. (3.118) can provide the necessary initial estimate of the eigenvalues.

Plate 3.6 Undamped free vibrations of a three-storey rigid frame

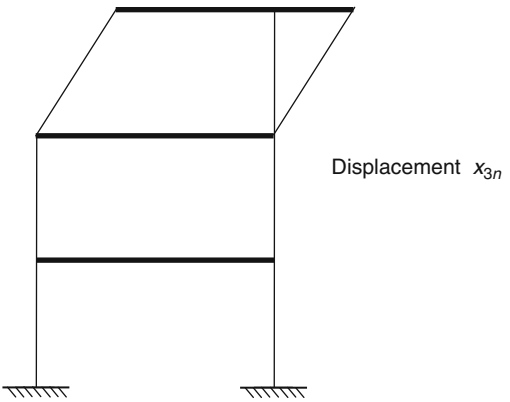
Data:



$$K = \frac{12EI}{L^3}$$



www.EngineeringBooksPDF.com



where E = dynamic value of Young's modulus,
I = relevant second moment of area,
L = distance between centres of floor levels = h within which column lies.

$$M_1 = 4,000\text{kg}$$
$$M_2 = M_3 = 1,000\text{kg}$$
$$k_1 = 2.0 \times 10^6\text{N/m}$$
$$k_2 = 1.0 \times 10^6\text{N/m}$$
$$k_3 = 0.5 \times 10^6\text{N/m}$$

Solution:

Sinusoidal vibrations $x = A\cos\omega\ t$

$A = X =$ maximum amplitude $\quad \dfrac{\delta x}{\delta t} = -\omega A \sin \omega t$

$\omega =$ frequency

$t =$ time

Lower columns: stiffness force contributions = $k_1\ (x_{1\text{n}} - x_{0\text{n}})$ acting to the left
Upper columns: stiffness force contributions = $k_2\ (x_{1\text{n}} - x_{2\text{n}})$ acting to the left
and so on

www.EngineeringBooksPDF.com

Force from floor 1 Mode 1	x_{0n} = amplitude of displacement at ground level "0"
Equation of dynamic equilibrium	$x_{1n}3x_{2n}$ = amplitude of displacement at first and second floor levels respectively
$-M_1\omega_n^2 x_{1n} + k_1(x_{1n} - x_{0n})$ $+k_2(x_{1n} - x_{2n}) = 0$	M_1, M_2, M_3 masses at 1, 2, 3 floors
If the columns are fixed $x_{0n} - 0$	n_0 = associated with amplitude of 0 level
The above equation becomes $(-M_1\omega_n^2 + k_1 + k_2)x_{1n} - k_2x_{2n} = 0$	n_1, n_2 related to resonance frequency of floors 1 and 2, respectively

Dynamic equilibrium of the second floor
Mode 2
Stiffness force contribution $= K_2(x_{2n} - x_{1n})$
(from lower columns)

Stiffness force (upper columns) $= K_3(x_{2n} - x_{3n})$
Similarly
Inertia force from floor 2 $= M_2 \dfrac{\delta^2 x_{2n}}{\delta t^2} = M_2(-\omega_n^2 x_{2n})$
The dynamic equilibrium equation is

$$- M_2\omega_n^2 x_{2n} + K_2(x_{2n} - x_{1n}) + K_3(x_{2n} - x_{3n}) = 0$$

or

$$- K_2x_{1n} + (-M_2\omega_n^2 + K_2 + K_3)x_{2n} - K_3x_{3n} = 0$$

A similar procedure is adopted as shown in mode 3.

The inertia force from floor 3. The dynamic equilibrium equation can similarly be written as

$$- M_3\omega_n^2 x_{3n} + K_3(x_{3n} - x_{2n}) = 0$$

or

$$- K_3x_{2n} + (-M_3\omega_n^2 x_{3n} + K_3)x_{3n} = 0$$

for the eigen solution of resonant vibration −3.

The systems of equations are grouped together in a matrix form for dynamic equilibrium

$$\begin{bmatrix} M_1\omega_n^2 + K_1 + K_2 & -K_2 & 0 \\ -K_2 & -M_2\omega_n^2 + (K_2 + K_3) & -K_3 \\ 0 & -K_3 & M_3\omega_n^2 + K3 \end{bmatrix} \begin{Bmatrix} x_{1n} \\ x_{2n} \\ x_{3n} \end{Bmatrix} = \begin{Bmatrix} 0 \\ 0 \\ 0 \end{Bmatrix}$$

www.EngineeringBooksPDF.com

Iteration is needed to produce a converging solution and that is a displacement Mode 2 such that $n = 2$ initial estimate for the mode shape

$x_{12} = 1$, $x_{22} = 0.2$, a standard computer program ISOPAR is considered

$\omega_2^2 = 700; x_{22} = 0.340$ ← computed – there is a difference between $x_{22} = 0.2$ trial and $x_{22} = 0.340$ computed. More trials are needed while keeping $x_{12} = 1$ constant throughout.

Trial 2

$x_{12}, x_{22} = 0.340$
computed $\omega_2^2 = 664.7; x_{22} = 0.380 \quad x_{22} = -$

Trial 3

$$x_{12} = 1, x_{22} = 0.380; \omega_2^2 = 654.8; x_{22} = 0.3925; x_{32} = -$$

Similarly	Computed values
Trial 4 $x_{12} = 1, x_{22} = 0.3925$	$\omega_2^2 = 651.8; x_{22} = 0.3965; x_{32} = -$
Trial 5 $x_{12} = 1, x_{22} = 0.3965$	$\omega_2^2 = 650.9; x_{22} = 0.3975; x_{32} = -$
Trial 6 $x_{12} = 1, x_{22} = 0.3975$	$\omega_2^2 = 650.6; x_{22} = 0.3975; x_{32} = -$
Trial 7 $x_{12} = 1, x_{22} = 0.3975$	$\omega_2^2 = 650.498; x_{22} = 0.3975; x_{32} = -1.3235$

Mode 1 Three Resonant Modes of Vibrations

$n = 1$ orthogonality between modes 3 and 1
when solved, if $x_{11} = 1.0 \rightarrow x_{21} = 2.1888; x_{31} = 3.6788$
Using above matrix $\omega_1^2 = 202.788\ (\text{rad/s})^2$

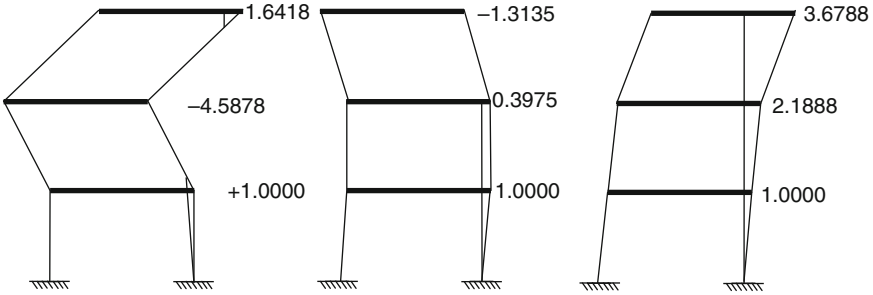
$$f_i = 2.2668\ \text{H}_z; \qquad T_1 = 0.44\,\text{s}$$

Similarly $\omega\frac{2}{2} = 650.498\ (\text{rad/s})^2$

$$f_2 = 4.05Hz; T_2 = 0.25s$$
$$x_{12} = 1.0; x_{22} = 0.3975; x_{32} = -1.3235$$
$$\omega_3^2 = 1896.0(rad/s)^2$$
$$f_3 = 6.915Hz; T_3 = 0.14s$$
$$x_{13} = 1.0; X_{23} = -4.578; x_{33} = 1.6421$$

They are given in the following diagram:

www.EngineeringBooksPDF.com



(a) M-1 mode-1 (b) M-2mode-2 (c) M-3 mode-3

Involving three masses, M_1, M_2 and M_3, the matrix relation can be written while knowing stiffnesses within the frame at all the positions of d.f.s.

$$\begin{bmatrix} M_1 & \omega_1^2 \\ M_2 & \omega_2^2 \\ M_3 & \omega_3^2 \end{bmatrix} \begin{Bmatrix} x_1 n \\ x_2 n \\ x_3 n \end{Bmatrix} = \begin{bmatrix} (k_1 + k_2)^{x_{1n}} & -k_1 x_{2n} & \\ -k_2 x_{1n} & (k_2 + k_3) k_{2n} & -k_3 x_{3n} \\ 0 & -k_3 x_{2n} & +k_3 x_{3n} \end{bmatrix}$$

Looking at the data given as of and, these matrices of non-linear equations can be solved by iterative methods in which the displacement mode shapes converge so that one of the optimum frequencies occurs of the frame. The first one has to obtain highest mode $n = 3$.

Take $x_{13}, x_{23} = -4$ and $x_{23} = 2$.

Compare with the original initial values $x_{13} = 1, x_{23} = -1$ and $x_{33} = 1$.

The values of ω_3^2 obtained from the first part of the above matrix shall come out as $1,748, x_{23} = -4.570$ and $x_{33} = 1.715$

The new mode shape $x_{13} = 1$; $x_{23} = -4.570$ and $x_{33} = 1.715$; this now will be used to give new

$\omega_3^2 = 1,892.78\ (\text{rad/s})^2$, similarly for others. The following relations of x_{13}, x_{23}, x_{33} trial values are compared with ω_3^2, x_{23}, x_{33} computed values.

	Trial values		Computed values		
Trials	x_{23}	x_{33}	x_{23}	x_{33}	ω_3^2
1	−4.000	2.000	−4.570	1.715	1,748.00
2	−4.570	1.715	−4.603	1.661	1,892.78
3	−4.603	1.661	−4.597	1.649	1,901.10
4	−4.597	1.619	−4.590	1.645	1,898.70
5	−4.592	1.645	−4.588	1.644	1,897.70
6	−4.5901	1.642	−4.589	1.641	1,897.30
7	−4.589	1.643	−4.589	1.641	1,897.20

Note: from trials 1–7, $x_{13} = 1.000$.

www.EngineeringBooksPDF.com

Similarly using the above matrix with the iterative technique indicated the above values are computed for x_{23}, x_{33} x_{23} and ω_3^2 and they are tabulated. The mass orthogonality between modes 3 and 2. The equation set up is $M_1\, x_{12}$ $x_{13} + M_2\, x_{22}\, x_{23} + M_3\, x_{32}\, x_{33} = 0$. Substituting values, then the relation can be easily found between x_{32} to x_{12} and x_{22}, x_{32} to x_{12} and x_{22}

The value of x_3 can be determined.

www.EngineeringBooksPDF.com

Chapter 4
Earthquake Response Spectra With Coded Design Examples

4.1 Introduction

The most important application in structural dynamics is in the analysis of the response of structures to ground shaking caused by an earthquake. The earthquake response is generally divided into two categories – linearly elastic and inelastic.

The response spectrum concept which is central to earthquake engineering together with procedures to evaluate the peak response of systems directly form the response spectrum. This then is followed by a study of the characteristics of the earthquake response spectra which generally lead into the design spectrum for the design of new buildings and safety evaluation of existing buildings against future earthquakes. The designers would be interested in response of yielding or inelastic system.

The ground acceleration is defined by numerical values at discrete time instants. These time instants should be closely spaced to describe accurately the highly irregular variation of acceleration with time. Typically, the time interval is chosen to be 1/100 to 1/50 of a second, requiring 1,500–3,000 ordinates to describe the ground motion.

The main cause of the structural damage during earthquake is its response to ground motions which is, in fact the input to the base of the structure. To evaluate the behaviour of the building under this type of loading condition, knowledge of structural dynamics is required. The static analysis and design can now be changed to a separate time-dependent analysis and design. The loading and all aspects of responses vary with time which result in an infinite number of possible solutions at each instant during the time interval. For an engineer the maximum values of the building response are needed for the structural design.

The response may be deflection, shear, equivalent acceleration, etc. The response curves are generally similar with a major variation occurring in the vertical ordinates. The variations definitely occur with the magnitude of the earthquake and location of the recording instruments. Accelerations derived from actual earthquakes are surprisingly high as compared with the force used in designs and the main reason is the effect of different degrees of damping.

M.Y.H. Bangash, *Earthquake Resistant Buildings*,
DOI 10.1007/978-3-540-93818-7_4, © M.Y.H. Bangash 2011

www.EngineeringBooksPDF.com

The recorded earthquake ground accelerations have no doubt similar properties to those of non-stationary random functions but owing to a lack of statistical properties related to such motions artificially generated accelerograms are used which are flexible for any duration. A typical artificially generated accelerogram prepared by the California Institute of Technology, USA, is shown in Fig. 4.1.

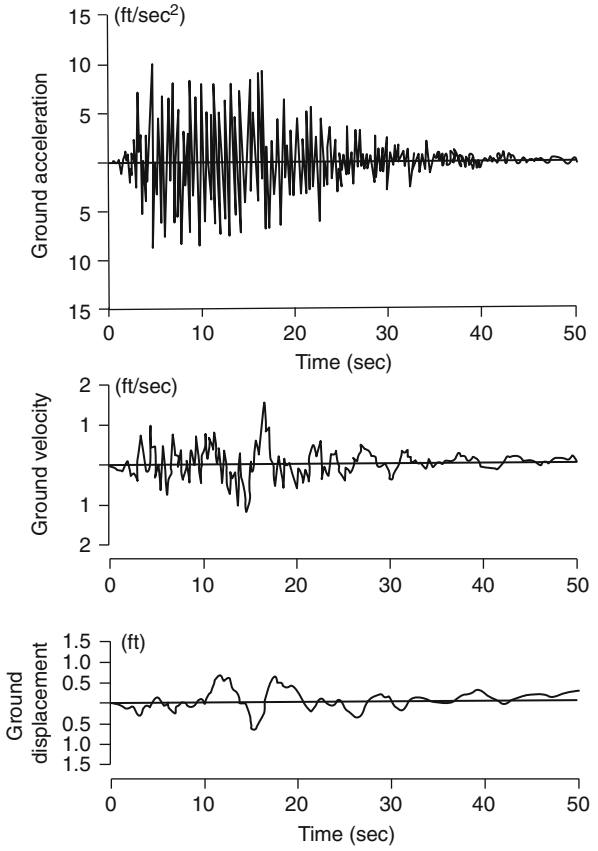


Fig. 4.1 Artificially generated accelerogram (California Institute of Tech, U.S.A.)

4.2 Fourier Spectrum

The frequency content of a function (accelerogram) can be exhibited by a standard method known as the *Fourier spectrum*. A typical single-degree-of-freedom oscillator is shown in Fig. 4.2 and is subjected to a base acceleration $\ddot{x}_g$, applied force $M\ddot{x}_g$, and the response is δ.

www.EngineeringBooksPDF.com

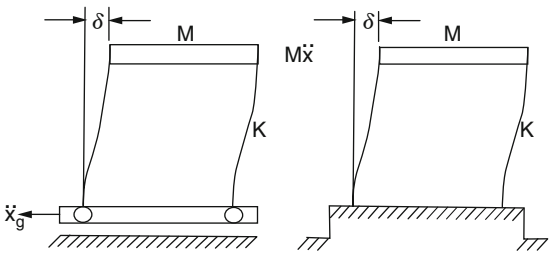


Fig. 4.2 A single-degree-of-freedom oscillator

The equation of motion is

$$M\ddot{\delta} + K\delta = -M\ddot{x}_g \tag{4.1}$$

where δ is the relative displacement and $\ddot{\chi}$ is the base acceleration.

The vibratory response is given for the relative displacement at time *'t'* by

$$\delta(t,\omega) = \frac{1}{\omega}\int_0^t \ddot{x}_g(\tau)\sin\omega(t-\tau)d\tau \tag{4.2}$$

$$\omega^2 = \frac{K}{M} = \left(\frac{2\pi}{T\eta}\right)^2$$

where T is the period.

The total energy is

$$E = \frac{1}{2}M\dot{\delta}^2 + \frac{1}{2}K\delta^2 \tag{4.3}$$

$$= \frac{1}{2}M\left[\left(\int_0^t \ddot{x}_g \sin\omega\tau d\tau\right)^2 + \left(\int_0^t \ddot{x}_g \cos\omega\tau d\tau\right)\right]^2 \tag{4.4}$$

The duration of $\ddot{\chi}$ from $t = 0$ to $t = t_1$, the square root of twice the energy per unit mass at that time t_1, is

$$\sqrt{\frac{2E(t,\omega)}{M}} = \left[\left(\int_0^t \ddot{x}_g \sin\omega\tau d\tau\right)^2 + \left(\int_0^{t_1} \ddot{x}_g \cos\omega\tau d\tau\right)^2\right]^{1/2} \tag{4.5}$$

where

$$\omega = \frac{2\pi}{T_\eta} = 2\pi f$$

www.EngineeringBooksPDF.com

A plot as a function of ω or T or f is the *Fourier amplitude spectrum*. In a normal situation the earthquake spectra are plotted as a function of T. On this basis Hudson and Housner (CIT(USA)) produced a plot for the Fourier spectrum of the ground acceleration component along with the recorded one at Taft, California (Fig. 4.1).

At the end $t = t_1, E(t_1, \omega)$ was the excitation value. The maximum value of the energy $E(t_m, \omega)$ will likely occur at $t_m < t_1$. if t_1 is changed to t_m, the value of $E(t_m, \omega)$ when plotted as a function of period or frequency becomes the *energy response spectrum*. If $\sqrt{2E(t_m, \omega)/M}$ as a velocity is plotted as a function of period frequency, it is called a *maximum velocity response spectrum*. This was then plotted for the Taft earthquake in California in Fig. 4.1. One can visualize that the amplitude of the Fourier spectrum is somewhat larger.

If the oscillator in Fig. 4.1 is subjected to viscous damping ζ and $\omega_n = \omega\sqrt{1-\zeta^2}$, then its response is

$$\delta(t, \omega, \zeta) = \frac{1}{\omega_n} \int_0^t \ddot{x}_g(\tau) e^{-\zeta\omega_n(t-\tau)} \sin \omega_n (t-\tau) d\tau \tag{4.6}$$

for $\zeta < 0.2$.

When $\omega = \omega_n$, the maximum value occurs at t_m, and then it is known as the *displacement response spectrum* S_d and is generally plotted as a function of period T for several values of ζ. The maximum velocity $\left|\dot{\delta}(t_\mathrm{m}, \omega, \zeta)\right|$ is called the *velocity response spectrum* S_v. The absolute acceleration spectrum is S_a and is given by

$$S_\mathrm{a} = \left(\frac{K}{M}\right) S_\mathrm{d} = \omega^2 S_\mathrm{d} = \left(\frac{2\pi}{T_\mathrm{n}}\right)^2 S_\mathrm{d} \tag{4.7}$$

The pseudo-velocity spectrum S_pv is derived when using the maximum displacement for zero kinetic energy and maximum strain energy $\frac{1}{2} K S_\mathrm{d}^2$

$$\frac{1}{2} M(\dot{\delta})^2 = \frac{1}{2} K S_\mathrm{d}^2 \tag{4.8}$$

The maximum relative velocity $\dot{\delta}$ would then be

$$\dot{\delta} = \sqrt{\frac{K}{M}}\, S_\mathrm{d} = \left(\frac{2\pi}{T\eta}\right) S_\mathrm{d} = S_\mathrm{pv} \tag{4.9}$$

Using the above-mentioned analytical expressions and recording certain well-known earthquakes, various researchers have produced response spectra. Figures 4.6, 4.7, 4.8, 4.9, 4.10, 4.11, 4.12, 4.13, 4.14, 4.15, 4.16 and 4.17 give these spectra plotted for a number of earthquake zones. In some cases various methods have been compared with those recorded from actual earthquakes.

www.EngineeringBooksPDF.com

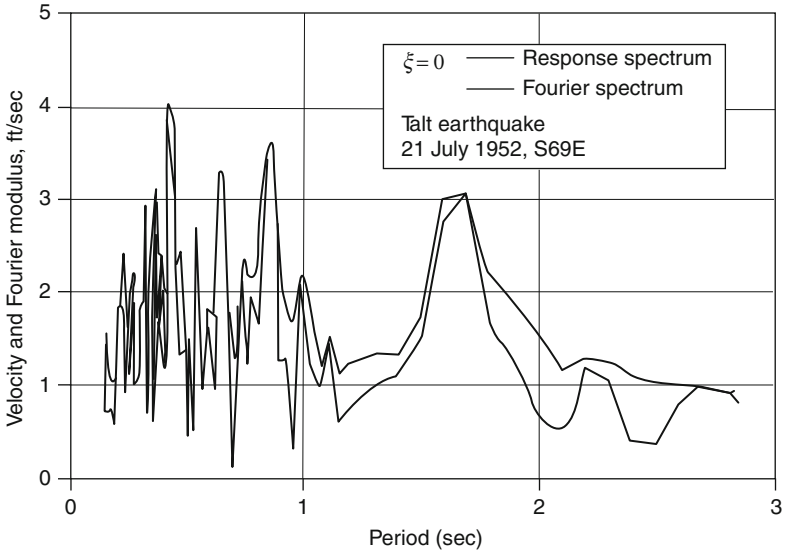


Fig. 4.3 Response spectrum based on Fourier spectrum of ground acceleration component S69E. Recorded 21 July 1952 at Taft, California

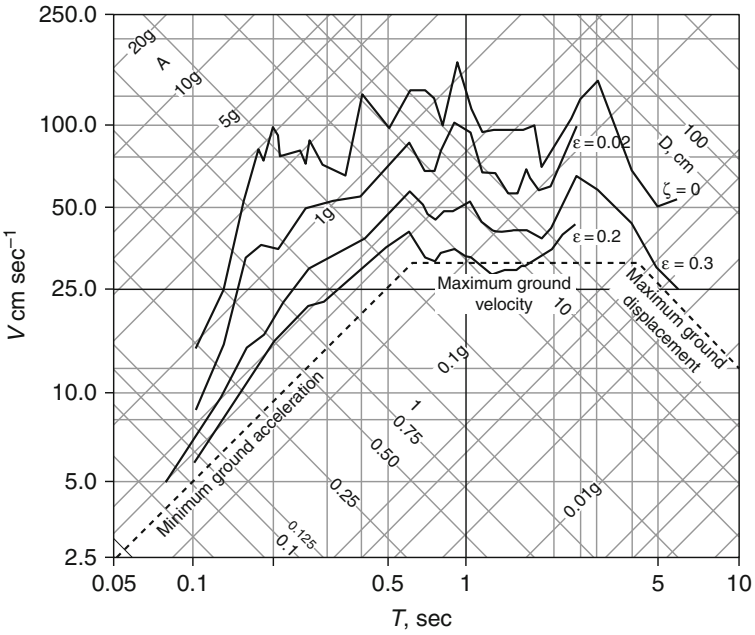


Fig. 4.4 Response spectra for elastic systems (May 1940 El-Centro Earthquakes, NS component) (after Blume, Newmark and Corning, 1960)

www.EngineeringBooksPDF.com

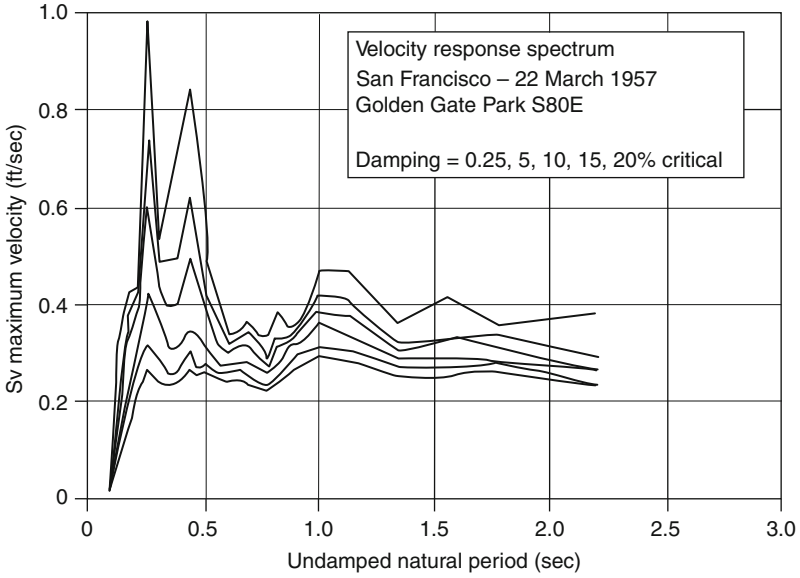


Fig. 4.5 Velocity response spectrum of the S80E component of ground acceleration. Recorded at Golden Gate Park, San Francisco

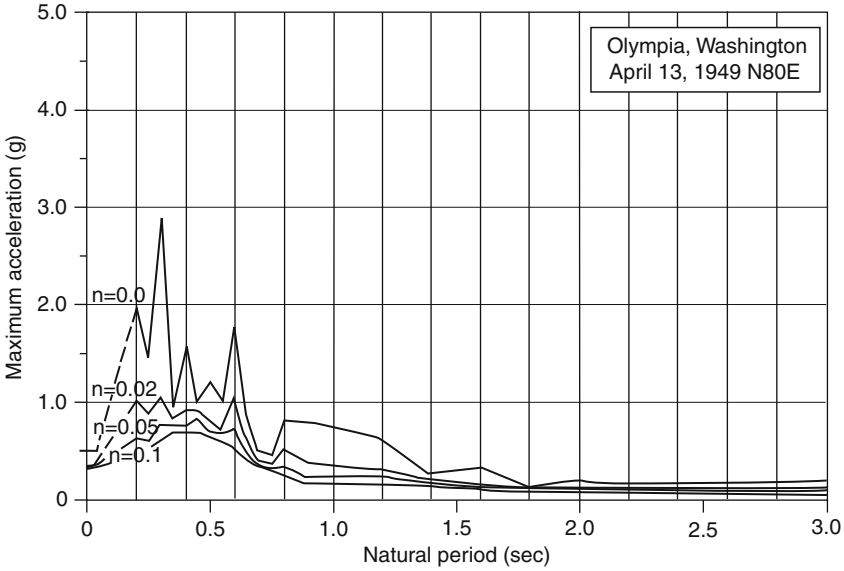


Fig. 4.6 Acceleration response spectrum of the N80E component of ground acceleration. Recorded at Olympia, Washington.

www.EngineeringBooksPDF.com

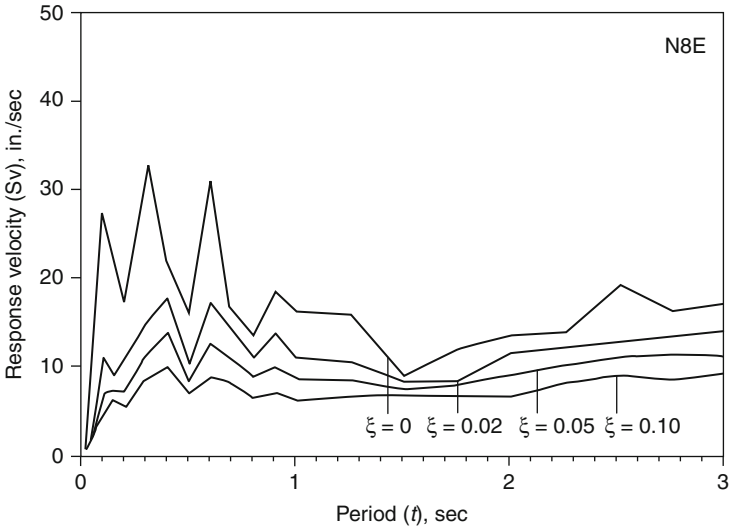


Fig. 4.7 Velocity response spectrum for ground acceleration. Recorded in Lima, Peru, 17 October 1966. Provided by G. Housner C.I.T. (U.S.A.)

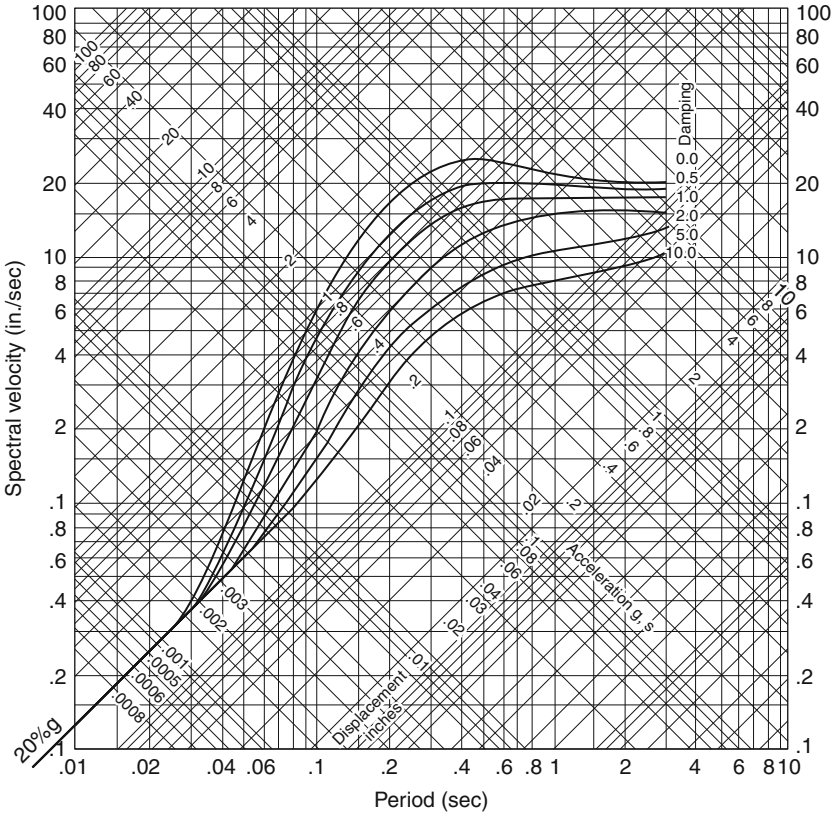


Fig. 4.8 Combined plot of design spectrum for acceleration, velocity and damping as a function of period and damping (20% *g* acceleration at zero period) C.I.T (U.S.A.)

www.EngineeringBooksPDF.com

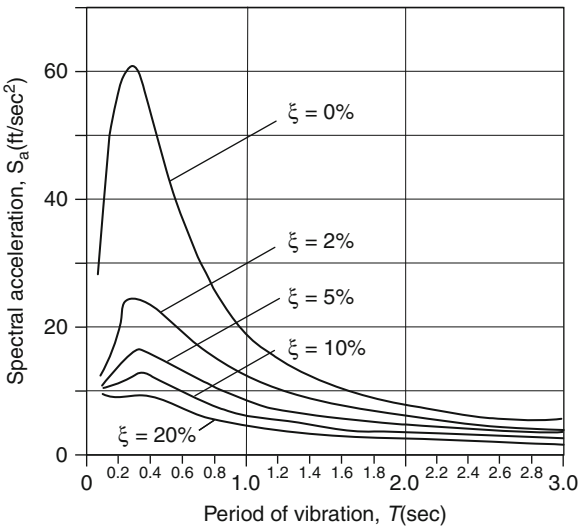


Fig. 4.9 Average acceleration response spectrum (El-Centro, 1940) (US Atomic Energy Report TID-7024, August 1963)

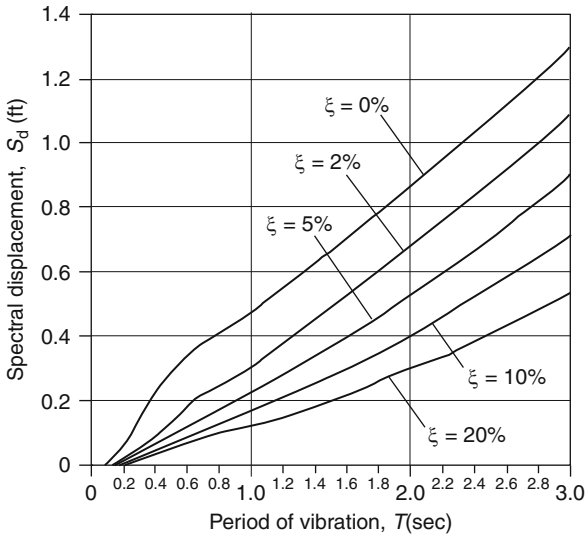


Fig. 4.10 Average displacement response spectrum (El-Centro, 1940) (US Atomic Energy Report TID-7024, August 1963)

www.EngineeringBooksPDF.com

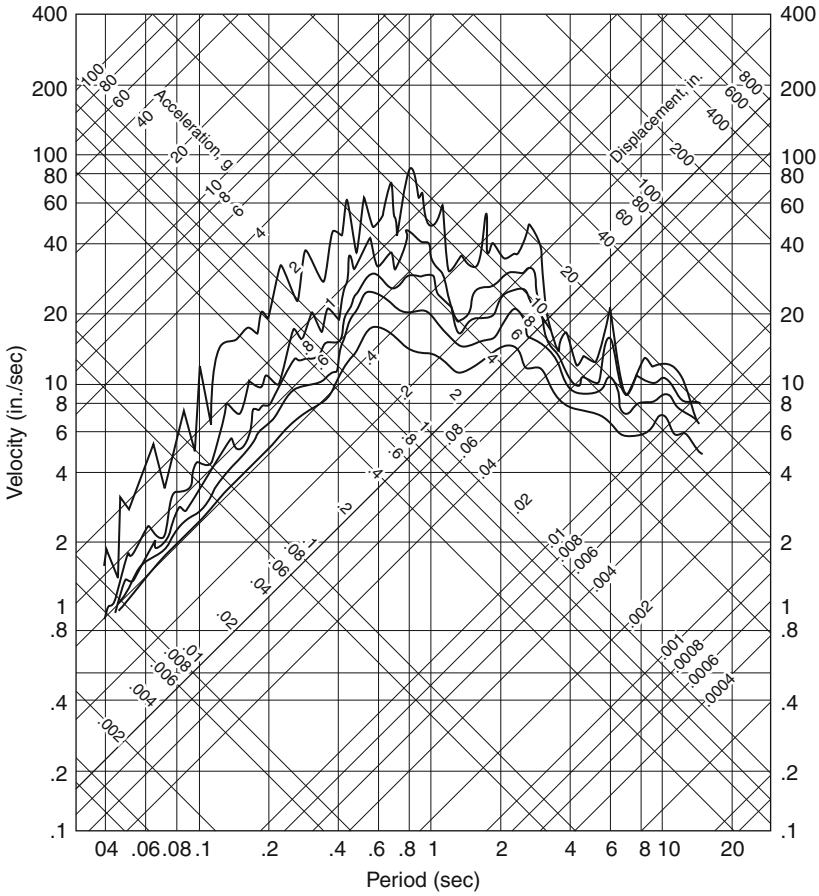


Fig. 4.11 Response spectra for Imperial Valley earthquake, 8 May 1940. Imperial valley county, U.S.A. and G. Housner of C.I.T. (U.S.A.)

www.EngineeringBooksPDF.com

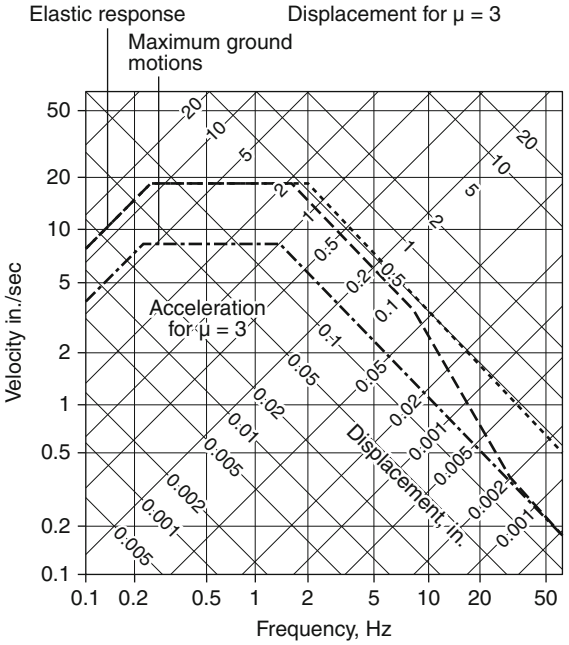


Fig. 4.12 Inelastic design spectra (Newmark and Hall, 1982)

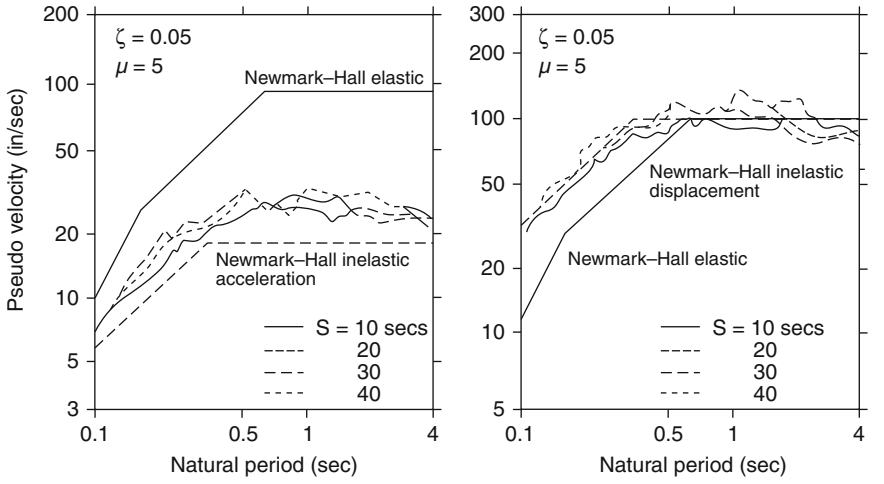


Fig. 4.13 Mean inelastic acceleration and displacement response for different strong ground motion durations (Lai and Biggs, 1980)

www.EngineeringBooksPDF.com

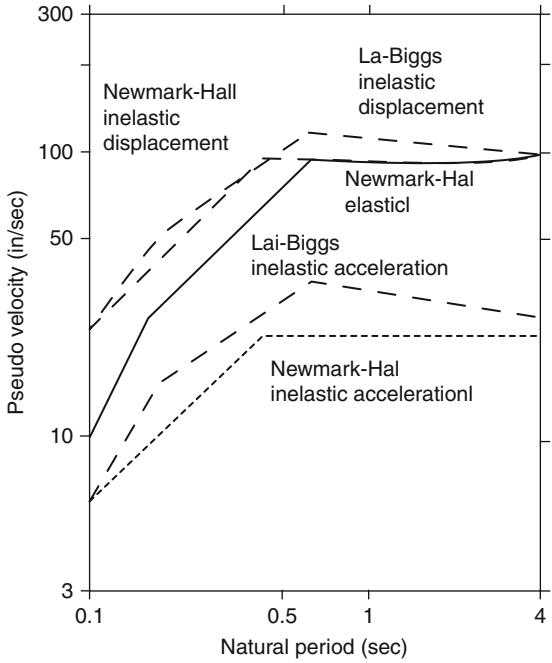


Fig. 4.14 Comparison of Lai–Biggs and Newmark–Hall inelastic spectra (from Lai and Biggs, 1980)

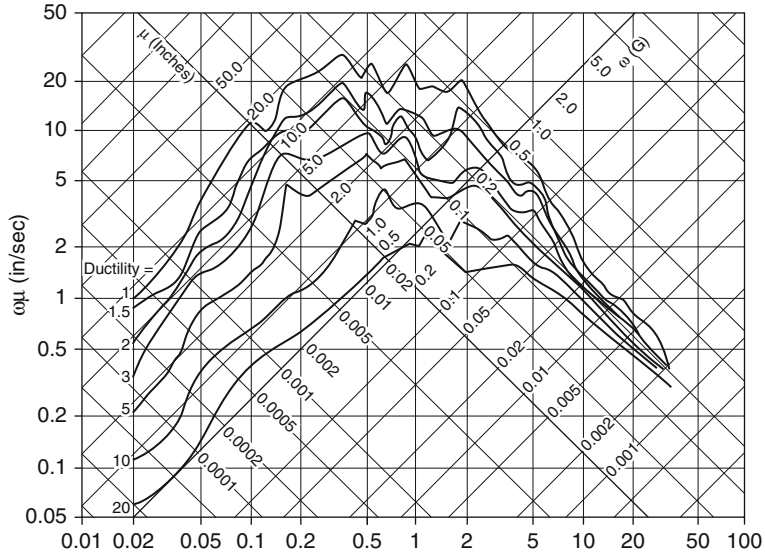


Fig. 4.15 Inelastic yield spectrum for the S90W component of El-Centro and the Imperial Valley earthquakes (El-Centro, 18 May 1940). Elastic–plastic systems with 5% damping (Riddle and Newmark)

www.EngineeringBooksPDF.com

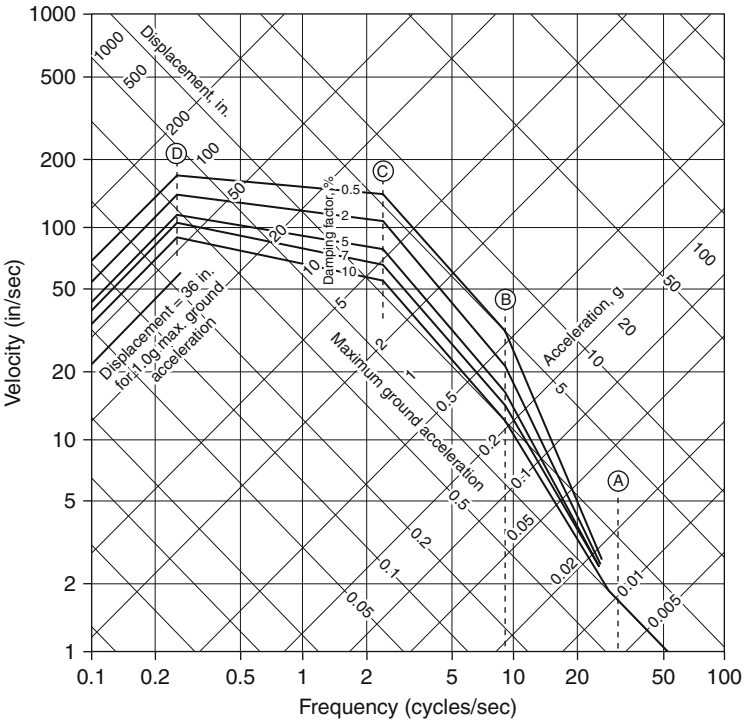


Fig. 4.16 NRC horizontal design spectra (1.0*g* horizontal ground acceleration) (with compliments of U.S.A.) NRC (Nuclear Regulatory Commission)

4.3 Combined Spectrum S_d-V-S_a

Each of the deformation, pseudo-velocity and pseudo-acceleration response spectra for a given ground motion contains the same information, no more and no less. The three spectra are simply different ways of presenting the same information on structural response. Knowing one of the spectra, the other two can be obtained by algebraic operations.

The need for a combined spectra has a great advantage. One of the reasons is that each spectrum directly provides a physically meaningful quantity. The deformation spectrum provides the peak deformation of a system. The pseudo-velocity spectrum is related directly to the peak strain energy stored in the system during the earthquake; the pseudo-acceleration spectrum is related directly to the peak value of the equivalent static force and base shear; the second reason lies in the fact that the shape of the spectrum can be approximated more readily for design purposes with the aid of all three spectral quantities rather than any one of them alone. For this purpose a combined

www.EngineeringBooksPDF.com

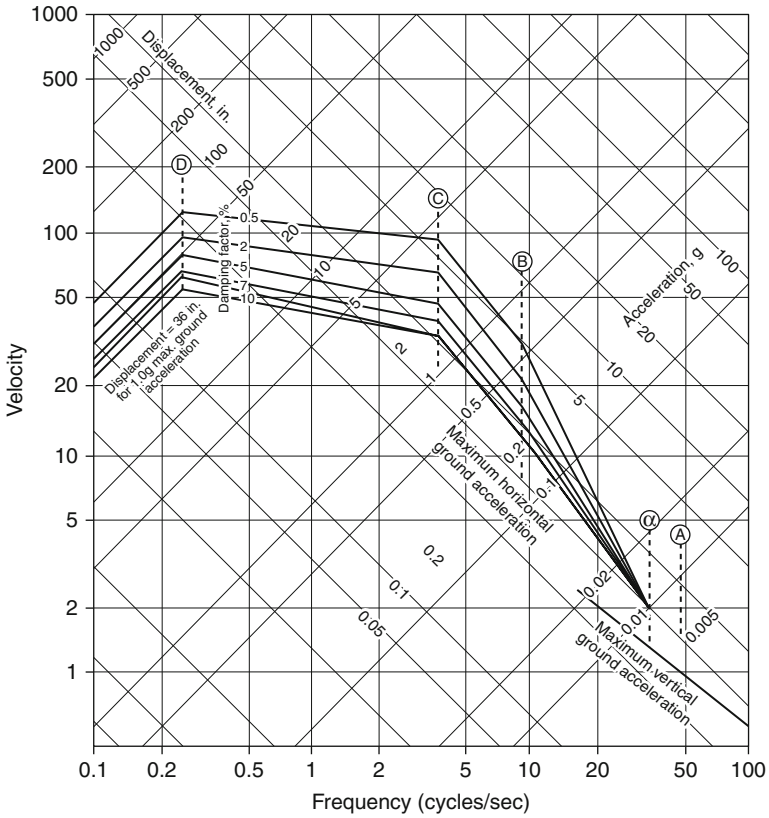


Fig. 4.17 NRC vertical design spectra (1.0*g* horizontal ground acceleration) (with compliments of Nuclear Regulatory Commission, Washington D.C., U.S.A. Provided by A.S. Veletsos and N.M. Newmark)

plot showing all three of the spectral quantities is especially useful. This type of plot was developed for earthquake response spectra, apparently for the first time, by A.S. Veletsos and N.M. Newmark in 1960.

4.4 Construction of Response Spectrum

The response spectrum for a given ground motion component $\ddot{x}_g(t)$ can be developed by implementation of the following steps:

1. Numerically define the ground acceleration $\ddot{x}_g(t)$; typically, the ground motion ordinates are defined every 0.02 s.
2. Select the natural vibration period T and damping ratio ζ of an SDF system.

www.EngineeringBooksPDF.com

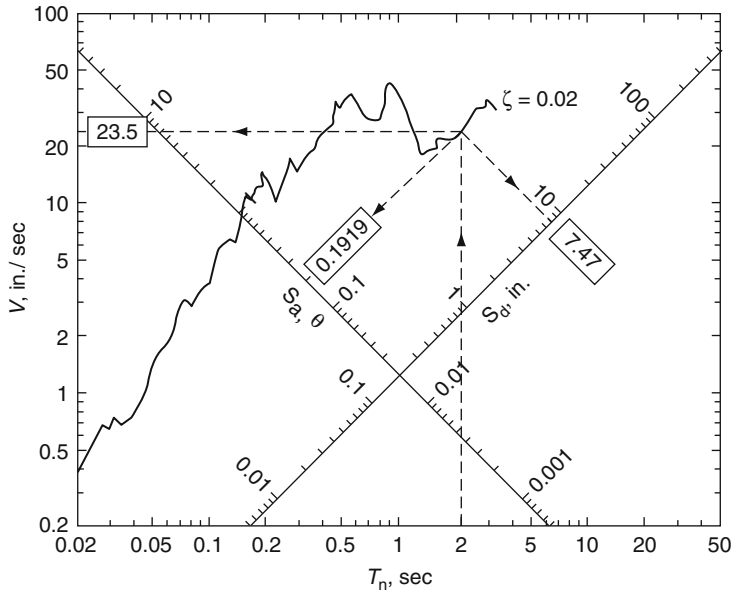


Fig. 4.18 Combined $S_d - V - S_a$ response spectrum for El-Centro ground motion; $\zeta = 2\%$

3. Compute the deformation response $\delta(t)$ of this SDF system due to the ground motion $\ddot{x}_g$ by any of the numerical methods. (In obtaining the responses, the exact solution for ground motion assumed to be piecewise linear over every $\Delta t = 0.02$ sec should be used.)
4. Determine u_o, the peak value of $u(t)$.
5. The spectral ordinates are $\delta_d = u_0$, $V = (2\pi/T_n)S_d$ and $S_a = (2\pi/T_n)^2 S_d$
6. Repeat steps 2–5 for a range of T and ζ values covering all possible systems of engineering interest.
7. Present the results of steps 2–6 graphically to produce three separate spectra like shown in Figs. 4.3–4.17 or a combined spectrum like the one in Fig. 4.18.

4.5 Design Examples

Conversion factors

Imperial	SI
1 ft	0.3048 m
1 kip	1,000 lbf
1 lbf	4.448 N = 0.4536 kgm/s^2
1 ft kip	1.356 kNm

www.EngineeringBooksPDF.com

4.5.1 Example 4.1 American Practice

A portal frame built in steel is shown in Fig. 4.19 The horizontal girder 25 ft (7.62 m) is infinitely stiff to prevent significant rotation at the top of the columns that are 15 ft high. The total weight inclusive of self-weight is 1.18 kips/ft. Using the following data and the design spectrum developed by Housner (Fig. 4.20), calculate the response of the structure for the earthquake design spectrum with and without 8 in concrete block masonry infill wall:

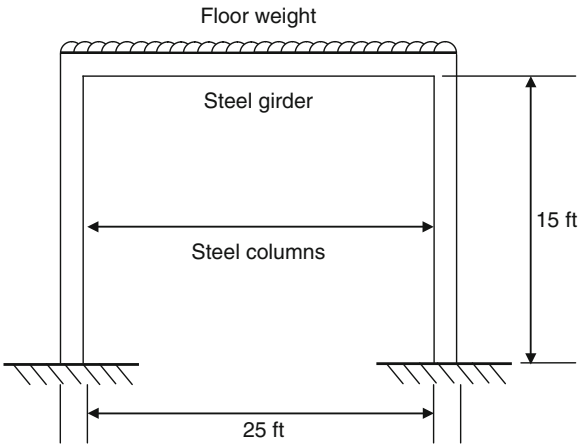


Fig. 4.19 A steel portal frame

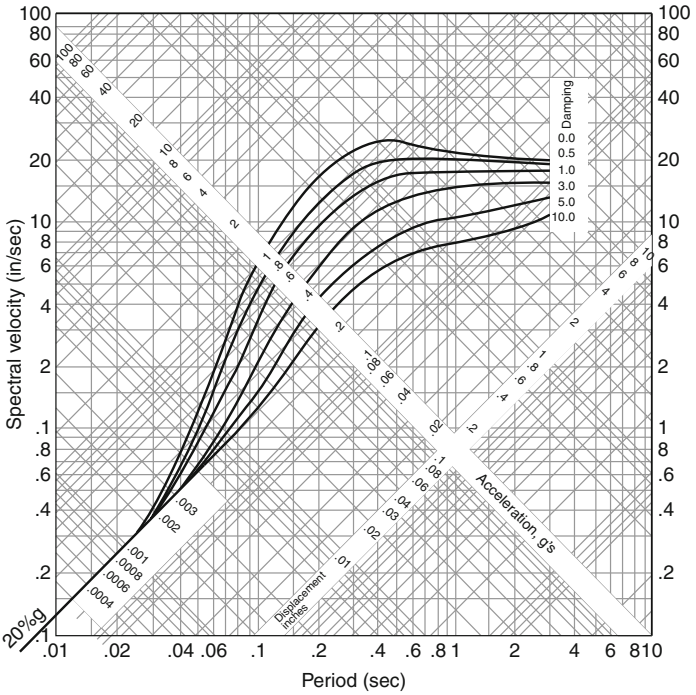


Fig. 4.20 Housner design spectra provided the late G. Housner 1960 C.I.T. (U.S.A.)

www.EngineeringBooksPDF.com

Steel:

$$I(\text{column}) = 56.4 \text{ in}^2$$

$$ES = 30 \times 10^6 \text{ lb/in}^2 \ (200\text{G N/m}^2)$$

Concrete block masonry:

$$E_\text{m} = 1{,}500\text{kip/in}^2$$

$$E_\text{v} = \text{shear modulus of elasticity } = 0.4E_\text{m}$$

$$\text{Masonry weight} = 100\text{lbf/ft}^2$$

Using the US code

$$K = \text{stiffness } = 2\left(\frac{12EI}{h^3}\right) = \frac{2(12)(30 \times 10^6)(56.4) \times 10^{-3}}{(15 \times 12)^3} = 6.963\text{kip/ft}$$

$$\omega_\text{n} = \sqrt{\frac{K}{M}} = \sqrt{\frac{\frac{6.963}{1.18 \times 25}}{386}} = 9.55 \text{ rad/s}$$

$$T_\text{n} = \frac{2\pi}{\omega_n} = 0.658 \approx 0.66 \text{ s}$$

Using 5% damping, from Housner's spectrum, $S_\text{v} = 10$ in/s. Thus,

$$S_\text{a} = \left(\frac{2\pi}{T_n}\right) S_\text{v} = 95.24\text{in/s}^2$$

$$S_\text{d} = \left(\frac{T_n}{2\pi}\right) S_\text{a} = \left(\frac{0.66}{2\pi}\right)^2 \times 95.24 = 1.05 \text{ in}$$

S_d is the relative displacement between the top and bottom of the column. Now

$$\text{Seismic coefficient} = \frac{\text{floor mass} \times \text{acceleration}}{\text{floor weight}}$$

$$= \frac{S_\text{a}}{g} = \frac{95.24}{386} \approx 0.25$$

The total shear force in the two columns at the ground level is equal to floor mass × acceleration of the mass.

www.EngineeringBooksPDF.com

Base shear

$$V = 0.250 \times 1.18 \times 25 = 7.375 \text{ kips}$$

or

$$V = KS_{\text{d}} = 6.963 \times 1.05 = 7.31 \text{ kips}$$

The difference between the two methods for the base shear is due to the difference between S_{a} and the true floor acceleration.

Force–deflection equation

$$\frac{\Delta c}{P} = \frac{h^3}{3E_M I} + \frac{1.2\,h}{AE_v} \qquad h = 15 \text{ ft} = 180\text{in}$$

$$= \frac{(180)^3}{3 \times 1500 \times \dfrac{7.62(300)^3}{12}} + \frac{1.2 \times 180}{(7.62 \times 300) \times 0.4 \times 1500}$$

$$= 2.337 \times 10^{-4}\text{in/kip}$$

$$K = \text{stiffness} = \frac{P}{\Delta c} = \frac{1}{2.337 \times 10^{-4}} = 4,279 \text{ kip/in}$$

One-half weight of the wall $= \frac{1}{2} \times 15 \times 25 \times 100 \text{ lbf/ft}^2 \times 10^{-3} = 18.75$ kips

$$K_{\text{T}} = \text{total spring constant} = 6.963 + 4,279 = 4,286 \text{ kip/in}$$

$$W_{\text{total}} = 1.18 \times 25 + 18.75 = 48.25 \text{ kips}$$

$$\omega_{\text{n}} = \sqrt{\frac{K}{M}} = \sqrt{\frac{4286}{\dfrac{48.25}{386}}} = 185.17 \text{ rad/s}$$

$$T_{\text{n}} = \frac{2\pi}{185.17} = 0.0339 \approx 0.034$$

$$V = S_{\text{a}} W = 0.24 \times 48.25 = 11.58 \text{ kips}$$

Using Housner's diagram (Fig. 4.20)

$$T_{\text{n}} = 0.03$$

$$S_{\text{v}} = 0.45 \text{ in/s}$$

$$S_{\text{a}} = 0.24 \text{ and } S_d = 0.0021\text{in}$$

www.EngineeringBooksPDF.com

4.5.2 Example 4.2 American and Other Practices

Using the following codes with respective conditions and criteria, calculate the base shear force for the framed buildings shown in Fig. 4.21. Use various codes given below while Chap. 2 gives various details.

(a) US code UBC-91
(b) Iran code ICSRDB 1988
(c) Australia code 1995
(d) India/Pakistan codes 1994
(e) Israel code 1994
(f) Japan code 1994
(g) Mexico code 1995
(h) European code 1995 (4.10)

4.5.2.1 US code UBC-91

$$V = \text{base shear force} = \frac{ZICW}{R_W}$$

$$Z = \text{zone } 3 = 0.3$$

$$I = 1.0$$

$$\sum W = 3 \times 800 + 700 = 3,100 \text{ kips}$$

$$R_W = \text{special moment} - \text{resisting frame } = 12(\text{RC frame})$$

$$S = \text{rock} = 1.0$$

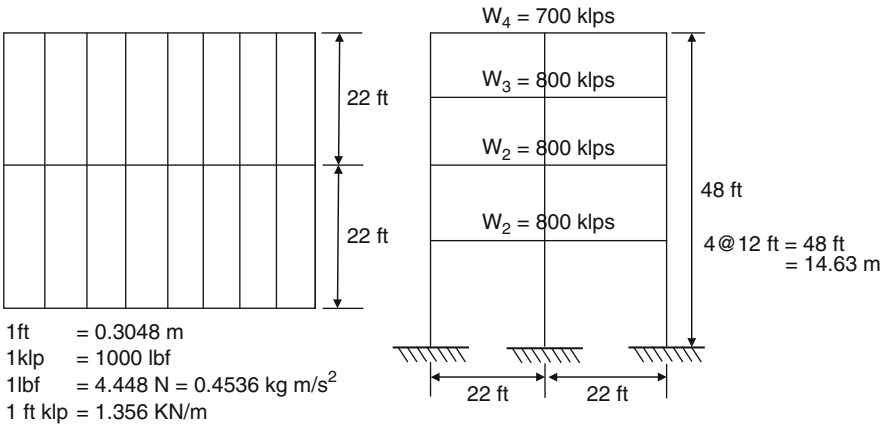


Fig. 4.21 A multistorey building frame using various codes

www.EngineeringBooksPDF.com

$$C = \frac{1.25S}{T_\eta^{2/3}} = \frac{1.25 \times 1}{\left[0.03 \times (48)^{3/4}\right]^{2/3}} = \frac{1.25 \times 1.0}{(0.55)^{2/3}} = 1.862$$

$$V = \frac{0.3 \times 1.0 \times 1.862 \times 3100}{12} = 144.305 \text{ kips}(642 \text{ kN})$$

4.5.2.2 Iran Code ICSRDB 1988

$$T_\eta = 0.07H^{3/4} = 0.07 \times (14.63)^{3/4} = 0.524$$

$$H_{(\text{metres})} = 0.3048 \times 48 = 14.63 \text{ m}$$

$$T_0 = \text{soil type } 1 = 0.3$$

$$\sum W = 3{,}100 \text{ kips} = 3{,}100 \times 10^3 \times \frac{4.448}{10^3} = 13{,}789 \text{ kN}$$

I = important factor = 1.0

R = behaviour coefficient = 7.0

A = design base acceleration = 0.35

$$B = \text{response coefficient} = 2\left(\frac{T_0}{T_\eta}\right)^{2/3} = \left(\frac{0.3}{0.524}\right)^{2/3} = 0.689$$

where $0.6 \leq B \leq 2.0$

$$C = \text{seismic coefficient} = \frac{ABI}{R} = \frac{0.35 \times 0.689 \times 1.0}{7.0} = 0.035$$

$$V = \text{base shear} = CW = 0.035 \times 13{,}789 = 475 \text{ kN}$$

4.5.2.3 Australia Code 1995

$$V = \text{total seismic base shear} = \frac{ISC}{R_f}\text{Gg}$$

$$\text{Gg} = 13{,}789 \text{ kN}$$

$$V_{\min} = 0.01Gg = 137.89 \text{ kN}$$

$$V_{\max} = \frac{2.5Ia}{R_f}Gg = \frac{2.5 \times 1 \times 0.10}{6} \times 13{,}789 = 575 \text{ kN}$$

$$V = \frac{1 \times 0.25 \times 0.67}{6} \times 13789 = 386.5 \text{ kN}$$

www.EngineeringBooksPDF.com

where

$$a = 0.10$$

$$I = 1.0$$

$$S\ (\text{soil}) = 0.67$$

$$R = 6$$

$$K_d = 5$$

$$C = \text{seismic design coefficient}$$

$$= \frac{1.25a}{T^{2/3}} = \frac{1.25 \times 0.10}{(0.252)^{2/3}} = \frac{1.25 \times 0.10}{0.498} = 0.251$$

$$T_\eta = \frac{h_\text{n}}{46} = \frac{48 \times 0.3048}{46} = 0.318 \text{ s}$$

or

$$T_\eta = \frac{48 \times 0.3048}{58} = 0.252 \text{ s} \quad \text{(adopt this value)}$$

4.5.2.4 India/Pakistan Codes 1994

Total weight of the building frame $\sum W = 13,789$ kN

$$\beta(\text{soil}) = 1.0$$

$$I = (\text{importance factor}) = 1.0$$

$K =$ (performance factor) $= 1.0$

$$T_\eta(\text{in} X - \text{direction}) = 0.1n = 0.1 \times 4 = 0.4 \text{ s}$$

$$T_\eta(\text{in y} - \text{direction}) = \frac{0.09H}{\sqrt{d}} = \frac{0.09 \times 14.63}{\sqrt{13.41}} = 0.36 \text{ sec}$$

Adopt $T_\eta = 0.4$ for maximum dimension, then $C = 0.9, \alpha_0 = 0.08$:

$$V = \text{base shear} = KC\beta I\alpha_0 W$$

$$= 1 \times 0.9 \times 1 \times 0.08 \times 13789 = 992.8 \text{ kN}$$

www.EngineeringBooksPDF.com

4.5.2.5 Israel Code 1994

$$T_\eta(\text{for concrete frame}) = 0.073H^{3/4} = 0.073\ (14.63)^{3/4} = 0.546\ \text{s}$$

$$\sum W = 13,789\ \text{kN}$$

$$K = \text{reduction factor} = 5.5$$
$$I = \text{importance factor} = 1.0$$
$$Z = \text{acceleration factor} = 0.1$$

S (soil) = 1.2

$$R_\text{a}(T_n) = \text{spectral amplification factor}$$
$$= \frac{1.25S}{T_\eta^{2/3}} = \frac{1.25 \times 1.2}{(0.546)^{2/3}} = 2.246$$

But

$$R_\text{a}(T_\eta) \geq 0.2\,K = 0.2 \times 5.5 = 1.1 < 2.246$$

Adopt $R_\text{a}(T_\eta) = 2.246$

$$C_\text{d} = \text{seismic coefficient} = \frac{R_aIZ}{K} = \frac{2.246 \times 1 \times 0.1}{5.5} = 0.041$$

$$C_\text{d} \geq \frac{SIZ}{\sqrt{3}\,K} = \frac{1.2 \times 1 \times 0.1}{\sqrt{3} \times 5.5} = 0.0295 \quad \text{(adopted)}$$

$$V = \text{base shear force}$$
$$= C_\text{d} \sum W_i = 0.0295 \times 13789 \approx 407\ \text{kN}$$

On the basis of $C_\text{d} = 0.041$

$$\frac{0.041}{0.0295} \times 407 \approx 565\ \text{kN}$$

www.EngineeringBooksPDF.com

4.5.2.6 Japan Code 1994

$$Q_i = C_i W_i = C_i \sum_{j=i}^{n} W_j$$

$$C_i = ZR_t A_i C_0$$

$$Z = 1.0(\text{for Tokyo})$$

$$C_0 = (\text{moderateearthquake}) = 0.2$$

$$T = h(0.02 + 0.1\gamma) = 14.63(0.02 + 0.1 \times 0) = 0.29 \text{ s}$$

($\gamma = 0$ since no steel components are present)

Solid profile I: rock

$$T_c = 0.4$$

$$R_t = 1.0$$

$$\alpha_i = \frac{W_i}{W_r} = 0.305$$

$$A_i = 1 + \left(\frac{1}{\sqrt{a_i}} - a_i\right)\frac{2T}{1+3T} = 1 + 0.467 = 1.467$$

$$C_i = 1.0 \times 1.0 \times 1.467 \times 0.2 = 0.2934$$

$$\sum W = 3,100 \text{ kips} = \frac{3,100 \times 10^3}{2240} = 1,384 \text{ tonne}$$

$$Q_i = V = 1,384 \times 0.2934 = 406 \text{ tonne}$$

4.5.2.7 Mexico Code 1995

Total weight $\Sigma W = 1,384$

$$C = \text{seismic coefficient}$$

$$Q' = \text{reduction factor for the moment} - \text{resisting frame}$$

$$= 0.8Q = 0.8(0.4) = 3.2 \quad (\text{along} X - \text{direction})$$

or

$= 0.8(3) = 2.4$ (along Y-direction)

Base shear

$$V_0 = 0.4(1,384)/3.2 = 173\text{t} \quad (\text{along X} - \text{direction})$$

$$V_0 = 0.4(1,384)/2.4 = 230.67\text{t} \quad (\text{along Y} - \text{direction})$$

www.EngineeringBooksPDF.com

4.5.2.8 Europe Code 1995

$$F_b = \text{seismic basic shear} = V = S_d(T_1)W$$
$$T = 0.29 \text{ s}$$
$$T_B \leq T \leq T_C$$
$$0.15 \leq 0.29 \leq 0.60$$
$$S_d(T_1) = a_g S \zeta B_0$$

where

$$B_0 = 2.5$$
$$\zeta = 0.7$$
$$S = 1.0(\text{for soil})$$
$$a_g = 0.1\,g$$
$$V = a_g S \zeta B_0 W = 0.1 \times 1.0 \times 0.7 \times 2.5 \times 13,789 = 2,413 \text{ kN}$$

4.5.3 Example 4.3 Algeria and Argentina Practices

A five-storey RC building is shown in Fig. 3.49 and is adopted as an office building. Using the seismic coefficient methods, determine seismic forces, storey shear forces and overturning moments. Use Algeria regulations RPA-88 and Argentina seismic code INPRES-CIRSOC 103.

Algeria Code

$$T = 0.1\,N = 0.1 \times 5 = 0.5 \text{ s}$$
$$A = \text{seismic coefficient} = 0.15$$
$$D = \text{dynamic amplification factor for firm soil}(T = 0.5 \text{ s}) = 1.42$$
$$B(\text{RCframe}) = \text{behaviourfactor} = 0.25$$
$$Q = \text{qualityfactor} = 1 + \sum_{q=1}^{6} P_q = 1 + 0.05 = 1.05$$
$$V = \text{base factor} = ADBQW$$
$$= 0.15 \times 1.42 \times 0.25 \times 1.05 \times (5 \text{ storeys} \times 1000 \text{ kN})$$
$$= 279.56 \text{ kN}$$

www.EngineeringBooksPDF.com

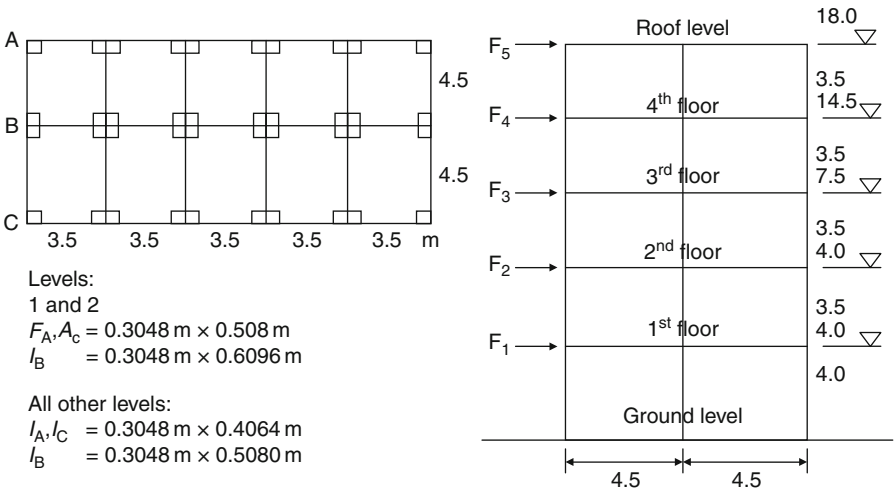


Fig. 4.22 A multi-Storey frame – Algevia and Argentina codes (Example 4.3)

Lateral forces (see Table 4.1)

$$F_k = \frac{(V - F_t) W_K h_K}{\sum_{i=1}^{N} W_i h_i}$$

$$F_t = 0 \text{ for } T_n = 0.5\text{s} < 0.7\text{s}$$

$$V_k = \text{storey shear} = F_t + \sum_{i=K}^{N} F_K$$

$$M_K = F_t(h_N - h_K) + \sum_{i=K+1}^{N} F_i(h_i - h_K)$$

$$\sum_{i=1}^{N} W_K h_K = 55,000$$

Table 4.1 Lateral forces for the five storeys

Level	W_K(kN)	h_k (m)	$W_K h_K$	F_K (kN)	V_K(kN)	M_K(kNm)
Roof level	1,000	18.0	18,000	91.49	91.49	0
4th floor	1,000	14.5	14,500	73.70	165.2	320.215
3rd floor	1,000	11.0	11,000	55.91	221.11	898.415
2nd floor	1,000	7.5	7,500	38.12	259.23	1,672.3
1st floor	1,000	4.0	4,000	20.33	279.56	2,579.6
Base		0.0		–	–	4,066.36

www.EngineeringBooksPDF.com

Sample F_K calculation for

$$\text{Roof}: \frac{18,000}{55,000} \times (V = 279.56) = 91.49 \text{ kN}$$

$$\text{4th floor}: \frac{14,500}{55,000} \times 279.56 = 73.70 \text{ kN}$$

Sample V_K calculations ($F_t = 0$) for
2nd floor: $279.56 - 20.33 = 259.23$kN
1st floor: 279.56 kN

Calculations for similar other floors:
Sample M_K calculations for
Roof: $M_k = 0$
fourth floor: $91.49(18.0 - 14.5) = 320.215$ kNm
third floor: $(91.49 + 165.2)(14.5 - 11.0) = 898.415$ kNm
second floor: $(91.49 + 165.2 + 259.23)(7.5 - 4.0) = 1672.3$ kNm

Argentina Code
(a) *Static load*
(Analysis done in kg units as suggested by the code):

$$\text{Seismic weights} = G_i + \eta L_i = 4 \text{ kN/m}^2 + 0.25 \times 8\text{kN/m}^2 = 6\text{kN/m}^2$$

$$\text{Total mass load} = 6 \times 166.5 \approx 1,000 \text{ kN}$$

As before
Total seismic weight (kg)

$$W = \frac{5 \times 1,000 \times 1\text{kg}}{0.009805} = 50.995 \times 10^5\text{kg}$$

$$\eta_i(\text{for the building}) = 0.25$$

$$\eta_i(\text{for roof}) = 0$$

Seismic zone 3, soil type 1 (rock)

$$\text{Plan area} = 9(4.5 + 4 \times 3.5)$$

$$= 166.5 \text{ m}^2$$

$$G = 4 \text{ kN/m}^2 \quad L_i = 18.5 \text{ m} = \text{Total length}$$

$$\text{Total number of floors} = 5 \text{ m}$$

There is no information about the density of the wall and it is therefore taken to be zero, i.e. $d = 0$:

www.EngineeringBooksPDF.com

$$T_{0e} = \text{fundamental period of vibration} = \frac{h_n}{100}\sqrt{\frac{30}{L} + \frac{2}{1+30d}}$$
$$= \frac{18.0}{100}\sqrt{\frac{30}{18.5} + 2} = 0.343 \text{ s}$$

(b) *Seismic coefficient*

A 5% damping for seismic zone 3, soil type 1 reinforced concrete-framed building with

$$a_s = 0.25 \quad b = 0.75 \quad T_1 = 0.20 \text{ s} \quad T_2 = 0.35 \text{ s}$$

In this case $T_1 < T < T_2$, hence

$$S_\text{a} = \text{horizontal seismic spectra pseudo} - \text{acceleration}$$
$$= b = 0.75$$

The seismic coefficient C is calculated as

$$C = \frac{s_\text{a}\gamma d}{R}$$
$$= \frac{0.75 \times 1.3}{5} = 0.195(\text{for RC structures withh ductility})$$
$$\gamma_d = \text{risk factor Group A} = 1.3$$
$$R = \text{reduction factors} = \mu = 5(\text{for} T \geq T_1)$$
$$V_0 = \text{base shear force} = CW$$
$$= 0.195 \times 50.995 \times 10^5 = 9.944 \times 10^5 \text{ kg}$$

Comparison with the Algeria code

$$V = 279.56 \text{ kN} = 28,512.239 \text{ kg} = 0.2 \times 10^5 \text{ kg}$$

The equivalence of

$$C = ADBQ = 0.056 < 0.195$$

And the factor for

$$V = \frac{9.944 \times 10^5}{0.2 \times 10^5} = 49.72$$

The tabulated values, assuming $\alpha = 1.0$ and $\alpha = 0.9$ for all levels and the base, respectively, are to be multiplied by 49.72. The frame is subjected to heavy

www.EngineeringBooksPDF.com

lateral loads and overturning moments and this building in Argentina will have to have a more robust design.

(c) *Torsional moment*

Table 4.1 is extended to include torsional moments. A column is created in Table 4.1 on the basis of

$$\begin{aligned} M_{ti} &= (1.5e_1 + 0.10L)V_i \\ &= 0.1LV_i \\ &= 0.1 \times 18.5V_i \\ &= 1.85V_i \end{aligned}$$

e_1 = distance from the CS at level i and the line of action of the shear force measured perpendicularly, assumed to be zero

all units in MKS, i.e. kg units.

The modified V column $\times$ 1.85 will give the M_{ti} values.

(d) *Storey drifts, lateral displacement and storey distortions*

K_i = stiffness at ith level $= 12EI_i/H_i^3$

$H_i = 3.5$ m storey height

$E_c = 2.1 \times 10^9 \text{kg/m}^2$

I_i = cross − sectional area moment of inertia for the storey column

(e) *Storey drift* Δ_i

Given by

$$\Delta = \frac{\mu V_i}{K_i}$$

Level	$V_i \times 10^4$ kg
Roof	0.9331
Fourth floor	1.8649
Third floor	2.2551
Second floor	2.6439
First floor	2.8512
Base	–

(f) I *for columns*

For floors 1 and 2:

$$I_A = I_C = \frac{1}{12} \times 0.3048(0.508)^3 = 3.3298 \times 10^{-3}\text{m}^4$$

$$I_B = \frac{1}{12} \times 0.3048(0.6096)^3 = 5.7539 \times 10^{-3}\text{m}^4$$

www.EngineeringBooksPDF.com

All other floors

$$I_A = I_C = \frac{1}{12}(0.3048)(0.4064)^3 = 1.7048 \times 10^{-3}\text{m}^4$$

$$I_B = \frac{1}{12}(0.3048)(0.5080)^3 = 3.3298 \times 10^{-3}\text{m}^4$$

Total

$$I = 6 \times I_A + 6I_B + 6I_C$$

(g) *K_i values for floor I*

Grids A and C:

$$\frac{12EI_i}{H_i^3} = \frac{12 \times 2.1 \times 10^9 \times 3.3298 \times 10^{-3}}{(4)^3}$$

$$= 1.3111 \times 10^6 \text{kg/m}$$

Grid B:

$$\frac{I_B}{I_A} \times K_i(\text{Grid A}) = \frac{5.7539 \times 10^{-3}}{3.3298 \times 10^{-3}} \times 1.3111 \times 10^6$$

$$= 2.266 \times 10^6 \text{kg/m}$$

$$K_i(\text{total})\text{floor} = 12 \times 1.3111 \times 10^6 + 6 \times 2.266 \times 10^6$$

$$= 29.3292 \times 10^6 \text{kg/m}$$

$$\Delta_i = \text{storey drift} = \frac{5V_i}{K_i} \quad \text{(total)}$$

	Δ_i(m)	M_{ti}(kg/m)
Roof	0.00196	1.726×10^4
Fourth	0.00392	3.450×10^4
Third	0.00474	4.172×10^4
Second	0.0056	4.891×10^4
First	0.0049	5.275×10^4
Base	–	–

(h) *Sample calculations for Δ_i/H_i*

$$\text{Roof level} = \frac{0.00196}{3.5} = 0.00056 \text{ (m)}$$

Floor	Δ_i/H_i
4	0.0011
3	0.0014
2	0.0016
1	0.001123

www.EngineeringBooksPDF.com

(i) K_i *values for all other floors*

$$\frac{12EI_i}{H_i^3} = 1$$

Grids A and C:

$$\frac{12 \times 2.1 \times 10^9 \times 1.7048 \times 10^{-3}}{(3.5)^3} = 1.002 \times 10^6 \text{kg/m}$$

Grid B:

$$\begin{aligned} I_B/I_A \times K_i(\text{Grid A}) &= \frac{3.3298 \times 10^{-3}}{1.7048 \times 10^{-3}} \times 1.002 \times 10^6 \\ &= 1.9571 \times 10^6 \text{ kg/m} \\ K_i(\text{total}) &= 12 \times 1.002 \times 10^6 + 6 \times 1.9571 \times 10^6 \\ &= 23.767 \times 10^6 \text{ kg/m} \end{aligned}$$

(j) Δ_i *(sample calculations)*

$$\text{First floor} = \frac{5 \times 2.8512 \times 10^4}{29.3292 \times 10^6} = 0.0049$$

(k) *Sample calculation for the lateral displacement* δ_i

$$\text{Second floor} = (0.0049 + 0.0056) = 0.0016(\text{m})$$

(l) *Sample calculations for* β_i *for* $P - \Delta$

$$\beta_i = \frac{P_i \Delta_i}{V_i H_i}$$

Floor 1:

$$\beta_1 = 0.00123 \frac{50.995 \times 10^5}{2.8512 \times 10^4} = 0.2200$$

All results are summarized in Table 4.2.

The maximum relative storey drift is $0.0056 < 0.014$ as allowed by the code. The conditions established for a $P - \Delta$ affect $\beta_i \geq 0.08$. Most values exceed this value, and it is necessary to carry out a $P - \Delta$ analysis, using a spectral modal analysis. The modal shear is used.

www.EngineeringBooksPDF.com

Table 4.2 Summary of results for Example 4.3

Level	Δ_i(m)	δ_i(m)	Δ_i/H_i relative drift	$W_i \times 10^5\,kg$	$\sum W_i \times 10^5\,kg$	$P-\Delta$ coeff. β_i
Roof	0.00196	0.02112	0.00056	10.199	10.199	0.0612
4	0.00392	0.01916	0.0011	10.199	20.398	0.1203
3	0.00474	0.011524	0.0014	10.199	30.597	0.1679
2	0.0056	0.0105	0.0016	10.199	40.796	0.2469
1	0.0049	0.0049	0.00123	10.199	50.995	0.2200
Base						

Table 4.3 Results for part (a) of Example 4.4

Floor	Lateral force (kips) (F)	Storey shear (kips) (V)	Storey moment (kipt ft) (M_0)
3	28	0	0
2	19	280	3,360
1	9	470	9,000
Base	0	560	15,720

4.5.4 Example 4.4 American Practice

(a) A three-storey shear wall building is to be designed against earthquake effects using US Uniform Building Code (UBC). Calculate the base shear, total lateral shear force and overturning moment at each level. Assume the storey height is 12 ft. Use the following data:

$$I = 1.0 \qquad Z_a = 1.0 \qquad S = 1.5$$
$$K = 1.33 \qquad T = 0.15\,\text{s}$$

For storey height (3.66 m) = 12 ft
Each floor weight = 1,000 kips (4,448 kN)

(b) If the shear wall is of reinforced masonry with peak ground acceleration $A_a = 0.4$ (for seismic coefficient $C_S = 2A_a/R$) and $A_v = 0.4$ (for lower value of base shear $C_S = 1.2A_vS/RT^{2/3}$) recalculate base shear, lateral shear force and overturning moment at each level when $S = S_1\,1.0$ for rock-like formation.

For part (a)

$$C = \frac{1}{15\sqrt{T}} = \frac{1}{15\sqrt{0.15}} = 0.171 > 0.12$$

use

$$C = 0.12$$
$$S = 1.5$$
$$C_S = 0.12 \times 1.5 = 0.18 > 0.14$$

www.EngineeringBooksPDF.com

and

$$C_S = 0.14$$

$$\sum W = 3 \times 1,000 = 3,000 \text{ kips } (13,344 \text{ kN}) \text{ or } 13,344\text{MN}$$

$$\text{Base shear} = V = Z_a ICSKW = 1 \times 1 \times 0.14 \times 1.33 \times 3,000$$

$$= 558.6 \text{ kips } (2485 \text{ kN})$$

Since $T \leq 0.75$ s
$F_t = 0$ at top
For lateral forces (Table 3.8) of the code:

$$F_i = \left(\frac{W_i h_i}{\sum_{i=1}^{3} W_i h_i} \right) V$$

For part (b)
$A_V = 0.4$
$R = 3.5$ for man sonry was
$A_a > 3$
$S = S_1 =$ seismic coefficient
$= 1.0$
= rock-like formation
Referring to Table 4.4

Table 4.4 Results for part (b) of Example 4.4

Floor	Lateral force (F) (kips)	Storey shear (V) (kips)	Storey moment (kipt ft)
3	340	0	0
2	230	340	4,080
1	120	570	10,920
Base	0	560	19,200

$$C_{S_{max}} = \frac{2(0.4)}{3.5} = 0.23$$

$$C_S = \frac{1.2AVS}{RT^{2/3}} = 0.49 > 0.23$$

$$V = 0.23 \times 3,000 = 690 \text{ kips } (3,069 \text{ kN})$$

4.5.5 *Example 4.5 American Practice*

Determine the base shear, storey shear, overturning moment and allowable inter storey displacement for nine-storey building with moment-resisting steel frame for an office in California as shown in Fig. 4.23. Use the US UBC-91 code and compare with UBC-85:

www.EngineeringBooksPDF.com

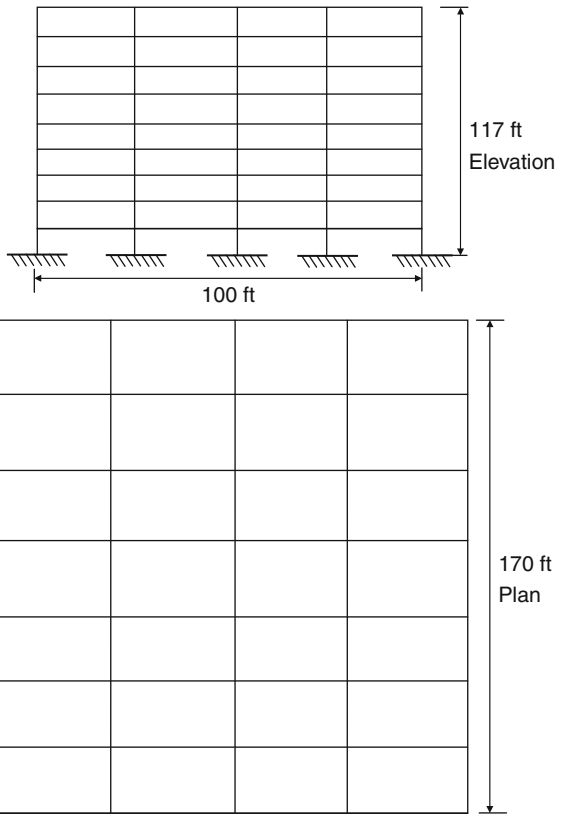


Fig. 4.23 Moment-resisting steel-framed building

Data

Storey height = 13 ft = h_x

Total load = 0.1 kip/ft^2 (all levels)

Soil profile type 2, i.e. $S_2 = 1.2$

Seismic coefficient $C = \frac{1}{15\sqrt{T}}$ or $C = \frac{1.25S}{T^{2/3}}$

Ductile moment frame and zone location: zone 4:

Base shear $V = Z_a IKCSW$ or $\frac{ZICW}{R_W}$

$$R_W = 12$$

For zone 4:

$$Z_a = 1$$

I = importance factor = 1.0 (for the office building)
K = ductile value = 0.67

www.EngineeringBooksPDF.com

$$C = \frac{1}{15\sqrt{T}}$$

$$T = C_t h_N^{3/4} = 1.25\,\text{s} \quad (\text{UBC} - 91)$$

$$T = 0.1\,N = 0.1 \times 9 = 0.9\,\text{s} \quad (UBC - 85)$$

$$S_2 = 1.2$$

$$C = \frac{(1.25 \times 1.2)}{(1.25)^{2/3}} = 2.39 \quad (\text{UBC} - 91)$$

$$C = \frac{1}{15\sqrt{0.9}} = 0.07 < 0.12 \quad (\text{UBC} - 85)$$

$$C = \frac{1}{15\sqrt{1.25}} = 0.061 < 0.12$$

$$C_S = 0.07(1.2) = 0.084 < 0.14$$

Comparison with UBC-85 leads to

$$\omega = 0.1(170)(100) = 1{,}700 \text{ kips/floor}$$

$$W = 9 \times 1700 = 15{,}300 \text{ kips}$$

$$Z = 1.0$$

$$I = 1.0$$

$$V = \frac{ZICW}{RW} = \frac{1 \times 1 \times 2.38 \times 15{,}300}{12}(\text{UBC} - 91)$$

$$= 3{,}034.5 \text{ kips}(13{,}497{,}456, \text{kN}) \text{ or} 13{,}497{,}456 \text{ MN} \approx 13.5 \text{ MN}$$

$$\frac{C}{RW} = \frac{2.38}{12} = 0.2 > 0.075$$

$$V = 1.0 \times 1.0 \times 0.67 \times 0.07 \times 1.2(15{,}300) \quad (\text{UBC} - 85)$$

$$= 861.1 \text{ kips } (3{,}830.2 \text{ kN})$$

(A) Based on UBC-85 sample calculations
Vertical distribution $T > 0.7$ s, i.e. 0.09 or 1.25 s:

www.EngineeringBooksPDF.com

$$F_t = 0.07 \times 0.9 \times 861.1\text{kips} = 54.25 \text{ kips}$$

$$0.25 \times V = 215.3 > 54.25$$

$$F_\text{t} = 54.2 \text{ kips}$$

$$V - F_\text{t} = 861.1 - 54.2 = 806.9 \text{ kips}$$

$$F_x = \text{lateral forces} = \frac{(V - F_t) W_x h_x}{\sum_{i=1}^{n} W_i h_i}$$

$$F_9 + F_t = \frac{806.9(1700)(117)}{994.5 \times 10^3} + 54.2 = 215.6 \text{ kips}$$

$$F_8 = \frac{806.9(1700)(104)}{994.5 \times 10^3} = 143.4 \text{ kips} (637.848 \text{ kN})$$

The results are summarized in Table 4.5.

Table 4.5 Individual and cumulative loading (UBC-85)

Level	h_x(ft)	W_x(kips)	$W_x h_x$(kip ft)
9	117	1,700	198,900
8	104	1,700	176,800
7	91	1,700	154,700
6	78	1,700	132,600
5	65	1,700	110,500
4	52	1,700	88,400
3	39	1,700	66,300
2	26	1,700	44,200
1	13	1,700	22,100
		15,300	$\Sigma 994.5 \times 10^3$

Storey shear

$$V_x = F_t \sum_{i=x}^{n} F_i$$

$$V_9 = 215.6 \text{ kips}$$

$$V_8 = 215.6 + 143.4 = 359 \text{ kips}$$

Overturning moment

$$M_x = F_\text{t}(h_\text{n} - h_x) + \sum_{i=1}^{n} F_i (h_i - h_x)$$

$$M_9 = 215.6 \times 13 = 2803 \text{ ft kips}$$

$$M_8 = 215.6(213) + 143.4(13) = 7469 \text{ ft kips}$$

Interstorey displacement

$$\Delta \leq 0.005 \, Kh = 0.005 \times 0.67 \times 13 = 0.04355 \text{ ft}$$

$$= 0.0133 \text{ m}$$

www.EngineeringBooksPDF.com

(B) Based on UBC-91 sample calculations

$$F_t = 0.07 \times 1.25 \times 3034.5 \text{ kips} = 265.52 \text{ kips} \leq 0.25 \times 3034.5$$
$$= 758.625 \text{ kips}$$
$$V - F_t = 3{,}034.5 - 265.52 = 2,768.98 \approx 2{,}769$$
$$F_9 + F_t = \frac{2,769(1,700)(117)}{994.5 \times 10^3} + 265.52$$
$$= 553.8 \text{ kips} + 265.52 = 819.32 \text{ kips}$$
$$F_8 = \frac{2,769(1,700)(104)}{994.5 \times 10^3} = 492.1 \text{ kips}$$

Storey shear

$$V_9 = 819.32 \text{ kips}$$
$$V_8 = 819.32 + 492.1 = 1{,}311.42 \text{ kips}$$

Overturning moment

$$M_9 = 8.19 \times 13 = 10{,}651.16 \text{ ft kips}$$
$$M_8 = 819.32(2 \times 13) + 492.1 = 26,223.32 \text{ ft kips}$$
$$\Delta = \text{allowable interstorey displacement (for 0.7s or greater)}$$
$$\nsucceq \frac{0.03}{R_w} \times \text{storey height } n \text{ or } 0.004 \times 13 = 0.052 \text{ ft } (0.016 \text{ m})$$

Table 4.6 gives the final comparative results.

Table 4.6 Comparative results for Example 4.5

Level	$F_i + F_t$(kips)		V_x (kips)		M_x (ft kips)	
9	215.6	(819.32)	215.6	(819.32)	2,803	(10,651)
8	143.6	(492.1)	359.0	(1,311.42)	7,469	(27,700)
7	125.5	(430.6)	484.5	(1,772.62)	13,768	(50,343)
6	107.6	(369.1)	592.1	(2,141.72)	21,466	(62,383)
5	89.7	(307.6)	681.8	(2,449.32)	30,329	(195,604)
4	71.7	(246.06)	754.5	(2,695.38)	40,125	(143,876)
3	53.8	(184.54)	807.3	(2,880)	50,619	(180,917
2	35.9	(123.03)	843.2	(2,893)	61,581	(219,558)
1	17.9	(61.515)	861.1	(2,955)	72,775	(258,998)
	861.1	(3,033.865)				

www.EngineeringBooksPDF.com

4.5.6 Example 4.6 American Practice

A two-by-two storey shear wall building is in a seismic environment. Using the following data and assuming that the natural frequencies fall into the constant acceleration range of the response spectra, calculate storey forces, overturning moments and displacement.

Data

storey height $= h$

floor weight $= W_S$

$$W_W = \text{weight of shear wall/unit length}$$

Floor is assumed to be infinitely rigid:

$$f_A = \text{natural frequency} = \sqrt{\frac{1.2EI/h^3}{1.54hM_w + 1.125M_s}}$$

Floor is assumed to be infinitely flexible:

$$f_{B_1} = \sqrt{\frac{0.4EI/h^3}{0.514hM_w + 0.281M_s}} \quad \text{(shear walls 1 and 3)}$$

$$f_{B_2} = \sqrt{\frac{0.4EI/h^3}{0.514hM_w + 0.562M_s}} \quad \text{(shear wall 2)}$$

where

$$M_s = \frac{W_s}{g}$$

$$M_w = \frac{W_w}{g}$$

Use the Rayleigh principle and assume that the shear wall mass is lumped at floor levels.

The deformation shape (see Fig. 4.24) is given by

$$\phi(z) = \frac{\delta_{max}}{3}\left(\frac{z^4}{L^4} - \frac{4z^3}{L^3} + 6\frac{z^2}{L^2}\right)$$

Specific deformation shape $= \phi(z) = \frac{1}{3}\left[\left(z^4/16\,h^4\right) - \left(z^3/2\,h^3\right) + \left(3z^2/2\,h^2\right)\right]$ for this building.

www.EngineeringBooksPDF.com

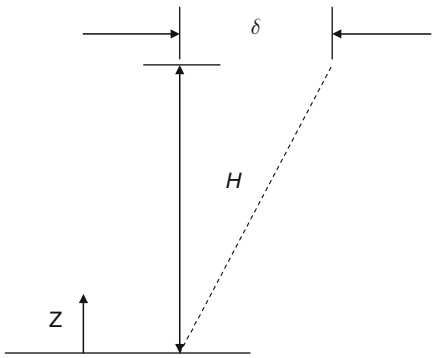


Fig. 4.24 Diagram for deformation shape calculation

The combined mass at the floor level is treated as W_{sw} to replace W_s:

$$W_{swA} = \sqrt{\frac{1.2EI/h^3}{0.281W_{sw}/g}} = \sqrt{1.03\frac{EI/h^3}{W_{sw}/g}}$$

$$W_{swB_1} = \sqrt{\frac{0.4EI/h^3}{0.281W_{sw}/g}} = \sqrt{1.19\frac{EI/h^3}{W_{sw}/g}} \quad \text{shear walls 1 and 3}$$

$$W_{swB_2} = \sqrt{\frac{0.4EI/h^3}{0.562W_{sw}/g}} = \sqrt{0.84\frac{EI/h^3}{W_{sw}/g}} \quad \text{shear wall 2}$$

$$W_{swB_1} > W_{swA} > W_{swB_2}$$

or

$$T_{B_1} < T_A < T_{B_2}$$

Deformation equation $\phi(z)$ applies when

$$\begin{matrix} z = h & \phi(z) = 0.354 \\ & > \{\phi_1\} = \begin{Bmatrix} 1.00 \\ 0.35 \end{Bmatrix} \\ z = 2h & \phi(z) = 1.00 \end{matrix}$$

For the first case $W = W_{sw}$
For the first case B_1 $W = \frac{1}{4}W_{sw}$
For the first case B_2 $W = \frac{1}{2}W_{sw}$

www.EngineeringBooksPDF.com

The lateral force at each level

$$F(z,t)_{\max} = M(z)\phi(z) \times \frac{W/g(1.0+0.354)}{W/g(1.0^2+0.354^2}S_a$$

$$= M(z)\phi(z) \times 1.204 \times S_a$$

$$F(z,t)_{\max} = 1.204\frac{W}{g} \times \phi(z)S_a$$

$$F(2h,t)_{\max} = 1.204\frac{W}{g} \times 1.0S_a = 1.204\frac{W}{g}S_a \quad \text{(level2)}$$

$$F(h,t)_{max} = 1.204\frac{W}{g} \times 0.354S_a = 0.426\frac{W}{g}S_a \quad \text{(level1)}$$

$$F(t) = \text{base} = 0$$

Storey shears

Level 2: 0

Level 1: $1.204\ \dfrac{W}{g}\ S_a$

Base: $(1.204 + 0.426)\ \dfrac{W}{g}\ S_a = 1.630\ \dfrac{W}{g}\ S_a$

Overturning moment

Level 2: 0

Level 1: $1.204\ \dfrac{W}{g}\ hS_a$

Base: $2.834\ \dfrac{W}{g}\ gS_a$

Lateral displacements $= 1.204\phi(z)S_d$

$$= \frac{1}{(f_1)^2}\phi(z)1.204S_a$$

Note that f_1^2 varies for each case.

Storey displacement

	A	B_1	B_2
$z = 2\,h$	$\dfrac{1.204S_a}{f_{A^2}}$	$\dfrac{1.204S_a}{f_{B_1}^2}$	$\dfrac{1.203S_a}{f_{B_2}^2}$
$z = h$	$\dfrac{0.426S_a}{f_A^2}$	$\dfrac{0.426S_a}{f_{B_1}^2}$	$\dfrac{0.426S_a}{f_{B_2}^2}$

4.5.7 Elastic Design Spectrum: Construction of Design Spectrum

In this section we introduce the concept of earthquake design spectrum for elastic systems and present a procedure to construct it from estimated peak values for ground acceleration, ground velocity and ground displacement.

The design spectrum should satisfy certain requirements because it is intended for the design of new structures, or the seismic safety evaluation of existing

www.EngineeringBooksPDF.com

structures, to resist future earthquakes. For this purpose the response spectrum for a ground motion recorded during a past earthquake is inappropriate. The jaggedness in the response spectrum, as seen in Fig. 4.25, is characteristic of that one excitation. The response spectrum for another ground motion recorded at the same site during a different earthquake is also jagged, but the peaks and valleys are not necessarily at the same periods. This is apparent from Fig. 4.26 where the response

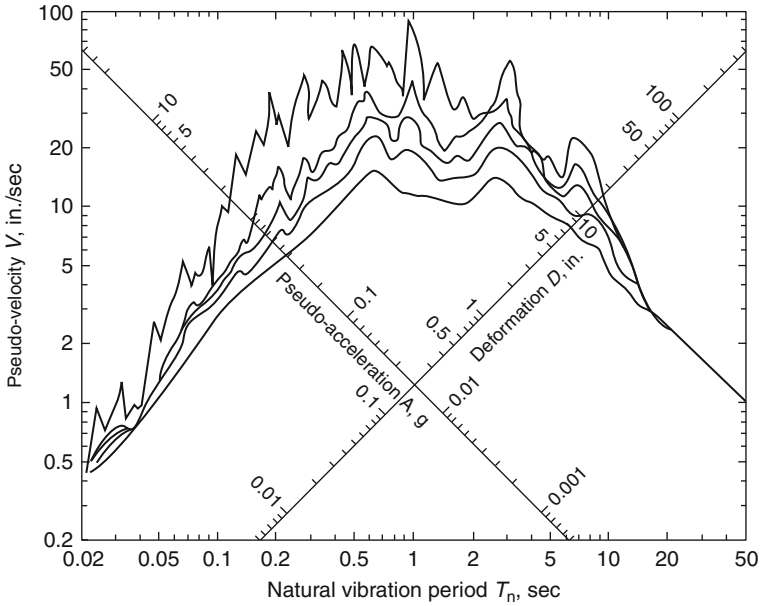


Fig. 4.25 Combined D-V-A response spectrum for El-Centro ground motion: $\zeta = 0$, 2, 5, 10 and 20%

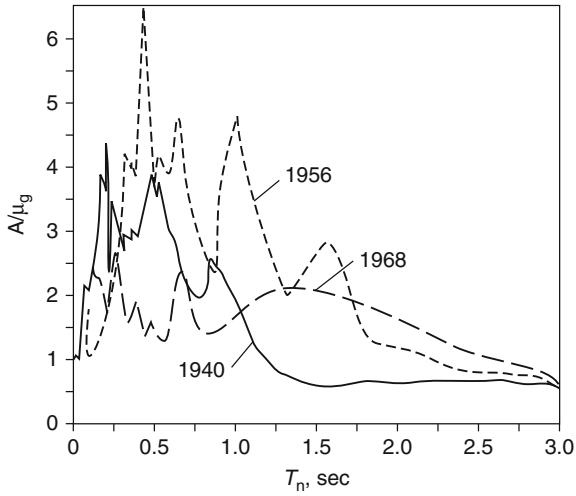


Fig. 4.26 Response spectra for the north–south component of ground motions recorded at the Imperial Valley Irrigation District substation, El-Centro, California, during earthquakes of 18 May 1940; 9 February 1956 and 8 April 1968. $Z = 2\%$. R. Riddle and N.M. Newmark (1979) California Institute of Technology, U.S.A

www.EngineeringBooksPDF.com

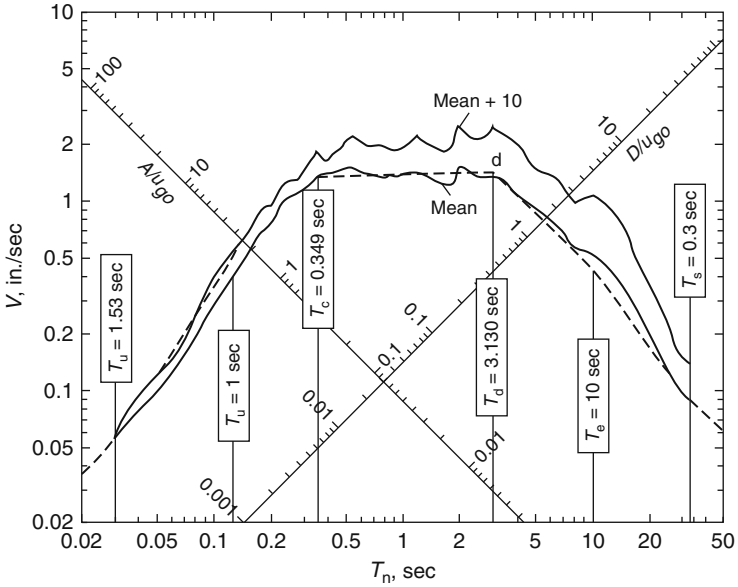


Fig. 4.27 Mean and mean $+1\,\sigma$ spectra with probability distributions for Vat $T_n = 0.25$, 1 and 4 s; $\zeta = 5\%$. *Dashed lines* show an idealized design spectrum. (Based on numerical data from R. Riddell and N. M. Newmark, 1979)

spectra for ground motions recorded at the same site during three past earthquakes are plotted. Similarly, it is not possible to predict the jagged response spectrum in all its detail for a ground motion that may occur in the future. Thus the design spectrum should consist of a set of smooth curves or a series of straight lines with one curve for each level of damping.

4.5.7.1 Procedure for Construction of Elastic Design Spectrum Based on American System: A Reference Is Made to Fig 4.28

1. Plot the three dashed lines corresponding to the peak values of ground acceleration $\ddot{u}_{go}$, velocity $\dot{u}_{go}$ and displacement u_{go} for the design ground motion.
2. Obtain from Table 4.7 or 4.8 the values of design ground motion.
3. Multiply $\ddot{u}_{go}$ by the amplification factor α_A to obtain for α_A, α_V, and α_D for the ζ selected.
4. Take $\ddot{u}_{go} = 1g, \dot{u}_{go} = 48\,\text{in/s}; u_{go} = 36\,\text{in} \rightarrow$ Plotted
5. From Table 4.7: Amplification factors for 81.1 percentile spectrum with 5% damping
6. $A = 1\text{ g} \times 2.71 = 2.71\ g$ – Constant A-branch
   $V = 48\text{ g} \times 2.30 = 110.74$ – Constant V-branch
   $D = 36 \times 2.01 = 72.4$ – Constant D-branch
7. The line A = 1*g* is plotted for $T_n < 1/33$ s and D = 36 in at 33 s.

www.EngineeringBooksPDF.com

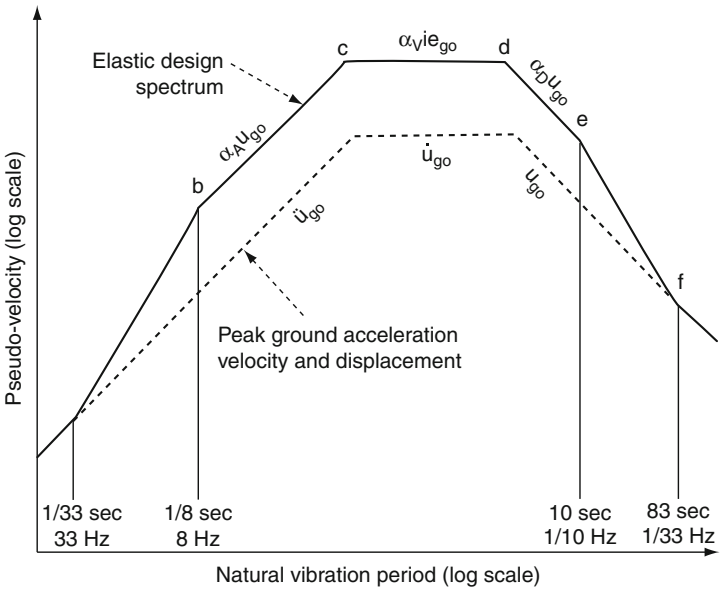


Fig. 4.28 Construction of elastic design spectrum

Table 4.7 Reinforcement designation and bar areas used in the USA

Bar size designation	Normal cross – sectional area (sq. in)	Weight 1b per ft	Nominal diameter (in)	British or European codes equivalent
#3	0.11	0.376	0.375	
#4	0.20	0.668	0.500	
#5	0.31	1.043	0.625	
#6	0.44	1.502	0.750	
#7	0.60	2.044	0.875	See Eurocode 2 BS 8110 for bar diameter designation
#8	0.79	2.670	1.000	
#9	1.00	3.400	1.128	
#10	1.27	4.303	1.270	
#11	1.56	5.313	1.410	
#14	2.25	7.650	1.693	
#18	4.0	13.600	2.257	

The elastic design spectrum provides a basis for calculating the design force and deformation for SDF systems to be designed to remain elastic. For this purpose the design spectrum is used in the same way as the response spectrum was used to compute peak response;

With the pseudo-velocity design spectrum known (Fig. 4.29). the pseudo-acceleration design spectrum and the deformation design spectrum are determined and plotted in Figs. 4.30 and 4.31 , respectively. Observe that A approaches

www.EngineeringBooksPDF.com

Table 4.8 ASTM metric reinforcing bars*

Bar size designation	Nominal dimensions Mass (kg/m)	Diameter (mm)
10 M	0.785	11.3
15 M	1.570	16.0
20 M	2.355	19.5
25 M	3.925	25.2
30 M	5.495	29.9
35 M	7.850	35.7
45 M	11.775	43.7
55 M	19.625	56.4

* ASTM A615M Grade 300 is limited to size Nos. 10 M through 20 M; otherwise 500 MPa for all the sizes. Check availability with local suppliers for Nos. 45 M and 55 M.

$\ddot{u}_{go} = 1\,g$ at $T_n = 0$ and D tends to $u_{go} = 36$ in at $T_n = 50$ s. The design spectrum can be defined completely by numerical values for T_a, T_b, T_c, T_d, T_e, and T_f, and equations for these periods–T_a, T_b, T_e, and T_f – are fixed, but others – T_c and T_d – depend on damping. The intersections of $A = 2.71g$, $V = 110.4$ in/s and $D = 72.4$ in are determined: $T_c = 0.66$ s and $T_d = 4.12$ s for $\zeta = 50\%$. Equations describing various branches of the pseudo-acceleration design spectrum are given in Fig. 4.30.

Repeating the preceding construction of the design spectrum for additional values of the damping ratio leads to Figs. 4.31, 4.32, 4.34 and 4.35. This then is the design spectrum for ground motions on firm ground with $\ddot{u}_{go} = 1\,g, \dot{u}_{go} = 48$ in/s

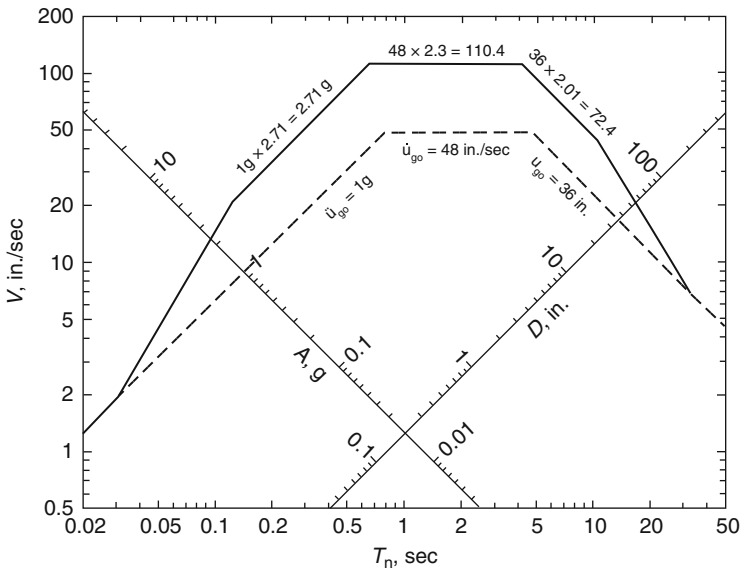


Fig. 4.29 Construction of elastic design spectrum (84.1th percentile) for ground motions with $\ddot{u}_{go} = 1\,g, \dot{u}_{go} = 48$ in/s; $u_{go} = 36$ in; $\zeta = 5\%$

www.EngineeringBooksPDF.com

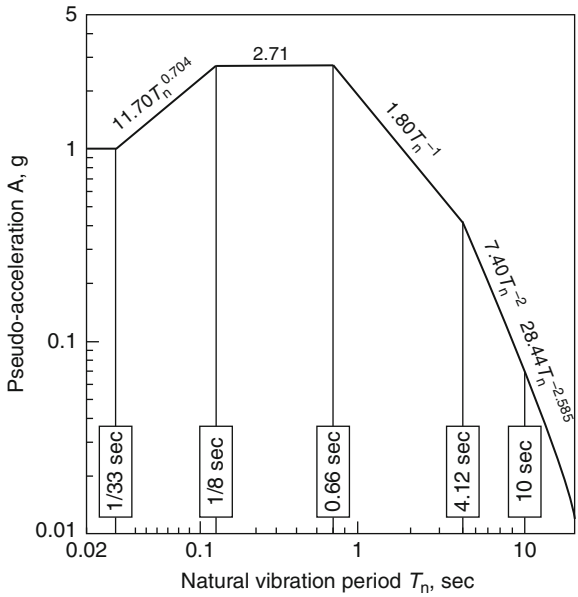


Fig. 4.30 Elastic pseudo-acceleration design spectrum (84.1th percentile) for ground motions with $\ddot{u}_{go} = 1\,g, \dot{u}_{go} = 48\text{in/s}$; $u_{go} = 36\,\text{in}; \zeta = 5\%$

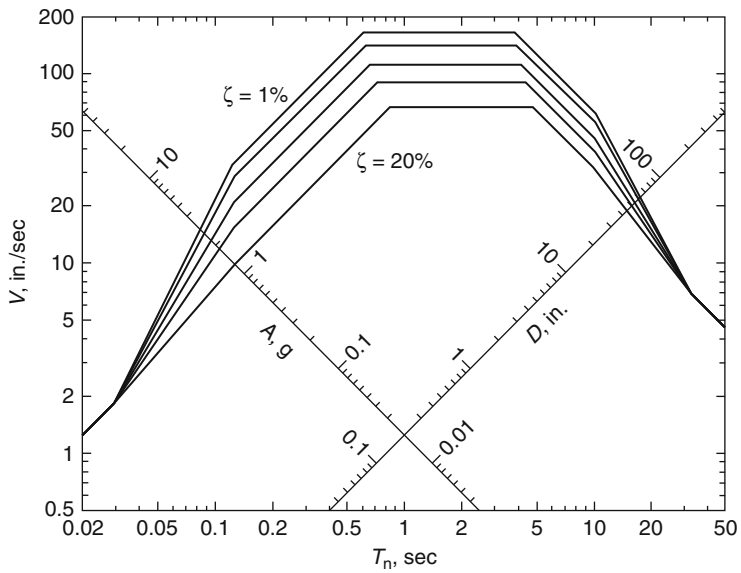


Fig. 4.31 Pseudo-velocity design spectrum for ground motions with $\ddot{u}_{go} = 1\,g$, $\dot{u}_{go} = 48$ in/s; $u_{go} = 36$ in; $\zeta = 1, 2, 5, 10$ and 20%

www.EngineeringBooksPDF.com

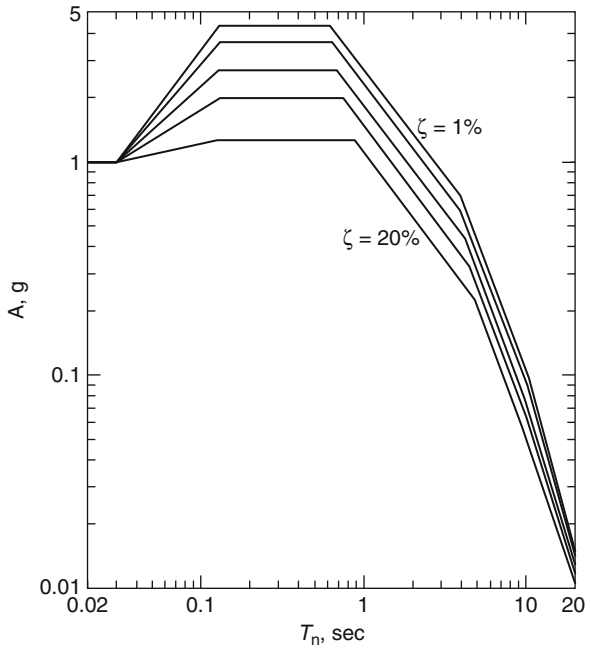


Fig. 4.32 Pseudo-acceleration design spectrum (84.1th percentile) for ground motions with $\ddot{u}_{go} = 1\,g, \dot{u}_{go} = 48\,\text{in/s}$; $u_{go} = 36\,\text{in}; \zeta = 1, 2, 5, 10$ and 20%

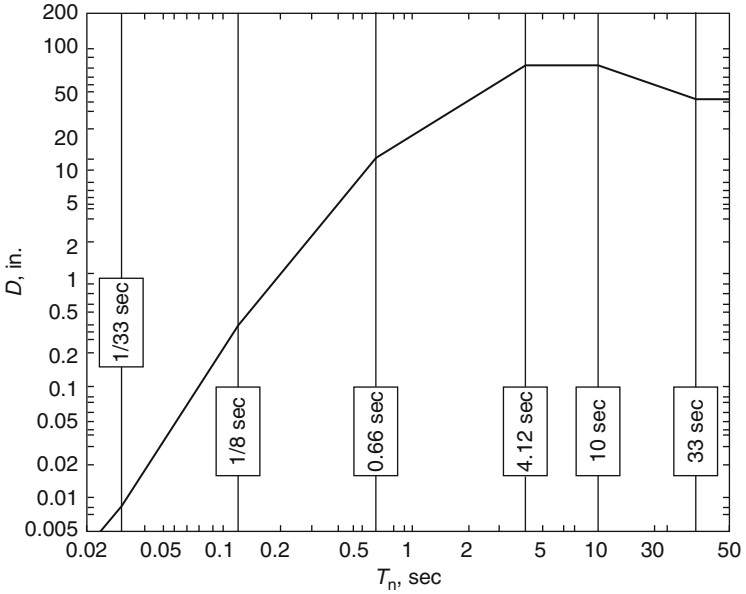


Fig. 4.33 Deformation design spectrum (84.1th percentile) for ground motions with $\ddot{u}_{go} = 1\,g, \dot{u}_{go} = 48$ in/s; $u_{go} = 36$ in; $\zeta = 5\%$

www.EngineeringBooksPDF.com

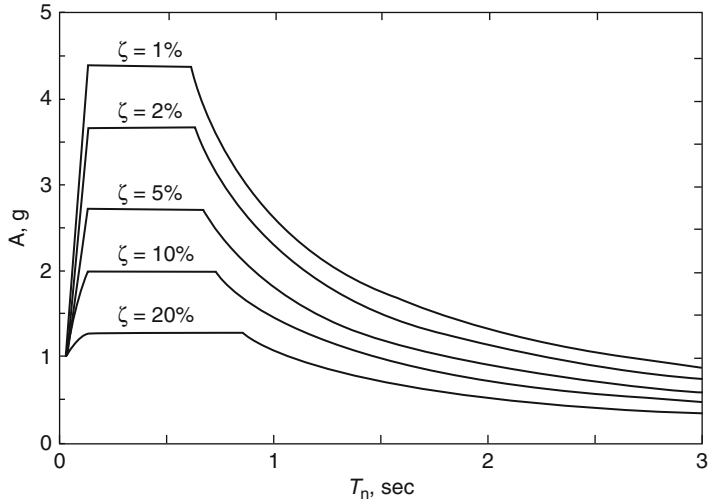


Fig. 4.34 Pseudo-acceleration design spectrum (84.1th percentile) for ground motions with $\ddot{u}_{go} = 1\,g, \dot{u}_{go} = 48$ in/s; $u_{go} = 36$ in; $\zeta = 1, 2, 5, 10$ and 20%

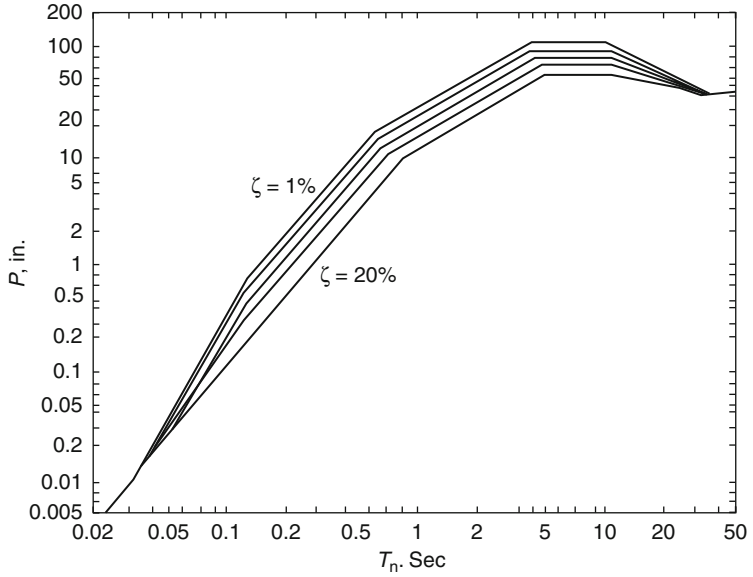


Fig. 4.35 Deformation design spectrum (84.1th percentile) for ground motions with $\ddot{u}_{go} = 1\,g, \dot{u}_{go} = 48$ in/s; $u_{go} = 36$ in; $\zeta = 1, 2, 5, 10$ and 20%

and $u_{go} = 36$ in in three different forms: pseudo-velocity, pseudo-acceleration and deformation.

The elastic design spectrum provides a basis for calculating the design force and deformation for SDF systems to be designed to remain elastic. For this

www.EngineeringBooksPDF.com

purpose the design spectrum is used in the same way as the response spectrum was used to compute peak response.

4.6 Earthquake Response of Inelastic Systems

4.6.1 General

Structures subjected to severe earthquake ground motion experience deformations beyond the elastic range. To a large extent, the inelastic deformations depend on the intensity of excitation and load deformation characteristics of the structure and often result in stiffness deterioration. Because of the cyclic characteristics of ground motion, structures experience successive loadings and unloadings and the force–displacement or resistance–deformation relationship follows a sequence of loops known as hysteresis loops. The loops reflect a measure of a structure's capacity to dissipate energy. The shape and orientation of the hysteresis loops depend primarily on the structural stiffness and yield displacement. Factors such as structural material, structural system and connection configuration influence the hysteretic behaviour.

A simple model which has extensively been used to approximate the inelastic behaviour of structural systems and components is the bilinear model shown in Fig. 4.36. In this model, unloadings and subsequent loadings are assumed to be parallel to the original loading curve. Strain hardening takes place after yielding initiates. Elastic–plastic (elasto-plastic) model is a special case of the bilinear model where the strain hardening slope is equal to zero. Other hysteretic models such as stiffness and strength degrading have also been suggested. The elastic–plastic model results in a more conservative response than other models. Because of its simplicity, it has been used in the development of inelastic response spectra.

Response spectra modified to account for the inelastic behaviour, commonly referred to as the inelastic spectra, have been proposed by several investigators.

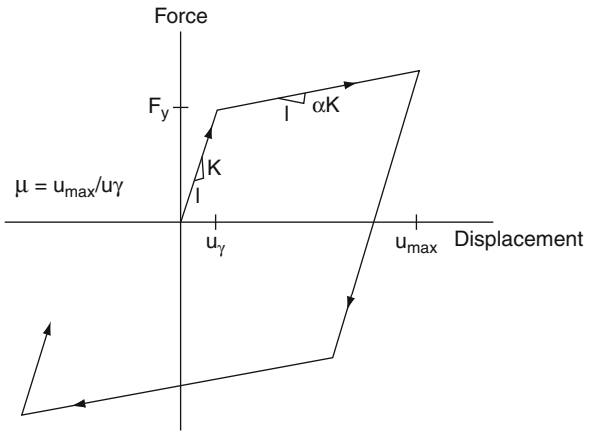


Fig. 4.36 Bilinear force–displacement relationship

www.EngineeringBooksPDF.com

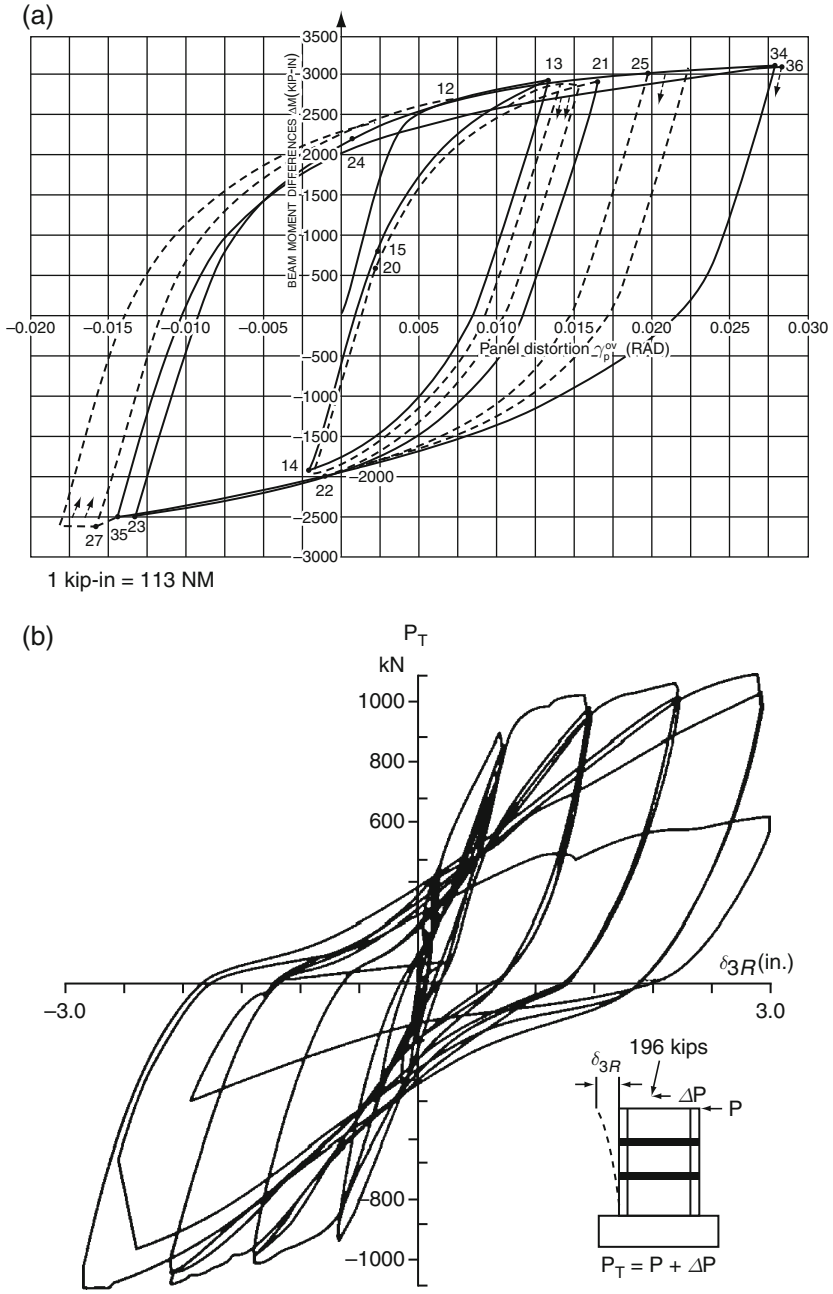


Fig. 4.37 Force–deformation relations

www.EngineeringBooksPDF.com

The use of the inelastic spectra in analysis and design, however, has been limited to structures that can be modelled as a single degree of freedom. Procedures for utilizing inelastic spectra in the analysis and design of multi-degree-of-freedom systems have also been developed to the extent that can be implemented in design. Similar to elastic spectra, inelastic spectra can usually be plotted on tripartite paper for a given damping and ductility or yield deformation. When the spectra are plotted for various ductilities, computations are repeated for several yield deformations using an iterative procedure such as *finite element* and other techniques to achieve the target ductility.

In the inelastic yield spectrum (IYS), the yield displacement is plotted on the displacement axis; in the inelastic acceleration spectrum (IAS), the maximum force per unit mass is plotted on the acceleration axis; and in the inelastic total displacement (ITDS), the absolute maximum total displacement is plotted on the displacement axis. For elastic–plastic behaviour, the inelastic yield spectrum and the inelastic acceleration spectrum are identical. Examples of inelastic spectra for a 5% damped elastic–plastic system for the S90W component of El-Centro, the Imperial Valley earthquake of 18 May 1940, are shown in Fig. 4.26. The figure indicates that for inelastic yield and acceleration spectra, the curves for various ductilities fall below the elastic curve (ductility of one), whereas for the inelastic total deformation spectra, they primarily fall above the elastic, particularly in the acceleration region. It should be noted that increasing the ductility ratio smoothes the spectra and minimizes the sharp peaks and valleys that are present in the plots.

A different presentation of inelastic spectra can always be conceived in a slightly different manner. The spectrum, referred to as the yield displacement spectrum (YDS), is plotted similar to the inelastic total deformation spectrum except that it is plotted for a given yield displacement instead of a given ductility. The ductility is obtained as the ratio of the maximum displacement to the yield displacement for which the spectrum is plotted. Their procedure offers an efficient computational technique, particularly when statistical studies are used to obtain inelastic design spectra.

Note: This concept is fully described in the archives on Imperial Valley in the Library of American Congress, Washington D.C.

4.6.2 De-amplification Factors

When inelastic deformations are permitted in design, the elastic forces can be reduced if adequate ductility is provided.

Hence they presented a set of coefficients referred to as “de-amplification factors” by which the ordinates of the elastic design spectrum are multiplied to obtain the inelastic yield spectrum. In addition it is worthwhile to note that artificial accelerograms with variable durations of strong motion presented a set of coefficients referred to as “inelastic acceleration response ratios” by which the ordinates of the elastic spectrum are decided to give the inelastic yield spectrum. Since these

www.EngineeringBooksPDF.com

two approaches are the inverse of one another, the reciprocal of the Lai–Biggs coefficients represents de-amplification factors. De-amplification factors can also be obtained from the Newmark–Hall procedures for estimating inelastic spectra.

The ductility factor R_μ is defined as the ratio of the elastic to the inelastic displacement for a system with an elastic fundamental period T and specified ductility μ such that

$$R_\mu(T, \mu) = \frac{u_y(T, \mu = 1)}{u_y(T, \mu)} \tag{4.11}$$

where uy is the yield displacement. Stated differently, R_μ is the ratio of the maximum inelastic force to the yield force required to limit the maximum inelastic response to a displacement ductility μ or the inverse of the de-amplification factors, stated earlier.

The relationship between displacement ductility and ductility factor has been the subject of several studies in recent years. Earlier studies by Newmark and Hall (2-87, 2-89) provided expressions for estimating the ductility factor R_μ for elastic–plastic systems irrespective of the soil condition. The expressions are

$$\begin{aligned} R_\mu(T \le 0.03\,\text{s}, \mu) &= 1.0 \\ R_\mu(0.12\,\text{s} \le T \le 0.5\,\text{s}, \mu) &= \sqrt{2\mu - 1} \\ R_\mu(T \ge 1.0\,\text{s}, \mu) &= \mu \end{aligned} \tag{4.12}$$

A linear interpolation may be used to estimate R_μ for the intermediate periods.

Using a statistical study of 15 ground motion records from earthquakes with magnitudes 5.7–7.7, they have developed relations for estimating R_μ for rock or stiff soils for 5% damping. Their proposed relationship is

$$R_\mu(T, \mu) = [c(\mu - 1) + 1]^{1/c} \tag{4.13}$$

where

$$c = \frac{T^a}{1 + T^a} + \frac{b}{T} \tag{4.14}$$

and a and b are parameters that depend on the strain hardening ratio α. Newmark and Hall together with Uans and Bertero recommend a = 1.00, 1.01 and 0.80 and b = 0.42, 0.37 and 0.29 for strain hardening ratios of 0 (elasto-plastic system), 2 and 10%, respectively.

Miranda and Bertero using 124 accelerograms recorded on different soil conditions developed equations for estimating R_μ for rock, alluvium and soft soil for 5% damping. They have not been given in this text. For details, a reference made to bibliography.

Comparisons of the de-amplification factors from the four procedures are shown in Fig. 4.38 for a 5% damping ratio and ductilities of 2 and 5. The figure

www.EngineeringBooksPDF.com

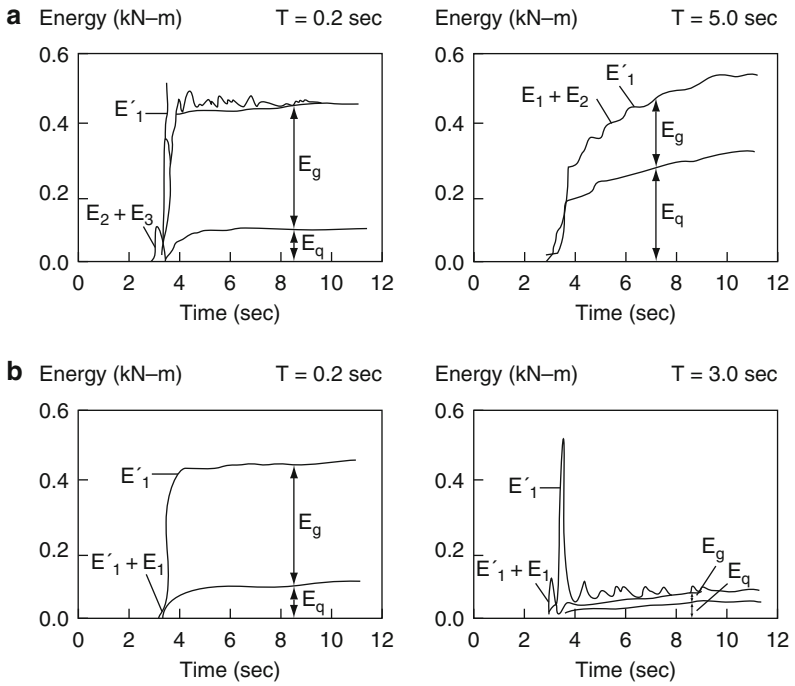


Fig. 4.38 (**a**) Absolute and (**b**) relative energy time histories for elastic–Plastic systems with 5% damping and ductility vatio of 5 subjeated to the 1986 San Salvador Carthquake (after Uans and Bertero)

indicates that the Riddell–Newmark de-amplification factors are in general the smallest (largest reduction in the elastic force) compared to the other three. Both Riddell–Newmark and Newmark–Hall de-amplification ratios remain constant over certain frequency segments, whereas that from Lai–Biggs follows parallel patterns. While the de-amplification ratios are affected by ductility, they are practically not influenced by damping. Since the elastic spectral ordinates decrease significantly with an increase in damping, there is a decrease in inelastic spectral ordinates.

4.6.3 Response Modification Factors

Current seismic codes recommend force reduction factors and displacement amplification factors to be used in design to account for the energy absorption capacity of structures through inelastic action. The force reduction factors (referred to as *R*-factors) are used to reduce the forces computed from the elastic design spectra. A recent study by the Applied Technology Council (ATC) proposes the following expression for computing the *R*-factors:

www.EngineeringBooksPDF.com

$$R = \frac{V_e}{V} = R_s R_\mu R_R \tag{4.15}$$

where V_e is the base shear computed from the elastic response (elastic design spectrum) and V is the design base shear for the inelastic response. The response modification factor R is the product of the following terms:

1. the period-dependent strength factor R_s which accounts for the reserve strength of the structure in excess of the design strength;
2. the period-dependent ductility factor R_μ which accounts for the ductile capacity of the structure in the inelastic range; and
3. the redundancy factor R_R which accounts for the reliability of seismic framing systems.

$$R^\mu(T,\mu) = \frac{\mu - 1}{\Phi(T,\mu)} + 1 \tag{4.16}$$

where

$$\Phi(T,\mu) = 1 + \frac{1}{T(10-\mu)} - \frac{1}{2T}\exp[-1.5(\ln T - 0.6)^2] \tag{4.16a}$$

For rock sites

$$\Phi(T,\mu) = 1 + \frac{1T_g}{T(12-\mu)} - \frac{2T_g}{5T}\exp[-2(\ln T - 0.2)^2] \tag{4.16b}$$

For alluvium sites

$$\Phi(T,\mu) = 1 + \frac{T_g}{3T} - \frac{3T_g}{4T}\exp[-2(\ln\frac{T}{T_g} - 0.25)^2] \tag{4.17}$$

For soft soil sites
and T_g is the predominant period of the ground motion defined as the period at which the relative velocity of a linear system with 5% damping is maximum throughout the entire period range.

4.6.4 Energy Content and Spectra

While the linear and nonlinear response spectra have been used for decades to compute design displacements and accelerations as well as base shears, they do not include the influences of strong motion duration, number of response cycles and yield excursions, stiffness and strength degradation or damage potential to structures. There is a need to re-examine the current analysis and design procedures, especially with the use of innovative protective systems such as seismic isolation and passive energy dissipation devices. In particular, the concept of

www.EngineeringBooksPDF.com

energy-based design is appealing where the focus is not so much on the lateral resistance of the structure but rather on the need to dissipate and/or reflect seismic energy imparted to the structure. In addition, energy approach is suitable for implementation within the framework of performance-based design since the premise behind the energy concept is that earthquake damage is related to the structure's ability to dissipate energy.

Housner was the first to recommend energy approach for earthquake-resistant design. He pointed out that ground motion transmits energy into the structure; some of this energy is dissipated through damping and nonlinear behaviour and the remainder stored in the structure in the form of kinetic and elastic strain energy. Housner approximated the input energy as one-half of the product of the mass and the square of the pseudo-velocity, $1/2\, m(\mathrm{PSV})^2$. His study provided the impetus for later developments of energy concepts in earthquake engineering.

For a nonlinear SDOF system with pre-yield frequency and damping ratio of ξ and respectively subjected to ground acceleration $\ddot{u}g = a(t)$, the equation of motion is given by

$$\ddot{x} + 2\zeta\dot{x} + F_S[X(t)] = -a(t) \tag{4.18}$$

where $F_s[x(t)]$ is the nonlinear restoring force per unit mass. Integrating (4.18) over the entire relative displacement history results in the following energy balance equation:

$$E_1 = E_k + E_D + E_S + E_H \tag{4.19}$$

where

$$E_1 = \text{Input energy} = \int_0^x a(t)dx = \int_0^1 a(t)\dot{x}dt \tag{4.20}$$

$$E_k = \text{Kinetic energy} = \int_0^x xdx = \frac{\dot{x}^2}{2} \tag{4.21}$$

$$\begin{aligned} E_D &= \text{Dissipative damping energy} \\ &= 2\beta\zeta \int_0^x \dot{x}dx = 2\zeta \int_0^t \dot{x}^2 dt \end{aligned} \tag{4.22}$$

$$\begin{aligned} E_S &= \text{Recoverable elastic strain energy} \\ &= \frac{F_S^2}{2\zeta^2} \end{aligned} \tag{4.23}$$

$$\begin{aligned} E_H &= \text{Dissipative plastic strain energy} \\ &= \int_0^x F_x dx - \frac{F_s^2}{2\omega^s} = \int_0^t F_s\dot{x}dt - \frac{F_S^2}{2\zeta^2} \end{aligned} \tag{4.24}$$

www.EngineeringBooksPDF.com

The energy terms in the above equations are given in energy per unit mass. Through the remainder of this section, the term "energy" refers to the energy per unit mass. The absolute energy terms E_D, E_S, and E_H are the same as their relative counterparts while the absolute input energy is given as $\int \ddot{X}_t \, dxg$ and the absolute kinetic energy is given as $\dot{x}_t^2/2$where x_t and x_g are the absolute and ground displacement, respectively. The absolute input energy represents the work done by the total base shear on the foundation displacement. The difference between the absolute and relative input and kinetic energies is given by

$$E_{I.\text{acs}} - E_{I.\text{rel}} =$$

$$E_{k.\text{abs}} - E_{k.\text{rel}} = \frac{\dot{x}_g^2}{2} + \dot{x}\dot{x}_g \tag{4.25}$$

Figure 4.38 shows energy time histories for a short-and a long-period elastic–-plastic structure using the relative and absolute energy terms. In addition, Uang and Bertero converted the input energy to an equivalent velocity such that

$$V_I = \sqrt{2E_I} \tag{4.26}$$

where E_I can be the relative or absolute input energy per unit mass. Figure 4.38 presents the relative and absolute input energy equivalent velocity spectra along with the peak ground velocity for three earthquake records. As the plots indicate, the relative and absolute input energies are very close for the mid-range periods (in the vicinity of predominant periods of ground motion). For longer and shorter periods, however, the difference between relative and absolute energies is significant.

4.6.5 Example 4.7 American Practice

For the collapse level, the earthquake spectral design requirements are the following:

$S_a = 0.60\,g$
$S_v = 21.5$ in/s
$S_d = 11.9$ in

Take 1 in = 25.4 mm

The elastic response spectrum for a 5% damped system ductility = 2%.
Correct the inelastic yield spectrum:

$$\text{Velocity region} = \frac{1}{\mu} = \frac{1}{2} = 0.5$$

$$\text{acceleration region} = \frac{1}{\sqrt{2\mu - 1}} = \frac{1}{\sqrt{4-1}} = 0.58$$

$$\text{displacement region} = \frac{1}{\mu} = \frac{1}{2} = 0.5$$

www.EngineeringBooksPDF.com

In summary

(1) $S_a(\text{inelastic}) = S_a(\text{elastic}) \times 0.58 = 0.348\,\text{g}$
Acceleration region
(2) $S_v(\text{inelastic}) = S_v(\text{elastic}) \times 0.5 = 10.75\,\text{in/s}$
Velocity region (0.273 m/s)
(3) $S_d(\text{inelastic}) = S_d(\text{elastic}) \times 0.5 = 5.95\,\text{in/s}$
Displacement region (0.151 m/s)
(4) The constant displacement line on three-way log paper. Draw the ground acceleration line on three-way log paper. Identify point on ground acceleration line corresponding to period of 0.03 s, i.e. point "a". Identify then point "b" on the constant acceleration line. Draw elastic spectrum similarly for 10% damping.

The plot and data are shown in Fig. 4.39.

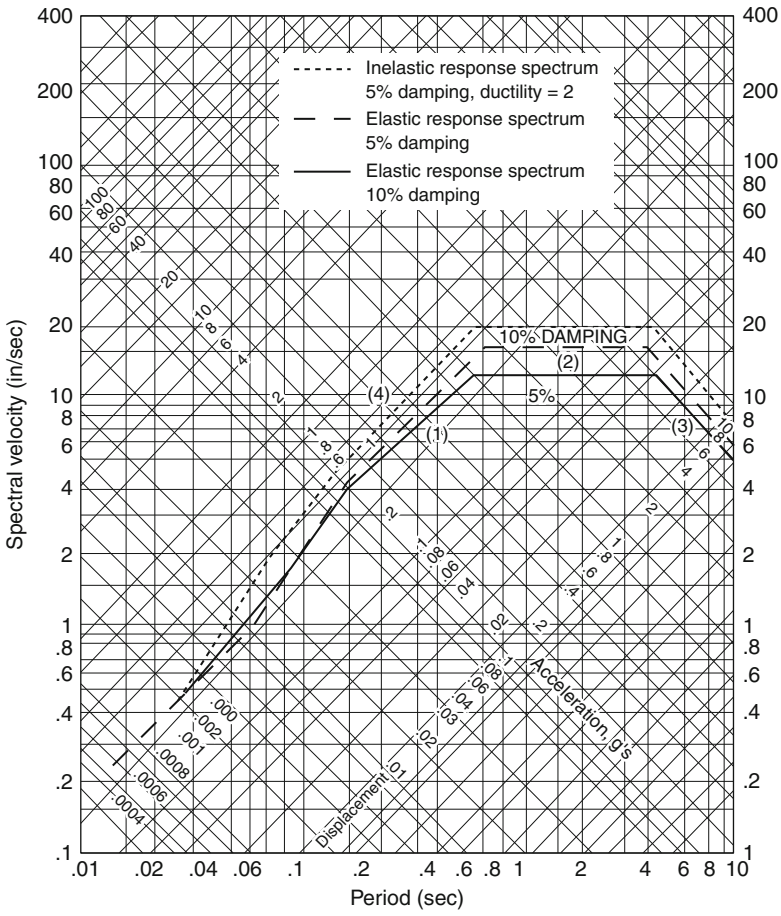


Fig. 4.39 Spectral velocity versus period

www.EngineeringBooksPDF.com

4.6.6 Example 4.8 American Practice

Using the following data and the Uniform Building Code (UBC) of the USA, design the beam–column connection and analyse the concrete ductile frame (Fig. 4.40) using UBC and ACI methods.

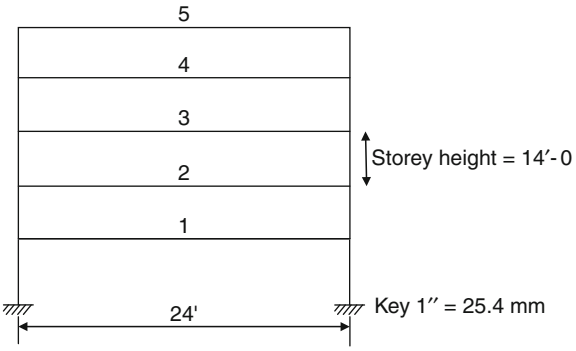


Fig. 4.40 Concrete ductile frame

Data
All beams 12 in × 28 in
All columns 16 in × 27 in
Working loads:

W_d = dead load = 70,000lbf
$f_c = 4,000\,\text{lbf/in}^2$
$f_y = 60,000\text{lbf/in}^2$
Z = zone 3 = 0.3
I(occupationfactor) = 1.25
C = seismic response = 1.0 for rock − like soil
R_w = system quality factor = 12 full ductile moment−resisting frames
$T = 0.15$ s

$$V = \left(\frac{\text{ZIC}}{R_w}\right) W \tag{4.27}$$

$$C = \frac{1.25}{(0.15)^{2/3}} = 4.43 > C = 2.75 \tag{4.28}$$

$$W = 5 \times W_s \tag{4.29}$$

If $T < 0.7$ s

F_t = horizontal force = 0

F_i = lateral earthquake forces in which

www.EngineeringBooksPDF.com

$$F_t = 0 \text{ at the } i\text{th level} = \left(\frac{W_i h_i}{\sum_{i=1}^{n} W_i h_i}\right) V \tag{4.30}$$

$$F_i = C_i V = 0.86 C_i W_s \tag{4.31}$$

Initial value to start with is

$$\sum_{i=1}^{n} = (1+2+3+4+5) W_s \quad (i = 5 \text{ at the topmost floor})$$

All floors need to be analysed for lateral forces, storey shears and storey moments.

Brief design notes and design formulae UBC and ACI

Relevant terms are

W_S = weight of one storey

R_W = system quality factor

W = total vertical weight of building = nW_S

S = site factor

C = seismic response = $(1.25/T)^3$

n = number of storeys

Step I

Determine earthquake zone, select UBC seismic coefficients Z,I,C,S,R_W. Determine period T by UBC method A or B.

Step II

Compute

$$V = \frac{ZIC}{R_W} W \quad \text{and} \quad V = F_t + \sum_{i=1}^{n} F_t \tag{4.32}$$

$F_t = 0$ when T = 0.7 s

$F_t = 0.97TC \leq 0.25\,V$

$T_n = C_t(hw)^{3/4}$

$C_t = 0.10\sqrt{AC}$

Step III

Tabulate base lateral force and each storey force F_i to F_n :

www.EngineeringBooksPDF.com

$$F_i = \frac{W_i h_i}{\sum_{i=1}^{n} W_i h_i} V \tag{4.33}$$

Find each storey shear and moment:

$$F_x = \frac{(V - F_i) W_n h_n}{\sum W h_i} \tag{4.34}$$

Step IV

Carry out a structural frame analysis to determine all shears and moments in the frame beams, columns and shear walls.

Step V

Revise where necessary the size and main reinforcement of the moment-resistant frame members: beams and beam–columns (beam–column when $P_{\mathrm{u}} > A_g f_c'/10$).

Step VI

Use strong column–weak beam concept, plastic hinges in beams and not columns: $\sum M_{\mathrm{col}\,\geq 6/5\mathrm{Mbm}}$ at joint.

Seismic beam shear forces:

$$\text{Beams}: \ \mathrm{V_L} = \frac{M^{-}_{\mathrm{prL}} + M^{+}_{\mathrm{prL}}}{t} + 0.75\frac{1.4D + 1.7L}{2} \tag{4.35}$$

$$V_{\mathrm{R}} = \frac{M^{+}_{\mathrm{prL}} + M^{-}_{\mathrm{prL}}}{l} - 0.75\frac{1.4D + 1.7L}{2} \tag{4.36}$$

Seismic column shear:

$$V_R = \frac{M_{\mathrm{prl}^4\mathrm{M}_{\mathrm{prz}}}}{h} \tag{4.37}$$

l = beam span

M_{prl} = probable moment of resistance

L = left, R = right } subscripts

h = column hight

$$\text{Hinges at beam } (\phi \mathrm{M_n}^{+} + \phi M_{\mathrm{n}}^{-})col \geq 6/5(\phi M_{\mathrm{n}}^{+} + \phi M_{\mathrm{n}}^{-})\mathrm{bm} \tag{4.38}$$

M_{n} = nominal moment strength

www.EngineeringBooksPDF.com

Step VII
Design longitudinal reinforcement.

(a) Beam–columns or columns:

$$0.01 \leq \rho_g \leq \frac{A_s}{A_g} \leq 0.06 \tag{4.39}$$

For practical considerations $\rho_g \leq 0.035$:

$$\rho_{\min} \leq \frac{200}{f_y} \geq \frac{3\sqrt{f'_c}}{f_c}(\text{for } +M) \geq \frac{6\sqrt{f'_c}}{f_y}(\text{for } -M) \tag{4.40}$$

(f_y is in lb/in^2 and $\rho \nrightarrow (0.025)$).

(b) Beams:

$$\begin{aligned} &M_n^+ \text{at joint face} \leq \frac{1}{2} M_n^- \text{at that face} \\ &M_{\text{n}}^+ \text{or } M_{\text{n}}^- \text{at any section } \geq \frac{1}{4} M_{\text{a, max}} \text{ at face} \end{aligned} \tag{4.41}$$

The above are material properties as adopted in Example 3.19.

Transverse confining reinforcement

(a) Spirals for columns:

$$\rho_s \geq \frac{0.12 f'_c}{f_{yh}} \quad \text{or} \quad \geq 0.45\left(\frac{A_g}{A_{ch}} - 1\right)\frac{f'_c}{f_{yh}} \tag{4.42}$$

whichever is greater.

(b) Hoop reinforcements for columns:

$$\begin{aligned} A_{\text{sh}} &\geq 0.09 s h_c \frac{f'_c}{f_{yh}} \\ &\geq 0.3 s h_c \left(\frac{A_g}{A_{ch}} - 1\right)\frac{f'_c}{f_{yh}} \end{aligned} \tag{4.43}$$

A_{g} = gross area
A_{ch} = core area to outside of spirals
h_{c} = column dimension

$s = \frac{1}{4}$ of smallest cross – sectional dimension or 4 in, whichever is smaller. Use standard tie spacing for the balance of the length where A_{sh} = area of transverse steel.

(c) Beams: Place hoop reinforcement over a length = $2h$ from face of columns. Maximum spacing: smaller of $s = \frac{1}{4}d, 8d_b$ main bar, $24d_b$ hoop or 12 m. If joint

www.EngineeringBooksPDF.com

confined on all four sides, 50% reduction in confining steel and increase in minimum spacing of ties to 6 in in columns is allowed. Use the standard size and spacing of stirrups for the balance of the span as needed for shear.

Beam–column connection (joint)

Available nominal shear strength ≥ applied V_u.

Confined on all faces:

$$V_n \leq 20\sqrt{f'_c}A_j \tag{4.44}$$

Confined on three faces or two opposite faces:

$$V_n \leq 15\sqrt{f'_c}A_j \tag{4.45}$$

All other cases:

$$V_n \leq 12\sqrt{f'_c}A_j \tag{4.46}$$

A_j = effective area at joint reduced by 25% for lightweight concrete. Horizontal shear is calculated if $1.25f_y$ applies for tensile reinforcement.

Development length, normal-weight concrete bar sizes #3 to 1 hooks the largest of

$$t_{dh} \geq f_y d_b / 65\sqrt{f'_c} \geq 8d_b \geq 6 \text{ in} \tag{4.47}$$

$$l_d = 2.5l_{dh} \text{ for 12 in or less concrete below straight bar}$$

$$l_d = 3.5l_{dh} \textit{ for} \geq 12\textit{in in one pour}$$

If bars have 90° hooks, $l_d = l_{dh}$. For lightweight concrete, adjust as in the ACI code. Bar designations and dimensions are given in Tables 4.7 and 4.8.

Design shear wall

$V_{uh} > 2A_{cv}\sqrt{f'c}$; use two reinforcement curtains in wall. If wall $f_c > 0.2f'_c$, provide boundary elements.

Available:

$$V_n = A_{cv}\left(\alpha_s\sqrt{f'_c} + \rho_n f_y\right) \tag{4.48}$$

$$\text{for } h_W/l_W \geq 2.0, \alpha_s = 2.0$$

$$\text{for } h_W/l_W = 1.5, \alpha_s = 3.0$$

Interpolate intermediate values of h_W/l_W.

Maximum allowance:

www.EngineeringBooksPDF.com

$$
\begin{aligned}
\upsilon_{\mathrm{n}} &= 8A_{\mathrm{cv}}\sqrt{f'_c} \quad \text{for total wall} \\
\upsilon &= 10A_{\mathrm{cp}}\sqrt{f'_c} \quad \text{for individual pier} \\
\rho_{\mathrm{v}} &= 0.0025 \\
A_{\mathrm{cv}} &= \text{net area of cross}-\text{section} \\
&= \text{thickness} \times \text{ length of section} \\
\phi &= 0.6 \\
V_{\mathrm{u}} &= \phi\, V_n \\
A_{\mathrm{cp}} &= \text{cross}-\text{sectional area of the individual pier}
\end{aligned}
\tag{4.49}
$$

Compressive strength:

$f'_c = 20\text{MPa}$
$f_{\mathrm{c}} = w_c^{1.5} 0.043\sqrt{f'_c}\text{MPa}$
$\phi = 0.9 \quad \text{for beam}$
$\phi = 0.07 \text{ or } 0.75 \text{ for columns}$

Design calculations

$$V = \frac{ZIC}{R_W} \quad (Z \text{ for zone } 3 = 0.3)$$
$R_W = 12$
$I = 1.25$
$$C = \frac{1.25}{T^{2/3}}$$
$S = 1.0$
$T = 0.7\,\text{s}$
$f_{\mathrm{t}} = 0$

Floor load (refer to Table 4.9)

$$W_{\mathrm{S}} = W_{\mathrm{D}} + W_{\mathrm{L}} = 70,000\,\text{lbf} + 80,000\,\text{lbf} = 150,000\,\text{lbf}$$

or

$$(31,383\,\text{kN}) + (359,467\,\text{kN}) = (673,297\,\text{kN})$$

Hence, base shear $V = 129{,}5851\text{bf}$.
The moment at each level is given in Table 4.9

www.EngineeringBooksPDF.com

Table 4.9 Data for loadings

Floor	C_i	$F = C_i W_s$ (ibf)	Storey shear (lbf)	Storey moment (lbf ft)
5	$C_5 = 5W_s/15W_s = 0.333$	45,960.0	0	0
4	$C_4 = 0.267$	36,850.8	45,960.0	643,440.0
3	$C_3 = 0.200$	27,603.6	82,800.0	1,802,640.0
2	$C_2 = 0.133$	18,356.4	110,400.0	3,348,240.0
1	$C_1 = 0.0066$	911.0	128,760.0	5,150,880.0
Base	$\delta = 0$	0	129,585.0	6,965,070.0

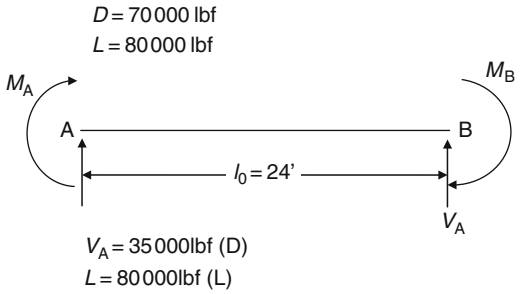


Fig. 4.41 Moment diagram for the design calculation

Seismic beam shear forces (Fig. 4.41)

$$V_L = \frac{M^-_{\text{prL}} + M^+_{\text{prR}}}{l_n} + 0.75\frac{1.4D + 1.7L}{2} = \frac{M_\text{A} + M_\text{B}}{l_\text{n}} + 0.75\frac{1.4D + 1.7L}{2} \tag{4.50}$$

Where l is the beam span and M_{pr} = probable moment of resistance. Now

$$V_L = \frac{M^+_{\text{prL}} + M_{\text{prR}}}{l} + 0.75\frac{1.4D + 1.7L}{2} \tag{4.51}$$

where L,R = left and right, respectively.

$$d = 27 - 2.5 = 24.5 \text{ in}$$

$$A_\text{s} = 4\,\text{in}^2$$

$$\rho = \frac{4}{12 \times 24.5} = 0.0136 < 0.025 \quad \text{(allowed by AC318)}$$

$$M_\text{n} = A_\text{s} f_\text{y}\left(d - \frac{a}{2}\right)$$

$$a = \frac{A_\text{s} f_\text{y}}{0.85 f'_\text{c} b} = \frac{4 \times 60,000}{0.85 \times 4,000 \times 12} = 5.9\text{in}$$

$$M_n = 4 \times 60,000\left(24.5 - \frac{5.9}{2}\right) = 5,172,000\,\text{lbf}$$

www.EngineeringBooksPDF.com

This value can be obtained from structural analysis of these frames. Hence

$$V_{\mathrm{L}} = \frac{5,172,000 + 5,172,000}{24 \times 12} + 0.75\left(\frac{1.4 \times 60,000 + 1.7 \times 75,000}{2}\right)$$

$$= 35,916.67 + 0.75\left(\frac{84,000 + 127,500}{2}\right)^2$$

$$= 35,916.67 + 79,312.5$$

$$= 115,229.171 \text{ bf}$$

$$V_{\mathrm{c}} = 2\sqrt{f'_c}\, b_w d = 2\sqrt{4,000} \times 12 \times 24.5 = 37,188.385\ 1 \text{ bf}$$

According to the ACI 318-95 code V_{c} can be zero under certain conditions. Now V_{n} at d_{n} from the face of the support (nominal shear strength)

$$= 115,229.17\left(\frac{12 - 28/12}{12}\right) = 92,826.\text{lbf}$$

$$V_{\mathrm{s}} = V_{\mathrm{n}} - V_c = 92,826.7 - 37,188.385 = 55,638.315\,\text{lbf}$$

$$V_{\mathrm{c}} = \text{seismic column shear force} = \frac{M_{\mathrm{pr1}} + M_{\mathrm{pr2}}}{h}$$

In the USA, generally the No. 4 (#4) hoop reinforcement is used:

#4 bar size, $A_{\mathrm{s}} = 0.2$ nominal diameter $= 0.375$ in

$$A_{\mathrm{v}} = 2 \times 0.2 = 0.40 \text{ in}^2$$

$$S = \frac{A_{\mathrm{v}} f_{\mathrm{v}} d}{V_{\mathrm{s}}} = \frac{0.40 \times 60,000 \times 24.5}{55,638.315} = 10.57 \text{ in}$$

Four closed hoops are placed at $10\frac{1}{2}$ in c/c on the critical section. When S is increased to

$$\frac{d}{2} = \frac{24.5}{2} = 12.25 \text{ in}$$

the code recommends curtailing stirrups at

$$\frac{V_{\mathrm{c}}}{2} = 18,594.193 \text{ lbf}$$

Confinement of reinforcement in the beam at the beam-column joint (Fig. 4.42) gives

www.EngineeringBooksPDF.com

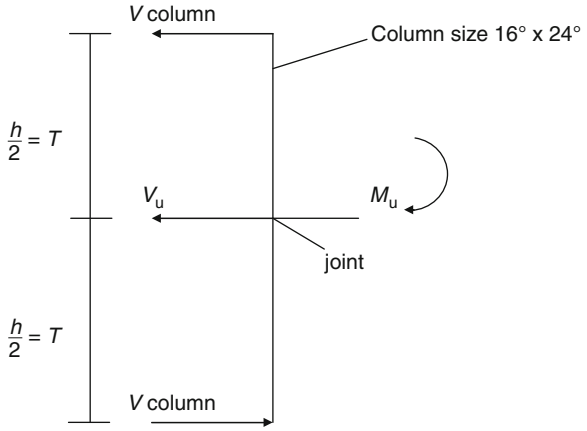


Fig. 4.42 Schematic of the beam-column joint

$$V_{\text{column}} = \frac{M_{\text{n}}}{(7+7)12} = \frac{5,172,000}{14 \times 12} = 30,785.714\,\text{lbf}$$

$$V_{\text{n}} \text{ at a joint} = A_{\text{s}} f_{\text{y}} - V_{\text{column}} = 4.0 \times 60,000 - 30,785.714 = 209,214.299\text{lbf}$$

V_{n} is allowable when $\leq 15\sqrt{f'_c} A_j$
where

$$A_{\text{j}} = \text{area at the joint} = 16 \times 24 = 384\text{in}^2$$

$$V_{\text{u}} = \text{allowable when } 0.85\left(15\sqrt{4,000} \times 384\right) = 309,650.23\text{lbf}$$

$$\text{actual } V_{\text{c}} = 129,585\text{lbf} \quad \text{(permitted)}$$

$$\text{column } d = 24 - 2.5 = 21.5\text{in}$$

$$V_{\text{c}} \text{ at the } A_{\text{j}} \text{ plane} = 2\sqrt{f'_{\text{c}}} \times 16 \times 21.5 = 2\sqrt{4,000} \times 16 \times 21.5 = 43,512.941\text{lbf}$$

$$V_{\text{c}} = \frac{V_{\text{u}}}{0.85} - V_c = \frac{309,650.23}{0.85} - 43,512.941 = 320,781.45\,\text{lbf}$$

$$S = \frac{A_v f_v d}{V_s} = \frac{0.4 \times 60,000 \times 21.5}{320781.45} \approx 0.643$$

www.EngineeringBooksPDF.com

Maximum allowable (Thus, nine # 4 bars)

$$S = d/4 = \frac{21.5}{4} = 5.375$$

Adopt 3 in {i.e. 4 in diameter}

$$8d_b = 8 \times \frac{9}{8} = 9 \text{ in}$$

$$d_b \times 24 = 24 \times \frac{1}{2} = 12 \text{ in (minimum)}$$

Thus, use four hoops plus two #4 cross-ties at 3 in c/c. The length of such hoops:

$$l_0 = 2h = 2 \times 28 = 56 \text{ in}$$

Reinforcement in the column at the beam-column joint
Whichever A_{sh} is greater should be adopted:

$$A_{sh} \geq 0.009 S h_c f'_c / f_{yh}$$

or

$$A_{sh} \geq 0.3 S h_c \left(\frac{A_{\text{g}}}{A_{\text{ch}}} - 1 \right) \frac{f'_{\text{c}}}{F_{\text{yh}}}$$

$$h_c = \text{column core}$$

$$= 24 - (2 \times 1.5 + 2 \times 0.5) = 20 \text{ in}$$

Try $S = 3$ in

$$A_{\text{sh}} = 0.09 \times 3 \times 20 \left(\frac{4000}{60,000} \right) = 0.36 \text{ in}^2$$

or

$$A_{\text{sh}} = 0.3 \times 3 \times 20 \left(\frac{16 \times 24}{11 \times 20} - 1 \right) \frac{4000}{60,000} 0.89 \text{ in}^2$$

Now, S (maximum allowable) $= \frac{1}{4} b = \frac{1}{4}$ small dimension or 4 in
$= \frac{1}{4} \times 16 = 4in$

Therefore, use #4 hoops at 3 in c/c and place the confining hoops in the column on both sides of the joint over a distance l_0 using the largest of

(a) depth of the member = 24 in
(b) $\frac{1}{6} \times$ clear span $= \frac{1}{6} \times 24 \times 12 = 48$ in
(c) 18 in

Thus, $l_0 = 48$ in; #4 hoops and cross-ties at 3 in c/c spacing (Fig. 4.43).

www.EngineeringBooksPDF.com

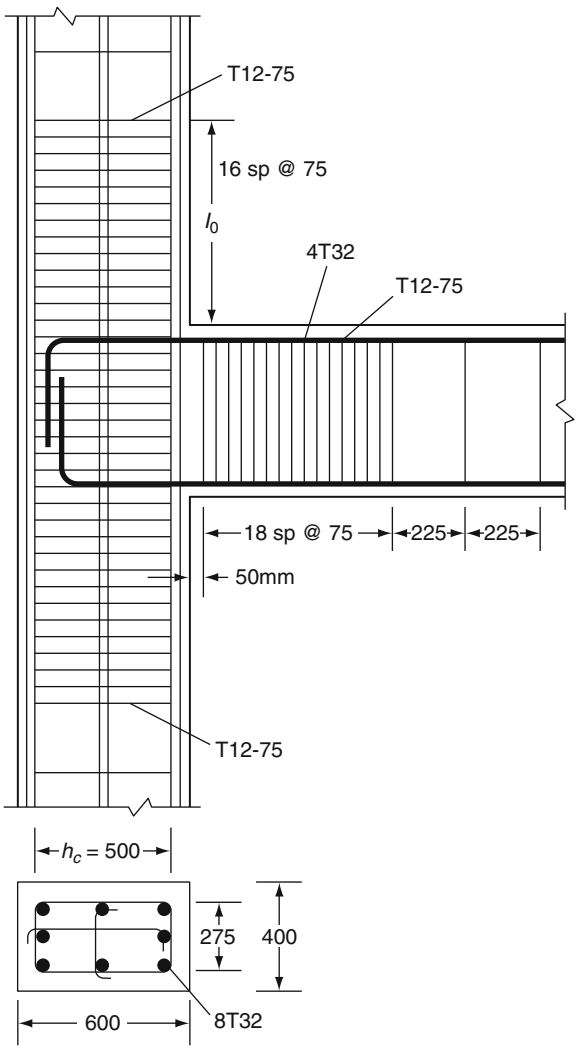


Fig. 4.43 Reinforcement in the column at the beam–column joint

4.6.7 Example 4.9 European Practice

The four-storey three-span concrete frame of a regular building is shown in Fig. 4.44. Adopting Eurocode 8 Parts 1–5 and the following data, design this frame for an earthquake environment.

Data

Concrete density (specific weight) $= 24kN/m^3$; concrete class C30

$E_{cm} =$ Young's modulus $= 30.5GPa\,(30.5 \times 10^6 kN/m^2)$

www.EngineeringBooksPDF.com

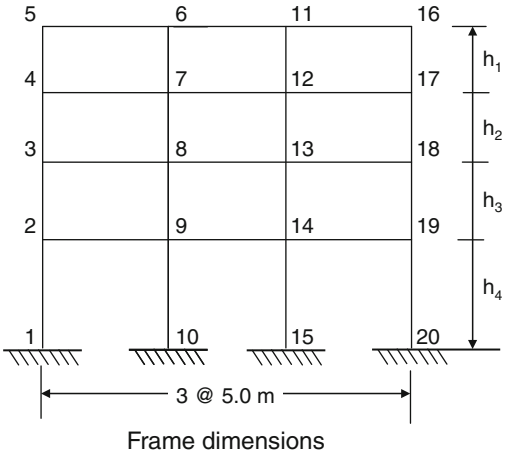


Fig. 4.44 Frame dimensions for Example 4.9

$$\text{v} = \text{Poisson}'\text{s ratio} = 0.2$$

$$f_{\text{ck}}/\gamma_c = \text{design compressive strength} = 30/1.5 = 20\ MPa\ (20MN/m^2)$$

$$T_{\text{Rd}} = \text{design shear strength} = 0.30\ MPa\ (0.3MN/m^2)$$

$$h_{\text{c}} = 3.0m$$

$$h_1 = 4.0m$$

All columns $1-2$ levels $= 500 \times 500$; all beams at $1-2$ levels $= 400 \times 400$.

All columns $2-3$ levels $= 500 \times 500$; all beams at $2-3$ levels $= 400 \times 400$.

All columns $3-4$ and $4-5$ levels $= 400 \times 400$.

All beams $3-4$ and $4-5$ levels $= 500 \times 500$.

Eurocode class
Steel class S400

$$f_{yd} = \text{design tensile strength} = f_{yk}/\gamma_s$$
$$= 400/1.15 = 348\ MPa\ (348\ MN/m^2)$$

Design loads

$$g = \text{dead load (floor, slabs, finishes, etc.)} = 6kN/m^2$$

$$G = 6kN/m^2 \times 5.0m = 30kN/m$$

www.EngineeringBooksPDF.com

Imposed or live loads

$$q_k = 2.0 kN/m^2$$

$$Q_k = 2 \times 5 = 10 kN/m$$

Design seismic action

Design response spectrum derived from

$$\delta_c(T) = I d_g s B_0 \left(\frac{T_B}{T}\right)^{K_{dt}} \frac{1}{q} \tag{4.52}$$

$I = 1.0$; $d_g = effective\ peak\ ground\ acceleration = 0.35\,g\ more\ than\ EI - Centro.$

$S = Site\ coefficient = 1.0$

$B_0 = amplification\ factor = 2.5$

$T_B = 0.4\,s$

$q = behavioural\ factor\ (Eurocode\ 8) = 3.5\ (assumed)$

$$\delta_e(T) = 1.0(0.35_g)(1.0)(2.5)\left(\frac{0.4}{T}\right)^{2/3}\left(\frac{1}{3.5}\right)$$

$$= 0.25_g\left(\frac{0.4}{T}\right)^{2/3} \quad (g \leq 0.25\,g)$$

Loads and inertial forces

$$\Sigma G_{kj} + \Sigma \psi_{Ei} Q_{ki} \tag{4.53}$$

$\psi_i = \psi_2 = 0.2$—the loads become quasi-static permanent live loads Q or $(30 + 0.2 \times 10) = 32$ kN/m

$$W_i/\text{floor} = 32(3 \times 5.0) = 480\,\text{KN}$$

Equal at all floors:

Floor $2 = 480 = W_2$
Floor $3 = 480 = W_2$
Floor $4 = 480 = W_2$
Floor $5 = 480 = W_2$

(Note that $h_i =$ interstorey height)

Seismic coefficient $= 0.25$

$$\gamma_i = \text{distribution factor} = h_i \frac{\Sigma W_i}{\Sigma W_i h_i} = h_i \frac{(1+1+1+1)W_i}{(4+7+10+13)W_i} = \frac{4}{34} h_i = 0.1176471 h_i \tag{4.54}$$

www.EngineeringBooksPDF.com

Horizontal forces at each level
The method has been demonstrated in other examples and the horizontal forces are computed (Fig. 4.45).

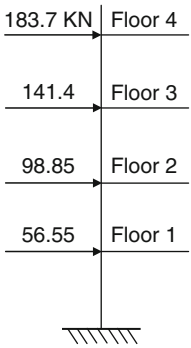


Fig. 4.45 Horizontal forces at each level of frame

Load combination for structural analysis
Eurocode 8 specifies at least two load combinations: (a) with the live load as the main variable action and (b) with the seismic load as the main action:

$$\left.\begin{array}{l}(a)\ S_{\mathrm{d}} = S(1.35G + 1.5Q_k) \\ (b)\ S_{\mathrm{d}} = S(G + \Sigma\psi_i Q_k + E)\end{array}\right\}\text{load combinations}$$

The frame has been analysed for these two loading cases using an IBM PC and the above data with the program STIFF. Design moments are based on the linear analysis of the building frame. Redistribution is permitted (see Fig. 4.46).

(A) Beams
From seismically considered situations, all beams shall be equally reinforced to cover 40 mm or 4 cm beams of 500×500.

$$M_{Rd} = \text{the ultimate bending moment at:}$$
$$\text{positive} = 240\text{kNm} > 145$$
$$\text{negative} = 355\text{kNm} \geq 265$$

See Table 4.10 for data.
Design shear forces
Conditions of static equilibrium at the beams subjected to vertical loads and end moments give design shear forces. The end moments must be from the actual reinforcement placed in beams. Eurocode 2 suggests the following beam analysis to evaluate moments and reactions. Each section at the end shall have two values of shear force – the maximum and the minimum value corresponding to positive and negative moments yielding at the hinges. The algebraic ratio between the maximum and the minimum values of the shear force at a section shall be denoted by "ζ". For the purposes of design the value of ζ shall not be taken as smaller than −1 (Fig. 4.47).

www.EngineeringBooksPDF.com

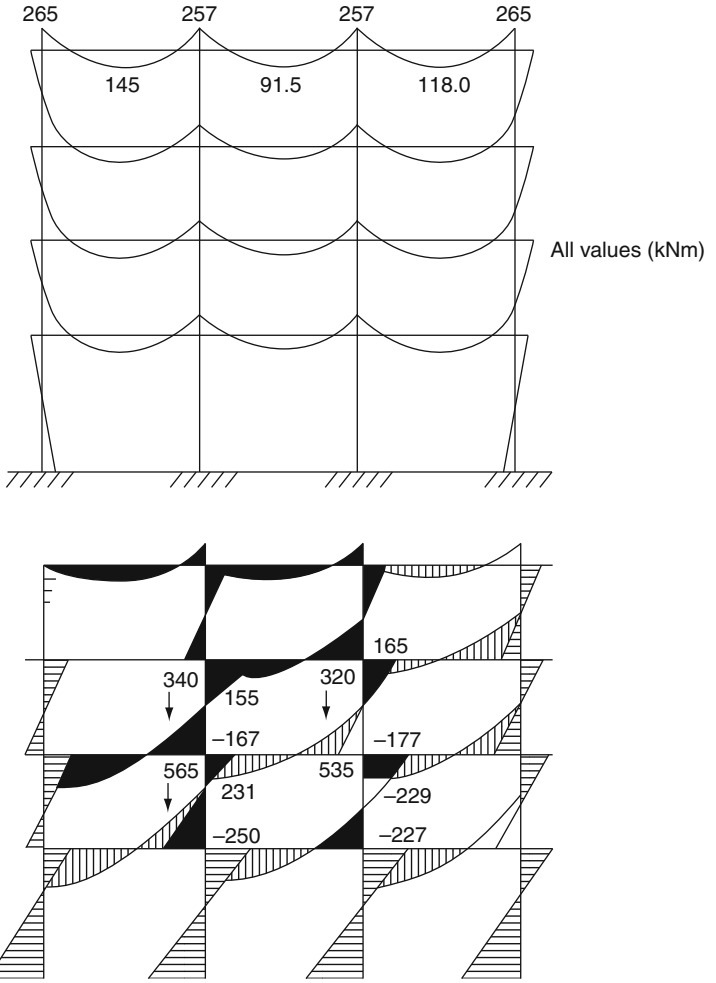


Fig. 4.46 Loading cases for structural analysis

Table 4.10 Beam loading

Main reinforcement	Eurocode	British code
At support	4 dia. 32 top	4T32
	3 dia. 25 bottom	3T25
At mid-span	2 dia. 32 top	2T32
	3 dia. 25 bottom	3T25

www.EngineeringBooksPDF.com

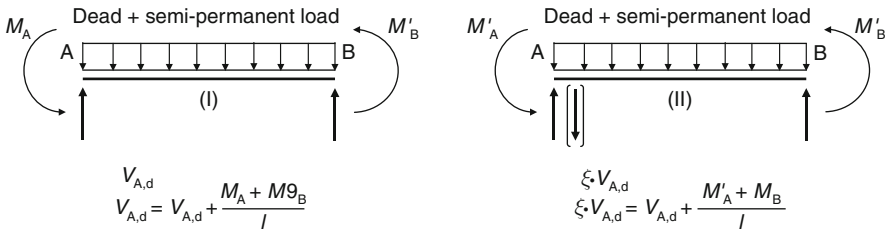


Fig. 4.47 Isolated moments and shears or reactions (Eurocode 2 requirements)

$$\omega \text{ or } \rho = 32\text{kN/m}$$

$$\begin{matrix} V_{i,\max} \\ V_{i,\min} \end{matrix} = 32 \times \frac{5}{2} \pm \frac{355 + 240}{5} = \begin{matrix} +199\text{kN} \\ -3.9\text{kN} \end{matrix}$$

$$\xi = \frac{-3.9}{199} = -0.0196 \approx 0$$

Resistance to shear (contribution of concrete) = 0
Vertical stirrups area

$$A_{\text{sw}} = \frac{V_{\max}}{0.9d}\left(\frac{1}{f_{\text{yd}}}\right)$$

$$= 13.83\text{cm}^2/\text{m} = 1383\text{mm}^2/\text{m}$$

Now:
2dia 10 − 125 A_{sw}=1,570mm^2/m (limited to a meter from the support)
(2T10 − 125) 2 legs of 10mm dia.

$$V_{\max} < V_{\text{Rdl}} = 6\tau_{\text{Rd}}.b_{\text{w}}.d = 6 \times 0.3 \times 500 \times 460 \times 10^{-3}$$

$$= 414\text{kN}$$

$$V_{\max} = 199\text{kN} < 414\text{kN} \quad \text{(permitted)}$$

(B) Columns

Critical columns are on the second and third floors, specifically the two at the centre. A reference is made to the loads and bending moment diagrams in Figs. 4.46 and 4.47 based on unfavourable combinations of loads. Only partially critical results are indicated from the linear structural analysis. For regular structures of three storeys or higher, the column moments due to the lateral forces alone shall be multiplied by a *dynamic magnification factor*.

For a planar frame such as this

$$\omega = 0.6T_1 + 0.85 \quad (1.2 \leq \omega \leq 1.8)$$

www.EngineeringBooksPDF.com

where T_1 is the fundamental period of the structure T_1 (Eurocode 8) is in the range of 0.4–0.6. Hence

$$\omega = 0.6(0.6) + 0.85 = 1.12 > 1.3$$

Therefore, $\omega = 1.3$ is retained.

Relative strength between columns and beams at joint
This requirement of Eurocode 8 is to be adhered to. Thus

$$\begin{aligned} M_b &= \text{sum of beam moments} = \left(M^+_{RD} + M^-_{RD}\right) \\ &= (240 + 355) = 595\text{kNm} \\ M_c &= \text{sum of column design moments} \\ &= 1.3(155 + 231) = 501.8\text{kNm} \end{aligned}$$

Reinforcement
Adverse combinations of axial force N and bending moment M can be adopted:
upper column

$$N = 320\text{kN}$$
$$M = 1.3 \times 177 = 230.1\text{kNm}$$

lower column

$$N = 565\text{kN}$$
$$M = 1.3 \times 227 = 295.1\text{kNm}$$

The section is therefore checked. Actual reinforcement provided in the section (avoiding traditional column calculations) is

8 dia. 25 and	12dia. 20	Eurocode
(8T25)	(12T20)	British standard
$A_s = 3,932\text{mm}^2$	$A_s = 3,760\text{mm}^2$	
Total $A_{s_{ToT}} = 7,692\text{mm}^2$		

The corresponding ultimate bending moments:
upper column

$$M_{Rd_u} = 265\text{kNm} > 230.1\text{kNm}$$

www.EngineeringBooksPDF.com

lower column

$$M_{\mathrm{Rd_L}} = 392\,\mathrm{kNm} > 295.1\,\mathrm{kNm}$$

Design shear forces
These are due to the contribution of the bending moments:
upper column

$$V = 1.3(167 + 177)/3 = 149.07\,\mathrm{kN}$$

lower column

$$V = 1.3(210 + 227)/3 = 189.37\,\mathrm{kN}$$

Shear resistance

$$N = 0.1 A_g f_{cd}$$

$$320 > 0.1 \times 0.4^2 \times 1670 = 26.72$$

$$535 > 0.1 \times 0.5^2 \times 1670 = 41.75$$

$$V_{cd} = 2\tau_{Rd} b_w d B_\ell$$

$$B_\ell = 1 + \frac{M_0}{M_d} \leq 2$$

$$M_0 = \text{decompression moment} = \frac{N_d}{A} W$$

$$M_d = \text{design moment}$$

Coefficient $B_\ell (1 \leq B_\ell \leq 2)$ takes into account the axial load.

Neglecting the reinforcement contribution the two cases are again considered as

upper column

$$B_\ell = 1 + \left(\frac{1}{M_{\mathrm{Rd_u}}} \times 320 \frac{0.4}{6} \right)$$

$$= 1 + \frac{1}{265} \times 320 \times \frac{0.4}{6} = 1.085 < 2$$

$$V_{cd} = 2 \times 300 \times 0.4^2 \times 1.085 = 104\,\mathrm{kN}$$

lower column

$$B_\ell = + \left(\frac{1}{M_{\mathrm{Rd_L}}} \times 535 \frac{0.5}{6} \right) = 1 + \frac{1}{392} \times 535 \times \frac{0.5}{6} = 1.114 \tag{4.55}$$

$$V_{cd} = 2 \times 300 \times 0.5^2 \times 1.114 = 167\,\mathrm{kN}$$

www.EngineeringBooksPDF.com

The shear force carried by the concrete is no different from the total shear force computed. Therefore, no change in reinforcement is needed.

Stability for a planar structure
The stability index is based on the secondary effects of storey shears and storey moments. Every floor condition has to be satisfied:

$$\theta = \frac{W\Delta_{el}q}{V_h} \leq 0.10 = \frac{\rho_{tot}dr}{V_{tot}h_i} \tag{4.56}$$

where

θ = deformability index⩾0.20

V = seismic design shear force across the storey

Δ_{el} = elastic interstorey drift due to actions

q = behaviour factor

h = floor height

W = vertical load above the storey in consideration ofθ⩾0.20

The above means that no inelastic analysis is needed for the $0.10 \leq \theta \leq 0.20$ elastic static approach; although conceptually inappropriate, it can provide extra strength:

$$W = 4 \times 480 = 1,920\text{kN}$$
$$q = 2.0$$
$$V = S_e(T_1)W = 0.27 \times 1920 = 518.4 \text{ kN}$$
$$h = 3\text{m or } 4\text{m}$$

Take $h = 3$m from the method given for the storey drift $\Delta_{el} = d\gamma = 0.006$:
$\theta = \frac{1920 \times 0.006 \times 2.0}{518.4 \times 3} = 0.0148148 \approx 0.014815 < 0.10$ (permitted)

With height h = 4m

$$\theta = \frac{3}{4} \times 0.014815 = 0.011 < 0.10 \quad \text{(permitted)}$$

Take the average:

$$\theta = \frac{0.14815 + 0.10}{2} = 0.013 < 0.10 \quad \text{(permitted)}$$

www.EngineeringBooksPDF.com

Thus

	$\Delta = \frac{0.010}{q} h(\mathrm{m})$	$\Delta_{el}(\mathrm{m})$
(1)	$= 0.010/2 \times 4.0 = 0.02$	0.006
(2)	$= 0.010/2 \times 3.0 = 0.015$	0.0055
(3)	0.015	0.0050
(4)	0.015	0.0040

The deformability condition is satisfied.

Note that for serviceability verification, the elastic drift Δ_{el} resulting from the application of horizontal forces or from the dynamic action shall at any storey satisfy the condition

$$\Delta_{el} \leq \frac{0.010}{q} \times h \tag{4.57}$$

For certain buildings, the indicated limits may be increased by 50% where significant damage is expected. Where the limits are exceeded separation of non-structural elements occurs. To take the drift without restraint

$$\Delta = 0.35\Delta_{el} \cdot q$$

Therefore,

$$\Delta = 0.35 \times 0.006 \times 2.0 = 0.0042\,\mathrm{m}$$

Maximum limit established by Eurocode 8 is

$$\begin{aligned} \Delta_{max} &= \frac{0.025}{q} h \\ &= \frac{0.025}{2.0} \times 3 = 0.0375\,\mathrm{m} \end{aligned} \tag{4.58}$$

or

$$\frac{0.025}{2.0} \times 4 = 0.05\,\mathrm{m} \quad (\text{this value adopted})$$

The values in the previous table are correct and do not exceed Δ_{max}.

Tensile reinforcement shall not be less than

$$\frac{1.4}{f_{yk}} \nrightarrow \frac{7}{f_{yk}} = \frac{1.4}{400} = 0.0035 \nrightarrow 0.006 \quad (\text{permitted})$$

The final structural details for Example 4.10 are given in Fig. 4.48

www.EngineeringBooksPDF.com

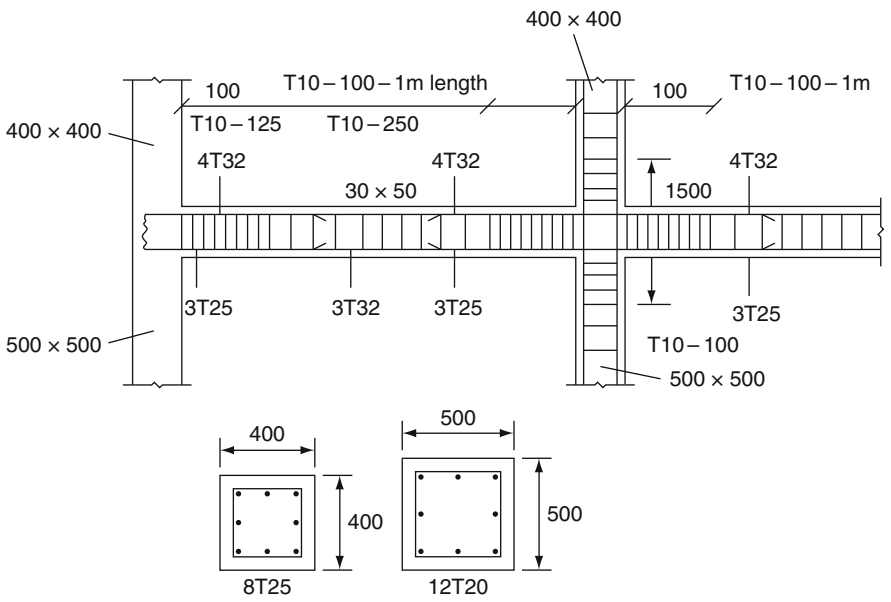


Fig. 4.48 Final structure details

4.6.8 Example 4.10 British Practice

For the response–time history using direct integration, the equation for the dynamic equilibrium, ignoring initial damping, is

$$\frac{M\delta^2 y}{\delta t^2} + Ky = F(t) \tag{4.59}$$

where M is the mass, K is the structure stiffness and $F(t)$ is the time-dependent force. Develop the direct integratio7n procedure that is generally met in

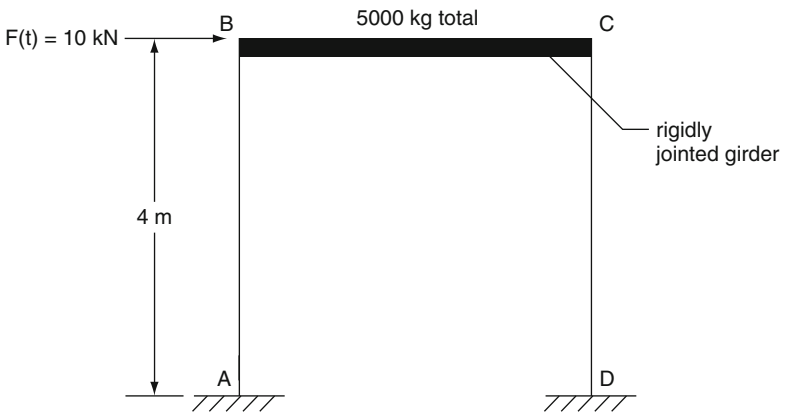


Fig. 4.49 Response analysis of a portal frame

www.EngineeringBooksPDF.com

earthquake analysis. A two-dimensional rigidly jointed steel frame with rigid support provides a single portal frame of 4 m height (Fig. 4.49). The horizontal girder to the two vertical members is infinitely stiff and carries a distributed mass of 500 kg. At the girder level an earthquake force of 10kN for 3 s exists. Using the following data, develop the response–time history for this frame:

I = second moment of area = $2 \times 10^3 \text{cm}^4$

E = Young's modulus for steel = 200 kN/mm^2

Initial time step = 0.015 s

c = damping of 10%

Construct the response of this portal over a period of 3 s indicating factors relating to frequency and amplitude of the dynamic response:

$$\frac{\delta^2 y}{\delta t^2}(\text{average acceleration at time } t=0) = \frac{\delta y/\delta t_{t=0.5} - \delta y/\delta t_{t=-0.5}}{\Delta t} \tag{4.60}$$

$$\frac{\delta y}{\delta t}(\text{average velocity at } t=+0.5) = \frac{y_{t=1} - y_{t=0}}{\Delta t} \tag{4.61}$$

$$\frac{\delta y}{\delta t}(\text{average velocity at } t=-0.5) = \frac{y_{t=0} - y_{t=-1}}{\Delta t} \tag{4.62}$$

$$\frac{\delta^2 y}{\delta t_{t=0}^2} = \frac{y_{t=1} - 2y_{t=0} + y_{t=-1}}{(\Delta t)^2} \tag{4.63}$$

At general time $t = \tau$. Hence

$$M\frac{y_{\tau+1} - 2y_\tau + y_{\tau-1}}{(\Delta t)^2} + Ky_\tau = F(t) \tag{4.64}$$

where y_τ = amplitude of displacement at $t = \tau$ and similarly others in the forward difference equations. For example, at time $t = \tau + 1$

$$y_{\tau+1} = y_\tau\left[2 - \frac{K(\Delta t)^2}{M}\right] - y_{\tau-1} + F(t)_\tau\left[\frac{(\Delta t)^2}{M}\right]^2 \tag{4.65}$$

Now

$$T = \text{natural period} = 2\pi\sqrt{\frac{M}{K}} \tag{4.66}$$

In order to calculate displacement at $t = +1$ one must obtain $y_{t=-1}$. One has to know the initial velocity $\delta y/\delta t = 0$, which is

$$\frac{y_{t=+1} - y_{t=-1}}{2\Delta t} \tag{4.67}$$

www.EngineeringBooksPDF.com

or

$$y_{t=-1} = y_{t=+1} - 2\Delta t \frac{\delta y}{\delta t_{t=0}} \tag{4.68}$$

The starting equation by making $\tau - 0$ becomes

$$y_1 = y_0 \left[\frac{2 - K(\Delta t)^2}{M}\right] - \left[y_1 - 2\Delta t \frac{\delta y}{\delta t_0}\right] + F(t)_0 \left[\frac{(\Delta t)^2}{M}\right] \tag{4.69}$$

By including damping $c = 10\%$, i.e. $c(\delta y/\delta t)$ in the generalized equation, then

$$M\frac{\delta^2 y}{\delta t^2} + c\frac{\delta y}{\delta t} + Ky = F(t)$$

Equation (4.69) becomes

$$y_{\tau+1}\left[1 + \frac{c\Delta t}{2\,M}\right] = y_\tau \left[2 - \frac{K(\Delta t)^2}{M}\right] - y_{\tau-1}\left[1 - \frac{c\Delta t}{2\,M}\right] + F(t)_\tau \left[\frac{(\Delta t)^2}{M}\right] \tag{4.70}$$

$y_{\tau+1}$ is computed from (4.70):

$$K(2\,\text{columns}) = \frac{2 \times 12EI}{L} = 1.5 \times 10^6 \text{ Nm}$$

$$T = 2\pi\sqrt{\frac{M}{K}} = 2\pi\sqrt{\frac{5000}{1.5 \times 10^6}} = 0.3635\,\text{s}$$

When $c = 10\%$, the maximum time-step interval $= 0.036 \approx 0.04$ s. The value of $\Delta t = 0.015$s is acceptable. $y_{\tau+1}$ is given by

$$y_{\tau+1} = \frac{y_\tau(1.9325) - y_{\tau-1}(0.974) + 4.5 \times 10^{-4} F(t)}{1.026}$$

For the initial case

$$y_1 = \frac{0 + 0 + 4.5 \times 10^{-4}}{2} = 2.25 \times 10^{-4}\text{m}$$

$$y_2 = \frac{2.25 \times 10^{-4}(1.9325) - 0 \times 0.974 + 4.5 \times 10^{-4}}{1.026} = 0.0008624\text{m}$$

$$y_3 = \frac{0.0008624(1.9325) - 2.25 \times 10^{-4} \times 0.974 + 4.5 \times 10^{-4}}{1.026}$$

$$= 0.0018493\text{m}$$

$$y_4 = \frac{0.0018493 \times 1.9325 - 0.0008624 + 4.5 \times 10^{-4}}{1.026} = 0.0031198\text{m}$$

www.EngineeringBooksPDF.com

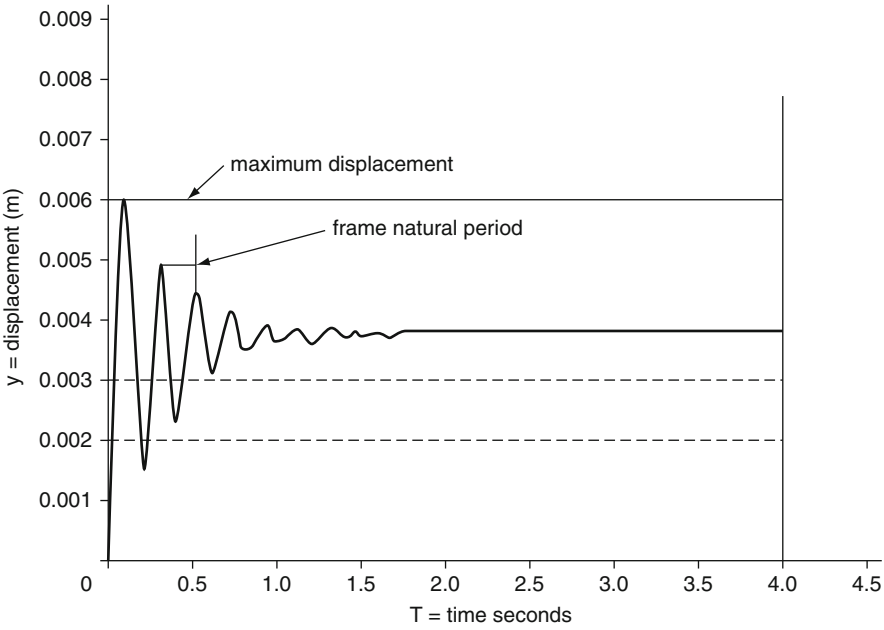


Fig. 4.50 Displacement– time relationship

These calculations are continued for other values of y. Figure 4.50 shows the cyclic nature of the response. The period of vibration is the same as the natural period of this frame. With damping of 10%, the displacement will have a static value reaching up to 4 s.

4.6.9 Yield Strength and Deformation from the Response Spectrum (American Practice)

Given the excitation of the El-Centro ground motion and the properties T_n and ζ of an SDF system, it is desired to determine the yield strength for the system consistent with a ductility factor μ. Corresponding to T_n, ζ and μ the value of A_y/g is read from the spectrum of Fig. 4.51 or 4.52. The desired yield strength can be obtained which is strength f_y. An equation for the peak deformation can be derived in terms of A_y as follows:

$$u_m = \mu u_y \tag{4.71}$$

where

$$u_y = \frac{f_y}{k} = \left(\frac{T_n}{2\pi}\right)^2 A_y \tag{4.72}$$

www.EngineeringBooksPDF.com

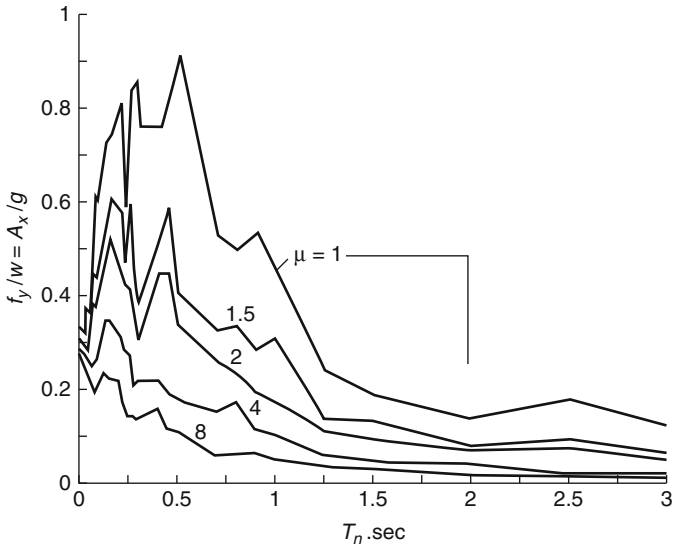


Fig. 4.51 Constant-ductility response spectrum for elasto-plastic systems and El-Centro ground motion

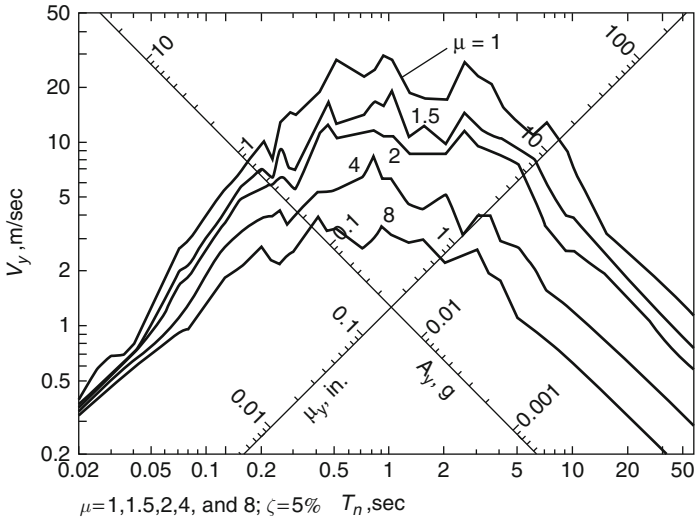


Fig. 4.52 Constant-ductility response spectrum for elasto-plastic systems and El-Centro ground motion

Putting (4.71) and (4.72) together gives the following equation:

$$u_m = \mu \left(\frac{T_n}{2\pi} \right)^2 A_y \tag{4.73}$$

www.EngineeringBooksPDF.com

Example 4.11 American Practice

Data $T_n = 0.5\,s$

Damping $\zeta = 5\%$

Ductility $\mu = 4$

Using Figs. 4.51 and 4.52 for the El-Centro ground motion, calculate the yield strength and deformation from the response spectrum or elasto-plastic system shown in the figures.

$A_y/g = 0.1789$

$$f_y = \text{the yield strength of an elasto-plastic system} = KU_y = m(w_n^2 u_y)$$
$$= mA_y = A_y/g = 0.1789w$$

where w = weight of the system

A = pseudo-acceleration response spectrum for linearly elastic systems

$$U_y = \frac{f_y}{k}\left(\frac{T_n}{2\pi}\right)^2 A_y = \left(\frac{0.5}{2\pi}\right)^2 \{0.179\,g\} \quad g = 386$$
$$= 0.437\,\text{in}(11.1\ \text{mm})$$
$$U_m = 4 \times 0.437 \approx 1.749\ \text{in}(44.5\ \text{mm})$$

4.7 Equivalent Static Force Method Based on Eurocode-8

4.7.1 General Introduction

Equivalent static response spectrum method and time history method are accepted by EC8 in order to evaluate seismic forces while treating at the same time the building which is symmetrical in elevation and plan.

One of the plan frame is taken as an example and shall be assumed moment-resisting rigid frame.

4.7.2 Evaluation of Lumped Masses to Various Floor Levels

Step 1 Lumped mass evaluation

(a) Roof: Mass of infill + mass of columns + mass of beams longitudinally and transversely of the floor + mass of slab + imposed load or action on roof wherever possible

(b) Mass of floor: Masses of all floors: seismic weight of each floor = full dead load + imposed load. Any weight supported between storeys

(c) Imposed loads or actions

(d) Total seismic weight of the building: $m = m_1 + m_2 + m_3 + \cdots$

www.EngineeringBooksPDF.com

Step 2 Determination of natural period

$$\text{For steel } C_t = 0.08$$
$$\text{For concrete } C_t = 0.075$$
$$T = C_t H^3/4$$

Step 3 Determination of design base shear V_B

$$V_B = a_g \zeta B_0 W \tag{4.74}$$

$$\text{and } V_B = A_R M(9.81) \leftarrow \text{for} T \rightarrow \frac{S_a}{G} = \frac{1}{T} \tag{4.75}$$

where $S = 1.0$

Soilsite : $B_0 = 2.5$

$\zeta = 0.1$

$a_g = 0.1\,g$ As an example, they may vary based on EC8

$$\begin{aligned} \text{Rocksite} : V_B = A_R W &= \frac{z}{2} I/R \frac{S_a}{g}(W) \\ &= \frac{z}{2} I/R \frac{S_a}{g}(M \times 9.81) \end{aligned} \tag{4.76}$$

Step 4 Vertical distribution of base shear
The design base shear (V_B) computed shall be distributed along the height of the building as per the expression

$$Q_i = V_B \frac{W_i H_i^2}{\sum_{i=1}^{n} W_i H_i^2} \tag{4.77}$$

where
Q_i = Design lateral forces at floor i
W_i = Seismic weights of the floor i
H_i = Height of the floor i, measured from base, and
n = Number of stories

The base shear force distribution can be determined as

$$Q_{1=V_1}\left(\frac{W_1 H_1^2}{W_1 H_1^2 + W_2 H_2^2 + W_3 H_3^2 + W_4 H_4^2}\right) \tag{4.78}$$

www.EngineeringBooksPDF.com

4.7.3 Response Spectrum Method

A: Frame without considering the stiffness of infills
A step-by-step procedure for analysis of the frame by response spectrum method is as follows.

4.7.3.1 Step 1: Determination of Eigenvalues and Eigenvectors

Mass matrix, M, and stiffness matrix, K, of the plane frame lumped mass model are

$$[M] = \begin{bmatrix} M_1 & 0 & 0 & 0 \\ 0 & M_2 & 0 & 0 \\ 0 & 0 & M_3 & 0 \\ 0 & 0 & 0 & M_4 \end{bmatrix}_{n \times n} \tag{4.79}$$

Note: The terms in a matrix can be of $n \times n$ terms ($n = 4$ as an example)
Column Stiffness of Storey

$$K = \frac{12EI}{L^3} \tag{4.80}$$

The lateral stiffness of each storey

$$k_1, k_2, k_3, \ldots, k_n \tag{4.81}$$

Stiffness of lumped mass modelled as

$$k = \begin{bmatrix} k_1 + k_1 & -k_2 & 0 & 0 \\ -k_2 & k_2 + k_3 & -k_3 & 0 \\ 0 & -k_3 & k_3 + k_4 & -k_4 \\ 0 & 0 & -k_4 & k_4 \end{bmatrix} \tag{4.82}$$

$n = 4$ for a case
The stiffness, mass matrices, eigenvalues and eigenvectors are

$$|K - \omega^2 m| = \begin{vmatrix} 2k - \omega^2 M & -k_2 & 0 & 0 \\ -k_2 & 2k - \omega^2 M & -k_3 & 0 \\ 0 & -k_2 & 2k - \omega^2 M & -k_3 \\ 0 & 0 & -k_4 & k - \omega^2 0.575M \end{vmatrix}_{n \times n} \tag{4.83}$$

$$= 0$$

www.EngineeringBooksPDF.com

where $\omega_n = \sqrt{K/m}$

$$(\omega_n^2)^4 - 8.3(\omega_n^2)(\omega^2) + 10.75(\omega^2)^2 - 4.45(\omega_n^2)(\omega^2)^3 + 0.575(\omega^2)^4 = 0 \quad (4.83a)$$

By solving the above equation, natural frequencies (eigen values) of various modes are eigenvalues

$$[\omega^2]_n = \begin{bmatrix} \omega_1^2 & & & \\ & \omega_2^2 & & \\ & & \omega_3^2 & \\ & & & \ddots .\omega_n^2 \end{bmatrix}_n \quad (4.84)$$

The quantity of ω_i^2 is called the ith eigenvalue of the matrix $\left[-M\omega_i^2 + K\right]\Phi_i$. Each natural frequency (ω_i) of the system has a corresponding eigenvector (mode shape), which is denoted by Φ_i. The mode shape corresponding to each natural frequency is determined from the equations

$$\begin{aligned} \left[-M\omega_1^2 + K\right]\Phi_1 &= 0 \\ \left[-M\omega_2^2 + K\right]\Phi_2 &= 0 \\ \left[-M\omega_3^2 + K\right]\Phi_3 &= 0 \\ \left[-M\omega_4^2 + K\right]\Phi_4 &= 0 \\ \vdots \quad & \quad \vdots \end{aligned} \quad (4.85)$$

$$\left[-M\omega_n^2 + K\right]\Phi_n = 0 \quad (4.85a)$$

4.7.3.2 Step 2: Determination of Modal Participation Factors

The modal participation factor of mode k is

$$\Gamma_k = \frac{\Sigma_{i=1}^n w_i \Phi_{ik}}{\Sigma_{i=1}^n w_i (\Phi_{ik})^2} \quad (4.86)$$

$$\Gamma_1 = \frac{\Sigma_{i=1}^4 W_i \Phi_{i1}}{\Sigma_{i=1}^4 W_i (\Phi_{i1})^2} = \frac{(W_1\Phi_{11} + W_2\Phi_{21} + W_3\Phi_{31} + W_4\Phi_{41})}{W_1(\Phi_{11})^2 + W_2(\Phi_{21})^2 + W_3(\Phi_{31})^2 + W_4(\Phi_{41})^2} \quad (4.87)$$

$$\Gamma_2 = \frac{\Sigma_{i=1}^4 W_i \Phi_{i2}}{\Sigma_{i=1}^4 W_i (\Phi_{i2})^2} = \frac{(W_1\Phi_{12} + W_2\Phi_{22} + W_3\Phi_{32} + W_4\Phi_{42})}{W_1(\Phi_{12})^2 + W_2(\Phi_{22})^2 + W_3(\Phi_{32})^2 + W_4(\Phi_{42})^2} \quad (4.88)$$

Similarly goes for $\Gamma_3 \ldots \Gamma_n$ (4.89)

www.EngineeringBooksPDF.com

where

g = Acceleration due to gravity,
Φ_{ik} = Mode shape coefficient at floor i in mode k, and
W_i = Seismic weight of floor i.

4.7.3.3 Step 3: Modal Masses

$$M_1 = \frac{\left[\Sigma_{i=1}^{4} W_i \Phi_{i1}\right]^2}{g\left[\Sigma_{i=1}^{4} W_i (\Phi_{i1})^2\right]} \tag{4.90}$$

Similarly for others up to nth mass M_n
Modal contributions of various modes

$$\begin{aligned} &\text{For model 1} = \frac{M_1}{M} \\ &\vdots \\ &\text{For model } n = \frac{M_n}{M} \end{aligned} \tag{4.91}$$

4.7.3.4 Step 4: Determination of Lateral Force at Each Floor in Each Mode

Q_{ik} = design lateral force at floor "i" in mode "k" is given by

$$A_k \Phi_{ik} \Gamma_k W_i \tag{4.92}$$

where A_k = design horizontal acceleration spectrum value using the natural period of vibration "T_k" of mode "k"

The design horizontal seismic coefficient for various modes are

$$A_{Rk} = \frac{Z}{2}\frac{I}{R}\frac{S_{ak}}{g} \quad \text{if it is rock} \tag{4.93}$$

Or if soil: $a_g S \zeta B_0$

4.7.3.5 Step 5: Determination of Storey Shear Forces in Each Mode

The peak shear force is given by

$$V_{ik} = \sum_{l=i+1}^{n} Q_{lk} \tag{4.94}$$

4.7.3.6 Step 6: Determination of Storey Shear Force due to All Modes

The peak shear force V_i in storey "i" due to all modes is obtained by combining those due to each mode in accordance with

www.EngineeringBooksPDF.com

(a) modal combination SRSS (square root of sum of squeares);
(b) complete quadratic combination (CQC) method.

If the building has no closely spaced modes, the peak response quality (λ) due to all modes considered shall be obtained as

$$\lambda = \sqrt{\Sigma_{k=1}^{r}(\lambda_k)^2} \tag{4.95}$$

where λ = absolute value of quantity in mode "k" and r is the number of modes under consideration.

Complete quadratic combination (CQC)

$$\lambda = \sqrt{\Sigma_{i=1}^{r}\Sigma_{i=1}^{r}(\lambda_k)^2} \tag{4.96}$$

where

r = Number of modes being considered,
P_{ij} = Cross-modal coefficient,
λ_i = Response quantity in mode i (including sign),
λ_j = Response quantity in mode j (including sign).

$$p_{ij} = \frac{8\zeta^2(1+\beta_{ij})\beta^{1.5}}{(1+\beta_{ij})^2 + 4\zeta^2\beta_{ij}(1+\beta_{ij})^2} \tag{4.97}$$

where

ζ = Modal damping ratio (in fraction),
β_{ij} = Frequency ratio ω_j/ω_i,
ω_i = Circular frequency in ith mode, and
ω_j = Circular frequency in jth mode.

Therefore, all the frequency ratios and cross-modal components can be presented in matrix form as

$$\beta_{ij} = \begin{bmatrix} \beta_{11} & \beta_{12} & \beta_{13} & \beta_{14} \\ \beta_{21} & \beta_{22} & \beta_{23} & \beta_{24} \\ \beta_{31} & \beta_{32} & \beta_{33} & \beta_{34} \\ \beta_{41} & \beta_{42} & \beta_{43} & \beta_{44} \\ \vdots & & & \vdots \\ \beta_{j1} & \beta_{j2} & \beta_{j3} & \beta_{j4} \end{bmatrix} = \begin{bmatrix} \omega_1/\omega_1 & \omega_2/\omega_1 & \omega_3/\omega_1 & \omega_4/\omega_1 \\ \omega_1/\omega_2 & \omega_2/\omega_2 & \omega_3/\omega_2 & \omega_4/\omega_2 \\ \omega_1/\omega_3 & \omega_2/\omega_3 & \omega_3/\omega_3 & \omega_4/\omega_3 \\ \omega_1/\omega_4 & \omega_2/\omega_4 & \omega_3/\omega_4 & \omega_4/\omega_4 \\ \omega_1/\omega_j & \cdots & \cdots & \omega_4/\omega_j \end{bmatrix} \tag{4.98}$$

$$\beta_{ij} = \begin{bmatrix} \beta_{11} & \cdots & \beta_{1j} \\ \vdots & & \vdots \\ \beta_{j1} & & \beta_{jj} \end{bmatrix} \tag{4.99}$$

www.EngineeringBooksPDF.com

4.7.3.7 Step 7 Determination of Lateral Forces at Each Storey

The design lateral forces Q_{roof} and Q_{i} at roof and the ith floor respectively, are given by

$$Q_{\text{roof}} = V_{\text{roof}} \quad Q_i = V_i - V_{j1} \tag{4.100}$$

SRSS Method

$$\begin{aligned} Q_{\text{roof}} &= V_n \\ Q_{\text{roof}} &= Q_{n-1} - Q_n \end{aligned} \tag{4.101}$$

CQC Method

$$Q_{\text{roof}} = Q_n = V_n \tag{4.102}$$

And then roof levels

$$Q_{n-1} - Q_n$$

Frame: Considering the stiffness of infills follow from column stiffness to the end procedures except here the stiffness of the infills is modelled as an equivalent diagonal strut in which the strut

$$B_{WS} = \frac{1}{2}\sqrt{\alpha_R^2 + \alpha_{L^1}^2} \tag{4.103}$$

where α_{R} and α_{L} are.

$$\alpha_{\text{R}} = \frac{\pi}{x}\left[\frac{E_f I_C H_1}{2E_m t \sin\ 2\theta}\right]^{1/4};\ \alpha_{\text{L}}\pi\left[\frac{E_f I_b l}{E_m t \sin\ 2\theta}\right]^{1/4} \tag{4.104}$$

where

$$\theta = \tan^{-1} H_1/l$$

where

E_{f} = Elastic modulus of the material of the frame
E_{m} = Elastic modulus of the masonry infill or wall
t = Thickness of the infill wall
H_1 = Height of the infill wall
l = Length of the infill wall
I_c = Moment of inertia of the column
B_{ws} = Width
l_{d} = Diagonal length of the strut = $\sqrt{H_1^2 + l^2}$

$$\text{Stiffness of the infill } = \frac{AE}{ld} m \cos^2\theta \tag{4.105}$$

www.EngineeringBooksPDF.com

4.7.4 Example 4.12 Step-by-Step Design Analysis Based on EC8

Case Study: The elevation and partial plan of a four-storey building frame in reinforced concrete is shown in Fig. 4.53.

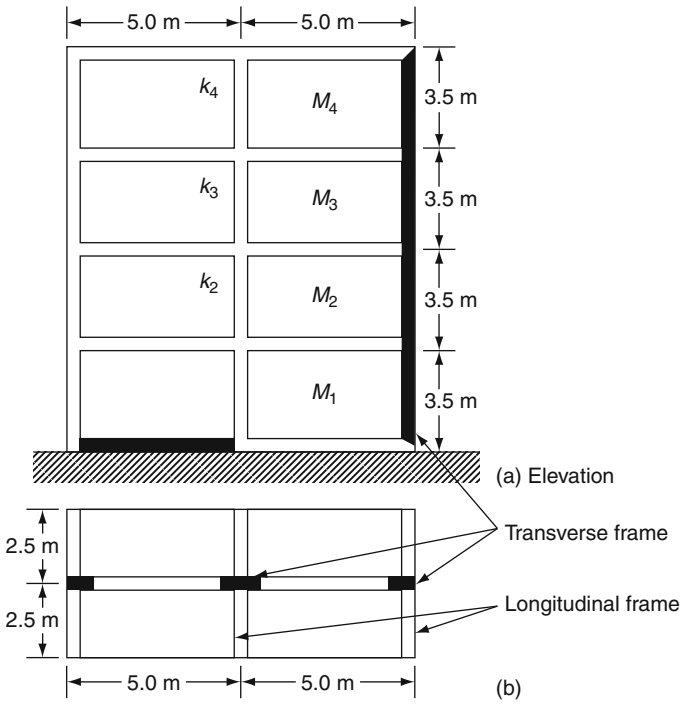


Fig. 4.53 Four-storey building

4.1 One plan frame needs to be analysed by equivalent static method and response spectrum method Analysis with and without infill wall.

Data: Seismic zone

No of storeys = 4
Floor height = 3.5 m; Total height H = 14 m
Infill wall: Longitudinal thickness = 250 mm
Transverse thickness = 150 mm
Action = 3.5 kN/m^2
Material C25 concrete; steel reinforcement Fe 130; $E_c = 22.36 \times 10^6$ kN/m^2
Beam size: Longitudinal: 450 × 250 mm throughout
Transverse: 350 × 250 mm throughout
Depth of slab: 100 mm

www.EngineeringBooksPDF.com

Column size: 450 × 250 mm
Intensity of infill = 250 kN/m^3

Earthquake forces shall be calculated for the fill dead load + percentage of imposed load. The roof imposed load shall be assumed as zero. The lumped masses are given in Step 2.

Step 1 Calculated values of lumped masses

Roof: Mass of infill of wall + mass of columns + mass of beams longitudinal and transverse direction of that floor + slab mass + imposed or action zero = 37,087 kg (363.82 kN)

First, second and third floors each = 64450 kg
With 50% imposed load for load greater than 3 kN/m^2
Check for soil and rock zones based on EC8

E_f = Elastic modulus of the material = 22,360 N/m^2
E_m = Elastic modulus of the masonry wall = 13,800 N/m^2
t = Thickness of the infill wall = 250 mm
H_1 = Height of the infill wall = 3.5 m
l = Length of the infill wall = 5.0 m

(A) Equivalent Static Method
Step 1 Seismic weight of the building

$$= M_1 + M_2 + M_3 + M_4$$
$$= 64,450 + 64,450 + 64,450 + 37,087 = 230,437 \text{ kg}$$

Step 2 Determination of natural period T

For concrete based on EC8 $C_4 = 0.075$; $H = 14$ m
From equivalent (4.74)

$$T = C_t H^{3/4} = 0.5423\text{s}$$

Step 3 Determination of design base shear for soil type

$$A_R = a_g S\zeta = 0.007$$

$$\text{Design base} V_B = a_g S\zeta B_0 W = 0.1(1.0)(0.7) = 0.007 B_0 W$$
$$= 0.007 \times 2.5 \times 230,437\text{kg}$$
$$= 40,326.475\text{kg}$$
$$= 395.4662 \text{ kN} \quad \text{Adopted}$$

www.EngineeringBooksPDF.com

Equation (4.75)
For rock

$$A_R = \frac{z\,1\,S_a}{2R\,g} = \frac{0.241}{2\quad 5}1.842$$

$$V_B = A_R W = 101.713\,\text{kN}$$

Step 4 Vertical distribution of base shear

$V_0 =$ Equation (4.77) is considered which takes the form of (4.78).
Equation (4.78) is solved
Load diagram values

$Q_1 = 17.040\,\text{kN}$	$V_1 = 156.882\,\text{kN}$
$Q_2 = 68.178\,\text{kN}$	$V_2 = 310.256\,\text{kN}$
$Q_3 = 153.124\,\text{kN}$	$V_3 = 378.417\,\text{kN}$
$Q_4 = 156.882\,\text{kN}$	$V_4 = 395.466\,\text{kN};\ V_B = 395.466\,\text{kN}$

Step 1 Determination of eigenvalues and eigenvectors

Mass matrix, evoking (4.79)

$$[M]_{4\times 4} = \begin{bmatrix} M_1 = 64,450 & & & \\ & M_2 = 64,450 & & \\ & & M_3 = 64,450 & \\ & & & M_4 = 37,087 \end{bmatrix} (\text{kN})$$

$$\text{Column stiffness} = \frac{12EJ}{L^3} = \frac{12(2,236\times 10^3)\left[\frac{0.25\times 0.3}{12}\right]}{(3.5)^3}$$

$$= 11,880.78\,\text{kN/m}$$

Each storey lateral stiffness

$$K_1 = K_2 = K_3 = K_4 = 3(11,880.78)$$

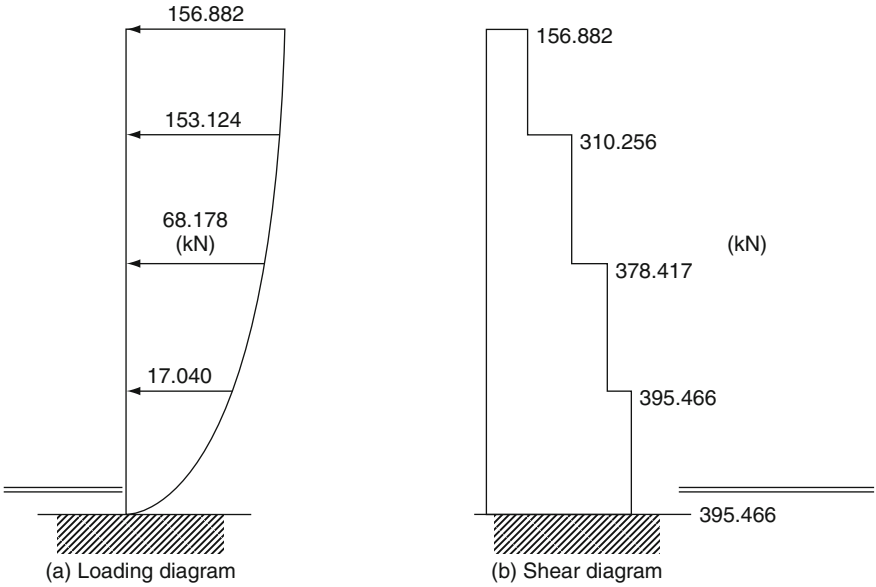
$$= 35,642.36\,\text{kN/m}$$

$$M_1 = M_2 = M_3, \text{etc.} 64218\,\text{kN} = 64,450$$

$$M_4 \rightarrow 37,087\,\text{kg} = 363.82\,\text{kN}$$

The stiffness of the lumped mass model is derived which is given below:

www.EngineeringBooksPDF.com



$$= \begin{bmatrix} 71,284.72 & -3,564.36 & 0 & 0 \\ -3,564.36 & 71,284.72 & -3564.36 & 0 \\ 0 & -3,564.36 & 71,284.72 & -3,564.36 \\ 0 & 0 & -3,564.36 & 3,564.36 \end{bmatrix} \text{kN/m}$$

The stiffness, mass matrices, eigenvalues and eigenvectors are calculated from (4.83). Solving this equation, eigenvalues, modal eigenvectors, mode shapes and natural periods under different modes are evaluated. The eigenvectors $\{\Phi\}$ are given as

$$\{\Phi\} = \{\Phi_1 \Phi_2 \Phi_3 \Phi_4\} = \begin{bmatrix} -0.0328 & 0.0795 & 0.0808 & -0.0397 \\ -0.0608 & 0.0644 & -0.0540 & 0.0690 \\ -0.0798 & -0.0273 & -0.0448 & -0.0799 \\ -0.0872 & -0.0865 & 0.0839 & 0.0696 \end{bmatrix}$$

$$(\omega_n^2)^4 - 8.3(\omega_n^2)^3 + 10.75(\omega_n^2)^2(\omega^2)^2 - 4.45(\omega_n^2)(\omega^2)^3 + 0.575(\omega^2)^4 = 0$$

Natural time period

$$T = \begin{bmatrix} 0.6977 & 0 & 0 & 0 \\ 0 & 0.2450 & 0 & 0 \\ 0 & 0 & 0.1636 & 0 \\ 0 & 0 & 0 & 0.1388 \end{bmatrix} \text{s}$$

www.EngineeringBooksPDF.com

Invoking (4.84)

$$[\omega^2]_n = \text{Eigenvalues} = \begin{bmatrix} \omega_1^2 & & & \\ & \omega_2^2 & & \\ & & \ddots & \\ & & & \omega_n^2 \end{bmatrix}_n$$

Equations (4.85) $[-M\omega_1^2 + K]\Phi_i$ are solved

Step 2 Equations (4.86), (4.87), (4.88) and (4.89) are solved for participation factors

$$\Gamma_1 = -14.40; \Gamma_2 = 4.30; \Gamma_3 = 1.95; \Gamma_4 = -0.68$$

Step 3 Determination of modal mass

The modal mass (M_k) of mode k is given by

$$M_k = \frac{\left[\Sigma_{i=1}^n W_i \Phi_{ik}\right]^2}{g\left[\Sigma_{i=1}^n W_i (\Phi_{ik})^2\right]}$$

$$M_1 = 207.60; M_2 = 18.54;\ M_3 = 3.82;\ M_4 = 0.47$$

Modal contributions of various modes

Mode 1 $\frac{M_1}{M} = 0.90\ (90\%)$

Mode 2 $\frac{M2}{M} = 0.0805\ (8.04\%)$

Mode 3 $\frac{M3}{M} = 0.0165\ (1.65\%)$

Mode 4 $\frac{M4}{M} = 0.002\ (0.2\%)$

Step 4 Determination of lateral force at each floor in each mode

$$Q_{ik} = A_k \Phi_{ik} \Gamma_k W_i \qquad \text{at floor } "i" \text{ in mode} "k"$$

where A_k = Design horizontal acceleration spectrum using the natural period of variation of mode "k"

Invoking (4.76)

$$A_{h1} = 0.343;\ A_{h2} = 0.060; A_{h3} = 0.060 = A_{hk}$$

For hard soil site → the code gives actual relations. The following are one specific relations chosen. They may vary for actual hard soil/rock cases.

www.EngineeringBooksPDF.com

$$\frac{S_a}{g} = \begin{cases} 1 + 1.5T; & 0.00 \le T \le 0.10 \\ 2.5; & 0.10 \le T \le 0.40 \\ 1.00/T; & 0.40 \le T \le 4.0 \end{cases}$$

$$\text{For } T_1 = 0.6978 \Rightarrow \frac{S_{a1}}{g} = 1.433$$

$$\text{For } T_2 = 0.2450 \Rightarrow \frac{S_{a2}}{g} = 2.5$$

$$\text{For } T_3 = 0.1636 \Rightarrow \frac{S_{a3}}{g} = 2.5$$

$$\text{For } T_4 = 0.1382 \Rightarrow \frac{S_{a4}}{g} = 2.5$$

Design lateral force in each mode

$$Q_{i1} = (A_1 \Gamma_i \phi_{i1} W_i)$$

$$[Q_{i1}] = \begin{bmatrix} (A_{h1}\Gamma_1\phi_{11}W_1) \\ (A_{h1}\Gamma_2\phi_{21}W_2) \\ (A_{h1}\Gamma_3\phi_{31}W_3) \\ (A_{h1}\Gamma_4\phi_{41}W_4) \end{bmatrix} = \begin{bmatrix} ((0.0343)(-14.40)(-0.0328)(64.45 \times 9.81)) \\ ((0.0343)(-14.40)(-0.0608)(64.45 \times 9.81)) \\ ((0.0343)(-14.40)(-0.0798)(64.45 \times 9.81)) \\ ((0.0343)(-14.40)(-0.0872)(37.08 \times 9.81)) \end{bmatrix}$$

$$= \begin{bmatrix} (10.275) \\ (19.043) \\ (25.018) \\ (15.720) \end{bmatrix} = \text{kN}$$

Similarly,

$$[Q_{i2}] = \begin{bmatrix} -43.44 \\ -35.199 \\ 14.920 \\ 27.207 \end{bmatrix}, \; [Q_{i3}] = \begin{bmatrix} -44.204 \\ 29.499 \\ 24.517 \\ -26.385 \end{bmatrix}, \; [Q_{i4}] = \begin{bmatrix} 21.749 \\ -37.722 \\ 43.675 \\ -21.878 \end{bmatrix}$$

www.EngineeringBooksPDF.com

Step 5 Determination of storey shear forces in each mode
The peak shear force is given by (4.94)

$$V_{i1} = \sum_{j=i+1}^{n} Q_{ik}$$

$$V_{i1} = \begin{bmatrix} V_{11} \\ V_{21} \\ V_{31} \\ V_{41} \end{bmatrix} \begin{bmatrix} (Q_{11} + Q_{21} + Q_{31} + Q_{41}) \\ (Q_{21} + Q_{31} + Q_{41}) \\ (Q_{31} + Q_{41}) \\ (Q_{41}) \end{bmatrix} = \begin{bmatrix} 70.056 \\ 59.781 \\ 40.738 \\ 15.720 \end{bmatrix} \text{kN}$$

Similarly,

$$V_{i2} = \begin{bmatrix} V_{12} \\ V_{22} \\ V_{32} \\ V_{42} \end{bmatrix} = \begin{bmatrix} -36.514 \\ 6.927 \\ 42.127 \\ 27.207 \end{bmatrix}, \; V_{i3} = \begin{bmatrix} V_{13} \\ V_{23} \\ V_{33} \\ V_{43} \end{bmatrix} = \begin{bmatrix} -16.572 \\ 27.632 \\ -1.867 \\ -26.385 \end{bmatrix},$$

$$V_{i4} = \begin{bmatrix} V_{14} \\ V_{24} \\ V_{34} \\ V_{44} \end{bmatrix} = \begin{bmatrix} 5.824 \\ -15.925 \\ 21.796 \\ -21.878 \end{bmatrix}$$

Step 6 Determination of storey shear force due to all modes

The peak storey shear force (V_i) in storey i due to all modes considered is obtained by combining those due to each mode in accordance with modal combination, i.e. SRSS (square root of sum of squares) or CQC (complete quadratic combination) method.

SRSS (square root of sum of squares)
If the building does not have closely spaced modes, the peak response quantity (λ) due to all modes considered shall be obtained as (4.95)

$$\lambda = \sqrt{\sum_{k=1}^{r} (\lambda_k)^2}$$

www.EngineeringBooksPDF.com

Using the above method, the storey shears are

$$\begin{aligned}
V_1 &= [(V_{11})^2+(V_{12})^2+(V_{13})^2+(V_{14})^2]^{\frac{1}{2}} \\
&= [(70.056)^2+(-36.154)^2+(-16.572)^2+(5.824)^2]^{\frac{1}{2}} = 80.930\,\text{kN} \\
V_2 &= [(V_{21})^2+(V_{22})^2+(V_{23})^2+(V_{24})^2]^{\frac{1}{2}} \\
&= [(59.781)^2+(6.927)^2+(27.632)^2+(5.824)^2]^{\frac{1}{2}} = 68.110\,\text{kN} \\
V_3 &= [(V_{31})^2+(V_{32})^2+(V_{33})^2+(V_{34})^2]^{\frac{1}{2}} \\
&= [(40.738)^2+(42.127)^2+(-1.867)^2+(21.796)^2]^{\frac{1}{2}} = 62.553\,\text{kN} \\
V_4 &= [(V_{41})^2+(V_{42})^2+(V_{43})^2+(V_{44})^2]^{\frac{1}{2}} \\
&= [(15.7202)^2+(27.207)^2+(-26.385)^2+(-21.878)^2]^{\frac{1}{2}} = 48.11\,\text{kN}
\end{aligned}$$

Similarly, using Eqs. (4.96), (4.97), (4.98) and (4.99), the CQC method yields the following results:

$$V_1 = 80.71;\ V_2 = 66.62;\ V_3 = 62.96;\ V_4 = 48.49$$

while keeping in mind

$$\beta_{ij} = \begin{bmatrix} \beta_{11} & \beta_{12} & \beta_{13} & \beta_{14} \\ \beta_{21} & \beta_{22} & \beta_{23} & \beta_{24} \\ \beta_{31} & \beta_{32} & \beta_{33} & \beta_{34} \\ \beta_{41} & \beta_{42} & \beta_{43} & \beta_{44} \end{bmatrix} = \begin{bmatrix} 1 & 0.0073 & 0.0031 & 0.0023 \\ 0.0073 & 1 & 0.0559 & 0.0278 \\ 0.0031 & 0.0559 & 1 & 0.2597 \\ 0.0023 & 0.0278 & 0.2597 & 1 \end{bmatrix}$$

Step 7 Determination of lateral forces at each storey

The design lateral forces Q_{roof} and Q_{i}, at roof and at ith floor, respectively, are calculated as

$$Q_{roof} = Q_i \text{ and } Q_i = V_i - V_{i+1}$$

Square root of sum of squares (SRSS)

$$\begin{aligned}
Q_{\text{roof}} &= Q_4 = V_4 = 46.499\,\text{kN} \\
Q_{\text{floor3}} &= Q_3 = V_3 - V_4 = 62.553 - 48.11 = 14.44\,\text{kN} \\
Q_{\text{floor1}} &= F_1 = V_1 - V_2 = 80.930 - 68.11 = 12.820\,\text{kN}
\end{aligned}$$

www.EngineeringBooksPDF.com

Complete quadratic combination (CQC)

$$Q_{\text{roof}} = F_4 = V_4 = 48.48 - 0 = 48.48\,\text{kN}$$
$$Q_{\text{roof3}} = F_3 = V_3 - V_4 = 62.95 - 48.48 = 14.47\,\text{kN}$$
$$Q_{\text{roof2}} = F_2 = V_2 - V_3 = 66.61 - 62.95 = 3.66\,\text{kN}$$
$$Q_{\text{roof1}} = F_1 = V_1 - V_2 = 80.70 - 66.61 = 14.09\,\text{kN}$$

Frame considering the stiffness of infills

The frame considered in the previous section is again analysed by considering the stiffness of infill walls. The infill is modeled as an equivalent diagonal strut.

All the above are still adopted except that the stiffness of the infill is included. Equations (4.103), (4.104) and (4.105) are utilized.

$$I_c = \text{Moment of inertia of columns} = \frac{1}{12}(0.25 \times 0.45^3) = 0.001893\,\text{m}^4$$
$$I_c = \text{Moment of inertia of columns} = \frac{1}{12}(0.25 \times 0.40^3) = 0.001333\,\text{m}^4$$
$$\alpha_h = \frac{\pi}{2}\left[\frac{22,360 \times 0.001893 \times 3.5}{2 \times 13,800 \times 0.25 \times \sin 2 \times 35}\right]^{1/4} = 0.611\,m$$
$$\alpha_l = \pi\left[\frac{22,360 \times 0.001333 \times 5.0}{13,800 \times 0.25 \times \sin 2 \times 35}\right]^{1/4} = 1.45\,m$$
$$B_{ws} = \frac{1}{2}\sqrt{\alpha_h^2 + \alpha_l^2} = 0.7885\,\text{m}$$
$$A = \text{Cross} - \text{sectional area of diagonal stiffness}$$
$$= B_{ws} \times t = 0.7885 \times 0.25 = 0.1972\,\text{m}^2$$
$$I_d = \text{Diagonal length of strut} = \sqrt{H_1^2 + l^2} = 6.103\ \text{m}$$

Therefore, stiffness of infill is

$$\frac{AE_m}{l_d}\cos^2\theta = \frac{0.1972 \times 13,800 \times 10^6}{6.103}0.819^2 = 299,086.078 \times 10^3\,\text{N/m}$$

For the frame with two bays there are two struts participating in one direction, total lateral stiffness of each storey

$$k_1 = k_2 = k_3 = k_4 = 3 \times 11,846.758 + 2 \times 299,086,078 = 633,712.430$$

www.EngineeringBooksPDF.com

Similarly the quadratic equations are formed as above:

$$\omega_1^2 = 1,442;\ \omega_2^2 = 11,698;\ \omega_3^2 = 26,227;\ \omega_4^2 = 36,719 \quad \text{are the eigenvalues.}$$

Eigenvectors Φ are of matrix form adopted, the natural frequency $[\omega]$ in rad/s is formulated.

Using the time period T matrix above, the modal participation factors are computed:

$$\Gamma_1 = 14.40;\ \Gamma_2 = 4.30;\ \Gamma_3 = 1.95;\ \Gamma_4 = -0.68$$

Similarly the modal masses are evaluated. The new values will be

$$M_1 = 207.60;\ M_2 = 18.54;\ M_3 = 3.82;\ M_4 = 0.47$$

In a similar manner the modal mass contributions are the same

$$\text{Mode 1} = \frac{M_1}{M} = 0.90\ (90\%);\ \text{Mode 2} = \frac{M_2}{M} = 8.04\%$$
$$\text{Mode 3} = \frac{M_3}{M} = 0.0165\ (1.65\%);\ \text{Mode 4} = \frac{M_4}{M} = 0.002\ (0.2\%)$$

Design force (lateral) at each floor in each member is the same

$$Q_{ik} = A_k \Phi_{ik} \Gamma_k W_i$$
$$T_1 = 2.5, T_2 = 1.871, T_3 = 1.581, T_4 = 1.491$$

S_{ag}

$$Q_{i1} = \begin{bmatrix} 1.7922 \\ 33.215 \\ 43.637 \\ 27.419 \end{bmatrix}; Q_{i2} = \begin{bmatrix} -32.511 \\ -26.342 \\ 11.167 \\ 20.360 \end{bmatrix} \text{(kN)}$$

$$\mathrm{Q_{i3}} = \begin{bmatrix} 1.7922 \\ 33.215 \\ 43.637 \\ 27.419 \end{bmatrix}; Q_{i4} = \begin{bmatrix} 1.7922 \\ 33.215 \\ 43.637 \\ 27.419 \end{bmatrix} \text{(kN)}$$

Hence the shear forces for the first mode (kN)

www.EngineeringBooksPDF.com

$$V_{i1} = \begin{bmatrix} V_{11} = 122.144 \\ V_{21} = 104.271 \\ V_{31} = 71.056 \\ V_{41} = 27.418 \end{bmatrix}; V_{i2} = \begin{bmatrix} V_{12} = -27.326 \\ V_{22} = 5.183 \\ V_{32} = 31.527 \\ V_{42} = 20.360 \end{bmatrix};$$

$$V_{i3} = \begin{bmatrix} V_{13} = -10.486 \\ V_{23} = 17.486 \\ V_{33} = -1.181 \\ V_{43} = -16.695 \end{bmatrix}; V_{i4} = \begin{bmatrix} V_{14} = 3.476 \\ V_{24} = -4.5041 \\ V_{34} = 13.007 \\ V_{44} = -13.056 \end{bmatrix}$$

Strong shear force due to all modes is similarly determined
(B) *Shear FORCE : Summary*

$$V_1 = 125.698\,\text{kN}$$
$$V_2 = 106.280\,\text{kN}$$
$$V_3 = 78.826\,\text{kN}$$
$$V_4 = 40.195\,\text{kN}$$

(C) *Summary of SRSS and CQC*
Following the above procedure based on SRSS and CQC methods, the following results have been summarized:

SRSS

$$Q_{\text{roof}} = Q_4 = V_4 = 40.195\,\text{kN}$$
$$Q_{\text{floor3}} = Q_3 = V_3 - V_4 = 38.630\,\text{kN}$$
$$Q_{\text{floor2}} = Q_2 = V_2 - V_3 = 27.453\,\text{kN}$$
$$Q_{\text{floor1}} = Q_1 = V_1 - V_2 = 19.418\,\text{kN}$$

CQC

40.961 kN
38.161 kN
26.852 kN
19.535 kN

www.EngineeringBooksPDF.com

www.EngineeringBooksPDF.com

Chapter 5
Dynamic Finite Element Analysis of Structures

5.1 Introduction

Because of the large number of computer runs required for dynamic analysis, it is very important that accurate and numerically efficient methods be used within computer programs. These methods have been described adequately. Equation of motion for various structures with seismic devices is given. Their functions are identified when various solution procedures are used. Some of the solution procedures popularly adopted by various resea rches are explained. A complete finite element procedure is given which can easily be linked to typical dynamic analysis chosen for a specific case study. These analyses are generally adopted by many well-known finite element computer packages. The analysis given has the flexibility to be adopted in any new package in the offing. Computer subroutines can be developed to link the main finite element analysis package with the performance of specific seismic devices. Many computerized finite element packages have such facilities. The purpose of this chapter is to give credit to the power of finite element in the use of earthquake-resistant structures.

Part A: Analysis with solution procedures

Dynamic Elastic Analysis with and without Seismic Devices

5.2 Dynamic Equilibrium

5.2.1 Lumped Mass system

The force equilibrium of a multi-degree-of-freedom lumped mass system as a function of time can be expressed by the following equation:

$$f(t)_1 + f(t)_D + f(t)_s = f(t) \tag{5.1}$$

in which the force vectors at time t are

$f(t)_1$ is a vector of inertia forces acting on the node masses
$f(t)_D$ is a vector of viscous damping forces

M.Y.H. Bangash, *Earthquake Resistant Buildings*,
DOI 10.1007/978-3-540-93818-7_5, © M.Y.H. Bangash 2011

www.EngineeringBooksPDF.com

$f(t)_S$ is a vector of forces carried by the structure
$f(t)$ is a vector of externally applied loads

Equation (5.1) is valid for both linear and non-linear systems if equilibrium is formulated with respect to the deformed geometry of the structure.
For linear analysis, Equation (5.1) can be written, in terms of nodal displacements, in the following form:

$$M_s\ddot{u}(t)_a + C\dot{u}(t)_a + K_s(t) = f(t) \tag{5.2}$$

in which M_s is the mass matrix (lumped or consistent), C is a viscous damping matrix (which is normally selected to approximate energy dissipation in the real structure) and K_s is the static stiffness matrix for the system of structural elements. The time-dependent vectors $u(t)_a, \dot{u}(t)_a$and $\ddot{u}(t)_a$ are the absolute nodal displacements, velocities and accelerations, respectively.

For seismic loading, the external loading $f(t)$ is equal to zero. The basic seismic motions are the three components of free-field ground displacements $u(t)_{ig}$ that are known at some point below the foundation level of the structure. Here, one can write Eq. (5.1) in terms of the displacements $u(t)$, velocities $\dot{u}(t)$ and accelerations $\ddot{u}(t)$ that are relative to the three components of free-field ground displacements.
Therefore, the absolute displacements, velocities and accelerations can be eliminated from Eq. (5.2) by writing the following simple equations:

$$u(t)_a = u(t) + I_x u(t)_{xg} + I_y u(t)_{yg} + I_z u(t)_{zg} \tag{5.3a}$$

$$\dot{u}(t)_a = \dot{u}(t) + I_x \dot{u}(t)_{xg} + I_y \dot{u}(t)_{yg} + I_z \dot{u}(t)_{zg} \tag{5.3b}$$

$$\ddot{u}(t)_a = \ddot{u}(t) + I_x \ddot{u}(t)_{xg} + I_y \ddot{u}(t)_{yg} + I_z \ddot{u}(t)_{zg} \tag{5.3c}$$

where I_i is a vector with ones in the 'i' directional degrees of freedom and zero in all other positions. The substitution of (5.3) into (5.2) allows the node point equilibrium equations to be rewritten as

$$m_s\ddot{u}(t) + c\ddot{u}(t) + k_s u(t) = -m_x\ddot{u}(t)_{xg} - m_y\ddot{u}(t)_{yg} - m_z\ddot{u}(t)_{zg} \tag{5.4}$$

where $m_i = m_s I_i$.

The simplified form of Eq. (5.4) is possible since the rigid body velocities and displacements associated with the base motions cause no additional damping or structural forces to be developed.

5.3 Solution of the Dynamic Equilibrium Equations

There are several different methods that can be used for the solution of (5.1). Each method has advantages and disadvantages that depend on the type of structure and loading.

www.EngineeringBooksPDF.com

5.3.1 Mode Superposition Method

The most common and effective approach for seismic analysis of linear structural systems is the mode superposition method. This method, after a set of orthogonal vectors are evaluated, reduces the large set of global equilibrium equations to a relatively small number of uncoupled second-order differential equation. The numerical solution of these equations involves greatly reduced computational time.

It has been shown that seismic motions excite only the lower frequencies of the structure. Typically, earthquake ground accelerations are recorded at increments of 200 points/s. Therefore, the basic loading data do not contain information over 50 cycles/s. Hence, neglecting the higher frequencies and mode shapes of the system does not introduce errors.

The dynamic force equilibrium, Equation (5.4), can be rewritten in the following form as a set of N second-order differential equations:

$$M\ddot{u}(t) + C\ddot{u}(t) + Ku(t) = F(t) = \sum_{j=1}^{N} f_j^* g(t)_j \tag{5.5}$$

All possible types of time-dependent loading, including wind, wave and seismic, can be represented by a sum of J space vectors f_j^*, which are not a function of time, and J time function $\mathbf{g}(t)_j$, where J cannot be greater than the number of displacements N.

The number of dynamic degrees of freedom is equal to the number of lumped masses in the system. Some publications advocate the elimination of all massless displacements by static condensation prior to the solution of Eq. (5.5). The static condensation method reduces the number of dynamic equilibrium equations to solve; however, it can significantly increase the density and the bandwidth of the condensed stiffness matrix.

For the dynamic solution of arbitrary structural systems, however, the elimination of the massless displacement is, in general, not numerically efficient. Therefore, the method of static condensation should be avoided and other methods can be used.

The fundamental mathematical method which is used to solve Eq. (5.5) is separation of variables. This approach assumes that the solution can be expressed in the following form:

$$u(t) = \Phi\, \ddot{Y}(t) \tag{5.6a}$$

where Φ is an "N by L" matrix containing L spatial vectors which are not a function of time and $\mathrm{Y}(t)$ is a vector containing L functions of time.

From Eq. (5.6a) it follows that

$$\dot{u}(t) = \Phi\, \dot{Y}(t) \tag{5.6b}$$

www.EngineeringBooksPDF.com

and

$$\ddot{u}(t) = \Phi \ddot{Y}(t) \tag{5.6c}$$

Prior to solution, it is necessary that the space functions satisfy the following mass and stiffness orthogonality conditions:

$$\Phi^{\mathrm{T}''} M \Phi = 1 \quad \text{and} \quad \Phi^{\mathrm{T}''} K \Phi = \Omega^2 \tag{5.7}$$

$\mathrm{T}'' = \mathrm{Transpose}$
where I is a diagonal unit matrix and Ω^2 is a diagonal matrix which may or may not contain the free vibration frequencies. It should be noted that the fundamentals of mathematics place no restrictions on these vectors, other than the orthogonality properties. Here, all space function vectors are normalized so that the *generalized mass* $\phi_n^{T''} M \phi_n = 1$.

After substitution of Eq. (5.6) into Eq. (5.5) and the premultiplication by $\Phi^{\mathrm{T}''}$ the following matrix of L equations are produced:

$$I\ddot{Y}(t) + d\dot{Y}(t) + \Omega^2 = \sum_{j=1}^{J} P_j g(t)_j \tag{5.8}$$

where $P_j = \Phi^{T''} f_j^*$ and are defined as the modal participation factors for time equation j. The term P_{nj} is associated with the nth mode.

For all structures the "square" matrix $[d]$ is not diagonal; however, in order to uncouple the modal equations it is necessary to assume that there is no coupling between the modes. Hence, it is assumed to be diagonal with the modal damping forms defined by

$$d_{nn} = 2\xi_n \omega_n \tag{5.9}$$

where ζ_n is defined as the ratio of the damping in mode n to the critical damping of the mode.

A typical uncoupled modal equation, for linear structural systems, is of the following form:

$$\ddot{y}(t)_n + 2\xi_n \omega_n \dot{y}(t)_n + \omega_n^2 y(t)_n = \sum_{j=1}^{J} P_{nj} g(t)_j \tag{5.10}$$

For three-dimensional seismic motion, this equation can be written as

$$\ddot{y}(t)_n + 2\xi_n \omega_n \dot{y}(t)_n + \omega_n^2 y(t)_n = P_{nx} \ddot{u}(t)_{gx} + P_{ny} \ddot{u}(t)_{gy} + P_{nz} \ddot{u}(t)_{gz} \tag{5.11}$$

where the three *mode participation factors* are defined by $P_{ni} = \phi_n M_i$ in which i is equal to x, y or z.

www.EngineeringBooksPDF.com

Prior to presenting the solution of Eq. (5.10) for various types of loading it is convenient to define additional constants and functions which are summarized in Table 5.2.

$$\ddot{y}(t) + 2\xi\omega\dot{y}(t) + \omega^2 y(t) = 0 \tag{5.12}$$

Table 5.1 Formulae for coefficients (Based on Wilson of the University of California, U.S.A.)

A reference is made to Fig. 5.1

$$A = e^{-\zeta\omega_n\Delta t}\left\{\frac{\zeta}{\sqrt{1-\xi^2}}\sin\omega_D\Delta t + \cos\omega_D\Delta t\right\}$$

$$B = e^{-\xi\omega_n\Delta t}\left\{\frac{1}{\omega_D}\sin\omega_D\Delta t\right\}$$

$$C = \frac{1}{K}\left\{\frac{2\xi}{\omega_n\Delta t} + e^{-\xi\omega_n\Delta t}\left[\left\{\frac{1-2\xi^2}{\omega_D\Delta t} - \frac{\xi}{\sqrt{1-\xi^2}}\right\}\sin\omega_D\Delta t - \left\{1 + \frac{\xi}{\omega_D\Delta t}\right\}\cos\omega_D\Delta t\right]\right\}^2$$

$$D = \frac{1}{K}\left\{1 - \frac{2\xi}{\omega_n\Delta t} + e^{-\xi\omega_n\Delta t}\left[\frac{2-\xi^2-1}{\omega_D\Delta t}\sin\omega_D\Delta t + \frac{2\xi}{\omega_n\Delta t} - \frac{2\xi}{\omega_D\Delta t}\cos\omega_D\Delta t\right]\right\}$$

$$A' = e^{-\xi\omega_n\Delta t}\left\{\frac{\omega_n}{\sqrt{1-\xi^2}}\sin\omega_D\Delta t\right\}$$

$$B' = e^{-\xi\omega_n\Delta t}\left\{\cos\omega_D\Delta t - \frac{\xi}{\sqrt{1-\xi^2}}\sin\omega_D\Delta t\right\}$$

$$C' = \frac{1}{K}\left\{-\frac{1}{\Delta t} + e^{-\xi\omega_n\Delta t}\left[\left\{\frac{\omega_n}{\sqrt{1-\xi^2}} + \frac{\xi}{\Delta t\sqrt{1-\xi^2}}\right\}\sin\omega_D\Delta t + \frac{1}{\Delta t}\cos\omega_D\Delta t\right]\right\}$$

$$D' = \frac{1}{K\Delta t}\left[1 - e^{-\xi\omega_n\Delta t}\left\{\frac{\xi}{\sqrt{1-\xi^2}}\sin\omega_D\Delta t + \cos\omega_D\Delta t\right\}\right]$$

The numerical solution for the dynamic equation $\omega_{n1} = \sqrt{K_1/M_1}$

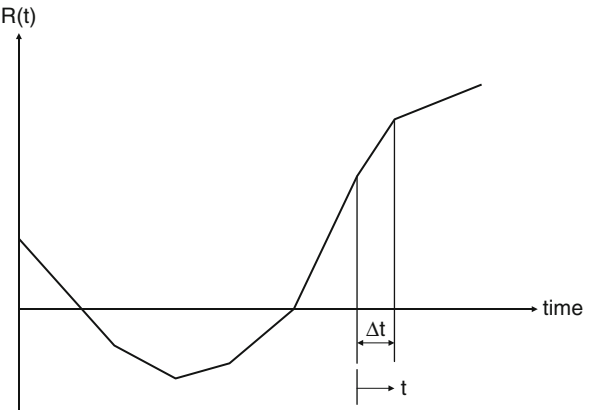


Fig. 5.1 Typical modal load function

www.EngineeringBooksPDF.com

Table 5.2 Summary of parameters used in dynamic Response Equations

Constants	$\omega_D = \omega\sqrt{1-\xi^2}\ \omega = \omega\xi\ \ \bar{\xi} = \frac{\xi}{\sqrt{1-\xi^2}}\ a_0 = \frac{2\xi}{\omega\Delta t}$
	$a_1 = 1 + a_0\ \ a_2 = -\frac{1}{\Delta t}\ \ a_3 = -\bar{\xi}a_1 - a_2/\omega_D\ \ a_4 = -a_1$
	$a_5 = -a_0\ a_6 = -\ a_2\ a_7 = -\bar{\xi}a_5 - a_6/\omega_D\ \ a_8 = -a_5$
	$a_9 = \omega_n^2 - \bar{\omega}^2\ \ a_6 = 2\bar{\omega}\omega$
	$\mathrm{S}(t) = e^{-\xi\omega t}\sin(\omega_D t)\ \ \mathrm{S}(t) = -\bar{\omega}(t) + \omega_D \mathrm{C}(t)$
	$\mathrm{C}(t) = e^{-\xi a x}\cos(\omega_D t)\ \mathrm{C}(t) = -\bar{\omega}C(t) - \omega_D S(t)$
	$\mathrm{A}_1(t) = (t) + \bar{\xi}S(t)\ \ S(t) = -a_9(t) - a_{10}C(t)$
Function	$\mathrm{A}_2(t) = \frac{1}{\omega_D}(t)\ \ \mathrm{C}(t) = -a_9(t) + a_{10}\mathrm{S}(t)$

in which the initial modal displacement y_0 and velocity $\dot{y}_0$ are specified duing previous loading acting on the structure. Note that the functions $S(t)$ and $C(t)$ given in Table 5.2 are solutions to Eq. (5.12).

The solution of (5.12) can now be written in the following compact form:

$$\begin{aligned} \mathrm{A}_3(t) &= \frac{1}{\omega^2}[a_1 + a_2 + a_3\mathrm{S}(t) + a_4\mathrm{C}(t)] \\ \mathrm{A}_4(t) &= \frac{1}{\omega^2}[a_5 + a_6 + a_7(t) + a_8\mathrm{C}(t)] \end{aligned} \tag{5.13}$$

This solution can be easily verified since it satisfies equation (5.12) and the initial conditions.

Typical modal loading $R(t)$ can be associated as

$$\ddot{y}(t) + 2\xi\omega\dot{y}(t) + \omega^2 y(t) = \mathrm{R}(t) \tag{5.14}$$

where the modal loading $R(t)$ is a piecewise linear function as shown in Fig. 5.1. and Table 5.2.

The recurrence formulas written to obtain the response in a single-degree-of-freedom system based on the interpolation of the excitation function are given below:

The coefficients A, B, C, D, A′, B′, C′, D′, depend on the system parameters and and on the time interval. Wilson of University of California gave these values which are listed in Table 5.1.

www.EngineeringBooksPDF.com

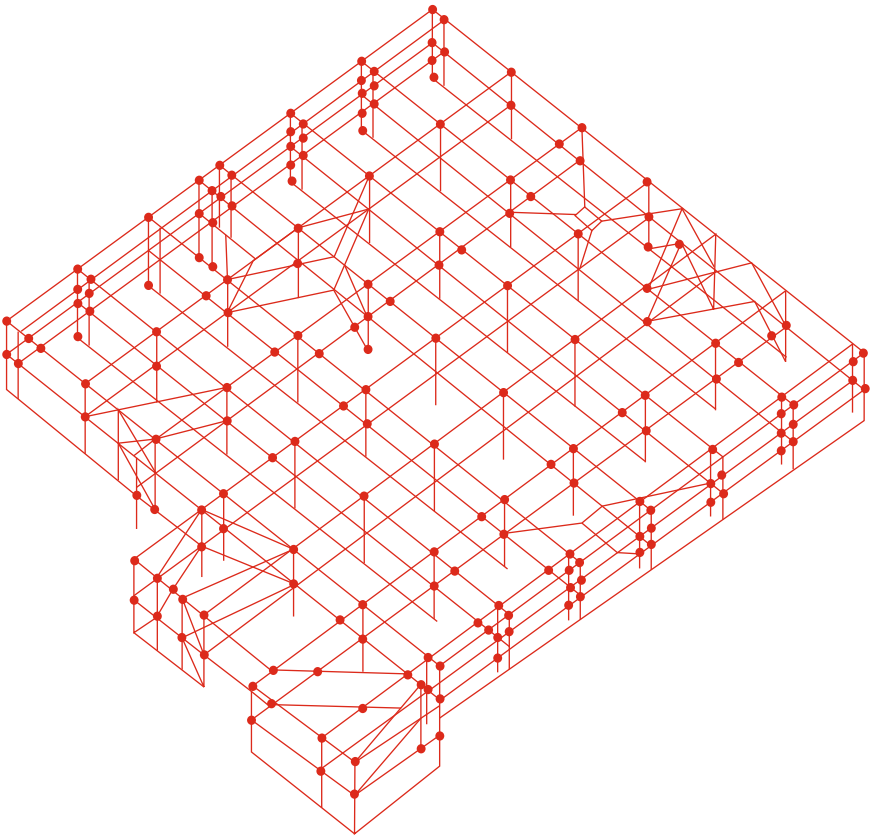


Fig. 5.2 View of the three-dimensional computer model of a frame or floor

Linear Interpolation of Excitation

The numerical solution for the equation is obtained as follows after determining the values:

$$\omega_n \sqrt{k_1/m_1} = \sqrt{\frac{m\mu^2}{1}} - 37.975\, rad/\sec$$

The time step is taken as the time step of the time history, i.e. $\Delta t = 0.01$ s
The coefficients obtained for equation are

$$A = 0.9296,\ B = 0.009597,\ C = 0.0000324,\ D = 0.0000164$$
$$A' = -13.812,\ B' = 0.8932,\ C' = 0.0047,\ D' = 0.004878$$

Substituting the coefficients obtained in the recurrence formulas for displacement and velocity, one gets the response of the uncoupled equation in normal coordinate (q).

www.EngineeringBooksPDF.com

5.4 Step-By-Step Solution Method

The most general solution method for dynamic analysis is an incremental method in which the equilibrium equations are solved at times Δt, $2\Delta t$, $3\Delta t$, etc. There are a large number of different incremental solution methods described in this chapter. In general, they involve a solution of the complete set of equilibrium equations at each time increment. In the case of non-linear analysis, it may be necessary to reform the stiffness matrix for the complete structural system for each time step. Also, iteration may be required within each time increment to satisfy equilibrium. As a result of the large computational requirements it can take a significant amount of time to solve structural systems with just a few hundred degrees of freedom.

In addition, artificial or numerical damping must be added to most incremental solution methods in order to obtain stable solutions. For this reason, engineers must be very careful in the interpretation of the results. For some non-linear structures, subjected to seismic motions, incremental solution methods are necessary.

For very large structural systems, a combination of mode superposition and incremental methods has been found to be efficient for systems with a small number of non-linear members as stated by Wilson of University of California.

The response of real structures, when subjected to large dynamic loads, often involves significant non-linear behaviour. In general, non-linear behaviour includes the effects of large displacements and/or non-linear material properties.

The more complicated problem associated with large displacements, which cause large strains in all members of the structures, requires a tremendous amount of computational effort and computer time to obtain a solution. However, certain types of large strains, such as those in rubber base isolators and gap elements, can be treated as a lumped non-linear element by the fast non-linear analysis (FNA) method.

5.4.1 Fundamental Equilibrium Equations

The global dynamic equilibrium equations, at time t, of an elastic structure with non-linear or energy-dissipating elements are of the following form:
Looking at Eq. (5.2) it is now rewritten as

$$M\ddot{U}(t) + C_{in}(t) + K_n(t) + R(t)_n = R(t) \tag{5.15a}$$

All elements in the equation have already been defined. In addition $R(t)$ is the external applied load where $R(t) = F(t) = \Sigma_j^N f_j g(t) j$. $R(t)N$ is the global mode force vector due to the sum of the forces in the non-linear elements and is

www.EngineeringBooksPDF.com

computed by iteration at time t. The solution of structural systems with a limited number of non-linear elements is summarized below.

The first step in the solution of Eq. (5.12) is to calculate a set of "m" orthogonal Ritz vectors, Φ , which satisfy the following equations of Eq. (5.7):

$$\Phi^{T''} M\ \Phi = 1 \quad \text{and} \tag{5.16a}$$

$$\Phi^{T''} K\ \Phi = \Omega^2 \tag{5.16b}$$

where I is a unit matrix and Ω^2 is a diagonal matrix in which the diagonal terms are defined.

The result is of great importance for the interpretation of the behaviour of isolated buildings and for their preliminary design: and for the usual spectral shapes, the isolation system can be designed for a maximum displacement equal to , and the superstructure for a shear coefficient equal to . These values could have been obtained with reference to a simple oscillator, whose mass is equal to the total mass of the superstructure and the stiffness and damping are equal to the corresponding quantities of the isolation system.

The interstorey drift, on which the damage produced by an earthquake depends, is proportional to the frequency ratio $\sqrt{B}$ and to the maximum base displacement.

5.4.2 Supplementary Devices

Supplementary devices are installed separately from isolators to complete the isolation system. Very often they are made of simple energy-dissipating elements (EDEs). EDEs are sometimes embodied in isolators to improve their energy-dissipating capabilities and avoid the use of separate devices. They have to be within the finite element systems equations.

5.4.2.1 Design Seismic Action Effects on Fixed-Base and Isolated Buildings

The stresses on fixed-base framed structure and on a similar isolated structure need to be compared in terms of base shear on the superstructure. Therefore, the ratio between the design spectral accelerations of a fixed-base structure multiplied by the effective mass ratio and that of a similar seismic-isolated structure divided by the behaviour factor of 1.5 for the superstructure is calculated, where is the period of the fixed-base structure and the period of the isolated structure. The effective mass ratio is taken as equal to 0.85, as prescribed for the equivalent linear static analysis, if the structure has at least two storeys and its vibration period is . It is taken equal to 1 for the isolated structure.

www.EngineeringBooksPDF.com

The comparison is referred to both the damage limit state (DLS). For the ULS of the fixed-base structure, the design spectral ordinate depends on the behaviour factor q, which is related to the ductility class and to the regularity of the superstructure along the height. The comparison is referred to the higher value of q for concrete structures. Thus, the case with

$$q = 4.5\alpha_v/\alpha_1 \tag{5.16c}$$

(ductility class high and regular frames) is examined, assuming the default value $\alpha_4/\alpha_1 = 1.3$. Reference is made to a typical rubber isolation system, having an equivalent viscous damping ratio equal to $\xi = 10\%$, resulting in a reduction factor of the spectral ordinate $n = 0.816$. The seismic force ratio as suggested by Wilson of the University of California is then given by

$$R_{ULS} = \frac{1.56 S_e(T_{\mathrm{bf}})}{Q S_e(T_{\mathrm{eff}})} \quad \begin{array}{l}\text{for } \mathrm{T_b} \le \mathrm{T_{bf}} \le 2\mathrm{T_c} \\ \text{and } \xi_{\mathrm{eff}} = 10\%\end{array} \tag{5.17}$$

As far as the DLS is, no reduction factor q has to be considered, and the seismic shear ratio becomes

$$R_{DLS} = 1.04\,\frac{S_e(T_{\mathrm{bf}})}{S_e(T_{\mathrm{eff}})} \quad \begin{array}{l}\text{for } \mathrm{T_b} \le \mathrm{T_{bf}} \le 2\mathrm{T_c} \\ \text{and } \xi_{\mathrm{eff}} = 10\%\end{array} \tag{5.18}$$

Looking at equations (5.17) and (5.18) it is clear that the period ratio plays a primary role in deciding the economic convenience of seismic isolation, as the spectral ratio depends mainly on it. Moreover, the advantages of seismic isolation are much more remarkable for the DLS, since no q factor enters into the equation, which results in the higher the effective period, the more favourable the RULS ratio becomes to seismic isolation. Focusing attention on the usual range of application of rubber isolation, and considering an isolation ratio of at least 2, it can be seen that the seismic force ratio RULS varies between 0.63 and 3.0 for ground type A and 0.54 and 1.5 for ground type D as suggested by Wilson of University of California.

As mentioned above, to obtain RULS, it is multiplied by about 4. Values of RULS much higher than 1 (ranging from 2.5 to 12 and from 2.2 to 6 for the situations above) are then obtained, emphasizing the significant advantages provided by seismic isolation in terms of non-structural damage control.

www.EngineeringBooksPDF.com

Solution Procedures

Several solution procedures are available for earthquake problems associated with finite element techniques. The most acceptable ones include implicit dynamic integration method and a number of others as described with this chapter. Runge–Kutta method is also widely used for the dynamic analysis problems. Loaddependent Ritz vector is also used for dynamic non-linear solutions. Typical methods, four is total, are listed in Table 5.3.

Table 5.3 Summary of non-linear solution algorithm

1. Runge-Kutta method
2. Non-Linear Algorithm using Ritz Vectors
3. Incremental method
4. Wilson-θ method

Note: There are many others, dependent various self programs selected by the commercial computer packages.

5.5 Runge–Kutta Method

5.5.1 Introduction

The very useful and flexible numerical method that one can describe was first introduced by C. Runge at the turn of the century and subsequently modified and improved by W. Kutta. It is essentially a generalization of Simpson's rule, and it can be shown that the error involved when integrating over a step of length h is of the order of h^5. The method is simple to use and, unlike the predictor–corrector method, allows adjustment of the length of the integration step from point to point without modification of the method which is useful for the solutions of stiff differential equations meted out in seismic problems.

The Runge–Kutta method readily extends to allow the numerical solution of simultaneous and higher-order equations. Suppose the equations involved are

$$\frac{\mathrm{d}y}{\mathrm{d}x} = f(x, y, z) \tag{5.19}$$

$$\frac{\mathrm{d}z}{\mathrm{d}x} = g(x, y, z) \tag{5.20}$$

subject to the initial conditions $y = y_0, z = z_0$ at $x = x_0$

www.EngineeringBooksPDF.com

Then, with a step of length h in x, define

$$\begin{aligned} k_{1n} &= f(x_n, y_n, z_n)h && \text{(a)} \\ k_{2n} &= f(x_n + \tfrac{1}{2}h, y_n + \tfrac{1}{2}K_{1n}, z_n + \tfrac{1}{2}K_{1n})h && \text{(b)} \\ k_{3n} &= f(x_n + \tfrac{1}{2}h, y_n + \tfrac{1}{2}k_{2n}, z_n + \tfrac{1}{2}K_{2n})h && \text{(c)} \\ k_{4n} &= f(x_n + h, y_n + k_{3n}, z_n + K_{3n})h && \text{(d)} \end{aligned} \tag{5.21}$$

and

$$\begin{aligned} K_{1n} &= g(x_n, y_n, z_n)h \\ K_{2n} &= g(x_n + \tfrac{1}{2}h, y_n + \tfrac{1}{2}k_{1n}, z_n + \tfrac{1}{2}K_{1n})h \\ K_{3n} &= g(x_n + \tfrac{1}{2}h, y_n + \tfrac{1}{2}k_{2n}, z_n + \tfrac{1}{2}K_{2n})h \\ K_{4n} &= g(x_n + h, y_n + k_{3n}, z_n + K_{3n})h \end{aligned} \tag{5.22}$$

The following formulae are then used to compute the increments Δy_n and Δz_n in y and z:

$$\Delta y_n = \frac{1}{6}(k_{1n} + 2k_{2n} + 2k_{3n} + k_{4n}) \tag{5.23}$$

and

$$\Delta z_n = \frac{1}{6}(K_{1n} + 2K_{2n} + 2K_{3n} + K_{4n}). \tag{5.24}$$

The values of y and z at the $(n + 1)$th step of integration are $y_{n+1} = y_n + \Delta y$, $z_{n+1} = z_n + \Delta z_n$.

These results may also be used to integrate a second-order equation by introducing the first derivative as a new dependent variable. Suppose $y'' - 2y' + 2y = 0$ with $y(0) = y'(0) = 1$. Then setting $y' = z$, the second-order equation is seen to be equivalent to the two first-order simultaneous equations $y' = z$ and $z' = 2(z - y)$, with $y(0) = 1$ and $z(0) = 1$ Eqs. with $h = 0.2$, $f \equiv z$, and $g \equiv 2(y - z)$ in determine $y'(0.2)$

$$\begin{aligned} k_{11} &= 0.2, & K_{11} &= 0 & \text{(a)} \\ k_{21} &= 0.2, & K_{21} &= -0.04 & \text{(b)} \\ k_{31} &= 0.196, & K_{31} &= -0.048 & \text{(c)} \\ k_{41} &= 0.1904, & K_{41} &= -0.0976 & \text{(d)} \end{aligned} \tag{5.25}$$

1. Initial Calculation – Prior to step-by-step solution
   a. Calculate "L" Load-Dependent Ritz vectors for the structure without the non-linear elements.
   b. Calculate the $n \times$ "L" B matrix, where *"n"* is the total number of degrees of freedom within all non-linear elements.
   c. Calculate 12 integration constants $\alpha_1 \ldots \alpha_{12}$

www.EngineeringBooksPDF.com

2. Non-linear solution at times Δt, $2\Delta t$, $3\Delta t$ --------
Taylor series to estimate solution at time

$$(t)_m = u(t-\Delta t)_m + \Delta t\, \dot{u}(t-\Delta t)_m + \frac{\Delta t}{2}\ddot{u}(t-\Delta t)_m \tag{5.26}$$

$$(t)_m = \dot{u}(t-\Delta t)_m + \Delta t\, \ddot{u}(t-\Delta t)_m \tag{5.27}$$

For iteration "i" calculate "n" non-linear deformations and velocities

$$\delta(t)^i = B\dot{u}(t)^i \quad \text{and} \quad \delta(t)^i = B\dot{u}(t)^i \tag{5.28}$$

Based on the deformation and velocity history in non-linear elements calculate "n" non-linear forces. $F(t_i)^n$
Calculate new modal force vector

$$\bar{F}(t)^i = F(t) - B^T F(t_i)^2 \tag{5.29}$$

Solve modal equation for new

$$u(t)^i, \quad \dot{u}(t)^i, \quad \ddot{u}(t)^i \tag{5.30}$$

Calculate error normalized

$$E_{rr} = \frac{\sum_{m=1}^{L} \left|\bar{f}(t)_m^i\right| - \sum_{m=1}^{L} \left|\bar{f}(t)_m^{i-1}\right|}{\sum_{m=1}^{L} \left|\bar{f}(t)_m^i\right|} \tag{5.31}$$

Where the tolerance *Tol* is specified

1. If $E_{rr} >$ Tol go to step with $i = i + 1$ (5.32)
2. If $E_{rr} <$ Tol go to step with $t = t + \Delta t$

5.6 Non-linear Response of Multi-Degrees-of-Freedom Systems: Incremental Method

The Wilson-θ method is suggested initially for the solution of the structure modelled by assuming that the acceleration varies linearly over the time interval from t to $t + \theta\delta t$, such that$\theta \geq 1$. For a value of $\theta \geq 1.38$, the Wilson-θ becomes unconditionally stable. Consider the difference between the dynamic equilibrium conditions at time t_i and $t_i + \theta\delta t$. The following incremental equations are obtained on the lines suggested earlier.

$$[M]\{\delta\ddot{u}_i\}_t + [C]\{\dot{u}\}_t\{\delta\dot{u}_i^{'}\}_t + [K_s]\{u\}\{\delta\dot{u}_i^{'}\}_t = \{\delta f_i(t)\} \tag{5.33}$$

www.EngineeringBooksPDF.com

where δ is the increment associated with the extended time $\theta\delta t$. Thus

$$\begin{aligned} c\{\delta u_1'\}^2 &= \{u(t_i+\theta\delta t)\} - \{u(t_i)\} \quad \text{(a)} \\ \{\delta \dot{u}_i'\} &= \{\dot{u}(t_i+\theta\delta t)\} - \{\dot{u}(t_2)\} \quad \text{(b)} \\ \{\delta \ddot{u}_i\} &= \{\ddot{u}(t_i+\theta\delta t) - \{\ddot{u}(t_i)\} \quad \text{(c)} \end{aligned} \tag{5.34}$$

The incremental force is given by

$$\{\delta F_2(t)\} = \{F(t_i+\theta\delta t)\} - \{F(t_i)\} \tag{5.35}$$

As shown in Fig. 5.3(a) and (b), both stiffness and damping are obtained for each time step as the initial values of the tangent to the corresponding curves. These coefficients are given as

$$\{k_{ij}\} = \{\delta F_{ti}/\delta u_j\} \tag{5.36}$$

$$\{c_{ij}\} = \{\delta F_{di}/\delta u_j\} \tag{5.37}$$

During the extended time step the linear expression for the acceleration is

$$\{\ddot{u}(t)\} = \{\ddot{u}_t\} + [\delta\ddot{u}_i/\theta\delta t(t-t_i)] \tag{5.38}$$

The value of $\delta\ddot{x}'t$ is taken from equation. Integration of equation gives the following equations:

$$\{\dot{u}(t)\} = \{\dot{u}_t\} + \{\ddot{\alpha}_1(t-t_i)\} + \frac{1}{2}\left\{\frac{\delta\ddot{u}'i}{\theta\delta t} \times (t-t_i)\right\} \tag{5.39}$$

$$\{u(t)\} = \{u_i\} + \{\dot{u}(t-t_i)\} + \left\{\frac{1}{2}\ddot{u}_i(t-t_i)^2\right\} + \left\{\frac{1}{6}\frac{\delta\ddot{u}}{\theta\delta t} \times (t-t_i)^3\right\} \tag{5.40}$$

At the end of the extended interval $t_i = t_i + \theta\delta t$, are equations reduced to

$$\delta\dot{u}_i = \ddot{u}_i\theta\delta t + \tfrac{1}{2}\delta\ddot{u}_i\theta\delta t \tag{5.41}$$

$$\delta u_i' = \dot{u}_i\theta\delta t + \tfrac{1}{2}\ddot{u}_i(\theta\delta t)^2 + \tfrac{1}{6}\delta\ddot{u}_i(\theta\delta t)^2 \tag{5.42}$$

The values of , and $\delta\alpha_i$ are given in (5.41) and (5.42). By substituting the expression for δu_i, from (5.41) into (5.42), the following equations are obtained:

$$\{\delta\ddot{u}_i'\} = \left\{\left[6/(\theta\delta t)^2\right]\delta\ddot{u}_i\right\}\left\{\left[(6/(\theta\delta t)^2\right]\dot{u}_i\right\} - 3\{\ddot{u}_i\} \tag{5.43}$$

$$\{\delta\ddot{u}_i'\} = \{(3/\theta\delta t)\delta\dot{u}_i\} - 3\{u_i\} - r_2\theta\delta t\{\ddot{u}_i\} \tag{5.44}$$

The incremental acceleration for the time interval δt can be obtained from

$$\{\delta(\ddot{u})\} = \{\delta\ddot{u}_i'/\theta\} \tag{5.45}$$

www.EngineeringBooksPDF.com

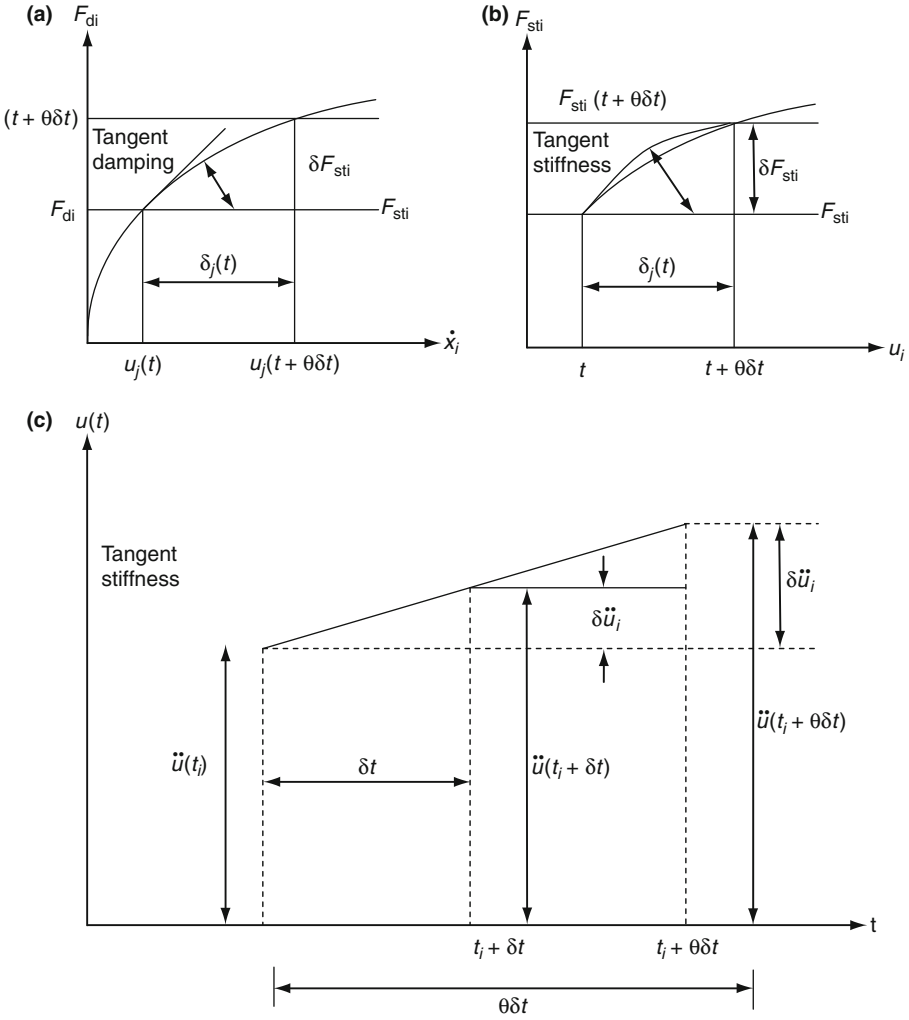


Fig. 5.3 Wilson-θ method; (**a**) values of c_{ij}; (**b**) value of k_{ij}; (**c**) linear acceleration

The incremental velocity and displacement for the time interval δt are given by

$$\{\delta u_i\} = \{\dot{u}_i \delta t\} + \tfrac{1}{2}\{\delta\ddot{u}_i \theta\delta t\} + \tfrac{1}{6}\{\delta\ddot{u}_i (\theta\delta t)^2\} \tag{5.46}$$

$\{u_{i+1}\} = \{u_i\} + \{\delta u_i\}$ at the end of the time step (5.47)

$$\{u_{i+1}\} = \{u_i\} + \{\delta u_i\}; t_{i+1} = t_i + \delta t \tag{5.48}$$

www.EngineeringBooksPDF.com

The following dynamic results:

$$\{\delta F_i(t)\} + \{M\}\{6/(\theta\delta t)\}\{u_i'\} + 3\{\ddot{u}_i\} + [C]\{3\{\dot{u}_i\} \\ +(3/\theta\delta t) + \tfrac{1}{2}\theta\delta t\{\ddot{u}_i\}\} = \{[K]_i + 6/\theta\delta t^2 + [M](\tfrac{3}{\theta}\delta t)[C]_i\} \times \{\delta u_i\} \tag{5.49}$$

Hence the initial acceleration for the next step is calculated at time $t + \delta t$ as

$$\{\ddot{u}_i + 1\} = [M]^{-1}[F_{i+1}(t)] - [C]_{i+1}\{u_{i+1}\} - [K]_{i+1}\{u_{i+1}\} \tag{5.50}$$

damping force vector

stiffness force vector

The procedure is repeated for t_{i+2}, etc. for the desired time.

5.7 Summary of the Wilson-θ Method

In order to summarize the Wilson-θ integration method, the following step-by-step solution should be considered with the dynamic, impact and explosion analysis of the structures.

(1) Assemble [K], [M] and [C]. (a)

(2) Set the initial values of and $F_0(t)$, u_0, $\ddot{u}_0$. (b)

(3) Evaluate $\ddot{x}_0$ using (c)

$$[M][\ddot{x}_0] = [F_0(t)] - [C]\{\dot{x}_0\} - [K]\{x_0\} \tag{d}$$

(4) Select a time step δt (usually taken as 1.4) and evaluate

$$\theta\delta t.a_1 = 3/(\theta\delta t), a_2 = 6/(\theta\delta t), a_3 = \theta\delta t/3, a_4 = 6(\theta\delta t)^2 \tag{e}$$

(5) Develop the effective stiffness matrix, $[K]_{eff}$

$$[K]eff = [K] + a_4[M] + a_1[C] \tag{f}$$

where $[K] = [\bar{K}]$ and 0 for elastic and plastic, respectively.

(6) Calculate $\delta F_i(t)$ for the time interval t_1 to $t_1 + \theta\delta t$

$$\{\delta F_i(t)\} = \{F(t)\}_{i+1} + [\{F(t)\}_{i+2} - \{F(t)\}_{i+1}(\theta - 1)] - \{F(t)\}i \tag{g}$$

(7) Solve the incremental displacement $\{\delta ui\}$ and the incremental acceleration $\{\delta\ddot{x}i'\}$ for the extended time interval $\theta\delta t$.

(8) Calculate $\{\delta\ddot{u}\}$.

(9) Calculate the incremental velocity and displacement.

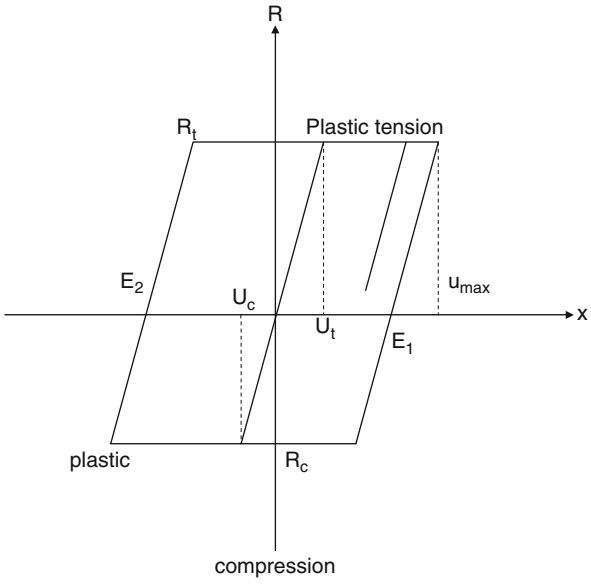
(10) Calculate $\{u_{i+1}\}$ and for the time $t_{t+1} = t_i + \delta t$ from equations and

www.EngineeringBooksPDF.com

(11) Calculate $\{\ddot{u}_{i+1}\}$ at time $t_{t-1} = t_i + \delta t$ from the dynamic equilibrium equation.

A typical numerical example is shown in Table 5.4 where quadratic and cubic functions are considered instead of the linear function.

Table 5.4 Elasto-plastic analysis



Increasing displacement $x > 0$
Decreasing displacement $x < 0$
(plastic) in tension $= R_t / K$
R_e are restoring forces in tension and compression, respectively
Let K = 3.35 kN/mm; $R_t = R_e$; M = 0.5 kNs^2/mm
= damping coefficient = 0.28 kNs/mm
$\dot{x} = 0$ in the initial case
= 0
u_t = 15/3.35 mm; = –4.48 mm;
$2\pi\sqrt{(M/K)} = 2\pi\sqrt{(0.5/3.35)} = 2.43$ s

For convenience, δt = 0.1s

$$[K]_{eff} = [\bar{K}] + a_4[M] + a_1[C]$$
$$= [\bar{K}]_p + (6/0.1)^2)0.5 + (3/0.1)0.28$$

where $[K]_p = 0$ for plastic

$$= [\bar{K}]_p + 350 + 8.4\{\delta F_2(t)\}$$
$$= [\bar{K}]_p + 308.4$$
$$\{\delta F_i(t)\} = \{\delta F(t)\} + \left(\tfrac{6}{\delta t} M + 3c\right)\dot{u} + \left(3M + \tfrac{\delta t}{2} c\right)\ddot{u}$$
$$= \{\delta F(t)\} + 3.84_u + .1514 + \ddot{u}$$

www.EngineeringBooksPDF.com

Table 5.4 (continued)

The velocity increment is given by

$$\begin{aligned}\delta\dot{u} &= (3/\delta t)\delta u_i - 3\dot{u}_i - (\delta t/2)\ddot{u}_i \\ &= (3/0.1)\delta u_i - 3\dot{u}_i(0.12)\ddot{u}_1 \\ &= 30\delta u_i - 3\dot{u}_i - 0.05\ddot{u}_i\end{aligned}$$

The results are obtained on the basis of the above two equations of force and velocity increment. The step-by-step procedure is covered in Section 3.4.6 and the results are tabulated as follows.

t $F(t)$ x $\dot{x}$ R $\ddot{x}$ $[\bar{K}_p]$ $[K_{eff}]$ $\delta F(t)$ $\delta\bar{F}(t)$ δx $\delta\dot{x}$

5.8 Dynamic Finite Element Formulation with Base Isolation

Seismic response of the base-isolated buildings, excited unidirectionally with these ground motions can be obtained by means of computer program ISOPAR-II. This program is given a detailed review in the Appendix.

The following assumptions are made in this software for the analysis of base-isolated buildings:

(i) The superstructure is elastic at all times and the non-linear behaviour is restricted in isolators only.
(ii) All framed substructures are connected at each floor level by a diaphragm, which is infinitely rigid in its own plane.
(iii) Each floor has three degrees of freedom (two translations and one rotation) attached to the centre of mass of each floor.
(iv) The isolation devices are rigid in the vertical direction and have negligible torsion resistance.

The equations of motion for the elastic superstructure are expressed in the following form familiar from the dynamic equations stated earlier inclusive of ground acceleration.

$$M_u + C_u + K_u = -MR\{\ddot{u}_g + \ddot{u}_b\} \tag{5.51}$$

where

M = mass matrix for superstructure
C = damping matrix for superstructure
K = stiffness matrix for superstructure
R = the matrix of influence coefficient
u = the vector of floor displacement relative to base
$\ddot{u}_b$ = the vector of base displacement relative to ground and
$\ddot{u}_g$ = the vector of ground acceleration

www.EngineeringBooksPDF.com

The equations of motion for the *base* are

$$\begin{aligned} R_M^T[\{\ddot{u}\} + R\{\ddot{u}_b + \ddot{u}_g\}] + [M_b]\{\ddot{u}_b + \ddot{u}_g\} \\ +[C_b]\{u_b\} + [\dot{k}_b]\{u_b\} + \{f\} = 0 \end{aligned} \tag{5.52}$$

where

M_b = mass matrix for base isolation system
C_b = damping matrix for base isolation system
K_b = stiffness matrix for base isolation system and
f = the vector containing the forces mobilized in the non-linear elements of the isolation system

Employing modal reduction

$$u = \phi u \tag{5.53}$$

where

ϕ = the modal matrix normalized with respect to the mass matrix and
u = the modal displacement vector relative to the base and combining equations the following equation is obtained:

$$\begin{aligned} &\begin{bmatrix} [I] & \phi^{T''} mR \\ R^{T''} m\phi & R^{T''} mR + \dot{M}_b \end{bmatrix} \begin{Bmatrix} \ddot{u} \\ \ddot{u}_b \end{Bmatrix} + \begin{bmatrix} 2\zeta_i \omega_i & 0 \\ 0 & C_b \end{bmatrix} \begin{Bmatrix} \ddot{u} \\ \dot{u}_b \end{Bmatrix} \\ &+ \begin{bmatrix} \omega_i^2 & 0 \\ 0 & R_b \end{bmatrix} \begin{Bmatrix} \dot{u} \\ u_b \end{Bmatrix} + \begin{Bmatrix} 0 \\ f \end{Bmatrix} = - \begin{bmatrix} \phi^{T''} mR \\ R^{T''} mR + m_b \end{bmatrix} (\ddot{u}_g) \end{aligned} \tag{5.54}$$

5.9 Added Viscoelastic Dampers (VEDs) in Seismic Buildings

5.9.1 Introduction

The effect of supporting braces on the controlled efficiency of VEDs is investigated. It is, on the basis if available evidence, considered that when sufficient stiffness cannot be provided for the supporting braces, if required, the flexibility of the brace should be considered in the design of the VED to achieve the desired performance of the building. Sometimes it is necessary, if compensation is needed, to reduce the size of the supporting brace to increase the additional VED size.

The viscoelastic damper (VED) is acknowledged as one of the most efficient energy-absorbing devices for building structures against dynamic loads such as earthquake or wind. Previous studies have shown that the efficiency of an added VED can be greatly enhanced by applying properly sized dampers to proper locations. Zhang and Soong and Shukla and Datta have proposed optimal location and size of the VED.

www.EngineeringBooksPDF.com

5.9.2 Generalized Equation of Motion when Dampers Are Used

Equations (5.1), (5.42) and (5.44) are modified to include the influence of the damper under consideration. The equation of motion of an n-degree-of-freedom building structure with supplementary dampers installed at different locations and subjected to ground excitations at the base can be written as

$$m_s\ddot{u}_s(t) + c_s\dot{u}(t) + k_s u_s(t) + \sum_{d=1}^{me} \bar{r}\, di\, p\, dr(t) = -m_s e_{gi}\ddot{u}_g(t) \tag{5.55}$$

where m_s, k_s and c_s, respectively, represent the $n \times n$ mass, stiffness, and inherent structural damping matrices of the building structure. $\ddot{u}_g(t)$ = ground acceleration time history; e = ground motion influence coefficients; and $u_s(t)$ = n-dimensional relative displacement response vector measured with respect to the base.

A dot over a quantity indicates time derivative of the quantity. $p_{dr}(t)$ represents the force in the damper at the dth location, and there are N number of possible locations where the devices can be installed on the structure. The influence of the damper force on the structure is considered through the n-dimensional influence vector. It is assumed that the structural system behaves linearly under earthquake-induced ground excitation.

5.9.3 System Dynamic Equation with Friction Dampers

The governing equation of motion given earlier in this chapter such as Eq. (5.1) can now be slightly modified for the whole system (superstructure of the building, sliding support and semi-active/passive dampers) and can be stated as without dampers (semi-active or passive) but sliding included of the building support

$$[m]\{\ddot{u}\} + [c]\{\dot{u}\} + \{P_d(u)\} = -[m][I]\{\ddot{u}_g\} \tag{5.56}$$

in which

$[m]$ = mass matrix; $[c]$ damping matrix
$\{u\}$ = linear case
$[k]$ = elastic stiffness matrix
$\{u\}^{T''}$ = displacement vector
I = identity matrix or unit diagonal matrix

The differential equations of motion (5.49) are solved in incremental form by employing the Newmark–Beta method assuming a constant average acceleration over a short time interval. In convergent process the Newton–Raphson method is used for the solution of the non-linear problem and the iteration

www.EngineeringBooksPDF.com

continues to a specified number of iterations or when the tolerance reaches an acceptable value. An energy tolerance is used to terminate the iterations if convergence is achieved. The Runge–Kutta method can also be used for these dynamic equations.

(a) Basic elements of the dampers

where f_i and y_i are the control force and the deformation of the damper–brace system, respectively, q_i is the horizontal displacement of the ith story, θ_i is the inclination angle of the brace, and are the stiffness of the brace, the stiffness and damping coefficient of the VED, respectively.

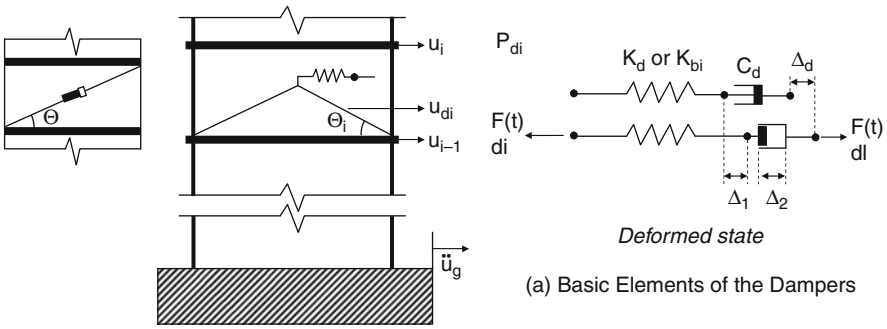


Fig. 5.4 Configuration of damper–brace system installed in a storey

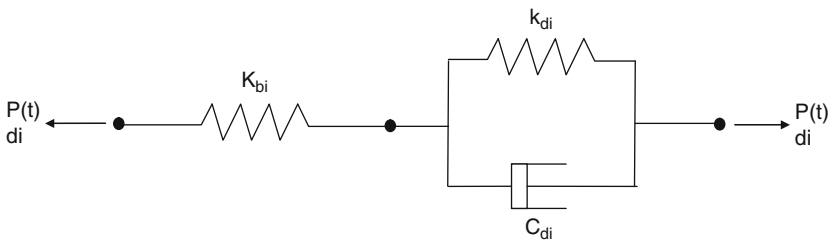


Fig. 5.5 Mathematical modelling of a VED and a supporting brace

5.9.3.1 Hysteretic Behaviour of a Semi-active Friction Damper

The energy dissipation characteristic of a damper is usually understood by its hysteresis loop. On the other hand, the hysteresis loop of a semi-active damper greatly depends on the control algorithm applied.

In other words, the same semi-active damper may have different hysteretic behaviours when using different control algorithms. In order to observe how the

www.EngineeringBooksPDF.com

proposed control method alters the hysteretic behaviour of a friction damper, in this subsection a single-degree-of-freedom structural system equipped with a semi-active friction damper under a harmonic load is investigated.

(a) Additional data for the building structures
f = natural frequency of the proposed building = 1 Hz computed
C = damping ratio = 0.05 or 5%

$$w(t)\ddot{u}_g = \text{ground excitation}$$
$$\ddot{u}_g(t) = 4.9\sin(2\pi t) m/\sec^2$$
$$\alpha = 0.99 \rightarrow \text{predictive control}$$
$$= 0.95 \text{ predictive control}$$
$$= 0.90 \text{ predictive control}$$

k_D = damper bracing stiffness = 3 × the building structure stiffness
Energy dissipation Ratios for three Earthquakes
El-Centro: PGA = 0.348 g (strong earthquake)
Kobe : PGA = 0.834 g (severe) 1 g = 9.8 m/s^2
Northridge: PGA = 0.843 g (severe)
R_d = energy dissipation ratio (%) = (E_1 = seismic input energy)/(F_D = Energy dissipated by the damper)

Table 5.5 indicates the masses up to 27 floors together with stiffness for each floor. The mass matrix [M] shall be 27 × 27 and [C] damping matrix and [K] stiffness matrix will be of the same order based on Table 5.5. The overall geometrical dimensions are not altered and are kept the same.

(b) Control for multiple friction dampers

Table 5.5 Comparison of energy dissipation ratios

Control method	Energy index	El-Centro (PGA = 0.348g)	Kobe (PGA = 0.834 g)	Northridge (PGA = 0.843 g)
Passive	E_1 (kN-m)	27.89	143.79	47.75
	F_D (kN-m)	15.81	115.39	35.76
	R_d (%)	56.70	80.25	75.37
Predictive	E_1 (kN-m)	21.82	129.25	53.95
α = 0.99	F_D (kN-m)	19.52	115.89	47.86
	R_d (%)	89.48	89.66	88.72
Predictive	E_1 (kN-m)	22.11	140.64	42.08
α = 0.95	F_D (kN-m)	17.17	109.29	32.67
	R_d (%)	77.66	77.71	77.63
Predictive	E_1 (kN-m)	22.07	142.23	38.10
α = 090	F_D (kN-m)	13.85	89.30	23.91
	R_d (%)	62.77	62.70	62.76

www.EngineeringBooksPDF.com

5.10 Non-linear Control of Earthquake Buildings with Actuators

5.10.1 Introduction

The actuators operate only when the velocity exceeds certain threshold values. They operate also in response to sensor signals at the same location. Normally in a controlled building one actuator is used on the base of the building and the other at its top.

The top position of an actuator is shown for the "Applause Tower" (Plate 5.1) as a typical example. Control performance of the AMD during earthquake in 1996 is to be looked at.

The structure is assumed to be base isolated.

The possibility of combining passive base isolation control systems and an active control system exerting control forces only on the base induces artificial damping without increasing stiffness to the isolated structure.

This section is concerned with a distributed-parameter structure mounted on a rigid base subjected to forces arising from ground motion during earthquakes.

5.10.2 Analysis Involving Actuators

The generalized equation of motion with dampers as given earlier can now be modified for this case. The right-hand side can be organized as follows:

$$M_s\ddot{u}_s + C_s\dot{u}_s + k_s u_s = Q_d + Q_c \tag{5.57}$$

where M_s, k_s, C_s, respectively, represent the n×n mass, stiffness and inherent structural damping matrices of this building structure. It is assumed that this building of a base-isolated structure consists of a distributed elastic structure clamped to a base in the form of a rigid slab capable of moving relative to the ground such that forces caused by ground motion are not transmitted to the base.

This means the base lies on a viscoelastic support modelled as a viscous damper and an elastic spring connected to the ground. Equations can now be treated as a single matrix equation which consists of two equations:

$$\begin{aligned} M_s\ddot{u}b + \phi^{T''}\ddot{u}_e + C_b\dot{u}b + K_b u_b &= C_b\dot{u}_g + K_b u_b + F \\ \phi\ddot{u}_b + M_e\ddot{u}_e + C_e\dot{u}_e + K_e u_e &= \bar{F}_{SW} + \bar{f}_c \end{aligned} \tag{5.58}$$

where

$$\begin{aligned} M_s &= \int_D \rho\phi\varphi^{T''}dD;\ c_b = \int_D \phi\,\phi^{T''}dD \\ k_b &= \int_D \phi\mathscr{L}\phi^{T''}dD \\ \bar{\phi} &= \int_D \rho\phi dD\ ;\ \bar{f}_c = \int_D \phi f_c dD \end{aligned} \tag{5.59}$$

www.EngineeringBooksPDF.com

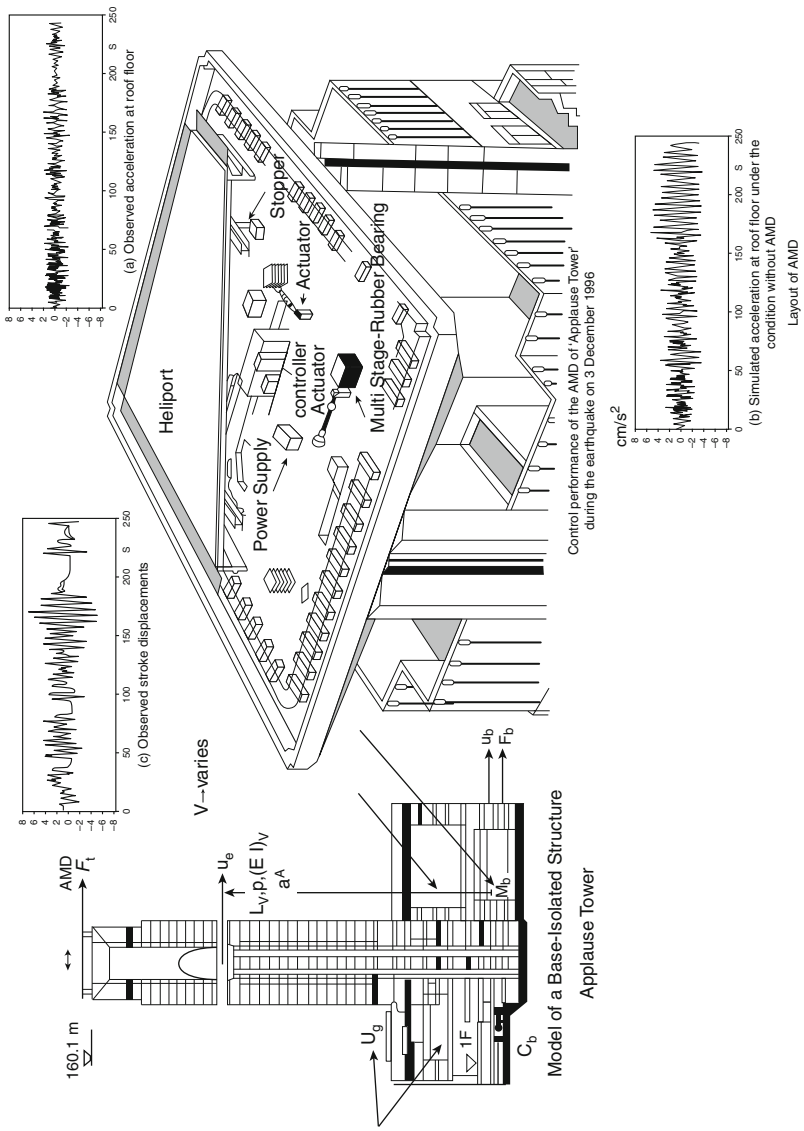


Plate 5.1 Applause tower
Note: Earthquake occuired on 3.12.1996 with compliments of moto institute, Tokyo, Japan
Also courtesy of Takenuka corp, Japan for Applause Tower compliments also from the owner Hanicyu Chayamachi Building owener (no address given)

www.EngineeringBooksPDF.com

Based on El-Centro earthquake, peak displacement u versus period is plotted in Plate 5.2 with and without dampers.

Peak displacement versus period

(a) The variation of the peak base displacement versus time period of the structure to the El-Centro earthquake excitation
(b) The variation of the peak base displacement versus time period of the structure to the Northridge earthquake excitation

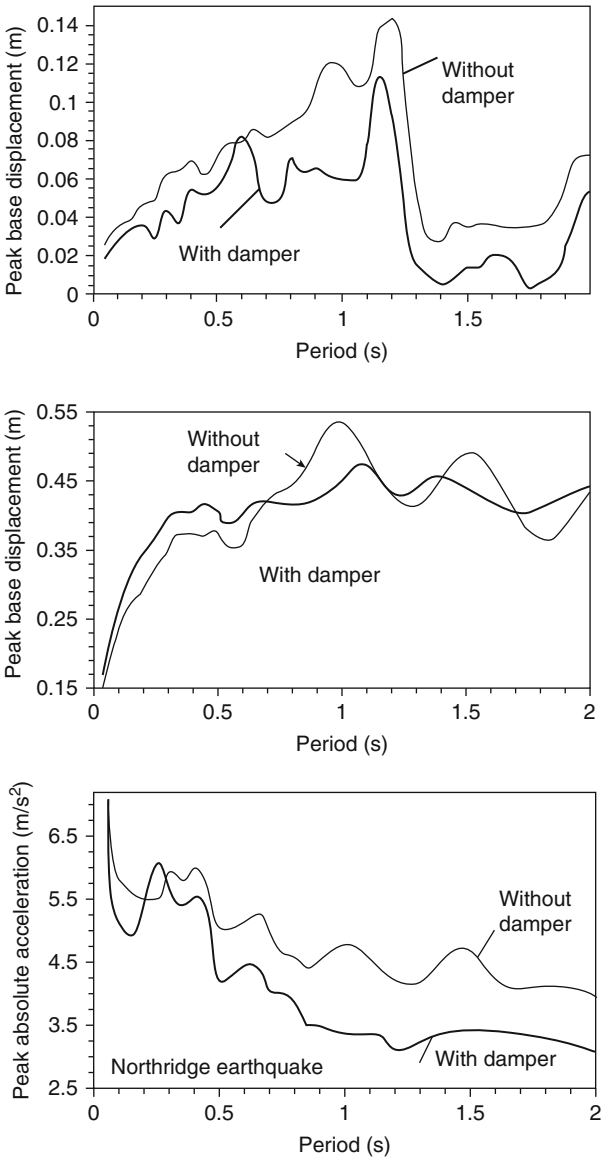


Plate 5.2 Displacement versus time; With and without dampers; Based on El-Centro earthquake

www.EngineeringBooksPDF.com

(c) The variation of the peak absolute acceleration of the superstructure versus time period of the structure to the Northridge earthquake excitation
(d) The comparison of peak absolute acceleration spectra of the superstructure versus time period of the structure with and without sliding
(e) The variation of the peak absolute acceleration of the superstructure versus time period of the structure to the El-Centro earthquake excitation.

5.10.2.1 Moments of Products of Inertia, Energies and Mass of Inertia

The moment and products of inertia with respect to the model centroid (the components of the inertia tensor) are

$$\begin{aligned} I'_{xx} &= I_{xx} - M\left[(Y_c)^2+(Z_c)^2\right] \\ I'_{yy} &= I_{yy} - M\left[(X_c)^2+(Z_c)^2\right] \\ I'_{zz} &= I_{zz} - M\left[(X_c)^2+(Y_c)^2\right] \\ I'_{xy} &= I_{xy} - MX_cY_c \\ I'_{yz} &= I_{yz} - MY_cZ_c \\ I'_{xz} &= I_{xz} - MX_cZ_c \end{aligned} \tag{5.60}$$

where typical terms are I'_{xx} = mass moment of inertia about the x axis through the model centroid and I'_{xy} = mass product of inertia with respect to the x and y axes through the model centroid.

It may be seen from the above development that only the mass (m_i) and the centroid (X_i, Y_i and Z_c) of each element are included. Effects which are not considered are

(a) the mass being different in different directions
(b) the presence of rotational inertia terms

Energies

Energies are available by setting

$$E_e^{po} = \begin{cases} \frac{1}{2}\sum_{i=1}^{NINT}\{\sigma\}^T\{\varepsilon^{el}\}\text{vol}_i + E_e^{pl} & \text{if element allows only displacement and rotational degree of freedom (DOF), and either is non-linear or uses integration points} \\ \frac{1}{2}\{u\}^T[K_e]\{u\} & \text{all other cases} \end{cases} \tag{5.61}$$

= potential energy

$$E_e^{ki} = \frac{1}{2}\{\dot{u}\}^T[M_e]\{\dot{u}\} \tag{5.62}$$

=kinetic energy

www.EngineeringBooksPDF.com

$$E_{\mathrm{e}}^{\mathrm{pl}} = \sum_{i=1}^{\mathrm{NINT}} \sum_{j=1}^{\mathrm{NCS}} \{\sigma\}^{\mathrm{T}} \{\Delta\varepsilon^{\mathrm{pl}}\} \, \mathrm{vol}_i \qquad (5.63)$$

$$= \text{plastic energy}$$

Mass Moments of Inertia

The computation of the mass moments and products of inertia as well as the model centroids is described in this section. The model centroids are computed as

$$\begin{aligned} X_c &= A_x/M \\ Y_c &= A_y/M \\ Z_c &= A_z/M \end{aligned} \qquad (5.64)$$

where typical terms are

$X_c = X$ coordinate of model centroid

$A_x = \sum_{i=1}^{N} m_i X_i$

$N =$ number of elements

$m_i =$ mass of element i

$X_i = X$ coordinate of the centroid of element i

$M = \sum_{i=1}^{N} m_i =$ mass of model centroid

The moments and products of inertia with respect to the origin are

$$I_{xx} = \sum_{i=1}^{N} m_i \left[(Y_i)^2 + (Z_i)^2 \right] \quad I_{zz} = \sum_{i=1}^{N} m_i \left[(X_i)^2 + (Y_i)^2 \right] \qquad (5.65)$$

$$I_{yy} = \sum_{i=1}^{N} m_i \left[(X_i)^2 + (Z_i)^2 \right] \quad I_{xy} = \sum_{i=1}^{N} m_i [(X_i)(Y_i)] \qquad (5.66)$$

$$I_{yz} = \sum_{i=1}^{N} m_i [(Y_i)(Z_i)] \qquad I_{xz} = \sum_{i=1}^{N} m_i [(X_i)(Y_i)] \qquad (5.67)$$

www.EngineeringBooksPDF.com

where typical terms are I_{xx} = mass moment of inertia about the x axis through the model centroid and I_{xy} = mass product of inertia with respect to the x and y axes through the model centroid.

5.11 Spectrum Analysis with Finite Element

This has been discussed earlier. The spectrum analysis is an extension to the pervious work and is written in a generalized term.

Spectrum analysis is an extension of the mode frequency analysis, with both base and force excitation options. The base excitation option is generally suitable for seismic and wave applications. A direction vector and a response spectrum table will be needed in addition to the data and parameters required for the reduced modal analysis. The response spectrum table generally includes displacements, velocities and accelerations. The force excitation is, in general, used for wind and space structures and missile/aircraft impact. It requires a force distribution and an amplitude multiplier table in addition to the data and parameters needed for the reduced modal analysis. A study of the mass distribution is made. Generally the masses are kept close to the reaction points on the finite element mesh rather than the (master) degrees of freedom. It is important to calculate the participation factors in relation to a given excitation direction. The base and forced excitations are given below:

$$\tilde{\gamma}_{\mathrm{i}} = \{\psi_i\}_{\mathrm{R}}^{\mathrm{T}''}[\mathrm{M}]\left\{\tilde{b}\right\} \text{ for the base excitation} \tag{5.68}$$

$$\tilde{\gamma}_i = \{\psi_i\}_{\mathrm{R}}^{\mathrm{T}''}\{F_{\mathrm{t}}\} \text{for the force excitation} \tag{5.69}$$

where $\left\{\tilde{b}\right\}$ = the unit vector of the excitation direction and $\{F_t\}$ = an input force vector.

The values of $\{\psi\}_R$ are normalized, and the reduced displacement vector is calculated from the eigenvector by using a mode coefficient $\tilde{M}$.

$$\{\tilde{u}\}_i = \left\{\tilde{M}_i\right\}\{\psi\}_i \tag{5.70}$$

where $\{\tilde{u}\}_i$ = reduced displacement vector and $[\tilde{M}_i]$ = the mode coefficient and where (a) for velocity spectra

$$\left[\tilde{M}_i\right] = \frac{[V_{si}]\{\tilde{\gamma}_i\}}{w_i} \tag{5.71}$$

(V_{si} = spectral velocity for the ith mode); (b) for force spectra

$$\left[\tilde{M}_i\right] = \frac{\left[\bar{f}_{si}\right]\{\tilde{\gamma}_i\}}{w_i^2} \tag{5.72}$$

www.EngineeringBooksPDF.com

($\bar{f}_{si}$ = spectral force for the ith mode); (c)

$$\left[\tilde{M}_i\right] = \frac{[a_{si}]\{\tilde{\gamma}_i\}}{w_i^2} \tag{5.73}$$

(a_{si} = spectral acceleration for the ith mode); (d)

$$\left[\tilde{M}_i\right] = \frac{[U_{si}]\{\tilde{\gamma}_i\}}{w_i^2} \tag{5.74}$$

(U_{si} = spectral displacement for the ith mode).
$\{U\}_i$ may be expanded to compute all the displacements, as was done in the case of superelement and substructuring of the equation.

$$\left[\frac{K}{K_R^{T''}}\right]\left[\frac{K_R}{K_{RR}}\right] \tag{5.75}$$

as was done above.

$$\{U\gamma'\}_i = [K\gamma', \gamma']^{-1}[K\gamma', \gamma]\{U_i\}_R \tag{5.76}$$

where $\{U\gamma'\}_i$ = the slave degree of freedom vector of mode i and $[K\gamma', \gamma']$, $[K\gamma', \gamma]$ = submatrix parts.
Sometimes an equivalent mass M_{ei} is needed for the ith mode since it may not be a function of excitation direction. This M_i^e is computed as

$$\left[M_i^e\right] = 1/\{\psi_i\}_R^{T''}\{\psi_i\}R \tag{5.77}$$

This is derived from the definition of the diagonal matrix of equivalent masses $[M^{\mathrm{e}}]$

$$[\psi]_R^{T''}\left[M^R\right][u]R = [I] \tag{5.78}$$

where $[I]$ = the identity matrix and $[\psi]_{\mathrm{R}}$ = a square matrix containing all mode shape vectors.

Where damping is included, the damping ratio $D_{\mathrm{R}i}$ for the data input, including damping C_{e}, is given for a matrix of coupling coefficient as

$$D_{Ri} = C_e w_i/2 \tag{5.79}$$

where ω_i is the undamped natural frequency of the ith mode.

In between the modes i and j, a modified damping ratio is needed to take into account the concrete structures subjected to wave and seismic effects.

$$D'_{Ri} = D_{Ri} + 2/t_e w_i \tag{5.80}$$

where t_{e} is the duration and T$''$ is transpose.

www.EngineeringBooksPDF.com

5.11.1 Calculation by Quadratic Integration

When the velocity varies linearly and the acceleration is constant across the time interval, appropriate substitutions are made into (A.34) giving
where f_1 , f_2 , f_3, = functions of time.

This results in an implicit time integration procedure. The only unknown is $\{u_t\}$ at each time point and this is calculated in the same way as in static analysis. Equation is then written as

$$\begin{aligned}&\left(\frac{2}{\Delta t_0 \Delta t_{01}}[m_0] + \frac{2\Delta t_0 + \Delta t}{\Delta t_0 \Delta t_{01}}[e] + [k_t]\right) u_t \\ &= \{F(t)\} + [ms]\left(-\frac{2}{\Delta t_0 \Delta t_1}\{u_{t-1}\} - \frac{2}{\Delta t_0 \Delta t_1}\{u_{t-2}\}\right) \\ &+ [c_t]\left(\frac{\Delta t_0}{\Delta t_0 \Delta t_1}\{u_{t-1}\} - \frac{\Delta t_0}{\Delta t_0 \Delta t_1}\{u_{t-2}\}\right)\end{aligned} \tag{5.81}$$

Where

$\Delta t_0 = t_0 - t_1$ t_0 = time of current iteration
$\Delta t_1 = t_1 - t_2$ t_1 = time of previous iteration
$\Delta t_2 = t_2 - t_3$ t_2 = time before previous iteration
t_3 = time before t_2
$\Delta t_2 = \Delta t_0 + \Delta t_1 = t_0 - t_2$

5.11.2 Calculation by Cubic Integration

Equation (5.82) becomes cubic and hence is written as

$$\begin{aligned}(a_1([m_0] + a_2[c_t] + [k_t])\{u_t\} &= \{F_1(t)\} \\ &+ [m_0](a_3\{u_{t-1}\}) - a_4\{u_{t-2}\} + a_5\{u_{t-3}\} \\ &+ [c_t](a_6\{u_{t-1}\} - a_7\{u_{t-2}\} + a_8\{u_{t-3}\})\end{aligned} \tag{5.82}$$

where a_1 to a_8 are functions of the time increments; these functions are derived by inverting a 4×4 matrix.

For clear-cut solutions, the size of the time step between adjacent iterations should not be more than a factor of 10 in non-linear cases and should not be reduced by more than a factor of 2 where plasticity exists.

5.11.3 Cubic Integration

$$\begin{aligned}&\left(\tfrac{2}{\Delta t^2}[ms]_R + \tfrac{1}{6\Delta t}[+k_t]_R\right)\{u_t\} = \{F(t)\} \\ &\quad + [ms]_R \tfrac{1}{\Delta t^2}\left(5\{u_{t-1}\}_R - 4\{u_{t-2}\}_R + \{u_{t-2}\}\right) \\ &\quad + [C_t]_R \tfrac{1}{\Delta t^2}\left(3\{u_{t-1}\}_R + \tfrac{3}{2}\{u_{t-2}\}_R + \tfrac{1}{3}\{u_{t-3}\}_R\right)\end{aligned} \tag{5.83}$$

www.EngineeringBooksPDF.com

5.11.4 Mode Frequency Analysis using Finite Element

The equation of motion for an undamped structure with no applied forces is written as

$$[M]\{\ddot{u}\} + [K_t']\{U_t\} = 0 \tag{5.84}$$

$[K_t']$ the structure stiffness matrix may include stress-stiffening effects. The system of equations is initially condensed down to those involved with the master (dynamic) degrees of freedom.

The number of dynamic degrees of freedom should at least be equal to two times the selected frequencies. The reduced form can be written as

$$[M]_R\{\dot{U}_t\}_R + [K_t']_R\{U_t\}_R = 0 \tag{5.85}$$

For a linear system, free vibrations of harmonic type are written as

$$\{u_t\}_R = \{\psi_i\}_R \cos w_i t \tag{5.86}$$

where $\{\psi_i\}R$ = the eigenvector representing the shape of the ith frequency; ω_i = the ith frequency (radians/unit time) and t = time.
Equation (5.86) assumes the form

$$\left(-\omega_i^2[M]_R + [K_t^1]_R\{\psi_i\}_R\right) = \{0\} \tag{5.87}$$

which is an eigenvalue problem with n values of ω^2 and n eigenvectors $\{\psi_i\}_R$ which satisfy Eq. (5.88), where n is the number of dynamic degrees of freedom. Using standard iteration procedures, () will yield a complete set of eigenvalues and eigenvectors.
Each eigenvector $\{\psi_i\}_R$ is then normalised such that:

$$\{\psi_i\}_R^{T''}[M]_R\{\psi_i\}_R = 1 \tag{5.88}$$

These n eigenvectors are now expanded to the full set of structure modal displacement degrees of freedom.

$$\{\psi_{\gamma' i}\}_R = \left[K_{\gamma'\gamma'}\right]^{-1}\left[K_{\gamma'\gamma}\right]\{\gamma_i\}_R \tag{5.89}$$

where $\{\psi_t\}_R$ = the slave degree of freedom vector of mode i and $\left[K_{\gamma'\gamma'}\right]$, $\left[K_{\gamma'\gamma}\right]$ are the submatrix parts.

The above dynamic analysis approach is generally adopted for structures subjected to normal dynamic loads, wind, wave and seismic loads. The above analysis, with modifications, is also applied to missile and aircraft explosions/

www.EngineeringBooksPDF.com

impact problems. Various steps need to included in the finite element analysis using the above concept.

Initialization

(1) Effective stiffness matrix

$$\left[K_0^*\right] = \left(6/6\tau^2\tau^2\right)[M] + (3/3\tau\tau)[C_0] + [K_0] \tag{A}$$

(2) Triangularize $\left[K_0^*\right]$

For each time step:

Calculation of displacement $\{U_{t+\tau}\}$

(1) Constant part of the effective load vector

$$\begin{aligned}\left\{R_{t+\tau}^*\right\} =& \{R_t\} + \theta(\{R_{t+\Delta t}\} - \{R_t\}) + \{F_t\} = [M] \\ &\times \left(\left(\frac{6}{\tau^2}\right)\{U_t\} + \frac{6}{\tau}\left\{\dot{U}_t\right\} + 2\left\{\ddot{U}_t\right\}\right) \\ &+ [C_0]\left(\frac{3}{\tau}\{U_t\} + 2\left\{\dot{U}_t\right\} + \frac{\tau}{2}\{U_t\} +\right)\end{aligned} \tag{B}$$

(2) Initialization $i = 0$, $\left\{\Delta P_{t\to t+\tau}^i\right\} = 0$

(3) Iteration

(a) $i \to i + 1$

(b) Effective load vector

$$\left\{R_{t+\tau TOT}^*\right\} = \left\{R_{t+\tau}^*\right\} + \left\{\Delta P_{t\to t+\tau}^{i-1}\right\} \tag{C}$$

(c) Displacement

$$\left\{U_{t+\tau}^i\right\}\left[K_0'\right]\left\{U_{t+\tau}^i\right\} = \left\{R_{t+\tau TOT}^*\right\} \tag{D}$$

(d) Velocity $\left\{U_{t+\tau}^2\right\} + (3/3\tau)\left(\left\{U_{t+\tau}^i\right\} - \{U_t\}\right) - 2\left\{\dot{U}_t\right\} - (\tau/2)\left\{\ddot{U}_t\right\}$

(e) Change of initial load vector caused by the non-linear behavious of the material $\left\{\Delta P_{t\to t+\tau}^i\right\}$

$$\begin{aligned}\left\{P_{t\to t+\tau}^i\right\} = &-[\Delta C_{0\to t}]\left(\left\{\dot{U}_{t+\tau}^i\right\} - \left\{\dot{U}_t\right\}\right) - \left\{\Delta C_{t\to t+\tau}^i\right\}\left\{\dot{U}_{t+\tau}^i\right\} \\ &\times[\Delta K_{0\to t}]\left(\left\{U_{t+\tau}^i\right\} - \{U_t\}\right) - \left\{\Delta K_{t\to t+\Delta t}^i\right\}\left\{U_{t+\tau}^i\right\}\end{aligned} \tag{E}$$

In fact, $\left\{\Delta P_{t\to t+\tau}^i\right\}$ is calculated using the initial stress method.

(f) Iteration convergence

$$\left\|\left\{\Delta P_{t\to t+\tau}^i\right\} = \left\{\Delta P_{t\to t+\tau}^{i-1}\right\}\right\| / \left\|\left\{\Delta P_{t\to t+\tau}^i\right\}\right\| < \text{toI} \tag{F}$$

or analogously, on stresses.

www.EngineeringBooksPDF.com

Note: $\{P\}$ could be any value of $\{F\}$.

Calculation of velocity, acceleration

Calculate new acceleration $\{\ddot{U}_{t+\Delta t}\}$, velocity $\{\dot{U}_{t+\Delta t}\}$, displacement $\{U_{t+\Delta t}\}$ and initial load $\{P_{t+\Delta t}\}$

$$\begin{aligned}[M]\{\ddot{U}_{t+\Delta t}\} + [C_0]\{U_{t+\Delta t}\} + [K_0]\{U_{t+\Delta t}\} \\ = \{R_{t+\Delta t}\} + \{P_t\} + \{\Delta P_{t\to t+\Delta t}\}\end{aligned} \tag{G}$$

$\{\Delta P_{t\to t+\Delta t}\}$ represents the influence of the nonlinearity during the time increment and is determined by iteration and satisfied for $t+\tau$, where $\tau = \theta\Delta t$ ($\theta > 1.37$ for an unconditionally stable method) applied to a linear problem. $[\Delta C_{0\to t}]$ and $[\Delta K_{0\to t}]$ represent the change of [C] and [K], respectively, from $t = 0$ to t.

To obtain the solution at time $t+\Delta t$, ( ) can be written as

$$\begin{aligned}[M]\{\ddot{U}_{t+\Delta t}\} + [C_0]\{U_{t+\Delta t}\} + [K_0]\{U_{t+\Delta t}\} \\ = \{R_{t+\Delta t}\} + \{F_t\} + \{\Delta F_{t\to t+\Delta t}\}\end{aligned} \tag{H}$$

$\{\Delta P_{t\to t+\Delta t}\}$ represents the influence of the nonlinearity during the time increment and is determined by iteration

$$\begin{aligned}\{\Delta P_{t\to t+\Delta t}\} = &- [\Delta C_{0\to t}]\{\Delta U_{t\to t+\Delta t}\} \\ &- [\Delta C_{t\to t+\Delta t}](\{U\} + \{\Delta U_{t\to t+\Delta t}\}) \\ &- [\Delta K_{0\to t}]\{\Delta U_{t\to t+\Delta t}\} \\ &- [\Delta K_{t\to t+\Delta t}](\{U_t\} + \{\Delta U_{t\to t+\Delta t}\})\ \ (I)\end{aligned} \tag{I}$$

$\{\Delta P_{t\to t+\Delta t}\}$ is calculated using the initial stress approach.

A modified Newton–Raphson or initial stress approach is adopted for solving these non-linear equations.

Reduced Linear Transient Dynamic Analysis

This is a reduced form of non-linear transient dynamic analysis. This analysis is carried out faster than the non-linear analysis since the matrix in such a case the matrix requires to be inverted once, and the analysis is reduced to a series of matrix multiplications and essential degrees of freedom (dynamic or master of freedoms) to characterize the response of the system.

Quadratic Integration

$$\begin{aligned}\left(\frac{1}{\Delta t^2}[M]_R + \frac{3}{2\Delta t}[C_t]_R + [K_t]_R\right)\{U_t\} &= \{F(t)\}_R \\ &+ [M]_R \frac{1}{\Delta t^2}(2\{U_{t-1}\}_R - \{U_{t-2}\}_R) \\ &+ \frac{1}{\Delta t}\left(2\{U_{t-1}\}_R - \frac{1}{2}\{U_{t-2}\}_R\right)\end{aligned} \tag{5.90}$$

The symbol R represents reduced matrices and vectors.

www.EngineeringBooksPDF.com

5.11.5 Dynamic Analysis: Time-Domain Technique

Dynamic analysis is a subject by itself. In this text a specific approach to the dynamic analysis of structures is discussed. The equations of motion are discretized in time. The direct integration technique and the Wilson-θ method are summarized. Where dynamic problems are tackled, the non-linear equations of motion (coupled or uncoupled) have been solved using these methods.

The dynamic equilibrium at the nodes of a system of structural elements is formulated at a given time t as

$$[M]\{\ddot{U}_t\} + [C_1]\{\dot{U}_t\} + K_t^1\{U_t\} = \{R_t\} \tag{5.91}$$

where $\{U_t\}$ and $\{R_t\}$ are the vectors of displacement and specified load, respectively. $[M]$ represents the mass matrix which is regarded as constant; $[C_t]$ and $\left[K_t^1\right]$ are the damping and stiffness matrices, respectively. The subscript t is used for quantities at time t and a dot denotes a derivative with respect to time.

To formulate Eq. (5.92), discretization with respect to time, using isoparametric finite elements, is performed. The simple applicable method is the numerical step-by-step integration of the coupled equations of motion. The response history is divided into time increments Δt, which are of equal length. The system is calculated for each Δt with properties determined at the beginning of the interval. Only one matrix based on M is excited. In addition, the direct integration technique allows a general damping matrix $[C_t]$ (which has to be specified explicitly) to be used without resorting to complex eigenvalues.

Discretization in the Time Domain

The equation of motion formulated at time $t = 0$ is written in the form

$$[M]\{\ddot{U}_0\} + [C_0]\{0\} + K_0^1\{U_0\} = \{R_0\} \tag{5.92}$$

where the subscript zero has been introduced. At time t, all quantities are known. Equation (?) is specified as

$$[Ms]\{\ddot{U}_t\} + [C_0] + [\Delta C_{0\to t}]\{\ddot{U}_t\} + \left[K_0^1\right] + [\Delta K_{0\to t}]\{U_t\} = \{R_t\} \tag{5.93}$$

or as

$$[Ms]\{\ddot{U}_t\} + [C_0]\{\dot{U}_t\} + K_0\{U_t\} = \{R_t\} + \{P_t\}\{F\}_t \tag{5.94}$$

where the initial load $\{P_t\}$ is specified by

$$\{P_t\} = -[\Delta C_{0\to t}]\{\dot{U}_t\} - [\Delta K_{0\to t}]\{\delta_t\} \tag{5.95}$$

To obtain the solution at time $t + \Delta t$ the equation is formulated as in Table 5.4.

www.EngineeringBooksPDF.com

5.11.5.1 Time History Method

Introduction

Two methods, namely equivalent force method and response spectrum method, have been explained in detail in the text. In Example 4.11 under case study 4.1, these methods have been supported by evaluation of equations. This example is now analysed using time history method. The dynamic response of the same plane frame given in Fig. 4.50 with the same infills to a specified time history compatible to EC-8 spectrum for 5% damping at the same rocky hard soil is examined. A hand calculation giving a step-by-step procedure for the analysis of the building frame by the time history using Tedesco et al. method is given in "Structure Dynamics – Theory and Applications, Addison-Wesley Longman 1999, Tedesco, J.W., McDougal, W.G. and Ross, C.A."

The same method and solutions are programmed in ISOPAR-BLAST under sub-program VUSAP-1. The following are the steps of this program.

Step 1: Modal Matrix Evaluation

The equation of motion for a multi-degree-of-freedom system produced in the text in many places is now reproduced as below to suit the analysis:

$$[M]\{\ddot{U}\} + [C]\{\dot{U}\} + [k_0]\{U\} = \{-\ddot{U}\}(t)[M]\{I\} \tag{5.96}$$

where $[M]$,$[K]$,[I],$\{I\}$ and $\{\ddot{U}_g\}$, respectively, are mass matrix, stiffness matrix, damping matrix, unit or identity matrix and ground acceleration.

The solution of equation of motion for any specified forces is difficult to obtain, mainly due to coupling of the variables $\{x\}$ in the physical coordinates. In mode superposition analysis or a modal analysis a set of normal coordinates, i.e. principal coordinates, are defined, such that, when expressed in those coordinates, the equations of motion become uncoupled. The physical coordinates $\{U\}$ may be related with normal or principal coordinates $\{g\}$ from the transformation expression as

$$\{U\} = [\Phi]\{q\} \quad [\Phi] \text{ is th modal matrix,} \tag{5.97}$$

Time derivatives of $\{U\}$ are

$$\{\dot{U}\} = [\Phi]\{\dot{q}\}; \quad \{\ddot{U}\} = [\Phi][\ddot{q}]$$

Substituting the time derivatives in the equation of motion and pre-multiplying by $[\Phi]^T$ results in

$$\begin{aligned}&[\Phi]^T[M][\Phi]\{\ddot{q}\} + [\Phi]^T[C][\Phi]\{\dot{q}\} + [\Phi]^T[K][\Phi]\{q\}\\ &= \left(-\ddot{U}_g(t)[\Phi]^T[M]\{I\}\right) + \{R_t\}\{P_t\}\end{aligned} \tag{5.98}$$

www.EngineeringBooksPDF.com

More clearly it can be represented as follows:

$$[M]\{\ddot{q}\} + [C]\{\dot{q}\} + [k]\{q\} = \{F_{\text{eff}}(t)\} \tag{5.99a}$$

where

$$[M] = [\Phi]^T[\mathrm{M}][\Phi] \tag{5.99b}$$

$$[C] = [\Phi]^T[C][\Phi] \tag{5.99c}$$

$$[K] = [\Phi]^T[k][\Phi] \tag{5.99d}$$

$$\{F_{\text{eff}}(t)\} = \left(-\ddot{U}_g(t)[\Phi]^T[M]\{I\}\right) + \{R_t\} + \{P_t\} \tag{5.100}$$

$[M]$, $[K]$ and $[C]$ are the diagonalized modal mass matrix, modal damping matrix and modal stiffness matrix, respectively, and $\{F_{\text{eff}}(t)\}$ is the effective modal force vector.

Mass and stiffness matrices are given as under

$[K]$ is the same as (4.8)

$[M]$ is the mass matrix derived in (4.78)

They are reproduced by sub-program of program ISOPAR from

$$\begin{aligned} K &= \begin{bmatrix} k_1 + k_2 & -k_2 & 0 & 0 \\ -k_2 & k_2 + k_3 & -k_3 & 0 \\ 0 & -k_3 & k_3 + k_4 & -k_4 \\ 0 & 0 & -k_4 & k_4 \end{bmatrix} \\ &= \begin{bmatrix} 1.2674 & -0.6337 & 0 & 0 \\ -0.6337 & 1.2674 & -0.6337 & 0 \\ 0 & -0.6337 & 1.2674 & -0.6337 \\ 0 & 0 & -0.6337 & 0.6337 \end{bmatrix} \times 10^6\,\text{kN/m} \end{aligned} \tag{5.101}$$

$$M = \begin{bmatrix} M_1 & 0 & 0 & 0 \\ 0 & M_2 & 0 & 0 \\ 0 & 0 & M_3 & 0 \\ 0 & 0 & 0 & M_4 \end{bmatrix} = \begin{bmatrix} 64.450 & 0 & 0 & 0 \\ 0 & 64.450 & 0 & 0 \\ 0 & 0 & 64.450 & 0 \\ 0 & 0 & 0 & 37.080 \end{bmatrix} \text{kN} \tag{5.102}$$

Natural frequencies and mode shape for the plane frame model

$$[\omega] = \begin{bmatrix} 37.975 & 0 & 0 & 0 \\ 0 & 108.157 & 0 & 0 \\ 0 & 0 & 161.947 & 0 \\ 0 & 0 & 0 & 191.621 \end{bmatrix} \text{rad/s}; \tag{5.103}$$

www.EngineeringBooksPDF.com

$$T = \begin{bmatrix} 0.1655 & 0 & 0 & 0 \\ 0 & 0.0581 & 0 & 0 \\ 0 & 0 & 0.0388 & 0 \\ 0 & 0 & 0 & 0.0328 \end{bmatrix} \text{Seconds}$$

$$\Phi_1 = \begin{bmatrix} -0.0328 \\ -0.0608 \\ -0.0798 \\ -0.0872 \end{bmatrix}, \Phi_2 = \begin{bmatrix} 0.0795 \\ 0.0644 \\ -0.0273 \\ -0.0865 \end{bmatrix}, \Phi_3 = \begin{bmatrix} 0.0808 \\ 0.0540 \\ -0.0448 \\ 0.0839 \end{bmatrix}, \Phi_4 = \begin{bmatrix} -0.0397 \\ 0.0690 \\ -0.0799 \\ 0.0696 \end{bmatrix}, \quad (5.104)$$

as in Example 4.5.11, Cass study 4.1, matrix $\{\Phi\}$.

Therefore, $[M]$, $[K]$ and $[C]$ are, while using equations (5.101b to 5.101d)

$$[M] = [\Phi]^T[M][\Phi] = \begin{bmatrix} 1 & 0 & 0 & 0 \\ 0 & 1 & 0 & 0 \\ 0 & 0 & 1 & 0 \\ 0 & 0 & 0 & 1 \end{bmatrix} \quad (5.105)$$

$$[K] = [\Phi]^T[k][\Phi] = \begin{bmatrix} 1442 & 0 & 0 & 0 \\ 0 & 11698 & 0 & 0 \\ 0 & 0 & 126227 & 0 \\ 0 & 0 & 0 & 36719 \end{bmatrix} \quad (5.106)$$

$$[C] = \text{diag}(2M_r\zeta_r\omega_r) = \begin{bmatrix} 3.7975 & 0 & 0 & 0 \\ 0 & 10.815 & 0 & 0 \\ 0 & 0 & 16.1947 & 0 \\ 0 & 0 & 0 & 19.1621 \end{bmatrix} \quad (5.107)$$

where Φ_{ik} = mode shape coefficient at floor i in mode k.

Step 2: Calculation of effective force vector

The excitation function is

$$\{F_{\text{eff}}(t)\} = \left(-\ddot{U}_g(t)[\Phi]^T[M]\{I\}\right) \text{ or } \left(-\ddot{U}_g(t)\Gamma_r\right)$$
$$\Gamma_r = \frac{\{\Phi\}_r^T[M]\{I\}}{\{\Phi\}_r^T[M]\{\Phi\}_r} = \frac{\{\Phi\}_r^T[M]\{I\}}{M_r} \quad (5.108)$$

www.EngineeringBooksPDF.com

Modal participation factors for th plane frame are $\Gamma_r = \begin{bmatrix} -14.40 \\ 4.30 \\ 1.95 \\ -0.68 \end{bmatrix}$, (5.109)

$$\{F_{\text{eff}}(t)\} = \left(-\ddot{U}_g(t)[\Phi]^T[M]\{I\}\right) = \begin{Bmatrix} -14.40 \\ 4.30 \\ 1.95 \\ -0.68 \end{Bmatrix}, \tag{5.110}$$

The compatible time history $\left\{\ddot{U}_g(t)\right\}$ as per spectra of EC-8 for 5% damping at rocky soil strata is given in Fig. 5.7.

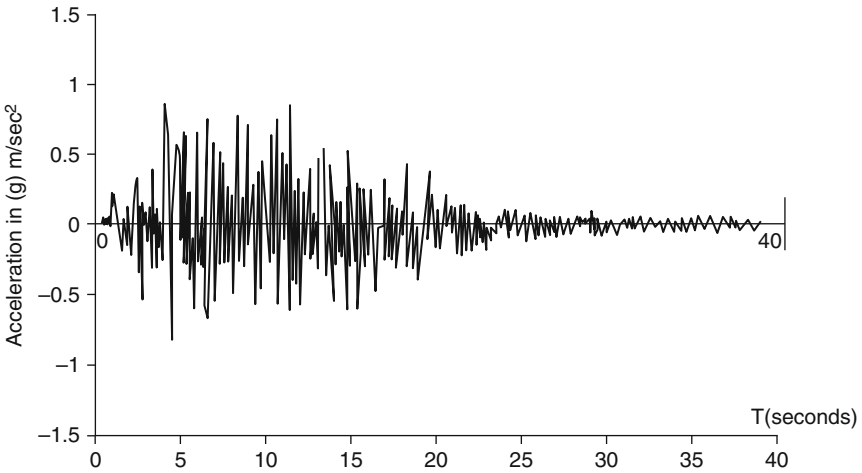


Fig. 5.7 Time history per EC-8 spectra (5% damping)

Step 3: Calculation of displacement response in normal coordinates

The uncoupled equations in the normal coordinates are

$$\begin{aligned} \ddot{q}_{10} + 3.9795\dot{q}_{10} + 1442q_{10} &= 14.40\ddot{U}_g(t) \quad \text{(a)} \\ \ddot{q}_{20} + 10.815\dot{q}_{20} + 11698q_{20} &= -4.30\ddot{U}_g(t) \quad \text{(b)} \\ \ddot{q}_{30} + 16.1947\dot{q}_{30} + 26227q_{30} &= -1.95(t) \quad \text{(c)} \\ \ddot{q}_{40} + 19.1621\dot{q}_{40} + 36719q_{40} &= 0.68\ddot{U}_g(t) \quad \text{(d)} \end{aligned} \tag{5.111}$$

This displacement response is normal coordinates can be computed from numerical methods started in the text. One of such methods is "piece wise linear

www.EngineeringBooksPDF.com

interpretation method" to evaluate the response of lined system developed in program ISOPAR (Figs. 5.8, 5.9, 5.10, and 5.11).

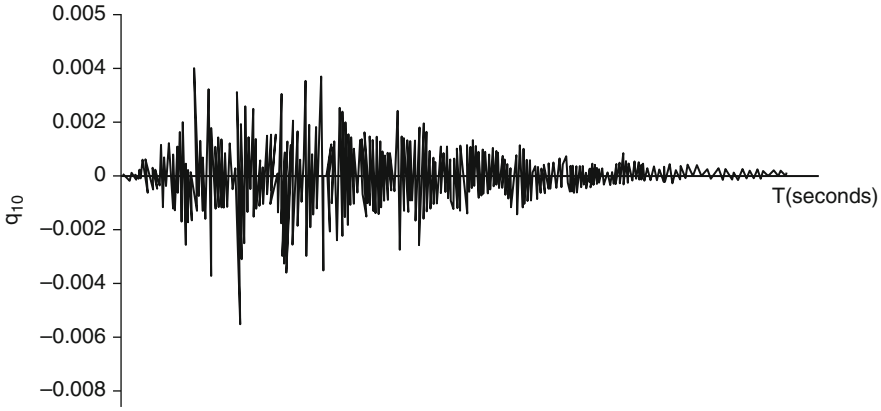


Fig. 5.8 Response history in q_{10} normal coordinates (displacement response)

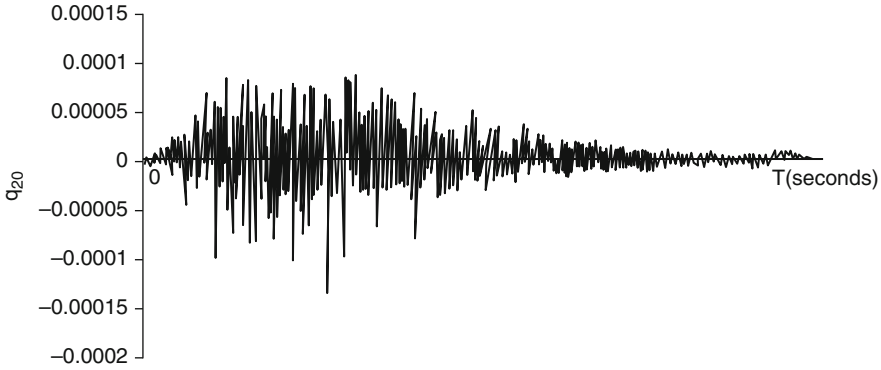


Fig. 5.9 Response history in q_{20} normal coordinates (displacement response)

Step 4: Displacement response in physical coordinates

Displacement response in physical coordinates $\{U\}$ is calculated from the transformation expression.

$$\{U_t\} = \sum_{r=1}^{n} \{\Phi\}_r q_r(t) \tag{5.112}$$

www.EngineeringBooksPDF.com

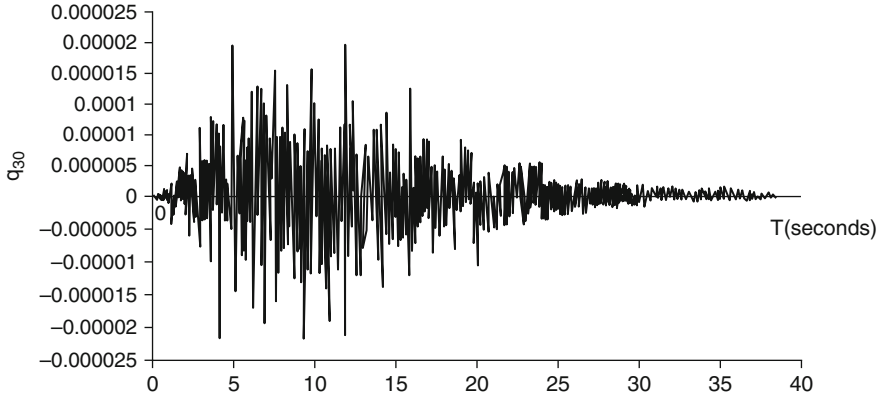


Fig. 5.10 Response history in q_{30} normal coordinates (displacement response)

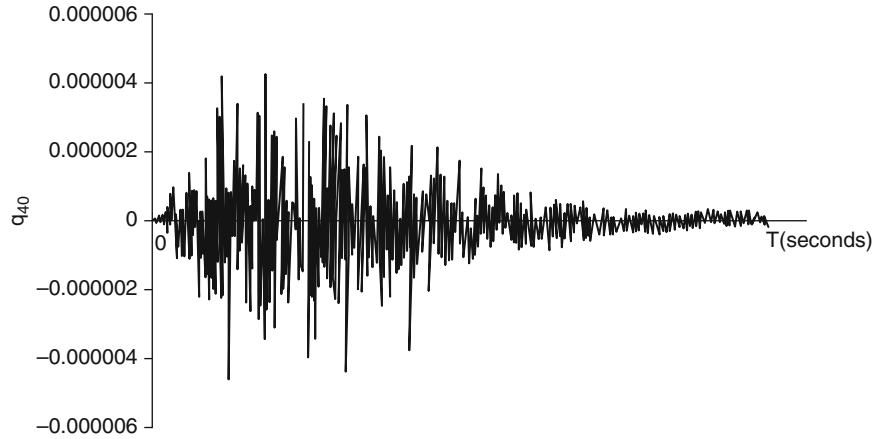


Fig. 5.11 Response history in q_{20} normal coordinates (displacement response)

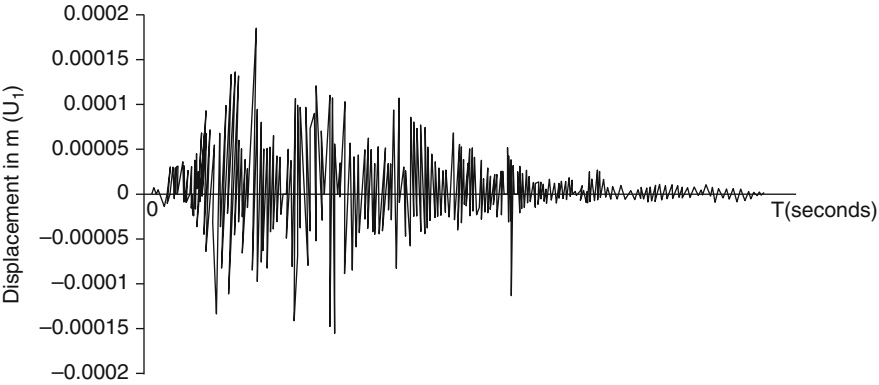


Fig. 5.12 First-storey displacement response in physical coordinates

www.EngineeringBooksPDF.com

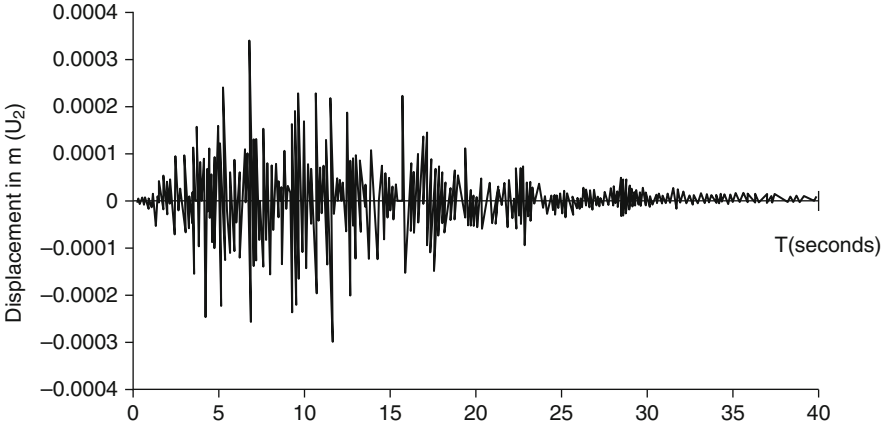


Fig. 5.13 Second-storey response displacement history in physical coordinates

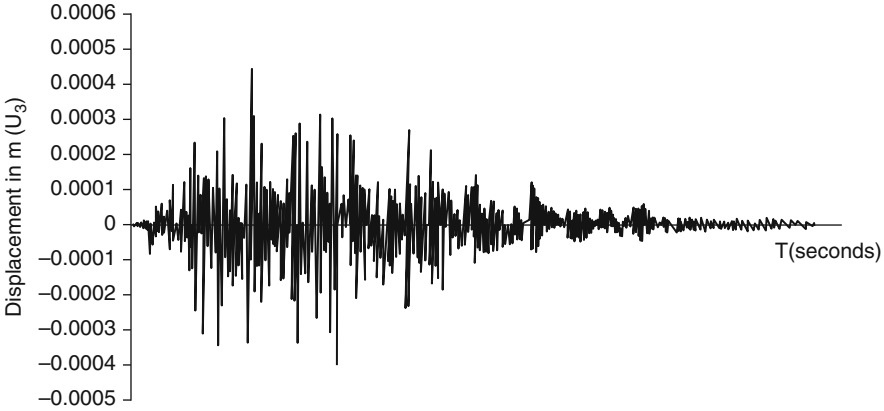


Fig. 5.14 Third-storey response displacement history in physical coordinates

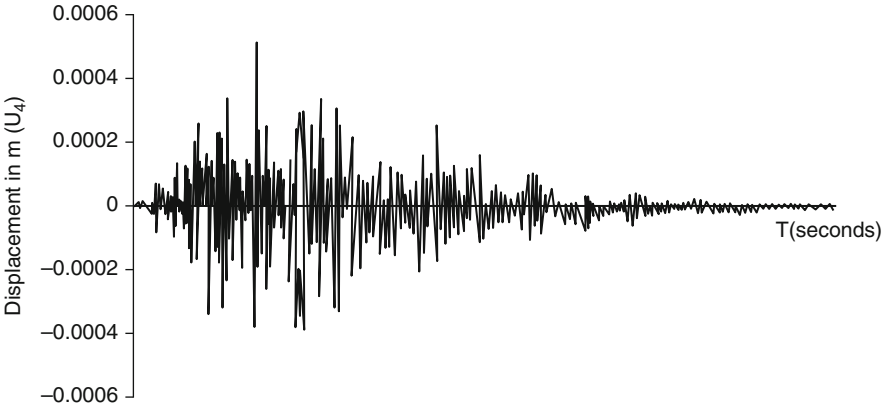


Fig. 5.15 Fourth-storey response displacement history in physical coordinates

www.EngineeringBooksPDF.com

$$\{U_t\} = \sum_{r=1}^{n} \{\Phi\}_r q_r(t) = \{\Phi\}_1 q_{10}(t) + \{\Phi\}_2 q_{20}(t) + \{\Phi\}_3 q_{30}(t) + \{\Phi\}_4 q_{40}(t)$$

$$= \begin{Bmatrix} -0.0328 \\ -0.0608 \\ -0.0798 \\ -0.0872 \end{Bmatrix} q_{10}(t) + \begin{Bmatrix} 0.0795 \\ 0.0644 \\ -0.0448 \\ -0.0839 \end{Bmatrix} q_{20}(t) + \begin{Bmatrix} 0.0808 \\ -0.0540 \\ -0.0448 \\ 0.0839 \end{Bmatrix} q_{30}(t) + \begin{Bmatrix} -0.0397 \\ 0.0690 \\ -0.0799 \\ 0.0696 \end{Bmatrix} q_{40}(t) \tag{5.113}$$

$$= \begin{Bmatrix} (-0.0328)q_{10}(t) + (0.0795)q_{20}(t) + (0.0808)q_{30}(t) + (-0.0397)q_{40}(t) \\ (-0.0608)q_{10}(t) + (0.0644)q_{20}(t) + (-0.0540)q_{30}(t) + (-0.0690)q_{40}(t) \\ (-0.0798)q_{10}(t) + (-0.0273)q_{20}(t) + (-0.0448)q_{30}(t) + (-0.0799)q_{40}(t) \\ (-0.0872)q_{10}(t) + (0.0865)q_{20}(t) + (0.0839)q_{30}(t) + (0.0696)q_{40}(t) \end{Bmatrix}$$

Step 5: Calculation of effective earthquake response forces at each storey

When the relative displacements of the masses $\{U_t\}$ have been established, the effective earthquake forces or the elastic restoring forces $F_s(t)$ acting at each mass M_i are determined from

$$\{F_s(t) = [k]\{U_t\}\}$$

$$= \begin{bmatrix} 1.2674 & -0.6337 & 0 & 0 \\ -0.6337 & 1.2674 & -0.337 & 0 \\ 0 & -6.337 & 1.2674 & -0.6337 \\ 0 & 0 & -0.6337 & 0.6337 \end{bmatrix} \times 10^6 \begin{Bmatrix} u_1(t) \\ u_2(t) \\ u_3(t) \\ u_4(t) \end{Bmatrix} \tag{5.114}$$

$$= \begin{bmatrix} 1267424U_1(t) - 633712U_2(t) \\ -633712U_1(t) + 1267424U_2(t) - 633712U_3(t) \\ -633712U_2(t) + 1267424U_3 - 633712U_4(t) \\ -633712U_3(t) + 633712U_4(t) \end{bmatrix}$$

Step 6: Calculation of storey shear

The storey shears are calculated as

$$\{V(t)\}[S][K]\{U(t)\} \tag{5.115}$$

where $[S]$ is the $(n \times n)$ upper triangular matrix given as

www.EngineeringBooksPDF.com

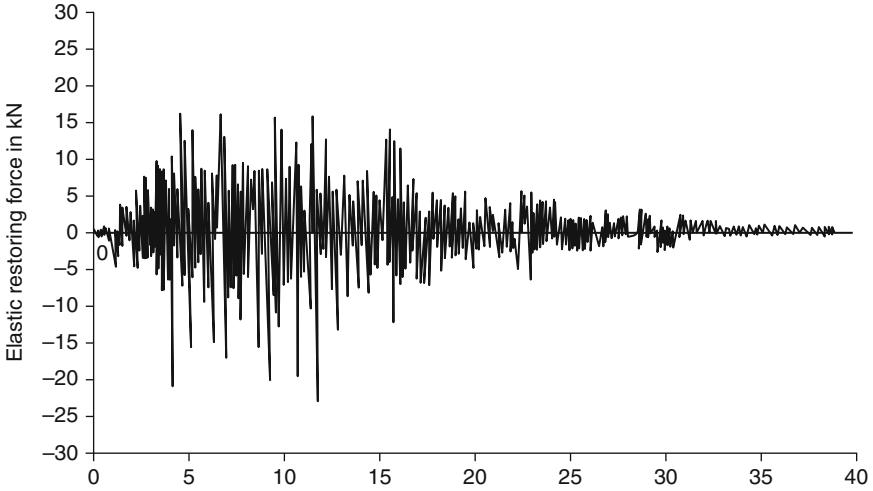


Fig. 5.16 Lateral load response at first storey (kN)

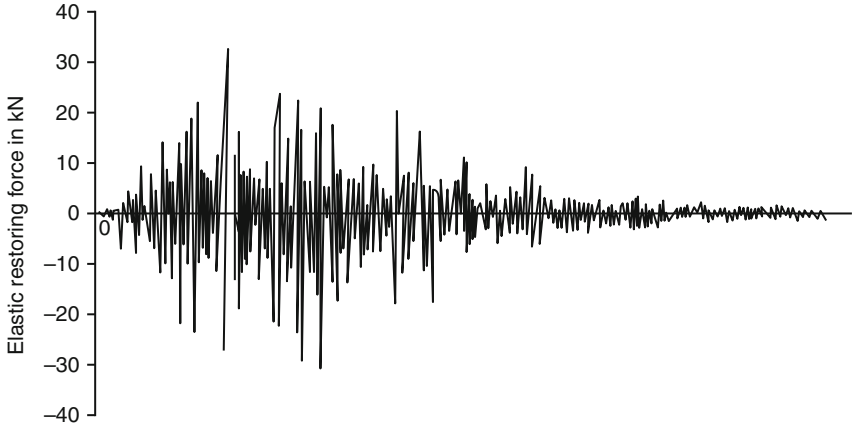


Fig. 5.17 Lateral load response first storey (kN)

$$[S] = \begin{bmatrix} 1 & 1 & 1 & . & . & 1 \\ 0 & 1 & 1 & . & . & 1 \\ 0 & 0 & 1 & . & . & 1 \\ . & . & . & . & . & . \\ . & . & . & . & . & . \\ 0 & 0 & 0 & . & . & 1 \end{bmatrix} \tag{5.116}$$

www.EngineeringBooksPDF.com

$$\{V(t)\} = \begin{bmatrix} 1 & 11 & 1 \\ 0 & 11 & 1 \\ 0 & 01 & 1 \\ 0 & 00 & 1 \end{bmatrix} \begin{bmatrix} 1.2674 & -0.6337 & 0 & 0 \\ -6.337 & 1.2674 & -0.337 & 0 \\ 0 & -0.6337 & 1.2674 & -0.6337 \\ 0 & 0 & -0.6337 & 0.6337 \end{bmatrix} \times 10^6 \begin{Bmatrix} U_1(t) \\ U_2(t) \\ U_3(t) \\ U_4(t) \end{Bmatrix} \quad (5.117)$$

Hence,

$$\begin{bmatrix} V_1(t) \\ V_2(t) \\ V_3(t) \\ V_4(t) \end{bmatrix} = \begin{bmatrix} 633712U_1(t) \\ -633712U_1(t) + 633712U_2(t) \\ -633712U_2(t) + 633712U_3(t) \\ -633712U_3(t) + 633712U_4(t) \end{bmatrix} \quad (5.118)$$

The storey shears at each storey are shown in Figs. 5.18 to 5.21.

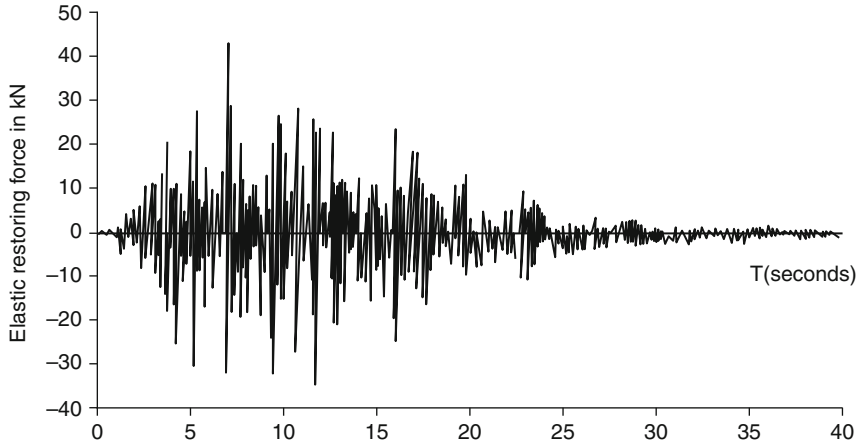


Fig. 5.18 Third-storey lateral load response (kN)

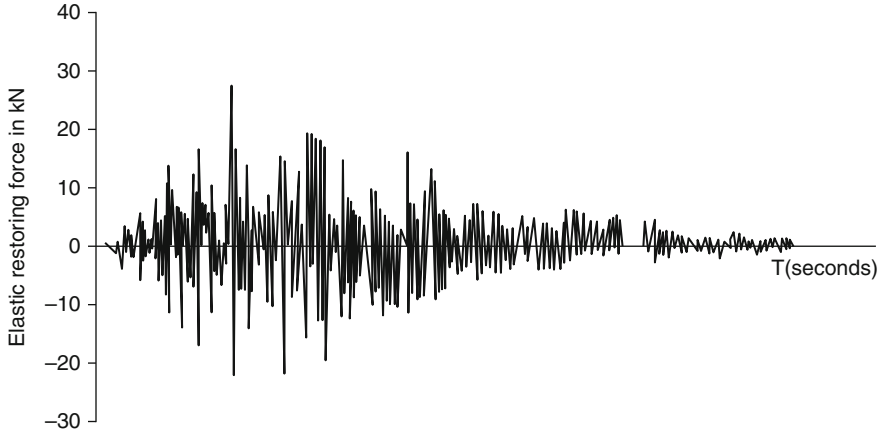


Fig. 5.19 Fourth-storey lateral load response (kN)

www.EngineeringBooksPDF.com

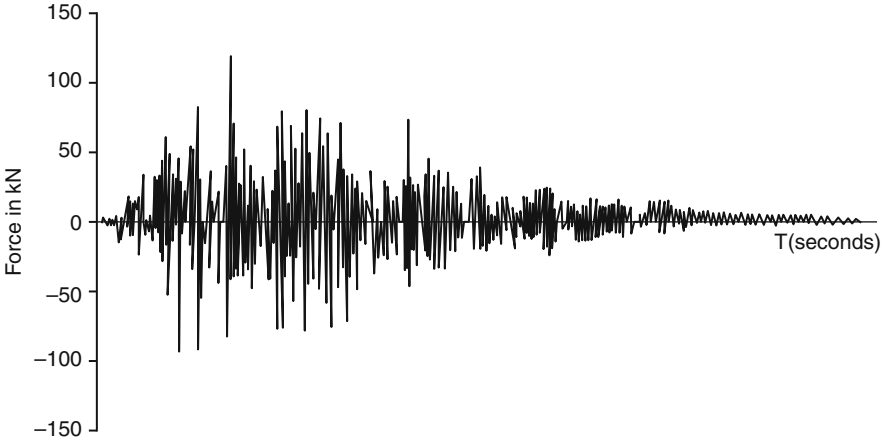


Fig. 5.20 Base shear lateral load response $V_1(t)(\text{kN})$ – first storey

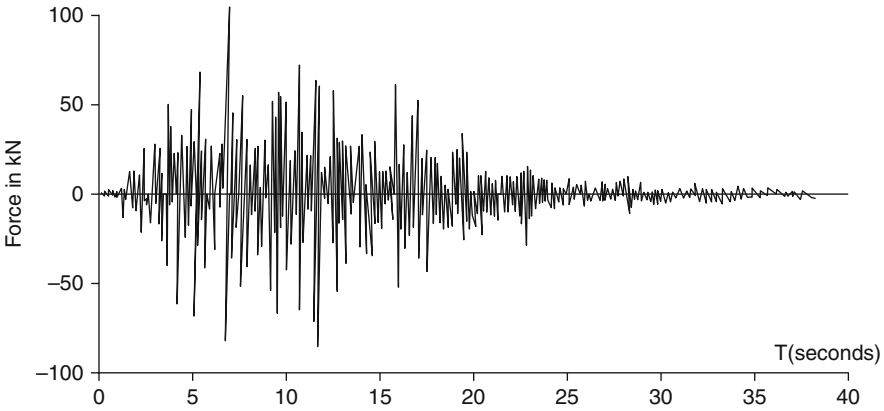


Fig. 5.21 Base shear lateral load response $V_2(t)(\text{kN})$ – second storey

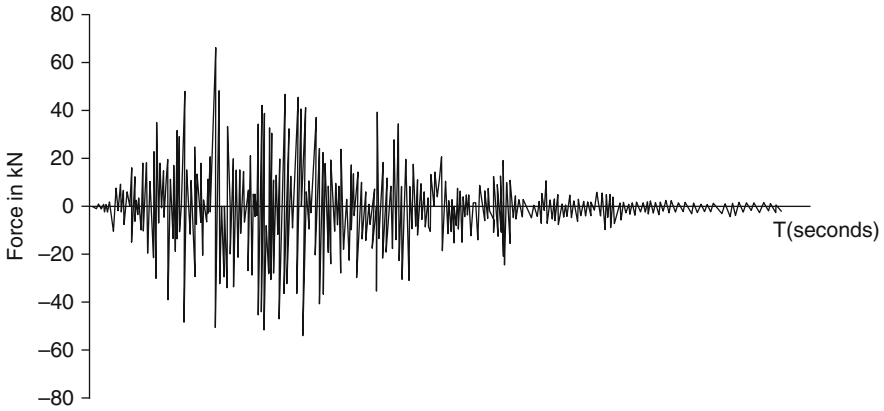


Fig. 5.22 Base shear lateral load response $V_3(t)(\text{kN})$ – third storey

www.EngineeringBooksPDF.com

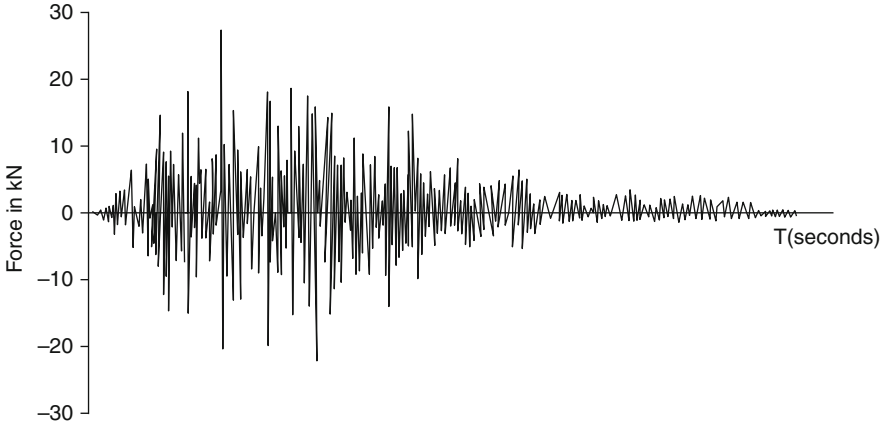


Fig. 5.23 Base shear lateral load response $V_4(t)$(kN) – fourth storey

Table 5.5 Summary of maximum response for the example structure

Position or location	$U_{max} \times 10^{-4}$(m)	F_{max} (KN)	V_{max} (KN)
1	1.90	23.4	120.40
2	3.54	32.88	104.47
3	4.68	43.86	72.10
4	5.13	28.64	28.24

Step 7: Calculation of maximum response

Maximum response of relative displacement, elastic restoring forces, storey shears at each storey in plane frame has been summarized in Table 5.5.

The total base shears $V_1(t)$ obtained from time history method is presented in Fig. 5.23. The maximum base shear obtained from time history analysis is 120.39 kN while from response spectrum analysis is 125.69 kN in Example 4.11 case study.

5.12 Sample Cases

5.12.1 Plastic Potential of the Same Form as the Yield Surface

$$f(J_2) = f(\delta_{ij}) = \frac{3}{2} = \frac{3}{2} S_{ij} S_{ij} \tag{5.119}$$

where
δ_{ij} = the Kronecker delta.
Differentiating

www.EngineeringBooksPDF.com

$$\begin{aligned}\frac{\partial f}{\partial \delta_{ij}} &= \frac{3}{2}\partial(S_{kl}S_{kl})/\partial\delta_{ij} \\ &= \frac{3}{2}S_{kl}\partial\delta_{mn}/\partial\delta_{ij} = 3S_{ij}\end{aligned} \tag{5.120}$$

The plastic strain increment is stated as

$$d\lambda\varepsilon_{ij}^{P} = \lambda S_{ij} \tag{5.121}$$

The equivalent plastic strain $\lambda\varepsilon^{-P}$ can be obtained as

$$d\lambda\varepsilon^{-P} = \left(\frac{2}{3}d\varepsilon_{ij}^{P}d\varepsilon_{ij}^{P}\right)^{1/2} \tag{5.122}$$

where

$$d\lambda = \frac{3}{2}\frac{d\varepsilon^{-P}}{\delta_{eq}}$$

5.12.2 von Mises Yield Surface Associated with Isotropic Hardening

The yield function f is written as

$$f = \frac{T}{2}(\sigma_{ij}) - \frac{1}{3}\sigma_{eq}^{2} \tag{5.123}$$

By differentiating,

$$df = (S_{ij}d\sigma_{ij}) - \frac{2}{3}\sigma_{\mathrm{eq}}(\partial\sigma_{\mathrm{eq}})/(d\varepsilon^{-P})\{d\varepsilon^{-P}\} \tag{5.124}$$

Using (5.91) onwards, the values of $d\lambda$ and $d\sigma$ given in (5.108) and (5.109) are given by

$$d\lambda = \left([D^{*}]_{i,j,k,l} - \frac{[D^{*}]S_{mn}S_{pq}[D^{*}]_{pqkl}}{\sigma_{ij}[D^{*}]_{i,j.k,l}S_{kl} + \left(\frac{2}{3}\sigma_{eq}\right)^{2}s_{H}}\right)\{D\varepsilon\}_{kl} \tag{5.125}$$

$$\text{When } d\{\Delta\in\}_{\mathrm{TOT}} = [D^{*}]^{-1}\{\Delta\delta\} + \frac{\delta f}{\delta S_{H}}\cdot d_{d} \tag{5.126}$$

$$0 = \left\{\frac{df}{d\delta}\right\}^{T} d\{\delta\} - Cd\lambda \tag{5.127}$$

$$d\{\sigma\} = [D^{*}]\{d\in\}_{\mathrm{TOT}} - \left\{\frac{\partial f}{\partial\sigma}\right\}^{T} d\lambda \tag{5.128}$$

www.EngineeringBooksPDF.com

Equation (5.133) is then substituted into (5.132), and (5.134) is obtained

$$0 = \frac{\partial f^T}{\partial \sigma}[D^*]\{d\varepsilon\}_{\mathrm{TOT}} - \left\{\frac{\partial f}{\partial \sigma}\right\}^T [D^*]\left\{\frac{\partial f}{\partial \sigma}\right\} d\lambda - C d\lambda \tag{5.129}$$

$$\text{As one knows } d\varepsilon_{ij} = d\bar{\varepsilon}_{ij} + d\varepsilon_{ij}^P \tag{5.130}$$

Equation (5.135) is then combined with (5.130), (5.131) and (5.125) to give the final value of $d\lambda$

$$d\lambda = \frac{\left\{\frac{\partial f}{\partial \sigma}\right\}^T [D^*]\{d\varepsilon\}_{\mathrm{TOT}}}{C + \left\{\frac{\partial f}{\partial \sigma}\right\}^T [D^*]\left\{\frac{\partial f}{\partial \sigma}\right\}} \tag{5.131}$$

Table 5.6 Analytical formulation of the steel anchors/studs

$[K_{\mathrm{TOT}}]\{\delta\}^* + \{F_{\mathrm{T}}\} - \{R_{\mathrm{T}}\} = 0$ (a)

where

$[K_{\mathrm{TOT}}] = [K_{\mathrm{l}}] + [K_{\mathrm{a}}]$ (b)

$$\{\delta\}^* = \begin{Bmatrix} \delta_{\mathrm{un}} \\ \delta_{\mathrm{b}} \end{Bmatrix} \quad \{F_{\mathrm{T}}\} = \begin{Bmatrix} F_{\mathrm{un}} \\ F_{\mathrm{b}} \end{Bmatrix} \quad \{R_{\mathrm{T}}\} = \begin{Bmatrix} R_{\mathrm{un}} \\ R_{\mathrm{b}} \end{Bmatrix}$$

$[K_{\mathrm{TOT}}]$ = total stiffness matrix
$[K_{\mathrm{e}}]$ = linear stiffness matrix
$[K_{\mathrm{a}}]$ = a stud stiffness matrix
$\{F_{\mathrm{T}}\}$ = total initial load vector
$\{R_{\mathrm{T}}\}$ = total external load vector

Subscript

un = quantities corresponding to unknown displacement (c)
b = quantities corresponding to restrained boundaries

$$[k_l]\{\delta_{\mathrm{un}}\} + \{F_{\mathrm{un}}\} = 0$$
$$\{\varepsilon\} = [B]\{\delta\}$$
$$\{\sigma\} = [D](\{\varepsilon\} - \{\varepsilon\})$$
$$\{S\} = \text{anchor shear forces}$$
$$= [K_{\mathrm{a}}]\{\delta_{\mathrm{un}}\}$$
$$\{F_{\mathrm{un}}\} = \int_v [B]^T[D]\{\varepsilon_0\}dv = \int_v [B]^T[D]\{\varepsilon_0\}\det[J]\mathrm{d}\xi\mathrm{d}\eta\mathrm{d}\zeta$$

The plastic buckling matrix is given by

$(K + \lambda K_{\mathrm{G}})F_{\mathrm{T}} = 0$ (d)

where K = the elasto-plastic stiffness matrix as a function of the current state of plastic deformation; and K_{G} = the initial stress geometric stiffness matrix.
The determinant

$|K + \lambda_{\mathrm{c}} K_{\mathrm{G}}| = 0$ (e)

The essential equation is characteristically triangularised for the ith loading step as

$(K^i + \lambda_{\mathrm{c}} K_{\mathrm{G}}^i)F_{\mathrm{T}}^i = 0 \;\; \lambda_{\mathrm{c}} = 1 + E_{\mathrm{ps}}$ (f)

E_{ps} is an accuracy parameter

www.EngineeringBooksPDF.com

Table 5.7 [K] – Shear and torsion included for line element

$$[D] = \begin{bmatrix}
\frac{EA}{L} & & & & & & & & & & & \\
0 & \frac{12EI_\xi}{L^3(1+\bar{\tau}_\eta)} & & & & & & & & & & \\
0 & 0 & \frac{12EI_\xi}{L^3(1+\bar{\tau}_\xi)} & & & & & & & & & \\
0 & 0 & 0 & \frac{GJ}{L} & & & & & & & & \\
0 & 0 & \frac{-6EI_\eta}{L^2(1+\tau_\xi)} & 0 & \frac{(4+\bar{\tau}_\xi)EI_\eta}{L(1+\bar{\tau}_\eta)} & & & & & & & \\
0 & \frac{6EI_\xi}{L^2(1+\bar{\tau}_\eta)} & 0 & 0 & 0 & \frac{(4+\bar{\tau}_\eta)EI_\xi}{L(1+\bar{\tau}_\eta)} & & & & & & \\
\frac{-EA}{L} & 0 & 0 & 0 & 0 & 0 & \frac{AE}{L} & & & & & \\
0 & \frac{-12EI_\xi}{L^3(1+\bar{\tau}_\eta)} & 0 & 0 & 0 & \frac{-6EI_\xi}{L^2(1+\bar{\tau}_\eta)} & 0 & \frac{12EI_\xi}{L^3(1+\bar{\tau}_\eta)} & & & & \\
0 & 0 & \frac{-12EI_\eta}{L^3(1+\bar{\tau}_\xi)} & 0 & \frac{6EI_\eta}{L^2(1+\bar{\tau}_\xi)} & 0 & 0 & 0 & \frac{12EI_\eta}{L^3(1+\bar{\tau}_\xi)} & & & \\
0 & 0 & 0 & \frac{-GJ}{L} & 0 & 0 & 0 & 0 & 0 & \frac{GJ}{L} & & \\
0 & 0 & \frac{6EI_\eta}{L^2(1+\bar{\tau}_\xi)} & 0 & \frac{(2-\bar{\tau}_\xi)EI_\eta}{L(1+\bar{\tau}_\xi)} & 0 & 0 & 0 & \frac{6EI_\eta}{L^2(1+\bar{\tau}_\xi)} & 0 & \frac{(4+\bar{\tau}_\xi)EI_\eta}{L(1+\bar{\tau}_\xi)} & \\
0 & \frac{6EI_\xi}{L^2(1+\bar{\tau}_\eta)} & 0 & 0 & 0 & \frac{(2-\bar{\tau}_\eta)EI_\xi}{L(1+\bar{\tau}_\eta)} & 0 & \frac{-6EI_\xi}{L^2(1+\bar{\tau}_\eta)} & 0 & 0 & 0 & \frac{(4+\bar{\tau}_\eta)EI_\xi}{L(1+\bar{\tau}_\eta)}
\end{bmatrix}$$

where

$\bar{\tau}_\eta = \frac{12EI_\xi}{GA_{s\eta}L^2} = 24(1+\nu)\frac{A}{A_{s\eta}}\left(\frac{T_\xi}{L}\right)^2 \quad \tau_\xi = \frac{12EI_\eta}{GA_{s\xi}L^2} = 24(1+\nu)\frac{A}{A_{s\xi}}\left(\frac{T_\eta}{L}\right)^2$

a_s = shear area T = torsional moment of inertia ρ = density ξ, η local axes are parallel to Z and Y axes

www.EngineeringBooksPDF.com

The factor C in (5.136) is an unknown factor defining the state of elasto-plasticity. When $C = 0$, (5.136) gives a value of $d\lambda$ for perfectly plastic situation with no hardening. The stress increments are given by

$$d\{\sigma\}_{\mathrm{TOT}} = [D^*] - \frac{[D^*]\left\{\frac{\partial f}{\partial \sigma}\right\}\left\{\frac{\partial f}{\partial \sigma}\right\}^T [D^*]}{C + \left\{\frac{\partial f}{\partial \sigma}\right\}^T [D^*]\left\{\frac{\partial f}{\partial \sigma}\right\}} \{d\varepsilon\}_{\mathrm{TOT}} \tag{5.132}$$

for the elasto-plastic case,

$$d\{\sigma\}_{\mathrm{TOT}} = [D^*] - [D_P] d\{\varepsilon\}_{TOT} \tag{5.133}$$

$$[D_P] = \frac{[D^*]\left\{\frac{\partial f}{\partial \sigma}\right\}\left\{\frac{\partial f}{\partial \sigma}\right\}^T [D]}{C + \left\{\frac{\partial f}{\partial \sigma}\right\}^T [D]\left\{\frac{\partial f}{\partial \sigma}\right\}} \tag{5.134}$$

The true stress increment in (5.139) is the difference between the stress increment $[D_P]\{d\bar{\varepsilon}\}_{\mathrm{TOT}}$ and the algebraic sum of stresses $[D]\{d\varepsilon\}$ due to elastic, creep, shrinkage, temperature, fatigue and other effects.

The matrix $[D]$ has the flexibility to include any concrete failure models described elsewhere in this book.

The parameter C is given by Hill [A.1] as

$$C = 4/9\sigma_{\mathrm{eq}}^2 S_{\mathrm{H}} \tag{5.135}$$

where S_{H} is the slope of the curve and represents hardening.

Where the influence of the studs, lugs and any other type of anchorages is to be included in the finite element analysis, the steps given in Table 5.8 are considered together with solid, panel and line elements.

$$f(\sigma, \varepsilon.\dot{\sigma}, \dot{\varepsilon}, S_{\mathrm{H}}) = 0 \tag{5.136}$$

where f is a definite representation of L_{F} and is a stress function. The only change is in the value of S_{H}, accounting for isotropic and anisotropic hardening and allowing the function f to be dependent not only on the present state of stress or strain, but also on the hardening history according to pre states of stress and strain. The value of $(\sigma, \dot{\sigma})$ and $\{\varepsilon, \dot{\varepsilon}\}$ must be in the plastic range, having total values of σ_{ij}^P and ε_{il}^P respectively.

When (5.124) is satisfied then the total differential of f is written as

$$df = \frac{\partial f}{\partial \sigma_{ij}^P} d\sigma_{ij}^P + \frac{\partial f}{\partial \varepsilon_{ij}^P} d\varepsilon^P + \frac{\partial f}{\partial S_H} dS_{\mathrm{H}} \tag{5.137}$$

The yield condition with ε_{ij}^P and S_{H} held constant can be interpreted as a yield surface in the multi-dimensional stress space.

www.EngineeringBooksPDF.com

Table 5.8 Stiffness coefficient and matrix for ISOPAR

The element pressure load vector in element coordinates is:

$$\{F_1^{\mathrm{Pr}}\} = \lfloor P_1 \quad P_2 \quad P_3 \quad P_4 \quad P_5 \quad P_6 \rfloor^{\mathrm{T}}$$

Value of stress stiffness coefficient (C_2)

Previous iteration resulted in a tensile stress	Previous iteration resulted in a compressive stress
1.0	0.0
1.0	$\frac{AE}{F \times 10^6}$
0.0	1.0
$\frac{AE}{F \times 10^6}$	1.0

$$F = \begin{cases} \text{for the first iteration : } AE\varepsilon^{in} \\ \text{for all subsequent iterations : the axial force} \\ \text{in the element as computed in the previous} \\ \text{stress pass of the element (output quantity)} \\ \text{FORC} \end{cases}$$

C_2 = value given in the table above.

The matrix for the tension-only or compression-only ISOPAR is given by:

$$[M_1] = \frac{M_{\mathrm{t}}}{2} \begin{bmatrix} 1 & & & & & & & & & & & \\ 0 & 1 & & & & & & & & & & \\ 0 & 0 & 1 & & & & & & & & & \\ 0 & 0 & 0 & 0 & & & & & & & & \\ 0 & 0 & 0 & 0 & 0 & & \text{Symmetric} & & & & & \\ 0 & 0 & 0 & 0 & 0 & 0 & & & & & & \\ 0 & 0 & 0 & 0 & 0 & 0 & 1 & & & & & \\ 0 & 0 & 0 & 0 & 0 & 0 & 0 & 1 & & & & \\ 0 & 0 & 0 & 0 & 0 & 0 & 0 & 0 & 1 & & & \\ 0 & 0 & 0 & 0 & 0 & 0 & 0 & 0 & 0 & 0 & & \\ 0 & 0 & 0 & 0 & 0 & 0 & 0 & 0 & 0 & 0 & 0 & \\ 0 & 0 & 0 & 0 & 0 & 0 & 0 & 0 & 0 & 0 & 0 & 0 \end{bmatrix}$$

When $f < 0$ the condition indicates a purely elastic change towards the inside of the yield surface. In cases where plastic flow does not occur, the increments of plastic strain $d\varepsilon_{ij}^P$ and the change of hardening parameter dS_{H} will be automatically zero, and hence, in the case of the unloading, (5.125) is reduced to

$$df = \frac{\partial f}{\partial \sigma_{ij}^P} d\left\{\sigma_{ij}^P\right\} < 0 \tag{5.138}$$

When $df = 0$, which is the case for neutral loading, no plastic strain changes occur and the hardening factor remains unchanged, then

$$df = \frac{\partial f}{\partial \sigma_{ij}^P} d\left\{\sigma_{ij}^P\right\} = 0 \quad d\left\{\varepsilon_{ij}^P\right\} = 0 \tag{5.139}$$

The quantity $d\sigma_{ij}$ is tangent to the surface for neutral loading. For the vector products to be zero, $\partial f / \partial \sigma_{ij}$ will be normal to the surface. When $d\sigma_{ij}$ is pointing

www.EngineeringBooksPDF.com

Table 5.9 Stiffness and mass matrices (courtesy STRUCOM, London)

Orders of degrees of freedom

The stiffness matrix in element co-ordinates is:

$$[K_1] = \begin{bmatrix} AE/L & & & & & & & & & & & \\ 0 & a_z & & & & & & & & & & \\ 0 & 0 & a_y & & & & & & & & & \\ 0 & 0 & 0 & GJ/L & & & & \text{Symmetric} & & & & \\ 0 & 0 & d_y & 0 & e_y & & & & & & & \\ 0 & c_z & 0 & 0 & 0 & e_y & & & & & & \\ -AE/L & 0 & 0 & 0 & 0 & 0 & AE/L & & & & & \\ 0 & b_z & 0 & 0 & 0 & d_z & 0 & a_z & & & & \\ 0 & 0 & b_y & 0 & c_y & 0 & 0 & 0 & a_y & & & \\ 0 & 0 & 0 & -GJ/L & 0 & 0 & 0 & 0 & 0 & GJ/L & & \\ 0 & 0 & d_y & 0 & f_y & 0 & 0 & 0 & c_z & 0 & e_y & \\ 0 & c_z & 0 & 0 & 0 & f_z & 0 & d_z & 0 & 0 & 0 & e_z \end{bmatrix}$$

where

A = cross-sectional area

E = Young's modulus

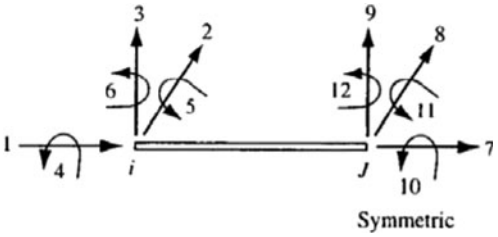
L = element length

G = shear modulus

$r_y = \sqrt{\frac{I_{yy}}{A}}$ = radius of gyration

$r_z = \sqrt{\frac{I_{zz}}{A}}$ = radius of gyration

$[M_1] = [M_t]$



Symmetric

Order of degrees of freedom

For uniform lateral pressure

$P_1 = P_4 = 0$

$P_2 = P_5 = -\frac{PL}{2}$

$P_3 = -P_6 = -\frac{PL^2}{12}$

P = uniform applied pressure (units = force/length)

Stress calculations

The centroidal stress at end i is:

$\sigma_i^{\text{dir}} = \frac{F_{x,i}}{A}$

where

σ_i^{dir} = centroidal strees

$F_{x,i}$ = axial force

The bending stress is

$\sigma_{\text{i}}^{\text{bnd}} = \frac{M_i t}{2I}$

where

σ_i^{bnd} = bending stress at end i

M_i = moment at end i

t = thickness of beam in element z direction

www.EngineeringBooksPDF.com

Table 5.10 Three-dimensional elastic beam (courtesy STRUCOM, London)

Element matrices and load vectors

All element matrices and load vectors are generated in the element co-ordinate system and must subsequently then be converted to the global co-ordinate system.

The element stiffness matrix is:

$$[K_1] = \frac{AE}{L}\begin{bmatrix} C_1 & 0 & 0 & -C_1 & 0 & 0 \\ 0 & 0 & 0 & 0 & 0 & 0 \\ 0 & 0 & 0 & 0 & 0 & 0 \\ -C_1 & 0 & 0 & C_1 & 0 & 0 \\ 0 & 0 & 0 & 0 & 0 & 0 \\ 0 & 0 & 0 & 0 & 0 & 0 \end{bmatrix}$$

to the outside of the surface the vector product will be positive; and this constitutes loading, with plastic flow taking place such that

$$df = \frac{\partial f}{\partial \sigma_{ij}^P} d\left\{\sigma_{ij}^P\right\} > 0 \tag{5.140}$$

The definition for the structural material stability postulates that during a load cycle that includes loading and unloading, the work performed has to be greater than zero, i.e.

$$d\varepsilon_{ij}^P d\sigma_{ij}^P \geq 0 \tag{5.141}$$

From (5.156) and (5.157) for ideally plastic material the plastic strain increment $d\varepsilon_{ij}^P$ is proportional to the stress gradient of the yield surface

$$d\varepsilon_{ij}^P = \frac{\partial f}{\partial \sigma_{ij}^P} d\lambda \tag{5.142}$$

where $d\lambda =$ a constant of proportionality.

Part B Plastic Flow Rule and Buckling

5.13 Plastic Flow Rule and Stresses During Elasto-plastic Staining Where particularly steel structures exist in seismic zones

Many materials have been examined, including concrete. They behave elastically up to a certain stage of the loading beyond which plastic deformation takes place. During this plastic deformation the state of strain is not uniquely determined by the state of stress, as stated previously. In a uniaxial state of stress a simple rule is required to initiate yielding at any Gaussian point of the isoparametric element. In the multiaxial state of stress, there are an infinite number of possible combinations of stresses at which yielding starts. These can be examined by the flow rule. Moreover, the flow rule supplements the elastic constitutive relationship, and the plastic strain increments are related to the plastic stress increments during the occurrence of plastic flow.

www.EngineeringBooksPDF.com

The yield criterion described by a failure surface in a multi-dimensional stress space is given by Bangash:

$$L_{\mathrm{F}}\left(\sigma_{ij}^{S}, \in^{P}, S_{\mathrm{H}}\right) = 0 \tag{5.143}$$

where

L_{F} = the yield functiont
σ_{ij}^{S} = the multi-dimensional stress state
$\in^{P}$ = accumulated plastic strain
S_{H} = strain hardening or softening parameter

The general form of the yield surface given by (5.121) allows either isotropic or kinematic hardening of the material. For a given previous history, $L_{\mathrm{F}}\left(\sigma_{ij}^{S}\right)$ is

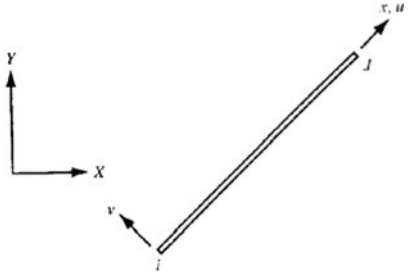
Table 5.11 Two-dimensional elastic beam (courtesy STRUCOM,London)

Element matrices and load vectors

The element stiffness matrix in element co-ordinates is:

$$[K_1] = \begin{bmatrix} \frac{AE}{L} & 0 & 0 & -\frac{AE}{L} & 0 & 0 \\ 0 & \frac{12EI}{L^3(1+\phi')} & \frac{6EI}{L^2(1+\phi')} & 0 & -\frac{12EI}{L^3(1+\phi')} & \frac{6EI}{L(1+\phi')} \\ 0 & \frac{6EI}{L^2(1+\phi')} & \frac{EI(4+\phi')}{L(1+\phi')} & 0 & -\frac{6EI}{L^2(1+\phi')} & \frac{EI(2-\phi')}{L(1+\phi')} \\ -\frac{AE}{L} & 0 & 0 & \frac{AE}{L} & 0 & 0 \\ 0 & -\frac{12EI}{L^3(1+\phi')} & \frac{6EI}{L^2(1+\phi')} & 0 & \frac{12EI}{L^3(1+\phi')} & -\frac{6EI}{L^2(1+\phi')} \\ 0 & \frac{6EI}{L^2(1+\phi')} & \frac{EI(2-\phi')}{L(1+\phi')} & 0 & -\frac{6EI}{L^2(1+\phi')} & \frac{EI(4+\phi')}{L(1+\phi')} \end{bmatrix}$$

where
A = cross-sectional area
E = Young's modulus
L = element length
I = moment of inertia
$\phi' = \frac{12EI}{GA^{\mathrm{s}}L^2}$
G = shear modulus
$A^{\mathrm{s}} = \frac{A}{F^{\mathrm{s}}}$ = shear area
F^{s} = shear deflection constant



Two-dimensional beam element centroidal axis

www.EngineeringBooksPDF.com

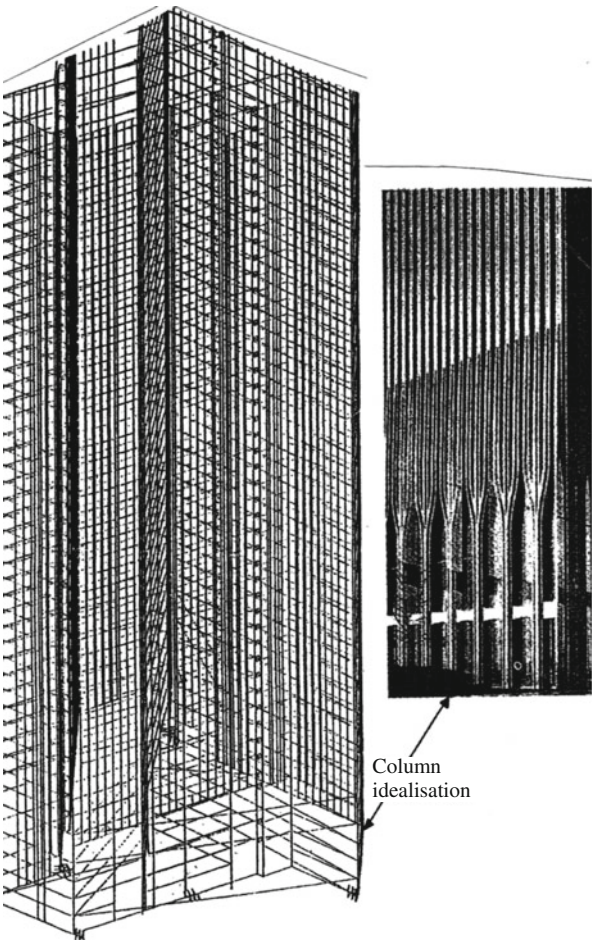


Fig. 5.24 Finite element mesh scheme for the WTC-1 analysis

always considered as a function of the current state of stress for which S_H is variable.

To give added generality, the plastic potential to which the normality principle is applicable is assumed as

$$L_Q\left(\sigma_{ij}^S, \in^P, S_{H0}\right) = 0 \tag{5.144}$$

This allows non-associated plasticity to be dealt with and associated rules to be obtained as a special case by making

$$L_H = L_Q \tag{5.145}$$

For a perfectly plastic material the yield surface of (5.121) remains constant. For a strain hardening material the yield surface must change with continued straining beyond the initial yield.

www.EngineeringBooksPDF.com

This phenomenon is included in (5.121) by allowing both L_F and S_H to be functions of the state of stress and the plastic deformation history. This means S_H will have a new value for every time-dependent yielding. Further, if the material is unloaded and then loaded again, additional yielding cannot take place, unless the current value of S_H has been exceeded.

A unified approach for arriving at the incremental stress–strain equation based on (5.121) can be written in a combined tensor form in three dimensions as the overall matrix is stored in the half-band form. Since the number of degrees of freedom is 15 at each story the dimensions of the stored matrix will be $(15 \times NS)$ by 30. The solution is obtained for the required number of loading cases and from the displacements thus obtained and the generalized member stiffness matrices. The stress resultants are found. Finally, the global load, stiffness and displacement relationships are obtained for the overall structures.

5.12.3 Dynamic Local and Global Stability Analysis

When the impact/blast occurs, there can be problem of combined torsional–flexural buckling of the building comprising the core, floors, columns and bracings. The elements of the building structures may be bolted or welded or in case of concrete connected with bars embedded to floors. The torsional buckling analysis can be combined with flexural buckling by adjusting the respective stiffness matrices. The torsional buckling was dealt with in detail already.

5.12.3.1 Dynamic Flexural Buckling

The eigenvalue buckling (bifurcation) is vital where steel is fully or partially anchored to the other elements such as aluminium or concrete. The eigenvalue buckling by bifurcation is represented by

$$\left([K] + \lambda_{ei}[K]_s\right)\{\psi\}_i = \{0\} \tag{5.146}$$

where

$[K]$ =stiffness matrix of the core complex
$[K]_S$= stress stiffness matrix
λ_{ei} = the ith eigenvalue (is to multiply load which generated $[K]_S$)
$\{\psi\}_i$= the ith eigenvector of displacement

To reduce the solution of (5.146) to its static and dynamic buckling (master) degrees of freedom, the matrix $[K]$ is reduced and $[K]_S$ is reduced in a manner identical to that by which the mass matrix is reduced. Hence (5.146) becomes

$$\left([K]_R + \lambda_{ei}[K]_s\right)\{\psi_i\}_R = \{0\} \tag{5.147}$$

where $[K]_R = \left[K_t^1\right]_R$ when blast problem is involved. The subscript 't' in C is a time-dependent matrix.

www.EngineeringBooksPDF.com

Since the building structures have specific geometry, the geometric stiffness matrix is involved. At the plasticity situation, the dynamic plastic stiffness matrix will now be $\left[K_t^{1P}\right]_R$. The overall plastic buckling matrix is now given by

$$\left(\left[K_t^{1P}\right]_R+\lambda_{ei}[K]_s\right)\{\psi_i\}_r=0 \tag{5.148}$$

where $\lambda_{ei} = I + E_{ps}$ and E_{ps} = accuracy parameters.

5.12.3.2 Inclusion of Torsional Buckling

For the torsional phenomena: Assuming that the core–floor–bracings complex has the final stiffness matrix $[K]_{\mathrm{TOT}}$, the matrix is algebraically added to $\left[K_t^{1P}\right]_R$. Hence,

$$[F]_{\mathrm{TOT}}=\left[K_t^{1P}\right]+[K]_{\mathrm{TOT}}+\lambda_{ei}[K_G],\{\Psi_i\}_R \tag{5.149}$$

The final buckling/torsional equation is given as

$$[K]_{\mathrm{TOT}}\{\delta\}^*+\{F_{\mathrm{T}}\}-\{R_{\mathrm{T}}\}=0 \tag{5.150}$$

where

$\{F_{\mathrm{T}}\}$ = total initial seismic load vector on each element of the complex
$\{R_{\mathrm{T}}\}$ = total external seismic load vector

$$\{\delta\}^*=\begin{Bmatrix}\delta_{\mathrm{un}}\\ \delta_{\mathrm{b}}\end{Bmatrix};\quad \{F_T\}=\begin{Bmatrix}F_{\mathrm{un}}\\ F_{\mathrm{b}}\end{Bmatrix};\quad \{R_T\}=\begin{Bmatrix}R_{\mathrm{un}}\\ \mathrm{R_b}\end{Bmatrix} \tag{5.150a}$$

In (5.151a) the subscripts '*un*' and '*b*' are defined as

un = quantities corresponding to unknown displacements
b = quantities corresponding to restrained boundaries

In (5.151b) if for simplicity reasons on mathematical equation

$$[K_l]=\left[K_t^{1P}\right]_R+[K]_{\mathrm{TOT}} \tag{5.150b}$$

then without geometric stiffness

$$[K_l]\{\delta_{\mathrm{un}}\}+\{F_{\mathrm{un}}\}=0 \tag{5.151}$$

When the influence of $[K_G]$ is taken into consideration, the overall plastic buckling/torsional criterion can now be given as

$$([K_l]+\lambda[K_G])F_{\mathrm{T}}=0 \tag{5.152}$$

www.EngineeringBooksPDF.com

where

$$\lambda = \lambda_{ei}\{\psi_i\}_R$$

$[K_l]$ = total plastic stiffness matrix as a function of the current state of plastic deformation
The determination

$$|K_l + \lambda K_G| = 0 \tag{5.153}$$

The essential equation is characteristically triangularized for the th loading step. It is essential to notice that a brief breakdown of the buckling phenomenon $\{\psi_i\}_R$ is related to the load vector $\mathrm{F_T}$ of the elements in (5.153) and

$$\{F_{\mathrm{un}}\} = \int [B]^T[D]\{\varepsilon_0\}d_{\mathrm{et}}[J]d\xi dnd\xi \tag{5.154}$$

5.13 Dynamic Analysis of Buildings in Three Dimensions

5.13.1 General Introduction

A framed tube is a thin-walled structure, which can be defined as one which is made up of thin plates joined along their edges. A precise quantitative definition for the thinness is not easy to give, except to say that the wall thickness is small compared to other cross-sectional dimensions, which are in turn small compared with the overall length of the structure. Shear walls of this type are extensively used in tall buildings, which typically exhibit another characteristic, namely that the walls are open sections, meaning that they do not have closed sections as, for example, box girders.

Compared to closed sections, open-section shear walls possess very little torsional rigidity and, therefore, must be given special consideration in their analysis and design. In a shear wall the shear stresses and strains are relatively much larger than those in solid rectangular columns. When shear walls twist, there is a so-called warping of the cross-section.

The framed tube buildings are very slender with a high width ratio in excess of 8.0. As mentioned the framed tube can be multi-dimensional. Various structural flooring systems are included. In order to achieve composite behaviour sometimes an attempt is made to limit the number of shear walls by interconnecting them with heavy floor systems.

Non-linear analyses of two- or three-dimensional structures are achieved by modelling prototype structures as assemblages of line members and panels. The line members may have axial, flexural, shearing and torsional properties, while the panels may carry in-plane direct and shear stresses in addition to

www.EngineeringBooksPDF.com

out-of-plane stress resultants. The analysis method employed is a matrix formulation of the stiffness or displacement type. In a general three-dimensional program, the coefficients, which relate the applied loading to six generalized displacements at the joint, are calculated, and a set of non-linear simultaneous equations is set up for each loading. Solutions of these equations result in the displacements of the joints, which are then used to calculate internal loads and stresses in the structural elements.

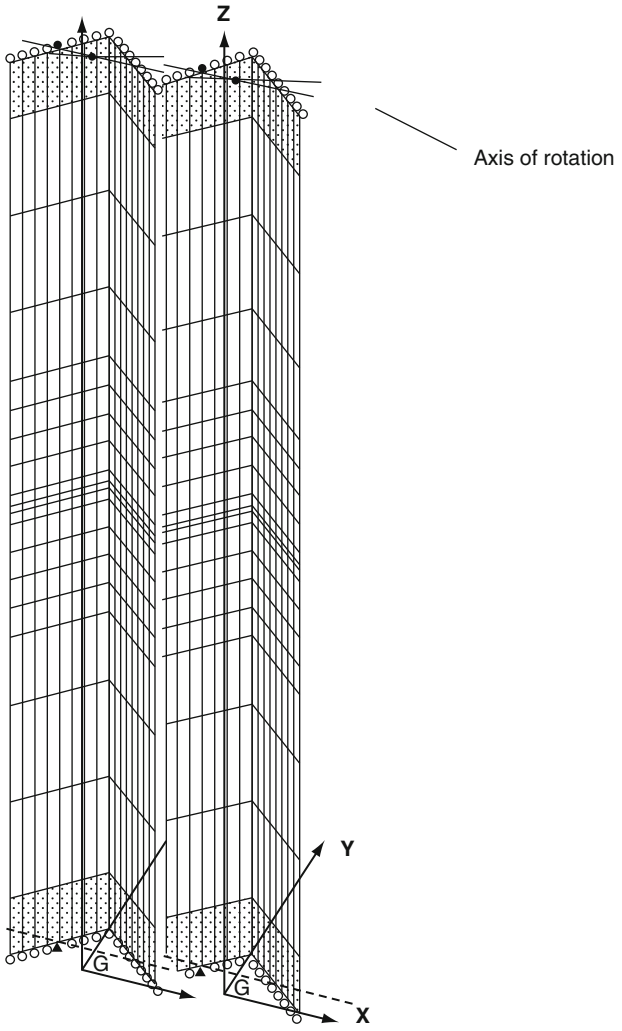


Fig. 5.25 Building frame in three dimensions using global axes on sectional elevation

www.EngineeringBooksPDF.com

Analytical solutions can be obtained for both frame and framed tube structures for high-rise buildings which mostly analysed as 3D structures are composed of relatively slender members which can be represented by properties along centroidal axis. Surface systems such as slabs and walls or frames are treated as an assemblage of finite elements. Many computer packages have the capability for mixing up different element types and are useful in idealizing problems of complex shape. External influences such as static, dynamic and blast load temperature and file can be considered in the design of such structures. The reader is advised to refer to Appendix IA for options.

Generation options are available for convenience of inputting large amounts of data. Many computer programs have plotting capabilities for the undeformed and deformed shape of the structure for verification of the model geometry and the structural behaviour of the system. The library of elements consists of elements from the basic linear element to the most sophisticated three-dimensional elements. Boundary elements in the form of spring supports can be incorporated. Loading options include gravity, thermal, in addition to the usual nodal loading consisting of either specified forces or displacements.

Among the dynamic analysis options, two of the most useful ones are eigenvalue analysis and response spectrum analysis. Wind, seismic and blast analyses by the response spectrum approach require the undamped free vibration mode shapes and frequencies of the system. The response spectrum analysis is obtained by solving the dynamic equilibrium equations by using the modal superposition method.

Data preparation involves defining the basic geometric dimensions of the structure by establishing joints or nodes on the structure.

5.13.2 Finite Element Analysis of Framed Tubular Buildings Under Static and Dynamic Load Influences

A tube is a three-dimensional structure and as such responds by bending about both its principal axes and rotation about a vertical axis. In analysing a quarter or half model, it is necessary to restrain the transverse bending and rotation of the tube. The kinematic restraints that preclude transverse movement and rotation of the model are shown in Fig. 5.26.

5.13.2.1 Lumping Technique

Many structural analyses have used lumping techniques to reduce the size of analytical models for computer analysis. The reduction in size was necessitated because even with large-capacity computers, there just was no economical way of solving very tall buildings with large numbers of joints. Before the structural analysis raises its eyebrows in surprise, it is well to bear in mind

www.EngineeringBooksPDF.com

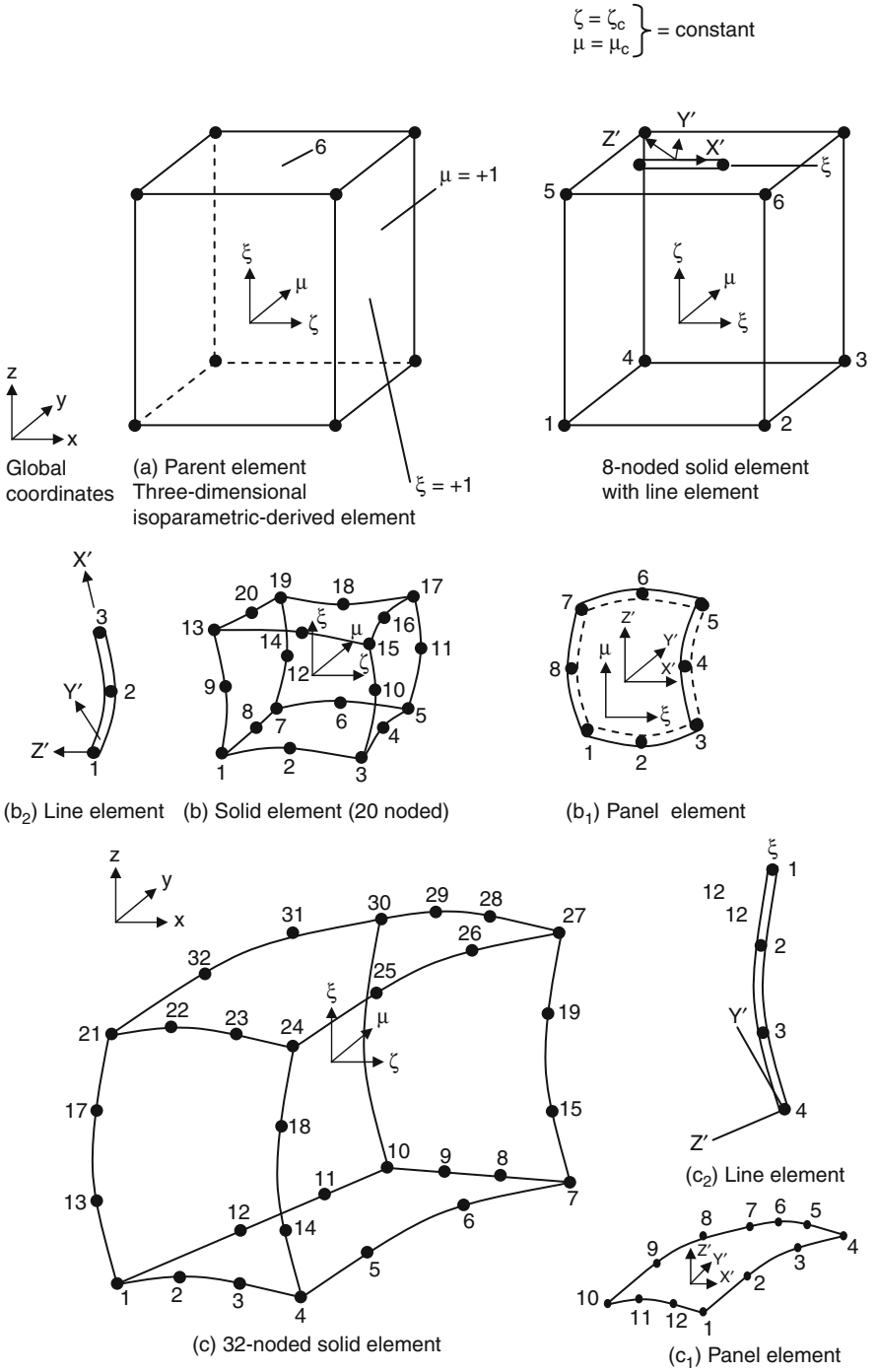


Fig. 5.26 Finite elements

www.EngineeringBooksPDF.com

that many notable buildings have been analysed using lumping techniques and they have been performing successfully over the years. Therefore, although the speed and capacity of modern mainframe computers are so vast as not to require lumping, introduction of desktop computers with relatively less capacity has once again required lumped computer modelling techniques. It is important to realise that as long as the essential features of the building are captured in the model, it makes very little difference whether a lumped or a full model is used for the analysis. Of course, there will be differences between the results of the two models, especially with regard to the stress resultants. Under impact and blast load effects, the authors found very little difference between the results of lumped and full models as discussed later on.

In this method of analysis, while looking at the entire structure, two floors are lumped into one floor, the moment of inertia and area of the girder in the lumped model should be twice their values in the prototype model. If n floors are lumped into one floor, the corresponding properties will be n times the prototype values. To keep the explanation simple, it is useful to introduce the following notations:

I_{cp} = moment of inertia of column in the unlumped model (prototype)
I_{cl} = moment of intertia of the column in the lumped model
L = length of girder which is the same in both models
h_{cp} = height of column in the unlumped model (prototype)
h_{cl} = height of the column in the lumped model
$\{u\}$ = element DOF vector
$\{\dot{u}\}$ = time derivative of element DOF vector
$\{K_e\}$ = element stiffness/conductivity matrix
$\{M_e\}$ = element mass matrix
NINT = number of integration points
NCS = total number of converged substeps
$\{\sigma\}$ = stress vector
$\{\varepsilon^{el}\}$ = elastic strain vector
$\{\Delta\varepsilon^{pl}\}$ = plastic strain increment
Vol_i = volume of integration points

Part C

5.14 Finite Element Modelling of Building Structures – Step by Step Formulations Incorporating All Previous Sections

5.14.1 Introduction

A step-by-step finite element analysis is developed in which a provision is made for elasto-plasticity, thermal creep, creep recovery and cracking

www.EngineeringBooksPDF.com

under static and dynamic conditions. Various concrete strength theories described in earlier chapters are included in the finite element analysis. These give facilities for the comparative study of results necessary for some sensitive structures. The analysis presented here also includes facilities for loading and unloading phenomena. Although greater emphasis is given to the use of isoparametric elements in the text, tables are provided which will assist in the automatic inclusion of other types of finite elements. Equations are set up in such a way that they can easily be replaced or modified to include other case studies. The initial stress or modified Newton–Raphson method is used for the major solution procedures. They together with acceleration and convergence procedures can easily solve non-linear, plasticity and cracking problems. Where dynamic problems exist, equations of motion are introduced in both linear and non-linear cases. Expressions for displacements, velocities and accelerations are then obtained. Direct integration and Wilson-θ methods have been used throughout for the time-dependent solutions of dynamically loaded structures. The main analysis of this chapter is supported by analyses given in various tables and appendices. For further study and additional information, the references cited in this chapter may be found useful.

5.14.2 Solid Isoparametric Element Representing Concrete

Three-dimensional isoparametric elements are used and the functions relating to coordinate systems are expressed as follows:

$$\begin{aligned} X &= \sum_{i=1}^{n} N_i(\xi,\eta,\zeta)X_i = N_1x_1 + N_2x_2 + \cdots = \{N\}^T\{X_n\} \\ Y &= \sum_{i=1}^{n} N_i(\xi,\eta,\zeta)Y_i = N_1y_1 + N_2y_2 + \cdots = \{N\}^T\{Y_n\} \\ Z &= \sum_{i=1}^{n} N_i(\xi,\eta,\zeta)Z_i = N_1z_1 + N_2z_2 + \cdots = \{N\}^T\{Z_n\} \end{aligned} \tag{5.155}$$

where $N_i(\xi,\eta,\zeta), i = 1$ to n, are the interpolation functions in the curvilinear coordinates ξ,η,ζ and X_i, Y_i and Z_i are the global X, Y, Z coordinates of mode i. The interpolation function N is also known as the shape function.

The terms $\{X_n\}, \{Y_n\}$ and $\{Z_n\}$ present the nodal coordinates and $\{N\}^T$ is dependent on ξ,η and ζ. Reference is made to Fig. 5.26 for important aspects of the mapping procedures. The most important aspect is to establish a one-to-one relationship between the derived and the parent element (Fig. 5.26). The necessary condition for a one-to-one relationship is the Jacobian determinant given in (5.157)

www.EngineeringBooksPDF.com

$$d[J] = \frac{\partial(X, Y, Z)}{\partial(\xi, \eta, \zeta)} = \begin{bmatrix} \frac{\partial X}{\partial \xi} & \frac{\partial X}{\partial \eta} & \frac{\partial X}{\partial \zeta} \\ \frac{\partial Y}{\partial \xi} & \frac{\partial Y}{\partial \eta} & \frac{\partial Y}{\partial \zeta} \\ \frac{\partial Z}{\partial \xi} & \frac{\partial Z}{\partial \eta} & \frac{\partial Z}{\partial \zeta} \end{bmatrix} \tag{5.156}$$

The Jacobian can also be written in a transported form, i.e. columns replace rows and vice versa.

5.14.3 The Shape Function

The relationship between displacements at any point in the local system (ξ, η, ζ) within the element and the nodal displacements is expressed in the most general form with the aid of a shape or interpolation function as

$$\begin{aligned} U(\xi, \eta, \zeta) &= N_1 u_1 + N_2 u_2 + \cdots (N)^T (u_n) = \sum_{i=1}^{n} N_i(\xi, \eta, \zeta) u_i \\ V(\xi, \eta, \zeta) &= N_1 v_1 + N_2 v_2 + \cdots (N)^T (v_n) = \sum_{i=1}^{n} N_i(\xi, \eta, \zeta) v_i \\ W(\xi, \eta, \zeta) &= N_1 w_1 + N_2 w_2 + \cdots (N)^T (w_n) = \sum_{i=1}^{n} N_i(\xi, \eta, \zeta) w_i \end{aligned} \tag{5.157}$$

where u_i, v_i and w_i are the nodal displacements in the X, Y, Z directions at node i.

The interpolation function N_i can also be expressed in terms of a local dimensionless coordinate system (ξ, η, ζ). Equation (5.159) is written in a more generalized form as

$$\bar{u} = \sum_{i=1}^{n} N_i \bar{u}_i \tag{5.158}$$

where $\bar{u}$ is any coordinate, $\bar{u}_i$ is the current value of $\bar{u}$ at node i and N_i is the shape function for node i.

5.14.4 Derivatives and the Jacobian Matrix

With the shape functions known, the global coordinates and displacements at any point within the element are expressed in terms of the nodal values (5.162) and (5.158):

www.EngineeringBooksPDF.com

$$X = \sum_{i=1}^{n} N_i X_i \quad Y = \sum_{i=1}^{n} N_i Y_i \quad Z = \sum_{i=1}^{n} N_i Z_i \tag{5.159}$$

$$U = \sum_{i=1}^{n} N_i u_i \quad V = \sum_{i=1}^{n} N_i v_i \quad W = \sum_{i=1}^{n} N_i w_i \tag{5.160}$$

where n is the number of nodes on element and X_i, Y_i, Z_i and u_i, v_i, w_i are the nodal coordinates and nodal displacements, respectively.

The derivatives of shape function with respect to global coordinates require the following transformation:

$$\begin{Bmatrix} \frac{\partial N_i}{\partial \xi} \\ \frac{\partial N_i}{\partial \eta} \\ \frac{\partial N_i}{\partial \zeta} \end{Bmatrix} = [J] \begin{Bmatrix} \frac{\partial N_i}{\partial X} \\ \frac{\partial N_i}{\partial Y} \\ \frac{\partial N_i}{\partial Z} \end{Bmatrix} \tag{5.161}$$

where i is the current node number.

$$\begin{Bmatrix} \frac{\partial N_i}{\partial X} \\ \frac{\partial N_i}{\partial Y} \\ \frac{\partial N_i}{\partial Z} \end{Bmatrix} = [J] \begin{Bmatrix} \frac{\partial N_i}{\partial \xi} \\ \frac{\partial N_i}{\partial \eta} \\ \frac{\partial N_i}{\partial \zeta} \end{Bmatrix} \tag{5.161a}$$

where

$$[J] = \begin{bmatrix} \frac{\partial X}{\partial \xi} & \frac{\partial Y}{\partial \xi} & \frac{\partial Z}{\partial \xi} \\ \frac{\partial X}{\partial \eta} & \frac{\partial Y}{\partial \eta} & \frac{\partial Z}{\partial \eta} \\ \frac{\partial X}{\partial \zeta} & \frac{\partial Y}{\partial \zeta} & \frac{\partial Z}{\partial \zeta} \end{bmatrix} \tag{5.161b}$$

where $[J]$ is a 3×3 Jacobian matrix. This matrix eventually plays a major role in the equilibrium equations:

$$\{F\} = [K]\{U\} \tag{5.162}$$

where

$\{U\}$ = the nodal displacement vector
$[K] = \sum_{i=1}^{n} [K_e]$ = the total stiffness matrix
$[k_e]$ = the element stiffness matrix
n = the number of elements

www.EngineeringBooksPDF.com

The determinant $d[J]$ as represented in (5.170) can be evaluated for a one-to-one relationship. Such derivatives of shape functions are given.

Displacement at nodes can now be expressed in the form of element displacement vectors:

$$\{U\} = \begin{Bmatrix} \{u_1\}_1 \\ \{u_2\}_2 \\ \vdots \\ \{u_n\}_n \end{Bmatrix} \tag{5.163}$$

The displacement field within each element can be expressed as

$$\{u\} = [N]\{u^e\} = \sum_{i=1}^{n} \left(N_i[I]\{u\}_i\right) \tag{5.164}$$

$\{u\}^e$= the element nodal displacement vector; $\{u\}_i$= the displacements at node i;
$[N]$ = the element shape function matrix; N_i = the shape functions of node i.

5.14.5 Determination of Strains

With the displacement known at all points within each element, the strains $\{\varepsilon\}$ can be expressed in the following form:

$$\{\varepsilon\} = \sum_{i=1}^{n} [B_i]\{u\}_i = [B]\{u\} \tag{5.165}$$

For the three-dimensional element the $[B]$ matrix of node i and $\{\varepsilon\}_{6\times1}$ are given below:

$$[B_i]_{6\times3} = \begin{bmatrix} \frac{\partial N_i}{\partial X} & 0 & 0 \\ 0 & \frac{\partial N_i}{\partial Y} & 0 \\ 0 & 0 & \frac{\partial N_i}{\partial Z} \\ \frac{\partial N_i}{\partial Y} & \frac{\partial N_i}{\partial X} & 0 \\ 0 & \frac{\partial N_i}{\partial Z} & \frac{\partial N_i}{\partial Y} \\ \frac{\partial N_i}{\partial Z} & 0 & \frac{\partial N_i}{\partial X} \end{bmatrix} \tag{5.166}$$

$$\{\varepsilon\}_{6\times1} = \left[\varepsilon_X, \varepsilon_Y, \varepsilon_Z, \gamma_{XY}, \gamma_{YZ}, \gamma_{ZX}\right]^{T^H} \tag{5.166a}$$

Appendix II gives full details of the coordinate transformations between Cartesian and curvilinear axes. The dimension of $[B]$ for 8-, 20- and 32-noded elements is 6×24, 6×60 and 6×96, respectively.

www.EngineeringBooksPDF.com

5.14.6 Determination of Stresses

The stresses $\{\sigma\}$ can be determined within each element from the strains as

$$\{\sigma\} = [D](\{\varepsilon\} - \{\varepsilon_0\} + \{\sigma_0\}) \tag{5.167}$$

where $\{\sigma_0\}$ = initial stresses; $\{\varepsilon_0\}$ = initial strains and $[D]$ = the material compliance matrix.

5.14.7 Load Vectors and Material Stiffness Matrix

Appendix III gives the material matrices $[D]$ for both concrete and steel. Now virtual displacement $\{du^e\}$ is applied at the nodes, and the sum of work done, dW, by the stresses and distributed body and surface forces over the element volume, vol, and surface, S, is given by

$$dW = \left[\{du^e\}^{T^H}\right]\left(\int_{\text{vol}} [B]^{T^H}\{\sigma\} d\ \text{vol} - \int_S [N]^{T^H}\{p\} d\ S - \int_{\text{vol}} [N]^{T^H}\{G\} d\ \text{vol}\right) \tag{5.168}$$

where $\{p\}$ = the surface force per unit surface area; $\{G\}$ = the force per unit volume and T^H = transpose of the matrix.

When the external work dW is related to the internal work dU

$$dW = dU \tag{5.169}$$

The element stiffness matrix $[K]$

$$[K] = \int_{\text{vol}} B^{T^H} DB d\ \text{vol} = \int_{-1}^{+1}\int_{-1}^{+1}\int_{-1}^{+1} B^{T^H} DB\ \det / d\xi d\eta d\zeta \tag{5.170}$$

The right-hand side of (5.170) is based on the Gaussian integration rule.

Equation (5.168) is valid for any virtual displacement $\{du^e\}$, thus it can be eliminated from both sides of (5.168a). Substituting equations (5.170) and (5.167) into (5.168) one obtains

$$\begin{aligned}\{P\}^e = &\left(\int_{\text{vol}} [B]^{T^H}[D][B] dV\right)\{u^e\} - \int_{\text{vol}} [B]^{T^H}[D]\{e_0\} dV \\ &+ \int_{\text{vol}} [B]^{T^H}\{\sigma_0\} dV - \int_S [N]^T\{p\} dS - \int_{\text{vol}} [N]^{T^H}\{G\} dV\end{aligned} \tag{5.171}$$

Table 5.10 gives miscellaneous loads and forces. Equation (5.185) is the force–displacement relation with stiffness transformation. The terms in (VI.17) are defined as the following:

The element stillness matrix

www.EngineeringBooksPDF.com

$$[K]^{\mathrm{e}}=\int_{\mathrm{vol}}[B]^{T^H}[D][B]dV=\int_{-1}^{+1}\int_{-1}^{+1}\int_{-1}^{+1}B^{T^H}DB\ \det J\ d\xi d\eta d\zeta \tag{5.171a}$$

The nodal force due to body force

$$[P_{\mathrm{b}}]^{\mathrm{e}}=-\int_{\mathrm{vol}}[N]^{T^H}[G]dV=-\int_{-1}^{+1}\int_{-1}^{+1}\int_{-1}^{+1}N^{T^H}G\det J\ d\xi d\eta d\zeta \tag{5.171b}$$

The nodal force due to surface force

$$\{P_s\}^{\mathrm{e}}=-\int_S[N]^{T^H}\{p\}dS \tag{5.171c}$$

The nodal force due to initial stress

$$\{P_{\sigma 0}\}^{\mathrm{e}}=-\int_{\mathrm{vol}}[B]^{T^H}[D]\{\varepsilon_0\}dV=-\int_{-1}^{+1}\int_{-1}^{+1}\int_{-1}^{+1}B^{T^H}D\sigma_0\det J\ d\xi d\eta d\zeta \tag{5.171d}$$

The nodal force due to initial strain

$$\{P_{\varepsilon_0}\}^{\mathrm{e}}=-\int_{\mathrm{vol}}[B]^{T^H}[D]\{\varepsilon_0\}dV=-\int_{-1}^{+1}\int_{-1}^{+1}\int_{-1}^{+1}B^{T^H}D\varepsilon_0\det J\ d\xi d\eta d\zeta \tag{5.171e}$$

Equation (VI.17) can be rewritten as

$$\{P^a\}^{\mathrm{e}}=[K]^{\mathrm{e}}\{u\}^{\mathrm{e}}+\{P_b\}^{\mathrm{e}}+\{P_s\}^{\mathrm{e}}+\{P_{\sigma_0}\}^{\mathrm{e}}+\{P_{\varepsilon_0}\}^{\mathrm{e}} \tag{5.171f}$$

The initial strain vector can be replaced, or the strains due to creep and shrinkage, $\{P^a\}^{\bar{\mathrm{e}}}$ or $\{P^a\}^{\bar{\mathrm{e}}}\mathrm{P}$, can be added to it. Hence these expressions can be added to (5.185). In addition, the strain in (5.171) can be the element swelling strain vector $\{P^{s'}\}^{\mathrm{e}}$. In the case of dynamic loadings applied to structures, an acceleration load vector $\{P^a\}^{\mathrm{e}}$ can be introduced into eqn (5.185) such that

$$\{P^a\}^{\mathrm{e}}=[M]\{A_n\}=\sum_{i=1}^{n}[M_{\mathrm{e}}]=P\sum_{i=1}^{n}[A_n]^{T^H}[A_n]d\xi d\eta d\zeta \tag{5.171g}$$

where $[M]$ = the total mass matrix; $[M_{\mathrm{e}}]$ = the element mass matrix and $\{A_n\}$ = the nodal acceleration vector. If large displacements are considered, the nodal vector $\{P^*\}^e$ can also be incorporated into Equation
Equation (5.171f) is the force–displacement relation for each element. For the whole structure the stiffness matrix and load vectors are assembled according to the nodal incidences; overall equilibrium equations can be written in the following form, as before:

$$[K]\{U\}=\{F\} \tag{5.172}$$

Equation (5.172) is solved for unknown displacements. The element strains can be obtained from nodal displacements. Linear material stresses are obtained from (5.167).

www.EngineeringBooksPDF.com

Table 5.12 Miscellaneous loads and forces [216]

Gravitational forces (surface forces)
Equivalent nodal force in the line of gravity Z-direction

$$\{P_s\}_i = \int_v \left[N^T\right]_i \begin{Bmatrix} 0 \\ 0 \\ -pg \end{Bmatrix} \mathrm{d\,vol}$$

$$= \sum_{i=1}^{n}\sum_{i=1}^{n}\sum_{i=1}^{n} [N]^T_{i,jk} \begin{Bmatrix} 0 \\ 0 \\ -pg \end{Bmatrix} |J|_{i,j,k} W_i W_j W_k$$

Body forces
Body force component per unit volume at (X, Y) point is

$$\begin{Bmatrix} f_x \\ f_y \\ f_z \end{Bmatrix} = \{\bar{f}\} = P_b \omega^2 \begin{Bmatrix} X \\ Y \\ 0 \end{Bmatrix}$$

$$0 \neq \int_v \{N\}^T \begin{Bmatrix} f_x \\ f_y \\ f_z \end{Bmatrix} \mathrm{d\,vol}$$

in the case of isoparametric elements.

Concentrated loads
Concentrated loads away from the point

$$\{P_{\sigma 0}\} = N_i(\xi_1, \eta_1, \zeta_1)P$$
$$\xi_1 = \xi\eta_1 = -\eta\zeta = +1$$

Distributed loads

$$\{Ps\} = \int_{-1}^{+1}\int_{-1}^{+1}\int_{-1}^{+1} N_i^{T''} [p_x, p_y, p_z,]^{T''} \begin{Bmatrix} \frac{\partial Y}{\partial \xi} & \frac{\partial Z}{\partial \eta} & -\frac{\partial Z}{\partial \xi} & \frac{\partial Y}{\partial \eta} \\ \frac{\partial Z}{\partial \xi} & \frac{\partial X}{\partial \eta} & -\frac{\partial Z}{\partial \eta} & \frac{\partial X}{\partial \xi} \\ \frac{\partial X}{\partial \xi} & \frac{\partial Y}{\partial \eta} & -\frac{\partial Y}{\partial \xi} & \frac{\partial X}{\partial \eta} \end{Bmatrix} \mathrm{d}\xi\ \mathrm{d}\eta \ \text{ for } \zeta = \pm 1$$

similarly for $\xi = \pm 1$; $\eta = \pm 1$.

The same procedure is adopted for choosing other element types. Appendix I gives data for some well-known elements.

If boundary conditions are specified on $\{U\}$ to guarantee a unique solution, (5.185) can be solved to obtain nodal point displacements at any node in the given structure. The equations with all degrees of freedom can be written as

$$\begin{bmatrix} K & K_{\bar{R}} \\ K_{\bar{R}}^{T^H} & K_{\bar{R}\bar{R}} \end{bmatrix} \begin{Bmatrix} U \\ U_{\bar{R}} \end{Bmatrix} = \begin{Bmatrix} F \\ F_{\bar{R}} \end{Bmatrix} \tag{5.173}$$

The subscript R represents reaction forces. The top half of (5.173) is used to solve for $\{U\}$.

$$\{U\} = -[K]^{-1}[K_{\bar{R}}]\{U_{\bar{R}}\} + [K]^{-1}\{F\} \tag{5.174}$$

The reaction forces $[F_R]$ are computed from the bottom half of the equation as

$$[F_{\bar{R}}] = [K_{\bar{R}}]^{T^H}\{U\} + \{K_{\bar{R}\bar{R}}\}\{U_{\bar{R}}\} \tag{5.175}$$

www.EngineeringBooksPDF.com

Equation (5.188) must be in equilibrium with Eqn. (5.189).

The Supplement and substructuring

For large structures with complicated features, a substructure (superelement) may be adopted on the lines suggested in (5.173). This superelement may then be used as a reduced element from the collection of elements. If subscripts γ and γ^l represent the retained and removed degrees of freedom of the equations partitioned into two groups, then the expressions in (5.187) can be written as

$$\begin{bmatrix} K_{\gamma\gamma} & K_{\gamma\gamma^l} \\ K_{\gamma^l\gamma} & K_{\gamma^l\gamma^l} \end{bmatrix} \begin{Bmatrix} U_\gamma \\ U_{\gamma^l} \end{Bmatrix} = \begin{Bmatrix} F_\gamma \\ F_{\gamma^l} \end{Bmatrix} \tag{5.176}$$

Equation (5.190) when expanded assumes the following form:

$$\{F_\gamma\} = \{K_{\gamma\gamma}\}\{U_\gamma\} + \{K_{\gamma\gamma^l}\}\{U_{\gamma^l}\} \tag{5.176a}$$

$$\{F_{\gamma^l}\} = \{K_{\gamma^l\gamma}\}\{U_\gamma\} + \{K_{\gamma^l\gamma}\}\{U_{\gamma^l}\} \tag{5.176b}$$

When a dynamic analysis is carried out, the subscript γ (retained) represents the dynamic degrees of freedom.

When (5.175b) is solved, the value of U_r' is then written, similarly to $(5.174)^{\cdot}$.

$$\{U_{\gamma^l}\} = \{K_{\gamma^l\gamma}\}\{F_{\gamma^l}\} - \{K_{\gamma^l\gamma^l}\}^{-1}\{K_{\gamma^l\gamma}\}\{U_\gamma\} \tag{5.177}$$

Substituting $\{U_{\gamma^l}\}$ into (5.176a)

$$\left[\left\{K_{\gamma\gamma}\right\} - \left\{K_{\gamma^l\gamma}\right\}\left\{K_{\gamma^l\gamma^l}\right\}^{-1}\left\{K_{\gamma^l\gamma}\right\}\right]\left\{U_\gamma\right\} = \left\{F_\gamma\right\} - \left\{K_{\gamma\gamma^l}\right\}\left\{K_{\gamma\gamma^l}\right\}^{-1}\left\{F_{\gamma^l}\right\} \tag{5.178}$$

or

$$[\bar{K}]\{\bar{U}\} = \{\bar{F}\} \tag{5.179}$$

where

$$[\bar{K}] = \left[K_{\gamma\gamma^l}\right] - \left[K_{\gamma\gamma^l}\right]\left[K_{\gamma^l\gamma^l}\right]^{-1}\left[K_{\gamma^l\gamma}\right] \tag{5.180}$$

$$\{\bar{F}\} = \left\{F_\gamma\right\} - \left[K_{\gamma\gamma^l}\right]\left[K_{\gamma^l\gamma^l}\right]^{-1}\left\{F_{\gamma^l}\right\}$$

$$\{\bar{U}\} = \left\{U_\gamma\right\} \tag{5.181}$$

and $\{\bar{K}\}$ and $\{\bar{F}\}$ are generally known as the substructure stiffness matrix and load vector, respectively.

In the above equations, the load vector for the substructure is taken as a total load vector. The same derivation may be applied to any number of independent load vectors. For example, one may wish to apply thermal, pressure, gravity and other loading conditions in varying proportions. Expanding the right-hand sides of (5.190a) and (5.190b)

www.EngineeringBooksPDF.com

$$\{F_\gamma\} = \sum_{i=1}^{n} \{F_{\gamma i}\} \tag{5.182}$$

$$\{F_{\gamma'}\} = \sum_{i=1} \{F_{\gamma' i}\} \tag{5.183}$$

where n = the number of independent load vectors.
Substituting into (5.181)

$$\{\bar{F}\} = \sum_{i=1}^{n} \{F_{\gamma\gamma'}\} - [K_{\gamma\gamma'}][K_{\gamma'\gamma'}]^{-1} \sum_{i=1}^{n} \{F_{\gamma' i}\} \tag{5.184}$$

The left-hand side of (5.185) is written as

$$\{\bar{F}\} = \sum_{i=1}^{n} \{\bar{F}_i\} \tag{5.185}$$

Substituting equation (5.185) into (5.186), the following equation is achieved:

$$\{\bar{F}_i\} = \{F_{\gamma i}\} - [K_{\gamma\gamma'}][K_{\gamma'\gamma'}]^{-1}\{F_{\gamma' i}\} \tag{5.186}$$

5.14.8 The Membrane Isoparametric Elements

The membrane steel plane element acting with a concrete element to form a composite section is adopted for many concrete structures, such as bridge decks, concrete pressure and containment vessels, offshore gravity of transmitting only the stresses in the plane while assuming a constant strain along the thickness. These elements are compatible with the one face of the solid isoparametric elements representing concrete. The element local, global and curvilinear coordinate systems are shown in Fig. 5.25. Available are details of shape functions. Knowing these functions, the strain–displacement relation can be obtained. The thickness d of the element is interpolated as

$$d = \sum_{i=1}^{n} N_i d_i \tag{5.187}$$

Where n = the number of nodes and d_i = the nodal thickness at node i.

As shown in Fig. 5.25, the local coordinate system x^I, y^I, z^I with corresponding nodal freedom u^I, v^I, w^I can be used to obtain the local strain field at that point.

$$\varepsilon_{x^I} = \frac{\partial u^I}{\partial x^I} \quad \varepsilon_{y^I} = \frac{\partial v^I}{\partial y^I} \quad \varepsilon_{x^I,y^I} = \frac{\partial u^I}{\partial y^I} + \frac{\partial v^I}{\partial x^I} \tag{5.188}$$

www.EngineeringBooksPDF.com

The x^I axis is tangential to the x_i axis, the z^I axis is normal to the plane of the element and the y^I axis is determined from the right-hand coordinate system. If $\hat{F}_\xi$ is the vector tangential to the ξ axis or the η axis, the vector is written as

$$\hat{F}_\xi = \begin{Bmatrix} \dfrac{\partial x^I}{\partial \xi} \\ \dfrac{\partial y^I}{\partial \xi} \\ \dfrac{\partial z^I}{\partial \xi} \end{Bmatrix} \tag{5.189}$$

Similarly the $\hat{F}_\eta$ vector, in matrix form, is written as

$$\hat{F}_\eta = \begin{Bmatrix} \dfrac{\partial x^I}{\partial \eta} \\ \dfrac{\partial y^I}{\partial \eta} \\ \dfrac{\partial z^I}{\partial \eta} \end{Bmatrix} \tag{5.190}$$

The vector normal to these vectors will be shown as

$$\hat{F}_{z^I} = \hat{F}_\xi \times \hat{F}_\eta = \begin{bmatrix} \dfrac{\partial y^I}{\partial \xi}\dfrac{\partial z^I}{\partial \eta} - \dfrac{\partial z^I}{\partial \xi}\dfrac{\partial y^I}{\partial \eta} \\ \dfrac{\partial z^I}{\partial \xi}\dfrac{\partial x^I}{\partial \eta} - \dfrac{\partial x^I}{\partial \xi}\dfrac{\partial z^I}{\partial \eta} \\ \dfrac{\partial x^I}{\partial \xi}\dfrac{\partial y^I}{\partial \eta} - \dfrac{\partial y^I}{\partial \xi}\dfrac{\partial x^I}{\partial \eta} \end{bmatrix} \tag{5.191}$$

The above vectors are normalized in order to obtain direction cosines:

$$\hat{F}_z = \frac{\hat{F}_z}{|\hat{F}_z|} \tag{5.192}$$

For the x^I axis

$$\hat{F}_{x^I} = \frac{\hat{F}_\xi}{|\hat{F}_\xi|}$$

and for the y^I axis

$$\hat{\hat{F}}_y = \hat{\hat{F}}_z \times \hat{\hat{F}}_x$$

www.EngineeringBooksPDF.com

where

$$|\hat{F}_z| = \sqrt{\left(\frac{\partial x^I}{\partial \xi}\frac{\partial z^I}{\partial \eta} - \frac{\partial z^I}{\partial \xi}\frac{\partial y^I}{\partial \eta}\right)^2 + \left(\frac{\partial z^I}{\partial \xi}\frac{\partial x^I}{\partial \eta} - \frac{\partial y^I}{\partial \xi}\frac{\partial z^I}{\partial \eta}\right)^2 + \left(\frac{\partial x^I}{\partial \xi}\frac{\partial y^I}{\partial \eta} - \frac{\partial y^I}{\partial \xi}\frac{\partial x^I}{\partial \eta}\right)^2} \quad (5.192a)$$

$$|\hat{F}_\xi| = \sqrt{\left(\frac{\partial x^I}{\partial \xi}\right)^2 + \left(\frac{\partial y^I}{\partial \xi}\right)^2 + \left(\frac{\partial z^I}{\partial \xi}\right)^2}$$

The direction cosines in a matrix form for the local orthogonal Cartesian system assume the following form:

$$\{\hat{F}\}_{3\times 3} = \begin{Bmatrix} \hat{\hat{F}}_{x^I} \\ \hat{\hat{F}}_{y^I} \\ \hat{\hat{F}}_{z^I} \end{Bmatrix} = \begin{bmatrix} \hat{F}_{x^I x} & \hat{F}_{y^I x} & \hat{F}_{z^I x} \\ \hat{F}_{x^I y} & \hat{F}_{y^I z} & \hat{F}_{z^I y} \\ \hat{F}_{x^I z} & \hat{F}_{z^I z} & \hat{F}_{z^I z} \end{bmatrix} \quad (5.193)$$

Derivatives

The local derivative of (5.188) must be obtained. To start with, sets of transformations are considered and the global derivatives are obtained:

$$\partial U_G = \begin{bmatrix} \frac{\partial u}{\partial x^l} & \frac{\partial v}{\partial x^l} & \frac{\partial w}{\partial x^l} \\ \frac{\partial u}{\partial y^l} & \frac{\partial v}{\partial y^l} & \frac{\partial w}{\partial y^l} \\ \frac{\partial u}{\partial z^l} & \frac{\partial v}{\partial z^l} & \frac{\partial w}{\partial z^l} \end{bmatrix} = J^{-1} \begin{bmatrix} \frac{\partial u}{\partial \xi} & \frac{\partial v}{\partial \xi} & \frac{\partial w}{\partial \xi} \\ \frac{\partial u}{\partial \eta} & \frac{\partial v}{\partial \eta} & \frac{\partial w}{\partial \eta} \\ 0 & 0 & 0 \end{bmatrix} \quad (5.194)$$

where

$$[J] = \begin{bmatrix} \frac{\partial x^I}{\partial \xi} & \frac{\partial y^I}{\partial \xi} & \frac{\partial z^I}{\partial \xi} \\ \frac{\partial x^I}{\partial \eta} & \frac{\partial y^I}{\partial \eta} & \frac{\partial z^I}{\partial \eta} \\ \hat{F}_{Z^I,x^d} & \hat{F}_{Z^I,y^d} & \hat{F}_{Z^I,z^d} \end{bmatrix} \quad (5.194a)$$

The next step is to obtain the local derivatives and they are summarized below:

$$\partial U_L = \hat{F}^{T^H} \partial \hat{U}_G \hat{F} = \sum_{i=1}^{n} \begin{bmatrix} \partial \hat{F}_1^i \partial u_1^i & \partial \hat{F}_1^i \partial u_2^i & \partial \hat{F}_1^i \partial u_3^i \\ \partial \hat{F}_2^i \partial u_1^i & \partial \hat{F}_2^i \partial u_2^i & \partial \hat{F}_2^i \partial u_3^i \\ \partial \hat{F}_3^i \partial u_1^i & \partial \hat{F}_3^i \partial u_2^i & \partial \hat{F}_3^i \partial u_3^i \end{bmatrix} \quad (5.195)$$

where

www.EngineeringBooksPDF.com

$$\partial F_1^i = \hat{F}_{x^l,x}\frac{\partial N_i}{\partial x} + \hat{F}_{x^l,y}\frac{\partial N_i}{\partial y} + \hat{F}_{x^l,z}\frac{\partial N_i}{\partial z} \tag{5.195a}$$

$$\partial F_2^i = \hat{F}_{y^l,x}\frac{\partial N_i}{\partial x} + \hat{F}_{y^l,y}\frac{\partial N_i}{\partial y} + \hat{F}_{y^l,z}\frac{\partial N_i}{\partial z}$$

$$\partial F_3^i = \hat{F}_{z^l,x}\frac{\partial N_i}{\partial z} + \hat{F}_{z^l,y}\frac{\partial N_i}{\partial y} + \hat{F}_{z^l,z}\frac{\partial N_i}{\partial z}$$

$$\partial u_1^i = \hat{F}_{x^l,x}u_i + \hat{F}_{x^l,y}v_i + \hat{F}_{x^l,z}w_i$$

$$\partial u_2^i = \hat{F}_{y^l,x}u_i + \hat{F}_{y^l,y}v_i + \hat{F}_{y^l,z}w_i$$

$$\partial u_3^i = \hat{F}_{z^l,x}u_i + \hat{F}_{z^l,y}v_i + \hat{F}_{z^l,z}w_i$$

Using (5.199) and (5.206) the strain value is computed as

$$\begin{aligned}\{\varepsilon\} &= \sum_{i=1}^{n}\begin{Bmatrix}\partial\hat{F}_1^i\partial u_1^i\\ \partial\hat{F}_2^i\partial u_2^i\\ \partial\hat{F}_2^i\partial u_1^i + \partial\hat{F}_1^i\partial u_2^i\end{Bmatrix}\\ &= [B]\{u^{\bar{e}}\}\\ &= \begin{Bmatrix}[B_1]\\ [B_2]\\ \vdots\\ [B_i]\\ \vdots\\ [B_n]\end{Bmatrix}\times\begin{Bmatrix}[u_1]\\ [u_2]\\ \vdots\\ [u_i]\\ \vdots\\ [u_n]\end{Bmatrix}\end{aligned} \tag{5.196}$$

In which $[B_i]$ and $[u_i]$ are given as

$$[B]_{3\times3} = \begin{bmatrix}\bar{\hat{F}}_{x^1,x}\partial\hat{F}_1^i & \hat{F}_{x^1,y}\partial\hat{F}_1^i & \hat{F}_{x^1,z}\partial\hat{F}_1^i\\ F_{y^1,x}\partial\hat{F}_2^i & \hat{F}_{y^1,y}\partial\hat{F}_2^i & \hat{F}_{y^1,z}\partial\hat{F}_2^i\\ \left(\hat{F}_{x^1,x}\partial\hat{F}_2^i + \hat{F}_{y^1,x}\partial\hat{F}_1^i\right) & \left(\hat{F}_{x^1,y}\partial\hat{F}_2^i + \hat{F}_{y^1,y}\partial\hat{F}_1^i\right) & \left(\hat{F}_{x^1,z}\partial\hat{F}_2^i + \hat{F}_{y^1,z}\partial\hat{F}_1\right)\end{bmatrix} \tag{5.197}$$

$$\{u_i\}_{3\times1} = \begin{Bmatrix}u_i\\ v_i\\ w_i\end{Bmatrix} \tag{5.198}$$

www.EngineeringBooksPDF.com

The local stresses at any point are written in the usual manner in the form of

$$\{\sigma\} = [D](\{\varepsilon\} - \{\varepsilon_0\}) \tag{5.199}$$

in which

$$\left\{\sigma^l\right\} = \left[\sigma_{x^l}, \sigma_{y^l}, T_{x^l y^l}\right]^{T^H} \quad \left\{\varepsilon_0^l\right\} = \left[\varepsilon_{x^l}, \varepsilon_{y^l}, 0\right]^{T^H} \tag{5.199a}$$

For the plane stress case, the elastic material matrix is given by

$$[D] = \frac{E_s}{1 - v_5^2} \begin{bmatrix} 1 & v_s & 0 \\ v_s & 1 & 0 \\ 0 & 0 & \frac{1-v_s}{2} \end{bmatrix} \tag{5.200}$$

where E_s and v_s are the modulus of elasticity and Poisson's ratio of steel. For $[D]$ in three-dimensional situations please refer to Appendix III. The element stiffness matrix for this element is given by

$$[K] = \int_{-1}^{+1} \int_{-1}^{+1} \int_{-1}^{+1} B^{T^H} DB \det J d\xi d\eta \tag{5.201}$$

Again (as before), the three-dimensional situation can occur in which case Eqn.(5.200) is modified. Other elements can be chosen to solve (5.201).

5.14.9 Isoparametric Line Elements

The method of derivation here for line elements is the same as for solid or membrane elements; the difference is only in the choice of displacement polynomials and the shape functions.

The line elements represent the conventional reinforcing bars or the prestressing tendons in concrete. The nodes of these elements depend on the type of solid elements used for concrete. They are given below:

(a) A 2-noded line element corresponds to an 8-noded solid element.
(b) A 3-noded line element corresponds to a 20-noded solid element.
(c) A 4-noded line element corresponds to a 30-noded solid element.

These line element nodes can be matched by placing them on top of the solid elements. Sometimes it is difficult to idealize them in this manner owing to the reinforcement layout. Such line elements can be placed in the body of the solid element. Where bond-slip analysis is carried out, these line elements can be placed on the nodes of the solid element or can be attached to spring elements as shown in Fig. 5.27.

www.EngineeringBooksPDF.com

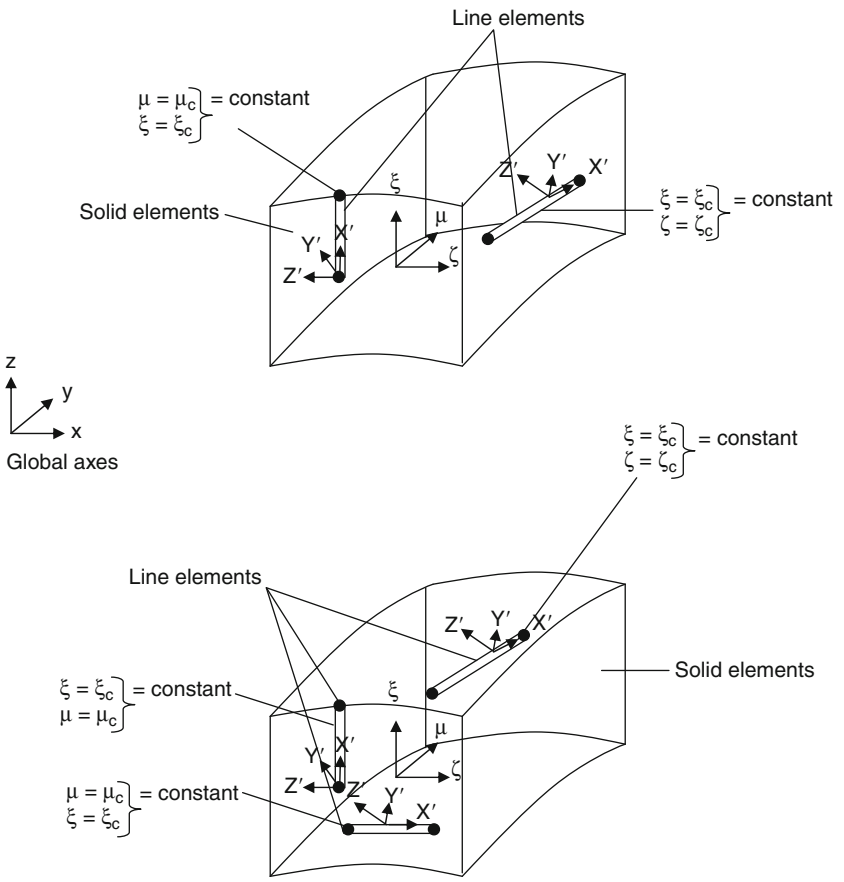


Fig. 5.27 Line elements in the body of a solid element

5.14.9.1 Two-, Three- and Four-Noded Elements

The shape functions and derivatives for the isoparametric line elements are given below:

(a) Two-noded line element

Shape functions	*Derivatives*
$N_1 = \frac{1}{2}(1-\xi)$	$\frac{\partial N_1}{\partial \xi} = -\frac{1}{2}$
$N_2 = \frac{1}{2}(1+\xi)$	$\frac{\partial N_2}{\partial \xi} = \frac{1}{2}$

(5.202)

www.EngineeringBooksPDF.com

(b) Three-noded line element (Fig. 5.6)

Shape functions	*Derivatives*
$N_1 = \frac{1}{2}(1-\xi)\xi$	$\frac{\partial N_1}{\partial \xi} = \xi - \frac{1}{2}$
$N_2 = 1 - \xi^2$	$\frac{\partial N_2}{\partial \xi} = 2\xi$
$N_3 = \frac{1}{2}(1+\xi)\xi$	$\frac{\partial N_3}{\partial \xi} = \xi + \frac{1}{2}$

(5.203)

(c) Four-noded line element (Fig. 5.6)

Shape functions	*Derivatives*
$N_1 = \frac{1}{3}(1-\xi)\left(2\xi^2 - \frac{1}{2}\right)$	$\frac{\partial N_1}{\partial \xi} = \frac{1}{3}\left(4\xi - 6\xi^2 + \frac{1}{2}\right)$
$N_2 = \frac{4}{3}\left(\xi^2 - 1\right)\left(\xi^2 - \frac{1}{2}\right)$	$\frac{\partial N_2}{\partial \xi} = \frac{4}{3}\left(3\xi^2 - \xi - 1\right)$
$N_3 = \frac{4}{3}\left(1 - \xi^2\right)\left(\xi + \frac{1}{2}\right)$	$\frac{\partial N_3}{\partial \xi} = \frac{4}{3}\left(1 - 3\xi^2 - \xi\right)$
$N_4 = \frac{1}{3}(1+\xi)\left(2\xi^2 - \frac{1}{2}\right)$	$\frac{\partial N_4}{\partial \xi} = \frac{1}{3}\left(4\xi + 6\xi^2 - \frac{1}{2}\right)$

(5.204)

The strain–displacement relation
At any point in the line element, the local Cartesian axis X^l is tangential to the curvilinear axis. The local strain in the axial direction at any point can be written as

$$\varepsilon_{x^l} = \partial U^l / \partial X^l \tag{5.205}$$

Using the displacement transformation, Equation (5.205) is written as

$$\varepsilon_{x^l} = \frac{1}{L}\left(l_1 \frac{\partial U}{\partial \xi} + m_1 \frac{\partial V}{\partial \xi} + n_1 \frac{\partial W}{\partial \xi}\right) \tag{5.205a}$$

www.EngineeringBooksPDF.com

where l_1, m_1, n_1 are the direction cosines of the X^l axis and are written as

$$\begin{aligned} l_1 &= \frac{\partial X}{\partial \xi}/L \\ m_1 &= \frac{\partial Y}{\partial \xi}/L \\ n_1 &= \frac{\partial Z}{\partial \xi}/L \end{aligned} \tag{5.205b}$$

$$L = \sqrt{(\partial X/\partial \xi)^2 + (\partial Y/\partial \xi)^2 + (\partial Z/\partial \xi)^2} \tag{5.205c}$$

U, V and W are the global nodal freedom at any node, and U^l is the local freedom in the X^l direction. It is related according to

$$U^l = l_l U + m_l V + n_l W \tag{5.206}$$

Equation (5.205) in terms of the shape function derivatives is now written as

$$\varepsilon_{x^l} = l_1 \sum_{i=1}^{n} \left[l_1 \frac{\partial N_i}{\partial \xi}, m_1 \frac{\partial N_i}{\partial \xi}, n_1 \frac{\partial N_i}{\partial \xi} \right] \begin{Bmatrix} U_i \\ V_i \\ W_i \end{Bmatrix} \tag{5.207}$$

where n is the number of nodes on the element.

$$\{\varepsilon_{x^l}\} = [B]\{U^e\} \tag{5.208}$$

Equation (5.207) is also written as

$$\begin{aligned} [B] &= [[B_1], [B_2], [B_3], \ldots [B_i], \ldots, \{B_n\}]^T \\ \{U^{\bar{e}}\} &= [[U_1], [U_2], [U_3], \ldots [U_i], \ldots, \{U_n\}]^T \end{aligned} \tag{5.209}$$

The stiffness matrix assumes the form

$$[K] = \int_{-1}^{+1} B^T E_S B A(\xi) L d\xi = \sum_{j=1}^{N} B_j^T E_s B_j L_j W_j A(\xi_j) \tag{5.210}$$

where

www.EngineeringBooksPDF.com

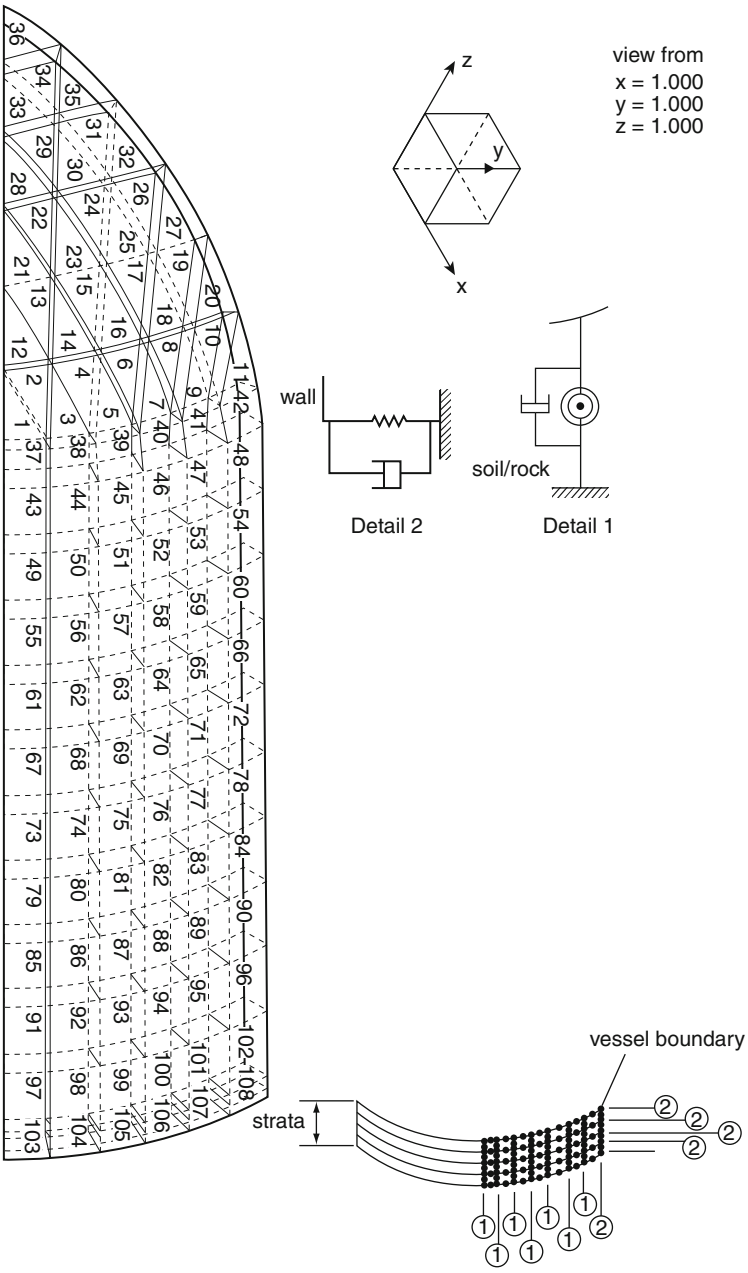


Fig. 5.28 Nonlinear model–Sizewell B vessel

www.EngineeringBooksPDF.com

$$A(\varepsilon_j) = \sum_{i=1}^{n} N_i A_j \tag{5.210a}$$

where A = the cross-sectional area at node j; n = the number of nodes on the element; N = the number of integration points and N_i = the shape function at node i.

The strain and stress are calculated as

$$\{\varepsilon_{x'}\} = [B]\{U^e\} \quad \{\sigma_{x'}\} = [E_S]\{\varepsilon_{x'}\} \tag{5.211}$$

where $\{U^{\bar{e}}\}$ is the global nodal displacement of the element.

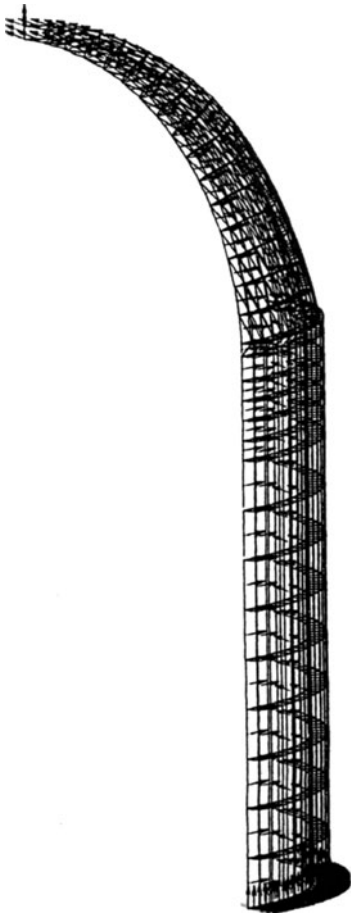


Fig. 5.29 Finite element mesh scheme for a concrete

www.EngineeringBooksPDF.com

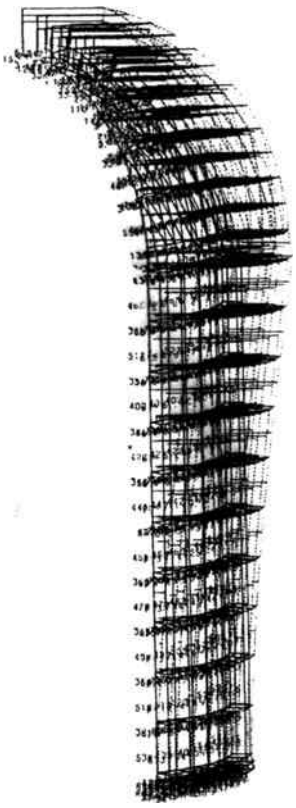


Fig. 5.30 Damage caused by implosion at a level 2.75 times the extreme loads (minimum safety factor 2.5)

www.EngineeringBooksPDF.com

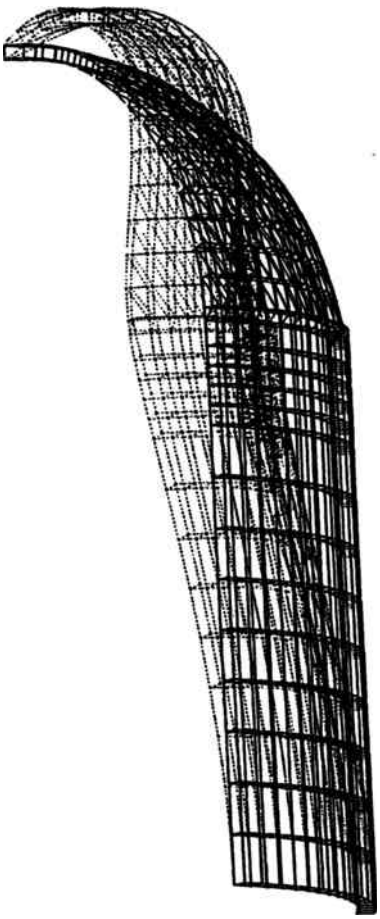


Fig. 5.31 Damage caused by implosion at a level 3.5 times the extreme loads (concrete cracked/scabbed; steel yielded/plastic)

www.EngineeringBooksPDF.com

5.14.10 Element Types, Shape Functions, Derivatives, Stiffness Matrices for Finite Element

Table 5.13 Shear and torsion included for line element

$$
[D] = \begin{bmatrix}
\frac{EA}{L} & & & & & & & & & & & \\
0 & \frac{12EI_\xi}{L^3(1+\bar{\tau}_\eta)} & & & & & & & & & & \\
0 & 0 & \frac{12EI_\xi}{L^3(1+\bar{\tau}_\eta)} & & & & & & & & & \\
0 & 0 & 0 & \frac{GJ}{L} & & & & & & & & \\
0 & 0 & \frac{-6EI_\eta}{L^2(1+\tau_\xi)} & 0 & \frac{(4+\bar{\tau}_\xi)EI_\eta}{L(1+\bar{\tau}_\eta)} & & & & & & & \\
0 & \frac{6EI_\xi}{L^2(1+\bar{\tau}_\eta)} & 0 & 0 & 0 & \frac{(4+\bar{\tau}_\eta)EI_\xi}{L(1+\bar{\tau}_\eta)} & & & & & & \\
\frac{-EA}{L} & 0 & 0 & 0 & 0 & 0 & \frac{AE}{L} & & & & & \\
0 & \frac{-12EI_\xi}{L^3(1+\bar{\tau}_\eta)} & 0 & 0 & 0 & \frac{-6EI_\xi}{L^2(1+\bar{\tau}_\eta)} & 0 & \frac{12EI_\xi}{L^3(1+\bar{\tau}_\eta)} & & & & \\
0 & 0 & \frac{-12EI_\eta}{L^3(1+\bar{\tau}_\xi)} & 0 & \frac{6EI_\eta}{L^2(1+\bar{\tau}_\xi)} & 0 & 0 & 0 & \frac{12EI_\eta}{L^3(1+\bar{\tau}_\xi)} & & & \\
0 & 0 & 0 & \frac{-GJ}{L} & 0 & 0 & 0 & 0 & 0 & \frac{GJ}{L} & & \\
0 & 0 & \frac{-6EI_\eta}{L^2(1+\bar{\tau}_\xi)} & 0 & \frac{(2-\bar{\tau}_\xi)EI_\eta}{L(1+\bar{\tau}_\xi)} & 0 & 0 & 0 & \frac{6EI_\eta}{L^2(1+\bar{\tau}_\xi)} & 0 & \frac{(4+\bar{\tau}_\xi)EI_\eta}{L(1+\bar{\tau}_\xi)} & \\
0 & \frac{6EI_\xi}{L^2(1+\bar{\tau}_\eta)} & 0 & 0 & 0 & \frac{(2-\bar{\tau}_\eta)EI_\xi}{L(1+\tau_\eta)} & 0 & \frac{-6EI_\xi}{L^2(1+\bar{\tau}_\eta)} & 0 & 0 & 0 & \frac{(4+\bar{\tau}_\eta)EI_\xi}{L(1+\bar{\tau}_\eta)}
\end{bmatrix}
$$

where

$$\bar{\tau}_\eta = \frac{12EI_\xi}{GA_{s\eta}L^2} = 24(1+\nu)\frac{A}{A_{s\eta}}\left(\frac{T_\xi}{L}\right)^2 \quad \bar{\tau}_\xi = \frac{12EI_\eta}{GA_{s\xi}L^2} = 24(1+\nu)\frac{A}{A_{s\xi}}\left(\frac{T_\eta}{L}\right)^2$$

A_s = shear area T = torsional moment of inertia p = density ξ, η local axes are parallel to Z and Y azes

www.EngineeringBooksPDF.com

Table 5.14 Chain rule

$$\begin{bmatrix} \frac{\partial u}{\partial X} \\ \frac{\partial u}{\partial Y} \\ \frac{\partial u}{\partial Z} \\ \frac{\partial v}{\partial X} \\ \frac{\partial v}{\partial Y} \\ \frac{\partial v}{\partial Z} \\ \frac{\partial w}{\partial X} \\ \frac{\partial w}{\partial Y} \\ \frac{\partial w}{\partial Z} \end{bmatrix} = \frac{1}{\det J} \begin{bmatrix} C_{11} & C_{12} & C_{13} & 0 & 0 & 0 & 0 & 0 & 0 \\ C_{21} & C_{22} & C_{23} & 0 & 0 & 0 & 0 & 0 & 0 \\ C_{31} & C_{32} & C_{33} & 0 & 0 & 0 & 0 & 0 & 0 \\ 0 & 0 & 0 & C_{11} & C_{12} & C_{13} & 0 & 0 & 0 \\ 0 & 0 & 0 & C_{21} & C_{22} & C_{23} & 0 & 0 & 0 \\ 0 & 0 & 0 & C_{31} & C_{32} & C_{33} & 0 & 0 & 0 \\ 0 & 0 & 0 & 0 & 0 & 0 & C_{11} & C_{12} & C_{13} \\ 0 & 0 & 0 & 0 & 0 & 0 & C_{21} & C_{22} & C_{23} \\ 0 & 0 & 0 & 0 & 0 & 0 & C_{31} & C_{32} & C_{33} \end{bmatrix} \begin{bmatrix} \frac{\partial u}{\partial \xi} \\ \frac{\partial u}{\partial \eta} \\ \frac{\partial u}{\partial \zeta} \\ \frac{\partial v}{\partial \xi} \\ \frac{\partial v}{\partial \eta} \\ \frac{\partial v}{\partial \zeta} \\ \frac{\partial w}{\partial \xi} \\ \frac{\partial w}{\partial \eta} \\ \frac{\partial w}{\partial \zeta} \end{bmatrix}$$

where

$$C_{11} = \frac{\partial Y}{\partial \xi}\frac{\partial Z}{\partial \xi} - \frac{\partial Z}{\partial \eta}\frac{\partial Y}{\partial \xi} \quad C_{12} = \frac{\partial Z}{\partial \xi}\frac{\partial Y}{\partial \zeta} - \frac{\partial Y}{\partial \xi}\frac{\partial Z}{\partial \zeta}$$

$$C_{13} = \frac{\partial Y}{\partial \xi}\frac{\partial Z}{\partial \zeta} - \frac{\partial Z}{\partial \xi}\frac{\partial Y}{\partial \zeta} \quad C_{21} = \frac{\partial Z}{\partial \xi}\frac{\partial X}{\partial \zeta} - \frac{\partial X}{\partial \xi}\frac{\partial Z}{\partial \zeta}$$

$$C_{22} = \frac{\partial X}{\partial \xi}\frac{\partial Z}{\partial \zeta} - \frac{\partial Z}{\partial \xi}\frac{\partial X}{\partial \zeta} \quad C_{23} = \frac{\partial Z}{\partial \xi}\frac{\partial X}{\partial \eta} - \frac{\partial X}{\partial \xi}\frac{\partial Z}{\partial \eta}$$

$$C_{31} = \frac{\partial X}{\partial \eta}\frac{\partial Y}{\partial \zeta} - \frac{\partial Y}{\partial \eta}\frac{\partial X}{\partial \zeta} \quad C_{32} = \frac{\partial Y}{\partial \xi}\frac{\partial X}{\partial \zeta} - \frac{\partial X}{\partial \xi}\frac{\partial Y}{\partial \zeta}$$

$$C_{33} = \frac{\partial X}{\partial \xi}\frac{\partial Y}{\partial \eta} - \frac{\partial Y}{\partial \xi}\frac{\partial X}{\partial \eta}$$

$\det[J]$ = the determinant of the Jacobian matrix.

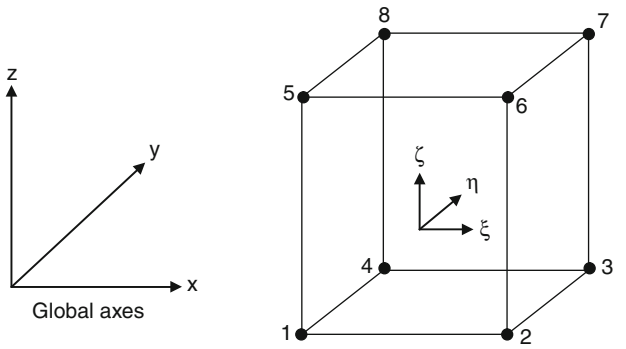
5.14.9.2 Line Element in the Body of a Solid Element

The procedure for the strain–displacement and the stiffness matrix is the same as for the other line elements. The element must lie parallel to one of the curvilinear axes (ξ, η, ζ) of the solid element. The element may be anywhere in the solid element with maximum curvilinear coordinates $\xi = \pm 1$, $\eta = \pm 1$ and $\zeta = \pm 1$. The displacement U inside the element is written as (Fig. 5.27)

www.EngineeringBooksPDF.com

Table 5.15 Solid isoparametric elements

Eight-noded solid element



Node i	Shape functions $N_i(\xi,\eta,\zeta)$	Derivatives		
		$\frac{\partial N_i}{\partial \xi}$	$\frac{\partial N_i}{\partial \eta}$	$\frac{\partial N_i}{\partial \zeta}$
1	$\frac{1}{8}(1-\xi)(1-\eta)(1-\zeta)$	$-\frac{1}{8}(1-\eta)(1-\zeta)$	$-\frac{1}{8}(1-\xi)(1-\zeta)$	$-\frac{1}{8}(1-\eta)(1-\xi)$
2	$\frac{1}{8}(1+\xi)(1-\eta)(1-\zeta)$	$\frac{1}{8}(1-\eta)(1-\zeta)$	$-\frac{1}{8}(1+\xi)(1-\zeta)$	$-\frac{1}{8}(1+\eta)(1-\eta)$
3	$\frac{1}{8}(1+\xi)(1+\eta)(1-\zeta)$	$\frac{1}{8}(1+\eta)(1-\zeta)$	$\frac{1}{8}(1+\xi)(1-\zeta)$	$-\frac{1}{8}(1+\eta)(1+\eta)$
4	$\frac{1}{8}(1-\xi)(1+\eta)(1-\zeta)$	$-\frac{1}{8}(1+\eta)(1-\zeta)$	$\frac{1}{8}(1-\xi)(1-\zeta)$	$-\frac{1}{8}(1-\eta)(1+\eta)$
5	$\frac{1}{8}(1-\xi)(1-\eta)(1+\zeta)$	$-\frac{1}{8}(1-\eta)(1+\zeta)$	$-\frac{1}{8}(1-\xi)(1+\zeta)$	$\frac{1}{8}(1-\eta)(1-\eta)$
6	$\frac{1}{8}(1+\xi)(1-\eta)(1+\zeta)$	$\frac{1}{8}(1-\eta)(1+\zeta)$	$-\frac{1}{8}(1+\xi)(1+\zeta)$	$\frac{1}{8}(1+\eta)(1-\eta)$
7	$\frac{1}{8}(1+\xi)(1+\eta)(1+\zeta)$	$\frac{1}{8}(1+\eta)(1+\zeta)$	$\frac{1}{8}(1+\xi)(1+\zeta)$	$\frac{1}{8}(1+\eta)(1+\eta)$
8	$\frac{1}{8}(1-\xi)(1+\eta)(1+\zeta)$	$-\frac{1}{8}(1+\eta)(1+\zeta)$	$\frac{1}{8}(1-\xi)(1+\zeta)$	$\frac{1}{8}(1-\eta)(1+\eta)$

$$\{U\} = [\bar{N}]\{U^{\bar{e}}\} = \sum_{i=1}^{n} [N_i][I]\{U_i\} \tag{5.212}$$

$$[\bar{N}] = [N(\xi, \eta_c, \zeta)](\text{solid element}) \tag{5.212a}$$

such that

$$\zeta = \zeta_c \quad \eta = \eta_c(\text{constant})$$

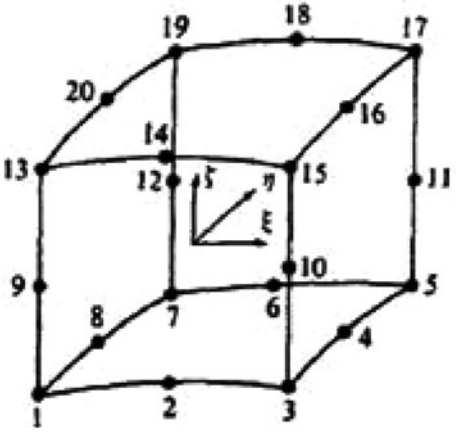
For the tangential directions of ξ and η

$$\hat{X}_\xi = \begin{Bmatrix} \frac{\partial X}{\partial \xi} \\ \frac{\partial Y}{\partial \xi} \\ \frac{\partial Z}{\partial \xi} \end{Bmatrix} (\text{at } \eta = \eta_c, \zeta = \zeta_c) \quad \hat{X}_\eta = \begin{Bmatrix} \frac{\partial X}{\partial \eta} \\ \frac{\partial Y}{\partial \eta} \\ \frac{\partial Z}{\partial \eta} \end{Bmatrix} (\text{at } \eta = \eta_c, \zeta = \zeta_c) \tag{5.213}$$

A normal $\hat{Z}^l$ axis vector and $\hat{X}^l$ axis and $\hat{Y}^l$ axis vectors are defined as

www.EngineeringBooksPDF.com

Table 5.16 Twenty-noded solid element



Node i	Shape functions $N_i(\xi,\eta,\zeta)$	Derivatives		
		$\frac{\partial N_i}{\partial \xi}$	$\frac{\partial N_i}{\partial \eta}$	$\frac{\partial N_i}{\partial \zeta}$
1	$\frac{1}{8}(1-\xi)(1-\eta)(1-\zeta)(-\xi-\eta-\zeta-2)$	$\frac{1}{8}(1-\eta)(1-\zeta)(2\xi+\eta+\zeta+1)$	$\frac{1}{8}(1-\xi)(1-\zeta)(2\eta+\xi+\zeta+1)$	$\frac{1}{8}(1-\xi)(1-\eta)(2\zeta+\eta+\xi+1)$
2	$\frac{1}{4}(1-\xi^2)(1-\eta)(1-\zeta)$	$-\frac{1}{2}(1-\eta)(1-\zeta)\xi$	$-\frac{1}{4}(1-\xi^2)(1-\zeta)$	$-\frac{1}{4}(1-\xi^2)(1-\eta)$
3	$\frac{1}{8}(1+\xi)(1-\eta)(1-\zeta)(\xi-\eta-\zeta-2)$	$\frac{1}{8}(1-\eta)(1-\zeta)(2\xi-\eta-\zeta-1)$	$\frac{1}{8}(1+\xi)(1-\zeta)(2\eta-\xi+\zeta+1)$	$\frac{1}{8}(1+\xi)(1-\eta)(2\zeta-\xi+\eta+1)$
4	$\frac{1}{4}(1+\xi^2)(1-\eta^2)(1-\zeta)$	$\frac{1}{4}(1-\eta^2)(1-\zeta)$	$-\frac{1}{2}(1+\xi)(1-\zeta)\eta$	$-\frac{1}{4}(1-\eta^2)(1+\xi)$
5	$\frac{1}{8}(1+\xi)(1+\eta)(1-\zeta)(\xi+\eta-\zeta-2)$	$\frac{1}{8}(1+\eta)(1-\zeta)(2\xi+\eta-\zeta-1)$	$\frac{1}{8}(1+\xi)(1-\zeta)(2\eta+\xi-\zeta-1)$	$\frac{1}{8}(1+\xi)(1+\eta)(2\zeta-\xi-\eta+1)$
6	$\frac{1}{4}(1-\xi^2)(1+\eta)(1-\zeta)$	$-\frac{1}{2}(1+\eta)(1-\zeta)\xi$	$\frac{1}{4}(1-\xi^2)(1-\zeta^2)$	$-\frac{1}{4}(1-\xi^2)(1+\eta)$

www.EngineeringBooksPDF.com

Table 5.16 (continued)

7	$\frac{1}{8}(1-\xi)(1+\eta)(1-\zeta)(-\xi+\eta-\zeta-2)$	$\frac{1}{8}(1+\eta)(1-\zeta)(2\xi-\eta+\zeta+1)$	$\frac{1}{8}(1-\xi)(1-\zeta)(2\eta-\xi-\zeta-1)$	$\frac{1}{8}(1-\xi)(1+\eta)(2\zeta-\eta+\xi+1)$
8	$\frac{1}{4}(1-\xi)(1-\eta^2)(1-\zeta)$	$-\frac{1}{4}(1-\eta^2)(1-\zeta)$	$-\frac{1}{2}(1-\xi)(1-\zeta)$	$-\frac{1}{4}(1-\eta^2)(1-\xi)$
9	$\frac{1}{4}(1-\xi)(1-\eta)(1-\zeta^2)$	$-\frac{1}{4}(1-\zeta^2)(1-\eta)$	$-\frac{1}{4}(1-\xi)(1-\zeta^2)$	$-\frac{1}{2}(1-\xi)(1-\eta)\zeta$
10	$\frac{1}{4}(1+\xi)(1-\eta)(1-\zeta^2)$	$\frac{1}{4}(1-\eta)(1-\zeta^2)$	$-\frac{1}{4}(1+\xi)(1-\zeta^2)$	$-\frac{1}{2}(1+\xi)(1-\eta)\zeta$
11	$\frac{1}{4}(1+\xi)(1+\eta)(1-\zeta^2)$	$\frac{1}{4}(1+\eta)(1-\zeta^2)$	$\frac{1}{4}(1+\xi)(1-\zeta^2)$	$-\frac{1}{2}(1+\xi)(1+\eta)\zeta$
12	$\frac{1}{4}(1-\xi)(1+\eta)(1-\zeta^2)$	$-\frac{1}{4}(1+\eta)(1-\zeta^2)$	$\frac{1}{4}(1-\xi)(1-\zeta^2)$	$-\frac{1}{2}(1-\xi)(1+\eta)\zeta$
13	$\frac{1}{8}(1-\xi)(1-\eta)(1+\zeta)(-\xi-\eta+\zeta-2)$	$\frac{1}{8}(1-\eta)(1+\zeta)(2\xi+\eta-\zeta+1)$	$\frac{1}{8}(1-\xi)(1+\zeta)(2\eta+\xi-\zeta+1)$	$\frac{1}{8}(1-\xi)(1-\eta)(2\zeta-\eta-\xi-1)$
14	$\frac{1}{4}(1-\xi^2)(1-\eta)(1+\zeta)$	$-\frac{1}{2}(1-\eta)(1+\zeta)\xi$	$-\frac{1}{4}(1-\xi^2)(1+\zeta)$	$\frac{1}{4}(1-\xi^2)(1-\eta)$
15	$\frac{1}{8}(1+\xi)(1-\eta)(1+\zeta)(\xi-\eta+\zeta-2)$	$\frac{1}{8}(1-\eta)(1+\zeta)(2\xi-\eta+\zeta-1)$	$\frac{1}{8}(1+\zeta)(1+\xi)(2\eta-\xi-\zeta+1)$	$\frac{1}{8}(1-\eta)(1+\xi)(2\zeta+\xi-\eta-1)$
16	$\frac{1}{4}(1+\xi)(1-\eta^2)(1+\zeta)$	$\frac{1}{4}(1-\eta^2)(1+\xi)$	$-\frac{1}{2}(1+\xi)(1+\zeta)\eta$	$\frac{1}{4}(1+\xi)(1-\eta^2)$
17	$\frac{1}{8}(1+\xi)(1+\eta)(1+\zeta)(\xi+\eta+\zeta-2)$	$\frac{1}{8}(1+\eta)(1+\zeta)(2\xi+\eta+\zeta-1)$	$\frac{1}{8}(1+\xi)(1+\zeta)(2\eta+\xi+\zeta-1)$	$\frac{1}{8}(1+\xi)(1+\eta)(2\zeta+\eta+\xi-1)$
18	$\frac{1}{4}(1-\xi^2)(1+\eta)(1+\zeta)$	$-\frac{1}{2}\xi(1+\eta)(1+\zeta)$	$\frac{1}{4}(1-\xi^2)(1+\zeta)$	$\frac{1}{4}(1-\xi^2)(1+\eta)$
19	$\frac{1}{8}(1-\xi)(1+\eta)(1+\zeta)(-\xi+\eta+\zeta-2)$	$\frac{1}{8}(1+\eta)(1+\zeta)(2\xi-\eta-\zeta-1)$	$\frac{1}{8}(1-\xi)(1+\zeta)(2\eta-\xi+\zeta-1)$	$\frac{1}{8}(1-\xi)(1+\eta)(2\zeta-\xi+\eta-1)$
20	$\frac{1}{4}(1-\xi)(1-\eta^2)(1+\zeta)$	$-\frac{1}{4}(1-\eta^2)(1+\zeta)$	$-\frac{1}{2}(1-\xi)(1+\zeta)\eta$	$\frac{1}{4}(1-\xi)(1-\eta^2)$

www.EngineeringBooksPDF.com

Table 5.17 Isoparametric membrane elements Four-noded membrane element

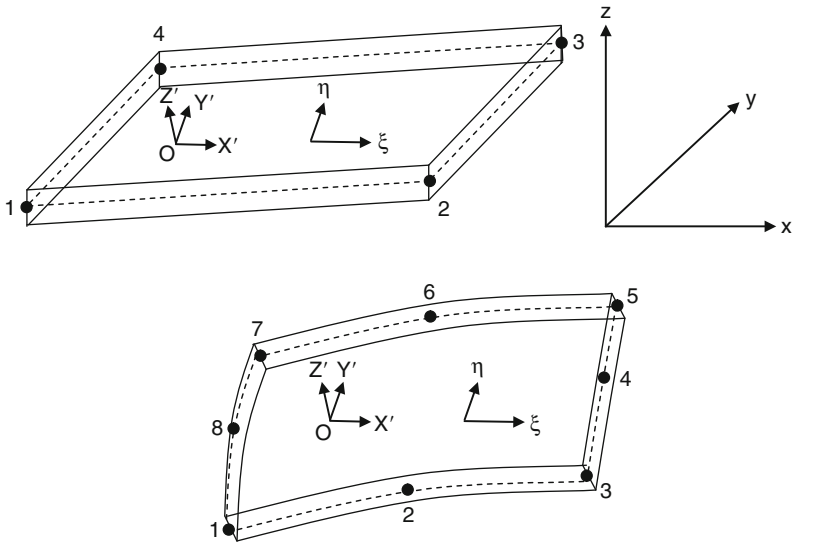
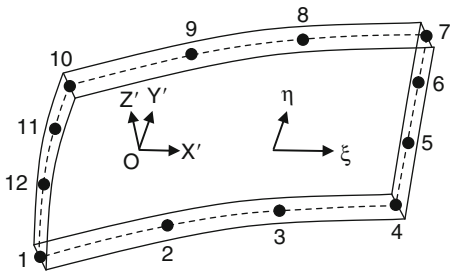


Table 5.18 Twelve-noded membrane element



Node i	Shape functions $N_i(\xi,\eta)$	Derivatives $\frac{\partial N_i}{\partial \xi}$	Derivatives $\frac{\partial N_i}{\partial \eta}$
1	$\frac{9}{32}(1-\xi)(1-\eta)\left[\xi^2+\eta^2-\frac{10}{9}\right]$	$\frac{9}{32}(1-\eta)\left[2\xi-3\xi^2-\eta^2+\frac{10}{9}\right]$	$\frac{9}{32}(1-\xi)\left[2\eta-3\eta^2-\xi^2+\frac{10}{9}\right]$
2	$\frac{9}{32}(1-\xi)\left(1-\xi^2\right)(1-\eta)$	$\frac{9}{32}(1-\eta)\left(3\xi^2-2\xi-1\right)$	$-\frac{9}{32}(1-\xi)\left(1-\xi^2\right)$
3	$\frac{9}{32}(1-\eta)\left(1-\xi^2\right)(1+\xi)$	$\frac{9}{32}(1-\eta)\left(1-2\xi-3\xi^2\right)$	$-\frac{9}{32}\left(1-\xi^2\right)(1+\xi)$
4	$\frac{9}{32}(1+\xi)(1-\eta)\left[\xi^2+\eta^2-\frac{10}{9}\right]$	$\frac{9}{32}(1-\eta)\left[2\xi+3\xi^2+\eta^2-\frac{10}{9}\right]$	$\frac{9}{32}(1+\xi)\left[2\eta-3\eta^2-\xi^2-\frac{10}{9}\right]$
5	$\frac{9}{32}(1+\xi)\left(1-\eta^2\right)(1-\eta)$	$\frac{9}{32}\left(1-\eta^2\right)(1-\eta)$	$\frac{9}{32}(1+\xi)\left(3\eta^2-2\eta-1\right)$
6	$\frac{9}{32}(1+\xi)\left(1-\eta^2\right)(1+\eta)$	$\frac{9}{32}\left(1-\eta^2\right)(1+\eta)$	$\frac{9}{32}(1+\xi)\left(1-2\eta-3\eta^2\right)$
7	$\frac{9}{32}(1+\xi)(1+\eta)\left[\xi^2+\eta^2-\frac{10}{9}\right]$	$\frac{9}{32}(1+\eta)\left[2\xi+3\xi^2+\eta^2-\frac{19}{9}\right]$	$\frac{9}{32}(1+\xi)\left[2\eta+3\eta^2+\xi^2-\frac{10}{9}\right]$
8	$\frac{9}{32}(1+\eta)\left(1-\xi^2\right)(1+\xi)$	$\frac{9}{32}(1+\eta)\left(1-2\xi-3\xi^2\right)$	$\frac{9}{32}\left(1-\xi^2\right)(1+\xi)$
9	$\frac{9}{32}(1+\eta)\left(1-\xi^2\right)(1-\xi)$	$\frac{9}{32}(1+\eta)\left(3\xi^2-3\xi-1\right)$	$\frac{9}{32}\left(1-\xi^2\right)(1-\xi)$
10	$\frac{9}{32}(1-\xi)(1+\eta)\left[\xi^2+\eta^2-\frac{10}{9}\right]$	$\frac{9}{32}(1+\eta)\left[2\xi-3\xi^2-\eta^2+\frac{10}{9}\right]$	$\frac{9}{32}(1-\xi)\left[2\eta+3\eta^2-\xi^2-\frac{10}{9}\right]$
11	$\frac{9}{32}(1-\xi)\left(1-\eta^2\right)(1+\eta)$	$-\frac{9}{32}(1+\eta)\left(1-\eta^2\right)$	$\frac{9}{32}(1-\xi)\left(1-2\eta-3\eta^2\right)$
12	$\frac{9}{32}(1-\xi)\left(1-\eta^2\right)(1-\eta)$	$-\frac{9}{32}(1-\eta)\left(1-\eta^2\right)$	$\frac{9}{32}(1-\xi)\left(3\eta^2-2\eta-1\right)$

www.EngineeringBooksPDF.com

$$\begin{aligned}\hat{Z}^l &= \left(\hat{X}_\xi \times \hat{X}_\eta\right)/\left|\hat{X}_\xi \times \hat{X}_\eta\right| \\ \hat{X}^l &= \hat{X}_\xi/\left|\hat{X}_\xi\right| \\ \hat{Y}^l &= \hat{Z}^l \times \hat{X}^l \\ \hat{F} = \left[\hat{X}^l, \hat{Y}^l, \hat{Z}^l\right]^{T^H} &= \begin{bmatrix} l_1 & l_2 & l_3 \\ m_1 & m_2 & m_3 \\ n_1 & n_2 & n_3 \end{bmatrix}\end{aligned} \tag{5.214}$$

Following (VI.35) onwards, the strains can be evaluated as

$$\varepsilon_{x^l} = \frac{\partial U^l}{\partial X^l} = \sum_{i=1}^{n} \bar{a}(l_1 U_i + m_1 V_i + n_1 W_i) = [B]\left\{U^{\bar{e}}\right\} \tag{5.215}$$

$$\bar{a} = l_1 \frac{\partial N_i}{\partial x} + m_1 \frac{\partial N_i}{\partial y} + n_1 \frac{\partial N_i}{\partial z} \tag{5.216}$$

Stresses are computed as

$$\left\{\sigma_x^l\right\} = \{E_s\}\left\{\varepsilon_x^l\right\} \tag{5.217}$$

This analysis is needed when the prestressing tendons or conventional reinforcement cannot be modelled as line elements lying at the nodes of the solid elements. They can then be located at the body of the concrete element. This analysis will replace the ones adopted for the other line elements.

5.14.9.3 Plastic Flow Rule and Stresses During Elasto-plastic Straining

Many materials have been examined, including concrete. They behave elastically up to a certain stage of the loading beyond which plastic deformation takes place. During this plastic deformation the state of strain is not uniquely determined by the state of stress, as stated previously. In a uniaxial state of stress a simple rule is

5.15 Criteria for Convergence and Acceleration

Convergence criteria

To ensure convergence to the correct solution by finer sub-division of the mesh, the assumed displacement function must satisfy the convergence criteria given below:

www.EngineeringBooksPDF.com

(a) Displacements must be continuous over element boundaries.
(b) Rigid body movements should be possible without straining.
(c) A state of constant strain should be reproducible.

Euclidean norm $\psi_i/R_i \leq C$. The term ψ_i represents the unbalanced forces and the norm of the residuals. With the aid of the iterative scheme described above, the unbalanced forces due to the initial stresses $\{\sigma_0\}$ become negligibly small. As a measure of their magnitude, the norm of the vector $\|\psi_i\|$ is used. The Euclidean norm and the absolute value of the largest component of the vector are written as

$$\begin{aligned} \|\psi_i\| &= \left(|\psi_1|^2 + \cdots + |\psi_n|^2\right)^{1/12} \\ \|R_i\| &= \left(\left|\{R_i\}^T\{R_i\}\right|\right)^{1/12} \end{aligned} \tag{5.218}$$

The convergence criterion adopted is

$$\|\psi_i\| = \max_i |\psi_1| < C = 0.001 \tag{5.219}$$

Uniform acceleration

Various procedures are available for accelerating the convergence of the modified Newton–Raphson iterations. Figure AV.1 shows the technique of computing individual acceleration factors, δ_1 and δ_2 are known. Then, assuming a constant slope of the response curve and from similar triangles, the value of δ_3 is computed:

$$\frac{\delta_1}{\delta_2} = \frac{\delta_2}{\delta_3} \quad \delta_3 = \delta_2 \frac{\delta_2}{\delta_1} \tag{5.220}$$

When δ_3 is added to δ_2, then the accelerated displacement δ_2' is expressed as

$$\delta_2' = \delta_2 + \delta_3 = \delta_2\left(1 + \frac{\delta_2}{\delta_1}\right) = \alpha\delta_2 \tag{5.221}$$

where the acceleration factor α is

$$\alpha = 1 + \frac{\delta_2}{\delta_1} \tag{5.222}$$

Generally the range of α is between 1 and 2. The value of α is 1 for zero acceleration, and the value of α reaches the maximum value of 2 when the slope of the $\delta - R$ curve approaches zero.

The acceleration factor α is computed individually for every degree of freedom of the system. The displacement vector obtained from the linear stiffness matrix $[k_0]$ is then multiplied by the $[\alpha]$ matrix having the above constants on its

www.EngineeringBooksPDF.com

diagonals. The remaining components of $[\propto]$ are zero. The accelerated displacement vector is then expressed as follows:

$$\{\Delta u_i^l\} = [a_{i-1}]\{\Delta u_i\} \tag{5.223}$$

From these accelerated displacement

$$\{\Delta \bar{u}_i\} = [k_0]^{-1}\{\psi_i\} \tag{5.224}$$

which results in a new set of acceleration factors. Now an estimate for the displacement increment is made in order to find the incremental stresses and total stresses. See Fig 5.32, 5.33, 5.34, 5.35, 5.36, 5.37

The residual forces needed to reestablish equilibrium can now easily be evaluated:

$$\{\psi_i\} = \int {}_v[B]^T\{\sigma_{0_T}\}\mathrm{d}V - \{R_i\} \tag{5.225}$$

where $\{R_i\}$ represents the total external load; dV is the volume.

A new displacement now results from

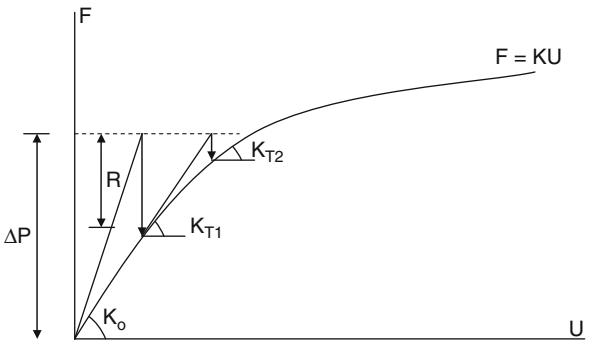


Fig. 5.32 Newton – Raphson method

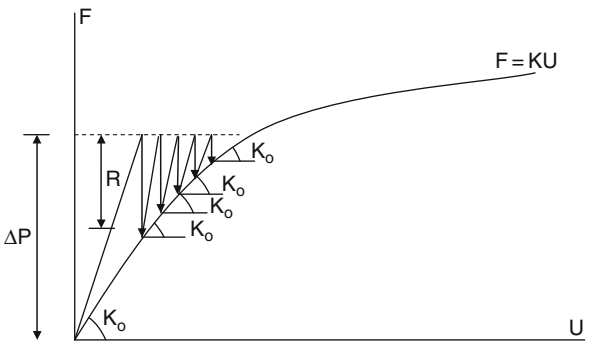


Fig. 5.33 Initial stress method
Note: ΔP is a specific value of F.

www.EngineeringBooksPDF.com

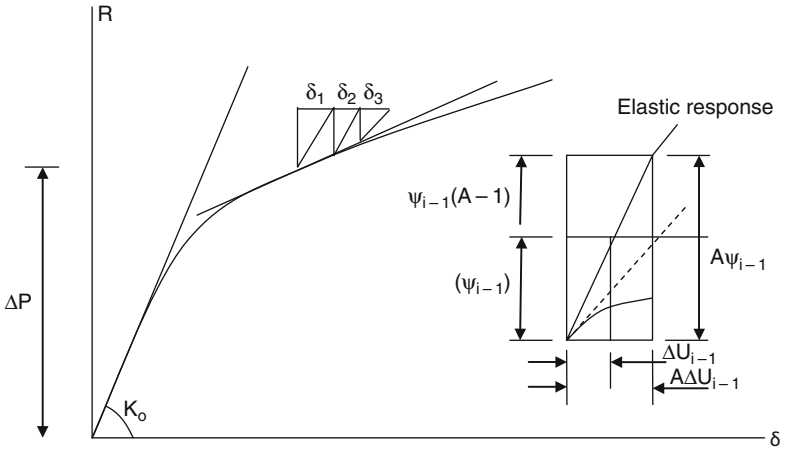


Fig. 5.34 Technique of computing acceleration factors

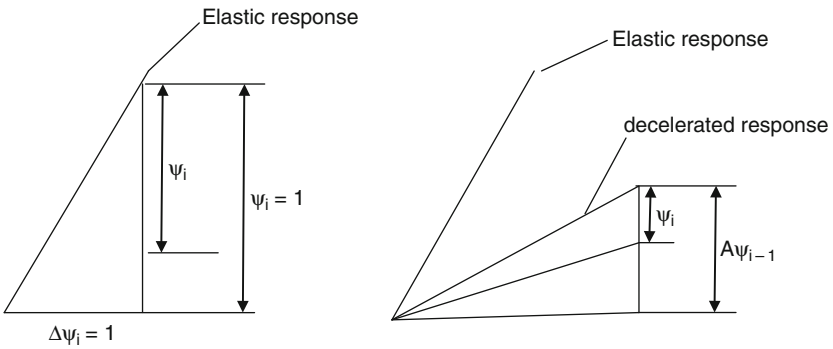


Fig. 5.35 Graphing representation

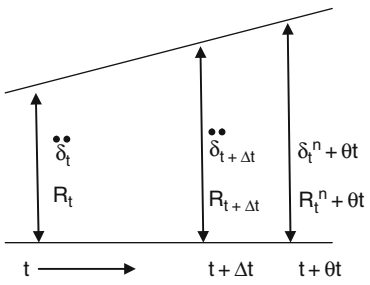


Fig. 5.36 Linear acceleration and load assumptions of the Wilson-θ method

www.EngineeringBooksPDF.com

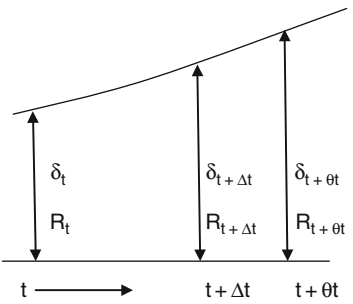


Fig. 5.37 Quadratic and cubic variation of velocity and displacement assumptions of the Wilson-θ method

$$\left\{\Delta_{u_{i+1}}\right\} = -[k_0]^{-1}\left\{\hat{\psi}_i\right\} \tag{5.226}$$

In order to carry out these iterative steps, numerical integration is required. First of all the evaluation of $\left\{\hat{\psi}_i\right\}$ from the initial stresses is required, and this requires integration over the elastic–plastic region only. The value of $\left\{\hat{\psi}_i\right\}$ is computed by carrying out the integration over the entire domain of the analysis. Since these kinds of accelerated steps unbalance the equilibrium, it has to be reestablished by finding the residual forces $\left\{\hat{\psi}_i\right\}$. Since the state of stress produced by the accelerated displacements is not in balance with the residual forces of the previous iteration, the new residual forces $\left\{\hat{\psi}_i\right\}$ of (AV.9) must balance $\{\sigma_T\}$ and $\{R_i\}$. Here the acceleration scheme is needed to preserve equilibrium, which will eventually make the equivalent forces over the whole region unnecessary. This is achieved by applying a uniform acceleration, i.e. the same acceleration factor $\bar{A}$ to all displacements, found by averaging the individual factors α_i

$$\bar{A} = \frac{1}{n}\sum_{i=1}^{n}\alpha_i \tag{5.227}$$

The force–displacement equation is then written by multiplying both sides with the scalar quantity $\bar{A}$ without disturbing the equilibrium:

$$\bar{A}\{\Delta u_i\} = [k_0]^{-1}\bar{A}\left\{\hat{\psi}_i\right\} \tag{5.228}$$

Now to evaluate $\left\{\hat{\psi}_{i+1}\right\}$, the previous value of $\left\{\hat{\psi}_i\right\}$ must be multiplied by $\bar{A}$ and the previously accelerated forces from the initial stresses $\{\sigma_0\}$ must be included such that

$$\left\{\hat{\psi}_{i+1}\right\} = \int_v [B]^T\{\sigma_{0_T}\}\mathrm{d}V - (A-1)\left\{\hat{\psi}_{i-1}\right\} \tag{5.229}$$

www.EngineeringBooksPDF.com

5.15.1 Introduction

Potential of interface elements in the engineering disciplines. In soil–structural interaction problems, interface elements play a very important role in bringing about close relations between various structural and soil/rock elements. In concrete mechanics examples can be cited such as the bond between concrete and reinforcements, softening and aggregate interlock in discrete cracks, friction in concrete connections, bedding of reinforced/plain/prestressed concrete structures in soils/rocks. This appendix reviews three methods which are recommended for both static and dynamic analysis.

5.15.2 Hallquist et al. Method

Hallquist et al. developed a useful concept of master and slave nodes sliding on each other. As shown in Fig. 5.38 slave nodes are constrained to slide on master segments after impact occurs and must remain on a master segment until a tensile interface force develops. The zone in which a slave exists is called a slave zone. A separation between the slave and the master line is known as void. The following basic principles apply at the interface:

(a) update the location of each slave node by finding its closest master node or the one on which it lies;
(b) for each master segment, find out the first slave zone that overlaps;
(c) show the existence of the tensile interface force.

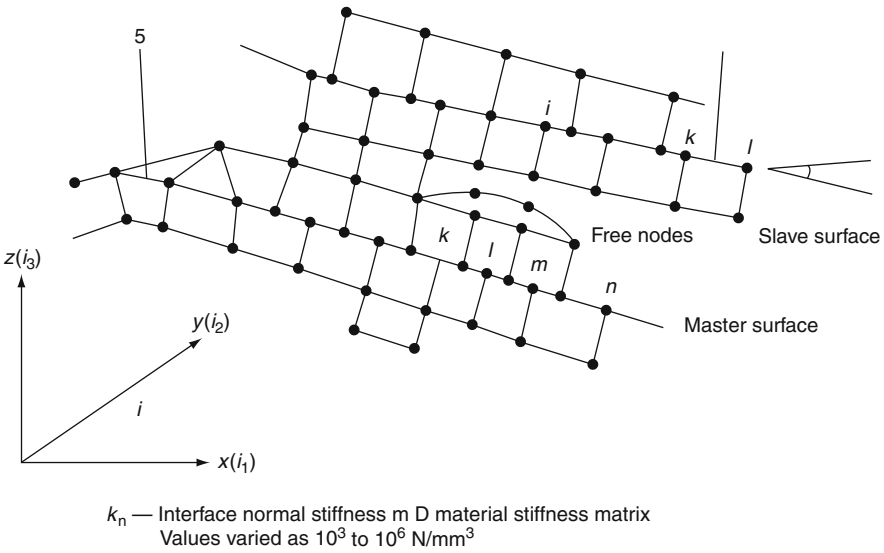


Fig. 5.38 Hallquist contact method (modified by Bangash)

www.EngineeringBooksPDF.com

Constraints are imposed on global equations by a transformation of the nodal displacement components of the slave nodes along the contact interface. Such a transformation of the displacement components of the slave nodes will eliminate their normal degrees of freedom and distribute their normal force components to the nearby master nodes. This is done using explicit time integration, as described in the finite element solution procedures. Thereafter impact and release conditions are imposed. The slave and master nodes are shown in Fig. 5.38. Hallquist et al. gave a useful demonstration of the identification of the contact point on the master segment to the slave node n_s and which finally becomes nontrivial during the execution of the analyses. When the master segment $\hat{t}$ is given the parametric representation and t is the position vector drawn to the slave node n_s, the contact point coordination must satisfy the following equations:

$$\begin{aligned} \frac{\partial \hat{r}}{\partial \xi}(\xi_c, \eta_c) \times [\hat{t} - \hat{r}(\xi_c, \eta_c)] = 0 \\ \frac{\partial \hat{r}}{\partial \eta}(\xi_c, \eta_c) \times [\hat{t} - \hat{r}(\xi_c, \eta_c)] = 0 \end{aligned} \tag{5.230}$$

where (ξ_c, η_c) are the coordinates on the master surface segment S_i. Where penetration through the master segment S_i occurs, the slave node η_s (containing its contact point) can be identified using the interface vector f_s

$$f_s = -lk_i\eta_i \quad \text{if } l<0 \tag{5.231}$$

to the degree of freedom corresponding to η_s, and

$$f_m^i = N_i(\xi_c\eta_c)f_s \quad \text{if } l<0 \tag{5.232}$$

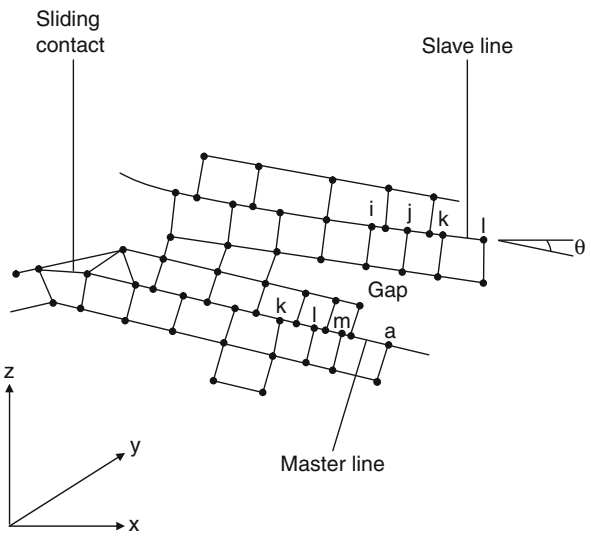


Fig. 5.39 Contact or gap element

www.EngineeringBooksPDF.com

where

$$l = \hat{n}_i \cdot [\hat{t} - \hat{r}(\xi_c, \eta_c)] < 0 \tag{5.233}$$

A unit normal

$$\hat{n}_i = \hat{n}_i(\xi_c, \eta_c); \quad \hat{t}_i = \hat{n}_i \sum_{j=1}^{n} N_j (F_1)^j(t) \tag{5.234}$$

$$k_i = f_{si} K_i A_i^2 / A_i^2 V_i \tag{5.235}$$

where

$(F_1)^j(t)$ = impact at the jth node
K = stiffness factor
K_i, V_i, A_i = bulk modulus, volume and face area, respectively
f_{si} = scale factor normally defaulted to 0.10
$N_i = \frac{1}{4}(1 + \xi\xi_i)(1 + \eta\eta_i)$ for a four-node linear surface

Bangash extended this useful analysis for other shape functions, such as N_i for 8-noded and 12-noded elements. On the basis of this theory and owing to the non-availability of the original computer source, a new sub-program CONTACT was written in association with the program ISOPAR. The sub-program CONTACT is in three dimensions.

$$\{\hat{F}_N\} = [K_{\gamma\gamma}]_i \{U_\gamma\}_i = [\sum k]\{\sum \Delta_i, \Delta_j, \ldots\} = \{\hat{F}_{i,j\ldots}\} + \{\pm\mu\hat{F}_n \ldots \pm \Delta_i \ldots\}$$

Δ_{sl} = distance of sliding

$$= (\Delta_j - \Delta_i) - \frac{\mu|\hat{F}_n|}{|K_{\gamma\gamma}|}$$

μ = friction

$$\{\hat{F}_{SN}\} \leq \mu\{\hat{F}_N\} \quad \text{no sliding}$$
$$\geq \mu\{\hat{F}_N\} \quad \text{sliding}$$
$$= 0 \quad \text{contact broken}$$

$$\theta = \cos^{-1}\frac{X}{\gamma} \quad \text{or} \quad \sin^{-1}\frac{Y}{\gamma}$$

Bibliography

Ali, H. M. and Abdel-Ghaffar, A. M. Modelling of rubber and lead passive-control bearings for seismic analysis. *J. Struct. Eng.* 1995; 121(7):1134–1144.

Bangash M.Y.H. Shock Impact and Explosion, Springer/Verlag 2009.

Bangash M.Y.H. and Bangash T. Shock Impact and Explosion Resistant. swedep Springer Verlag.

www.EngineeringBooksPDF.com

Barbat, A. H. and Bozzo, L. M. Seismic analysis of base isolated buildings. *Arch. Comput. Methods Eng*. 1997; 4(2):153–192.

Barbat, A. H. and Miquel-Canet, J. *Estructuras Sometidas a Acciones Sismicas*. Centro Internacional de Metodos Numericos en Ingenieria CIMNE, Barcelona 1994.

Barbat, A., Oller, S., Onate, E., and Hanganu, A. Viscous damage model for Timoshenko beam structures. *Int. J. Solids Struct*. 1997; 34(30):3953–3976.

Bathe, K. J. *Finite Element Procedures*. Prentice-Hall, NJ, 1996.

Bhatti, M. A., Pister,K. S., and Polak, E. Optimization of control devices in base isolation system for aseismic design. *Structural Control* (Leipholz, H. H. E., ed.). North-Holland Publishing Co., Amsterdam, The Netherlands, 1979; pp. 127–138.

Chopra and Chandrasekaren. Absorber system for earthquake excitation. *Proc. 4th World Conf. Earthquake Eng*., Chile, 1969; Vol. II, pp. 139–148.

CSO Volume 7 (User), Book 1: Fortuoi Write Ups, Computing Services Office, University of Illinois, Urbana, IL, 1974.

Den Hartog, J. P. *Mechanical Vibrations* (4th edn.). McGraw-Hill, New York, 1956.

Dong, R. G. Vibration-absorber effect under seismic excitation. *J. Struct. Div*. (ASCE) 1976; 102:2021–2031.

Feng, M. Q. Application of hybrid sliding isolation system to buildings. *J. Engrg. Mech*. 1993; 119(10):2090–2108.

Feng, M. Q., Shinozuka, M., and Fujii, S. Friction-controllable sliding isolation system. *J. Engrg. Mech*. (ASCE) 1993; 119(9):1845–1864.

Fuller, K. N. G., Gough, J., Pound, T. J., and Ahmadi, H. R. High damping natural rubber seismic isolators. *J. Struct. Control* 1997; 4(2):19–40.

Fur, L. S., Yang, H. T. Y., and Ankireddi,S. Vibration control of tall buildings under seismic and wind loads. *J. Struct. Engrg*. (ASCE) 1994; 122(8):948–957.

Gadala, M. S. Alternative methods for the solution of hyperelastic problems with incompressibility. *Comp. Struct*. 1992; 42(1):1–10.

Govindjee, S. and Simo, J. C. 'Mullins' effect and the strain amplitude dependence of the storage modulus. *Int. J. Solids Struct*. 1992; 2(14/15):1737–1751.

Gupta,Y. P. and Chandrasekaren, A. R. Absorber system for earthquake excitation. *Proc. 4th World Conf. Earthquake Eng*., Santiago, Chile II, 1969; pp. 139–148.

Hanganu, D. A. *Analisis no lineal estatico y dinamico de estructuras de hormigon armado mediante modelos de dano*. Ph.D. Thesis, Escuela Tecnica Superior de Ingenieros de Caminos Canales y Puertos de Barcelona, Universidad Politecnica de Cataluna, 1997.

Heinsbroek, A. G. T. J. and Tijsseling, A. S. *Seismic Isolation and Response Control for Nuclear and Non-Nuclear Structures*. Structural Mechanics in Reactor Technology, SMiRT11, Tokyo, Japan 1991.

Hermann, L. R., Hamidi, R., Shafigh-Nobari, F., and Lim, C. K. Nonlinear behaviour of elastromeric bearings, I: Theory. *J. Eng. Mech*. 1988; 114(11):1811–1830

Hermann, L. R., Hamidi, R., Shafigh-Nobari, F., and Ramaswamy, A. Nonlinear behaviour of elastomeric bearings. II:FE analysis and verification. *J. Eng. Mech*. 1998; 114(11): 1831–1853.

Housner, G.W. Intensity of Earthquake ground shaking near the causative fault. Proc. 3rd world conference on Earthquake Engineering, NewZealand, Vol 1, pp. III. Jan. 1965, 94–115.

Hwang, J. S. and Ku, S. W. Analytical modelling of high damping rubber bearings. *J. Struct. Eng*. 1997; 123(8):1029–1036.

Jagadish, K. S., Pradas, B. K. R., and Rao, P. V. The inelastic vibration absorber subjected to earthquake ground motions. *Eng. Struct. Dyn*. 1979; 7:317–326.

Jalihal, P., Utku, S., and Wada, B. K. Active base isolation in buildings subjected to earthquake excitation. *Proc. 1994 Int. Mech. Eng. Cong. Exposition*, Chicago, Illinois, 1994; DSC-Vol. 55-1, pp. 381–388.

www.EngineeringBooksPDF.com

Jangid, R. S. Seismic response of sliding structures to bi-directional earthquake excitation. *Earthquake Eng. Struct. Dyn.* 1996; 25:1301–1306.

Jangid, R. S. Response of pure-friction sliding structures to bi-directional harmonic ground motion. *Eng. Struct.* 1997; 19:97–104.

Kaliske, M., Gebbeken, N., and Rothert, H. A generalized approach to inelastic behaviour at finite srains-Application to polymeric material. *Proc. 5th Int. Conf. Comput. Plasticity*, Centro Internacional de Metodos Numericos en Ingenieria CIMNE, Barcelona, 1997; pp. 937–944.

Kaynia, A. M., Veneziano, D., and Biggs, J. M. Seismic effectiveness of tuned mass dampers. *J. Struct. Div.* (ASCE) 1981; 107:1465–1484.

Kelly, J. M. Control devices for earthquake-resistant structural design. *Structural Control* (Leipholz, H. H. E., ed.). North-Holland Publishing Co., Amsterdam, The Netherlands, 1979; pp. 391–413.

Kelly, J. M. *Dynamic and Failure Characteristics of Bridgestone Isolation Bearings*. Earthquake Engineering Research Center, College of Engineering, University of California, Berkley, 1991.

Kelly, J. M. *Final Report on the International Workshop on the Use of Rubber-Based Bearing for the Earthquake Protection of Buildings*. Earthquake Engineering Research Center, College of Engineering, University of California, Berkley 1995.

Kelly, J. M., Leitmann, G., and Soldatos, A. G. Robust control of base-isolated structures under earthquake excitation. *J. Optim. Theory Appl.* 1987; 53(2):159–180.

Koh, C. G. and Kelly, J. M. Viscoelastic stability model for elastometric isolation bearings. *J. Struct. Eng.* 1989; 115(2):285–302.

Krieg, R. D. and Krieg, D. N. Accuracy of numerical solution methods for the elastic, perfectly plastic model. *Pres. Ves. Technol.* 1977; 99:510–515.

Lead hula-hoops stabilize antenna. *Eng. News-Record* July 22 1976; 10.

Li, Z., Rossow, E. C., and Shah, S. P. Sinusoidal forced vibration of sliding masonry system. *Struct. Eng.* (ASCE) 1989; 115:1741–1755.

Liaw, T. C., TIan,Q. L., and Cheung, Y. K. Structures on sliding base subjected to horizontal and vertical motions. *Struct Eng.* (ASCE) 1988; 114:2119–2129.

Lin, B. C. and Tadjbakhsh, I. G. Effect of vertical motion on friction driven systems. *Earthquake Eng. Struct. Dyn.* 1986; 14:609–622.

Loh,C. H. and Chao, C. H. Effectiveness of active tuned mass damper and seismic isolation on vibration control of multi-storey building. *J. Sound Vibration* 1996; 193(4):773–792.

Lu, L. Y. and Yang, Y. B. Dynamic response of equipment in structures with sliding support. *Earthquake Eng. Struct. Dyn.* 1997; 26:61–77.

Luco, J. E., Wong, H. L., and Mita, A. Active control of the seismic response of structures by combined use of base isolation and absorbing boundaries. *Earthquake Eng. Struct. Dyn.* 1992; 21(6):525–541.

Luft, R. W. Optimal tuned mass dampers for buildings. *J. Struct. Div.* (ASCE) 1979; 105: 2766–2772.

McNamara, R. J. Tuned mass dampers for buildings. *J. Struct. Div.* (ASCE) 1977; 103: 1785–1798.

Meirovitch, L. *Dynamics and Control Of Structures*. Wiley-Interscience, New York, 1990.

Meirovitch, L. *Principles and Techniques of Vibrations*. Prentice-Hall, Inc., Englewood Cliffs, NJ, 1997.

Miyama, T. Seismic response of multi-storey frames equipped with energy absorbing storey on its top. *Proc. 10th World Conf. Eng.*, Madrid, Spain, 19–24 July 1992; Vol. 7, pp. 4201–4206.

Mokha, A., Constantinou, M. C., and Reinhorn, A. M. Verification of friction model of Teflon bearings under triaxial load. *Struct. Eng.* (ASCE) 1993; 119:240–261.

www.EngineeringBooksPDF.com

Molinares, N. and Barbat A. H. *Edificios con aislamiento de base no lineal*. Monografias de Ingenieria Sismica 5, Centre Internacional de Metodos Numericos en Ingenieria, CIMNE, Barcelona 1994.

Moore, J. K. *A nonlinear finite element analysis of elastomeric bearings*, Ph.D. Thesis, Department of Civil Engineering, University of California at Davis, 1982.

Morman, K. The generalized strain measure with application to non-homogeneous deformations in rubber-like solids. *J. Appl. Mech*. 1986; 53:726–728.

Mostaghel, N., Hejazi, M., and Tanbakuchi, J. Response of sliding structure to harmonic support motion. *Earthquake Eng. Struct. Dyn*. 1983; 11:355–366.

Mostaghel, N. and Khodaverdian, M. Dynamics of resilient-friction base isolator (R-FBI). *Earthquake Eng. Struct. Dyn*. 1987; 15:379–390.

Mostaghel, N. and Tanbakuchi, J. Response of sliding structures to earthquake support motion. *Earthquake Eng. Struct. Dyn*. 1983; 11:729–748.

Nagarajaiah, S., Li, C., Reinhorn, A., and Constantinou, M. 3D-BASIS-TABS: version 2.0 computer program for nonlinear dynamic analysis of three dimensional base isolated structures. *Technical Report NCEER-94-0018*, National Centre for Earthquake Engineering Research, University, Buffalo, 1994.

Nagarajaiah, S., Reinhorn, A. M., and Constantinou, M. C. Nonlinear dynamic analysis of 3-D-Base-isolated structures. *J. Struct. Eng*. 1991; 117(7):2035–2054.

Newmark, N.N. A method of computation for structural dynamics. J. Eng. Mech, Div. Asck, Vol 85, Nov. EM3, July 1959, pp. 67–94.

Newmark, N.M. and Rosen Blueth E., Fundamentals of earthquake engineering, Prentice Hall, Inc. Englewood chipps, N.I 1971., pp. 162–163.

Odgen, R. W. *Nonlinear Elastic Deformations*. Ellis Horwood, Chichester, England, 1984.

Oller, S. *Modelizacion Numerica de Materiales Friccionales*. Monografia 3, Centro Internacional de Metodos Numericos en Ingenieria CIMNE, Barcelona, 1991.

Oller, S., Onate, E., Miquel, J., and Botello, S. A plastic damage constitutive model for composite materials. *Int. J. Solids Struct*. 1996; 33(17):2501–2518.

Onate, E. *Calculo de estructuras por el Metodo de los Elementos Finitos*. Centro Internacional de Metodos Numericos en Ingenieria CIMNE, Barcelona, 1992.

Ormondroyd, J. and Den Hartog, J. P. The theory of the dynamic vibration absorber. *Trans*. (ASME) 1928; APM-50-7:9–22.

Pu, J. P. and Kelly,M. Active control and seismic isolation. *J. Eng. Mech. ASCE* 1991; 117(10):2221–2236.

Qumaroddin, M., Rasheeduzzafar, Arya,A. S., and Chandra, B. Seismic response of masonry buildings with sliding substructure. *Struct. Eng. ASCE* 1986; 112:2001–2011.

Reinhorn, A. M., Soong, T. T., and Wen, C. Y. Base isolated structures with active control. *Recent Advances in Design, Analysis, Testing and Qualification Methods. ASME PVP* 1987; 127:413–419.

Rofooei, F. R. and Tadjbakksh, I. G. Optimal control of structures with acceleration, velocity, and displacement feedback. *J. Engrg. Mech. ASCE* 1993; 119(10): 1993–2010.

Salomon, O. *Estructuras con sistema de aislamiento sismico*. Analisis por Elementos Finitos. Master's Thesis, Escuela Tecnica Superior de Ingenieros de Caminos Canales y Puertos de Barcelona, Universidad Politecnica de Cataluna, 1995.

Salomon, O., Oller, S. and Barbat, A. Modelling of laminated elastomeric passive-control bearing for seismic analysis. *Fourth World Cong. Comput. Mech.,* Buenos Aires, Argentina, 1998.

Simo, J. C. A framework for finite strain elastoplasticity based on maximum plastic dissipation and the multiplicative decomposition: Part 2 computational aspects. *Comp. Methods Appl. Mech. Eng*. 1988; 68:1–31.

Simo, J. C. Algorithms for static and dynamic multiplicative plasticity that preserve the classical return mapping schemes of the infinitesimal theory. *Comp. Methods Appl. Mech. Eng*. 1992; 99:61–112.

www.EngineeringBooksPDF.com

Simo, J. C. and Taylor, R. L. Quasi-incompressible finite elasticity in principal stretches. Continuum basis and numerical algorithms. *Comp. Methods Appl. Mech. Eng.* 1991; 85:273–310.

Skinner, R. I., Robinson,W. H., and McVerry, G. *An Introduction to Seismic Isolation*. Wiley, Chichester, 1993.

Sladek, J. R. and Klingner, R. E. Effect of tuned-mass dampers on seismic response. *J. Struct. Div.* (ASCE) 1983; 109:2004–2009.

Sner, M. and Utku, S. Active-passive base isolation system for seismic response controlled structures. *Proc. 36th AIAA/ASME/ASCE/AHS/ASC Struct. Struct. Dyn. Mat. Conf. AIAA/ASME Adaptive Struct.* Forum Part 4 (of 5), New Orleans, Louisiana, 1995; pp. 2350–2359.

Sussman, T. and Bathe, K. A finite element formulation for nonlinear incompressible elastic and inelastic analysis. *Comp. Struct.* 1987; 26(1/2):357–409.

Tower's cables handle wind, water tank damps it. *Eng. News-Record* Dec. 9 1971; 23.

Tuned mass dampers steady sway of skyscrapers in wind. *Eng. News-Record* Aug. 18 1977; 28–29.

Villaverde, R. Earthquake response of systems with nonproportional damping by the conventional response spectrum method. *Proc. 7th World Conf. Earthquake Eng.*, Istambul, Turkey 1980; Vol. 5, pp. 467–474.

Villaverde, R. Reduction in seismic response with heavily-damped vibration absorbers. *Earthquake Eng. Struct. Dyn.* 1985; 13:33–42.

Villaverde, R. Seismic control of structures wih damped resonant appendages. *Proc. 1st World Conf. Struct. Control*, Los Angeles, California, USA, 1994; WP4-113–WP4-119.

Villaverde, R. and Koyama, L. A. Damped resonant appendages to increase inherent daming in buildings. *Earthquake Eng. Struct.* 1993; 22:491–507.

Villaverde, R. and Martin, S. C. Passive seismic control of cable-stayed bridges with damped resonant appendages. *Earthquake Eng.* 1995; 24:233–246.

Villaverde, R. and Newmark, N. M. *Seismic response of light attachments to buildings*. SRS No. 469, University of Illinois, Urbana, IL, 1980.

Watari, A. and Sano, I. Optimum tuning of the dynamic damper to control response of structures to earthquake ground. *Sixth World Conf. Earthquake Eng.*, New Delhi, India, 1977; Vol. 3, pp. 157–161.

Westermo, B. and Udwadia, F. Periodic response of a sliding oscillator system to harmonic excitation. *Earthquake Eng. Struct. Dyn.* 1983; 11:135–146.

Wirsching, P. H. and Campbell, G. W. Minimal structural response under random excitation using vibration absorber. *Earthquake Dyn.* 1974; 2:303–312.

Wirsching, P. H. and Yao, J. T. P. Safety design concepts for seismic structures. *Comput. Struct.* 1973; 3:809–826.

Yang, J. N., Danielians, A., and Liu, S. C. Aseismic hybrid control systems for building structures. *J. Engrg. Mech.* (ASCE) 1991; 117(4): 836–853.

Yang, J. N., Danielians, A., and Liu, S. C. Aseismic hybrid control of nonlinear and hysteretic structures, I. *J. Engrg. Mech.* (ASCE) 1992a; 118(7):1423–1440.

Yang, J. N., Danielians, A., and Liu,S. C. Aseismic hybrid control of nonlinear and hysteretic structures, I. *J. Engrg. Mech.* (ASCE) 1992b; 118(7):1441–1456.

Yang, Y. B., Lee, T. Y., and Tsai, I. C. Response of multi-degree-of-freedom structures with sliding supports. *Earthquake Eng. Struct. Dyn.* 1990; 19:739–752.

Younis,C. J. and Tadjbakhsh, I. G. Response of sliding structure to base excitation. *Eng. Mech.* (ASCE) 1984; 110:417–432.

www.EngineeringBooksPDF.com

Chapter 6
Geotechnical Earthquake Engineering and Soil–Structure Interaction

6.1 General Introduction

In earthquake engineering, geotechnics plays a prime part. To begin with the knowledge of soil mechanics for areas related to seismic history is essential. The understanding of basic dynamics as given in earlier chapters is a must. It is vital that shaking of the soft ground in earthquakes must have historical records. The rupture of fault as a cause of earthquake must be treated as a part of seismological knowledge. Earthquake waves are as P- and S-waves, love wave and Rayleigh wave. The engineer must know the response of elastic ground to surface excitation, seismic wave energy and the wave transmission and reflection at interface. To assess the behaviour of particularly heavy structures in earthquakes, the soil must be related to the overall performance of structures. The following are clearly essential to perform the soil–structure interaction.

(a) The intensity of earthquake motion and motion records
(b) Time history of the ground motion and power of acceleration–time history
(c) Earthquake magnitude and acceleration and duration
(d) Effects of local soil conditions on maximum acceleration
(e) Significance of outcrop motion
(f) Response of multilayered ground and amplification of motion of particularly alluvium surface and at the top hill
(g) Direction of seismic criteria force
(h) Damping ratio in soils
(i) Direction of seismic inertia force and wave propagation modulus in soils
(j) Variation of shear modulus at the interface of soil layers
(k) Rate-dependent nature of clays
(1) Non-linear cyclic behaviour of undisturbed soils
(m) Dilutancy of sand under cyclic loading
(n) Seismic devices when existing together with elasto-plasticity of soils
(o) Subsidence and liquefaction and sand boiling induced by earthquakes
(p) Floating of embedded parts
(q) Correlation between shear strain energy and excess pore water pressure
(r) Behaviour of soil undergoing cyclic undrained loading from earthquakes

M.Y.H. Bangash, *Earthquake Resistant Buildings*,
DOI 10.1007/978-3-540-93818-7_6, © M.Y.H. Bangash 2011

www.EngineeringBooksPDF.com

(s) Post-liquefaction behaviour of sandy ground
(t) Displacement/deformation of liquefied subsoil
(u) Soil densification

One can see how appropriately seismic loading characterizes a number of factors including earthquake source, travel path effects, local site effects and the effect of soil–structure interaction (SSI). The SSI analysis evaluates the collective response of the systems to a specified free-field ground motion. The inertial interaction and kinematics interaction are the most important effects in the global finite element investigation of SSI. The methodologies of soil–structure interaction analysis involve

(1) Foundation input motion (FIM)
(2) Impedance function, meaning stiffness and damping characteristics of foundation soil
(3) The substructure approach, knowing each step is independent of the other

Many computerized analyses exist to solve heavy structural problems such as containment buildings. The problem of SSI can be grouped into two main categories, namely the wave scattering problem and the impedance problem. The reduction of the former problem can only be achieved through observations on the seismic wave field. The reduction of uncertainties associated with the latter problem can be accomplished by test correlation studies using the data during forced vibration tests.

6.2 Concrete Structures – Seismic Criteria, Numerical Modelling of Soil–Building Structure Interaction and Isolators

6.2.1 Structural Design Requirements for Building Structures

6.2.1.1 Introduction to the Design Basis

The seismic analysis and design procedures to be used in the analysis and design of concrete structures and their components shall be as prescribed in various codes. The design ground motions can occur along any direction of a structure. The design seismic forces, and their distribution over the height of the structure, shall be established by a specific code and the corresponding internal forces in the members of the concrete structure shall be determined using a linearly elastic model. An approved alternative procedure may be used to establish the seismic forces and their distribution, in which case the corresponding internal forces and deformations in the members shall be determined using a theoretical model.

Individual members shall be designed and sized for the shears, axial forces and moments determined in accordance with these provisions, and connections shall develop the strength of the connected members or the forces. The

www.EngineeringBooksPDF.com

foundation shall be designed to accommodate the forces developed or the movement imparted to the structure by the design ground motions. In the determination of the foundation design criteria, special recognition shall be given to the dynamic nature of the forces, the expected ground motions and the design basis for strength and energy dissipation capacity of the structure. The foundations can be flexible or rigid. In the layout the foundations shall have the isolators carefully arranged to offset damaging seismic forces.

6.2.2 *Structure Framing Systems*

The basic structural framing systems to be used are indicated in Table 6.1. Each type is subdivided by the types of vertical element used to resist lateral seismic forces. The structural system used shall be in accordance with the seismic performance category and height limitations indicated in the table. The appropriate response modification coefficient, R, and the deflection amplification factor, C, indicated in Table 6.1 shall be used in determining the base shear and design storey drift.

Table 6.1 Structural systems

Basic structural system and seismic force-resisting system	Response modification coefficient R[a]	Deflection amplification factor C_d[b]	Structural system limitations and building height (ft) limitations Seismic performance category			
			A and B	C	D[d]	E[e]
Bearing wall system						
Light frame walls with shear panels	$6\frac{1}{2}$	4	NL[c]	NL	160	100
Reinforced concrete shear walls	$4\frac{1}{2}$	4	NL	NL	160	100
Reinforced masonry shear walls	$3\frac{1}{2}$	3	NL	NL	160	100
Concentrically braced frames	4	$3\frac{1}{2}$	NL	NL	160	100
Plain concrete shear walls	$1\frac{1}{2}$	$1\frac{1}{2}$	NL	[g]	NP[c]	100
Building frame system						
Eccentrically braced frames, moment-resisting connections at columns away from link	8	4	NL	NL	160	100
Eccentrically braced frames, non-moment-resisting connections at columns away from link	7	4	NL	NL	160	100

www.EngineeringBooksPDF.com

Table 6.1 (continued)

Basic structural system and seismic force-resisting system	Response modification coefficient R[a]	Deflection amplification factor C_d[b]	Structural system limitations and building height (ft) limitations Seismic performance category			
			A and B	C	D[d]	E[e]
Composite eccentrically braced frames (C-EBF)	8	4	NL	NL	160	100
Light frame walls with shear panels	7	$4\frac{1}{2}$	NL	NL	160	100
Concentrically braced frames	5	$4\frac{1}{2}$	NL	NL	160	100
Composite concentrically braced frames (C-CBF)	5	$4\frac{1}{2}$	NL	NL	160	100
Reinforced concrete shear walls	$5\frac{1}{2}$	5	NL	NL	160	100
RC shear walls composite with steel elements	$5\frac{1}{2}$	5	NL	NL	160	100
Plain (unreinforced) masonry shear walls	$1\frac{1}{2}$	$1\frac{1}{2}$	NL	[f]	NP	NP
Plain concrete shear walls	2	2	NL	[g]	NP	NP
Dual system with an intermediate moment frame of reinforced concrete or an ordinary moment frame of steel capable of resisting at least 25% of prescribed seismic forces						
Concentrically braced frames	5	$4\frac{1}{2}$	NL	NL	160	100
Composite concentrically braced frames (C-CBF)	5	$4\frac{1}{2}$	NL	NL	160	100
Reinforced concrete shear walls	6	5	NL	NL	160	100
RC shear walls composite with steel elements	6	5	NL	NL	160	100
Special moment frames of reinforced concrete	$2\frac{1}{2}$	$2\frac{1}{2}$	NL	NL	NL	NL

key 1ft = 0.3048m

Note: Data collected from the archives of the British Library and organised them in the given format

www.EngineeringBooksPDF.com

Table 6.1 (continued)

Basic structural system and seismic force-resisting system	Response modification coefficient R[a]	Deflection amplification factor C_d[b]	Structural system limitations and building height (ft) limitations Seismic performance category			
			A and B	C	D[d]	E[e]
Moment-resisting frames system						
Special moment frames of reinforced concrete	8	5	NL	NL	NL	NL
Composite special moment frames (C-SMF)	8	$5\frac{1}{2}$	NL	NL	NL	NL
Intermediate moment frames of reinforced concrete	5	$4\frac{1}{2}$	NL	NL	NP	NP
Composite ordinary moment frames (C-OMF)	$4\frac{1}{2}$	4	NL	NL	160	100
Composite partially restrained frames (C-PRF)	6	$5\frac{1}{2}$	160	160	100	NP
Ordinary moment frames of reinforced concrete	3	$2\frac{1}{2}$	NL[h]	NP	NP	NP
Dual system with a special moment frame capable of resisting at least 25% *of prescribed seismic forces*						
Eccentrically braced frames, moment-resisting connections at columns away from link	8	4	NL	NL	NL	NL
Eccentrically braced frames, non-moment resisting connections at columns away from link	7	4	NL	NL	NL	NL
Composite eccentrically braced frames (C-EBF)	8	4	NL	NL	NL	NL
Concentrically braced frames	6	5	NL	NL	NL	NL
Special concentrically braced frames– steel	8	$6\frac{1}{2}$	NL	NL	NL	NL
Composite concentrically braced frames (C-CBF)	6	5	NL	NL	NL	NL
Reinforced concrete shear walls	8	$6\frac{1}{2}$	NL	NL	NL	NL

www.EngineeringBooksPDF.com

Table 6.1 (continued)

Basic structural system and seismic force-resisting system	Response modification coefficient R[a]	Deflection amplification factor C_d[b]	Structural system limitations and building height (ft) limitations Seismic performance category			
			A and B	C	D[d]	E[e]
RC shear walls composite with steel elements	8	$6\frac{1}{2}$	NL	NL	NL	NL
Steel plate-reinforced composite shear walls	8	$6\frac{1}{2}$	NL	NL	NL	NL

[a]Response modification coefficient R for use through the provisions.
[b]Deflection amplification factor C_d.
[c]NL = not limited and NP = not permitted. If' using metric units, 100 ft approximately equals 30 m and 160 ft approximately equals 30 m.
[d] For descriptions of building systems limited to buildings with a height of 240 ft (70m) or less.
[e]For building systems limited to buildings with a height of 160 ft (50 m) or less.
[f]Structures excluded.
[g]Plain concrete shear walls shall have nominal reinforcement.
[h]Ordinary moment frames of reinforced concrete are not permitted as part of the seismic force-resisting system in seismic performance category B buildings founded on soil profile type E or F.
Note: Data collected from the archives of the British Library in London and finally placed them in the given format.

6.2.2.1 Dual System

For a dual system, the moment frame shall be capable of resisting at least 25% of the design forces. The total seismic force resistance is to be provided by the combination of the moment frame and the shear walls or braced frames in proportion to their rigidities.

6.2.2.2 Combinations of Framing Systems

Different structural framing systems are permitted along the two orthogonal axes of the building. Combinations of framing systems shall comply with the requirements of this section.

6.2.2.3 Combination Factor

The response modification coefficient R in the direction under consideration at any storey shall not exceed the lowest response modification factor R for the seismic force-resisting system in the same direction considered above that storey.

6.2.2.4 Combination Framing Detailing Requirements

The detailing requirements of the higher response modification coefficient R shall be used for structural components common to systems having different response modification coefficients.

www.EngineeringBooksPDF.com

6.2.2.5 Seismic Performance Categories A, B and C

The structural framing system for buildings assigned to seismic performance categories A, B and C shall comply with the building height and structural limitations in Table 6.1.

6.2.2.6 Seismic Performance Category D

The structural framing system for a building assigned to seismic performance category D shall comply with the above provisions and the additional provisions of this section.

6.2.2.7 Limited Building Height

The height limit in Table 6.2 may be increased to 240 ft (70 m) in buildings that have concrete cast-in-place shear walls. Such buildings shall have braced frames or shear walls arranged in one plane such that they resist no more than the following portion of the seismic forces in each direction, including torsional effects:

Table 6.2 Plan structural irregularities

Irregularity type and description	Seismic performance category application
1. *Torsional irregularity* To be considered when diaphragms are rigid in relation to the vertical structural elements that resist the lateral seismic forces	D and E
Torsional irregularity Shall be considered to exist when the maximum storey drift, computed including accidental torsion, at one end of the structure transverse to an axis is more than 1.2 times the average of the storey drifts at the two ends of the structure	C, D and E
2. *Re-entrant corners* Plan configurations of a structure and its lateral force-resisting system contain re-entrant corners, where both projections of the structure beyond a re-entrant corner are greater than 15% of the plan dimension of the structure in the given direction	D and E
3. *Diaphragm discontinuity* Diaphragms with abrupt discontinuities or variations in stiffness, including those having cut out or open areas greater than 50% of the gross enclosed diaphragm area, or changes in effective diaphragm stiffness of more than 50% from one storey to the next	D and E
4. *Out-of-plane offsets* Discontinuities in a lateral force resistance path, such as out-of-plane offsets of the vertical elements	D and E
5. *Non-parallel systems* The vertical lateral force-resisting elements are not parallel to or symmetric about the major orthogonal axes of the lateral force-resisting system	C, D and E

www.EngineeringBooksPDF.com

(a) 60% where the braced frame or shear walls are arranged only on the perimeter.
(b) 40% where some of the braced frames or shear walls are arranged on the perimeter.
(c) 30% for other arrangements.

6.2.2.8 Interaction Effects

Moment-resisting frames that are enclosed or adjoined by more rigid elements not considered to be part of the seismic force-resisting system shall be analysed and designed so that the action or failure of those elements will not impair the vertical.

6.2.2.9 Deformational Compatibility

Every structural component not included in the seismic force-resisting system in the direction under consideration shall be designed to be adequate for the vertical loadcarrying capacity and the induced moments resulting from the design storey drift.

6.2.2.10 Special Moment Frames

A special moment frame that is used but not required by Table 6.1 is permitted to be discontinued and supported by a more rigid system with a lower response modification coefficient. Where a special moment frame is required by Table 6.1., the frame shall be continuous to the foundation.

6.2.2.11 Seismic Performance Category E

The framing systems of buildings assigned to category E shall conform to the code requirements for category D and to the additional requirements and limitations of this section. The height limitation shall be reduced from 240 to 160 ft (from 70 to 50 m).

6.2.2.12 Seismic Building Configuration

Buildings shall be classified as regular or irregular based on the criteria in this section. Such classification shall be based on the plan and vertical configuration.

6.2.2.13 Plan Irregularity

Buildings having one or more of the features given in Table 6.2 shall be designated as having plan structural irregularity and shall comply with the requirements in the codes.

www.EngineeringBooksPDF.com

6.2.2.14 Vertical Irregularities

Buildings having one or more of the features given in Table 6.3 shall be designated as having vertical irregularity and shall comply with the requirements in the relevant sections of the code.

Table 6.3 Vertical structural irregularities

Irregularity type and description	Seismic performance category application
1. *Stiffness irreg4larity – soft storey* A soft storey is one in which the lateral stiffness is less than 70% of that in the storey above or less than 80% of the average stiffness of the three storeys above	D and E
2. *Weight (mass) irregularity* Mass irregularity shall be considered to exist where the effective mass of any storey is more than 150% of the effective mass of an adjacent storey. A roof that is lighter than the floor below need not be considered	D and E
3. *Vertical geometric irregularity* Vertical geometric irregularity shall be considered to exist where the horizontal dimension of the lateral force-resisting system in any storey is more than 130% of that in an adjacent storey	D and E
4. *In-plane discontinuity in vertical lateral force-resisting elements* An in-plane offset of the lateral force-resisting elements greater than the length of those elements or a reduction in stiffness of the resisting element in the storey below	D and E
5. *Discontinuity in capacity–weak storey* A weak storey is one in which the storey lateral strength is less than 80% of that in the storey above. The storey strength is the total strength of all seismic- resisting elements sharing the storey shear for the direction under consideration	B, C, D and E

6.3 Combination of Load Effects

The effects on the building and its components due to gravity loads and seismic forces shall be combined in accordance with the factored load combinations as presented in ANSI and ASCE 7 except that the effect of seismic loads E shall be as defined herein. For other codes a reference is made for combination of load effects.

The effect of seismic load E shall be defined as follows for load combinations in which the effects of gravity and seismic loads are additive:

$$E = Q_E + 0.5\, C_a D \tag{6.1}$$

www.EngineeringBooksPDF.com

where E is the effect of horizontal and vertical earthquake-induced forces; C_a" is the seismic coefficient based on the soil profile type and the values of C_a as determined; D is the effect of dead load and Q_E is the effect of horizontal seismic forces.

The effect of seismic load E shall be defined by (6.2) as follows for load combinations in which the effects of gravity counteract seismic load:

$$E = Q_E - 0.5C_aD \tag{6.2}$$

where E, Q_E, C_a and D are as defined above.

The load factor on E need not be taken as greater than 1.0 in factored load combinations when using the seismic loads as defined in these provisions.

For columns supporting discontinuous lateral force-resisting elements, the axial force in the columns shall be computed using the most critical load combinations. Load combinations including seismic loads shall also be investigated, except that the effect of seismic load E shall be defined by (6.3) as follows:

$$E = \left(\frac{2R}{5}\right)Q_E + 0.5\,C_aD \tag{6.3}$$

where E, Q_E, C_a and D are as defined above and R is the response modification coefficient as given in Table 6.1. The axial forces in such columns need not exceed the capacity of other elements of the structure to transfer such loads to the column.

Brittle materials, systems and connections shall be designed using the most critical load combinations. Load combinations including seismic loads shall also be investigated, except that the effect of seismic load E shall be defined by (6.6) as follows:

$$E = \left(\frac{2R}{5}\right)Q_E - 0.5\,C_aD \tag{6.4}$$

where E, R, Q_E, C_a and D are as defined above.

The factor ($2\ R/5$) shall be equal to or greater than 1.0. The term $0.5\ C_a$ is permitted.

6.4 Deflection and Drift Limits

The design storey drift Δ as determined shall not exceed the allowable storey drift Δ_a as obtained for any torsional effects (Table 6.4). All portions of the building shall be designed and constructed to act as an integral unit in resisting

www.EngineeringBooksPDF.com

Table 6.4 Allowable storey drift Δ_a (in or mm)

Building	Seismic Hazard	Exposure group	
	I	II	III
Buildings, other than masonry shear wall or masonry wall frame buildings, four storeys or less in height with interior walls, partitions, ceilings and exterior wall systems that have been designed to accommodate the storey drifts	0.025 h_{sx}[a,b]	0.020 h_{sx}	0.015 h_{sx}
Masonry cantilever shear wall buildings	0.010 h_{sx}	0.010 h_{sx}[c]	0.010 h_{sx}
Other masonry shear wall buildings	0.007 h_{sx}	0.007 h_{sx}[c]	0.007 h_{sx}
Masonry wal4 frame buildings	0.010 h_{sx}[c]	0.013 h_{sx}	0.010 h_{sx}
All other buildings	0.020 h_{sx}	0.015 h_{sx}	0.010 h_{sx}

[a] h_{sx} is the storey height below level x.
[b] There shall be no drift limit for single-storey buildings with interior wall partitions, ceilings and exterior wall systems that have been designed to accommodate the storey drifts.
[c]Buildings in which the basic structural system consists of masonry shear walls designed as vertical elements cantilevered from their base foundation support which are so constructed that moment transfer between shear walls (coupling) is negligible. Data collected from the Library of ASCE, (U.S.A.)

seismic forces unless separated structurally by a distance sufficient to avoid damaging contact under total deflection.

6.5 Equivalent Lateral Force Procedure

6.5.1 General

This section provides the required minimum standards for the equivalent lateral force procedure of seismic analysis of buildings. For purposes of analysis, the building is considered to be fixed at the base.

6.5.2 Seismic Base Shear

The seismic base shear V in a given direction shall be determined in accordance with the following equation:

$$V = C_3 W \tag{6.5}$$

where C_3 is the seismic response coefficient and W is the total dead load and applicable portions of other loads listed below.

(a) In areas used for storage, a minimum of 25% of the floor live load shall be applicable. Floor live load in public garages and open parking structures is not applicable.

www.EngineeringBooksPDF.com

(b) Where an allowance for particular load is included in the floor load design, the actual partition weight or a minimum weight of 10 psf (0.5 kN/m^2) of floor area, whichever is greater, shall be applicable.
(c) Total operating weight of permanent equipment.

6.5.2.1 Calculation of Seismic Response Coefficient

When the fundamental period of the building is computed, the seismic response coefficient C_S; shall be determined in accordance with the following equation:

$$C_S = (1.2\,C_V))/(RT^{2/3}) \tag{6.6}$$

where

C_V = the seismic coefficient based on the soil profile type and the value of A_V
R = the response modification factor
T = the fundamental period of the building (s).

A soil–structure interaction reduction is permitted when determined using the generally accepted procedures approved by the regulatory agency.

Alternatively, the seismic response coefficient need not be greater than the following:

$$C_S = (2.5\,C_V)/R \tag{6.7}$$

where R is as above and C_s is the seismic coefficient based on the soil profile type and the value of A_a.

6.5.3 Period Determination

The fundamental period T of the building in the direction under consideration shall be established using the structural properties and deformational characteristics of the resisting elements in a properly substantiated analysis. The fundamental period T shall not exceed the product of the coefficient for upper limit on calculated period C_u from Table 6.5 and the approximate fundamental period T_a determined from the appropriate requirements.

6.5.3.1 I Approximate Fundamental Period for Concrete and Steel Moment-Resisting Frame Buildings

The approximate fundamental period, T_a in seconds, shall be determined from the following equation:

$$T_a = C_T h_n^{3/4} \tag{6.8}$$

www.EngineeringBooksPDF.com

Table 6.5 Coefficient for upper limit on calculated period

Seismic coefficient C_V	Coefficient C_U
≥0.4	1.2
0.3	1.3
0.2	1.4
0.15	1.5
0.1	1.7
0.05	1.7

where $C_T = 0.039$ for moment-resisting frame systems of reinforced concrete in which the frames resist 100% of the required seismic force and are not enclosed or adjoined by more rigid components that will prevent the frames from deflecting when subjected to seismic forces (the metric coefficient is 0.0731); $C_T = 0.020$ for all other building systems (the metric coefficient is 0.0488) and $h_n =$ the height (ft or m) above the base to the highest level of the concrete structures.

Alternatively, the approximate fundamental period, T_a in seconds, shall be determined from the following equation for concrete structures and moment-resisting frame buildings not exceeding 12 storeys in height and having a minimum storey height of 10 ft (3 m).

$$T_a = 0.1\,N$$

where N is the number of storeys.

6.5.4 Vertical Distribution of Seismic Forces

The lateral forces F_x (kip or kN) induced at any level shall be determined from the following equations by all codes:

$$F_x = C_{vx} V \tag{6.9}$$

and

$$C_{vx} = \frac{W_x h_x^k}{\sum_{i=1}^{n} W_i h_i^k} \tag{6.10}$$

where

C_{vx} = vertical distribution factor
V = total design lateral force or shear at the base of the building (kip or kN)
W_i and W_x = the portion of the total gravity load of the building W located or assigned to level i or x
h_i and h_x = the height (ft or m) from the base to level i or x and

www.EngineeringBooksPDF.com

$K=$ an exponent related to the building period as follows:
For buildings having a period of 0.5 s or less, $k=1$
for buildings having a period of 2.5 s or less, $k = 1$
for buildings having a period between 0.5 and 2.5 s, k shall be 2 or shall be determined by linear interpolation between 1 and 2.

6.6 Horizontal Shear Distribution

The seismic design storey shear in any storey V_x (kip or kN) shall be determined from the following equation:

$$V_x = \Sigma^x F_i \tag{6.11}$$

where F_i is the portion of the seismic base shear V (kip or kN) induced at level i.

The seismic design storey, V_x (kip or kN), shall be distributed to the various vertical elements of the seismic force-resisting system in the storey under consideration, based on the relative lateral stiffness of the vertical-resisting elements and the diaphragm.

6.6.1 Torsion

The design shall include the torsional moment, M (kip-ft or kNm), resulting from the location of the structure (masses plus the accidental torsional moments, M_{ta} (kip-ft or kNm)) caused by assumed displacement of the base each way from its actual location by a distance equal to 5% of the dimension of the building perpendicular to the direction of the applied forces.

Buildings of seismic performance categories C, D and E, where type 1 torsional irregularity exists. shall have the effects accounted for by increasing the accidental torsion at each level by a torsional amplification factor A_x determined from the following equation

$$A_x = \left(\frac{\delta_{\max}}{1.2\,\delta_{\text{avg}}}\right) \tag{6.12}$$

where $\delta_{\max}$ is the maximum displacement at level x (in or mm) and δ_{avg} is the average of the displacements at the extreme points of the structure at level x (in or mm).

The torsional amplification factor A_x is not required to exceed 3.0. The more severe loading for each element shall be considered for design.

www.EngineeringBooksPDF.com

6.6.2 Overturning (determined by all codes)

The building shall be designed to resist overturning effects caused by the seismic forces. At any storey, the increment of overturning moment in the storey under consideration shall be distributed to the various vertical force-resisting elements in the same proportion as the distribution of the horizontal shears to those elements.

The overturning moments at level x, M_x (kip-ft or kNm), shall be determined from the following equation:

$$M_x = \tau \Sigma_{i=x}^{n} F_i (h_i = h_x) \tag{6.13}$$

where

F_i = the position of the seismic base shear V included at level i,
h_i and h_x = the height (ft or m) from the base to level i or x,
τ = 1.0 for the top 10 storeys,
τ = 0.8 for the 20th storey from the top and below, and
τ = a value between 1.0 and 0.8 determined by a straight line interpolation for storeys between the 20th and 10th storeys below the top.

The foundations of buildings except inverted-type structures shall be designed for the foundation overturning design moment, M (kip-ft or kNrn), at the foundation soil interface determined using the equation for the overturning moment at level M (kip-ft or kNm) with an overturning moment reduction factor T of 0.75 for all building heights.

6.7 Drift Determination and $P-\Delta$ Effects

Storey drifts and, where required, member forces and moments due to $P-\Delta$ effects shall be determined in accordance with this section.

6.7.1 Storey Drift Determination (determined by all codes)

The design storey drift shall be computed as the difference between the deflections at the top and bottom of the storey under consideration. The deflections of level x at the centre of the mass, δ_x (in or mm), shall be determined in accordance with the following equation:

$$\delta_x = C_\mathrm{d} \delta_{xc} \tag{6.14}$$

where

C_d = the deflection amplification factor
δ_{xc} = the deflections determined by an elastic analysis (in or mm)

www.EngineeringBooksPDF.com

Where applicable, the design storey drift, Δ (in or mm) shall be increased by the incremental factor relating to the $P-\Delta$ effects.

6.7.2 P–Δ Effects (determined according to all codes)

$P-\Delta$ effects on storey shears and moments the resulting member forces and moments, and the storey drifts induced by these effects are not required to be considered when the stability coefficient θ, as determined by the following equation, is equal to or less than 0.10:

$$\theta = (P_x\Delta)/(V_x h_{sx} C_d) \tag{6.14a}$$

where

P_x = the total vertical design load at and above level x (kip or kN); when calculating the vertical design load for purposes of determining $P-\Delta$ the individual load factors need not exceed 1.0
Δ = the design storey drift occurring simultaneously with $V\sim$ (in or mm)
V_x = the seismic shear force acting between level x and $x-1$ (kip or kN)
h_{sx} = the storey height below level x (ft or m)
C_d = the deflection amplification factor

The stability coefficient B shall not exceed $\theta_{\max}$ determined as follows:

$$\theta_{\max} = 0.5/(\beta C_\mathrm{d}) \leq 0.25 \tag{6.14b}$$

where β is the ratio of shear demand to shear capacity for the storey between level x and $x-1$. The ratio may be conservatively taken as 1.0.

When the stability coefficient θ is greater than 0.10 but less than or equal to $\theta_{\max}$ the incremental factor is related to $P-\Delta$.

To obtain the storey drift for including the $P-\Delta$ effect, the design storey drift determined shall be multiplied by $1.0/(1-\theta)$. When θ is greater than $\theta_{\max}$ the structure is potentially unstable and shall be redesigned.

6.8 Modal Analysis Procedure: Codified Approach

6.8.1 Introduction

A reference is made to the model analysis in Chap. 4 with examples. This section provides required standards for the modal analysis procedures of seismic analysis of structures. The symbols used in this method of analysis have the same meaning as those for similar terms with the subscript m denoting quantities in the mth mode. The structure shall be modelled as a system of masses lumped at

www.EngineeringBooksPDF.com

various levels with each mass having one degree of freedom – that of lateral displacement in the direction under consideration.

The analysis shall include, for each of two mutually perpendicular axes, at least the lowest three modes of vibration or all modes of vibration with periods greater than 0.4 s. The number of modes shall equal the number of storeys for buildings less than three storeys in height.

The required periods and mode shapes of the building in the direction under consideration shall be calculated by established methods of structural analysis for the fixed–base condition using the masses and elastic stiffnesses of the seismic force–resisting system. A reference is made to Chap. 5 for modal and Chap. 6 for other analyses and solution procedures.

6.8.2 Modal Base Shear as by Codified Methods

The portion of the base shear contributed by the mth mode, Vm, shall be determined from the following equations:

$$V_m = C_{\mathrm{sm}} \bar{W}_n \tag{6.15}$$

$$\bar{W}_{\mathrm{m}} = \frac{\left(\sum_{i=l}^{n} w_i \phi_{im}\right)}{\sum_{i=l}^{n} w_i \phi_{im}^2} \tag{6.16}$$

where

C_{sm} = the modal seismic response coefficient determined below
W_{m} = the effective modal gravity
w_i = the portion of the total gravity load of the building at level i and
ϕ_{im} = the displacement amplitude at the ith level of the building when vibrating in its mth mode.

The modal seismic response coefficient C_{sm} shall be determined in accordance with the following equation:

$$C_{\mathrm{sm}} = (1.2\, C_v)/(R T_m^{2/3}) \tag{6.17}$$

where

C_v = the seismic coefficient based on the soil profile type and the value A_v
R = the response modification factor determined from Table 6.1 and
T_m = the modal period of vibration (in seconds) of the mth mode of the building.

The modal seismic design coefficient C_{sm} is not required to exceed 2.5 times the seismic coefficient C_a divided by the response modification factor R.

The following are the exceptions.

www.EngineeringBooksPDF.com

(a) The limiting value is not applicable to seismic performance category 0 and E buildings with a period of 0.7 s or greater located on soil profile type E or F sites.
(b) For buildings on sites with soil profile type D, E or F, the modal seismic design coefficient C_{sm} for modes other than the fundamental mode that have periods less than 0.3 s is permitted to be determined by the following equation:

$$C_{\mathrm{sm}} = \frac{C_{\mathrm{a}}}{R}(1.0 + 5.0\,T_m), \tag{6.18}$$

where R and T_{m} are as defined above and C_a is the seismic coefficient based on the soil profile type and the value of $A_{\mathrm{a.}}$
(c) For buildings where any modal period of vibration T_{m} exceeds 4.0 s, the modal seismic design coefficient C_{sm} for that mode is permitted to be determined by the following equation:

$$C_{\mathrm{sm}} = \frac{3C_{\mathrm{a}}}{RT_{\mathrm{m}}^{4/3}} \tag{6.19}$$

where R and T_m are as defined above and C_a is the seismic coefficient based on the soil type and the value of A_v.

The reduction due to soil structure–concrete interaction may be used.

6.8.3 Modal Forces, Deflection and Drifts

The modal force F_{xm} at each level shall be determined by the following equations:

$$F_{\mathrm{vm}} = C_{vxm}V_{\mathrm{m}} \tag{6.20}$$

and

$$C_{vxm} = \frac{w_x\phi_{\mathrm{vm}}}{\sum_{i=l}^{n} w_i\phi_{i\mathrm{m}}} \tag{6.21}$$

where $C_{v\mathrm{sm}}$ = the vertical factor in the mth mode except that for buildings where the gravity load is concentrated at a single level, it shall be taken as equal to W.

The reduced based shear V shall in no case be taken as less than 0.7 V.

V_{m} = the total design lateral force or shear at the base in the mth mode
w_i,w_x = the portion of the total gravity load of the building W located or assigned to level i or x

www.EngineeringBooksPDF.com

ϕ_{xm} = the displacement amplitude at the xth level of the building when vibrating in its mth mode and
ϕ_{im} = the displacement amplitude at the 8_{xm} level of the building when vibrating in its mth mode.

$$\delta_{\mathrm{xm}} = C_{\mathrm{d}}\delta_{xem} \tag{6.22}$$

and

$$\delta_{\mathrm{xe}m} = \left(\frac{g}{4\pi^2}\right)\left(\frac{T_m^2 F_{xm}}{W_x}\right) \tag{6.23}$$

where

C_d = the deflection amplification factor determined from Table 6.1
δ_{xem} = the deflection level x in the mth mode at the centre of the mass at level x determined by an elastic analysis
g = the acceleration due to gravity (rt/s^2 or rtl/s^2)
T_{m} = the model period of vibration in seconds of the mth mode of the building
F_{xm} = the portion of the seismic base shear in the mth mode induced at level x and
W_x = the portion of the total gravity load of the building W located or assigned to level x.

The modal drift in a storey Δ_{m} shall be computed as the difference between the deflections δ_{xm} at the top and bottom of the storey under consideration.

6.8.4 Soil–Concrete Structure Interaction Effects

6.8.4.1 General

The provisions set forth in this section may be used to incorporate the effects of soil–concrete structure interaction in the determination of the design earthquake forces and the corresponding displacement of the building. The use of these provisions will decrease the design values of the base shear lateral forces and overturning moments but may increase the computed values of the lateral displacements and the secondary forces associated with the $P-\Delta$ effects. The coded method of soil-concrete structure interaction can be compared with the results obtained from the finite element analysis given in Chap. 5.

6.8.4.2 Equivalent Lateral Forces Procedure

The following provisions are supplementary to those presented above.

www.EngineeringBooksPDF.com

6.8.4.3 Base Shear

To account for the effects of soil–concrete structure interaction, the base shear V determined may be reduced to

$$V = V - \Delta V \tag{6.24}$$

The reduction ΔV shall be computed as follows:

$$\Delta V = \left[C_s - C_s \left(\frac{0.05}{\beta} \right)^{0.4} \right] \bar{W} \tag{6.25}$$

where

C_s = the seismic response coefficient computed using the fundamental natural period of fixed-base structure T or T_a, or the seismic response coefficient computed using the fundamental natural period of flexibly supported structure (T)
β = the fraction of critical damping for the structure–foundation system
W = the effective gravity load of the building which shall be taken as 0.7 W, except that for buildings where the gravity load is concentrated at a single level, it shall be taken as equal to W.

The reduced base shear V shall in no case be taken as less than 0.7 V.

6.8.4.4 Effective Structural Period

The effective period T shall be determined as follows:

$$\bar{T} = T \sqrt{\left(1 + \frac{k}{K_y} \right) \left(1 + \frac{K_y \bar{h}^2}{K_0} \right)} \tag{6.26}$$

where

T = the fundamental period of the concrete structures
$\bar{k}$ = the stiffness of the concrete structure when fixed at the base
$\bar{h}$ = the effective height of the structure which shall be taken as 0.7 times the total height

$$\bar{k} = 4\pi^2 \left(\frac{\bar{W}}{gT^2} \right) \tag{6.27}$$

$\bar{h}$ except that for buildings where the gravity load is effectively concentrated at a single level, it shall be taken as the height to that level; K_y is the lateral stiffness of the foundation defined as the static horizontal force at the level of the

www.EngineeringBooksPDF.com

foundation necessary to produce a unit deflection at that level, the force and the deflection being measured in the direction in which the structure is analysed; K_θ is the rocking stiffness of the foundation defined as the static moment necessary to produce a unit average rotation of the foundation, the moment and rotation being measured in the direction in which the structure is analysed and g is the acceleration due to gravity.

The foundation stiffnesses K and K_θ shall be computed by established methods using soil properties that are compatible with the soil strain levels associated with the design earthquake motion. The average shear modulus G for the soils beneath the foundation at large strain levels and the associated shear wave velocity V_s needed in these computations shall be determined from Table 6.6.

Table 6.6 Values of G/G_o and V_s/v_{so}

	Ground ≤0.10	Acceleration ≤ 0.15	Coefficient ≤0.20	≤0.30
Value of G/G_o	0.81	0.64	0.49	0.42
Value of V_s/v_{so}	0.90	0.80	0.70	0.65

V_{so} = the average shear wave velocity for the soils beneath the foundation at small strain levels (10^{-3}% or less)

$G_0 = \gamma v^{2}_{so}/g$ = the average shear modulus for the soils beneath the foundation at small strain levels and

γ = the average unit weight of the soils

For concrete structures supported on mat foundations that rest at or near the ground surface or are embedded in such a way that the side wall makes contact with the soil, it cannot be considered to remain effective during the design ground motion; the effective period of the building may be determined as follows:

$$T = T\sqrt{1 + \frac{25\alpha r\bar{h}}{u_s^2 T^2}\left(1 + \frac{1.12 r\bar{h}^2}{r_m^3}\right)} \tag{6.28}$$

where α = the relative weight density of the structure and the soil defined by

$$\alpha = \frac{\bar{W}}{\gamma A_0 h} \tag{6.29}$$

r_a and r_m = characteristic foundation lengths defined by

$$r_a = \sqrt{\frac{A_0}{\pi}} \tag{6.30}$$

and

$$r_m = \sqrt[4]{\frac{4I_0}{\pi}} \tag{6.31}$$

www.EngineeringBooksPDF.com

The quantity r is a characteristic foundation length that shall be determined as follows.

For $\bar{h}/L_0 \leq 0.5$

$$r = r_m = \sqrt[4]{\frac{4I_0}{\pi}} \tag{6.32}$$

For

$$\bar{h}/L_0 \leq 0.5 \tag{6.33}$$

where

L_o = the overall length of the side of the foundation in the direction being analysed
A_o = the area of the load-carrying foundation and
I_o = the static moment of inertia of the load-carrying foundation

For intermediate values of h/L_o the value of r shall be determined by linear interpolation.

6.9 Methods of Analysis Using Soil-Structure Interaction

6.9.1 General Introduction

Dynamic analysis may be used for the design of any concrete structures interacting with soils. Some analyses are given below:

(a) response-spectrum analysis with and without seismically isolated structures
(b) time-history analysis with and without seismically isolated structures

These methods have been dealt with in Chap. 5.

6.9.2 Response-Spectrum Analysis

Response-spectrum analysis shall be performed using a damping value equal to the effective damping of the isolation system or 30% of critical, whichever is less. This method is given in Chap. 5.

Response-spectrum analysis is used to determine the total design displacement, and the total maximum displacement shall include simultaneous excitation of the model by 100% of the most critical direction of ground motion and 30% of the ground motion on the orthogonal axis. The maximum displacement of the isolation system shall be calculated as the vectorial sum of the two orthogonal displacements.

www.EngineeringBooksPDF.com

The design shear at any storey shall not be less than the storey shear obtained using the value of V_s taken as equal to the base shear obtained from the response-spectrum analysis of the direction of interest.

6.9.3 Time-History Analysis

Time-history analysis shall be performed with at least three appropriate pairs of horizontal time-history components as defined.

Each pair of time histories shall be applied simultaneously to the model, considering the most disadvantageous location of mass eccentricity. The maximum displacement of the isolation system shall be calculated from the vectorial sum of the two orthogonal components at each time step.

The parameter of interest shall be calculated for each time-history analysis. If three time-history analyses are performed, the maximum response of the parameter of interest shall be used for design. If seven or more time-history analyses are performed, the average value of the response parameter of interest shall be used for design. For each pair of horizontal ground of components, the square root sum of the squares (SRSS) of the 5% damped spectrum of the scaled horizontal components shall be constructed. The motions shall be scaled such that the average value of the SRSS spec4ra does not fall below 1.3 times the 5% damped spectrum of the design earthquake (or maximum capable earthquake) by more than 10% in the period range of *TI* from minus 1.0 s to *TI* plus 1.0.

Time histories developed for sites within 15 km of a major active fault shall incorporate near-fault phenomena. In both cases the analyses shall be performed using specific earthquake input.

The design earthquake shall be used to calculate the total design displacement of the isolation system and the lateral forces and displacements of the isolated structure. The maximum capable earthquake shall be used to calculate the total maximum displacement of the isolation system. The details of this method are given in Chap. 5.

6.9.4 Characteristics of Interaction

The interaction effects in the approach used here are expressed by an increase in the fundamental natural period of the structure and a change (usually an increase) in its effective damping. The increase in period results from the flexibility of the foundation soil, whereas the change in damping results mainly from the effects of energy dissipation in the soil due to radiation and material damping. These statements can be clarified by comparing the responses of rigidity and elastically supported systems subjected to a harmonic excitation of the base. Consider a linear structure of weight W, lateral stiffness k and coefficient of viscous damping c (shown in Fig. 6.1) and assume that it is

www.EngineeringBooksPDF.com

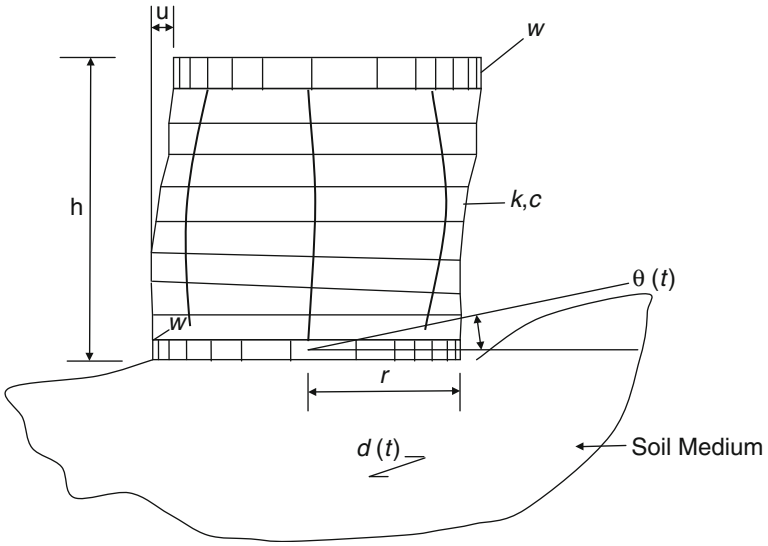


Fig. 6.1 Structure–soil interaction

supported by a foundation of weight W_0 at the surface of a homogeneous elastic half-space.

As an example, the foundation weight and the weight of the structure are assumed for a circular footing to be uniformly distributed over a circular area of radius r. The base excitation is generally specified by the free-field motion of the ground surface. This is taken as horizontally directed motion with a period T_0 and an acceleration of amplitude a_m. The rotation of the foundation is θ and the displacement to the base of the top of the structure designated as u.

The response spectra for $h/r = 1$ and $h/r = 5$ for the structure can be plotted as shown in Figs. 6.2 and 6.3. The solid lines represent response spectra for the steady-state amplitude of the total shear for different values of ϕ_0 –the relative flexibility parameter for the soil and the structure concerned. The results are displayed in a dimensionless form, the abscissa representing the ratio of the period of the excitation T_0 to the fixed-base natural period of the system T and the ordinate showing the ratio of the amplitude of the actual base shear V to the amplitude of the base shear. The value of $m = W/g$ in a product ma_m where a_m is the acceleration amplitude of the free-field ground motion. The inclined scales represent deformation amplitude of the superstructure. They are the plots produced by Veletsos and Meek.

Having given the background to the seismic criteria and the soil–concrete structure interaction, it now becomes essential to present mathematical data on the site seismic response. They are given in Figs. 6.1, 6.2 and 6.3.

www.EngineeringBooksPDF.com

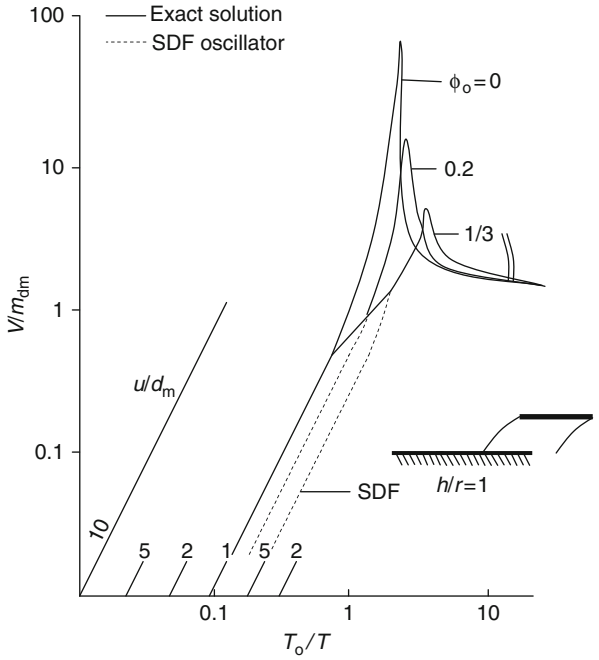


Fig. 6.2 A comparative study of exact and SDF oscillator result (h/r = 1)

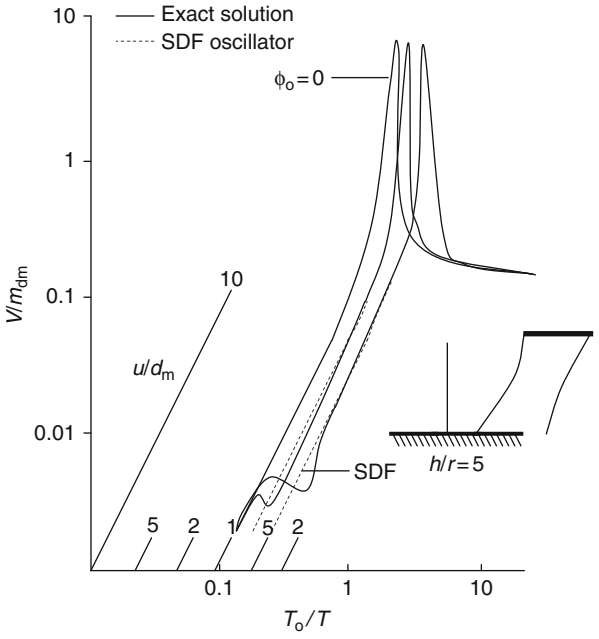


Fig. 6.3 A comparative study of exact and SDF oscillator results (h/r = 5)

www.EngineeringBooksPDF.com

6.10 Site Response – A Critical Problem in Soil–Structure Interaction Analyses for Embedded Structures

6.10.1 Vertical Earthquake Response and P–*Δ Effect*

The methodology for vertical and horizontal response analysis is the same in principle. However, the difference in vibrational properties of the structure has str4ng influences in response analysis. At least the following three influences exist.

First, the amplitude and spectral contents of earthquake motion vary with the magnitude and distance of the earthquake, but differently in the horizontal and vertical directions; the relative amplitude of the vertical motion is higher for sites in the epicentral region.

Second, the possible variation for both amplitude and frequency content is to be considered when analysing the response in the vertical direction.

Third, the vertical vibration response of vertical members is mainly from axial forces while the horizontal response is from the shear and bending forces. The hysteretic property for different loads may be different, especially in the non-linear range; the $P-\Delta$ effect will produce a descending branch in the force–deformation curve.

6.10.2 P–*Δ Effects*

In an elastic system, P–Δ may also introduce non-linearity. This effect is very important for high-rise structures and inelastic structures.

For a single mass system as shown in Fig. 6.4 the $P-\Delta$ effect is the secondary moment produced by the axial force $F(t)$ and the vertical inertial force $M(\ddot{v} + \ddot{v}_g)$ on the deflection u, which is equivalent to an additional horizontal force

$$[F(t) + M(\ddot{v} + \ddot{v}_g)]u/H \tag{6.34}$$

where $\ddot{v}_g$ is the vertical ground acceleration and $\ddot{v}$ is the relative vertical acceleration of the mass. Because vertical vibration is also considered, there are now two degrees of freedom and two equations of motion

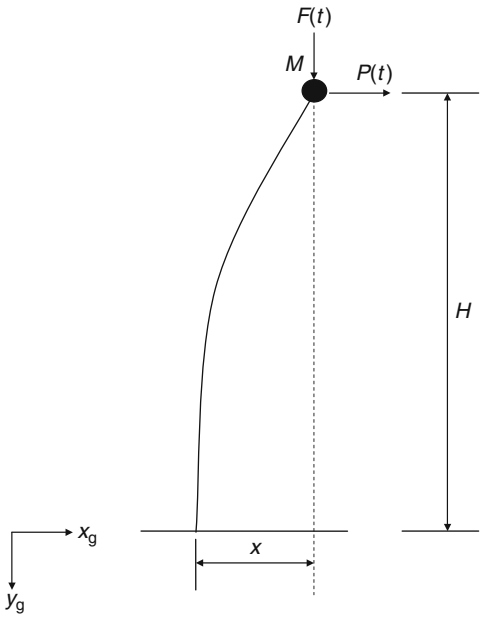
$$M\ddot{u} + C_u\dot{u} + K_u = P(t) - M\ddot{u}_g - [F(t) + M(\ddot{v} + \ddot{v}_g)]u/H \tag{6.35}$$

$$M\ddot{v} + C_v\dot{v} + k_v v = F(t) - M\ddot{v}_g \tag{6.36}$$

where C_u, C_v are, respectively, the damping coefficient and stiffness of the system in the horizontal and vertical directions. It is seen here that the last term in (6.38) makes the problem non-linear.

www.EngineeringBooksPDF.com

Fig. 6.4 $P-\Delta$ effects



$$
\begin{aligned}
&M\ddot{u} + C_u\dot{u} + K_u = P - M\ddot{u}_g = p(t) \\
&\quad = a_0 + \sum [a_j \cos \omega_j t + b_j \sin \omega_j t] \qquad (j = l, \infty) \\
&quad \quad = \sum C_j \exp(i\omega_j t) \qquad\qquad (j = -\infty, \infty)
\end{aligned} \tag{6.37}
$$

where coefficient $C_j = (a_j - \mathrm{ib_j})/2$ for $j > 0$ or $C_\mathrm{j} = (a_j = ib_j)/2$ for $j < 0$ is complex and $C_0 = a_0$; $i = (-1)^{1/2}$; $\omega_{-j} = \omega_j$; $C_j = C_{-j}$, the Fourier development gives the following result:

$$
\begin{aligned}
p(t) &= \Sigma C_j \exp(i\omega_j t) \\
C_j &= \frac{1}{T_\mathrm{P}} \int_0^{T_\mathrm{p}} p(t) \exp(-i\omega_t t) \mathrm{d}t
\end{aligned} \tag{6.38}
$$

where T_p is the total duration of motion, as shown in Fig. 6.6, including a dynamic part and a quiescent part and the latter is added for the convenience of fast Fourier transform (FFT) computation. In FFT, the total duration T_p is divided into N intervals of I, and $N = 2M$, where M and N are integers. The most commonly used N values are 1024, 2048 or 4096. The selection of $\Delta t = T_\mathrm{p}/N < T_{\min}/z$ is controlled by high-frequency components and T_p should be several times the greater period considered.

www.EngineeringBooksPDF.com

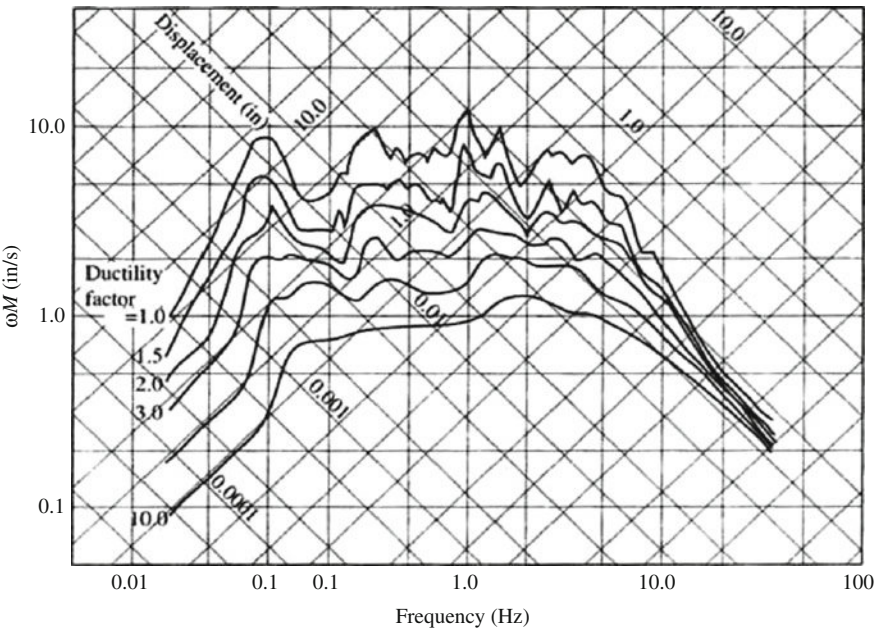


Fig. 6.5 Frequency spectra

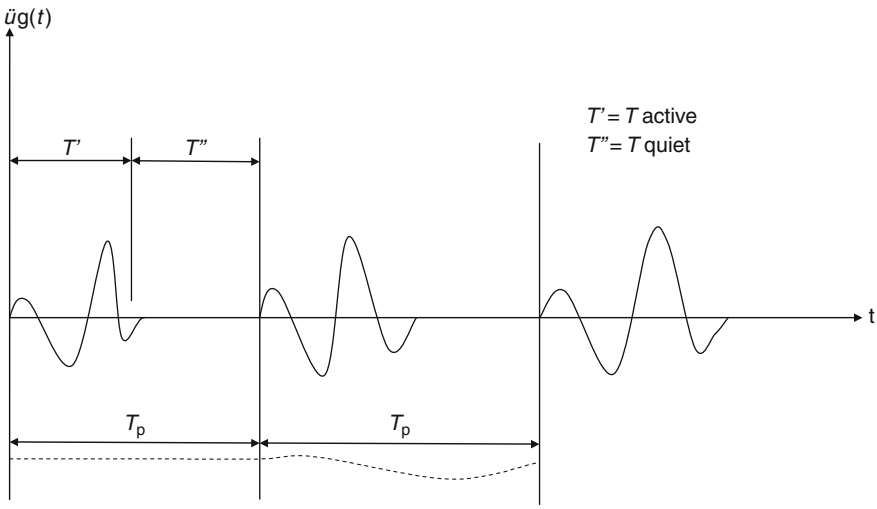


Fig. 6.6 Acceleration–time relationship

www.EngineeringBooksPDF.com

6.10.2.1 The Use of Transfer Function

The transfer function plays an important role in frequency domain analysis as described in Chap. 5. It is the ratio of the stationary response to the simple harmonic input. Where $p(t) = C\exp(i\omega t)$, the stationary response of an SDF system is

$$u(t) = H(i\omega)C\exp(i\omega t) \tag{6.39}$$

and the transfer function is then

$$H(i\omega) = \frac{u(t)}{p(t)} = \frac{1}{-m\omega^2 + iC\omega + k} \tag{6.40}$$

$$= \frac{(1/k)}{1 - \beta^2 + 2i\xi\beta} \tag{6.41}$$

where $\beta = \omega_0$ is the ratio of the input motion frequency ω and the natural frequency $\omega_0 = (\mathrm{k/m})^{1/2}$ of the system. The transfer function is complex; its modulus $[H(i\omega)]$ is the ratio of the amplitudes of the response and the input, and the phase angle of $H(i\omega)$ is the difference between the phase angles of the response and the input. There are many transfer functions. For earthquake motion $u_g(t)$

$$\ddot{u} + 2\xi\omega_0\dot{u} + \omega^2 u_0 = \ddot{u}_{\mathrm{g}} \tag{6.41a}$$

and the transfer function of the relative displacement $u(i)$ of the system to the input $\ddot{u}$

$$Hu(i\omega) = (\omega_0^2 - \omega^2 + 2i\xi\omega_0\omega)^{-1} = \left[\left(\omega_0^2 - \omega^2\right)^2 + 4\xi^2\omega_0^2\omega^2\right]^{-1/2}\exp(i\phi)$$
$$\phi = \tan^{-1}\left[(2\xi\omega_0\omega)/\left(\omega_0^2 - \omega^2\right)\right] \tag{6.41b}$$

From relations between the spectra of a function and its derivative, it is easy to find the transfer functions of relative velocity $u(t)$ and the absolute acceleration $\ddot{u}(t) + \ddot{u}_g(t)$ to $\ddot{u}_g(t)$. With the transfer function found, the corresponding response in the time domain can be obtained from (6.41b)

$$u(t) = \sum H_u(i\omega_j)C_j(\omega)\exp(i\omega_j t) \tag{6.42}$$

6.10.3 Frequency Domain Analysis of an MDF System

The procedure is exactly the same as for the SDP system. Consider the earthquake motion.

www.EngineeringBooksPDF.com

The Fourier transformation of this equation is

$$(-\omega^2 M + i\omega C + K)U(i\omega) = -MI\ddot{U}_g(i\omega) \tag{6.43a}$$

or, in terms of the transfer function matrix,

$$H(i\omega) = U^0(i\omega) \tag{6.43b}$$

which is the ratio of the stationary system response matrix $u(t) = U^0(i\omega)\exp(i\omega t)$ to input in the frequency domain and hence

$$U(i\omega) = H(i\omega)^* I\ddot{U}_g(i\omega) \tag{6.43c}$$

The computation of transfer function matrix $H(i\omega)$ is time consuming. The response matrix $u(t)$ can then be found from $U(i\omega)$ by a Fourier transformation. To avoid the computation of $H(i\omega)$, the model response in frequency domain can be found

$$Q_j(i\omega) = H_j(i\omega)\ddot{U}_g(i\omega) \tag{6.43d}$$

After finding the model response $Q_j(t)$ in the time domain by Fourier transformation, the total response can be found.

As mentioned before, any other response can be found in the same way if the corresponding transfer function is used.

Instead of finding the structural response for a given ground motion $U_g(t)$ in the step-by-step integration method, the response spectrum method finds the maximum structural response from the given response spectrum $S_a(\omega)$ of the ground motion.

6.10.4 Some Non-linear Response Spectra

In the linear case, because of the approximate relation,

$$S_a = \omega S_v = \omega S_d \tag{6.44}$$

Note: All three spectra can be plotted on one tripartite grid diagram. These approximations do not hold in the non-linear case; there are then three possible non-linear response spectra. This method can be compared with the methods shown in Chap. 5.

It is noted that for the non-linear yield response spectrum, the ordinate is not displacement response but the yield deformation which produces the displacement response $U_{max} = \mu u_y$ where $\mu = [u_{max}/u_y]$ is the ductility factor. The corresponding approximation in this case is

$$S_a = \omega S_v = \omega S_d \tag{6.45}$$

www.EngineeringBooksPDF.com

And the yield strength of the concrete structure is

$$P_{\mathrm{y}} = P_{\max} = ku_{\mathrm{y}} = m\omega^2 u_{\mathrm{y}} \tag{6.46}$$

In an ideal elasto-plastic system, P_y is the maximum internal force elastic limit of the deformation capacity u_y which the system should have in order to limit the spectral acceleration, velocity and displacement to not over $\omega^2 u_y$, ωu_y and u_y, respectively. Here u_y and ductility factor It are requirements of the capacity for the system. Finally, four structural factors (natural period, damping ratio, type of hysteretic curve and the ductility factor μ) and three ground motion parameters (peak acceleration A, velocity V and displacement D) are obtained for analysis.

6.10.5 Soil–Structure Interaction Numerical Technique

Soil–structure interaction (SSI) was first studied a long time ago in analysis of the vibration of machinery foundations but has developed greatly in the past two decades because of the rapid advances in computer technology. It may be classified into time and frequency domains in methodology or total structure concept or substructure and hybrid structure in structural decomposition. Most investigators have adopted frequency–domain analysis which has the following advantages.

(a) It is convenient to consider the frequency-dependent foundation impedance when the whole system is divided into structure and ground.
(b) The transmitting boundary for a finite element model or wave propagation theory is frequency dependent.

Generally speaking, SSI analysis consists of four fundamental problems as follows:

(i) The free-field problem: the rock (ground) motion is found from other given motions.
(ii) The scattering problem: the response of the ground is studied with the structure removed at the contacts (Fig. 6.6) of the structure and ground. The different contact points of the hybrid structure are studied, including the foundation soil and the remaining half-space.
(iii) Impedance: the displacements $U_{\mathrm{c}}(\omega)\exp(i\omega t)$ at the contact points are found for forces applied at the contact point $F_{\mathrm{c}}(\omega)\exp(i\omega t)$. The impedance matrix $Is(\omega) = \mathrm{C}^{-1}(\omega)$ or the flexibility matrix $C(\omega)$ of the ground is defined in the following ratio:

$$U_c(\omega) = C(\omega)F_c(\omega) \tag{6.47}$$

www.EngineeringBooksPDF.com

If the foundation of the structure is on the ground surface, the ground substructure is a half-space; for the case with only one horizontal layer on top of homogeneous space, there is an analytical solution for $C(w)$.

(iv) Finally, there is the soil–structure interaction (SSI) system.

6.10.6 Substructure Method in the Frequency Domain

Moreover, the methods of substructuring in finite element is fully described in Chap. 5. Figure 6.7a shows the FF system of the total structure or the frequency domain analysis. This method is also called the method of impedance, which divides the system into two substructures (substructures 1 and 2) at the contact surface as shown in Fig. 6.7b, c, studies their responses separately first and combines them later to satisfy the continuity condition. It has been used in both time and frequency domains.

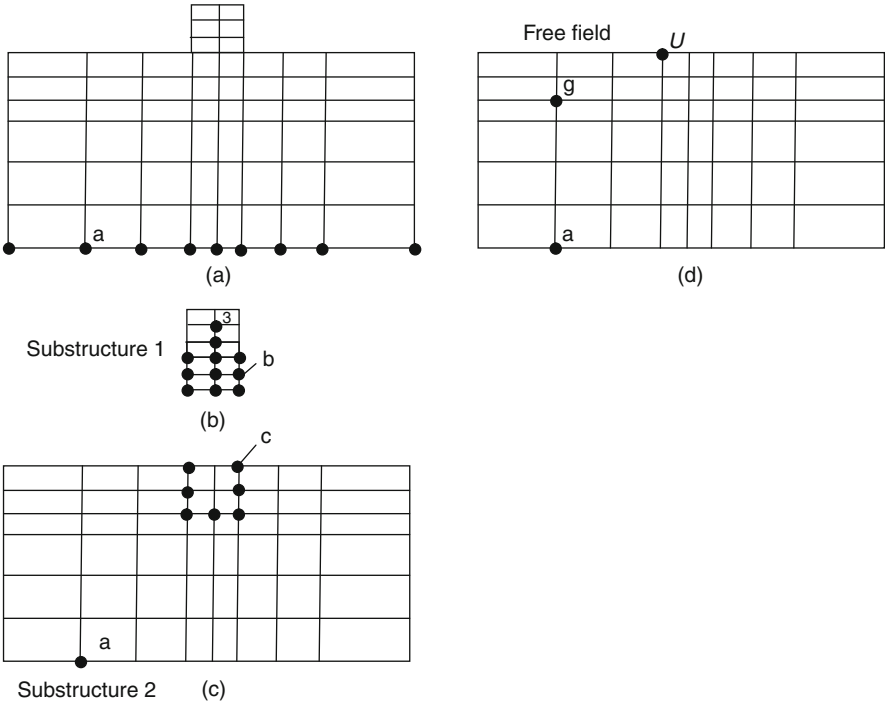


Fig. 6.7 A total structure and substructures

www.EngineeringBooksPDF.com

Let the known motion be a general three-dimensional time history $ug(t)$, whose frequency domain expression is $U_g(\omega)$ at some depth below the surface. The four primary problems are encountered:

(a) Free-field response: the input motion $u_a(t)$ or $U_a(\omega)$ is evaluated as bedrock point "a" in Fig. 6.8d, the lower boundary of the ground substructure for given motional point g. Let the analysis use Din operator L_1^*:

$$L_1^* : u_a(t), U_a, (\omega) = u(t), U_{\mathrm{g}}^0(\omega) \tag{6.48}$$

(b) Scattering problem: the response of substructure 2 is studied (Fig. VIII.8(c)). Let there be an operator L_{i}^*:

$$L_2^* : u_{\mathrm{g}}^0(t), U^0(\omega) = u_{\mathrm{a}}(t), U_{\mathrm{a}}(\omega) \tag{6.49}$$

(c) mpedance problem: the response of substructure 2 is studied (Fig. 6.8(c)) under an external excitation $f_c(t) = F_c(\omega)F_c(i\omega t)$ acting along one direction at any point c. The response at point c, $u_c(t) = U_c(\omega)\exp(i\omega t)$ for a given force $f_b(\omega) = F_b(\omega)\exp(i\omega t)$ at point c is

$$U_c(\omega) = C(\omega)F_c(\omega) \quad F_c(\omega) = I_s(\omega)U_c(\omega)C(\omega) \tag{6.50}$$

(d) The response $u_b(t)$ or $U_b(\omega)$ of substructure 1 under external forces $f_{\mathrm{b}}(t) = F_b\,(\omega)\exp(i\omega t)$ is studied at contact point b:

$$F_b(\omega) = M_b(\omega)\omega^2\, U_b(\omega) \tag{6.51}$$

where $M_b(\omega)$ is the equivalent, frequency-dependent mass matrix of the superstructure.

The four primary problems are four steps to find the operators L_1*, L_2*, $C(\omega)$ or $I_s(\omega)$ and $M_b(\omega)$. The final solution is only an assemblage of the four to satisfy the compatibility requirement at the boundary points b and c.

The continuity condition at boundary points b and c is that the displacement $u_b(t)$ or $U_b(\omega)$ is equal to the sum of displacements $u_c{}^0(t)$ or $U_c{}^0(\omega)$ of substructure 2 and the displacements $u_c(t)$ or $U_c(w)$ due to the SSI effect of substructure 1 on substructure 2:

$$u_b(t) = u_c^0(t) + u_c(t) \text{ or} b(\omega) = U_c^0(\omega) + U_c(\omega) \tag{6.52}$$

The equilibrium condition requires that the sum of forces $f(t)$ or $F_c(\omega)$ between the ground and foundation and the forces $f_b(t)$ or $F_b(\omega)$ between the structure and foundation resist the inertial force $f_i(t)$ or $F_i(\omega)$ of the rigid foundation, i.e.

$$u_b(t) = u_c^0(t) + u_c(t) \text{ or } F_c(\omega) = M_0\ \omega^2 U_b(w) + F_b(\omega) \tag{6.53}$$

where $M_0W^2U_b(\omega)$ is the Fourier transform of the inertial force $f_i(t)$ and M_0 the mass matrix of the rigid foundation.

www.EngineeringBooksPDF.com

From these Fourier equations it is finally found that

$$U_b(\omega) = \{I - \omega^2 C(\omega)[M_0 + M_{\mathrm{b}}(\omega)]\}^{-1} U_c^0(\omega) \tag{6.54}$$

or

$$U_b(\omega) = \{I_s(\omega) - \omega^2[M_0 + M_b(\omega)]\}^{-1}\, U_c^0(w) \tag{6.55}$$

$$F_c^0(\omega) = I_s(\omega) U_c^0(\omega) \tag{6.56}$$

where I is the identity matrix. If three-dimensional ground motion is considered, a rigid foundation has six components: three translational and three rotational, and I is 6×6. Equation (6.54) clearly shows the interactions. The effect of input motion $u_g(t)$ is represented by $U_c^0(\omega)$, the foundation input motion obtained by operators L_1 and L_2; the interaction of the superstructure foundation and ground by the term $C(\omega)[M_0 + M_b(\omega)]$ and $U_b(\omega)$ is the result of the input motion on the soil–structure system, from which the structural response is obtained.

In (6.55), $F_c^0(\omega) = I_s(\omega)U_c^0(\omega)$ is the driving force vector which includes the forces and moments from the rigid foundation on the ground when points c of the substructure 2 tend to deform and the foundation resists the deformation. Equations (6.55) and (6.56) are easier to use than Eq. (6.54).

6.11 Mode Superposition Method – Numerical Modelling

The alternative numerical method under mode superposition given in Chap. 5 can be adopted for superstructures.

Mode superposition method is a method of using the natural frequencies and mode shapes from the modal analysis to characterize the dynamic response of a structure to transient or steady harmonic excitations.

The equations of motion may be expressed as stated before in Chap. 5:

$$[M]\{\ddot{u}\} + [C]\{\ddot{u}\} + [K]\{u\} = \{F\} \tag{6.57}$$

$\{F\}$ is the time-varying load vector given by

$$\{F\} = \{F^{\mathrm{nd}}\} + s\{F^S\} \tag{6.58}$$

where $\{F^{\mathrm{nd}}\}$ is the time-varying nodal forces; s is the load vector scale factor and $\{F\}$ is the load factor from the modal analysis.

The procedure of setting modal coordinates are clearly established as indicated in Chap. 5. Equation (6.57) is then reset and orthogonality conditions are established. Normality conditions given in (6.59) are established:

$$\{\phi_i\}^{\mathrm{I}}\{M\}\{\phi_j\} = 1 \tag{6.59}$$

www.EngineeringBooksPDF.com

Using damping terms, the circular frequency for mode j, w_j, is evaluated as

$$w_j \sqrt{(k_j/M_j)} \tag{6.60}$$

The rest of the procedure is clearly established.

The complete mode shape can be derived for each sector from modal displacements. The displacement component (x,y,z) at any point in the global structures is then given by

$$u_i = A \cos\left[\alpha\left(\frac{T}{N} - 1\right) + \bar{\phi}\right] \tag{6.61}$$

where $\frac{T}{N}$ sector number; $A = U_A / \cos \bar{\phi}$

$\phi = \tan^{-1}(U_{B,i} / U_{A,i})$

$U_{B,i} \ni U_{A,i}$ = modal analysis component displacement values at point "i"

As identification Chap. 5, the analysis requires mass moment of inertia, products of inertia and energies in order to evaluate stress–strain at any point "i". They are given as below as a repeat if one wants to use the method indicated in this chapter.

6.12 Mass Moments of Inertia

The computation of the mass moments and products of inertia as well as the model centroids is described in this section. The model centroids are computed as

$$\begin{aligned} X_c &= A_x/M \\ Y_c &= A_y/M \\ Z_c &= A_z/M \end{aligned} \tag{6.62}$$

where typical terms are

X_c = X coordinate of model centroid

$A_x = \sum_{i=1}^{N} m_i X_i$

N = number of elements

m_i = mass of element i

X_i = X coordinate of the centroid of element i

$M = \sum_{i=1}^{N} m_i$ mass of model centroid

www.EngineeringBooksPDF.com

The moments and products of inertia with respect to the origin are

$$I_{xx} = \sum_{i=1}^{N} m_i[(Y_i)^2 + (Z_i)^2] \qquad I_{zz} = \sum_{i=1}^{N} m_i[(X_i)^2 + (Y_i)^2] \tag{6.63}$$

$$I_{yy} = \sum_{i=1}^{N} m_i[(X_i)^2 + (Z_i)^2] \qquad I_{xy} = -\sum_{i=1}^{N} m_i[(X_i)(Y_i)] \tag{6.64}$$

$$I_{yz} = -\sum_{i=1}^{N} m_i[(Y_i)(z_i)] \qquad I_{xz} = -\sum_{i=1}^{N} m_i[(X_i)(z_i)] \tag{6.65}$$

where typical terms are I_{xx} = mass moment of inertia about the X axis through the model centroid and I_{xy} = mass product of inertia with respect to the X and Y axes through the model centroid.

The moment and products of inertia with respect to the model centroid (the components of the inertia tensor) are

$$\begin{aligned}
I'_{xx} &= I_{xx} - M[(Y_c)^2 + (Z_c)^2] \\
I'_{yy} &= I_{yy} - M[(X_c)^2 + (Z_c)^2] \\
I'_{zz} &= I_{zz} - M[(X_c)^2 + (Y_c)^2] \\
I'_{xy} &= I_{xy} + MX_cY_c \\
I'_{yz} &= I_{yz} + MY_cZ_c \\
I'_{xz} &= I_{xz} + MX_cZ_c
\end{aligned} \tag{6.66}$$

where typical terms are I'_{xx} = mass moment of inertia about the X axis through the model centroid and I'_{xy} = mass product of inertia with respect to the X and Y axes through the model centroid.

It may be seen from the above development that only the mass (m_i) and the centroid (X_i, Y_i, and Z_c) of each element are included. Effects which are not considered are

(a) the mass being different in different directions;
(b) the presence of rotational inertia terms.

www.EngineeringBooksPDF.com

6.12.1 Energies

Energies are available by setting

$$E_{\mathrm{e}}^{\mathrm{po}} = \begin{cases} \frac{1}{2}\sum_{i=1}^{\mathrm{NINT}} \{\sigma\}^{\mathrm{T}}\{\varepsilon^{\mathrm{el}}\}\mathrm{vol}_i + E_{\mathrm{e}}^{\mathrm{pl}} & \text{if element allows only displacement and rotational degrees of freedom (DOF) and either is non-linear or uses integration points} \\ \frac{1}{2}\{u\}^{\mathrm{T}}[K_e]\{u\} & \text{all other cases} \end{cases} \quad (6.67)$$

= potential energy

$$E_{\mathrm{e}}^{\mathrm{ki}} = \frac{1}{2}\{\dot{u}\}^{\mathrm{T}}[M_{\mathrm{e}}]\{\dot{u}\} \quad (6.68)$$

= kinetic energy

$$E_{\mathrm{e}}^{\mathrm{pl}} = \sum_{i=l}^{\mathrm{NINT}}\sum_{j=l}^{\mathrm{NCS}}\{\sigma\}^{\mathrm{T}}\{\Delta\varepsilon^{\mathrm{pl}}\}\,\mathrm{vol}_i \quad (6.69)$$

= plastic energy

where

{u} = element DOF vector
$\{\dot{u}\}$ = time derivative of element DOF vector
[K_e] = element stiffness/conductivity matrix
[M_e] = element mass matrix

6.13 Modelling of Isolators with Soil–Structure Interaction

6.13.1 Introduction

The design process for an isolation system will generally begin with a preliminary design using parameters from a previous project or from data from a manufacturer to estimate the possible maximum displacement of the system and minimum values of various controlling quantities (such as shear strain) and also for estimating the structural base shear, stability of the isolators and possibility of uplift. After this preliminary design process is completed, examples of the final design of the isolators will be ordered and subjected to the code-mandated prototype test programme.

An innovative design strategy called "seismic isolation" provides an economic practical alternative for the design of new structures and the seismic rehabilitation of existing buildings, bridges and industrial equipment. Rather than resisting the large forces generated by earthquakes,

www.EngineeringBooksPDF.com

seismic isolation decouples the structure from the ground motion and thus reduces earthquake forces by factors of 5–10. This level of force reduction is very significant because it may eliminate the ductility demand on a structural system.

The principle of seismic isolation is to introduce flexibility at the base of a structure in the horizontal plane, while at the sametime introducing damping elements to restrict the amplitude or extent of the motion caused by the earthquake. The essential feature is to ensure that the period of structure is well above that of the predominant earthquake input.

The advantages of seismic isolation include

(a) the ability to eliminate ductility demand;
(b) significant reduction of structural and non-structural damage;
(c) enhancement of the safety of the building contents, occupants and architectural facades;
(d) reduction of seismic design forces.

Seismic isolation should be considered if any of the following situations apply:

(i) increased building safety, post-earthquake operability and business survivability are desired;
(ii) reduced lateral design forces are desired;
(iii) alternative forms of construction with limited ductility capacity (such as precast and prestressed concrete) are desired in an earthquake region;
(iv) an existing structure is not currently safe for earthquake loads.

Seismic isolation gives the option of providing a building with better performance characteristics than all current codes give. It therefore represents a major step forward in the seismic design of civil engineering structures. In the case of building retrofit, the need for isolation may be more obvious: the structure may simply not be safe in its present condition. In such cases, seismic isolation should be compared with alternative solutions, such as strengthening, to determine the cost-effectiveness.

Structures are generally suitable for seismic isolation if the following conditions exist:

(1) height of structure is two storeys or greater (unless unusually heavy);
(2) site clearance permits horizontal displacements at the base of about 6″ (152 mm);
(3) geometry of structure is not slender in elevation;
(4) lateral wind loads or other non-seismic loads are less than approximately 10% of the weight of the structure;
(5) site ground motion is not dominated by long-period components.

New impetus was given to the concept of seismic isolation by the successful development of mechanical energy dissipators and elastomers with high-

www.EngineeringBooksPDF.com

damping properties. Mechanical energy dissipators, when used in combination with a flexible isolation device, can control the response of the structure by limiting displacements and forces, thereby significantly improving seismic performance.

6.13.2 Isolation System Components

Base isolation is now a mature technology and is used in many countries, and there are a number of acceptable isolation systems, the construction of which is well understood. Most systems used today incorporate either elastomer bearings with the elastomer being either natural rubber or neoprene, or sliding bearings, with the sliding surface being Teflon and stainless steel (although other sliding surfaces have been used). Systems that combine elastomeric bearings and sliding bearings have also been proposed and implemented. Some systems of base isolation are given in earlier chapters and in Chap. 5.

6.13.3 Numerical Modelling of Equations of Motion with Isolators

As mentioned in the previous sections, the elements used for base isolation structures (high-damping rubber bearings, lead-rubber bearings, hysteretic and viscous dampers) behave in the non-linear range under horizontal forces. Therefore, the non-linear behaviour of these isolation systems themselves has to be included in the discrete mathematical model of an isolated structure. The dynamic equilibrium equations of an elastic system with non-linear isolators and energy-dissipating elements are given by the following expression:

$$M\ddot{U}(t) + C\dot{U}(t) + KU(t) + R_N(t) = R(t) \tag{6.70}$$

This is to be compared with the formulation in Chap. 5 for non-usage of isolators, where M, K and C are the mass matrix, the stiffness matrix and the damping matrix, respectively, for the whole elastic system. $R(t)$ is a time-varying load and $R(t)_N$ presents a vector of nodal forces in the non-linear isolators and the dissipating elements (dampers).

The more economical way of solving (6.70), through transformation of (6.70) into generalized modal coordinates, is as follows:

$$IX(t) + \Lambda X(t) = \Omega_X(t) = F(t) - F_N(t) \tag{6.71}$$

www.EngineeringBooksPDF.com

where

$$\phi^{\mathrm{T}} M\phi = I \tag{6.72}$$

$$\phi^{\mathrm{T}} K\phi = \mathrm{diag}[\omega^2] = \Omega^2 \tag{6.73}$$

$$F_N(t) = \phi^{\mathrm{T}} R(t)_N \tag{6.74}$$

where $F_N(t)$ versus $\Delta(t)$ can be related.

If C is assumed to be proportional damping, then $\Lambda = \varphi^T C\varphi = \mathrm{diag}[2\xi_i\omega_i]$, where ξ represents a modal damping ratio. The transformation matrix φ can represent either the eigen or the Ritz vectors for the whole model without the non-linear elements. Further direct integration of the system of equations can be done by means of the modal superposition method where only the first few vectors that participate in the total response of the system need to be included in the direct integration.

During the integration of (6.70) the loads in the non-linear elements are calculated at the end of each time step. The loads are then transformed into modal loads and are added on the right side of Eq. (6.70). Iteration is performed within each time step until the loads converge.

If linear isolators and viscous dampers are used to isolate the structure, matrix C will not be proportional to matrices $\boldsymbol{M}$ and $\boldsymbol{K}$ and will be given as follows:

$$C = C_{\mathrm{d}} + C = \mathrm{diag}[2\xi_i\omega_i] + C$$

By substituting matrix C, the system assumes the following form:

$$x_i + 2\xi_i\omega_i x + \omega^2 x_i = f_i - \sum_{i-1}^{m} C_{ij}X_j \qquad i = 1, 2, \ldots, m$$

6.13.4 Displacement and Rotation of Isolation Buildings

Plate 6.1 gives building displacement and rotation phenomena with isolation systems, with pads, rollers and the kinds; the phenomenon on soil–structure interaction is shown (Plate 6.1a,b,c).

Plate 6.1a Resilient-friction base isolation system. The resilient-friction base isolation (R-FBI) bearing attempts to overcome the problem of the high friction coefficient of Teflon on stainless steel at high velocities by using many sliding interfaces in a single bearing. Thus, the number of layers divides the velocity between the top and bottom of the bearing so that the velocity at each face is small, maintaining a low friction coefficient (Plate 6.1d). In addition to the sliding elements, there is a central core of rubber that carries no vertical load but provides a restoring force. This is shown in Plate 6.1d.

www.EngineeringBooksPDF.com

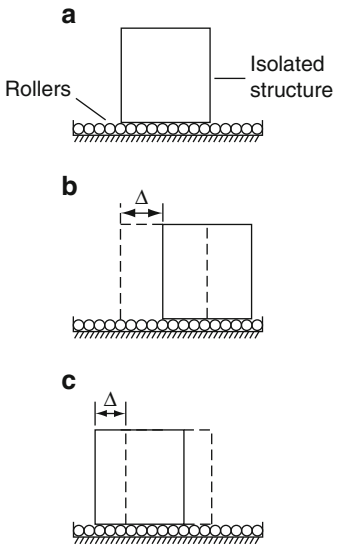


Plate 6.1a Concrete structure–displacement phenomena

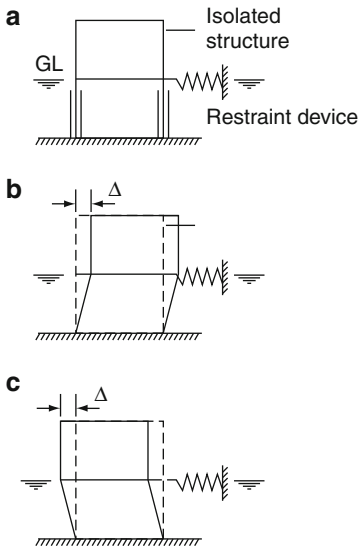


Plate 6.1b Displacement of isolated structures

www.EngineeringBooksPDF.com

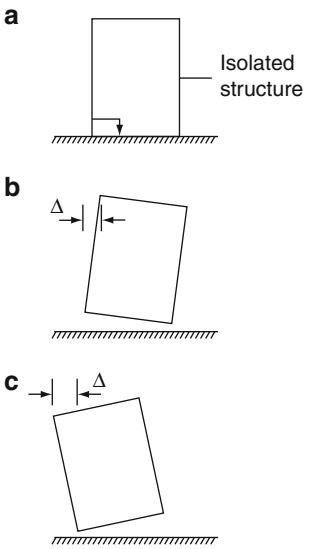


Plate 6.1c Displacement and rotation of concrete structures

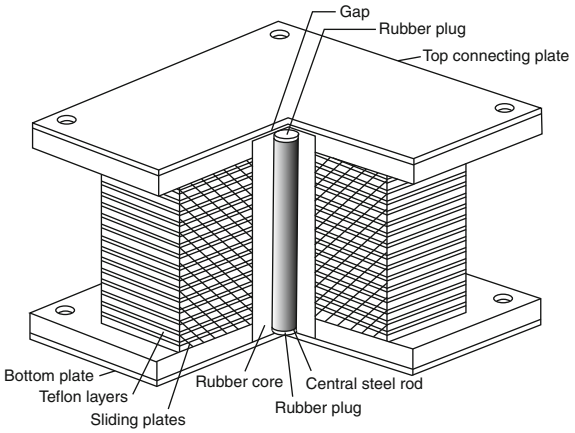


Plate 6.1d Isolators with low friction

6.13.4.1 Reactor Containment Building

The actual cross-section of the TVA prestressed concrete containment building is given in Figs. 6.8 and 6.9. The finite element model is given in Fig. 6.10 using soil-structure interaction concept described in this chapter using the kobe earthquake in Japan; the complete deformed containment building with cracks in concrete and complete failure of prestressing tendons is shown in Fig. 6.11. This is the damage model for the Kobe earthquake of frequency 8.5–9.5 Hz.

www.EngineeringBooksPDF.com

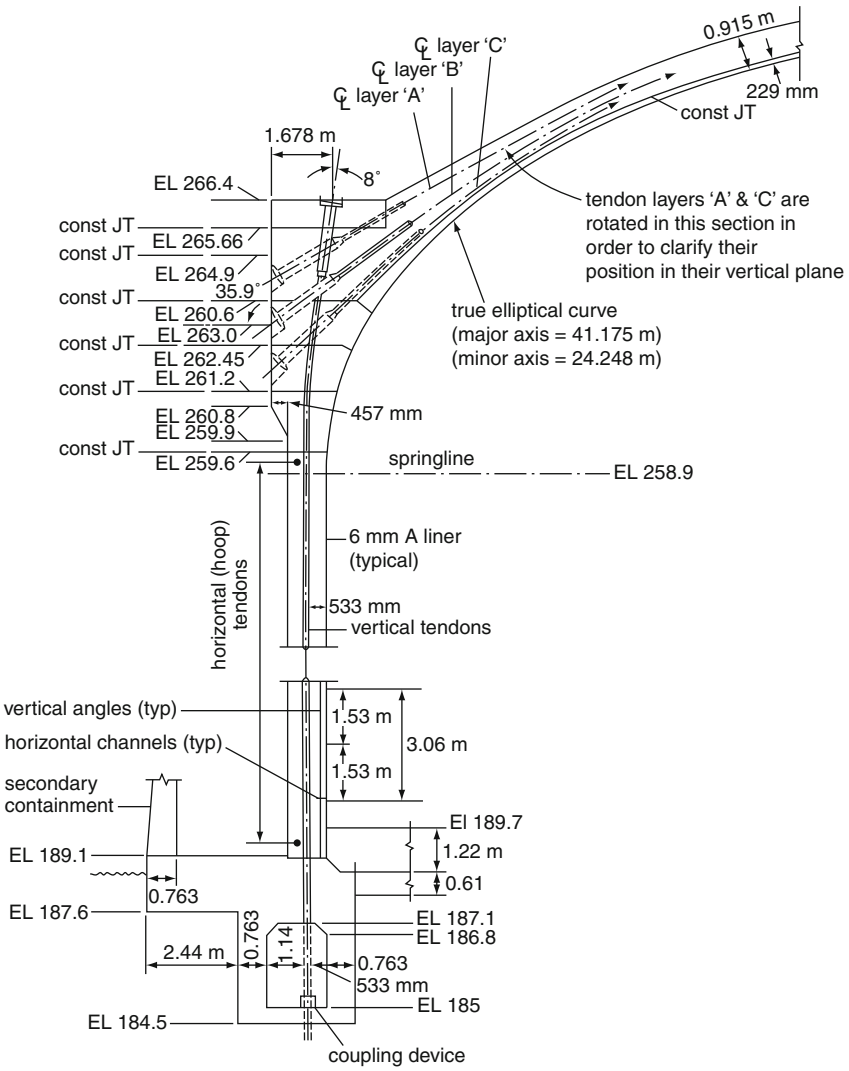


Fig. 6.8 Typical section – wall and dome (courtesy of TVA and Bellefonte NPS)

www.EngineeringBooksPDF.com

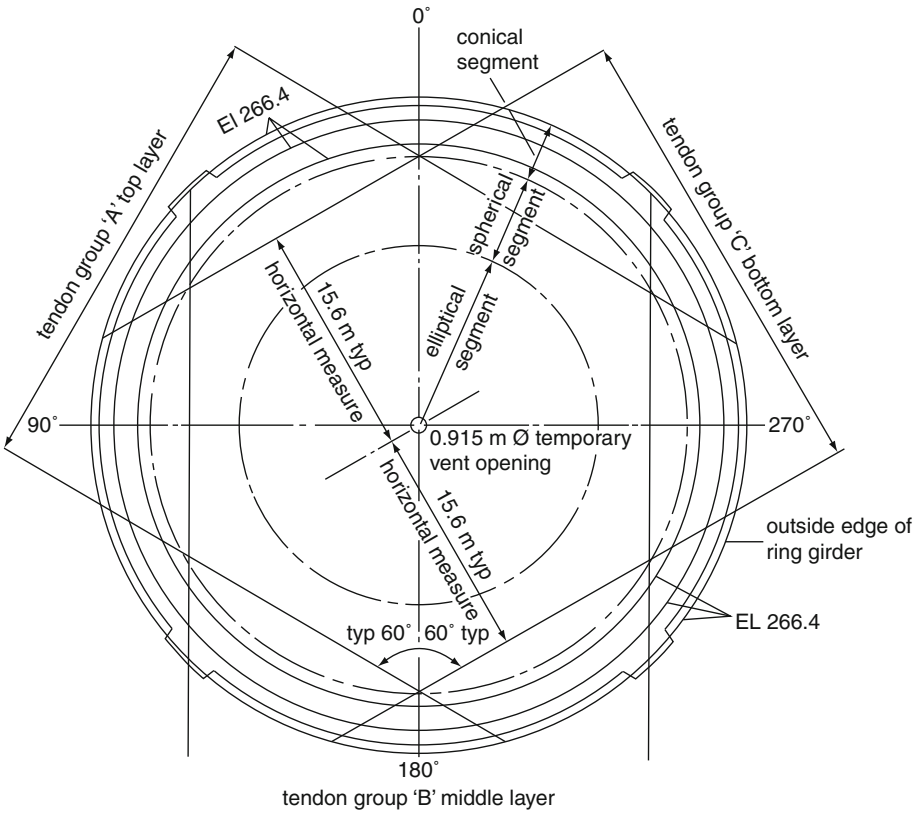


Fig. 6.9 Plan of the dome. (Note: The typical dome tendon spacing is 978 mm, measured horizontally. The final prestressing force for each tendon group is 5453.25 kN/m)

www.EngineeringBooksPDF.com

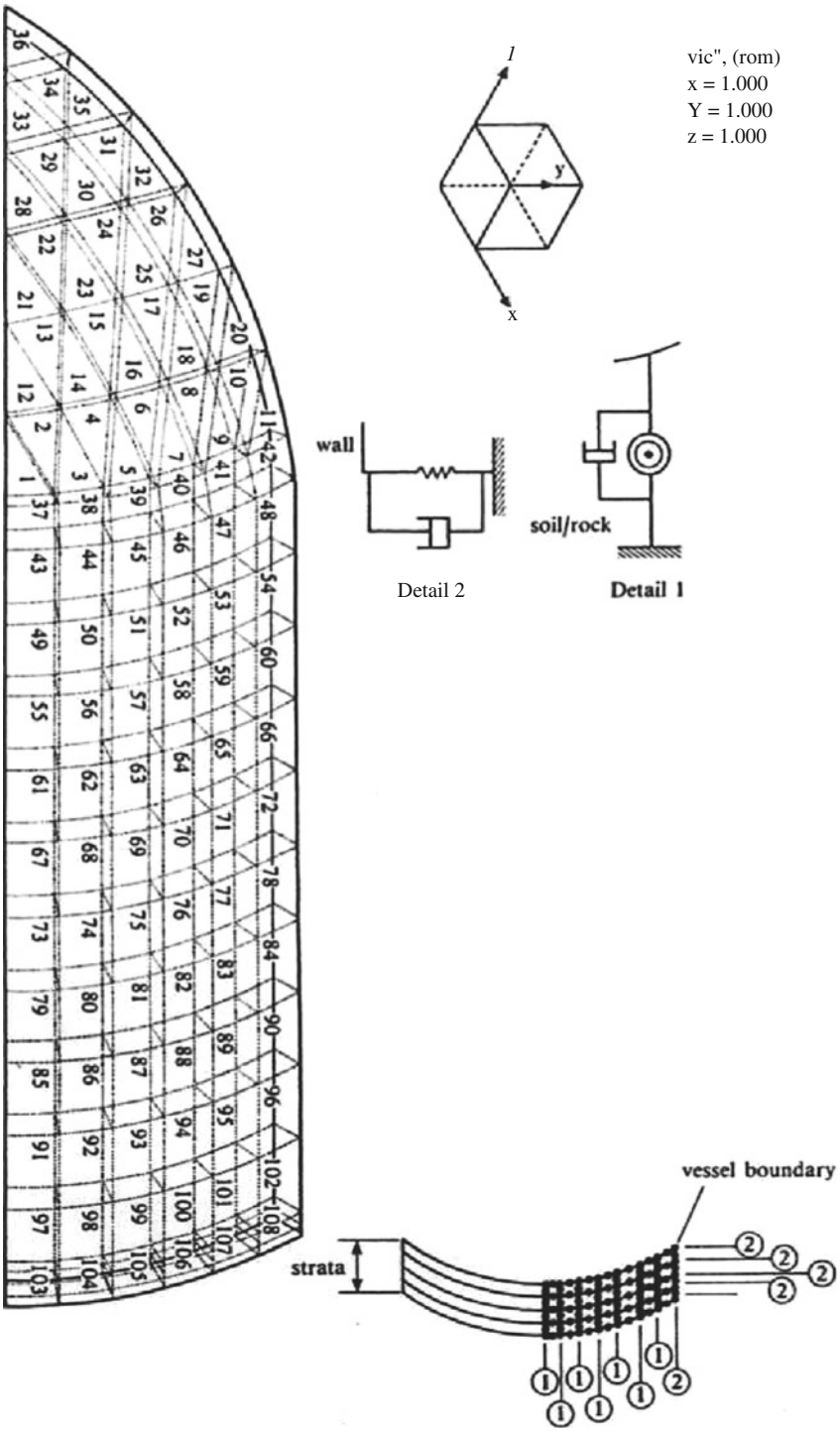


Fig. 6.10 *Non-linear model* - Bellefonte

www.EngineeringBooksPDF.com

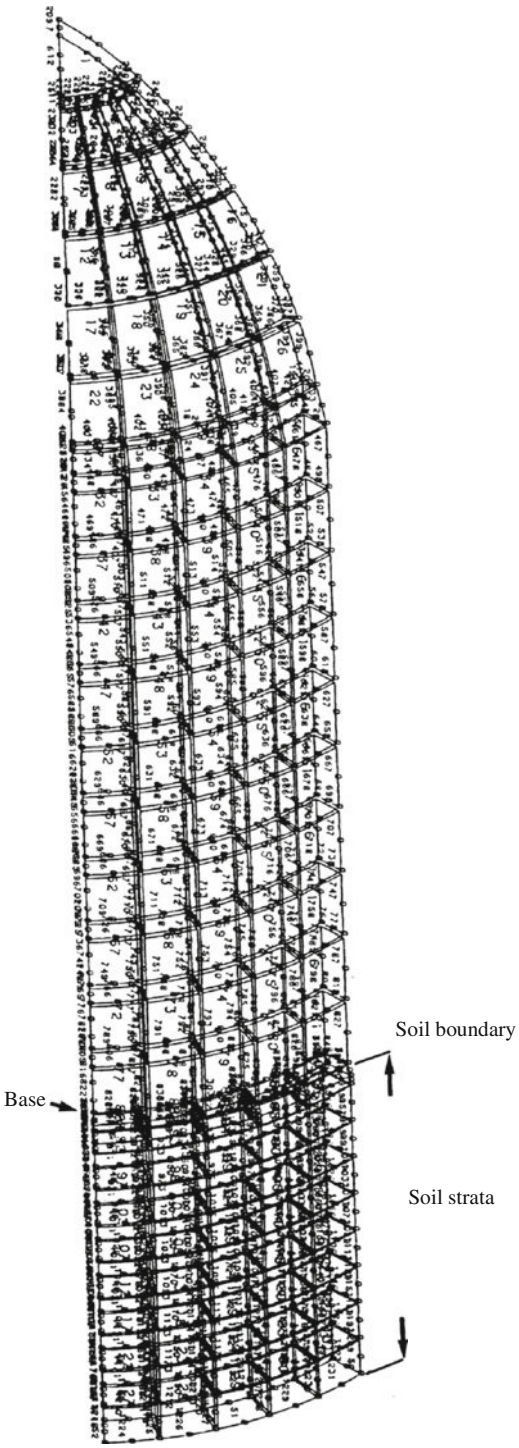


Fig. 6.11 Finite elements for the Bellefonte vessel

www.EngineeringBooksPDF.com

for containment vessels subjected to internal pressures up to 344.75 kN/m^2 along with dead, live and prestressing loads. The idealized strata in case of the Bellefonte vessel are given in Fig. 6.11 for the vessel parameters shown in Figs. 6.9 and 6.10.

(i) Missile loads (Y_m). In nuclear plant design, components and equipment should be protected against loss of function due to plant-generated and extreme environmental missile. Where a containment building is close to a major airport the damage caused by a otential missile such as an aircraft crash should be considered.

Bibliography

Akiyama, H. *Earthquake Resistant Limit-State Design for Buildings*. University of Tokyo Press, Tokyo, Japan, 1985.

Bendat, J. S. and Piersol, A. G. *Random Data: Analysis and Measurement Procedures*. John Wiley and Sons, Inc., New York, 1971.

Berg, G. V. and Thomaides, T. T. Energy consumption by structures in strong-motion earthquakes. *Proc. 2nd World Conf. Earthquake Eng*., Tokyo and Kyoto, 1960; pp. 681–696.

Blackman, R. and Tuckey, J. W. *The Measurement of Power Spectra from the Point of View of Communication Engineering*. Dover Publications, New York, 1959.

Caughey, T. K. and Stumpf, H. J. Transient response of a dynamic system under random excitation. *J. Appl. Mech*. 1961; 28:563–566.

Chaboche, L. J. Constitutive equation for cyclic plasticity and cyclic viscoplasticity. *Int. J. Plasticity* 1989; 5:247–301.

Clough, R. W. Analysis of structural vibrations and dynamic response. *Proc. 1st US-Japan Symp. Recent Adv. Matrix Meth. Struct. Anal. Design*, Tokyo (1969), University of Alabama Press, 1971.

Corotis, R. B. *Time-dependent power spectra and first passage probabilities*. MIT Civil Engineering Research Report R7D-78, Massachusetts Institute of Technology, Cambridge, MA, 1970.

Corotis, R. B., Vanmarcke, E. H., and Cornell, C. A. First passage of nonstationary random processes. *J. Eng. Mech. Div*.(ASCE) 1972; 98:401–414.

Craig, R. and Bampton, M. Coupling of structures for dynamic analysis. *AIAA J*. 1968; 6:1313–1319.

Fajfar, P. and Vidic, T. Consistent inelastic design spectra: hysteretic and input energy. *Earthquake Eng. Struct. Dyn*. 1994; 23:523–537.

Goel, S. C. and Berg, G. V. Inelastic earthquake response of tall steel frames. *J. Struct. Div*. (ASCE) 1968; 94:1907–1934.

Housner, G. W. Limit design of structures to resist earthquakes. *Proc. First World Conf. Earthquake Eng*., Berkeley, CA, 1956; Vol. 5, pp. 1–11.

Housner, G. W. Behavior of structures during earthquakes. *J. Eng. Mech. Div*.(*ASCE*) 1959; 85(4):109–129.

Housner, G. W. and Jennings, P. C. The capacity of extreme earthquake motions to damage structures. *Structural and Geotechnical Mechanics: A volume honoring NM Newmark* (Hall, W. J., ed.). Prentice-Hall, Englewood Cliff, NJ, 1975; pp. 102–116.

Japan Road Association. *Design Specification for Highway Bridges*, Part V (Seismic Design). Maruzen Press, Tokyo, 1998.

Kato, B. and Akiyama, H. Energy input and damages in structures subjected to severe earthquakes. *J. Struct. Const. Eng*.(AU) 1975; 235:9–18 (in Japanese).

Kausch, H. H. *Polymer Fracture* (2nd revised edn). Springer-Verlag, Berlin, 1987.

www.EngineeringBooksPDF.com

Kausel, E., Roesset, J. M., and Waas, G. Dynamic analysis of footings on layered media. *J. Eng. Mech. Div.* (ASCE) 1975; 101:679–693.

Kuwamura, H., Kirino, Y., and Akiyama, H. Prediction of earthquake energy input from smoothed Fourier amplitude spectrum. *Earthquake Eng. Struct. Dyn.* 1994; 23: 1125–1137.

Lee, T. H. and Wesley, D. A. Soil-structure interaction of nuclear reactor structures considering through-soil coupling between adjacent structures. *Nucl. Eng. Design* 1973; 24: 374–387.

Leger, P. and Dussault, S. Seismic-energy dissipation in MDOF structures. *J. Struct. Eng.* (ASCE) 1992; 118(5):1251–1269.

Lewangamage, C. S. *Measurement of strain field of continua by image analysis and its application to understanding behavior of rubber*. Master Thesis, The University of Tokyo, Japan, 2001.

Lewangamage, C. S., Abe, M., Fujino, Y., and Yoshida, J. Characteristics of rubber used in seismic isolation by digital and thermal image analysis. *Proc. 9th Int. Symp. Smart Struct. Mater.*, San Diego, USA, 2002; Vol. 9.

Luco, E., Hadjian, A. H., and Bos, H. D. The dynamic modeling of the half-plane by finite elements. *Nucl. Eng. Design* 1974; 31:184–194.

Luco, J. E. Torsional response of structures to obliquely incident seismic SH waves. *Int. J. Earthquake Eng. Struct. Dyn.* 1976; 4:207–219.

Lyon, R. H. *Statistical Energy Analysis of Dynamical Systems*. MIT Press, Cambridge, MA, 1975.

Lysmer, J. and Richart, F. E. Dynamic response of footings to vertical loading. *J. Soil Mech. Found. Div.* (ASCE) 1966; 92(SM1):65–91.

Mahin, S. A. and Lin, J. Construction of inelastic response spectrum for single-degree-of-freedom system. *Report No. UCB/EERC-83/17*, Earthquake Engineering Research Center, University of California, Berkeley, CA, 1983.

Mori, A., Carr, A. J., Cooke, N., and Moss, P. I. Compression behaviour of bridge bearings used for seismic isolation. *Eng. Struct.* 1996; 18(5):351–362.

Ogawa, K., Inoue, K., Nakashima, M. A study on earthquake input energy causing damages in structures. *J. Struct. Construct. Eng.* (AU) 2000; 530:177–184 (in Japanese).

Ohi, K., Takanashi, K., and Tanaka, H. A simple method to estimate the statistical parameters of energy input to structures during earthquakes. *J. Struct. Const. Eng.* (All) 1985; 347:47–55 (in Japanese).

Ordaz, M., Huerta, B., and Reinoso, E. Exact computation of input-energy spectra from Fourier amplitude spectra. *Earthquake Eng. Struct. Dyn.* 2003; 32:597–605.

Page, C. H. Instantaneous power spectra. *J. Appl. Phys.* 1952; 23(I):103–106.

Parmelee, R. A., Perelman, D. S., Lee, S. L., and Keer, L. M. Seismic response of structure-foundation systems. *J. Eng. Mech. Div.* (ASCE) 1968; 94:1295–1315.

Press, W. H., Flannery, B. P., Teukolsky, S. A., Vetterling, W. T. *Numerical Recipes in* C. Cambridge University Press, Cambridge, 1988.

Rejcba, C. Design of elastomer bearings. *PCI J.* 1964; 9:62–78.

Richardson, J. D. *Forced vibrations of rigid bodies on a semi-infinite elastic medium*. Ph.D. Dissertation, Nottingham University, England, 1969.

Richart, F. E., Woods, R. D., and Hall, J. R. *Vibration of Soils and Foundations*. Prentice-Hall, Englewood Cliffs, NJ, 1970.

Riddell, R. and Garcia, J. E. Hysteretic energy spectrum and damage control. *Earthquake Eng. Struct. Dyn.* 2001; 30:1791–1816.

Scanlan, R. H. Seismic wave effects on soil-structure interaction. *Int. J. Earthquake Eng. Struct. Dyn.* 1976; 4:379–388.

Scanlan, R. H. and Sachs, K. Earthquake time histories and response spectra. *J. Eng. Mech. Div.*(ASCE) 1974; 100:635–655.

Shinozuka, M. Maximum structural response to seismic excitations. *J. Eng. Mech. Div.* (ASCE) 1970; 96(EM5):729–738.

www.EngineeringBooksPDF.com

Stallybrass, M. P. A variational approach to a class of mixed boundary-value problems in the forced oscillations of an elastic medium. *Proc. 4th US Nat. Cong. Appl. Mech.* 1962; 391–400.
Takewaki, I. Optimal damper placement for minimum transfer functions. *Earthquake Eng. Struct. Dyn.* 1997; 26:1113–1124.
Takewaki, I. Probabilistic critical excitation for MDOF elastic-plastic structures on compliant ground. *Earthquake Eng. Struct. Dyn.* 2001a; 30:1345–1360.
Takewaki, I. A new method for non-stationary random critical excitation. *Earthquake Eng. Struct. Dyn.* 2001b; 30:519–535.
Takewaki, I. Critical excitation method for robust design: a review. *J. Struct. Eng.*(ASCE) 2002a; 128(5):665–672.
Takewaki, I. Robust building stiffness design for variable critical excitations. *J. Struct. Eng.* (ASCE) 2002b; 128(12):1565–1574.
Takizawa, H. Energy-response spectrum of earthquake ground motions. *Proc. 14th Nat. Disaster Sci. Symp.*, 1977; pp. 359–362, Hokkaido (in Japanese).
Tanabashi, R. Personal view on destructiveness of earthquake ground motions and building seismic resistance. *J Architect. Buil. Sci.* (AB) 1935; 48:599 (in Japanese).
Tanabashi, R. Studies on the nonlinear vibrations of structures subjected to destructive earthquakes. *Proc. First World Conf. Earthquake Eng.*, Berkeley, CA, 1956; Vol. 6, pp. 1–16.
Treloar, L. R. G. *The Physics of Rubber Elasticity* (3rd edn). Clarendon Press, Oxford, 1975.
Uang, C. M. and Bertero, V. V. Evaluation of seismic energy in structures. *Earthquake Eng. Struct. Dyn.* 1990; 19:77–90.
Uchida, K., Miyashita, T., and Nagata, S. *Earthquake response analysis of a nuclear power plant reactor building with a circular base mat*. Annual Report of the Kajima Institute of Construction Technology, 21, 98–99, first published in Japanese in June 1973.
Veletsos, A. S. and Ventura, C. E. O. Modal analysis of non-classically damped linear systems. *Earthquake Eng. Struct. Dyn.* 1986; 14:217–243.
Veletsos, A. S. and Wei, Y. T. Lateral and rocking vibration of footings. *J. Soil Mech. Found. Div.* (ASCE) 1971; 97:1227–1248.
Yamashita, Y., Kawabata, S. Strain energy density approximation formula for carbon-filled rubber. *Jpn. Rubber Assoc.* 1992; 65:517–527 (in Japanese).
Zahrah, T. F. and Hall, W. J. Earthquake energy absorption in SDOF structures. *J. Struct. Eng.*(ASCE) 1984; 110(8):1757–1772.

www.EngineeringBooksPDF.com

www.EngineeringBooksPDF.com

Chapter 7
Response of Controlled Buildings – Case Studies

7.1 Introduction

This chapter deals with a number of buildings constructed with different materials, vertical and plain dimensions and variable floor areas. The height of a building is measured to its eaves level. The classification of building structure can be identified as made up of reinforced concrete with or without prestressing elements, structural steel, steel–concrete composite and many others in combination. The building can be built as three-dimensional moment frame with shear walls with individual spread footings or mat systems and RC/steel pile foundation. The building cited on site may have a different foundation or ground properties. Where ground properties are unknown, the analysis for soil structure interaction is based on Chap. 6 and Chap. 7, as per details given in Table 7.1. Various devices for the buildings have been described in this text and they have been used to make the building as controlled structures. For checking various buildings irrespective of how tall they are, the devices such as isolators, dampers contribute to control acceleration, displacement, velocity and the total drift. A comparative study is made between the designer's results and results produced by the author. In many areas the collaboration is excellent between the results given by the original designers and those evaluated by the author using three different computer packages, namely, programs ISOPAR, ETAB and SAP2000. Some results are presented in graphical form and some are compared in tabulated form as a comparative study of individual test cases for various constructed facilities. Seismic waveforms such as El-Centro NS and Taft EW have been adopted for cases where the information was not available. In some cases the waveform for Kobe earthquake has been used to evaluate various parameters. The reader has a choice to adopt any specific waveform for building in seismic area where information cannot, for some reason, be obtained.

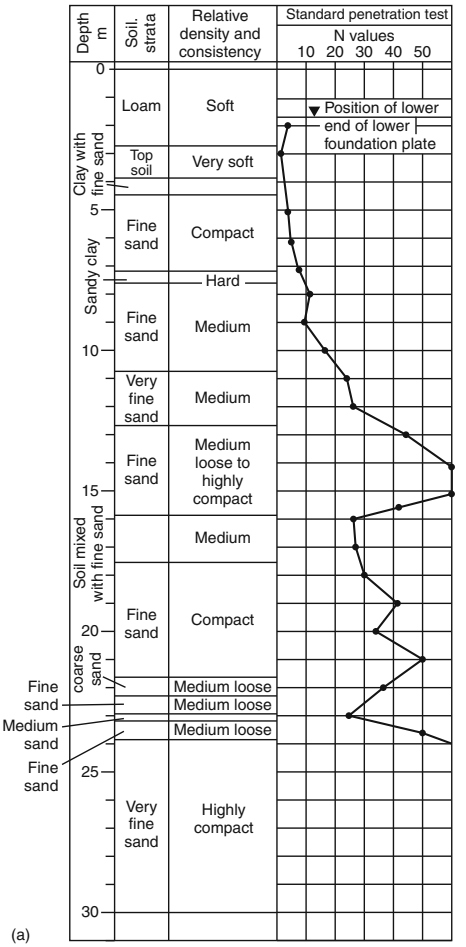
The author has analysed quite a few buildings of constructed facilities as controlled structures and related their displacement, velocities and acceleration to the height and total floor areas. The obvious problems are the intricate layouts of buildings and the relevant positioning of devices and

M.Y.H. Bangash, *Earthquake Resistant Buildings*,
DOI 10.1007/978-3-540-93818-7_7, © M.Y.H. Bangash 2011

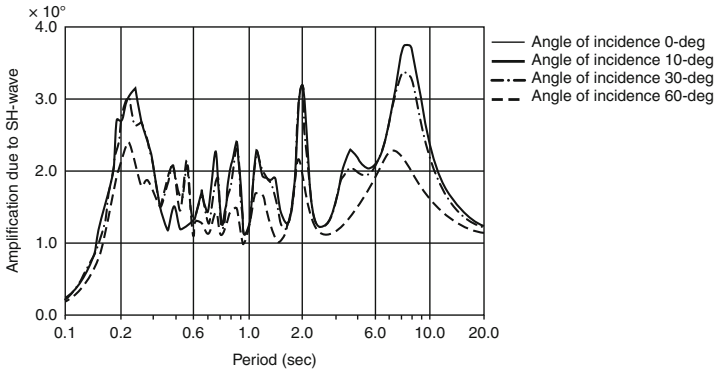
www.EngineeringBooksPDF.com

Table 7.1 Foundation properties

Foundation strata



(a)



(b) Analytical value of ground periodic properties and amplification properties due to multiple reflections of SH waves

Data provided by Moto Institute, Tokyo(1988)
Note: For all analyses and design, the above is assumed. Where foundation soils do vary, the test results, if different, must be obtained for a site

www.EngineeringBooksPDF.com

their quantities. What the author has done is to reanalyse the existing constructed facilities with and without devices. Displacement, velocities, acceleration and storey drift were examined. If they are excessive without devices based on codified methods and practical limitations imposed, a simple numerical relation will give the number of devices needed to control the building. A random permutation and combination approach has been adopted. This random method of algebra would decide and confirm the initial numberof devices needed to make the building stand up to specific seismic waveform, with reduced displacements and accelerations of floors and foundation levels. The reduction of storey drift will then confirm the analysis to an acceptable level. It is envisaged that calculated initial numbers of devices may be lightly more or less depending upon the geometric locations available in the overall layout. The author has noted that in such circumstances, the final prepared controlled structure has to be reanalysed using specific analysis. In many cases, the author has used dynamic nonlinear time integration approach to reanalyse the building structure. The reanalysis will confirm whether or not its results will comply with the code limitations. At the reanalysis stage, the number of constructed facilities was checked again for displacement, velocity and acceleration and storey drift with known seismic devices at each floor level where such devices could also easily be accommodated. The net results are within 10% accuracy when author's results were compared with those of the designers of the existing facilities. The results are summarized for each building of constructed facility in the form of data, tables and graphs.

7.2 Building With Controlled Devices

Examples of response-controlled structures found in various countries are known. The Japanese ones are first in parts (A) and (B) and Table 7.1 and part (C) to (H). The listing is just few types known to the author;

(A)
1. Buildings with laminated rubber support
2. Buildings with sliding supports
3. Buildings with sway-type hinged columns
4. Buildings with double columns
5. Buildings with dampers (viscoelastic, friction)
6. Buildings with dynamic dampers
7. Buildings with sloshing-type dampers

www.EngineeringBooksPDF.com

(B) Building (Data provided by various companies)	Type
1. Yachiyodai Unitika Menshin	Laminated rubber
2. Okumura Group, Namba Research Center, office wing	Laminated rubber
3. Obayashi Group, Technical Research Center, 61 Laboratory	Laminated rubber
4. Oires Industries, Fujizawa plant, TC Wing	Laminated rubber
5. Takenaka Komuten Funabashi Laminated Taketomo Dormitory	Laminated rubber
6. Kajima Constructions, Technical Research Center Nishi Chofu Acoustic Laboratory	Laminated rubber
7. Christian Data Bank	Laminated rubber
8. Tohoku University, Menshin Building	Laminated rubber
9. Fujita Industries, Technical Research Laboratory, 6th Laboratory	Laminated rubber
10. Shibuya Shimizu No. 1 Building	Laminated rubber
11. Fukumiya Apartments	Laminated rubber
12. Shimizu Construction, Suchiura Branch	Laminated rubber
13. Toranomon San-Chome Building	Laminated rubber
14. Department of Science and Technology, Inorganic Material Laboratory, Vibration –free Wing	Laminated rubber
15. A Certain Radar	Sliding support
16. Taisei Construction Technical Research Center, J Wing	Sliding support
17. Chamber of Commerce and Culture	Friction damper
18. Chib Port Tower	Dynamic damper
19. Toyana Park Observatory	Dynamic damper
20. Gold Tower	Sloshing damper
21. Yokohama Marine Tower	Sloshing damper

A typical two-storey building in Japan with devices located (Plate 7.1) will be tested against the random method of algebra approach.

(C) Buildings with laminated rubber support (menshin structure)
Structures using laminated rubber support in their foundations are the most popular type of response-controlled structures found within and outside Japan. It is common to use laminated rubber along with other types of dampers. Laminated rubber is used to extend the fundamental period of a building in the horizontal direction so that the seismic input is reduced while the dampers absorb the incident seismic energy. Sometimes, laminated rubber is also used to reduce the vertical microseisms.

www.EngineeringBooksPDF.com

Regarding building size, buildings in the USA are constructed mostly of steel while in Japan one finds RCC structure with four to five stories. There is also one example of a 14-storied RCC structure.

(D) Buildings with sliding support
Sliding-support structures are generally used for computer room floors. Examples using sliding supports for the entire building are very few and only recent. This type of structure is not able to return to its original position. When using sliding supports the position of a building after an earthquake will be different from the one before the earthquake.

(E) Buildings with double columns
Columns of low stiffness are provided in the foundation of a building. The basic considerations are the same as those for the laminated rubber support. There are few examples of this technique, one in New Zealand and one in Japan (Tokyo Science University).

(F) Buildings with dampers (viscoelastic, friction)
Various types of dampers are installed in a multistoried structure, thus absorbing the incident seismic energy. In the USA, buildings using viscoelastic dampers (VEM) have been in use for some time to reduce the response to strong winds. In Japan, steel dampers and friction dampers are used in multistoried buildings.

(G) Buildings with dynamic dampers
Dynamic dampers convert the vibration energy of an earthquake or wind into kinetic energy allowing the dynamic damper to absorb the input energy. It is used to reduce the vibrations of machinery. In the USA this technique is mainly used to reduce the deformation of a building due to wind, while in Japan, it is used to absorb the wind as well as earthquake energy. In Japan, this technique is used for tower-type structures of lesser mass.

(H) Buildings with sloshing-Type dampers
The incident vibration energy is absorbed as the kinetic energy of water (or fluid) using the phenomenon of sloshing of liquids. In Japan, this technique is mainly used for tower-type structures to reduce building deformation due to wind or earthquake.

7.2.1 Special Symbols with Controlled Devices

Plate No. 7.1 briefly gives the symbols adopted for some devices.

www.EngineeringBooksPDF.com

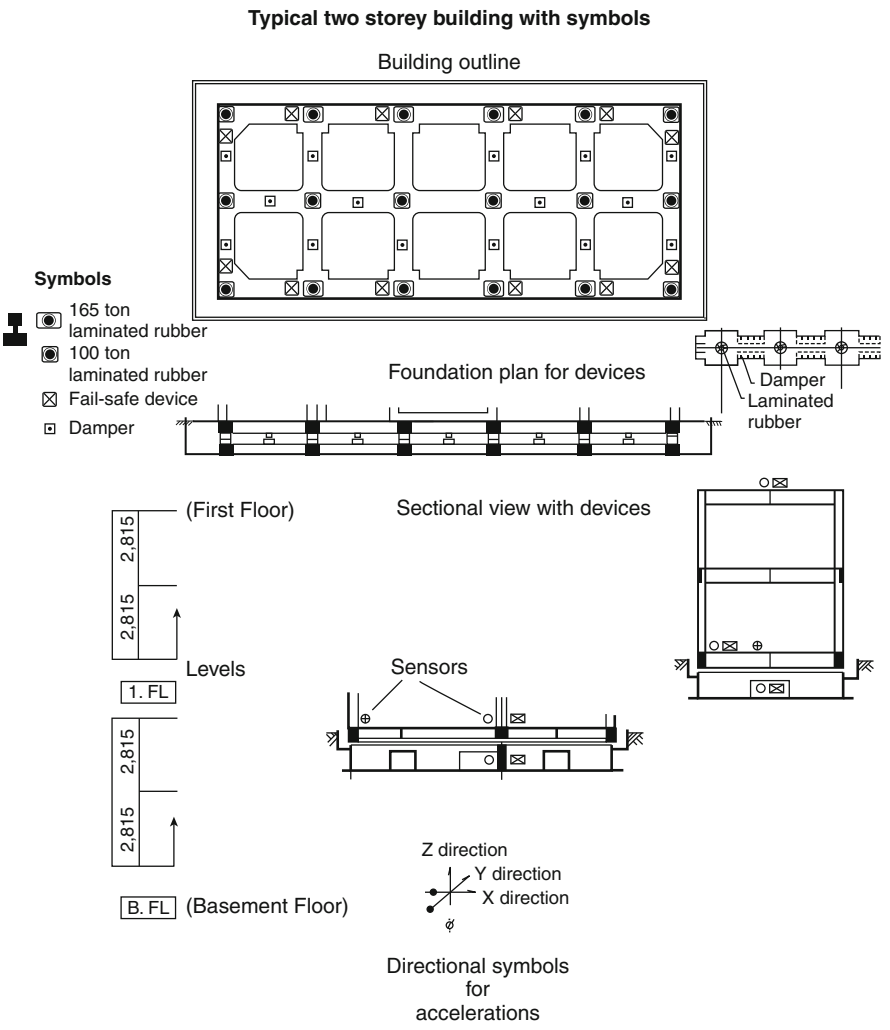


Plate 7.1 Typical two-storey building with symbols

7.2.2 Seismic Waveforms and Spectra

Table 7.2 briefly gives typical data on a waveform, i.e. Japan-A Similar data can exist for other seismic waveforms. In this chapter El-Centro NS and Taft EW waveforms have been commonly used for exercises. A similar method can be adopted for other wave forms.

www.EngineeringBooksPDF.com

Table 7.2 Earthquakes for which seismic waveforms and spectra have been adopted in Japan.

No.	Date and time of the earthquake	Epicentre	Hypocentre Lat.	Long.	km	Magnitude
1.	4, Oct. 1985, 21:25	Southern Ibaraki prefecture	140∠09.5′	35∠52.1′	78	6.1
2.	4, Jul. 1986, 08:29	Eastern Saitama prefecture	139∠26.9′	35∠52.1′	149	4.8
3.	20, Sept. 1986, 12:04	Northern Ibaraki prefecture	140∠39.6′	36∠28.4′	56	5
4.	9, Jan. 1987, 22.16	Central Iwate prefecture	141∠47′	39∠51′	71	6.9
5.	6, Feb. 1987, 22:16	Off Fukushima prefecture	141∠54′	36∠59′	31	6.7
6.	22, Feb. 1987, 5:39	Border of Saitama and Ibaraki prefecture	139∠47′	36∠03′	85	4.4
7.	7, Apr. 1987, 09:40	Off Fukushima prefecture	141∠54′	37∠17′	37	6.6
8.	10, Apr. 1987, 19:59	South Ibaraki prefecture	139∠52	36∠08′	57	5.1
9.	17, Apr. 1987, 16:33	Northern Chiba prefecture	140∠08′	35∠46′	75	5.1
10.	23, Apr. 1987, 0.5:13	Off Fukushima prefecture	141∠37′	37∠04′	49	6.5
11.	30, Jun. 1987, 18:17	Southwest Ibaraki prefecture	140∠06′	36∠12′	55	5.1
12.	17, Dec. 1987, 11:08	Off eastern Chiba prefecture	140∠29′	35∠21′	58	6.7
13.	18, Feb. 1988, 14:43	Off Eastern Chiba prefecture	140∠11′	4∠51′	75	5.0
14.	18, Feb. 1988, 17:10	Eastern Kanagawa refecture	139∠31′	35∠30′	44	3.5
15.	18, Mar. 1988, 05:34	Eastern Tokyo	139∠39	35∠40′	99	6.0

Note: Building No. 1 – Yachiyodai Unitika Apartments; 2 – Kajima Constructions, Technical Research Center, Environmental and Vibration Laboratory; 3 – Takenaka Technical Research Center, Large prototype; 4 – Okumura Group, Tsukuba Research Center, Administrative Wing; 5 – Obayashi Group, Technical Research Center, 61st Test Wing; 6 – Oires Technical Center; 7 – Takenaka Komuten, Funabashi Taketomo Dormitory; 8 – Tohoku University Building; 9 – Chiba Port Tower; 10 – Mongumi test structure.
Note: Information collected and placed in order. With compliments from above sources 1–15.

www.EngineeringBooksPDF.com

7.2.3 Maximum Acceleration and Magnification

Again eight buildings were chosen by the Japanese companies to evaluate and compare the maximum acceleration and magnification at various floor levels of these buildings from basement level to the roof level. These figures are given in Table 7.3.

7.2.4 Three-Dimensional Simulation of the Seismic Wave Field

In regions such as Japan, there is a strong interaction between the details of the seismic force and the three-dimensional building structure, particularly with the presence of subduction zones. Wherever possible modelling of the wave field in three dimensions can then provide a useful means of simulating the likely effect of major earthquakes. Subduction along the Nankai trough is responsible for very large earthquakes, such as a magnitude 8.0 event. In the three-dimensional analysis using non-linear time integration approach, a hybrid pseudo-spectral/finite element approach is used for the region. Assume the region is 820 × 410 km in horizontal dimensions and 125 km in depth. The mesh of optimum nature is 512 × 256 × 160 points with a horizontal mesh increment of 1.6 km and a vertical increment of 0.8 km can be adopted. The minimum S-wave velocity for the superficial layer in the three-dimensional mould is 3 km/s. The P-wave front is an outer rampart to the larger 'S' disturbance. A reference is made to Table 7.1 for layer positioning

In some cases accurate wave fields have been correctly evaluated. The numerical values of accelerations for case studies have been stated. In the 55-storey building, the seismic wave field mesh scheme interacts with suitable finite element gap between the building and the foundation strata.

7.3 Evaluation of Control Devices and the Response-Control Technique

7.3.1 Initial Statistical Investigation of Response-Controlled Buildings

The response-control technique restricts or controls the response of buildings to external vibrations. The responses to be restricted or controlled are acceleration, velocity and displacement. It is possible to control or restrict the stresses developed in structural material by controlling the above responses.

The extent of restriction or control of response of buildings to external forces using response-control techniques can be set at any level, unlike in earlier wind- and earthquake-resistant structural methods. As a result, the response-control

www.EngineeringBooksPDF.com

Table 7.3 Maximum acceleration and magnification

	Yachiyodal Unitika Menshin Apartments *	Kajima Acoustic Laboratory Building *	Okumura Group Research Laboratory Building *	Obayashi Group Laboratory *	Oires Industries Technical Center *	Takenaka Komuten, Funabashi Taketomo Dormitory *	Chiba Port Tower *	Mongumi Menshin Type test Structure *
RF	34.7	42.9	45.7	11.6	29.0	23.1	414	16.3
	(44.7)	(54.4)	(66.5)	(10.9)	(45.0)	(23.3)	(410)	(15.8)
IF		48.9	10.4	26.0	27.0	171	15.5	
		(63.4)	(10.6)	(43.0)	(22.4)	(148)	(15.3)	
BA	131.3	34.7	40.8	20.4	29.0	64.4		20.6
	(123.3)	(42.4)	(50.3)	(21.5)	(62.0)	(86.4)		(31.3)
GI			54.6	39.0	54.0			
			(82.6)	(43.8)	(72.0)			
RF	0.26	1.23	1.12	0.57	1.0	1.36		0.79
	(0.36)	(1.28)	(1.32)	(0.51)	(0.73)	(0.27)		(0.50)
BA			0.74	0.52	0.54			
			(0.61)	(0.49)	(0.86)			

Upper row NS (Y); Lower row EW (X), Max. Acc: gal

*Note: Information from The data collected each building has been normalised in the above Table. The author received with compliments.

www.EngineeringBooksPDF.com

technique is most effective in solving the technical problems encountered during design, which are mentioned below:

1. Ensuring safety of structures under emergency conditions
2. Reduction in the cross-sectional area of structural materials
3. Preventing vibrations, sliding or rolling of household appliances
4. Preventing damage or peeling of non-structural materials
5. Restricting irregular vibrations
6. Maintaining nonerratic performance of machines and gadgets

Plate 7.1 gives the classification of structural control devices and, evaluation items for isolators and dampers.

The emphasis is to gather together existing guided examples and case studies of constructed facilities. Statistical curves are then needed for various parameters in order to facilitate the number of devices needed in the building. Tables 7.1, 7.2, 7.3, 7.4, 7.5, and 7.6 give examples of response-controlled structures in Japan and other countries. The data given therein would go some way to assist statistical charts needed for the quick evaluation of the numbers and other related parameters of seismic devices. In the preparation of such charts, where information could not be obtained, the author has adopted other constructed facilities in which randomly placed devices such as isolators and dampers were analysed using linear and non-linear analyses mentioned in this text. The data were transferred to match up with existing constructed facilities, thus filling the gaps existing in the information. The buildings were built in concrete, steel composite and timber. Graphs 7.1 to 7.6 are the outcome of such statistical and numerical analyses and are intended to be used for

Table 7.4 Permutations and Combinations of Devices

A or B or C

When we get to the next picture we have only two to choose from:

B C or A C A B

Finally, for the last picture there is no choice – it is the one that remains. So get the six permutations

A B C	B A C	C A B
A C B	B C A	C B A

www.EngineeringBooksPDF.com

Table 7.5 Guided examples of response-controlled structures in Japan and other countries

No.	Name of building	Location	No. of floors	Built-up area, m^2	Structure	Application	Year of construction	Remarks	Controlling devices
1	M.I.E. building					Computer room floor		Ball bearing support	35*
2.	Dynamic floor					Computer room floor		Teflon sheets	30
3.	Fudochokin Bank (now Kyowa Bank)	Himeji	+3,−1	791	RCC	Bank branch	1934	Sway-type hinge column	40*
		Shimonoseki	+3	641	RCC	Bank branch	1934		
4.	Tokyo Science University	Tokyo	+17, −1	14,436	Steel	School	1981	Double columns	15
5.	Union House	Auckland, New Zealand	+12, −1		RCC	Office	1984	Double columns	–
6.	Pestalochi Elementary School	Skopje, Yugoslavia	+3		RCC	School	1969	Rubber	200*
7.	Foothill Law and Justice Center	California, USA	+4, −1		Steel	Court	1986	Laminated rubber	150*
8.	W. Clayton Building	Wellington, New Zealand	+4		RCC	Office	1983	Laminated rubber	150*
9.	Cruas Atomic Power Plant	France			RCC	Atomic furnace	1984	Laminated rubber	–
10.	Kousberg Atomic Power Plant	South Africa			RCC	Atomic furnace	1983	Laminated rubber	–
11.	Hachiyodai Apartments	Chiba, Japan	+2	144	RCC	Housing	1983	Laminated rubber	–
12.	Okumura group, Namba Research Center; Office wing	Tochigi, Japan	+4	1,330	RCC	Research Centre	1986	Laminated rubber	–

Data collected from the British Library, London (1991)

www.EngineeringBooksPDF.com

Table 7.5 (continued)

No.	Name of building	Location	No. of floors	Built-up area, m^2	Structure	Application	Year of construction	Remarks	Controlling devices
13.	Tohoku University, Shimazu Construction Laboratory	Miyagi, Japan	+3	200	RCC	Observatory	1986	Laminated rubber, viscous response control	113*
14.	Obayashi group Technical Research Center, 61st Laboratory	Tokyo	+5, –1	1,624	RCC	Laboratory	1986	Laminated rubber	–
15.	Oires Industries Fujizawa Plant, TC wing	Kanagawa, Japan	+5	4,765	RCC	Laboratory	1986	Laminated rubber	–
16.	Funabashi Taketomo Dormitory	Chiba, Japan	+3	1,530	RCC	Dormitory	1987	Laminated rubber	–
17.	Kashima Construction Research Laboratory, West Chofu, Acoustic Laboratory	Tokyo	+2	655	RCC	Research laboratory	1986	Laminated rubber	–
18.	Christian Data Bank	Kanagawa Japan	+2	293	RCC	Data centre		Laminated rubber	120*
19.	Chiba Port Tower	Chiba, Japan	125 m	2,308	Steel	Tower	1986	Dynamic response control	–
20.	Sydney Tower	Australia	325 m		Steel	Tower	1975	Dynamic response control	–
21.	Citicorp Center	New York, USA	+59		Steel	Office	1977	Tuned mass response control	15*
22.	Hitachi Headquaters	Tokoyo	+20, –3	57,487	Steel	Office	1983	Steel response control	10*

www.EngineeringBooksPDF.com

Table 7.5 (continued)

23.	World Trade Center	New York, USA	+110		Steel	Office	1976	VEM damper (viscous elastic mass)	35*
24.	Columbia Center	Seattle, USA	+76		Steel	Office	1985	VEM damper (viscous elastic mass)	
25.	Radar Construction	Chiba, Japan			Steel	Instrument platform	1980	Roller bearing	35
26.	Christchurch chimney	Christchurch, New Zealand	35 m		RCC	Chimney		Steel response control	60*
27.	Commerce, Cultural	Saitama, Japan	+30		Steel	Office	1987	Friction response control	38
28.	Fujita Industries Technical Research Laboratory (6th)	Kanagawa, Japan	+3	3,952	RCC	Research center		Laminated rubber	80*
29.	Shibuya Shimizu No. 1 Building	Tokoyo	+5, −1	3,385	RCC	Office		Laminated rubber	80*
30.	Fukumiya Apartments	Tokoyo	+4	682	RCC	Cooperative housing		Laminated rubber	–
31.	Lambeso C.E.S	France	+3	4,590	RC prefab	School	1978	Laminated rubber	–

Note: + Indicates floors above ground and – indicates floors below ground.

* Compared and tested on the basis of dynamic non-linear three-dimensional finite element Analysis.

Note: Data collected from sources

Note: Data collected from cases 1 to 12 from locations given in the Table and place them in given order. With compliments from organisations mentioned in items No. 1 to 31. The author acknowledges the data with thanks.

www.EngineeringBooksPDF.com

Table 7.6 Case studies of earthquake constructed facilities

Item	Hachiya apartments ‡	Christian data center Ø ‡	Okumura group Ø Ø
Designed by	Tokyo Building Research Center	Tokyo Building Research Center, Unitika	Tokyo Building Research Center, Okumura group
Year of approval; No. 455	2 November 1982; Kana 61	19 November 1985; Tochi 37	24 December 1985;
No. of floors	+2	+2, −1	+4
Built-up area, m^2	60.18	226.21	348.18
Application	Housing (residential)	Data house	Research centre
Structure	RCC frame (shear wall)	RCC frame (shear wall)	RCC frame
Foundation	Raft foundation with cast in situ piles	Deep foundation	RCC cast in situ raft
Isolator: Dimensions, mm	82 × 300 dia	Rubber 5 thick × 300 dia (12 layers)	Rubber 7 thick thick × 500 dia (14 layers)
Numbers	(6) (computed 7)	(32) (28)	(25) (21)
Supporting force	$\sigma =$ 45 kg/cm^2, 0.5 t/cm (32 t)	$\sigma =$ 60 kg/cm^2, 0.5 t/cm (42.5 t)	$\sigma =$ 60 kg/cm^2, 0.86 t/cm (120 t)
Response-control device	Friction force between PC plates	Uses plastic defomation of steel bars bent to make a loop (8 nos)	Uses plastic deformation of steel bars bent to make a loop (12 nos)
Shear force coefficient used in design	0.2	0.15	0.15
Fundament period Small deformation	1.83 cm	1.4 cm	1.4 cm
Large deformation		1.9 cm	2.1 cm
Incident seismic wave	El-Centro 1940 (NS) Hachinohe 1968 (NS) Hachinohe 1986 (EW) Taft 1952 (EW)	El-Centro 1940 (NS) Hachinohe 1968 (NS) Taft 1952 (EW)	El-Centro 1940 (NS) Taft 1952 (EW) Hachinohe 1968 (NS)
Input level	300 gal	300 gal, 450 gal	300 gal, 450 gal

Note: (*) computed and tested on the basis of dynamic non-linear three-dimensional analysis using finite element.
(Ø) Actually provided.
Note: Data collected from the archives British Library for Huchiya apartments (‡), christian data center [Ø‡] and okumura group [Ø Ø], with compliments.

www.EngineeringBooksPDF.com

evaluating the initial number of devices, displacements, velocities and accelerations for various heights and floor areas of the buildings. This procedure has cut down the time and effort of making decisions regarding devices and building final displacement, velocity and acceleration. The exact analysis for a particular building will be carried out both with and without such devices. The extent of control within specified limitations will be known. The limitations on the following will be adhered to:

(a) Response acceleration
(b) Response relative displacement (using linear, non-linear and damage analyses)
(c) Response material stress
(d) Physical positioning of devices in a specific layout in three dimensions

The variables concerning (d) shall require the knowledge of total building floor area, standard area per floor, floor height and final building height. Once the total number of devices **"S"** is known from the graph, the next step is to initially spread these devices across the building structure when the above requirements are met. Various methods are available and their boundary conditions must be such that the requisite number must easily be accommodated after the analytical decisions are made. In this text the selected method is based on permutation and/or combination. The permutation is for single-type device and combination is for two or more types of devices placed in sequence or in others to reduce drift, acceleration and velocity commensurate with the codified methods and clauses noted in design practices. This method cuts down the time and cost involved in arriving at the optimum choice finally placed before a specific computer program to assess and meet the targets given by designers and clients. It is therefore necessary to remind the reader about the method.

7.3.2 Permutations and Combinations

7.3.2.1 Permutations

A permutation for the devices of identical shape, make and performance shall be the "rearrangement number" or "order" in specific area of a floor from an ordered list **"S"** required for a building within specific seismic zone. The rearrangement of devices in permutation will finally determine the optimum positions, when put to a specific analysis-cum-computer program, such that the targets are met.

For example, the number of permutations for devices {1, 2}, namely {1, 2} and {2,1}, shall be $2! = 2 \times 1 = 2 \leftarrow$ two places two permutations in two positions; $3! = 3 \times 2 \times 1 = 6 \leftarrow$ three places and six permutations in three positions for the devices to be placed at the floor level. In order to further explain, the 3! would be in the following six set-up and in six orders as

www.EngineeringBooksPDF.com

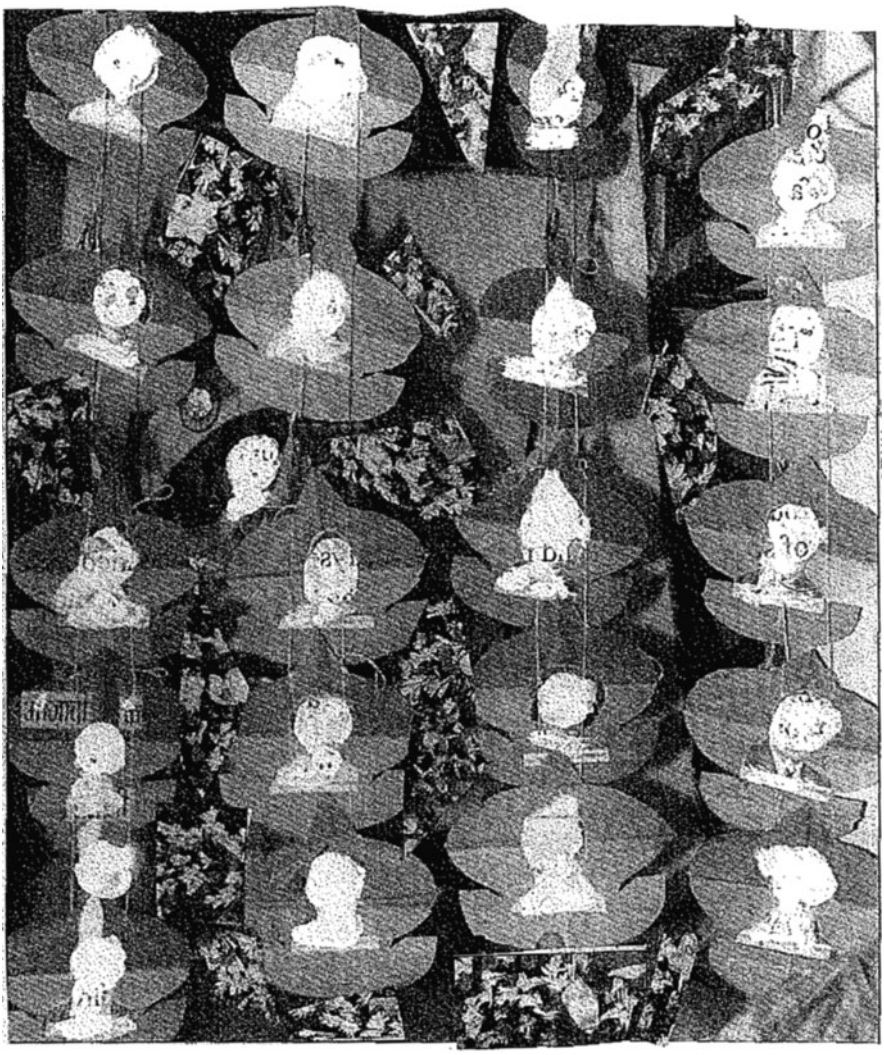


Plate 7.2 Random Distribution of Seismic Devices in Buildings

$$\{1,2,3\},\{1,3,2\},\{2,1,3\},\{2,3,1\},\{3,1,2\} \text{ and } \{3,2,1\}$$

The positioning of the devices shall be arranged in this order, provided the space allocated in a floor or in between the floors lately thoroughly analysed by the **algorithm** is sufficient. The examples and graphs can initially test the arrangements. Assuming this order is finally adopted, the results can be assessed and the order can reduce the response for specific earthquake-

www.EngineeringBooksPDF.com

induced input. The same concept is taken further for a greater permutation n! If the quantities are large, they can be ordered in subsets. The number of ways of obtaining an ordered subset of 'K' number of H^2 devices for "m" floors out of n floors, columns, trusses and walls can be decided upon, since some floors may not need them.

$$P_k = \text{the number of ways of obtaining ordered subset of devices} = n!/\{n-k\}! \tag{7.1}$$

For example, when $n = 4$ and $(n-k) = 2$, then

$$4!/2! = \left(\frac{4\times 3\times 2\times 1}{(2\times 1)}\right) = 12 \qquad 2 \text{ subsets of } (1,2,3,4), \text{ namely}$$

$$\{1,2\},\{1,3\},\{1,4\},\{2,1\},\{2,3\},\{2,4\},\{3,1\},\{3,2\},\{3,4\},\{4,1\},\{4,2\} \text{ and } \{4,3\} \tag{7.2}$$

The devices are initially located in the subset formation and the analysis is carried out accordingly as given in Eq. (7.2). One must consider the limitation on the positions for total number of devices forming the order list "S". A computer program "SUBSET" is needed to initially reject the number of redundant devices without which the target with few can be easily achieved. For example, for 10 devices in the number computed, the target on acceleration, displacement and materials stress can be achieved with three devices, the most favourable for permutation can be $10 \times 9 \times 8 = 720$ and the remaining are left out, i.e. $(7 \times 6 \times 5 \times 4 \times 3 \times 2 \times 1)$; then in a generalized manner

$$10 \times 9 \times 8 \frac{10!}{(10-3)!} \tag{7.3a}$$

or

$$P_r = \frac{n!}{(n-r)!} \tag{7.3b}$$

where r choices are discarded and $(n\text{-}r)!$ is adopted

r = devices decided to be placed at important zones, if geometrically or structurally acceptable.

7.3.2.2 Combinations

The above analysis has considered the optimum positioning and permutation of devices on, say, a floor. The order they were, numerically and geometrically, is important. What if the order of devices is not really important? Consider as above the positioning of the three devices which had six permutations. If these three devices are the same in each permutation for positioning, they were, say,

www.EngineeringBooksPDF.com

all A, B and C, however they are positioned. "*They were only one combination*". Hence for 3!, i.e. six permutations, they have one combination. Three devices will be "*one set*". The same will be true for "*each group*" of three devices as above as choosing 720 permutations when choosing 3 devices from "10". So the number 3! of sets of 3 from 10 can be arranged in combinations as $\frac{720}{3!} = 120$.

In general, it can be further written in shorthand as

$$\text{number of combinations} = \frac{\text{total number of permutations for positioning devices}}{\text{number of permutations of each set of devices}} \tag{7.4}$$

In the same way that permutations have shorthand, combinations have similar shorthand. All one has to do is to divide the total number of permutations by the number of permutations in each set. So, the right-hand side of the following equation is the same as the equation for the number of permutations except for an additional $r!$ term in the divisor which corrects the number of permutations of each set of devices for true positioning.

$$\begin{matrix} C = n! \\ r!(n-r)! \end{matrix} \tag{7.5}$$

7.4 Permutations and Combinations of Devices

When one talks of permutations and combinations one often uses the two terms interchangeably (Suggestion: "When talking of permutations and combinations, these terms are oftentimes used interchangeably.") In mathematics, however, the two each have very specific meanings, and this distinction often causes problems. (Suggestion: In mathematics, however, each of these terms carries a distinctive meaning, which can cause confusion.")

In brief, the permutation of a number of devices is the number of different ways they can be placed, i.e. which is first, second, third, etc. If one wishes to choose some device from a larger number of devices, the way one positions the chosen device is also important. With combinations, on the other hand, one does not consider the order in which devices were chosen or placed, just which devices were chosen. They could be devices chosen from Plate 7.1.

One can summarise them as
Permutations – position important (although choice may also be important)
Combinations – chosen devices important, which may help one to remember which is which and the difference between them for the purpose of recognition in devices

As mentioned above, there is an important difference between permutations and combinations. In this case, for permutations the order of events is

www.EngineeringBooksPDF.com

important: Order 1 is different from Order 2. For combinations, however, it does not matter which device was chosen first. A reference is made to Plate 7.2 and also referring to Plate 7.1, in this example, there are two permutations of devices A, B $\neq$ B, A but only one combination, i.e. (A, B = B, A).

Assuming the engineer has three devices now [*A*], [*B*] and [*C*]. How many different permutations are there to place them at "suitable places"? When one considers the first device, one can easily choose from all three to be placed in position or location of importance by the engineer. When the engineer gets to the next device, there is no choice and it is the one that remains to be placed in a zone of great importance from the response analysis carried out on a building completely free of devices. So one can get six permutations as given below. The arrangement is as in Table 7.4 for the devices given in Plate 7.3.

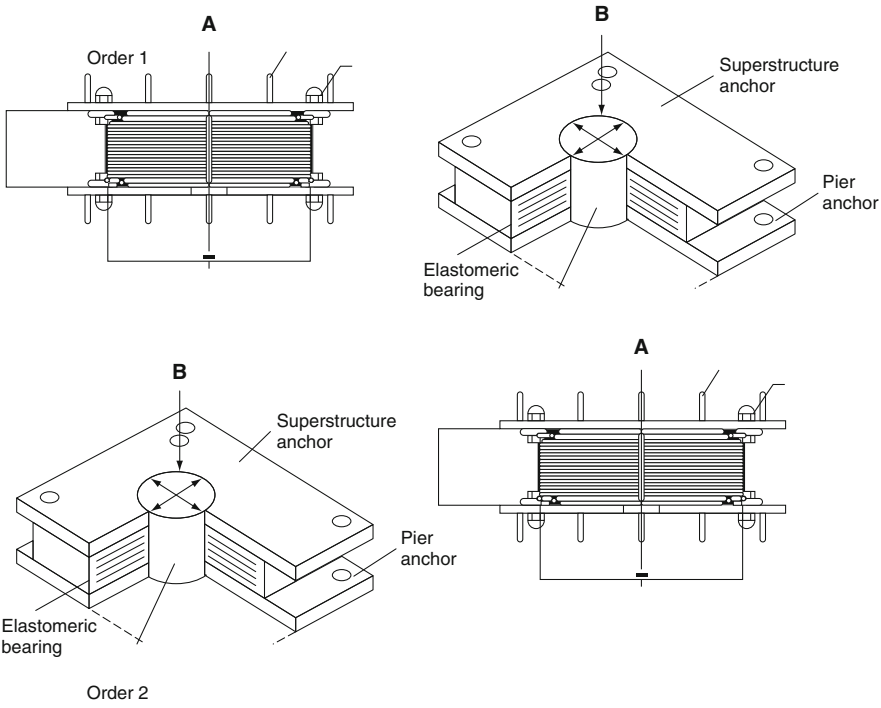


Plate 7.3 Devices in permutations

www.EngineeringBooksPDF.com

A representation of a permutation as a product of permutation device cycles is unique (up to the ordering of the cycles). An example of a cyclic decomposition is the permutation (4, 2, 1, 3) of (1, 2, 3, 4). This is denoted (2) (143) corresponding to the disjoint permutation cycles (2) and (143). There is a great deal of freedom in picking the representation of a cyclic decomposition of devices since (a) the cycles are disjoint and can therefore be specified in any order and (b) any rotation of a given cycle specifies the same cycle. Therefore, (431) (2), (314) (2), (143) (2), (2) (431), (2) (143) and (2) (143) all describe the same permutation for the devices. This concept reduces the "jump" in combinations.

Another notation that explicitly identifies the positions occupied by devices before and after application of a permutation on $\boldsymbol{n}$ device uses a $\mathbf{2} \times \boldsymbol{n}$ matrix, where the first row is **(123** . . .$\boldsymbol{n}$**)** and the second row is the new arrangement. For example, the permutation which switches elements 1 and 2 and fixes 3 would be written for devices as

$$\begin{matrix} 123 \\ 213 \end{matrix} \tag{7.6}$$

Any permutation is also a product of transpositions. Permutations are commonly denoted in lexicographic or transposition order. There is a correspondence between a permutation and a pair of *Young* tableaux known as the *Schensted* correspondence.

The number of wrong permutations of $\boldsymbol{n}$ devices is [n!/e] where [x] is the nint function. A permutation of $\boldsymbol{n}$ ordered devices in which no device is in its natural place is called a derangement (or sometimes a complete permutation) and the number of such permutations is given by the subfactorial $\mathbf{!}\boldsymbol{n}$.

Using

$$(\boldsymbol{x}+\boldsymbol{y})^n = \sum_{r=0}^{x} \binom{n}{r} \boldsymbol{x}^{\boldsymbol{n}-\boldsymbol{r}} \boldsymbol{y}^{\boldsymbol{r}} \tag{7.7}$$

with $x = y = 1$ gives

$$2^x = \sum_{r=0}^{x} \binom{n}{r} \tag{7.8}$$

So the number of ways of choosing 0, 1,. . ., or $\boldsymbol{n}$ at a time is 2^n where $\boldsymbol{n}$ is the number of devices.

The set of all permutations of a set of devices 1, . . ., $\boldsymbol{n}$ can be obtained using the following recursive procedure as given below:

www.EngineeringBooksPDF.com

$$
\begin{array}{cccccc}
 & 1 & 2 & & & \\
 & / & & & & \\
2 & 1 & & & & \\
 & 1 & & 2 & 3 & \\
 & & & / & & \\
 & 1 & 3 & 2 & & \\
 & / & & & & \\
3 & 1 & & 2 & & \\
| & & & & & \\
3 & 2 & & 1 & &
\end{array} \tag{7.9}
$$

$$
\begin{array}{cccccc}
 & \backslash & & & & \\
 & 2 & 3 & 1 & & \\
 & & & \backslash & & \\
 & 2 & & 1 & 3 &
\end{array} \tag{7.10}
$$

This method of dispersing the devices becomes very useful. Several positions will give many solutions when put to the relevant computer program. The controlled building will be analysed for positions of devices in an earthquake zone. The one that gives optimum $P-\Delta$ and decreased responses will be the optimum solution for the safety of the building. This means the target has been achieved and a certificate is issued for safety when all the results are satisfactory. Thus the positioning of devices can be acceptable. Tables 7.5, 7.6, 7.7, 7.8, 7.9, and 7.10 show the building areas with the number of floors for buildings at different towns made with different materials that have been checked for seismic devices. No information was available to check for a number of devices needed as part of control. Based on permutation/combination and available spaces or locations, the numbers noted are computed once. Some of them have been checked using three-dimensional dynamic non-linear analysis and the number of devices cited give controlled performances.

Case Study on Nachiyodai Unitika Apartments

Two-storey building designed by Unitika Inc.
Yachiyo city, Japan

Building data: reinforced concrete building (Ref: Plate 7.3)
Total floor area $= 2\{5.63\ (6.080 + 4.280)\} = 116.6536\ \text{m}^2 \approx 116.654\ \text{m}^2$
Total height $= 6.50\ \text{m} = n(\text{m})$; type of earthquake El-Centro NS
Seismic waveform $=$ 300gal–500gal

Total floor area $= 116.654\ \text{m}^2$ and $h = 6.50$ m, the number of LR (isolators) required $= 12$ (maximum). Initially they are located as

Upper structure and the raft foundation $= 6$
first floor $= 6$
Dampers needed (friction type) $= 3$

www.EngineeringBooksPDF.com

Table 7.7 Case studies of earthquake constructed facilities

	(3)	(4)	(5)
Item	Obayashi Group Technical Research Center *	Dieres Industries Fujizawa site TC wing *	Funabashi Taketomo Dormitory *
Designed by	Obayashi Group	Oires Industries, Symiono Constructions, Yasui Building Designers	Takenaka Komyten
Year of approval; No.	27 February 1986; Tok. 30	7 April 1986; Kana 21	24 June 1986; Chi 43
No. of floors	+5	+5	+3
Built-up area, m^2	351.92	1136.5	719.28
Application	Laboratory	Research laboratory and office	Dormitory
Structure	RC	RC	RC
Foundation	PHC tie (cement grout method)	Concrete in situ raft (earth-drilling method)	Concrete in situ raft (earth-drilling method)
Isolator: Dimensions, mm	Rubber 4.4 thick × 740 dia (61 layers)	Rubber 10 thick × 24 dia (H = 363), OD =650, 700, 750, 800	Rubber 7 thick × 670 dia (19 layers) (H = 187) Rubber 8 thick x 700 dia (18 layers) (H = 195)
Numbers	14 (15*)	35 (38*)	14 (17*) supporting
Supporting force	200 t		200 t → 6 nos 150 t → 8 nos
Response-control device	Uses elasto-plastic recovery of steel bars (96 Nos.)	Lead plug inserted in laminated rubber	Viscous damper (8 Nos.)
Shear force coefficient used in design	0.5	0.2	0.15
Fundamental period Small deformation	X = 1.33 cm Y = 1.24 cm	X = 0.895 cm Y = 0.908 cm (at 50% deflection)	X = 2.09 cm

www.EngineeringBooksPDF.com

Table 7.7 (continued)

Large deformation	$X = 3.12$ cm $Y = 3.08$ cm	$X = 2.143$ cm $Y = 2.148$ cm (at 100% deflection)	$Y = 2.10$ cm
Incident seismic wave	El-Centro 1940 (NS) Hachinohe 1968 (NS) Hachinohe 1968 (EW) Taft 1952 (EW) Man-made earthquake 2 waves	El-Centro 1940 (NS) Hachinohe 1968 (NS) Hachinohe 1968 (EW) Taft 1952 (EW) KT 008 1980 (NS) Man-made earthquake 2 waves	El-Centro 1940 (NS) Taft 1952 (EW) Tokyo 1o1 1956 (NS) Hachinohe 1968 (NS) Man-made earthquake 4 waves
Input level	25 cm/sec, 50 cm/s	25 cm/sec, 50 cm/s	25 cm/sec, 50 cm/s

Note: (*) computed and tested on the basis of dynamic non-linear three-dimensional analysis using finite element.
* Note: Data collected with the compliments of respective companies.

www.EngineeringBooksPDF.com

Table 7.8 Case studies of earthquake constructed facilities

Item				
		Kashima Constructions Research Center (reapplied) * Center, Nishi Chofu Acciystus	Christian Data Apartments *	Fukumiya *
Designed by		Kashima Constructions	Tokyo Building Research Center	Okumura Group
Design requirements		Reduce seismic input and insulate (isolate) from Earth's vibrations	Antiseismic. Prevent any damage to stored goods	Safety of building. Added value in business
Year of approval; No. Tok 473		5 December 1986;		3 March 1987; Tok 44
No. of floors		+2	+2	+4
Built-up area, m^2		379.10	149.43	225.40
Application		Research laboratory	Data house	Cooperative housing
Structure		RC	RC	RC
Foundation		Concrete in situ raft (deep foundation)	Deep foundation	Concrete in situ raft (miniature earth-drilling method)
Isolator: Dimensions, mm		320 × 1340 (48 thick × 5 dial); 308 × 1080 (38 thick × 6 dia) (25 layers)	4 thick × 435 dia	
Dnamic Non-linear F.E. Analysis	Numbers	18	12	
	Supporting force	165 t: 1340 dia 100 t: 1080 dia	$\sigma = 60$ kg/cm^2; 0.55 t/cm (90 t)	
	Respones-control device	Elasto-plastic damper using mild steel 14T15	Uses plastic deformation of steel bars bent to make a loop6T8	Uses plastic deformation of steel bars bent to make a loop 7T10

www.EngineeringBooksPDF.com

Table 7.8 (continued)

Shear force coefficient used in design	0.2	0.15	0.2
Primary Small period deformation	$X = 0.828$ cm $Y = 0.809$ cm	1.3 cm	1.4 cm
Large deformation	1.80 cm	1.9 cm	2.2 cm
Incident seismic wave	EI Centro 1940 (NS) Taft 1952 (EW) Tokyo 101 1956 (NS) Sendai THO38-1 1978 (EW)	EI Centro 1940 (NS) Taft 1952 (EW) Hachinohe 1968 (NS)	EI Centro 1940 (NS) Taft 1952 (EW) Tokyo 101 1956 (NS) Hachinohe 1968 (NS)
Input level	25 cm/s, 50 cm/s	300 gal, 450 gal	25 cm/s, 50 cm/s

NOTE: (*) computed and tested on the basis of dynamic non-linear three-dimensional analysis using finite element.
( ) Actually provided.
* Data collected from these companies and presented in the given format. With compliments from these constructors in Japan.

www.EngineeringBooksPDF.com

Table 7.9 Case studies of earthquake constructed facilities

Item			
		Shibuya Shimizu Building No. 1 ‡ *	Fujita Industries 6th Laboratory ‡ *
Design requirements		Protect the main building and OA equipment installed therein	Protect the main building and the equipment stored therein such as laboratory equipment and computers
Year of approval; No		13 March 1987; Tok 52	14 May 1987; Kana 23
No. of floors		+5, −2	+3
Built-up area, m^2		560.30	102.21
Application		Office	Research laboratory
Structure		RCC	RCC
Foundation		Concrete in situ raft (earth-drilling method)	PHC pile (type A, B) cement grout method
Isolator: Dimensions, mm		5.0 thick × 620 dia (50 layers); 6.0 thick × 740 dia (45 layers)	4.0 thick × 450 dia (44 layers)
Numbers		20	4
Supporting force		100–150 t 620 200–250 t: 740 dia	
Response-control device		Elasto-plastic damper using (49*) mild steel bars (48 Nos.) (57*)	
Shear force coefficient used in design		0.15: Basement, 1st floor; 0.183: 3rd floor; 0.205: 5th floor	0.15: 1st floor, 0.17: 2nd floor; 0.20: 3rd floor
Fundamental period	Small deformation	$X = 1.30$ cm $Y = 1.24$ cm	1.35 cm] Dynamic finite Element Analysis
	Large deformation	$X = 2.99$ cm $Y = 2.97$ cm	
Incident: seismic wave		El-Centro 1940 (NS) Taft 1952 (EW) Hachinohe 1968 (NS) Hachinohe 1968 (EW) Sdkanrig, Sdkantig, Sdansrig } man-made seismic wave	El-Centro 1940 (NS) Taft 1952 (EW) Hachinohe 1968 (NS) Hachinohe 1968 (EW) Artm 79L00 (seismic wave)
Input level		25 cm/s, 50 cm/s	25 cm/s, 50 cm/s

NOTE: (*) computed and tested on the basis of dynamic non-linear three-dimensional analysis using finite element.
( ) Actually provided.
‡ * Data from the designers with compliments.

From the graph, these are the items needed to begin with subject to complete analysis as outlined in this text in general and Chap. 5 in particular.

Application of the permutation/combination method

$$\mathrm{S} = 12,\ \mathrm{LR/floor} = 6\,n; n! = 6! = 6 \times 5 \times 4 \times 3 \times 2 \times 1$$
$$(n-k)! = 3! = 3 \times 2 \times 1$$

www.EngineeringBooksPDF.com

Table 7.10 Case studies of earthquake constructed facilities

Item	(11)	(12)
	Inorganic Materials Research Center, Vibration-free Wing	Shimizu Constructions, Chuchiura Branch, new building
1	2	3
Designed by	Secretariat of the Ministry of Construction, Planning Bureau	Shimizu Constructions
Design requirements	Protect the main building and research equipment stored therein	
Year of approval	June 1987	June 1987
No. of floors	+1	+4
Built-up area, m^2	8,341 (old – 7,725; new – 616)	170.366
Application	Research centre	Office, company housing
Structure	RCC	RCC
Foundation	PHC raft (type A) blast method	PHC raft (type B, C) method using earth auger
Isolator: Dimensions, mm	3.2 thick × 420 dia (62 layers)	6.0 thick × 450 dia; 6.0 × 500; 6.0 × 550 (31 layers)
Number	32	14
Supporting force	65 t (max 80 t)	51–165 t
Response-control device	Elasto-plastic damper using mild steel bars (108 nos.) (112*)	Lead plug inserted in laminated rubber (112*)
Shear force coefficient used in design	0.15	All floors 0.15
Fundamental period — Small deformation	$X = 1.17$ cm $Y = 1.17$ cm	$X = 0.77$ cm $Y = 0.77$ cm Dynamic Finite Element Analysis
Large deformation	$X = 2.26$ cm $Y = 2.26$ cm	$X = 2.33$ cm $Y = 2.33$ cm
Incident seismic wave	El-Centro 1940 (NS) Taft 1952 (EW) Hachinohe 1968 (NS) Hachinohe 1968 (EW) Tsukuba 85 NS Tsukuba 85 EW Tsukuba 86 NS Tsukuba 86 EW (Observed seismic waves)	El-Centro 1940 (NS) Taft 1952 (EW) Hachinohe 1968 (NS) Ibaragi 606 1964 (NS)
Input level	25 cm/s, 50 cm/s	35 cm/s, 50 cm/s

NOTE:(*) computed and tested on the basis of dynamic non-linear three-dimensional analysis using finite element.
( ) Actually provided.
Data under 1,2,3 are obtained by the author with compliments.

$$P_k = \frac{n!}{(n-k)!}$$
$$= 120$$
$$C_r^n = \frac{120}{3 \times 2 \times 1} = 20 \text{ positioning for combination}$$

The requisite floors:

$$\text{S} + \text{Dampers} = 12 + 7 = 19 \approx 20$$
$$\uparrow$$

Two floors are okay — adopted — computed

www.EngineeringBooksPDF.com

These are now to be tested for a given layout using the program ISOPAR and then finally checked against the design given by Unita Inc., Japan.

Data for Raft foundation For soil–structure interaction
Ground property
Foundation depth Raft foundation. Formation GL-1.15 m
Soil property and *N* value

GL-m	0–2.8	2.8–3.9	3.9–10.8	10.8–12.7	12.7
Soil	Red loam	Red above loam	fine sand	very fine sand	Fine sand loam below
N value	<4	1.4	4–17	25–27	>50
Permissible pile resistance 6.0 t/m^2 = 60 KN/m^2					

Outline of the structure

Foundation

Ground type:	Raft foundation, supported directly on loam-type soil. Formation depth:
Foundation structure:	GL-1.15 m
Maximum contact:	Long term: 4.81 t/m^2 = 48.1 KN/m^2
Pressure:	Short term: –

Case Study 7.1 A Two-Storey Building
Description of the structure
A reference is made to Plate 7.4. It is an RCC framed structure with the following details of the elements:

www.EngineeringBooksPDF.com

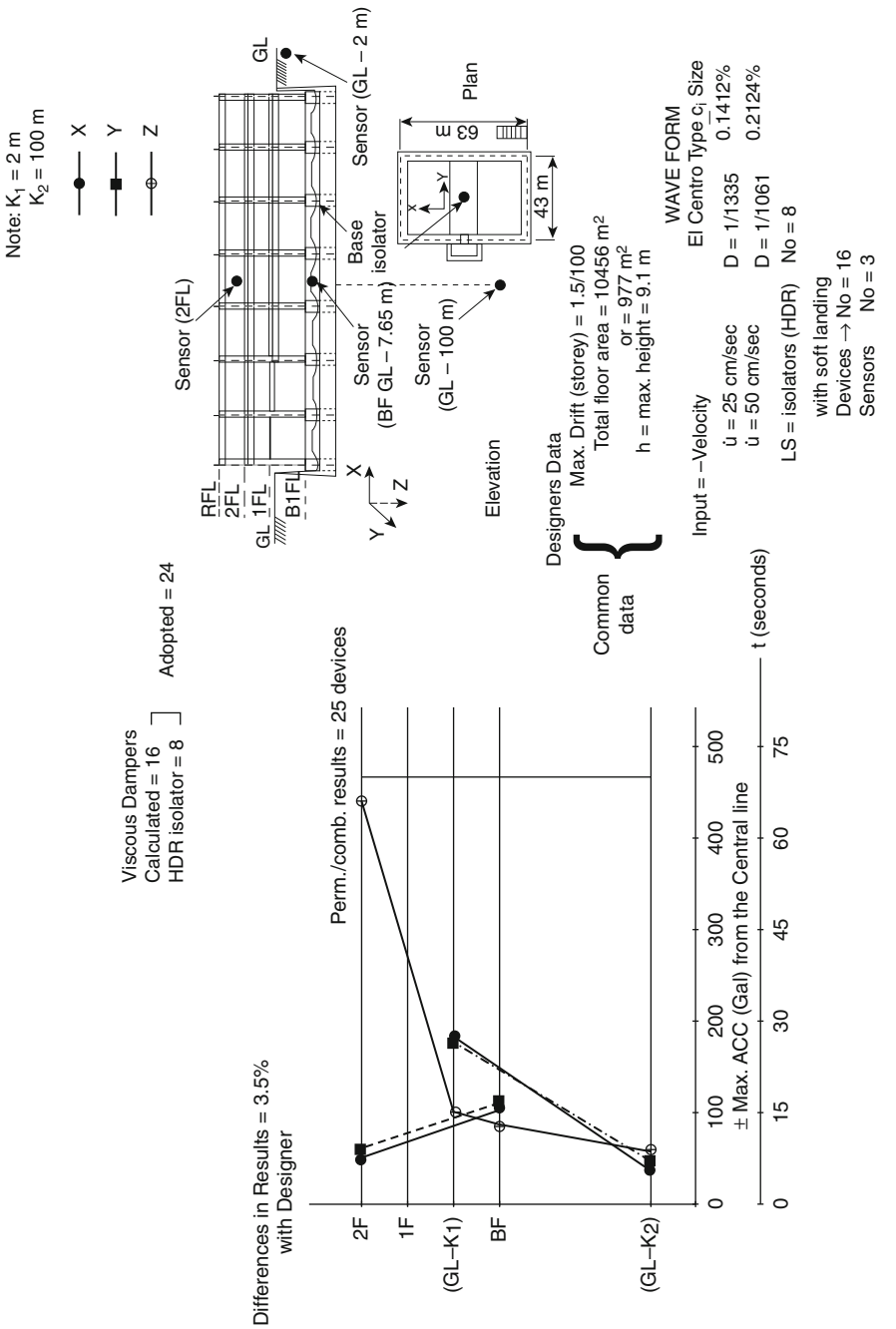


Plate 7.4 Test Case 7.1 Case Study I

www.EngineeringBooksPDF.com

(continued)

1. With load bearing and other RC walls of 1.5 m on raft foundation	
2. Column 450 × 450 common to each floor	
3. Beam	300 × 550 for raft 500 × 550 mm for two floors 600 × 550 mm for floors
4. Floor	RCC cast in situ concrete 120 cm
5. Roof	RCC cast in situ concrete 120 cm
6. Non-bearing walls > 150 cm as above	
Isolators (6 nos)	Each isolator consists of rubber – natural rubber 5 thick × 300 dia (12 layers); steel plate – SUS 304; insertion plate – PL2 × 300 dia (11 layers); flange plate 22 × 500 × 500 SS41 (JIS G 3101 type 2); base plate 9 × 500 × 500; fixing bolt H.T.B F10T (JIS B 1186) M20
Damping device	Friction damper – uses the frictional forces acting between the PC plate for dry and the side walls

Method of analysis

Dynamic non-linear analysis with and without above devices has been carried out. The data for the soils are incorporated in the soil–structure interaction analysis to cater for the ground effects. Hallquist gap element for the raft has been adopted in the soil–structural analysis. The author has no data from Unitika Inc. to indicate whether or not soil–structure interaction was included in their analysis. Program ISOPAR has assumed the characteristic loads for the building (1.4Gk + 1.6Gk) did exist in the overall analysis. Time integration approach has been adopted for the solution of equations, the details of which are given in the text. For the hysteresis loop, the isolators are assumed to be of high damping natural rubber.

Results

Table 7.10 for this two-storey building gives a comparative study between this work and that of Unitika Incorporation. The results seem to be quite close to one another. Moreover the computed response peak was 0.083 g and the spectral peak was 0.5 g. When the damping is raised to 2% from 0.10, for 66 KN the maximum occurred at one place and the corresponding deflection of the isolator was 635 mm. The shear stress–strain for the device is shown in Table 10.1. The results do indicate that the maximum drift is reduced and the two-storey building is doing extremely well and is safe.

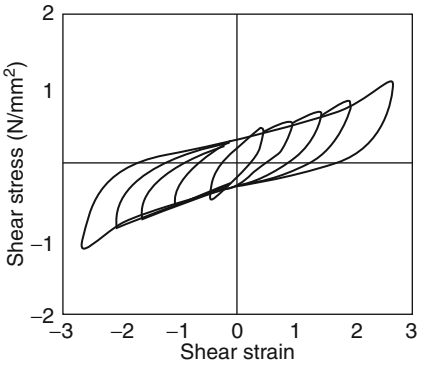
www.EngineeringBooksPDF.com

A Comparative Study of Results
Hysteresis Loop

Table 7.11 Analysis Type Case Study 7.1 Finite element three-dimensional seismic waveform TYPE: El-Centro 300–450gal degrees of freedom

	UNITIKA, Japan TYPE	*X	*Y	*Z	Program ISOPAR *X	*Y	*Z
1	Fundamental period T (sec)	1.83	1.83	–	1.778	1.778	0.01
	(a) Mode 1	0.05	0.07	–	0.045	0.0458	0.009
	(b) Mode 2						
2	Damping Constant (∈ or β)	0.10	0.10	–	0.10	0.10	0.10
3	Isolator HRD type	√	√	–	√	√	√
4	Shear coefficient	0.244 (F2)	0.244 (F2)	–	0.251(F2)	0.251 (F2)	0.031 (F2)
	C_i (building)	0.200 (F1)	0.200 (F1)	–	0.210 (F2)	0.210 (F1)	0.01 (F1)
5	Seismic load (%)						
	(a) Rigid frame	35 (F2); 27 (F1)	39 (F2); 53 (F1)		33 (F2); 25 (F1)	36 (F2); 51 (F1)	–
	UNIKA, Japan				Program ISOPAR		
	(b) Shear wall	65 (F2); 73 (F1)	61 (F2); 47 (F1)		67 (F2); 75 (F2)	64 (F2) 49 (F1)	– –
6	Device	14 cm	–				
	Umax	0.17 (NS)	–				
		21 cm	–				
		0.25 (NS)	–				
7	Upper structure $\ddot{U}$max						
	(a) Foundation 300 gal input (cm/s^2)	168			176	158	158
	Ci	0.17 (NS)			0.18 (NS)	0.18 (NS)	0.18 (NS)
	(b) Fißtfloot 450 gal input (cm/s^2)	252			261	236	136
	Ci	0.25 (NS)			0.245 (NS)	0.245 (NS)	0.245 (NS)

Hysteresis loop



X* – Along the length
Y* – Along width
Z* – Vertical axis
A_{total} = 116.654 m^2
H = Effective building height = 6.5 m
Rubber bulk modulus = 2500 MN/m^2
Rubber shear modulus = 0.55 MN/m^2

www.EngineeringBooksPDF.com

Case Study 7.2
Obayashi-Gumi Technical Research Center Laboratory 61 Designed By Obayashi-Gumi Ltd, Tokyo, Japan

Building Data:	Reinforced concrete rigid frame building with RCC seismic wall
Total floor area:	1623.89 m^2, total height = 22.80 m = h (m)
Area/floor:	328.75m^2, Type of earthquake waveform: El-Centro with acceleration amplitude 300–450 cm/s^2
Total floors:	above ground = 5 Penthouse = 1
Dampers – 24 nos, they are positioned. as a set of 4 Total No = 96.	
Isolators – 14 no, with ABCD permutation + combination Total No computed = 98	

Soil Property And Foundation Data
Note: These data are used for soil–structure interaction analysis

Soil property and N value		Ground property Foundation depth PHC pile	Formation GL-1.775 m Pile depth, formation GL-7.0 m
GL-m	0–0.7 m	0.7–6.2 m	> 6.2 m
Soil type	Red loam	Loam	Gravel
N value	–	2.3	>50
Permissible pile resistance		PHC pile (Type A, B) cement grouting method (method approved by Ministry of Construction under Section 38 of its regulations) 45 dia 66t/pile (long term); 132 t/pile (short term)	

Outline of the structure

Foundation

Ground type, foundation structure	PHC pile supported directly in fine sand layer at GL-6.2 m		
Maximum contact pressure (Pile resistance)		Long term	Short term
	PHC pile (type A, B) 450 dia		
	Side column	90 t	138 t
	Corner column	200 t	257 t

www.EngineeringBooksPDF.com

(continued)

Main Structure	
Structural features	The device is placed between RCC upper structure and the foundation
Frame classification Bearing walls, other wall	*X* direction: RCC rigid frame; *Y* direction: RCC aseismic wall RCC structure
Material for columns	RCC structure; column – B × D = 600 × 550, 650 × 550;
Beams, sections	Beam – B × D = 300, 450 × 700; 300, 450, 500 × 800; Concrete – Fc = 270, Steel bars: deformed bars – SD30, SD35 (JIS G 3112)
Columns, beams, joints	RCC structure
Floor	PRC rib slab, PRC flat slab (cast in situ concrete structure)
Roof	PRC rib slab (cast in situ RCC structure)
Non-bearing wall	Outlet wall – ALC plate; inner wall – Glass fibre-reinforced Foam gypsum plate
Fire-proof coating	–
	Structural design
Device	
Laminated rubber	Each consists of Rubber – natural rubber 4.4 thick × 740 dia (61 layers); steel plate: insertion plate – SS41 (JIS G 3101) PL – 24 – 30 × 985 (top and bottom); fixing bolt – H.T.B. F10T (JIS B 1186) M24
Steel rod damper	Each set consists of Steel rod – SCM 435 (JIS G 4105) three beams (span 20 cm, 45 cm, 20 cm); bearing – SUJ2 (JIS H 5105); steel plate – SS41 (JIS G 3101 type 2); base plate 4 PL – 19 × 230 × 360; Fixing bolt – PC steel rod type A (JIS G 3109) 4 numbers, 13 dia.

Steel and concrete building : Two storey
Results SAP2000
Time history non-linear analysis: Three-dimensional
D = max. Diff. = 1.52/100
Ci = 0.22 cm
U = Velocity m/s = 50 cm/s
Ü = Acceleration; x = 3 200Gal
y = 200 Gal
z = 50 Gal
t = 130 cm

Case Study 7.3 Four-storey building No. of degrees = 6

Seismic waveform: El-Centro NS and Taft EW
Major analysis is non-linear time integration.
Data: Case Studies C, covering five different cases:

1 RC building C1: h = height = 14 m; A = total area = 1100 m^2;
Devices: 12-Isolators, 13.free-sliding pot bearing

2. Steel building C2: h = height = 19 m; A = total area = 4500 m^2
Devices: 32 YE dampers

www.EngineeringBooksPDF.com

(continued)

3.	RC building C3:	h = height = 15 m; A = total area = 8000 m^2
	Devices:	80 hysteric steel damper
4.	RC building C4:	h = height = 13.92 m; A = total area = 636.764 m^2
	Devices:	14 LRB with lead plug
5.	RC building C5:	h = height = 11.57 m; A = total area = 681.8 m^2
	Devices:	12 R500/steel plates, bolts, 7 sets of steel rod dampers
C1	Input level = 0.25 g; max drift = 1/7500; U_{max}max. top displacement = 14.10 cm	
C2	Input level = 1.40 g; max drift = 1.5/00; U_{max}. top displacement = 15.20 cm	
C3	Input level = 200 g; max drift = 1/500; U_{max}. top displacement = 18.10 cm	
C4	Input level = 35 cm/s; max drift = 1/500; U_{max}. top displacement = 15.80 cm	
C5	Input level = 50 cm/s; max drift = T/500; U_{max}. top displacement = 14.90 cm	

Case Study 7.4 Five-storey building

Seismic waveform: El-Centro NS and Taft EW
Data: Case studies C
Nursing Home Building (RCC): C1 h = height = 19.40 m; total area = 5504.6 m^2;
Devices: 18 isolators, rubber bearings
Shibuya Shimizu Building (RCC): C2 h = height = 16.45 m; total area = 3385.0 m^2;
Devices: 20 isolators, 108 feel dampers
Obayashi R&D Center: C3 h = height = 22.8 m; total area = 1624.0 m^2;
Devices: 14 isolators, 96 feel dampers
Centro P. Del rione Traianoc C4 h = height = 14.5 m; total area = 90,000 m^2;
Devices: 624 isolators, multi-layered elastomeric
IMFR Gervasutta Hospital C5 h = height = 21.0 m; total area = 2000 m^2;
Devices: 52 HDE isolators
Nursing Home Building (Tamari and Tokita, 2005)

www.EngineeringBooksPDF.com

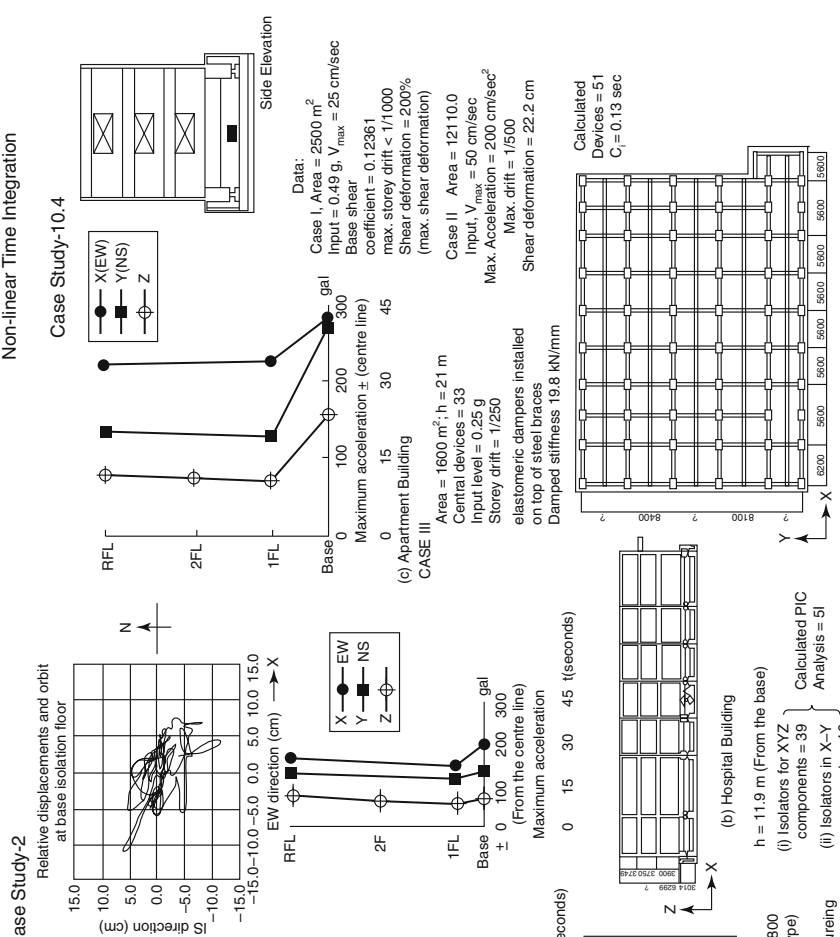


Plate 7.5 Case Study 7.5 Two-storey building

www.EngineeringBooksPDF.com

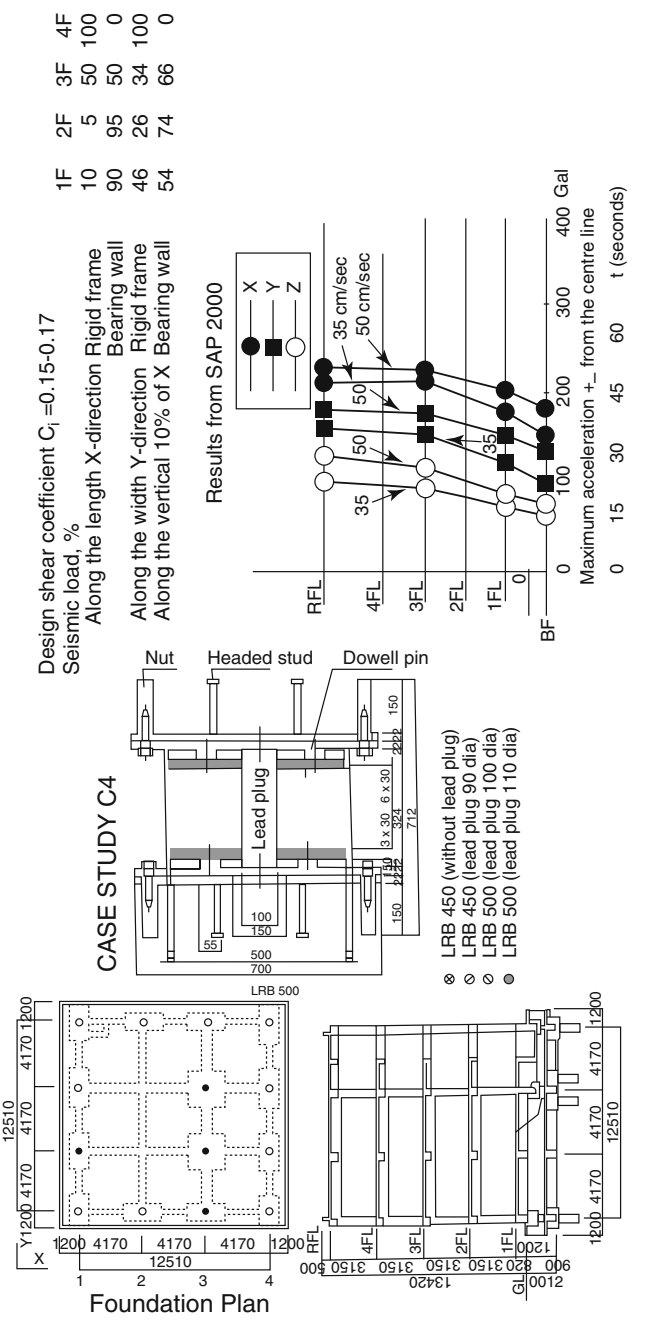


Plate 7.6 Case Study 7.6 Three-storey building

www.EngineeringBooksPDF.com

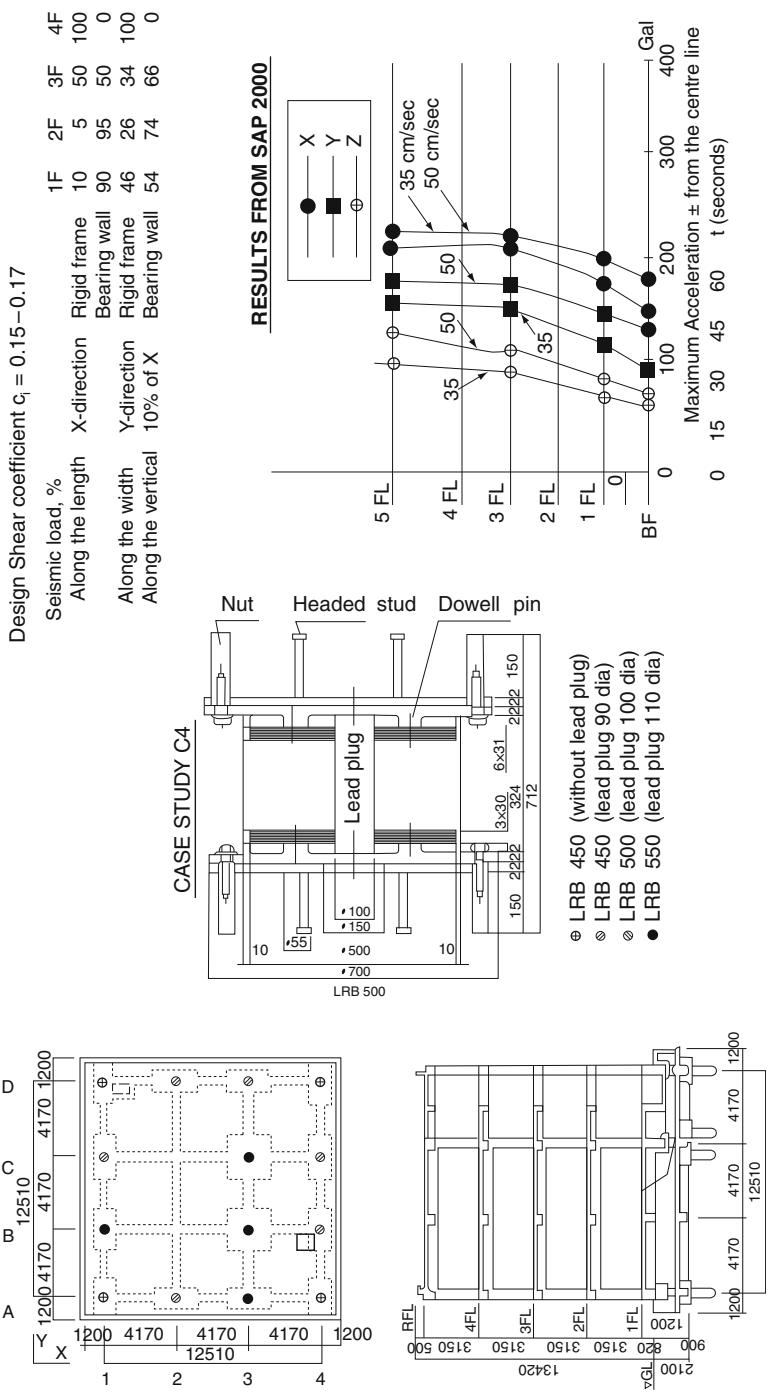


Plate 7.7 Sesmic waveform: El-centro NS and Taft Ew

www.EngineeringBooksPDF.com

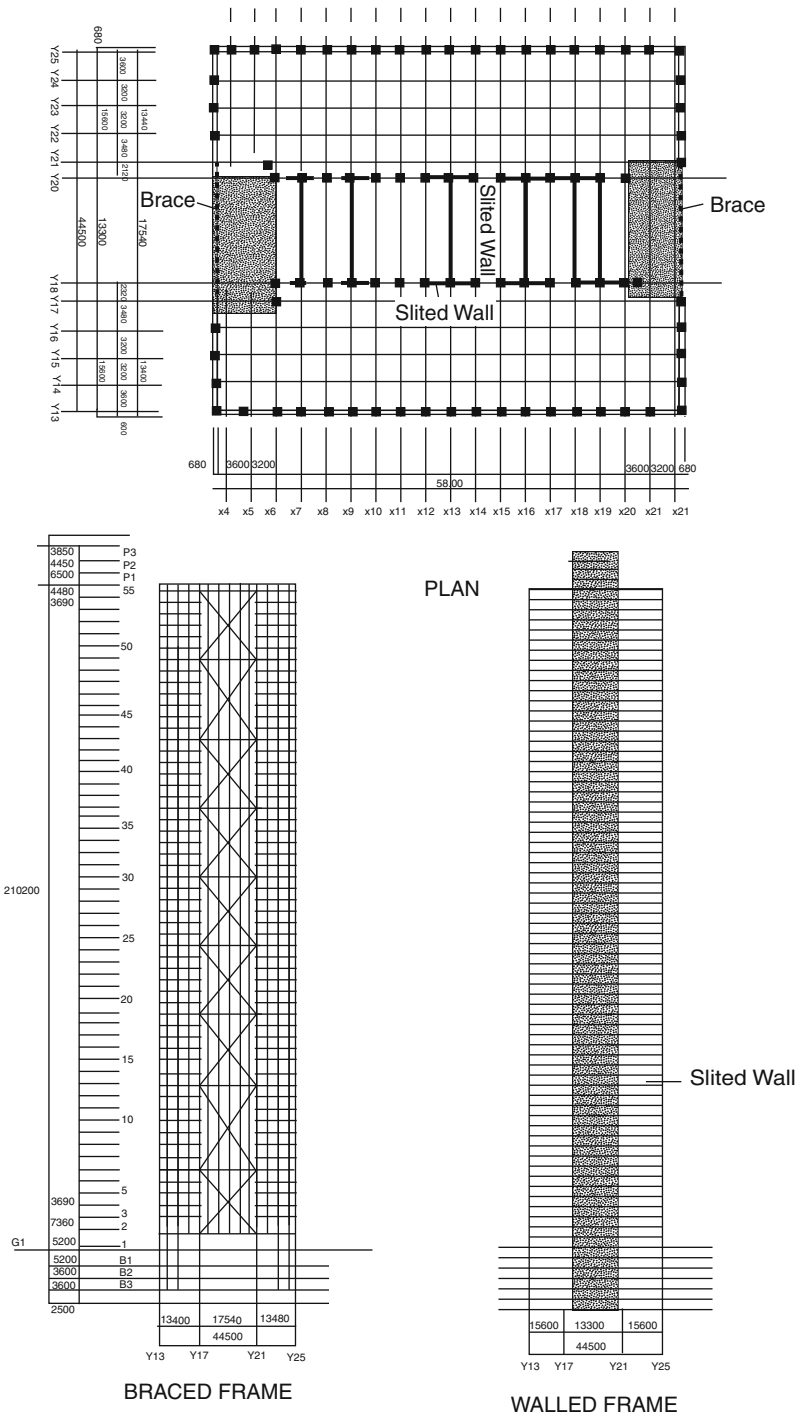
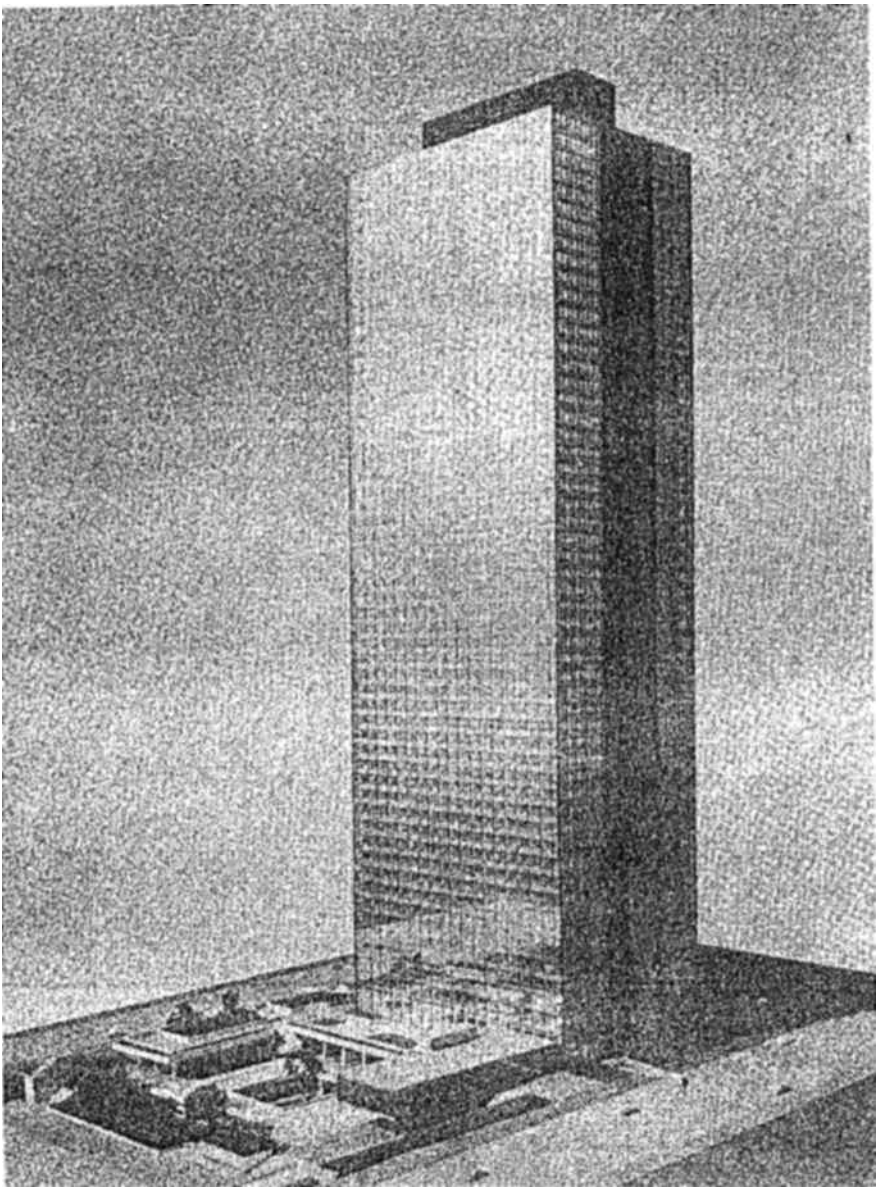


Plate No 7.8 Plan and Elevations of SMB Building

www.EngineeringBooksPDF.com



www.EngineeringBooksPDF.com

Case Study 7.5 Obayashi-Gumi Technical Research Center Laboratory Designed by Obayashi-Gumi Ltd, Tokyo, Japan

Building Data: - Reinforced concrete rigid frame building with RCC aseismic wall

- Total floor area: 1623.89 m^2; total height = 22.80 m = h (m)
- Area/floor = 328.75 m^2
- Type of earthquake waveform: El-Centro with accelerations amplitude 300–400 cm/s^2
- Total floors: 5 above ground, 1 penthouse
- Dampers: 24 nos in sets of 4 are positioned. Total no. = 96
- Isolators: 14 nos are positioned

with A, B, C, D permutation and combination
The total number computed = 98

Soil Property and Foundation Data

Note: These data are used for soil–structure interaction analysis

		Ground property Foundation depth PHC file		Formation GL-1.775 m Pile depth Formation GL-7.0 m
Soil property and N value				
GL-m	0–0.7 m	0.7–6.2 m	>6.2 m	
Soil type	Red Loam	Loam	Gravel	
N value:	–	2–3	>50	
Permissible pile resistance	PHC pile (Type A, B) cement grouting method (method approved by Ministry of Construction under Section 38 of its regulations) 45 dia 66 t/pile (long time); 132 t/pile (short term)			

Case Study 7.6 A Comparative Study of Results
Analysis type: Seismic Waveform type Degree of Freedom
Finite element Three-Dimensional El-Centro 300–345 gal 6/floor

S.No.	Obayashi-Gumi Ltd, Tokyo, Japan DIRECTION Type				Program ISOPAR and Graph G-type Direction		
		X^*	Y^*	Z^*	X^*	Y^*	Z^*
1	Fundamental period (s)						
	(a) mode 1	3.12	3.08	–	2.92	3.01	1.05
	(b) mode 2	0.42	0.25	–	0.39	0.22	0.01
2	Damping constant (ξ & β)	0.02	0.01	–	0.015 25 cm/s	0.02 50 m/s	0.001
3	Shear coefficient C_i building	0.122 (F1) Input 25 cm/s	0.120 (F1)	–	0.119 (F1)	0.119 (F1)	0.100

www.EngineeringBooksPDF.com

(continued)

S.No.	Obayashi-Gumi Ltd, Tokyo, Japan DIRECTION Type	X*	Y*	Z*	Program ISOPAR and Graph G-type Direction X*	Y*	Z*
		0.172 (F1) Input 50 cm/s	0.172 (F1)		0.172 (F1)	0.169 (F1)	0.100
4	Seismic load %						
	(a) Rigid frame	100%	100%		Fure-Storey rigid frame analysis in three-dimensional bending, shear, axial effects using SAP 2000 dynamic, non-linear		
	(b) Shear wall	100%	100%				
5	–				100%	100%	100%
6	**Device** U_{max}						
	(a) Input 25 m/s	11.7 cm	11.1 cm		10.67	10.91 cm	0.51 cm
	(b) Input 50 m/s	23.3 cm	23.4 cm		21.25	23.4 cm	0.98 cm
7	**Upper structure** $\ddot{U}_{max}$At foundation level						
	(a) Input 25 cm/s	220 cm/s^2	184 cm/s^2		198 cm/s^2	179 cm/s^2	17.2 cm/s^2
	(b) Input 50 cm/s	267 cm/s^2	267 cm/s^2		238 cm/s^2	270 cm/s^2	27.0 cm/s^2
8	Max. shear coefficient C_i						
	(a) Input 25 cm/s	0.135	0.134		0.132 (F1)	0.132 (F1)	0.110
	(b) Input 50 cm/s	0.182	0.189		0.175 (F1)	0.180 (F1)	0.110

Hysteresis loop as shown in Plate 7.9.

Case Study 7.7 Shibuya Shimizu Building - I

Designed by Obayashi - Gumi Ltd, Tokyo, Japan

Building Data's

- Six Storey with Penthouse
- Reinforced concrete rigid frame building with RCC antiseismic wall
- Total floor area = 3385.09 m^2, total height = 21.05 m = h cm
- Area/floor = 567.8 m^2, types of earthquake: El-Centro, Taft
- Total floors : Above ground 5
  Below ground 1
  Penthouse 1
- Isolators No. 20-A
- Damper No. 108-B
- Steel rod
- With AB permutation combination P/C. Total no 130 – calculated and 130 $\approx$ 108 adopted in practice.

www.EngineeringBooksPDF.com

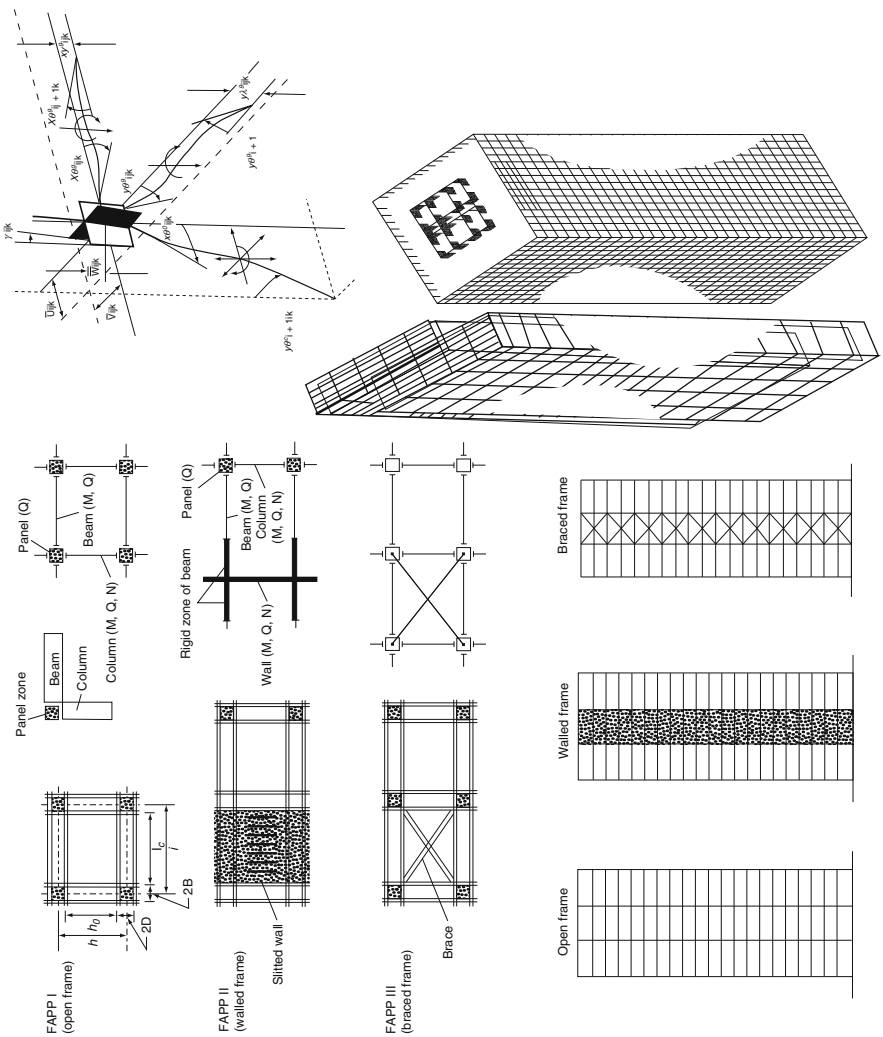


Plate 7.9 Five-Storey Building with Basement

www.EngineeringBooksPDF.com

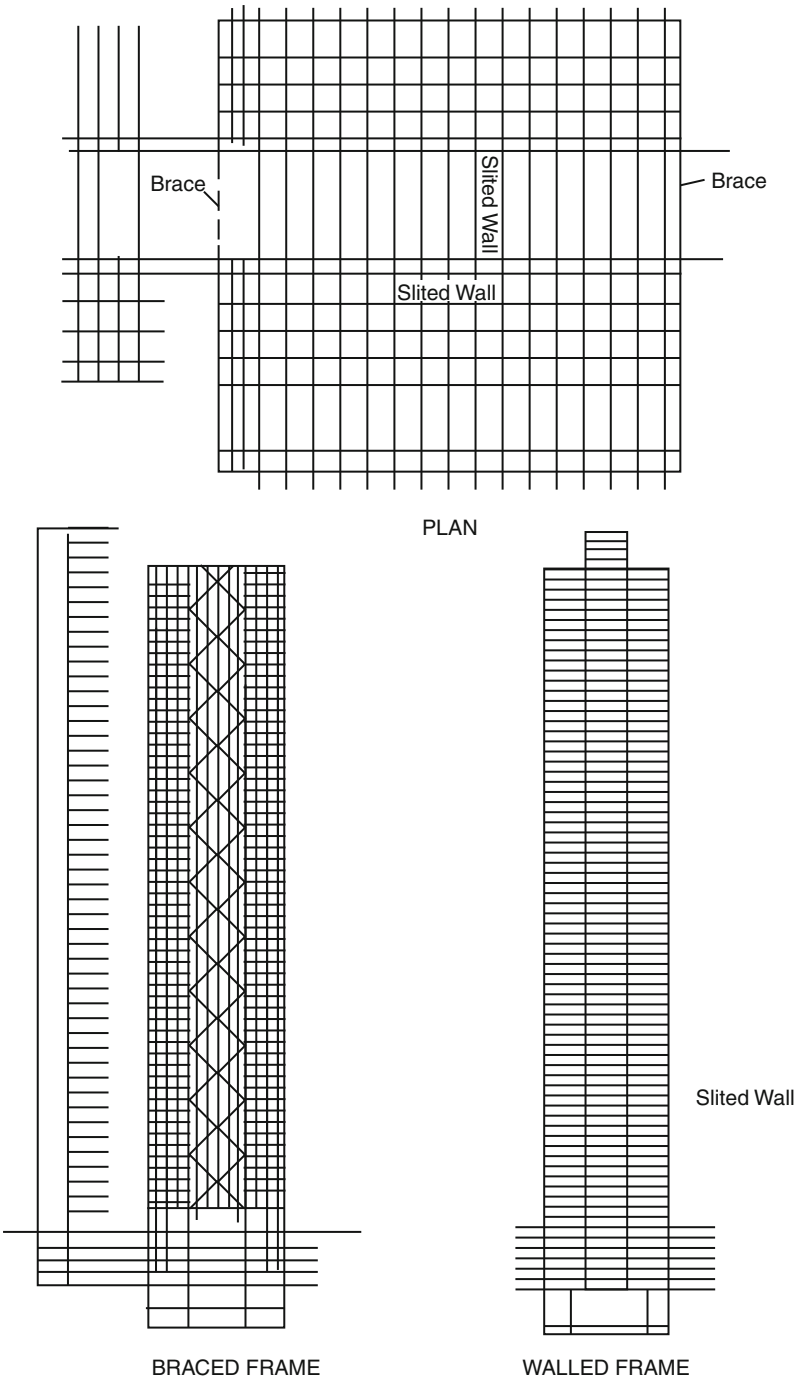


Plate No 7.10 Six-Storey Building with Penthouse

www.EngineeringBooksPDF.com

Soil Property and Foundation Data

For Soil–Structural Interaction

Note: These data are used for soil–structural interaction analysis

GL-m	0–1.0	1.0–6.7	6.7–10.4	10.4–13.2	13.2–15.4	15.4–18.7	18.7–20.0	20.0–25.4	25.4–30.2
Soil	Red loam	Loam	Clay loam	Tuff Clay	Sandy silt	Silt	Very fine sand	Gravel	Clay
N value	–	4–23	3–6	8	4–5	5–8	23	50	>50

Permissible pile Resistance	Cast in situ concrete pile (earth drill method): Long term 160 t/pile 1,200 dia 280 t/pile		
	Outline of the Structure		
Foundation			
Ground type and foundation structure	Pile foundation: Cast in-situ pile supported directly on gravel layer at GL-20.0 m		
Maximum contact pressure (pile resistance)	Cast in situ concrete pile.		
	900 dia at side column	1,200 dia at middle column	1,200 dia at corner column
	Long term		
	156 t/pile	235 t/pile	264 t/pile
	Short term		
	199 t/pile	261 t/pile	382 t/pile
Main structure			
Structural features	It is a menhin structure where the menhin device is placed between the RCC upper structure and the foundation		
Frame classification	Along the length: RCC rigid frame Along the width: RCC antiseismic wall		
Bearing wall, other walls materials for columns	Column – B × D = 400 × 450, 450 × 450, 500 × 500, 450 × 350		
Beams, sections	Beams – B × D = 220 × 750, 220 – 250 × 1050, 220 – 250 × 1,150, 250 × 400; Steel bars – deformed bars SD35 (JIS G 3,112); concrete – FC = 210 kg/cm^2 (for foundation and foundation beam)		
Columns, beams, joints	RCC rigid structure		
Floor	Cast in situ RCC structure		
Roof	Cast in situ flat slab structure		
Non-bearing walls	Outer wall – ALC plate; Inner wall – ALC plate		
Fire-proof coating			
	Structural Design		
Laminated rubber (20 nos)	100–150 ton (8 nos). Each consists of rubber – natural rubber 5 thick × 620 dia (50 layers); steel plate; insertion plate – SS41 (JIS G 3101); flange plate – SS41 (JIS G 3101); 20–28 × 830 dia (top and bottom); fixing bolt – high-tension bolt FBT (JIS B 1186) M24		
	200–250 ton (12 nos). Each consists of Rubber – natural rubber 6 thick × 740 dia (45 layers); steel plate: insertion plate SS41 (JIS G 3101) 3.1 × 740 dia (44 Nos); flange plate – SS41 (JIS G 3101) 24–30 × 985 dia (top and bottom); fixing bolt – High-tension bolt FBT (JIS B 1186) M24.		
	Rubber properties: Rubber hardness: 40 ± 5 25% shear modulus (kg/cm^2): 3.4 ± 1.0		

www.EngineeringBooksPDF.com

(continued)

Steel rod dampers (108 nos)	Elongation (%): >500 Tensile strength (kg/cm^2): > 200 Shear elasticity modulus (kg/cm^2): 5.6 Young's modulus (kg/cm^2): 11.5 Each consists of steel rod – SCM435 (JIS G 4105) three continuous beams (span 20 cm, 45 cm, 20 cm); bearing – SUJ2 (JIS G 4805); steel plate – SS41 (JIS G 3101); base plate – four plates: 16 × 180 × 260; fixing bolt: high-tension Bolt FBT (JIS B 1186) 4 – M16.

Case Study 7.8 A Comparative Study of Results
Analysis Study Seismic waveform type Degree of freedom
Dynamic non-linear F.E El-Centro Traft 7

	Obayashi-Gumi Ltd; Tokyo, Japan				PROGRAM ISORAR and graph G-Type		
S.No	DIRECTION TYPE	*X	*Y	*Z	DIRECTION *X	*Y	*Z
1.	Fundamental Period T (sec)	2.09	2.97	–	-		
(a) mode 1	2.99		–	2.89	2.87	0.33	
(b) mode 2	0.33	0.17	–	0.31	017	0.078	
2.	Damping	0.02 (50 cm/s)		–	0.02	0.02	–
	(ξ & β)	0.01 (25 cm/s)		–	0.01	0.01	–
3.	Shear coefficient (C_i)	0.15 (F1)	0.15 (F1)	–	0.145 (F1)	0.137 (F1)	0.130 (F1)
		0.183 (F2)	0.183 (F2)	–	0.179 (F2)	0.173 (F2)	0.123 (F2)
		0.205 (F3)	0.205 (F3)	–	0.205 (F3)	0.200 (F3)	0.200 (F3)
4.	Seismic load %	– (F2)	1 1 (F1)	–			
	(a) Rigid frame	100 (F1),	↓	–	} The	same as	item 4
	(b) Bearing wall	100 (F3)	99 (β) 99	–	}		
		100 (F5),	1 (3F) 99	–			
		100 (β)	2 (5F) 99	–			
5.	-						
6.	Device U_{max}						
	(a) Input 25 cm/sec	8.31 cm	28.89 cm	–	7.89 cm	8.00 cm	0.075 cm
	(b) Input 50 cm/sec	24.4 cm	23.9 cm	–	23.5 cm	23.1 cm	0.08 cm
	(a) C_i 25 cm/sec	0.101	0.106	–	0.101	0.102	0.02
	(b) C_i 50 cm/sec	0.191	0.192	–	0.189	0.183	0.035
7.	Upper structure Ü A foundation level						
	(a) Iinput 25 cm/s	147.3 cm/s^2	106.8 cm/s^2	–	141.3 cm/s^2	103.3 cm/s^2	10.70 cm/s^2
	(b) Input 50 cm/s	198.5 cm/s^2	187.2 cm/s^2	–	188 cm/s^2	177 cm/s^2	10.99 cm/s^2
8.	Max shear C_i						
	a. Input 25 cm/s	0.108	0.106	–	0.107	0.105	0.04
	b. Input 50 cm/s	0.193	0.192	–	0.190	0.191	0.07

www.EngineeringBooksPDF.com

Case Study 7.9 Six-Storey Buildings

Analysis: Non-Linear Timer Integration

Seismic waveform El-Centro NS and Taft EW; Kobe Data
Case Study C

Post and Telecommunication Center Japan C1: h = height = 37.95 m; A = Total area = 7305 m^2
Devices: LRB = 131; 90 steel dampers

Solano County, California C2: h = height = 28.0 m; A = total area = 4,700 m^2;
Devices: FVD = 20

Inagi Hospital, Inagi, Japan C3: h = height = 35.81m; A = total area = 18,518 m^2;
Devices: LRB isolators = 84; 42 steel dampers

University of Basilicata, Italy C4: h = height = 25m; A = total area = 12,500 m^2;
Devices: LRB isolators = 80

Guangzhou University Building, China C5: h = height = 22.5 m; A = total area = 23,452.6 m^2;
Devices: LRB isolators = 209

Results from SAP2000
Post and Telecommunication Building, Kobe, Japan
Insert drawing of plan of base isolation floor.

C1C1 = Input level 25 cm/s; maximum drift = 1/5,000 and 25 cm
U, top displacement = 13.5; $\mathring{U}$ = 90 cm/s
$\ddot{U}$ = 300 cm/s^2
C2C2 = Input level 25 cm/s; maximum drift = 13.98 cm; U = 36 cm; $\mathring{U}$ = 24.5 cm/s
$\ddot{U}$ 375 cm/s^2
C3C3 = Input level 50 cm/s; max drift = 1/1,780; U = 35 cm; $\mathring{U}$ = 25 cm/s;
$\ddot{U}$ = 200 cm/s^2
C4C4 = Input level 25 cm/s; max drift = 1/500; U = 20 cm; $\mathring{U}$ = 250 cm/s;
$\ddot{U}$ =168 cm/s^2
C5C5 = Input level 25 cm/s; max drift = 1/1,906; U = 21 cm; $\mathring{U}$ = 30 cm/s
$\ddot{U}$ = 220 cm/s

Case Study 7.10 Six-Storey Building
Analysis: Non-linear Time Integration

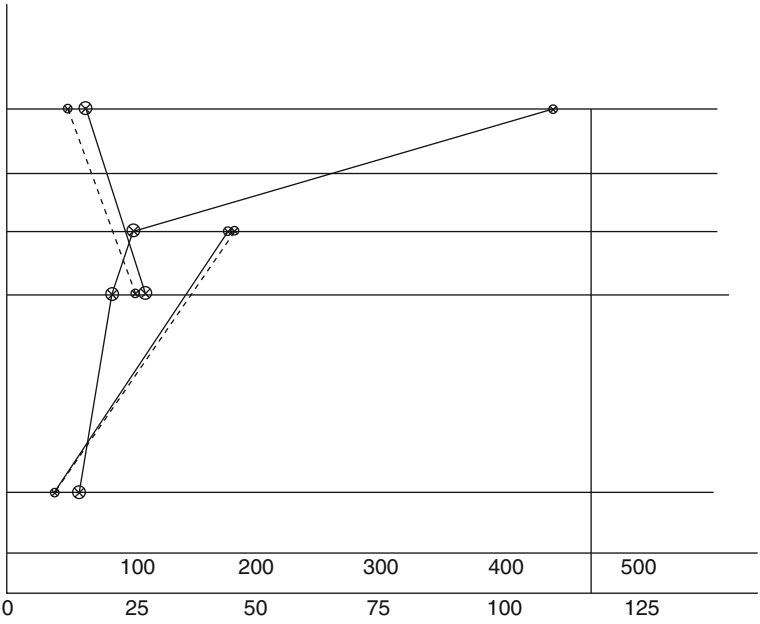
Data: Case Studies C
1. Post & Telecommunication Centre C1:
   h = height = 37.95 m; A = total area = 730,500 m^2;
   Devices: LRB = 131; 90 steel dampers
2. Solano County, California C2:
   h = height = 28.00 m; A = total area = 4,700 m^2
   Devices: FVD = 20

www.EngineeringBooksPDF.com

3. Inagi Hospital, Inagi, Japan C3:
   h = height = 35.81 m; A = total area = 18,518 m^2
   Devices: LRB isolators = 84; 42 steel dampers
4 University of Basilicata, Italy C4:
   h = height = 25.0 m; A = total area = 12,500 m^2
   Devics: LRB isolators = 80
5 Guangzhou University Building, China C5:
   h = height = 22.5 m; A = total area = 23,452 m^2
   Devices: LRB isolators = 209

Results from SAP 2000

C1 Input level = 25 cm/s; max drift = ...and 25 cm; U_{max}. top displacement = 13.50 cm; U = 40 cm/s; Ü = 300 cm/s^2
C2 Input level = 25 cm/s; max drift = 13.98 cm; U_{max}. top displacement = 36 cm/s; Ú = 24.5 cm/s; Ü = 375 cm/ s^2
C3 Input level = 50 cm/s; max drift = 17.80 cm; U_{max}.top displacement = 35 cm; Ú = 25 cm/s; Ü = 200 cm/ s^2
C4 Input level = 25 cm/s; max drift = 1/500; U_{max}. top displacement = 1/500; U = 20 cm; Ú = 250 cm/sec; Ü = 168 cm/s^2
C5 Input level = 220 g; max drift = 1/1,406; U_{max}. top displacement = 21 cm Ú = 30 cm/sec; Ü = 220 cm/s^2



Post & Telecommunication Building, Kobe, Japan

www.EngineeringBooksPDF.com

Case Study 7.11 Seven-Storey Building
Seismic WaveForm : El-Centro NS and TAFT, EW
DATA: CASE STUDY C

Insert floor plan drawing?	
System Plaza Isogo,	C1: h = height = 30.3 m; A = total area = 9,242.13 m^2
Yokohama city, Japan	Devices: Isolators = 24; devices computed = 58
	Dampers = 28
	Lead steel 52 Adopted
Yinhe Building	C2: h = height = 18.9 m; A = total area = 130,000 m^2
Wulumugi city,China	Devices: LRB isolators = 123; Adopted 206
	Dampers = 86
	Devices computed P/C
	LRB + dampers = 200
RESULTS: SAP2000	
	C1 Input level = 50 cm/s; storey drift = 1/200
	U = 39 cm/s; $\mathring{U}$ = 50 cm/s; $\ddot{U}$ = 264 cm/s^2
	C2 Input level = 400 gal; storey drift = 22 cm
	$\mathring{U}$ = 50 cm/s; $\ddot{U}$ = 400 cm/s^2; C_i = 0.21
Insert graph from excel?	

www.EngineeringBooksPDF.com

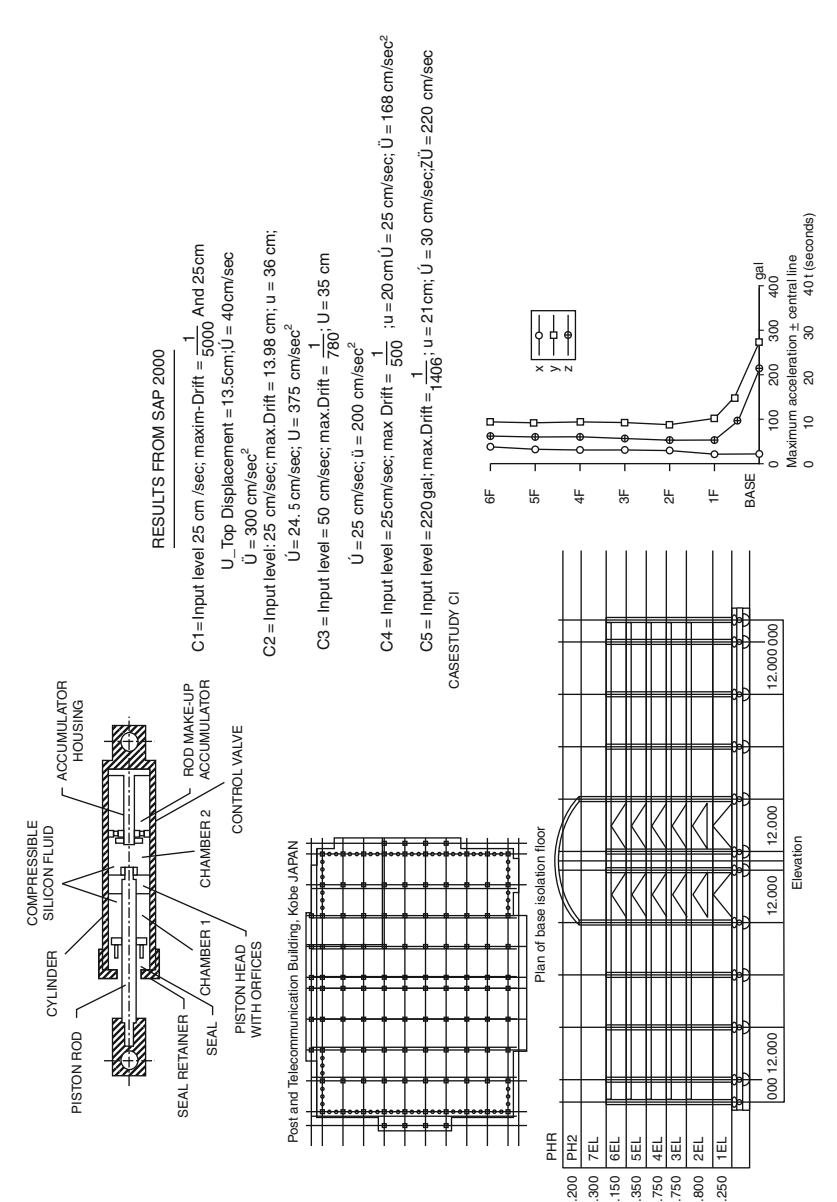
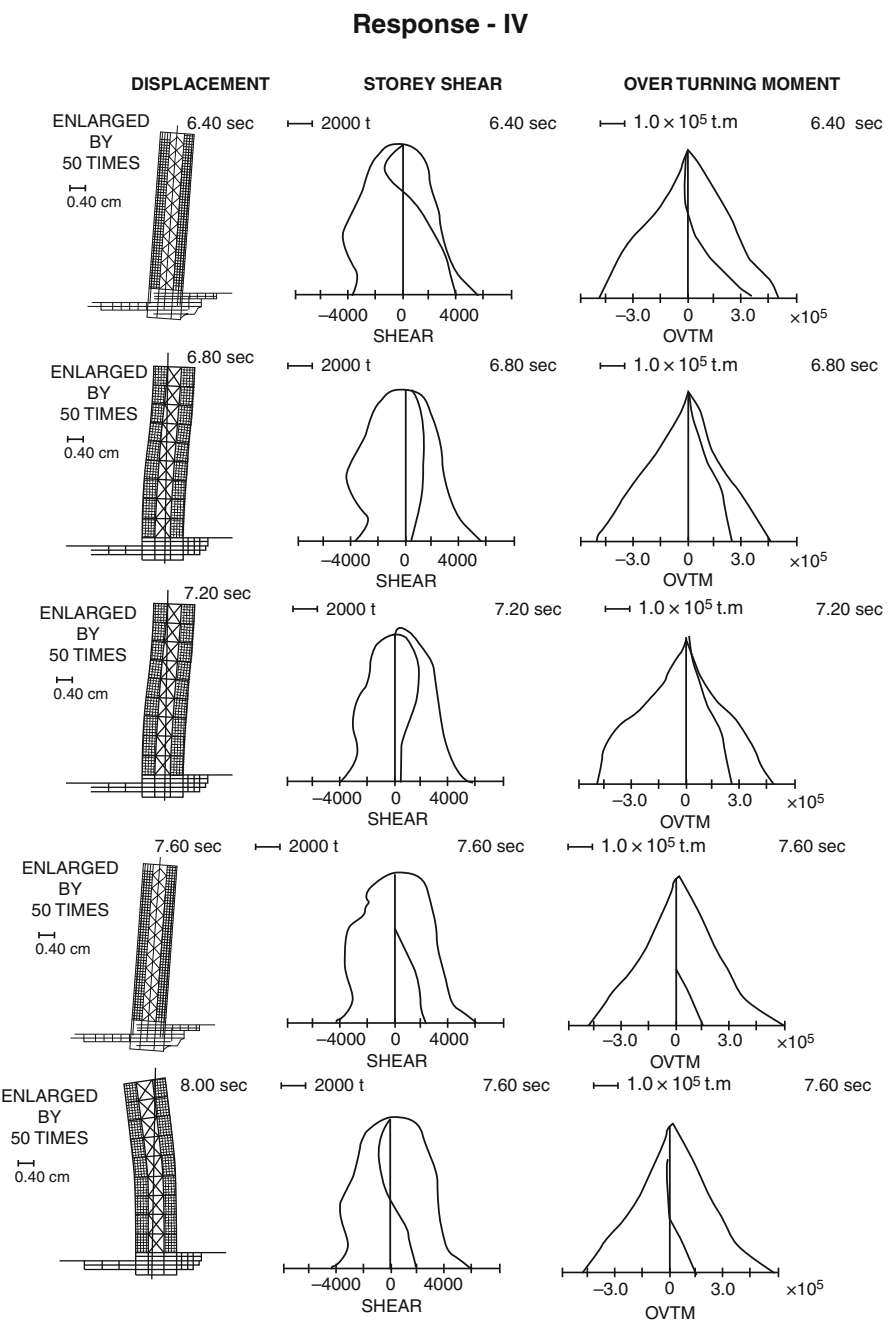


Plate 7.11 Seismic WaveForm: El-Centro NS and TAFT EW

www.EngineeringBooksPDF.com



Animated earthquake response 4

Plate 7.12

www.EngineeringBooksPDF.com

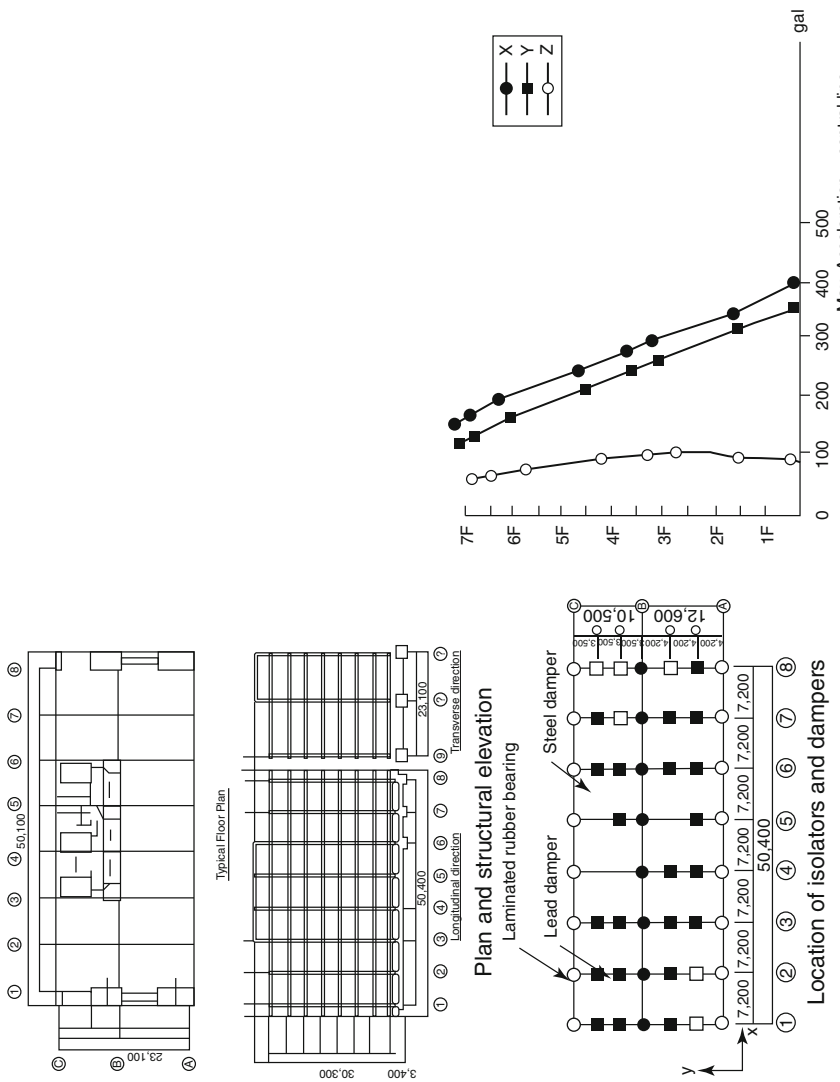


Plate 7.13 Seven-storey building. Acceleration and velocity response spectra (Courtesy of Japan Seismological Society, Tokyo, 1995, Fig. 6)

www.EngineeringBooksPDF.com

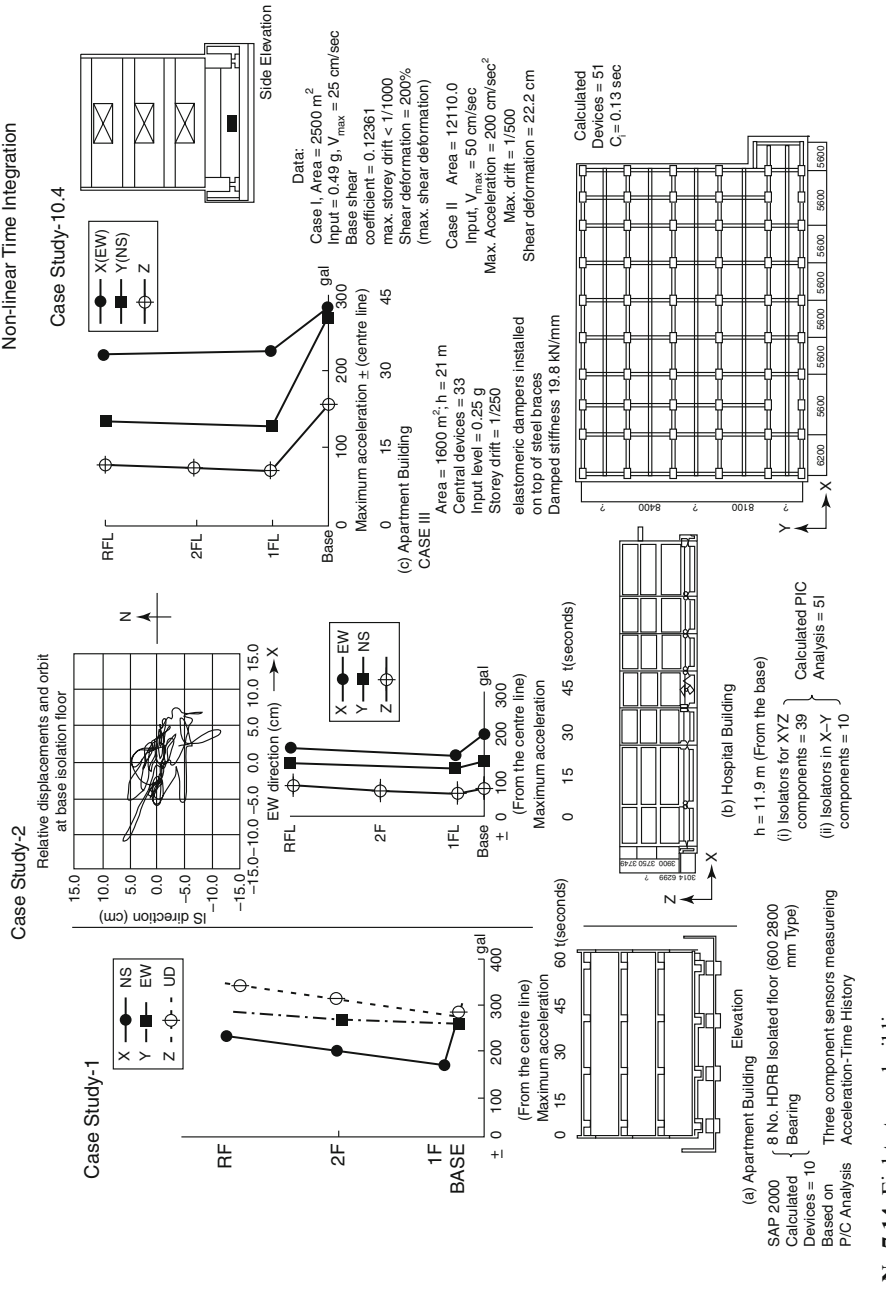
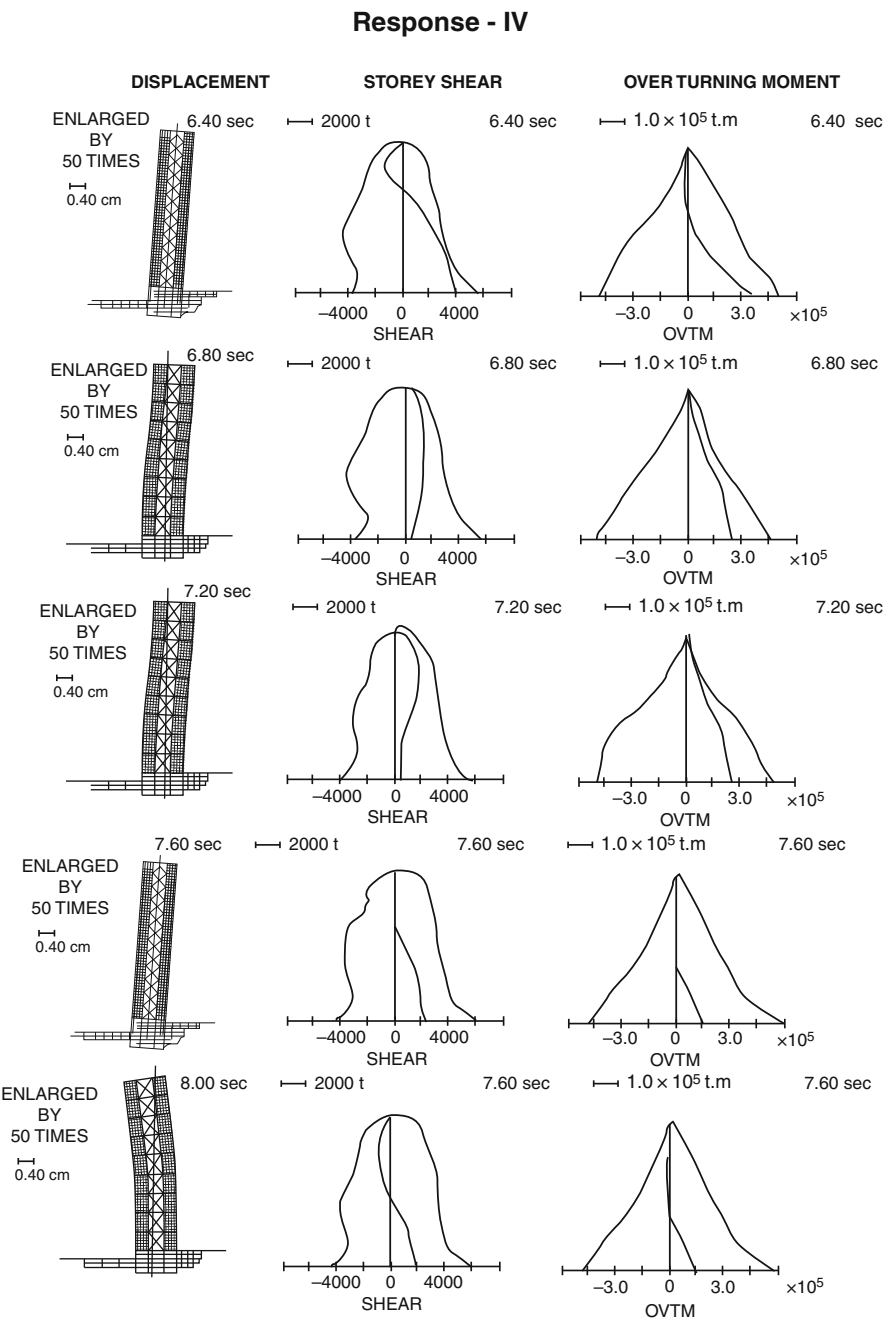


Plate No 7.14 Eight-storey buildings

www.EngineeringBooksPDF.com



Animated earthquake response 4

Plate No 7.15

www.EngineeringBooksPDF.com

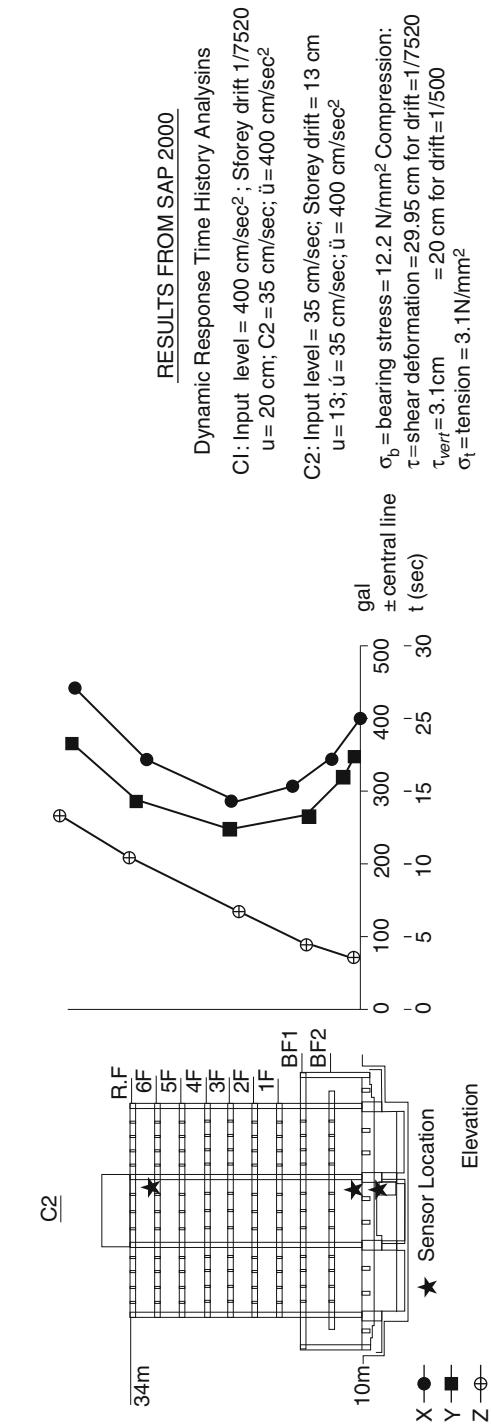


Plate 7.16 SMB – comparative assessment using the El-Centro and Kobe earthquakes

www.EngineeringBooksPDF.com

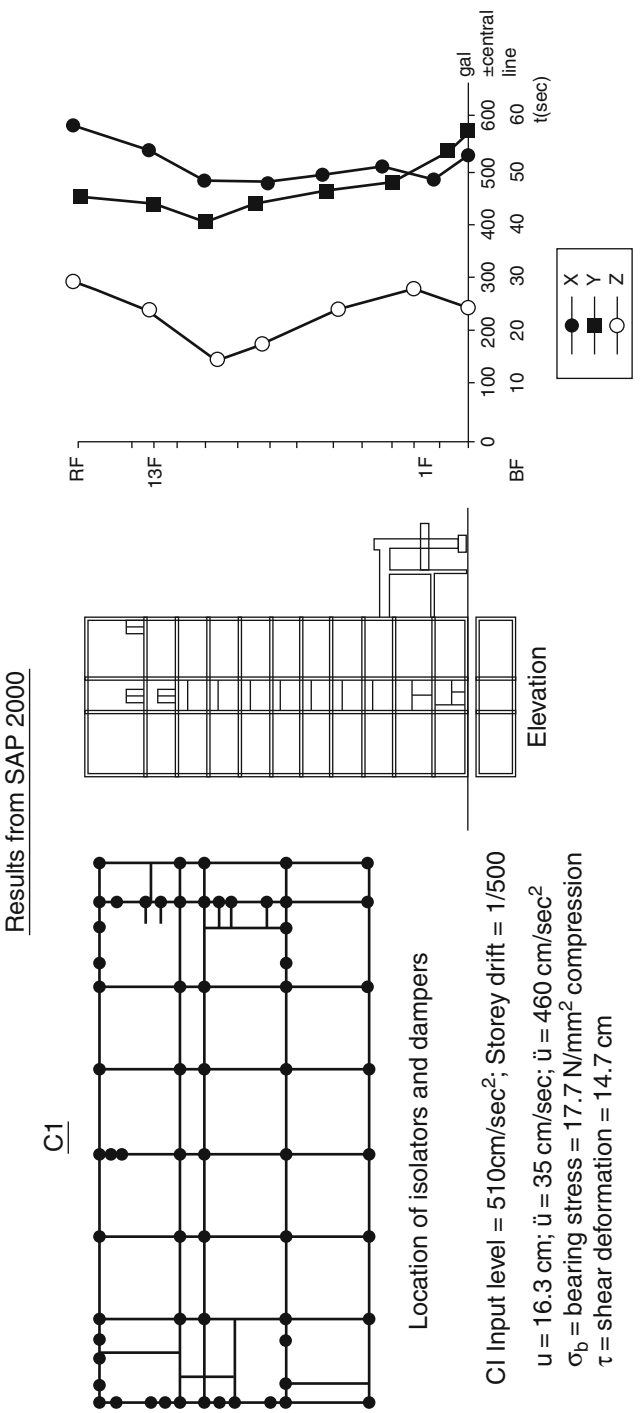
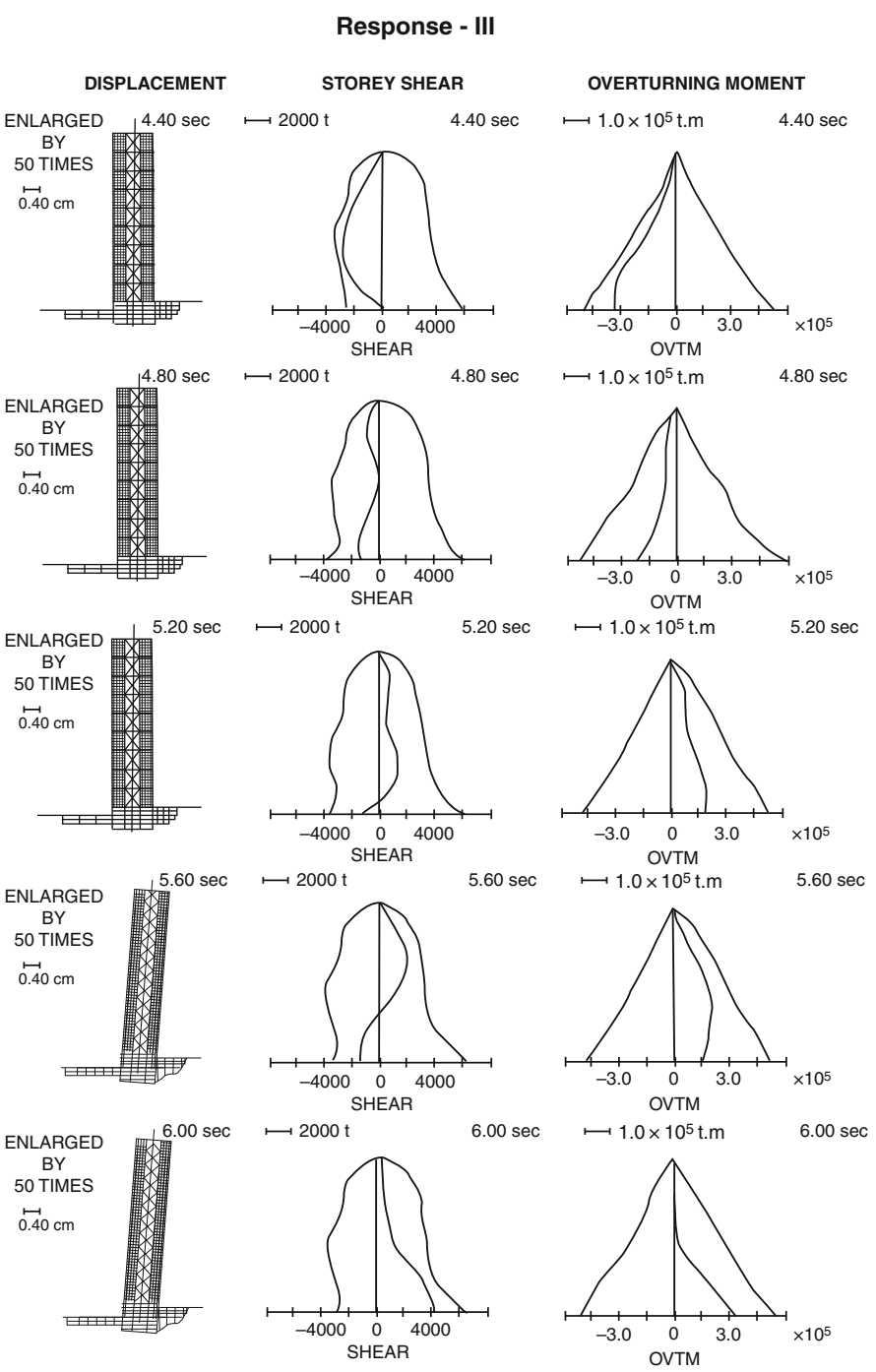


Plate No 7.17 Thirteen-storey building

www.EngineeringBooksPDF.com



Animated earthquake response 3

Plate No 7.18

www.EngineeringBooksPDF.com

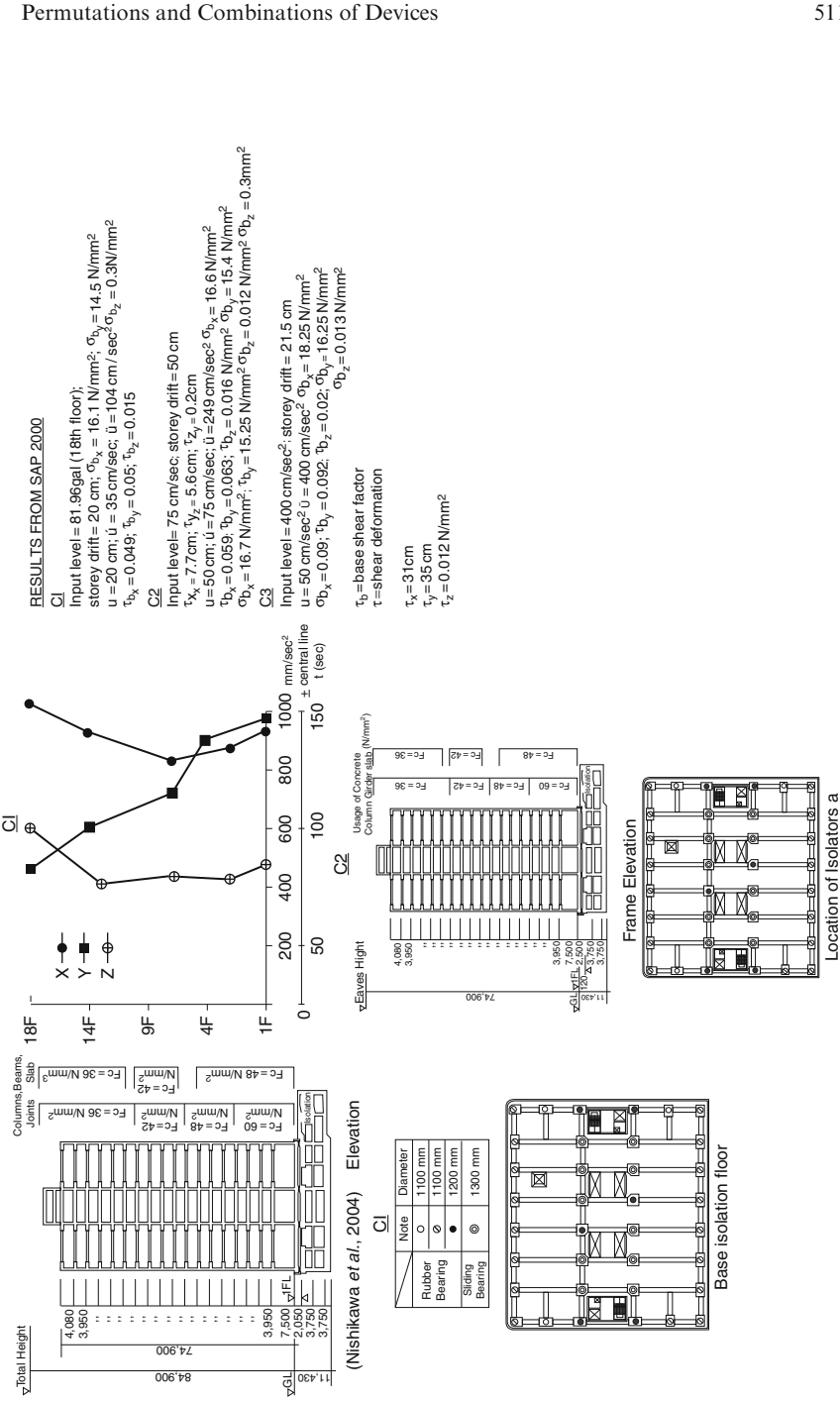


Plate No 7.19

www.EngineeringBooksPDF.com

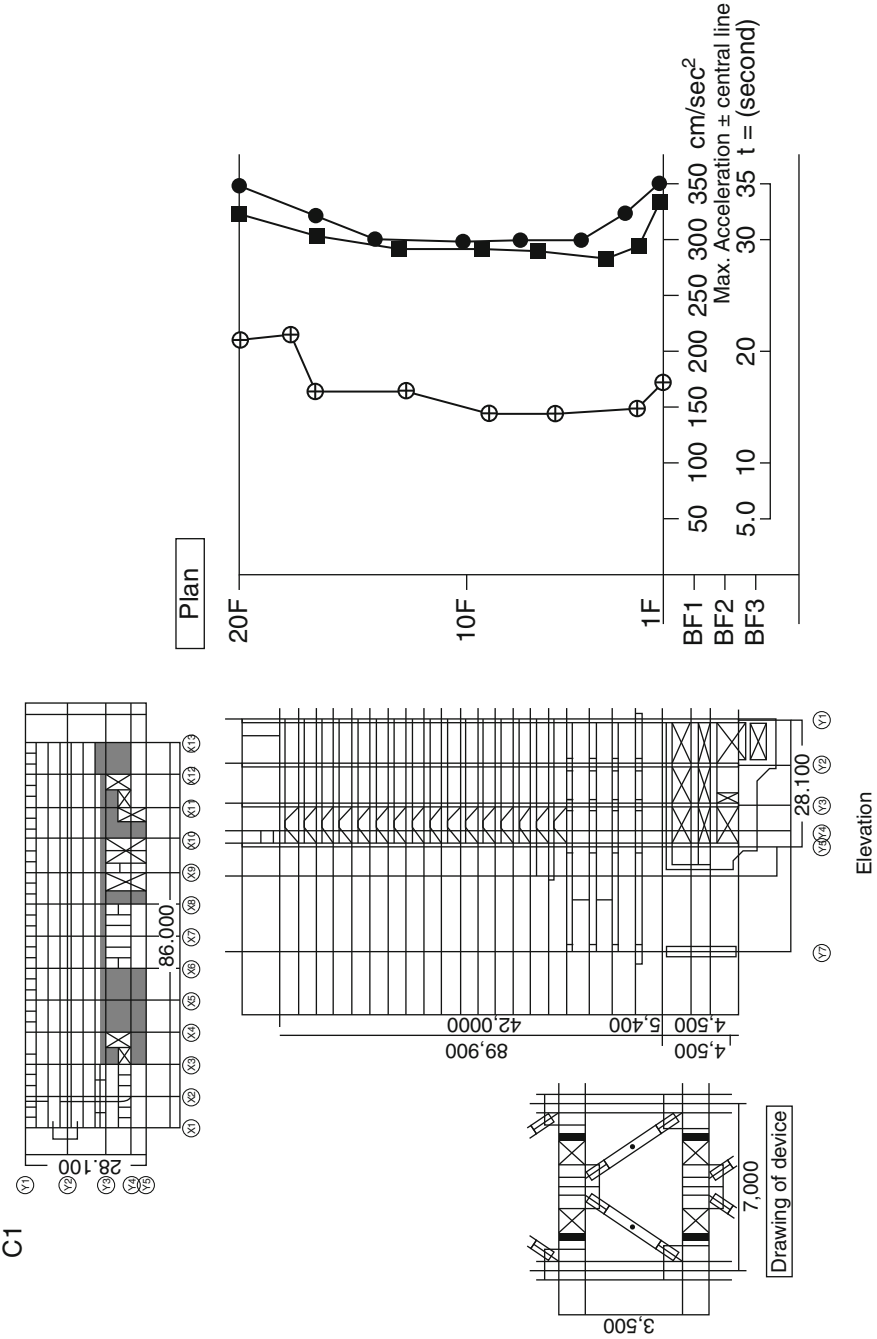


Plate 7.20

www.EngineeringBooksPDF.com

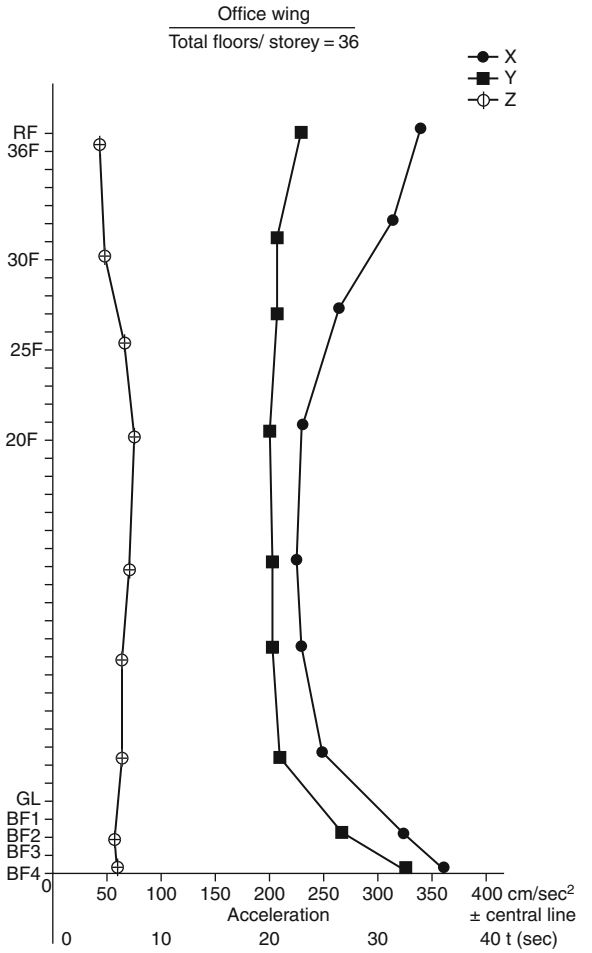


Plate 7.21

www.EngineeringBooksPDF.com

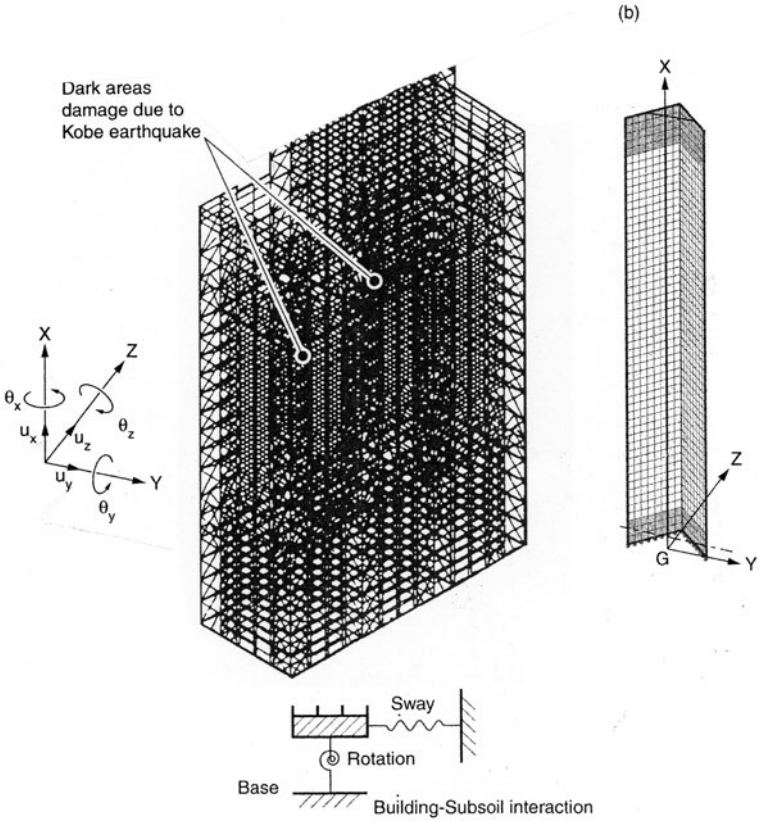


Plate 7.22 *(a) Finite element mesh scheme for the SMB Building. (b) Building substructure (total No. of 20 substructures)*

Data: Case Studies C

1. C1 USC University Hospital, California, USA:
   h = height = 33.5 m; A = total area = 3,995 m^2; devices: LRH = 68; IHR = 8
2. C2 Kadokania Head Office, Tokyo, Japan:
   h = height = 30.4 m; A = total area = 8016 m^2; devices: HDR isolators = 16
3. C3 Shanghai International Circuit, China:
   h = 34.82 m; A = total area = 13,000 m^2; devices: Pot bearing elastomer = 4
4. C4 Linhailu Housing Completion, China:
   h = height = 34.10 m; A = total area = 202.3 m; devices: isolators = 22

www.EngineeringBooksPDF.com

5. C5 University Hospital Building, Northridge:
   $h = 35.0$ m; A = total area = 6,308.5 m; devices: LR isolators = 68; N.R = 81
   Total = 177 Adopt

C5: University Building Northridge, USA	Devices from P/C computed as
	= HDR isolators = 24
	= LR isolators = 70
	= LR/NR = 78
	Total = 172

Results from SAP2000
Analysis: Non-linear Time Integration

C1: Input level = 0.45 g; Storey drift = 6.5/1,000
U = 26.67 cm; $\mathring{U}$ = 60 cm/s; $\ddot{U}$ = 350 cm/s^2

C2: Input level = 75 cm/sec; Storey drift = 1/1,360
U = 37.1 cm; $\mathring{U}$ = 75 cm/sec; $\ddot{U}$ = 500 m/s^2

C3: Input level = 200 cm/sec; Storey drift = 1/100
U = 20 cm; $\mathring{U}$ = 35 cm/sec^2; $\ddot{U}$ = 250 cm/s^2

C4: Input level = 400 gal; Storey drift =
U = 16.7 cm; $\mathring{U}$ = 50 cm/s; $\ddot{U}$ = 400 cm/s^2

C5: Input level = 350 gal; Storey drift = 20 cm
U = 18.9 cm; $\mathring{U}$ = 29 cm/s; $\ddot{U}$ = 359 gal

C5: Shear deformation and strain = 20 cm; C_3 case = 6 cm; C_5 case.
τ_{vert} = 3.2 mm
σ_b = bearing stress = 10 N/mm^2 compression.

Case Study 7.12 Twelve Storey building
Seismic waveform: El-Centro; Taft EW; Isobe 1995
Data Case Study C

1. C1 King County Court House, Washington, USA:
   h = height = 65.0 m; A = total area = 55,560 m^2;
   Devices: steel braces = 40; steel dampers = 96; device from P/C = 105 (adopted)
2. C2 Education Mansion, Nanjing, China:
   h = height = 46.80 m; A = total area = 8,500 m^2
   Devices: viscous and non-viscous dampers = 64; device from P/C = 71 (adopted)

www.EngineeringBooksPDF.com

Results from SAP2000

C1 Input level = 400 cm/s; storey drift = 18.2 cm; U_{max}. top displacement = 25.2 cm; $\dot{U}$ = 35 cm/s; $\ddot{U}$ = 0.35 g
C2 Input level = 510 cm/s^2; max drift = 1/140; U_{max}. top displacement = 13 cm/s; $\dot{U}$ = 35 cm/s; $\ddot{U}$ = 510 cm/s^2

σ_b = bearing stress = 11.9 N/mm^2 compression.
τ = shear deformation = 28.5 N/mm^2
τ_{vert} = 2.95 mm
δ_t = tension = 2.95 N/mm^2

Case Study 7.13 Eighteen-Storey Building
Seismic waveform, El-Ccentro NS, Taft EW

Data Case Study C

1. C1 Office Building, Sendai, Japan:
   h = height = 84.9 m; A = total area = 32,801.20 m^2;
   Devices: sliding and R. bearings = 36
2. C2 Sendai Mori Building, Japan:
   h = height = 74.9 m; A = total area = 43,193 m^2
   Devices: isolators = 26; sliding bearings = 10
3. C3 Sendai Mori Building, Japan:
   h = height = 51.9 m; A = total area = 160,000 m^2
   Devices: ME isolators = 110; leach dampers = 110

Results from SAP2000
C1 Input level = 81.96 gal (18th floor); storey drift = 20.0 cm;
C2
C3
σ_b =
τ =
τ_{vert} =
δ_t

Case Study 7.14 ToranoMon San-Chome building
Designed by Shimizu Construction, Tokyo, Japan

Building Data
Reinforced concrete rigid frame building with non-bearing walls. Refs. Plate 7
Total floor area = 3372.989 m^2; building height = 29.70 m
Area/floor = 392.352 m^2; type of earthquake: El-Centro Taft

www.EngineeringBooksPDF.com

Seismic Waveforms

Initial velocity	El-Centro (1940)	Taft (1952)
35 cm/s	358 cm/s^2	348 cm/s^2
50 cm/s	551 cm/s^2	497 cm/s^2
Total floors above ground = 8		
Total: Isolators	= 12 with A and B permutation and combination	
Rod damper	= 23	
Total number calculated = 35 = 25 No. actually adopted		

Soil Property and Foundation Data
Note: This is used for soil-structure interaction

GL-m	0–8.7	8.7–21.4	21.4–39.3	>39.3
Soil layer	Clay with fine sand	Fine sand	Sand pebbles	Fine sand
N value	9–31	11–50	> 50	> 50

Permissible pile resistance	Cast in situ concrete pile: resistance (t/pile): 3000 dia – 900; 2,700 dia – 850; 2,400 dia – 710; 2,200 dia – 620; 1,300 dia – 270; short-term resistance: twice the long-term resistance
Foundation	
Ground type and foundation structure	Cast in situ concrete pile is supported directly on gravelly soil layer at GL-23m
Maximum contact pressure (pile resistance)	1,300 dia – 253 t; 2,200 dia – 605 t; 2,400 dia – 661 t; 2,700 dia – 787 t; 3,000 dia – 851 t
Main structure	
Structural features	It is a structure where the device consisting of laminated rubber bearing and steel damper is placed between the RCC upper structure and the foundation
Frame classification	*X* direction: RCC rigid frame and RCC antiseismic wall *Y* direction: RCC rigid frame and RCC antiseismic wall
Material for column	RCC structure, column – B × D 700 × 700, 900 × 1000
Beams, sections	Beam B × D = 500 × 700 – 500 × 1000; Concrete – common concrete, FC = 240 kg/cm^2; Steel bars – deformed Bars SD30A, SD53 (JIS G 3112)
Columns, beams, joints	RCC rigid structure
Floor	RCC slab
Roof	RCC slab
Non-bearing wall	Outer wall – RCC structure; Inner wall – RCC structure, concrete block structure

Structural Design

The device			
Laminated rubber	Each laminated rubber assembly consists of		
OD of laminated rubber	880 dia	960 dia	1030 dia
Inner rubber	Natural rubber		
Thickness	5.4	6.2	6.0
Layers	36	30	30

www.EngineeringBooksPDF.com

(continued)

Outer rubber	Special synthetic rubber 8 mm thick		
Inner steel plate	SPHC (JIS G 3131)		
Thickness	2.2	2.2	2.2
Layers	35	29	29
Outer steel plate			
(flange plate) Type I	SS41 (JIS G 3106)		
Thickness	28	32	32
Layers	2 layers, top and bottom		
Type II	SM50A (JIS G 3101)		
Thickness	41	47	32
Layers	2 layers, top and bottom		
Fixing bolt	SS41 (JIS G 3101)		
Type I	8-M30	8-M36	8-M36
Type II	16-M30	16-M36	8-M36
Rubber properties	Inner rubber	Outer rubber	
Hardness (JIS A type)	$40^0 \pm 5$	60 ± 5	
Stress at 25% elongation (kg/cm^2)	3.4 ± 10	6.0 ± 2.0	
Tensile strength (kg/cm^2)	200 min	120 min	
Shear elongation (%)	500 min	600 min	
Steel rod damper	Each set consists of Steel rod – SS45C (JIS G 4501), dia 35 min length 994 min; piston – SS41 (JIS G 3101) dia 160 mm length 300 mm; dia 235 mm, length 60 mm (ends); cylinder – SS41 (JIS G 3101), dia 235 mm, length 290 mm, thickness 32.5 mm; steel rod fixing plate – SS41 (JIS G 3101), dia 600 mm; thickness 60 mm; flange – SS41 (JIS G3101), dia 600 mm, thickness 40 mm; fixing bolt – SS41 (JIS G 3101), 8-M36		

Design Details

A Comparative Study of Results

Case Study 7.15

Analysis type Seismic waveform type → El-Centro and Taft Degree of freedom 9

Dynamic non-linear FE Type of analysis

S. No				Program Isopars		
Direction				Direction		
Type	X*	Y*	Z*	X*	Y*	Z*
1 Fundamenta period T(sec)						
(a) mode 1	1.62	1.52	–	1.59	1.50	0.06
(b) mode 2	2.61	2.57		2.52	2.98	0.39
2 Damping (ξ & β)	1% (upper structure)	0%		1%	1%	0%
3 Shear coefficient C_i	0.150 (LF)	0.150 (LF)				
	0.191 (IF) 0.296 (TF)	0.191 (IF) 0.296 (TF)		} same	AS 3 →	→

www.EngineeringBooksPDF.com

(continued)

S. No	Direction			Program Isopars		
	Type	X*	Y*	Z*	X*	Y*	Z*
4	Seismic load %						
	(a) Rigid frame	35 (LF); 62 (IF) 108 (TF)	4 (LF), 18 (IF) 45 (TF)				
	(b) Pressure wall	65 (LF); 38 (IF) 8 (TF)	96 (LF), 82 (IF) 55 (TF)		} same	AS →	→
5	Device U_{max}						
	(a) Input 35 cm/s	12.5 cm (Taft)	12.4 cm (Taft)		11.71 cm (El-Centro)	11.67 cm (El-Centro)	0.05 cm (El-Centro)
6	(b) Input 50 cm/s	18.4 cm	23.10 cm		17.93 cm (El-Centro)	21.75 cm (El-Centro)	1.25 cm (El-Centro)
7	Upper structure	146 cm/s^2	132 cm/s^2		138 cm/s^2	128 cm/s^2	50 cm/s^2
	Ü at foundation	203 cm/s^2	189 cm/s^2		198 cm/s^2	190 cm/s^2	75 cm/s^2
8	Max shear C_i 1st floor						
	(a) Input 35 cm/s	0.113	0.118		0.114	0.120	0.110
	(b) Input 50 cm/s	0.164	0.186		0.170	0.190	0.113

Case Study 7.16 Nine-Storey building
Seismic WaveForm: El-Centro NS TAFT EW, KUBA 1995

Data: Case Studies C

1. C1 Tonghui Gardens, Beijing, China:
   h = 33.2 m, A = 480 m^2; devices: LRB isolators
2. C2 Government Office Building:
   h = 46 m, A = 6,680 m^2 = 4,200; devices: lead dampers = 600
   Kushiro Japan

Devices computed from C/P = 4,900 (adopted)

Results from Dynamic Response, Time History Analysis SAP2000

C1: Input level = 400 cm/s^2; storey drift = 1/7520;
U = 20 cm, $\mathring{U}$ = 35 cm/s, $\ddot{U}$ = 400 cm/s^2

C2 : Input level = 35 cm/s, storey drift = 13 cm;
U = 13 cm, $\mathring{U}$ = 35 cm/s, $\ddot{U}$ = 400 cm/s^2

σ_b = bearing stress = 12.2 N/mm^2 compression
τ = shear deformation = 29.95 cm for drift = 1/7500
τ_{vert} = 3.1 cm = 20 cm for drift = 1/500
σ_t = tension = 3.1 N/mm^2

Case Study 7.17 Thirteen-Storey building
Seismic WaveForm El-centro NS, TAFT EW; KOBE

www.EngineeringBooksPDF.com

Data: Case Study C

Suqian Renfanzhihui Building, Seqian City, China

C1: h = height = 48.9m, A = total area = 12,300 m^2

Devices: LE and friction sliding isolators = 65
Viscous dampers = 4
= 69 Adopted

Computed from P/C 63
6
69

Case Study 7.18 Nine-storey building
Seismic Waveform: El-Centro NS; Taft EW, Kuba, 1995

Data Case Study
1. C1 Tonghui Gardens, Beijing, China:
   h = 33.2 m, A = 480,000 m^2; devices: LRB isolators
2. C2 Government Office Building, Kushiro, Japan:
   h = 46 m, A = 6,680 m^2 = 4,200; devices: lead dampers = 600
   Devices computed from C/P = 4,900 (adopted)

Results from Dynamic Response, Time History Analysis SAP2000

C1: Input level = 400 cm/s^2; storey drift = 1/7520;
U = 20 cm, $\dot{U}$ = 35 cm/s, $\ddot{U}$ = 400 cm/s^2

C2: Input level = 35 cm/s, storey drift = 13 cm;
U = 13 cm, $\dot{U}$ = 35 cm/s, $\ddot{U}$ = 400 cm/s^2

σ_b = bearing stress = 12.2 N/mm^2 compression
τ = shear deformation = 29.95 cm for drift = 1/7500
τ_{vert} = 3.1 cm = 20 cm for drift = 1/500
σ_t = tension = 3.1 N/mm^2

Case Study 7.19 Thirteen-Storey building
Seismic Waveform: El-Centro NS; Taft EW, Kuba, 1995

Data: Case Study
1. C1 Seqian Renfanzhihui Building, Seqian City, China
   h = height = 33.2 m, A = total area = 480,000 m^2;
   Devices: LE and Friction sliding isolators = 65, viscous dampers = 4
   → 69 adopted

Computed from PC 63
6
69

www.EngineeringBooksPDF.com

Results from SAP2000

C1: Input level = 510 cm/s^2, storey drift = 1/500;
U = 16.3 cm, $\mathring{U}$ = 35 cm/s, $\ddot{U}$ = 460 cm/s^2
σ_b = bearing stress = 17.7 N/mm^2 compression
τ = shear deformation = 14.7 cm

Case Study 7.20 Twenty-Storey Building
Seismic Waveform: El-Centro NS; Taft EW, Kuba, 1995

Data: Case Study

1. C1 Shinagawa Station Building, Minatoku, Japan
   h = height = 90.4 m, A = total area = 62,754.200 m^2;
   Devices: Steel unbonded braces and hysteric steel dampers = 195

   Computed from PC

$$\overline{189}$$

Results from SAP2000

C1 : Input level = 50 cm/s^2, storey drift = 1/100;
U = 18.4 cm, $\mathring{U}$ = 50 cm/s, $\ddot{U}$ = 259 cm/s^2

Ci = max shear coefficient = 20

τ_{bx} = 0.051; τ_{by} = 0.061; τ_{bz} = 0.017
σ_{bx} = 18.1 N/mm^2; σ_{by} = 15.7 N/mm^2; σ_{bz} = 0.147 N/mm^2
σ_b = bearing stress
τ = shear deformation
τ_{vert} =
σ_t = tension

Case Study 7.21 Eight-Storey Building
Seismic waveform: El-Centro NS; Taft EW, Kuba, 1995

Data: Case Studies C

1. C1 USC University Hospital California, USA:
   h = height = 33.5 m, A = total area = 3,995 m^2; devices: LRH = 68; IHR = 8
2. C2 Kadokawa Head Office, Tokyo, Japan:
   h = height = 30.4 m, A = total area = 8,016 m^2; devices: HDR isolators = 16
3. C3 Shanghai International Circuit, China:
   h = height = 34.82 m, A = total area = 13,00 m^2; devices: pot-bearing elastomer = 4
4. C4 Linhaitu Housing Comletion, China:
   h = height = 34.1 m, A = total area = 2,002.3 m^2; devices: isolators = 22
5. C5 University Hospital Building, Northridge:
   h = height = 35.0 m, A = total area = 6,308.5 m^2; devices: LRH isolators = 68; N.R = 81

www.EngineeringBooksPDF.com

Devices computed from P/C:

= HDR isolators	= 24
= LR isolators	= 70
= LR/NR	= 78
	172

Results from SAP2000
Analysis Non-linear Time Integration

C1: Input level = 0.45 g; storey drift = 6.5/1,000;
$U = 25.67$ cm, $\dot{U} = 60$ cm/s, $\ddot{U} = 350$ cm/s^2

C2: Input level = 75 cm/s, storey drift = 1/1360;
$U = 37.1$ cm, $\dot{U} = 75$ cm/s, $\ddot{U} = 500$ cm/s^2

C3: Input level = 200 cm/cm^2; storey drift = 1/1000;
$U = 20.0$ cm, $\dot{U} = 35.0$ cm/s, $\ddot{U} = 250$ cm/s^2

C4: Input level = 400 gal, storey drift = 20 cm
$U = 16.7$ cm, $\dot{U} = 50$ cm/s, $\ddot{U} = 400$ cm/s^2

C5: Input level = 350 gal, storey drift =
$U = 18.7$ cm, $\dot{U} = 29$ cm/s, $\ddot{U} = 3{,}590$ cm/s^2

σ_b = bearing stress = 10.0 N/mm^2 compression
τ = shear deformation and strain = 20.0 cm for C3 case
= 6.0 cm for C5 case

τ_{vert} = 3.2 mm
σ_t = tension = 3.1 N/mm^2

Case Study 7.22 Eight Story Building
Seismic Waveform: El-Centro NS; Taft EW, Kuba, 1995

Data: Case Studies C

1. C1 Los Angeles City Hall, LA, USA:
   h = height = 42.0 m, A = total area = 100,406.7 m^2;
   Devices: Isolators (HDR + SLB = viscous dampers) = 526 actually placed
   Isolators (HDR + SLB = viscous dampers) = *59 (calculated)

C1: Input level = MCE (10% in 100 years); storey drift = 3/1000;
$U = 53.30$ cm, $\dot{U} = 35$ cm/s, $\ddot{U} = 0.35$ g

Results from SAP2000 and Program ISOPAR for checking results
*using permutation/combination and finally checked by time history analysis

$\tau_{bx} = 0.071$; $\tau_{by} = 0.019$; $\tau_{bz} = 0.020$
$\sigma_{bx} = 20.2$ N/mm^2; $\sigma_{by} = 17.7$ N/mm^2; $\sigma_{bz} = 0.158$ N/mm^2
$C_i = 0.31$

Total floors/storeys = 36

www.EngineeringBooksPDF.com

7.5 Seismic Design of Tall Buildings in Japan – A Comprehensive Study

7.5.1 General Introduction

Kiyushi Muto in his report (MUTO Report 73-1-1, May 1973) laid out a comprehensive method for the planning and design of tall buildings ($h \leq 45$m and $h > 45$m) in Japan. In order to obtain horizontal seismic coefficients, Tables 10.14 and 10.15 give preliminary calculations based on an old Japanese code. In the same section, the work has been modified by including the effects of vertical acceleration. The SMB building of 55 storeys is taken as a study case (Plate 7.8).

The Muto Institute has provided a flow chart (Fig. 7.1) which indicates the AIJ guidelines for the seismic analysis and design of tall buildings in Japan. It is suggested that preliminary design planning be checked and analysed against several earthquakes. Dynamic analysis is performed using a rigorous vibration model in conjunction with structural stiffness. A series of computer programs have been developed (FAPP I to FAPP IV) for steel structures. Figures 7.9 and gives a brief illustration of what these computer programs can do. Examples in Table 3.18 indicate the response control in actual tall buildings.

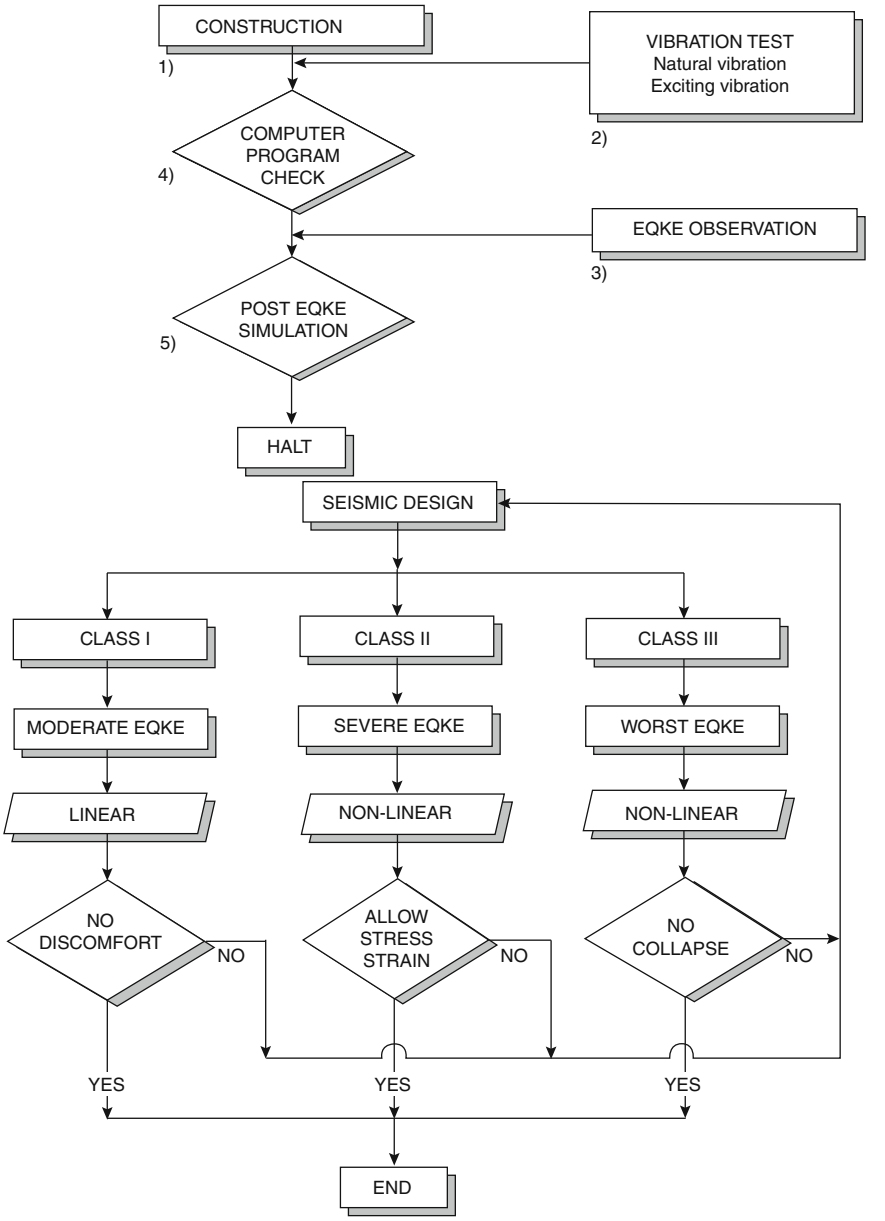
After developing a sound technique for planning, testing various buildings and obtaining a criterion for the seismic analysis of tall buildings, the Muto Institute took up the case of the Shinjuku Mitsui Building (SMB) in Tokyo, a 55-storey, 225m high office building as shown in Plate 7.8. Typical floor areas are 58.4×44.5m. The building has sufficient stiffness against strong winds and typhoons, which frequently occur in Japan. The stiffness of this building was assessed initially by a value given by the fundamental natural period $T_1 = 0.1N$ where N is the number of storeys. Hence $T_1 = 0.1 \times 55 = 5.5$ seconds. Various layouts and schemes were considered but T_1 was not sufficient in the transverse direction. The final suitable design layout is shown in the Muto Report.

The El-Centro Earthquake was considered as the basis for the animated earthquake response of the SMB building.

7.5.2 Resimulation Analysis of SMB Based on the Kobe Earthquake Using Three-Dimensional Finite Element Analysis

The earthquake of 17 January 1995 that occurred in the area of Kobe in southwestern Japan, also known as the Hanshin or Hyogo-Ken Nanbu Earthquake, caused extensive damage and numerous casualties. The magnitude of this earthquake was $M = 7.2$. Various universities and institutes in Japan reported crust deformations, the foreshocks, with around 6,000 events

www.EngineeringBooksPDF.com



Note: Consideration should be paid on the strong wind effects together with earthquake motion

Fig. 7.1

www.EngineeringBooksPDF.com

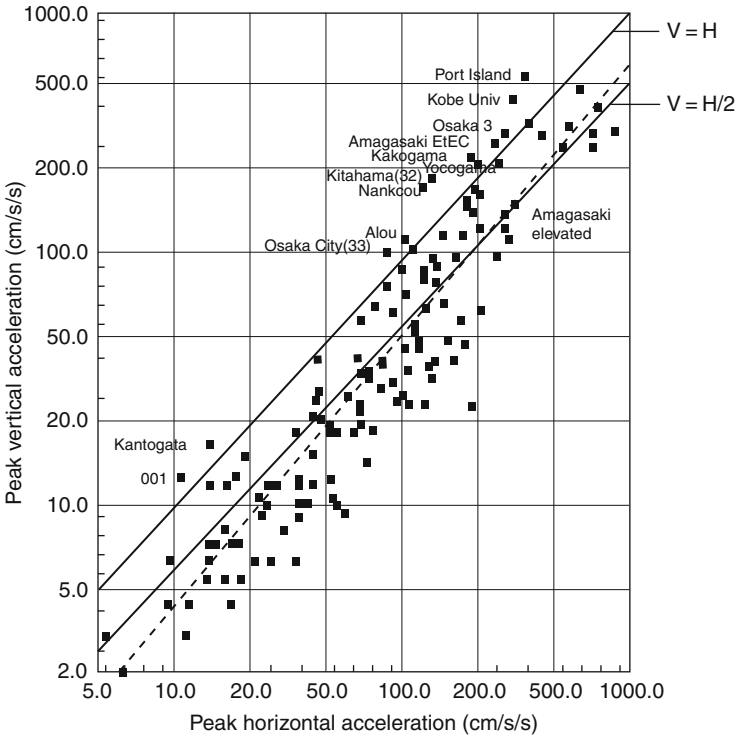


Fig. 7.2 Plots of peak horizontal acceleration versus peak vertical acceleration (courtesy of Japan Seismological Society, Tokyo, 1995, Fig. 4)

immediately after these shocks, irregular recordings of electromagnetic signals of both high and low frequency and disturbances in seawater temperature.

For the first time it became clear how important the peak vertical acceleration is in conjunction with peak horizontal acceleration. Figures 10.2 and 10.3 produced by the Seismological Society of Japan give acceleration and velocity

7.5.2.1 Data I

Maximum horizontal acceleration	818 gal
Maximum vertical acceleration	447 gal
Maximum horizontal velocity	40 kine
Maximum vertical velocity	90 kine
Maximum horizontal displacement	11 cm
Maximum vertical displacement	21 cm

www.EngineeringBooksPDF.com

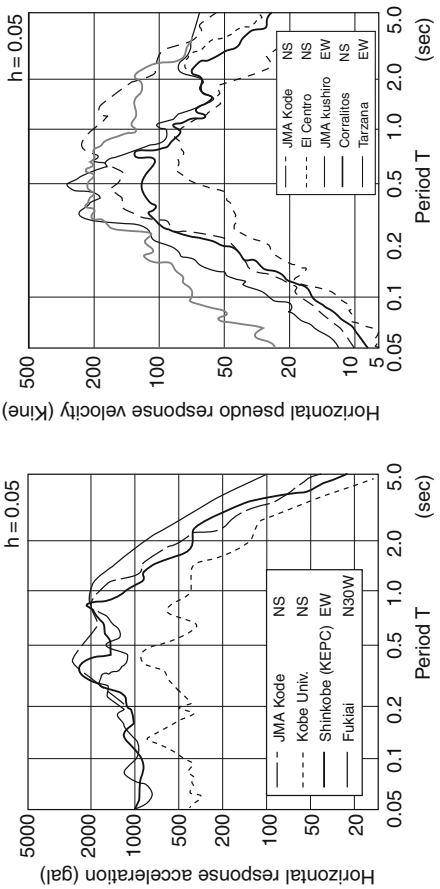


Fig. 7.3 Acceleration and velocity response spectra (courtesy of Japan Seismological Society, Tokyo, 1995, Fig. 6)

www.EngineeringBooksPDF.com

A Comparative Study of Results

Case Study 7.23 Thirty-Two-Storey Building
Analysis Type

Dynamic Non-linear Time Integration	Seismic Waveform Type of Analysis	El-Centro 300–345 gal	Degrees of Freedom: 32

	Hikken Sekki Co, Ltd				ISOPAR and G-Graph		
	DIRECTION				DIRECTION		
S. No.	Type	*X	*Y	*Z	*X	*Y	*Z
1	Fundamental period T(s)	2.88	2.76	–	2.77	2.73	0.51
	(a) mode 1						
	(b) mode 2	1.07	1.02		1.07	1.02	0.21
2	Damping	0.02	0.02	–	0.02	0.02	0.02
3	Shear coefficient (C_i)	0.10	0.10	–	0.10	0.10	0.10
4	Seismic load %	80 (F1)	60 (F2)	–			
	(a) Rigid frame	70 (F2)	70 (F2)	–			
	(b) Bearing walls	20 (F1)	40 (F1)	–			
		30 (F1)	30 (F1)				
5	Device U_{max} and C_i	–	–	–	10.87 cm	10.23 cm	0.06 cm
	(a) Input 50 cm/s C_i	–	–		18.89	20.35	1.30
	(b) Input 300 cm/s C_i	–	–				
6	Upper Structure	–	–	–	170 cm/	170 cm/	50 cm/s^2
	Ü	0.088	0.091	–	s^2	s^2	0.110
	(a) Input 50 cm/s C_i				0.114	0·120	
	(b) Input 518 cm/s C_i	–	–	–	350 cm/	189 cm/	56 cm/s^2
		0.147	0.153	–	s^2	s^2	0.113
					0.140	0.230	

Hysteresis Loop

Case Study 7.24 Thirty-Six-Storey Building

Building Data:

- Industrial Cultural Centre, Omiya City, Japan
- Designed by Hikken Sekki Co, Ltd, Tokyo, Japan
- Above ground: Steel rigid frame with steel plate walls–total floors: 36 (offices)
- Below ground: RCC rigid frame, using RCC and steel walls–total floors: 17 (hotel)
- All types of walls antiseismic
- A = total floor area = 105060.16 m^2
- Standard area/floor: 2119.64 m^2(office)
  707.40 m^2 (hotel)

www.EngineeringBooksPDF.com

(continued)

–Total number of isolators:	12	
–Dampers:	6	Total number of isolators and dampers evaluated
	18	from P/C-evaluated Non-linear Time Analysis = 21

H = building height	Office wing	136.550 m
	Hotel wing	57.050 m
H = max height of the structure	Office wing	140.050 m
	Hotel wing	57.050 m
Standard floor height	Office wing	3.8 m
	Hotel wing	3.2 m
Height of first floor	Office wing	5,500 m
	Hotel wing	–
Height of the equipment floor	Office wing (13th floor)	5,500 m
	Hotel wing	–
Height of basement floor	Office wing	5,800 m
	Hotel wing (B1 floor)	5,800
Floors		
Above ground	Office wing	31
	Hotel wing	13
Below ground	Office wing	4
	Hotel wing	3
Penthouse	Office wing	1
	Hotel wing	1

Soil Property and Foundation Data

Note (used also for soil–structure interaction)

Soil Property and *N* value

	GL-m	Soil layer	*N* value
	0.0–5.0	Loam and clay (lm. DT)	1–5
	5.0–10.0	Sandy soil, cohesive soil (D_c2, D_c1)	3–34
	10.0–26.0	Sandy soil ± (D2)	16–44
	26.0–41.0	Cohesive soil (D_c2, D_c3)	4–44
	41.0–43.0	Alternate layers of gravel, sandy soil and cohesive soil	14–50
	43.0–48.0	Cohesive soil ± (D_c4)	10–15
	48–63	Sandy soil ± (D3)	30–50
Permissible ground resistance	Pile resistance: 250t/m^2		

www.EngineeringBooksPDF.com

Ground Property

Foundation depth	Office wing	25.250 m
	Hotel wing	17.450 m
Ground type, foundation structure	Pile foundation	
Maximum contact pressure (Pile resistance)	210 t/m^2(pile)	

Main Structure

Structural features	In both *X* and *Y* directions, rigid frames containing antiseismic steel plate walls at the core are provided
Frame classification	Structure above ground: RCC rigid frames using steel plate walls; Structure below ground: RCC rigid frame using RCC antiseismic walls and steel frames
Bearing walls, other walls	Structure above ground: Steel plate antiseismic walls Structure below ground: RCC antiseismic walls
Material for columns, beams, sections	Structure above ground: Column – 600×600 with a box-like cross-section; Beam-welded I section with depths of 850, 1200, 1500 Structure below ground: Column – 1100×1100 and 1000×1000; Beam – 850×1200 and 850×900 Steel frame – SM50; Steel bars – SD35, SD30; Concrete – Floor above ground: light concrete strength – 180 kg/cm^2 (sp. gr. 1.75, 1.85); Floor below first floor: common concrete strength – 210 kg/cm^2
Columns, beams, joints	Structure above ground: Beam flange welded at site. Beam web fixed with HT bolts and columns welded at site; Structure below ground: Steel sections fixed with HT bolts (columns and beams, factory welded)
Floor	Structure above ground: RCC slab Structure below ground: RCC slab
Roof	Cast in situ concrete structure
Non-bearing walls	Outer wall – Precast concrete structure; Inner wall – Light steel frame with laminated PB

7.5.3 Data I

Maximum horizontal acceleration = 818 gal
Maximum vertical acceleration = 447 gal
Maximum vertical velocity = 40 kine
Maximum horizontal velocity = 90 kine

www.EngineeringBooksPDF.com

7.5.4 Data II

In the finite element analysis dynamic equations given in the Appendix, the damping ratio is 10%. Isoparametric four-noded solid elements are used for the finite element discretization. The following gives additional data:

1. SBM 55-storey frame and floors
   Floor: Four-noded solid elements (55,500)
   Frame: Four-noded line elements (220,000)
2. Soil–structure interaction
   2,400 nodes on ground surface
   2,200 nodes on ground–structure interface
   ] Computer CRAY-3

Reference is made to the soil–structure analysis in Chap. 6.

7.5.4.1 Provision of Controlled Devices

(a) Total number of isolators = 1,650 computed with P/C and non-linear time integration
Total number of HAD type = 1,620 provided by designers (HRD)
Total number of dampers:
(b) Viscoelastic computed = 335
Viscoelastic provided = 365*
(c) Viscous computed = 155 with P/C calculation and non-linear time integration
Viscous provided = 159* by the designers
(d) Sensors = 80

*Note: Positions available in the building where the devices could easily be accommodated.

Results based on ISOPAR-II

Ground period	$T_c = 0.6$ sec
Primary design period T	$T_{x1} = 2.88$; $T_{y1} = 2.76$; $T_{z1} = 1.35$
Design shear coefficient C_i	Along the length: 0.10; along the width: 010; distribution pattern: it includes the shear distribution as obtained from the vibration response analysis
Horizontal seismic intensity at the foundation K	The seismic intensity K at 1F: 0.10; the seismic at GL-40m = 0. In between, it is interpolated assuming a straight line relationship
Maximum storey drift	3/1000

Maximum horizontal and vertical displacements respectively 11cm and 21cm

www.EngineeringBooksPDF.com

$\tau_{bx} = 0.10$; $\tau_{by} = 0.10$; $\tau_{bz} = 0.022$
$\sigma_{bx} = 25.3\ \text{N/mm}^2$; $\sigma_{by} = 19.3\ \text{N/mm}^2$; $\sigma_{bz} = 0.23\ \text{N/mm}^2$

Acceleration time relation is drawn in 10.16, giving values in three directions X, Y and Z.

7.5.4.2 Finite Element Analysis: Non-linear Time Integration

Programs ISOPAR and SAP2000 have been used to check each other's validated results and to check certain specialized data and results.

The finite element mesh scheme with boundary conditions defined is shown in Plate 7.23. The step-by-step time integration analysis is adopted as part of this dynamic finite element analysis. The loadings given by the Muto Institute in Fig. . ...are adopted as the input data to the three-dimensional finite element analysis.

For reasons of economics in the overall performance of time-consuming solution procedures, the entire structure is divided into seven No. 8 substructures. The loading on one substructure from the Muto seismic analysis is given in Fig. 7.4. All columns are 500×500 mm box-type fully welded and rigidly connected to a girder. The transverse framing consists of wall frames, open frames and braced frames. Dead weight is assumed to be 115 kg/m^2(1.045 KN/m^2). A non-linear earthquake of 0.5 g was assumed for this study.

Due to the inclusion of vertical acceleration simultaneously with the horizontal acceleration, the approach is completely changed. If this building were located in the Kobe region during the earthquake, the damage to the floors and frames would be in the ratio of three times the damage if vertical acceleration were not ignored. The deformation shear and overturning moments by the Program ETABS, checked by Programs ISOPAR and SAP2000 for the animated earthquake responses, would be *on average four times more*. A comparative study of the displacement–time function graph (Fig. 10.5) indicated a marked difference for the Kobe earthquake. All seismic devices were placed and functionable.

The SM building is taken as an example for the three-dimensional dynamic finite element analysis in which material and geometric non-linearity are considered. Figure 10.16 shows ductility models for the various materials adopted. These models are included in the program ISOPAR (extended three-dimensional analysis of building systems) developed by Wilson et al. at the University of California. The building is idealized as independent frames and sub-frames interconnected by a flooring system adopted by the Muto Institute. Axial, bending and shear deformations are included within each column made of 500×500 welded box-type members. Beams, girders and vertical panel elements allow discontinuity. The loadings evaluated accurately by the Muto Institute for the SBM building have been modified to include the effects of both horizontal and vertical acceleration. Non-linear earthquakes of 0.5 g are considered for Kobe and other earthquake locations, assuming the SMB is sited in these areas as well.

www.EngineeringBooksPDF.com

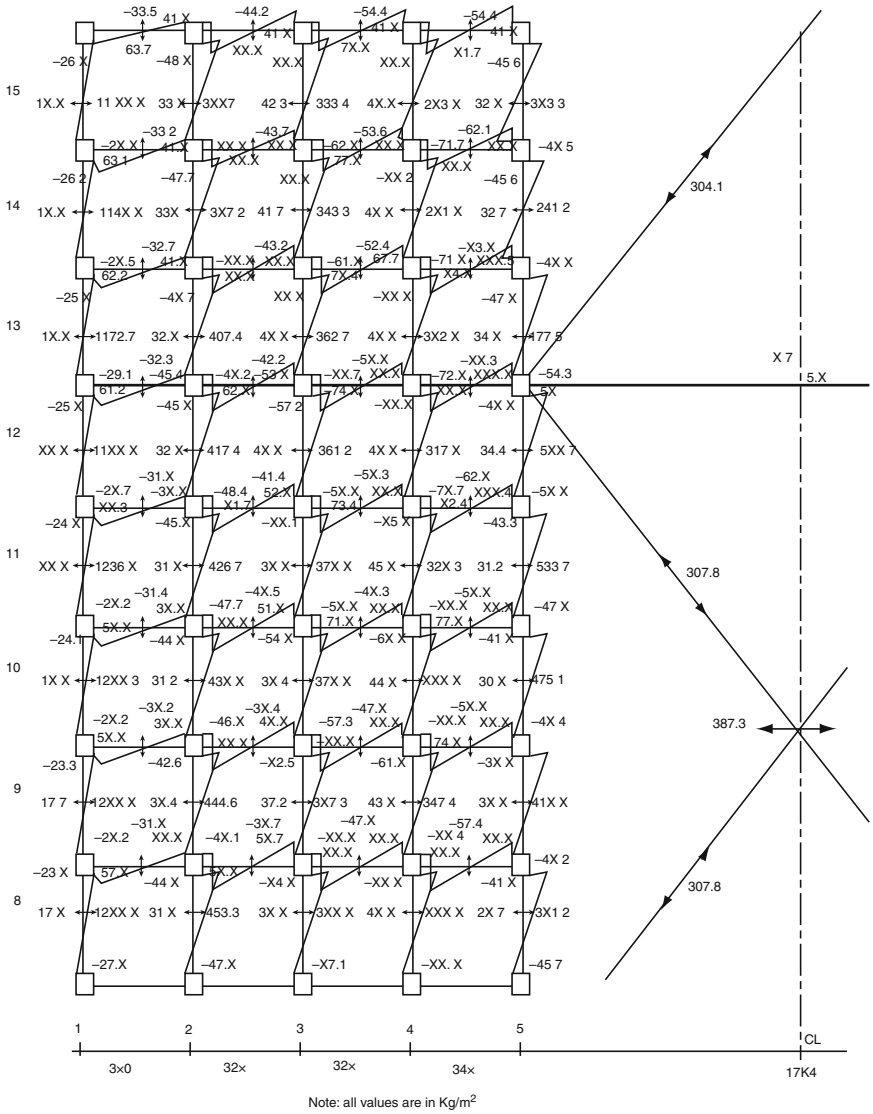


Fig. 7.4 Stress diagram for seismic load

www.EngineeringBooksPDF.com

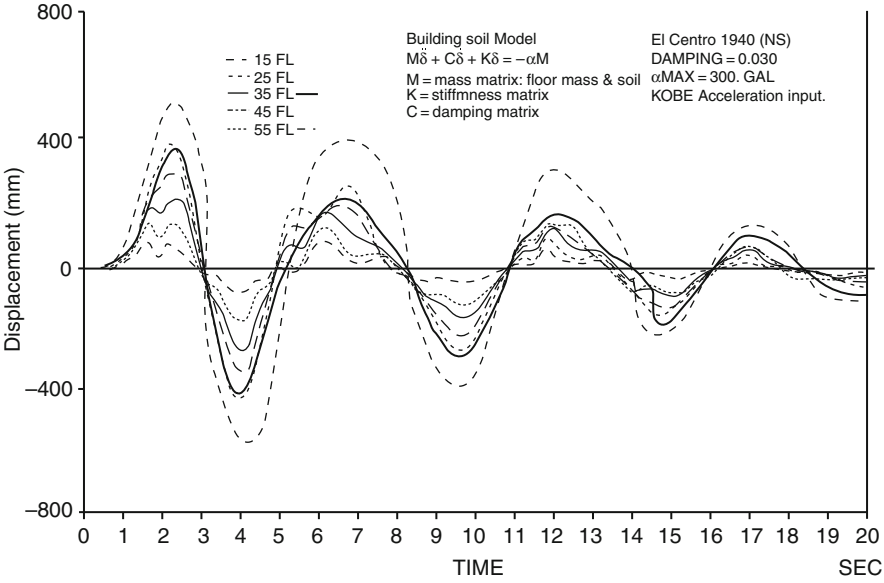


Fig. 7.5 Displacement–time history (Kobe)

Figure 10.7 shows a comparative assessment of modes based on the El-Centro and Kobe earthquakes. In all cases vertical acceleration is included simultaneously with horizontal acceleration. Table 7.12 shows a comparative safety assessment of the SMB building subjected to various earthquakes. The effects on this building due to the Kobe earthquake are enormous. The damage is predicted. Owing to massive outputs, only Table 7.13 summarizes the strength reduction and excessive storey drift under various earthquakes without devices.

In addition, the same building was put to the other waveform apart from El-Centro (NS) and Taft (EW) such as Tokyo101 (NS) and Sandai (NS). For linear earthquake of intensity 0.10 g, using constant damping of 0.030 and considering soil–structure interaction, the values of acceleration and shear are plotted against strorey height. They are shown in Plate 10.12 for the SMB building. Again, non-linear earthquake response was considered for El-Centro (NS) waveform with four intensities of 0.1, 0.3 and 0.5 g. Soil–structure interaction effect was considered again ($\alpha M = 100, 300, 500$). The results have been obtained using Program ETABS. Both shear and storey drift are plotted for floor heights. No devices in these results were considered. The reader can fudge the performances of the SMB building with and without devices. These results are given in Plate 10.13. Next, for the same building, Program ETAB was used to compare storey drift and overturning moments for the earthquakes with and without devices for various storey heights in Plate 10.14. The

www.EngineeringBooksPDF.com

Table 7.11 BRI Standard for $H > 45\ m$

Seismic force

$$F = C_1 . W$$

$$C_1 = C_0 . Z. I$$

Where C_0 = basic shear coefficient

$$C_0 = 0.2S \text{ for } T < G + 1.75 \text{ sec}$$

$$= \frac{0.35S}{T - G} \text{ for } T \leq G + 1.75 \text{ sec}$$

T = fundamental natural period

G = soil factor
= –0.75, 0, 0.5, 0.75

S = construction factor
= 0.9, 1.0

Z = zoning factor
= 1.0, 0.9, 0.8

I = importance factor

Lateral seismic force

$$f_i = {}_1f_i + {}_2f_i + {}_3f_i$$

$${}_1f_i = \alpha C_1 Wx$$

$${}_2f_i = \beta C_1 Wx. \frac{W \cdot x}{\sum_{x=0}^{h} Wx \cdot x}$$

$${}_3f_i = \gamma C_1 W$$

where

Wx = ith floor lumped load

W = total load

x = height of ith floor

$\alpha = (2 - T)/2(T < 2), 0(T \geq 2)$

$\beta = T/2(T < 2), (12 - T)/10(T \geq 2)$

$\gamma = 0(T < 2), (T - 2)/10(T \geq 2)$

www.EngineeringBooksPDF.com

Table 7.12 Seismic load in Japan (horizontal co-efficient)

Building code for $H \leq 45$ m

seismic force

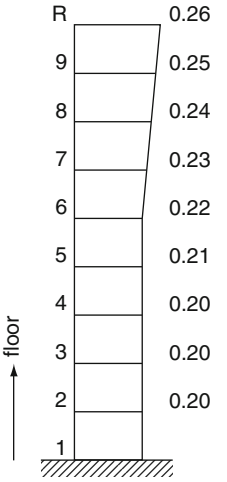
$$f_i = kW_i$$

where k = seismic coefficient
W_i = ith floor lumped load

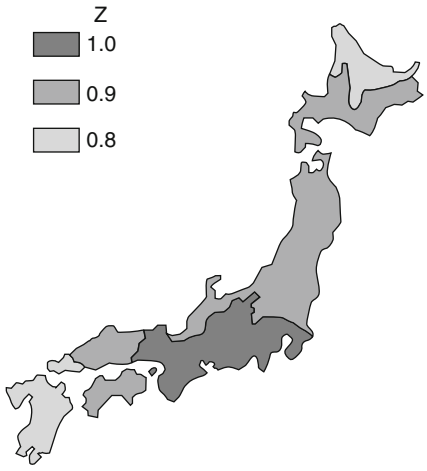
seismic coefficient

$$k = k_0 \,.\, Z \,.\, S$$

where k_0 = 0.2 for $H \leq 16$ m
i = increment = 0.1 every 4 m over 16 m
Z = zoming factor = 1.0, 1.9, 0.8
S = soil and constuction factor
= 0.6, 0.8,1.0, 1.5(rock → soft soil)



Fundamental seismic coefficient K_0



Zoning factor Z

www.EngineeringBooksPDF.com

Table 7.14 SMB – comparative safety assessment

	Strength reduction factor of design stresses*		Storey drift factor on top of design drift		Storey shear strength reduction factor from the design factor +	
Earthquake*	Longitudinal	Transverse	Longitudinal	Transverse	Longitudinal	Transverse
El-Centro	0.76	0.87	1.80	1.82	0.71	0.73
Taft	0.72	0.83	1.73	1.74	0.84	0.85
San-Fernando	0.89	0.88	1.65	1.70	0.81	0.82
Koyna	0.84	0.83	1.36	1.56	0.79	0.80
Mexico	0.79	0.81	1.71	1.75	0.77	0.80
Tokyo	0.73	0.75	1.69	1.73	0.78	0.81
Kobe	0.92	0.89	1.93	1.94	0.83	0.69

*Non-linear earthquake (0.5 g), elasto-plastic spectra, 5% damping and vertical acceleration included.
+ Designer reported in Muto Report

www.EngineeringBooksPDF.com

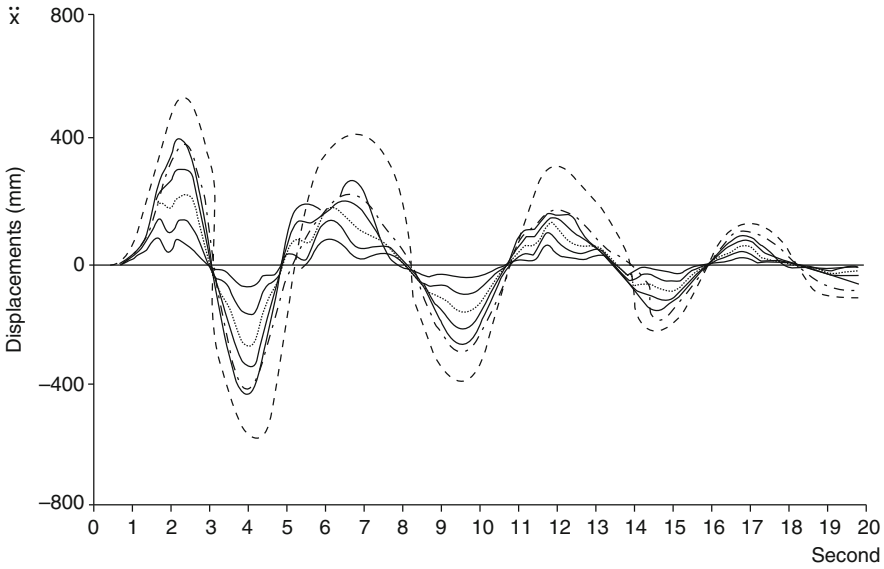


Fig. 7.6 ($\ddot{x}$-T relations for SMB Building-A comparative study)

www.EngineeringBooksPDF.com

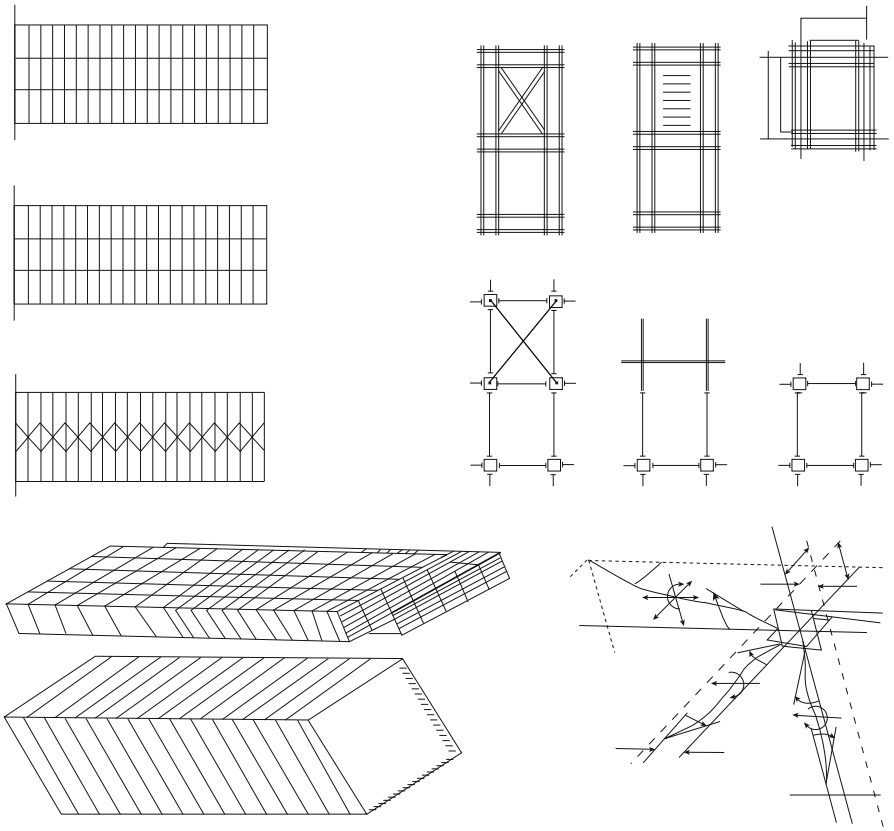


Fig. 7.7 (Source: MUTO Institute, Tokyo, Japan. Professor: MUTO)

www.EngineeringBooksPDF.com

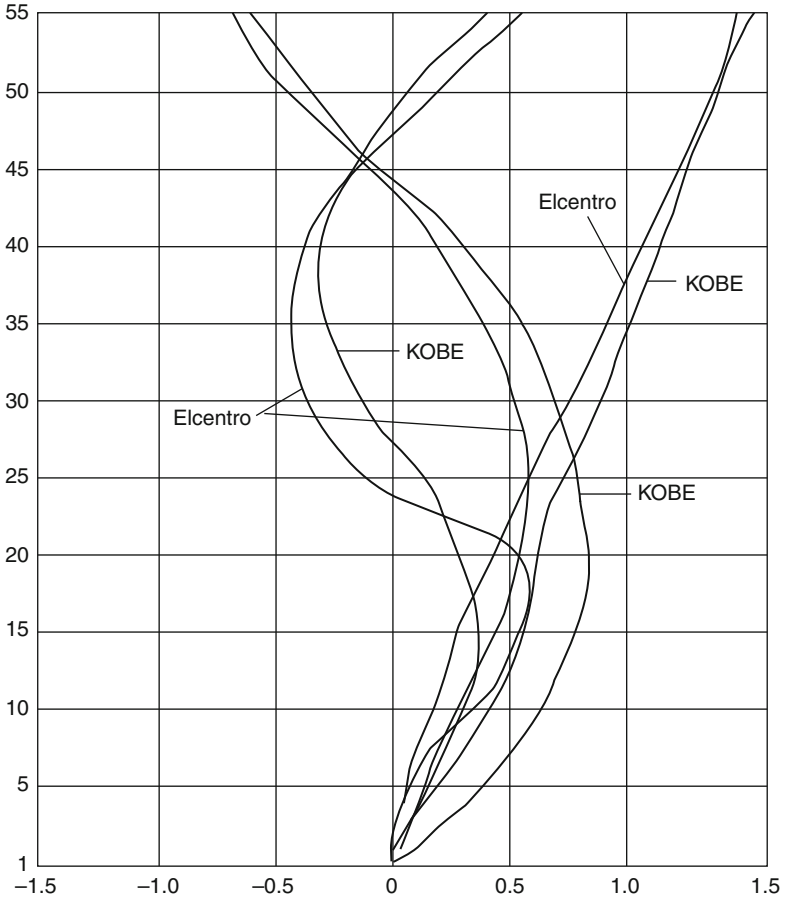


Fig. 7.8

www.EngineeringBooksPDF.com

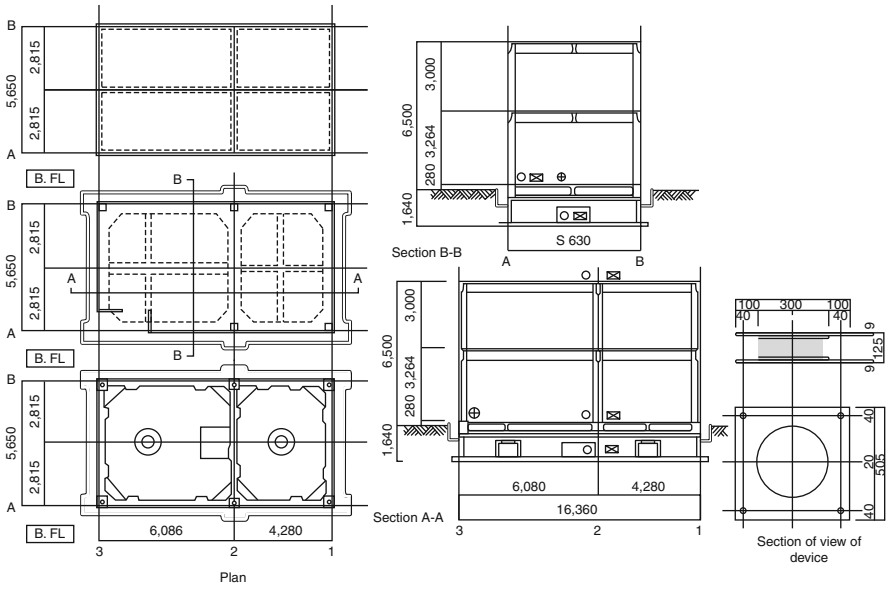


Fig. 7.9 (Source: MUTO Institute, Tokyo, Japan. Professor: MUTO)

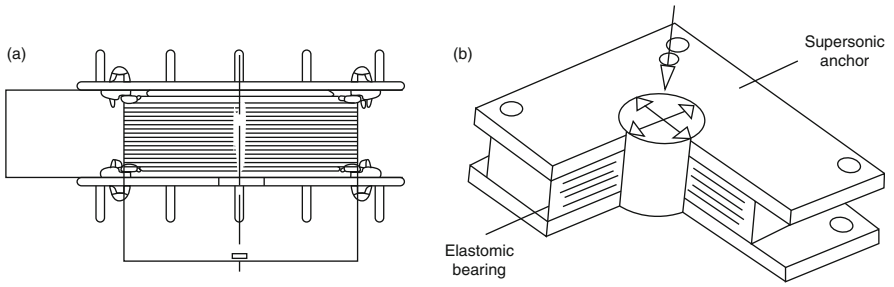


Fig. 7.10 (Source: MUTO Institute, Tokyo, Japan. Professor: MUTO)

www.EngineeringBooksPDF.com

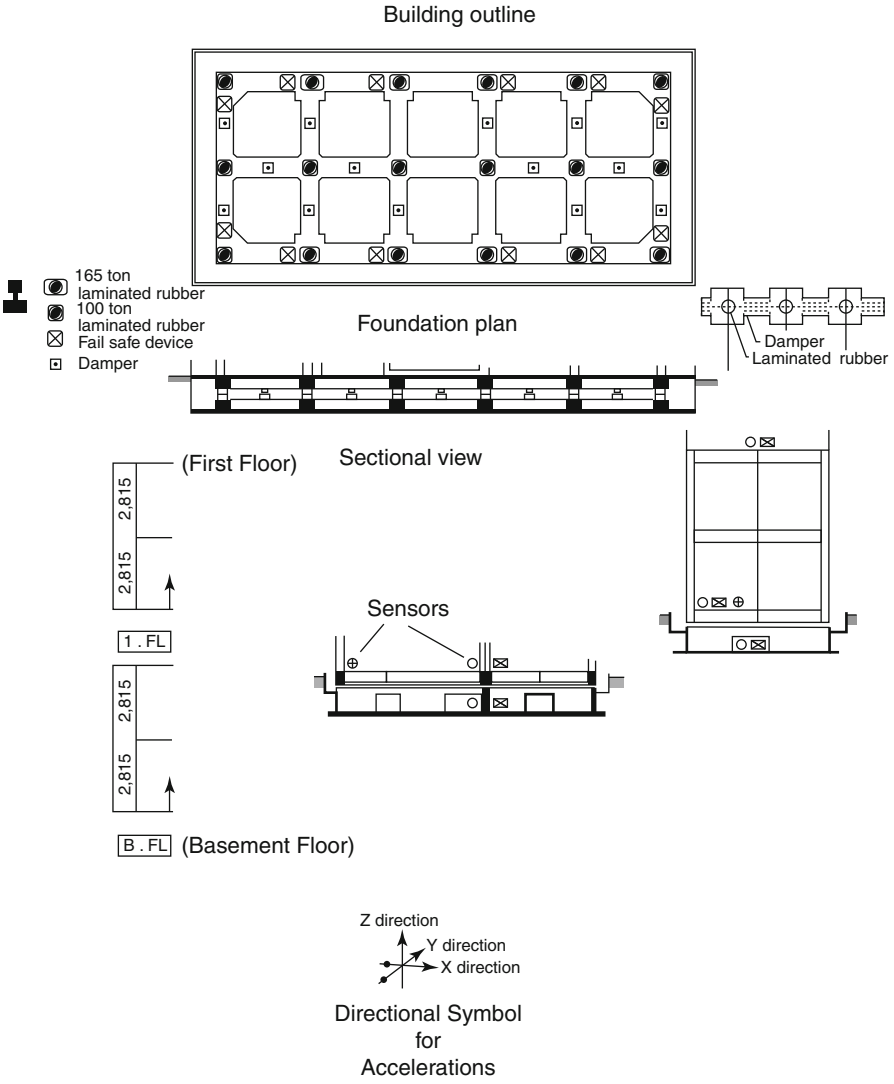


Fig. 7.11 (Source: MUTO Institute, Tokyo, Japan. Professor: MUTO)

www.EngineeringBooksPDF.com

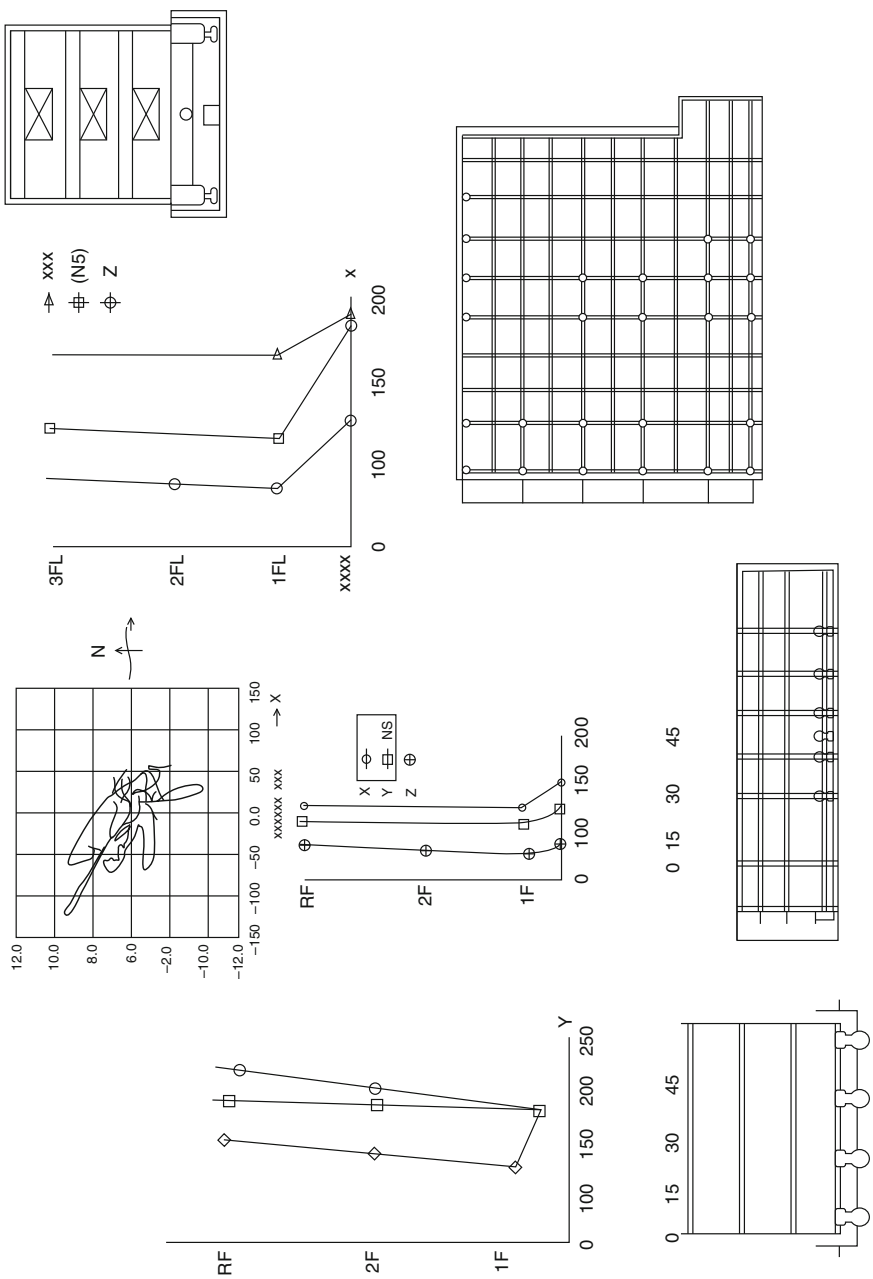


Fig. 7.12 (Source: MUTO Institute, Tokyo, Japan. Professor: MUTO)

www.EngineeringBooksPDF.com

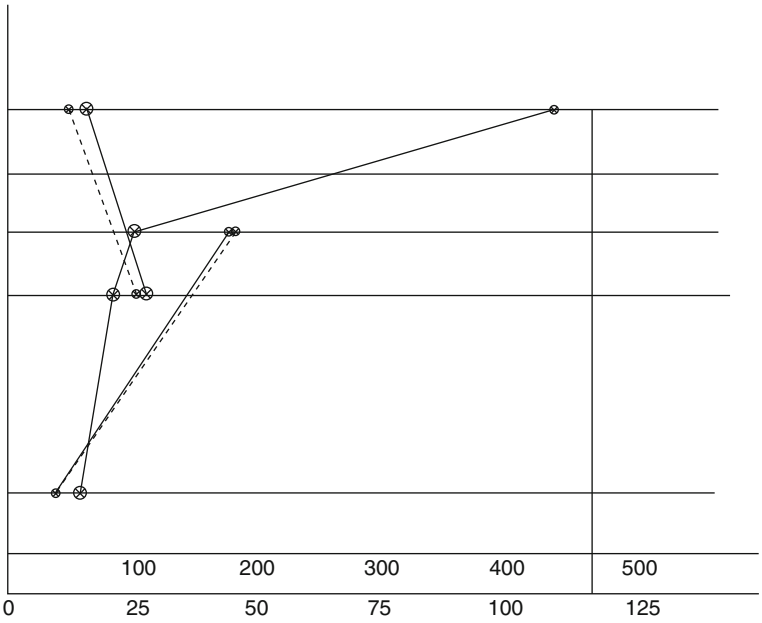


Fig. 7.13 (Source: MUTO Institute, Tokyo, Japan. Professor: MUTO)

www.EngineeringBooksPDF.com

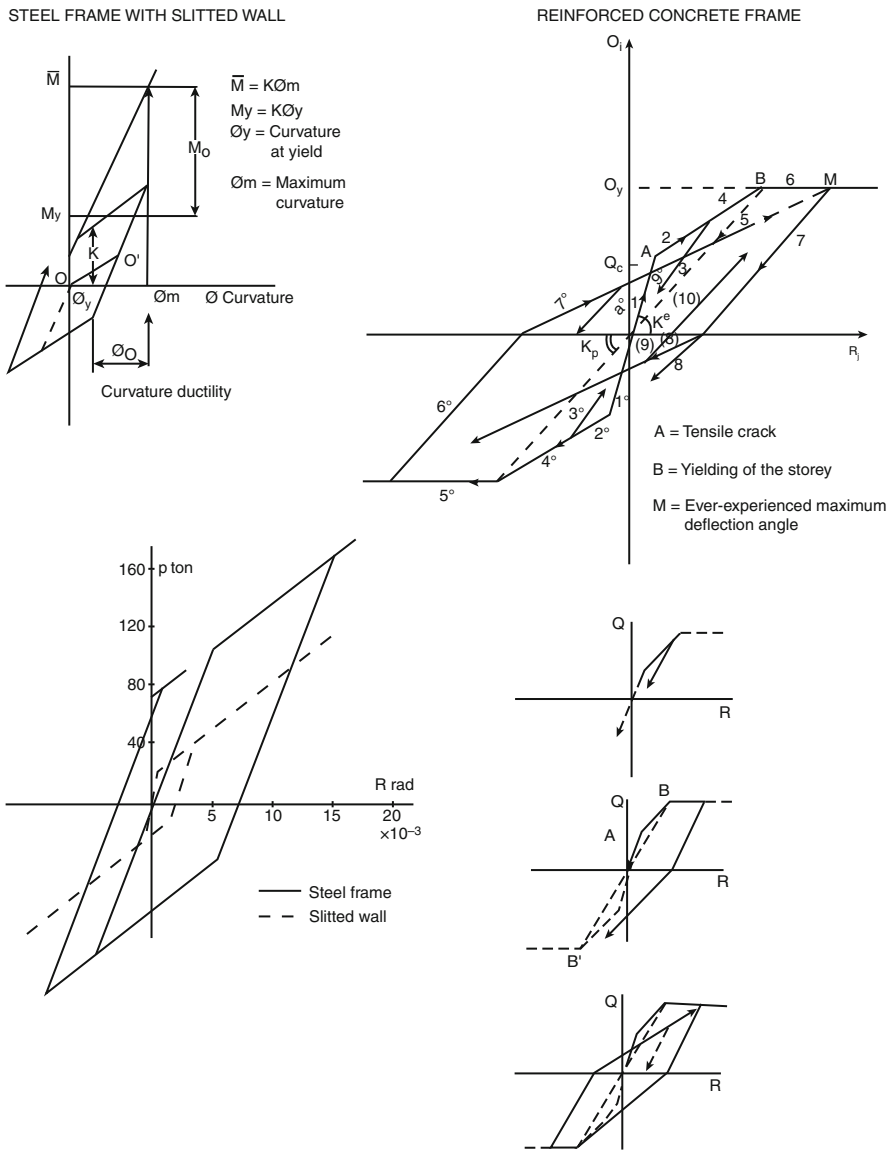


Fig. 7.14 (Source: MUTO Institute, Tokyo, Japan. Professor: MUTO)

www.EngineeringBooksPDF.com

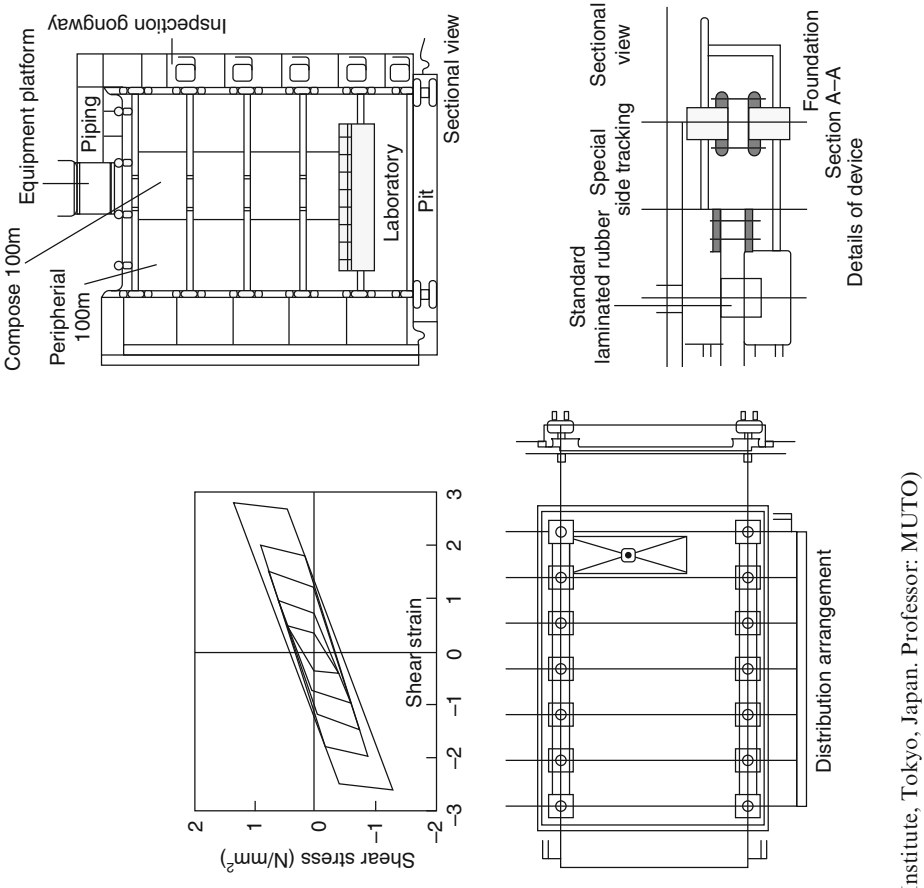


Fig. 7.15 (Source: MUTO Institute, Tokyo, Japan. Professor: MUTO)

www.EngineeringBooksPDF.com

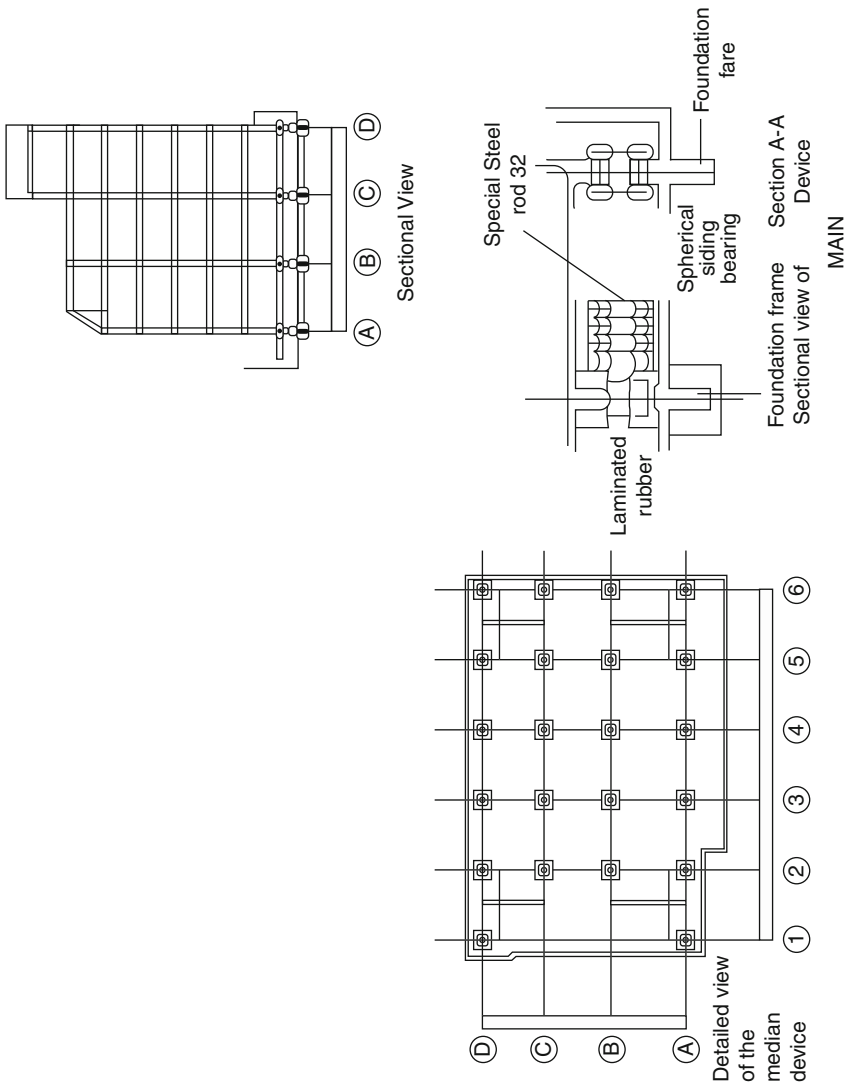


Fig. 7.16 (Source: MUTO Institute, Tokyo, Japan. Professor: MUTO)

www.EngineeringBooksPDF.com

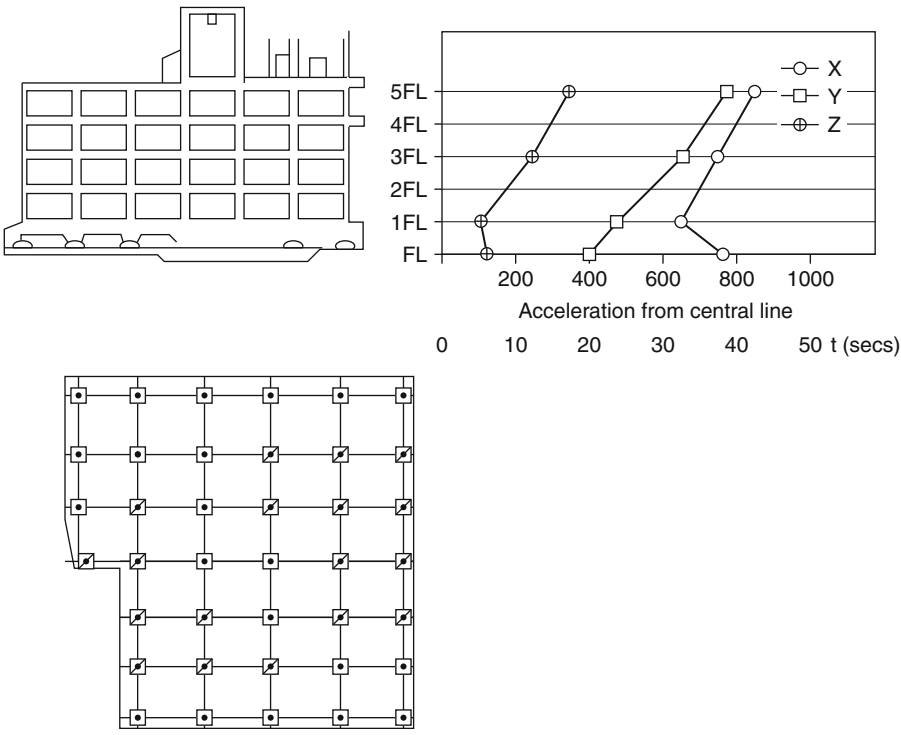


Fig. 7.17 (Source: MUTO Institute, Tokyo, Japan. Professor: MUTO)

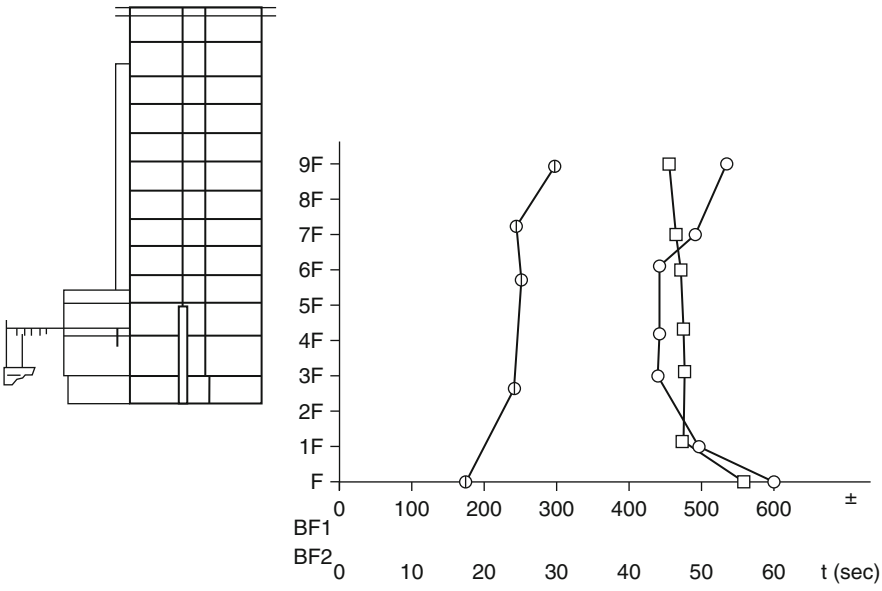
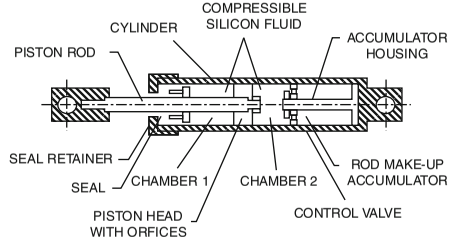


Fig. 7.18 (Source: MUTO Institute, Tokyo, Japan. Professor: MUTO)

www.EngineeringBooksPDF.com



RESULTS FROM SAP 2000

C1 = Input level 25 cm /sec; maxim-Drift = $\frac{1}{5000}$ And 25cm

U_Top Displacement = 13.5cm; $\dot{U}$ = 40cm/sec

$\ddot{U}$ = 300 cm/sec^2

C2 = Input level: 25 cm/sec; max.Drift = 13.98 cm; u = 36 cm;

$\dot{U}$ = 24. 5 cm/sec; U = 375 cm/sec^2

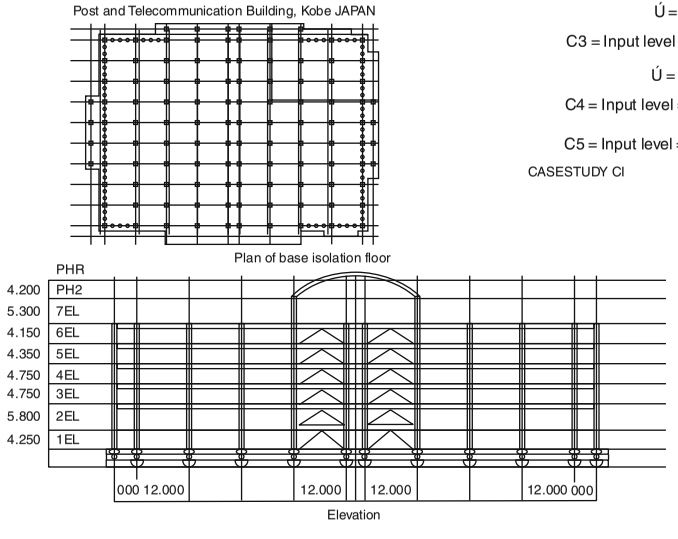
C3 = Input level = 50 cm/sec; max.Drift = $\frac{1}{780}$; U = 35 cm

$\dot{U}$ = 25 cm/sec; $\ddot{u}$ = 200 cm/sec^2

C4 = Input level = 25cm/sec; max Drift = $\frac{1}{500}$; u = 20cm $\dot{U}$ = 25 cm/sec; $\ddot{U}$ = 168 cm/sec^2

C5 = Input level = 220 gal; max.Drift = $\frac{1}{1406}$; u = 21 cm; $\dot{U}$ = 30 cm/sec; $Z\ddot{U}$ = 220 cm/sec

CASESTUDY CI



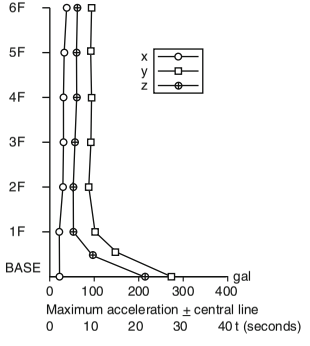


Fig. 7.19 (Source: MUTO Institute, Tokyo, Japan. Professor: MUTO)

www.EngineeringBooksPDF.com

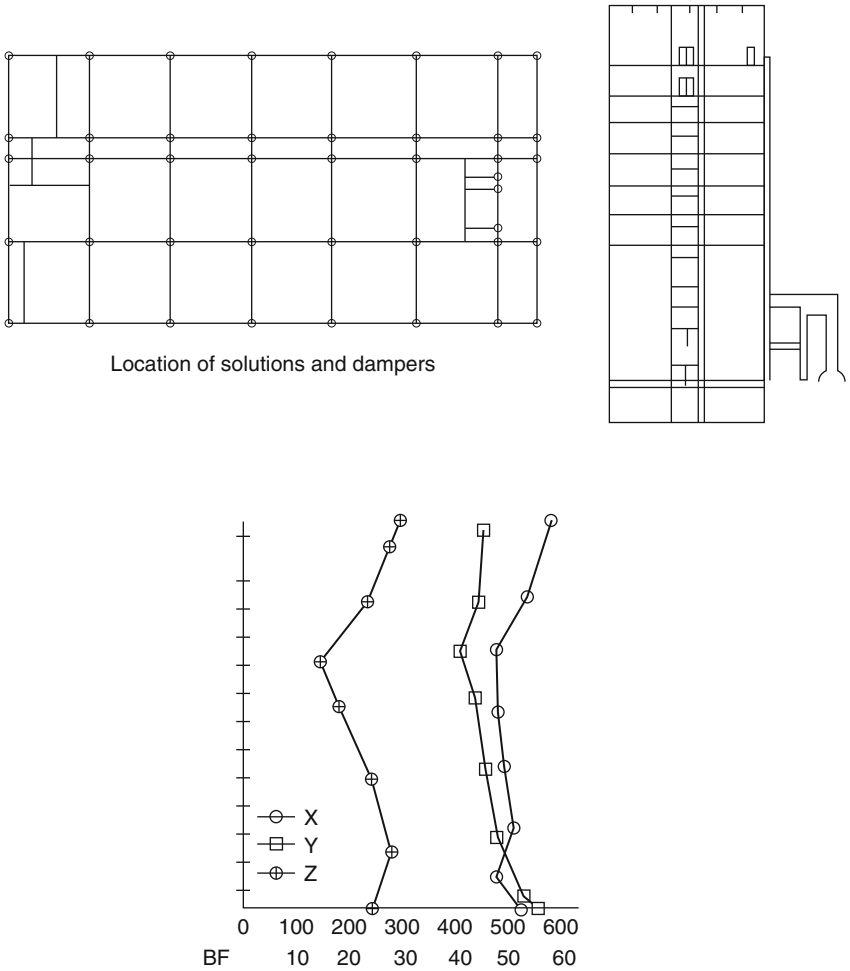


Fig. 7.20 (Source: MUTO Institute, Tokyo, Japan. Professor: MUTO)

www.EngineeringBooksPDF.com

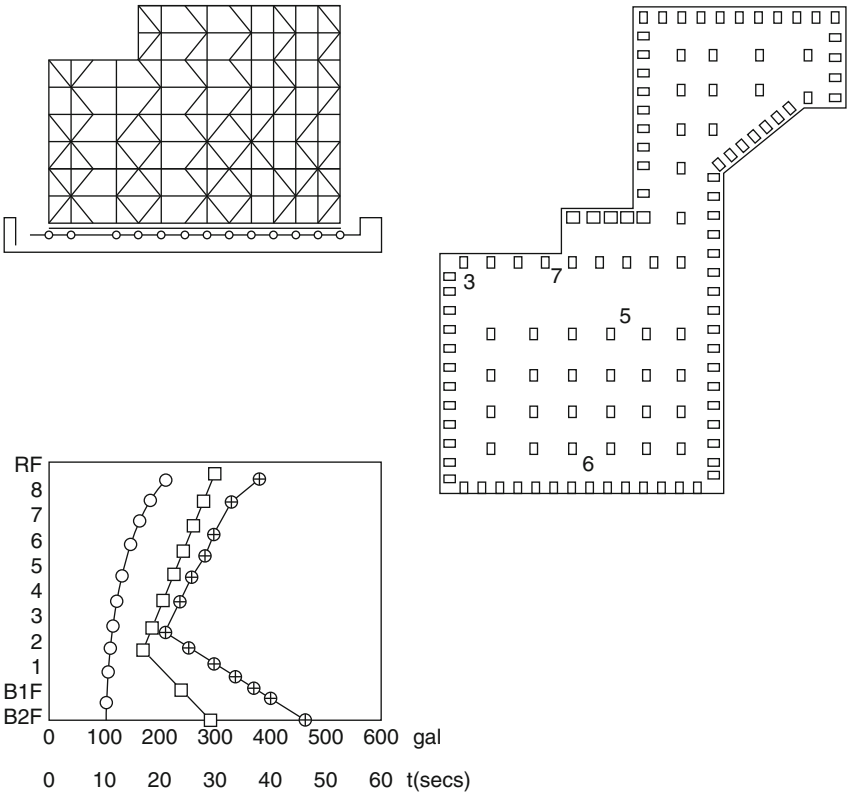


Fig. 7.21 (Source: MUTO Institute, Tokyo, Japan. Professor: MUTO)

www.EngineeringBooksPDF.com

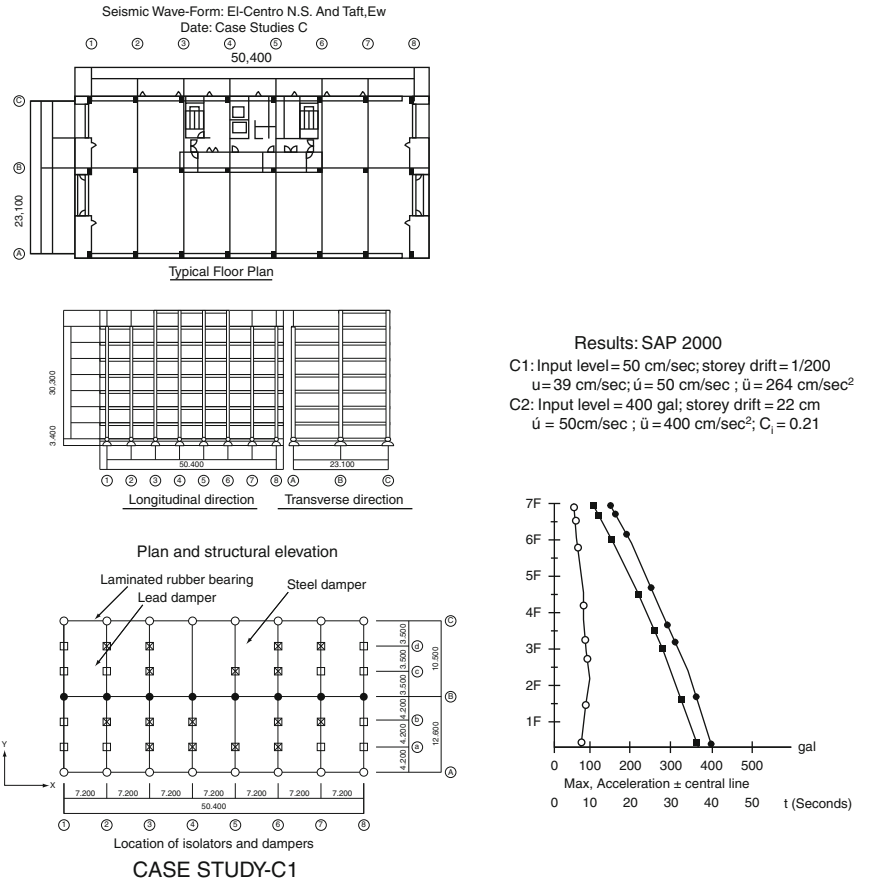


Fig. 7.22 (Source: MUTO Institute, Tokyo, Japan. Professor: MUTO)

www.EngineeringBooksPDF.com

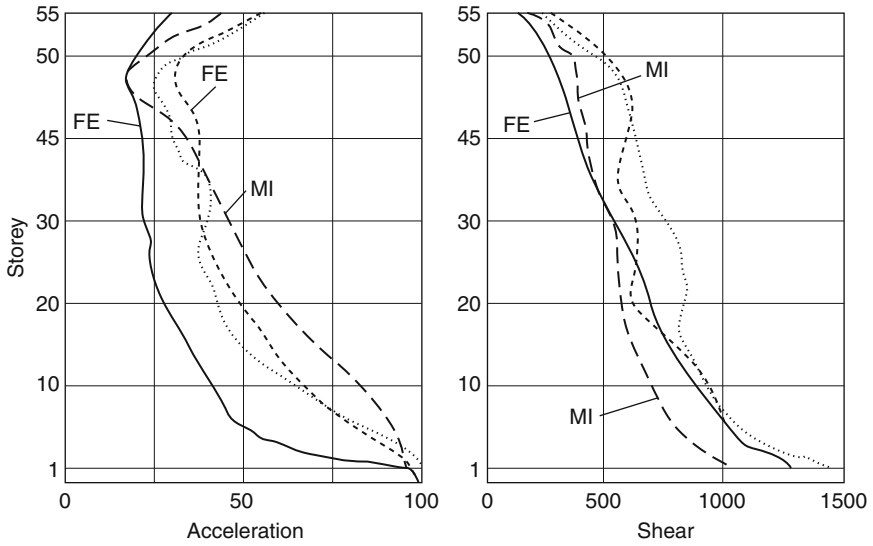


Fig. 7.23 Linear earthquake response-A comparative study
FE-Finite Element Analysis By Bangash using El-centro
MI-Muto Institute, Japan, using Taft $\xi = 3\%$ damping

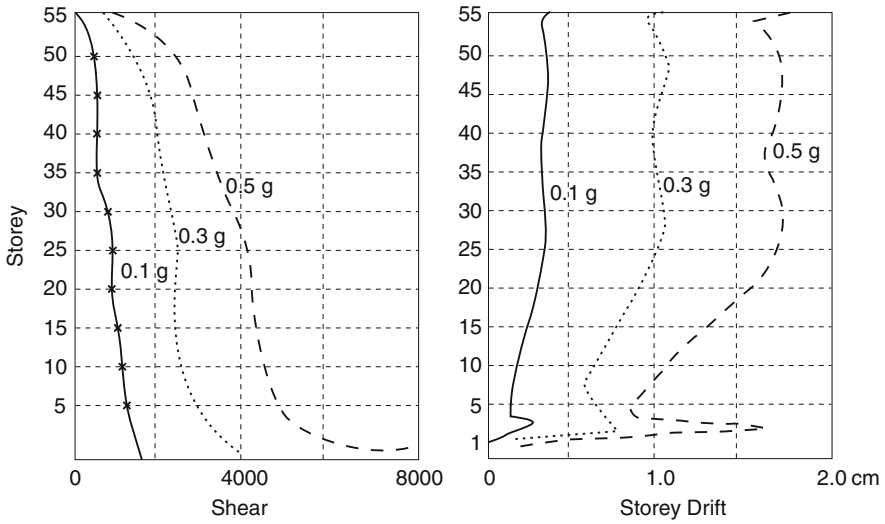


Fig. 7.24 Non-linear earthquake response-A comparative study
Intensity marked 0.1, 0.3, 0.5g.
Results from F.E. $\xi = 3\%$ damping

www.EngineeringBooksPDF.com

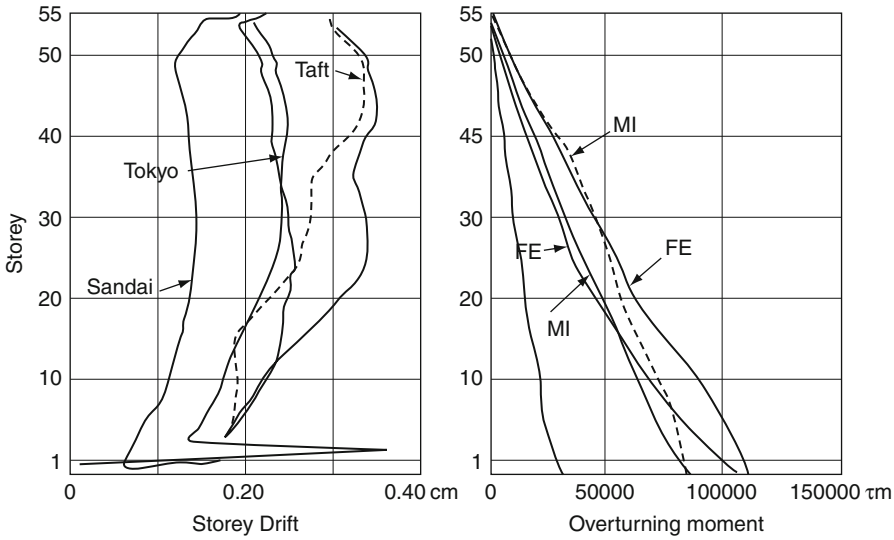


Fig. 7.25 Comparative Study of Earthquakes
Results from F.E. and Muto Institute M.I
FE-Finite Element
MI-Muto Institute, Japan

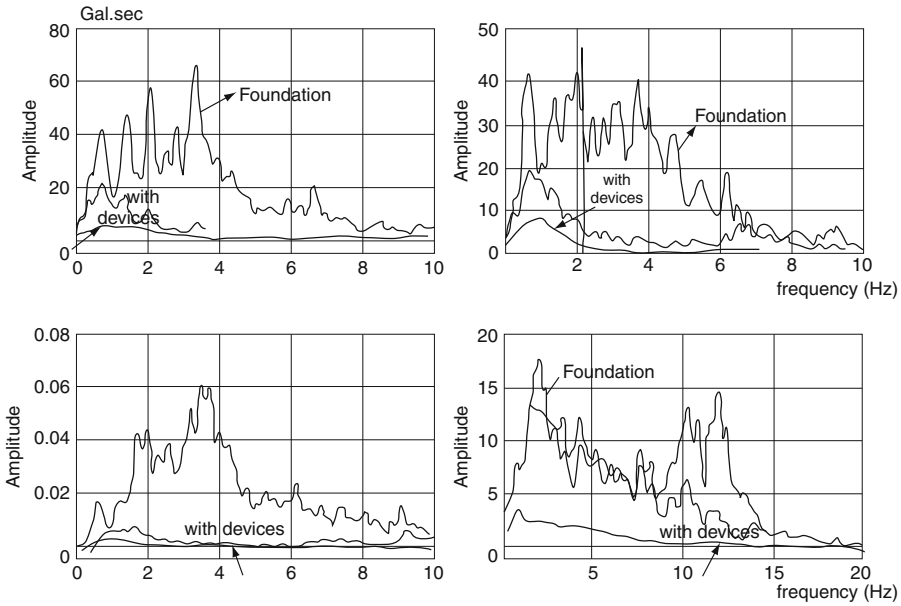


Fig. 7.26 Amplitude versus frequency-A comparative Study
Note: Floors are not represented

www.EngineeringBooksPDF.com

damping of 0.03 is kept constant taking into consideration the soil–structure interaction effects.

Then it is necessary to check Fourier spectrum in each direction for the SMB building with and without seismic devices using Program ETAB. Plate 7.15 shows these results.

It is concluded that vertical acceleration is important and cannot now be ignored. Since the SMB building is not actually in the Kobe region, the building is safe and the existing design features are adequate even if the vertical acceleration parameters are included. In the Kobe region this type of building would receive superficial damage but would not collapse due to specific layout techniques adopted by the Muto Institute, Japan.

www.EngineeringBooksPDF.com

Chapter 8
Seismic Criteria and Design Examples Based on American Practices

8.1 General Introduction

This chapter briefly contains the design criteria provided in UBC-97. A table is provided for various structural systems and is followed by the structural design requirements for framing systems, performance categories, building configurations, including plan and vertical structural irregularities. As action is given on combination of load effects, it became necessary to give the American views on deflection and drift limits. This is followed by equivalent lateral force procedure, period determination and seismic base shear. Vertical distribution of seimic forces and horizontal base shear distribution, torsion and overturning moments are fully described and supported by design equations. Next $P - \Delta$ effects, modal forces, deflection and drifts are given due consideration. Soil– structure interaction effects given earlier in the text are briefly mentioned to remind the designer that it necessarily has to be dealt with. They are described in Chap. 6.

This chapter gives away design examples based on the criteria given in UBC-97.

8.2 Structural Design Requirements for Structures

8.2.1 Introduction to the Design Basis

The seismic analysis and design procedures to be used in the analysis and design of structures and their components shall be as prescribed in various codes. The design ground motions can occur along any direction of a structure. The design seismic forces and their distribution over the height of the structure shall be established by a specific code and the corresponding internal forces in the members of the structure shall be determined using a linearly elastic model. An approved alternative procedure may be used to establish the seismic forces and their distribution, in which case the corresponding internal forces and deformations in the members shall be determined using a theoretical model.

M.Y.H. Bangash, *Earthquake Resistant Buildings*,
DOI 10.1007/978-3-540-93818-7_8, © M.Y.H. Bangash 2011

www.EngineeringBooksPDF.com

Individual members shall be designed and sized for the shears, axial forces and moments determined in accordance with these provisions, and connections shall develop the strength of the connected members or the forces. The foundation shall be designed to accommodate the forces developed or the movement imparted to the structure by the design ground motions. In the determination of the foundation design criteria, special recognition shall be given to the dynamic nature of the forces, the expected ground motions and the design basis for strength and energy dissipation capacity of the structure. The foundations can be flexible or rigid. In the layout the foundations shall have the isolators carefully arranged to offset damaging seismic forces. The most comprehensive work is given on numerical modelling in the author's book on *Earthquake Resisting Buildings*, published by Springer-Verlag, Germany.

8.3 Drift Determination and *P*–Δ Effects

Storey drifts and, where required, member forces and moments due to $P-\Delta$ effects shall be determined in accordance with this section.

8.3.1 Storey Drift Determination

The design storey drift shall be computed as the difference between the deflections at the top and bottom of the storey under consideration. The deflections of level x and the centre of the mass δx (in or mm) shall be determined in accordance with the following equation:

$$\delta_x = C_\mathrm{d}\delta_{xc} \tag{8.1}$$

where

C_d = the deflection amplification factor
δ_{xc} = the deflection determined by an elastic analysis (in or mm).

Where applicable, the design storey drift Δ (in or mm) shall be increased by the incremental factor relating to the $P-\Delta$ effects.

8.4 *P*–Δ Effects

$P-\Delta$ effects on storey shears and moments the resulting member forces and moments and the storey drifts induced by these effects are not required to be considered when the stability coefficient θ, as determined by the following equation, is equal to or less than 0.10:

www.EngineeringBooksPDF.com

$$\theta = (P_x \Delta)/(V_x h_{sx} C_d) \tag{8.2}$$

where

P_x = the total vertical design load above level x (kip or kN); when circulating the vertical design load for purpose of determining $P - \Delta$, the individual load factors need not exceed 1.0
Δ = the design storey drift occurring simultaneously with V_x (in or mm)
V_x = the seismic shear force acting between level x and $x-1$ (kip or kN)
h_{sx} = the storey height below level x (ft or m)
C_d = the deflection amplification factor

The stability coefficient θ shall not exceed θ_{max}, determined as follows:

$$\theta_{max} = 0.5/(\beta C_d) \leq 0.25 \tag{8.3}$$

8.5 Modal Forces, Deflection and Drifts

The modal force F_{xm} at each level shall be determined by the following equations:

$$F_{xm} = C_{vxm} V_m \tag{8.4}$$

8.6 Soil–Concrete Structure Interaction Effects

8.6.1 General

The provisions set forth in this section may be used to incorporate the effects of soil–concrete structure interaction in the determination of the design earthquake forces and the corresponding displacement of the building. The use of these provisions will decrease the design values of the base shear lateral forces and overturning moments but may increase the computed values of the later displacements and the secondary forces associated with the $P - \Delta$ effects. The procedure is given elaborately in Chap. 6.

8.7 Equivalent Lateral Forces Procedure

The following provisions are supplementary to those presented above.

www.EngineeringBooksPDF.com

8.7.1 Base Shear

To account for the effects of soil–concrete structure interaction, the base shear determined may be reduced to

$$V = V - \Delta V \tag{8.5}$$

The reduction ΔV shall be computed as follows:

$$\Delta V = \left[C_s - C_s \left(\frac{0.05}{\beta} \right)^{0.4} \right] \overline{W} \tag{8.6}$$

where

C_s = the seismic response coefficient computed using the fundamental natural period of fixed base structure T or T_a or the seismic response coefficient computed using the fundamental natural period of flexibly supported structure (T)

β = the fraction of critical damping for the structure–foundation system. A reference is made to Fig. 8.1

W = the effective gravity load of the building which shall be taken as 0.7 except that for buildings where the gravity load is concentrated at a single level, it shall be taken as equal to W.

The reduced base shear V shall in no case be taken as less than 0.7 V.

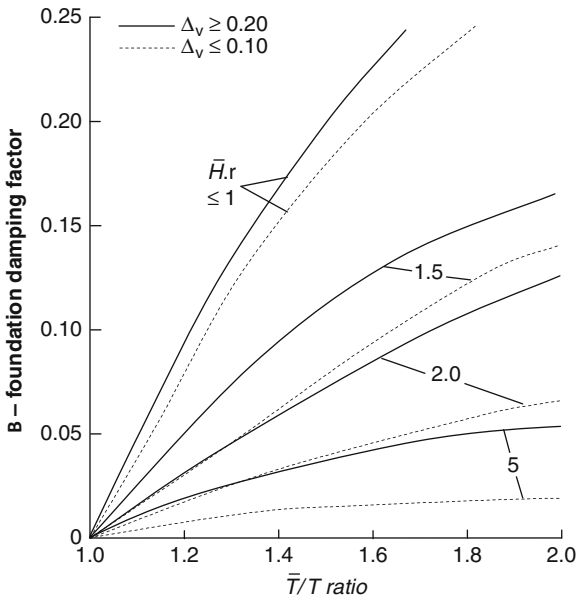


Fig. 8.1 Foundation damping factors

www.EngineeringBooksPDF.com

8.7.2 Effective Structural Period

The effective period T shall be determined as follows:

$$\overline{T} = T\sqrt{\left(1 + \frac{\overline{k}}{K_y}\right)\left(1 + \frac{K_y\overline{h^2}}{K\theta}\right)} \tag{8.7}$$

where

T = the fundamental period of the concrete structures
$\overline{k}$ = the stiffness of the concrete structure when fixed at the base
$\overline{h}$ = the effective height of the structure which shall be taken as 0.7 times the total height

$$\overline{k} = 4\pi^2\left(\frac{\overline{W}}{gT^2}\right) \tag{8.8}$$

$\overline{h}$ except that for buildings where the gravity load is effectively concentrated at a single level, it shall be taken as the height to that level; K_y is the lateral stiffness of the foundation defined as the static horizontal force at the level of the foundation necessary to produce a unit deflection at that level, the force and the deflection.

Being measured in the direction in which the structure is analysed K_θ is the rocking stiffness of the foundation defined as the static moment necessary to produce a unit average rotation of the foundation, the moment and rotation being measured due to in the direction in which the structure is analysed, and g is the acceleration gravity.

The foundation stiffness K and K_θ shall be computed by established methods using soil properties that are compatible with the soil strain levels associated with the design earthquake motion. The average shear modulus G for the soils beneath the foundation at large strain levels and the associated shear wave velocity v_s needed in these computations shall be determined from Table 8.3.

V_{so} = the average shear wave velocity for the soils beneath the foundation at small strain levels (10^{-3}% or less)
$G_0 = \gamma v^2_{so}/g$ = the average shear modulus for the soils beneath the foundation at small strain levels and
γ = the average unit weight of the soils

8.7.2.1 Effective Damping

The effective damping factor for the structure–foundation system β shall be computed as follows:

www.EngineeringBooksPDF.com

$$\overline{\beta} = \beta_0 + \frac{0.05}{\left(\frac{\overline{T}}{T}\right)^3} \tag{8.9}$$

where $\beta_0 =$ the foundation damping factor as specified in Fig. 8.1.

The value corresponding to $A_v = 0.15$ in Fig. 8.1 shall be determined by averaging the results obtained from the solid lines and the dashed lines.

The quantity is a characteristic foundation length that shall be determined as follows:

$$r = r_a = \sqrt{\frac{A_0}{\pi}} \tag{8.10}$$

$$\begin{aligned} &\text{For } \frac{\overline{h}}{L_0} \geq 1 \\ &r = r_m = \sqrt[4]{\frac{4I_0}{\pi}} \end{aligned} \tag{8.11}$$

where

$L_0 =$ the overall length of the side of the foundation in the direction being analysed
$A_0 =$ the area of the load-carrying foundation and
$I_0 =$ the static moment of inertia of the load-carrying foundation

For intermediate values of h/L_0 the value of r shall be determined by linear interpolation

Design calculation (US Code)

Design Example 8.1

A two-storey building with a mason –γy shear wall is located 10 km from the epicentre with an earthquake magnitude greater than 7.0. Use the following data:

Total height = 9.15 m ; $R = 4.5$
Each floor = 4.0 m; soil type S_D
$V_g =$ acceleration = 304.8 m/s

Calculate, using UBC seismic code,
(a) Total design shear
(b) The vertical distribution of the base shear to these two storeys

Solution UBC→7 code

$V =$ base shear $= \dfrac{3.0\,C_a}{R} \cdot W$

$Z = 0.4$

$C_a =$ acceleration-controlled seismic response coefficient = 0.44 Na
= 0.44(1.0) = 0.44

$W = W_1 + W_2$ Level II→W_2

www.EngineeringBooksPDF.com

(continued)

Design calculation (US Code)
$W_1 = 2{,}446$ KN; W_2 Level I$\rightarrow W_1$
Total $W = 2{,}446 + 1{,}557 = 4{,}003$ N
$V = 1{,}174.21$ N
$F_x = \dfrac{3.0\, c_a}{R}.w_i$
$F_1 = 717.49$ N $F_2 = 456.425$ N
V (soil level) = 1,174.21 N
The foundations shall be designed for this lateral force $V = 1{,}174.21$

Design Calculations (US Code)	
Design Example 8.2 A four-storey steel frame is located in seismic zone 4. Its a moment-resisting type and has equal storey height of 4.0 m. Anatural period $T = 0.7$ s. The load distribution and displacement are identified in Fig. 8.2. Determine (a) Design level response displacement in the third storey (b) Maximum inelastic response in storey 1 (c) Drift ratio in top storey (d) If there is 18 mm movement accommodated in storey II calculate design level response drift.	
Solution	
Δ_s = design level response(third storey) = $\Delta_{III} - \Delta_{II} = 42 - 25$ mm = 17 mm	UBC-97
Δ_m = max-inelastic response displacement in storey 1 = $\Delta_m = 0.7$ R $\Delta_s = 60$ mm	
$\Delta_m > 0.20\, hs \leftarrow hs$ = storey height = 80 mm > 60 mm O.K.	$R = 8.5$
Design level response storey drift in the top storey	Δ_S = first storey = 10 mm
$\Delta_s = \Delta_{IV} - \Delta_{III} = 55 - 42$ mm = 13 mm	
Δ_{SR} = The storey drift ratio = 0.033	UBC-97: Sec 1627
Δ_{MR} = The maximum allowable design level response storey drift ratio for each storey	
$= \dfrac{0.02\, hs}{hs} = 0.20$	
If the movement of 18 mm is accommodated, then	
$\Delta = \Delta_m = 0.7R\Delta_{s_{11}}$	
Δ_{s11} = second-storey drift	
$\dfrac{\Delta}{0.07R} = \dfrac{18\text{ mm}}{0.7(0.85)} = 3$ mm	
$\Delta_{II} - \Delta_I = 25 - 10 = 15$ mm > 3 mm	

www.EngineeringBooksPDF.com

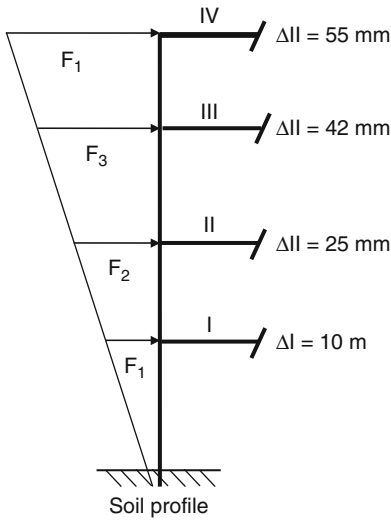


Fig. 8.2 Four-storey load–displacement

Design calculations (US Code)

Design Example 8.3

A 10-storey building 30.5 m high has a total estimated weight of 66.8×10^3 N. It has a location in seismic zone 4 and at a distance of 5 km from the epicentre. The building frame is a moment-resistant type constructed on soil type S_B (UBC-97). Using the following data and criteria defined by UBC-97, determine the total design base shear following the recommended static lateral force procedure:

$C_t = 0.0853$; $I = 1.00$; $C_a = 0.4$ Na; $C_v = 0.4$ N

$N_a = 1.2$; $N_v = 1.6$; $R = 8.5$; $z = 0.4$

Solution:

$V =$ total base shear $== \left(\dfrac{C_D.I}{RT}\right) W$

where r = seismic response modification factor

I = importance factor

C_v = seismic response coefficient

W = seismic dead load

T = natural period $= C_t(C_t)^{3/4} = 1.13$ — UBC-97

$C_a = 0.4(1.2) = 0.48$; $C_v = (0.4)\ (1.6) = 0.64$ — 1630.2.2

V = total base shear = 4,451 N — Item 1

V = minimum base shear $= 0.11\ C_a\, IW = 3{,}527$ N — Method A

For (zone4) $= \left\{\dfrac{0.82N_v.I}{R}\right\} \cdot (W) = 4,024 > 3527$ N

The total design base shear cannot be less than 4,024 N. Hence $V = 4{,}451$ N must be used.

$V_{\max} = \left[\dfrac{2.5C_a 1}{R}\right] W = 9,430.6 > 4,451$ N

The design base shear is 4,451 N.

www.EngineeringBooksPDF.com

Design calculations (US Code)

Design Example 8.4

The horizontal stiffness of a single isolator is defined by $K_H = GA$, where G is the shear modulus of a rubber, A is the full cross-sectional area of the pad. And t_r is the total thickness of the pad rubber. Assuming the diameter of the isolator = 24″ and the design displacement is 11.43″, calculate the value of the period T_D.

$t_r = 1.50''$ note 1 inch = 25.4 mm

$g = 38.4$; $T = 0.73$ s

D_D = design displacement = 11.43″

$G = 7.35$ Kips/in^2

Solution

$A = \frac{\pi\phi^2}{4} = \frac{\pi(24)^2}{4} = 425\,\text{in}^2$

Total rubber thickness $= \dfrac{D}{t_r} = \dfrac{11.43}{1.50} = 7.6$

$$K_H = \frac{7.35(452)}{384} = 8.65\,\text{Kip/in}$$

$$T_D = 2.5\sqrt{\frac{7.35}{8.65}} = 2.3\,\text{s}$$

$T_D \geq 3T_{\text{fixedbase}} = 3(0.7) = 2.1$

Hence $T_D = 2.3 > 2.1$ OK.

The isolator initial parameter OK.

www.EngineeringBooksPDF.com

www.EngineeringBooksPDF.com

Chapter 9
Design of Structural Elements Based on Eurocode 8

9.1 Introduction

This chapter covers only the requirements related to Eurocode 8. Other codes, for comparison, currently in existence is briefly given. Prior to the design calculations an emphasis is placed on the types of superstructure and structural systems, classifications of the seismic zones. A preference is given to the EC8 requirements in this chapter. At the time of writing this chapter calculations have been attempted to design structural elements using EC8. Some relevant equations are given and they have been referred to while carrying out design of structural elements. The reader is advised to Study Chaps. 2, 4 and 5 as well and grab the basic methods and related calculations.

9.2 Existing Codes

A reference is made to Chap. 2 regarding existing codes. The following list cover more or less the codes followed by other countries in case the designers need a comparative study of seismic code requirements:

Algeria	Earthquake Resistance Regulations RPA (2002)
Australia	Minimum Design Load on Structures AS1170 Part 4 (1996)
Austria	Design Loads in Building ONoRmB4015 Part 1 (1999)
Bulgaria	Code for Design of Buildings and Structures in Seismic Regions (1996)
Canada	National Building Code of Canada (1996)
Chile	–
China Peoplès Republic of	Code for Seismic Design of Buildings (2001)
Colombia	–
Costa Rica	–
Croatia	Similar to Yugoslavia and revised in 1999
Cuba	–
Dominican Republic	Provisional and Recommendations for Seismic Analysis of Structures (2004)

M.Y.H. Bangash, *Earthquake Resistant Buildings*,
DOI 10.1007/978-3-540-93818-7_9, © M.Y.H. Bangash 2011

www.EngineeringBooksPDF.com

Ecuador	Manual de adise n de Esstructureas sismo. Resistentes para tusvs guil (2000)
Egypt	Regulations for Earthquake-Resistant Design of Buildings in Egypt (1996)
El Salvador	–
Ethiopia	–
France	NF Po6013 (AFNOR Buildings) (1997)
Germany	German Standard Din 4144 Building in German Earthquake Area (2002)
Ghana	Code for the Seismic Design of Concrete Structure (1990)
Greece	Greek code for Seismic-Resistant Structures EAK 2000 (2000)
Hungary	Dimensioning Directives for Seismic Effects, MI-04.133-81-Now Eurocode 8 (2005)
India	Criteria for Earthquake Design of structures, Part 1, BIS (2002) IS 1893-1 (2002)
Indonesia	–
Iran	Iranian Code for Seismic-Resistant Design of Buildings (1998)
Israel	Design Provision for Earthquake Resistance of Structures SI 413 (1998)
Italy	Technical Rules for Construction in Seismic Zones (2002), Now Eurocode 8 (2005)
Japan	Earthquake-Resistant Design Method for Building Part (2) 2000 (other versions)
Jordan	Jordan Code for Loads and Forces (1990)
Korea	Building Code for Structural Regulations (2000)
Macedonia	–
Mexico	–
Nepal	Nepal National Building Code NBC (2004)
New Zealand	General Structural Design and Design Loadings for Buildings NZS4203 (2004)
Nicaragua	–
Norway	Following the Eurocode 8 (2005)
Panama	–
Peru	–
Philippines	–
Portugal	Following the Eurocode 8 (2005)
Romania	Seismic Building Code (2000), now following the Eurocode 8 (2005)
Russian Federation	Seismic Building Code 2000
Slovenia	Following the Eurocode 8 (2005)
Spain	Following the Eurocode 8 (2005)
Switzerland	Standard STA 160, Action on Structures (2003), now Following the Eurocode 8 (2005)
Chinese Taiwan	Building Code for Earthquake-Resistant Structures (2002)
Thailand	–
Turkey	Specification for Structures to be Built in Disaster Areas (2000)
United States of America	Minimum Design Loads for Building and Structures ASCE-7 (2002)

www.EngineeringBooksPDF.com

Venezuela	–
Yugoslavia	Following the Eurocode 8 (2005)
Eurocode 8	Design Provisions for Earthquake Resistance of Structures (2005)
ISO 3010	International Standard Base for Design of Structures: Seismic Actions (2001)
(former) Yugoslavia	Code of Technical Regulations for the Design and Construction of Building in Seismic Regions (1981)

9.2.1 Explanations Based on Clause 4.2.3 of EC8 Regarding Structural Regularity. A Reference is Made to Eurocode 8: Part 1 – Design of Structures for Earthquake Resistance

Note: This brief is refered to the extended version of clause 4.2.3 of the code

(i) Criteria for regularity in plan:

$$\text{The slenderness ratio } \lambda = L_{\max}/L_{\min} \leq 4$$

where $L_{\max}$ = larger dimensions in plan; $L_{\min}$ = smaller dimensions in plan in order to meet the above condition:

The total length of the building = 5 m; the width of the building = 16 m

One has divided the total length (5 m) of the building into three separate independent portions, two external units of 42 m = 84 m; and the central unit of 21 m = 21 m, thus totalling 10 m with a clear gap between the units; 4 m has been left so that the earthquake force on each unit will not affect the adjacent one due to collision as explained in this text. The overall area is 114×21 m. In our case, $\lambda = 42/16 = 2.65 < 4$.

So, it satisfies the criteria for regularity in plan:

(ii) Criteria for regularity in elevation:
If the building is regular in plan, with slight deviation in central unit, it will satisfy the criteria for elevation in plan.

(iii) Criteria for well-distributed and relatively rigid cladding:
The criteria is satisfied by providing with well-distributed rigid cladding on the roof and vertical sides.

9.2.2 Seismological Actions (Refer Clause 3.2 of EC8)

The construction area is in the earthquake zone of 'strong' intensity which is equivalent to the *Modified Mercalli (MM) scale between VII and VIII and Richer scale between* 6.2 *and* 6.8
Assumed: in our case, horizontal ground acceleration = $0.1g$

www.EngineeringBooksPDF.com

For most of the application of EN 1998, the hazard is described in terms of a single parameter, i.e. the value of the reference peak ground acceleration on type A ground, $a_g R$.

The reference peak ground acceleration, chosen by the National Authorities for each seismic zone, corresponds to the reference return period of the seismic action for the no-collapse requirement (or equivalently the reference probability of exceedance in 50 years) chosen by the National Authorities (see Chap. 14). An importance factor = 1.0 is assigned to this reference period.

Low sensitivity is recommended

(i) when the design ground acceleration on type A ground, $a_g \leq 0.08\,g$ or
(ii) when the product $a_g \times S \leq 0.1\,g$

In the analysis a_g is the same as $\ddot{u}_g$ or $\ddot{X}g$. This is convenient in the analytical formulation.

The basic representation of the seismic action is given in Clause 3.2.2 using ground type based on Table 3.1 of EC8.

9.3 Avoidance in the Design and Construction in Earthquake Zones: Contributing Factors Responsible for Collapse Conditions

Many buildings collapse during earthquakes due to many contributing factors. Prior to the design of buildings, it is necessary to

1. *Avoid soft storey ground floors*: Walls existing in the upper floors are omitted in the ground floor but replaced by columns. This means the *ground floor* is soft in the horizontal direction. In such constructions the columns receive damage due to the cyclic displacements between the building upper parts and the vibrating or moving soil. A storey mechanism sometimes exists by the developing plastic hinges at the top and the bottom of columns with a large concentration of plastic deformations at their ends. Hence the collapse inevitably occurs.
2. *Avoid soft storey upper floors*: Once the lateral bracing is weakened, omitted altogether or the horizontal resistance is substantially reduced above a particular floor, a dangerous sway mechanism occurs and hence the collapse is inevitable.
3. *Avoid a symmetric bracing*: When the centre of the building mass and the centre of resistance do not coincide, definitely twist occurs. This develops torsion in the horizontal plane about the centre of the stiffness. Great relative displacement occurs between the bottom and top of the columns in particular, by keeping them far apart from the centre of stiffness. Failure normally occurs.
4. *Avoid bracing offsets*: Horizontal bracing offsets in-plane at the bottom plan or out-of-plane at the top plan do cause position of the bracing changes from one storey to another, thereby developing bending moments and shear forces. They, in the case of being continuous, definitely reduce seismic resistance. Bracing offsets must be avoided.

www.EngineeringBooksPDF.com

5. *Avoid columns and masonry walls mixed system*: Mixed system of concrete steel column walls is unfavourable because

   (a) Columns with slabs and beams develop frames with small horizontal stiffness than masonry wall.
   (b) Failure of masonry wall due to seismic actions or deflection will be unable to carry gravity loads and inertia loads.

   The collapse is inevitable.

6. *Avoid bracing of frames with masonry infills*: The frames structure is relatively flexible and somewhat ductile. However, the unreinforced masonry is stiff and fragile. The two in combination will cause a damage scenario under the effect of small deformations.

   The combination of these two different incompatible construction does perform poorly. The masonry fails due to the shear or sliding diagonal cracks that develop which indicates seismic failures. The framed structure will have totally different performance as stated earlier. The failure is imminent.
7. *Avoid short columns*: Shear is a problem in short columns. Shear failure occurs reaching plastic moment capacity. Short columns are to be avoided.
8. *Avoid partially filled frames*: The infill of parapet walls into a frame structure without the addition of joints can cause shear failure like a short column. A sway mechanism and P–Δ effect can occur when sufficient shear strength exists.

9.4 Superstructure and Structural Systems

9.4.1 Regularity

To offer a better resistance to earthquakes, the constructions should preferably have simple forms on the one hand and a distribution of the masses and rigidities as regular as possible in the plan and in elevation on the other hand.

9.4.2 Structural Systems

In general, the constructions should have lateral load-resisting system at least in two horizontal directions. These systems should be arranged in order to

- take up sufficient vertical load enough to ensure their stability.
- ensure a direct transmission of the forces to the foundations.
- minimize the torsion action effects.

The lateral load-resisting systems should have a regular configuration and form a continuous and coherent structural system as monolithic as possible. On the other hand, this system should be sufficiently redundant in order to ensure an important margin between the elastic limit and the rupture threshold of the structure.

www.EngineeringBooksPDF.com

A Particular attention should be given to the design and execution of all the connections, keeping in mind the effects of any failure at this level on behaviour of the structure.

9.4.2.1 Reinforced Concrete Structures/Buildings

(a) Moment-resisting space frames without rigid masonry infill walls

The concerned buildings should not exceed seven storeys or 23 m in height in zone I low seismicity; six storeys or 20 m in height in zone II moderate seismicity; two storeys or 8 m in height in zone III high seismicity.

(b) Moment-resisting space frames with rigid masonry infill walls

Here the structure is composed uniquely of the frames capable of carrying all forces due to the vertical and horizontal loads. The fill thickness shall not exceed without loading 10 cm except for the exterior masonry infill panels or for separating walls between two premises where a second wall of 5 cm is accepted on the interior side.

The concerned building shall not exceed six storeys or 20 m height in zones I and II and two storeys or 18 m in height in zone III.

(c) Structural lateral load-resistant system composed of vertical load-carrying shear walls in reinforced concrete.

They are walls and wall cum frames. The lateral case will have walls carrying more than 20% vertical loads. The lateral loads are carried by the walls alone.

(d) RC building entirely braced by RC core

Here the building is completely braced by the RC rigid core which carries all horizontal loads.

(e) Dual bracing systems composed of walls and frames with justification frame wall interaction.

(i) Here the shear walls carry less than 20% of vertical loads.
(ii) The horizontal loads are jointly carried by the shear walls and the frames.
(iii) The frames resist less than 25% of the storey shear in addition to forces due to vertical loads.

(f) Moment-resisting frames system braced by RC shear walls. In this case the shear walls carry less than 20% of vertical loads plus total forces due to horizontal loads.

The buildings are limited to 10 storeys or 33 m maximum height. In zone III, the frames shall have the capacity to resist not less than 25% of the storey shear force due to the vertical loads.

Steel Structure or Buildings

(a) Structures or buildings braced with ordinary moment resisting the height of all the buildings does not exceed five storeys or 17 m in height.

www.EngineeringBooksPDF.com

(b) Ductile moment-resisting space frame systems. They alone resist the total horizontal loads.
(c) Structures or buildings braced by concentric braced frames.

The height of the building in this case is limited to five storeys or 17 m in height.
The complete structure carries total vertical load.
The moment-resisting space frames alone resist the total horizontal loads.

(d) Structures or buildings braced by the X-braced frame:
In this system of a braced node, the axis of the diagonal, the beam and the column are convergent to one point located in the centre of the node. In this type of frame only those diagonals which are in tension contribute to the resistance and the dissipative behaviour.
(e) Structures or buildings with V-braced frames
Here the beams of each braced frame are continuous and the point of the intersection of the diagonal axis of the braced frame is located on the axis of the beam. The resistance and the capacity of dissipation are provided by the joint participation of both the in-tension and in-compression diagonals.
(f) The moment-resisting frames and the braced frames should be designed to resist horizontal loads according to their relative rigidities considering the interaction at all levels. The ductile moment-resisting frames should have the capacity to alone resist not less than 25% of the global horizontal loads.
(g) Structural system braced with ductile frames and X-braced frames
In this system, the dual bracing system is a combination of ductile moment-resisting space frames and concentric V-braced frames.
(h) Vertical cantilever frame system
This category of structure with small degree of redundancy concerns essentially classical one-storey frames with rigid transversal beam and slender structure (tube) type where the resistant structural elements are essentially the columns located on the periphery of the structure.
These particular structures have a dissipative behaviour located uniquely at the ends of the columns.
(i) Steel frame structure braced by diaphragm
These structures resist the seismic actions by the diaphragm effect of vertical element (walls) and horizontal element (floors). The level of dissipative behaviour of these structures depends on the capacity of ductile shear resistance of these walls and floors that can be achieved with various materials and technologies (cold-formed ribbed sheet, reinforced masonry wall, plain concrete or reinforced concrete wall, etc.
The walls should be fixed to the steel frame in order to consider the connections as rigid.
(j) Steel frame structure braced by reinforced concrete core
Same definition as for reinforced concrete frames structural system.
(k) Steel frame structure braced by reinforced concrete shear walls
Same definition as for reinforced concrete frames structural system.

www.EngineeringBooksPDF.com

(l) Steel framed structure braced with dual system composed of a reinforced concrete core and braced steel frames and/or steel moment-resisting frames in periphery.

(m) System including transparencies (soft storeys)

The most illustrative examples are given by the reception levels or lobbies of hotel (rare separation walls or storey height more important than for the current storeys) or absence of separation walls at some storeys for some special reasons (commended to make all the arrangement for mitigating the unfavourable predictable effects).

9.5 Response Spectra Based on EU Code 8

The response spectrum (elastic) is given in Fig. 9.1. The expression for the design spectrum $S_d(T)$ normalized by the acceleration of gravity "g" can be defined by the following expression:

$$0 \leq T \leq T_B : S_d(T) = \propto .S.\left[1 + \frac{T}{T_B}.\left(\frac{B_0}{q}\right) - 1\right] \tag{9.1}$$

$$T_B \leq T \leq T_C : S_d(T) = \propto .S.\frac{B_0}{q} \tag{9.2}$$

$$T_C \leq T \leq S_d(T)\begin{cases} \geq \propto .S\frac{B_0}{q}. \\ \geq [0.20]. \propto \end{cases}\left[\frac{T_C}{T}\right]k_{d2} \tag{9.3}$$

EU CODE – 8

Seismic Action

Characterization of the motion at a point.

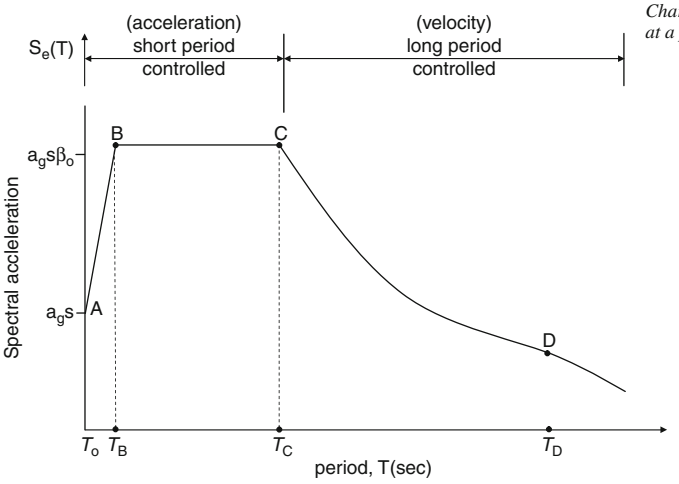


Fig. 9.1 Response spectra

www.EngineeringBooksPDF.com

$$T_{D\leq}T : S_d(T)\begin{cases} \geq \propto .S\frac{B_0}{q}.\left[\frac{T_C}{T_D}\right]_{k_{d_1}} \left[\frac{T_D}{T}\right]k_{d\,z} \\ \geq [0,20].\propto \end{cases} \tag{9.4}$$

Note Sometimes $S_e(T)$ is written for the elastic spectrum instead of $S_d(T)$ in (9.1), (9.2), (9.3) and (9.4)

The behaviour factor q is an approximation of the ratio of the seismic forces experienced by the completely elastic structure with 5% viscous damping.

Three types of soil profiles are defined: A, B, C, ordered with decreasing overall stiffness; from profile A – C there is a shift of the corner period towards higher values, while the maximum amplification is essentially unaffected, with only a 10% reduction foreseen for subsoil class C.

The values suggested in EC8 for the parameters defining the elastic response spectrum are given in Table 9.1.

Table 9.1 Parameters of elastic response spectrum (code Table 2.3.1)

Soil class	S	β_0	K_1	K_2	T_B	T_C	T_D
A	1.0	2.5	1.0	2.0	0.10	0.40	3.0
B	1.0	2.5	1.0	2.0	0.15	0.60	3.0
C	0.9	2.5	1.0	2.0	0.20	0.80	3.0

The correction factor for damping is given by the expression of the code equation (2.3.2).

$$\eta = (\Gamma/2+\xi\ )^{\frac{1}{2}} \geq 0.7 \tag{9.5}$$

The rotational response spectrum about the axis i has the form of code equation (2.3.3) which is

$$s_{ci}^{\theta} = \{_{w/c}S_e(T)\} \tag{9.6}$$

$S_e(T)$ is site dependent; the expression c is the S-wave velocity.

The peak ground displacement d_g is given by

$$d_{g=}[0,05].a_g.s.T_C.T_D \tag{9.7}$$

With the values of a_g, s, T_C, T_D as defined, where

$S_d(T)$ ordinate of the design spectrum, which is normalized by g

$\propto$ ratio of the design ground acceleration a_g to the acceleration of gravity

$$(\propto= a_g/g) \tag{9.7a}$$

q behaviour factor

K_{d1}, k_{dz} exponents which influence the shape of the design spectrum for a vibration period greater than T_C, T_D, respectively. Values of the parameters

www.EngineeringBooksPDF.com

Table 9.2 Values of k_{d1} and k_{d2}

Subsoil class	K_{d1}	K_{d2}
A	(2/3)	(5/3)
B	(2/3)	(5/3)
C	(2/3)	(5/3)

$B_{O.}T_BT_{C.}T_{D.}S$ are given earlier. The values of the parameters K_{d1}, k_{dz} are given in Table 4.2 of the code, given as Table 9.2.

The design spectrum as defined above is not sufficient for the design of structure with base-isolation or energy-dissipation systems.

The comparative equations for normalized spectral acceleration are

(a) Elastic spectrum:

$$\frac{S_e}{a_g s N} \tag{9.8}$$

(b) Inelastic spectrum versus time T

$$\frac{S_d}{a_g s} \tag{9.9}$$

9.5.1 The Behaviour Factor q

Table 9.3 (code Table 2.3.2) gives the factor q for RC, steel piers or columns, abutments and arches.

Two further cases for possible reduction value of q have to be considered. One is related to the amount of design normalized axial force $\eta k = N/A_k * f_{ck}$.

When ηk exceeds 0.3 (it must not be >0.6) q is linearly reduced to 1 for $\eta k = 0.6$.

The second depends on the intended location of plastic hinges being accessible for inspection and repair or not. In the later case the q-values are divided by a factor of 1.4.

For pile foundations where accessibility is questionable at best, a q-value of 2.5 is given (1.5 for inclined piles), provided the piles are detailed for ductility.

For the combination of modal maxima, both SRSS and CQC rules are given with respective range of applicability. The maximum action effects can be evaluated as

$$E = \sqrt{\left(E_x^2 + E_y^2 + E_z^2\right)} \tag{9.10}$$

www.EngineeringBooksPDF.com

Table 9.3 Maximum values of behaviour factor q (code Table 2.3.2)

	Seismic behaviour	
Ductile elements	Limited ductile	Ductile
Reinforced concrete piers		
Vertical in bending ($a_s^* \geq 3.5$)	1.5	3.5
Squat ($a_s = 1.0$)	1.0	1.0
Inclined struts in bending	1.2	2.0
Steel piers		
Vertical in bending	1.5	3.5
Inclined struts in bending	1.2	2.0
with normal bracing	1.5	2.5
with eccentric bracing		3.5
Abutments	1.0	1.0
Arches	1.2	2.0

$*a_a = H/L$ is the aspect ratio of the column for $1.0 < a_s < 3.5$. The q-factor may be obtained by linear interpolation

9.6 Seismic Design Philosophy of Building Frames Using Eurocode 8

9.6.1 General Introduction

This section examines procedures recommended in Eurocode 8 in the seismic design of steel-framed buildings. Buildings maybe designed according to EC8 based on non-dissipative and dissipative behaviour. The non-dissipative design implies "elastic response" and is normally limited to areas of low seismicity. The dissipative lateral forces result from an idealized responsive spectrum. This requirement for ductility uses capacity design approaches.

Two fundamental seismic design levels are considered in EC8 namely "no collapse" and "damage limitation" which essentially refer to ultimate and serviceability states, respectively. No collapse corresponds to seismic action based on a recommended probability of exceedance of 10% in 50 years, or return period of 475 years, whilst damage limitation relates to a recommended probability of 10% in 10 years, or return period of 95 years.

For ultimate limit design in elastic performance is incorporated through the value of q to obtain an acceleration design spectrum S_d; in order to avoid inelastic or non-linear analysis, linear spectral accelerations are generally divided by q, excepting some modification for $T < T_b$ to account for inherent properties, to reduce the design forces.

The shape of inelastic design spectrum for various values of "q" can be plotted. The difference between the elastic spectrum and inelastic spectrum for various values of behaviour factor "q" is identified. In the absence of detailed evaluation, the following values are recommended:

www.EngineeringBooksPDF.com

(a) For DCM (ductile class medium – value of $q = 4$, moment frame:

$$\frac{5 \propto u}{\propto 1}(\text{multistorey}) = 1.3 \tag{9.11}$$

(b) For DCH (ductile class high - value of $\frac{5 \propto \text{u}}{\propto 1}$, moment frame (9.12)

$$\text{Single portal frame} = \frac{\propto u}{\propto 1} - 1.1, \text{ moment frame}$$

$$\text{Single - span multistorey frame} \frac{\propto \text{u}}{\propto 1} = 1.2, \text{ moment frame} \tag{9.13}$$

(c) In case of DCM $\frac{\propto u}{\propto 1} \leq 1.6$

(d) For cross-sections in dissipative zones

$$\left.\begin{array}{l}\text{DCM } (1.5 < q \leq 2.0) = \text{class I, II or III} \\ \qquad\qquad\qquad\qquad\qquad\qquad \}\text{DCH} = 4.0\end{array}\right. \tag{9.14}$$

$$\text{DCM}(2.0 < q \leq 4.0) = \text{class I. II} \tag{9.15}$$

$$\text{DCH}(q > 4.0) = \text{class I} \qquad \}\text{DCM} = 4.0 \tag{9.16}$$

According to Sect 6.13 EN 1998-1:2004, the value of $(M_{Ed,}col)$, the design moment for columns of the frames, can be calculated from

$$M_{Ed,}col = M_{Ed}, G + 1.1\gamma_{OV}\Omega M_{Ed,}E \tag{9.17}$$

where

M_{Ed}, G = gravity loads or actions causing bending moment
$M_{Ed,}E$ = lateral earthquake pressure forces casing bending moments
γ_{OV} = the material overstrength factor, i.e. ratio of the actual to design yield strength of steel 1.25

The value of 1.1 in (9.17) takes into account strain rate and strain hardening effects, the parameter Ω, the beam overstrength factor at any zone is given by

$$\Omega_i = \frac{M_{PI}}{M_{Ed^i}} Rdi_i$$

where

M_{Ed^i} = design in the beam part of beam i
$M_{pi,}Rd.i$ = corresponding plastic moment capacity

In reality, the gravity moments $(M_{EA,G})$ remain constant and only the lateral seismic moments $(M_{EA,E})$ are magnified with more severe events. Consequently, a more accurate definition for Ω should take the form

www.EngineeringBooksPDF.com

$$\Omega_{\text{mod}.i} = \frac{M_{PI-}M_{EA.G.i}}{M_{Ed,E.i}} = \frac{M_{pi.Rd.i} - M_{Ed.G.i}}{M_{Edi} - M_{Ed.G.i}} \tag{9.18}$$

In addition to the design moments from (9.1) columns should be checked for co-existing axial and shear forces similarly obtained from

$$N_{Ed.col} = N_{Ed.G+}1.1\,\gamma_{OV}\Omega N_{EAE} \tag{9.19}$$

$$V_{Ed,col} = V_{Ed.G+}1.1\,\gamma_{OV}\Omega N_{EAE} \tag{9.20}$$

where " Ω" is defined before (i.e. based on the beam flexural overstrength).

The redistribution factor $\frac{\propto u}{\propto 1}$, shall be incorporated into the column equation leased on the frame redistribution capabilities. When the columns are braced, capacity designing requirements axial load $(N_1(Ed.m))$ should be determined from

$$N_{Ed.m} = N_{Ed.G+}1.1\,\gamma_{OV}\Omega \mathrm{N}_{\mathrm{EAE}} \tag{9.21}$$

where $N_{Ed.G}$ and N_{EAE} are axial forces due to gravity loads and lateral seismic forces, respectively, for the beam or column member under consideration. Within the seismic design situation, $N_{Ed.G}$ results from gravity action only whilst N_{EAE} is due to lateral earthquake loads. For braced frames, "Ω" is a braced overstrength determined as minimum over all the braces, of

$$\Omega = \frac{N_{pi.Rd.i}}{N_{Ed.i}} \tag{9.22}$$

where $N_{Ed.i}$ and $N_{pi.Rd.i}$ are the design axial force and plastic capacity, respectively, for brace "i". Beams and columns should then be checked for buckling or yielding based on $N_{Ed.m}$ considering interaction effects from any co-existing moment (M_{EA}) in the seismic condition.

The relative bending stiffness of columns in proposition to the lateral stiffness of tension braces at the lowest storey by β is given as

$$\beta = \frac{\Sigma \frac{L_c}{L_C^3}}{\Sigma \frac{A_d}{L_d}\cos\boldsymbol{\phi}} = \frac{L_d \Sigma I_C}{L_C^3 \cos\boldsymbol{\phi} \Sigma A_d} \tag{9.23}$$

where A_d and L_d are the area and length of the diagonal braces, respectively; I_C and L_C are second moment of area and height of columns, respectively; ϕ is the angle between the diagonal and horizontal projections. The simplified version of (9.23) applies if L_d, L_c and $\boldsymbol{\phi}$ are constant.

The relationship between (β) and the normalized ductility demand (μ_r) can be defined as

www.EngineeringBooksPDF.com

$$\mu_r = \frac{d_{r.\max} n}{\Delta_{\text{top}}} \tag{9.23a}$$

where $d_{r.\max}$ is the maximum interstorey drift within the fame, 'n' is the number of storeys and Δ_{top} is the drift at the frame top.

9.7 Load Combinations and Strength Verification

The seismic load combinations required by Eurocode 8 can be summarized as follows.

In Eurocode 8, the "design action effect" (i.e. the ultimate load) is taken as due to the unfactored combination of dead plus earthquake loads, plus a reduced amount of variable loads, such as live or snow loads. Wind loads are never included with the seismic loads: that is, ψ_2 is always taken zero for wind loads. Using Eurocode notation, this is expressed as

$$\underset{\text{Design action effect}}{E_d} = \underset{\text{Dead}}{\sum G_{kj}} + \underset{\text{Earthquake}}{A_{Ed}} + \underset{\text{Reduced variable load}}{\Sigma \psi_{ai} Q_{ki}} \tag{9.24}$$

9.7.1 Design Strength

The material safety factors γ_M as defined in EC2, EC3 and EC4 for fundamental load combination shall also be used for strength verification under seismic load combinations and capacity design effect.

Note: The material safety factors are repeated here for ease of reference

Reinforced concrete

Concrete	$\gamma_c = [1.5]$
Reinforcing steel	$\gamma_s = [1.15]$
Structural steel	$\gamma_{MO} = [1.1]$
Plastic resistance of cross-section	$\gamma_{m1} = [1.1]$
Resistance of net section at bolt holes	$\gamma_{m2} = [1.25]$
Bolts, rivets, pins, welds, slip	$\gamma_m = [1.25]$

9.7.2 Capacity Design Effects: Method Stated in the Eurocode-8

(1) For structures of ductile behaviour, capacity, design effects (F_c) shall be calculated by analysing the intended flexural mechanism actions and a level of seismic action at which all intended flexural hinges have developed bending

www.EngineeringBooksPDF.com

moment equal to an appropriate upper fractile of their flexural resistance, called moment overstrength M_O.

(2) The moment overstrength of section shall be calculated as

$$M_O = \gamma_O + M_{Rd} \tag{9.25}$$

where

γ_o is the value overstrength factor

M_{Rd} is the design flexural strength of the section, in the selected direction and sense, based on the actual section geometry and reinforcement configuration (γ_m values for fundamental load combinations). In demanding M_{Rd}, the interaction with the axial force and eventually with the bending moment in the other direction, both resulting from the combination of permanent actions (gravity loads and prestressing) and the design seismic action in the same direction and sense, shall be considered.

(3) *P* The value of the overstrength factor shall be taken in general as

$$\gamma_o = 0.7 + 0.2q \tag{9.26}$$

where q is the relevant behaviour factor.

In the case of reinforced concrete sections, with special confining reinforcement according to clause 6.2.1 of the code in which the value of the normalized axial force

$$\eta_k = \frac{N_{Ed}}{A_C f_{ck}} \tag{9.27}$$

exceeds 0.1,the value of overstrength factor shall be increased to

$$\gamma_o = \left[1 + 2(\eta_k - 0.1)^2\right](0.7 + 0.2q) \tag{9.28}$$

where

N_{Ed} is the value of the axial force at the plastic hinge corresponding to the design seismic combination, which is positive if compressive

A_C is the area of section and

f_{ck} is the characteristic concrete strength.

(4) Within members containing plastic hinge(s), the capacity design bending moment, M_C, at the vicinity of the hinge shall not be assumed greater than the relevant design flexural resistance M_{Rd} of the hinge assesses according to clause 5.6.3.1.

www.EngineeringBooksPDF.com

9.7.3 Design Provisions for Earthquake Resistance of Structures

The elastic spectrum is made up of four portions: increasing response acceleration, constant response acceleration, constant response velocity and constant response displacement, separated by the values of three "corner" periods. The four branches are given by the following expression:

$$0 \le T \le T_B: \qquad S_e(T) = a_g.S\left[1 + \frac{T}{T_B}.(\eta.\beta_o - 1)\right] \tag{9.29}$$

$$T_B \le T \le T_C: \qquad S_e(T) = a_g.S\ \eta.\beta_o \tag{9.30}$$

$$T_C \le T \le T_D: \qquad S_e(T) = a_g.S\ \eta.\beta_o\left[\frac{T_C}{T}\right]^{K_1} \tag{9.31}$$

$$T_C \le T: \qquad S_e(T) = a_g.S\ \eta.\beta_o\left[\frac{T_C}{T_D}\right]^{K_1}.\left[\frac{T_D}{T}\right]^{k_2} \tag{9.32}$$

where T is the vibration period of a linear single-degree-of-freedom system

$S_e(T)$	is the ordinate of the elastic spectrum
a_g	is the design value of effective peak ground acceleration
β_o	is the spectral amplification factor for damping ratio 5%
S	is a factor depending on the soil class
η	is the correction factor for damping values different from 5%
$K_1.K_2$	exponents of descending branches for spectrum
T_B, T_C	limits of the constant spectral acceleration
T_D	value defining the beginning of constant displacement range of the spectrum

Note: The M_{Rd} curve shown in Fig. 9.2 corresponds to a pier with variable cross-section (increasing downwards). In case of constant cross-section M_{Rd} is also constant.

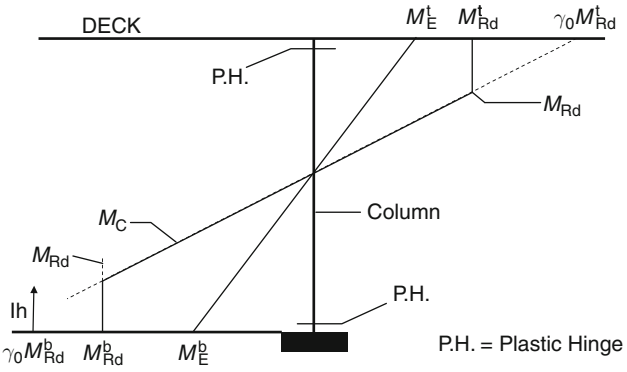


Fig. 9.2 Capacity design moments within member containing plastic hinge(s)

www.EngineeringBooksPDF.com

(5) Capacity design effects shall be calculated in general for each sense of the seismic action in both the longitudinal and transverse directions. A relevant procedure and simplifications are given in Annex G.

9.7.4 Second-Order Effects

In case of linear analysis, second-order effects may be estimated using displacement:

$$d_E = 0.5(1 + q)d_{Ee} \tag{9.33}$$

where q is the behaviour factor and d_{Ee} are the seismic displacement obtained from the first-order elastic analysis.

9.7.5 Resistance Verification of Concrete Sections

(a) Design effects

(1) When the resistance of a section depends significantly on the interaction of more than one action effects (e.g. bending moments and axial force) it is sufficient that the ultimate limit state conditions, given in the respective clauses, are satisfied separately by the extreme (max or min) value of each action, taking into account the interaction with the coincidental accompanying values of the other actions.

(b) Structure of limit ductile behaviour

(1) P

$$E_d \leq R_d \tag{9.34}$$

where

E_d is the design action effect under the seismic load combination including second-order effects and

R_d is the design resistance of the section.

(2) (P) In regions of moderate to high seismicity ($a_1 g \geq [0.10\, g]$) the shear resistance of potential plastic hinges shall be verified according to 5.6.3.4.

(c) Structures of ductile behaviour
Flexural resistance of sections of plastic hinges

(1)

$$M_{Ed} \leq M_{Rd} \tag{9.34a}$$

where

M_{Ed} is the design moment under the seismic load combination, including second-order effects and

www.EngineeringBooksPDF.com

M_{Rd} is the design flexural resistance of the section, taking into account the interaction of the accompanying design effects (axial force and eventually the bending moment in the other direction).

(2) P The longitudinal reinforcement of the member containing the hinge shall remain constant and fully active at least over the length l_h indicated in Fig. 9.2.

(d) Flexural resistance outside the region of plastic hinges

(1) $$M_C \leq M_{Rd} \tag{9.35}$$

where

M_C is the capacity design moment as defined in Clause 5.3 and
M_{Rd} is the design resistance of the section, taking into account the interaction of the corresponding design effects (axial force and eventually the bending moment in the other direction).

(e) Shear resistance of elements outside the region of plastic hinges

(1) Verification of web diagonal compression

$$V_C \leq V_{Rdz} \tag{9.36}$$

(2) Verification of shear reinforcement

$$V_C \leq V_{Cd} + V_{wd} \tag{9.37}$$

where V_C is the shear force resulting from capacity design as per Clause 5.3.
Design shear resistance shall be calculated according to EC2 part 1

$$\begin{gathered} V_{Rdz} \\ V_{Cd} = V_{Rdl} \\ V_{wd} \end{gathered}$$

Note: Formulae are repeated here, in concise form, to facilitate cross-reference

$$V_{Rdz} = 0.5 v f_{cd} b_w 0.9d \qquad with \;\; v = 0.7 - \frac{fck}{200} \geq 0.5 \tag{9.38}$$

$$V_{cd} = V_{Rd1} = [\tau_{Rd} k(1.2 - 40\rho_1) + 0.15\sigma_{cp}] b_w d \tag{9.39}$$

where

$$\tau_{Rd} = 0.035 f_{ck^{\frac{2}{3}}}$$

$$k = 1.6 - d \geq 1$$

www.EngineeringBooksPDF.com

$\rho_1 = \left(\frac{A_{sl}}{b_w d}\right) > 0.02$ is the ratio of longitudinal tension reinforcement

$\sigma_{cp} = \frac{N_{Ed}}{A_c}$ is the average normal stress under the design seismic effects, and d is the depth of the section in metres

$$V_{wd} = \left(\frac{A_{sw}}{s}\right) 0.9 d f_{ywd} \tag{9.39a}$$

where

A_{sw} and s are the area and spacing of the stirrups, respectively,
f_{ywd} is the design yield strength of the shear reinforcement and
b_w is the width of the web of the section.

(e) Shear resistance of plastic hinges

(1) Verification of diagonal compression

$$V_C < V_{Rde} \tag{9.40}$$

where

V_{Rde} is the shear resistance corresponding to the compressive concrete strength after degradation

$$= 0.275 v f_{ck} b_{wc} d_c \tag{9.40a}$$

where

$$\upsilon = 0.7 - f_{ck}/200 \geq 0.5 \text{ and} \tag{9.41}$$

b_{mc} and d_c are confined web width and depth of the section, respectively.

(2) Verification of shear reinforcement

$$V_c \leq V_{cde} + V_{wd} \tag{9.42}$$

where V_{cde} is the contribution of the concrete after degradation and is equal to

$$\begin{aligned} &V_{cde} 0 \text{ if } \eta_k \leq 0.1 && (a) \\ &V_{cde} = 2.5 \tau_{Rd} b_{wc} d_c \text{ for } \eta_k > 01 && (b) \\ &\text{with } \eta_k = \tfrac{N_{Ed}}{A_{cc} f_{ck}} && (c) \end{aligned} \tag{9.43}$$

V_{wd} is the contribution of reinforcement calculated according to 5.6.33 (2) of the code
N_C is the design axial force and is positive if compressive and

www.EngineeringBooksPDF.com

A_{CC} is the confined (core) concrete area of the section.

(3) In circular sections the effective shear area b_{wc}, d_c may be assumed equal to the confined concrete area πD_{sp}^2 and d_c may be assumed equal to D_{sp} where D_{sp} is the spiral diameter.

(4) Verification of sliding shear

$$V_c \leq A_v f_{yd} + \min N_{Ed} \tag{9.44}$$

where A_V is the total distributed longitudinal reinforcement with a design and strength f_{yd}.

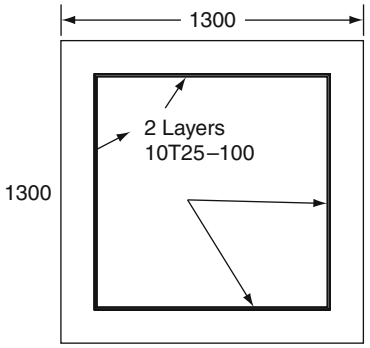
(5) The above verification (9.44) is not applicable in squat wall-type elements with shear ratio $\alpha_s = \frac{M}{Vd} < 2.0$ for such cases, which are quite rare in bridges; the relevant provisions of EC8/Part 1.3 shall be applied.

Design Calculations

Q.9.1 **Design of RC Columns Based on Eurocode 8** 1.1–3.2

Data:

H = column height = 4 m
Square cross-section = 1,300 X1,300 (mm)
Weight on column from superstructure = 4,000 kN
Subsoil class = A (based on (EC8) assumed
Acceleration = $\ddot{U} = a_g = 400$ gal
Strength of concrete = f_{ck} = 24 N/mm^2;
concrete strain = 0.0035
Strength of reinforcement = f_{yk} = 35 N/mm^2
Young's modulus = Ec = 25 N/mm^2
Cross-sectional area = A = 1.69 m^2
Diameter of longitudinal bars = T25 (A_S = 491 mm^2)



γ_c = concrete material factor = 1.50

γ_c = reinforcement material factor = 1.15

from yield and ultimate moments and the values of M_u and M_Y are given as Clause EC8/2 Annex C2

M_Y = 17,880 kNm; ϕ_Y =0.00140/m

M_u = 23,210 kNm: M_u =0.00556/m

www.EngineeringBooksPDF.com

$$I_{un} = \frac{1.3 \times 1.3^2}{12} = 0.2380\,\text{m}^4$$

$$I_{cr} = \frac{My}{(E_c \phi_y)} = \frac{17{,}880}{25} \times (10^6 \times 0.0014)^{-1} = 0.510\,\text{m}^4$$

$T =$ fundamental period: $I_{\text{eff}} = 0.08 \times I_{un} + I_{cr} = 0.529\text{m}^4$

K for column $= 3\,\frac{E_c I_{\text{eff}}}{H^2} = \frac{3 \times 25 \times 10^6 \times 0.529}{4^3} = 619{,}922\ (\text{kN/m})$

$$M = W_u + 0.5\,W_p = 4{,}000 + 0.5(4 \times 1.69 \times 25)$$
$$= 4{,}000 + 84.4 = 4{,}084.4$$

$$T = \sqrt[2\pi]{\frac{M/g}{K}}$$

$$\sqrt[2\pi]{\frac{4084.4/9.81}{619922}} = 0.1629 \approx 0.163$$

Design spectrum analysis with soil condition A

$$0 \le T \le T_B \quad S_e(T) = a_g.s\left[1 + \frac{T}{T_B}(\eta\beta_0 - 1)\right]$$

Design Calculations

$a_g = 400 \times 1.3 = 520\,\text{gal};\ a = \frac{a_g}{G} = \frac{520}{980} = 0.531$ EC B/2 -4.1.6

$S = 1.0;\ \beta_0 = 2.5 \quad K_{dt} = \frac{2}{3}$

Table 4.1, q is fixed as 3.5 for height $=$ 4.0 m and the length is 1.3, so EC 8/2-4.2.1.4

$\frac{4}{13} \approx 3.077 \le 3.50$

$T_B = 0.40\,s, T = 0.163\,s$

$S_e(T) = 0.6915 > 0.20 \times 0.106$

$S_e(T)$*is fixed as* 0.69

Verification of flexural resistance at the base of the column (the plastic hinge region)

MA $=$ the applied moment at the base of the column

$$= \left\{4{,}000 \times \frac{4(4 \times 1.69 \times 25)4}{2\}(0.69)} = 11{,}273\,\text{kNm}$$

The maximum elastic displacement at the top of the column

$d_{E\text{elastic}} = 0.5\,(1 + q)\,d_{Ee} = 0.5(1 + 3.6) \times 0.018 = 0.0414\,\text{m}$

Δm, the additional moment (second-order effect)

$4{,}000\,d_E = 4{,}000 \times 0.0414 = 165.6\,\text{kNm}$
$M_{AT} =$ the total applied moment $= M_A + \Delta M = 16{,}413.6\,\text{KNM}$

www.EngineeringBooksPDF.com

$M_y < 17,880$ OK

Calculation for the length of plastic EC 8/2.6.2.1.4

η_k = normalized axial force

$A_C = 1.69\,\text{m},^2 f_{ck} = 25\,\text{Nmm}^2$

$N_{Ed} = 4,000 + (1.69 \times 4 \times 25)$

$\text{N}_{\text{Ed}} = 4000 + (1.69 \text{ x } 4 \text{ x } 25)$ EC 8/2.6.2.1.4

$N_{Ed}/(A_c.f_{ck}) = \frac{4.169 \times 10^3}{1 \times 25 \times 10^3 \times 1.69} = 4,169\,\text{kN}$

$0.0987 < 0.1$

$\eta_k = 0.0987 \approx 0.0988$

The length of the plastic hinge is larger if one of the following:
(a) The depth of the column = 1.3 m

(b) The distance from the point of maximum moment where the moments is reduced by 20%

$= 4 \times 0.2 = 0.8\,\text{m}$

The depth is kept as 1.3 m

Verification of the shear resistance in the plastic hinge region EC8/2.5.6.3.4
The shear force resulting from The Capacity Design EC8/2.5.3

Since $\eta_k < 0.1, \gamma_0 = 0.7 + 0.2q$
$0.7 + 0.2 \times 0.5 = 1.4$
V_C = applied shear force in the capacity design effects

$\gamma_0 V = 4\,(4,000 + 1.69 \times 4 \times 25) \times 0.69 = 4027.25\,\text{kN}$ EC.5.6.3.4(1)

For diagonal compression

$V_{Rde} = 0.275\,\text{VF}_{CK} b_{wc} d_c$

$0.275(0.4 - \frac{24}{200})24 \times 1,150 \times 1,150 = 5,061.4 > 4,072.25 = V_C$ OK

www.EngineeringBooksPDF.com

Design Calculations

For transverse reinforcement 2 Legs. T16
($\phi = 15.9\,\text{mm}\ A_s = 201\,\text{mm}^2$) are provided in the horizontal plane with vertical spacing 150 mm, i.e. 2LT16-150

EC.5.6.3.4(2)

The shear resistance corresponding to the yield of shear reinforcement

$$V_{cde} + V_{wd} = 0 + \left[\frac{A_{sw}}{S}\right]0.9dfy_{wd}$$

$$= 0 + \left(201 \times \frac{12}{150}\right)0.9 \times 1150$$

$$= \left(\frac{345}{1.15}\right) = 3,450\,\text{kN}$$

EC8/2.6.2.1.3

Minimum amount of confining reinforcement in plastic hinge region

The transverse reinforcement ratio ρ_w is given by

$\rho_w = A_{sw}/s.b$ where A_{sw} = total area of ties in one direction
Confinement $= 201 \times 12 = 2,412\,\text{mm}^2$

$= \frac{2,412}{150 \times 1,150}$

EC8/2-6.2.1

$= 0.01398$

$w_{wd} = \frac{\rho_w f_{yd}}{f_{cd}}$ = $f_{yd} = f_{yk}/\gamma$

$0.01398 \times 300/16$ $345/1.15$

$= 0.262$ $= 300$

EC8/2-6.2.1.3

$w_{wd}, r \geq 1.74\frac{A_c}{A_{cc}}(0.009M_c + 0.17)\eta_k$ $f_{cd} = \frac{f_{ck}}{\gamma_c}$

$w_{wd}.r = 0.0914$ $-0.07 \geq w_w$ $24/241.501.50$
$= 16$

$A_C = 1.69\,\text{m},^2 A_{CC} = 1.3225\,\text{m},^2 \mu_c = 13$

The corresponding w_{wd} is $0.166 > w_{wd,r} = 0.01914$
The bar diameter for transverse reinforcement is decreased to

T10 ($[(A]_s = 126.7\,\text{mm}^2$) instead of T16 $[(A]_s = 201\,\text{mm}^2$)

w_{wd} decreases to 0.106 and greater than $w_{wd.}dr$, hence it can be used.
Requirement for bucking of longitudinal reinforcement to prevent bucking in the plastic region

$A_t/S = A_s f_{ys}/1.6f_{yt}\,\text{mm}^2/\text{m}$ A_t = area of one tie leg

ΣA_sTwice cross-sectional area A_s = sum of the area by one tie leg of the longitudinal bars of longitudinal T-25 bars (mm^2)

($A_s = 419\,\text{mm}^2$)
Hence $A_t/S = 614\,\text{mm}^2/\text{m}; s = 0.15\,\text{m}$

www.EngineeringBooksPDF.com

Design Calculations	Sheet No. 9.4 Code Clause

$A_t > 120.5\,\text{mm}^2$ f_{ys} = yield of longitudinal bars EC8/2-5.6.3.3(1)
f_{yt} = yield of tie

For diagonal compression

$$V_R, d, 2 = 0.5\vartheta \quad f_{cd} b_w 0.9d$$
$$= 6,243 > V_c = 4{,}265$$

The shear resistance corresponding to the yield shear reinforcement can be obtained as EC8/2-5.6.3.3(2)

$$V_{cd} + V_{wd} = [\tau_{Rd} k(1.2 + 40\rho_1) + 0.15\delta_{cp}] b_w d$$

$$\tau_{Rd} = 0.035 f_{ck}^{\frac{2}{3}} = \frac{0.291\,\text{N}}{\text{mm}^2}.k = 1.6\,\text{dcms} \geq 1, \text{ take } k = 1$$

$$d = 1.1\,\text{m}, \rho_1 = A_{s1}/b_w d = 0.01707$$

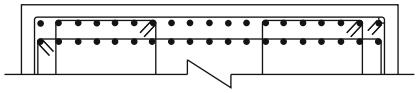
$$\delta_{cp} = N_{ED}/A_C = 4,000 \times 10^2/1,300 \times 1,300 = \frac{2.367\,\text{N}}{\text{mm}^2}$$

$$V_{cd} = [0.291 \times 1(1.2 + 40 \times 0.01707) + 0.15 \times 2.367 \times 1,300 \times 1,100]$$
$$= 126.84 \times 10^4\,\text{kN}$$
$$V_{wd} = (A_{SW}/S)0.9 d f y_{wd} = 3,968\,\text{kN}$$

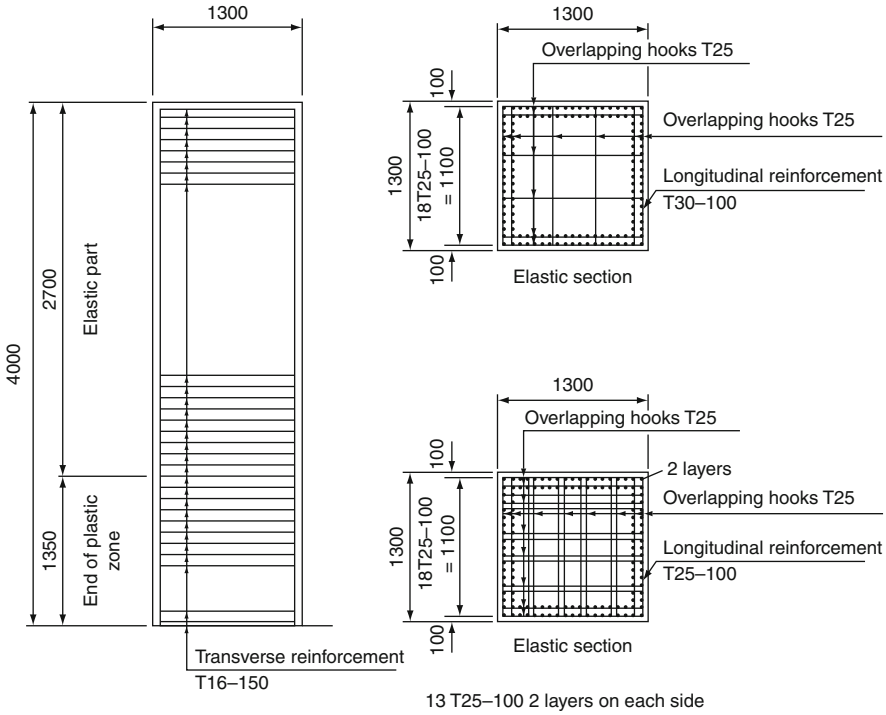
Shear resistance $= V_{cd} + V_{wd} = 496.64 \times 10^5\,\text{kN} > V_C = 4,027.25\,\text{kN}$

Shear resistance outside the plastic $= 4,027.25\,\text{kN}$ hinge region is satisfied.

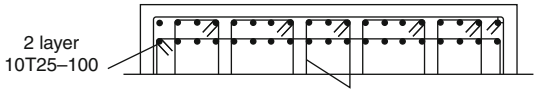
www.EngineeringBooksPDF.com



Detailing of overlapping hooks
for general section



13 T25–100 2 layers on each side
(design required 1025–100)



Detailing of overlapping hooks
for plastic hinge section

Case (a)
H = 7m; a_g = 400 gal
H = 4m; a_g = 400 gal

www.EngineeringBooksPDF.com

Design Calculations

Q.9.2

Problem 9.2 One-storey frame made in concrete has four numbers of columns each having a rectangular cross-section 700 mm by 600 mm as shown in Fig. 9.3.

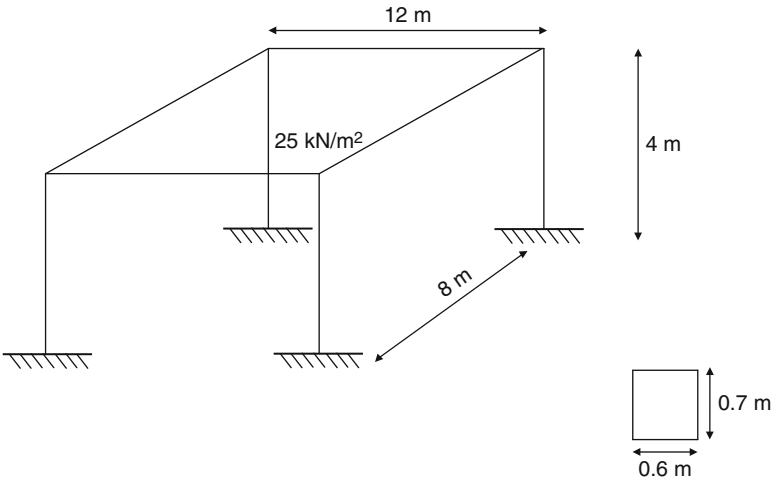


Fig. 9.3 One-storey frame under earthquake

$E = 3.2 \times 10^7\,\text{kN/m}^2$. The design response spectrum parameters are given below:

$$\alpha = 0.4; S = 1,\ q = 3.5; \beta_o = 2.5; \gamma = 1; T_B = 0.15; T_c = 0.45; T_D = 3.05$$

Showing the frame is subjected to the design earthquake using EC8,calculate

(a) fundamental vibration of this frame in the X, Y, Z directions;
(b) equivalent forces F_x, F_y,F_z induced in the frame (static);
(c) the inelastic deflection and check that the deflections in (c) meet the serviceability limit state

Solution

(a) $T = \frac{2\pi}{w} = 2\pi\sqrt{\text{M/K}}$

$W = 25 \times 12 \times 8 = 2,400\,\text{kN}$

$M = \frac{2,400}{9.82} = 244.64\,8(\text{kg.}/\text{s}^2\text{m})$

$M = \frac{2,400}{9.82} = 244.648\,(\text{kg.s}^2/\text{m})$

$= I_X = \frac{bd^3}{12}; I_X = 0.01715\,\text{m}^4; I_Y = 0.0126\,\text{m}^4$

$K_X = 4\ (12\,EI_Y/L^3) = 0.3024 \times 10^4\,\text{kN/m}$

www.EngineeringBooksPDF.com

Design Calculations

Note:

$L = 4\,\text{m}$

$A = 0.6 \times 0.7 = 0.42\,\text{m}^2 \quad K_Y = 4\left(\frac{12\,EI_X}{L^3}\right) = 0.416 \times 10^6\,\text{kN/m}$

$K_z = \frac{4\,EA}{H} = 4\left[\frac{32\times10^6\times0.42}{4}\right] = 13.44 \times 10^6\,\text{kN/m}$

$T_X = \frac{2\pi}{w} = \sqrt[2\pi]{\frac{m}{K_x}} = 0.01787\,s$

$T_y = \sqrt[2\pi]{\frac{m}{K_y}} = 0.1581\,s$

$T_z = \sqrt[2\pi]{\frac{m}{K_z}} = 0.0268\,\text{s}$

(b) $F_X; F_Y; F_Z$

$F = ma$

$F_X = MS_dT_x(i) \qquad a = S_d(t)g$

$S_d(T_X) = \frac{\propto S\beta_o}{q}g \qquad 0.1 < 0.1787 < 0.4$

$\frac{0.4\times1\times2.5}{3.5}g = 0.286.39\,g$

From

$F_x = 244.648 \times 0.286 \times 9.81 = 686.39\,\text{kN}$

$F_Y = 656.399\,\text{kN}$

$F_z = MS_d(T_z) \times 0.7\,g, \qquad T_z = 0.0268 < 0.15\,s$

reduction factor $= 0.7$

$0 \le T \le T_B$

$0 \le 0.268 \le 0.1$

$S_d(0.268) = a_s\left[1 + \frac{T}{T_B}\left(\frac{\beta_0}{q} - 1\right)\right]$

$= 0.4\left[1 + \frac{0.268}{0.1}\left(\frac{2.5}{3.5} - 1\right)\right] = 0.324$

$F_z = 244.648 \times 0.3241 \times 0.7 \times 9.81 = 544.409\,\text{kN}$

$dx.e = \frac{F_x}{K_x} = \frac{686.399}{0.3024\times10^6} = 2.2675 \times 10^{-3}\,\text{m}$

(c)

$\text{d}x = \text{d}xe(q) = 7.936 \times 10^{-3}\,\text{m}$

$\text{d}r \le \frac{h}{250}; \text{d}r = 0.016$

$\text{d}x < \text{d}r$

$7.936 \times 10^{-3}\text{m} < 0.016\,\text{m}$ OK

Note: The individual column checking procedure as given in Example 9.1 shall be carried out. This is not given in this solution owing to lack of space for repetitive work.

www.EngineeringBooksPDF.com

Design Calculations

Q.9.3

Problem 9.3 The frame in Fig. 9.4 is now modified by providing two additional columns pinned at the ground level and increasing the horizontal span to 14 m with 6 m width as shown in the figure. The frame is loaded with 5.2 KN/m^2 Each column has a cross-section 0.75 m × 0.65 m. Determine

(i) the natural periods vibration in X, Y, Z directions based on EC8
(ii) the static equivalent forces $F_x; F_Y; F_Z$ induced in the frame based on the rules provided by EC8
(III) The inelastic deflection dx.dy caused by the EC8 earthquake defined by the following parameters of the design response spectrum:

$\alpha = 0.4;\ q = 3.5;\ \beta_o = 2.5;\ T_B = 0.1;\ T_c = 0.4;\ T_D = 3.0;\ S = 1;\ \gamma = 1$

For vertical motion, use the reduction factor. Check to see that the values of deflection meet the serviceability limit state. Assume the value of E, as

$E = 3.2 \times 10^7\ \text{kN/m}^2$

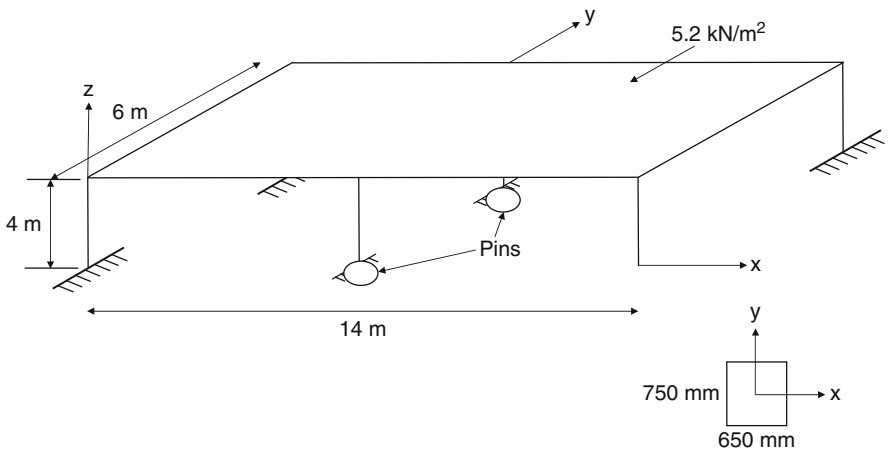


Fig. 9.4 Concrete slab supported by six columns

www.EngineeringBooksPDF.com

Design Calculations

Q.9.3

Solution

(i) $M = 5.2 \times 14 \times 6 = 436.8$

$$M = \frac{436.8}{9.81} = 44.526\,\text{kgs}^2/\text{m}$$

$$K_x = \frac{4\times 12\,EL_x}{L^3} + 2\,\frac{[3EI_y]}{L^3} \qquad I_X = \frac{0.65\times 0.75^3}{12} = 0.02285$$

$$= \frac{4\times 12\times 32\times 10^6(0.01716)}{4^3} + 2\times\frac{32\times 10^6(0.01716)}{4^3} = 0.4636\times 10^6\,\text{kN/m}$$

where

$$I_Y = \frac{0.75(0.65)^3}{12} = 0.01716\,\text{m}^4$$

$$K_y = 0.61669\times 10^6\,\text{kN/m}; \quad K_z = 6\left(\frac{EA}{L}\right) = 23.4\times 10^6\text{kN/m}$$

$T_X = 0.06$ s; $T_Y = 0.052$ s; $T_Z = 0.0085$ s

All of them are less than 1; hence it is stiff.

(ii) $T_E = 0.1$; $T_C = 0.4$; $T_D = 3.0$

$F = ma$

$F_x = S_d(T_x)M$

If $S_1d(T_1x = 0.06 \quad 0 \le 0.06 \le 0.1)$

$$S_d = a_1\left[1 + \frac{T}{T_s}\left(\frac{\beta_0}{q} - 1\right)\right] = 0.331$$

So from Fig. 9.3

$$F_x = 44.526\times 0.4\times 9.81 = 174.72\,\text{kN}$$

$S_d\,(T_Y - 0.052)$

$$S_d(y) = a_s\left[1 + \frac{T}{T_s}\left(\frac{\beta_0}{q} - 1\right)\right] = 0.3405$$

$$F_y = 44.526\times 0.341\times 9.81 = 148.95\,\text{kN}$$

$$S_d(z) = (T = 0.0085) = 0.3902$$

$$F_Z = 44.526\times 0.341\times 9.81\times 0.7 = 119.28\,\text{kN}$$

$$dx(e) = \frac{F_x}{k_x} = \frac{174.72}{0.4634\times 10^6} = 3.77\times 10^{-4} \approx 0.4\,\text{mm}$$

$\text{d}x\ (\text{in}) = \text{d}x(e)\times q = 0.14\,\text{mm}$ $\qquad \text{d}r = \frac{h}{250} = 0.016$

$\text{d}r > \text{d}x$

$$\text{d}y(e) = \frac{F_Y}{K_Y} = 2.414\times 10^{-4}\,\text{m}$$

$\text{d}y\,(\text{in}) = 8.448\times 10^{-4} = 0.8123$; $\text{d}r > \text{d}y$

www.EngineeringBooksPDF.com

Design Calculations

Example 9.4 A two-storey building consists of three such frames along X- direction as shown in Fig. 9.5. The dimensions in plan are 12 m × 12 m. The height of each floor is 4 m with a total height of 8 m.The two numbers of each bay c/c of columns is 6 m is both *X* and *Y* directions. Using the following data
(i) Calculate T_1 and T_2, the period of vibrations in the *X*-direction
(ii) Check the calculation of T_1 against the EC8.
(iii) Total horizontal forces on the frame induced based on EC8
Data:

$$[K] = \text{Structural stiffness matrix} = \begin{bmatrix} (k_{11}) & (k_{12}) \\ 527.33 & -264.67 \\ (k_{21}) & (k_{22}) \\ -264.67 & 264.67 \end{bmatrix} \times 10^6 \mathbf{N/m}$$

Circular frequencies:

$\omega_1 = 35.0728$ rad/s

$\omega_2 = 56.5788$ rad/s

SRSS Method is adopted as stated in this text

Parameters forming design response spectrum

$\propto = 3.75;\ \beta_0 = 2.5;\ T_B = 0.1;\ T_C = 0.4;\ T_D = 3.0;\ S = 1;\ \gamma_1 = 1$

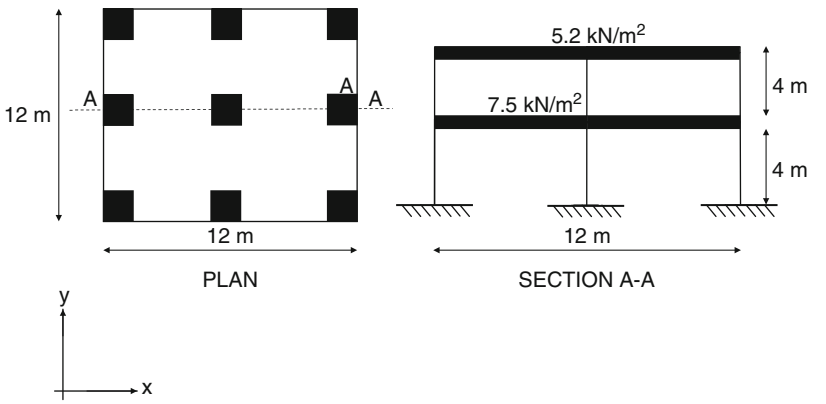


Fig. 9.5 A two-storey two-bay frame

www.EngineeringBooksPDF.com

Design Calculations

Q.9.4

(i) w_1 *and* w_2 are known

$T_1 = \frac{2\pi}{w_1} = 0.17914$ s

$T_2 = \frac{2\pi}{w_2} = 0.0725$ s

(ii) EC8 formula

$T_1 = C_t H_t^{3/4}$

$= 0.07\text{s}\, H^{\frac{3}{4}}$

$= 0.3567$ s

Around twice

$W_{1\text{total}} = 5.2 \times 144 = 748.8$ kN $\quad M_1 = 76.330\,\text{kgs}^2/\text{m}$

$W_{2total} = 7.5 \times 144 = 1,080$ kN; $\quad M_2 = 110.092\,\text{kgs}^2/\text{m}$

$T_B = 0.1; \quad T_C = 0.4; \quad T_D = 3$

$S_d(T_1 = 0.17914)$

$$S_d = aS\frac{\beta_o}{q} = 0.233$$

$T_B < T \leq T_C$

$s_d(T_2 = 0.075)$

$$S_d = aS\left[1 + \frac{T}{T_B}\left(\frac{\beta_o}{q} - 1\right)\right] = 0.2625$$

$0 < T < T_E$

$(K_{11} - M_1 w_1^2)\phi_{11} + k_{12}\phi_{21} = 0$

Modal values $\phi_{11} = 0.6577$

$(K_{11} - M_1 w_2^2)\phi_{12} + K_{12}\phi_{21}$

$\phi_{12} = -1.08606$

$\Gamma_1 = \text{participation factor} = \dfrac{M_1\phi_{11} + \phi_{21}}{M_1\phi_{11}{}^2 + M_2\phi_{21}{}^2}$

$= 1.1963$

$\Gamma_2 = \text{participation factor} = \dfrac{\text{M}_1\phi_{12} + \text{M}_2\phi_{22}}{\text{M}_1\phi_{12}^2 + \text{M}_2\phi_{22}^2} = -0.1962$

$$\begin{Bmatrix} F_{11} \\ F_{21} \end{Bmatrix} = \Gamma_1 S_d(T_1)\begin{bmatrix} w_1 & 0 \\ 0 & w_2 \end{bmatrix}\begin{bmatrix} \phi_{11} \\ \phi_{21} \end{bmatrix}$$

$(F_{ij})_{\max} = \Gamma_j S_d(T_j, E_j)[w]\phi_{ij}$

$F_{11} = \Gamma_1 s_d(T_1)[w_1]\phi_{11} = 137.274$ kN

$F_{21} = \Gamma_1 S_d(T_1)[w_2]\phi_{11} = 326.944$ kN $=$ F_{12}

$$\begin{Bmatrix} F_{12} \\ F_{22} \end{Bmatrix} = \Gamma_1 S_d(T_1)\begin{bmatrix} w_1 & 0 \\ 0 & w_2 \end{bmatrix}\begin{bmatrix} \phi_{12} \\ \phi_{22} \end{bmatrix}$$

$F_{22} = (-38.57)$ kN; $F_1 = \sqrt{(F_{11}^2 + F_{21}^2)} = 354.593$ kN

$\text{F}_1 = \sqrt{(F_{21}^2 + F_{22}^2)} = 329.211\,kN$

www.EngineeringBooksPDF.com

9.8 Analysis and Design of a Steel Portal Frame under Seismic Loads. A Reference is Made to Fig. 9.6.

It is assumed that the portal frame has been designed against the wind. Only live, dead and seismic loads are involved using Eurocode 1: Part 1-1 Design criteria are needed but only produce guidelines for this frame if one wishes to design this frame using Eurocode-8.

9.8.1 Data on Loadings

Characteristic dead loads (G_k) and imposed loads based on Eurocodes 1: Part 1-1

Roof: A reference is made to a portal frame in Fig. 9.6 and 9.7.

Total dead weight	= 7.85KN/m on roof beam or load
Dead load/m of column	= 6.56KN/m
Characteristic live load	= 15KN/m
Total dead load DL_{TOT}	= 131.45KN
Total live load LL_{TOT}	= 260.6KN

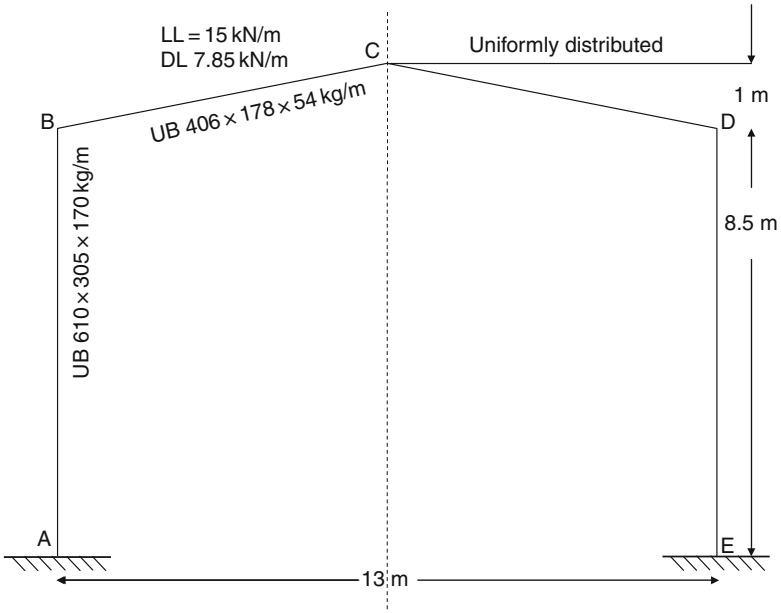


Fig. 9.6 A steel portal frame under loads (DL + LL)

www.EngineeringBooksPDF.com

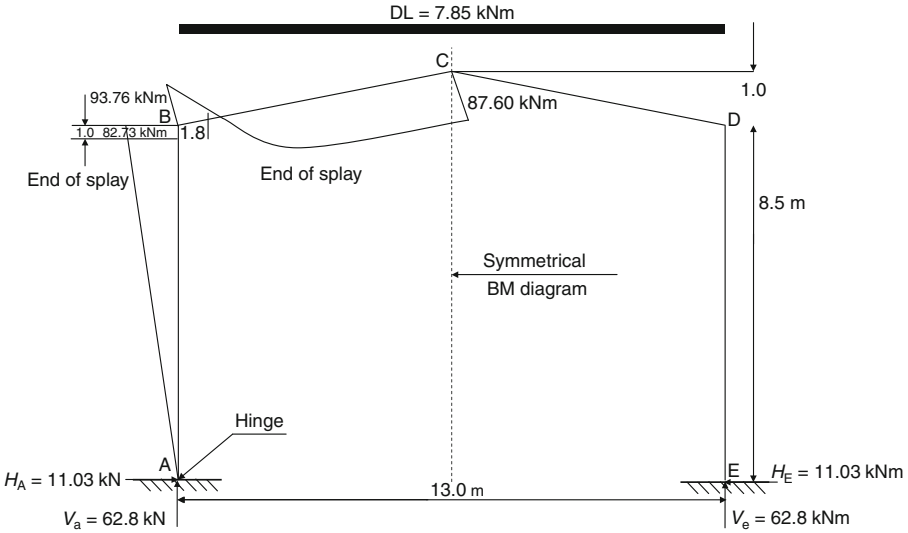


Fig. 9.7 BM diagram for dead loads

9.8.2 Bending Moments, Vertical and Horizontal Reactions

(a) Due to dead load

$M_{BA} = M_{DE} = 93.76$ kNm; H_A at base $= 11.03$KN;
$M_{CB} = M_{CD} = 87.60$ kNm $V_A = V_E = 51$KN

(b) Live load

$M_{BA} = 135$kNm
$M_{DE} = -96.22$kNm
$E_2 = 7$KN Seismic force at mid height of the column and
$M_{BA(seismic)} - M_{DE} = 29.75$kNm
$V_A = VE_{(seismic)} = -5.654$KN
$H_A = H_E = 7$KN
Design Base Shear $= F_{BD} = 0.366$ Mg

Recommended methods of analysis is stiffness and flexibility methods for the portal frame $= 39$KN

9.8.3 Ultimate Design Moments and Shears (Moment-Capacity Design)

Section UB610×305×170 kg/m; steel grade S275
Class I
$\delta_{uv} = 1.25$
fy $\not\geq 378$ W/mm^2

www.EngineeringBooksPDF.com

Max. ultimate design moment at YY axis = M_{ED} = 844kNm
Max. ultimate shear = 95KN
Max. Axial thrust = 194KN

Follow the eurocode EC-8 and Eurocode-3, check this frame for the seismic combination of actions and prove that the frame is safe.

Guidelines for solution

1. Develop the BM diagram for live load and to account for the base force due to seismic action.
2. Total load on the column of frame.
3. Choose the analysis such as

   (a) Flexibility method
   (b) Stiffness method
   (c) Handbook formulae (Kleinlogel Rahman Formula).

4. Assume member size given above and carry out solutions for moments shear and axial effects using one of the above method. Draw BM diagram at caves level due to the combination of seismic loads.
5. Check for seismic combination of actions for columns and pure in parts and beams.
6. Classify the section, in this will come out to be class 1 while checking the flang and web.
7. Carry out moment capacity design using EC-5 and EC-8.
8. Check the size UB610×305×170 kg/m; steel grade S = 275.
9. Check for the dissipative zones expected to yield before other zones.
10. Check shear buckling resistance and buckling resistance to compression on all load combinations.
11. Check the plastic moment of resistance, plastic moment capacity, shear and buckling effects such as for shear and

Conclusion. For columns UB 610×305×179 kg/m; S = 275 is ok.
For beam UB 406×178×54 kg/m is ok.

www.EngineeringBooksPDF.com

Design Calculations

Example 9.5. A three-storey three-bay frame made in concrete is shown in Fig. 9.6. The frame is fixed to the foundations. The natural frequencies w_j and the modal matrix for this frame are given below:

$$\text{Natural frequency } w_j = \begin{bmatrix} w_1 \\ w_2 \\ w_3 \end{bmatrix} = \begin{bmatrix} 16.568 \\ 44.250 \\ 73.240 \end{bmatrix} \text{ rad/s}$$

$$\text{Modal matrix} \left[\phi_{ij}\right] = \begin{bmatrix} 0.5350 & 1.000 & 0.2230 \\ 0.9019 & -0.2287 & -0.9153 \\ 1.000 & -0.7610 & 1.000 \end{bmatrix}$$

(i) Evaluate periods of vibrations T_1, T_2 and T_2.
(ii) Calculate the participation factors Γ and the effective modal masses μ_m for each mode and total modes asked for in EC8
(ii) Total horizontal forces induced in the frame when the design response spectrum using the parameters $\propto = 0.35$; $q = 3.75$; $\beta_o = 2.5$; $T_B = 0.1$; $T_C = 0.4$; $T_D = 3.0$; $S = 1$
Uses SRSS combination of modes are adopted

Design Calculations

$T_1 = \frac{2\pi}{w_;}$ $T_1 = 0.3794\,\text{s}$; $T_2 = 0.143\,\text{s}$; $T_3 = 0.0856$

(i), (ii) $\Gamma_1 =$ participating factor at 1

$$\frac{M_1\phi_{11} + M_2 + \phi_{21} + M_2 + \phi_{31}}{M_1{\phi_{11}}^2 + M_2{\phi_{21}}^2 + M_2 + {\phi_{31}}^2} = 1.2258$$

$$\Gamma_2 = \frac{M_1\phi_{12} + M_2\phi_{22} + M_3 + \phi_{32}}{M_1{\phi_{12}}^2 + M_2{\phi_{22}}^2 + M_3{\phi_{32}}^2} = 0.3380$$

$$\Gamma_3 = \frac{M_1\phi_{12} + M_2\phi_{23} + M_3 + \phi_{32}}{M_1{\phi_{12}}^2 + M_2{\phi_{22}}^2 + M_3{\phi_{32}}^2} = 0.3099$$

$M_1 = 427.569\,\text{kg}$; $M_2 = 30.913\,\text{kg}$

$M_3 = 0.2306\,\text{kg}$

$90\%\, E_{m_1} = 412.84377\,\text{kg}$
$Em_1 > 90 Em_1$ same repeated for M_2 and M_3
(iii) $T_B = 0.1$; $T_C = 0.4$; $T_D = 3$

$S_d(T_1 = 0.3793)$
for $T_B < T \leq T_C$
$S_d = \propto S\beta_{o/q} = 0.233$
$S_d(T_2 = 0.142)$; $S_d = 0.233$
$s_d(T_3 = 0.0857)$
For $0 \leq T \leq T_B$
$S_d = \propto_s \left[1 + \frac{T}{T_B}\left(\frac{\beta_o}{q} - 1\right)\right] = 0.25$

www.EngineeringBooksPDF.com

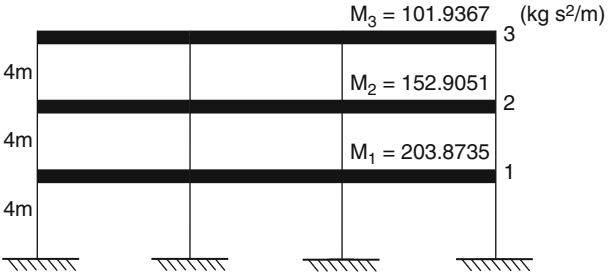


Fig. 9.8 A three bay three-storey frame

$$\begin{Bmatrix} F_{11} \\ F_{21} \\ F_{32} \end{Bmatrix} = \Gamma_1 S_{d1} \begin{bmatrix} w_1 & 0 & 0 \\ 0 & w_2 & 0 \\ 0 & 0 & w_3 \end{bmatrix} \begin{Bmatrix} \phi_{11} \\ \phi_{21} \\ \phi_{31} \end{Bmatrix}$$

$F_{11} = 305.30\,\text{kN} \rightarrow \text{F}_1$

$F_{21} = 386.5\,\text{kN} \rightarrow \text{F}_{21}$

$F_{31} = 385.590\,\text{kN} \rightarrow \text{F}_{31}$

www.EngineeringBooksPDF.com

Chapter 10
Earthquake – Induced Collision, Pounding and Pushover of Adjacent Buildings

10.1 General Introduction

The pounding of adjacent structures during earthquakes has been receiving considerable attention in recent years. This is because adjacent structures with inadequate clear spacing between them have suffered considerable structural and non-structural damage as a result of their collision during major earthquakes. The different dynamic characteristics of adjacent buildings make then vibrate out of phase, and pounding occurs if there is a lack of sufficient space between them. However, building code provisions for seismic separations in seismically active regions are not applicable, not only in the old parts of the cities but also in many cases in new buildings, due to socioeconomic implications. Moreover, pounding between adjacent structures is a highly complex phenomenon, and its accurate modelling requires great details of information of the structures in conjunction with a very reliable analytical method. In general, inelastic and plastic deformation, local crushing as well as impact-induced fracturing may occur at contacts during impact and pounding.

In this chapter the phenomenon of mutual interaction between neighbouring buildings and the parameters that are affecting it are described thoroughly. The required separation distance between adjacent buildings in order to reduce pounding is studied as well as the building code provisions for seismic separations. Earthquake ground motion spatial variation effects on relative linear elastic response of adjacent buildings and their vibration characteristics are analysed and also analytical solutions for the relative impact velocity are derived when adjacent buildings collide. Finally, the contact impact model is treated by the Lagrange multiplier method, which enforces compatibility of displacements for the bodies coming into contact. Many other methods including the modal analysis given in Chap. 5 have also been recommended.

It has been observed, during powerful earthquakes, that in neighbouring buildings, which are tangential to each other or have small separation distance between them so that they can collide with each other, their dynamic behaviour is mutually influenced in an important scale. In these conditions the phenomena that are developed from the impact have as a result the mutual interaction of these buildings and also the drastic change of their dynamic response.

M.Y.H. Bangash, *Earthquake Resistant Buildings*,
DOI 10.1007/978-3-540-93818-7_10, © M.Y.H. Bangash 2011

www.EngineeringBooksPDF.com

During these phenomena, the presence of defects is possible, not only in the building itself but also in the secondary elements of the mutually impacted buildings. The defects of the building can be developed in positions that are crucial for the behaviour of buildings, having as a possible result some or total collapse of the buildings.

This phenomenon is called *mutual interaction between neighbouring buildings under the conditions of seismic actions*.

If the neighbouring buildings do not come in contact with each other, because the separation distance between them is big enough, but they are founded in soft soils then there is still the possibility of mutual interaction in their dynamic behaviour. In this case the mutual interaction is immediate, via the soil of the foundation.

For example, poundings between structures have been observed in the Alaska earthquake of 1964, San Fernando earthquake of 1971, Mexico City earthquake of 1985, Loma Prieta earthquake of 1989 in California, Kobe earthquake of 1995, Taiwan Chi-Chi earthquake of 1999, the Sequenay earthquake of 1988 in Canada, the 1992 Erzincan earthquake in Turkey and the 1992 Cairo earthquake. Recently many earthquakes occurred in Turkey, Iran and Pakistan. The earthquake in 2006 has destroyed Margalla Tower in Islamabad, Pakistan, and prior to collapse, the adjacent floors–walls interacted, eventually causing a total collapse.

The influence of the following factors when collision occurs between adjacent buildings need to be examined in detail if possible:

1. The sizes of the building masses that impact or pound
2. The stiffness and damping of each building
3. The number of storeys of each building and in the height that the pounding impact occurs
4. The separation distance between the adjacent buildings must be such that mutual pounding does not occur
5. The surface of the impact
6. The elastic–plastic behaviour of the buildings and their plasticity and cracking levels
7. The simulation on the foundation of the buildings
8. The intensity and the dynamic characteristics of the

Apart from item 4, information does exist in each case mentioned in items 1–3 and 5–8.

Initially, a simplified model of several adjacent buildings in a block was used to study the pounding of such buildings due to strong earthquakes. Considerable structural damage and even some collapses have sometimes been attributed to this effect. Each building is modelled as a SDOF system and pounding is simulated using impacted elements. A parametric investigation of this problem shows that *the end* structural elements almost always have substantial *increases in their response while for "interior" elements the opposite often happens*. This explains why high percentages of corner buildings have collapsed in many earthquakes. Moreover, the *effects of gap size, structural strength, relative mass size as well as impact element damping and stiffness* need to be investigated.

www.EngineeringBooksPDF.com

It is proposed to model pounding first between two adjacent buildings, with natural periods T_1 and T_2 and damping ζ_1 and ζ_2 under harmonic earthquake excitation, as non-linear Hertzian impact between two SDOF systems. Analytical solution for the impact velocity can be derived for the case of rigid impacts. Inelastic impact will also be modelled by incorporating a coefficient of restitution. For more general cases of non-rigid impacts, numerical simulations can be carried out to examine the applicability of the analytical solution for rigid impacts and to investigate the maximum impact velocity.

An effective solution for studying the pounding response of adjacent buildings during earthquakes can be carried out using the Lagrange multiplier approach by which the geometric compatibility conditions due to contact are enforced. The energy and momentum balance criteria for contacting buildings are satisfied according to the laws of impact covering post-impact conditions, which can also take into account local energy absorption phenomena during collision. A solution scheme is proposed which can be incorporated easily into existing computer programs for static and dynamic analysis of buildings as proposed in earlier chapters with and without seismic devices.

In many practical applications building structures are often constructed with narrow gaps between adjacent but independent substructures. Examples include mechanical equipment within nuclear power plants, multi-span highway bridges and multistorey offices and parking structures. When responding to dynamic loads, the different dynamic characteristics of the individual units make them vibrate out-of-phase and mutual impact therefore occurs if the original gap size is too small.

In this chapter a simplified MDOF numerical model for analysis of the lateral collision between adjacent buildings subjected to base excitation is suggested along with others. This model is based on the assumption that when the adjacent building structural elements are collided with relatively high velocity and/or the local stiffness at the location of contact is much higher than global stiffness of the involved systems, then the duration of each collision can be assumed as zero, and the change in potential energy of the system is negligible. As a result, the constraints between the structural elements are removed and the original system is replaced by pairs of colliding masses. The principle of conservation of momentum and the coefficient of restitution is applied to each floor independently to uniquely determine the incremental velocities corresponding to each impact. The problem, therefore, turns to be a set of MDOF systems subjected to a series of sudden change in velocities. BANG-F has a solution scheme described in the text. It is interesting to note the following papers by Chopra A. K and Goel R.K. The reader must note these:

(a) A modal pushover analysis procedure for estimating seismic demands for buildings. *Earthquake Eng. Struct. Dyn.* 2002; 31, 561–582.
(b) A modal pushover analysis procedure to estimate seismic demands for unsymmetric-plan buildings. *Earthquake Eng. Struct. Dyn.* 2004; 33, 903–927.

Here some improved pushover analysis (MPA) procedure which retains (a) conceptual simplicity and computational attractiveness modal approach is

www.EngineeringBooksPDF.com

adopted. In paper (b) a comprehensive MPA procedure with invariant force distribution is given for unsymmetrically planned building. Here again modal approach is adopted. The reader is already familiar with the modal procedure earlier. Where seismic devices are employed, the right equation of motion in Chopra A.K. et al. formulation be adopted, particularly for non-linear analysis. Where interation analysis can be carried out for pushover with non-equal heights of buildings, a reference is made to the following paper: C.G Kara Yannis and Maria. J. Favvata, Earthquake induced interaction between adjacent reinforced concrete structures with non-equal heights, *Earthquake Engng. Struct. Dyn.* 2005; 34, 1–20.

Here the authors developed a paper on the influence of structural pounding on the ductility requirement and the seismic behaviour of RC structures designed according to EC2 and EC8 with non-equal heights.

10.2 Analytical Formulation for the Pushover

It is indeed very difficult to decide which method is to be used successfully to achieve the economic pushover results. The floors are modelled as adjacent masses. If the buildings are of equal heights or of unequal heights, the equations of equilibrium can be established. Building with equal heights having adjacent masses can be treated as a *contact impact case* such that each pair of masses vibrates initially along the line joining their centres. They should then collide head on while moving along the same straight line after collision. The collision is generally inelastic such that the local energy absorption phenomenon during impact can be taken into account. The second Newton's law can be used for generalizing equations of equilibrium for any case of building configurations. Again the buildings with and without seismic devices can easily be devised using dynamic equations. Such equations are with and without devices.

The generalized equilibrium equation for a pair of buildings can be written as

$$[m_a]^t\{\ddot{u}\}_a^t+[c]_a^t\{\dot{u}\}_a^t+[k]_a^t\{u\}_a^t=-[m_a]^t\{I\}\ddot{x}_g-\{F\}^t-\text{Building ``a''} \quad (10.1)$$

$$[m_b]^t\{\ddot{u}\}_b^t+[c]_b^t\{\dot{u}\}_b^t+[k]_b^t\{u\}_b^t=-[m_b]^t\{I\}\ddot{x}_g-\{F\}^t-\text{Building ``b''} \quad (10.2)$$

such that one has to look for

$$\{u\}_a-\{u\}_b\leq d \quad (10.3)$$

where $\{u\}$, $\{\dot{u}\}$ and $\{\ddot{u}\}$ are the displacement, velocity and acceleration of each building such as buildings (a) and (b).

$\ddot{x}_g =$ acceleration of support
$\{I\} =$ influence coefficient column vector

www.EngineeringBooksPDF.com

$[c]=$ damping matrix $[k]=$ structural stiffness matrix
$\{F\}=$ final force stiffness matrix
$\{0\}=$ zero matrix as a column matrix

In (8.3) if the final displacement is equal to or less than $\{d\}$, the collision will not occur. In all cases

$$\{F\} \geq 0$$

If any of the floor is untouched, all kinematic terms are treated constant. Where the floors are in contact, the linear and non-linear impact momentum law with normal velocity u_{nol} which can be treated as common will be at the end of approach.

10.3 Linear Response

The basic conditions of contact along the generic surfaces are that no material overlap can occur, and as a result contact forces are developed that act along the region of contact. Here, attention is focused on the planar case of frictionless contact without sliding. Furthermore, the developments are restricted to a node-to-node contact, which imposes the consideration of additional nodes in the case of slab-to-column contact. In this context, with reference to Fig. 10.1 the constraint equation of the two nodes *j, l* in contact is written as

$$u_1^{(j)} - u_1^{(l)} = \delta_{jl} \tag{10.4}$$

where $u_1^{(j)}$, $u_1^{(l)}$ are the nodal displacements in direction x_1 of nodes *j, l*, respectively.

Since this is a constrained problem, the governing equilibrium equations are derived by invoking stationarity of the total potential function:

$$\Pi = \frac{1}{2}\{u\}_{\text{TOT}}^{T}[K]_{\text{TOT}}\{u\}_{\text{TOT}} - \{F\}_{\text{TOT}}^{T}\{u\}_{\text{TOT}} \tag{10.5}$$

subject to the geometric constraints $[K_\lambda]\{u\} = \{\delta\}$.

This is transformed to an unconstrained optimization problem of the Lagrangian functional

$$L(u,\lambda) = \frac{1}{2}\{u\}_{\text{TOT}}^{T''}[K]_{\text{TOT}}\{u\}_{\text{TOT}} - \{F\}^{T}\{u\}_{\text{TOT}} + \{\lambda\}_{\text{TOT}}^{T''}[[K_\lambda]_{\text{TOT}}\{u\}_{\text{TOT}} - \{\delta\}] \tag{10.6}$$

with the necessary conditions given as

$$\nabla_u L(u,\lambda) = [K]_{\text{TOT}}\{u\}_{\text{TOT}} - \{F\}_{\text{TOT}} + [K_\lambda]_{\text{TOT}}^{T''}\{\lambda\} = 0 \tag{10.7}$$

where

T″ is the transpose
TOT – Total matrix

www.EngineeringBooksPDF.com

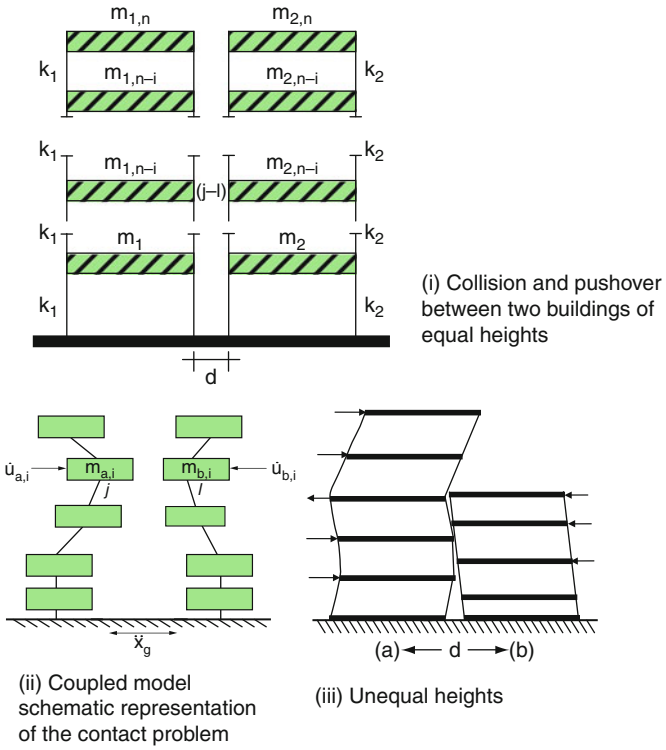


Fig. 10.1 A pushover analysis of buildings using the Lagrange multiplying formulation

$$\nabla_u L(u, \lambda) = [K]_{\text{TOT}}\{u\} - \{d\} = 0 \tag{10.8}$$

or

$$\begin{bmatrix} [K] & [K_\lambda^{T''}] \\ [K_\lambda] & [0] \end{bmatrix} \begin{bmatrix} \{u\}_{\text{TOT}} \\ \{\lambda\} \end{bmatrix} = \begin{bmatrix} F \\ d \end{bmatrix} \tag{10.9}$$

The symbols are defined as:

$\{u\}$ = vector of nodal displacement of the two buildings in contact;
$\{\lambda\}$ = vector of nodal contact forces;
$\{F\}$ = vector of nodal external forces;
$[K]$ = A (n x n) combined stiffness matrix of the two buildings;
T'' = Transpose.

A reference is made to Chap. 5 for the linear response analysis.

www.EngineeringBooksPDF.com

The compatibility conditions of contact are expressed by (10.7) in which $\{d\}$ is the vector of initial nodal gaps and the contact matix $[K_\lambda]_{\text{TOT}} =$ a $(m_t \times n_t)$ matrix of the form.

$$\begin{bmatrix} \ldots 1 \ldots \ldots -1 \\ \ldots\ldots 1 \ldots\ldots\ldots -1 \ldots \\ \ldots\ldots\ldots\ldots\ldots\ldots \\ \ldots\ldots 1 \ldots\ldots -1 \ldots\ldots \end{bmatrix} \begin{bmatrix} u_{a,i} \\ u_{kj} \end{bmatrix} = \{d\} \tag{10.10}$$

The dimension m corresponds to the total number of constraints or the total number of nodal pairs of contact.

Non-linear response

A reference is made in the text for non-linear response.

To generate the equilibrium conditions for iteration i at increment $i + \Delta t$, stationarity of the following Lagrangian functional is invoked:

$$L^{(i)}(u, \lambda) = \Pi^{(i)} - \sum_k W_k^{(i)} \tag{10.11}$$

where

$\Pi^{(i)} =$ incremental potential leading to the incremental equilibrium equations without contact conditions for iteration $t + \Delta t$;

$\sum_k W_k^{(i)} =$ incremental potential of the contact forces at iteration i.

In the present case $W_k^{(i)}$ for the pair k of contacting nodes j, l takes the form

$$\begin{aligned} W_x^{(i)} = &\left[\{ {}^{t+\Delta^k}\lambda_k^{u=1} \}_{\text{TOT}}^{T''} \left(\{\Delta_{uj}^{(i)}\}_{\text{TOT}} - \{\Delta_u^{(i)}\}_{\text{TOT}} + \{\delta_\lambda^{(l-1)}\} \right)_{\text{TOT}} \right] \\ &+ \{\Delta\lambda_K^{(i)}\}_{\text{TOT}}^{T''} \left(\{\Delta_{uj}^{(i)} - \{\Delta_{uj}^{(i)}\}_{\text{TOT}} + \{\delta_\lambda^{(i-1)}\}_{\text{TOT}} \right. \end{aligned} \tag{10.12}$$

The governing finite element equations are obtained by substituting (10.12) into (10.11) and invoking stationarity conditions (10.6) and (10.7), then the equilibrium equations for iteration I at increment $t + \Delta t$ are

$$\begin{aligned} &\left[\begin{bmatrix} {}^{t+\Delta t}K^{(i-1)} & [0] \\ [0] & [0] \end{bmatrix}_{\text{TOT}} + \begin{bmatrix} 0 & {}^{t+\Delta t}\left[k_\lambda{}^{(i=1)\text{T}''}\right] \\ {}^{t+\Delta t}[k_\lambda{}^{(i=1)}] & 0 \end{bmatrix} \right] \begin{bmatrix} \Delta u^{(i)} \\ \Delta\lambda^{(i)} \end{bmatrix}_{\text{TOT}} = \\ &\begin{bmatrix} {}^{t+\Delta t}F^{(i-1)} \\ 0 \end{bmatrix}_{\text{TOT}} - \begin{bmatrix} {}^{t+\Delta t}F^{(i-1)} \\ 0 \end{bmatrix}_{\text{TOT}} + \begin{bmatrix} {}^{t+\Delta t}\left\{ R_\lambda{}^{(i-1)} \right\} \\ {}^{t+\Delta t}\left\{ \delta_\lambda{}^{(i-1)} \right\} \end{bmatrix}_{\text{TOT}} \end{aligned} \tag{10.13}$$

in which

$[{}^{t+\Delta t}K^{(i-1)}] =$ tangent stiffness matrix after iteration $i-1$;

$[{}^{t+\Delta t}K_\lambda{}^{(i-1)}] =$ contact matrix for the effect of the contact conditions of the m pairs of nodes;

www.EngineeringBooksPDF.com

$\{^{t+\Delta t}F^{(i-1)}\}$ = vector of nodal point forces equivalent to element stresses;
$\{^{t+\Delta t}R_{\lambda}{}^{(i-1)}\}$ = vector of updated contact forces;
$\{^{t+\Delta t}\delta_{\lambda}{}^{(i-1)}\}$ = vector of overlapping distances of adjacent nodes;
$\{\Delta u^{(i)}\}$ = vector of incremental displacements;
$\{\Delta\lambda^{(i)}\}$ = vector of incremental contact forces.

The contact matrix is identical to that of Eq. (10.9) while the vector of uploaded contact forces for the kth pair of nodes j, l is given by

$$\left\{{}^{t+\Delta t}R_k^{(i-1)}\right\} = \begin{bmatrix} t+\Delta t_{\lambda_k^{(i-1)}} \\ -t+\Delta t_{\lambda_k^{(i-1)}} \end{bmatrix} \tag{10.14}$$

When the Lagrange multiplier method is used to enforce the compatibility constraints of the corresponding displacements due to contact, the typical equilibrium equation of motion can then be written (Ref: Chap. 5)

$$[M]_{\text{TOT}}\{\ddot{u}\} + [C]_{\text{TOT}}\{\dot{u}\} + [K]\{u\}_{\text{TOT}} = \{F(t)\}_{\text{TOT}} \tag{10.15}$$

It is transformed, for linear response, as in the manner shown below:

$$\begin{bmatrix} M & 0 \\ 0 & 0 \end{bmatrix}\begin{bmatrix} \ddot{u} \\ 0 \end{bmatrix}_{\text{TOT}} + \begin{bmatrix} C & 0 \\ 0 & 0 \end{bmatrix}_{\text{TOT}}\begin{bmatrix} \dot{u} \\ 0 \end{bmatrix}_{\text{TOT}} + \begin{bmatrix} K & K_{\lambda}^{T\prime\prime} \\ K_{\lambda} & 0 \end{bmatrix}_{\text{TOT}}\begin{bmatrix} u \\ \lambda \end{bmatrix}_{\text{TOT}} = \begin{bmatrix} F(t) \\ \delta \end{bmatrix}_{\text{TOT}} \tag{10.16}$$

For non-linear response the dynamic equilibrium equations for iteration i at time increment $t + \Delta t$ are expressed as

$$\begin{aligned} &\begin{bmatrix} M & 0 \\ 0 & 0 \end{bmatrix}\begin{bmatrix} \Delta\ddot{u}^{(i)} \\ 0 \end{bmatrix} + \begin{bmatrix} C & 0 \\ 0 & 0 \end{bmatrix}_{\text{TOT}}\begin{bmatrix} \Delta\dot{u}^{(i)} \\ 0 \end{bmatrix}_{\text{TOT}} \\ &\quad + \left[\begin{bmatrix} {}^{t+\Delta t}K^{(i-1)} & 0 \\ 0 & 0 \end{bmatrix}_{\text{TOT}} + \begin{bmatrix} 0 & {}^{t+\Delta t}K_{\lambda}^{(i-1)T\prime\prime} \\ {}^{t+\Delta t}K_{\lambda}^{(i-1)} & 0 \end{bmatrix}\right]\begin{bmatrix} \Delta_u^{(i)} \\ \Delta_{\lambda}^{(i)} \end{bmatrix}_{\text{TOT}} = \\ &\quad \begin{bmatrix} {}^{t+\Delta t}F^{(t+\Delta t)} \\ 0 \end{bmatrix}_{\text{TOT}} - \begin{bmatrix} [M] & 0 \\ 0 & 0 \end{bmatrix}_{\text{TOT}}\begin{bmatrix} {}^{t+\Delta t}\ddot{u}^{(i-1)} \\ 0 \end{bmatrix}_{\text{TOT}} - \\ &\begin{bmatrix} [C] & 0 \\ 0 & 0 \end{bmatrix}_{\text{TOT}}\begin{bmatrix} {}^{t+\Delta t}\dot{u}^{(i-1)} \\ 0 \end{bmatrix}_{\text{TOT}} - \begin{bmatrix} {}^{t+\Delta t}\{F\}^{(i-1)} \\ 0 \end{bmatrix}_{\text{TOT}} + \begin{bmatrix} {}^{t+\Delta t}\{R\}_{\lambda}^{(i-1)} \\ {}^{t+\Delta t(i-1)}\{d\}_{\lambda} \end{bmatrix}_{\text{TOT}} \end{aligned} \tag{10.17}$$

in which $\{\Delta u^{(i)}\}$, $\{\Delta\dot{u}^{i}\}$ and $\{\Delta\ddot{u}^{i}\}$ are vectors of incremental displacements, velocities and accelerations, respectively, in iteration i.

The time integration of dynamic response is performed with the *Newmark* method in which the displacement and velocity vectors at time $t + \Delta t$ are given as

$$\left\{{}^{t+\Delta t}u\right\} = \{t_u\} + {}^{t}\dot{u}^{\Delta t} + \left[\left(\frac{1}{2}-\beta\right)\{'\ddot{u}\} + \beta\left\{{}^{t+\Delta t}\ddot{u}\right\}\right]\Delta t^2 \tag{10.18}$$

www.EngineeringBooksPDF.com

$$\left\{{}^{t+\Delta t}\dot{u}\right\} = \left\{{}^{t}\dot{u}\right\} + \left[(1-\gamma)\left\{{}^{t}\ddot{u}\right\} + \gamma\left\{{}^{t+\Delta t}\ddot{u}\right\}\Delta t\right] \tag{10.19}$$

The implicit *Newmark* scheme requires the solution of the following system in each time step for the linear problem:

$$\begin{bmatrix} [\hat{K}] & [K_\lambda^T] \\ [K_\lambda] & [0] \end{bmatrix}_{\text{TOT}} \begin{bmatrix} u^{t+\Delta t} \\ t+\Delta t_\lambda \end{bmatrix}_{\text{TOT}} = \begin{bmatrix} \left\{t+\Delta t_{\hat{R}}\right\} \\ \{d\} \end{bmatrix}_{\text{TOT}} \tag{10.20}$$

where

$$[\hat{K}]_{\text{TOT}} = \begin{bmatrix} [\hat{K}_a] & & \\ & [\hat{K}_b] & \\ & & \vdots \end{bmatrix}, \{\tilde{R}\} = \begin{bmatrix} \{\hat{R}_a\} \\ \{\hat{R}_b\} \\ \vdots \end{bmatrix}_{\text{TOT}} \tag{10.21}$$

$$\begin{bmatrix} {}^{t+\Delta t}[K]^{(i-1)} & {}^{t+\Delta t}[K]_\lambda^{(i-1)} T'' \\ {}^{t+\Delta t}[K]_\lambda^{(i-1)} & 0 \end{bmatrix}_{\text{TOT}} \begin{bmatrix} \{\Delta u\}^{(i)} \\ \{\Delta\lambda\}^{(i)} \end{bmatrix}_{\text{TOT}} = \begin{bmatrix} \left\{{}^{t+\Delta t}\hat{R}\right\} \\ 0 \end{bmatrix}_{\text{TOT}} - \begin{bmatrix} {}^{t+\Delta t}\{F\}^{(i-1)} \\ 0 \end{bmatrix} + \begin{bmatrix} {}^{t+\Delta t\Delta t}\{R\}_\lambda^{(i-1)} \\ {}^{t+\Delta t}\{d\}_\lambda^{(i-1)} \end{bmatrix} \tag{10.22}$$

which again can be solved following the steps of the linear case. Formation and factorization of the tangent stiffness matrix should be performed preferably at the beginning of each time step. The procedure described may exploit basic routines of standard static and dynamic analysis of buildings and thus can be incorporated into existing programs with minor alterations. A reference is made to Chap. 5.

The values of the Lagrange multipliers, computed in step 7 of the above algorithm, are dependent on the time increment Δt and therefore cannot be interpreted as the real contact forces during impact as in the static case. The impact which is produced by the contact forces, however, is independent of the integration time step and gives a real interpretation of the physical meaning of the Lagrange multipliers.

10.3.1 Post-contact Conditions

A reference is made to Chap. 5 for inelastic or elastoplastic solutions under dynamic loads. Particularly, the involving of gap elements in the analytical procedure can be considered after this analysis.

The dynamic aspects of post-contact conditions, however, require special attention. An accurate dynamic contact solution must fulfil the conditions that the total energy of the system of contacting buildings is conserved for perfectly elastic impact and the impulse–momentum relationship is satisfied for each building. In case of partially elastic impact, the energy balance condition is

www.EngineeringBooksPDF.com

properly modified by the introduction of the coefficient of restitution e. This coefficient accounts for local energy absorption mechanisms.

Each of (10.1) or (10.2) will have two parts covering instant time when impact occurs and to the time when an impact or collision ends, the impact forces $F_{i,ta}$ and $F_{i,te}$:

$$F_{i,t'}/F_{i,t} = \frac{\dot{u}_{b,i}(t') - \dot{u}_{a,i}(t')}{\dot{u}_{a,i}(t) - \dot{u}_{b,i}(t)} = e \tag{10.23}$$

The final velocities are then computed together with the loss of energy

$$\dot{u}_{b,i}t' = \dot{u}_{b,i}(t) + (1+e)[m_{b,i}(t) - m_{a,i}\dot{u}_{b,i}(t)]/(m_{a,i} + m_{b,i}) \tag{10.24}$$

The loss of kinetic energy will then be written as

$$\begin{aligned} \mathrm{KE(loss)} = &\frac{1}{2}\left[\frac{m_{a,i}m_{b,i}}{m_{a,i} + m_{b,i}}\right](1-e^2)(\dot{u}_{a,i}(t) - \dot{u}_{b,i}(t))^2 \\ &- \text{ when } e = 1, \text{ elastic bodies} \end{aligned} \tag{10.25}$$

It is interesting to note from Eq. (8.3) when $e=0$ completely plastic impact two equations can be arrived at:

$$\{d\dot{u}_a(t)\} = \{\dot{u}_a(t') - \dot{u}_a(t)\} \tag{10.26}$$

$$\{d\dot{u}_b(t)\} = \{\dot{u}_b(t') - \dot{u}_b(t)\} \tag{10.27}$$

$$t_k \le t \le t_{k+1} \qquad k = 1, 2, 3, \ldots t_1 = 0$$

The decomposition is in two parts. One is caused by $\ddot{x}_g$ with initial conditions at time t and another is free vibration contributed by incremental velocities due to impact.

The energy loss vanishes for the impact of completely elastic bodies ($e=1$), and the maximum loss is induced for completely plastic impact ($e=0$). Finally, the rebound velocities are obtained from

$$\dot{u}'_{a,i} = \dot{u}_{a,i} - (1+e)\frac{m_{b,i}(\dot{u}_{a,i} - \dot{u}_{b,i})}{m_{a,i} + m_{b,i}} \tag{10.28}$$

$$\dot{u}'_{b,i} = \dot{u}_{b,i} + (1+e)\frac{m_{a,i}(\dot{u}_{a,i} - \dot{u}_{b,i})}{m_{a,i} + m_{b,i}} \tag{10.29}$$

First, one considers the special case in which the distance of separation between the two buildings is ${}^t d = 0$ (at time t). Following the algorithm presented in the previous section and the integration formulae, the buildings separate in time step $t + 2\Delta t$ when

$$0 < \beta < \frac{1}{4}(2\gamma + 1) \tag{10.30}$$

www.EngineeringBooksPDF.com

with the following velocities

$$\dot{u}'_{a,i} = \dot{u}_{a,i} - \frac{m_{b,i}(\dot{u}_{a,i} - \dot{u}_{b,i})}{\beta(m_{a,i} + m_{b,i})} \tag{10.31}$$

$$\dot{u}'_{b,i} = \dot{u}_{b,i} + \frac{m_{a,i}(\dot{u}_{a,i} - \dot{u}_{b,i})}{\beta(m_{a,i} + m_{b,i})} \tag{10.32}$$

Equating the above velocities with the analytical ones Eqs. (10.28) and (10.29) and taking into account the expression for unconditional stability discussed in the text by *Newmark* method

$$\gamma \geq \frac{1}{2}, \quad \beta \geq \frac{1}{4}(\frac{1}{2} + \gamma)^2 \tag{10.33}$$

The following values for β, γ are given as

$$\beta = \frac{1}{1+e}, \quad \gamma = \frac{3-e}{2(1+e)} \tag{10.34}$$

The two buildings separate in time $t + 3\Delta t$ when

$$\frac{1}{4}(2\gamma + 1) < \beta < \frac{5 + 6\gamma + \sqrt{13 + 12\gamma - 12\gamma^2}}{12} \tag{10.35}$$

with rebound velocities

$$\dot{u}'_{a,i} = \dot{u}_{a,i} - \frac{(6\beta - 2\gamma - 1)m_{b,i}(\dot{u}_{a,i} - \dot{u}_{b,i})}{2\beta^2(m_{a,i} + m_{b,i})} \tag{10.36}$$

$$\dot{u}'_{b,i} = \dot{u}_{b,i} - \frac{(6\beta - 2\gamma - 1)m_{a,i}(\dot{u}_{a,i} - \dot{u}_{b,i})}{2\beta^2(m_{a,i} + m_{b,i})} \tag{10.37}$$

Since the rebound velocities are now functions of both β and γ, the expression for β, γ is much more involved than those of the previous case. Repeating the above discussion for the general case, the following conditions must be satisfied for separation after time $t + \Delta t$:

$$(2\beta - 2\gamma - 1)(\dot{u}_{a,i} - \dot{u}_{b,i} - d) < 2\beta(\dot{u}_{a,i} - \dot{u}_{b,i}) \tag{10.38}$$

with rebound velocities

$$\dot{u}'_{a,i} = \dot{u}_{a,i} - \frac{m_{b,i}(\dot{u}_{a,i} - \dot{u}_{b,i} - d)}{\beta(m_{a,i} + m_{b,i})} \tag{10.39}$$

$$\dot{u}'_{b,i} = \dot{u}_{b,i} - \frac{m_{a,i}(\dot{u}_{a,i} - \dot{u}_{b,i} - d)}{\beta(m_{a,i} + m_{b,i})} \tag{10.40}$$

www.EngineeringBooksPDF.com

The corresponding expressions for β, γ become

$$\beta = \frac{1}{1+e}\frac{\dot{u}_{a,i} - \dot{u}_{b,i} - d'}{\dot{u}_{a,i} - \dot{u}_{b,i}}, \qquad \gamma > \frac{(3-e+)(u_{a,i} - u_{b,i}) - 2d'}{2(1+e)(u_{a,i} - u_{b,i})} \tag{10.41}$$

where $d' = d/\Delta t$. When inequality (10.38) is not satisfied separation is realized after time $t + 2\Delta t$ under more complicated conditions.
In the case of perfectly elastic contact ($e = 1$) and ${}^{t}d = 0$, the values $\beta = 1/2$, $\gamma = 1/2$ produce the analytical rebound velocities from Eq. (8.13) and Eq. (8.14) after separation at time $t + 2\Delta t$. Incidentally these values for β, γ lead to coincident analytical and computational velocities when ${}^{t}d \neq 0$, but separation is now taking place in time step $t + 3\Delta t$.

10.4 Calculation of Building Separation Distance

10.4.1 Minimum Separation Distance Required to Avoid Structural Pounding

A reference is made to the Time-History Formulation in Chap. 5. The emphasis in structural pounding problems is on the "relative displacement" of potential pounding location of adjacent buildings. If $u_{ai}(t)$ and $u_{bi}(t)$ are the displacement time histories and $Z(t)$ is the relative displacement time history of two adjacent buildings (a), (b) at the potential pounding position, then $Z(t)$ can be expressed as stated earlier:

$$Z(t) = U_{b,i} - U_{a,i} = d \tag{10.42}$$

where d separation distance.
The minimum distance required to avoid pounding, "$\bar{e}$", can be written as

$$\bar{e}_{\text{reqd}} = Z(t)_{\text{sup}} \tag{10.43}$$

where subscript "sup" is a maximum value of the entire range of the relative displacement time history. Hence pounding does occur when $Z(t) < \bar{e}_{\text{reqd}}$. This is the value of "d".

The UBC-97 requires that separation shall allow for the maximum inelastic response displacement Δ_m when adjacent buildings are separated. Its value shall be greater than "d". The value of Δ_m based on UBC-97 is given as

$$\Delta_m = 0.7R\Delta_s \tag{10.44}$$

in which R is the numerical coefficient representative of the inherent over-strength and global ductility capacity of lateral-force-resisting systems and Δ_s

www.EngineeringBooksPDF.com

is the design level response displacement, which is the total drift or total storey drift that occurs when the structure is subjected to the design seismic forces.

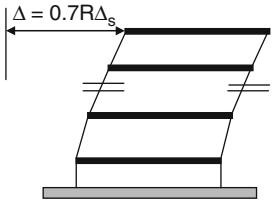
When a structure adjoins a property line not common to a public way, that structure shall be set back from the property line by at least the displacement Δ_M of that structure. In other words, adjacent buildings shall be separated by at least Δ_{MT} which can be determined by the ABS (absolute sum) expression

$$\Delta_{MT} = \Delta_{\mathrm{MA}} + \Delta_{\mathrm{MB}} \tag{10.45}$$

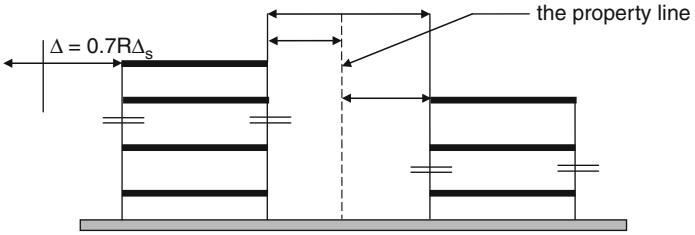
in which Δ_{MA} and Δ_{MB} are the inelastic displacements of the adjacent buildings (a) and (b), respectively.

In addition, adjacent buildings on the same property shall be separated by at least Δ_{MT} which can be determined by the square root of the sum of the squares (SRSS) expression

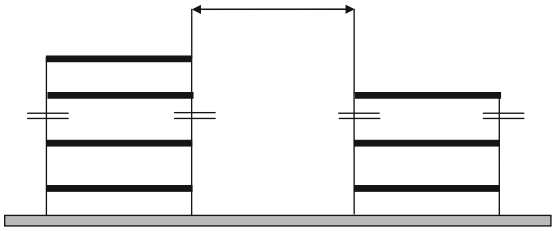
$$\Delta_{MT} = \sqrt{[(\Delta_{MA})^2 + (\Delta_{MB})^2]} = d \tag{10.46}$$



(a) Maximum inelastic displacement of a building



(b) Separation distance of adjacent buildings on different property



(c) Separation distance of adjacent buildings on the same property

Fig. 10.2 Minimum building separation specified by the UBC-97 (with compliments of UBC-97)

www.EngineeringBooksPDF.com

Note that the use of the ABS and SRSS combination methods, implied by the UBC, provides an upper limit of the required separation distance of adjacent buildings to avoid pounding Fig. 10.2. This can easily be checked using Time-History method of Chap. 5.

These methods generally overestimate the required separation distance. The SRSS method ignores the cross-correlation of the responses of adjacent buildings and provides a conservative estimate for Δ_{MT}. The ABS method considers the entire out-of-phase motion, regardless of the relative magnitudes of the periods of buildings and provides a more conservative estimate for Δ_{MT}.

10.5 Data for Buildings

A reference is made to the two buildings in Fig. 10.3. Two buildings – 10 storeys, three bays and 4 storeys, three bays – are chosen for the pushover study. The following data for the respective buildings are summarized in Table 10.1 for an earthquake of 0.4G.

10.6 Discussion on Results

As stated in Table 10.1, two types of case studies have been examined. And they are

1. Two building steel frames of equal heights with three bays. Two 10-storey buildings of heights 30 m with inter-floor heights 3.0 m. They have three bays in each frame with 3–6 m spacing.

Table 10.1 Data for two buildings (Fig. 10.3)

10 Storeys – three Bays 1. Case Study 1: 10 DOF Pushover: equal heights	4 Storeys - three Bays 1. Case Study 2: 10 DOF Pushover: unequal heights
(a) 2 No. 10 storeys – 3 Bays $h = 3$ m $H = 30$ m	1 No. 10 storeys – 3 Bays and 1 No. $h = 3$ m $H = 12$ m
(b) T = period = 1.144 s 10 storeys	T = period = 0.576 s 4 storeys
(c) $V_{\text{design}} = 2{,}567$ kN base shear (single bay)	$V_{\text{design}} = 2{,}050$ kN base shear (single bay)
(d) K = stiffness = 7,081 kNcm (single)	K = stiffness = 4,710 Ncm (single)
(e) mass of each storey = 45.5×10^3	mass of each storey = 45.5×10^3
(f) mean ductility $U_s = 5.0$	mean ductility Us = 4.0
(g) E = Young's modulus = 2.06×10^7 kN/m^2	E = Young's modulus = 2.06×10^7 kN/m^2
(h) $d = 7.5$ m	$d = 7.5$m
(i) $K_\phi = 2.225 \times 10^8$ kNm/rad	$K_\phi = 2.225 \times 10^8$ kNm/rad (hard soil)
(j) $X_g = 0.1$ g sin ωt	$X_g = 0.1$ g sin ωt
(k) K_s = internal spring value $= 0.5 \times 10^7$ kN/m	K_s = internal spring value $= 0.5 \times 10^7$ kN/m
(l) $I_\phi = 4.55$ tm^2 (torsional moment of inertia)	$I_\phi = 4.55$ tm^2 (hard soil)

www.EngineeringBooksPDF.com

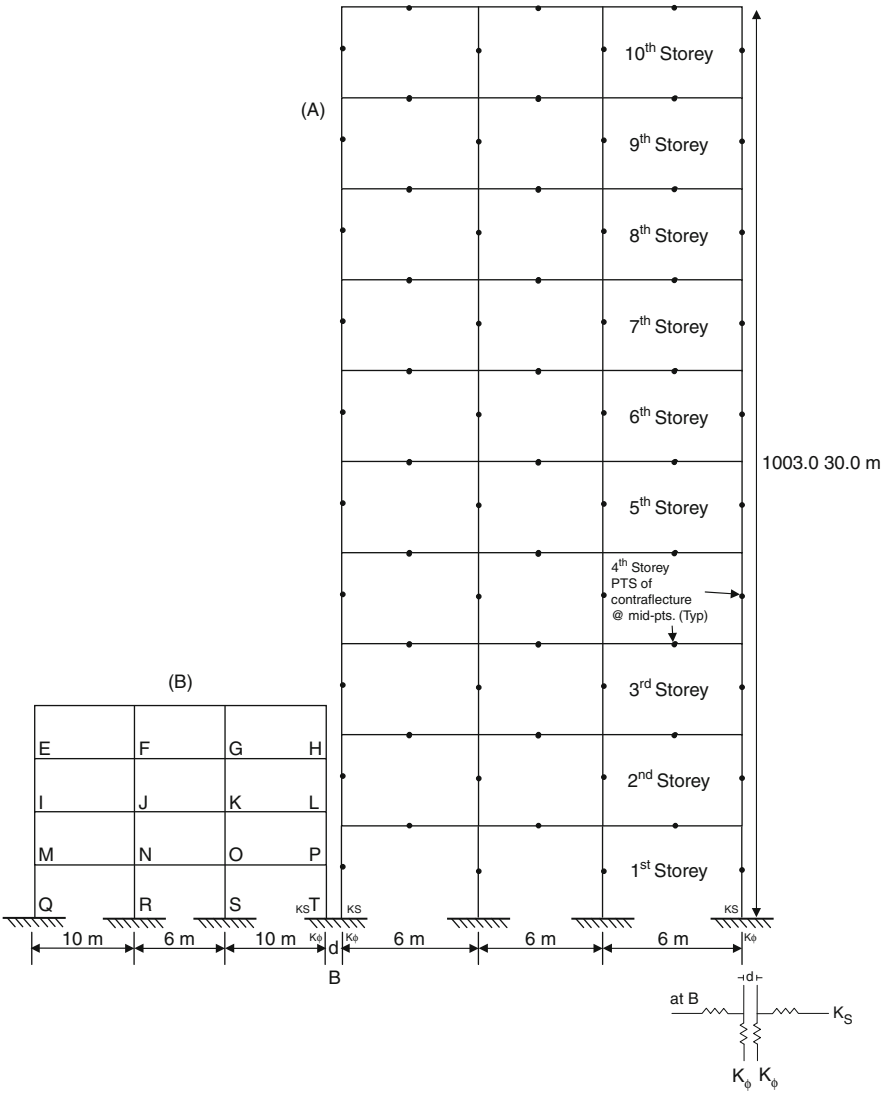


Fig. 10.3 The two building frames

2. Two- to four-storey steel frames, each associated with the 10-storey frame. The floor height is 3 m with three bay exteriors have two spans of 10 m each with an internal bay of 6 m.

The soils are represented by springs K_s and K_ϕ stiffness representing lateral and rotational displacement. Table 10.2 gives the details of the generalized stiffness matrices. While preparing individual input data for the structural elements forming the building frames, the individual dimensions are taken into

www.EngineeringBooksPDF.com

Table 10.2 Generalised Matrices for Building Elements

$$|K|_{\text{Element}} =$$

$$\frac{1}{det}\begin{bmatrix} \left(\frac{L}{EI}+C\right) & -\left(\frac{L^2}{2EI}+B\right) & -\left(\frac{L}{EI}+C\right) & \left(B-\frac{L^2}{2EI}+CL\right) \\ -\left(\frac{L^2}{2EI}+B\right) & \left(\frac{L^3}{3EI}+\frac{L}{GA_s}+\frac{N}{K_c}+A\right) & \left(\frac{L^2}{2EI}+B\right) & \left(\frac{L^3}{6EI}+BL-\frac{L}{GA_s}+\frac{N}{K_c}+A\right) \\ -\left(\frac{L}{LI}+C\right) & \left(\frac{L^2}{2EI}+B\right) & \left(\frac{L}{EI}+C\right) & \left(\frac{L^2}{2EI}+B\right) \\ \left(B-\frac{L^2}{2EI}+CL\right) & \left(\frac{L^3}{6EI}+BL-\frac{L}{GA_s}+\frac{N}{K_c}+A\right) & \left(\frac{L^2}{2EI}+B\right) & \left(\frac{L^3}{3EI}+\frac{L}{GA_s}+\frac{N}{K_c}+A\right) \end{bmatrix}$$

$$\begin{matrix} u_1\theta_1 & u_2\theta_2 & u_3\theta_3 & u_4\theta_4 & u_5\theta_5 & u_f\theta_f \end{matrix}$$

$$\begin{bmatrix} K_{11} & K_{12} & 0 & 0 & 0 & 0 \\ K_{11} & K_{11}+K_{12} & K_{23} & 0 & 0 & 0 \\ 0 & K_{32} & K_{22}+K_{33} & K_{34} & 0 & 0 \\ 0 & 0 & K_{43} & K_{33}+K_{44} & K_{45} & 0 \\ 0 & 0 & 0 & K_{54} & K_{44}+K_{55} & K_{5f} \\ 0 & 0 & 0 & 0 & K_{f5} & K_{55}+K_{ff} \end{bmatrix}$$

$$K_{5f} = \frac{EI_5}{1+4\lambda_5}\begin{bmatrix} -\frac{12}{h_5^2} & -\frac{6}{h_5^2} \\ \frac{6}{h_5^2} & \frac{2}{h_5^2}(1-2\lambda_5) \end{bmatrix};\ k_{ff} = \begin{bmatrix} K_u & 0 \\ 0 & K\phi \end{bmatrix} \quad K_{f5} = K_{sf}^T$$

$$A = \left(\frac{1}{I_c}-\frac{1}{I}\right) \quad \frac{L^2 L_u}{E} \quad \sum_{i=1}^{N}\left(\frac{2i-1}{2N}\right)^2$$

$$B = \left(\frac{1}{I_c}-\frac{1}{I}\right)\frac{LL_u}{E}\sum_{i=1}^{N}\left(\frac{2i-1}{2N}\right) \qquad C = \left(\frac{1}{I_c}-\frac{1}{I}\right)\frac{NL_u}{E}$$

$$\det = \frac{L^4}{12E^2I^2}+\frac{L}{EI}\left(\frac{L}{GA_s}+\frac{N}{K_c}\right)+\frac{AL}{EI}+C\left(\frac{L^3}{3EI}+\frac{L}{GA}+\frac{N}{K}+A\right)-\frac{BL^2}{EI}-B^2$$

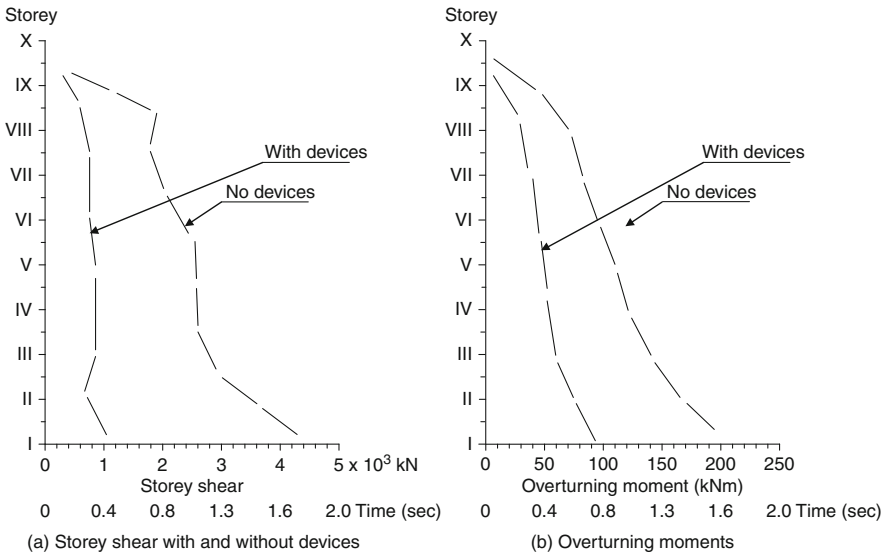


Fig. 10.4 Response quantities: 10-storey steel building, computed moments with (4% drift)

www.EngineeringBooksPDF.com

consideration. Table 10.2 for K (element) in used to cover every element and to formulate eventually a global matrix for any frame. Program "IDEAS" has been used to prepare the input preparation for the program F-Bang, which is the three-dimensional dynamic finite non-linear element program. The global matrix $[K]_{TOT}$ becomes huge for the program to solve. The solution procedures are discussed in text. Wilson - θ is used and finally checked by Runge–Kutta method.

First two 10-storey framed buildings exist at $d = 7.5$ m space. Figure 10.4 (i) and (ii) gives the comparative results for storey shear and overturning moment for the 10-storey buildings with a critical $d = 7.5$ m. The results are with and without seismic devices. Comparative study of time-dependent displacements are given for the 10-storey and 4-storey buildings with the same

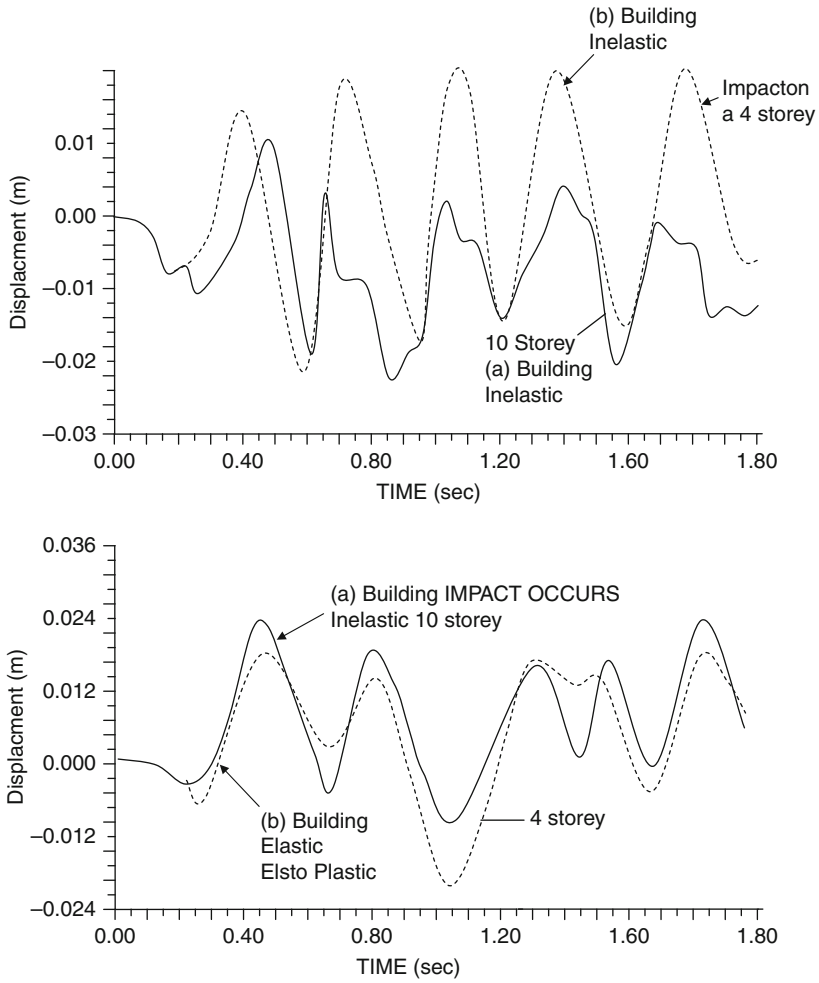


Fig. 10.5 Comparative studies of displacements

www.EngineeringBooksPDF.com

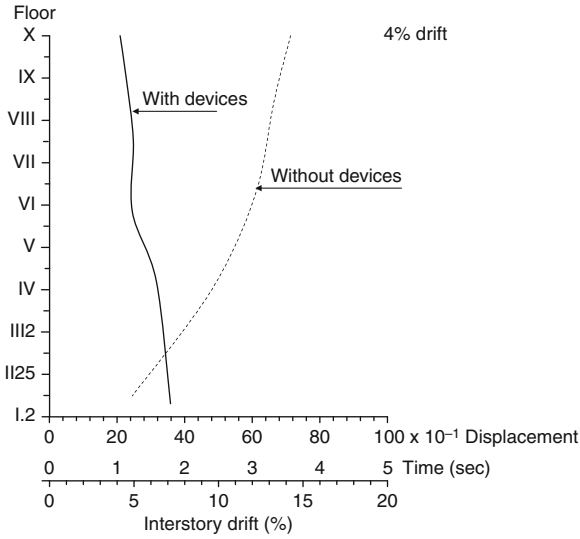


Fig. 10.6 Interstorey drift versus for a 10-storey building

value of $d = 7.5$m (Fig. 10.5). When the impact occurs independently on each building, it is necessary to give out these results without placing seismic devices in any position. Figure 10.6 gives the interstorey drift with and without seismic devices. The output from program F-Bang is quite enormous. Due to lack of space, it was not possible to produce other results which include the interaction between cladding and the floors. The stress distribution up to plasticity level on each member of building has been calculated. The joints were independently analysed for dynamic stresses, strains, plasticity and cracks and their extensions. However, the output containing these quantities can easily be available as soon as such cases are analysed. Just to conclude this section, the reader must realize that apart from the line elements, the walls, floors with connections took 3.5 h for F-Bang to analyse and create an output. The total number of line elements are 670 for steel-framed buildings with 1,970 isoparametric elements (20 noded isoparameters elements. Stated in chapter 5 and appendices.) for cladding and 3,150 isoparametric (20 noded) elements for each floor, giving over 35,000 solid elements since the floor slab was made in RC panels, which put bar elements concrete to be 1,357. Hence the reinforcement amount 10,378,100 nodes for all the elements. One can see the enormous nodal points to cater for. Maybe these will come out in other editions, if space is provided.

Bibliography

ACI Committee 318. *Building Code Requirements for Structural Concrete* (ACI 318-95) and Commentary (ACI 318R-95), American Concrete Institute, Detroit, 1995.

www.EngineeringBooksPDF.com

Allahabadi, R., and Powell, G.H. DRAIN-2DX user guide. *Report No. UCB/EERC-88/06*, Earthquake Engineering Research Center, University of California, Berkeley, CA, 1988.

American Society of Civil Engineers. *Prestandard and Commentary for the Seismic Rehabilitation of Buildings*, FEMA-356, Federal Emergency Management Agency, Washington, DC, 2000.

Anagnostopoulos, S.A. Building pounding re-examined: How serious a problem is it? *Proceedings of the 11th World Conference on Earthquake Engineering,* Acapulco, Mexico, 1996.

Anagnostopoulos, S.A. Earthquake induced pounding: State of the art. *Proceedings of the 10th European Conference on Earthquake Engineering 1995;* Vol. 2: 897–905.

Anagnostopoulos, S.A. Pounding of buildings in series during earthquakes. *Earthquake Eng. Struct. Dyn.* 1988; 16:443–456.

Anagnostopoulos, S.A., and Spiliopoulos, K.V. An investigation of earthquake induced pounding between adjacent buildings. *Earthquake Eng. Struct. Dyn.* 1992; 21:289–302.

Arnold, C., and Reitherman, R. *Building Configuration and Seismic Design*. Wiley, New York, 1982.

Athanasiadou, C.J., Penelis, G.G., and Kappos, A.J. Seismic response of adjacent buildings with similar or different dynamic characteristics. *Earthquake Spectra* 1994; 10.

Aydinoglu, M.N. An incremental response spectrum analysis procedure based on inelastic spectral displacements for multi-mode seismic performance evaluation. *Bullet. Earthquake Eng.* 2003; 1:3–36.

Benjamin, J.R., and Cornell, C.A. *Probability, Statistics, and Decision for Civil Engineers*. McGraw-Hill, New York, 1970; 684pp.

Bertero, V.V. Observation on structural pounding. *Proceeding of the International Conference on Mexico Earthquake,* ASCE, 1986; 264–287.

Bracci, J.M., Kunnath, S.K., and Reinhorn, A.M. Seismic performance and retrofit evaluation for reinforced concrete structures. *J. Struct. Eng.* (ASCE) 1997; 123(1):3–10.

Building Seismic Safety Council. *NEHRP Guidelines for the Seismic Rehabilitation of Buildings, FEMA-273 and Commentary FEMA-274*. Federal Emergency Management Agency, Washington, DC, 1997.

Chintanapakdee, C., and Chopra, A.K. Evaluation of modal pushover analysis for generic frames. *Pacific Earthquake Engineering*. Research Center, University of California, Berkeley, 2002, to be published.

Chintanapakdee, C., and Chopra, A.K. Evaluation of modal pushover analysis using generic frames. *Earthquake Eng. Struct. Dyn.* 2003; 32:417–442.

Chintanapakdee, C., Chopra, A.K. Seismic response of vertically irregular frames: Response history and modal pushover analysis. *J. Struct. Eng.* (ASCE) 2004; 130(8), 1177–1185.

Chopra, A.K. *Dynamic of Structures: Theory and Applications to Earthquake Engineering* (2nd ed.). Prentice-Hall, Englewood Cliffs, NJ, 2001; 844pp.

Chopra, A.K. and Goel, R. Modal pushover analysis of SAC building, *Proceedings SEAOC Convention*, San Diego, California, 2001.

Chopra, A.K., and Goel, R.K., A modal pushover analysis procedure to estimating seismic demands for buildings: Theory and preliminary evaluation. *PRRE Report 2001/03,* Pacific Earthquake Research Center, University of California, Berkeley.

Chopra, A.K., and Goel, R.K., A modal pushover analysis procedure to estimating seismic demands for buildings. *Earthquake Eng. Struct. Dyn.* 2002; 31: 561–582.

Chopra, A.K., and Goel, R.K. Capacity-demand-diagram methods based on inelastic design spectrum. *Earthquake Spectra* 1999; 15(4):637–656.

De Stefano, M., and Rutenberg, A. Predicting the dynamic response of asymmetrical multistorey wall-frame structures by pushover analysis: Two case studies. *Proceedings of the 11th European Conference on Earthquake Engineering*. Balkema Rotterdam, 1998.

Elnashai, A.S. Advanced inclastic static (pushover) analysis for earthquake applications. *Struct. Eng. Mech.* 2001; 12(1):51–69.

www.EngineeringBooksPDF.com

Eurocode 2. *Design of Concrete Structures- Part 1. General Rules and Rules for Building*. CEN, Technical Committee 250/SG2, ENV 1992-1-1, 1991.

Eurocode 8. *Structural in Seismic Regions, Design – Part 1. General and Building*. CEC, Report EUR 12266 EN, May 1994.

Fajfar, P., and Fischinger, M. N2- a method for nonlinear seismic analysis of regular structures. *Proceedings of the 9th World Conference on Earthquake Engineering,* Tokyo-Kyoto, Japan, 1988; 5:111–116.

Goel, R.K., and Chopra, A.K. Period formulas for moment-resisting frame buildings. *J. Struct. Eng*. (ASCE) 1997; 123(11):1454–1461.

Gupta, A., and Krawinkler, H. Estimation of seismic drift demands for frame structures. *Earthquake Eng. and Struct. Dyn*. 2000; 29:1287–1305.

Gupta, B., and Kunnath, SK. Adaptive spectra-based pushover procedure for seismic evaluation of structures. *Earthquake Spectra* 2000; 16(2):367–392.

International Code Council. *2000 International Building Code*. Falls Church, Virginia, 2000.

Kilar, V., and Fajfar, P. Simple push-over analysis of asymmetric buildings. *Earthquake Eng. Struct. Dyn*. 1997; 26:233–249.

Kim, B, and D'Amore, E. Pushover analysis procedure in earthquake engineering. *Earthquake Spectra* 1999; 13:417–434.

Krawinkler, H., and Seneviratna, GDPK. Pros and cons of a pushover analysis of seismic performance evaluation. *Engineering Structures* 1998; 20:452–464.

Krawinkler, H., and Nassar, A.A. Seismic design based on ductility and cumulative damage demands and capacities. In *Nonlinear Seismic Analysis and Design of Reinforced Concrete Buildings* (Fajfar, P. and Krawinkler, H., eds.). Elsevier Applied Science, New York, 1992.

Kunnath, S.K., and Gupta, B. Validity of deformation demand estimates using nonlinear static procedures. *Proceedings of U.S. Japan Workshop on Performance-Based Earthquake Engineering Methodology for Reinforced Concrete Building Structures,* Sapporo, Hokkaido, Japan, 2000; 117–128.

Maison, B. and Bonowitz, D. How safe are pre-Northridge WSMFs? A case study of the SAC Los Angeles nine-storey building. *Earthquake Spectra* 1999; 25(1):31–46.

Matsumori, T., Otani, S., Shiohara, H., and Kabeyasawa, T. Earthquake member deformation demands in reinforced concrete frame structures. *Proceedings of U.S. –Japan Workshop on Performance-Based Earthquake Engineering Methodology for Reinforced Concrete Building Structures,* Maui, Hawaii, 2000; 79–94.

Miranda, F. Seismic evaluation and upgrading of existing buildings. *Ph.D. Dissertation*, Department of Civil Engineering, University of California, Berkeley, CA, 1991.

Moghadam, A.S., and Tso, W.-K. Pushover analysis for asymmetrical multistorey buildings. *Proceedings of the 6th U.S. National Conference on Earthquake Engineering,* EERI, Oakland, CA, 1998.

Newmark, N.M., and Hall, W.J. *Earthquake Spectra and Design*. Earthquake Engineering Research Institute, Berkeley, CA, 1982; 103pp.

Ohtori, Y., Christenson, R.E, Spencer, Jr B.R, and Dyke, SJ. Benchmark Control Problems for Seismically Excited Nonlinear Buildings, http://www.nd.edu/~quake/, Notre Dame University, Indiana, 2000.

Paret, T.F., Sasaki, K.K., Eilbeck, D.H., and Freeman, S.A. Approximate inelastic procedures to identify failure mechanisms from higher mode effects. *Proceedings of the 11th World Conference on Earthquake Engineering,* Acapulco, Mexico, Paper No. 966, 1996.

Rosenblueth, E., and Meli, R. The 1985 earthquake: Causes and effects in Mexico City. *Concrete Int*. (ACI) 1986; 8(5):23–24.

Sasaki, K.K., Freeman, S.A., and Parent, T.F. Multimode pushover procedure (MMP) – a method to identify the effects of higher modes in a pushover analysis. *Proceedings of the 6th U.S. National Conference on Earthquake Engineering,* Seattle, Washington, 1998.

www.EngineeringBooksPDF.com

Skokan, M.J., and Hart, G.C. Reliability of non-linear static methods for the seismic performance prediction of steel frame buildings. *Proceedings of the 12th World Conference on Earthquake Engineering*, Paper No. 1972, Auckland, New Zealand, 2000.

Vidie, T., Fajfar, P., and Fischinger, M. Consistent inelastic design spectra: Strength and displacement. *Earthquake Eng. Struct. Dyn.* 1994; 23(5):507–521.

Villaverde, R. Simplified response spectrum seismic analysis of non-liner structures. *J. Struct. Eng. Mech.*, ASCE 1997; 123:256–265.

Westermo, B.D. The dynamic of interstructural connection to prevent pounding. *Earthquake Eng. Struct. Dyn.* 1989; 18:687–699.

www.EngineeringBooksPDF.com

www.EngineeringBooksPDF.com

Additional Extensive Bibliography

Analysis and Design of Buildings and Their Materials

1. ECCS Advisory Committee 1. *Multi-storey Buildings in Steel – The Swedish Method* (ECCS Publication No. 75). European Convention for Constructional Steelwork, Brussels, 1995.
2. Mullet, D. L. *Slim Floor Design and Construction* (SCI-Publication – 110). The Steel Construction Institute, Ascot (Berkshire), 1992.
3. Mullet, D. L. and Lawson, R. M. *Slim Floor Construction using Deep Decking* (SCI-Publication-127). The Steel Construction Institute, Ascot (Berkshire), 1993.
4. Bogaard van de, A. W. A. M. J. and Eldik van, C. H. Verdiepingbouw in staal en beton-Staalskelet met geintegrerdde liggers en kanaalplaten (Multi-storey buildings in steel and concrete-Steel frame with built-in beams and hollow core slabs, Dutch), Staalbouw Instituut, Rotterdam, 1995.
5. Eurocode 1. *Basis of Design and Actions on Structures, Part 1: Basis of Design*. CEN/TC250/N80, Draft July 1992.
6. Eurocode 3. *Design of Steel Structures, Part 1.1: General Rules and Rules for Buildings*. CEN, prENV, 1993-1-1.
7. ECCS Advisory Committee 5. *Essentials of Eurocode 3. Design Manual for Steel Structures in Building* (ECCS Publication No. 65). European Convention for Constructional Steelwork, Brussels, 1991.
8. Verburg, W. H. Geintegreerde liggers-Rekenmodel voor de doorsnedecontrole volgens NEN 6770 (Built-in beams – Calculation model for member analysis according to the Dutch code NEN 6770). *Bouwen met Staal* 1992; 107:7–12.
9. Wyatt, T. A. *Design Guide on the Vibration of Floors* (SCI-Publication -076). The Steel Construction Institute, Ascot (Berkshire), 1989.
10. Precast Prestressed Hollow Core Floors (FIP Recommendations). Thomas Telford, London, 1988.
11. Anderson, J. Ljudisolering I bjälklag bestaende av stalbalk och haldäckeselement (Sound insulation in floor built-up from steel beam and hollow core slab, Swedish), SBI Rapport 160: 1. Stalbyggnadsintute, Stockholm, 1992.
12. Anderson, J. Ljudisolering i bostadshus med stalstomme a (Sound insulation in residential building with steel frame, Swedish), SBI Publikation 144. Stalbyggnadsinstitutet, Stockholm, 1992.
13. Eurocode 3. *Design of Steel Structures, Part 1.2: Fire Resistance*. CEN, prENV 1993-1-2.
14. ECCS Technical Committee 3. *European Recommendations for the Fire Safety of Steel Structures*. European Convention for Constructional Steelwork, Elsevier, Amsterdam/Brussels, 1983.
15. Saiidi, M. *Constructability of Reinforced Concrete Joints*. ACI Publication SCM-14 (86), Sec. VI, March 1986.

M.Y.H. Bangash, *Earthquake Resistant Buildings*,
DOI 10.1007/978-3-540-93818-7, © M.Y.H. Bangash 2011

www.EngineeringBooksPDF.com

16. Saiidi, M., Ghusn, G., and Jiang, Y. Five-spring element for biaxially bent R/C columns. *J. Struct. Div.* (ASCE) February 1989; 115:398–416.
17. Saiidi, M. and Sozen, M. A. *Simple and Complex Models for Nonlinear Seismic Response of Reinforced Concrete Structures*. Civil Engineering Studies, Structural Research Series no 465, Department of Civil Engineering, University of Illinois, Urbana, 1979.
18. Sakino, K. and Ishibashi, H. *Experimental Studies on Concrete Filled Square Steel Tubular Short Columns Subjected to Cyclic Shearing Force and Constant Axial Force*. Transactions of the Architectural Institute of Japan, no. 353, July 1985; 81–89.
19. Sakino, K. and Tomii, M. Hysteretic behavior of concrete filled square steel tubular beam-columns failed in flexure. *Transactions Japan Concrete Institute*, 1981; 3:439–446.
20. Sakino, K., Tomii, M., and Watanabe, K. Sustaining load capacity of plain concrete stub columns confined by circular steel tube. *Proc. Int. Specialty Conf. Concrete Filled Steel Tubular Struct.*, Harbin, China, August 1985; 112–118.
21. SANZ. *Code of Practice for the Design of Concrete Structures* (NZS 3101 Part 1). Standards Association of New Zealand, Wellington, 1982.
22. Sargin, M. *Stress-Strain Relationships for Concrete and Analysis of Structural Concrete Sections*, Study no. 4. Solid Mechanics Division, University of Waterloo, Ontario, Canada, 1971.
23. Schickert, G. and Winkler, H. *Results of Test Concerning Strength and Strain of Concrete Subjected to Multiaxial Compressive Stress*. Die Bundesanstalt für Materialprüfung (BAM), Berlin, Germany, 1977; p. 123.
24. Schlaich, J., et al. Toward a consistent design of structural concrete. *PCI J.* 1987; 2(3):74.
25. Schlaich, J. and Schaefer, K. *Konstruieren in Stahlbetonbau (Detailing in Reinforced Concrete Design), Betonkalender*, Part 2. W. Ernst, Berlin, Germany, 1984; pp. 787–1005.
26. Schlaich, J., Schaefer, K., and Jennewein, M. Toward a consistent design of structural concrete. *PCI J.* May–June 1987; 3:774–750.
27. Schlaich, J. and Weischede, D. Detailing reinforced concrete structures. *Proc. Can. Struct. Concrete Conf.*, Department of Civil Engineering, University of Toronto, Toronto, Ontario, 1981; pp. 171–198.
28. Schmidt, W. and Hoffman, E. S. 9000 psi Concrete – Why? Why Not? *Civil Engineering* (ASCE), 1975; Vol. 45, pp. 52–55.
29. Schuster, J. *Helical Stairs*. Julius Hoffman, Stuttgart, Germany, 1964.
30. Scott, B. D., Park, R., and Priestley, M. J. N. Stress-strain behavior of concrete by overlapping hoops at low and high strain rates. *ACI J.* January–February 1982; 79(1):13–27.
31. Scott, W. T., *Reshoring a Multistory Concrete Frame: A Practical Approach, Analysis and Design of High-Rise Concrete Buildings*, ACI Special Publication SP-97. American Concrete Institute, Detroit, 1985; pp. 277–301.
32. SEAOC. *Recommended Lateral Force Requirements and Commentary*. Structural Engineers' Association of California, San Francisco, 1975.
33. Sekin, M. and Uzumeri, S. M. Exterior beam-column joints in reinforced concrete frames. *Proc. VIIth World Conf. Earthquake Eng.*, Istanbul, Turkey, September 1980; 6:183–190.
34. Shah, S. P. New reinforced materials in concrete. *ACI J.* October 1974; 71(10):627.
35. Shah, S. P. (ed.). *Fatigue of Concrete Structures* (ACI Special Publication SP-75). American Concrete Institute, Detroit, 1982; pp. 133–175.
36. Shah, S. P. and Rangan, B. V. Fiber reinforced concrete properties. *ACI J.* February 1971; 68(2):126–135.
37. Shah, S. P., et al. Cyclic loading of spirally reinforced concrete. *J. Struct. Eng.* (ASCE) July 1983; 109(ST7):1695–1710.
38. Sheikh, S. A. and Uzumeri, S. M. *Properties of Concrete Confined by Rectangular Ties*. Bulletin d'Inforamtion, no.132, Comité Euro-International du Béton, Paris, France, 1979; pp. 53–60.

www.EngineeringBooksPDF.com

39. Sheikh, S. A. and Uzumeri, S. M. Strength and ductility of tied concrete columns. *J. Struct. Div.* (ASCE) May 1980; 106(ST5):1079–1102.
40. Siev, A. Analysis of free straight multiflight staircases. *J. Struct. Div.* (ASCE) 1962; 88(ST3):207–232.
41. Smith, K. N. and Vantsiotis, A. S. Shear strength of deep beams. *ACI J.* 1982; 79:201–213.
42. Somerville, G. *The Behavior and Design of Reinforced Concrete Corbels, Shear in Reinforced Concrete* (ACI Special Publication SP-42). American Concrete Institute, Detroit, 1974; pp. 477–502.
43. Stang, H. and Shah, S. P. Failure of fiber reinforced composites by pull-out fracture. *J. Mater. Sci.*, March 1986; 21:953–957.
44. Steven, R. F. Encased stanchions. *Struct. Eng.* February 1965; 43(2):59–66.
45. Suaris, W. and Shah, S. P. Properties of concrete and fiber reinforced concrete subjected to impact loading. *J. Struct. Div.* (ASCE) July 1983; 103(ST7):1717–1741.
46. Subedi, N. K. Reinforced concrete deep beams: a method for analysis. *Proc. Inst. Civil Eng.* (London) 1988; 85:1–30.
47. Paulay, T., Priestley, M. J. N., and Synge, A. J. Ductility in earthquake resisting squat shear walls. *ACI J.* 1982; 79(4):257–269.
48. Paulay, T. and Santhakumar, A. R. Ductile behaviour of coupled shear walls. *J. Struct. Div.* (ASCE) 1976; 102(ST1):93–108.
49. Paulay, T. and Taylor, R. G. Slab coupling of earthquake resisting shear walls. *ACI J.* 1981; 78(2):130–140.
50. Paulay, T. and Uzumeri, S. M. A critical review of the seismic design provisions for ductile shear walls of the Canadian code and commentary. *Can. J. Civ. Eng.* 1975;2(4)592–601.
51. Pfeifer, D. W., Magura, D. D., Russell. H. G., and Corley, W. G. *Time Dependent Deformations in a 70 Story Structure, Designing for Effects of Creep and Shrinkage in Concrete Structures* (ACI Special Publication SP-76). American Concrete Institute, Detroit, 1971; pp. 159–185.
52. Portland Cement Association. *Design of Deep Girders* (Publication ISO79.01D). PCA, Skokie, III, 1980.
53. Potucek, W. Die Beanspruchung der Stege von Stablbetonplattenbalken durch Querkraft und Biegung (Stresses in Webs of Reinforced Concrete T-Beams Subjected to Flexure and Shear). *Zement und Beton* 1977; 22(3):88–98.
54. Potyondy, J. G. Concrete filled tubular steel structures in marine environment. *Proc. Int. Specialty Conf. Concrete Filled Steel Tubular Struct.*, Habin, China, August 1985; 27–31.
55. Priestley, M. J. N. and Park, R. *Strength and Ductility of Bridge Substructures*. Research Report 84-20, Department of Civil Engineering, University of Canterbury, Christchurch, New Zealand, 1984; 120.
56. Priestley, M. J. N., and PARK , R. J. N., Concrete Filled Steel Tubular Piles under Seismic Loading, Proceedings of the International Specialty Conference on Concrete Filled Steel Tubular Structures, Harbin, China, August 1985; pp. 96–103.
57. Priestley, M. J. N., Park, R., and Potangaroa, R. T. Ductility of spirally-confined concrete columns. *J. Struct. Div.* (ASCE) January 1981; 107(ST1):181–202.
58. PTI. *Design of Post-Tensioned Slabs*. Post-Tensioning Institute, Glenview, III, 1984.
59. Ragan, H. S. and Warwaruk, J. Tee members with large web openings. *PCI J.* August 1967; 12(4):52–65.
60. Ramakrishnan, V. and Ananthanarayana, Y. Ultimate strength of deep beams in shear. *ACI J.* 1968; 65:87–98.
61. Ramakrishnan, V. and Josifek, C. performance characteristics and flexural fatigue strength on concrete steel fiber composites. *Proc. Int. Symp. Fiber Reinforced Concrete*, Madras, India, Oxford and IBH Publishing, New Delhi, December 1987; pp. 2.73–2.84.
62. Ramakrishnan, V., et al. A compressive evaluation of concrete reinforced straight steel fibres with deformed ends glued together bundles. *ACI J.* May–June 1980; 77(3):135–143.

www.EngineeringBooksPDF.com

63. Rausch, E. Design of inclined reinforcement to resist direct shear; Direct shear in concrete structures. *Der Bauingenieur* (Heidelberg) April 1922; 3(7):211–212; August 1931; 12(32/33):257.
64. Raush, E. Design for shear in reinforced concrete structures. *Der Bauingenieur* (Heidelberg) 1963; 38:257.
65. Rawdon de paiva, H. A. and Siess, C. P. Strength and behavior of deep beams in shear. *J. Struct. Div.* (ASCE) 1965; 91:19–41.
66. Regan, P. E. Shear in RC beams. *Mag. Concrete Res.* March 1969; 21(66):31–42.
67. Reinhardt, H. W. and Walraven, J. C. Cracks in concrete subject to shear. *J. Struct. Div.* (ASCE) January 1982; 108(ST1):207–224.
68. Rice, P. F. and Hoffman, E. S. *Structural Design Guide to the ACI Building Code*. Van Nostrand Reinhold, New York, 1985.
69. Ritter, W. Die Beauweise Hennebique (Hennebique's construction method). *Schweizerische Bauzeitung* (Zurich) 1899; 17:41–43, 49–52, 59–61.
70. Rogowsky, D. M. and Macgregor, J. G. The design of reinforced concrete deep beams. Concrete Int.: Design Construct. 1986; 8(8):49.
71. Rogowsky, D. M., Macgregor, J. G., and Ong, S. Y. Test of reinforced concrete deep beams. *ACI J.* July–August 1986; 83(4):614–623.
72. Roik, K., Bergmann, R., Bode, H., and Wagenknecht, G. Tragfahigkeit von ausbetonierten Hohlprofilstützen aus Baustahl, Technical Report no. 75-4, Institut für Konstruktiven Ingenieurbau, Ruhr-Universität Bochum, Germany, May 1975.
73. Romualdi, J. P. and Baston, G. R. Mechanics of crack arrest in concrete. *J. Eng. Mech. Div.* (ASCE) June 1963; 89(EM3):147–168.
74. Romualdi, J. P. and Mandeo, J. A. Tensile strength of concrete affected by uniformly distributed and closely spaced short lengths of wire reinforcement. *ACI J.* June 1964; 61(6):657–670.
75. Rosman, H. G. Approximate analysis of shear walls subjected to lateral loads. *ACI J.* 1964; 61:717–733.
76. Russell, H. G. *High-rise Concrete Buildings: Shrinkage, Creep, and Temperature Effects*, Private Communication, 1985.
77. Saenz, L. P. and Martin, I. Slabless tread-riser stairs. *ACI J.* 1961; 58:353.
78. Mattock, A. H. Design proposals for reinforced concrete corbels. *PCI J.* May–June 1976; 21(3):8–42.
79. Mattock, A. H., et al. The behavior of reinforced concrete corbels. *PCI J.* March–April 1976; 21(2):52–77.
80. Mayfield, B., Kong, F. K., Bennison, A., and Davies, J. C. D. T. Corner joint details in structural lightweight concrete. *ACI J.* May 1971; 68(5):366–372.
81. Mccormac, C. W. *Design of Reinforced Concrete*, 2nd edn. Harper & Row, New York, 1986; Chapter 14.
82. Mehmel, A. and Freitag, W. Tests on the load capacity of concrete brackets (in German). *Der Bauingenieur* (Heidelberg) 1967; 42(10):362–369.
83. Meinheit, D. F. and Jirsa, J. O. Shear strength of reinforced concrete beam-column connections. *J. Struct. Div.* (ASCE) 1983; 107(ST11):2227–2244.
84. Meyers, V. J. *Matrix Analysis of Structures*. Harper & Row, New York, 1983.
85. Mindess, S. *The Fracture of Fiber Reinforced and Polymer Impregnated Concretes: A Review, Fracture Mechanics of Concrete*. Elsevier Applied Science Publishers, Amsterdam, The Netherlands, 1983; pp. 481–501.
86. Mindess, S. and Young, J. F. *Concrete*. Prentice Hall, Englewood Cliffs, NJ, 1981; Chapter 18.
87. Mitchell, D. and Collins, M. P. Diagonal compressions field theory – a rational model for structural concrete in pure torsion. *ACI J.* August 1974; 71(8):396–408.
88. Mitchell, D. and Cook, W. D. Preventing progressive collapse of slab structures. *J. Struct. Eng.* (ASCE) July 1984; 110(ST7):1513–1532.

www.EngineeringBooksPDF.com

89. Mochle, J. P., Diebold, J. W., and Zee, H. L. Experimental study of a flat- plate building model. *Proc. 18th World Conf. Earthquake Eng*., San Francisco, CA, July 1984; Vol. IV, pp. 355–362.
90. Moersch, E., *Der Eisenbetonbau-Seine Theorie und Anwendung* (Reinforced Concrete Construction-Theory and Application), 3rd edn. K. Wittwer, Stuttgart, 1908; 5th edn., Vol. 1, Part 2, 1922.
91. Moersch, E. *Concrete Steel Construction*, English translation by E. P. Goodrich. McGraw-Hill, New York, 1909; 368 pp. (Translation from 3rd edition of Der Eisenbentonbau; 1st edition 1902).
92. Mohammadi, J. and Yazbeck, G. J. Strategies for Bridge Inspection using probabilistic models. *Structural Safety and Reliability* (Aug, A. H.-S., Shinozuka, M., and Schueller, G. I., eds.). American Society of Civil Engineers, New York, 1990; Vol. 3, pp. 2115–2122.
93. Mokhtar, A. S., et al. Stud shear reinforcement for flat concrete plates. *ACI J*. September–October 1985; 82(5):676–683.
94. Moretto, O. *Reinforced Concrete Course* (Curso de Hormingon Armado), 2nd edn. Libreria El Ateneo, Buenos Aires, Argentina, 1971.
95. Moretto, O. *Deep Foundations – Selected Synthesis of the Present State of the Knowledge about Soil Integration*. Revista Latinoamericana de Geotecnia, Caracas, Venezuela, July–September, 1975.
96. Moretto, O. Foundations of the bridges over the Parana River in Argentina. *Proc. 5th Pan American Conf. Soil Mech. Found. Eng*., Buenos Aires, Argentina, 1975; Vol. v.
97. Morishita, Y., Tomii, M., and Yoshimura, K. Experimental studies of bond strength in concrete filled circular steel tubular columns subjected to axial loads. *Transactions Japan Concrete Institute* 1979; 1:351–358.
98. Morishita, Y., Tomii, M., and Yoshimura, K. Experimental studies on bond strength in concrete filled square steel tubular columns subjected to axial loads. *Transactions Japan Concrete Institute*, 1979; 1:359–366.
99. Morishita, Y. and Tomii, M. Experimental studies on bond strength between square steel tube and encased concrete core under cyclic shearing force and constant axial force. *Transactions Japan Concrete Institute* 1982; 4:363–370.
100. Morrison, D. G. and Sozen, M. A. *Response of Reinforced Concrete Plate-Column Connections to Dynamic and Static Horizontal Loads*. Civil Engineering Studies, Structural Research Series no. 490, University of Illinois, Urbana, April 1981.
101. Morrison, J. K., et al. Analysis of the debonding and pull-out process in frame composites. *J. Eng. Mech. Div*. (ASCE) February 1988; 114:277–294.
102. Mphonde, A. C. and Frantz, G. C. *Shear Test of High- and Low- strength Concrete Beams with Stirrups* (ACI Special Publication SP-87). American Concrete Institute, Detroit, pp. 179–196.
103. Mueller, P. *Failure Mechanisms for Reinforced Concrete Beams in Torsion and Bending*. International Association for Bridge and Structural Engineering Publications, 1976; Vol. 36, pp. 147–163.
104. Naaman, A. E. and Shah, S. P. Pullout mechanism in steel fiber reinforced concrete. *J. Eng. Mech. Div*. (ASCE) August 1976; 102(ST8):1537–1548.
105. Naaman, A. E., et al. Probabilistic analysis of fiber reinforced concrete. *J. Eng. Mech. Div*. (ASCE) April 1974; 100(EM2):397–413.
106. Nasser, K. W., Acavalos, A., and Daniel, H. R. Behavior and design of large opening in reinforced concrete beams. *ACI J*. January 1967; 64(1):25–33.
107. Mansur, M. A., et al. Ultimate torque of R/C beam with large openings. *J. Struct. Eng*. (ASCE) August 1983; 109(8):2602–2618.
108. Mansur, M. A., et al. Collapse loads of R/C beams with large openings. *J. Struct. Eng*. (ASCE) November 1984; 110(11):1887–1902
109. Mansur, M. A., et al. Design method for reinforced concrete beams with large openings. *ACI J*. July–August 1985; 82(4):517–524.

www.EngineeringBooksPDF.com

110. Marti, P., *Zur Plastischen Berechnung von Stahlbeton* (on Plastic Analysis of Reinforced Concrete). Institute of Structural Engineering, ETH Zurich, Switzerland, 1980; Report no. 104, 176 pp.
111. Marti, P. *Strength and Deformations of Reinforced Concrete Members under Torsion and Combined Actions*. Bulletin d'information, no. 146. Comité Euro-International du Béton, January 1982; pp. 97–138.
112. Marti, P. Basic tools of reinforced concrete beam design. *ACI J*. January–February 1985; 82:46–56; also, Discussion November–December 1985; 82(6):933–935.
113. Marti, P. Truss models in detailing. *Concrete International: Design Construction* October 1985; 8(10):66–68.
114. Marti, P. Staggered shear design of simply supported concrete beams. *ACI J*. January–February 1986; 83(1):36–42.
115. Marti, P. Staggered shear design of concrete bridge girders. *Proc. Int. Conf. Short Medium Span Bridges*, Ottawa, ON, Canada, August 1986; Vol. 1, pp. 139–149.
116. Marti, P. Design of concrete slabs for transverse shear. *ACI Struct. J*. 1986; 84(1).
117. Marti, P. Personal Communication, 1990.
118. Marti, P. and Kong, K. Response of reinforced concrete slab elements to torsion. *J. Struct. Eng*. (ASCE) May 1987; 113(ST5):976–993.
119. Martinez, S., Nilson, A. H., and Slate, F. O. Spirally-reinforced high-strength concrete columns. *ACT J*. September–October 1982; 81:431–442; Research report no. 82-101, Department of Structural Engineering, Cornell University, Ithaca, NY, August, 1982.
120. Mast, R. F. Auxiliary reinforced in concrete connections. *ASCE Proc*. June 1968; 94(ST6):1485–1504.
121. Matsui, C. strength and behavior of frames with concrete filled square steel tubular columns under earthquake loading. *Proc. Int. Specialty Conf. Concrete Filled Steel Tubular Struct*., Harbin, China, August 1985; pp. 104–111.
122. Matsui, C. Local bucking of concrete filled steel square tubular columns. *IABSE-ECCS Symp*., Luxembourg, September 1985; pp. 269–276.
123. Kotsovos, M. D. An analytical investigation of the behavior of concrete under concentration of load. *Mater. Struct*. (RILEM) September–October 1981; 14(83):341–348.
124. Kotsovos, M. D. A fundamental explanation of the behavior of RC beams in flexure based on the properties of concrete under multiaxial stress. *Mater. Struct*. (RILEM) November–December 1982; 15:529–537.
125. Kotsovos, M. D. Effect of testing techniques on the post-ultimate behavior of concrete in compression. *Mater. Struct*. (RILEM) 1983:16:3–12.
126. Kotsovos, M. D. Mechanisms of 'shear' failure. *Mag. Concrete Res*. June 1983; 35(123):99–106.
127. Kotsovos, M. D. Behavior of RC beams with shear span to depth ratios between 1.0 and 2.5. *ACI J*. May–June 1984; 81(3):279–286.
128. Kotsovos, M. D. Deformation and failure of concrete in a structure. *Int. Conf. Concrete Under Multiaxial Conditions* (RILEM-CEB-CNRS), Toulouse, France, May 1984.
129. Kotsovos, M. D. Behavior of reinforced concrete beams with a shear span to depth ratio greater than 2.5. *ACI J*. 1986; 83:1026–1034.
130. Kotsovos, M. D. Shear failure of reinforced concrete beams. *Eng. Struct*. 1987; 9:32–38.
131. Kotsovos, M. D. *Shear Failure of RC Beams: A Reappraisal of Current Concepts*. Bulletin, d'information, no. 178/179. Comité Euro-International du Béton, Paris, France, 1987; pp. 103–112.
132. Kotsovos, M. D. Compressive force path concept: basis for ultimate limit state reinforced concrete design. *ACI J*. 1988; 85:68–75.
133. Kotsovos, M. D. Design of reinforced concrete deep beams. Struct. Eng. 1988; 66:28–32.
134. Kotsovos, M. D. Designing RC beams in compliance with the concept of the compressive force path (in preparation).

www.EngineeringBooksPDF.com

135. Kotsovos, M. D. Behavior of RC beams designed in compliance with the compressive force path (in preparation).
136. Kotsovos, M. D. Shear failure of RC beams (in preparation).
137. Kotsovos, M. D. Behavior of RC beams with shear span to depth ratios greater than 2.5 (in preparation).
138. Kotsovos, M. D. *The Use of Fundamental Properties of Concrete for the Design of RC Structural Members*. Research Project Sponsored by Nuffield Foundation, Award No. 890BA, Imperial College.
139. Hillerborg, A. Analysis of fracture by means of the fictitious crack model. *Int. J. Cement Composite* 1980; 2:177–184.
140. Hoff, G. C. Bibliography on fiber reinforced concrete. *Proc. Int. Symp. Fiber Reinforced Concrete*, Madras, India, Oxford and IHB Publishing, New Delhi, December 1987; pp. 8.3–8.163.
141. Hognestad, E., *A Study of Combined Bending and Axial Loading in Reinforced Concrete Members*. Bulletin no. 399, Engineering Experiment Station, University of Illinois, Urbana, November 1951.
142. Holmes, M. and Martin, L. H. *Analysis and Design of Structural Connections, Reinforced Concrete and Steel*. Ellis Horwood Ltd., West Sussex, UK, 1983
143. Hsu, T. T. C. Softened truss model theory for shear and torsion. *ACI Struct. J.* November–December 1988; 85(6):624–635.
144. Hurd, M. K. *Formwork for Concrete*, 4th edn. ACI Special Publication SP-4, American Concrete Institute, Detroit, 1979.
145. Hurd, M. K. and Courtois, P. D. Method of analysis for shoring and reshoring in multistory buildings. *Second Int. Conf. Forming Econ. Concrete Building*, ACI Special Publication, SP-90, American Concrete Institute, Detroit, 1986; pp. 91–100.
146. IABSE. *Colloquium on Plasticity in Reinforced Concrete*. International Association of Bridge and Structural Engineers, Copenhagen, Introductory Report, Vol. 28, 172 pp, Final Report, Vol. 29, 360 pp., 1979.
147. IAEE. *Earthquake Resistant Regulations – A World List*. International Association for Earthquake Engineers, Tokyo, Japan, 1984; p. 904.
148. Iqbal, M. and Derecho, A. T. *Inertial Forces over Height of Reinforced Concrete Structural Walls During Earthquakes, Reinforced Concrete Structures Subjected to Wind and Earthquake Forces*. ACI Special Publication SP-63, American Concrete Institute, Detroit, 1980; pp. 173–196.
149. Japan Concrete Institute. *Method of Test for Flexural Strength and Flexural Toughness of Fiber Reinforced Concrete*. Japan Concrete Institute, 1983; pp. 45–51.
150. Jeng, Y. S. and Shah, S. P. Crack propagation of steel fiber reinforced mortar and concrete. *Proc. Int. Symp. Fibrous Concrete CI*, The Construction Press Ltd., Lancaster, UK, 1986.
151. Johnston, C. D. Properties of steel fiber reinforced mortar and concrete. *Proc. Int. Symp. Fibrous Concrete CI*, The Construction Press Ltd., Lancaster, UK, 1980.
152. Johnston, C. D. Definition and measurements of flexural toughness parameters of fiber reinforced concrete. *Cement Concrete Aggr.* CCAGDP, ASTM (Winter) 1982; 4(2):53–60.
153. Johnston, C. D. Steel fiber reinforced concrete – present and future in engineering construction. *J. Composites* April 1982; pp. 113–121.
154. Johnson, E. and Savre, T. I. *Tests on Brackets in Concrete* (in Norwegian). Norwegian Building Research Institute, Oslo, Report no. 2/1976, 1976; p. 31.
155. Kaba, S. A. and Mahin, S. A. *Refined Modeling of Reinforced Concrete Columns for Seismic Analysis*. Earthquake Engineering Research Center, University of California, Berkeley, Report no. UCB/EERC-84/03, April 1984.

www.EngineeringBooksPDF.com

156. Kani, G. N. J. The riddle of shear and its solution. *ACI J*. April 1964; 61(4):441–467.
157. Karshenas, S. and Ayoub, H. An investigation of live loads on concrete structures during construction. *Proc. I COSSAR'89, 5th Int. Conf. Struct. Safety Reliability*, San Francisco, CA, 1989; pp. 1807–1814.
158. Kato, B., Akiyama, H., and Kitazawa, S. *Deformation Characteristics of Box-shaped Steel Members Influenced by Local Buckling* (in Japanese). *Transactions Architect. Inst. Jpn*. June 1978; 268:71–76.
159. Kienberger, H. *Diaphragm Walls as Load Bearing Foundations*. Institute of Civil Engineers, London, UK, 1975.
160. Kemp, E. L. and Mukherjee, P. R. Inelastic behavior of corner knee joints. *Consulting Engineer*, October 1968; pp. 44–48.
161. Knowles. R. B. and Park, R. Strength of concrete filled steel tubular columns. *J. Struct. Div*. (ASCE) December 1969; 95(ST12):2565–2587.
162. Kollegger, J. and Mehlhorn, G. Material model for cracked reinforced concrete. *Proc. IABSE Colloquium Comput. Mech. Concrete Struct*., Delft, The Netherlands, August 1987; pp. 63–74.
163. Kong, F. K. and Evans, R. H. *Reinforced and Prestressed Concrete*, 2nd edn. The English Language Book Society and Nelson, 1980, pp. 162–179.
164. Kong. F. K., Robins, P. J., and Cole, D. F. Web reinforcement effects on deep beams. *ACI J*. 1970; 67:1010–1017.
165. Kong, F. K., et al. Design of reinforced concrete deep beams in current practice. *Struct. Eng*. 1975; 53(4):73–180.
166. Kormeling, H. A., et al. Static and fatigue properties of concrete beams reinforced with continuous bars and with fibers. *ACI J*. January–February 1980; 77(1):36–43.
167. Kotsovos, M. D. Fracture processes of concrete under generalized stress states. *Mater. Struct*. (RILEM) November–December 1979; 12(72):431–437.
168. ACI Committee 207. ACI Manual of Concrete Practice, Part 1, 1986.
169. ACI Committee 209. Prediction of creep, shrinkage, and temperature effects in concrete structures. *Designing for Creep and Shrinkage in Concrete Structures* (ACI Special Publication SP-76). American Concrete Institute, Detroit, 1982; pp. 139–300.
170. ACI 228. In-place methods for determination of strength of concrete, American Concrete Institute. *ACI Mater. J*. September–October 1988; F85(5):446–471.
171. ACI. *Building Code Requirements for Reinforced Concrete* (ACI 318–83). American Concrete Institute, Detroit, 1983.
172. ACI Committee 318. *Building Code Requirements for Reinforced Concrete*. American Concrete Institute, Detroit, 1983; 111 pp.
173. ACI 318. *Building Code Requirements for Reinforced Concrete (ACI 318–89) and Commentary* (ACI 318R–89). American Concrete Institute, Detroit, 111 pp., 1989.
174. ACI 347. *Recommended Practice for Concrete Formwork*. American Concrete Institute, Detroit, 1978; 37 pp.
175. ACI 363. State-of-the-art on high strength concrete. *ACI J*. July–August 1984; 81(4):364–411.
176. ACI Committee 544. State of the art report on fiber reinforced concrete. *ACI J*. November 1973; 70(11):729–744.
177. ACI Committee 544. Measurements of properties of fiber reinforced concrete. *ACI J*. July 1978; 75(7):283–289.
178. ACI Committee 544. Measurements of properties of fiber reinforced concrete. *ACI J*. November–December, 1988; pp. 583–593.
179. ACI-ASCE Committee 352. *Revised recommendations for the Design of Beam-Column Joints*. American Concrete Institute, Detroit, draft. No. 11, 1984; 34 pp.
180. ACI-ASCE Committee 352. Recommendations for design of beam-column joints in monolithic reinforced concrete structures. *ACI J*. May–June 1985; 82(3): 266–283.

www.EngineeringBooksPDF.com

181. Computational mechanics of concrete structures: advances and applications. *Transactions of IABSE Colloquium* Delft 87, Delft, August 1987; pp. 113–120.
182. Pruijssers, A. F. Shear resistance of cracked concrete subjected to cyclic loading. *Computational Mechanics of Concrete Structures: Advances and Applications*, Transactions of IABSE Colloquium Delft 87, Delft, August 1987; pp. 43–50.
183. Walraven, J. C. Aggregate interlock under dynamic loading. *Darmstadt Concrete* 1986; 1:143–156.
184. Yoshikawa H. et al. Analytical model for shear slip of cracked concrete. *J. Struct. Eng. Am. Soc. Civ. Engrs*. April 1989; 115(4):771–788.
185. Li, B. and Maekawa, K. Contact density model for cracks in concrete. Computational mechanics of concrete structures: advances and applications. *Transactions IABSE Colloquium Delft* August 1987; 87:51–62.
186. Bazant, Z. P. and Gambarova, P. G. Crack shear in concrete: crack band micro plane model. *J. Struct. Eng. Am. Soc. Civ. Engrs* September 1984; 110(9):2015–2035.
187. Riggs, H. R. and Powell, G. H. Rough crack model for analysis of concrete. *J. Eng. Mech.* (ASCE) May 1986; 112(5):448–464.
188. Bazant, Z. P. and Oh, B. H. Microplane model for progressive fracture of concrete and rock. *J. Eng. Mech.* (ASCE) 1985; 111(4):559–582.
189. Gambarova, Z. P. and Floris, E. Microplane model for concrete subject to plane stresses. *Nucl. Eng. Design* 1986; 97:31–48.
190. Bazant, Z. P. and Prat, P. C. Microplane model for brittle-plastic material: I. Theory; II. Verification. *J. Eng. Mech.* (ASCE) 1988; 114(10):1672–1702.
191. Feensra, P. H., et al. Numerical study on crack dilatancy. I. Models and Stability analysis; II. Applications. *J. Eng. Mech.* (ASCE) April 1991; 117(4):733–753, 754–769.
192. Cedolin, L. and Dei Poli, S. Finite element studies of shear critical R/C beams. *J. Eng. Mech. Div.* (ASCE) June 1977; 103(EM3):395–410.
193. Kemp, E. L. and Mukherjee, P. R. Inelastic behavior of corner knee joints. *Consulting Engineer*, October 1968; pp. 44–48.
194. Knowles, R. B. and Park, R. Strength of concrete filled steel tubular columns. *J. Struct. Div.* (ASCE) December 1969; 95(ST12):2565–2587.
195. Tassions, T. and Vintzeleou, E. Concrete-to-concrete friction. *J. Struct. Eng.* (ASCE) April 1987; 113(4):832–849.
196. Isenberg, J. and Adham, S. Analysis of orthotropic reinforced concrete structures. *J. Struct. Div.* (ASCE) December 1970; 96(ST12):2607–2623.
197. Duchon, N. B. Analysis of reinforced concrete membranes subject to tension and shear. *ACI J.* September 1972; 69(9):578–583.
198. Collins, M. P. Towards a rational theory for reinforced concrete members in shear. *J. Struct. Div.* (ASCE) April 1978; 104(ST4):649–666.
199. Perdikaris, P. C. and White, R. N. Shear modulus of precracked R/C panels. *J. Struct. Eng.* (ASCE) February 1985; 111(2):270–289.
200. Tanabe, T. and Yoshikawa, H. Constitutive equations of a cracked reinforced concrete panel. Computational mechanics of concrete structures: advances and applications. *Transactions IABSE Colloquium Delft* August 1987; 17–34.
201. Vintzeleou, E. N. and Tassios, T. P., Mathematical Models for dowel action under monotonic and cyclic conditions. *Mag. Conc. Res.* March 1986; 38(134):13–22.
202. Soroushian, P., et al. Bearing strength and stiffness of concrete under reinforcing bars. *ACI Mater. J.*, Technical Paper No. 84-M19, May–June 1987; pp. 179–184.
203. Johnston, D. W. and Zia, P. Analysis of dowel action. *J. Struct. Div.* (ASCE) May 1971; 97(ST5):1611–1630.
204. Giuriani, E. On the axial stiffness of a bar in cracked concrete. *Bond in Concrete* (Bartos, P. ed.). Applied Science Publishers, London, 1982.
205. Brenna, et al. Studie Ricerche, 11/89. School for the Design of RC Structures, Politecnico di Milano, Milan, Report, 1990.

www.EngineeringBooksPDF.com

206. Di Prisco, et al. Non-linear modeling of dowel action of a bar immersed in a concrete mass of infinite extent (in Italian). Studie Ricerche, 10/88. School for the Design of RC structures, Politecnico di Milano, Milan, 1989.
207. Jimenez-Perez, R., et al. Bond and dowel capacities of reinforced concrete. *ACI J*. Symposium Paper, No. 76004, Jan. 1979.
208. Mehlhorn, G. Some developments for finite element analyses of reinforced concrete structures. *Computer Aided Analysis and Design of Concrete Structures*, *Proc. 2nd Int. Conf.,* Zell-am-See, April, 1990; pp. 1319–1336.
209. Mehlhorn, G. et al. Nonlinear contact problems – a finite element approach implemented in ADINA. *Computers Struct*. 1985; 21(1/2):69–80.
210. Mehlhorn, G. and Keuser, M. Isoparametric contact elements for analysis of reinforced concrete structures. Finite Element Analysis of Reinforced Concrete Structures. *Am. Soc. Civ. Engrs*. 1986; 329–347.
211. Miguel, P. F. A discrete-crack model for the analysis of concrete structures. *Computer Aided Analysis and Design of Concrete Structures*, *Proc. 2nd Int. Conf*., Zell-am-See, April 1990; pp. 897–908.
212. Bathe, K.-J. et al. Nonlinear analysis of concrete structures. *Computers Struct*. 1989; 32(3/4):563–590.
213. Grootenboer, H. J. et al. Numerical models for reinforced concrete structures in plane stress. *Heron J*. 1981; 26(1c):83.
214. Hibbit, H. D. et al. ABAQUS Manuals: V.1: User's Manual, Version 4.5, 1984, Version 4.8, 1989, Providence, RI.
215. Blaauwendraad, J. Realizations and restrictions. Applications of numerical models to concrete structures. *Finite Element Analysis of Reinforced Concrete Structures* (Mever, C. and Okamura, H., eds.). ASCE, New York, 1986; pp. 557–578.
216. Wang, Q. B. et al. Failure of reinforced concrete panels – how accurate the models must be. *Computer Aided Analysis and Design of Concrete Structures, Proc. 2nd Int. Conf*., Zell-am-See, April 1990; pp. 153–163.
217. Sarne, Y. *Material Nonlinear Time-Dependent Three Dimensional Finite Element Analysis of Reinforced and Prestressed Concrete Structures*. Thesis submitted to the Department of Civil Engineering, Massachusetts Institute of Technology, in partial fulfillment of the requirements for the Degree of Doctor of Philosophy, Cambridge, MA, 1974.
218. Kotsovos, M. D. and Newman, J. B. A mathematical description of the deformational behavior of concrete under complex loading. *Mag. Conc. Res*. June 1979; 31(107):67–76.
219. Darwin, D. and Pecknold, D. A. Nonlinear biaxial stress strain law for concrete. *J. Eng. Mec*. (ASCE) April 1977; 103:229–241.
220. Schickert, G. and Winckler, H. Results of test concerning strength and strain of concrete subjected to multiaxial compressive stresses. *Deutscher Ausschuss für Stahlbeton* (Berlin) 1977; 277.
221. Traina, L. A. Experimental stress-strain behavior of a low strength concrete under multiaxial states of stress. AFWL-TR-82-92, Air Force Weapons Laboratory, Kirtland Air Force Base, New Mexico, 1982.
222. Saenz, L. Equation for the stress-strain curve of concrete. *ACI J*. September 1964; 61:1229–1235.
223. Kupfer, H. et al. Behavior of concrete under biaxial stresses. August 1973; 99:853–866.
224. William, K. J. and Warnke, E. P. Constitutive model for the triaxial behavior of concrete. *IABSE Proc*. 1975; 19:1–31.
225. Eberhardsteiner, J., et al. *Triaxales Konstitutive Modellieren von Beton*. Report, Institute for Strength of Materials, Technical University of Vienna, 1987.
226. Sargin, M. *Stress-strain relationship for concrete and the analysis of structural concrete sections*. No. 4, Solid Mechanics Division, University of Waterloo, 1971.
227. Van Mier, J. G. M. Strain-softening of concrete under multiaxial loading conditions. Dissertation, Eindhoven University, 1984.

www.EngineeringBooksPDF.com

228. Dafalias, Y. F. and Popov, E. P. Plastic internal variable formalism of cyclic plasticity. *Appl. Mech. Am. Soc. Civ. Engrs*. 1976; 43:645–651.
229. Dafalias, Y. F. and Herrmann, L. R. Bounding surface formulation of soil plasticity. *Soil Mechanics – Transient and Cyclic Loads*. (Pande G. N. and Zienkiewicz O. C. eds.). Wiley, New York, 1982.
230. Fardis, N. M., et al. Monotonic and cyclic constitutive law for concrete. *J. Eng. Mech*. (ASCE) 1983; 109:516–536.
231. Spooner, D. C. and Dougill, J. W. A quantitative assessment of damage sustained in concrete during compressive loading. *Mag. Conc. Res*. 1975; 27:151–160.
232. Resende, L. A damage mechanics constitutive theory for the inelastic behavior of concrete. *Comp. Meth. Appl. Mech. Engng*. 1987; 60:57–93.
233. Krajcinovic, D. Constitutive equations for damaging materials. *J. Appl. Mech*. (ASME) 1983; 50:355–360.
234. Bažant, Z. P. and Kim, S. S. Plastic-fracturing theory for concrete. *J. Eng. Mech*. (ASCE) June 1979; 105: 407–428.
235. Han, D. J. and Chen, W. F. Strain-space plasticity formulation for hardening softening materials with elastoplastic coupling. *Int. J. Solids Struct*. 1986; 22(8):935–950.
236. Lemaitre, J. Coupled elastoplasticity and damage constitutive equations. *Comp. Meth. Appl. Mech. Engng*. 1985; 51:31–49.
237. Bažant, Z. P. and Prat, P. C. Microplane model for brittle-plastic material – Parts I and II. *J. Eng. Mech*. (ASCE) 1988; 114(10):1672–1702.
238. Bažant, Z. P. and Ožbolt, J. Nonlocal microplane model for fracture, damage and size effect in structures. *J. Eng. Mech*. (ASCE) 1990; 116(11):2485–2505.
239. Pramono, E. and William, K. Fracture energy-based plasticity formulation of plain concrete. *J. Eng. Mech*. (ASCE) June 1989; 115.
240. Lubliner, J. et al. A plastic-damage model for concrete. *Int. J. Solids Struct*. 1989; 25(3).
241. Bažant, Z. P. and Oh, B. H. Microplane model for progressive fracture of concrete and rock. *J. Eng. Mech*. (ASCE) 1985; 111.
242. Bažant, Z. P. and Prat, P. C. Microplane model for brittle-plastic material: I theory, II verification. *J. Eng. Mech*. (ASCE) October 1988; 114:1689–1702.
243. Chen, W. F. *Plasticity in Reinforced Concrete*. McGraw-Hill, New York, 1982.
244. Scordelis, A. C., Nilson, A. H., and Gerstle, K. *Finite Element Analysis of Reinforced Concrete*. State of the Art Report, American Society of Civil Engineers, New York, 1982.
245. Bažant, Z. P. and Bhat, P. Endochronic theory of inelasticity and failure of concrete. *J. Eng. Mech*. (ASCE) August 1976; 102:701–722.
246. Elwi, A. A. and Murray, D. W. A 3D hypoelastic concrete constitutive relationship. *J. Eng. Mech*. (ASCE) August 1979; 105:623–641.
247. Buyukozturk, O. and Shareef, S. S. Constitutive modeling of concrete in finite element analysis. *Comp. Struct*. 1985; 21(3):581–610.
248. Stankowski, T. and Gerstle, K. H. Simple formulation of concrete behavior under multi-axial load histories. *ACI J*. March–April 1985; 82(2):213–221.
249. Shafer, G. S. and Ottosen, N. S. An invariant-based constitutive model. *Structural Research Series 8506*. Department of Civil Environmental and Architectural Engineering, University of Colorado, Boulder, 1985.
250. Vermeer, P. A. and De Borst, R. Non-associated plasticity for soils, concrete and rocks. *Heron J*. 1984; 29:1–64.
251. Han, D. J. and Chen, W. F. A nonuniform hardening plasticity model for concrete materials. *J. Mech. Mat*. 1985; 4:283–302.
252. Fardis, M. N. and Chen, E. S. A cyclic multiaxial model for concrete. *Comput. Mech*. 1986; 1:301–315.
253. Chen, E. S. and Buyukozturk, O. Constitutive model for concrete in cyclic compression. *J. Eng. Mech*. (ASCE) 1985; 111:797–814.

www.EngineeringBooksPDF.com

254. Yang, B. et al. A bounding surface plasticity model for concrete. *J. Eng. Mech.* (ASCE) March 1985; 111:359–380.
255. Comité Euro-International du Béton. *Concrete Under Multiaxial States of Stress. Constitutive Equations for Practical Design.* CEB, Lausanne, 1983, Bulletin d'Information 156.
256. Krajcinovic, D. Continuous damage mechanics. *Appl. Mech. Rev.* 1984; 37:1–6.
257. Lemaitre J. How to use damage mechanics. *J. Nucl. Eng. & Design* 1984; 80:233–245.
258. Resende, L. and Martin, J. B. A progressive damage continuum model for granular materials. *Comp. Meth. Appl. Mech. Eng.* 1984; 42:1–18.
259. Krajcinovic, D. and Fonseka, G. U. The continuous damage theory of brittle materials. *J. Appl. Mech. Am. Soc. Mech. Engrs.* 1981; 48:809–824.
260. Mazars, J. Description of the multiaxial behavior of concrete with an elastic damaging model. *Proc. RILEM Symp. Concrete Under Multiaxial Conditions*, INSA-OPS Toulouse, May 1984.
261. Dougill, J. W. On stable progressively fracturing solids. *Z. Angew. Math. Phys.* 1976; 27:423–437.
262. Gerstle, K. H., et al. Behavior of concrete under multiaxial stress states. *J. Eng. Mech.* (ASCE) December 1980; 106:1383–1403.
263. Dulacska, H. Dowel action of reinforcement crossing cracks in concrete. *ACI J.* December 1972; 69(69–70):745–757.
264. Furuchi, H. and Kakuta, Y. Deformation behavior in dowel action of reinforcing bars. *Transactions Japan Concrete Institute* 1985; 7:263–268.
265. Krefeld, W. J. and Thurston, C. W. Contribution of longitudinal steel to shear resistance of reinforced concrete beams. *ACI J.* March 1966; 63(14):325–344.
266. Dei Poli, S. et al. Dowel action as a means of shear transmission in R/C elements: a state-of-art and new test results (in Italian), *Studi e Richerche*, 9/87. School for the Design of R/C Structures, Politeccnico di Milano, Milan, 1988; pp.217–303.
267. Dei Poli, S. et al. Shear transfer by dowel action in R/C elements: the effects of transverse reinforcement and concrete cover (in Italian), *Studi e Ricerche*, 10/88. School for the Design of R/C Structures, Politecnico di Milano, Milan, 1989; pp.9–76.
268. Di Prisco, M. and Gambarova, P. G. Test results and modelling of dowel action in normal, high-strength and fiber reinforced concrete. *Proc. 1st B. Abbyal Environment. Speciality Conf. Can. Soc. Civil Eng. – CSCE*, 2, Hamilton (Ontario), May 1990; pp.702–722.
269. Paschen, H. and Schonhoff, T. *Investigations on Shear Connectors Made of Reinforcing Steel Embedded in Concrete* (in German). DAfSt, Report 346, Berlin, 1983; pp.105–149.
270. Vintzeleou, E. N. and Tassios, T. P. Behavior of dowels under cyclic deformations. *ACI Struct. J.* Technical Paper No. 84–S3, January–February 1987; pp.18–30.
271. Giuriani, E. and Rosati, G. P. Behaviour of concrete elements under tension after cracking. *Studi e Ricerche*, 8/86. School for the Design of RC Structures, Politecnico di Milano, Milan, 1987.
272. Fardis, M. N. and Buyukozturk, O. Shear transfer model for reinforced concrete. *J. Eng. Mech.* (ASCE) April 1979; 105(EM2):255–275.
273. Leombruni, P. et al. *Analysis of Cyclic Shear Transfer in Reinforced Concrete with Application to Containment Wall Specimens.* MIT0CE R79-26, June 1979.
274. Jimenez-Perez, R. et al. *Shear Transfer Across Cracks in Reinforced Concrete*. Cornell University, Department of Structural Engineering, Report 78–4, August 1978.
275. Laible, J. P. et al. Experimental investigation of seismic shear transfer across cracks in concrete nuclear containment vessels. ACI Special Publication SP53, Detroit, 1977; pp.203–226.
276. Bažant, Z. P. and Gambarova, P. G. Rough cracks in reinforced concrete *J. Struct. Div.* (ASCE) April 1980; 106(ST4):819–842.
277. Gambarova, P. G. Shear transfer by aggregate interlock in cracked reinforced concrete subject to repeated loads (in Italian). *Studi e Ricerche*, 1/79. School for the Design of R/C Structures, Politecnico di Milano, Milan, 1980; pp.43–70.

www.EngineeringBooksPDF.com

278. Gambarova, P. G. and Karakoc, C. A new approach to the analysis of the confinement role in regularly cracked concrete elements. *Trans. 7th SMiRT Conf.* II Paper H5/7, Chicago, August 1983; pp.251–261.
279. Gambarova, P. G. Shear transfer in R/C cracked plates (in Italian). *Trans. 1983 Meet. Ital. Soc. R/C and P/C Struct. – AICAP*, Bari, May 1983; pp.141–156.
280. Dahlblom, O. and Ottosen, N. S. Smeared crack analysis using a generalized fictitious crack model. *J. Eng. Mech.* (ASCE) January 1990; 116(1):55–76.
281. Gupta, A. K. and Maestrini, S. R. Post-cracking behavior of membrane reinforced concrete elements including tension-stiffening. *J. Struct. Eng.* (ASCE) April 1989; 11(4):957–976.
282. Hillerborg, A. Numerical methods to simulate softening and fracture of concrete. *Fracture Mechanics of Concrete: Structural Application and Numerical Calculation* (Sih, G. C. and Di Tommaso, A., eds.). Martinus Nijhoff Publishers, Dordrecht, Netherlands, 1984; pp. 141–170.
283. Bažant, Z. P. and Cedolin, L. Blunt crack propagation in finite element analysis. *J. Eng. Mech.* (ASCE) April 1979; 105(EM2):297–315.
284. Okamura, H. and Maekawa, K. Non-linear analysis and constitutive models of reinforced concrete. *Proc. 2nd Int. Conf. Computer Aided Analysis and Design of Concrete Structures*, Zell-am-See, April 1990; pp.831–850.
285. Rots, J. G. and Blaauwendraad, J. Crack models for concrete: discrete or smeared Fixed, multi-directional or rotating? *Heron J.* 1989; 34(1):59.
286. Bažant, Z. P. and Oh, B. H. Crack band theory for fracture of concrete. *Mater. Struct.* 1983; 16:155–177.
287. Bažant, Z. P. Mechanics of distributed cracking. *Appl. Mech. Rev.* (ASCE) 1986; 39(5):675–705.
288. Cervenka, V. Constitutive model for cracked reinforced concrete. *ACI J. Proc.* November–December 1985; 82(6):877–882.
289. Crisfield, M. A. and Wills, J. Analysis of R/C panels using different concrete models. *J. Eng. Mech.* (ASCE) March 1989; 115(EM3):578–597.
290. Barzegar, F. Analysis of RC membrane elements with anisotropic reinforcement. *J. Struct. Eng.* (ASCE) March 1989; 115(3):647–665.
291. Barzegar, F. and Ramaswamy, A. A secant post-cracking model for reinforced concrete with particular emphasis on tension stiffening. *Proc. 2nd Int. Conf. Computer Aided Analysis and Design of Concrete Structures*, Zell-am-See, April 1990; pp. 1001–1016.
292. De Borst, R. and Nauta, P., Non-orthogonal cracks in a smeared finite element model. *Eng. Comput.* 1985; 2:354–46.
293. Cervenka, V. *Constitutive Model for Cracked Reinforced Concrete Under General Load Histories*. CEB, March 1987; pp. 157–167 (Bulletin d'Information 178/179).
294. Vecchio, F. J. and Collins, M. P. The modified compression-field theory for reinforced concrete elements subjected to shear. *ACI J. Proc.* March–April 1986; 83(2):219–231.
295. Kolmar, W. *Beschreibung der Kraftübertragung über Risse in nichtlinearen Finite Elemente Berechnungen von Stahlbetontragwerken*. Technische Hochschule Darmstadt, December 1986; p. 193.
296. Gupta, A. K. and Akbar, H. Cracking in reinforced concrete analysis. *J. Struct. Eng.* (ASCE) August 1984; 110(8):1735–1746.
297. Balakrishnan, S. and Murray, D. W. Prediction of R/C panel and deep beam behaviour by NLFEA. *J. Struct. Eng.* (ASCE) October 1988, 114(10):2323–2342.
298. Hu, H.-T. and Schnobrich, W. C. Nonlinear analysis of cracked reinforced concrete. *ACI Struct. J. Proc.* March–April 1990; 87(2):199–207.
299. Btroud, A. H. *Approximate Calculation of Multiple Integrals*. Prentice Hall, Englewood Cliffs, NJ, 1971.
300. Bežant, Z. P. Parallel viscous element and damage element coupling as a model for rate effect in concrete fracture. Note privately communicated to M. Jirasek, S. Beissel and J. Ožbolt, June, 1991.

www.EngineeringBooksPDF.com

301. De Borst, R. Continuum models for discontinuous media. *Proc. Int. Conf. Fracture Processes Brittle Disordered Materials*, Noordwijk, The Netherlands, 1991; p. 18.
302. Bažant, Z. P. (T. A. Jaeger (ed.). Numerically stable algorithm with increasing time steps for integral-type aging creep. *First Int. Conf. Struct. Mech. Reactor Technol.*, West Berlin, Part H, 1971; Vol. 4, p. 17.
303. Bažant, Z. P. and Chern, J. C. Strain softening with creep and exponential algorithm. *J. Eng. Mech.* (ASCE) 1985; 113(3):381–390.
304. Puaudier-Cabot, G. and Bažant, Z. P. Nonlocal damage theory. *J. Eng. Mech.* (ASCE) 1987; 113:1512–1533.
305. Sinha, B. P. et al. Stress-strain relations for concrete under cyclic loading. *J. Am. Concr. Inst.* 1964; 61(2):195–211.
306. Reinhardt, H. W. and Cornelissen, H. A. W. Post-peak cyclic behavior of concrete in uniaxial tensile and alternating tensile and compressive loading. *Cement Concr. Res.* 1984; 14:263–278.
307. Eligehausen, R. and Ožbolt, J. Size effect in concrete structures. *RILEM-CEB Workshop on Application of Fracture Mechanics in Concrete*, Turin, 1990; p. 38.
308. Ožbolt, J. and Bažant, Z. P. Microplane model for cyclic triaxial behavior of concrete. *J. Eng. Mech.* (ASCE) 1992; 118(7):1365–1386.
309. Hillerborg, A., et al. Analysis of crack formation and crack growth in concrete by means of fracture mechanics and finite elements. *Cement Concr. Res.* 1976; 6:773–782.
310. Duda, H. *Bruchmechanische Verhalten von Beton unter monotoner und zyklischer Zugbeanspruchung*. Thesis, T. H. Darmstadt, 1990.
311. Petersson, P. E. *Crack Growth and Development of Fracture Zones in Plain Concrete and Similar Materials*. Report TVBM-1006, Thesis, Division of Building Materials, University of Lund, Sweden, 1981.
312. Gustafsson, P. J. Fracture mechanics studies of nonyielding materials like concrete. *Report TVBM-1007*, Thesis, Division of Building Materials, University of Lund, Sweden, 1985.
313. Gopalaratnam, V. S. and Shah, S. P. Softening response of plain concrete in direct tension. *ACI J.* 1985; 82(27):310–323.
314. Cornelissen, H. A., W. et al. Experiments and theory for the application of fracture mechanics to normal and lightweight concrete. *Fracture Toughness and Fracture Energy of Concrete* (Wittmann, F. H. ed.). Elsevier, Amsterdam, 1986; pp. 565–575.
315. Rots, J. G., et al. Smeared crack approach and fracture localization in concrete. *Heron J.* Delft, 1985; 30(1):1–48.
316. Gylltoft, K. Fracture mechanics model for fatigue in concrete. *RILEM Mater. Struct.* 1984; 17(97):55–58.
317. Reinhardt, H. W., et al. Tensile tests and failure analysis of concrete. *J. Struct Eng.* (ASCE) 1986; 1112(11):2462–2477.
318. Yankelevsky, D. Z. and Reinhardt, H. W. Uniaxial behaviour of concrete in cyclic tension. *J. Struct. Eng.* (ASCE) 1989; 115(1):166–182.
319. Suzuki, T., Kimura, M., Aburakawa, M., and Ogata, T. Elasto-plastic behaviors of concrete-filled square steel tubular columns and their connections with beams – tension-type connections with long through bolts (in Japanese). *Trans. Architect. Inst. Japan*, December 1985; 358:63–70.
320. Suzuki, T., Kimura, M., Ogawa, T., and Itoh, H. Elasto-plastic behaviors of concrete filled square steel tubular columns and their connections with beams – outstanding diaphragm connections (in Japanese). *Trans. Architect. Inst. Japan* 1986; 359:93–101.
321. Suzuki, T., Kimura, M., Ogawa, T., and Itoh, H., Elasto-plastic behaviors of concrete filled square steel tubular columns and their connections with beams – outstanding diaphragm connections (in Japanese). *Trans. Architect. Inst. Japan* December 1986; 358:63–70.
322. Swann, R. A. *Flexural Strength of Corners of Reinforced Concrete Portal Frames*. Report in TRA 434, Cement and Concrete Association, London, U.K., 1969.

www.EngineeringBooksPDF.com

323. Swartz, S. E., et al. *Structural Bending Properties of High Strength Concrete*. ACI Spec Publication SP-87, American Concrete Institute, Detroit, 1985; pp. 147–178.
324. Tan, K. H. *Ultimate Strength of Reinforced Concrete Beams with Rectangular Openings under Bending and Shear*. Thesis, National University of Singapore, 1982.
325. Tanaka, H., et al. Anchorage of transverse reinforcement in rectangular reinforced concrete columns in seismic design. *Bull. NZ Soc. Earthquake Eng*. June 1985; 18(2):165–190.
326. Taylor, H. P. J. *Shear stresses in RC Beams without Shear Reinforcement*. Technic Report TRA 407, Cement and Concrete Association, London, February 1968; 23 pp.
327. Terzaghi, K. *Coefficients of Subgrade Reactions*. Geotechnique, London, December 1955.
328. Thurlimann, B. Grob, J., and Luchinger, P. *Torsion, beigung und schub in stahlbeton-tregern (torsion, flexure and shear in reinforced concrete girders)*. Institute of Structural Engineering, ETH Zurich, Switzerland, 1975; 170 pp.
329. Thurlimann, B. and Luchinger, P. Steifigkeit von gerissenen stahlbetonbalken unter torsion und biegung (stiffness of cracked reinforced concrete beams subjected to torsion and flexure). *Beton und Stahlbetonbau*, June 1973; 68(6):146–152.
330. Thurlimann, B., Marti, P., Pralong, J., Ritz, P., and Zimmerli, B. *Anwendung der plastizitåtstheorie auf stahlbeton (application of the theory of plasticity to reinforced concrete)*. Institute of Structural Engineering, ETH Zurich, Switzerland, 1983; 252 pp.
331. Timoshenko, S. *Strength of Materials*. Van Nostrand Co., New York, 1965.
332. Tomii, M. Bond check for concrete-filled steel tubular columns, *Proc. U.S. Japan Joint Sem. Composite Mixed Construct*., Washington, DC, July 1984; pp. 195–204.
333. Concrete filled steel tube structures. *Proc. Natl. Conf. Plan. Design Tall Buildings*, ASCE-IABSE, Tokyo, Japan, August; pp. 55–72.
334. Tomii, M. and Sakino, K. Experimental studies on the ultimate moment of concrete filled square steel tubular beam-columns. *Trans. Architect. Inst. Japan* January 1979; 275:55–63.
335. Tomii, M. and Sakino, K. Elasto-plastic behavior of concrete filled square steel tubular beam-columns. *Trans. Architect. Inst. Japan* June 1979; 280:111–120.
336. Tomii, M. and Sakino, K. Experimental studies on concrete filled square steel tubular beam-columns subjected to monotonic shearing force and constant axial force. *Trans. Architect. Inst. Japan* July 1979; 281:81–90.
337. Tomii, M., Sakino, K., and Kiyohara, K. Experimental studies on plain concrete columns subjected to monotonic shearing force and constant axial force. *Trans. Architect. Inst. Japan* September 1981; 307:46–55.
338. Tomii, M., Sakino, K., Watanabe, K., and Xiao, Y. Lateral load capacity of reinforced concrete short columns confined by steel tube – experimental results of preliminary research. *Proc. Int. Specialty Conf. Concr. Filled Steel Tubular Struct*., Harbin, China, August 1985; pp. 19–26.
339. Tomii, M., Sakin, K., Xiao, Y. and Watanabe, K., Earthquake – resisting hysteretic behavior of reinforced concrete short columns confined by steel tube-experimental results of preliminary research. *Proc. Int. Specialty Conf. Concrete Filled Steel Tubular Struct*., Harbin, China, August 1985; pp. 119–125.
340. Tomii, M., Yoshimura, K. and Morishita, Y. Experimental studies on concrete filled steel tubular stub columns under concentric loading. *Proc. Int. Colloquium Stability Struct. Under Stat. Dyn. Loads*, SSRC/ASCE, Washington, DC, March 1977; pp. 718–741.
341. Tomii, M., Yoshimura, K. and Morishita, Y. A method of improving bond strength between steel tube and concrete core cast in circular steel tubular columns. *Transactions Japan Concrete Institute* 1980; 2:319–326.
342. Tomii, M., Yoshimura, K. and Morishita, Y. A method of improving bond strength between steel tube and concrete core cast in square and octagonal steel tubular columns. *Transactions Japan Concrete Institute* 1980; 2:327–334.

www.EngineeringBooksPDF.com

343. Trost, H. The calculation of deflections of reinforced concrete members – a rational approach, designing for creep and shrinkage in concrete structures. *ACI* Special Publication SP-76, American Concrete Institute, Detroit, 1982; pp. 89–108.
344. UBC. Uniform building code (chapter 23, section 2312: earthquake regulations). *International Conference of Building Officials*, Whittier, CA, 1982.
345. Constantinou, M. C., Soong, T. T., and Dargush, G. F. *Passive Energy Dissipation Systems for Structural Design and Retrofit*. MCEER-State University of New York at Buffalo, 1998.
346. SEAONC, Structural Engineers Association of Northern California. *Tentative Seismic Design Requirements for Passive Energy Dissipation Systems*, San Francisco, CA, 1993.
347. Paulay, T. and Priestly, M. J. N. *Seismic Design of Reinforced Concrete and Masonry Buildings*. Wiley, New York, 1992.
348. Aiken, I. D. and Kelly, J. M. *Earthquake Simulator Testing and Analytical Studies of Two Energy-Absorbing Systems for Multistory Structures*. Technical Report UCB/EERC-90/03, University of California at Berkeley, 1990.
349. Whitaker, A. S., Bertero, V., Alonso, J., and Thompson, C. *Earthquake Simulator Testing of Steel Plate Added Damping and Stiffness Elements*. Technical Report EERC-89/02, University of California at Berkeley, 1990.
350. Lobo, R. F., Shen, J. M., Reinhorn, K. L., and Soong, T. T. *Inelastic Response of Reinforced Concrete Structures with Viscoelastic Braces*. Technical Report NCEEC-0006, National Center for Earthquake Engineering Research, Buffalo, NY, 1993.
351. Reinhorn, K. L., Li, C., and Constantinou, M. C. Experimental and Analytical Investigation of Seismic Retrofit of Structures with Supplemental Damping. Technical Report NCEEC-95-0001, National Center for Earthquake Engineering Research, Buffalo, NY, 1995.
352. Dolce M. Passive control of structure. *Proc. 10th Euro. Conf. Earthquake Eng.*, Vienna, 1994.
353. Housner, G. W., et al. Structural control: past, present and future. *J. Eng. Mech.* (ASCE) 1998; 123(9):897–971.
354. Duerig, T. W., Melton, K. N., Stoeckel, D., and Wayman, C. M. (eds.). *Engineering Aspects of Shape Memory Alloys*. Butterworth-Heinemann Ltd., London, 1990.
355. Whittaker, A. S., Krumme, R. C., and Hayes, J. R. *Structural Control of Building Response Using Shape Memory Alloys*. Report No. 95/22, Headquarters US Army Corps of Engineers, Washington, DC, USA, 1995.
356. Graesser, E. J. and Cozzarelli, F. A. Shape memory alloys as new materials for aseismic isolation. *J. Eng. Mech.* (ASCE) 1991; 117:2590–2608.
357. Hodgson, D. E. and Krumme, R. C. Damping in structural applications. *Proc. 1st Int. Conf. Shape Memory Superelastic Technol.*, Pacific Grove, CA, USA, 1994.
358. Dolce, M. and Cardone, D. Mechanical behavior of SMA elements for seismic applications – Part 1 Martensite and austenite NiTi bars subjected to torsion. *Int. J. Mech. Sci.* 2001; 43(11):2631–2656.
359. Dolce, M. and Cardone, D. Mechanical behavior of SMA elements for seismic applications – Part 2 Austenite NiTi wires subjected to tension. *Int. J. Mech. Sci.* 2001; 43(11):2657–2677.
360. Various Authors. *Brite-Euram MANSIDE Project – Workshop Proceedings*, National Seismic Survey, Rome, Italy, 1999.
361. Dolce, M., Cardone, D., and Mametto, R. Implementation and testing of passive control devices based on shape memory alloys. *Earthquake Eng. Struct. Dyn.* 2000; 29(7):945–968.
362. Cardone, D., Coelho, E., Dolce, M., and Ponzo, F. Experimental behavior of RC frames retrofitted with dissipating and re-centering braces. *J. Earthquake Eng.* 2004; 8(3):361–396.
363. CEN, European Committee for Standardisation. Eurocode 8: *Design Provision for Earthquake Resistance of Structures*. Part 1.1: General Rules, Seismic Actions and Rules for Buildings, ENV, 1998-1-1.

www.EngineeringBooksPDF.com

364. CEN, European Committee for Standardisation. Eurocode 2: *Design of Concrete Structures*. Part 1-1: General Rules and Rules for Building, ENV, 1992-1-1.
365. Woo, K., El Atter, A., and White, R. N. *Small-Scale Modeling Techniques for Reinforced Concrete Structures Subjected to Seismic Loads*. Technical Report No. NCRRR 88-0041, State University of New York at Buffalo, 1988.
366. Dolce, M., Cardone, D., and Nigro, D. Experimental tests on seismic devices based on shape memory alloys. *Proc. 12th World Conf. Earthquake Eng*., Auckland, New Zealand, 30 Jan.–4 Feb. 2000.
367. Braga, F. and D'anzi P. Steel braces with energy absorbing devices: a design method to retrofit reinforced concrete existing buildings. *Strengthening and Repair of Structures in Seismic Areas*. Ouest Editions Presses Academiques, Nice, 1991; pp. 146–154.
368. Prakash, V., Powell, G. H., and Campbell, S. DRAIN-3DX: base program description and user guide-version 1.10. Report No. UCB/SEMM-94/07. Department of Civil Engineering, University of California at Berkeley, CA, 1994.
369. Cardone, D. and Dolce, M. Dynamic behavior of R/C frame equipped with seismic devices based on shape memory alloys. *Ingegneria Sismica* (Patron editore) 1999; 3:16–35 (in Italian).
370. Chopra, A. K. *Dynamics of Structures*. Prentice-Hall, London, 1995; p. 729.
371. FEMA356. *Prestandard and Commentary for the Seismic Rehabilitation of Buildings*. Federal Emergency Management Agency, Washington DC, 2000.
372. Akton, A. E., Bertero, V. V., Chowohury, A. A., and Nagashima, T. *Experimental and Analytical Predictions of the Mechanical Characteristics of a 1/5-Scale Model of a 7-Story R/C Frame-Wall Building Structure*. Report UCB/EERC No. 83/13, University of California, Berkeley, 1983.
373. Stafford Smith, B. Methods or predicting the lateral stiffness and strength of multi-story infilled frames. *Building Science*. Pergamon Press, Oxford, UK, 1967: Vol. 2, pp. 247–257.
374. Klinger, R. E. and Bertero, V. V. Earthquake resistance of infilled frames. *J. Struct. Div*. 1978; 104(ST6):973–989.
375. Mainstone, R. J. and Weeks, G. A. The influence of bounding frame on the racking stiffness and strength of brick walls. *Proc. 2nd Int. Brick Masonry Conf*., Stoke on Trent, UK, 1970; pp. 165–171.
376. Ministero dei Lavori Pubblici. Norme tecniche per la progettazione, esecuzione e collaudo degli edifici in muratura e per il loro consolidamento. D.M.LL.PP. del 20/11/1987.
377. Applied Technology Council. *NEHRP Guidelines for the Seismic Rehabilitation of Buildings*, Ballot Version (ATC-33). Washington, DC, P[Building Seismic Safety Council] 1996 (FEMA 273-274), 400/A665/ no. 33/ 1996/ Ref.
378. Elnashai, A. S., et al. Experimental and Analytical Investigations into the Seismic Behavior of Semi-Rigid Steel Frames. Department of Civil Engineering, Imperial College of Science and Technology and Medicine, London, 1996; 209p. (ESEE no. 96-7), 400/E83/96-7.
379. Kramer, S. L. *Geotechnical Earthquake Engineering*. Prentice Hall, Upper Saddle River, NJ, 1996; 653p. 400/K72/1996.
380. Erberik, M. A. and Haluk, S. *Influence of Earthquake Ground Motion Characteristics on Structural Damage and Seismic Response Reduction*. Earthquake Engineering Research Center, Middle East Technology University, Ankara, Turkey, 1996; 117 Ivs. (METU/EERC 96-04). 400/M53/96-04.
381. Tsai, K. C. and Wu, S. *Behavior and Design of Seismic Moment Resisting Beam-Column Joints*. Center for Earthquake Engineering Research, National Taiwan University, Taipei, 1993; 120p. (CEER 82-10). 400/N27/82-10.
382. Pressure Vessels and Piping Division, ASME, Chung, H. H., and Saleem, M. A. (eds.). Seismic, Shock and Vibration Isolation, 1996: presented at the 11996 *ASME Pressure Vessels and Piping Conference*, Montreal, Quebec, Canada, Jull 21–26, 1996; 139p. (PVP Vol. 341). 480/S437/1996.

www.EngineeringBooksPDF.com

383. Hamada, M. and O'Rourke, T. *Proc. 6th Japan-US Workshop Earthquake Resistant Design Lifeline Facilities and Countermeasures against Soil Liquefaction*, Waseda University, Tokyo, Japan, Jun. 11–13, 1996. National Center for Earthquake Engineering Research, Buffalo, NY, 1996; 754p. (NCEER-96-0012). 500/N24/96-12.
384. Cheok, G. S. and Stone, W. C. *Performance of 1/3-Scale Model Precast Concrete Beam-Column Connections Subjected to Cyclic Inelastic Loads* (Report no. 4). US Department of Commerce, National Institute of Standards and Technology, Gaithersburg, MD, June 1994; 59p. (NISTIR 5436). 500/N57/5436.
385. Kelly, J. M. *Earthquake-Resistant Design with Rubber*, 2nd edn. Springer, London, New York, 1997; 243p. 525/K45/1997.
386. Stewart, J. P. *An Empirical Assessment of Soil Structure Interaction Effects on the Seismic Response of Structures*. PhD thesis, University of California, Berkeley, California, 1996; 210p. 535/S748/1996.
387. Structural Engineers Association of Northern California. *Current Design Issues in Structural Engineering Practice*, 1996 Fall Seminar, November 6, 13, & 20. The Association, San Francisco, 1996; 1v. 600/C877/1996.
388. Han, S. *Wave Propagation in Discontinuous Rock Mass*. Department of Geotechnical Engineering, Nagoya University, Nagoya, Japan, 1989; 122p. 305.4/H26/1989.
389. Applied Technology Council. *ATC TechBrief*. The Council, Redwood City, California, 1996; 400/A6654.
390. Applied Technology Council. *Case Studies in Rapid Postearthquake Safety Evaluation of Buildings*. The Council, Redwood City, California. 1996; 295p. (ATC 20-3). 400/A665/20-3.
391. Diaz, R. F. C. *Hidrologia Para Ingenieros*. Pontificia University, Catolica del Peru, Fondo Editorial, Lima, 1994; 396p. 400/C52/1994.
392. US National Science Foundations; Polish Academy of Sciences. *Civil Infrastructure Systems Research for the Next Century: A Global Partnership in Research*. Strata Mechanics Research Institute of the Polish Academy of Sciences (PAS), Cracow, Poland, October 2–4, 1996. Washington, DC, NSF, 1996; 253p.
393. Challenges Associated with Existing Facilities, February 12–15, 1997, Austin Texas. EERI, Oakland, California, 1997; 1v. 400/E27/1997.
394. Assessment of Earthquake Engineering Research and Testing Capabilities in the United States. Earthquake Engineering Research Institute, Oakland, California, 1995. (Publication no. WP-01A). 400/E275/WP-01A.
395. Hu, Y.-X. and Dong, W. *Earthquake Engineering*. Spon, London, 1996; 410p. 400/H8/1996.
396. Ishihara, K. (ed.). Earthquake geotechnical engineering. *Proc. IS-Tokyo '95/the 1st Int. Conf. Earthquake Geotech. Eng.*, Tokyo, 4–16 November 1995. A.A. Balkema, Rotterdam, 1995; 3v. 400/I5657/1995.
397. Unjoh, S., et al. *Proc. 4th US–Japan Workshop Earthquake Protect. Syst. Bridges*, December 9 and 10, 1996. Public Works Research Institute, Tsukuba Science City, Japan, 1996; 349p. (Technical memorandum of PWRI; no. 3480). 400/J191/3196.
398. Vance, V. L. and Smith, H. A. *Effects of Architectural Walls on Buildings Response to Ambient and Seismic Excitations*. The John A. Blume Earthquake Engineering Center, Stanford, California, 1996; 206p. (Report no. 117). 400/J54/no. 117.
399. Basoz, N. and Kiremidjian, A. S. *Risk Assessment for Highway Transportation Systems*. The John A. Blume Earthquake Engineering Center, Stanford, California, 1996; 257p. (Report no. 118). 400/J54/no. 118.
400. Ozkan, G. and Mengi, Y. A *Boundary Element Method for Axisymmetric Elastodynamic Analysis*. Middle East Technical University, Earthquake Engineering Research Center, Ankara, Turkey, 1996; 131p. (METU/ EERC 96-05). 400/M53/95-05.
401. Budnitz, R. J., Apostolakis, G., Boore, D. M., Cluff, L. S., Coppersmithm, K. J., Cornell, C. A., and Morris, P. A. *Recommendations for Probabilistic Seismic Hazard Analysis: Guidance on Uncertainty and Use of Experts*. US Nuclear Regulatory Comm'n., Washington, DC, 1997; 2v. (NUREG/CR-6372). 400/N87/CR-6372.

www.EngineeringBooksPDF.com

402. Bardet, J. P., et al. *North American-Japan Workshop on the Geotechnical Aspects of the Kobe, Loma Prieta, and Northridge Earthquakes*, Osaka, Japan, 22–24 January 1996. California, Department of Civil Engineering, Los Angeles, 1997; 126p.
403. Ellingwood, B., et al. *Reliability-Based Condition Assessment of Steel Containment and Liners*. US Nuclear Regulatory Comm'n., Washington, DC, 1996; 96p. (NUREG/CR-5442). 400/N87/CR-5442.
404. Talwani, P., Kellog, J. N., and Trenkamp, R. *Validation of Tectonic Models for an Intraplate Seismic Zone, Charleston, South Carolina with GPS Geodetic Data*. US Nuclear Regulatory Comm'n., Washington, DC, 1997; 41p. (NUREG/CR-6529). 400/N87/CR-6529.
405. ASME, Ma, D. C., et al. *Pressure Vessels and Piping Division, Seismic Engineering, 1995*: presented at the 1995 Joint ASME/JSME Pressure Vessels and Piping Conference, Honolulu, Hawaii, July 23–27, 1995. American Society of Mechanical Engineers, New York, 1995; 462p. (PVP vol. 312). 400/ S43/1995.
406. Tajima, K. and Kawashima, K. *Modification of Acceleration, Velocity and Displacement Response Spectra in terms of Damping Ratio*. Tokyo Institute of Technology, Tokyo, 1996; 137p. (TIT/EERG 96-3).
407. Chen, I.-H., et al. *Summary Report on Semi-Active Base Isolation Control*. Department of Civil Engineering, University of Michigan, Ann Arbor, Michigan, 1994; 1v. (UMCEE 94-38) 400/U423/94-38.
408. Lafave, J. M. and Wight, J. K. *Behavior of Reinforced Concrete Exterior Wide Beam-Column-Slab Connections Subjected to Lateral Earthquake Loading*. Department of Civil Engineering, University of Michigan, Ann Arbor, Michigan, 1997; 173p. (UMCEE 97-01) 400/U423/97-01.
409. Rai, D. C. and Goel, S. C. *Seismic Evaluation and Upgrading of Existing Steel Concentric Braced Structures*. Department of Civil Engineering, University of Michigan, Ann Arbor, Michigan, 1997; 99lvs. (Report UMCEE 97-03) 400/U423/97-03.
410. Sato, Y., et al. *Strong-Motion Earthquake Records on the 1994 Hokkaido-Toho-Oki Earthquake in Port Areas*. Port and Harbour Research Institute, Nagase, Yokosuka, Japan, 1996; 341p. (Technical note of the Port and Harbour Research Institute, Ministry of Transport, Japan, no. 853).
411. Huang, M. J. (ed.). *Proc. SMIP97 Seminar on Utilization for Strong-Motion Data, Los Angeles*, California, May 8 1997. California Division of Mines and Geology, Sacramento, California, 1997; 127p. (415.1/S45/1997).
412. Duval, A.-M. *Détermination de la réponse d'un site aux seismes a l'aide du bruit de fond: Evaluation Experimental*. Laboratoire central des ponts et chausses, Paris, 1996; 264p.
413. Terzaghi, K., et al. *Soil Mechanics in Engineering Practise*, 3rd edn. Wiley, New York, 1996; 549p. (465/T45/1996).
414. Guha, S. *Dynamic Characteristics of the Deep Old Bay Clay Deposits in the East San Francisco Bay Area*. University Microfilms International, Ann Arbor, Michigan, 1996; 259p.
415. ASME, Chung, H. H., and Saleem, M. A. (eds.). *Seismic, Shock and Vibration Isolation*, 1996: presented at the 1996 ASME Pressure Vessels and Piping Conference, Montreal, Quebec, Canada, July 21–26, 1996. American Society of Mechanical Engineers, New York, 1996; 139p. (PVP vol. 341) 480/S437/1996.
416. Fang, H.-Y. *Foundation Engineering Handbook*, 2nd edn. Chapman & Hall, New York, 1991; 923p. (485/F688/1991).
417. Szczesiak, T. Die Komplemetarmethode: ein neus Verfahren in der dynamishen Boden-Struktur-Interaktion. Birkhauser Verlag, Basel, Boston, 1996; 30p. (500/E35/224).
418. Kratzig, W. B. and Niemann, H. *Dynamics of Civil Engineering Structures*. A.A. Balkema, Rotterdam, Brookfield, 1996; 630p.
419. Rodriguez, M. and Calistrillon, E. *Manual de evaluacion postsismical dela seguridad structural de edificiones*. Inst. de Ingenieria, UNAM, Cayoacan, Mexico, 1995; 57p. (Series del Inst. de Ingenieria no. 569).

www.EngineeringBooksPDF.com

420. Reinhorn, A. M., et al. *Modeling of Masonry Infill Panels for Structural Analysis*. National Center for Earthquake Engineering Research, Buffalo, NY, 1995; 1v. (NCEER 95-0018). 500/N24/95-18.
421. Roa, R. S., et al. *Retrofit of Nonductile Reinforced Concrete Frames Using Friction Dampers*. National Center for Earthquake Engineering Research, Buffalo, NY, 1995; 1 v. (NCEER 95-0020).
422. Mylonakis, G., et al. *Parametric Results for Seismic Response of Pile-Supported Bridge Bents*. National Center for Earthquake Engineering Research, Buffalo, NY, 1995; 1 v. (NCEER 95-0021).
423. Costley, A. C. and Abrams, D. P. *Dynamic Response of Unreinforced Masonry Buildings with Flexible Diaphragms*. National Center for Earthquake Engineering Research, State University of New York, Buffalo, NY, 1996; 1 v. (NCEER-96-0001) 500/N24/96-01.
424. Seligson, H. A., et al. *Chemical Hazards, Mitigation and Preparedness in Areas of High Seismic Risk: A Methodology for Estimating the Risk of Post-Earthquake Hazardous Materials Release*. National Center for Earthquake Engineering Research, Buffalo, NY, 1996; 1v. (Technical report NCEER 96-0013) 500/N24/96-13.
425. Mander, J. B., et al. *Response of Steel Bridge Bearings to Reversed Cyclic Loading*. National Center for Earthquake Engineering Research, Buffalo, NY, 1994; 193p. (Technical report NCEER-96-0014).
426. Youd, T. L. and Beckam, C. J. *Highway Culvert Performance During Past Earthquakes*. National Center for Earthquake Engineering, Buffalo, NY, 1996; 94p. (Technical report NCEER-96-0015).
427. Bradfor, M. A. and Wright, H. D. *Short and Long-Term Behavior of Axially Loaded Composite Profiled Walls*. University of New South Wales, Sydney, 1996; 20p. (UNICIV report no. R-359).
428. Shenton, H. W., III. *Guidelines for Prequalification, Prototype and Quality Control Testing of Seismic Isolation Systems*. National Institute of Science and Technology, Boulder, CO, 1996; 136p. (NISTIR 5800).
429. Detwiler, R. J., Bhatty, J. I., and Bhattacharja, S. *Supplementary Cementing Materials for Use in Blended Cements*. Portland Cement Ass'n., Skokie, III, 1996; 96p. (Research and Development Bulletin RD112T).
430. Burg, R. G. *The Influence of Casting and Curing Temperature on the Properties of Fresh and Hardened Concrete*. Portland Cement Ass'n., Skokie, III, 1996; 13p. (Research and Development Bulletin RD113T).
431. Stark, D. *The Use of Recycled-Concrete Aggregate from Concrete Exhibiting Alkali-Silica Reactivity*. Portland Cement Ass'n., Skokie, III, 1996; 14p. (Research and Development Bulletin RD114).
432. Gajda, J. *Development of a Cement to Inhibit Alkali-Silica Reactivity*. Portland Cement Ass'n., Skokie, III, 1996; 53p. (Research and development bulletin RD115T).
433. Duan, M.-Z. and Chen, W.-F. *Proposed Design Guidelines for Construction Code Requirements of Concrete Buildings*. School of Civil Engineering, Purdue University, West Lafayette, IN, 1996; 60 lvs. (CE-STR-96-16).
434. Budek, A., Benzoni, G., and Priestly, M. J. N. *An Analytical Study of the Inelastic Seismic Response of Reinforced Concrete Pile-Columns in Cohesionless Soil*. Structural Systems Research Project, University of California, San Diego, La Jolla, California, 1995; 174p. (SSRP-95/13).
435. Seible, F. *Structural Response Assessment of Soil Nail Wall Facings: Executive Summary of Experimental and Analytical Investigations*. Structural Systems Research Project, University of California, San Diego, La Jolla, California, 1996; 44 lvs. (Report; SSRP-96/01).
436. Benzoni, G., et al. *Seismic Performance of Circular Reinforced Concrete Columns Under Varying Axial Load*. Structural Systems Research Project, University of California, San Diego, La Jolla, California, 1996; 174p. (SSRP-96/04).

www.EngineeringBooksPDF.com

437. Nagdi, K. *Rubber as and Engineering Material: Guideline for Users*. Hanser Publishers, Munich, New York, 1993; 302p.
438. Technical Committee of Nordic Concrete Research Meeting 1996. *Proc. Nordic Concrete Res. Meeting*, Espoo, Finland, 1996. Norsk Betongforening, Oslo, 1996; 340p.
439. Helmuth, R. A. and Wes, P. B. *Reappraisal of the Autoclave Expansion Test*. Construction Technology Laboratories, Portland Cement Ass'n., Skokie, I11, 1996; 44p. (PCA R & D serial no. 1955).
440. Sozen, M. A. and Moehle, J. P. *A Study of Experimental Data on Development and Lap-Splice Lengths for Deformed Reinforcing Bars in Concrete*. The S&M Partnership, Urbana, I11, 1990; 109 lvs.
441. Comit E. Euro-international Du B. Eton. *RC Elements Under Cyclic Loading: State of the Art Report*. American Society of Civil Engineers, Publications Sales Department [distributor], New York; T. Telford, London, UK, 1996; 190p.
442. Comit E. Euro-international Du B. Eton. *RC Frames Under Earthquake Loading State of the Art Report*. American Society of Civil Engineers, New York; T. Telford, London, UK, 1996; 303p.
443. NOAA, National Geophysical Data Center. *The Behavior of Columns During Earthquakes*. The Center, Boulder, CO, 1996.

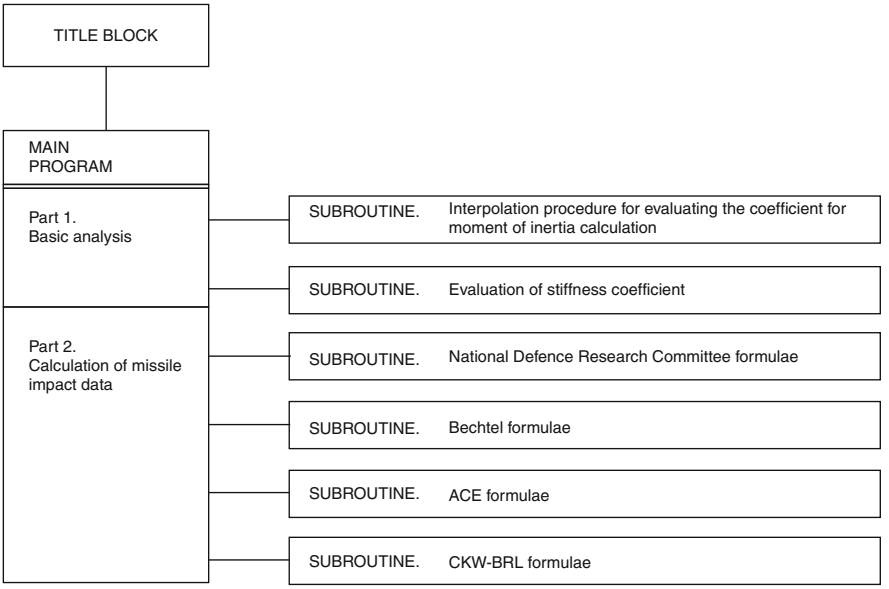
www.EngineeringBooksPDF.com

www.EngineeringBooksPDF.com

Appendix A
Subroutines for Program ISOPAR and Program F-Bang

Program Structural Layout

Andrew Watson main programmer (supervised by M.Y.H. Bangash)



www.EngineeringBooksPDF.com

```
      REAL I,B,T,F,D,K,V,P,N,PN,PT,AY,AX,EC,ES,X,Y,Q,Q1,S,ME,MPUA,C
      REAL NTP,KL,NSF,FC,W,DIA,VEL,FCI,KCPFI,WI,DIAI,VELI,PENEI
      REAL PENET,RAT,PERF,SCAB,SSCAB,HSCAB,ACEP,ACPER,CKPEN,CKPER
      WRITE (6,1)
 1    FORMAT (1H/,'Put in your values of B(cm),T(cm),D(cm)'/
     +        1H/,'B (Unit width of slab ,cm)'/
     +        1H/,'T (Overall depth of slab ,cm)'/
     +        1H/,'D (Depth to reinforcing steel ,cm)')
      READ (5,*) B,T,D
      CALL INTN (F)
      I=0.5000*(((B*(T*T*T))/12)+F*B*(D*D*D))
      WRITE (6,2)
 2    FORMAT (1H/,'The average moment of inertia,Ia(cm4/cm) ,is')
      WRITE (6,3) I
 3    FORMAT (1H/,F30.2)
      CALL INT (Q)
      WRITE (6,17)
17    FORMAT (1H/,'Key in the value of Q that corresponds to'/
     +        1H/,'your calculated value of X/Y. This is the '/
     +        1H/,'required Stiffness Coefficient')
      READ (5,*) Q
      WRITE (6,12)
12    FORMAT (1H/,'Put in your values of V,EC(MPa),Y(m)'/
     +        1H/,'V (Poissons Ratio for concrete ,usually 0.17'/
     +        1H/,'EC (Elastic modulus of concrete ,MPa)       '/
     +        1H/,'Y (Length of slab ,m)                       ')
      READ (5,*) V,EC,Y
      K=((12*EC*I)/(((Q*Y*Y)*(1-(V*V)))*1000000000))
      WRITE (6,5)
 5    FORMAT (1H/,'The value of K (MN/mm) is')
      WRITE (6,6) K
 6    FORMAT (1H/, F30.2)
      WRITE (6,7)
 7    FORMAT (1H/,'Input the following data :         '/
     +        1H/,'WD (The Weight Density of the concrete ,Kg/m3)'/
     +        1H/,'T (The overall depth of the slab ,m)'/
     +        1H/,'X (The width of the slab ,m)')
      READ (5,*) WD,T,X
      MPUA=((WD*T)/9.81)
      WRITE (6,8)
8     FORMAT (1H/,'The mass per unit area of the slab is, (Kg.sec2/m3')
      WRITE (6,9) MPUA
9     FORMAT (1H/,F5.1)
      ME=((MPUA*3.142*X*X*9.81)/(6*4*1000))
      WRITE (6,10)
10    FORMAT (1H/,'The effective mass is one sixth of the mass'/
     +        1H/,'within the circular yield pattern.         '/
     +        1H/,'Effective mass is ,N.sec2/mm')
      WRITE (6,11) ME
11    FORMAT (1H/,F4.2)
450   FORMAT(1H/,'Key in the corresponding F value')
      READ (5,*) Y1
      WRITE (6,500)
```

www.EngineeringBooksPDF.com

```
 500  FORMAT (1H/,'Key in the value of PN from the table that is'/
     +       1H/,'just higher than your calculated value of PN')
      READ (5,*) X3
      WRITE (6,550)
 550  FORMAT(1H/,'Key in the corresponding F value')
      READ (5,*) Y2
      WRITE (6,600)
 600  FORMAT (1H/,'Key in your calculated value of PN')
      READ (5,*) X2
      F=((((X2-X1)/(X3-X1))* (Y2-Y1))+Y1)
      WRITE (6,700)
 700  FORMAT(1H/,'The value of F you require is')
      WRITE (6,800) F
 800  FORMAT(1H/,F8.5)
      RETURN
      END
      SUBROUTINE INT (Q)
      WRITE (6,1000)
1000  FORMAT (1H/,'Key in the length,X (m),& width,Y (m) ,of the slab')
      READ (5,*) X,Y
      Q1=X/Y
      WRITE (6,1100)
1100  FORMAT (1H/,'You require a Q value that corresponds with this'/
     +       1H/,'calculated value of X/Y')
      WRITE (6,1200) Q1
1200  FORMAT (1H/,F4.2)
      WRITE (6,1300)
1300  FORMAT (1H/,'The table you use is dependant on support'/
     +       1H/,'conditions at the sides')
      WRITE (6,1400)
1400  FORMAT (1H/,'SIMPLY SUPPORTED ON       FULLY FIXED ON ALL  '/
     +       1H/,'ALL FOUR SIDES            FOUR SIDES'/
     +       1H/,'X/Y VALUES |Q VALUES      X/Y VALUES |Q VALUES'/
     +       1H/,'===========|========      ===========|========'/
     +       1H/,'    1.0    | 0.1391          1.0    | 0.0671 '/
     +       1H/,'    1.1    | 0.1518          1.2    | 0.0776 '/
     +       1H/,'    1.2    | 0.1624          1.4    | 0.0830 '/
     +       1H/,'    1.4    | 0.1781          1.6    | 0.0854 '/
     +       1H/,'    1.6    | 0.1884          1.8    | 0.0864 '/
     +       1H/,'    1.8    | 0.1944          2.0    | 0.0866 '/
     +       1H/,'    2.0    | 0.1981        INFINATE | 0.0871 '/
     +       1H/,'    3.0    | 0.2029                           '/
     +       1H/,'  INFINATE | 0.2031                           ')
      RETURN
      END
      SUBROUTINE NDRC (PENET,PERF,SCAB)
      REAL NSF,KCPFI,FC,W,DIA,VEL,FCI,WI,DIAI,VELI,PENET,PENET,RAT,T
      WRITE (6,1998)
1998  FORMAT (1H/,'Input,T,the overall depth ,mm')
      READ (5,*) T
      WRITE (6,2000)
2000  FORMAT (1H/,'Input the relevant missile shape factor ,NSF'/
     +       1H/,'For flat nosed missiles, NSF=0.72'/
     +       1H/,'For blunt nosed missiles, NSF=0.84'/
```

www.EngineeringBooksPDF.com

```
     +       1H/,'For sperical nosed missiles, NSF=1.00'/
     +       1H/,'For very sharp nosed missiles, NSF=1.14')
      READ (5,*) NSF
      WRITE (6,2100)
2100  FORMAT (1H/,'Input the following :'/
     +       1H/,'FC The ultimate concrete compressive strength,N/mm2'/
     +       1H/,'W (The weight of the missile, N)'/
     +       1H/,'DIA (The circular section diameter, mm)'/
     +       1H/,'VEL (The impact velocity, m/sec)')
      READ (5,*) FC,W,DIA,VEL
      FCI=(FC/0.007)
      KCPFI=(180/SQRT(FCI))
      WI=((2*W)/9)
      DIAI=(DIA/25.4)
      VELI=(VEL/0.3048)
      PENEI=(SQRT((4*KCPFI*NSF*WI*DIAI)*((VELI/(1000*DIAI))**1.8)))
      PENET=(PENEI*25.4)
      RAT=(PENET/DIA)
      IF (RAT.LT.2.0) THEN
      GO TO 2200
      ELSE IF (RAT.GT.2.0) THEN
      GO TO 2400
      END IF
2200  WRITE (6,2300)
2300  FORMAT (1H/,'The missile penetration using the NDRC (National'/
     +       1H/,'Defence Research Committee) Formula for'/
     +       1H/,'''x/d'' less than or equal to 2.0 is ,(mm)')
      WRITE (6,2350) PENET
2350  FORMAT (1H/,F6.1)
      GO TO 2700
2400  PENEI=(((KCPFI*NSF*WI)*((VELI/(1000*DIAI))**1.8))+DIAI)
      PENET=(PENEI*25.4)
      WRITE (6,2450)
2450  FORMAT (1H/, 'The missile penetration using the NDRC (National'/
     +       1H/,'Defence Research Committee) Formula for'/
     +       1H/,'''x/d'' greater than 2.0 is ,(mm)')
      WRITE (6,2470) PENET
2470  FORMAT (1H/,F6.1)
2700  WRITE (6,2710)
2710  FORMAT (1H/,'The ''x/d''ratio is')
      WRITE (6,2720) RAT
2720  FORMAT (1H/,F5.3)
      IF (RAT.LT.1.35) THEN
      GO TO 2800
      ELSE IF (RAT.GT.1.35) THEN
      GO TO 2900
      END IF
2800  PERF=(DIA*((3.19*RAT)-(0.718*RAT*RAT)))
      GO TO 3000
2900  PERF=(DIA*(1.32+(1.24*RAT)))
3000  WRITE (6,3100)
3100  FORMAT (1H/,'The Perforation,calculated using the NDRC, is ,mm')
      WRITE (6,3200) PERF
```

www.EngineeringBooksPDF.com

```
3200  FORMAT (1H/,F5.1)
      IF (PERF.LT.T) THEN
      GO TO 3300
      ELSE IF (PERF.GT.T) THEN
      GO TO 3400
      END IF
3300  WRITE (6,3350)
3350  FORMAT (1H/,'This value is less than the overall depth.The'/
     +       1H/,'slab adequately resists collapse due to perforation')
      GO TO 3500
3400  WRITE (6,3450)
3450  FORMAT (1H/,'This value is greater than the overall depth.The'/
     +       1H/,'slab will collapse due to perforation')
3500  IF (RAT.LT.0.65) THEN
      GO TO 3600
      ELSE IF (RAT.GT.0.65) THEN
      GO TO 3700
      END IF
3600  SCAB=(DIA*((7.91*RAT)-(5.06*RAT*RAT)))
      GO TO 3800
3700  SCAB=(DIA*(2.12+(1.36*RAT)))
3800  WRITE (6,3850)
3850  FORMAT (1H/,'The Scabbing thickness,calculated using NDRC, is ,mm')
      WRITE (6,3860) SCAB
3860  FORMAT (1H/,F5.1)
      IF (SCAB.LT.T) THEN
      GO TO 3900
      ELSE IF (SCAB.GT.T) THEN
      GO TO 4000
      END IF
3900  WRITE (6,3950)
3950  FORMAT (1H/,'This value is less than the overall depth.The'/
     +       1H/,'slab will not collapse due to scabbing')
      GO TO 4100
4000  WRITE (6,4050)
4050  FORMAT (1H/,'This value is greater than the overall depth.The'/
     +       1H/,'slab will collapse due to scabbing')
4100  RETURN
      END
      SUBROUTINE BTEL (SSCAB, HSCAB)
      REAL W,VEL,DIA,FC,FCI,WI,DIAI,VELI,SSCI,HSCI,SSCAB,HSCAB
      WRITE (6,5000).
5000  FORMAT (1H/,'Input the following:'/
     +       1H/,'W (The weight of the missile,N)'/
     +       1H/,'VEL (The impact velocity of the missile,m/sec)'/
     +       1H/,'DIA (The diameter of the missile,mm)'/
     +       1H/,'FC (The concrete compressive strength,N/mm2)')
      READ (5,*) W,VEL,DIA,FC
      FCI=(FC/0.007)
      WI=((2*W)/9)
      DIAI=(DIA/25.4)
      VELI=(VEL/0.3048)
      SSCI=((15.5*(WI**0.4)*(VELI**0.5))/(SQRT(FCI)*(DIAI**0.2)))
      HSCI=((5.42*(WI**0.4)*(VELI**0.65))/(SQRT(FCI)*(DIAI**0.2)))
```

www.EngineeringBooksPDF.com

```
      SSCAB=(SSCI*25.4)
      HSCAB=(HSCI*25.4)
      WRITE (6,5100)
5100  FORMAT (1H/,'Using the BECHTEL formula the slab thickness'/
     +        1H/,'to prevent scabbing from a solid missile is,mm')
      WRITE (6,5200) SSCAB
5200  FORMAT (1H/,F6.1)
      WRITE (6,5300)
5300  FORMAT (1H/,'Using the BECHTEL formula the slab thickness to'/
     +        1H/,'prevent scabbing from a hollow missile is,mm')
      WRITE (6,5400) HSCAB
5400  FORMAT (1H/,F5.1)
      RETURN
      END
      SUBROUTINE ACE (ACEP,ACPER)
      REAL W,DIA,VEL,FC,FCI,DIAI,WI,VELI,ACEPI,APFI,ACEP,ACPER,EPI
      WRITE (6,6000)
6000  FORMAT (1H/,'Input the following:'/
     +        1H/,'W (The weight of the missile,N)'/
     +        1H/,'DIA (The diameter of the missile,mm)'/
     +        1H/,'VEL (The impact velocity of the missile,m/sec)'/
     +        1H/,'FC (The concrete compressive strength,N/mm2)')
      READ (5,*) W,DIA,VEL,FC
      FCI=(FC/0.007)
      WI=((2*W)/9)
      DIAI=(DIA/304.8)
      VELI=(VEL/0.3048)
      ACPI=((282*WI*(DIAI**0.215)*((VELI/1000)**1.5))/(FCI*DIAI**2))
      EPI=(0.5*DIAI)
      ACEPI=(ACPI+EPI)
      APFI=((1.23*DIAI)+(1.07*ACEPI))
      ACEP=(ACEPI*25.4)
      ACPER=(APFI*25.4)
      WRITE (6,6100)
6100  FORMAT (1H/,'The penetration depth using the ACE formula is,mm')
      WRITE (6,6200) ACEP
6200  FORMAT (1H/,F5.1)
      WRITE (6,6300)
6300  FORMAT (1H/,'Thickness to prevent perforation using ACE is,mm')
      WRITE (6,6400) ACPER
6400  FORMAT (1H/,F5.1)
      RETURN
      END
      SUBROUTINE CKW (CKPEN,CKPER)
      REAL W,DIA,VEL,WI,DIAI,VELI,CKPEI,CKPRI,CKPEN,CKPER
      WRITE (6,7000)
7000  FORMAT (1H/,'Input the following:'/
     +        1H/,'W (The weight of the missile,N)'/
     +        1H/,'DIA (The diameter of the missile,mm)'/
     +        1H/,'VEL (The impact velocity of the missile,m/sec)')
      READ (5,*) W,DIA,VEL
      WI=((2*W)/9)
      DIAI=(DIA/25.4)
      VELI=(VEL/0.3048)
```

www.EngineeringBooksPDF.com

```
      CKPEI=((6*WI*(DIAI**0.2)*((VELI/1000)**1.333333))/(DIAI**2))
      CKPRI=(1.3*CKPEI)
      CKPEN=(CKPEI*25.4)
      CKPER=(CKPRI*25.4)
      WRITE (6,7100)
7100  FORMAT (1H/,'The penetration using the CKW-BRL formula is,mm')
      WRITE (6,7200) CKPEN
7200  FORMAT (1H/,F5.1)
      WRITE (6,7300)
7300  FORMAT (1H/,'Thickness to prevent perforation using CKW-BRL,mm')
      WRITE (6,7400) CKPER
7400  FORMAT (1H/,F5.1)
      RETURN
      END
```

Blast Loading Program

```
>LIST10.410
    10 REM ''INITIALIZE PRINTER''
    20 VDU2,1,27,1,64,3
    30 REM ''DISABLE PAPER END DETECTOR''
    40 VDU2,1,27,1,56,3
    50 REM ''SELECT PRINT STYLE 24''
    60 VDU2,1,27,1,33,1,56,3
    70 REM ''SET LEFT MARGIN - 4 SPACES''
    80 VDU2,1,27,1,108,1,4,3
    90 REM ''SET LINE SPACING - 35/216INCHES''
   100 VDU2,1,27,1,51,1,38
   110 PRINT:VDU3:INPUT ''DO YOU REQUIRE PRINT-OUT ON PAPER? ENTER Y FOR Y
ES AND N FOR NO '':A1$:IF A1$=''Y'' THEN VDU2
   120 PRINT ''BLAST LOADING PROGRAM:''
   130 VDU2,1,27,1,33,1,53,3:IF A1$=''Y'' THEN VDU2
   140 PRINT ''BY N.M. ALAM (1987)''
   150 VDU2,1,27,1,106,1,10,3:IF A1$=''Y'' THEN VDU2
   160 PRINT ''------------------------------'':PRINT:GOTO 180
   170 PRINT:VDU3:INPUT ''DO YOU REQUIRE PRINT-OUT ON PAPER? ENTER Y FOR Y
ES AND N FOR NO '';A1$
   180 VDU2,1,27,1,33,1,0,3:VDU2,1,27,1,108,1,8,3:IF A1$=''Y'' THEN VDU2
   190 PRINT ''------------------------------------------------------------
----------'':VDU2:PRINT:VDU2,1,27,1,106,1,18,3
   200 INPUT ''OPERATOR'S NAME'';N$;''RUN NUMBER'';N1:INPUT ''DATE'';N1$
   210 IF A1$=''Y'' THEN VDU2:VDU21:PRINT ''OPERATOR'S NAME: '';N$;TAB(36);''R
UN NUMBER: '';N1;TAB(52);''DATE: '';N1$:VDU6
   220 VDU2,1,27,1,106,1,15,3:IF A1$=''Y'' THEN VDU2
   230 PRINT ''------------------------------------------------------------
----------'': PRINT:IF A1$=''Y'' THEN VDU2
   240 PRINT ''DESIGN OF A WALL, IN A HIGH EXPLOSIVE ENVIRONMENT. THE DESI
GN AIM IS''
   250 PRINT ''TO LIMIT THE DAMAGE RESULTING FROM BLAST LOADS IN CONNECTIO
N WITH AN''
   260 PRINT ''ACCIDENTAL EXPLOSION.''
   270 PRINT:VDU2:PRINT:VDU3:IF A1$=''Y'' THEN VDU2
```

www.EngineeringBooksPDF.com

```
   280 REM DETERMINE THE WORST CASE LOADING ON THE WALL. THE WALL WILL
   290 REM BE LOADED BY BLAST WAVES AND BY THE BUILD-UP OF QUASI-STATIC
   300 REM PRESSURE WITHIN THE ENCLOSED VOLUME.
   310 PRINT ‘‘B L A S T  W A V E  LOADING:’’
   320 VDU2,1,27,1,106,1,20,3:IF A1$=‘‘Y’’ THEN VDU2
   330 PRINT ‘‘------------------------------’’
   340 PRINT
   350 REM LOADING FROM THE BLAST WAVE IS INFLUENCED BY THE CHARGE
   360 REM LOCATION. A CHARGE LOCATED ADJACENT TO A SIDE WALL WILL
   370 REM GIVE A REFLECTION OFF THE SIDE WALL AS WELL AS THE FLOOR
   380 REM AND PRODUCE HIGHER LOADS.
   390 PRINT ‘‘FOR  W O R S T  CASE LOADING A CHARGE REFLECTION FACTOR O
F  2,’’
   400 PRINT ‘‘FROM BOTH FLOOR AND WALL SHOULD BE USED.’’
   410 PRINT
>LIST420,860
   420 VDU2,1,27,1,106,1,15,3
   430 INPUT ‘‘CHARGE REFLECTION FACTOR (WALL) ’’;C1
   440 INPUT ‘‘CHARGE REFLECTION FACTOR (FLOOR)’’;C2
   450 INPUT ‘‘CHARGE WEIGHT (kg of TNT)’’;W
   460 IF A1$=‘‘Y’’ THEN VDU2
   470 VDU21:PRINT ‘‘CHARGE REFLECTION FACTOR (WALL) ? ’’;C1
   480 PRINT ‘‘CHARGE REFLECTION FACTOR (FLOOR)? ’’;C2
   490 PRINT ‘‘CHARGE WEIGHT (kg of TNT)? ’’;W:VDU6
   500 LET W1=C1*C2*W
   510 PRINT
   520 VDU2,1,27,1,106,1,15,3:IF A1$=‘‘Y’’ THEN VDU2
   530 PRINT ‘‘EFFECTIVE CHARGE WEIGHT = ’’;W1;‘‘kg of TNT’’
   540 PRINT:PRINT
   550 PRINT ‘‘*** CALCULATION OF CHARGE STAND OFF ***’’
   560 PRINT
   570 PRINT ‘‘CHARGE STANDOFF IS THE DISTANCE FROM THE WALL BEING DESIGNE
D  TO THE’’
   580 PRINT ‘‘EDGE OF THE HIGH EXPLOSIVE AREA, PLUS THE CHARGE RADIUS.’’
   590 PRINT
   600 VDU2,1,27,1,106,1,15,3
   610 INPUT ‘‘DISTANCE FROM WALL TO EDGE OF HIGH EXPLOSIVE AREA (m)’’;D
   620 INPUT ‘‘SPHERICAL CHARGE RADIUS (m)’’;D1
   630 IF A1$=‘‘Y’’ THEN VDU2
   640 VDU21:PRINT ‘‘DISTANCE FROM WALL TO EDGE OF HIGH EXPLOSIVE AREA (m)
?  ’’;D
   650 PRINT ‘‘SPHERICAL CHARGE RADIUS (m)? ’’;D1:VDU6
   660 LET R=D+D1
   670 PRINT
   680 VDU2,1,27,1,106,1,15,3:IF A1$=‘‘Y’’ THEN VDU2
   690 PRINT ‘‘STANDOFF DISTANCE = ’’;R;‘‘m’’
   700 PRINT:PRINT
   710 PRINT ‘‘*** SCALED STANDOFF DISTANCE ***’’
   720 PRINT
   730 LET R1=R/(W1^(1/3))
   740 LET R7=INT(R1*1000+0.5)/1000
   750 PRINT ‘‘SCALED STANDOFF DISTANCE = ’’;R7;‘‘m/kg’’;
   760 VDU2,1,27,1,83,1,0,3:IF A1$=‘‘Y’’ THEN VDU2
   770 PRINT ‘‘1/3’’:VDU2,1,27,1,84,3:IF A1$=‘‘Y’’ THEN VDU2
```

www.EngineeringBooksPDF.com

```
   780 PRINT
   790 VDU2,1,27,1,106,1,15,3:IF A1$=‘‘Y’’ THEN VDU2
   800 PRINT ‘‘FOR THIS SCALED STANDOFF DISTANCE-REFER TO FIGURE 4 FOR THE
REFLECTED’’
   810 PRINT ‘‘PRESSURE AND REFLECTED IMPULSE VALUES.’’
   820 PRINT
   830 VDU2,1,27,1,106,1,15,3
   840 INPUT ‘‘REFLECTED PRESSURE Pr (kPa) ’’;P
   850 INPUT ‘‘VALUE FOR ir/W∧1/3 (kPa.sec/kg∧1/3) ’’;I
   860 IF A1$=‘‘Y’’ THEN VDU2
>LIST870.1340
   870 VDU21:PRINT ‘‘REFLECTED PRESSURE Pr (kPa)? ’’;P
   880 PRINT ‘‘VALUE FOR ir/W’’;
   890 VDU6:VDU2,1,27,1,83,1,0,3:IF A1$=‘‘Y’’ THEN VDU2
   900 VDU21:PRINT ‘‘1/3’’;
   910 VDU6:VDU2,1,27,1,84,3:IF A1$=‘‘Y’’ THEN VDU2
   920 VDU21:PRINT ‘‘ (kPa.sec/kg’’;
   930 VDU6:VDU2,1,27,1,83,1,0,3:IF A1$=‘‘Y’’ THEN VDU2
   940 VDU21:PRINT ‘‘1/3’’;
   950 VDU6:VDU2,1,27,1,84,3:IF A1$=‘‘Y’’ THEN VDU2
   960 VDU21:PRINT ‘‘)? ’’;I:VDU6
   970 LET I1=W1∧(1/3)∗I
   980 LET I2=INT(I1∗1000+0.5)/1000
   990 PRINT
  1000 VDU2,1,27,1,106,1,15,3:IF A1$=‘‘Y’’ THEN VDU2
  1010 PRINT ‘‘REFLECTED IMPULSE ON WALL ir = ’’;I2;‘‘kPa.sec’’
  1020 PRINT
  1030 PRINT ‘‘BLAST WAVE LOADING IS IDEALIZED AS A TRIANGULAR PULSE WITH
ZERO RISE’’
  1040 PRINT ‘‘TIME.’’
  1050 PRINT
  1060 PRINT ‘‘*** LOAD DURATION ***’’
  1070 PRINT
  1080 LET T=2∗I1/P
  1090 LET T5=INT (T∗1E5+0.5)/1E5
  1100 PRINT ‘‘LOAD DURATION = ’’;T5;‘‘sec’’
  1110 VDU2,1,27,1,51,1,210,3:IF A1$=‘‘Y’’ THEN VDU2
  1120 PRINT:PRINT
  1130 VDU2,1,27,1,51,1,42,3:IF A1$=‘‘Y’’ THEN VDU2
  1140 PRINT ‘‘QUASI-STATIC LOADING:’’
  1150 VDU2,1,27,1,106,1,27,3:IF A1$=‘‘Y’’ THEN VDU2
  1160 PRINT ‘‘------------------------------’’
  1170 PRINT
  1180 PRINT ‘‘*** VOLUME OF ROOM ***’’
  1190 PRINT:VDU3
  1200 INPUT ‘‘LENGTH OF ROOM (m)’’;L
  1210 INPUT ‘‘WIDTH OF ROOM (m)’’;L1
  1220 INPUT ‘‘FLOOR TO CEILING HEIGHT (m)’’;L2
  1230 IF A1$=‘‘Y’’ THEN VDU2
  1240 VDU21:PRINT ‘‘LENGTH OF ROOM (m)? ’’;L
  1250 PRINT ‘‘WIDTH OF ROOM (m)? ’’;L1
  1260 PRINT ‘‘FLOOR TO CEILING HEIGHT (m)? ’’;L2:VDU6
  1270 LET V=L∗L1∗L2
  1280 LET V1=INT(V∗1000+0.5)/1000
```

www.EngineeringBooksPDF.com

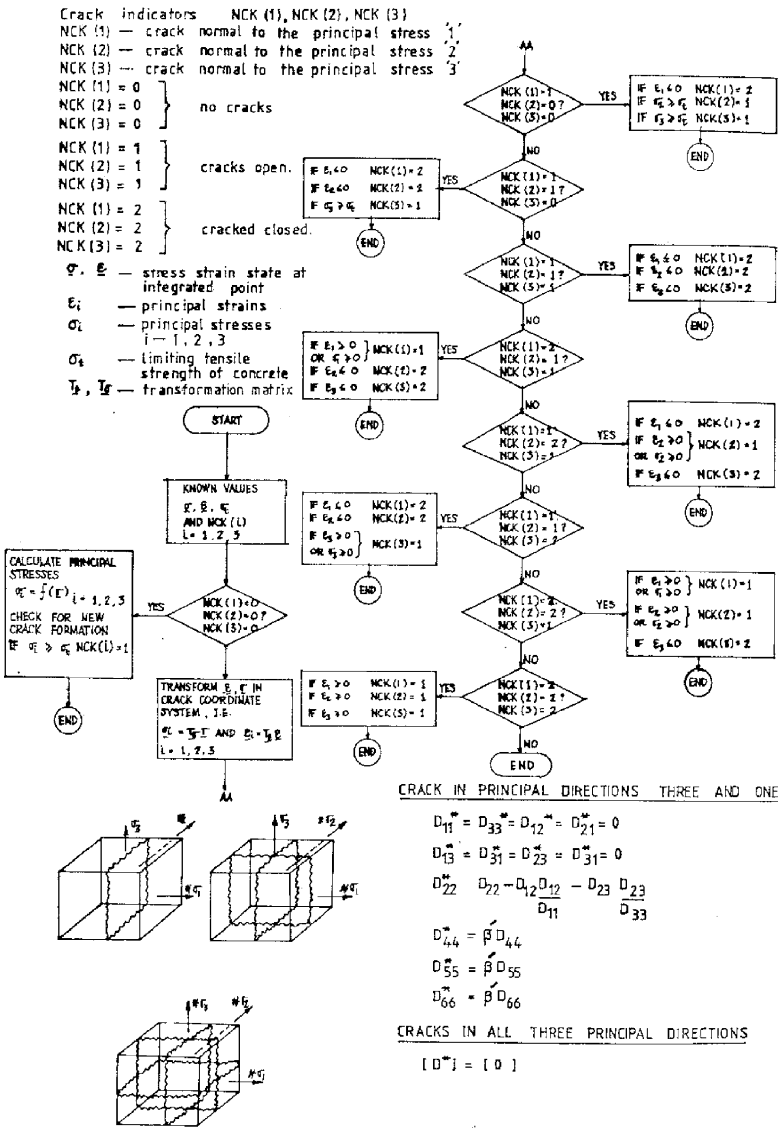
```
  1290 PRINT
  1300 VDU2,1,27,1,106,1,15,3:IF A1$=‘‘Y’’ THEN VDU2
  1310 PRINT ‘‘VOLUME OF ROOM = ’’;V1;‘‘m’’;
  1320 VDU2,1,27,1,83,1,0,3:IF A1$=‘‘Y’’ THEN VDU2
  1330 PRINT ‘‘3’’:VDU2,1,27,1,84,3:IF A1$=‘‘Y’’ THEN VDU2
  1340 LET D3=W/V
>LIST3600,3990
  3600 LET T6=INT(T3*1E5+0.5)/1E5
  3610 PRINT ‘‘PERIOD OF THE SYSTEM = ’’;T6;‘‘sec’’
  3620 PRINT
  3630 PROCdisplay
  3640 VDU2,1,27,1,51,1,210,3:IF A1$=‘‘Y’’ THEN VDU2
  3650 PRINT:PRINT:VDU2,1,27,1,106,1,20,3:IF A1$=‘‘Y’’ THEN VDU2
  3660 VDU2,1,27,1,51,1,31,3:IF A1$=‘‘Y’’ THEN VDU2
  3670 PRINT ‘‘*** NUMERICAL INTEGRATION ***’’
  3680 PRINT ‘‘*** FOR ONE DEGREE OF FREEDOM SPRING-MASS SYSTEM ***’’
  3700 PRINT
  3720 PRINT ‘‘TO INTEGRATE THE EQUATION OF MOTION, A TIME STEP LESS THAN
OR EQUAL’’
  3730 PRINT ‘‘TO ONE-TENTH OF THE FUNDAMENTAL PERIOD IS ADEQUATE IN MOST
INSTANCES.’’
  3740 PRINT:PRINT
  3750 VDU2,1,27,1,106,1,25,3
  3760 INPUT ‘‘CHOSEN VALUE FOR TIME STEP (sec)’’;T4
  3770 IF A1$=‘‘Y’’ THEN VDU2
  3780 VDU21:PRINT ‘‘CHOSEN VALUE FOR TIME STEP (sec)? ’’;T4:VDU6
  3790 PRINT
  3800 VDU2,1,27,1,106,1,10,3
  3810 INPUT ‘‘SPECIFY TIME AT WHICH CALCULATIONS SHOULD TERMINATE (sec) ’’
;N
  3820 IF A1$=‘‘Y’’ THEN VDU2
  3830 VDU21:PRINT ‘‘SPECIFY TIME AT WHICH CALCULATIONS SHOULD TERMINATE (
sec)? ’’;N:VDU6
  3840 VDU2,1,27,1,33,1,15:VDU2,1,27,1,108,1,10,3:IF A1$=‘‘Y’’ THEN VDU2:PR
INT:PRINT:VDU2,1,27,1,106,1,20,3:IF A1$=‘‘Y’’ THEN VDU2
  3850 PRINT TAB(1);‘‘COL 1’’;TAB(14);‘‘COL 2’’;TAB(27);‘‘COL 3’’;TAB(41);‘‘COL
4’’;TAB(55);‘‘COL 5’’;TAB(66);‘‘COL 6’’;TAB(76);‘‘COL 7’’
  3860 PRINT
  3870 VDU2,1,27,1,106,1,15,3:IF A1$=‘‘Y’’ THEN VDU2
  3880 PRINT TAB(1);‘‘TIME:’’;TAB(55);‘‘ACC.:’’;TAB(66);‘‘VEL.:’’;TAB(76);
‘‘DISP .:’’
  3890 VDU2,1,27,1,106,1,20,3:IF A1$=‘‘Y’’ THEN VDU2:PRINT ‘‘--------------
------------------------------------------------------------------------’’
  3900 PRINT:VDU2,1,27,1,106,1,15,3:IF A1$=‘‘Y’’ THEN VDU2
  3910 LET E1=0
  3920 LET E2=0
  3930 FOR S=0 TO N STEP 14
  3940 LET E=F4*1000-((F4*1000/T)*S)
  3950 IF E<0 THEN LET E=0
  3960 IF S=0 THEN LET Q=0:Q1=0:Q2=0
  3970 LET U=K1*1000*(Q+T4*Q1+((T4^2/4)*Q2))
  3980 LET U1=E-U
  3990 LET U2=U1/(0.66*M7+0.25*K1*1000*T4^2)
```

www.EngineeringBooksPDF.com

```
>LIST4000,4460
  4000 LET U3=Q1+0.5*(U2+Q2)*T4
  4010 LET U4=Q+0.5*(U3+Q1)*T4
  4020 IF S=0 THEN LET U3=0:U4=0
  4030 LET 01=INT(S*1E5+0.5)/1E5
  4040 LET 02=INT(E*100+0.5)/100
  4050 LET 03=INT(U*100+0.5)/100
  4060 LET 04=INT(U1*100+0.5)/100
  4070 LET 05=INT(U2*1000+0.5)/1000
  4080 LET 06=INT(U3*1E4+0.5)/1E4
  4090 LET 07=INT(U4*1E5+0.5)/1E5
  4100 LET G=01:PROCtable:PRINT TAB(2-G1);G;
  4110 LET G=02:PROCtable:PRINT TAB(19-G1);G;
  4120 LET G=03:PROCtable:PRINT TAB(32-G1);G;
  4130 LET G=04:PROCtable:PRINT TAB(46-G1);G;
  4140 LET G=05:PROCtable:PRINT TAB(57-G1);G;
  4150 LET G=06:PROCtable:PRINT TAB(66-G1);G;
  4160 LET G=07:PROCtable:PRINT TAB(76-G1);G
  4170 LET Q=U4
  4180 LET Q1=U3
  4190 LET Q2=U2
  4200 LET E1=U4
  4210 IF E2<E1 THEN LET E2=E1
  4220 NEXT S
  4230 VDU2,1,27,1,51,1,210,3:IF A1$=''Y'' THEN VDU2
  4240 PRINT:PRINT
  4250 VDU2,1,27,1,51,1,40,3:IF A1$=''Y'' THEN VDU2
  4260 PRINT
  4270 VDU2,1,27,1,33,1,0,3:IF A1$=''Y'' THEN VDU2
  4280 VDU2,1,27,1,108,1,8,3:IF A1$=''Y'' THEN VDU2
  4290 PRINT ''*** MAXIMUM DISPLACEMENT OBTAINED FROM INTEGRATION PROCEDURE
***''
  4300 LET E3=E2*1000
  4310 LET E4=INT (E3*100+0.5)/100
  4320 PRINT
  4330 VDU2,1,27,1,106,1,15,3:IF A1$=''Y'' THEN VDU2
  4340 PRINT ''MAXIMUM CENTRE DISPLACEMENT OF WALL = '';E4;''mm''
  4350 PRINT:PRINT
  4360 PRINT ''*** DUCTILITY RATIO ***''
  4370 LET H=E2/(R5/K)
  4380 LET H4=INT(H*100+0.5)/100
  4390 PRINT
  4400 VDU2,1,27,1,106,1,15,3:IF A1$=''Y'' THEN VDU2
  4410 PRINT ''DUCTILITY RATIO = '';H4
  4420 PRINT:PRINT
  4430 PRINT ''*** MAXIMUM HINGE ROTATION AT THE SUPPORT ***''
  4440 PRINT
  4450 VDU2,1,27,1,106,1,15,3:IF A1$=''Y'' THEN VDU2
  4460 LET H1=E2/(L2/2)
>LIST4470,4900
  4470 LET H2=ATN(H1)
  4480 LET H3=H2*360/(2*3141592654)
  4490 LET H5=INT (H3*100+0.5)/100
  4500 PRINT ''MAXIMUM HINGE ROTATION AT THE SUPPORT = '';H5;'' DEGREES''
```

www.EngineeringBooksPDF.com

Program ISOPAR



CRACK IN PRINCIPAL DIRECTIONS THREE AND ONE

$$D^{**}_{11} = D^{**}_{33} = D^{**}_{12} = D^{**}_{21} = 0$$

$$D^{**}_{13} = D^{**}_{31} = D^{**}_{23} = D^{**}_{32} = 0$$

$$D^{**}_{22} \quad D_{22} - D_{12}\frac{D_{12}}{D_{11}} - D_{23}\frac{D_{23}}{D_{33}}$$

$$D^{**}_{44} = \beta D_{44}$$

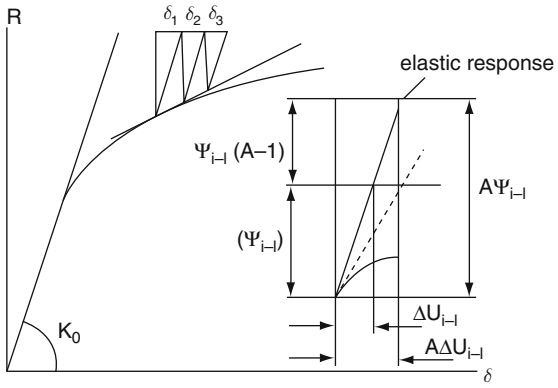
$$D^{**}_{55} = \beta D_{55}$$

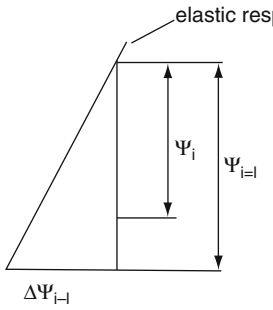
$$D^{**}_{66} = \beta D_{66}$$

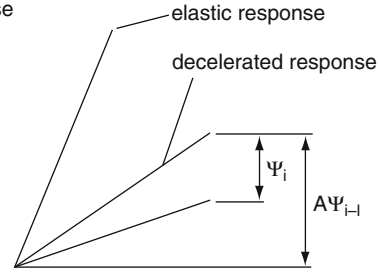
CRACKS IN ALL THREE PRINCIPAL DIRECTIONS

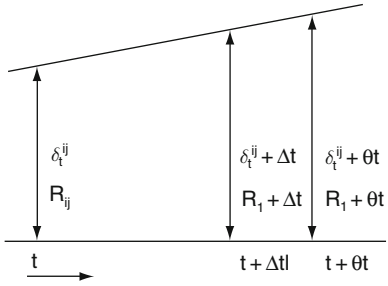
$$[D^{**}] = [0]$$

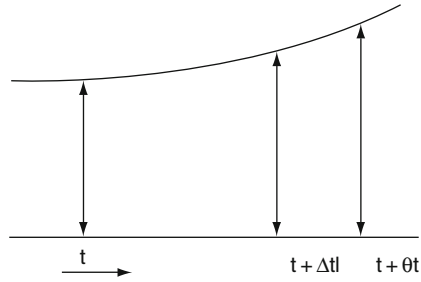
www.EngineeringBooksPDF.com












```
  4510 PRINT:PRINT:PRINT
  4520 VDU3
  4530 INPUT ‘‘DO YOU WANT TO RUN THE INTEGRATION PROCEDURE AGAIN? ENTER Y
  FOR YES AND N FOR NO ’’;Z1$
  4540 IF A1$=‘‘Y’’ THEN VDU2
  4550 VDU21:PRINT ‘‘DO YOU WANT TO RUN THE INTEGRATION PROCEDURE AGAIN? ’’
;Z1$:VDU6
  4560 IF Z1$=‘‘Y’’ THEN GOTO 3650
  4570 PRINT:PRINT
  4580 VDU3
```

www.EngineeringBooksPDF.com

```
  4590 INPUT ‘‘DO YOU WANT TO RUN THE PROGRAMME AGAIN FROM THE START? ENTER
Y FOR YES AND N FOR NO ’’;Z$
  4600 IF A1$=‘‘Y’’ THEN VDU2
  4610 VDU21:PRINT ‘‘DO YOU WANT TO RUN THE PROGRAMME AGAIN FROM THE START
? ’’;Z$:VDU6
  4620 IF Z$=‘‘Y’’ THEN GOTO 170
  4630 PRINT:PRINT
  4640 PRINT ‘‘                        ***  E  N  D  *** ’’
  4650 VDU3
  4660 END
  4670 DEF PROCtable
  4680 LET G$=STR$(G)
  4690 LET J=0
  4700 LET J=J+1
  4710 LET G1$=RIGHT$(G$,J)
  4720 LET G2$=LEFT$(G1$,1)
  4730 LET G7$=LEFT$(G$,1)
  4740 LET G3$=MID$(G$,2,1)
  4750 IF G7$=‘‘−’’ THEN LET G3$=MID$(G$,3,1)
  4760 IF G2$=‘‘.’’ THEN GOTO 4790
  4770 IF LEN(G1$)=LEN(G$) THEN GOTO 4810
  4780 GOTO 4700
  4790 LET G1=LEN(G$)-LEN(G1$)
  4800 IF G2$=‘‘.’’ THEN GOTO 4820
  4810 LET G1=LEN(G$)
  4820 IF G3$=‘‘E’’ THEN LET G1=G1−3
  4830 ENDPROC
  4840 DEF PROCdisplay
  4850 VDU3
  4860 PRINT ‘‘PRESS ANY KEY TO CONTINUE(EXCEPT CONTROL KEYS SUCH AS >BREA
K<, >ESCAPE<, ETC.’’
  4870 key$=GET$
  4880 CLS
  4890 IF A1$=‘‘Y’’ THEN VDU2
  4900 ENDPROC
```

Ottosen Model

```
      IMPLICIT REAL*8(A−H,O−Z)
      COMMON/MTMD3D/DEP(6,6),STRESS(6),STRAIN(6),IPT,NEL
      DIMENSION PAR(3,5),FS(6,6),FSTPOS(6,6),PROP(1),SIG(1),
      @         DVI1DS(6),DVJ2DS(6),DVJ3DS(6),DVTHDS(6)
      OPEN (UNIT=5,FILE=‘PARAMETERS’,STATUS=‘OLD’)
      READ (5,*,END=3700)((PAR(IF,JF),JF=1,5),IF=1,3)
3700  CLOSE (5)
      PK = PROP(3)/PROP(4)
      IP = 0
      JP = 0
      IF (PK .LE. 0.08) IP = 1
      IF (PK .EQ. 0.10) IP = 2
      IF (PK .GE. 0.12) IP = 3
      IF (PK .LT. 0.10) JP = 1
```

www.EngineeringBooksPDF.com

```
      IF (PK .GT. 0.10) JP = 2
      IF (IP .EQ. 0) GOTO 3800
      A = PAR(IP,2)
      B = PAR(IP,3)
      PK1 = PAR(IP,4)
      PK2 = PAR(IP,5)
      GOTO 3909
3800  SUB1 = PK-PAR(JP,1)
      SUB2 = PAR(JP + 1,1)-PAR(JP,1)
      A = SUB1*(PAR(JP*1,2)-PAR(JP,2))/SUB2+PAR(JP,2)
      B = SUB1*(PAR(JP*1,3)-PAR(JP,3))/SUB2+PAR(JP,3)
      PK1 = SUB1*(PAR(JP*1,4)-PAR(JP,4))/SUB2+PAR(JP,4)
      PK2 = SUB1*(PAR(JP*1,5)-PAR(JP,5))/SUB2+PAR(JP,5)
3900  VARI1 = SIG(1)+SIG(2)+SIG(3)
      VARJ2 = 1.0/6.0*((SIG(1)-SIG(2))**2+(SIG(2)-SIG(3))**2+
     @       (SIG(3)-SIG(1))**2)+SIG(4)**2+SIG(5)**2+SIG(6)**2
      VARI13 = VARI1/3.0
      VI131 = SIG(1)-VARI13
      VI132 = SIG(2)-VARI13
      VI133 = SIG(3)-VARI13
      VARJ3 = VI131*(VI132*VI133-SIG(5)**2)-SIG(4)*(SIG(4)*VI133
     @       -SIG(5)*SIG(5))+SIG(6)*(SIG(4)*SIG(5)-SIG(6)*VI132)
      VAR3TH = 1.5*3.0**(0.5)*VARJ3/VARJ2**1.5
      IF (VAR3TH .GE. 0.0) GOTO 4000
      ALAM = 22.0/21.0-1.0/3.0*ACOS(-PK2*VAR3TH)
      TOTLAM = PK1*COS(ALAM)
      DFD3TH = PK1*PK2*VARJ2**0.5*SIN(ALAM)/(3.0*PROP(4)*
     @         SIN(ACOS(-PK2*VAR3TH)))
      GOTO 4100
4000  ALAM = 1.0/3.0*ACOS(PK2*VAR3TH)
      TOTLAM = PK1*COS(ALAM)
      DFD3TH = PK1*PK2*VARJ2**0.5*SIN(ALAM)/(3.0*PROP(4)*
     @         SIN(ACOS(PK2*VAR3TH)))
4100  DFDI1 = B/PROP(4)
      DFDJ2 = A/PROP(4)**2+TOTLAM/(PROP(4)*VARJ2**0.5)
      DVI1DS(1) = 1.0
      DVI1DS(2) = 1.0
      DVI1DS(3) = 1.0
      DVI1DS(4) = 0.0
      DVI1DS(5) = 0.0
      DVI1DS(6) = 0.0
      DVJ2DS(1) = 1.0/3.0*(2.0*SIG(1)-SIG(2)-SIG(3))
      DVJ2DS(2) = 1.0/3.0*(2.0*SIG(2)-SIG(1)-SIG(3))
      DVJ2DS(3) = 1.0/3.0*(2.0*SIG(3)-SIG(1)-SIG(2))
      DVJ2DS(4) = 2.0*SIG(4)
      DVJ2DS(5) = 2.0*SIG(5)
      DVJ2DS(6) = 2.0*SIG(6)
      DVJ3DS(1) = 1.0/3.0*(VI131*(-VI132-VI133))+2.0*VI132*VI131-
     @            2.0*SIG(5)**2*SIG(4)**2*SIG(6)**2
      DVJ3DS(2) = 1.0/3.0*(VI132*(-VI131-VI133))+2.0*VI131*VI133-
     @            2.0*SIG(6)**2*SIG(4)**2*SIG(5)**2
      DVJ3DS(3) = 1.0/3.0*(VI133*(-VI131-VI132))+2.0*VI131*VI132-
     @            2.0*SIG(4)**2*SIG(5)**2*SIG(6)**2
      DVJ3DS(4) = -2.0*VI133*SIG(4)+2.0*SIG(5)*SIG(6)
```

www.EngineeringBooksPDF.com

```
      DVJ3DS(5) = −2.0∗VI131∗SIG(5)+2.0∗SIG(4)∗SIG(6)
      DVJ3DS(6) = −2.0∗VI132∗SIG(6)+2.0∗SIG(4)∗SIG(5)
      CONVJ2 = 3.0∗3.0∗∗0.5/(2.0∗VARJ∗1.2)
      VJ3J2 = VARJ3/VARJ2∗∗0.5
      DVTHDS(1) = CONVJ2∗(−0.5∗VJ3J2∗(2.0∗SIG(1)−SIG(2)−SIG(3))+
      @           DVJ3DS(1))
      DVTHDS(2) = CONVJ2∗(−0.5∗VJ3J2∗(2.0∗SIG(2)−SIG(1)−SIG(3))+
      @           DVJ3DS(2))
      DVTHDS(3) = CONVJ2∗(−0.5∗VJ3J2∗(2.0∗SIG(3)−SIG(1)−SIG(2))+
      @           DVJ3DS(3))
      DVTHDS(4) = CONVJ2∗(−3.0∗VJ3J2∗SIG(4)+DVJ3DS(4))
      DVTHDS(5) = CONVJ2∗(−3.0∗VJ3J2∗SIG(5)+DVJ3DS(5))
      DVTHDS(6) = CONVJ2∗(−3.0∗VJ3J2∗SIG(6)+DVJ3DS(6))
      DO 4200 IS = 1,6
      FS(IS,1) = DFDI1∗DVI1DS(IS)+DFDJ2∗DVJ2DS(IS)∗
                 DFD3TH∗DVTHDS(IS)
4200  FSTPDS(1,IS) = FS(IS,1)
      RETURN
      END
```

Main Program for Non-linear Analysis

```
C
        SUBROUTINE NONSTR(TEL,IGAUS,TEM)
C------------          THIS SUBR. CALC. THE INCREMENTAL
C------------          AND UPDATED STRESS, LOADING AND UNLOADING
C------------          AND CRACK FORMATION
C
£INSERT COMMON.FF
C
C-----       IF POINT IS ALREADY CRUSHED DO NOT DO ANY CALCULATION
        IF(NCRK(IGAUS,IEL).EQ.999)GO TO 555
C
C
C            CRACK INDICATOR
        NCR=NCRK(IGAUS,IEL)
C                  LOADING - UNLOADING INDICATOR
        IUNL=IUNLOD(IGAUS,IEL)
C
C--------          CRACK WIDTH(IN TERMS OF STRAINS)
C        DO 5 J=1,3
C        CRW(J)=CWI(J,IGAUS)
C5      CONTINUE
C
C----------           COPY ANGL INTO DC
        DO 7 J=1,9
        DO(J)=ANGL(J,IGAUS,IEL)
7       CONTINUE
C
        CALL RZERO(CET,6)
C
C---------------        STRESSES CURRENT AND TOTAL
```

www.EngineeringBooksPDF.com

```
        DO 10 J=1,6
        STG(J)=SIGT(J,IGAUS,IEL)
        STB(J)=STG(J)+SIG(J)
10      CONTINUE
C
        IF(NCR.EQ.0)GO TO 30
C
C----------            TRANSFORMATION MATRIX IN CRACK DIRECTIONS
        DO 20 J=1,3
        DC1(J)=ANGL(J,IGAUS,IEL)
        DC2(J)=ANGL(J+3,IGAUS,IEL)
        DC3(J)=ANGL(J+6,IGAUS,IEL)
20      CONTINUE
C
        CALL TRANSF (3)
C---------------          TRANSFORM STB STRESS IN CRACK DIRECTION
C---------------          ALSO INCREMENTAL STRESS SIG
        CALL MVECT(QM,STB,CET,6,6)
C
         CALL MVECT(QM,SIG,STC,6,6)
C
C---------------                TRANSF. TOTAL STRAIN IN CRACK DIR.
C
        CALL TRANSF(1)
        DO 21 J=1,6
        AJ(J)=ECT(J,IGAUS)
21      CONTINUE
C
        CALL MVECT(QM,AJ,ECA,6,6)
C
C
        GO TO 50
C
30      CONTINUE
C------------                 CALC. PRINCIPAL STRESSES DUE TO STB
        CALL PRINCL(2,IGAUS,STB)
        CET(1)=PS1(IGAUS)
        CET(2)=PS2(IGAUS)
        CET(3)=PS3(IGAUS)
        KKOO=1
        IF(KKOO.EQ.1)GO TO 40
C----------          PRINCIPAL STRAINS
        DO 38 J=1,6
        ECB(J)=ECT(J,IGAUS)
38      CONTINUE
C
        CALL PRINCL (1,IGAUS, ECB)
        ECA(1)=EP1(IGAUS)
        ECA(2)=EP2(IGAUS)
        ECA(3)=EP3(IGAUS)
40      CONTINUE
C
C
C-----          CALCULATE EQUIVALENT STRAIN
```

www.EngineeringBooksPDF.com

```
C
        EQSTN=SIGEFF(ECB)
C---------------          CHECK FOR CONCRETE CRUSHING
C        EC1=ECA(1)+ECU
C        EC2=ECA(2)+ECU
C        EC3=ECA(3)+ECU
C        IF(EC1.LT.0.0 .OR. EC2.LT.0.0 .OR. EC3.LT.0.0)GO TO 888
C
        CRUSH=EQSTN - ECU
        IF(CRUSH .GT. 0.0) GO TO 888
C
   50   CONTINUE
C
C-----       CALC. AND UPDATE CRACK INDICATOR
C
C
        CALL CRACK(CET,ECA,NCR,CRW)
C
C----------            STORE UPDATED VALUES IN ARRAYS
        NCRK (IGAUS,IEL)=NCR
        DO 41 J=1,9
        ANGL(J,IGAUS,IEL)=DC(J)
   41   CONTINUE
C
C        DO 42 J=1,3
C        CWI(J,IGAUS)=CRW(J)
C  42      CONTINUE
C
        IF(NCR.EQ.0)GO TO 110
        DO 105 J=1,3
        DC1(J)=ANGL(J,IGAUS,IEL)
        DC2(J)=ANGL(J+3,IGAUS,IEL)
        DC3(J)=ANGL(J+6,IGAUS,IEL)
   105  CONTINUE
        CALL TRANSF(1)
        DO 106 J=1,6
        ECB(J)=EC(J)
   106  CONTINUE
C
        CALL MVECT (QM,ECB,EC,6,6)
C
C
   110  CONTINUE
C--------         GO TO APPROPRIATE CONCRETE COMPRESSION CRITERION
        IF (ICOMP.EQ.1)GO TO 98
C---------            CALC. UNIAXIAL STRAINS
        DO 308 J=1,3
        IF (ENU(J).LT.1.E-15)GO TO 306
        EIU(J)=SIG(J)/ENU(J)
        GO TO 308
   306  CONTINUE
        EIU(J)=0.0
   308  CONTINUE
C---------------              EQUIV. STRESS AT PREVIOUS UNLOADED POINT
```

www.EngineeringBooksPDF.com

```
        SEQ=SIGY(IGAUS,IEL)
C--------------                    CALC. EFFECTIVE STRESS DUE TO CURRENT
C-------------                    AND TOTAL STRESS
        SIGEF2=SIGEFF(ECT(1,IGAUS))
         DO 109 J=1,6
        ECB(J)=ECT(J,IGAUS)-ECRT(J)
   109  CONTINUE
        SIGEF1=SIGEFF (ECB)
        FLOA=SIGEF2-SIGEF1
        IF(IUNL .EQ. 1) GO TO 60
C           IUNL=0 --- ON THE EQUIV. CURVE
C
        IF(SIGEF2 .GE. SEQ)GO TO 43
C--------------             UNLOADING AT THIS POINT
        RFACT=(SEG-SIGEF1)/FLOA
C--------------             NON-LINEAR STRAIN
        DO 35 J=1,6
        ECB (J)=RFACT*EC(J)
   35     CONTINUE
C-----            MEAN NON-LINEAR STRAIN
        DO 201 J=1,3
        ETU(J,IGAUS)=ETU(J,IGAUS)+0.5*RFACT*EIU(J)
   201     CONTINUE
        CALL DMATL(STB,IEL,IGAUS,TEM)
C--------------                       INCREMENTAL STRESS ASSOCIATED WITH -ECB
        CALL MVECT (DDS,ECB,AJ,6,6)
C--------------                     ELASTIC STRAIN
        DO 36 J=1,6
        ECB(J)=(1.0-RFACT)*EC(J)
   36     CONTINUE
        IUNLOD(IGAUS,IEL)=1
C-------------             ELASTIC STRESS INCR.
        CALL DMATL(CET,IEL,IGAUS,TEM)
        CALL MVECT(DOS,ECB,STA,6,6)
C---------- TOTAL STRESS INCREMENT
        DO 37 J=1,6
        SIG(J)=STA(J)+AJ(J)
   37     CONTINUE
C
          DO 202 J=1,3
          ETU(J,IGAUS)=ETU(J,IGAUS)+EIU(J)-0.5*RFACT*EIU(J)
   202     CONTINUE
        GO TO 99
   43     CONTINUE
C--------------       LOADING AT THIS POINT
C-----          MEAN UNIAXIAL STRAIN
        DO 203 J=1,3
        ETU(J,IGAUS)=ETU(J,IGAUS)+EIU(J)*0.5
   203     CONTINUE
        CALL DMATL(STB,IEL,IGAUS,TEM)
C--------------           STRESS INCREMENT
C
C       CALL MVECT(DDS,EC,SIG,6,6)
```

www.EngineeringBooksPDF.com

```
C-----           ACCUMULATE TOTAL UNIAXIAL STRAIN
        DO 205 J=1,3
          ETU(J,IGAUS)=ETU(J,IGAUS)+EIU(J)*0.5
   205    CONTINUE
        GO TO 99
C
   60     CONTINUE
C--------------           NOT ON THE EQUIV. CURVE
        IF(SIGEF2 .GT. SEQ)GO TO 70
C------------         ELASTIC UNLOADING
        CALL DMATL(CET,IEL,IGAUS,TEM)
C-------------          ELASTIC STRESS
        CALL MVECT(DOS,EC,SIG,6,6)
C-----            ACCUMULATE UNIAXIAL STRAIN
          DO 206 J=1,3
        ETU(J,IGAUS)=ETU(J,IGAUS)+EIU(J)
   206    CONTINUE
        GO TO 99
   70     CONTINUE
C------------        LOADING PARTLY ELASTIC PARTLY NON-LINEAR
        FRAC=(SEQ-SIGEF1)/FLOA
C-----------           ELASTIC STRAIN
        DO 71 J=1,6
        ECB(J)=FRAC*EC(J)
   71     CONTINUE
        CALL DMATL(CET,IEL,IGAUS,TEM)
        CALL MVECT(DDS,ECB,STA,6,6)
C---------------           STRESS AT THE CURVE
        DO 72 J=1,6
        AJ(J)=STG(J)+STA(J)
   72     CONTINUE
C-----            MEAN UNIAXIAL STRAIN
          DO 207 J=1,3
        ETU(J,IGAUS)=ETU(J,IGAUS)+0.5*EIU(J)*(1.+FRAC)
   207     CONTINUE
C
        IUNLOD(IGAUS,IEL)=0
C-----------       STRAIN ASSOCIATED WITH NON-LINEAR CURVE
        DO 73 J=1,6
        ECB(J)=(1.0-FRAC)*EC(J)
   73     CONTINUE
        CALL DMATL(AJ,IEL,IGAUS,TEM)
C-------           STRESS INCR.
        CALL MVECT(DDS,ECB,STB,6,6)
C----------------          TOTAL INCREMENTAL STRESS
        DO 74 J=1,6
        SIG(J)=STA(J)+STB(J)
   74     CONTINUE
C
        DO 208 J=1,3
          ETU(J,IGAUS)=ETU(J,IGAUS)+0.5*EIU(J)*(1.-FRAC)
   208    CONTINUE
        GO TO 99
   98     CONTINUE
```

www.EngineeringBooksPDF.com

```
C--------        STRESS INCREMENT ON THE BASIS OF ENDOCHRONIC THEORY
C
        DO 1223 J=1,6
        SIGG(J)=SIG(J)
        ECC(J)=EC(J)
   1223 CONTINUE
        CALL ENDOST(IEL,IGAUS,SIGG,ECC)
C
   99   CONTINUE
        IF(NCR.EQ.0)GO TO 50
        DO 91 J=1,6
        AJ(J)=SIGT(J,IGAUS,IEL)
   91     CONTINUE
        CALL TRANSF(3)
        CALL MVECT(QM,AJ,STG,6,6)
C----------           TRANSFORM LOCAL STRESSES IN GLOBAL DIRN
        CALL TRANSF(2)
        DO 92 J=1,6
        STG(J)=STG(J)+SIG(J)
   92   CONTINUE
C----------             RELEASE STRESSES ACROSS THE OPEN CRACKS
        CALL GETNCK (NCR,NCK)
        IF(NCK(1).EQ.1)STG(1)=0.0
        IF(NCK(2).EQ.1)STG(2)=0.0
        IF(NCK(3).EQ.1)STG(3)=0.0
        CALL MVECT(QM,STG,STA,6,6)
C
        DO 94 J=1,6
        SIGT(J,IGAUS,IEL)=STA(J)
   94    CONTINUE
C
        GO TO 999
90      CONTINUE
        DO 100 J=1,6
        SIGT(J,IGAUS,IEL)=SIGT(J,IGAUS,IEL)+SIG(J)
100      CONTINUE
        GO TO 999
888      CONTINUE
C-----------            CRUSHING OF CONCRETE
        NCRK(IGAUS,IEL)=999
C---------           RELEASE STRESSES
        DO 101 J=1,6
        SIGT(J,IGAUS,IEL)=0.0
101       CONTINUE
C
        GO TO 555
999     CONTINUE
C-----       CHECK THAT THE CURRENT STATE OF STRESS IS
C-----       INSIDE THE FAILURE SURFACE
        CALL PRINCL(2,IGAUS,SIGT(1,IGAUS,IEL))
        CET(1)=PS1(IGAUS)
        CET(2)=PS2(IGAUS)
        CET(3)=PS3(IGAUS)
        IF(CET(1).GT.0.0 .OR.CET(2).GT.0.0 .OR.CET(3).GT.0.0)
```

www.EngineeringBooksPDF.com

```
      1                                                    GO TO 555
      CALL CONCR1(CET)
C      IF(ICOMP.EQ.2)     CALL CONCR3(CET)
      BRING=1.0
      IF(FF.GT.1.0001)BRING=BRING/FF
      DO 553 J=1,6
      SIGT(J,IGAUS,IEL)=BRING*SIGT(J,IGAUS,IEL)
  553 CONTINUE
C
  555 CONTINUE
      RETURN
      END
C
      SUBROUTINE ASSLOD(IEL,NER,ELOD)
£INSERT COMMON.FF
C
C-----------          TO ASSEMBLE LOAD VECTOR
C
      DO 95 J=1,NER
      M1=(MCODE(J,IEL)-1)*NDF
C------              ELASTO-PLASTIC STRAIN INCR.
      DO 88 J=1,3
      ECM(J)=FPROP*ECM(J)
  88  CONTINUE
      CALL SBINST (ECM,NSUB,SGMT(1,IGAUS,I1))
C-----  ADD ELASTIC STRESS INCR
      DO 94 J=1-3
      SGMT(J,1GAUS,I1)=SGMT(J.IGAUS,I1)+SGM(J)
  94  CONTINUE
      NYM(IGAUS,I1)=2
99    CONTINUE
      RETURN
      END
C
      SUBROUTINE MEMDAT(I1,IGAUS,STD)
£INSERT COMMON.FF
C
C------------              TO CALC. ELAS TO - PLASTIC MATERIAL MATRIX
C-----------              AT STRESS LEVEL,STD FOR MEMBRANE ELEMENTS
C
C
C------------              CALC. ELASTIC MATERIAL MATRIX
C
      CALL DMEMB
C-----------              CHECK WHETHER CURRENT POINT IS PLASTIC
      IF(NYM(IGAUS,I1).NE.1)GO TO 50
C
C
      EFF=ZMISE(STD)
      SX=(2.*STD(1)-STD(2))/3.
      SY=(2.*STD(2)-STD(1))/3.
      FAC=EFF/1.5
C
C------------               CALC. (DF/D(STD) = AJ
```

www.EngineeringBooksPDF.com

```
        AJ(1)=SX/FAC
        AJ(2)=SY/FAC
        AJ(3)=2.*STD(3)/FAC
C
C------------              CALC. DENOMINATOR OF PLASTIC MATRIX
C                     DENOM=AJ(T)*DJ*AJ + HARDG
C
        CALL MVECT(DJ,AJ,STC,3,3)
C
        DENOM=0.0
        DO 10 J=1,3
        DENOM=DENOM+AJ(J)*STC(J)
10       CONTINUE
C
        DENOM=DENOM+HARDG
C
C-----------               CALC. ELASTO-PLASTIC MATERIAL MATRIX AND
C-----------               STORE IT INTO DJ
        DO 30 J=1,3
        DO 20 K=1,3
        DJ(J,K)=DJ(J,K)-STC(J)*STC(K)/DENOM
20       CONTINUE
30       CONTINUE
C
50       CONTINUE
C
        RETURN
        END
C
C
        SUBROUTINE SBINST(ECL,NSUB,STA)
C-----      STRESS INCR IS CALCULATED USING SUB-INCREMENTAL
C-----      METHOD,ALSO STRESS STA IS UPDATED
£INSERT COMMON.FF
        DIMENSION ECL(1)
        RSUB=NSUB
        DO 3 J=1,3
        ECB(J)=ECL(J)/RSUB
   3    CONTINUE
        SIGY1=ZMISE(STA)
C-----       LOOP OVER SUB-INCREMENTS
        DO 70 ISUB=1,NSUB
C------------              CALC. ELASTO-PLASTIC MATERIAL MATRIX -DJ
C
        SX=(2.*STA(1)-STA(2))/3.
        SY=(2.*STA(2)-STA(1))/3.
        FAC=SIGY1/1.5
C
C------------              CALC. (DF/D(STA) = AJ
        AJ(1)=SX/FAC
        AJ(2)=SY/FAC
        AJ(3)=2.*STA(3)/FAC
C
C------------              CALC. DENOMINATOR OF PLASTIC MATRIX
```

www.EngineeringBooksPDF.com

```
C                    DENOM=AJ(T)*DJ*AJ + HARDG
C
        CALL MVECT(DJ,AJ,STC,3,3)
C
        DENOM=0.0
        DO 10 J=1,3
        DENOM=DENOM+AJ(J)*STC(J)
10        CONTINUE
C
        DENOM=DENOM+HARDG
C-----------               CALC. ELASTO-PLASTIC MATERIAL MATRIX AND
C-----------               STORE IT INTO DJ
        DO 30 J=1,3
        DO 20 K=1,3
        DJ(J.K)=DJ(J,K)-STC(J)*STC(K)/DENOM
20      CONTINUE
30       CONTINUE
C-----       CALC. DLAMB AND EQUIV. PLASTIC STRAIN INCREMENT
        DLAMB=0.0
        DO 64 J=1,3
        DLAMB=DLAMB+STC(J)*ECB(J)
   64   CONTINUE
        DLAMB=DLAMB/DENOM
C-----       UNLOADING IS PLASTIC INSIDE A SUBINCREMENTS
C        IF(DLAMB.LT.0.0)CLAMB=0.0
        BB=0.0
        DO 65 J=1,3
        BB=BB+AJ(J)*STA(J)
   65   CONTINUE
        EQSTN=DLAMB*BB/SIGY1
        CALL MVECT(DJ,ECB,STB,3,3)
        DO 60 J=1,3
        STA(J)=STA(J)+STB(J)
   60   CONTINUE
C-----       CALC. UPDATED YIELD SURFACE
        SIGY2=ZMISE(STA)
        SIGY1=SIGY1+HARDG*EQSTN
        FACT=1.0
        IF(SIGY2.GT.SIGY1)FACT=SIGY1/SIGY2
C-----       UPDATE STRESS VECTOR
        DO 62 J=1,3
        STA(J)=STA(J)*FACT
   62   CONTINUE
C
   70   CONTINUE
        RETURN
        END
C
        SUBROUTINE STELST(I)
£INSERT COMMON.FF
C
C---------              CALC. ELASTO-PLASTIC STRESS INCR AND UDATE
C---------              CURRENT STRESS AND PLASTIC INDICATOR
          N=LRF(I)
```

www.EngineeringBooksPDF.com

```
C
        I1=I-(NTE1+NTE2)
C
        T1=SIGGT(I1)
        T2=T1+STRV
        T1=RABS(T1)
        T2=RABS(T2)
C
        FACL=T2-T1
        IF(FACL.EQ.0.0)GO TO 99
C-----------              CHECK FOR LOADING OR UNLOADING AT THIS POINT
C
         IF(ISPL(I1).EQ.1)GO TO 40
C-----        POINT ELASTIC BEFORE
        IF(T2.LT.YIELST(I1))GO TO 50
C-----       TRANSITION ZONE - LOADING
C-----------        FRACTION OF ELASTIC STRAIN INCR.
        FRAC=(YIELST(I1)-T1)/FACL
C
        ISPL(I1)=1
C*--------        ELASTIC STRESS INCREMENT
        STRV=STRV+FRAC
C*--------        STRESS AT YIELD SURFACE
        SIGGT(I1)=SIGGT(I1)+STRV
C*--------         PLASTIC STRAIN INCR.
        STRNV=(1.0-FRAC)*STRNV
        GO TO 45
C
   40   CONTINUE
C-----       POINT PLASTIC BEFORE
        IF(T2.GT.YIELST(I1))GO TO 45
        GO TO 50
   45   CONTINUE
        EPSMOD=ZESBAR(I)
C--------         CALC. PLASTIC STRESS INCR. AND UPDATE STRESS
        STRVPL=STRNV*EPSMOD
        STRV=STRV+STRVPL
        SIGGT(I1)=SIGGT(I1)+STRVPL
C
        GO TO 99
C
   50     CONTINUE
C---------              UNLOADING AT THIS POINT
C
C-------         CHECK IF POINT WAS PLASTIC IN PREVIOUS ITERATION
        IF(ISPL(I1).EQ.1)GO TO 55
        SIGGT(I1)=SIGGT(I1)+STRV
        GO TO 99
   55   CONTINUE
C-----       CHECK THAT THE UNLOADING IS REAL
        STRV=ZESBAR(I)*STRNV
        T2=SIGGT(I1)+STRV
        T2=RABS(T2)
        IF(T2.GT.YIELST(I1))GO TO 45
```

www.EngineeringBooksPDF.com

```
        FACL=T2-T1
        IF(FACL.EQ.0.0)GO TO 99
        FRAC=(YIELST(I1)-T1)/FACL
C-------------               PLASTIC STRESS INCR.
        STRPL=FRAC*STRV
        ISPL(I1)=2
C
C-------------               ELASTIC STRESS INCR.
        STREL=ZESBAR(I)*(1.0-FRAC)*STRNV
        STRV=STRPL+STREL
C
        SIGGT(I1)=SIGGT(I1)+STRV
99       CONTINUE
        RETURN
        END
C
        SUBROUTINE INCLNE(I,NER)
£INSERT COMMON.FF
C-----------------------------------------------------------------
C
        IF(JRADL.NE.0)GO TO 10
        IF(NBC.GT.0)GO TO 188
   10   CONTINUE
        JP=NER*NDF
        I1=I-(NTE1+NTE2)
        LET=IDENT(I)
        DO 13 J=1,NER
        IJ=MCODE(J,I)
        IF(LET.GT.2)IJ=LCODE(J,I1)
13      LC(J)=IJ
        DO 3 J=1,3
        DO 3 K=1,3
3       C(J,K)=0.0
        IF(JRADL.NE.0)GO TO 31
        C(1,1)=RCOS(SHY)
        C(2,2)=RCOS(SHY)
        C(3.3)=1.0
        C(1,2)= -RSIM(SHY)
        C(2,1)=RSIN(SHY)
31      DO 132 J=1,NER
        M1=LC(J)
        IF(JRADL.NE.0)GO TO 17
        M1=(M1-1)*NDF
        JS=0
        DO 26 K=1,6
        Q(K,J)=QM(J,K)
26      CONTINUE
C
        CALL MPPODT(Q,O,OOS,6,6,6)
25      CONTINUE
        RETURN
        END
C
        SUBROUTINE PRINCL(NEP.M.CET)
```

www.EngineeringBooksPDF.com

```
£INSERT COMMON.FF
C
C-------------------------------------------------------------------------------
C                          THIS SUBROUTINE CALCULATES THE PRINCIPAL STRAINS
C                          PRINCIPAL STRESSES AND DIRECTION COSINES
C                       NEP=2 - PRINCIPAL STRESS AND D.C.
C                            NEP=1 - PRINCIPAL STRAINS ONLY
        LL=0
        DO 10 J=1,6
        IF(RABS(CET(J)).GT.1.OE-15)LL=1
10      CONTINUE
C
        IF(NEP.EO.1)GO TO 20
        PS1(M)=0.0
        PS2(M)=0.0
        PS3(M)=0.0
        GO TO 30
20      CONTINUE
        EP1(M)=0.0
        EP2(M)=0.0
        EP3(M)=0.0
30      CONTINUE
C
        IF(LL.EQ.0)GO TO 999
C
        G1= CET(1)
        G2= CET(2)
        G3= CET(3)
        G4= CET(4)
        G5= CET(5)
        G6= CET(6)
        ZNV1 = G1 + G2 + G3
        ZNV2 = G1*G2 + G2*G3 + G3*G1 - G4*G4 - G5*G5 - G6*G6
        ZNV3 = G1+G2*G3+2.0 *G4*G5*G6 -G1*G5*G5 - G2*G5* G6
     1         - G3*G4*G4
        BB = - ZNV1
        CW = ZNV2
        CD = - ZNV3
C       FIND ALL ROOTS OF CUBIC EQUATION AA*X*3 + BB*X*2 + CC*X + DD
C       FIRST ROOT (X5) IS FOUND BY NEWTON'S METHOD USING 0 AS
C       FIRST APPROX. THEN SOLVE QUADRATIC BY STANDARD FORMULA
C       ERR IS THE ACCUR ACY REQUIRED FOR ROOT X5
        ERR = 1E-6
        X1 = 0.0
        CORT=2.0*ERR
        MGG=0
1000    B1 = BB + X1
        MGG=MGG+1
        IF(MGG.GT.35)GO TO 2000
        B2 = CW + X1*B1
        IF(RABS(CORT).LT. ERR)GO TO 2000
        B3 = CD+ X1 * B2
        C3 = ( X1 + B1) * X1 + B2
        IF( RABS(C3) .LT. 1E-30) C3 = 1.0
```

www.EngineeringBooksPDF.com

```
      CORT=B3/C3
      X1=X1-CORT
      GO TO 1000
2000  X5 = X1
C
C     SECOND PART - FIND ROOTS OF QUADRATIC
C                   X**2 + B1*X + B2 = 0.0
C
      DIP = B1*B1 - 4.0*B2
      IF(DIP .LT. 0.0) GO TO 3000
      SD = RSORT (DIP)
      X6 = (SD - B1) * 0.5
      X7 = - (SD + B1) * 0.5
      GO TO 335
3000  X6 = - 0.5 * B1
      X7 = 0.5 * RSQRT (-DIP)
      WRITE(JOUT, 800) I,M
800   FORMAT(/,15X, 9HCONJUGATE, 215)
335   CONTINUE
C                   PRINCIPAL STRESSES AND DIRECTION COSINES
C          DC1,DC2,DC3 ARE THE DIRECTION COSINES OF
C          PRINCIPAL STRESSES PS1, PS2, PS3
      IF (X5 .GE. X6 .AND. X6 .GE. X7) GO TO 430
      IF(X5 .GE. X7 .AND. X7 .GE. X6) GO TO 431
      IF(X6 .GE. X6 .AND. X5 .GE. X7) GO TO 432
      IF(X6 .GE. X7 .AND. X7 .GE. X5) GO TO 433
      IF(X7 .GE. X5 .AND. X5 .GE. X6) GO TO 434
      IF(X7 .GE. X6 .AND. X6 .GE. X5) GO TO 435
430   X1 = X5
      X2 = X6
      X3 = X7
      GO TO 438
431   X1 = X5
       X2 = X7
      X3 = X6
      GO TO 438
432   X1 = X6
      X2 = X5
      X3 = X7
      GO TO 438
433   X1 = X6
      X2 = X7
      X3 = X5
      GO TO 438
434    X1 = X7
      X2 = X5
      X3 = X6
      GO TO 438
435   X1 = X7
      X2 = X6
      X3 = X5
438   CONTINUE
      IF(NEP.EQ.1)GO TO 99
C----------       PRINCIPAL STRESSES
```

www.EngineeringBooksPDF.com

```
        PS1(M)=X1
        PS2(M)=X2
        PS3(M)=X3
        DO 440 IS = 1,3
        GO TO (443 , 445 ,447) ,IS
443     AS1 = G1 - X1
        AS2 = G2 - X1
        AS3 = G3 - X1
        GO TO 444
445     AS1 = G1 - X2
        AS2 = G2 - X2
        AS3 = G3 - X2
        GO TO 444
447     AS1 = G1 - X3
        AS2 = G2 - X3
        AS3 = G3 - X3
444     CONTINUE
        AK=G4
        BK= G5
        CK= G6
        YAP1=AS2*CK-BK*AK
        YAP2=AK*AK-AS1*AS2
        IF(YAP1 .EQ. 0.0 ) YAP1=1.0
        IF(YAP2 .EQ. 0.0 ) YAP2=1.0
        BJM1=    (BK*BK-AS2*AS3)/YAP1
        BJM2= (AS1*BK-AK*CK) /YAP2
        BJ1 = BJM1*BJM1
        BJ2 = BJM2*BJM2
        ZIP = RSQRT( BJ1 + BJ2 + 1.0)
         IF ( ZIP .LT. 0.0 ) ZIP=1.0
        DC3(IS)= 1.0 / ZIP
        DC1(IS)= BJM1 * DC3(IS)
        DC2(IS)= BJM2 * DC3(IS)
440     CONTINUE
        GO TO 999
   99   CONTINUE
C-----------         PRINCIPAL STRAINS
        EP1(M)=X1
        EP2(M)=X2
        EP3(M)=X3
   999  CONTINUE
        RETURN


       SUBROUTINE RESIDL(1)
       DIMENSION XJ(6)
       COMMON/MEM/SP(20),SJ(3,3)
       DIMENSION TF(60)
       COMMON/TOR/ SV(146),TE(20),CET(6),CTE,DTIME,TIME
       COMMON/REL/ U(438),P(438),PP(438),UU(438)
       COMMON/AAA/ NEL,NNP,NEQ,NHBD,NBC,NTE1,NTE2,NTE3,NTE4,
      1 NNE1,NNE2,NNE3,NNE4,NDF,NRF,NRS,DET3,NGP,INCORE,JRADL
       COMMON/BBB/ D(6,6),D1(6,6),E(12,3),POIS(12,6),MCODE(128,8),
      1         EK(24,24) ,H(6,24),LRF(128),IDENT(128)
```

www.EngineeringBooksPDF.com

```
      COMMON/CCC/ X(146),Y(146),Z(146),NZN(438),NFIX(10)
     1 ,AST(12),EST(12),DIA(12),SIGT(1,8,6),ECR(1,1,1)
      COMMON/CAP/ GE1(27),GE2(27),GE3(27),WE(4),W(14),NG1
      COMMON/ABC/ PS1(14),PS2(14),PS3(14),SIG(14,6),EC(14,6)
C--------------------    THIS SUBR. CALCULATES RESIDUAL FORCE DUE TO CREEP
      JP=NNE1*NDF
      CALL DMAT(1)
      DO 13 J=1,JP
13    TF(J)=0.0
      M=0
      DO 28 J1=1,NG1
      DO 28 J2=1,NG1
      DO 28 J3=1,NG1
      M=M+1
      CALL ISOP2(1,J1,J2,J3,3,4)
      DOS=DETJ*WE(J1)*WE(J2)*WE(J3)
      DO 18 J=1,6
      SUM=0.
      DO 17 K=1,6
17    SUM=SUM+D1(J,K)*ECP(M,K)
18    XJ(J)=SUM
      DO 20 J=1,JP
      SUM=0.
      DO 19 JK=1,6
19    SUM=SUM+H(JK,J)*XJ(JK)
20    TF(J)=TF(J)+SUM*DOS
28    CONTINUE
C
      DO 35 J=1,NNE1
      M1=(MCODE(1,J)-1)*NDF
      JJ=(J-1)*NDF
      DO 35 K=1,NDF
      JJ=JJ+1
      M1=M1+1
35    P(M1)=P(M1)+TF(JJ)
      RETURN
      END



      SUBROUTINE ROTATE(NK)
      COMMON/AAA/ NEL,NNP,NEQ,NHBD,NBC,NTE1,NTE2,NTE3,NTE4,
1    1 NNE1,NNE2,NNE3,NNE4,NDF,NRF,NRS,DETJ,NGP,INCORE,JRADL
      COMMON/CCC/ X(146),Y(146),Z(146),NZN(438),NFIX(10)
     1 ,AST(12),EST(12),DIA(12),SIGT(1,8,6),ECR(1,1,1)
      COMMON/REL/ O(438),P(438),PP(438),UU(438)
C-------    MULTIPLY BY ROTATION MATRIX IN LOAD VECTOR
      SHY=22.5/57.29
      CS=COS(SHY)
      SN=SIN(SHY)
      DO 1 JI=1,NNP
      IF(JRADL.EQ.1)GO TO 81
      LK=(JI-1)*NDF
      DO 2 KL=1,NDF
```

www.EngineeringBooksPDF.com

```
      LK=LK+1
      IF(NZN(LK).LT.0)GO TO 4
2     CONTINUE
      GO TO 1
81    RR=SQRT(X(JI)*X(JI)+Y(JI)*Y(JI))
      CS=X(JI)/RR
      SN=Y(JI)/RR
4     JJ=(JI-1)*NDF
      IF(NK.EQ.2)GO TO 50
      S1=P(JJ+1)*CS+P(JJ+2)*SN
      S2=P(JJ+2)*CS-P(JJ+1)*SN
      P(JJ+1)=S1
      P(JJ+2)=S2
      GO TO 1
50    CONTINUE
      S1=U(JJ+1)*CS-U(JJ+2)*SN
      S2=U(JJ+2)*CS+U(JJ+1)*SN
      U(JJ+1)=S1
      U(JJ+2)=S2
1     CONTINUE
      RETURN
      END



       SUBROUTINE DMAT(I)
       COMMON/BBB/ D(6,6),D1(6,6),E(12,3),POIS(12,6),MCODE(128,8),
      1            EK(24,24) ,H(6,24),LRF(128),IDENT(128)
       N= LRF(I)
       IF(DIME.EQ.N) RETURN
       LIME=N
C     DUE TO SYMMETRY OF THE COMPLIANCES, THREE RELATION EXIST
       POIS(N,4) = POIS(N,1)* E(N,2)/ E(N,1)
       POIS(N,5) = POIS(N,2)* E(N,3)/ E(N,2)
       POIS(N,6) =POIS(N,3)* E(N,3)/ E(N,1)
       RAT = 1- POIS(N ,1)* POIS(N,4)-POIS(N,3)* POIS(N,6)-POIS(N,2)
      1*POIS(N,5) -POIS(N,1) * POIS(N,2)*POIS(N,3) -
      2     POIS(N,4) * POIS(N,5) * POIS(N,6)
13     D1(1,1)= (1 -POIS(N,2) * POIS(N,5))* E(N,1)/ RAT
       D1(1,2)= (POIS(N,1) + POIS(N,3) * POIS(N,5))*E(N,2)/RAT
       D1(1,3)= (POIS(N,3) + POIS(N,1) * POIS(N,2))*E(N,3)/RAT
       D1(2,2)= (1- POIS(N,3)* POIS(N,6))*E(N,2)/RAT
       D1(2,3)= (POIS(N,2) + POIS(N,3)*POIS(N,4))*E(N,3)/RAT
       D1(2,1)   = D1(1,2)
       D1(3,1) =D1(1,3)
       D1(3,2) = D1(2,3)
       D1(3,3)= (1-POIS(N,1)*POIS(N,4))* E(N,3)/RAT
       E11 = 0.5 *(E(N,1)/ (1+ POIS(N,1)))
       E22 = 0.5 *(E(N,1)/ (   POIS(N,1) + E(N,1)/E(N,2)))
       D1(4,4)=  0.5 * (E11 +E22)
       E31 = 0.5 * (E(N,2)/(1+ POIS(N,2)))
       E32 = 0.5 * (E(N,2)/(E(N,2)/ E(N,3) + POIS(N,2)))
       D1(5,5)= 0.5 * (E31+ E32)
       E42 = 0.5 *(E(N,3) /(1+ POIS(N,6)))
```

www.EngineeringBooksPDF.com

```
      E43 = 0.5 * (E(N,3)/(E(N,3)/E(N,1) + POIS(N,6)))
      D1(6,6) = 0.5 * (E42 +E43)
      RETURN
      END



      SUBROUTINE GAUSS
      COMMON/CAP/ GE1(27),GE2(27),GE3(27),WE(4),W(14),NG1
      COMMON/AAA/ NEL,NNP,NEQ,NHBD,NBC,NTE1,NTE2,NTE3,NTE4,
     1  NNE1,NNE2,NNE3,NNE4,NDF,NRF,NRS,DETJ,NGP,INCORE,JRADL
      IF(NGP.EQ.8)GO TO 25
      NG1=3
      GE1(1)=0.77459666924
      GE2(1)=GE1(1)
      GE3(1)=GE1(1)
      GE1(3)= -GE1(1)
      GE2(3)= -GE1(1)
      GE3(3)= -GE1(1)
      GE1(2)=0.0
      GE2(2)=0.0
      GE3(2)=0.0
      WE(1)=0.55555555555556
      WE(2)=0.88888888888889
      WE(3)=WE(1)
      GO TO 33
25    CONTINUE
      NG1=2
      WE(1)=1.0
      WE(2)=1.0
      WE(3)=1.0
      GE1(1)=0.57735026918
      GE1(2)= -GE1(1)
      GE2(1)=GE1(1)
      GE2(2)= -GE1(1)
      GE3(1)=GE1(1)
      GE3(2)= -GE1(1)
33    CONTINUE
      RETURN
      END



      SUBROUTINE  ELSTIF(1)
      COMMON/AAA/ NEL,NNP,NEQ,NHBD,NBC,NTE1,NTE2,NTE3,NTE4,
     1  NNE1,NNE2,NNE3,NNE4,NDF,NRF,NRS,DETJ,NGP,INCORE,JRADL
      COMMON/CAP/ GE1(27),GE2(27),GE3(27),WE(4),W(14),NG1
      COMMON/BBB/ D(6,6),D1(6,6),E(12,3),POIS(12,6),MCODE(128,8),
     1          EK(24,24) ,H(6,24),LRF(128),IDENT(128)
      COMMON/CCC/ X(146),Y(146),Z(146),NZN(438),NFIX(10)
     1  ,AST(12),EST(12),DIA(12),SIGT(1,8,6),ECR(1,1,1)
      DIMENSION ES(3,24),S(3,3),C(3,3)
      SHY=22.5
      SHY=(3.14/180.)*SHY
```

www.EngineeringBooksPDF.com

```
      JP=NDF*NNE1
      DO 12 IS =1,24
      DO 12 JS =1,24
12    EK(IS,JS) =0.0
      CALL DMAT(I)
      IF( NGP .EQ. 14 ) GO TO 23
C
C                  (2×2×2) AND (3×3×3) GAUSS INTEGRATION
C
      DO 39   J1 = 1 , NG1
      DO  39   J2 = 1 , NG1
      DO  39   J3 = 1, NG1
      CALL ISOP2(I,J1,J2,J3,3,1)
      DOS = WE(J1)*WE(J2)*WE(J3)*DETJ
      DO 17 N1=1,6
      DO 17 N2 =1,6
17    D(N1,N2)=DOS*D1(N1,N2)
      DO 38 II=1, JP
      DO 38 JJ=1, JP
      IF (II.GT.JJ)GO TO 2522
      EIKJ = 0.0
      DO 37 IJ=1,6
      HTDIK = 0.0
      DO 36 JI=1,6
      HTDIK = HTDIK + H(JI,II) * D(JI,IJ)
36    CONTINUE
      EIKJ = EIKJ + HTDIK * H(IJ,JJ)
37    CONTINUE
      EK(II,JJ) = EK(II,JJ) + EIKJ
2522  CONTINUE
38    CONTINUE
39    CONTINUE
      GO TO 333
23    CONTINUE
      DO21 M=1, NGP
       CALL ISOP2(I,M,M,M,3,1)
C
C   MATERIAL PROPERTY MATRIX ^D^, ^D^ IS MULTIPLIED BY
C   WEIGHTING COEFFICIENTS AND DET. OF JACOBIAN DETJ
C
      DOS= W(M)*DETJ
      DO 18 N1=1,6
      DO 18 N2=1,6
18     D(N1,N2)=DOS*D1(N1,N2)
      DO 6  II= 1,24
      DO 5 JJ =1, 24
      IF(II .GT. JJ) GO TO 5
      EIKJ =0.0
      DO 4 IJ =1,6
      HTDIK =0.0
      DO 3 JI = 1, 6
      HTDIK = HTDIK + H( JI, II)*D(JI,IJ)
C
C          H(JI,II)= TRANSPOSE OF  H(II,JI)
```

www.EngineeringBooksPDF.com

```
C
3       CONTINUE
        EIKJ =EIKJ +HTDIK *H(IJ,JJ)
4       CONTINUE
        EK(II,JJ) = EK(II,JJ) +EIKJ
5       CONTINUE
6       CONTINUE
21      CONTINUE
333     CONTINUE
        DO 2523 II=1,JP
        DO 2523 JJ=1,JP
2523    EK(JJ,II)=EK(II,JJ)
C       CALL BOUNDC(JP,NNE1 ,I)
        RETURN
        C(1,1)=COS(SHY)
          C(2,2)=COS(SHY)
          C(1,2)= -SIN(SHY)
        C(2,1)=SIN(SHY)
        C(3,3)=1.0
        C(1,3)=0.
        C(3,1)=0.
        C(2,3)=0.
        C(3,2)=0.
        DO 132J=1,NNE1
        M1=(MCODE(I,J)-1)*NDF
        JS=0
        DO 110K=1,NDF
        M1=M1+1
        IF(NZN(M1).LT.0)JS=1
110     CONTINUE
        IF(JS.EQ.0)GO TO 132
        IS=(J-1)*NDF
        DO 116JI=1,NNE1
        JN=(JI-1)*NDF
        DO 112N=1,NDF
        DO 112NN=1,NDF
        IJ=JN+NN
        SUM=0.
        DO 111NJ=1,NDF
        IN=IS+NJ
111     SUM=SUM+C(NJ,N)*EK(IN,IJ)
112     ES(N,IJ)=SUM
116     CONTINUE
        DO 122N=1,NDF
        DO122NN=1,NDF
        SUM=0.
        DO 123NJ=1,NDF
        IN=IS+NJ
123     SUM=SUM+ES(N,IN)*C(NJ,NN)
122     S(N,NN)=SUM
        DO124N=1,NDF
        DO124NN=1,NDF
        IN=IS+NN
124     ES(N,IN)=S(N,NN)
```

www.EngineeringBooksPDF.com

```
      DO 125KJ=1,NDF
      JM=IS+KJ
      DO 125JK=1,JP
125   EK(JM,JK)=ES(KJ,JK)
132   CONTINUE
      RETURN
      END


      SUBROUTINE ISOP2(1,J1,J2,J3,NEJ,NF)
      COMMON/AAA/ NEL,NNP,NEQ,NHBD,NBC,NTE1,NTE2,NTE3,NTE4,
     1 NNE1,NNE2,NNE3,NNE4,NDF,NRF,NRS,DETJ,NGP,INCORE,JRADG
      COMMON/DGE/S(20,3),CC(3,20),C(3,3)
      COMMON/BBB/ D(6,6),D1(6,6),E(12,3),POIS(12,6),MCODE(128,8),
     1         EK(24,24) ,H(6,24),LRF(128),IDENT(128)
      COMMON/MEM/ SP(20),SJ(3,3)
      COMMON/CCC/ X(146),Y(146),Z(146),NZN(438),NFIX(10)
     1 ,AST(12),EST(12),DIA(12),SIGT(1,8,6),ECR(1,1,1)
      COMMON/CAP/ GE1(27),GE2(27),GE3(27),WE(4),W(14),NG1
C
      JP=NNE1*NDF
      DO 80 J=1,6
      DO 80 K=1,JP
80    H(J,K)=0.0
      S1= 1.0 + GE1(J1)
      S2= 1.0 - GE1(J1)
      S3= 1.0 + GE2(J2)
      S4= 1.0 - GE2(J2)
      S5= 1.0 + GE3(J3)
      S6= 1.0 - GE3(J3)
      IF(NNE1 .EQ. 20 .OR.NNE1.EQ.32 ) GO TO 34
C
      A=0.125
      IF(NEJ .GT. 2 )GO TO 81
      SP(1)=A*S2*S4*S6
      SP(2) = A*S1*S4*S6
      SP(3)=A*S1*S3*S6
      SP(4)=A* S2*S3*S6
      SP(5)=A*S2*S4*S5
      SP(6)=A*S1*S4*S5
      SP(7)=A*S1*S3*S5
      SP(8)=A*S2*S3*S5
      IF(NEJ .EQ. 1) RETURN
81    CONTINUE
      S(1,1) = - A * S4 * S6
      S(1,2) =  -A * S2 * S6
      S(1,3) =  -A * S4 * S2
      S(2,1) =   A * S4 * S6
      S(2,2) =    -A * S1 * S6
      S(2,3) = - A * S1 * S4
      S(3,1) =   A * S3 * S6
      S(3,2)  =  A * S1 * S6
      S(3,3)  = - A * S1 * S3
      S(4,1)  = -A * S3 * S6
```

www.EngineeringBooksPDF.com

```
      S(4,2)  =   A * S2 * S6
      S(4,3)  =  - A * S2 * S3
      S(5,1)  =  - A * S4 * S5
      S(5,2)  =    -A * S2 * S5
      S(5,3)  =    A * S2 * S4
      S(6,1)  =    A * S4 * S5
      S(6,2)  =    -A * S1 * S5
      S(6,3)  =    A * S1 * S4
      S(7,1) =       A * S3 * S5
      S(7,2) =     A * S1 * S5
      S(7,3) =       A * S1 * S3
      S(8,1) =     - A * S3 * S5
      S(8,2) =     A * S2 * S5
      S(8,3) =       A * S2 * S3
      GO TO 38
34    CONTINUE
      S7= S1*S2
      S8 = S3*S4
      S9 = S5*S6
      S11 = GE1(J1)
      S12 = GE2(J2)
      S13 = GE3(J3)
      IF (NNE3 .EQ. 32 ) GO TO 36
      IF (NEJ .GT. 2 )GO TO 82
C
C         SHAPE FUNCTIONS FOR 20-NODE ELEMENT
      SP(1) = A* S2* S3 *S6 *(-S11+ S12- S13-2)
      SP(2) = 2*A* S7* S3*S6
      SP(3) = A* S1* S3* S6*(S11 +S12-S13 -2)
      SP(4) = A*2*S1*S8* S6
      SP(5) = A*S1*S4* S6* (S11-S12 -S13 -2)
      SP(6)= 2*A*S7* S4* S6
      SP(7)=  A* S2*S4* S6*(-S11- S12-S13-2)
      SP(8)= 2*A*S2* S8 *S6
      SP(9)=  2*A*S2*S3* S9
      SP(10) = 2*A*S1* S3* S9
      SP(11)= 2*A*S1* S4*S9
      SP(12)= 2*A*S2*S4* S9
      SP(13) =  A* S2* S3* S5*(-S11 +S12 +S13-2)
      SP(14) =  2*A * S7* S3* S5
      SP(15) = A* S1* S3 *S5* (S11+S12+ S13-2)
      SP(16) = 2*A*S1* S8*S5
      SP(17) = A*S1* S4*S5 * ( S11-S12+S13 -2)
      SP(18) =  2*A* S7* S3*S5
      SP(19)=  A*S2*S4 *S5*(-S11-S12 +S13-2)
      SP(20) = 2*A* S2* S8* S5
C-------------------------------------------------------
B2    CONTINUE
      IF(NEJ .EQ. 1) RETURN
      S(1,1) = 0.125 * S3 * S6 *(2.0*S11+1.0-(S12-S13))
      S(1,2) = 0.125 * S2 * S6*(2.0*S12-1.0-S11-S13)
      S(1,3) = 0.125* S2*S3*(2.0*S13+1.0-S12 + S11)
      S(2,1) = -0.5*S11*S3*S6
      S(2,2) = 0.25* S7*S6
```

www.EngineeringBooksPDF.com

```
S(2,3) = −0.25*S7*S3
S(3,1) = 0.125*S3*S6*(2.0*S11−1.0+S12 − S13)
S(3,2) = 0.125*S1*S6*(2.0*S12−1.0+S11−S13)
S(3,3) = 0.125*S1*S3*(2*S13 + 1.0− S11−S12)
S(4,1) = 0.25*S6*S8
S(4,2) = −0.5*S12*S1*S6
S(4,3) = − 0.25*S1*S8
S(5,2) = 0.125*S1*S6*(2*S12 +1.0−S11+S13)
S(5,3) = 0.125*S1*S4*(2*S13+1.0−S11+S12)
S(5,1) = 0.125*S4*S6*(2*S11−1.0−S12−S13)
S(6,1) = −0.5*S4*S6*S11
S(6,2) = −0.25*S7*S6
S(6,3) = −0.25 * S7*S4
S(7,1) = 0.125*S4*S6*(2*S11+1.0+S12+S13)
S(7,2) = 0.125*S2*S6*(2.0*S12+1.0+S11+S13)
S(7,3) = 0.125*S2*S4*(2.0*S13+1.0+S11+S12)
S(8,1)  = - 0.25*S8*S6
S(8,2) =-0.50*S12*S2*S6
S(8,3)  = - 0.25* S2 * S8
S(9,1)  = - 0.25*S3*S9
S(9,2)  =  0.25*S2*S9
S(9,3) = -0.5*S13*S2*S3
S(10,1) =  0.25*S3*S9
S(10,2) =  0.25*S1*S9
S(10,3)=-0.5*S13*S1*S3
S(11,1) =  0.25*S4*S9
S(11,2) = -0.25*S1*S9
S(11,3)=-0.5*S1*S4*S13
S(12,1) = -0.25*S4*S9
S(12,2) = -0.25*S2*S9
S(12,3)=-0.5*S13*S2*S4
S(13,1)=0.125*S3*S5*(2*S11+1.0− S12−S13)
S(13,2)= 0.125*S2*S5*(2*S12−1.0+S13−S11)
S(13,3)=0.125*S2*S3*(2.0*S13−1.0+S12−S11)
S(14,1)= −0.5*S11*S3*S5
S(14,2) = 0.25*S7*S5
S(14,3)= 0.25*S7*S3
S(15,1)=0.125*S3*S5*(2.0*S11+S12+S13−1.0)
S(15,2)=0.125*S1*S5*(2.0*S12+S11+S13−1.0)
S(15,3)=0.125*S1*S3*(2.0*S13+S11+S12−1.0)
S(16,1) = 0.25*S8*S5
S(16,2)= −0.5*S12*S1*S5
S(16,3) = 0.25*S8*S1
S(17,1)=0.125*S4*S5*(2 *S11+S13−S12 −1.0)
S(17,2) =0.125*S1*S5*(2.0*S12−S11 −S13+1.0)
S(17,3) =0.125*S1*S4*(2.0*S13 +S11−S12−1.0)
S(18,1)=-0.5*S4*S5*S11
S(18,2)= -0.25*S7*S5
S(18,3)= 0.25*S7*S4
S(19,1)= 0.125*S4*S5*(2.0*S11+S12−S13+1.0)
S(19,2)=0.125*S2*S5*(2.0*S12+S11−S13+1.0)
S(19,3)=0.125*S2*S4*(2.0* S13−S11−S12−1.0)
S(20,1)= − 0.25*S8*S5
S(20,2)= −0.5*S12*S2*S5
```

www.EngineeringBooksPDF.com

```
      S(20,3) = 0.25*S2*S8
      GO TO 38
36    CONTINUE
38    CONTINUE
      P1=0.0
      P2=0.0
      P3=0.0
      P4=0.0
      P5=0.0
      P6=0.0
      P7=0.0
      P8=0.0
      P9=0.0
      DO 44 J = 1,NNE1
      M1 = MCODE(I,J)
       P1 = P1 + S(J,2)*Y(M1)
      P2 = P2 + S(J,3)*Z(M1)
      P3 = P3 + S(J,2)*Z(M1)
      P4 = P4 + S(J,3)*Y(M1)
      P5 = P5 + S(J,1)*Z(M1)
      P6 = P6 + S(J,1)*Y(M1)
      P7 = P7 + S(J,3)*X(M1)
      P8 = P8 + S(J,2)*X(M1)
      P9 = P9 + S(J,1)*X(M1)
44    CONTINUE
      SJ(1,1) = P1*P2-P3*P4
      SJ(1,2)= P3*P7 -P8* P2
      SJ(1,3) = P8*P4 -P1*P7
      SJ(2,1)= P4*P5- P2*P6
      SJ(2,2) =P2*P9-P5*P7
      SJ(2,3)= P7*P6-P4*P9
      SJ(3,1)= P6*P3 - P5*P1
      SJ(3,2) = P5*P8-P9*P3
      SJ(3,3) = P9*P1 - P6*P8
      IF(NEJ .EQ. 2) RETURN
C   DETERMINANT  OF  JACOBIAN
C
      DETJ = (P9 * (P1* P2 - P3 * P4 ) + P8 * ( P4 * P5 - P2 * P6)
     1          + P7 * ( P3 * P6 - P1 * P5))
      IF(DETJ .LE. 0.0) WRITE(3,133) 1
C
C   JACOBIAN    INVERSION
C
      DO 75 N1=1,3
      DO 75 N2 =1,3
75    C(N2,N1)=SJ(N1,N2)/DETJ
C
      DO 45 K=1,3
      DO 45 J=1,NNE1
      CC(K,J)=0.0
45    CONTINUE
C
      DO 47 K=1,3
      DO 47 J=1,NNE1
```

www.EngineeringBooksPDF.com

```
      DO 46 N1=1,3
46    CC(K,J) = CC(K,J) + C(K,N1)*S(J,N1)
47    CONTINUE
C
C                    STRAIN-DISPLACEMENT MATRIX
      DO 54 N1=1,NNE1
      N2 = (N1-1)*NDF
      L1 = N2+1
      L2 = N2+2
      L3=N2+3
      H(1,L1)=CC(1,N1)
      H(4,L1+1)=CC(1,N1)
      H(6,L1+2)=CC(1,N1)
      H(2,L2)=CC(2,N1)
      H(4,L2-1)=CC(2,N1)
      H(5,L2+1)=CC(2,N1)
      H(3,L3)=CC(3,N1)
      H(5,L3-1)=CC(3,N1)
      H(6,L3-2)=CC(3,N1)
54    CONTINUE
      IF(NF .EQ. 4) RETURN
C
C     ---------- MODIFY ^H^ MATRIX FOR INCLINED BOUNDARY CONDITIONS
C
      PHI=22.5*3.14155/180.0
      CS=COS(PHI)
      SN=SIN(PHI)
      DO 68 J=1,NNE1
      IF(JRADL.EQ.1)GO TO 63
      JH=(MCODE(I,J)-1)*NDF
      DO 332KP=1,NDF
      JH=JH+1
      IF(NZN(JH).LT.0)GO TO 64
332   CONTINUE
      GO TO 68
63    M1=MCODE(I,J)
      RR=SQRT(X(M1)*X(M1)+Y(M1)*Y(M1))
      CS=X(M1)/RR
      SN=Y(M1)/RR
64    NJ=J
      N2=(NJ-1)*NDF
      L1=N2+1
      L2=N2+2
      L3=N2+3
      C1=CC(1,NJ)
      C2=CC(2,NJ)
      C3=CC(3,NJ)
C
      H(1,L1)=CS*C1
      H(1,L2)=-SN*C1
      H(2,L1)=SN*C2
      H(2,L2)=CS*C2
      H(3,L3)=C3
      H(4,L1)=CS*C2+SN*C1
```

www.EngineeringBooksPDF.com

```
      H(4,L2)=CS*C1-SN*C2
      H(5,L1)=SN*C3
      H(5,L2)=CS*C3
      COMMON/FF/ SIGG1(110),SIGG2(110)
      COMMON/TOR/ SV(146),TE(20),CET(6),CTE,DTIME,TIME
      COMMON/BBB/ D(6,6),D1(6,6),E(12,3),POIS(12,6),MCODE(128,8),
     1              EK(24,24),H(6,24),LRF(128),IDENT(128)
      COMMON/ABC/ PSI(14),PS2(14),PS3(14),SIG(14,6),EC(14,6)
     1,DC1(14,3), DC2(14,3), DC3(14,3),ECP(14,6)
      COMMON/LID/ SK(438,84)
      COMMON/BON/ NNODE, NEUB,NETB,NBLOK, NDISK1,NDISK2,NDISK3
      COMMON/REL/ U(438),P(438),PP(438),UU(438)
      COMMON/CCC/ X(146),Y(146),Z(146),NZN(438),NFIX(10)
     1,AST(12),EST(12),DIA(12),SIGT(1,8,6),ECR(1,1,1)
      COMMON/AAA/ NEL,NNP,NEQ,NHBD,NBC,NTE1,NTE2,NTE3,NTE4,
     1 NNE1,NNE2,NNE3,NNE4,NDF,NRF,NRS,DEIJ,NGP,INCORE,JRADL
      COMMON/CAP/ GE1(27),GE2(27),GE3(27),WE(4),W(14),NG1
C   ISOPARAMETRIC ELEMENTS REPRESENT       CONCRETE OF THE VESSEL
C
C   LINE ELEMENTS REPRESENT PRESTRESSING CABLES AND REINFORCEMENTS
C   LINKAGE ELEMENTS REPRESENT NON-LINEAR BOND
        OPEN(UNIT=20,DEVICE='DSK',ACCESS='SEQINOUT',FILE='NSA20.TMP',
     1   DISPOSE='DELETE',PROTECTION=''011)
        OPEN(UNIT=21,DEVICE='DSK',ACCESS='SEQINOUT'
     1 ,FILE='NSAR21.TMP',  DISPOSE='DELETE',PROTECTION=''011)
        OPEN(UNIT=22,DEVICE='DSK',ACCESS='SEQINOUT',FILE='NSAR22.TMP',
     1  DISPOSE='DELETE',PROTECTION=''011)
      IELST=1
      IELST=0
      CALL INPUT
      DO 500 I=1,NTE1
       DO 500 J=1,NGP
      DO 500 K=1,6
      SIGT(I,J,K)=0.0
      ECR(1,J,K)=0.
500   CONTINUE
      DO 501 J=1,NGP
      PS1(J)=0.
      PS2(J)=0.
      PS3(J)=0.
      DO501K=1,6
      SIG(J,K)=0.
      EC(J,K)=0.0
501    CONTINUE
      CALL GAUSS
      CALL ASSEMB
      CALL DECOMP
       DO 1000 NPR=1,1
      CALL LOAD
      CALL ROTATE(1)
      DO 3 JJ=1,NEQ
      IF( NZN(JJ) .NE. 0 ) P(JJ)=0.0
3     CONTINUE
      NLI=0
```

www.EngineeringBooksPDF.com

```
502    CONTINUE
       NLI=NLI+1
       TIME=0.
       IF(NGI.EQ.1)GO TO 612
       IF(IELST.EQ.0)GO TO 612
C---------------SPECIFY A TIME INCREMENT IN DAYS
C--------------DTIME=0.777 TO TERMINATE THE ITERATION
       READ(1,507)DTIME
       IF(DTIME-0.777)549,550,549
507    FORMAT(F0.0)
549    CONTINUE
       WRITE(3,508)DTIME
508    FORMAT(///,40X,'TIME INCREMENT(IN DAYS)=',F12.5)
       TIME=TIME+DTIME
       TT=TIME
       DT=DTIME
       DO 509 I=1,NTE1
       CALL CREEP(I,DT,TT,2)
C      DO 510J=1,NGP
C      DO 510 K=1,6
C510   ECR(I,J,K)=ECR(I,J,K)+ECP(J,K)
       CALL RESIDL(I)
509    CONTINUE
       CALL ROTATE(1)
612    CONTINUE
       CALL RHVECT
       CALL RESOLV
C-------      TRANSFORM INCLINED DISPL. IN GLOBAL SYSTEM-----------------
       CALL ROTATE(2)
       DO 503 J=1,NEQ
       P(J)=0.
503    UU(J)=UU(J)+U(J)
       DO 504 I=1,NEL

       CALL STRESS(I,NLI)
       GO TO (515,515,516)IDENT(I)
515    CONTINUE
       DO 505 J=1,NGP
       DO 505 K=1,6
       SIGT(1,J,K)=SIGT(1,J,K)+SIG(J,K)
505    CONTINUE
       GO TO 504
516    CONTINUE
       SIGG2(I)=SIGG2(I)+SIGG1(I)
504    CONTINUE
       CALL OUTPUT
       IF (IELST.EQ.0)GO TO 550
       GO TO 502
550    CONTINUE
1000   CONTINUE
       CLOSE(UNIT=20)
       CLOSE(UNIT=21)
       CLOSE(UNIT=22)
       STOP
```

www.EngineeringBooksPDF.com

```
      END
      COMMON/FF/ SIGG1(110),SIGG2(110)
      COMMON/TOR/ SV(146),TE(20),CET(6),CTE,DTIME,TIME
      COMMON/BBB/ D(6,6),D1(6,6),E(12,3),PDIS(12,6),MCODE(128,8),
     1           EK(24,24) ,H(6,24),LRF(128),IDENT(128)
      COMMON/ABC/ PS1(14),PS2(14),PS3(14),SIG(14,6),EC(14,6)
     1,DC1(14,3), DC2(14,3), DC3(14,3),ECP(14,6)
      COMMON/LID/ SK(438,84)
      COMMON/BON/ NNODE, NEUB,NETB,NBLOK, NDISK1,NDISK2,NDISK3
      COMMON/REL/ U(438),P(438),PP(438),UU(438)
      COMMON/CCC/ X(146),Y(146),Z(146),NZN(438),NFIX(10)
     1 ,AST(12),EST(12),DIA(12),SIGT(1,8,6),ECR(1,1,1)
      COMMON/AAA/ NEL,NNP,NEQ,NHBD,NBC,NTE1,NTE2,NTE3,NTE4,
     1 NNE1,NNE2,NNE3,NNE4,NDF,NRF,NRS,DETJ,NGP,INCORE,JRADL
      COMMON/CAP/ GE1(27J,GE2(27),GE3(27),WE(4),W(14),NG1
C   ISOPARAMETRIC ELEMENTS REPRESENT  CONCRETE OF THE VESSEL
C
C   LINE ELEMENTS REPRESENT PRESTRESSING CABLES AND REINFORCEMENTS
C   LINKAGE ELEMENTS REPRESENT NON-LINEAR BOND
       OPEN(UNIT=20,DEVICE='DSK',ACCESS='SEQINOUT',FILE='NSA20.TMP',
     1   DISPOSE='DELETE',PROTECTION=''011)
       OPEN(UNIT=21,DEVICE='DSK',ACCESS='SEQINOUT'
     1 ,FILE='NSAR21.TMP', DISPOSE='DELETE',PROTECTION=''011)
        OPEN(UNIT=22,DEVICE='DSK',ACCESS='SEQINOUT',FILE='NSAR22.TMP',
     1   DISPOSE='DELETE',PROTECTION=''011)
      IELST=1
      IELST=0
      CALL INPUT
      DO 500 I=1,NTE1
       DO500 J=1,NGP
      DO 500 K=1,6
      SIGT(I,J,K)=0.0
      ECR(1,J,K)=0.
500   CONTINUE
      DO 501 J=1,NGP
      PS1(J)=0.
      PS2(J)=0.
      PS3(J)=0.
      DO501K=1,6
      SIG(J,K)=0.
      EC(J,K)=0.0
501    CONTINUE
      CALL GAUSS
      CALL ASSEMB
      CALL DECOMP
       DO 1000 NPR=1,1
      CALL LOAD
      CALL ROTATE(1)
      DO 3 JJ=1,NEQ
      IF( NZN(JJ) .NE. 0 ) P(JJ)=0.0
3     CONTINUE
      NLI=0
502   CONTINUE
      NLI=NLI+1
```

www.EngineeringBooksPDF.com

```
      TIME=0.
      IF(NLI.EQ.1)GO TO 612
      IF(IELST.EQ.0)GO TO 612
C--------------SPECIFY A TIME INCREMENT IN DAYS
C-------------DTIME=0.777 TO TERMINATE THE ITERATION
      READ(1,507)DTIME
      IF(DTIME-0.777)549,550,549
507   FORMAT(F0.0)
549   CONTINUE
      WRITE(3,508)DTIME
508   FORMAT(///,40X,'TIME INCREMENT(IN DAYS)=',F12.5)
      TIME=TIME+DTIME
      TT=TIME
      DT=DTIME
      DO 509 I=1,NTE1
      CALL CREEP(I,DT,TT,2)
C     DO 510J=1,NGP
C     DO 510 K=1,6
C510  ECR(I,J,K)=ECR(I,J,K)+ECP(J,K)
      CALL RESIDL(I)
509   CONTINUE
      CALL ROTATE(1)
612   CONTINUE
      CALL RHVECT
      CALL RESOLV
C-------      TRANSFORM INCLINED DISPL. IN GLOBAL SYSTEM-----
      CALL ROTATE(2)
      DO 503 J=1,NEQ
      P(J)=0.
503   UU(J)=UU(J)+U(J)
      DO 504 I=1,NEL

      CALL STRESS(I,NLI)
      GO TO(515,515,516)IDENT(1)
515   CONTINUE
      DO 505 J=1,NGP
      DO 505 K=1,6
      SIGT(1,J,K)=SIGT(1,J,K)+SIG(J,K)
505   CONTINUE
      GO TO 504
516   CONTINUE
      SIGG2(I)=SIGG2(I)+SIGG1(I)
504   CONTINUE
      CALL OUTPUT
      IF(IELST.EQ.0)GO TO 550
      GO TO 502
550   CONTINUE
1000  CONTINUE
      CLOSE(UNIT=20)
      CLOSE(UNIT=21)
      CLOSE(UNIT=22)
      STOP
      END
```

www.EngineeringBooksPDF.com

```
      SUBROUTINE FLOW(FF ,A1)
      COMMON/JJ/ELE(100)
      DIMENSION      AA1(6) , AA2(6) , AA3(6) , A1(6) ,A2(6)
      COMMON/AAA/ NEL,NNP,NEQ,NHBD,NBC,NTE1,NTE2,NTE3,NTE4,CCC,CCT,
     1 NNE1,NNE2,NNE3,NNE4,NDF,NRF,NRS,DETJ,NITER,NLY,NTYPE,YY1,YY2
       CCY=0.7*CCC
      AKF = CCT/CCC
      IF( AKF .EQ. 0.08) GO TO 41
      IF( AKF .EQ. 0.10) GO TO 42
      IF( AKF .EQ. 0.12) GO TO 43
41    AMM = 1.8076
      BMM = 4.0962
      CMM = 14.4863
      DMM = 0.9914
      GO TO 44
42    AMM = 1.2759
      BMM = 3.1962
      CMM = 11.7365
      DMM = 0.9801
      GO TO 44
43    AMM = 0.9218
      BMM = 2.5969
      CMM = 9.9110
      DMM = 0.9647
44    CONTINUE
      ZNZ2= A1(1)+A1(2)+A1(3)
      ZNZ1=0.33333334*ZNZ2
      SS1 = A1(1) -ZNZ1
      SS2 = A1(2) -ZNZ1
      SS3 = A1(3) -ZNZ1
C
C          ZNY2, ZNY3 ARE SECOND AND THIRD INVARIANTS OF
C          DEVIATORIC STRESSES
C
      ZNY2 = 0.5 * ( SS1 * SS1 + SS2 * SS2 + SS3*SS3) + A1(4)*A1(4)
     1         + A1(5)* A1(5) + A1(6) * A1(6)
      IF(ZNY2 .EQ. 0.0 > ZNY2=1.0
      ZNY3 = SS1*SS2*SS3 + 2.0*A1(4)*A1(5)*A1(6)
     1              - SS1*A1(5) * A1(5) - SS2*A1(6)*A1(6)
     1              - SS3 *A1(4) * A1(4)
      QOS3 = 1.50*1.732 * ZNY3 / (ZNY2**1.50)
      IF(QOS3 .GE. 0.0) GO TO 46
      LAMD = CMM * COS(1.047 - ACOS(-DMM*QOS3)*0.3334)
      GO TO 47
46    LAMD = CMM * COS(0.3334* ACOS(DMM * QOS3))
47    FF = AMM*ZNY2/(CCY*CCY ) *LAMD*SQRT(ZNY2)/CCY+ BMM*ZNZ2/CCY-1.0
      GO TO 17
2     CONTINUE
C--------------- MOHR COULOMB YIELD CRITERIA-----
C
      AJ1=A1(1)+A1(2)+A1(3)
      AJ=AJ1/3.0
      SX=A1(1)-AJ
      SY=A1(2)-AJ
```

www.EngineeringBooksPDF.com

```
      SZ=A1(3)-AJ
      AJ2=0.5*(SX*SX+SY*SY+SZ*SZ)+A1(4)+A1(4)+A1(5)*A1(5)+A1(6)*A1(6)
100   FORMAT(//,5X,5F12.3)
      WRITE(2.100)AJ1,SX,SY,SZ,AJ2
      FF=3.0*AJ2+CCY*AJ1+0.2*AJ1*AJ1
      FF=3.0*FF
       FF=FF-CCY**2
       AJ2=SQRT(AJ2)
       FF=SQRT(3)*AJ2-CCY
17    CONTINUE
      RETURN
      END


          SUBROUTINE INPUT
          COMMON/GSS/ ZETA(27), ETA(27), ZI(27), W(27), NGP
          COMMON/AAA/ NEL,NNP,NEQ,NHBD,NBC,NTE1,NTE2,NTE3,NTE4,CCC,CCT,
        1  NNE1,NNE2,NNE3,NNE4,NDF,NRF,NRS,DETJ,NITER,NLI,NTYPE,YY1,YY2
          COMMON/CCC/ X(125),Y(125),Z(125),NFIX(55),NZN(55),
        1  AST(12),EST(12),DIA(12),ELINE(6,6),ELINK(6,6)
          COMMON/BBB/ D(6,6),D1(6,6),E(12,3),POIS(12,6),MCODE(20,8),
        1       EK(24,24),H(6,24),LRF(20),IDENT(20)
          COMMON/BPP/   BS1(20),BS2(20),BS3(20),SL1(20),SL2(20),SL3(20)
          COMMON/BIR/ SLOPH,SLOPV,SLOPS,NPOINTS,ELE(20)
          COMMON/OOO/ FF,ECU,BETA
C   INPUT  DATAS FOR ISOPARAMETRIC ELEMENT
C
C         READ  AND PRINT NODAL CO-ORDINATES
C
          READ(1, 10)NNP,NTE1,NTE2,NTE3,NNE1,NNE2,NNE3,NRF,NBC,NDF,NGP,NRS,
        1  NNE4 ,NTE4
          NEL = NTE1+NTE2+NTE3+NTE4
          WRITE (2,15) NEL,NNP,NTE1,NTE2,NTE3,NNE1,NNE2,NNE3,NRF,NBC,NDF,NGP
        1,  NRS
          WRITE(2,30)
          DO  8  I= 1,NNP
          READ(1,40) X(I), Y(I),Z(I)
B         WRITE(2,50) I, X(I),Y(I),Z(I)
C
C   READ AND PRINT CONNECTIVITY ARRAYS
C
          WRITE(2,60)
          NEXT =NTE1+1
          NUMB = NTE1 + NTE2
          JNUMB = NUMB + 1
          MAMP = NTE1 + NTE2+NTE3
          JMAM = MAMP + 1
          IF(NTE1 .EQ. 0)GO TO 312
          DO 3 I = 1, NTE1
          READ(1,65) (MCODE(I,J),J=1,NNE1),LRF(I),IDENT(I)
3         WRITE(2,66)I, (MCODE(I,J),J=1,NNE1),LRF(I),IDENT(I)
312       CONTINUE
          IF(NTE2 .EQ. 0) GO TO 313
          DO 7 I = NEXT, NUMB
```

www.EngineeringBooksPDF.com

```
      READ(1,106)(MODDE(I,J),J=1,NNE2),LRF(I),IDENT(I)
7     WRITE(2,107)I,(MCODE(I,J),J = 1,NNE2),LRF(I), IDENT(I)
313   CONTINUE
      IF(NTE3 .EQ. 0) GO TO 57
      DO  56  I = JNUMB , MAMP
      READ(1,67) (MCODE(I,J),J=1,NNE3),LRF(I), IDENT(I)
56    WRITE(2,68) I, (MCODE(I, J),J=1,NNE3), LRF(I),IDENT(I)
57    CONTINUE
      IF(NTE4 .EQ. 0) GO TO 311
      DO  13  I = JMAM, NEL
      READ(1,69) (MCODE(I,J),J=1,NNE4), LRF(I),IDENT(I)
13    WRITE(2,70)I, (MCODE(I,J),J=1,NNE4), LRF(I),IDENT(I)
311   CONTINUE
C
C           CALCULATE  HALF - BANDWIDTH
C
      JHBD = 1
      DO  266  I = 1, NEL
      LET = IDENT(I)
      GO TO (256,257,258,260) LET
256   NER = NNE1
      GO TO 259
257   NER = NNE2
      GO TO 259
258   NER = NNE3
      GO TO 259
260   NER=NNE4
259   MET = 10000
      JET = 1
      DO 266 J = 1, NER
      IF (MCODE(I , J) .LT. MET)  MET = MCODE(I,J)
      IF (MCODE(I, J) .GT. JET)   JET = MCODE(I,J)
      IF ((JET - MET). GT. JHBD)  JHBD = (JET - MET )
266   CONTINUE
      NHBD = (JHBD + 1)*NDF
      WRITE(2,207) NHBD
      WRITE(2,75)
      DO 11 I = 1, NRF
      READ(1, 80)    ( E(I, J), J=1,3),(POIS(I,M),M=1,3)
11    WRITE(2,85)I,( E(I,J), J=1,3),(POIS(I,M),M=1,3)
      WRITE(2, 90)
      DO 12 I = 1, NBC
      READ(1,95)NZN(I) , NFIX(I)
12    WRITE(2,100) NZN(I),NFIX(I)
C
C   READ  YOUNG'S  MODULUS  FOR  PRESTRESSING  STEEL
      WRITE (2,81)
      DO 14 I =1 , NRS
      READ(1, 71) EST(I), DIA(I)
   14 WRITE(2,72)  I , EST(I), DIA(I)
C
C                              READ PLASTIC CONSTANTS
C
      READ(1,31) CCC,CCT,YY1,YY2,BETA,ECU,NLI,NTYPE
```

www.EngineeringBooksPDF.com

```
31        FORMAT(6F0.0,210)
          WRITE(2,32)CCC,CCT,YY1,YY2,BETA,ECU,NLI,NTYPE
C----------------   READ DATAS OF BOND LINKAGE ELEMENTS-------------------
C
          READ(1,211) NPOINTS
          IF(NPOINTS.EQ.0)GO TO 307
          WRITE(2,216)
          DO 356 I=1,NPOINTS
          READ(1, 217) BS1(I), SL1(I)
356       WRITE(2,218) I,BS1(I),SL1(I)
          WRITE(2,212)
          DO 358 I=1,NTE4
          READ(1,213) ELE(I)
358       WRITE(2,214)I, ELE(I)
          SLOPS=8.0**10
          SLOPV =8.0**10
          SLOPH=(BS1(2)-BS1(1))/(SL1(2)-SL1(1))
307       CONTINUE
211       FORMAT(10)
212       FORMAT(//////,5X,15HLINKAGE ELEMENT,5X,14HAVERAGE LENGTH)
213       FORMAT(F0.0)
214       FORMAT(5X, 15,14X,F12.4)
216       FORMAT(/////,25X,12HCURVE POINTS,5X,11HBOND STRESS,11HSLIP VALUES)
217       FORMAT(2F0.0)
218       FORMAT(25X,15,10X,F10.4,10X,F10. 9)
32        FORMAT(1H1,20X,33H CONCRETE COMPRESSIVE STRENGTH  =, F12.4//
         1  20X, 32H CONCRETE TENSILE STRENGTH     =,F12.4//
         1  20X, 35H YIELD STRESS OF PRESTRESSING WIRE  =,F12.4//
         1  20X, 34H YIELD STRESS OF REINFORCEMENT     =,F12.4//
         1    20X, 33H     SHEAR FACTOR                =, F5.3//
         1   20X, 33H     CONCRETE FAILURE STRAIN      =, F6.5//
         1   20X, 34H       NO. OF LOAD INCREMENTS      =, 15//
         1   20X, 34H    NO. OF TYPE-1 STEEL ELEMENTS   =,15)
C
C
C
C
10        FORMAT(1410)
15        FORMAT(1H1,20X,37HNUMBER OF ELEMENTS                    =, 15//
        1           20X, 37HNO OF NODAL POINTS                    =,15//
        2           20X, 37HNO OF TYPE 1 ELEMENT                  =,15//
        3           20X, 37HNO OF TYPE 2 ELEMENT                  =,15//
        4           20X, 37HNO OF TYPE 3 ELEMENT                  =,15//
        5           20X, 37HNO OF NODESIN TYPE1 ELEMENT           =,15//
        6           20X, 37HNO OF NODESIN TYPE2 ELEMENT           =,15//
        7           20X, 37HNO OF NODESIN TYPE3 ELEMENT           =,15//
        8           20X, 36HSECTION REFERENCE FOR TYPE1 ELEMENT =,15//
        9           20X, 37HNO OF BOUNDARY CONDITIONS             =,15//
        1           20X, 35H NO OF DEGREES OF FREEDOM PER NODE    =,15//
        1           20X, 37HNO OF GASS POINTS FOR INTEGRATION     =,15//
        1           20X, 38HSECTION REFERENCE FOR TYPE3 ELEMENT    =,15////)
30        FORMAT(5X,5HNODES,10X,12HX-COORDINATE,10X,12HY-COORDINATE,
        1       10X,12HZ-COORDINATE)
40        FORMAT(3F0.0)
```

www.EngineeringBooksPDF.com

```
50        FORMAT(5X, 15, 13X, F10.4,12X, F10.4, 12X,F10.4)
60        FORMAT(1H1,5X,11HELEMENT NO.,10X,33HCONNECTIVITY   ARRAYS (NODE N
         10S),
         1       10X, 17HSECTION REFERENCE,3X,17HEL IDENTIFICATION)
65         FORMAT(1010)
66        FORMAT(5X,15,5X,815,18X,13,14X,15)
67        FORMAT(410)
68        FORMAT(5X,15,12X,216,39X,13,14X,15)
69        FORMAT(410)
70        FORMAT(5X,15,12X,216,12X,15,28X,15)
71        FORMAT(2F0.0)
72        FORMAT(8X,15,11X,F12.3,12X,F10.6)
75        FORMAT(1H1, 3X,17HSECTION REFERENCE,5X,38H ELASTIC MODULUS OF
        1  CONCRETE  ,27H* * * * *POISSION'S RATIOS * * * *)
80        FORMAT(6F0.0)
81        FORMAT(/////////, 5X,11HSECTION REF,8X,14HYOUNGS MODULUS,BX,
        1   13HDIA. OF STEEL)
85        FORMAT(8X,13, 12X, F10.2,2X,F10.2,2X,F10.2,4X,F4.3,2X,F4.3,2X,F4.3
        1,2X,F4.3,2X,F4.3,2X,F4.3)
90        FORMAT(1H1, 5X, 10HZERO NODES, 10X,11HCONSTRAINTS)
95        FORMAT(210)
100       FORMAT(5X,15,14X,16)
105       FORMAT(F15.4)
106       FORMAT(810)
107       FORMAT(5X,15, 5X, 615,28X,13,14X,15)
207        FORMAT(///////,15X,20HHALF BANDWIDTH IS =, 5X,15)
          RETURN
          END
```

SOC Listing

```
*     LIST 8
*     CARCS COLUMN
*     FCRIRAN NCRM
C     VERSION CURRENT OCTOBER 1969
      CLICHE COMMON
COMMON WHICH CAN VARY WITH TIME
       COMMON NC, JN, LN, TT, IR, LX, ENI, RN(12C2), DRMX(1202), VMX(1202
     1), PX(1202), QMX(1202), SIGR(1202), SIGT(1202), XMU(1202), AM(1202
     2), C1(1202), CR(1202), DV(1202), DVC(1202), EC(1202), ISV(1202),
     3 P(1202), Q(1202), CK(1202), TK(1202), VN(1202), VO(1202), AMU(120
     42), E(1202), I(1202), R(1202), V(1202), TC(12), TIC(12), RPL(25),
     5 CT, DTH, DTN, DTPR, EPP, ETOT, FDT, HDTI, IL, IPI, IPU, ITCX,
     6 IBANK, NCD, PJM, PTS, CXT, RJH, STR, SXN, TPR, HDTH, TTS
COMMON WHICH REMAINS THE SAME FOR DURATION OF PROBLEM
      COMMON CPLOT, IEPLOT, IRPLOT, IHEAC(8), GR, DXT, PLOD(100), GAS(27
     128), PT(400), FMU(400), DPM(400), PTC(200), FMC(200), DPC(200),
     2 EK(200), EP(200), DEK(200), CK(200), CP(200), CKP(200), AK(10),
     3 VI(10), RM(10), AMZ(10), AM1(10), AM2(10), GXK(10), PZO(10), P1(1
     40), P2(10), GSL(10), GCT(10), SE(0), EF(10), EV(10), GSI(10),
     5 IT(10), ITT(10), IP(10), RB(11), RHO(11), GK(10), CF, CCN, HCCN,
     6 IRZ, REZF, IWRT(4), PPR(61), TP(61), IVR, IALF
```

www.EngineeringBooksPDF.com

```
COMMON WHICH IS USED FOR GENERAL CALCULATION BUT NOT SAVEC
       COMMON ABF(4004), ABA(4004), ABB(4004), BF(200), EN(11), OCH(11),
     1 ENC(11), EDP(6), FDT(6), EDTL(6), ING(25), FNG(25), IDN(4), PRI,
     2 IC(2), MC(2), ID(8), A, ABS, AMC, AME, AMPI, B, BARK, C, CKL, CRC
     3, CIC, CZC, CAVR, CRTI, CVEL, CVRC, D, DP, CU, CEC, DRI, CR2, DRH,
     4 CRS, DIV, DV1, DVK, EW, EDV, EKL, ETA, ETW, EJTW, ERCU, FA, FST,
     5 FSTM, FSTR, G1, G2, GAM, GLN, GMI, GMU, IBX, III, IIJ, IPB, IPDT,
     6 ITER, ITOT, ITIME, ITOTL, ITSTP, J, K, L, LL, LP, M, N, NN, NP,
     7 NCYC, CFF, PCT, PL3, PL4, PQ1, PC2, PBAR, CO, CS, QKS, QSAV, R21,
     8 R22, RDR, RH1, RH2, ROR, RZI, RACT, RII21, RH22, RMV1, RMV2, SK,
     9 SLC, SLE, SLP, SMU, SDSP, SLP1, STAB, TV, TAR, TBR, TFR, TK1
       COMMON TK2, TO1, TQ2, TRR, TERK, VCC, VDV, VM1, VM2, VN1, VNH,
     1 VOL1, VOL2, WT, YN1, RIX(10), GW, F, S, AD, AF, CA, CB, DC, CD,
     2 KIM, ZETA, LIL
      COMMON CT(1202), EKS(1202)
      EQUIVALENCE (YN1, RIX(1))
      EQUIVALENCE (ION(4),PRI)
      EQUIVALENCE (ING,FNG)
      END CLICHE
      USE COMMON
C     READ 68 AND WRITE 6A
      CALL REGST
      N=.LOC.ABF(1)
      J=.LOC.ZETA
      N=J-N
      DC 1 LIL=1,N
      ABF(LIL)=C.
   1  CONTINUE
      CALL REWIND (16)
      CALL CLOCK (MO(1), MO(2))
      CRTI=1.
      NCYC=J=5
      L=16
   2  BLFFER IN (16,1) (DPLOT,IALF)
   3  IF (UNIT,16,M) 3, ,219,219
      CALL RECEOF (16)
      J=5
   4  BUFFER IN (16,1) (NC,TTS)
   5  IF (UNIT,16,M) 5, ,22C,220
      BACKSPACE FILE 16
      CALL BSPACE (16)
      CALL FSPACE (16)
      READ INPUT TAPE 2, 95C, (ID(J), J=1,8)
      READ INPUT TAPE 2, 951, GW, ITIME, A, STR
      STR=100,*STR
      CALL ASSIGN (7,0,10HSCCPLOTBUF,4020C)
      SET UP RUNNING TIME
      IF (ITIME) ,7,7
      IF (IBANK) 6, ,6
      IBANK=-ITIME
   6  ITIME=IBANK
   7  IBX=1
      TTS=MAX1F(GW*1000.,TTS)
 ECK  FOR RIGHT TAPE
```

www.EngineeringBooksPDF.com

```
      DC 8 J=1,8
      IF (IHEAD(J)-ID(J)) ,8,
      WRITE OUTPUT TAPE 3, 954, (IHEAD(J), J=1,8)
      CALL ERROR (0.)
   8  CONTINUE
      K=6
      IF (A) , ,9
      CALL WRSO
      GO TO 1C
   9  CALL RECEOF (6)
      CALL BSPACE (6)
   10 CALL WRST
      CALL WRTEOF (6)
      CALL BSPACE (6)
      CALL BANDP (ICN(1), ICN(3))
      B=ICN(2)
      B=B/PRI
      A=B-40.
      ICN(1)=A
      IF (ITIME) , ,11
      ITIME=ION(1)
      GO TO 12
   11 ITIME=XMINOF(ION(1), ITIME)
   12 ITOTL=8
      IF (NC) 13, ,13
CLE   1 CONSTANTS INITIALIZED
      CALL BANDP (ION(1), ION(3))
      A=ION(2)
      A=A/PRI
      ITOT=A
      ITCT=ITCTL-ITOT
      GO TO 15
CHECK CLOCK FOR TIME STOP -- INCREMENT COUNTER
C     EVERY 20 CYCLES GOES TO 10 INSTEAC OF 11
   13 ITSTP=0
      CALL BANDP (ICN(1), ICN(3))
      A=ION(2)
      A=A/PRI
      ITCT=A
      ITCT=ITOTL-ITCT
   14 ITSTP=ITSTP+1
CALCULATE DELTA T
      A=1.1*DTH
      B=(SQRTI(SXN))/3.
      B=MINIF(B, A)
      DT=.5*(B+DTH)
      DTH=B
CHECK FOR PRESSURE PROFILE
   15 IF (IPO-2) 20,16,
C     OUTER PRESSURE PROFILE
      L=1
      GO TO 17
C     INNER PRESSURE PROFILE
   16 L=LX
```

www.EngineeringBooksPDF.com

```
   17 TK(L)=0.
   18 A=DIMF (TP(IPI+1),TT)
      IF (A) 19, ,19
      IPI=IPI+1
      IF (TP(IPI+1)) , ,18
      IPO=1
      GO TO 20
   19 A=TT-TP(IPI)
      B=TP(IPI+1)-TP(IPI)
      P(L)=PPR(IPI)+(PPR(IPI+1)-PPR(IPI))*A/B
      EPP=EPP+(PJM*HDT1+P(L)*DTN)*V(L-1)*CCN*(3.*RJH*RJH+FDT*V(L-1)*V(
     11))
      ETOT=EPP+ENI
CYCLE CONSTANT INITIALIZATION
   20 PCT=BARK=0.
      TT=TT+DTH
      HDTI=.5*DT
      HDTH=.5*DTH
      DTN=DTH-HDTI
      FDT=HDTP*HDTH
      L=IR
      SXN=DXT
      QXT=ABSF(QXT)
      VCC=1.0E-3*QXT/SQRTI(AK(L)*RHC(L+1))
      VCC=MINIF(VCC,1.0E-8)
      QXT=1.
      PC1=P(JN)+Q(JN)
      TC1=TK(JN)+CK(JN)
      IF (I(JN)) ,21,
      DR1=DR(JN-1)-CR(JN)+RN(JN-1)-RN(JN)
      R21=DR(JN-1)+CR(JN)+RN(JN-1)+RN(JN)
      VCL1=VN(JN)-DVO(JN)
      VM1=(VOL1-DV(JN))/AM(JN)
      TK1=TQ1*VM1/R21
      RMV1=DR1/VM1
      RH1=R(JN-1)+V(JN-1)*HDTH
      RH21=RH1*RH1*V(JN-1)
CALCULATION OF J-LINES BEGINS HERE
   21 CC 144 J=JN,LN
      GAM=0.
      III=(I(J)-1)/10C+1
      EC(J)=E(J)
      VC(J)=V(J)
CALCULATE EQUATIONS OF MOTION
      IF (R(J)) 218,27,
      PC2=P(J+1)+Q(J+1)
      TC2=TK(J+1)+QK(J+1)
      IF (I(J+1)) ,28,
      CR2=CR(J)-DR(J+1)+RN(J)-RN(J+1)
      R22=DR(J)+DR(J+1)+RN(J)+RN(J+1)
      VCL2=VN(J+1)-DVC(J+1)
      VM2=(VOL2-DV(J+1))/AM(J+1)
      TK2=TQ2*VM2/R22
      RMV2=DR2/VM2
```

www.EngineeringBooksPDF.com

```
      IF (I(J)) ,29,
      ROR=(TK2*DR1+TK1*DR2)/(DR1+DR2)
      RCR=.5*(RMV1+RMV2)
   22 A=(PQ1-PQ2)/RDR
      IF (V(J)) ,23,
      VCC=1.E-2C
   23 DV1=DT*(1.333333333*(TQ1-TQ2)/RDR+A+8.*RCR+GR)
      V(J)=V(J)-DV1
      IF (ABSF(V(J))-VCC) 30,30,
   24 C=DTH*V(J)
      RH2=R(J)+.5*C
      RH22=RH2*RH2*V(J)
      DR(J)=DR(J)+C
      R(J)=RN(J)+DR(J)
      CRS=R(J-1)-R(J)
      IF (I(J)) ,113,
   25 C=(V(J)-V(J-1))*(V(J)*(V(J-1)+V(J))+V(J-1)*V(J-1))
      C=DTH*(3.*(RH22-RH21)+FDT*C)
      DV(J)=DV(J)+C
      VN1=VOL1-DV(J)
      VNH=VN1+.5*C
      D=(DV(J)+DVC(J))/VN1
      AMP1=D+1.
      EDV=C/VN(J)
      DVK=C/VNH
      FTA=VN(J)/VNH
      VCV=VN(J)*C/(VN1*(VN1+C))
      DU=V(J-1)-V(J)
      DRH=RH1-RH2
      IF (CU) ,26,26
      ERCU=ETA*DU*RHO(L+1)
      QSAV=ERCU*DU
   6  TER=3.*CTH*CU/DRH
      TERK=DVK+TER
      IF (III-3) 31,31,
      IF (I(J)-40C) 116,125,125
CALCULATE BOUNDARY CONDITIONS
   7  RH2=RH22=0.
      GO TO 25
   8  RCR=.5*RMV1
      ROR=TK1
      GO TO 22
   9  RDR=.5*RMV2
      ROR=TK2
      GO TO 22
CALCULATIONS MADE WHEN LITTLE OR NO ACTIVITY EXISTS
   10 V(J)=0.
      IF (V(J-1)) 24, ,24
      RH2=R(J)
      RH22=0.
      IF (III-3) 113,113,
      IF (III-4) ,24,
      C=DR1*(R(J-1)*R21+R(J)*R(J))
      PCT=C*P(J)+PCT
```

www.EngineeringBooksPDF.com

```
      GO TO 113
CALCULATE SLOPE AND PRESSLRE FOR I LESS THAN 300
   11 N=IT(L)+1
      NP=IP(L)+1
      PL3=SLP=SMU=0.
      IF (XMU(J)-2.*GCT(L)*AM2(L)) ,47,47
      IF (XMU(J)) 56, ,
      IF (D-XMU(J)) 32, ,
      XMU(J)=C
      GO TO 42
      IF (XMU(J)-AM1(L)) 42,42,
      IF (III-2) 34, ,
      IF (P(J)) , ,34
      IF (XMU(J)-AM2(L)) 33, ,
      XMU(J)=.98*AM2(L)
      XMU(J)= -XMU(J)
      GO TO 56
      IF (XMU(J)-AM2(L)) ,48,48
      IF (D-.95*XMU(J)) ,42,42
  PECIAL UNLOAdING SCHEME - A -
      IF (D-AM1(L)) , ,35
      SLP=AK(L)
      GO TO 41
   35 CC 36 K=NP,NP+38
      IF (P(J)-PT(K)) 37,37,
      IF (FMU(K+1)-FMU(K)) 37,37,
   36 CONTINUE
      K=NP+38
   37 SLE=DPM(K)
      DO 38 K=N,N+18
      IF (P(J)-PTC(K)) 39,39,
      IF (FMC(K+1)-FMC(K)) , ,38
      SLC=SLE
      GO TO 40
   38 CONTINUE
      K=N+18
   39 SLC=DPC(K)
   40 SLP1=SLE+XML(J)*(SLC-SLE)/AM2(L)
      SLP=SLP1-AM1(L)*(SLP1-AK(L))/C
   41 PL3=P(J)+SLP*VDV
      GO TO 65
CALCULATE ELASTIC P-MU TABLE - B -
   42 ABS=D
      CALL PSUB
      GO TO 65
      ENTRY PSUB
      DO 44 K=NP,NP+38
      IF (ABS-FMU(K)) ,45,43
      PL3=PT(K-1)+(ABS-FML(K-1))*DPM(K)
      GO TO 46
   43 IF (FMU(K+1)-FMU(K)) 45,45,
   44 CONTINUE
      K=NP+38
   45 PL3=PT(K)+(ABS-FMU(K))*DPM(K)
```

www.EngineeringBooksPDF.com

```
   46 SLP=DPM(K)
      RETURN PSUB
CALCULATE CRUSHED P-MU TABLE
   47 XMU(J)=MAX1F(D, XMU(J))
   48 SLP=AK(L)*.C1
      ABS=D
      DC 51 K=N-1,N+18
      IF (D-FMC(K)) 49, ,50
      PL3=PTC(K)
      SLP=DPC(K)
      GO TO 52
   49 IF (K-N) 52, ,
      PL3=PTC(K-1)+(D-FMC(K-1))*DPC(K)
      SLP=DPC(K)
      GO TO 52
   50 IF (FMC(K+1)-FMC(K)) , ,51
      CALL PSUB
      GO TO 52
   51 CONTINUE
      CALL PSUB
   52 IF (D-.985*XMU(J)) ,65,65
      ABS=XMU(J)
      PL4=PL3
      SLP1=SLP
      CALL PSUB
      GAM=.5*PL3*XMU(J)/(1.+XMU(J))
      GAM=GXK(L)*(GAM-EF(L))/(EV(L)-EF(L))
      IF (GAM), ,53
      PL3=PL4
      SLP=SLP1
      GO TO 65
   53 GAM=MIN1F(GAM,GXK(L))
      ABS=C
      IF (D) , ,54
      PL4=GSL(L)*C
      PL3=SLP=0.
      SLP1=GSL(L)
      GO TO 55
   54 CALL PSUB
   55 DP=GAM*(E(J)-.5*PL3*D/AMP1)
      PL4=PL4+DP
      SLP=SLP1+.5*GAM*((PL4+P(J))/ETA-(.5*(B+AMU(J))*SLP+PL3/ETA))/ETA
      PL3=PL4
      IF (SLP) ,65,65
      SLP=.01*AK(L)
      GO TO 65
CALCULATE S.L.S.
   56 IF (D-AMZ(L)) , ,57
      PL3=0.
      SLP=AK(L)
      GO TO 65
   57 DO 58 K=N,N+18
      IF (P(J)-PTC(K)) 62, ,
      IF (FMC(K+1)-FMC(K)) 59,59,
```

www.EngineeringBooksPDF.com

```
   58 CONTINUE
   59 DO 60 K=NP,NP+38
      IF (P(J)-PT(K)) 61, ,
      IF (FMU(K+1)-FMU(K)) 61,61,
   60 CONTINUE
      K=NP+38
   61 ABS=FMU(K-1)+(P(J)-PT(K-1))/DPM(K)
      SLP=DPM(K)
      GO TO 63
   62 ABS=FMC(K-1)+(P(J)-PTC(K-1))/CPC(K)
      SLP=DPC(K)
   63 IF (D-ABS) ,64,64
      IF (ABS-AMZ(L)) ,64,
      SLP=(D-AMZ(L))*SLP/(ABS-AMZ(L))
   64 PL3=P(J)+SLP*VDV
      IF (PL3) ,65,65
      PL3=0.
  - EXIT -
   65 IF (E(J)-EF(L)) ,66,66
      ABF(IBX+1)=V(J)
      A=ISV(J)
      ABF(IBX+2)=SIGNF(C1(J),A)
      ABF(IBX+3)=AMU(J)
      ABF(IBX+4)=P(J)
      ABF(IBX+5)=TK(J)
      IBX=IBX+7
  209 CONTINUE
      IF (IEPLOT) 211,211,
      ABF(IBX-1)= -100.
      ABF(IBX)=ETCT
      DC 210 N=1,6
      ABF(IBX+1)=EDTL(N)
      IBX=IBX+1
  210 CONTINUE
      IBX=IBX+1
      GO TO 212
  211 ABF(IBX-1)= -10.
  212 IF (ITSTP-2C) 14,13,13
  213 L=2
CALCULATE BALANCE OF REAL TIME IN ACCOUNT (NEG. RUNNING TIME) AND RESET
  214 IF (IBANK) 215,215,
      IBANK=IBANK-ITOT
  215 III=2
C - EMPTY PLOT BUFFER ONTO 68 BEFORE TERMINATICN
      IF (DPLCT) 216,216,
      CALL PLTOUT
C - WRITE FINAL DUMP ON 68
  216 K=16
      CALL WRST
      K=6
      CALL PLOTE
      CALL WRST
      CALL WRTEOF (6)
      CALL UNLOAD (6)
```

www.EngineeringBooksPDF.com

```
      CALL CLCCK (IC(1),IC(2))
      WRITE OUTPUT TAPE 3, 966, ITOT, IC(1),IC(2)
      WRITE OUTPUT TAPE 3, 967
      CALL OOND3A(3)
      CALL OOND3A(61)
      IF (L-1) ,217,
      READ INPUT TAPE 2, 971, L
      IF (L-8) 217, ,217
C - CALL PLOT
      CALL CHAIN (5,5)
C - UNLOAD TAPES - CALL EXIT - NO PLOT
  217 CALL UNLOAD (16)
      CALL EXIT
CREATE IF RADIUS NEGATIVE
        OUTPUT TAPE 3, 968, J-1
        ERROR (1.)
        ROUTINES
  219 CALL TSTR
      GO TO (221,2,2,2), J
  220 CALL TSTR
      GO TO (221,4,4,4), J
  221 WRITE OUTPUT TAPE 3, 972
      PRINT 972
      CALL OOND3A(3)
      CALL OOND3A(61)
      CALL EXIT
C     MAIN CODE TAPE SUBRCUTINES
      ENTRY TSTO
      CALL BSPACE (K)
      DO 900 M=1, (5-N)
      CALL WRBLNK (K)
  900 CONTINUE
      N=N-1
      RETURN TSTO
      ENTRY WRSC
      N=5
  901 BUFFER OUT (K, 1) (DPLOT,IALF)
  902 IF (UNIT, K, M) 902,904, ,
      CALL TSTO
      IF (N-1) 901, ,901
      WRITE OUTPUT TAPE 3, 908, K
      IF (K-6) 903, ,903
      RETURN WRSO
  903 CALL OOND3A(3)
      CALL OOND3A(61)
      CALL EXIT
  904 CALL WRTEOF (K)
      RETURN WRSO
      ENTRY WRST
      N=5
  905 BUFFER CUT (K,1) (NC,TTS)
  906 IF (UNIT,K,M) 906,907, ,
      N=N-1
      IF (N-1) 905, ,905
```

www.EngineeringBooksPDF.com

```
  907 RETURN WRST
      ENTRY TSTR
      CALL BSPACE (L)
      J=J-1
      RETURN TSTR
      FORMAT STATEMENTS
  908 FORMAT ( 7H1 TAPE ,13,38H IS BAD, PLEASE REPLACE IT AND RESTART)
  950 FORMAT (8A1C)
  951 FORMAT (E7.C,17,2E7.0)
  952 FORMAT (///35H ENERGY TOTALS PER ORIGINAL REGIONS)
  953 FORMAT (///33H ENERGY TOTALS PER MATERIAL STATE)
  954 FORMAT (60H TAPE 68 AND CARD I.D. ARE NOT THE SAME, PROBLEM TERMIN
     1IATED///22H TAPE IS FOR PROBLEM ,8A10)
  956 FORMAT (1H1/8H SOC II ,7A10,4A10//, 9H STARTED ,1A8, 4H ON ,1A8/)
  957 FORMAT (1H1/8A1C,4A10)
  958 FORMAT (///43H N CYCLE  DELTA T(N)  DELTA T(N+.5)   TIME//1X,16,
     11X,3E14.5//42H   DELTA T CONTROLLED BY ZONE WITH RADIUS =,E14.5)
  960 FORMAT (//69H     KINETIC ENERGY     INTERNAL ENERGY     GRAVITY
     1    TOTAL ENERGY//(4E18.10))
  961 FORMAT (///17H ENERGY INPUT IS ,E18.10)
  962 FORMAT (///35H THIS IS A PRESSURE PROFILE PROBLEM)
  963 FORMAT (///36H VOLUME WEIGHTED CAVITY PRESSURE IS ,E12.5)
  964 FORMAT (18H BAD ENERGY CHECK/)
  966 FORMAT (26H PROBLEM TERMINATED AFTER ,16,8H SECONDS///13H THE TIME
     1 IS ,1A8,13H THE MACHINE ,1A8)
  967 FORMAT (1H1)
  968 FORMAT (1H1///19H NEGATIVE R AT J = ,14,14H CHECK PROBLEM)
  971 FORMAT (11)
  972 FORMAT (65H 3 BAD READS OF 68, CHECK TAPE AND UNIT, THEN RESTART
     1THIS JOB )
  973 FORMAT (60H ERROR IN THIS PROBLEM.   DO NOT TRY TO CONTINUE OR RES
     1TART.)
  974 FORMAT (1H1///47H SLOPE LESS THAN OR EQUAL TO ZERO. CHECK INPUT//)
     1//117H CYCLE DELTA T(N) DELTA T(N+.5) J STATE P(N+1)
     2SLOPE     MU(N+1)     P(N)     MU(N)     MU MAX//1X,16,
     32E12.5,216,5E13.5,E12.5)
  975 FORMAT (1H1///30H MU-E/SLOPE GREATER THAN 1.501///60H     MU-E
     1     SLOPE     MU N+1     PRESSURE     LOC.//4E14.5,11)
  976 FORMAT (1H1///30H MU-C/SLOPE GREATER THAN 1.501///60H     MU-C
     1     SLOPE     MU N+1     PRESSURE     //4E14.5)
  977 FORMAT (45H END OF TAPE SENSED - DUMP TAKEN - RECORD = ,13)
      END
*     LIST8
*     CARDS COLUMN
*     FORTRAN     PLTC
      SUBROUTINE PLIOUT
      USE COMMON
      CALL REWIND (7)
      BUFFER IN (7,1) (ABA(1),ABA(4C04))
      M=4005
      J=1
      DO 7 N=1,IPB
    1 IF (UNIT,7,K) 1,2,,100
      WRITE OUTPUT TAPE 3, 103, N, IPB
```

www.EngineeringBooksPDF.com

```
  103 FORMAT (20H END TAPE ERROR - N=,I3,6H I PB =,I3)
      GO TO 2
  100 IF (I0 CHECK,7) ,102
      WRITE OUTPUT TAPE 3, 101, N, IPB
  101 FORMAT (20H PARAITY ERROR - N =,I3,6H I PB =,I3)
      GO TO 2
  102 WRITE OUTPUT TAPE 3, 104, N, IPB
  104 FORMAT (20H WORD COUNT ERROR,N=,I3,6H IPB =,I3)
    2 IF (N-IPB) ,3,3
      BUFFER IN (7,1) (ABA(M),ABA(M+4003))
    3 BUFFER OUT (16,1) (ABA(J),ABA(J+4003))
    4 IF (UNIT,16,K) 4,5,,
      WRITE OUTPUT TAPE 3, 900
      IF (M-1) , ,6
      M=4005
      J=1
      GO TO 7
    6 M=1
      J=4005
    7 CONTINUE
    8 CALL REWIND (7)
      BUFFER OUT (16,1) (ABF(1), ABF(4004))
    9 IF (UNIT,16,K) 9,10,,
      WRITE OUTPUT TAPE 3, 900
   10 CALL WRTEOF (16)
      RETURN
  900 FORMAT (51H BAD TAPE READ/WRITE, PLOT MAY HAVE SOME BAD POINTS)
      END
*     LIST 8
*     CARDS COLUMN
*     FORTRAN     RPLOT
      SUBROUTINE RPLOT
      USE COMMON
      A=R(JN)
      DO I J=JN,LN
      IF (I(J)-390) 1, ,
      B=R(J-1)
      LP=J-1
      GO TO 2
    1 CONTINUE
      B=R(LN)
      LP=LN
    2 YN1=GW=V(J)
      F=S=P(JN)
      AD=AF=TK(JN)
      DA=CB=EO(JN)=P(JN)+1.3333333*TK(JN)
      DC=CD=VO(JN)=P(JN)-.66666667*TK(JN)
      DC 3 J=JN+1,LP
      YN1=MAX1F(YN1,V(J))
      Gh=MIN1F(GW,V(J))
      F=MAX1F(F,P(J))
      S=MIN1F(S,P(J))
      AD=MAX1F(AD,TK(J))
      AF=MIN1F(AF,TK(J))
```

www.EngineeringBooksPDF.com

```
      VO(J)=P(J)-.66666667*TK(J)
      EO(J)=P(J)+1.3333333*TK(J)
      DA=MAX1F(DA,EO(J))
      DB=MIN1F(DB,EO(J))
      DO=MAX1F(DC,VO(J))
      DD=MIN1F(DD,VO(J))
    3 CONTINUE
      K=LP-JN+1
      DO 12 J=1,10, 2
      IF (RIX(J)-RIX(J+1)) 12,12,
      CALL SETCH (10.,2.,0, 0, 0, 0)
      GO TO (4,5,6,8,9), J/2+1
    4 WRITE OUTPUT TAPE 100, 450, (IHEAD(N), N=1,8), TT
      L=JN+12020
      GO TO 7
    5 WRITE OUTPUT TAPE 100, 451, (IHEAD(N), N=1,8), TT
      L=JN
      GO TO 7
      6 WRITE OUTPUT TAPE 100, 452, (IHEAD(N), N=1,8), TT
      L=JN+3606
    7 CALL MAPG(B, A, RIX(J+1), RIX(J))
      CALL TRACE (R(JN), P(L), K)
      GO TO 11
    8 WRITE OUTPUT TAPE 100, 453, (IHEAD(N), N=1,8), TT
      L=JN
      GO TO 10
    9 WRITE OUTPUT TAPE 100, 454, (IHEAD(N), N=1,8), TT
      L=JN+8414
   10 CALL MAPG (B, A, RIX(J+1), RIX(J))
      CALL TRACE (R(JN), EOIL), K)
   11 CALL FRAME
   12 CONTINUE
      RETURN
  450 FORMAT (8A1C/30H VELOCITY VERSUS RADIUS AT T =  ,E12.5)
  451 FORMAT (8A1C/30H PRESSURE VERSUS RADIUS AT T =  ,E12.5)
  452 FORMAT (8A1C/31H K-R THETA VERSUS RADIUS AT T =  ,E12.5)
  453 FORMAT (8A1C/30H RADIAL STRESS VERSUS R AT T =  ,E12.5)
  454 FORMAT (8A1C/34H TANGENTIAL STRESS VERSUS R AT T =  ,E12.5)
      END
*         LIST 8
*         CARDS COLUMN
*         FORTRAN
          SUBROUTINE BANDP (IBA,ITL)
          USE COMMON
C
C         CALL BANDP(A,B)
C         STORES ASCII USER NUMBER IN A(1)
C         STORES NUMBER OF SECONDS IN BANK ACCOUNT IN A(2) INTEGER
C         STORES TL IN B(1) INTEGER SECONDS
C         STORES PRIORITY IN B(2) FLOATING PT
C
          COMMON /GOBCOM/ GCOM
          ADDRESS ZETA
          DIMENSION IBA(2), ITL(2)
```

www.EngineeringBooksPDF.com

```
          ZETA=0
          KIM = (2401B.SHL.48).LN.((.LOC.ERROR) .SHL.30) .UN.(.LOC.IBA(1))
          GCOM=(1004B.SHL.18).UN.(.LOC.KIM)
          GO TO ZETA
ERROR     GO TO OK
          GO TO ERROR
OK        IBA(2) =IBA(2) / 1000000
          KIM =(2403B.SHL.48).UN.((.LOC.ERR) .SHL.30 ) .UN.(.LOC.ITL(1))
          GCOM=(1004B.SHL.18).UN.(.LOC.KIM)
          GO TO ZETA
ERR        GO TO THRU
          GO TO ERR
THRU      ITL(1)= ITL(1) / 1000000
          RETURN
          END
*     LIST 8
*     CARDS COLUMN
*     FORTRAN     ERRCR
      SUBROUTINE ERROR (ERR)
      USE COMMON
      CALL UNLOAD (16)
      CALL UNLOAD (6)
      IF (CRTI) 1, ,1
      CALL PLOTE
    1 IF (ERR) 3,3,
      WRITE OUTPUT TAPE 3, 100, NC, DT, DTH, TT, RADT
      DO 2 J=JN,LN
      I(J)=XSIGNF(I(J),ISV(J))
    2 CONTINUE
      WRITE OUTPUT TAPE 3, 101, (J-1, DR(J), R(J), V(J), AMU(J), P(J),
     1 Q(J), TK(J), QK(J), E(J), I(J), J=JN,LN+1)
    3 CALL OOND3A (3)
      CALL OOND3A (61)
      CALL EXIT
  100 FORMAT (18H1 ERROR PRINTOUT///43H N CYCLE   DELTA T(N) DELTA T
     1(N+.5) TIME///X,I6,1X,3E14.5//42H DELTA T CONTROLLED BY ZONE WIT
     2H RADIUS =,E14.5)
  101 FORMAT (///120H   J   DELTA R     RADIUS   VELOCITY   MU
     1 PRESSURE   SHOCK   k  R-THETA   K SHOCK   ENERGY   ST
     2 ATE//(1X,14,9E12.5,17))
       END
```

www.EngineeringBooksPDF.com

Appendix B
KOBE (Japan) Earthquake Versus Kashmir (Pakistan) Earthquake

B.1. KOBE Earthquake versus Kashmir Earthquake

The summary of the Japan meteorological Agency (JMA) has produced intensity scale and range exists from 0 to 7. Mostly the areas come under disastrous (No. 6) to very disastrous (No.7). Number 7 where collapse of more than 30 % of wooden houses falling of objects, wavy deformation observed in horizon. The Kashmir Earthquake was similar. Despite all these the brick houses together with stoney ones, collapse like house of card. The Kobe Earthquake is known also as Hyogo-Ken Manbu. Although various spring dampers were used. In Kashmir no such things existed. The damage could have been more, had Kashmir not having stoney mountains or it had plane areas like KOBE. Based on modified Marcalli (MM) of XII, and JMA 7, the positional scale of KOBE lies between them. The disaster level in Azad Kashmir was much more it did not have modern construction of houses, roads and amenities. Many thousands of human beings were carelessly killed or mammed in Kashmir since it did not have plane area to have access to when compared with that of KOBE.

B.1 Data comparison

Serial Number	KOBE				Kashmir		
(1)	M_L = Magnitude = 7.6 on Richter Scale			↔	Magnitude = 7.6 on Richter Scale		
(2)	Hypo-depth = 10 Km			↔	Hypo-depth = 16 km		
(3)	M_W = Moment Magnitude = 6.9			↔	7.2		
(4)	M_S = Surface Magnitude = 6.9			↔	7.2		
(5)	Epicentre Location = 34.527 N, 135.005E			↔	40.35 N 123.00		
(6)	Fault line 50 km long SE (affecting small areas)			↔	100 km long NS (affecting large areas)		
(7)	Accumulated stress Equivalent to "2 No" Earthquake M_L = 8.5 or larger			↔	Accumulated stress Equivalent "4 No" Earthquake M_L = 8.5 or larger		
	Acceleration			↔	*Velocity*		
(8)	(Max) (cm/s/s)			*Component*	(Max) (CMax) (cm/s)		
	N-S	EW	UD	↔	N-S	EW	UD
	818.0	617.3	332.2	↔	55.1	344 cm/s	20.6 cm/s

www.EngineeringBooksPDF.com

B.1 (continued)

Serial Number	KOBE		Kashmir
(9)	*Energy*	↔	*Energy*
	More Eg. Less than Kashmir. Acceleration greater or lesser less energy. Separation time less between horizontal wave and slowing moving surface wave is longer and hence less impact and less destructive	↔	More E_S, greater from 16 km depth. More energy E_s transferred to the surface. Separation time is sharper. More impact, more destruction
(10)	Vertical component of acceleration = 21%	↔	Vertical component of acceleration 30%
(11)	Peak ground acceleration from site within 10 km from zone of intense destruction, the fault zone of KOBE Earthquake		
	Kobe Motoyama	↔	*Kashmir*
	PGA (g) = 0.79		*Muzzafar Abad* PGA (g) = 0.83
	* Estimate distance from fault line = 1 km		* Estimate 2 km distance
	Kobe University		*Border Area*
	PGA(g) = 0.31		PGA (g) = 0.32 to 0.33
	* Distance = 3 km		*Distance = 3 km
	* Distance from site within 10 km of the zone fo destruction.		

www.EngineeringBooksPDF.com